Lars Olof Björn *Editor*

Photobiology

The Science of Light and Life

Third Edition

Springer

Photobiology

Lars Olof Björn
Editor

Photobiology

The Science of Light and Life

Third Edition

Springer

Editor
Lars Olof Björn
School of Life Science
South China Normal University
Guangzhou
China

Department of Biology
Lund University
Lund
Sweden

ISBN 978-1-4939-1467-8 ISBN 978-1-4939-1468-5 (eBook)
DOI 10.1007/978-1-4939-1468-5
Springer New York Heidelberg Dordrecht London

Library of Congress Control Number: 2014958587

Preface

I started my first photobiological research project in the spring of 1957. My scientific interest ever since has been focused on photobiology in its many aspects. Because I have been employed as a botanist, my own research has dealt mostly with the photobiology of plants, but throughout this time, I have been interested in other aspects such as vision, the photobiology of skin, and bioluminescence. A first edition of the present book was published in 2002 and a second edition in 2008. This third edition is much expanded and completely updated. Eight new authors have been recruited among my eminent colleagues.

It has not been possible to cover all aspects of photobiology in one volume, but I feel that we have managed to catch a fair and well-balanced cross section. Many colleagues promised to help, but not all lived up to their promises. To those who did and who are coauthors to this volume, I direct my thanks; I think that they have done an excellent job.

Living creatures use light for two purposes: for obtaining useful energy and as information carrier. In the latter case, organisms use light mainly to collect information but also (e.g., by coloration and bioluminescence) for sending information, including misleading information, to other organisms of their own or other species. Collection of free energy through photosynthesis and collection of information through vision or other photobiological processes may seem to be very different concepts. However, on a deep level, they are of the same kind. They use the difference in temperature between the sun and our planet to evade equilibrium, i.e., to maintain and develop order and structure.

Obviously, all of photobiology cannot be condensed into a single volume. My idea has been to first provide the basic knowledge that can be of use to all photobiologists and then give some examples of special topics.

Thus, this book is intended as a start, not as the final word. There are several journals dealing with photobiology in general and an even greater number dealing with special topics such as vision, photodermatology, or photosynthesis. There are several photobiology societies arranging meetings and other activities. And last but not least, up-to-date information can be found on the Internet. The most important site apart from the Web of Science, Scopus, Google Scholar, and other scientific databases is the homepage for the International Union of Photobiology http://iuphotobiology.com/societies.html, which has links to a number of regional and national organizations for photobiology.

The subtitle of this book may be somewhat misleading. There is only one science. But I wanted to point out that the various disciplines dealing with light and life have more in common than is perhaps generally realized. I hope that the reader will find that the same principles apply to seemingly different areas of photobiology. For instance, we have transfer of excitation energy between chromophores active in photosynthesis, in photorepair of DNA, and in bioluminescence. Cryptochromes, first discovered as components in light-sensing systems in plants, are involved in the human biological clock and probably in the magnetic sense of birds and other animals, and they have evolved from proteins active in DNA photorepair.

Many colleagues have been helpful in the production of this book. Three of my coauthors—Professors Helen Ghiradella, Govindjee, and Anders Johnsson—who are also close friends have earned special thanks because they have helped with more chapters than those who bear their names. Helen has also helped to change my Scandinavian English into the American twist of the

islanders' tongue, but we have not changed the dialect of those who are native English speakers. Govindjee has contributed not only with his knowledge of photobiology but also with his great experience in editing. Drs. Margareta Johnsson and Helena Björn van Praagh have helped with improvements and corrections, and Professor Allan Rasmusson at our department in Lund has been very helpful when I and my computer have had disagreements. I have enjoyed the friendliness and help of other colleagues in the departments in Lund and Guangzhou. The staff of our biology library in Lund has been very helpful and service minded. Several colleagues, among them Stig Allenmark, DainisDravins, Dmitri Lapotko, Sandra Pizarello, and Eric Warrant, have reviewed sections that deal with their own research areas. I deeply regret that one author, Gernot Renger, unexpectedly passed away before being able to complete his chapter. I wish to express my thanks to the publisher and printer staff for their support during the production of this book.

Many others have helped, but special thanks go to my wife and beloved photobiologist Gunvor, who has supported me during the work and put up with papers and books covering the floor in our common home; to her I dedicate those chapters of the book that bear my name.

There are several new chapters in the third as compared to the second edition: Chap. 11, Photoactive proteins; Chap. 13, Photoreceptive proteins and their evolution; Chap. 14, Signaling crosstalk under the control of plant photoreceptors; Chap. 17, Photosynthetic light harvesting; Chap. 25 Light-promoted infection; Chap. 27, Role of ultraviolet radiation in the origin of life. On the other hand, some chapters present in the second edition had to be skipped either for space limitation or for other reasons: Photosynthetic light harvesting, charge separation, and photoprotection: The primary steps; Photoperiodism in insects and other animals; Light treatment in medicine. The former chapter "Spectral tuning in biology" has been divided into two, one dealing with pigments and the other one with structural color. However, it will still be possible to obtain pdf files of chapters from the second edition from the publisher.

Lund, Sweden
March 2014

Lars Olof Björn

Photobiology

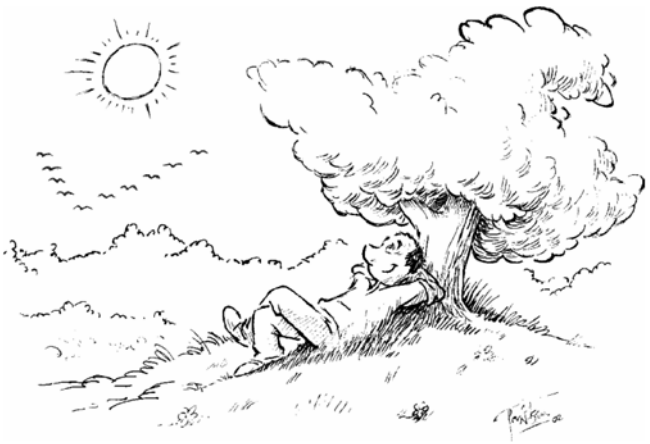

(Drawing by Per Nilsson)

I am lying on my back beneath the tree,
dozing, looking up into the canopy,
thinking: what a wonder!—I can see!

But in the greenery above my face,
an even greater miracle is taking place:
Leaves catch photons from the sun
and molecules from air around.
Quanta and carbon atoms become bound.
Life, for them, has just begun.

The sun not only creates life, it also takes away
mostly by deranging DNA.
Damage can be, in part, undone
by enzymes using photons from the sun.

Summer nears its end, already 'cross the sky
southward aiming birds are flying by.

Other birds for travel choose the night
relying on the stars for guiding light.
Imprinted in their little heads are Gemini,
Orion, Dipper, other features of the sky.
There is room for clocks that measure
day and night,
Correct for movement of the sky
and tell the time for flight

Deep into oceans, into caves
the sun cannot directly send its waves.
But through intricacies of foodweb's maze,
oxygen from chloroplasts, luciferin,
luciferase,
at times, in place,
where night and darkness seem to reign,
solar quanta emerge as photons once again.
L.O. Björn 2002

Contents

Contributors

Lars Olof Björn School of Life Science, South China Normal University, Guangzhou, China

Department of Biology, Lund University, Lund, Sweden

Wolfgang Engelmann Department of Botany, University of Tübingen, Tübingen, Germany

Helen Ghiradella Department of Biology, University at Albany, Albany, NY, USA

Govindjee Biochemistry, Biophysics and Plant Biology, Department of Plant Biology, University of Illinois, Urbana, IL, USA

Charlotte Helfrich-Förster Lehrstuhl für Neurobiologie und Genetik, Biozentrum Universität Würzburg, Würzburg, Germany

Pirjo Huovinen Universidad Austral de Chile, Instituto de Ciencias Marinas y Limnológicas, Valdivia, Chile

Lei Jiang School of Life Science, South China Normal University, Guangzhou, China

Anders Johnsson Department of Physics, Norwegian University of Science and Technology (NTNU), Trondheim, Norway

Richard E. Kendrick Department of Plant Science, Wageningen University, Wageningen, The Netherlands

Shuichi Kinoshita Graduate School of Frontier Biosciences, Osaka University, Osaka, Japan

Shaoshan Li School of Life Science, South China Normal University, Guangzhou, China

Miriam Liedvogel Max-Planck-Institute for Evolutionary Biology, Ploen, Germany

Richard L. McKenzie National Institute of Water and Atmospheric Research, (NIWA), Omakau, Central Otago, New Zealand

Tihana Mirkovic Department of Chemistry, University of Toronto, Toronto, ON, Canada

Curtis D. Mobley Sequoia Scientific, Inc, Bellevue, WA, USA

Rachel Muheim Department of Biology, Lund University, Lund, Sweden

Mary Norval Biomedical Sciences, University of Edinburgh Medical School, Edinburgh, Scotland, UK

Qiu Qiu Department of Research and Development, Guangzhou Water Quality Monitoring Center, Guangzhou, China

Gregory D. Scholes Department of Chemistry, University of Toronto, Toronto, ON, Canada

Department of Chemistry, Princeton University, Princeton, NJ, USA

Yutao Wang School of Life Science, South China Normal University, Guangzhou, China

James L. Weller School of Plant Science, University of Tasmania, Hobart, Tasmania, Australia

The Nature of Light and Its Interaction with Matter

1

Lars Olof Björn

1.1 Introduction

The behavior of light when it travels through space and when it interacts with matter plays a central role in the two main paradigms of twentieth-century physics: relativity and quantum physics. As we shall see throughout this book, it is also important for an understanding of the behavior and functioning of organisms.

1.2 Particle and Wave Properties of Light

The strange particle and wave properties of light are well demonstrated by a modification of Young's double-slit experiment. In Young's original experiment (1801), a beam of light impinged on an opaque screen with two parallel, narrow slits. Light passing through the slits was allowed to hit a second screen. Young did not obtain two light strips (corresponding to the two slits) on the second screen but instead a complicated pattern of several light and dark strips. The pattern obtained can be quantitatively explained by assuming that the light behaves as waves during its passage through the system.

It is easy to calculate where the maxima and minima in illumination of the last screen will occur. We can get some idea of the phenomenon of *interference* by just overlaying two sets of semicircular waves spreading from the two slits (Fig. 1.1), but this does not give a completely correct picture.

For the experiment to work, it is necessary for the incident light waves to be in step, i.e., the light must be spatially coherent. One way of achieving this is to let the light from a well-illuminated small hole (in one more screen) hit the screen with the slits. The pattern produced (Fig. 1.2) is a so-called interference pattern or, to be more exact, a pattern produced by a combination of *diffraction* (see the next section) in each slit and *interference* between the lights from the two slits. It is difficult to see it if white light is used, since each wavelength component produces a different pattern. Therefore, at least a

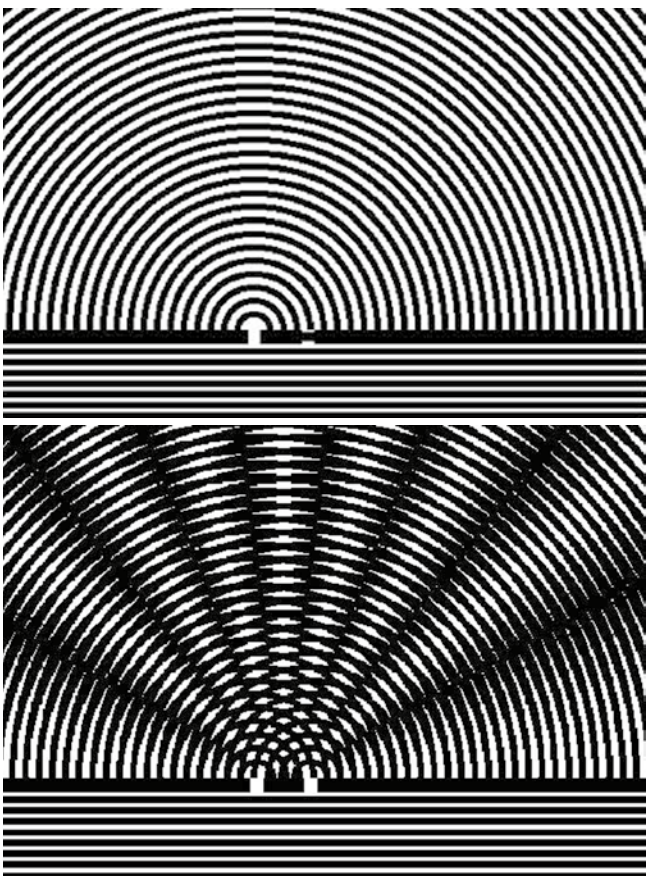

Fig. 1.1 (*Top*) Light waves impinge from below on a barrier with only one slit open and spread from this in concentric rings. (*Bottom*) Light waves impinge from below on a barrier with two slits open. The two wave systems spreading on the other side interfere and in some sectors enhance, in others extinguish one another. The picture is intended only to simplify the understanding of the interference phenomenon and does not give a true description of the distribution of light

L.O. Björn
School of Life Science, South China Normal University, Guangzhou, China

Department of Biology, Lund University, Lund, Sweden
e-mail: Lars_Olof.Bjorn@biol.lu.se

L.O. Björn (ed.), *Photobiology: The Science of Light and Life*,
DOI 10.1007/978-1-4939-1468-5_1,

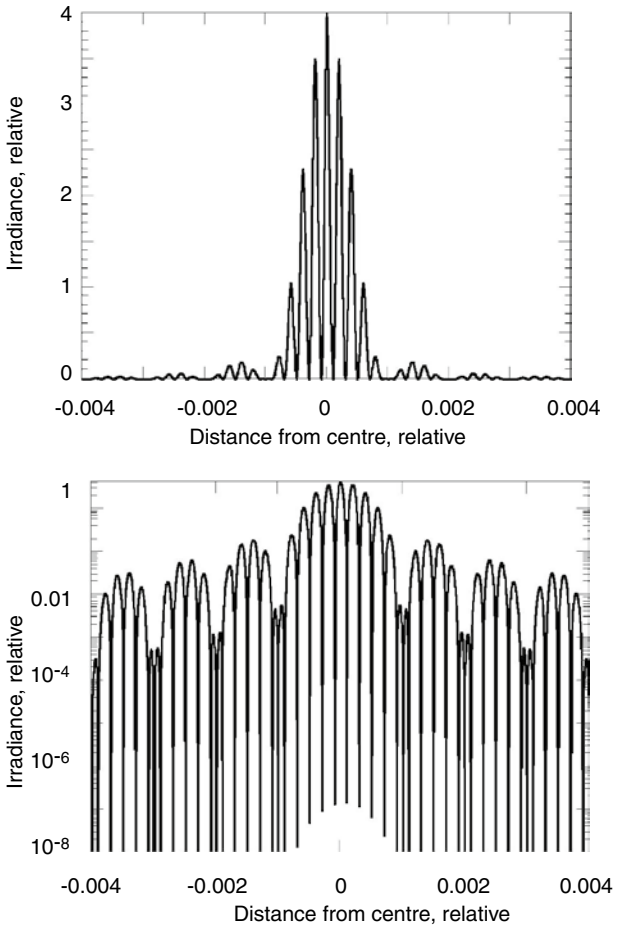

Fig. 1.2 Interference pattern produced in Young's double-slit experiment (computer simulation). The width of each slit is 1 mm, the distance between slit centers 4 mm, and the wavelength 0.001 mm (1 μm). The distance from the center of the screen is along the horizontal axis and the irradiance ("light intensity") along the vertical axis, both in relative units. Note that the vertical scale is linear in the upper diagram and logarithmic in the lower one

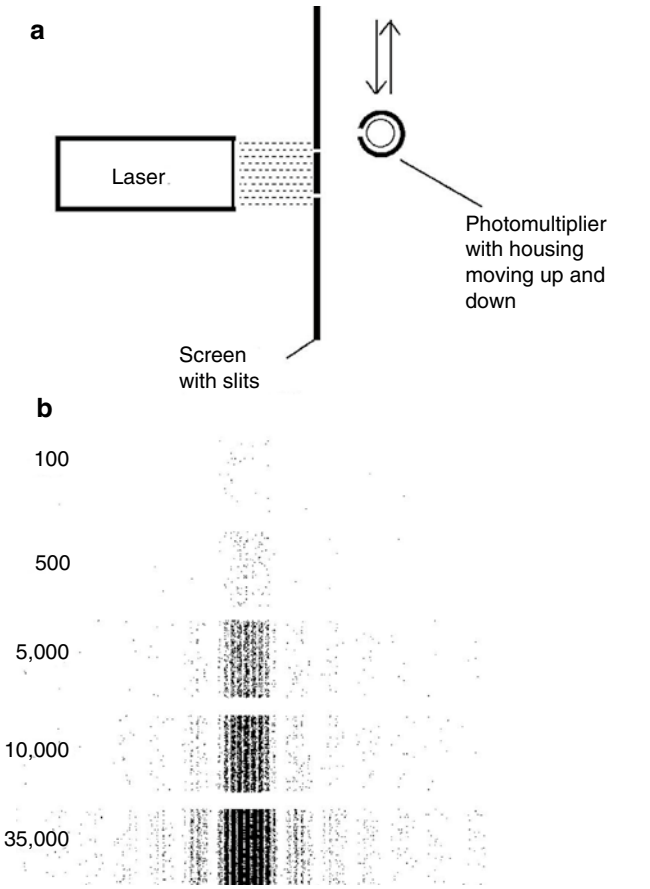

Fig. 1.3 (**a**) Double-slit experiment set up to count single photons. The sketch is not to scale. In a real experiment, the distance of the photomultiplier from the screen with slits would be greater, and the opening in the photomultiplier housing smaller. (**b**) Simulation of the pattern of photon hits on a screen behind a double slit arranged in the same way as in Fig. 1.2. The number of photons is indicated for each experiment. Although the photon hits take place randomly and cannot be predicted, the interference pattern emerges more and more clearly with increasing number of photons

colored filter should be used to limit the light to a narrower wave band. The easiest way today (which Young could not enjoy) is to use a laser (a simple laser pointer works well), giving at the same time very parallel and very monochromatic light, which is also sufficiently strong to be seen well.

In a direction forming the angle α with the normal to the slitted screen (i.e., to the original direction of the light), waves from the two slits will enhance each other maximally if the difference in distance to the two slits is an integer multiple of the wavelength, i.e., $d \cdot \sin \alpha = n \cdot \lambda$, where d is the distance between the slits, λ the wavelength, and n a positive integer (0, 1, 2, …). The waves will cancel each other completely when the difference in distance is half a wavelength, i.e., $d \cdot \sin \alpha = (n + 1/2) \cdot \lambda$. To compute the pattern is somewhat more tedious, and we need not go through the details. The outcome depends on the width of each slit, the distance between the slits, and the wavelength of light. An example of a result is shown in Fig. 1.2.

So far so good—light behaves as waves when it travels. But we also know that it behaves as particles when it leaves or arrives (see later). The most direct demonstration of this is that we can count the photons reaching a sensitive photocell (photomultiplier).

But the exciting and puzzling properties of light stand out most clearly when we combine the original version of Young's experiment with the photon counter. Instead of the visible diffraction pattern of light on the screen, we could dim the light and trace out the pattern as a varying frequency of counts (or, if we so wish, as a varying frequency of clicks as in a classical Geiger counter) as we move the photon counter along the projection screen (Fig. 1.3a). Since we count single photons, we can dim the light considerably and still be able to register the light. In fact, we can dim the light so much that it is very, very unlikely that more than *one photon at a time* will be in flight between our light source and the photon counter. This type of experiment has actually been

performed, and it has been found that a diffraction pattern is still formed under these conditions. We can do the experiment also with an image-forming device such as a photographic film or a charge-coupled diode (CCD) array as the receiver and get a picture of where the photons hit. A computer simulation of the outcome of such an experiment is shown in Fig. 1.3b.

If you think a little about what this means, you will be very puzzled indeed. For the diffraction pattern to be formed, we need *two* slits. But we can produce the pattern by using only one photon at a time. There can be no interaction between two or more photons, which have traveled different paths, e.g., one photon through one slit and another photon through the other slit. The experiment shows that each photon "must be aware" of both slits, or, in other words, must have traveled through both slits. I know of no other physics experiment that demonstrates more clearly than this one that light is not waves or particles. The wave and the particle are both *models*, incomplete pictures or imaginations of the nature of light. The limitations of our senses and our brain prevent us from getting closer to reality than this, simply because it has not made sense during our evolution to get closer to reality. This limitation does not prevent us from using our models very successfully as long as we use them in a correct way.

Not only light behaves in this way but also electrons, atoms, and molecules. Arndt et al. (1999) passed a beam of fullerene (C_{60}) through a double slit and got a similar pattern, and Sclafani et al. (2013) used a diatom frustule to diffract phthalocyanine molecules.

Let us take one more example to make clear how "weird" (i.e., counterintuitive) the scientific description of the behavior of light is. When I was younger I used to watch the Andromeda galaxy using my naked eyes (now it is difficult, not only because my vision has worsened, but because there is so much electric light around where I live). I could see the galaxy because atoms in it had emitted light about 2 million years earlier. The photons, after having traveled through empty space, interacted with rhodopsin molecules in my eyes. But no photon started on its course following a straight line toward the earth. It traveled as an expanding wave. Just before interacting with the rhodopsin molecule in my eye, the photon was *everywhere* on a wavefront with a radius of 2 million light years. The energy of the photon was not localized until it came into contact with my eye.

1.3 Light as Particles and Light as Waves and Some Definitions

When we are dealing with light as waves, we assign a wavelength to each wave. Visible light has wavelengths in a vacuum in the range 400–700 nm (1 nm equals 10^{-9} m), while ultraviolet radiation has shorter and infrared radiation longer waves.

Photobiologists divide the ultraviolet part of the spectrum into ultraviolet A (UV-A) with 315–400 nm wavelength, UV-B with 280–315 nm wavelength, and UV-C with <315 nm wavelength. You may see other limits for these regions in some publications, but these are supported by the Comité Internationale de l'Eclairage (CIE), which introduced the concepts. Just as everybody should use the same internationally agreed-upon length of the meter, everybody should honor the definitions of UV-A, UV-B, and UV-C; otherwise, there is a risk for chaos in the scientific literature. Plant photobiologists, for whom the spectral region 700–750 nm is especially important, call this radiation "far-red light." They also call the region 400–700 nm "photosynthetically active radiation," or PAR, rather than visible light. Just as radiation outside this band is perfectly visible for some organisms such as some insects, birds, and fish (and some light in the range 400–700 nm invisible to many animals), so radiation with wavelengths shorter or longer than "photosynthetically active radiation" is photosynthetically active to many organisms.

Natural light never has a single wavelength but can rather be regarded as a mixture of waves with different wavelengths.

When we characterize light by its wavelength, we usually mean the wavelength in a vacuum. When it travels through a vacuum, the velocity of light is always *exactly* 299,792.4562 km/s, irrespective of wavelength and the movement of the radiation source in relation to the observer. The reason that this value is exact is that the velocity of light in a vacuum links our definitions of the meter and the second. This velocity is usually designated c and wavelength λ (the Greek letter lambda). A third property of light which we should keep track of is its frequency, i.e., how many times per time unit the wave (the electric field) goes from one maximum (in one direction) to another maximum (in the same direction). Frequency is traditionally designated ν (Greek letter nu), and in a vacuum we have the following relation between the three quantities just introduced: $c = \lambda \cdot \nu$, or $\lambda = c/\nu$, or $\nu = c/\lambda$. When light passes through matter (such as air or water or our eyes), the velocity and wavelength decrease in proportion, and frequency remains unchanged. Sometimes the wave number, i.e., $1/\lambda$, is used for the characterization of light. It is usually symbolized by ν with a line (bar) over it, and a common unit is cm^{-1}.

When we think of light as particles (photons), we assign an amount of energy (E) to each photon. This energy is linked to the wave properties of the light by the relations $E = h \cdot \nu$, where h is Planck's constant, 6.62617636 J·s (joule-seconds). It also follows from the preceding that $E = h \cdot c/\lambda$. We can never know the exact wavelength, frequency, or energy of a single photon.

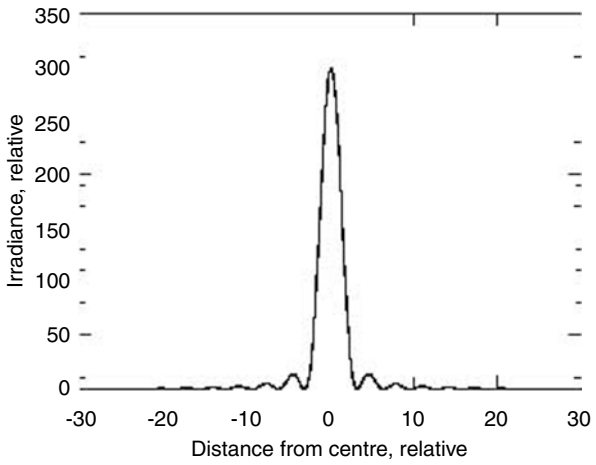

Fig. 1.4 Diffraction pattern in a single slit (the pattern from a round hole looks similar but is slightly different)

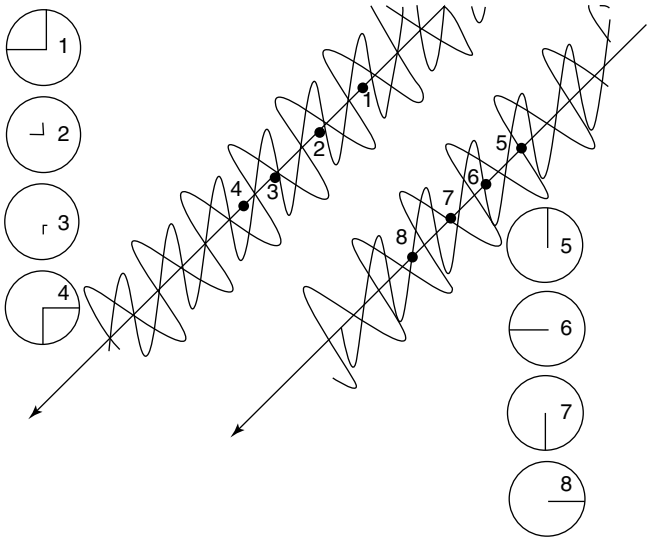

Fig. 1.5 In the *upper left part* of the figure, a plane-polarized light beam, composed of one vertically and one horizontally polarized component, is depicted in perspective and also "head-on" at different points (or at one point at different moments). Numbered points in the perspective drawing correspond to the numbers on the "head-on" drawings. Only the electric components of the electromagnetic fields are shown (*wavy lines* in the perspective drawing, *straight lines* in the "head-on" drawings). In the *lower right part* of the drawing, the same is shown for a circularly polarized beam

1.4 Diffraction

We usually think of light traveling in straight lines if there is nothing in its way. We have seen in Young's double-slit experiment that it does not always do that. In fact, the great physicist Richard Feynman has shown that its behavior is best understood if we think of it as always traveling every possible way at the same time and components traveling those different ways interfering with one another at every possible point.

We do not have to have two slits to show how the light "bends" near edges. This "bending" is called diffraction in scientific terminology. It is very important to take diffraction into account to understand some biological phenomena, such as the vision of insects (see Chap. 15). Light is diffracted in any small opening and also near any edge. To compute the diffraction pattern, we can make use of something called Huygens' principle (sometimes the Huygens-Fresnel principle). It states that we can think of propagating light as a sum of semispherical waves emanating from a wavefront. If the wavefront is flat, the semispherical waves emanating from it add up to a new flat wavefront. But if something stops some of the semispherical waves, the new wavefront is no longer flat. In Fig. 1.1 (top) we illustrate this in one plane. Flat waves impinge from below on a screen with an opening. Many semicircular waves start out from the opening. Along a line from the middle of the opening, the resulting wavefront is flat, but at the edges the semicircular waves produce a bent pattern. We have calculated this pattern more exactly in Fig. 1.4.

1.5 Polarization

Light waves are *transverse*, i.e., the oscillation is perpendicular to the direction of wave propagation and the direction of the light (this is in contrast to sound waves, in which particles vibrate in the line of wave propagation). In the case of light, there are no vibrating particles but a variation in electric and magnetic fields. The electric and magnetic fields are both perpendicular to the direction of propagation but also perpendicular to one another. When the electric fields of all the components of a light beam are parallel, the beam is said to be *plane-polarized*. The *plane of polarization* is the plane that contains both the electrical field direction and the line of propagation.

If we add two beams which travel in the same direction and are both plane-polarized and have the same *phase* (i.e., the waves are in step) but different planes of polarization, the resulting light is also plane-polarized with its plane of polarization at an intermediate angle.

Light can also be circularly polarized, in which case the electrical field direction spirals along the line of propagation. Since such a spiral can be left- or right-handed, there are two kinds of circular polarization, left-handed and right-handed (Fig. 1.5).

Circularly polarized light can be regarded as the sum of two equally strong plane-polarized components with right angles between the planes of polarizations and a 90° *phase difference* between the components. On the other hand, plane-polarized light can be regarded as a sum of equally strong left- and right-handed components of circularly polarized light. There are several animations available on the internet that explain this better than a stationary illustration can, e.g.:
http://en.wikipedia.org/wiki/Circular_polarization
http://ja01.chem.buffalo.edu/~jochena/research/opticalactivity.html

http://www.photophysics.com/tutorials/circular-dichroism-cd-spectroscopy/1-understanding-circular-dichroism
http://www.enzim.hu/~szia/cddemo/edemo7.htm
(accessed August 16, 2013)

Natural light, such as direct sunlight, is often almost unpolarized, i.e., a random mixture of all possible polarizations. After reflection in a water surface, the light becomes partially plane-polarized. Skylight is a mixture of circularly and plane-polarized light, which we call elliptically polarized light. We cannot directly perceive the polarization of the light we see. Insects do and often use the polarization of skylight as an aid in their orientation. Plants in many cases react differently to plane-polarized light depending on its plane of polarization. This holds for chloroplast orientation in seed plants, mosses, and green algae and also for growth of fern gametophytes. A good treatise on the subject (in German) is provided by W. Haupt (1977).

1.6 Statistics of Photon Emission and Absorption

Usually the members of a population of excited molecules can be expected to emit photons independently of one another, i.e., the time of emission of one photon does not depend on the time of emission of another photon. One exception to this rule occurs when stimulated emission becomes significant, as happens in a laser. Another exception is when there is cooperation between different parts of a cell (e.g., when a dinoflagellate flashes), between different cells in an organism (e.g., when a firefly flashes), or between different individuals in a population (e.g., when fireflies in a tree send out synchronized flashes). The examples in the last sentence are very obvious. However, careful study of the statistics of photon emission offers a very sensitive way of detecting cooperation between different parts of a biological system, and we shall therefore dwell a little on this subject, which also has a bearing on the reliability of measurement of weak radiation in general.

When photons are emitted independently of one another, the distribution of emission events in time is a Poisson distribution, just as in the case of radioactive decay. This means that if the mean number of events in time Δt is x, then the probability of getting exactly n events in the time Δt is $p = e^{-x} \cdot x^n / n!$. In this formula, n! stands for factorial n, i.e., $1 \cdot 2 \cdot 3 \cdot 4 \ldots$ n. Thus 1! = 1, 2! = 2, 3! = 6, 4! = 24, and so on. By definition 0! = 1.

We are familiar with the Poisson distribution of events from listening to a Geiger–Müller counter. That events are Poisson-distributed in time means that they are completely randomly distributed in time. When one event takes place does not depend on when a previous event occurred. One might think that there cannot be much useful information to be extracted from such a random process, but such a guess is wrong. The reader is probably already familiar with some of the useful things we can learn from the random decay of atomic nuclei. We can, in fact, use our knowledge of how Poisson statistics work for determining the number of photons required to trigger a certain photobiological process. The remarkable thing is that we can do this even without determining the number of photons we shine on the organism that we study.

The principle was first used by Hecht et al. (1942) to determine how many photons must be absorbed in the rods of an eye to give a visual impression. Their ingenious experiment was a bit complicated by the fact that our nervous system is wired in such a way that several rods have to be triggered within a short time for a signal to be transmitted to the brain (thereby avoiding false signaling due to thermal conversion of rhodopsin). We shall demonstrate the principle with a simpler example, an experiment on the unicellular flagellate *Chlamydomonas* (Hegemann and Marwan 1988). This organism swims around with two flagella, and it reacts to light by either stopping ("stop response") or by changing swimming direction ("turning response").

All one has to do is to take a sample of either light-adapted or dark-adapted *Chlamydomonas* cells, subject them to a flash of light, and note which fraction of the cells either stop or turn. The experiment is then repeated several times, with the flash intensity varied between experiments. The absolute fluence in each flash need not be determined, only a relative value. If one possesses a number of calibrated filters, no light measurement at all need be performed. Then the fraction of reacting cells for each flash is plotted against the logarithm of the relative flash intensity. It turns out that (for dark-adapted cells) the curve so obtained, if plotted on a comparable scale, has the same shape as the curve labeled $n = 1$ in Fig. 1.6. This holds for both stop response and for turning response, and it means that both responses can be triggered by a single photon. If the experiment is carried out within 20 min of removing the cells from strong light, the stop-response curve has a shape similar to the curve labeled $n = 2$ in Fig. 1.6, meaning that in this case two photons are required.

The curves in Fig. 1.6 have been computed in the following way (let, as before, x be the average number of events recorded in a large number of trials): the curve for $n = 1$ is the probability (p) of absorption of at least one photon, which is one minus the probability for absorption of no photon or $p = 1 - e^{-x} \cdot x^1 / 1! = x / e^x$. The curve for $n = 2$ follows the formula $p = 1 - e^{-x} \cdot x^1 / 1! - e^{-x} \cdot x^2 / 2!$, the curve for $n = 3$ follows the formula $p = 1 - e^{-x} \cdot x^1 / 1! - e^{-x} \cdot x^2 / 2! - e^{-x} \cdot x^3 / 3!$, etc.

1.7 Heat Radiation

The term heat radiation is sometimes (erroneously) used synonymously with infrared radiation. We shall use it here as the energy emitted when the energy of the random heat

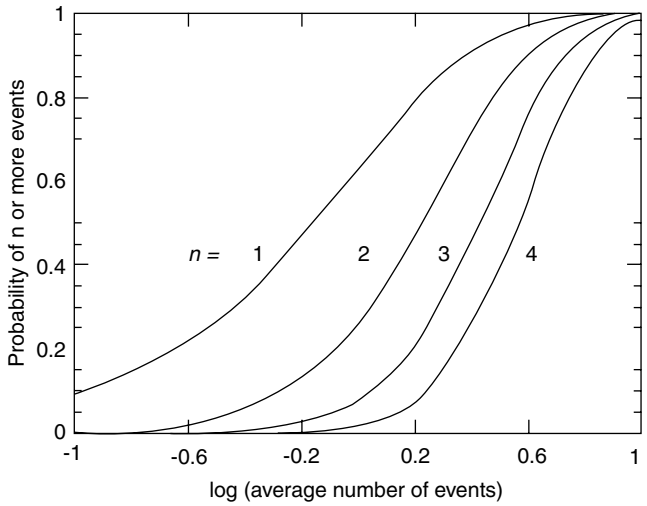

Fig. 1.6 The probability that at least a certain number (n) of absorption events will occur during a sampling time plotted against the logarithm of the average number of events that would occur during a large number of similar samplings. It is seen that the shape of the curves depends on the value of n. If at least n absorption events are necessary for inducing a process, one can determine the number n by plotting the frequency of successful inductions against the logarithm of fluence and compare the shape of the curve obtained with the above diagram

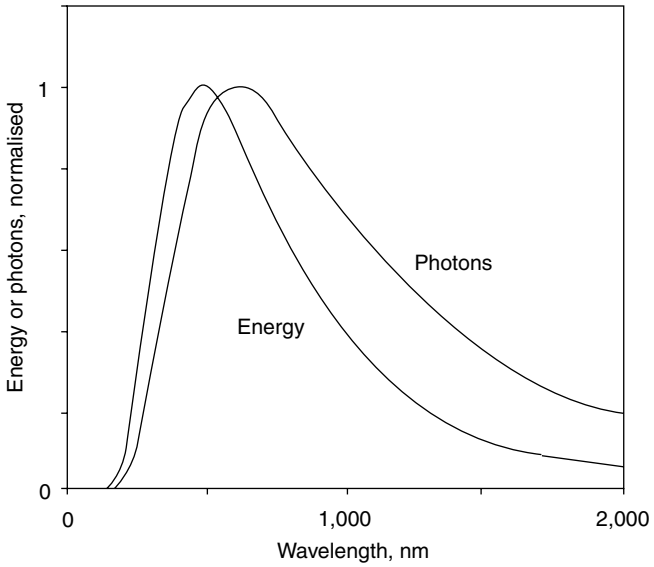

Fig. 1.7 Blackbody radiation (5,000 K) plotted as photons per wavelength interval and as energy per wavelength interval

movement of the particles in condensed matter (solids, liquids, or compressed gases) is converted to radiation. It is easiest to think of heat radiation as the glow of a hot body (lamp filament or the sun), but our own bodies also emit heat radiation, as does, in fact, a lump of ice or even a drop of liquid nitrogen. A body that is cooler than its environment absorbs more radiation than it emits, but still it radiates according to Planck's radiation law, to be described below. Heat radiation may be infrared, visible, or ultraviolet and, if we go to exotic objects in the cosmos, even outside this spectral range.

The starting point of the quantum theory was the attempt to explain the spectrum of the radiation emitted by a glowing body. To derive a function that matched the observed spectrum, Planck had to assume that the radiation is emitted in packets (quanta or photons) of energy $h{\cdot}\nu$, where ν stands for frequency (which is also the velocity of light divided by the wavelength) and h is a constant, Planck's constant = $6.62620{\cdot}10^{-34}$ J·s. Planck's radiation law was derived for an ideal blackbody, best approximated by a hollow body with a small hole in it. With modifications it can be used for other bodies as well. The sun radiates almost as a blackbody.

Planck's formula can be written in different ways, depending on whether we consider radiation per frequency interval or per wavelength interval and whether we express the radiation as power (energy per time) or number of photons (per time). Furthermore, we may be interested in the radiation density inside a hollow body (mostly for theoretical purposes) or the radiation flux leaving a body (for most applications).

$$\text{Energy density per frequency interval} = \left(8\pi h / c^3\right) \cdot \nu^3 / \left(\mathrm{e}^{h\nu/kT} - 1\right)$$

$$\text{Photon density per frequency interval} = \left(8\pi / c^3\right) \cdot \nu^2 / \left(\mathrm{e}^{h\nu/kT} - 1\right)$$

$$\text{Energy density per wavelength interval} = 8\pi hc \cdot \lambda^{-5} / \left(\mathrm{e}^{h\nu/kT} - 1\right)$$

$$\text{Energy density per wavelength interval} = 8\pi\lambda^{-4} / \left(e^{h\nu/kT} - 1\right)$$

These functions are mostly plotted with ν or λ as the independent variable and T as a parameter. It should be noted that even for the same T, the functions all have maxima at different values of ν or λ (see Fig. 1.7, which shows the plots of energy per wavelength interval and photons per wavelength interval for 5,000 K).

These examples are shown merely as an illustration of the fact that the maxima occur at different locations depending on which principle you use for plotting the spectra. This is not only true for heat radiation; it holds for all emission spectra, also for fluorescence emission spectra for instance. The most common sin of people publishing about fluorescence is that they do not understand this. They write "fluorescence, relative" on their vertical axis without further specification and do not realize that not even the shape of their spectrum, nor the positions of maxima, will be defined in such graphs. The second most common way of sinning is to spell fluorescence incorrectly.

You can see from Fig. 1.8 that the maxima occur at longer wavelengths when the temperature is lower and also that the total radiation is less in that case. In fact, the wavelength of the maximum is inversely proportional to the absolute temperature (Wien's law), while the total photon emission is proportional to the third power of the absolute temperature (i.e., to T^3) and the total energy emission to the fourth power (T^4, Stefan–Boltzmann's law). Wien's and Stefan–

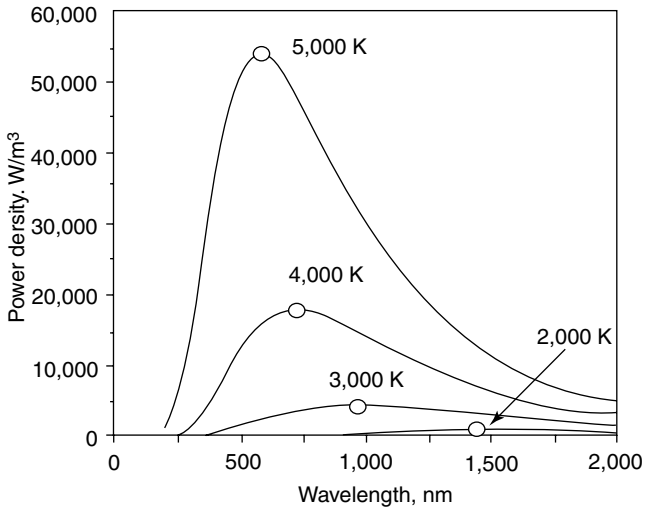

Fig. 1.8 Blackbody radiation plotted as power per wavelength interval for different temperatures. Note that since the graphs show power (i.e., energy per time) per area and per wavelength interval, the dimension is power per volume and the unit W/m^3. The maximum of each curve is indicated by a *circle*

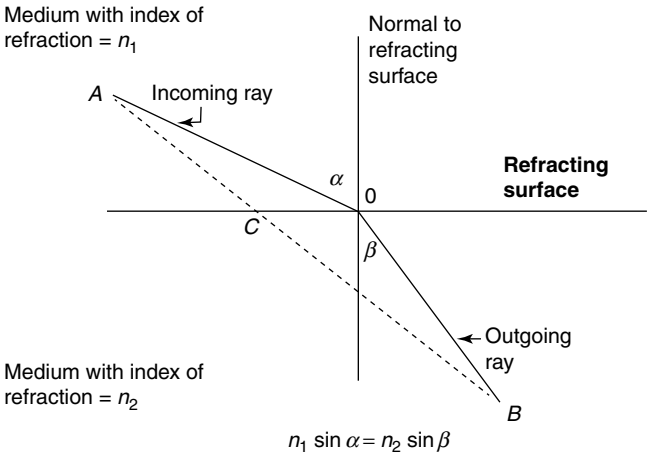

Fig. 1.9 Refraction of light in a plane interface between transparent materials

Boltzmann's laws can both be derived from Planck's radiation formula but were found experimentally before Planck did his theoretical derivation.

The formulas shown above refer to radiation density in a closed cavity with radiating walls. The *fluence rate*, or amount of radiation per unit of time and unit of *cross-sectional* area falling from all directions on a sphere in this cavity, is obtained by multiplying the radiation density by the velocity of light. (Do not worry if you have some difficulty with this here. We shall return later to the concept of fluence rate, which is quite important in photobiology and often misunderstood.) Suppose that the sphere in the cavity is ideally black (absorbing all the radiation falling on it) and has the same temperature as the walls. The second law of thermodynamics states that (assuming that no heat energy is generated or consumed in the sphere) the sphere must stay at the same temperature as the walls and it must radiate the same amount of radiation (distributed in the same way across the spectrum) as it receives. Therefore its *excitance* (radiation given off per unit of time and unit of *surface* area) is the energy density given by the formulas above multiplied by the velocity of light and divided by 4 (since the *surface* area of the sphere is four times the *cross-sectional* area).

To obtain the excitance of a non-blackbody (such as a glowing tungsten filament in a light bulb or your own body), the excitance computed for a blackbody should be multiplied by the *emissivity*. The emissivity varies quite a lot with wavelength, so the multiplication must be carried out separately for each wavelength value in which you are interested. The emissivity also varies somewhat with temperature. The *absorptivity*, or the ability to absorb radiation, is identical to the emissivity; otherwise, the second law of thermodynamics would be violated.

It may seem that this is a little too much physics for a biology book, but an understanding of the basic physical principles is very helpful when it comes to the experimental work in photobiology. What has just been described can be used for calibrating measuring equipment in the photobiology laboratory.

1.8 Refraction of Light

From school you should be familiar with Snell's law. This describes how light is refracted at an interface between two media with different indices of refraction (refractive indices), say n_1 and n_2. Figure 1.9, in which we assume $n_1 < n_2$, will serve as a reminder. If you need further explanation, you will have to look in other books.

The refractive index can be regarded as the inverse of the relative velocity of light in the medium in question, i.e., it is the velocity in a vacuum divided by that in the medium. It can be shown that Snell's law is equivalent to the statement that the light takes the fastest path possible between any two points on the rays shown. Compared to a straight line (dashed in Fig. 1.9) between point A on the upper ray and point B on the lower ray, you can see that the light goes a longer distance (solid line) in the medium with refractive index n_1 (lower index, higher velocity) than in the medium with refractive index n_2 (higher index, lower velocity), i.e., AO > AC and OB < CB. The refractive index is a pure number (no unit, as it is the ratio of two velocities). As we have used it here, it is a real number (the usual type of number we use in most calculations, represented as a decimal number). In more advanced optical theory, the refractive index is a complex ("two-dimensional") number.

As for the values of α and β in relation to one another, the figure looks the same if the light direction is reversed. However, this does not hold any longer when reflection is taken into account or when we consider the amount of light in the beams.

Throughout most of the spectrum the refractive index decreases with wavelength, but there are spectral regions (where absorption bands occur) where it increases steeply with wavelength; this phenomenon is, for historical reasons, called *anomalous dispersion*, although it is quite normal. In general, the change in refractive index with wavelength is called *dispersion*.

In some crystals and many biological materials, the refractive index is different depending on direction and plane of polarization of the light. Such a medium is termed *birefringent*. Birefringence occurs in plant cell walls and other structures where elongated molecules are arranged in a certain direction. Measurement of birefringence has been an important method in elucidating the arrangement of molecules in such cases. Media that are originally *isotropic* (with the same properties in different directions and thus not birefringent) may become birefringent by stretching or squeezing, application of electric fields, or other treatments.

When light passes through a birefringent medium of suitable thickness, it becomes circularly or elliptically polarized because of the phase difference that develops between the components of different plane polarization.

1.9 Reflection of Light

Reflection may be *specular* (from a shiny, smooth surface or interface) or *diffuse* (from a more or less rough surface or interface). Diffuse reflection is very important in biology, but we shall limit ourselves here to specular reflection at interfaces between dielectric (nonmetallic) media.

The angle of incidence is always equal to the angle of reflection, but the amount of light reflected (as opposed to refracted) depends on the polarization of the light. The plane in which both the incident and the reflected rays (and the normal to the reflecting surface) lie is called the *plane of incidence*. The component of the light with an electric field parallel to this plane is designated by //; that with an electric field perpendicular to the plane of incidence by +. The fractions, *R*// and *R*+, of the irradiance of these components that are reflected are given by Fresnel's equations in which α is the angle of incidence (equal to the angle of reflection) and β the angle of transmission (see Fig. 1.9 in the section on refraction):

$$R// = \left[\tan(\alpha-\beta)/\tan(\alpha+\beta)\right]^2$$

$$R+ = \left[\sin(\alpha-\beta)/\sin(\alpha+\beta)\right]^2$$

The reflected fraction of unpolarized light is the mean of the two ratios. For normal incidence ($\alpha = \beta = 90°$) another set of equations has to be used, since with the equations above, divisions by zero would occur. In this case there is no distinction between *R*// and *R*+:

$$R = \left[(n_1 - n_2)/(n_1 + n_2)\right]^2$$

As an example of use of the last equation, let us consider the reflection in a glass plate ($n_2 = 1.5$) in air ($n_1 = 1$). When light strikes the glass plate (perpendicularly), $R = [(1-1.5)/(1+1.5)]^2 = [-0.5/2.5]^2 = 0.04 = 4$ %. When the light strikes the second interface (from glass to air), the value of *R* comes out the same again, because since the expression is squared, it does not matter in this case which of the indices you subtract from the other one. Thus 96 % of the 96 % of the original beam, or 92.16 %, will be transmitted in this "first pass." It can be shown that after an infinite number of passes between the two surfaces, the reflected fraction will be $R[1+(1-R)/(1+R)] = 2.0.04/(1+0.04) = 7.69$ % and the transmitted fraction 92.31 %. For most practical purposes, we may estimate a reflection loss at normal incidence of about 8 % in a clean glass plate or glass filter, but if the refractive index is exceptional, this value may not hold. If the glass is not clean, it certainly does not.

The multiple internal reflection is not of much effect in a single glass plate, but I wanted to mention it here, because the effect is taken advantage of in so-called interference filters to be described in a later section.

Going back to the case of $\alpha < 90°$, we find by division, member by member, of the equations above that *R*// divided by *R*+ is $[\cos(\alpha-\beta)/(\cos(\alpha+\beta)]^2$. This ratio will always be > 1, so *R*// > *R*+, or, in other words, the component of light with the electric field perpendicular to the plane of incidence and parallel to the interface will be more easily reflected than the other component. The interface can act as a polarizing device. It can be shown that the reflected beam becomes completely polarized when $\tan\alpha = n_2/n_1$, because none of the light polarized parallel to the plane of incidence is reflected (Fig. 1.10). The angle $\alpha = \arctan(n_2/n_1)$ is called the *Brewster* angle.

If a beam strikes a flat interface obliquely from the side where the refractive index is highest, the outgoing beam will have a greater angle to the normal than the ingoing (according to Snell's law). If the angle of incidence is increased more and more, an angle will eventually be reached when the outgoing beam is parallel to the interface. At greater angles of incidence, there will be total reflection, i.e., all light will be reflected, and none transmitted. The smallest angle of incidence at which total reflection occurs is called the *critical angle*.

If an object with higher refractive index immersed in the medium with lower refraction index comes very close to the reflecting interface (at a distance less than a wavelength), then light energy can "tunnel" through and interact with that object. It is a principle exploited for, e.g., fingerprint readers and some special kinds of microscopy (see Chap. 5).

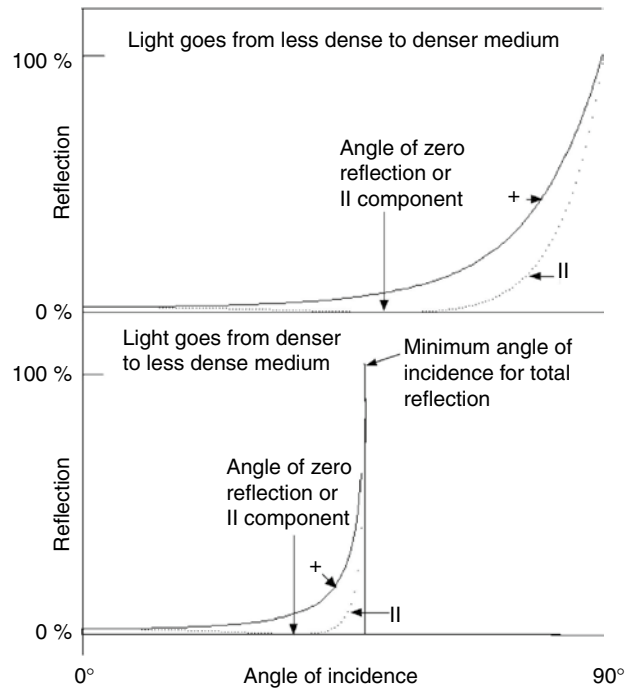

Fig. 1.10 Percent of light reflected for different angles of incidence for light going from air ($n=1$) to water ($n=1.33$, *top*) and from water to air (*bottom*) and for light polarized with the electric vector in the plane of incidence (II) or perpendicular to the plane of incidence (+). For II-polarized light, no light is reflected for a certain angle of incidence (the Brewster angle). For light going from the denser medium (water) to the less dense medium, total reflection occurs for angles of incidence larger than the critical angle

1.10 Scattering of Light

Although, strictly speaking, reflection and refraction are also a result of scattering (absorption and reemission of electromagnetic energy by material oscillators), we do, in practice, use the term scattering in a more restricted sense for processes that tend to change the propagation of light from an ordered way to a random one. We can distinguish three types of scattering named after three distinguished scientists: Mie scattering, Rayleigh scattering, and Raman scattering.

Mie scattering is caused by particles larger than the wavelength of the light and having a refractive index different from that of the continuous phase in which they are suspended. Typical examples are water droplets (clouds, fog) or dust in the atmosphere, or the result of mixing a solution of fat in acetone with water. Almost any animal or plant tissue is a strong Mie scatterer due to the boundaries between cells and between different parts of the cells and, in the case of plant tissue, between cells and intercellularies. Mie scattering is nothing other than repeated reflection and refraction at numerous interfaces. As we have seen, light of different wavelengths is not reflected or refracted in exactly the same way, but most of these differences cancel out in Mie scattering, and there is no strong wavelength dependence of this phenomenon.

Rayleigh scattering is caused by the interaction of light with particles smaller than the wavelength of the light. The particles may even be individual molecules or atoms. In this case there are no interfaces at which reflection or refraction can take place. However, the closer the wavelength of the light is to an absorption band of the scattering substance (i.e., the closer the frequency of the light is to a natural oscillating frequency in the matter), the more strongly the electrons in the matter "feel" the light and the greater is the probability that the electromagnetic field is disturbed when it sweeps by. Most substances have their strongest absorption bands in the far ultraviolet. Therefore, in the infrared, visible, and near ultraviolet regions, Rayleigh scattering increases very steeply toward shorter wavelength. Ultraviolet is scattered more strongly than blue, which in turn is scattered more strongly than red. The blue color of the sky is due to more blue than red light being scattered out of the direction of the direct sunlight. To be more precise, Rayleigh scattering is inversely proportional to the fourth power of the wavelength, i.e., proportional to $1/\lambda^4$.

In Rayleigh scattering the direction of the electrical field is not changed. If, for instance, a horizontal beam, vertically polarized (i.e., with the electric field vertical), is scattered, the electric field remains vertical. But light can never propagate in the direction of its electric field (remember, it is a transverse wave). This means that the light is not scattered up or down, only in horizontal directions. If, on the other hand, the incident light is not polarized, it is scattered in all directions but with different polarizations.

In both Mie and Rayleigh scattering, the wavelength of the light remains unchanged. In Raman scattering, on the contrary, either part of the photon energy is given off to the scattering particles (which in this case are molecules) or some extra energy is taken up from the particles. The amount of energy taken up or given off corresponds to energy differences between vibrational levels in the molecule. Raman scattering can be used as an analysis method and is also a source of error in fluorescence analysis, but we do not need to consider it in photobiological phenomena, since it is always very weak.

1.11 Propagation of Light in Absorbing and Scattering Media

We shall consider here first the simplest case: a light beam (irradiance I_o) that perpendicularly strikes the flat front surface of a homogeneous nonscattering but absorbing object. The most common objects of this kind that we deal with in the laboratory are spectrophotometer cuvettes and glass filters. A small fraction of the incident light is specularly reflected at the surface according to Fresnel's equation (see Sect. 1.9). For simplicity, we disregard this in this section. In spectrophotometry, reflection is taken care of by comparing a sample with a reference cuvette having approximately the same reflectivity as the sample cuvette.

At depth x within the object, the irradiance (see Chap. 2 for definitions of irradiance and other terms) will be $I_x = I_o \cdot e^{-Kx}$, where K is the linear absorption coefficient. The relationship is known as Lambert's law and follows mathematically from the conditions that (1) the light is propagated in a straight line and (2) the probability of a photon being absorbed is the same everywhere in the sample.

In spectrophotometry we also make use of Beer's law, which states that under certain conditions, K is a product of the molar concentration of the absorbing substance and its molar absorption coefficient (or, in the case of several absorbing substances, the sum of several such products).

However, we are concerned now not with spectrophotometry, but with the propagation of light in living matter. Almost invariably, we will be facing complications caused by intense scattering. A general quantitative treatment of scattering is so complicated as to be useless for the photobiologist. All it would lead to would be a system of equations with mostly unknown quantities.

A simplified theory, which has been found very useful as a first approximation, is the Kubelka–Munk theory (Kubelka and Munk 1931). It should be observed that this theory is valid only for "macro-homogeneous" objects, i.e., those that on a macroscopic scale are uniform and isotropic, with absorption and scattering coefficients that can be determined. Seyfried and Fukshansky (1983) have shown how the theory can be modified for an object consisting of several macro-homogeneous layers. Specular reflection at the surfaces has to be dealt with separately. Uncertainty in the specular reflection leads to uncertainties in the absorption and scattering coefficients if they, as proposed by Seyfried and Fukshansky, are determined from overall reflection and transmission by the object. In any case, the method is good enough to demonstrate here the general features of light propagation in media that both absorb and scatter light.

Suppose that we can determine, with sufficient confidence, the reflectance R (except for specular reflectance) and transmittance T of our sample. The linear absorption coefficient K and the linear scattering coefficient S, as well as the fluence rate at any point inside the sample, can then, with some effort, be computed from the system of equations:

$$
\begin{aligned}
R &= 1/\left[a + b \cdot \coth\left(bSd\right)\right] \\
T &= \mathrm{b}/\left[a \cdot \sinh\left(bSd\right) + b \cdot \cosh\left(bSd\right)\right] \\
a &= \left(S + K\right)/S \\
b &= \sqrt{\left(a^2 - 1\right)} \\
I_x &= I_\mathrm{o} \cdot T \cdot \left[\begin{matrix}\left\{\left(a+1\right)/b\right\} \cdot \sinh\left\{bS \cdot \left(d - x\right)\right\} \\ + \cosh\left\{bS \cdot \left(d - x\right)\right\}\end{matrix}\right].
\end{aligned}
$$

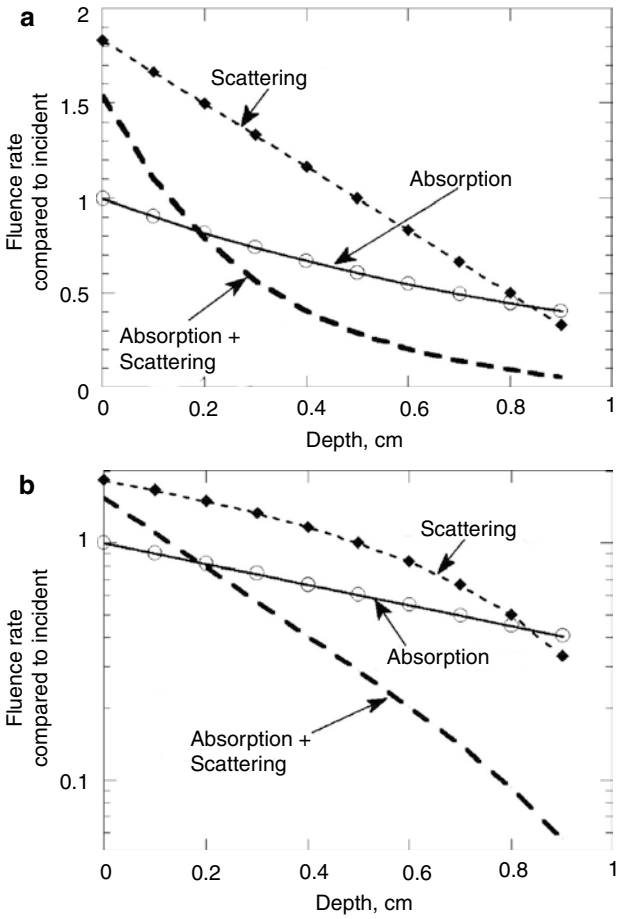

Fig. 1.11 Decrease of fluence rate with depth. The decrease of fluence rate with depth of penetration in a 1-cm-thick slab of a medium with absorption only (linear absorption coefficient 1 cm^{-1}), scattering only (linear scattering coefficient 5 cm^{-1}), and one with both absorption (1 cm^{-1}) and scattering (5 cm^{-1}). The values were computed using the Kubelka–Munk theory and assuming isotropic incident light. In the upper frame, the fluence rate scale is linear, and in the lower one, logarithmic. Note that in a scattering medium, fluence rate can exceed the fluence rate of the incident light (**a** is a linear plot; **b** has a logarithmic vertical scale)

Here I_o is the fluence rate incident from one side, and I_x the fluence rate at depth x of a sample of overall thickness d. The so-called hyperbolic operators sinh, cosh, and coth are defined by the following relationships: $\sinh(y) = (e^y - e^{-y})/2$; $\cosh(y) = (e^y + e^{-y})/2$; $\coth(y) = \cosh(y)/\sinh(y)$. If light is incident from both sides, the last equation has to be modified.

To demonstrate, without too much computation, the effect of scattering, we shall assume that we have determined K and S. For any sample thickness, d, we can then compute I_x as a function of x.

Note the following features in the examples of computer outputs (Figs. 1.11 and 1.12):

1. When S is given a low value (0.01), the Kubelka–Munk curve coincides with the Lambert curve (and is therefore invisible).

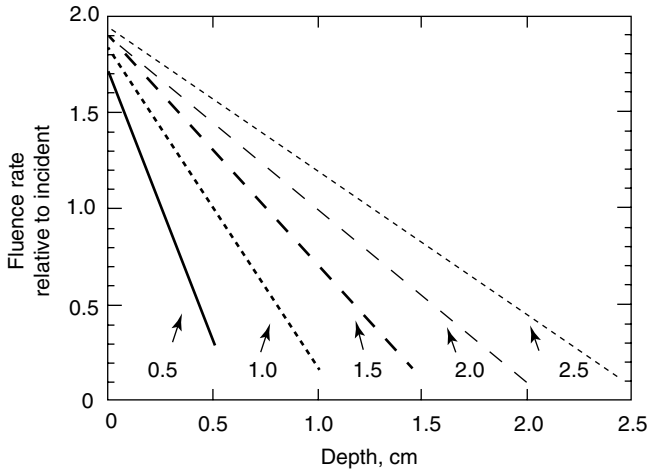

Fig. 1.12 Decrease of fluence rate in layers of the indicated thickness (in cm) of a purely scattering medium (no absorption); the linear scattering coefficient is 5 cm^{-1} in all cases. Note that the fluence rate decreases more quickly in a thin scatterer because there is less backscatter of light

2. When *S* has a value similar to or higher than *K*, i.e., when scattering is appreciable compared to absorption, the fluence rate in the sample near the illuminated side is higher than the incident fluence rate. This is no violation of the law of energy conservation; the sample does not create any new light. However, the concentration of photons is increased by their bouncing back and forth.

The expediency with which the Kubelka–Munk equations can be evaluated using a computer must not cause us to forget the limitations of the Kubelka–Munk theory. One severe restriction is that only diffuse incident light or light with an incidence angle of 60° is considered. We need only enter three constants, *K*, *S*, and thickness of the scattering medium, to describe the scattering object. A more complete description would give more realistic results, but apart from the difficulty in choosing the correct constants, the equations and algorithms would rise in complexity very fast. More complete theories are described by Star et al. (1988) and Keijzer et al. (1988).

1.12 Spectra of Isolated Atoms

We shall deal in this section with isolated atoms (which are not part of di- or polyatomic molecules and also not close to one another for other reasons, such as high pressure). They can increase their internal energy by absorbing photons and also give off energy by emitting photons. They can absorb or emit only very particular photons, whose energy corresponds very exactly to differences between energy levels in the atom. The simplest case is the hydrogen atom, and it has been found that its energy levels are inversely proportional to $1/n^2$, where *n* represents positive integers (1, 2, 3, …). The possible energy

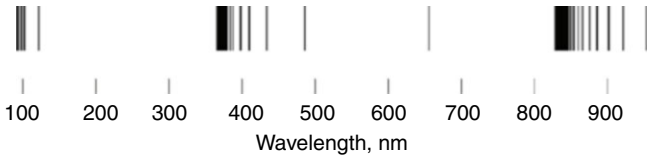

Fig. 1.13 Spectrum of atomic hydrogen (computer simulation)

jumps are then proportional to the energy differences $1/n^2–1/m^2$, where n = 1, 2, 3, …and m = n + 1, n + 2, etc. Since, according to the relationships $E = h\nu$ and $\lambda = c\nu$, the energy (*E*) of a photon is inversely proportional to wavelength (λ), the wavelengths of light which can be absorbed or emitted by a hydrogen atom are given by $1/\lambda = R\cdot(1/n^2–1/m^2)$ (see Fig. 1.13). The proportionality constant is called the reduced Rydberg constant. It is slightly dependent on the mass of the atom's nucleus, and for ordinary hydrogen, it amounts to 0.0109677581 nm^{-1}.

In ordinary hydrogen gas, the atoms are combined in pairs. However, when an electric current runs through the gas, the pairs are split and photon emission from energized (excited) free hydrogen atoms takes place. In the laboratory we use lamps containing heavy hydrogen (deuterium), for instance, in the spectrophotometer. We use the continuous part of the spectrum in the ultraviolet (as well as continuous emission in the ultraviolet arising from molecular deuterium) for measuring ultraviolet absorption of samples. We can use the two first lines of the Balmer series, for which $n = 2$ (Hα at 656 nm and Hβ at 486 nm), for wavelength calibration. In the program on which Fig. 1.13 is based, an approximate Rydberg constant in between that for light and heavy hydrogen was used. In nature, Hα, Hβ, and some other hydrogen lines appear in the spectrum from the sun as absorption lines (Fraunhofer lines), because of the presence of nonexcited hydrogen atoms in the atmosphere of the sun outside the glowing photosphere. Light of these particular wavelengths is therefore almost absent in the daylight spectrum. The absence of Hα light from daylight should make it possible to measure other light (e.g., fluorescence) at this wavelength in full daylight. However, the chlorophyll fluorescence from plants is weak at such a short wavelength.

One other case where the photobiologist is concerned with the spectrum of isolated atoms is when he or she uses low-pressure mercury lamps. We shall return to this in Chaps. 3 and 25.

1.13 Energy Levels in Diatomic and Polyatomic Molecules

The energy relations immediately become much more complex when we proceed from single atoms to molecules consisting of two atoms each, i.e., diatomic molecules. The

simplest example of such a molecule (if we disregard the hydrogen molecular ion H_2^+) is the hydrogen molecule, H_2.

In the molecule we have, in addition to the electronic energy described for the atom, vibrational and rotational energy. In diatomic molecules, the bond between the atoms, mediated by the electrons, can be regarded as an elastic string or spring, which stretches and contracts. At one instant the nuclei of the two atoms move toward one another. When the positively charged nuclei come close enough, their mutual electric repulsion becomes strong enough to reverse the motion, and the distance between the nuclei starts to increase. The nuclei move apart until the attractive force from the negatively charged electrons becomes strong enough to reverse the motion again.

This oscillating movement of the nuclei has some resemblance to that of a pendulum, but one difference is that it is asymmetrical. The force on the nuclei is not proportional to the distance from a symmetry point, and therefore, the molecule is an inharmonic oscillator rather than a harmonic one.

The changes in energy due to changes in oscillating movement are smaller than (the largest) energy jumps due to electronic transitions (changes in electronic energy).

In molecules consisting of more than two atoms each, there are also oscillations due to the bending of bonds, but we shall disregard this in the following.

The molecule can also absorb or emit energy by changing its state of rotation. In diatomic molecules, only rotation around an axis perpendicular to the bond contributes to the rotational energy, but in more complicated molecules, we must consider three axes of rotation, all perpendicular to one another.

All these energy changes are quantized, i.e., only certain energy changes are possible. However, because the vibrational and rotational energy amounts are much smaller than the electronic energy amounts and are combined with them, the molecules have apparently continuous absorption and emission bands rather than lines. At equilibrium, the number of molecules (N_x, N_y) "occupying various energy states" as the jargon goes, i.e., having various amounts of energy (E_x, E_y), is related to the energy differences between the states by the formula $N_x / N_y = e^{(E_y - E_x)/(kT)}$.

We shall now restrict the discussion to the stretching vibrations and their interaction with the electronic energy transitions. At one point in the stretching oscillation, the force acting on the nuclei is zero (the repulsive and attractive forces compensate one another exactly). All the vibrational energy is then kinetic (translational) energy. In contrast, when the distance between the nuclei is either minimal or maximal, i.e., at the inner and outer turning points, the velocity is zero, and therefore, the kinetic energy is zero. All the vibrational energy is then potential (positional) energy. In between, the kinetic and potential parts of the energy change in such a way that their sum is constant.

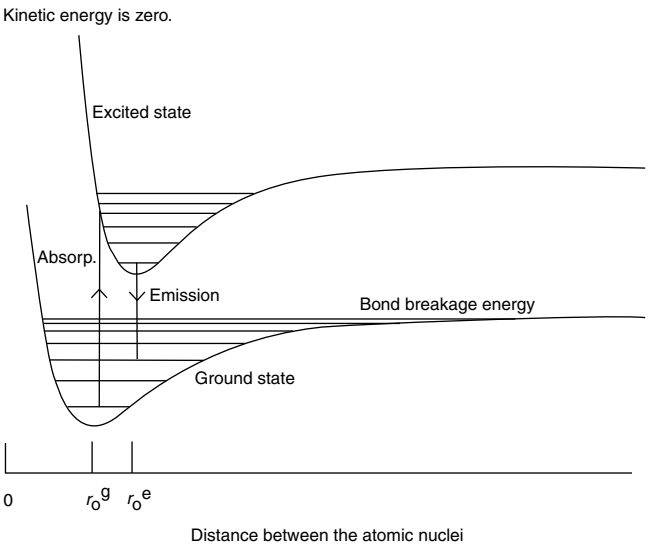

Fig. 1.14 The potential energies (vertical coordinate) of the electronic ground state and the first excited state are shown by the *curves* as functions of the distance between the atomic nuclei in a diatomic molecule (horizontal coordinate). The equilibrium distances (lowest potential energy) for the ground and excited states are denoted by r_o^g and r_o^e, respectively. At this distance the potential energy is minimal, and the kinetic energy (distance between *curves and horizontal lines*) is maximal. However, the molecule never comes to rest at this position. Even at zero absolute temperature, the vibrations continue (*lowest horizontal lines on the curves*)

In Fig. 1.14, the distance between the atomic nuclei is plotted in the horizontal direction (lowest values to the left) and the energy of the molecule in the vertical direction (lowest values at the bottom). The curved lines show the potential energy for various distances and for two different electronic states of the molecule. The various horizontal lines within the curved lines show the total energy for various vibrational states and for the two electronic states. The turning point in the oscillating movement of the nuclei is where these horizontal lines reach the curves. For these interatomic distances, the kinetic energy is zero.

Looking at Fig. 1.14 and the lengths of the vertical lines in it, we get some understanding of why absorption maxima occur at shorter wavelengths (higher photon energy) than emission maxima (this difference is referred to as the "Stoke's shift"). The maxima, which we can determine experimentally, of course, correspond to the wavelengths and photon energies of the most likely transitions. Later we will see how one can look at the same phenomenon from quite a different point of view.

A macroscopic pendulum moves most slowly near the turning points. If it were possible to get snapshots of the molecule at random times, one would therefore expect most of the snapshots to show the atoms near the turning points. However, the quantum physics is more complicated than that. For the lowest vibrational state, the zero state, it is quite

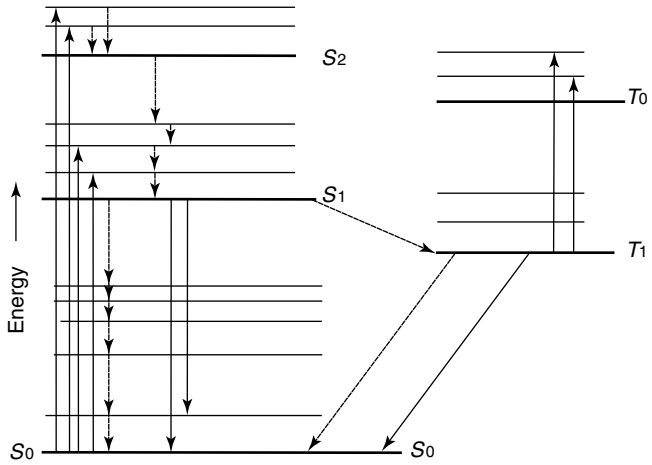

Fig. 1.15 Jablonski diagram: the *thick horizontal lines* indicate electronic energy states, the *thin horizontal lines* above each thick line vibrational substates. Associated with each electronic state, and indicated by *thinner lines* above the *thick lines*, are several vibrational energy levels. The higher up in the diagram, the higher energy the *lines* indicate. The *solid upward arrows* represent absorption of photons (light energy), and the *down pointing solid lines*, emission of photons (either spontaneous or stimulated emission). The *wider arrow* to the far *left* indicates that energy increases upward in the diagram. T_o the *left* in the figure the system of singlet states (S_o, S_1, S_3, with only paired electrons), to the *right* the system of triplet states (T_1, T_2, containing unpaired electrons). *Arrows with short dashes* indicate radiationless transitions within each state system. *Arrows with long dashes* indicate intersystem transitions (intersystem crossing). In the singlet system, radiative de-excitation (fluorescence) can take place only from the lowest excited state, since all other states are very short-lived. The transition from a triplet state to the ground level (S_o) does not take place easily, since an electron has to change spin. Thus the T_1 state (the lowest triplet state) is long-lived, and the radiative de-excitation from T_1 results in phosphorescence. This Jablonski diagram is not intended to depict energy relations in a particular molecule, but only general principles. A Jablonski diagram for the oxygen (O_2) molecule would, however, look radically different, since for this molecule the lowest-lying level represents a triplet state

the opposite, and the probability is greatest that the molecule will be near the state of zero potential energy and maximum kinetic energy. Thus, when for some reason a molecule changes electronic state, in most cases, the transition will occur from near the midpoint of the line for the lowest vibrational state. The vertical line to the left in Fig. 1.14 shows a likely transition from the lower electronic state to the higher electronic state, and the line to the right shows a likely transition from the higher electronic state to the lower one. The upward transition could be associated with absorption of photons, and the downward one by emission of photons.

In order to illustrate the various energy levels and transitions between them, it has become customary to use a kind of diagram named after Aleksander Jabłonski (pronounced Jabwonski). In such a diagram (see Fig. 1.15), the electronic energy levels (energy states of the molecule) are indicated by thick horizontal lines, the overlayered vibrational states by thinner horizontal lines, and state transitions by arrows.

Note that the downward pointing solid arrows (light emission) are generally shorter than the upward pointing ones (light absorption) corresponding to the fact that light emission is generally of longer wavelength (lower photon energy) than light absorption. This is, however, a matter of statistical distribution, and in stimulated emission, the wavelength is the same for absorbed and emitted light.

Stimulated emission is a phenomenon theoretically stipulated by Einstein but observed much later. According to Einstein, a molecule can be transformed by light absorption in two ways: either from a lower to a higher energy state, as we have described before, or from a higher to a lower state. In the latter case two photons are emitted (stimulated emission) for each one absorbed, and all three photons are of the same wavelength. The reason that it took a long time for stimulated emission to be observed is that the concentration of molecules in sufficiently high energy states is usually low, and the probability for stimulated emission therefore low. The transitions are described using so-called Einstein coefficients, B_{12}, B_{21}, and A_{21}. If, in a certain radiation field of energy density $r(\nu)$ for the frequency (ν), the number of molecules in the lower energy state is N_1, in the upper state N_2, then the probability of upward transitions is $B_{12}{\cdot}\rho(\nu){\cdot}N_1$, and the probability of downward stimulated transitions is $B_{21}{\cdot}\rho(\nu){\cdot}N_2$, but there are also spontaneous downward transitions with a probability $A_{21}{\cdot}N_2$. Because of the spontaneous downward transitions, N_1 is generally much larger than N_2. When light intensity is increased more and more, N_2 gradually approaches N_1 but cannot be caused to exceed it by light absorption alone (see Fig. 1.16).

The most important applications of stimulated emission are the laser (acronym for *l*ight *a*mplification by *s*timulated *e*mission of *r*adiation) and some types of high-resolution optical microscopy, to be described later.

Apart from the changes in vibrational and rotational energy, there are other causes of the "broadening" of spectra mentioned above (from line spectra to band spectra). More complicated molecules are usually (and the biomolecules always) in a condensed phase (liquid or solid) rather than in a low-pressure gas.

The different molecules in the phase affect one another in complicated ways so that the energy levels of one molecule are not the same as those of its neighbors. Finally, the different molecules are not identical (as a collection of isolated atoms of the same kind are) since they, even if they correspond to a single chemical formula, may have different *conformations*, e.g., an extended or folded chain of atoms. This results in continuous absorption and emission spectra.

Because, at ordinary temperatures, transitions between different conformational states take place readily, we do not experience molecules with different conformations as different kinds of molecules. By greatly lowering the temperature, we may prevent the transitions between different

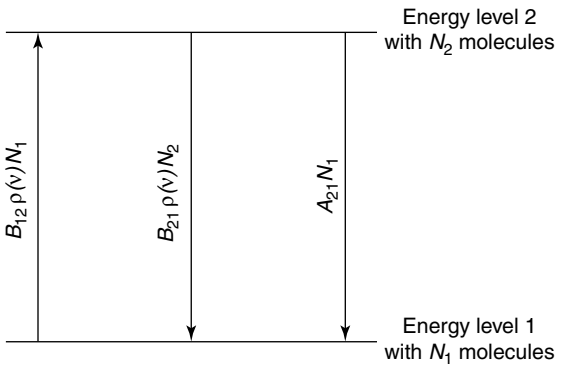

Fig. 1.16 Simplified energy level diagram (Jablonski diagram) for a molecule to explain stimulated emission. The *arrows* symbolize transitions between the two levels, by (from *left* to *right*) absorption, stimulated emission, and spontaneous emission. The probability of a transition is proportional to the population (N_1 or N_2) of molecules from which the transition takes place. Absorption and stimulated emission are also proportional to the energy density, $\rho(\nu)$, at the frequency (ν), which corresponds to the energy difference ($\Delta E = h\nu$) between the levels. (The energy density, in turn, is the product of the speed of light and the fluence rate.) For each one of these transition probabilities, there is also a proportionality factor (called an Einstein coefficient), i.e., B_{12} for absorption, B_{21} for stimulated emission, and A_{21} for spontaneous emission. Einstein showed that $B_{12} = B_{21}$ and $A_{21} = B_{21} \cdot 8\pi \cdot h\nu^3/c^3$. In the steady state, the upward and the total downward transition rates are the same, i.e., $B_{12} \cdot \rho(\nu) \cdot N_1 = B_{21}\rho(\nu) \cdot N_1 = B_{21} \cdot \rho(\nu) \cdot N_2 + A_{21} \cdot N_2$, from which follows $N_2/N_1 = \rho(\nu)/[\rho(\nu) + 8\pi \cdot h\nu^3/c^3]$. It follows from this that for low energy densities (weak light), N_2/N_1 and also N_2 increase proportionally to the light but also that N_2/N_1 cannot exceed 1 even if the light is very strong. A so-called inverted population of molecules with $N_2/N_1 > 1$, which is necessary for laser action, can only be obtained in other ways than by simple light absorption from one energy state to another one

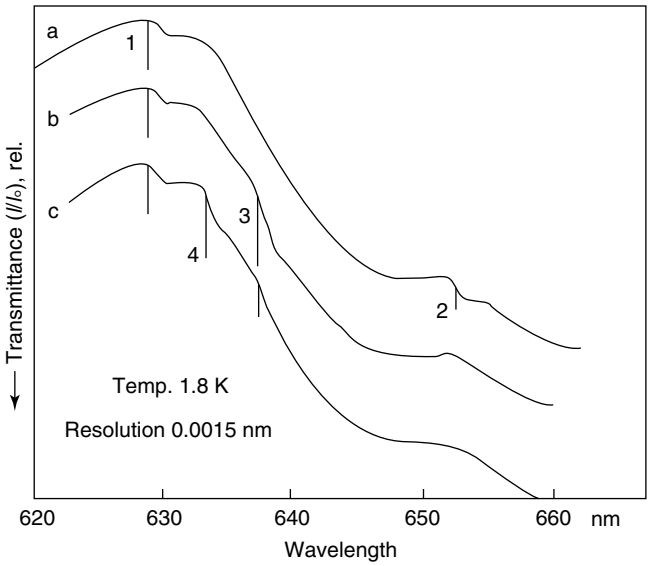

Fig. 1.17 A solution of C-phycocyanin was irradiated with a strong laser beam. Various wavelengths were used in the order indicated by the numbers and the *vertical lines* on the curves. These *lines* are, in fact, narrow dips or "holes" in the absorption spectra caused by depopulation of specific molecular states by the laser light. Note that irradiation with light of shorter wavelength following one with light of longer wavelength causes a repopulation of the less energetic state (corresponding to the longer wavelength). For instance, irradiation 3 practically cancels the effect of irradiation 2 (but not that of irradiation 1 at an even shorter wavelength than 3). Similarly, irradiation 4 partly cancels the effect of irradiation 3 (From Friedrich et al. 1981, modified)

conformational states as well as between different vibrational and rotational states, and it becomes possible to selectively deplete one state by monochromatic light from a laser. In this way one may "burn holes" in an absorption spectrum and see which portion of a spectrum is associated with a particular state (Fig. 1.17).

Even at a temperature of absolute zero, the oscillation continues with all molecules in the lowest vibrational state, the zero state. In fact, even at room temperature, the majority of the molecules are in this state, but a substantial fraction is in higher states.

Even at moderately lowered temperatures, absorption spectra (as well as fluorescence spectra) are sharpened (Fig. 1.18). This effect is often taken advantage of in spectroscopic investigations of biological samples containing several substances with similar spectra, such as cytochromes or chlorophyll proteins.

It should be understood that a molecule can appear in an electronically excited state for reasons other than having absorbed light or ultraviolet radiation. In rare cases, the collisions with other molecules can give a molecule sufficient energy for transition to an excited state. Chemical reactions may also produce reactants in electronically excited states, which can lose their energy by emission of light. This is how chemiluminescence works, and bioluminescence, which will be described later, is biochemical chemiluminescence.

1.14 Quantum Yield of Fluorescence

It has been already mentioned that a molecule in the excited state may lose its energy in various ways as light by radiative de-excitation. This process is called fluorescence if the transition is from a singlet excited state to a singlet ground state, and phosphorescence if the transition is from a triplet excited state to a singlet ground state or from a singlet excited state to a triplet ground state (the most important example of the latter is phosphorescence of singlet oxygen). It can also lose energy as vibrations to neighboring molecules (thermal de-excitation). Singlet excited states can disappear by "intersystem crossing" to produce triplet states; this happens, e.g., sometimes with chlorophyll molecules. And finally, energy may be lost through chemical reactions. Thus, the total rate of disappearance of singlet excitation can be described as the sum of the rates for the different de-excitation "pathways." In most cases, each molecule "acts on its own," so the kinetics of disappearance of singlet excitate states is of first order (in contrast, de-excitation of singlet oxygen is mixed first and second order at higher concentrations). It can thus be described by a

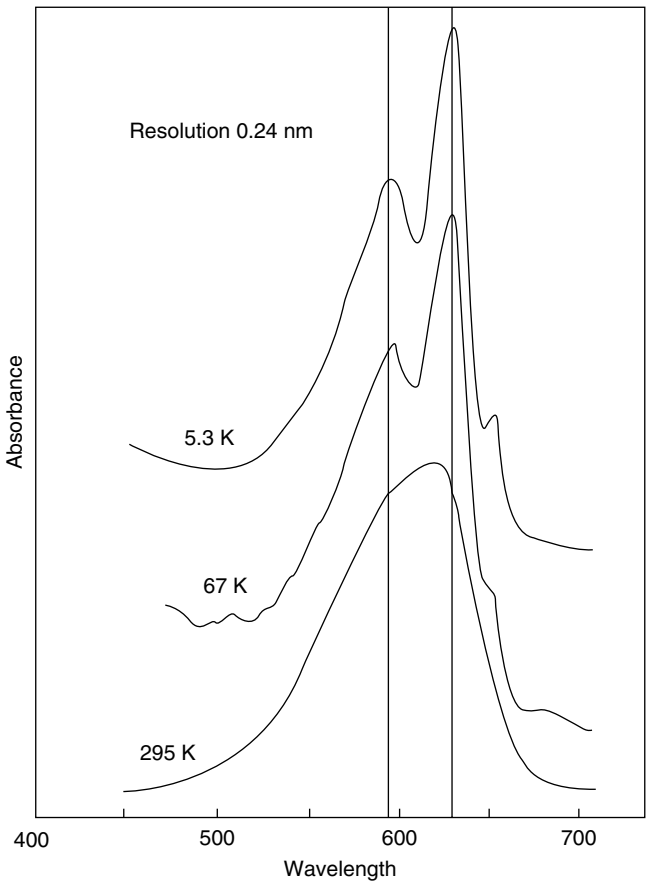

Fig. 1.18 Absorption spectra of C-phycocyanin at various temperatures (Redrawn from Friedrich et al. 1981)

first order rate constant k, which is a sum of the rate constants for the different pathways:

$$k = k_{\mathrm{f}} + k_{\mathrm{th}} + k_{\mathrm{ic}} + k_{\mathrm{ch}},$$

where f stands for radiative de-excitation (usually fluorescence), th for thermal de-excitation, ic for intersystem crossing, and ch for chemical de-excitation. Under steady illumination, a steady state develops, so the rate of excitation by absorption of photons equals the total rate of de-excitation. Therefore, the ratio of the number of photons emitted as fluorescence to the number of photons absorbed will be

$$\phi_f = k_{\mathrm{f}} / k = k_{\mathrm{f}} / \left(k_{\mathrm{f}} + k_{\mathrm{th}} + t_{\mathrm{ic}} + k_{\mathrm{ch}}\right).$$

The quantity φ_{f} is called the quantum yield of fluorescence. In the same way, we have a quantum yield for each de-excitation path; for example, also for the chemical deactivation,

$$\phi_{\mathrm{ch}} = k_{\mathrm{ch}} / k = k_{\mathrm{ch}} / \left(k_{\mathrm{f}} + k_{\mathrm{th}} + t_{\mathrm{ic}} + k_{\mathrm{ch}}\right).$$

The different pathways compete with one another. Therefore, the chlorophyll fluorescence from a plant, which is usually weak and invisible, increases if we add a poison that stops photosynthesis, the main pathway for chemical de-excitation. The fluorescence from chlorophyll becomes even stronger and clearly visible if we extract the chlorophyll and illuminate it dissolved in an organic solvent as acetone. Then we have not only completely stopped chemical de-excitation but also decreased thermal de-excitation.

Studying the changes of fluorescence from chlorophyll is an important way to investigate the functioning of the photosynthetic apparatus. In this context, one often uses the terms photochemical quenching and nonphotochemical quenching, respectively, for the chemical and thermal de-excitations competing with fluorescence.

1.15 Relationship Between Absorption and Emission Spectra

A simple relationship between absorption and emission spectra of even very complicated molecules was first hinted at by E. H. Kennard (1918) and later elaborated upon mostly by B. I. Stepanov. The relationship is most commonly referred to as the Stepanov (1957) relationship. The basic idea is that it is of no consequence to the future behavior of a molecule in which way it reached a certain state. From this it follows that any emission from an excited (energy-rich) electronic state of any kind of molecule in thermal and conformational equilibrium with its surroundings must have the same spectrum, whether the molecule reached the energy-rich state by collisions with its neighbors, or by absorbing a photon, or as a result of a chemical reaction. More specifically, the shape of the fluorescence spectrum (excited state reached by absorption of photons) is identical to the shape of the heat radiation spectrum from that kind of molecule. The heat radiation spectrum follows Planck's law for a blackbody, modified by the emissivity of the substance. But the emissivity, as was already mentioned, is the same as the absorptivity, which has the same spectral dependence as the experimentally measured absorption coefficient. Thus (fluorescence spectrum) = (absorption spectrum) × (blackbody spectrum). The multiplication sign here stands for *convolution*, i.e., multiplication of pairs of values throughout the spectrum. The fluorescence spectrum will then be expressed as photons per wavelength interval, energy per frequency interval, etc., depending on how the blackbody spectrum is entered into the equation.

The Stepanov relationship breaks down when heat energy cannot easily diffuse away from the emitting molecule. This happens in solid media or liquids of high viscosity and is always the case at low temperatures. Conversely, by comparing a fluorescence and an absorption spectrum, it can be found out whether or not the molecules in the excited state are in thermal and conformational equilibrium with the surroundings at the time of photon emission. An example of the

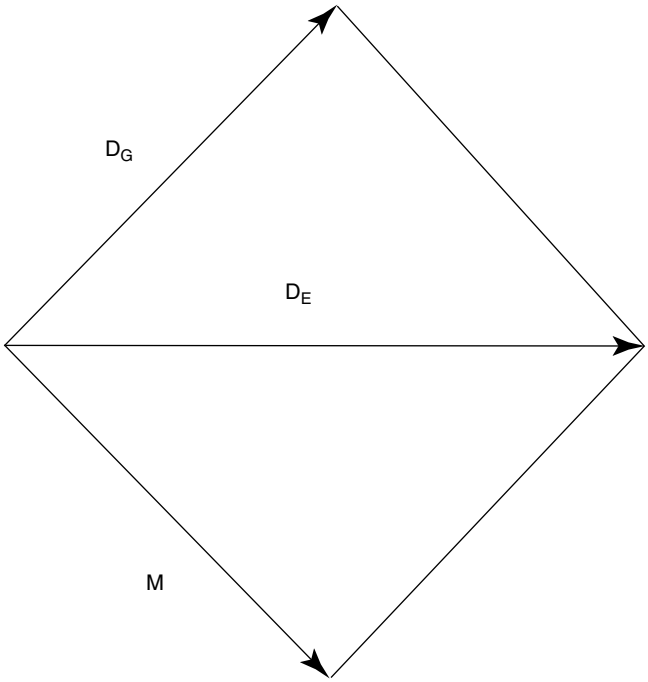

Fig.. 1.19 The transition moment **M** for a transition from the ground state to an excited state is the vectorial difference between the dipole moments of the molecule in the excited state **(D_E)** and in the ground state **(D_{EG})**

application of these ideas to a biological system is provided by Björn and Björn (1986).

1.16 Molecular Geometry of the Absorption Process

In a molecule, the center of positive charge (associated with the nuclei) may, or may not, coincide with the center of negative charge (associated with the electrons). If the center of positive charge does not coincide with the center of negative charge, the molecule is a dipole. Unless molecules are symmetrical, as are CCl_4 or CH_4, they are more or less strong dipoles.

A dipole is characterized by a dipole moment. This is a vector having direction and magnitude. The magnitude is the distance between positive and negative charge centers times the amount of charge. The direction of the dipole moment is from the negative to the positive charge center. Like other vectors, the dipole moment is often symbolized by an arrow (Fig. 1.19).

When a molecule is electronically excited, the negative charge is generally displaced in relation to the positive charge, i.e., there is a change in dipole moment. This change in dipole moment is called the transition moment and often symbolized by **M.** Like the dipole moment, it is a vector; in fact, it is the dipole moment of the excited state **(D_E)** minus the dipole moment of the ground state **(D_G).** Symbolizing the vectors by arrows, we may describe the subtraction as shown in Fig. 1.19.

The magnitude of the transition moment can be estimated from the absorption spectrum of the compound in question. Denoting the molar absorption coefficient by ε, the refractive index of the solvent by n, and light velocity divided by wavelength (frequency, c/λ) by ν, the oscillator strength (the square of the magnitude of the transition moment) is approximately $1.0222\times10^{-62} n \,\mathrm{x}\, \int[\varepsilon(\nu)/\nu]\ \mathrm{d}\nu\ \ \mathrm{C^2\,m^2}$, where integration is carried out over the absorption band. If we let ε instead stand for molecular cross section in m^2, the formula becomes $2.673\times10^{-25} n\ \mathrm{x}\int[\varepsilon(\nu)/\nu]\ \mathrm{d}\nu\ \ \mathrm{C^2\ m^2}$. C is the symbol for coulomb. For further details, see Knox (2003).

In most cases of excitation by light absorption, the probability of absorption is proportional to the square of the component of the transition moment in the direction of the electric field of the light. (There are cases of interaction between electrons and the magnetic field of the light rather than the electric field, but these cases are of little interest in photobiology.) Expressed in another way, the probability is proportional to $|\mathrm{M}|^2\cos^2\alpha$, where α is the angle between the transition moment and the direction of the electric vector of the light wave, i.e., the direction in the plane of polarization which is perpendicular to the direction of light propagation.

To those of you who think this is hard to follow, remember that the probability of absorption depends on how the molecule is oriented in relation to the direction of the light and (for plane-polarized light) the plane of polarization. For absorption of light by molecules in ordinary solutions, this is of no consequence, since the molecules (except in special cases) have random directions. For absorption of light by molecules in living cells, it is sometimes very important, since these molecules may be very accurately aligned. In such cases, light polarized in a direction parallel to the transition moment of the absorbing molecule is more strongly absorbed than light polarized in other directions. This phenomenon is called (absorption) dichroism.

In the same molecule there may be transition moments with different directions. For example, in the chlorophyll molecule, two transition moments are nearly at right angles to one another. The transition moment for emission of fluorescence may have a direction different from that for excitation of fluorescence. By measuring the polarization of fluorescence from molecules irradiated by polarized light, one can gain information about the angle between the transition moments.

1.17 Transfer of Electronic Excitation Energy Between Molecules

Transfer of electronic excitation energy from compound A to compound B may be symbolized as $\mathrm{A^* + B \rightarrow A + B^*}$. The energy quantum to be transferred must have a size such that it can be given off by A, i.e., corresponding to the energy of

a photon within the fluorescence band of A. Furthermore, it must be of a size that can be taken up by B, i.e., correspond to the energy of a photon within the absorption band of B. There are a few photobiological phenomena in which this energy transfer is actually mediated by a photon. As an example, we may mention the transfer of energy from luciferin in the lantern of a firefly female to the rhodopsin in the eye of a firefly male. However, in the majority of cases, the radiation transfer is radiationless, a process that is much more efficient at short range. Very few of the photons emitted by firefly females happen to be absorbed in rhodopsin molecules of firefly males. The advantage of energy transfer by photons is that it can take place over distance. We also all depend on the energy transfer taking place directly between atoms in the sun and chlorophyll molecules in plants, but also, this is a very wasteful process in the sense that a very small fraction of the photons emitted by the sun end up in chlorophyll molecules. On the other hand, once the quantum has been caught by a chlorophyll molecule (or a molecule of phycoerythrin or phycocyanin), it is channeled from molecule to molecule with an efficiency of practically 100 % by radiationless energy transfer (Fig. 1.20).

There are two main mechanisms for radiationless energy transfer: *exciton coupling* and the *Förster mechanism*. Exciton coupling occurs in a pure form in the photosynthetic antennae of green photosynthetic bacteria like *Chloroflexus*. The so-called chlorosomes of these bacteria contain rods made up of bacteriochlorophyll and carotenoid molecules. The pigment molecules are so tightly packed together that the whole rod behaves almost as a single pigment molecule; the energy is delocalized. This phenomenon, called *exciton coupling*, provides very fast transfer of the energy to the reaction center.

In other cases, chromophores may just pairwise be close enough to share energy and form what is called *exciplexes*. When exciplexes are formed, the energy levels split up.

The other mechanism, the Förster mechanism or resonance transfer, or dipole–dipole interaction, takes place in the phycobilisomes, pigment antennae of cyanobacteria and red algae composed of phycoerythrin, phycocyanin, allophycocyanin, and linker peptides holding the complex together (phycoerythrin is not always present, and in some cases, there are also other phycobiliproteins, such as phycoerythrocyanin). Only a few of the chromophores in the phycobilisomes are close enough to form exciplexes. A special section will be devoted to the Förster mechanism because it is so important.

Fig. 1.20 Demonstration of energy transfer in phycobilisomes prepared from a cyanobacterium. The chemical composition is exactly the same in the two test tubes, except for the concentration of the phosphate buffer in which the phycobilisomes are suspended. The test tubes are illuminated with *green light* (absorbed mainly by phycoerythrin), and the *yellow* and *red color* is due to fluorescence of the phycobiliproteins. In the test tube to the *left*, the phosphate concentration is low, the phycobilisomes are dissociated with large distances between the various phycobiliproteins, and the fluorescence is directly emitted by phycoerythrin. In the test tube to the right, the phosphate concentration is high (0.15 M), the phycobiliproteins are close together in undissociated phycobilisomes, and energy is transferred from phycoerythrin, via phycocyanin, and finally emerges as red fluorescence from allophycocyanin. Such "fluorescence resonance energy transfer" (FRET) is nowadays exploited in a number of applications, such as a method for DNA sequencing (Phycobilisome preparation by Dr. Gunvor Björn, photo by the author)

1.18 The Förster Mechanism for Energy Transfer

Thus, the transition of the molecule from one electronic energy state to another causes a change in the electrical field around it. Conversely, a change in the electric field can cause the transition from one energy state to another one. The field change caused by the transition in one molecule can cause the opposite transition in a neighboring molecule. This is the essence of energy transfer by dipole–dipole interaction, the Förster mechanism for energy transfer.

Just as the field change from the transition taking place in one molecule (the donor) drops off with the third power of the distance, so the sensitivity of the other molecule (the acceptor) to a field change drops off with the third power of

the distance. The combined effect is a sixth power relationship: the rate of dipole–dipole energy transfer between two molecules is inversely proportional to the sixth power of the distance.

We are now ready to have a look at a simplified Förster's formula:

$$\text{Energy transfer rate} = \text{factor } \phi \left(\text{overlap initegral}\right) \cdot \cos^2 \alpha / \left(r^6\right).$$

Here φ is the fluorescence quantum yield in the absence of the acceptor (see Sect. 1.15), α is the angle between the transition moments of the molecules, r is the distance, and the overlap integral is the convolution (pointwise product) of the donor fluorescence spectrum by the acceptor absorption spectrum, integrated over the whole spectral region in common.

1.19 Triplet States

Our description of molecular energy states so far has been aimed primarily at explaining the properties and processes associated with so-called singlet states. A molecule is said to be in a singlet state when all its electrons are grouped in pairs, so that the two electrons in each pair have opposite *spins*. Spin is a property of an electron or other charged particle that makes it act like a small magnet to produce a magnetic field. Positively charged particles such as atomic nuclei also have spin.

Because all electrons in a molecule in a singlet state occur in pairs, and the electrons in each pair have opposite spins, the electrons produce no net magnetic field. Most molecules like to be in a singlet state, so usually the ground state, the most stable state, having the lowest electronic energy, is a singlet state. A notable exception is the dioxygen molecule (making up ordinary oxygen in the air), which we shall come back to later.

However, it can occasionally happen that when a molecule has been excited from its ground (singlet) state to an excited singlet state, an electron "flips over," i.e., changes spin. Let us take a concrete and important example—the chlorophyll a molecule (Fig. 1.18). Like other chlorophyll forms, chlorophyll a has two prominent absorption bands corresponding to two electronic transitions with high probability. For chlorophyll a, these absorption bands are in the blue and red parts of the spectrum. In a collection of chlorophyll a molecules, be it in the plant or in solution, most of the molecules are in the ground state. Absorption of a photon of red light transforms a ground state molecule to the first excited singlet state. Absorption of a photon of blue light transforms a molecule from the ground state to the second excited singlet state. A molecule in the second excited singlet state very rapidly transfers some of its electronic energy to vibrational energy (heat) and lands in the first excited singlet state. Then various things can happen. The most "exciting" (pardon the expression) of the possibilities is that an electron completely leaves the molecule. This is the key step in photosynthesis and the key step in the whole living world. Another possibility is that the molecule "shakes off" more energy, heats its environment even more, and returns to the ground state. A third possibility is that it emits a photon, which carries away the excess energy and also returns the molecule to the ground state. A fourth possibility, which is realized in only a small fraction of the cases, is that the molecule is transferred from the first excited singlet state to the first (excited) triplet state. Although this happens after only a small fraction of excitations, it is important, and if plants were not specially equipped to handle such events, they would not survive.

A change from a singlet to a triplet state, which involves a spin change, a "flip" of an electron, is sometimes referred to as "intersystem crossing," because singlet and triplet states can be considered to be two types of states. Intersystem crossings are still sometimes also called "forbidden transitions," because early theories did not include the rare occasions when they occur.

Also, the change from the excited triplet state to the (singlet) ground state is "forbidden." In fact, it does occur (as many forbidden things do in our society). In any case, it does not take place quickly, or, in other words, the excited triplet state has a long lifetime. A triplet molecule does not easily react with a singlet molecule, but if it meets another triplet molecule, things are different. The magnetic fields created by the unpaired electrons interact. Even if the triplet molecules should not react chemically, they can exchange energy and become two singlet molecules. But because creation of a triplet state is in most cases a rare event, most triplet molecules are in low concentration, and the chance that two will meet is not great. We shall now come to a very important exception to this rule, already mentioned above.

1.20 The Dioxygen Molecule

The molecules of ordinary oxygen that we breathe have very remarkable properties. The most remarkable, important, and unusual of them all is that dioxygen molecules have a triplet ground state. From what will follow, the reader might get the impression that this is very unfortunate, because it makes oxygen a bit difficult to handle for organisms and imposes many threats. We shall deal with some of these in the chapters on phototoxicity and photosynthesis. But as is the case with many properties of the surprising and exciting world which we inhabit, if things were not exactly as they are, we would not be around. Just think for a moment that if the dioxygen in the air were in the singlet state, what would happen? We all know that oxygen under certain circumstances can react with organic

matter such as wood or our own bodies. Not only single houses or trees, but whole towns and forests have sometimes burned down. When oxygen oxidizes organic matter, large amounts of energy are released as heat. Processes that release energy usually take place quite easily. But for a house to catch fire, something has to get hot to start with. Once fire has started, other things get hot, and the fire is not easy to extinguish. Why is it that the fire does not start spontaneously?

The answer is that dioxygen consists of triplet molecules, and triplet molecules do not easily react with singlet molecules. Only after things get hot and some of the organic molecules get into states with lone electrons does a reaction with oxygen take place. When this happens, heat is released, more organic molecules acquire unpaired electrons and can react with oxygen, and so on.

Since we know that electrons like to join to pairs, one would expect that two oxygen atoms combine to a dioxygen molecule by joining two unpaired electrons to a pair. Instead, they combine to form a molecule with two lone electrons, a diradical.

1.21 Singlet Oxygen

Singlet dioxygen exists, but its lowest electronic state has more energy than the triplet ground state. Singlet oxygen can be produced by reaction of ordinary triplet oxygen with another compound in the triplet state, provided the energy of that other molecule is high enough. As we can see from Fig. 1.21, the energy of triplet chlorophyll (in relation to the singlet ground state of chlorophyll) is high enough to transfer oxygen from its triplet ground state to an excited singlet state called $^1\Delta g$, according to the following scheme:

$$\text{Chlorophyll}\ (\text{excited triplet}) + O_2\ (\text{ground state}) \rightarrow \text{Chlorophyll (ground state)}$$

The singlet so created is very reactive and can attack various other singlet molecules in the cell. If the plant did not have special systems both for preventing as much as possible the formation of singlet oxygen (this is the role of carotene in the plant cell) and for ameliorating the effects of it if it is formed, the plant could not survive for long, as shown in mutants lacking these protective systems.

In addition to chlorophyll, many other pigments, when illuminated, can form triplet states and generate singlet oxygen. We shall deal with this further in the chapter on phototoxicity.

The electronic configurations of various O_2 molecules and O_2 ions are shown schematically in Fig. 1.22.

1.22 Some Aspects of Light Recently Attracting Increased Interest

In this section, we shall briefly mention aspects of light that have recently attracted increased interest and provide references for further study.

1.22.1 Surface Plasmons

Surface plasmons constitute a form of energy which can be described as intermediate between light and electrical energy. Plasmons occur in the interface between an electrically conducting medium and an electrical insulator. They are not known to have direct relevance for biology but are used in biological research, e.g., for nano-tweezers (see Chap. 5, Juan et al. 2012; Dionne et al. 2012). For further information about plasmons, see Lakowicz (2006) and Berweger et al. (2012).

1.22.2 Orbital Angular Momentum of Light

This should not be confused with the ordinary angular momentum of photons due to their spin, neither should light having orbital angular momentum be confused with circularly polarized light. It can be generated only using special methods. So far, it has been important mostly for manipulation of very small particles (Grier 2003). Possibly, it can have relevance for the origin of chirality of biological molecules, but there is no evidence for this.

1.22.3 Coherence

Coherent light is light in which the waves corresponding to different photons are in step, and such light is best known as emitted by lasers. Recently, there has been much discussion concerning whether coherent energy transport might occur in photosynthetic systems even after absorption of incoherent light and of what importance that may be. We refer to Fassioli et al. (2012) and Kassal et al. (2013) for an introduction to the literature.

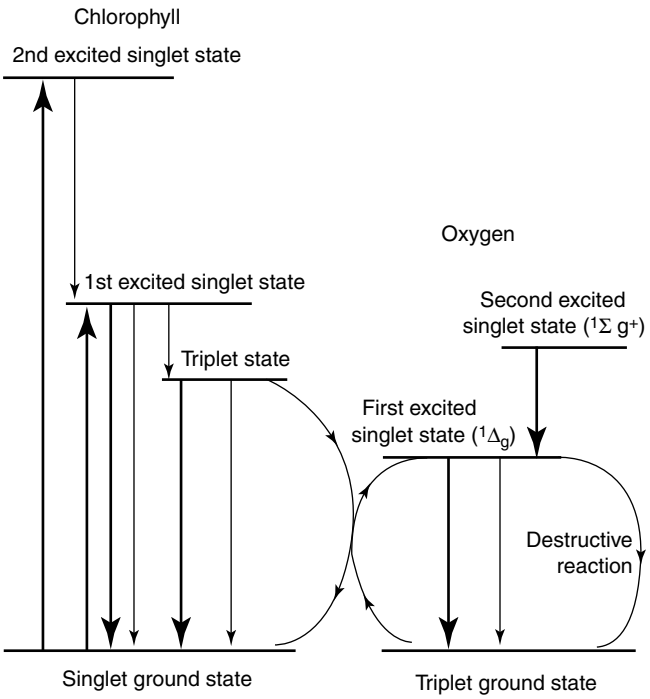

Fig. 1.21 The various energy states (*horizontal lines*) of chlorophyll (*left*) and molecular oxygen (*right*) and their energy transitions (*arrows*). Energy is plotted upward, i.e., a *high horizontal line* depicts a high energy state. Only the most important electronic levels are indicated, and the vibrational levels have been omitted. *Thicker lines* depict energy transitions associated with absorption (*upward arrows*) or emission (*downward arrows*) of light. The *long upward arrow* from the ground state of chlorophyll to the second excited state represents absorption of blue light; the *shorter upward arrow* from the ground state to the first excited state absorption of red light. *Thin arrows* represent radiationless transitions, in which energy is either transformed to heat (*straight arrows*) or reaction with another molecule (*curved arrows*) takes place. Emission of light can take place either as fluorescence (rapid light emission from singlet to singlet state) or as phosphorescence (slow light emission associated with change from singlet to triplet, as in chlorophyll at low temperature, or from triplet to singlet—in oxygen gas even at room temperature)

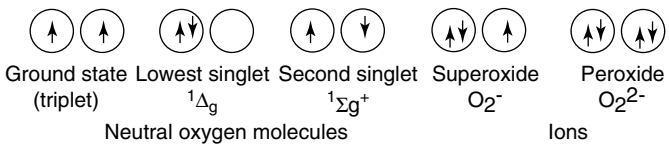

Fig. 1.22 The electronic configurations in various forms of neutral dioxygen (*left*) and dioxygen ions of biological importance (*right*). Only the "antibonding" (π^*) electrons are shown, since all lower orbitals are similar (completely filled) for all the species. *Arrows* of opposite directions represent electrons of opposite spin

References

Alonso M, Finn EJ (1967) Fundamental university physics, vol 2, Fields and waves. Addison-Wesley, Reading

Arndt M, Nairz O, Vos-Andreae J, Keller C, van der Zouw G., Zeilinger, A (1999) Wave–particle duality of C60 molecules. Nature 401, 680–682

Berweger S, Atkin JM, Olmon RL, Raschke MB (2012) Light on the tip of a needle: plasmonic nanofocusing for spectroscopy on the nanoscale. J Phys Chem Lett 3:945–952

Björn LO, Björn GS (1986) Studies on energy dissipation in phycobilisomes using the Kennard-Stepanov relation between absorption and fluorescence emission spectra. Photochem Photobiol 44:535–542

Dionne JA, Harry A, Atwater HA (2012) Plasmonics: metal-worthy methods and materials in nanophotonics. Mater Res Bull 37:717–724

Fassioli F, Olaya-Castro A, Scholes GD (2012) Coherent energy transfer under incoherent light conditions. J Phys Chem Lett 3:3136–3142

Friedrich J, Scheer H, Zickendraht-Wendelstadt B, Haarer D (1981) High-resolution optical studies on C-phycocyanin via photochemical hole burning. J Am Chem Soc 103:1030–1035

Grier DG (2003) A revolution in optical manipulation. Nature 424:810–816

Haupt W (1977) Bewegungsphysiologie der Pflanzen. Georg Thieme Verlag, Stuttgart

Hecht E (1987) Optics, 2nd edn. Addison Wesley, Reading

Hecht S, Shlaer S, Pirenne MH (1942) Energy, quanta and vision. J Gen Physiol 25:819–840

Hegemann P, Marwan W (1988) Single photons are sufficient to trigger movement responses in Chlamydomonas reinhardtii. Photochem Photobiol 48:90–106

Juan ML, Righini M, Romain Quidant R (2011) Plasmon nano-optical tweezers. Nat Photonics 5:349–356

Kassal I, Yuen-Zhou J, Rahimi-Keshari S (2013) Does coherence enhance transport in photosynthesis? J Phys Chem Lett 4: 362–367

Keijzer M, Star WM, Storchi PRM (1988) Optical diffusion in layered media. Appl Optics 27:1820–1824

Kennard EH (1918) On the thermodynamics of fluorescence. Phys Rev 11:29–38

Knox RS (2003) Dipole and oscillator strengths of chromophores in solution. Photochem Photobiol 77:492–496

Kubelka P, Munk F (1931) Ein Beitrag zur Optik der Farbanstriche. Phys Rev 11:672–683

Lakowicz (2006) Plasmonics in biology and plasmon-controlled fluorescence. Plasmonics 1:5–33

Sclafani M, Juffmann T, Knobloch C, Arndt M (2013) Quantum coherent propagation of complex molecules through the frustule of the alga Amphipleura pellucida. New J. Phys 15:083004. (http://iopscience.iop.org/1367-2630/15/8/083004)

Seyfried M, Fukshansky L (1983) Light gradients in plant tissue. Appl Optics 22:1402–1408

Star WM, Marijnissen JPA, van Gemert MJC (1988) Light dosimetry in optical phantoms and in tissues: I. Multiple flux and transport theory. Phys Med Biol 33:437–454

Stepanov BI (1957) A universal relation between the absorption and luminescence spectra of complex molecules. Dokl Akad Nauk SSSR 112:830–842 (Engl. transl. Soviet Phys. Doklady, 2, 81–84)

Principles and Nomenclature for the Quantification of Light

2

Lars Olof Björn

2.1 Introduction: Why This Chapter Is Necessary

This chapter will not deal with measuring equipment or measuring techniques, but with basic concepts of light quantification. This topic seems confusing, not only to the layman and the student, but also to the expert. Some reasons for this confusion are as follows:

1. The layman and beginning student erroneously regard the "amount" or "intensity" of light as something that can be completely described by a number.
   Such a view disregards the following:
   (a) Light consists of components with different wavelengths. A full description of the light would thus give information about the "amount" of light of each wavelength.
   (b) Light has direction. The simplest case is that all the light we are considering has the same direction, i.e., the light is collimated; the rays are all parallel. Another case is that light is isotropic, i.e., all directions are equally represented. Between these extremes, there is an infinite number of possible distributions of directional components.
   (c) Light may be polarized—either circularly polarized or plane polarized. In the rest of this chapter, we shall disregard this complication, but one should always be aware of the fact that a device such as a photocell may be differentially sensitive to components of different polarization, and polarization may be introduced by part of the experimental setup, such as a monochromator or a reflecting surface.
   (d) Light may be more or less coherent, with light waves "going in step." We will not address this complication in this chapter.
   (e) People often disregard or neglect or confuse the concept of time. We must decide whether we want to express an *instantaneous* or a *time-integrated* quantity, e.g., *fluence rate* or *fluence*, and *power* or *energy*. Power means energy per time unit.
2. Light is of interest for people investigating or working with widely different parts of reality. Experts in different fields have used different concepts and different nomenclature, partially depending on what properties of light have been interesting for them and partly due to the whims of historical development. Only rather recently have there been serious attempts to achieve a uniform nomenclature, and the process is not yet complete.

2.2 The Wavelength Problem

As we cannot always quantify light by giving the complete spectral distribution, we have to quantify it in some simpler way. From the purely physical viewpoint, there are two basic ways. Either we express a quantity related to the number of photons or a quantity related to the energy of light. For a light of single wavelength, the energy of a photon is inversely proportional to the wavelength and the proportionality constant is Planck's constant multiplied by the velocity of light.

There is an ultimate way of calibration only for the energy of light. For this we can use a hollow heat radiator of known temperature, which will radiate in a way predictable by basic physics. Using such a radiator, a photothermal device, such as a thermopile or a bolometer (see Chap. 4), can be calibrated, and then any kind of light can be measured with it and expressed in energy or power units. We can use it for measuring a series of "monochromatic" (i.e., narrow-band) light beams, and they, in turn, can be used for calibrating other measuring devices in either energy or photon units.

Actinometers, i.e., photochemical devices, seem to count photons, but in this case the ability of photons to cause a response (the quantum yield) varies with wavelength.

L.O. Björn
School of Life Science, South China Normal University, Guangzhou, China

Department of Biology, Lund University, Lund, Sweden
e-mail: Lars_Olof.Bjorn@biol.lu.se

L.O. Björn (ed.), *Photobiology: The Science of Light and Life*,
DOI 10.1007/978-1-4939-1468-5_2, © Springer Science+Business Media New York 2015

We can also use photomultipliers as photon counters, but we should be aware that they do not, strictly speaking, count photons, but impulses caused by photons. Some impulses are not caused by incident photons, but by electrons knocked out from the photocathode by the heat vibration of the atoms in it. We try to minimize this by cooling the photocathode. Furthermore, all photons do not have the same ability to knock out electrons from the photocathode and cause pulses to be counted. This ability is wavelength dependent. Therefore, we cannot use photon counting as an independent calibration method.

The units for expressing light as photons are as follows:

1. Photons (number of photons).
2. Moles of photons (the symbol is mol), which is $6.02217 \cdot 10^{23}$ photons, or a unit derived from this, such as micromole of photons ($6.02217 \cdot 10^{17}$ photons). The symbol for the latter is μmol.

Either of these can be expressed per time and/or per area or (rare in biological contexts) per volume.

The unit for energy is joule (J). Energy per time is power, and joule per second is watt (W). Both can be expressed per area (or, rarely in biological contexts, per volume, i.e., energy density or power density).

You should note that simply giving a value followed by "W/m^2" without further qualification is not defined, since one cannot be sure what kind of area you are expressing with m^2. Is it a flat area or a curved one? If it is flat, what is its direction? This brings us to the topic of the next section.

2.3 The Problem of Direction and Shape

Most light-measuring systems are calibrated using light of (approximately) a single direction, i.e., collimated light. However, light in nature, where most plants live, is not collimated. If the sky is cloudless and unobstructed, the rays coming directly from the sun are rather well collimated, but in addition there is skylight and light reflected from the ground and various objects. A plant physiologist who wants to understand how plants use and react to light has to take this into account.

Traditionally, most measuring devices can be regarded as having a flat sensitive surface, and when we calibrate the instrument, we generally position this surface perpendicularly to a collimated calibration beam. A plant leaf is also flat, so in the first approximation we can measure light in single-leaf experiments with a flat device with the same direction as the leaf. But a whole plant is far from flat (except in very special cases). Different surfaces on the plant have different directions. Ideally we should know the detailed directional (and spectral) distribution of the light impinging on the plant, but this is not possible in practice. Since a plant is a three-dimensional object, it would in most cases be better to determine the light using a device having a spherical shape and equally sensitive to light from any direction. This brings us to the distinction between

1. Irradiance, i.e., radiation power incident on a flat surface of unit area, and
2. Energy fluence rate (or fluence rate for short), i.e., radiation power incident on a sphere of unit cross section. The term fluence rate was introduced by Rupert (1974).

Both these concepts have their correspondences in photon terms. For case 1 the nomenclature is not settled, but it would be logical to use the term photon irradiance. Many people, especially in the photosynthesis field, use the term photon flux density and the abbreviation PFD (PPFD for photosynthetic flux density; see below). For case 2 the term photon fluence rate is well accepted among plant physiologists, but hardly among scientists in general.

Energy fluence is the energy fluence rate integrated over time. By fluence is meant as the same thing as energy fluence.

We shall now compare irradiance and energy fluence for different directional distributions of light (see Fig. 2.1):

1. Collimated light falling perpendicularly to the irradiance reference surface. In this case, the flat surface of unit area and the sphere of unit cross-sectional area will intercept the light equally, and irradiance will be the same as fluence rate.
2. Collimated light falling at an angle α to the normal of the irradiance reference plane. In this case, the light intercepted by the flat surface of unit area will be less than that intercepted by the sphere of unit cross-sectional area. The irradiance will be cos(α) times the fluence rate. Since cos(α) is less than unity, the irradiance in this case will be lower than the fluence rate.
3. Completely diffuse light falling from one side only. The ratio of irradiance to fluence in this case will be an average of cos(α) for all angles α from 0 to $+\pi/2$ weighted by sin(α), i.e., $\int \sin(\alpha)\cdot\cos(\alpha)\cdot dx / \int \sin(\alpha)\cdot dx$ with the integral running from 0 to $+\pi/2$, and this is equal to 1/2. Thus, the irradiance in this case is half the fluence rate. The reason we have to weight cos(α) by sin(α) is that all values of α are not equally "common" and do not have the same probability. The various directions may be thought of as corresponding to points on a big sphere, the center of which is the point of measurement. The sphere can be thought of as divided into a pile of rings, and each ring (corresponding to a value of α) has a radius, and hence a circumference proportional to sin(α).
4. Completely diffuse light from both sides, i.e., isotropic light. The sphere is then hit by light over its whole surface, but for the flat receiver we still count only one surface (irradiance is defined in this way), so irradiance is one quarter of the fluence rate in this case. We can easily remember this if we think that the area of a circle is one quarter of the area of a sphere with the same radius.

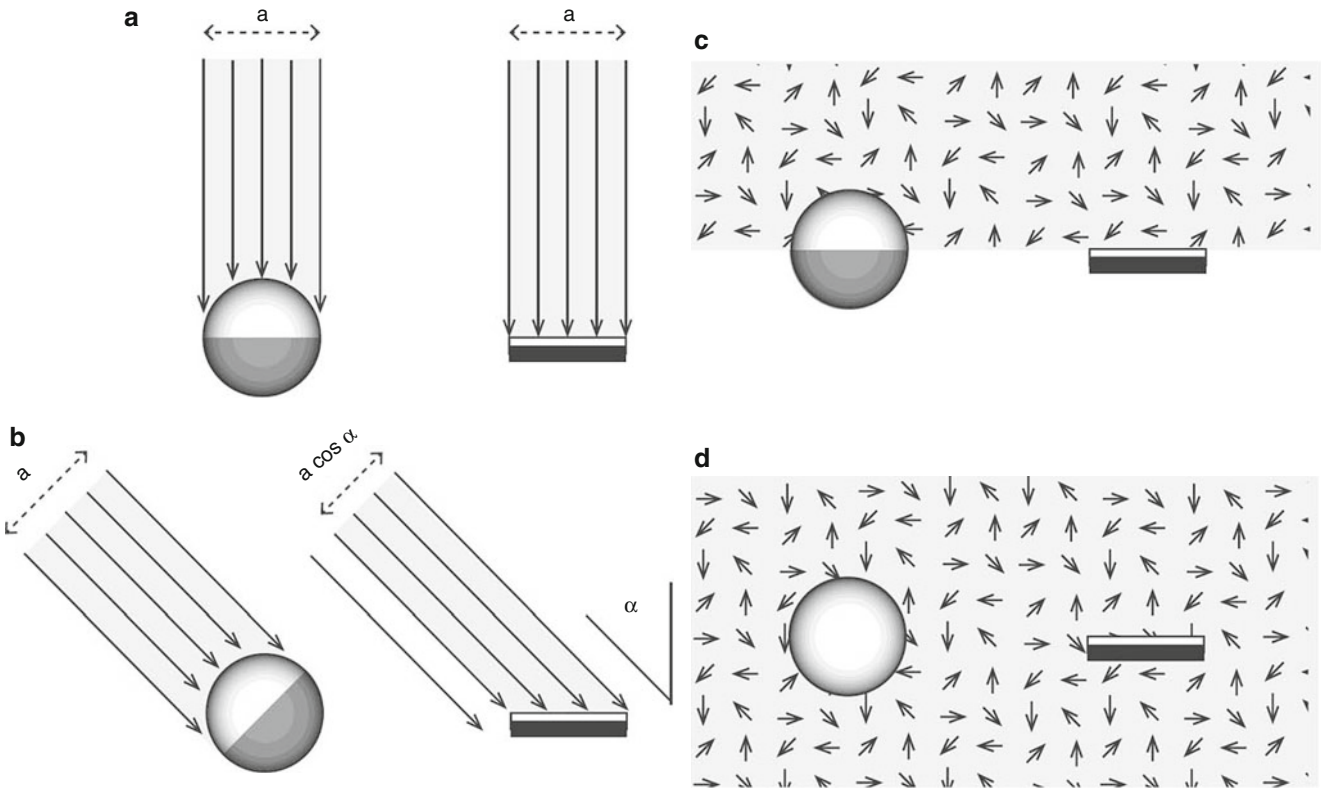

Fig. 2.1 The concepts of irradiance and fluence rate. In (**a**) the incident light is perpendicular to the surface of the flat irradiance sensor. In this case, fluence rate and irradiance are equal. In (**b**) the incidence angle is α. The irradiance sensor then intercepts only the fraction cos α of what the fluence rate sensor does. In (**c**) the light is diffuse, but incident only from above. Then the fluence rate is twice the irradiance. In (**d**) the sensors are immersed in diffuse radiation from all directions, but the irradiance sensor senses radiation only from above. In this case the fluence rate is four times the irradiance (Courtesy Pedro J. Aphalo and Eva Rosenqvist)

We may now make a table of various quantities associated with light measurements (Table 2.1).

In all the above cases, we add the word "spectral" before the various terms if we wish to describe the spectral variation of the quantity. We may thus write, e.g., spectral fluence rate on the vertical axis of a spectrum of light received by a spherical sensor.

What we here have called fluence rate is termed *actinic flux* by atmospheric scientists. Two more terms with the same meaning are *space irradiance* and *scalar irradiance*. The term space irradiance was introduced by Grum and Becherer (1979). The term *spherical irradiance* has been used in similar contexts, but means one quarter of the fluence rate. *Vectorial irradiance* is just the same as irradiance. The reader should use just one system of terms, preferably irradiance and fluence rate, but may encounter all these other terms in the literature.

Few instruments on the market, and very few spectroradiometers, are designed for direct measurement of fluence rate. Most of them are constructed for irradiance measurements and a few for measurement of radiance (see below). But Björn (1995) and Björn and Vogelmann (1996) have shown how irradiance meters can be used for estimation of fluence rate.

Table 2.1 Various quantities associated with light measurements

	Flat receiver	Spherical receiver
Instantaneous values		
Energy system	(Energy) irradiance Unit: W m^{-2}	(Energy) fluence rate Unit: W m^{-2}
Photon system	Photon irradiance (=photon flux density) Unit: mol m^{-2} s^{-1}	Photon fluence rate Unit: mol m^{-2} s^{-1}
Time integrated values		
Energy system	(Energy density) Unit: J m^{-2}	(Energy) fluence Unit: J m^{-2}
Photon system	–	Photon fluence Unit: mol m^{-2}

So far we have been dealing with light falling on a surface, either a flat or a spherical one. But we may need to express other quantities, for instance, the total power (energy per time unit) output of a light source. The unit for this is, of course, W (watt). The power emission per unit area of the source is called the *radiant excitance* and is measured in W/m^2 (just like irradiance and fluence rate, so beware of confusing them). The power emission takes place in different

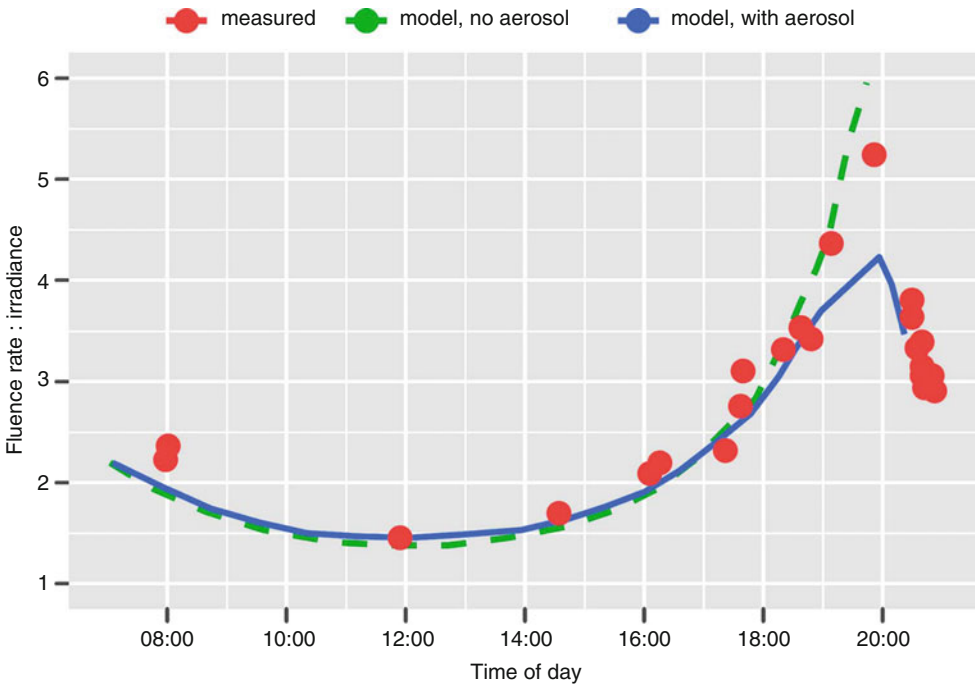

Fig. 2.2 The variation of the ratio of fluence rate to irradiance over a clear summer day in southern Sweden. Presence of small particles in the air (aerosol) dampens the variation. The graph is for cloudless conditions and 400–700 nm ("PAR" spectral band, see Fig. 2.3). For ultraviolet radiation, especially for UV-B radiation, the variation is smaller, because even clean air scatters this radiation to make it to a large extent diffuse. For overcast conditions, the variation is also smaller than for clear skies (Measurements and calculations by the author, plot by Pedro J. Aphalo and Eva Rosenqvist)

directions; in total there is a solid angle of 4π steradians (sr) surrounding a source. Usually the emission is not equally distributed in all directions, so for a certain direction we might like to specify the power emission per steradian. This quantity is called the *radiant intensity* in that direction, and the unit is W/sr. (Note that the term intensity is often (erroneously) used in another and usually not well-defined sense). The radiant intensity per area unit on a plane perpendicular to the light is called *radiance*, and the unit is W/sr/m^2. The official definition of radiance (usually denoted by L) is as follows: radiant power (P), leaving or passing through a small transparent element of surface in a given direction from the source about the solid angle θ, divided by the solid angle and by the orthogonally projected area of the element in a plane normal to the given beam direction, $\mathrm{d}S \cos\theta$. With mathematical symbols we write: $L = \mathrm{d}^2P/(\mathrm{d}\Omega\, \mathrm{d}S \cos\theta)$ for a divergent beam propagating in an elementary cone of the solid angle Ω containing the direction θ.

If we integrate the radiance over all 4π radians for both Ω and θ, we get back to the fluence rate that we are already familiar with.

Fortunately, the average photobiologist need not keep all these concepts in his or her head at all times. You can look them up when needed. However, you must be clear over the meaning of irradiance and fluence rate and not confuse these two concepts. As a practical illustration of how the ratio of fluence rate to irradiance can vary under natural conditions, see Fig. 2.2.

A comprehensive list of recommended units, concepts, and symbols for photo-science is published by Braslavsky et al. (2007).

2.4 Biological Weighting Functions and Units

Section 2.3 concludes the physical quantification of light. However, there has been a need for additional concepts in connection with organisms and biological problems. Traditionally there has been a special system related to the human perception of light. We can here limit ourselves to *illuminance*, which is expressed in lux. Neglecting the historical development, we can say that lux is the integrated spectral irradiance weighted by a special weighting function. This weighting function is precisely described mathematically, but can be thought of as the average (photopic, i.e., related to strong light vision mediated by cones) eye spectral sensitivity for a large number of people. (Rarely we also see the expression "scotopic lux," which is the corresponding term using the scotopic visibility weighting function.) The photopic visibility function has its maximum at 555 nm, and for this wavelength 1 W/m^2 equals 683 lx. For all other wavelengths, 1 W/m^2 is less than 683 lx. Illuminance integrated over a flat area is called *luminous flux*, and the unit is lumen. Thus lux is lumen per square meter. In older American literature the unit foot-candle (f.c.) is used instead of lux. Foot-candle equals lumen per square foot, and since there are 3.2808399 ft in a meter, there are $3.2808399^2 = 10.763910$ square feet in a square meter, and also 10.763910 lx in a foot-candle. There are also a number of other photometric concepts and units, which we seldom need in photobiology. Many of them are defined in the *Handbook of Chemistry and Physics*.

Similarly we may, for purposes other than vision (reading light, working light), weight the spectral irradiance by other functions. These functions approximate various photobiological action spectra (see Chap 8). One special function is zero below 400 nm and above 700 nm, and unity from 400 to 700 nm. This describes by definition photosynthetically active radiation, or PAR. Usually one uses the spectral photon irradiance to weight by this function, and this is the meaning of the often used term PPFD, photosynthetic photon flux density. To assume photosynthetic zero action outside the range 400–700 nm and the same action for all components within the range is, of course, physiologically speaking an approximation, but an approximation that people have agreed upon, just as the definition of lux involves an approximation that holds well only for photopic (cone) vision.

Other weighting functions are used for "sunburn" meters to yield "sunburn units," but in this field we have to watch out for various "units" used by various people. One kind of sunburn meter used much in the past is the Robinson-Berger meter, but recently a new agreement has been reached for using a weighting spectrum more closely resembling the true sunburn action spectrum (for Caucasian skin). One weighting function to determine safe working conditions shown in Fig. 2.3 is damaging UV. This particular function was agreed upon in 1991 by the International Radiation Protection Association (IRPA) and the International Commission on Nonionizing Radiation Protection (ICNIRP). Another, slightly different function for similar purposes was devised by the American Conference of Governmental Industrial Hygienists (ACGIH).

In reality, of course, different kinds of damage, such as damage to the cornea and to the lens of the eye and to skin of persons with different pigmentation, have different action spectra. Also the standard PAR is an approximation to reality, since different plants, and even the same plant in different states, have different action spectra for photosynthesis.

There are numerous other weighting spectra in use for estimating radiation with other biological actions. We shall address some of them in the chapter on ultraviolet radiation effects.

Some meters, such as lux meters, sunburn meters, and meters for PAR, are constructed with spectral responses approximating the weighting functions and can therefore directly yield the values we want without spectral decomposition of the light. For more precise work, and in the case of, e.g., UV inhibition of plant growth, it is necessary to measure (using a spectroradiometer) each wavelength component separately and weight by the weighting function using arithmetics (usually computers are used).

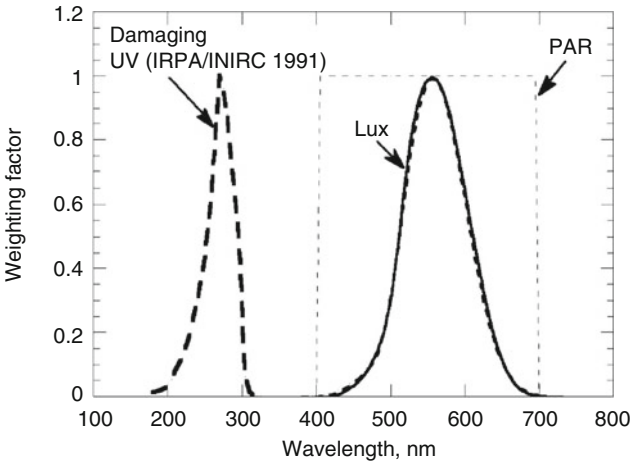

Fig. 2.3 Examples of weighting functions. The damaging UV function is one devised by the International Radiation Protection Association (*IRPA*) and the International Commission on Nonionizing Radiation Protection (*ICNIRP*) and thus having a certain official status. *PAR* stands for photosynthetically active radiation, and this weighting factor is unity from 400 to 700 nm and zero outside this interval. This weighting function is applied more often to photon irradiance or photon fluence rate than to energy irradiance and energy fluence rate. The Lux function is that used for conversion of W/m^2 to lux (or W to lumen). The maximum is here made unity to allow plotting together with the other functions, but in absolute units it corresponds to 683 lx per W at 555 nm. The Lux graph in fact consists of two plots, so close that they hardly can be distinguished in the diagram—both the official values from a table and an analytical approximation consisting of the difference between two Gauss functions: weighting factor = $\exp[-(555-\lambda)/63.25]^2 - \exp[-(495-\lambda)/30]^2/6.8$, where λ stands for wavelength in nm

References

Björn LO (1995) Estimation of fluence rate from irradiance measurements with a cosine corrected sensor. J Photochem Photobiol B Biol 29:179–183

Björn LO, Vogelmann TC (1996) Quantifying light and ultraviolet radiation in plant biology. Photochem Photobiol 64:403–406

Braslavsky SE et al (2007) Glossary of terms used in photochemistry. 3rd ed. (International Union of Pure and Applied Chemistry recommendations 2006). Pure Appl Chem 79:293–465. Available at http://www.iupac.org/reports/III/2002-024-1-300_rec061012.pdf or http://www.iupac.org/reports/1993/homann/index.html

Grum F, Becherer RJ (1979) Optical radiation measurements. Academic Press, New York, pp 14–15

Handbook of chemistry and physics (many editions). CRC Press, Cleveland. http://en.wikipedia.org/wiki/CRC_Handbook_of_Chemistry_and_Physics

Rupert CS (1974) Dosimetric concepts in photobiology. Photochem Photobiol 20:203–212

Generation and Control of Light

3

Lars Olof Björn

3.1 Introduction

Any photobiological experimental setup consists of three main parts: a light source, a light path, and a target. The biological object under investigation may form the light source, part of the light path, or, as in the most common case, the target. In the following, we shall treat the nonbiological components of the experimental setup.

3.2 Light Sources

3.2.1 The Sun

Almost all the natural light at the surface of the earth comes from the sun (this holds, of course, also for moonlight). The sun, on the whole, radiates as a glowing blackbody at a temperature of about 6,000 K. We have already mentioned the absence of some wavelength components from sunlight due to absorption in the outer cooler layers of the sun. Sunlight is further modified by the Earth's atmosphere before it reaches ground level. More about this and other natural light conditions will follow in Chaps. 6 and 7.

3.2.2 Incandescent Lamps

The light from an incandescent lamp originates at the surface of a glowing filament, which nowadays is, almost invariably, made from tungsten. It is heated by an electric current flowing through it. In order not to be destroyed (oxidized) by the oxygen in the air, the filament is enclosed in an envelope made of glass or quartz. The envelope is either evacuated (most commonly for small lamps) or filled with an inert gas or iodine vapor.

The spectral composition of the emitted light is strongly dependent on the temperature of the filament. As a first approximation, the spectrum varies with temperature as does that of blackbody radiation (Planck's law). However, due to the wavelength dependence of the emissivity of tungsten, more shortwave radiation is emitted than from a blackbody of the same temperature. The filament is, in most cases, coiled, which makes it somewhat "blacker" (more like a glowing cavity) than a smooth tungsten surface would be.

In most cases, it is desirable to obtain as much as possible of the radiation toward the short-wavelength end of the spectrum, i.e., to operate the lamp with as high a filament temperature as possible (the temperature can be increased by increasing the voltage). However, this results in a shorter life of the lamp, because the tungsten evaporates more quickly (and condenses again on the envelope, which blackens it). As a rule of thumb, an increase of the voltage by 10 % above the recommended voltage will decrease the lamp life to one third (i.e., by two thirds).

The lamp life at a certain filament temperature can be increased by making the filament thicker. Thereby, a certain power (wattage) is reached at a lower voltage (using a higher current). A further advantage of low-voltage lamps is, in many cases, that the filament is shorter. Quite often a small ("point-like") light source is desirable in optical systems.

A gas-filled envelope permits a higher filament temperature than an envelope with vacuum. A mixture of argon and nitrogen is the most common choice (old-fashioned household bulbs). The addition of iodine ("halogen lamps" or "quartz–iodine lamps") permits an even higher temperature. This is because the iodine vapor combines with the tungsten vapor. The compound is decomposed again when the molecules hit the hot filament, which is thereby continuously regenerated. For the regeneration to work properly, the temperature of the envelope must be so high that the tungsten iodide cannot condense on it. Therefore, such lamps are manufactured with a very small envelope made of quartz, which can withstand high temperature.

L.O. Björn
School of Life Science, South China Normal University, Guangzhou, China

Department of Biology, Lund University, Lund, Sweden
e-mail: Lars_Olof.Bjorn@biol.lu.se

L.O. Björn (ed.), *Photobiology: The Science of Light and Life*,
DOI 10.1007/978-1-4939-1468-5_3,

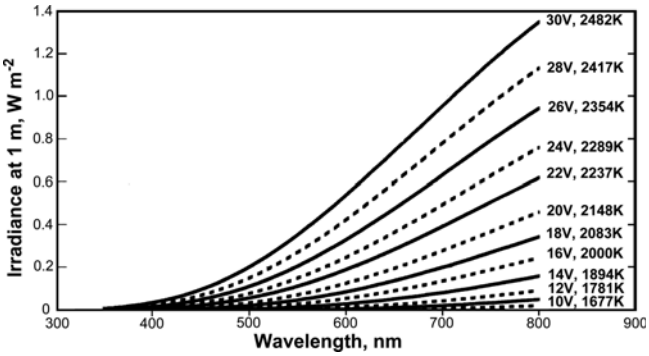

Fig. 3.1 Emission spectra of an incandescent lamp with a nominal rating of 24 V run at different voltages, with computed filament temperatures indicated. The lowest dashed curve corresponds to 8 V and 1,547 K

The advantages of incandescent lamps are their low cost, no requirement for complex electrical circuitry, and stability. The main disadvantage is that the emission at the short-wavelength end of the spectrum is low and the spectrum is strongly dependent on the current through the lamp and therefore difficult to keep absolutely constant. A method to estimate the spectrum of an incandescent lamp fed with direct current (within the spectral range where the glass or quartz envelope does not absorb appreciably) has been devised by Björn (1971). The principle is as follows: using a small current and measuring both the current through and the voltage across the lamp, the room temperature resistance of the lamp is measured (this is essentially the resistance of the tungsten filament). After the lamp has been powered up (with direct current), the current and voltage are measured again. From this, the "hot" resistance is computed. The temperature of the glowing filament can be computed from the ratio between room temperature resistance and "hot" resistance, and from this (using the Planck formula for a blackbody radiator and the known temperature- and wavelength-dependent emissivity of tungsten), the spectrum can be computed.

Using these principles, emission spectra for a lamp with a 24 V rating operated at various voltages were computed (Fig. 3.1) according to Björn (1971).

3.2.3 Electric Discharges in Gases of Low Pressure

In a gas discharge lamp, an electric current is flowing through a gas. The gas emits light, the spectral composition of which depends on the gas. When the gas has a low pressure, it emits a line spectrum, i.e., only light of certain wavelengths is represented (in contrast to the continuous spectrum emitted by an incandescent lamp).

The basic parts of a gas discharge lamp are a gas enclosed in a transparent envelope and the two electrodes necessary for the conduction of current to and from the gas. In addition to this, it is often necessary with other parts, such as heating filaments, to release enough electrons to start the current through the gas or to vaporize, e.g., mercury or sodium when vapors of these metals are to be used as emitting gas.

The electric resistance of an incandescent lamp increases when the current through it increases, since tungsten has a higher resistivity the higher the temperature. Thus, an incandescent lamp is self-regulating and burns in a stable way as long as the voltage is constant. In a gas discharge lamp, the reverse holds: its electric resistance decreases with increasing current. Therefore, such a lamp has to be connected to some kind of circuitry limiting the current. In the case of direct current, a series resistor is often used, and in the case of alternating current, a choke.

Gas discharge lamps containing mercury vapor of very low pressure emit most of their energy as ultraviolet radiation of wavelength 253.7 nm. This wavelength is close to the absorption maximum of nucleic acids, and the radiation is also absorbed by the aromatic amino acids in proteins and many other biological molecules. The photons are also energetic enough to initiate many chemical reactions, and therefore, this kind of radiation is very destructive for living matter. Low-pressure mercury lamps with quartz envelopes (which transmit this kind of radiation, in contrast to glass envelopes) are therefore used as sterilization (germicidal) lamps.

Fluorescent lamps are similar lamps, but with glass envelopes, which on the inner surfaces have a fluorescent layer converting the UV radiation to visible light (or, in certain cases, to UV radiation of longer wavelength than the original emission).

Glow lamps are a kind of low-pressure gas discharge lamp, usually containing neon. Lamps containing the element to be measured are used for atomic absorption spectroscopy. Low-pressure sodium lamps, emitting almost monochromatic light at 589 nm, have been used extensively as sources of outdoor working light, because they give more visible light per unit of energy input than any other type of lamp. To a large extent, they have been abandoned, mostly because our color vision cannot be used with monochromatic light.

Microwave radiation is used for the energy input in some other gas-filled lamps, such as "electrodeless" high-pressure xenon lamps.

3.2.4 Medium- and High-Pressure Gas Discharge Lamps

If the vapor pressure in a mercury lamp is increased, more and more of the emission at 253.7 nm is reabsorbed, and finally, very little of this radiation escapes from the vapor.

Instead, spectral lines of longer wavelength emerge (medium-pressure mercury lamps). At even higher pressures, the spectral lines are broadened to bands (high-pressure mercury lamps), and finally, a continuous spectrum results (superhigh-pressure mercury lamps).

Deuterium (heavy hydrogen) lamps of medium pressure are used as light sources for spectrophotometry in the ultraviolet region.

Lamps containing xenon of high pressure are used to obtain a strong continuous emission from 300 nm and into the infrared. Depending on the composition of the envelope, more or less of shorter wavelength, ultraviolet also escapes. Xenon lamps come in a great variety of types. We use lamps running at about 24 V on direct current (but ignited with about 2,000 V = danger!!) and wattages (rated powers) from 150 to 900 W. Xenon lamps of higher wattage are often water cooled. Electrodeless xenon lamps are also manufactured. They are powered by microwave radiation.

Because xenon lamps with UV-transparent envelopes cause conversion of oxygen to ozone, such lamps must be provided with exhausts to transport the ozone out of the building. The same holds for high-pressure mercury lamps with UV-transparent envelopes.

All high-pressure lamps are dangerous because they can explode. They must therefore never be operated without protective housing. Even when cold, they should be handled with care, using eye protection and other appropriate safety measures.

3.2.5 Flashlamps

Electronic flashes are xenon lamps through which a capacitor is discharged when a special triggering pulse has ionized the gas. The energy available is proportional to the capacitance of the capacitor and to the square of the voltage to which it has been charged. In many cases, it is desirable to have a short flash duration. This requires that the impedance of the circuit is low (short leads) and the capacitance low (high voltage has to be applied to the capacitor to get enough energy with a low capacitance). It is also necessary to prevent the circuit from oscillating and causing multiple flashes. Ordinary photographic flashes have a flash duration of about 1 ms. If they are "automatic," i.e., combined with a light-sensing photodiode and appropriate circuitry, the flash will be cut off when a certain amount of light energy has been emitted.

3.2.6 Light-Emitting Diodes

Light-emitting diodes (LEDs) are used in applications where very strong light is not needed, for instance, as indicator lights and displays. However, the maximum output power available from LEDs is increasing, and LEDs are the cheapest devices that can be modulated very rapidly: using an appropriate circuit, they can be switched on and off in a few nanoseconds. For this reason, they were used early as light sources for measuring variable fluorescence in plants. Initially, the trouble with this was that only red-emitting diodes were intense enough and their red light is not easy to efficiently separate from the chlorophyll fluorescence. Now sufficiently intense blue-emitting diodes are also available.

LEDs of several spectral emission types are presently manufactured: ultraviolet A, B, and C and blue, green, yellow, red, and infrared. It should be noted that they are not monochromatic light sources and especially the shortwave rated LEDs often have a broadband emission of longer wavelength than the nominal emission. For some types, the emission spectrum changes with operating current. LEDs are powered by a low-voltage source (e.g., a 1.5 V battery; some types need up to 5 V) in series with a resistor limiting the current to the rated value. Proper polarity should be observed.

Traditional LEDs contain inorganic semiconductors such as GaN, InGaN, SiC, and GaAsP (see Table 3.1). Very recently, several laboratories and companies have started to develop organic light-emitting diodes (OLEDs), which will probably widen the range of spectral types available. Roithner also markets a range of infrared-emitting diodes with emission peak wavelengths to greater than >4.5 µm. A LED emitting at 210 nm has been constructed (Taniyasu et al. 2006) but as of this writing not yet commercially available. An interesting new development is the construction of a LED that can generate a single photon at a time (Yuan et al. 2002).

3.2.7 Lasers

Laser is an acronym for light amplification by stimulated emission of radiation. Stimulated emission occurs when a photon causes a molecule in an excited state to emit a second photon. Stimulated emission as such requires no special equipment. It occurs regularly when photons of the proper energy encounter excited molecules. However, as a rule, excited molecules are very rare compared to molecules in the ground state (remember the equilibrium concentration formula, $N_y/N_x = \exp(E_x - E_y)/kT$). To get light amplification by stimulated emission, we must have more stimulated emission than light absorption, which means that we must have more molecules in the proper excited state than in the ground state. This can be achieved in different ways but never by "direct lift" from the ground state by absorption of light. Various lasers employ indirect "optical pumping" (sometimes by another laser), electrical energy, or chemical reactions. For a laser to work, photon losses must also be

Table 3.1 Examples of LEDs and where to obtain them

Peak wavelength (nm)	Semiconductors	Company and URL
237–365	AlGaN/GaN	Sensor Electronic Technology, Inc. www.s-et.com
370–390	GaN	Nichia America
460	GaN	www.nichia.co.jp/en
470, 505, 525	SiC/GaP	LEDtronics
574, 595, 611	InGaAlP	www.ledtronics.com
630	GaAsP/GaP	
660	GaAlAs/GaAlAs	
660, 700, 720	GaAlAsP	Roithner Lasertechnik
780, 810, 905	GaAlAsP	http://www.roithner-laser.com/
375–1550	InGaN AlGaAs/AlGaAs	Epitex http://www.epitex.com/
240–415	InGaAsP	Spectrecology http://www.spectrecology.com/ (All accessed Aug. 17, 2013)

minimized by a suitable optical configuration, often involving mirrors.

Laser light has some unusual properties:

1. Laser light is coherent in the sense that the light constitutes very long wave trains, contrary to ordinary light, where each photon can be regarded as a limited wave packet independent of other photons.
2. Laser light can be made very collimated (all rays very parallel).
3. Laser light is usually very monochromatic (very narrow spectral bandwidth) or consists of a small number of such very narrow bands.
4. Laser light may be (but is not necessarily) plane polarized.
5. The light from some types of lasers is given off in extremely short pulses of extremely high power (energy per time unit). However, this does not hold for all lasers. Some lasers emit light continuously and have very feeble power.

Even lasers of low power, such as the helium–neon laser, should be handled with some caution. This is because the beam is so narrow, parallel, and monochromatic that if it hits your eye all its power will be focused onto a very small area of your retina and blind that particular spot.

One kind of laser that is in everyday use is the continuous helium–neon laser, emitting at 632.8 nm and a few infrared wavelengths. Dye lasers are advantageous in many cases because the wavelength can be selected over a wide range (within the fluorescence band of the dye used, and the dye can be changed if necessary). You may sometimes encounter a YAG laser. YAG is the acronym for yttrium aluminum garnet, containing trivalent neodymium ions in $Y_3Al_5O_{12}$. They are very powerful emitters of infrared radiation of 1,060 nm wavelength. For photobiological purposes, they are sometimes combined with frequency doublers made of potassium phosphate crystals, so that green light of 530 nm wavelength is obtained. The wavelength can be further changed either by letting the light undergo Raman scattering or by using it as a power source for a dye laser. Diode lasers are photodiodes emitting coherent light. They are now the most common lasers, used in CD players and other optical readout devices and laser pointers. They are available from 370 nm in the UV-A band to the long-wavelength red.

3.3 Selection of Light

In many cases, you do not want to use light as it comes from your light source. You may wish to remove some parts of the spectrum or select just a narrow spectral band or select light with a certain polarization, or you might wish to modulate the light in time, for instance, quickly change from darkness to light or obtain a series of light pulses. The first three sections below will deal with wavelength selection. A review of filters and mirrors of interest to biologists is provided by Stanley (2003).

3.3.1 Filters with Light-Absorbing Substances

The simplest devices for modifying the spectral composition of light are filters with light-absorbing substances that remove certain components from the spectrum. These color filters may be solid or liquid.

Cheap filters, which are quite useful for some purposes, consist of colored plastic (e.g., Plexiglas or cellulose acetate). Colored cellophane is not recommended as it is rather unstable, and cellulose acetate has to be used with great caution since it bleaches with time. It must also be realized that

all these substances transmit far-red light and infrared radiation freely. Thus, a piece of green Plexiglas does not transmit just green light. It is very instructive to put one, two, three, etc. sheets of green Plexiglas on an overhead projector and watch the effect (or look through the sheets toward an incandescent lamp). One or two sheets look clearly green, after which the color becomes indescribably dirty and finally shifts to deep red. This is because far-red light is transmitted even more freely than green light, and when practically all the green light (to which our eyes are most sensitive) is gone, we see the remaining far-red, which is otherwise hidden by the green. Remember that plants, contrary to our eyes, are more sensitive to far-red light than to green!

Undyed cellulose acetate can be used as a cutoff filter to remove UV-C radiation but retain UV-A and UV-B. The exact absorption depends on the thickness and must be checked regularly because the filter changes, especially in front of a UV radiation lamp. A more stable alternative is a special type of uncolored Plexiglas, number FBL.2458 (from Röhm GmbH, ordinarily used in front of the UV radiators in Solaria).

A great variety of gelatin filters for photographic use are manufactured by Ilford, Kodak, and other companies. They may also be very unstable in strong light and also freely transmit far-red light.

From an optical viewpoint, some solutions are much better filters than anything that can be made in solid form, but solutions are in many cases inconvenient to use. Thick layers may be required for the optical properties you want, and the liquid filters may therefore become bulky. Furthermore, some of the most useful colored substances are, unfortunately, carcinogenic or toxic in other ways.

One useful substance, which is not particularly dangerous, is water (see Figs. 3.2 and 3.3). It can be used for removing infrared radiation and thus avoid heating by light from incandescent and xenon lamps. Addition of copper sulfate increases the absorption of far-red. Copper sulfate should be used only with distilled water, and the solution should be acidified with sulfuric acid to avoid precipitation of cupric carbonate.

Solutions of potassium dichromate (carcinogenic!) are very good for removing light of wavelength shorter than about 500 nm, as one might want to do in, e.g., studies of fluorescence. For this purpose, it is far superior to glass filters or any filters containing organic compounds because of the total lack of fluorescence. We use it for filtering away the blue excitation light when we study the red chlorophyll fluorescence from plants.

Containers (cuvettes) for solutions of copper sulfate or potassium dichromate can be made by gluing together pieces of ordinary clear Plexiglas. Be sure that the glue has dried thoroughly and throughout before you pour your solution into the cuvettes, or you will lose more time than you are

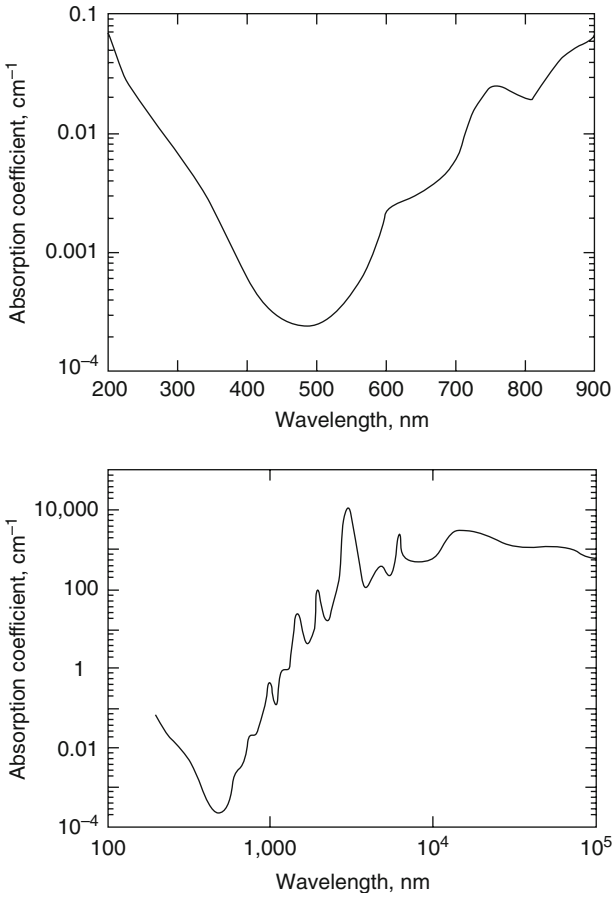

Fig. 3.2 The absorption spectrum of pure water plotted in two different ways (Data from Hale and Querry (1973), replotted)

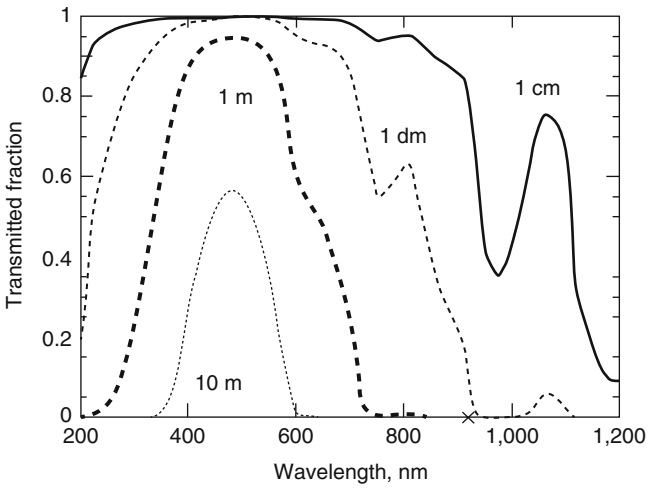

Fig. 3.3 The fraction of light of various wavelengths absorbed by (pure) water layers of the thicknesses indicated. Ten-meter filters are not very practical in the laboratory, but 10 and even 100 m of water are natural light filters for many organisms. The transmission in natural waters differs from that in chemically pure water and will be dealt with in Chap. 7 (Calculated from data of Hale and Querry (1973))

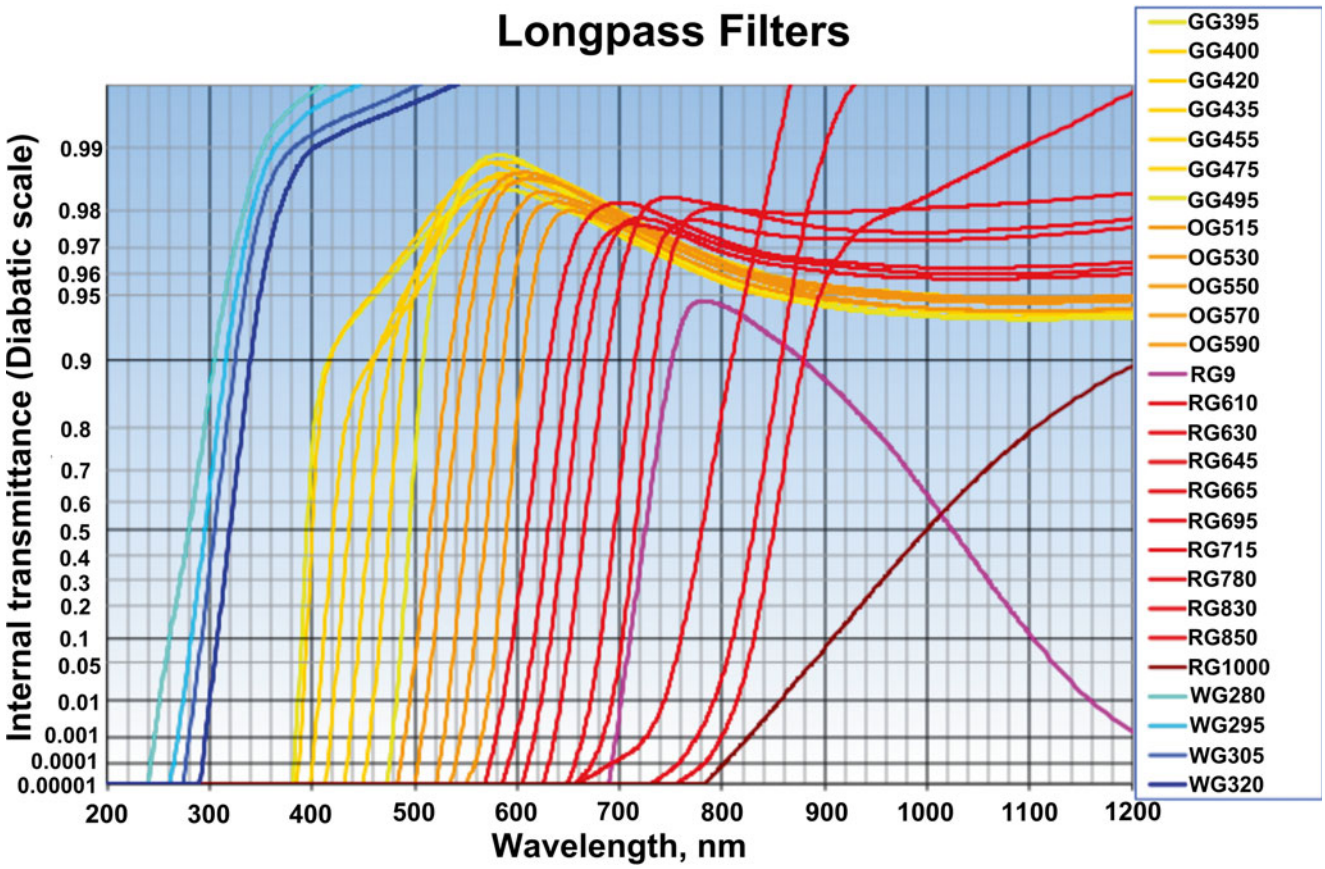

Fig. 3.4 Cutoff filters made of glass, manufactured by Schott & Gen., Mainz. Note that the vertical transmission scale is not linear. The filters absorb short-wavelength and transmit long-wavelength light. The diagram, drawn for 1-mm (WG 230 to GG 395)- or 3-mm (GG 400 to RG 1,000)-thick filters, does not take reflection (roughly 0.08 or 8 %) into account. The "diabatic" transformation of the vertical scale emphasizes the low- and high-transmittance portions. Mathematically, it means that scale is linear with the expression {1–log[log(1/transmittance)]}

trying to save. It is best to test for leaks using distilled water before you put your solutions in. Distilled water can be removed again from the leaks, but crystals cannot!

Cobalt chloride and nickel sulfate (nasty, carcinogenic, toxic, and in the case of nickel allergenic) dissolved in water or aqueous ethanol make very good broadband filters for the UV-B region, but because the substances are so dangerous, I do not recommend them unless you really know what you are doing and are sure that your cuvettes will not leak. Detailed descriptions of solution filters, especially for isolating lines of the mercury spectrum, can be found in Calvert and Pitts (1966), Rabek (1982), and Gahr et al. (1995).

Colored glass filters are made by several companies. My personal experience is mainly with filters manufactured by Schott & Gen. (Mainz, Germany) and Corning (USA). A large assortment of such filters is available (Fig. 3.4), so a catalog should be consulted before ordering. Of the filters from Schott, I have most often found BG12 and BG18 useful for isolating broadband blue light, and a series of cutoff filters, which cut off the short end of the spectrum (cutoff wavelengths from 250 to 780 nm) but transmit light of longer wavelength. For a particular kind of glass, the cutoff point can be varied by having filters of different thickness or using several filters in tandem.

All the filters absorbing the unwanted light convert the absorbed energy to heat. If the light to be filtered is strong, the filters may become overheated and be destroyed. Organic substances may be decomposed, plastic may melt or burn, solutions may boil, and glass may crack. The risk for these unwanted effects is considerably less in the case of interference filters.

3.3.2 Interference Filters

An interference filter removes the unwanted radiation from a beam not by absorption, but by reflection. It does not contain any colored substances but instead a number of partially reflecting and partially transmitting interfaces. Some interference filters contain very thin metal films; others are made from alternating layers of transparent compounds of high and low refractive indices. The complete theory for interference filters is complicated. However, its essence is that when the spacing between the layers is a quarter of a wavelength, destructive interference will occur in the

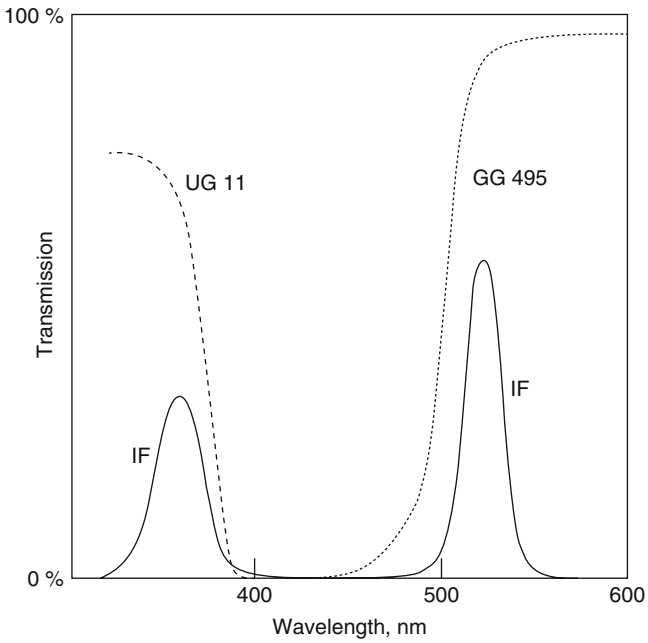

Fig. 3.5 The transmission spectrum for an interference filter (*IF*) with two transmission peaks. The ratio between the two peak wavelengths in this case is 3:2. Either one of the transmission bands can be selected by combining the interference filter with suitable glass filters: UG 11 for the short-wavelength band or GG 495 for the long-wavelength band

reflected beam, so no light is reflected for this particular wavelength. Instead, light of this wavelength is transmitted. Light with twice or three times (or any integer times) the basal wavelength will also be transmitted, since there will be layer distances corresponding to a quarter of these wavelengths. The reader is referred to Sect. 9.10, which deals with a very similar topic.

Interference filters of the type just described will thus allow several narrow spectral bands to pass through, with wavelengths 4, 8, 12, … times the distance between interfaces. By combining interference and glass filters, one of the bands can be selected (Fig. 3.5). When using such combination filters, it is essential (at least if strong light is to be filtered) that the interference part of the filter faces the incident light. If the absorbing glass part is hit by the unfiltered light, the filter might become overheated.

For the filter to function properly, the light to be filtered must be nearly perpendicular to the filter, or the transmitted band will be broadened and shifted to longer wavelength. Thus, only collimated (parallel) light, not diffuse light or light from an extended light source (e.g., a fluorescent tube), can be efficiently filtered by an interference filter.

Even if interference filters do not heat up as easily as absorbing filters, care should be taken so that their temperature does not rise by conduction from other parts of your apparatus. They should also be protected from moisture. When not in use, they should be kept in a desiccator with dry silica gel.

The half-band width of a spectral band is defined as the difference in wavelength (or frequency) between the two points in the spectrum where the band is half the maximum height. Photobiologists often use interference filters with half-band widths of about 15 nm. This gives a reasonable compromise between spectral purity and amount of light transmitted. For some purposes, filters with half-band widths up to 50 nm are useful. There are also interference filters with half-band widths as small as a fraction of a nanometer. They are used, e.g., by astronomers for photographing the sun using light emitted by a single kind of atom.

Continuous interference filters (also called spectral wedges) transmit light of different wavelengths at different points on the filter. They are usually oblong, with different wavelengths along their length. Also, circular spectral wedges have been manufactured.

There are interference filters other than the narrow band type. One useful type is Calflex (see http://www.linos.com/pages/no_cache/home/shop-optik/planoptik/filter/?sid = 12664&cHash = c8035311a6). One version of it transmits almost the full visible range and reflects ultraviolet and infrared (including far-red).

3.3.3 Monochromators

For high spectral purity of light, yet flexibility in the choice of wavelength, a monochromator is the device of choice. A very simple monochromator can be made from a continuous interference filter between two slits (Fig. 3.6). Light of different wavelength is obtained simply by sliding the interference filter. However, this arrangement is not suitable when a small half-band width (high-purity light) is required.

In earlier times, most monochromators contained a prism as the dispersing element (i.e., the component deflecting the light differently depending on wavelength). Gratings were too difficult to make and hence expensive. New methods, however, allow the mass production of high-quality gratings, and nowadays, practically all monochromators for the near infrared, visible, and ultraviolet regions use a reflection grating as the dispersing element.

The basic theory for a grating is best understood as an extension of Young's double-slit experiment. Using a computer, we can investigate the effect of increasing the number of slits more and more. An essential part of a program for this consists of the three equations relating wavelength (λ), deflection angle (θ), and relative fluence rate (I) to the width (b), number (n), and distance (a) of the slits:

$$\alpha = (a \cdot \pi / \lambda) \cdot \sin\theta$$
$$\beta = (b \cdot \pi / \lambda) \cdot \sin\theta$$
$$I = 4\left[\sin\beta \cdot \sin(n \cdot \alpha) / (\alpha \cdot \beta)\right]$$

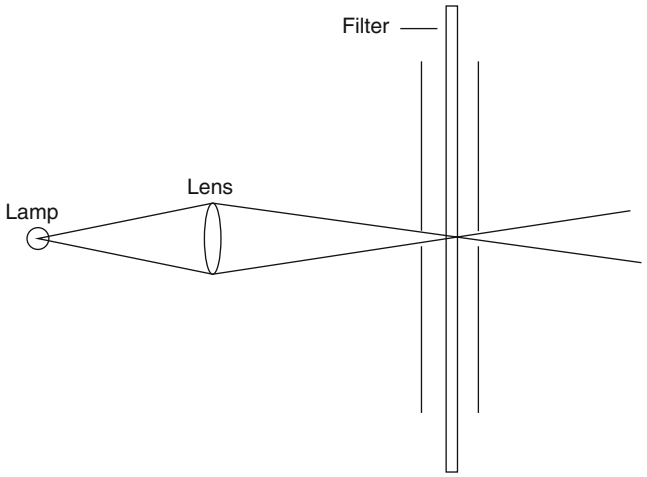

Fig. 3.6 Simple monochromator consisting of an interference filter between two slits. It is here combined with a simple illuminator consisting of a lamp and a lens, providing light which is almost perpendicular to the filter, which is essential for proper function

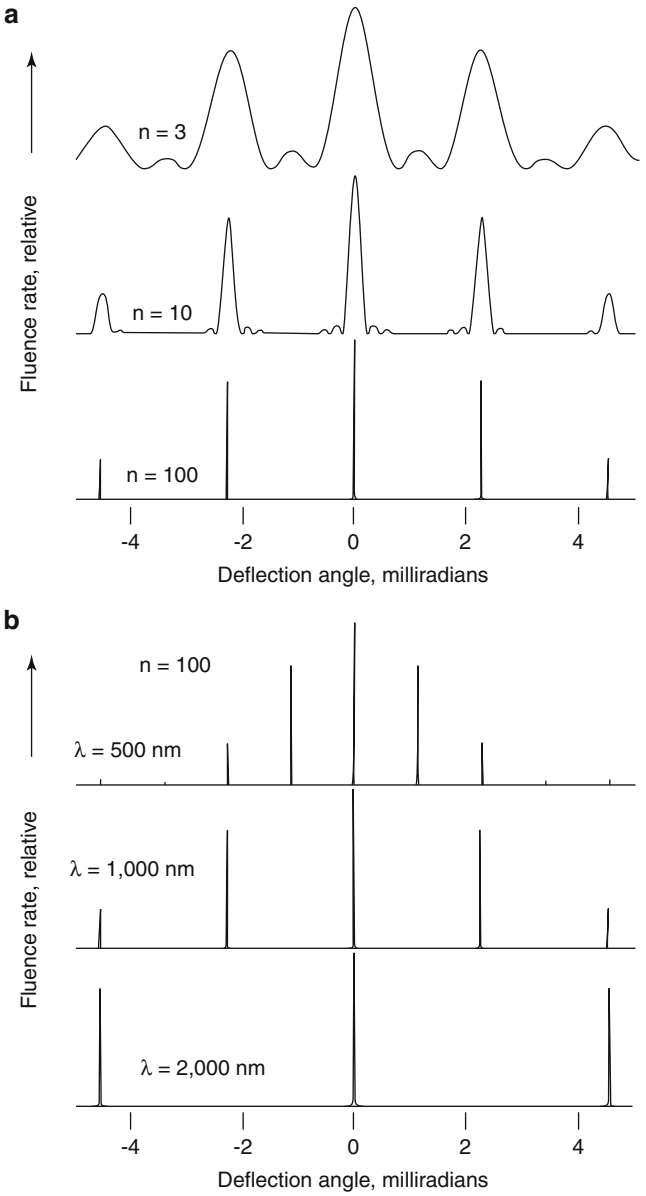

Fig. 3.7 (**a**) Computed diffraction patterns from n slits ($n = 1$, 10, or 100). With increasing slit number, the peaks become sharper. The slit width is 0.3 mm, the slit distance 1 mm, and the wavelength 1,000 nm. (**b**) As in (**a**), but with slit number kept constant and the wavelength varied. With increasing wavelength, the deflection angle increases

The highest central peak (nondeflected light) in Fig. 3.7a is called the first-order light. With mixed input light, this includes all wavelengths. The two peaks on each side of it is the first-order light and so on.

Comparing the last three printouts (Fig. 3.7b), we see that the deflection angles increase with wavelength. We can see that the second-order light with wavelength 500 nm is deflected to the same angle as the first-order light with wavelength 1,000 nm. Likewise, fourth-order light of 500 nm wavelength, second-order light of 1,000 nm wavelength, and first-order light of 2,000 nm wavelength are all deflected to the same angle. As will be explained later, this has important consequences for photobiological experimentation.

Transmission gratings in the form of multiple slits are seldom used, except as here for teaching the theory of gratings. Instead, mirrors with grooves, called reflection gratings, are made in many variants, usually as replicas, i.e., copies molded in plastic from very expensive originals. The principle of operation is essentially the same, except that the light exits on the same side of the grating where it enters.

Modern reflection gratings have the added refinement of blaze. This means that the grooves are not symmetrical but shaped in such a way that the direction of specular reflection coincides with the diffraction direction for a certain wavelength—the blaze wavelength. That makes a grating particularly efficient for this wavelength. If you have a choice, you should select a grating with a blaze wavelength near the wavelength you are particularly interested in or for which it is difficult to get sufficiently strong light. For a lamp–monochromator combination like the one shown in Fig. 3.8, it is usually preferred to have a low blaze wavelength to compensate for the lower lamp output in the UV and blue regions. On the other hand, in equipment for the analysis of light (monochromator–photomultiplier combinations in spectroradiometers or the emission units of spectrofluorometers), it may be advantageous to use a high blaze wavelength to compensate for the lower sensitivity of the photocell for long-wavelength light.

A grating monochromator, in addition to the grating, consists of an entrance slit, an exit slit, and optics, which forms an image of the entrance slit at the exit slit via reflection in the grating. In Fig. 3.8, we see a schematic diagram of one type of monochromator suitable for photobiological use. In this case, a plane grating is combined with a concave

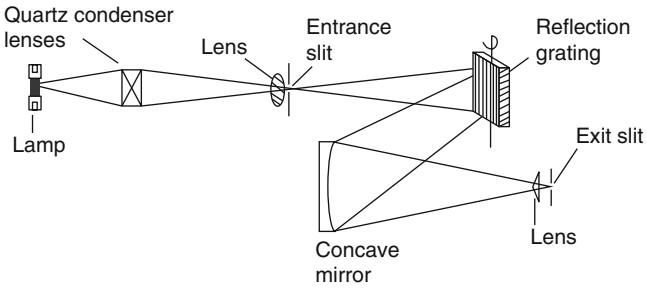

Fig. 3.8 Schematic diagram for a monochromator used for photobiology experiments

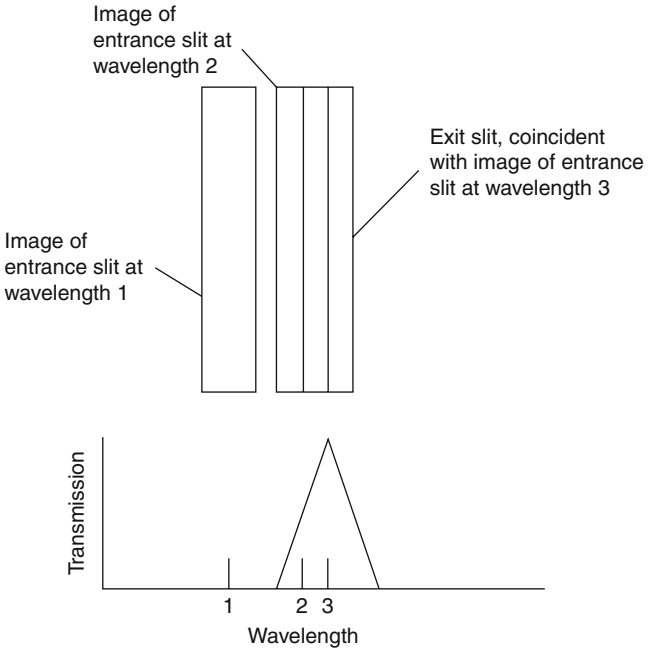

Fig. 3.9 Images of the entrance slit for different wavelengths in relation to the exit slit (*above*), and the ideal transmission function, neglecting diffraction in entrance and exit slits. If the slit is narrow, with a width approaching the wavelength, diffraction will take place (see Fig. 3.4)

mirror. Another solution is to use a concave grating, which focuses the light without any concave mirror. The wavelength of light leaving the exit slit is changed by rotating the grating. The monochromator is shown in combination with an illumination unit consisting of a lamp and a lens.

When using a grating monochromator, one should be aware of the fact that despite the name, with a certain setting, it transmits light of more than one wavelength:

First, we have the problem of light of various orders (first, second, etc.) mentioned above. The wavelength scale on the monochromator is valid for only a certain order, usually the first. When the dial is set at 300 nm, second-order light of 150 nm wavelength may also be transmitted.

Second, the spectral composition of the light within one spectral transmission band depends on the size of the slits. A compromise has to be made in choosing the slits: The wider they are, the more light is transmitted (Fig. 3.9), but the narrower they are, the higher the spectral purity (which is, in many cases, important). The best compromises are found when the image of the entrance slit (in monochromatic light) just covers the exit slit. In this case, the spectral transmission band shape would be triangular were it not for diffraction at the slits and imperfections in the construction. In reality, the spectral band transmitted will be of a somewhat rounded triangular shape (see Chap. 4).

An interesting new development is the construction of acousto-optic tunable interference filters (see Tran 1997 for a review). Such a filter is in a way intermediate between an interference filter and a grating. The basic principle is that a sound wave in a crystal creates regions of alternating low and high refractive index, which causes diffraction of a light beam. In this way, the unit functions as a grating. But unlike a grating, it need not be rotated for changing the wavelength of light exiting in a certain direction. This can be done by changing the frequency of the sound wave, which is generated piezoelectrically. This makes possible very rapid scanning over a spectral range by changing the frequency of the driving voltage.

References

Björn LO (1971) Simple methods for the calibration of light measuring equipment. Physiol Plantarum 25:300–307

Calvert JG, Pitts JN Jr (1966) Photochemistry. Wiley, New York

Gahr A, Weil L, Niessner R (1995) Polychromatic actinometry with filter solutions. Water Res 29:2125–2137

Hale GM, Querry MR (1973) Optical constants of water in the 200 nm to 200 µm wavelength region. Appl Opt 12:555–563

Rabek JF (1982) Experimental methods in photochemistry and photophysics, part 2. Wiley, Chichester

Stanley CM (2003) Filters and mirrors for applications in fluorescence microscopy. Methods Enzymol 360:394–415

Taniyasu Y, Kasu M, Makimoto T (2006) An aluminium nitride light-emitting diode with a wavelength of 210 nm. Nature 441:325–328

Tran CD (1997) Principles and analytical applications of acousto-optic tunable filters, an overview. Talanta 45:237–248

Yuan ZL, Kardynal BE, Stevenson RM, Shields AJ, Lobo CJ, Cooper K, Beattie NS, Ritchie DA, Pepper M (2002) Electrically driven single-photon source. Science 295:102–105

The Measurement of Light

4

Lars Olof Björn

4.1 Introduction

There are three principal types of light-sensitive devices in common use, based upon three different effects of light on matter: photothermal, photoelectric, and photochemical devices. We shall describe these and their uses and then go on to describe a more complex device, the spectroradiometer.

4.2 Photothermal Devices

Photothermal devices have slow response and low sensitivity. Their great advantage is that, unlike photoelectric and photochemical devices, they have the same response per energy unit throughout a very wide spectral range. Their principle of operation is that the light to be measured is allowed to be absorbed by a target. The temperature of the target is raised by the absorbed energy, and the temperature rise is taken as a measure of the amount of energy absorbed.

4.2.1 The Bolometer

In a bolometer, the target is a temperature-dependent resistor. The resistivity of all materials is temperature dependent. In the first bolometers, thin platinum foils, blackened with colloidal platinum for efficient absorption of light, were used. The resistivity of platinum rises with temperature. The platinum foils were freely suspended in the air, and these bolometers were very sensitive to air currents.

In the bolometers commonly used in photobiology laboratories today, the targets are thermistors, that is, semiconductor resistors with a large negative temperature coefficient. They are protected by a window made from sapphire, lithium fluoride, or other materials with a wide spectral transmittance range. The light target is part of a Wheatstone bridge, so that small changes in resistance can be recorded.

The setup is schematically depicted in Fig. 4.1. Of the four resistor arms of the bridge, one is variable, so that the bridge can be balanced (same potential at the top as at the bottom and no current flowing through the meter) with

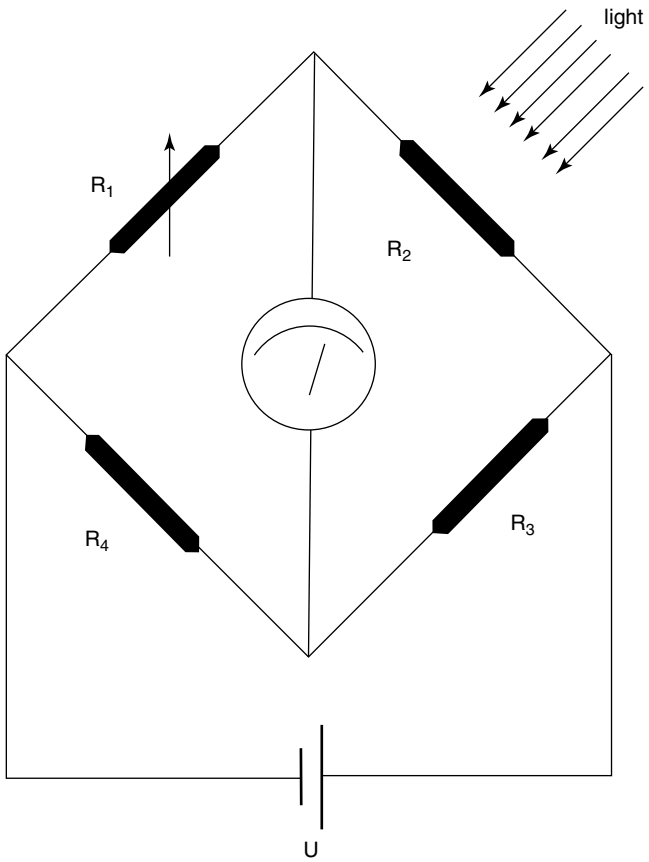

Fig. 4.1 Schematic diagram of a bolometer. It is connected to a voltage source with voltage U

L.O. Björn
School of Life Science, South China Normal University, Guangzhou, China

Department of Biology, Lund University, Lund, Sweden
e-mail: Lars_Olof.Bjorn@biol.lu.se

L.O. Björn (ed.), *Photobiology: The Science of Light and Life*,
DOI 10.1007/978-1-4939-1468-5_4, © Springer Science+Business Media New York 2015

the target resistor shielded from light. In general, the potential difference between the top (R_1/R_2 junction) and bottom (R_3/R_4 junction) will be $U[R_2/(R_1+R_2)-R3/(R_3+R_4)]$, so that when the bridge is balanced $R_2/(R_1+R_2)=R_3/(R_3+R_4)$. We now remove the light shield and allow the light to be measured to fall on R_2. This resistor now heats up and changes its resistance by the amount ΔR_2. The concomitant change in potential between "up" and "down" will be $U\cdot\Delta R_2/(R_1+R_2)$, and change in current flowing through the meter will be proportional to the resistance change of the target.

Disregarding heating by the current flowing through it, the energy taken up by the target consists of the light to be measured plus heat radiation from the surroundings, assumed to be at absolute temperature T_a. The heat radiation received is proportional to T_a^4 (Stefan–Boltzmann's law). The radiation energy given off by the target (at absolute temperature T_t) is proportional to T_t^4. When equilibrium has been reached, we thus have the relationship for the irradiance of the light to be measured (k_1 and k_2 are constants):

$$\text{Irradiance} = k_1\cdot T_a^4 = k_1\cdot T_t^4$$

or

$$\text{Irradiance} = k_1\cdot\left(T_t^4-T_a^4\right)=k_1\cdot\left(T_t^2+T_a^2\right)\cdot\left(T_t+T_a\right)\cdot\left(T_t-T_a\right)\approx k_2\cdot\left(T_t-T_a\right)$$
$$=k_2\cdot\Delta T.$$

Thus, the irradiance is proportional to the temperature change of the target resistor and thus, as shown previously, proportional to the current flowing through the meter.

Irradiances down to about 1 W/m^2 can be measured with a standard bolometer. At lower irradiances, the drift problems become serious. When a low irradiance is to be measured, it is best to connect the bolometer to a strip-chart recorder or computer to keep track of the drift of the baseline. A suitable procedure is to expose the bolometer to the light for 30 s, then shield it for the same period for recording of the baseline, then expose it again, etc. Prolonged exposure decreases the reading, because the balancing resistors (not directly exposed to the light) heat up by heat conduction.

The calibration of a bolometer can be easily checked as described by Björn (1971). For highest accuracy, a special standard lamp should be used in the way specified in the directions supplied with it. For information regarding standard lamps, see the section on spectroradiometers.

4.2.2 The Thermopile

A thermocouple is a couple of junctions between two metals. Wherever two metals are in contact, a temperature-dependent potential difference exists. A thermopile consists of several thermocouples (each one with two junctions) connected in series, as shown in Fig. 4.2. Of each couple of junctions, one is shielded from and the other one exposed to the light to be measured. The sensitivity and speed of response are increased by attaching small light-absorbing (and heat-radiating) shields to the junctions, and these shields should be blackened for efficient absorption (and reradiation).

For optimal results, the input resistance of the current measuring meter should be matched to the resistance of the thermopile, which is of the order of 10–100 ohm. A thermopile is usable down to about the same irradiance as a bolometer. As for the bolometer, the output current is proportional to the irradiance.

4.2.3 Thermopneumatic Devices

The principle of pneumatic thermal radiation detectors is that the radiation heats a gas. The resulting expansion can be detected by the movement of an enclosing membrane. In one of the early devices, the Golay detector, the movement was detected optically. Sensors based on this principle, used principally for infrared radiation, are still being refined, and very small movements of the membrane can be detected interferometrically. Pneumatic detectors are often used in connection with chopped or pulsating light. In this case, the periodic expansion of the gas can be detected by a microphone. Many biologists have come in contact with this principle when measuring carbon dioxide, for instance, in the measurement of photosynthesis and respiration. An infrared gas analyzer (IRGA; Fig. 4.3) for such measurements often works in a differential mode.

External air passes through an optical cell ("reference cell"), then through the cell with the biological sample ("sample cell"), and finally through a second optical cell. A beam of infrared radiation passes alternatingly through one or the other of the cells. From there the radiation continues into an analyzing cell, partitioned by a flexible membrane. This cell contains the same kind of gas as the one being measured. Depending on how much radiation there remains after absorption in the reference cell and the sample cell, the gas in the two halves of the analyzing cell is heated more or less and temporarily expands in a corresponding way. Usually

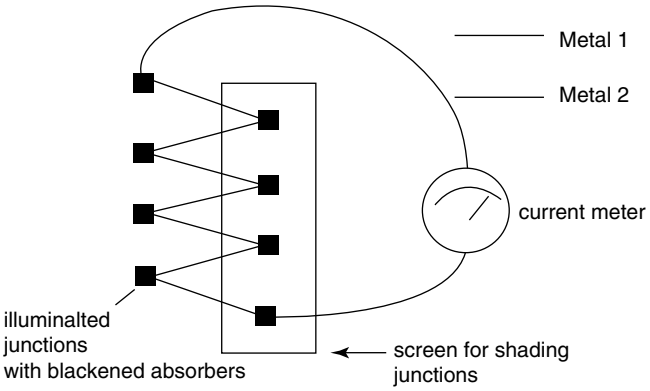

Fig. 4.2 Schematic diagram of thermopile with current meter

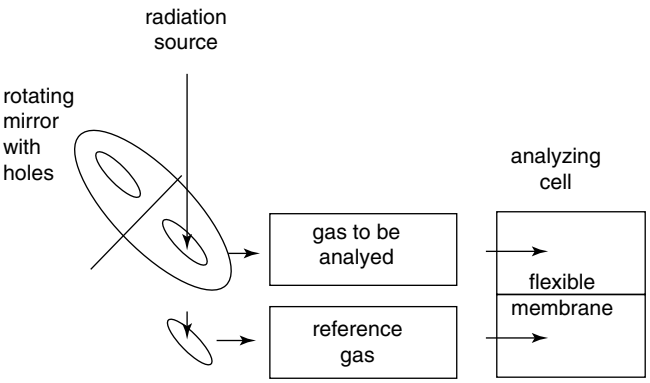

Fig. 4.3 Principle for an infrared gas analyzer (IRGA), very schematic. Infrared radiation passes alternatingly through a cell with reference gas, for instance, ambient air, and alternatingly through a cell with gas to be analyzed, for instance, air that has passed a compartment with plants taking up carbon dioxide. Depending on how much radiation remains to be absorbed in the two halves of the analyzing cell, the flexible membrane separating the two halves is deflected to a greater or lesser extent

the heating and expansion is different in the two halves, which causes the membrane to vibrate in relation to how the radiation is deflected through the reference cell and the sample cell. By making the membrane form one plate in an electrical capacitor, this vibration can give rise to an electrical signal proportional to the difference in gas concentration in the sample cell and the reference cell.

Evans (2005) has suggested that some beetles use the thermopneumatic principle for detecting infrared radiation.

4.3 Photoelectric Devices

A great number of photoelectric devices exist. They can be divided into two main categories, depending on whether they exploit an outer photoeffect (at a metal surface in vacuum or gas) or an inner photoeffect inside a solid semiconductor.

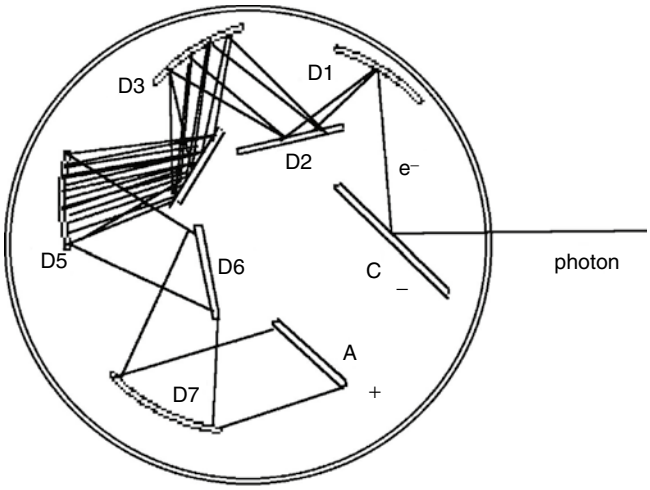

Fig. 4.4 Diagram of (side-on) photomultiplier

4.3.1 A Device Based on the Outer Photoelectric Effect: The Photomultiplier

Although many kinds of photocells (as well as television camera tubes, image intensifiers, etc.) utilize the outer photoeffect, we shall limit ourselves here to a description of the photomultiplier, a device extensively used by photobiologists. Figure 4.4 shows the basic principle. Inside an evacuated envelope of glass or quartz, there are a number of metal plates. The one marked C is the photocathode. It is held at a large negative potential relative to ground (wires connected to electrical circuitry not shown). The surface of the photocathode exposed to the light to be measured is covered with a layer of special metals. Usually a mixture of several metals, some of which are alkali metals, is used. Depending on the particular metal alloy, photomultipliers have different spectral responses.

When a photon hits the photocathode, an electron is released from the metal (as is known from chemistry, alkali metals are especially prone to losing electrons; they have a low *work function*). Because the photocathode is at a low electric potential, the electron does not return to the surface. Instead, it is accelerated toward another metal plate nearby, which is held at a higher potential, dynode 1 (D1). In flight the electron acquires such a velocity that when it hits the dynode, it releases two or three electrons from it. They travel on to dynode 2 (at an even higher potential) where further electrons are released. Photomultipliers are constructed with up to 12 dynodes in series, and at each dynode, more electrons are added. Finally, the electron swarm is collected at the final plate, the anode (A in Fig. 4.4). This is usually maintained close to ground potential. The electrons flowing to the anode represent an electrical current, which also flows

through the wire connected to the anode (not shown), and this can be recorded and used as a measure of the light incident on the photocathode.

Contrary to the thermoelectric devices described in the previous section, photomultipliers have different sensitivities to different kinds of light. Furthermore, they are rather unstable. Their great advantage lies in the high light sensitivity: even individual photons can be recorded by some photomultipliers under suitable conditions. Provided the electronic circuitry to which they are connected has a low time constant, photomultipliers also have a short response time (although different photomultipliers differ in this respect).

The diagram shows a so-called side-on photomultiplier. There are also other designs. A common one is the end-on photomultiplier, where the photocathode consists of a thin, semitransparent metal film on the inside of the flat end of the cylindrical envelope. In this type, the spectral response is also dependent on the thickness of the film, which usually varies somewhat over the surface. Photomultipliers require an operating voltage of 500–5,000 V; in many cases about 1,000 V is used. The different electrodes are given their proper voltages by a chain of resistors between the negative high voltage lead and ground. The output current is very strongly dependent on the operating voltage, which must therefore be held very constant (with N dynodes and operating voltage U, the output current is roughly proportional to U^N).

The output is not always measured as a current. As the incident irradiance is lowered, the discontinuous nature (quantization) of light becomes more and more apparent. At very low light levels, it becomes advantageous to record individual photons by counting the pulses of current flowing to the anode. The measurement of very weak light is further dealt with in Sect. 4.7.

Photomultipliers are made with different cathode layers for different spectral ranges from the ultraviolet to the near infrared (to about 900 nm). Photomultipliers sensitive to light of long wavelength generally have a higher dark current (dark noise) than others. The noise level can be decreased (to achieve a better signal-to-noise [S/N] ratio) by lowering the temperature. Liquid nitrogen, dry ice, or Peltier coolers are generally used for this. Cooling must be combined with precautions to avoid dew on the optical components.

4.3.2 Devices Based on Semiconductors (Inner Photoelectric Effect)

In the inner photoelectric effect, absorption of a photon inside a solid semiconductor results in the separation of a positive charge from a negative one.

Photoconductive cells with a semiconductor as the light-sensitive element have been used extensively in the past. Among these lead sulfide cells for measurements in the near infrared, for which no photomultipliers or other suitable photocells were available, and cadmium sulfide cells for photographic exposure meters can be mentioned. Photoconductive cells are variable resistors and require an external source of voltage for creation of a current that can be measured. They have a slow response and are not used much for scientific measurements.

Photodiodes and phototransistors, on the other hand, can be made to have a very rapid response. For very long wavelengths (>1,000 nm), they also compete with photomultipliers in terms of sensitivity. The so-called avalanche photodiode can be regarded as a semiconductor equivalent to the photomultiplier. Photodiodes are often preferred in applications where photomultipliers could also be used, because photodiodes are small, cheap, and rugged and do not require high voltages. In combination with special electronics, it is nowadays possible to detect single photons of 1,550 nm wavelength using an avalanche photodiode (Namekata et al. 2006), and this is possible also with special, cooled photomultipliers (Skovsen et al. 2006). Photodiode arrays have become popular for recording a whole spectrum at one time (each diode in the array measures one spectral band).

Two main types of barrier layer cells are in current use: the selenium cell and the silicon cell. They are similar in principle but differ in their spectral response: the selenium cell is most sensitive to green and blue light, and the silicon cell, to red and far-red light. The general principle is shown in Fig. 4.5.

Because selenium barrier layer cells have a spectral sensitivity somewhat resembling that of the human eye, they are used in photometers (lux meters) for measurement of visible light at, for example, working places. By combination with suitable filters, the spectral sensitivity curve can be made to almost completely match the curve for scotopic vision (which defines illuminance). In earlier days, such cells were also used for photographic exposure meters, where they have now been replaced by cadmium sulfide photoconductive cells and, more recently, by photodiodes.

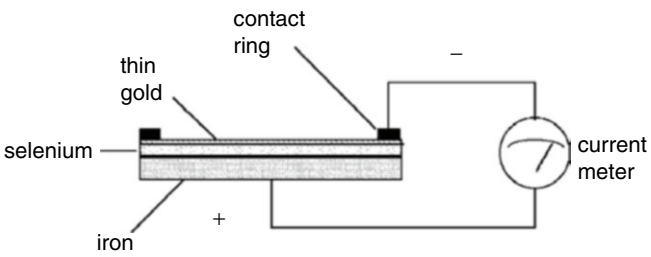

Fig. 4.5 Selenium barrier layer cell with required circuitry. Note that the device generates its own operating voltage and does not require any battery or other external voltage source

4.4 Photochemical Devices: Actinometers and Dosimeters

Chemical systems for measurement of light and ultraviolet radiation are called actinometers. (The best known photochemical device for recording light is photographic film. This has also been used for quantitative measurements, but it will not be further discussed here. Other chemical systems are usually better suited for quantitative measurements of radiation.)

Actinometers have the advantage of not having a need for calibration by the user and thus do not require the purchase of an expensive standard lamp with an expensive power supply. Standardization has usually been taken care of by those who have designed the actinometer. Another advantage is that the geometry can more easily be adjusted to the measurement problem. The shape of a liquid actinometer can easily be made to correspond to the overall shape of the irradiated object under study. In many cases, it is of interest to study a suspension or solution that can be put in an ordinary cuvette for spectrophotometry or fluorimetry, and the actinometer solution can be put into a similar cuvette.

A large number of actinometers have been devised. Kuhn et al. (1989) list and briefly describe and give references to 67 different systems involving gaseous, liquid, and solid phases. Of these they recommend five. In general, actinometers are sensitive to short-wave radiation and insensitive to long-wave radiation. Insensitivity to long-wave radiation can be both a drawback and an advantage, but by choosing the best actinometer for the purpose, one can avoid the disadvantages. One advantage of using an actinometer insensitive to long-wave radiation is that one can work under illumination visible to the human eye, without disturbing the measurement. We shall give an introduction below to a few different actinometers, not all of which are mentioned by Kuhn et al. (1989), and then go on to describe more in detail the most popular one for ultraviolet radiation—the potassium ferrioxalate or potassium iron(III) oxalate actinometer:

1. The potassium iodide actinometer (Rahn 1997) is sensitive primarily to UV-C radiation (wavelength <280 nm) and with slight sensitivity also for short-wave UV-A. It is suitable for determining the 253.7 nm radiation from low-pressure mercury lamps (bactericidal lamps), since the contribution from other spectral lines of the lamp will be negligible (but the ferrioxalate actinometer works almost as well for this purpose). It can be handled in ordinary incandescent light (not light from unshielded quartz–iodine lamps). The reaction on which this actinometer is based is the oxidation of iodide ion by iodate ion to form iodine, or rather triiodide ion (I_3^-).
2. An actinometer sensitive to visible light (photosynthetically active radiation) has been described by Wegner and Adamson (1966). It works up to above 700 nm and is based on potassium tetrathiocyanatodiamminechromate (III), $K[Cr(NH_3)^2(SCN)_4]$. The latter can rather easily be prepared from the commercially available Reinecke's salt, that is, $NH_4[Cr(NH_3)_2(SCN)_4]$. Irradiation causes the uptake of water and release of thiocyanate, which can be measured spectrophotometrically after addition of an Fe(III) salt.
3. Two more actinometers that have recently been used in biological contexts are the 2-nitrobenzaldehyde actinometer (Allen et al. 2000) and the oxalic acid/uranyl sulfate actinometer (Mirón et al. 2000). A different version of the latter one preferable for small radiation doses is among those recommended by Kuhn et al. (1989).
4. As already mentioned, the most popular actinometer for ultraviolet radiation (and for violet and blue radiation as well) is the ferrioxalate actinometer. The description below will be sufficient for the experimenter starting in the field. For more detailed information, one should consult Parker (1953), Hatchard and Parker (1956), Lee and Seliger (1964), and Goldstein and Rabani (2007). Complete recipes have also been published by, for example, Seliger and McElroy (1965) and Jagger (1967).

In the ferrioxalate actinometer, the following photochemical reaction is exploited:

$$\tfrac{1}{2}\left(COO^-\right)_2 + Fe^{3+} + \text{photon} \rightarrow CO_2 + Fe^{2+}$$

or

$$\text{Oxalate ion} + \text{Fe(III) ion} + \text{light} \rightarrow \text{carbon dioxide} + \text{Fe(II) ion}.$$

The quantum yield for this reaction (i.e., the number of iron ions reduced per photon absorbed) is slightly wavelength dependent but close to 1 in the spectral region, 250–500 nm, where the ferrioxalate actinometer is used. Usually a 1-cm layer of 0.006 M ferrioxalate solution is used. Quantum yield and the fraction of the radiation (perpendicular to the 1 cm layer) absorbed are shown in Table 4.1.

The quantum yields for 0.15 M actinometer solution are 0.952 of the above values. Irradiation of the side walls of the

Table 4.1 Quantum yield and the fraction of radiation (perpendicular to 1-cm layer) absorbed

Wavelength	Quantum yield	Fraction absorbed	Quantum yield × fraction absorbed
253.7	1.26	1	1.260
300.0	1.26	1	1.260
313.3	1.26	1	1.260
334.1	1.26	1	1.260
365.6	1.26	1	1.260
404.7	1.16	0.92	1.067
435.0	1.11	0.49	0.544
509.0	0.85	0.02	0.017

cuvette should be avoided, that is, the beam should be smaller than the cross section of the cuvette.

The amount of Fe(II) formed can be measured spectrophotometrically after addition of phenanthroline, which gives a strongly absorbing yellow complex with Fe(II) ions.

The ferrioxalate for the actinometer is prepared by mixing 3 volumes of 1.5 M $(COOK)_2$ with 1 volume of 1.5 M $FeCl_3$ and stirring vigorously. This step and all the following involving ferrioxalate should be carried out under red light (red fluorescent tubes). The precipitated $K_3Fe(C_2O_4)_3 \cdot 3H_2O$ should be dissolved in a minimal amount of hot water, and the solution allowed to cool for crystallization (this crystallization should be repeated twice more).

Following is a recipe for the three solutions required for carrying out actinometry (see Goldstein and Rabani 2007 for a different procedure and other quantum yields):

Solution A: Dissolve 2.947 g of the purified and dried Fe(III) oxalate in 800 ml distilled water, add 100 ml 0.5 M sulfuric acid, and dilute the solution to 1 l. This gives 0.006 M actinometer solution, which is suitable for measurement of ultraviolet radiation. For visible light, which is only partially absorbed, it may be advantageous to use 0.15 M Fe(III) oxalate instead, that is, 73.68 g per liter solution.

Solution B: The phenanthroline solution to be used for developing the color with Fe(II) ions should be 0.1 % w/v 1:10 phenanthroline monohydrate in distilled water.

Solution C: Prepare an acetate buffer by mixing 600 ml of 0.5 M sodium acetate with 360 ml of 0.5 *M* H_2SO_4.

Solution A is irradiated with the light to be measured. The geometries of the container and of the light are important and must be taken into account when evaluating the result. The simplest case is when the light is collimated, the container a flat spectrophotometer cell, the light strikes one face of the cell perpendicularly, and no light is transmitted. Even in this case, one has to distinguish whether the cell or the beam has the greater cross section and correct for reflection in the cell surfaces. The irradiation time should be adjusted so that no more than 20 % of the iron is reduced.

After the irradiation, two volumes of the irradiated solution are mixed with two volumes of solution B and one volume of solution C and then diluted to 10 volumes with distilled water. After 30 min, the absorbance at 510 nm is measured against a blank made up in the same way with unirradiated solution A.

Example of calculation: 4 ml of 0.006 M actinometer solution are irradiated in a flat quartz container by parallel rays of UV-B impinging at right angles to one surface (and not able to enter any other surface). The radiation cross section intercepted by the solution is 2 cm^2. Five minutes of irradiation produces 0.6 µmol Fe(II).

Throughout the UV-B region, the quantum yield is 1.26. Reflection from the surface is estimated to be 7 % (by application of Fresnel's law). None of the radiation penetrates the solution to the rear surface, since the solution thickness is well over 1 cm. Therefore, 0.6 mmol corresponds to $0.6/(1.26 \cdot 0.93)$ µmol = 0.512 µmol radiation incident on 2 cm^2 in 5 min, and the photon irradiance (quantum flux density, in this case equal to the photon fluence rate, since the rays are parallel and at right angles to the surface) is $0.512/(2 \cdot 5)$ µmol/cm^2/min^1 = 5.10 nmol/cm^2/min^1 or $5.12 \cdot 10^4/60$ nmol/m^2/s^1 = 853 nm/m^2/s^1.

The great limitation of the ferrioxalate actinometer is that it is not sensitive to long wavelength light (in many cases this is also an advantage; one reason being that red working light can be used without interference with the measurements). Several actinometers sensitive to longer wavelengths have been designed. Warburg, for instance, used one based on chlorophyll. A modern, red-sensitive actinometer has been described by Adick et al. (1989).

Chemical or biological systems, mostly in the solid state, for recording light, and ultraviolet radiation in particular, are widely employed for estimating exposure of people, leaves in a plant canopy, and other objects which for various reasons are not easily amenable to measurements with electronic devices. These chemical devices are generally referred to as *dosimeters* rather than actinometers, even if there is no defined delimitation between these categories. Construction, calibration, and use of chemical and other dosimeters have been the subject of frequent reviewing (Bérces et al. 1999; Horneck et al. 1996; Marijnissen and Star 1987). Their radiation-sensitive components can be either chemical substances (natural like DNA or provitamin D or artificial) or living cells (e.g., various spores and bacteria). A critical evaluation of two kinds of dosimeters was recently performed by Seckmeyer et al. (2012).

4.5 Fluorescent Wavelength Converters ("Quantum Counters")

As stated earlier, photomultipliers have the advantage of being very sensitive as well as the disadvantage of having wavelength-dependent sensitivity. Fluorescent wavelength converters or "quantum counters" are solids or solutions, usually used in conjunction with photomultipliers, to obtain devices which are sensitive yet have a sensitivity per photon that is independent of wavelength over a certain interval. The idea is to use a solution that has an absorbance high enough that all photons (except those reflected) will be absorbed and that has a high fluorescence yield. Incident light of any wavelength distribution within certain limits is then converted, photon for photon, to light of a fixed wavelength distribution (the fluorescence spectrum of the "quantum counter"), to which the photomultiplier has a fixed sensitivity. One of the major uses of "quantum counters" is calibration of excitation units of spectrofluorometers. The "quantum counter" most widely used consists of a concentrated solution of rhodamine B in ethylene glycol. It is useful for wavelengths up to 600 nm.

4.6 Spectroradiometry

4.6.1 General

A spectroradiometer is an apparatus with which you can measure the spectrum of light, that is, either the spectral irradiance, the spectral fluence rate, or the spectral radiance as a function of wavelength (or frequency, which is equivalent but less commonly used by biologists). It consists of three main parts: (1) input optics, different for spectral irradiance, spectral fluence rate, or spectral radiance; (2) a monochromator or, preferably, a double monochromator; and (3) a transducer for converting the light signal to an electrical signal. The latter may be, in some cases, a photodiode but is usually a photomultiplier. In some spectroradiometers, instead of a monochromator, there is a spectrograph that projects a whole spectrum, and the transducer is a diode array, charge-coupled device (CCD, see Sect. 4.8), complementary metal–oxide–semiconductor (CMOS), or a multichannel plate, which samples the whole spectrum at once. The latter arrangement has the advantage of speed and synchronous sampling of all spectral channels, but is not always suitable. In particular, it is very unsuitable for measuring ultraviolet radiation in daylight, in which case stray light problems must be minimized by use of a double monochromator.

A complete spectroradiometer system also requires some facility for frequent recalibration, as especially photomultipliers have very bad long-term stability.

4.6.2 Input Optics

Before deciding on input optics, we need to decide what quantity we wish to measure. For spectral radiance, we need input optics with which we can sample a very narrow solid angle. This can be some kind of telescope, but for most purposes, it is sufficient to have a tube with a terminal stop that determines the sampling angle and a few internal baffles and an inner matte black surface to avoid reflections inside the tube to reach the monochromator entrance slit Fig. 4.6.

For spectral fluence rate, we need a device that samples all directions with equal sensitivity. This is an ideal that cannot really be fulfilled, but it can be approached. Using input optics for irradiance, it is possible to combine several measurements to obtain the fluence rate (Björn 1995; Björn and Vogelmann 1996).

For spectral irradiance measurements, we need input optics, which has a "cosine response," meaning that the sensitivity, or the efficiency of sampling, for a certain direction should be proportional to the cosine of the angle between that direction and the optical axis. The concept of "cosine response" is graphically explained in Fig. 4.7.

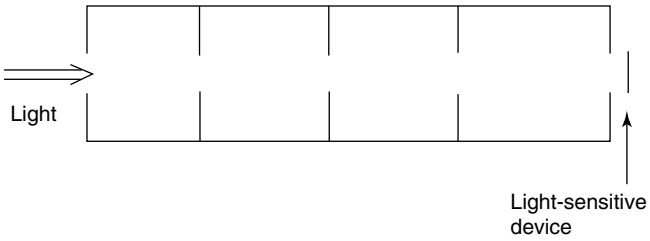

Fig. 4.6 Input optics for radiance (narrow-angle) measurements, consisting of a tube with stops and internal baffles, and inside painted dull black to prevent internal reflections

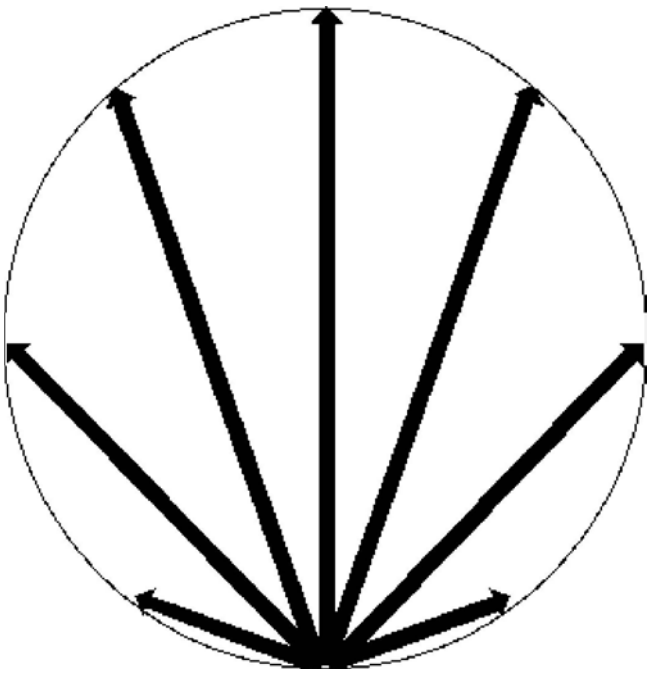

Fig. 4.7 Cosine sensitivity of a receiver. The sensitivity is greatest straight up in this case and decreases proportionally to the cosine of the angle to the vertical. In the horizontal direction, the sensitivity is zero

As a first crude device to reach this situation, one could let the light to be measured strike a strongly scattering but translucent plate above the entrance slit of the monochromator. Suitable materials for this include ground quartz or fused silica or Teflon, depending on the spectral range. A flat plate is, however, not very satisfactory, especially for large deviations from the optical axis. For measuring irradiance of light from an extended light source, for instance, an overcast sky, light at these large angles is very important, since the "amount of sky" corresponding to a certain angular deviation from the optical axis is proportional to the sine of the angle. Somewhat better results are obtained using a hemispherical scattering dome over the slit. The only device that works well is an integrating sphere (Fig. 4.8), and to work well it must be well designed. Details on this subject are provided by Optronic Laboratories (1995, 2001); Schneider and Young 1998).

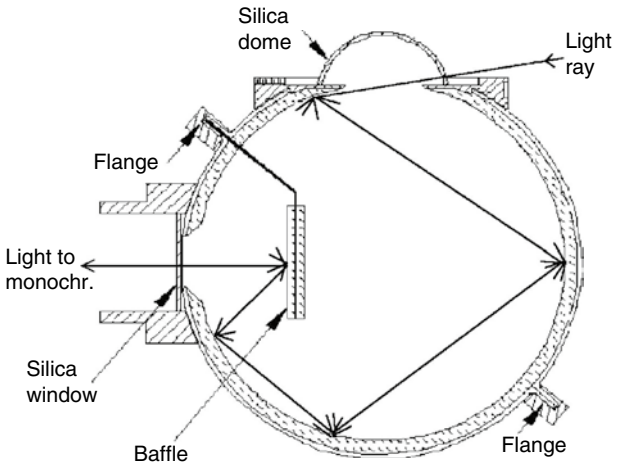

Fig. 4.8 Integrating sphere used as input optics for spectroradiometric irradiance measurements. On top is a silica dome, which can be omitted if the instrument is to be used only indoors or in good weather conditions. *Below* that is the opening in the sphere that defines the area over which the irradiance measurement is taken and the direction of the reference surface. A light ray has been drawn that strikes this at a low angle. It is important that the walls of the sphere taper off to an edge to allow rays at such low angles to enter the sphere. The ray strikes the inner diffusely reflecting wall. From the point where it strikes, light is scattered in all directions. We have followed one possible path through the sphere, but the little "brushes" at each scattering point are meant to indicate that there are many possibilities. Eventually the light strikes the backside of the baffle, which serves as the direct light source for the monochromator (see Fig. 4.9)

In some cases, we are more interested in the shape of a spectrum than in the absolute light level, and then the angular sensitivity function is less important. We may also be interested in measuring light in places where it is not easy to put the spectroradiometer itself (such as underwater or inside the mouth). In that case, the best choice may be to use fiber optics at the input end of the spectroradiometer. Even then one may add, for instance, a small scattering device at the tip of the fiber optic conductor to collect light from different directions. Single light-conducting fibers may even be used to measure light inside plant or animal tissues (Vogelmann and Björn 1984).

4.6.3 Example of a Spectroradiometer

We show here (Fig. 4.9), as an example of a spectroradiometer often used by biologists, the construction of Model 754 from Optronic Laboratories.

Spectroradiometers for measurement of UV-B radiation in daylight do not work well with a single monochromator, mainly because spectral irradiance in the UV-B region changes very rapidly with wavelength. Very small amounts of radiation outside the intended band can therefore ruin the measurement. When two monochromators are used in tandem, it is of course very important that their wavelength settings agree throughout the scan. The only way to achieve this

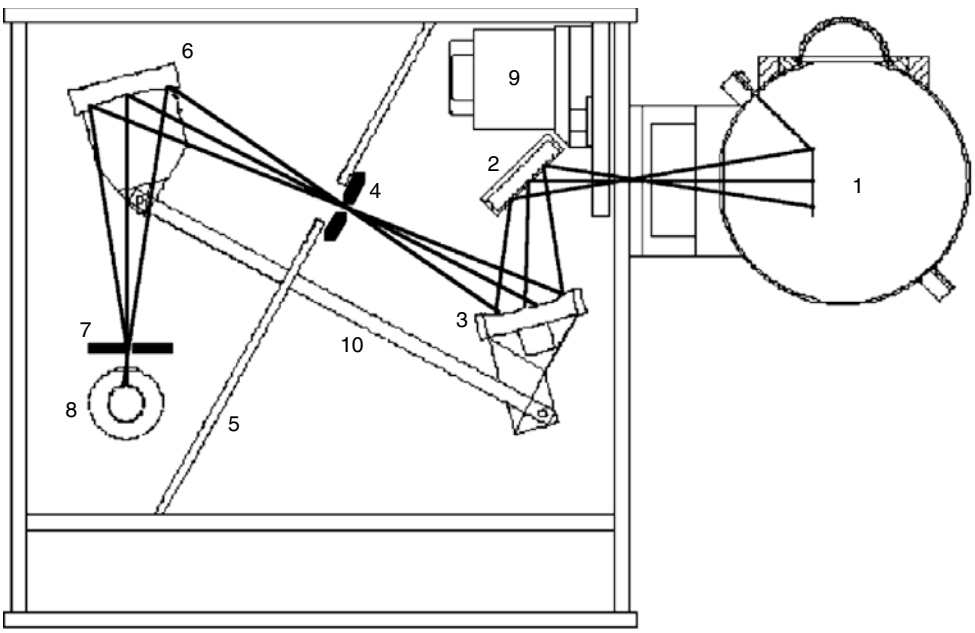

Fig. 4.9 Diagram of spectroradiometer (Optronic Laboratories model 754), simplified to enhance the important optical parts. Light from the integrating sphere (*1*, see Fig. 4.8) enters the light-tight box through a slit (entrance slit for the first monochromator, not specifically shown) and is deflected by the mirror (*2*) to the first grating (*3*). The chosen wavelength band leaves this first monochromator unit through the exit slit (*4*) in the wall (*5*) separating the two monochromators. This slit (4) is also the entrance slit for the second monochromator. The second grating (*6*) again disperses the light and deflects the chosen wavelength band onto a slit (*7*) in front of the photomultiplier (*8*). A stepper motor (*9*) turns the grating to change the wavelength. The rotating grating supports are connected by a bar (*10*), thus assuring that they follow one another with high fidelity

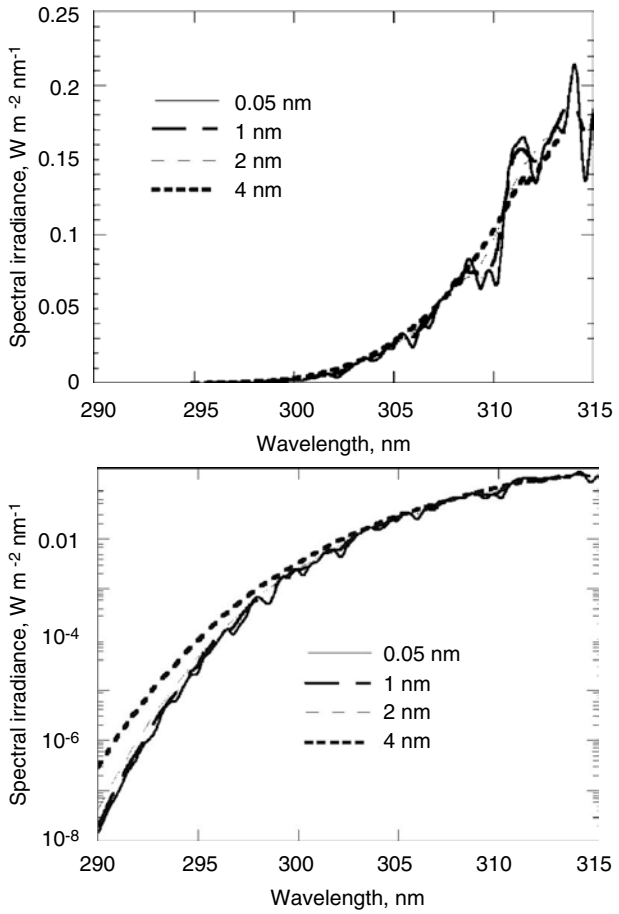

Fig. 4.10 A portion of the ultraviolet daylight spectrum in Lund at noon on June 15, plotted with three different half-bandwidths (modeled values). Left frame with linear, right frame logarithmic spectral irradiance scale. In the *linear plot*, we can see how the fine structure is gradually smoothed out, while the semilogarithmic plot shows more clearly how systematic positive errors develop in the short-wavelength part. With 4 nm bandwidth, the error is more than an order of magnitude for part of the spectrum

is to have both built on a single baseplate and be driven by a single wavelength drive mechanism.

Because biological chromophores have rather broad spectra, the fine structure of the daylight spectrum or the spectrum of any other light is not of great importance. Still, it is important that the bandwidth of the measuring system is not too great, that is, that the slits in the monochromator are not wide when daylight UV-B radiation is to be measured. This is because the spectrum is so steep in this region. Figure 4.10 illustrates this: when the bandwidth is increased above 1 nm, values in the short-wavelength part of the UV-B band start being too high. Errors are also introduced in the calibration (see below) if the bandwidth is too great.

Information about other types of spectroradiometers of interest for biologists is available from the following websites (accessed on August 17th, 2013):

http://www.oceanoptics.com/products/usb2000uvvis.asp
http://www.eoc.csiro.au/instrument/html/terrestrial/asd_fieldspec.htm
http://www.spectralevolution.com/portable_spectroradiometer.html

A relatively new development in spectroradiometer construction is to use a diode array to capture the whole spectrum simultaneously, instead of a photomultiplier in combination with a mechanical scanning system. These instruments have the advantage of speed and lack of any mechanical problems and also consume less energy (which is of importance for field equipment). However, the problems with stray light are larger than for the more conventional instruments. Thus they are generally not useful for daylight measurements below 300 nm, and below 350 nm a stray light correction must often be applied to reach an acceptable accuracy.

4.6.4 Calibration of Spectroradiometers

4.6.4.1 Wavelength Calibration with Lamps

This is the simple part but important. If the wavelength is not correct, then everything else will be wrong, too. The wavelength error should be less than 1 nm; for measurements of daylight UV-B radiation, it should preferably be much less.

For such calibration, any medium pressure mercury lamp works well, even an ordinary fluorescent lamp. Easily recognizable spectral lines occur at 253.7, 265.2, 312.6 + 313.2, 334.1, 365.0, 365.4, 366.3, 404.7, 435.8, 491.6, 496.0, 546.1, 577.0, 579.1, 623.4, and 690.7 nm. The short-wavelength bands do not penetrate the envelopes of most fluorescent lamps.

4.6.4.2 Irradiance Calibration with Standard Lamps

Usually, a spectroradiometer is calibrated using a lamp with a known output at different wavelengths. The most commonly used lamp is a 1 kW tubular quartz–iodine incandescent lamp. The reason to use such a powerful lamp is to obtain sufficient output in the ultraviolet region, and a lamp of this power can be used down to 250 nm. (For shorter wavelengths usually deuterium standard lamps are used.)

Using transfer standards, these standard lamps are ultimately calibrated against cavity radiators held at a well-determined temperature and designed so they follow as closely as possible the theoretical Planck blackbody radiation formula (see Chap. 1). When you purchase such a lamp, you will obtain a table of the spectral irradiance obtainable at certain wavelengths at certain distance using a specific geometry and also information about the accuracy. You will be surprised at (1) the wide uncertainty limits compared to most other kinds of physical measurements (typically 3.5 %

at 250 nm) and (2) the high price of the lamp. After all, it looks almost like the lamp you have in the overhead projector in your lecture hall. What you should consider at this moment of surprise is that the lamp has been preburned and selected to be particularly stable and the effort and cost involved in calibrating it as accurately as possible. You should buy a second similar but uncalibrated lamp at a much lower cost, calibrate this as a working standard against your expensive lamp, and only occasionally use your expensive lamp to check your working standard.

The disadvantage of using a 1 kW lamp (apart from the heat it produces in your usually small calibration room) is that it requires a direct current of 8 A to run at 125 V, and quite a big power supply is needed to produce this with good accuracy. It is very important that you really run it at the specified current at which it was calibrated. An error of 0.1 % in the current produces a 1.2 % error in the spectral irradiance at 250 nm and a 0.6 % error at 400 nm. It is important that the current is as ripple-free (has as little ac component) as possible. The best way of measuring the current is to measure the voltage across a precision resistor of, say, 0.1 ohm in the lamp circuit with a good digital voltmeter.

Calibration of a spectroradiometer is a tricky thing. When you calibrate it with your standard lamp, you usually put the standard lamp on the optical axis. Suppose that you calibrate two spectroradiometers in this way with the same standard lamp in the same setup, so that they show the same result when you measure light from a lamp in the laboratory. Then you take the spectroradiometers outdoors and measure the daylight. You will then likely find that the two spectroradiometers show different results. This can have different causes, but the two major ones are probably that (1) the temperature is different and the two spectroradiometers have different temperature dependencies and (2) they have different off-axis sensitivities, and you are now measuring a very extended light source rather than an almost point-like standard source.

It is recommended that you recalibrate a spectroradiometer about once a month. This interval can be modified according to the experience you obtain over time with your particular instrument under your particular working conditions. If you move your instrument around, you should perform a rather easy wavelength check at each new location.

4.6.4.3 Irradiance Calibration with an Improvised Standard Lamp

Björn (1971) devised a method to use an ordinary tubular incandescent lamp as a standard lamp without prior optical calibration of the lamp, just relying on electrical measurements. The basic idea is that the temperature of the lamp filament is calculated from the increase in electrical resistance when it heats up from room temperature; calculate the spectrum of the glowing filament from its temperature using Planck's radiation formula with appropriate corrections for the (temperature and wavelength-dependent) emissivity of tungsten. This method is not recommended if calibrated standard lamps are obtainable for the experimenter.

4.6.4.4 Calibration Without a Standard Lamp

Considering the cost of standard lamps, their instability, and the difficulty of ensuring the same standard everywhere in the world, it would be good if a radiation source were available free of charge so that everyone could use the same radiation source. There is such a radiation source: the sun.

4.6.4.5 Wavelength Calibration Using Daylight

The sun is essentially a heat radiator, thus radiating an essentially continuous spectrum, while a line spectrum is more suitable for wavelength calibration. However, some of the outer layers of the sun have a temperature that is low enough to reabsorb light from the inner layers and still hot enough to contain single atoms, not united to molecules. They produce the so-called Fraunhofer lines in daylight, which are absorption spectral lines of these free atoms. The wavelengths of these Fraunhofer lines can be looked up in various sources. Here we just mention the two due to hydrogen, which are most suitable for wavelength calibration in the visible region: 486.1344 nm (Fraunhofer F line) and 686.9955 nm (Fraunhofer C line).

4.6.4.6 Irradiance Calibration Using the Sun

Surprisingly, the sun can also be used for irradiance calibration. This is surprising because we have the variable terrestrial atmosphere between ourselves and the sun, and this atmosphere is not the same everywhere. If we are on a mountain, there is less atmosphere between us and the sun than at sea level, and other factors also contribute to different attenuation of the sunlight at different places and times. However, these difficulties can be circumvented, provided the atmosphere is reasonably clear and stable over a day.

Consider first two (unrealistically) simple cases (Fig. 4.11). We have no clouds in the sky. In the first case the sun is directly overhead, and the light is attenuated by, as the jargon in the field goes, one air mass. At a certain wavelength, the spectral irradiance from the direct sunlight can be written as $I_1 = I_e \cdot e^{-a}$, where I_e is the corresponding extraterrestrial spectral irradiance, that is, the spectral irradiance just outside the terrestrial atmosphere. The spectral irradiances we consider here are in the direction of the sun (light falling on a plane perpendicular to the direction to the sun). We consider only the direct sunlight, that is, not that scattered in the atmosphere or reflected from the ground. In the second case, the sun is at an angle of 60° to the vertical, that is, the zenith angle of the sun is 60°. In this case, the light path through the atmosphere is twice as long as in the first case. The irradiance then must be (provided the Lambert–Beer law is valid)

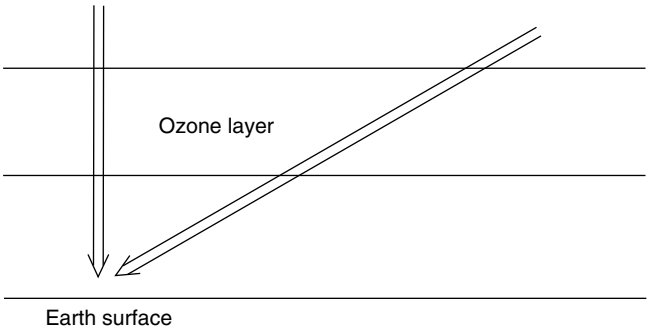

Fig. 4.11 Effect of atmosphere on sunlight from different directions. If scattered light is excluded so only the direct beam is considered, the length of the path of light through the atmosphere is longer for obliquely incident light, in proportion to the cosine of the incidence angle

$I_2 = I_e.e^{-2a}$, since the light is now attenuated by two air masses. Only when the scattered light is excluded by a narrow-angle input does the Lambert–Beer law hold (see Sect. 1.11). The ratio between the two irradiances below the atmosphere is then $I_2/I_1 = e^{-a}$, and this ratio we should be able to determine without absolute calibration of the spectroradiometer. But knowing e^{-a}, we can now calibrate the spectroradiometer against the extraterrestrial irradiance using the relationship $I_1 = I_e \cdot e^{-a}$.

This is the principle of the Langley calibration method. In practice, it is a bit more complicated than described here. One has to take spectra of the sun over at least 1 day and preferable over several days when the weather is stable and the sky without clouds. For the Lambert–Beer law to be valid, one has to measure the *direct* sunlight and exclude skylight as well as possible. One way of doing this is to measure the sunlight through a narrow baffled tube (Fig. 4.6) following the sun. Another way is to take a difference reading, that is, the difference between the total daylight and the daylight when shadowing the sun. One then plots the logarithm of the reading against the air mass (the air mass is proportional to one over the cosine of the zenith angle). This gives a nearly straight-line relationship, which can be extrapolated to zero air mass, corresponding to the reading that would have been obtained outside the atmosphere. For high accuracy one must apply various corrections (especially for large zenith angles), for instance, for the refraction (bending) of the light rays in the atmosphere and for the curvature of the earth and for the fact that different attenuators in the atmosphere do not have the same height distribution (especially for the fact that ozone, absorbing at short wavelengths, is higher than most attenuators). One must also take into account the variation of the sun–earth distance over the year, but this is easy. With decreasing wavelength, the difficulties increase (e.g., due to the rapidly changing ozone attenuation, the strong wavelength dependence of ozone absorption, less constant output of the sun at short wavelengths, and the smaller signal in relation to instrument noise). Below 300 nm this method cannot be used at all. Details of the method with different variations and comparisons with other calibration methods can be found in Schmid and Wehrli (1995), Wilson and Forgan (1995), Schmid et al. (1998), Slusser et al. (2000), Adler-Golden and Slusser (2007), and Chen et al. (2013).

4.7 Special Methods for Measurement of Very Weak Light

4.7.1 Introduction

Only methods based on photomultipliers will be reviewed here, but photomultipliers can be used in different ways. We shall not touch upon imaging of very weak light, which is important in many contexts from astronomy to biology. Photomultipliers can be used in the following main ways.

4.7.2 Direct Current Mode

This is the "classical way" described in Sect. 4.3.1. The dc component of the anode current is measured. If the light is steady or varies only slowly, an amplifier with a long time constant can be used to obtain a "smoothed" or averaged value of the current; alternatively, this averaging can, of course, be achieved using a computer. Then the light is shut off and the dark current is measured in the same way. With the photomultiplier connected to suitable electronic circuitry, the difference between "light" and "dark" currents is proportional to the light to be measured.

If the light is very weak, this does not work well. This is because the difference between "light" and "dark" currents will be a small difference between two larger terms, and a small relative error in any of them will result in a larger relative error in the difference. Furthermore, for a weak light, a long time will be required to get a reliable value of the light current, and in the meantime the dark current might drift.

4.7.3 Chopping of Light and Use of Lock-In Amplifier

In this mode, for instance, a rotating shutter or mirror is used to cut the light into short pulses separated by darkness of similar duration. A special amplifier amplifies the current during the light and dark periods separately, and the difference is continuously computed, or electric charges from the two sets of periods are stored for integration of the difference over time. In this way, the effect of drift with time of the dark current is minimized. In this way, much weaker light can be measured than is possible in the direct current mode. It is, for

example, easy to measure the light emitted from a plant leaf (as a reversal of the photosynthetic process; see Sect. 26.8) for tens of minutes after the leaf has been placed in "darkness." However, "ultraweak luminescence" (Sect. 26.9) can hardly be measured with this method.

4.7.4 Measurement of Shot Noise

Shot noise is the "noise" of the dc signal from the photomultiplier arising from the quantized nature of light, that is, the current pulses generated by the single photons. Yoh-Han Pao et al. (1966) suggested that the shot noise, treated as an ac signal, could be used as a measure of the light. Later experiments indicate that the signal-to-noise ratio for this method is somewhat better than for the lock-in method. However, because of the advantages of the method to be described below, this method has not been used much.

4.7.5 Pulse Counting

The dominating technique today for measuring very weak light is to count the current pulses generated in a photomultiplier by single photons. All pulses of the anode current, however, are not due to photons. Electrons are also released both from the photocathode and from the dynode surfaces by thermal energy. This is what gives the dark current in the dc mode. One great advantage of the pulse counting method is that pulses due to thermal emission from the dynodes can be filtered off, because they are smaller than those coming from the photocathode, since they have gone through fewer amplification steps Alfano and Ockman (1968). To achieve this, the pulses from the anode go to a pulse discriminator, which allows only pulses above a certain amplitude to pass. The pulses passing through are then shaped to a uniform amplitude and pulse shape, so they can be more accurately counted.

However, this cannot be done in a perfect way. Some photon-induced pulses are discarded, and some spurious pulses are passed. Some photons do not give rise to any pulses at all, because the quantum efficiency of the photocathode is lower than one (even in the spectral region where it is highest). And there is no way by which thermal pulses arising in the photocathode can be distinguished from light-induced pulses. Therefore, a photomultiplier can never be used as an absolute photon-counting device. To estimate the true number of photons arriving at the photocathode, the photomultiplier has to be calibrated, and a correction has to be made for "dark pulses."

Just as in a Geiger counter, there is a certain minimum time necessary for two pulses to be counted separately. Since the pulses are Poisson distributed in time, the counting efficiency starts to decline gradually when the photon absorption rate increases over a certain limit. The absolute standard error of the number of pulses recorded, according to Poisson statistics, is proportional to the square root of the number of pulses counted and the relative error proportional to one over this square root. With absolute standard errors of e_l for the light count and e_d for the dark count, the standard error of the difference between light and dark counts is the square root of $(e_l{}^2 + e_d{}^2)$.

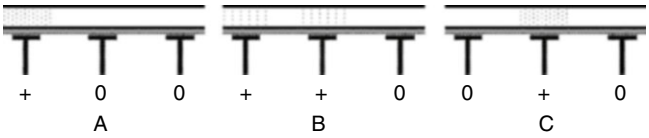

Fig. 4.12 The principle for a charge-coupled device (CCD). A small part of the CCD is shown at three different times (**a**–**c**). Electrodes are shown as **T**. In A, light has released electrons (shown as *dots*) in a doped silicon plate near the leftmost electrode. A wave of positive electrical potential (shown with the *plus signs*) is passed along the electrodes from *left* to *right*, and the electrons follow this positive wave through the silicon and can finally be collected sequentially from each location at a collection electrode at the right end (or edge, if it is a two-dimensional CCD)

4.8 A Sensor for Catching Images: The Charge-Coupled Device

There are different kinds of electronic sensors for recording images, but only the most commonly used one will be described here: the charge-coupled device (CCD). Most readers have probably used a CCD already as part of a digital camera. But a CCD is useful everywhere when you wish to record light in one or two dimensions. In Chap. 29, we show how it can be used for recording spectra. The principle for a CCD is shown in Fig. 4.12.

References

Adick H-J, Schmidt R, Brauer H-D (1989) A chemical actinometer for the wavelength range 610–670 nm. J Photochem Photobiol 49A:311–316

Adler-Golden SM, Slusser JR (2007) Comparison of plotting methods for solar radiometer calibration. J Atmos Ocean Technol 24:935–938

Alfano RR, Ockman N (1968) Methods for detecting weak light signals. J Opt Soc Am 58:90–95

Allen JM, Allen SK, Baertschi WW (2000) 2-Nitrobensaldehyde: a convenient UV-A and UV-B chemical actinometer for drug photostability testing. J Pharm Biomed Anal 24:167–178

Bérces A, Fekete A, Gáspár P, Grof P, Rettberg P, Hornedk G, Rontó G (1999) Biological UV dosimeters in the assessment of biological hazards from environmental radiation. J Photochem Photobiol B Biol 53:36–43

Björn LO (1971) Simple methods for the calibration of light measuring equipment. Physiol Plant 25:300–307

Björn LO (1995) Estimation of fluence rate from irradiance measurements with a cosine corrected sensor. J Photochem Photobiol B Biol 29:179–183

Björn LO, Vogelmann TC (1996) Quantifying light and ultraviolet radiation in plant biology. Photochem Photobiol 64:403–406

Chen M, Davis J, Tang H, Ownby C, Gao W (2013) The calibration methods for multi-filter rotating shadowband radiometer: a review. Front Earth Sci 7:257–270

Evans WG (2005) Infrared radiation sensors of Melanophila acuminata (Coleoptera: Buprestidae): a thermopneumatic model. Ann Entomol Soc Am 98:738–746

Goldstein S, Rabani J (2007) The ferrioalate and iodide-idodate actinometers in the UV region. J Photochem Photobiol A: Chem. doi:10.10/6/jjphotochem, 2007.06.006

Hale GM, Querry MR (1973) Optical constants of water in the 200 nm to 200 μm wavelength region. Appl Opt 12:555–563

Hatchard CG, Parker CA (1956) A new sensitive actinometer. II. Potassium ferrioxalate as a standard chemical actinometer. Proc Roy Soc A235:518–536

Horneck G, Rettberg P, Rabbow E, Strauch W, Seckmeyer G, Facius R, Reitz G, Strauch K, Schott JU (1996) Biological dosimetry of solar radiation for different simulated ozone column thicknesses. J Photochem Photobiol 32:189–196

Jagger J (1967) Introduction to research in ultraviolet photobiology. Prentice-Hall, Englewood Cliffs

Kuhn HJ, Braslavsky SE, Schmidt R (1989) Chemical actinometry. Pure Appl Chem 61:187–210

Lee J, Seliger HH (1964) Quantum yield of the ferrioxalate actinometer. J Chem Phys 40:519–523

Marijnissen JPA, Star WM (1987) Quantitative light dosimetry in vitro and in vivo. Lasers Med Sci 2:235–242

Mirón AS, Grima EM, Sevilla JMF, Chisti Y, Camacho FG (2000) Assessment of the photosynthetically active incident radiation on outdoor photobioreactors using oxalic acid/uranyl sulfate chemical actinometer. J Appl Phycol 12:385–394

Namekata N, Sasamori S, Inoue S (2006) 800 MHz Single-photon detection at 1550-nm using an InGaAs/InP avalanche photodiode operated with a sine wave gating. Opt Express 14:10043–10049

Optronic Laboratories (2001) Standard spheres and sphere standards. Application note (A15). Downloadable from http://goochandhousego.com/wp-content/uploads/2014/01/A15_STANDARD-SPHERES-AND-SPHERE-STANDARDS_2-01_GH.pdf

Optronics Laboratories (1995) Improving integrating sphere design for near-perfect cosine response. Application note (A9). Downloadable from http://goochandhousego.com/download/improving-integrating-sphere-design-for-near-perfect-cosine-response/

Pao Y-H, Zitter RN, Griffith JE (1966) New method of detecting weak light signals. J Opt Soc Am 56:1133–1135

Parker CA (1953) A new sensitive chemical actinometer. I. Some trials with potassium ferrioxalate. Proc Roy Soc London 220A:104–116

Rahn RO (1997) Potassium iodide as a chemical actinometer for 254 nm radiation: use of iodate as an electron scavenger. Photochem Photobiol 66:450

Rolfe J, Moore SE (1970) The efficient use of photomultiplier tubes for recording spectra. Appl Optics 9:63–71

Ryer AD (1997) Light measurement handbook. International Light, Inc., Technical Publications Dept, Newburyport, ISBN 0-9658356. Downloadable from http://www.intl-light.com/handbook/

Schmid B, Wehrli C (1995) Comparison of sun photometer calibration by use of the Langley technique and the standard lamp. Appl Optics 34:4500–4512

Schmid B, Spyak PR, Biggar SF, Wehrli C, Sekler J, Ingold T, Mätzler C, Kämpfer N (1998) Evaluation of the applicability of solar and lamp radiometric calibrations of a precision sun photometer operating between 300 and 1025 nm. Appl Optics 37:3923–3941

Schneider WE, Young R Spectroradiometry methods. Application note (A14), pp 49. Optronics Laboratories, Orlando (1998). Downloadable from http://www.goochandhousego.com/wp-content/uploads/2013/12/A14_SPECTRORADIOMETRY-METHODS_1-98_GH.pdf

Seckmeyer S, Klingebiel M, Riechelmann S, Lohse I, McKenzie RL, Liley JB, Allen MW, Siani A-M, Casale GR (2012) A critical assessment of two types of personal UV dosimeters. Photochem Photobiol 88:215–222

Seliger HH, McElroy W (1965) Light: physical and biological action. Academic, New York

Skovsen E, Snyder JW, Ogilby PR (2006) Two-photon singlet oxygen microscopy: the challenges working with single cells. Photochem Photobiol 82:1187–1197

Slusser J, Gibson J, Bigelow D, Kolinski D, Disterhoft P, Lantz K, Beaubie A (2000) Langley method of calibrating UV filter radiometers. J Geophys Res 105:4841–4849

Vogelmann TC, Björn LO (1984) Measurement of light gradients and spectral regime in plant tissue with a fiber optic probe. Physiol Plant 60:361–368

Wegner EE, Adamson WW (1966) Photochemistry of complexions. III. Absolute quantum yields for the photolysis of some aqueous chromium (III) complexes. Chemical actinometry in the long wavelength visible region. J Am Chem Soc 88:394–404

Wilson SR, Forgan BW (1995) In situ calibration technique for UV spectral measurements. Appl Optics 34:5475–5484

Light as a Tool for Biologists: Recent Developments

5

Lars Olof Björn

5.1 Introduction

Light has, of course, been exploited by scientists as far back as there has been any science. Until recently, almost everything we knew about the universe beyond the lower terrestrial atmosphere was information carried by light. Since Bunsen's time, optical spectroscopy has provided information about things as small as atoms and as large as galaxies. Spectrometry (absorption or fluorescence) or optical microscopy, or both, has been important for most biologists. The following account will therefore not attempt to be comprehensive but will focus on a few recent developments of interest for biologists. A good guide to much of the pre-2003 literature is provided by *Methods in Enzymology* (Elsevier) Vol. 360 and 361 (2003).

5.2 Optical Tweezers and Related Techniques

When we hear the word tool, we probably first see in our minds something we can hold in the hand, like a hammer, pliers, or tweezers. We use tweezers to handle things that are too small for our fingers to manipulate. But mechanical tweezers, and even traditional micromanipulators, are too large for particles smaller than single cells. Such objects can be handled with optical tweezers, invented by Ashkin (1970).

The description in Fig. 5.1 applies to light beams that are most intense in the center and with irradiance tapering off towards the periphery approximately as a Gauss function (as may be recalled from elementary statistical theory) does. But another type of beam has also been tried for optical forceps, a so-called Bessel beam. This beam has a complicated cross section. True Bessel beams cannot be produced, but an approximation can be made by focusing an ordinary beam from a laser (approximate Gauss beam), not with an ordinary lens, but with a conical lens. A Bessel beam has the advantage that the irradiance is kept high over a longer distance,

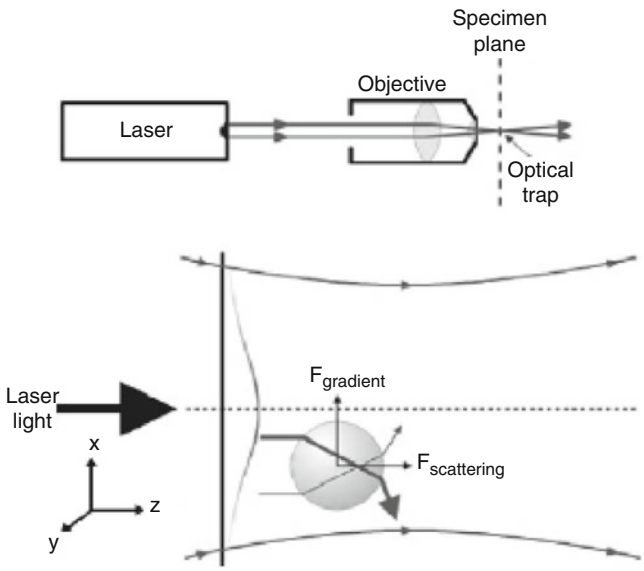

Fig. 5.1 A simple form of optical tweezers. A particle is trapped in the focus of a laser beam. The picture shows how a strong ray of light is bent downwards by a transparent (or at least semitransparent, as all sufficiently small biological objects are) sphere. This gives an upward force acting on the sphere. If the sphere from the beginning is a little off-center in the beam, the corresponding ray giving a downward force is weaker, and the resulting force will be towards the beam center. Bending of both rays will also produce a force on the sphere towards the right, since they both decrease the rightward momentum of the light and this must be compensated for by the sphere's momentum. Light absorption as well as back reflection will give a force in the direction of the light, but for small objects, this will be a small effect. Light refraction will be more important for the forces along the light beam. There is a gradient in light refraction, and if the particle starts to move past the focus, a restoring force is created (see Fig. 5.2) (Slightly modified from Stanford University's URL http://www.stanford.edu/group/blocklab/Optical%20Tweezers%20Introduction.htm)

L.O. Björn
School of Life Science, South China Normal University, Guangzhou, China

Department of Biology, Lund University, Lund, Sweden
e-mail: Lars_Olof.Bjorn@biol.lu.se

L.O. Björn (ed.), *Photobiology: The Science of Light and Life*,
DOI 10.1007/978-1-4939-1468-5_5,

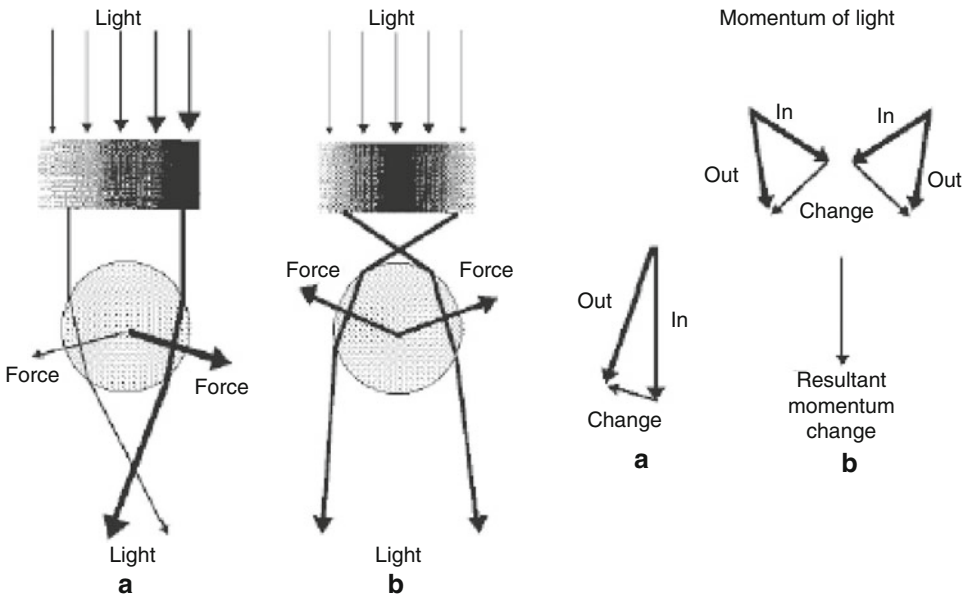

Fig. 5.2 Diagrams showing the refraction of light in a transparent sphere (*left*) and the resulting change in momentum of the light (*right*). The forces on and movements of the sphere are such that they compensate for the change in momentum of the photons. Surprisingly, the amount of momentum transfer has even recently been a matter of much discussion among physicists (e.g., Loudon and Barnett 2006). The diagrams to the right show how the momentum change can be computed graphically by subtraction and addition of vectors

not only in a focal spot. Therefore, it can be used to manipulate particles in directions perpendicular to the beam, while they can move freely along the beam.

In another method, instead of "clamping" particles in a spot (as with Gaussian beams) or along a Bessel beam, a kind of "optical washboard" or "corrugated surface" is produced, and this can be "shaken" so that particles move along the surface, with different speeds depending on size (Paterson et al. 2005). For this, a Bessel beam is used.

Using holograms, any light distribution can be created and used for manipulating objects (Grier and Roichman 2006), and light in combination with sheets of certain polymers can be used to transport materials over microscopic distances (Stiller et al. 2004). Dorman (2007) exemplifies the use of optical tweezers in biology.

5.3 Use of Lasers for Ablation, Desorption, Ionization, and Dissection

The reader has probably already heard or read about the "light scalpel" that doctors use for some kinds of surgery. Laser beams can be used for killing cancer cells, for fixing retinae that have come loose, and for several other medical purposes.

Lasers also have many uses related to this in nonmedical biology. One of the most important applications is to make large molecules, such as protein molecules, available for mass spectrometry, for determination of molecular mass and content of, e.g., phosphate groups (Krüger et al. 2006; Marshall et al. 2002).

The methods of evaporating the samples are referred to as laser ablation (any removal of material from a solid or liquid surface) and laser desorption (Peterson 2007). In addition, molecules and molecular fragments can be ionized by the laser beam, and the resulting electric charge is, of course, an important factor in mass spectrometry. A new method combining the use of laser and electrospray ionization (ESI) is electrospray-assisted laser desorption ionization (ELDI) (Huang et al. 2006).

Laser beams can also be used for microdissection of biological specimens (Nelson et al. 2006). There are two main methods for this: "laser capture microdissection" (LCM) and "laser cutting." Several commercial instruments are marketed for each of these. In the former method, a film of ethyl–vinyl–acetate is locally heated by an infrared laser beam, melted, and glued to the structure one wishes to pull away from the rest of the sample. In laser cutting, an ultraviolet laser beam (a 337-nm nitrogen laser is suitable) is used to cut out the desired structure.

5.4 Fluorescent Labeling

In classical light microscopy, biological structures in most cases had to be stained with various pigments to become clearly visible. Gradually, methods became more sophisticated, so that it became possible to determine the chemical makeup of various cell structures by staining them with specific colored compounds ("cytochemistry"). A great leap forward was taken when pigments were combined with antibodies, which make very specific associations with cell structures and particularly with proteins. In the microscopy methods to be described in the following sections, labeling with fluorescent pigments plays an important role, and these pigments are commonly combined with antibodies to make the labeling of cell constituents specific. Antibodies are best for rather large molecules, while for small metabolites,

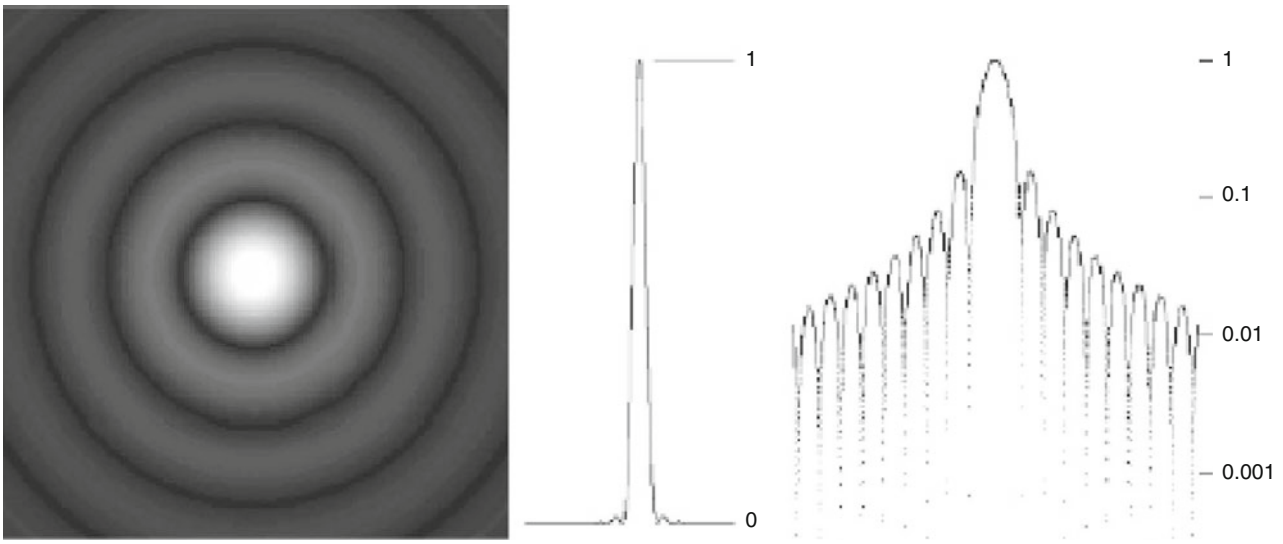

Fig. 5.3 The Airy disk: the real appearance and graphs of the radiance distribution on logarithmic and linear scales

specific RNA species can be used in combination with fluorescent molecules (Paige et al. 2012).

Many fluorescent compounds have been used in this way. One particular compound has become particularly important—the so-called green fluorescent protein (GFP). It is produced by the jellyfish *Aequorea victoria* (see Chap. 26). It has a major excitation peak at 395 nm and a minor excitation peak at 475 nm. The emission peak is in the green region at 509 nm, which makes it very suitable for visual detection of fluorescence. Another somewhat similar protein is produced by the sea pansy *Renilla reniformis.*

The advantage with a protein is that it can be used as a reporter for gene expression. For this purpose, the gene for GFP is fused with a regulator gene to be studied and inserted into the genome of the organism under study. The first publication (Chalfie et al. 1994) introducing this technique has, at the time of this writing, been cited 2,532 times. Tsien (1998) has written an early review of the subject, which is also well cited.

Fluorescent proteins with other emission spectra can be obtained in different ways: (1) by extracting and cloning proteins from other organisms, such as the red-emitting pigment from the railroad worm (Viviani 1999) or various proteins from corals (Verkhusha and Lukyanov 2004); (2) by changing amino acids in the protein by genetic engineering or chemically modifying the chromophore (Heim 1994; Shkrob et al. 2005); (3) by photoactivation or phototransformation, i.e., by various photochemical reactions of the protein (see below); and (4) by combining two proteins with different fluorescence properties so that energy absorbed by one can be transferred to the other one. By labeling a sample simultaneously with proteins having different fluorescence properties, regulation of different genes can be studied in the same sample (e.g., Jiang et al. 2006).

Proteins can also be made to change their fluorescence spectra by light treatment (e.g., Ando 2002; Elowitz et al. 1997; Habuchi et al. 2005; Lukyanov et al. 2005). The exact mechanism for this color change varies from case to case. It can be due to a conformational change of the protein or to photochemical change of an amino acid in the protein.

The fluorescence quantum yield of GFP is so high that single molecules can be registered (e.g., Cotlet et al. 2006; Peterman et al. 1999).

A recent comprehensive review (Fricker et al. 2006) describes a number of special methods in quantitative fluorescence microscopy which we shall not recount here. They include quantitative imaging of gene expression, in vivo imaging of mRNA localization and dynamics, methods for protein localization, level and turnover, and protein–protein interactions. One method for judging the proximity of two protein molecules is to study the resonance energy transfer between chromophores attached to them (see Chap. 1). Still another novel microscopy method using fluorescence is "fluorescent speckle microscopy" (Danuser and Waterman-Storer 2006) for the study of macromolecule dynamics (such as cytoskeleton assembly/disassembly) in living cells.

5.5 Abbe's Diffraction Limit to Spatial Resolution in Microscopy

We have seen in Chap. 1 that light is diffracted when passing through an opening. This diffraction limits the resolution of conventional light microscopy. A bright point will not be imaged as a point but as a diffraction pattern, somewhat similar to what we have encountered in the section on diffraction in slits, but with a circular shape, a so-called Airy disk (Fig. 5.3).

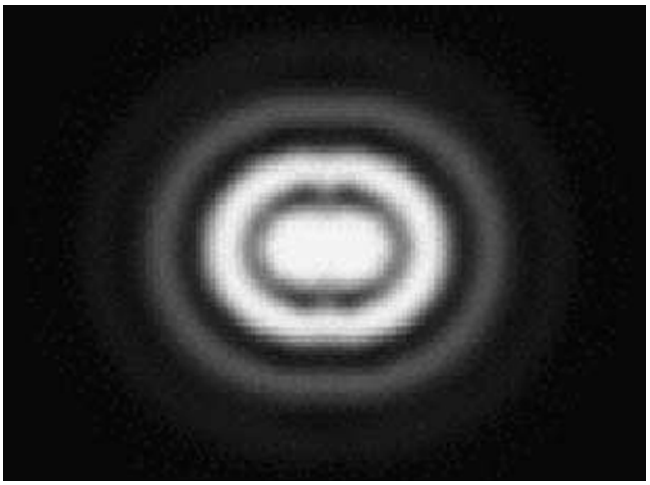

Fig. 5.4 Image of two bright spots at the minimum resolvable distance

More than 130 years ago, Ernst Abbe showed that the smallest distance between two points (Fig. 5.4) that can be resolved by a conventional light microscope is $s = 1.22 \cdot \lambda / (2 \cdot n \cdot \sin\alpha)$, where λ is the wavelength of the light used, n the refractive index of the medium between the objective lens and the object, and α the half-angle of the objective lens subtended at the object plane. The so-called numerical aperture, $n \cdot \sin\alpha$, is often stated on the objective of a microscope, so it is easy to estimate s. With immersion oil as the medium between the objective and the object and a high-quality immersion objective, the numerical aperture can be made as high as 1.4.

With light for which the human eye has a high sensitivity and resolution, 500 nm, we get $s = 1.22 \cdot 500/(2 \cdot 1.4)$ nm = 218 nm = 0.218 μm. The brightness distribution for this case, which is considered to be the limit for resolution of two points, is shown in Fig. 5.4.

Using a longer wavelength, while diminishing the resolution, has the advantage of better penetration and less scattering in most biological specimens.

The resolution can be further improved by using ultraviolet radiation instead of visible light (since the Airy disk will be smaller with a lower wavelength) and still further by using electrons instead of photons (electron microscopes use wavelengths in the nanometer range, but the numerical aperture is less favorable).

An improvement in factual resolution for biological specimens was achieved with the invention of the confocal microscope, but this is merely a way of improving focusing and reducing disturbing scattered light. The ultimate resolution is still set by Abbe's criterion.

More recently, however, Abbe's diffraction limit has been broken through, in more than one way, and resolutions of only a few tens of nanometers achieved using visible light (see below).

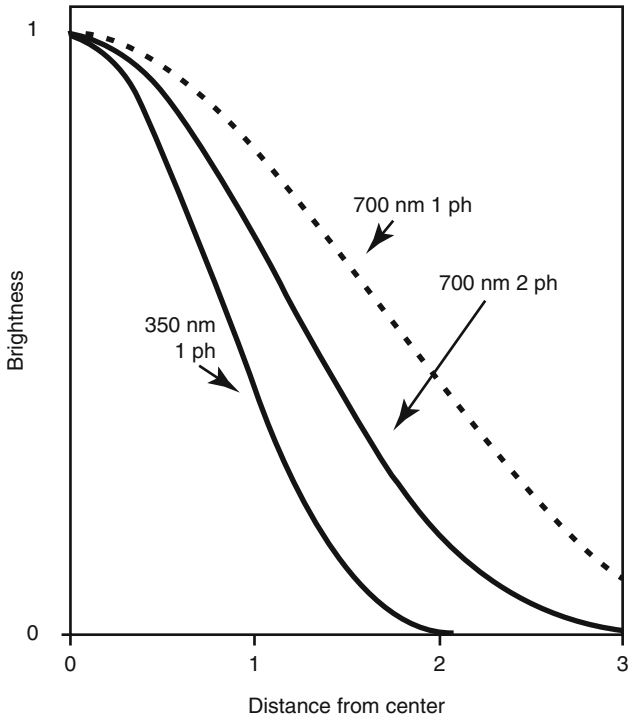

Fig. 5.5 Brightness of a small fluorescing spot as imaged with one-photon fluorescence (350 and 700 nm) and two-photon fluorescence (700 nm)

5.6 Two-Photon Excitation Fluorescence Microscopy

In this technique, the biological specimen is stained with antibodies to which a fluorescent pigment has been attached. The antibodies attach to the structures that one wishes to study, such as a specific protein. The method utilizes the fact that fluorescence can be induced not only by light of a wavelength corresponding to an absorption band of the fluorescent pigment but also by light of twice that wavelength (photons with half the energy of the energy gap in the Jablonski diagram), provided the concentration of photons is high enough that two of them will be absorbed by the same molecule within a short enough time. If the equipment is suitably adjusted, this happens only in the center of the laser beam with which fluorescence is excited. The specimen must be examined point by point by a scanning laser beam. In two-photon microscopy, in order to use the same absorption band of the fluorescent pigment as in one-photon microscopy, the wavelength must be doubled. Doubling of the wavelength alone would worsen the resolution by a factor of two. Since, for two-photon excitation, the fluorescence brightness is proportional to the square rather than the first power of the fluence rate of the exciting light, this disadvantage is only partly compensated for, as shown in Fig. 5.5.

An important advantage with two-photon excitation is that less bleaching occurs than with one-photon excitation.

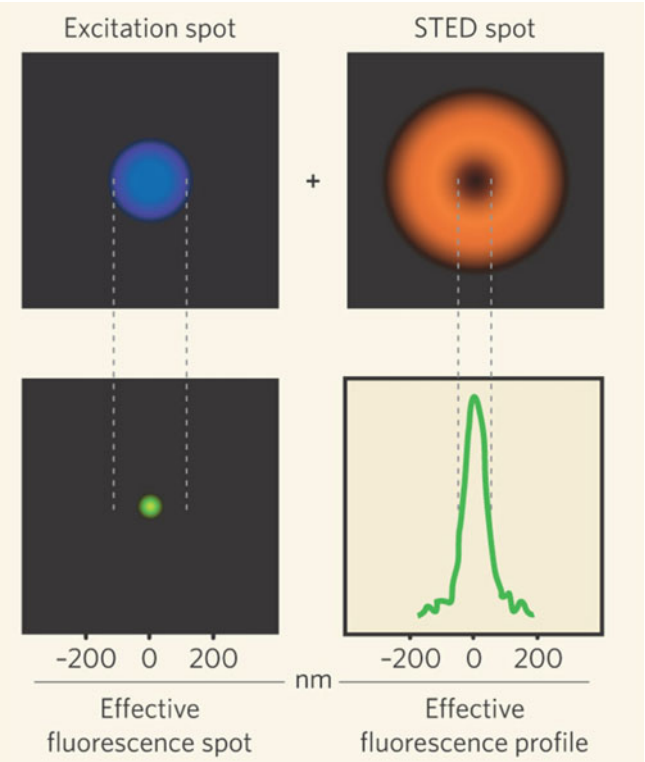

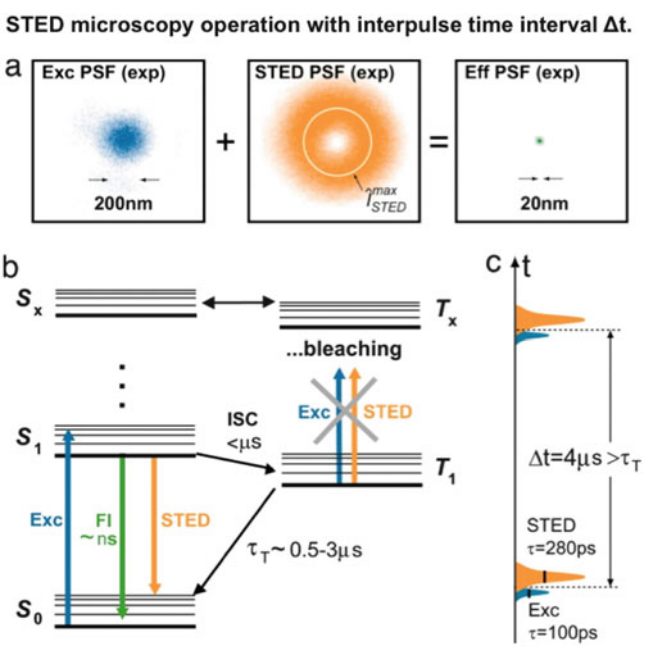

Fig. 5.6 The principle for STED (*Left picture* reprinted by permission from Macmillan Publishers Ltd: Simpson (2006), Copyright 2006 STED microscopy operation with interpulse time interval ?t. (**a** *Left* and *Center*) (**a**). Measured spots for excitation (*blue*) and STED (*orange*) pulses resulting in 22-nm STED spot. (**b**). Conversions between pigment energy levels. If time between *blue* and *orange* pulses is too short, excitation of triplet pigment causes bleaching. (**c**). With pulse interval long enough the triplet state has decayed and bleaching is prevented. *Right* STED microscopy operation with interpulse time interval Δt. (**a**). Measured spots for excitation (*blue*) and STED (*orange*) pulses resulting in 22-nm STED spot. (**b**). Conversions between pigment energy levels. If time between *blue* and *orange* pulses is too short, excitation of triplet pigment causes bleaching. (**c**). With pulse interval long enough the triplet state has decayed and bleaching is prevented. (Reprinted, with permission, from Donnert et al. (2006))

5.7 Stimulated Emission Depletion

Another method, stimulated emission depletion microscopy (STED microscopy or STEM), also uses fluorescent labeling of the specimen in the same way but a different method for exciting the fluorescence. In this method, too, the specimen is scanned spot by spot by a laser beam, which excites fluorescence (Fig. 5.6). Diffraction of the beam causes the illuminated spot to have a minimum diameter of about 200 nm if blue light of 470-nm wavelength is used. Immediately after the pulse of blue light and before any appreciable amount of fluorescence light has had time to be emitted, a second pulse, now of a higher wavelength, hits the sample. The time between the pulses is long enough for the excited pigment to decay to the lowest vibrational level of the first excited singlet state. The wavelength of the second pulse is such that it causes the pigment to return to the ground level via stimulated emission (the same phenomenon that takes place in a laser). The second pulse has a ring-shaped cross section, i.e., the intensity in the center is almost zero. Thus, the depletion of the excited state will take place around the circumference of the excited spot, and fluorescence will be emitted only from the most central part.

A problem with this method is that since very strong light has to be used, and thus a high concentration of excited state, a triplet state is easily formed, resulting in chemical reactions that destroy the pigment (bleaching). This problem can be circumvented by suitable choice of pigment and irradiation protocol.

5.8 Near-Field Microscopy

A completely different approach for breaking the diffraction limit in microscopy was suggested long ago (Synge 1928), but was first implemented in a practically useful way by Betzig and Chichester (1992). The principle is to either collect or deliver the viewing light so close to the specimen that the light has had no space to spread by diffraction (Figs. 5.7 and 5.8).

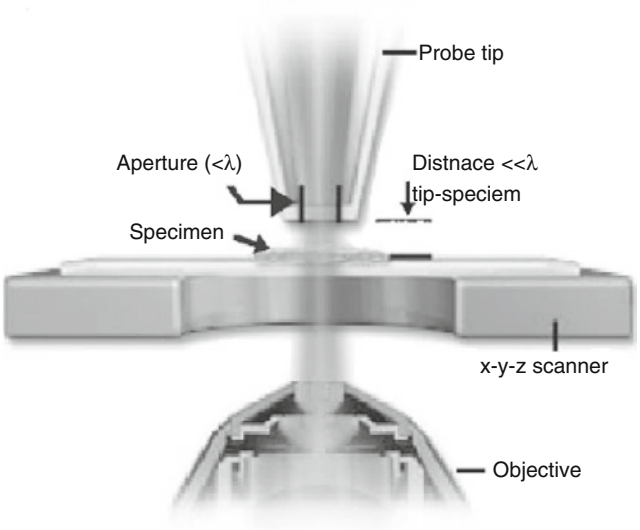

Fig. 5.7 Near-field microscopy (Slightly modified from http://www.olympusmicro.com/primer/tecniques/nearfieldintro.html. Courtesy of Dr. Michael W. Davidson)

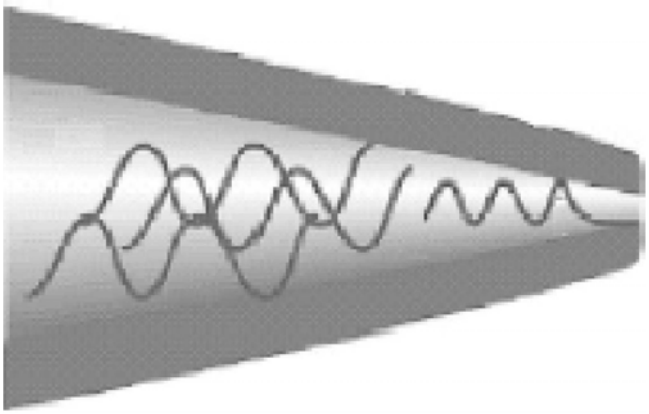

Fig. 5.8 Tapered and aluminum-coated glass fiber for near-field microscopy, schematic. Light waves are squeezed together until there is no room for them to propagate further. But a so-called evanescent electromagnetic field still protrudes a short distance beyond the tip of the fiber, and if a scattering medium is brought into this region, the light energy can propagate into the "far field" and be registered with a photomultiplier. The same device can work in the opposite direction, and sample photons from the evanescent field of the sample if this is illuminated (Modified from http://www.azonano.com/details.asp?ArticleID=1205)

Betzig and Chichester (1992) introduced the use of a very thin light-conducting fiber for this purpose. The light aperture at the end of the fiber is much less than the wavelength of light, about 25–100 nm in diameter, and the distance between the fiber tip and the sample often even less, 5–50 nm. Also, in this method, the specimen has to be probed point by point, and an image is obtained by scanning (Fig. 5.9). The method is sometimes referred to as near-field scanning optical microscopy (NSOM). Because the probe is so close to the sample, with a few modifications the setup can also be used for atomic (shear) force microscopy.

5.9 Optoacoustic Tomography and Microscopy

Both light and sound can be used for imaging. Light has an advantage over sound in that it can give more specific contrast, perceived by us as color. For scientific purposes, one can use light of specific wavelength for rather specific imaging of chemical compounds, such as hemoglobin, oxyhemoglobin, or nucleic acid. One drawback of light for imaging of biological objects is that it is almost completely scattered within a short distance (less than 1 mm) in biological tissue, and some light does not even penetrate very deep.

Sound also has advantages over light for biological imaging. Ultrasonic imaging for medical purposes was pioneered by Hellmuth Hertz at Lund University (http://en.wikipedia.org/wiki/Carl_Helmut_Hertz) and has been extensively used for imaging of hearts, bowels, nasal sinuses, livers, and fetuses. Many animals, such as dolphins and bats, have of course used sound for imaging long before that. Sound penetrates much deeper than light in biological tissue, and the scattering is a thousandfold lower than that of light. Another advantage is that it travels more slowly, and one can therefore more easily determine the distance to a reflecting structure by measuring the time of travel from source to receiver and thus map organs in three dimensions. The wavelength of the sound waves cannot be made as short as of light, and therefore the spatial resolution is limited, and the contrast is not as great and in particular not as discriminatory (colorful) as that of light.

The optoacoustic technique combines the advantages of optical and acoustical imaging. In this technique, the object is illuminated with light, but it is an acoustic signal that forms the image.

If a light-absorbing object is exposed to a very short (nanosecond range) pulse of light (a laser is used for this), its temperature is transiently slightly increased, and it undergoes a rapid, small expansion. This creates a pressure pulse, in other words a sound wave, that travels out from the object. If we have pressure receivers ("microphones") placed at four points around the object, we can calculate the position of the object after recording the time of arrival of the pressure pulse to the four receivers. This is the basic principle of optoacoustic imaging. In case we are pursuing photoacoustic computed tomography (see below), it does not matter if the light is diffuse when it reaches the object to be imaged, since the imaging is not done by the light, but by the sound. To image an extended three-dimensional object is, of course, a bit more complicated and involves a lot of sophisticated mathematics and

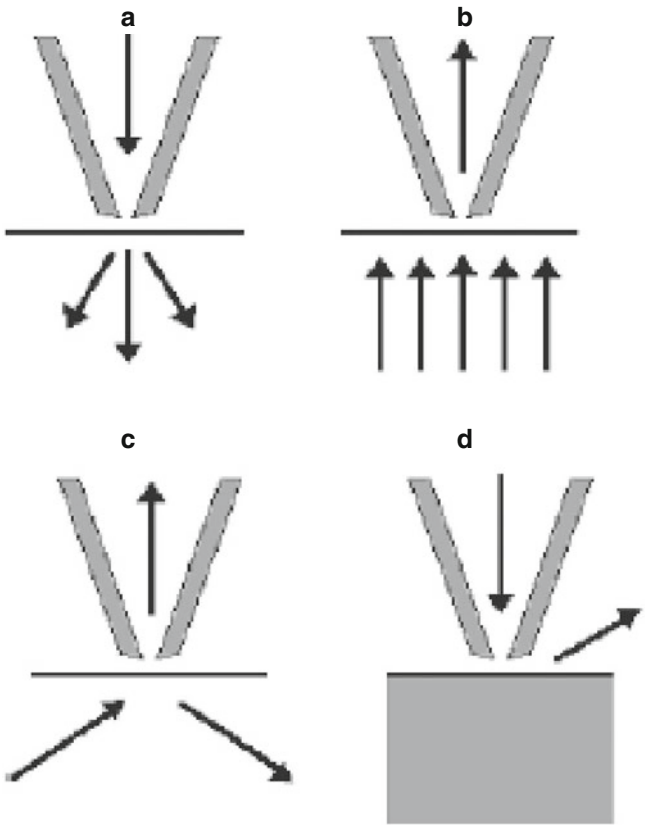

Fig. 5.9 Four methods for scanning near-field microscopy. (**a**, **b**) Light is either delivered (**a**) from the tapered fiber or collected (**b**) by it. (**c**) How "frustrated" total reflection is used. All light coming from below undergoes total reflection except where the evanescent field from structures in the sample comes sufficiently close to the fiber. (**d**) Light delivered from the fiber is scattered from structures in the sample only if they come within reach of the evanescent field, and then the scattered light can be picked up by a photomultiplier or photodiode

equipment. There are three main branches of photoacoustic imaging techniques: photoacoustic microscopy (PAM), photoacoustic computed tomography (PACT), and photoacoustic endoscopy (PAE).

For photoacoustic microscopy, a laser pulse is focused onto a spot not very far from the surface of a tissue, and a sound receiver is focused onto the same spot, either from the same or the opposite side, so it is a kind of confocal microscopy. The specimen is then scanned by moving the focusing spot in a raster-like way, repeating the laser pulses to cover the whole area of interest.

For photoacoustic computed tomography, the laser pulses are not focused but are distributed across the whole specimen, and the receiver is moved around to receive sound pulses from all sides. A computer program transforms the received pressure signals to a three-dimensional image of the object. Both methods are described in more detail by Wang (2009) and Wang and Hu (2012), who also provide many references.

5.10 Further Methods for "Super-Resolution Microscopy"

A large number of other methods for "super-resolution microscopy" have recently been developed and are being developed. A good overview is available on the Internet at http://en.wikipedia.org/wiki/Super_resolution_microscopy (accessed on August 24, 2013).

5.11 Optical and Photoacoustic Detection of Malaria Infection via Vapor Nanobubbles

Over 200 million people are infected by malaria every year, and about 600,000 die. The sooner infection is detected, the greater the chance of survival, but until now, diagnosis can be made only from blood samples. Recently, Lukianova-Hleb et al. (2013) have described a new noninvasive and rapid method for the first transdermal detection of malaria infection as low as 0.00034 %, so far tested on animals (and on infected humans and human blood cells in vitro). It depends on the photothermal properties of an excretion product from the malaria parasite, *Plasmodium falciparum*.

Plasmodium develops inside red blood cells, which contain mainly hemoglobin. The parasite metabolizes the protein part of the molecule, but the heme content far exceeds what the organism needs and must be disposed of. This results in formation of nanoparticles of modified heme, so-called hemozoin. These particles have a well-ordered, almost crystalline structure and, for this reason, have an absorption spectrum that differs from that of hemoglobin or of amorphous or dissolved heme. This allows to efficiently generate a vapor nanobubble around hemozoin with a laser pulse. Furthermore, when a short laser pulse is applied, a vapor nanobubble spectral narrowing takes place, similar to that which has been observed for gold nanoparticles: a short and intense laser pulse applied at the absorption maximum creates a gas bubble around the nanoparticle (Lukianova-Hleb et al. 2013). This event can be recorded either as a pressure pulse (photoacoustic method) or as increased light scattering, using a second (probe) laser pulse applied a short time after the first (actinic) pulse. It is likely that the photoacoustic method will prove to be the more useful for noninvasive detection of malaria infection in the human body.

Figure 5.10 shows that the action spectrum for the vapor nanobubble signal from hemozoin is quite different from that of the absorption spectrum of healthy blood. By choosing 672 nm as the wavelength for the laser pulse, one can avoid any interference from undamaged hemoglobin. No photoacoustic signal is obtained for any wavelength if hemozoin is not present, as is shown by the green curve. Figure 5.11 shows the kind of images that are obtainable with this technique and

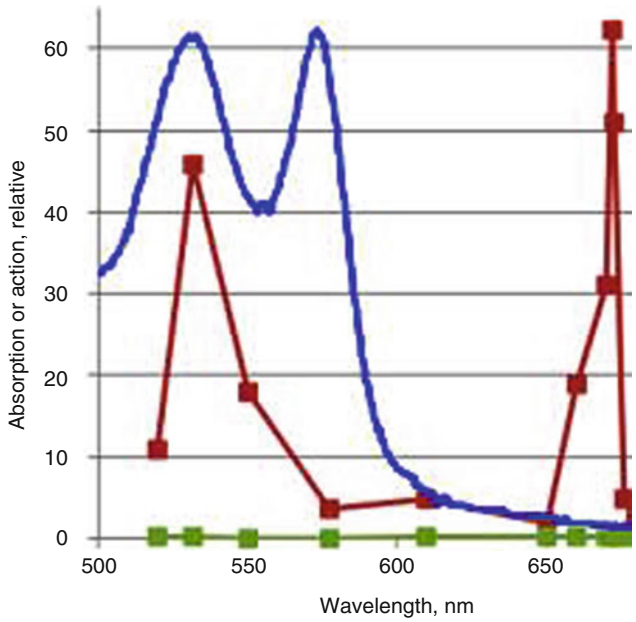

Fig. 5.10 Photoacoustic signal from an infected red blood cell containing hemozoin (*red*) and a healthy cell (*green*). The *blue curve* shows the absorption spectrum of an oxygenated blood, corrected for scattering and normalized to the same maximum as the *red curve* (Data from Lukianova-Hleb et al. (2014), redrawn)

how the hemozoin-containing cells can be destroyed by a laser pulse.

5.12 Quantum Dots

"Quantum dots" is a rapidly expanding field. A search for this term on the Web of Science in September 2014 gave 1,55,500 hits, the first two from 1986. Although the term quantum dot had not yet been coined, a few earlier publications, such as Brus (1984) and Rosetti et al. (1982), do in fact deal with them. During the past decade, each year an average of 926 more papers on the subject have been published than in the preceding year. The main application in biology is for fluorescent labeling of cell constituents. Overviews of biological applications are provided by Michalet et al. (2005), Du et al. (2006), Klostranec and Chan (2006), and Xu et al. (2006). Before going further into biological applications, it is necessary to begin with a general introduction to quantum dots.

A quantum dot is a semiconductor (or sometimes a metal) nanostructure that confines mobile charges, negative electrons, and/or positive holes, in all directions. In this respect, the concept resembles the somewhat older ones, quantum well and quantum wire. However, a quantum well confines the charges in just one dimension and allows them to move freely in the other two, while a quantum wire allows the charges to move freely in one direction. The restriction can have various causes, such as electric potential gradients or interfaces between different materials. Quantum dots usually consist of 100–100,000 atoms. The smallest ones are slightly less than 2 nm across and the largest ones of interest to biologists about 15 nm. Some of them share many properties with atoms, such as having discrete energy levels. Because the charges are spatially confined, quantum dots have optical properties which differ from the properties of larger objects of the same materials. The same principles apply here as for the double bond systems with π electrons described in the chapter on spectral tuning in biology. Thus, smaller size corresponds to a smaller optical wavelength, and just by choosing size, a quantum dot can be tuned, so it absorbs or emits light of a certain wavelength, without adjustment of chemical composition.

Although many scientists regard quantum dots to be semiconductors by definition, structures that behave in much the same way may also be constructed of some metals (Zheng et al. 2007), and therefore, it may also be acceptable to speak about metal quantum dots.

The most popular quantum dot material so far for basic and applied work has been cadmium selenide, CdSe. In biological contexts, the main disadvantage of this material is its toxicity due to release of cadmium ions, but with appropriate coating (cladding), this disadvantage can be decreased (Bakalova et al. 2005; Derfus et al. 2004; Hardman 2006). There are also other reasons to provide the quantum dot core with a cladding. It increases the quantum yield for emission and may modify the wavelength. Quantum dots with CdSe cores are usually coated with ZnS and outside this a shell of something else Bakalova et al. (2006). The outermost layer can be configured with ligands to biological structures, for instance, polynucleotides or antibodies.

The photon energy ($E=h\nu$) and thus the wavelength ($\lambda=c/\nu$) of the light emitted from a quantum dot depend mainly on two quantities, the energy gap E_{bulk} in the bulk material of which the (core of) quantum dot is made and the extra energy arising from confinement of the mobile charge, E_{conf}: $hc/\lambda=E=E_{bulk}+E_{conf}$.

A somewhat simplified derivation from the time-independent Schrödinger equation of a formula for the emission wavelength of a spherical quantum dot with mobile electrons and holes, as, for instance, one made of CdSe, leads to $E_{conf}=h^2/(6.513\bullet 8m_eR^2)$, where m_e is the electron mass and R the radius of the quantum dot. The value of E_{bulk} varies, of course, with the material, and for CdSe, it is $3.85\cdot10^{-19}$ J. Using this relationship, we can produce the solid curve in Fig. 5.12.

As seen in Fig. 5.12, with increasing quantum dot size, the emission wavelength approaches a limiting value. Emission wavelengths up to 700 nm can be obtained with CdSe as core material (Wang and Seo 2006), and other types of quantum dots can be produced that emit above 1,000 nm (see Michalet et al. 2005 for examples). Because, in practice,

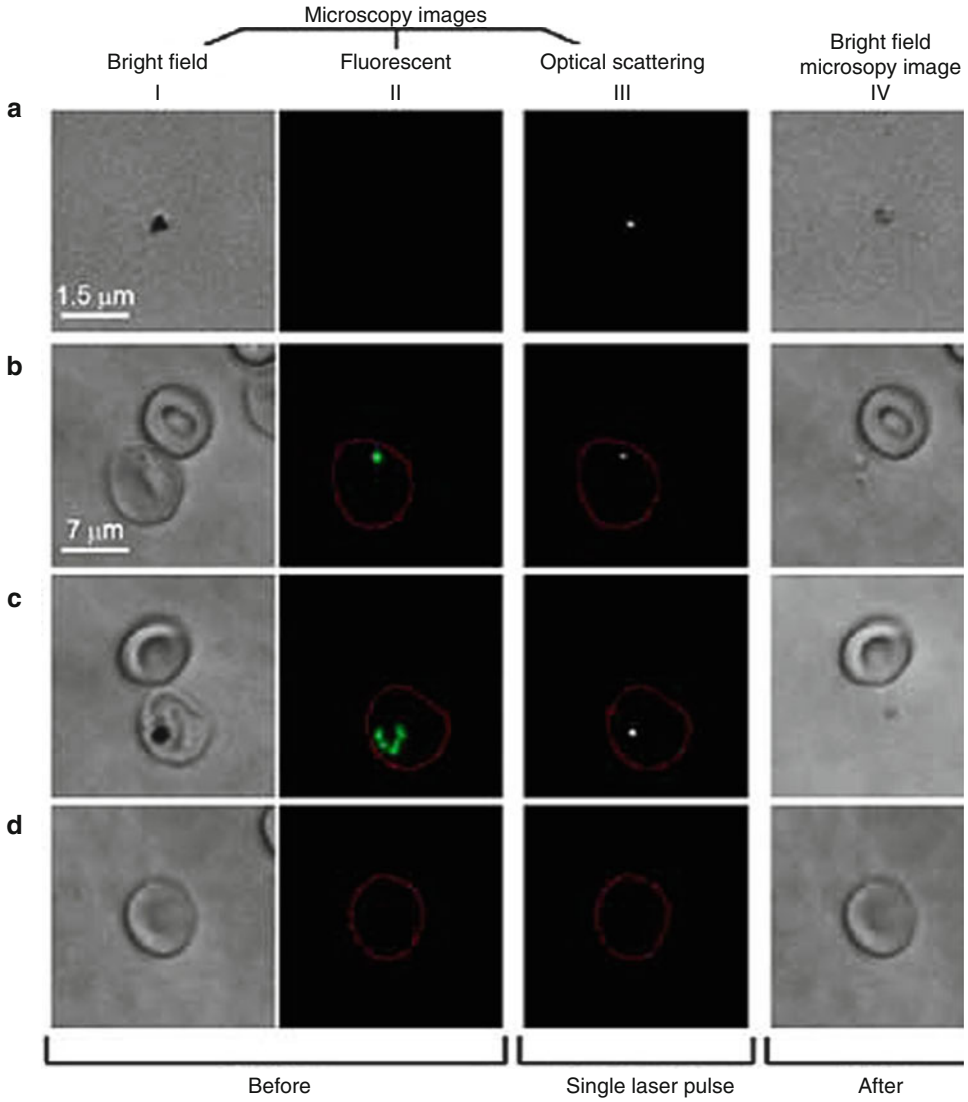

Fig. 5.11 Pulsed laser (532 nm, 40 mJ·cm^{-2}) exposure of isolated hemozoin and cultured human blood cells results in hemozoin-dependent nanobubble generation, which is detectable optically and acoustically and results in infected cell destruction. (**a**) Hemozoin nanoparticles in water. (**b**) Uninfected (*top*) and *P. falciparum* early ring stage–infected (*bottom*) human red blood cells. (**c**) Uninfected (*top*) and *P. falciparum* mature schizont stage–infected (*bottom*) human red blood cells. (**d**) Uninfected human RBC. (*I*) Bright field image shows cells before laser pulse. (*II*) SYBR green I fluorescence image reveals parasite presence before laser pulse. (*III*) Time-resolved optical scattering images of nanobubbles. (*IV*) Bright field images after laser pulse (From Lukianova-Hleb et al. (2014))

all quantum dots in a preparation do not have exactly the same dimensions, the emission is spread out over a spectral band of finite width. However, quantum dots have emission bands more narrow than most fluorescent molecules. The absorption spectrum is, on the other hand, quite wide (Fig. 5.13), so different types of quantum dots can be excited with the same kind of light, which is an advantage when one wishes to image quantum dots emitting different colors at the same time in the same sample.

The power dependence with the quantum dot radius raised to −2 based on the simplified theory is not universal, and Brus (1984) and more recently Wang and Seo (2006) and Cademartiri et al. (2006) derived more accurate relationships. One of these (more relevant for CdSe quantum dots) is shown in Fig. 5.10 (dashed curve).

The main advantages of using quantum dots rather than molecular fluorescent labels are (1) greater stability against bleaching, (2) higher fluorescence quantum yield and therefore stronger fluorescence, (3) more narrow emission bands, and (4) the possibility of continuously tuning of the emission wavelength and choosing any desired value. The first two properties make it possible to follow single-labeled macromolecules as they move around in a cell, are taken up, or are excreted. The second two properties make it possible to label several different kinds of molecule in different colors in the same preparation.

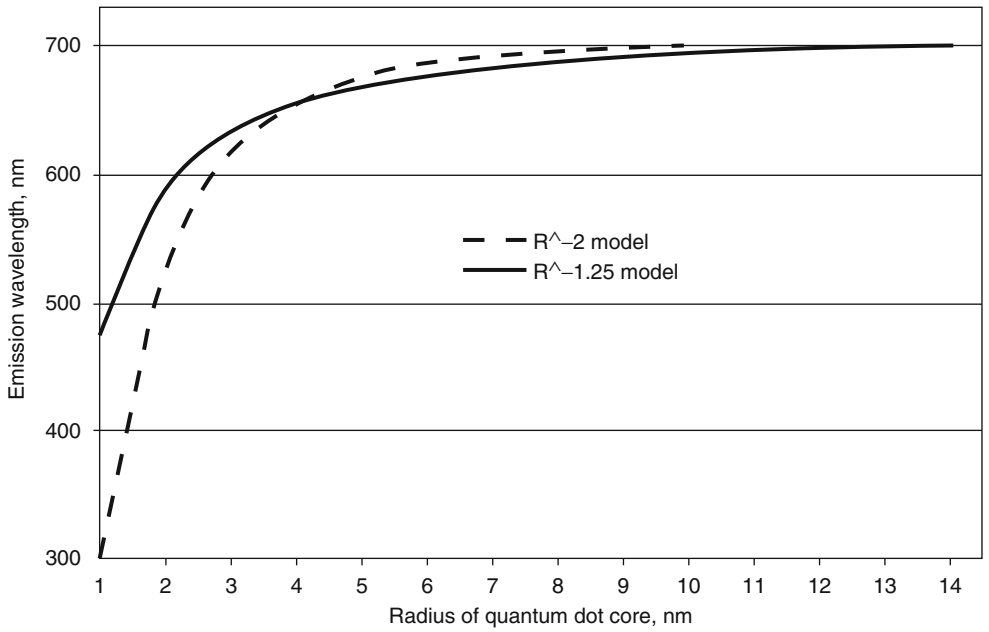

Fig. 5.12 Emission wavelength versus quantum dot radius for spherical CdSe quantum dots without cladding, computed as described in the text. The *solid line* is for the empirical model with exponent −1.25, the *dashed line* for the theoretical model with exponent −2. An E_{bulk} value of $2.78781 \cdot 10^{-19}$ J is used here

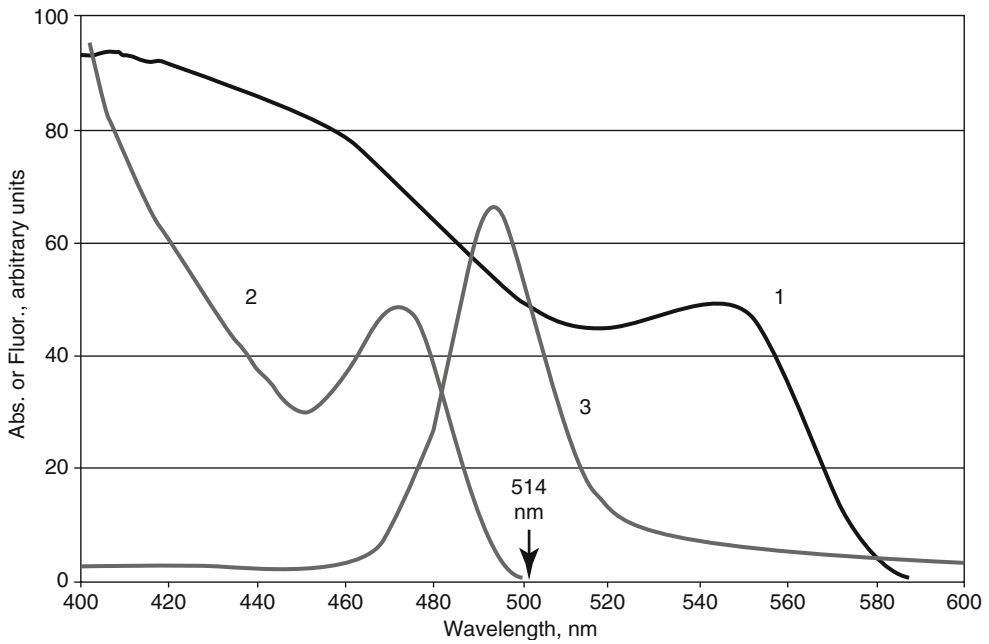

Fig. 5.13 Phototuning of CdSe quantum dots with SiO_2 shells. (*1*) Absorption spectrum of the original quantum dots. The vertical axis does not show absorbance in this diagram, but absorption coefficient divided by scattering coefficient, but this does not make much difference in shape of the spectrum. These original quantum dots have an absorption maximum at 553 nm and an emission maximum at about 572 nm. After photoetching for 20 h with 514-nm light, the absorption spectrum changes to *curve 2* and the emission spectrum to *curve 3*. Quantum dots with other emission maxima can be obtained by photoetching with light of other wavelengths. In every case, the absorption spectrum changes so that absorption becomes practically zero at the etching wavelength (Redrawn and simplified, after Torimoto et al. (2006))

The fluorescence yield of small CdSe quantum dots can be increased to >0.5 by careful control of temperature, Cd/Se ratio, and other factors during production (Donega et al. 2003) and following treatment with ultraviolet radiation (Bakalova et al. 2005). McBride et al. (2006) show that structural relations between the CdSe core and the ZnS shell are important. The quantum yields decrease with increasing quantum dot size (increasing wavelength), which is attributed to decreasing overlap between the wave functions for electrons and holes. Larger quantum dots, on the other hand, absorb more excitation light. Quantum dot size and thus emission wavelength can be varied by varying the duration of crystal growth time at high temperature and also by adjusting the temperature (190–270 °C) for crystal growth (Wang and Seo 2006). A particularly elegant method to tune cadmium selenide quantum dots with SiO_2 shells has been devised by Torimoto et al. (2006), who use monochromatic light of selected wavelengths to etch the quantum dots (by photochemical oxidation of the selenium) until they stop absorbing the etching light. The peak emission will then be at about 20 nm lower wavelength than the etching light. This procedure should also help to decrease the size variation between the particles and thus result in a narrower emission spectrum. The SiO_2 shell serves to prevent the particles from coalescing.

Because of the extremely low detection limits of quantum dot fluorescence labels, they can be employed for various forensic purposes, such as detection of anthrax spores (Park et al. 2006), specific DNA traces (Raymond et al. 2005), or fingerprints (Bouldin et al. 2000; Menzel et al. 2000). Specificity and suppression of background fluorescence interference can be improved by monitoring the fluorescence lifetime (Bouldin et al. 2000).

Among applications on the medical side, early cancer detection (Nida et al. 2005; Chu et al. 2006; Hu et al. 2006; Li et al. 2006) deserves special mention.

One of the most interesting properties discovered during the study of single quantum dots is that even if they are steadily illuminated, they usually do not fluoresce continuously, but intermittently. In other words, they "turn on and off," a phenomenon known as blinking. Although of great theoretical interest, we shall not expand on the reasons for blinking here. In some cases, blinking may be a disadvantage, for instance, if quantum dots are used for tracking molecules which move rapidly in unpredictable ways, but in most cases, it is not a problem because of the high speed of on and off switching. In other cases, blinking can be taken advantage of. For instance, blinking makes it possible to determine whether light comes from a single or two quantum dots (by determining whether the blinks have just one light level or two) and to determine the distance between two quantum dots, even if they are too close to be resolved in the microscope (Lagerholm et al. 2006). Blinking can be suppressed by covering the quantum dots in a special way (Hammer et al. 2006).

For some applications, it may be of advantage to make the quantum dots emit light without being themselves illuminated, and this is possible to achieve by supplying energy in some other way (So et al. 2006). If the quantum dots are tuned to emit very long-wavelength radiation, they may be visible (by instruments) even if buried deep in the body, something that may be of great value for tracing cancers.

Because of the possibility of seeing individual quantum dots, many different molecules have been individually tagged with them, for instance, DNA (Crut et al. 2005) and RNA (Chan et al. 2005) molecules and ion channels (O'Connell et al. 2006; Nechyporuk-Zloy et al. 2006). Since quantum dots can be counted, they have also been used for counting molecules. For such a count to be reliable, however, one has to be able to ascertain that all molecules become labeled, and O'Connell et al. (2006) have worked out a procedure to check if this is the case, using two labels with different colors and seeing how many two-color labeled points there are in relation to those labeled with one color only. In their particular case, they determined that a membrane channel protein could be labeled with a maximum of two quantum dots.

By conjugating quantum dots to signal peptides (used by cells to target proteins to correct organelles), the quantum dots can be directed to specific organelles (Hoshino et al. 2004). Many other examples of adaptations of quantum dot surfaces for different cellular targets are described by Medintz et al. (2005). Mutations in DNA can be detected with a method employing quantum dots (Yeh et al. 2006).

Many different types of quantum dots are now commercially available. Some of them are so easy to make that several student experiments for this have been worked out, both for CdS and for CdSe quantum dots (Fig. 5.14) (Kippeny et al. 2002; Boatman et al. 2005; Winkler et al. 2005). Traditionally, CdSe quantum dots have been manufactured at high temperature using poisonous organic solvents, but Deng et al. (2006) show that it is also possible to work below 100 °C and use water as solvent. In addition to production by these "wet" methods, there exists a "dry" method for manufacture of another kind of quantum dots for the electronics industry.

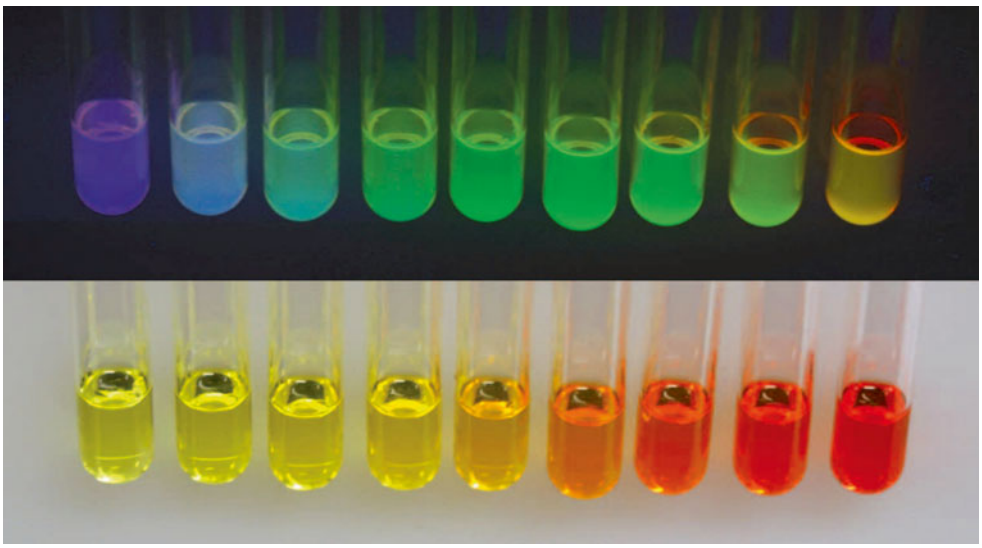

Fig. 5.14 CdSe quantum dots prepared in a student experiment. The *top picture* shows fluorescent colors with UV-A excitation, the *bottom* one the absorptive colors under white light. CdSe quantum dots can be prepared emitting fluorescence at longer wavelength, up to 700 nm (From Boatman et al. 2005 with permission from *J Chem Educ*. Vol. 82, No. 11, pp. 1697–1699; copyright ©2005, Division of Chemical Education, Inc.)

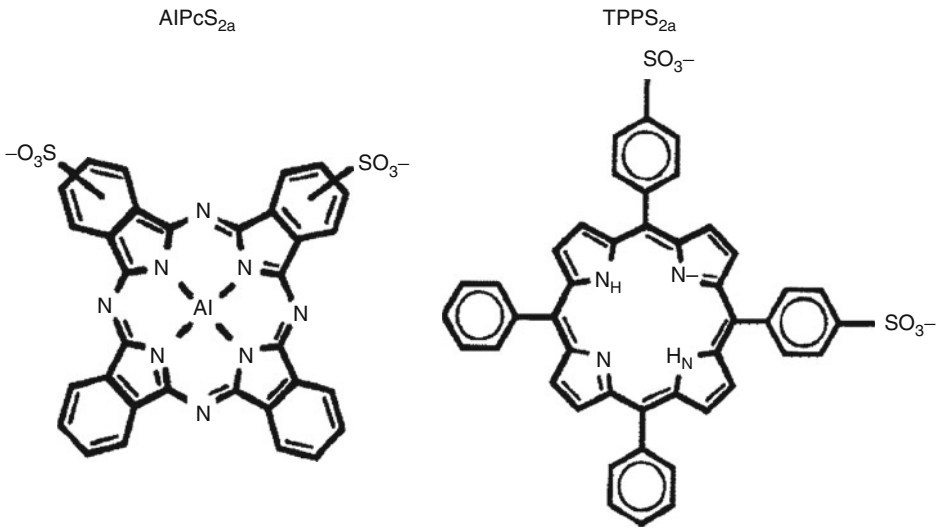

Fig. 5.15 Two photosensitizers that become specifically localized to endocytic vesicle membranes after being taken up into cells. TPPS2a is *meso*-tetraphenylporphine with two sulfonate groups on adjacent phenyl rings, and AlPcS2a is aluminum phthalocyanine with two sulfonate groups on adjacent rings (From Høgset et al. (2004))

5.13 Photochemical Internalization

Photochemical internalization is a technique for delivering macromolecules or other particles to the cytoplasm of cells. Molecules that would otherwise be excluded from the cell can be made to pass through the cell by being combined with a suitable molecule or atom group that causes it to be taken up into a vesicle by endocytosis. A problem with this is that the material taken up in a cell remains in membrane vesicles and may eventually end up in lysosomes and be broken down there. The enclosing membrane can, however, be punctured by photochemical production of singlet oxygen (Berg et al. 1999). Singlet oxygen is very short lived in vivo (Moan and Berg 1991) and therefore does not diffuse more than a few nanometers (20 nm at most) before being destroyed. Therefore, the photodynamic attack on the vesicle membrane is most efficient if the sensitizing pigment is incorporated into the vesicle membrane. Some photosensitizers have, in fact, been found which after uptake in cells become specifically localized to lysosome membranes (Fig. 5.15). The photosensitizer may be administered together with the

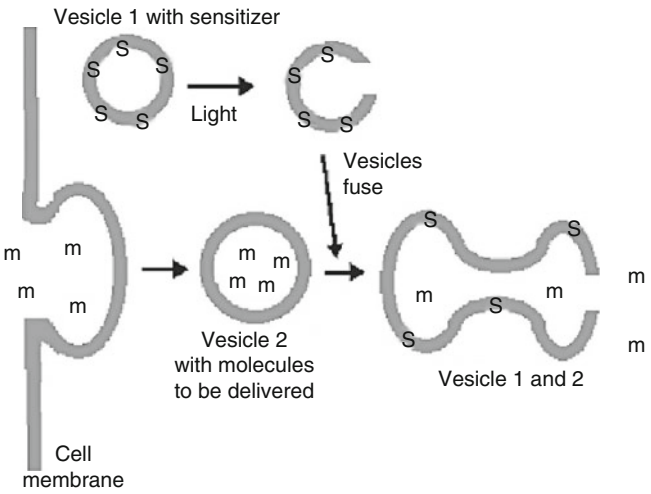

Fig. 5.16 Photochemical internalization using preloaded sensitizer. The cell is first treated with sensitizer(*s*) and the vesicles containing sensitizer punctured with light. When then the molecules (*m*) to be delivered to the cytosol are taken up by endocytosis, the endocytosis vesicles fuse with the already punctured vesicles, and the molecules are released to the cytosol (Redrawn and modified from Høgset et al. (2004))

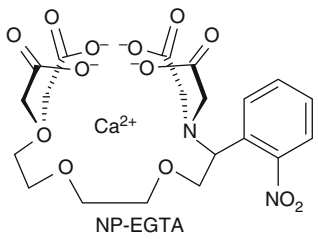

Fig. 5.17 Nitrophenyl ethylene glycol-bis(2-aminoethyl) *N*,*N*,*N*′,*N*′-tetraacetic acid, an example of a substance that can be used to deliver caged calcium ions

substance to be taken up. Alternatively, as shown in Fig. 5.16, the cell may be preloaded with the sensitizer and lysosomes punctured with light.

When afterwards the substance is taken up by endocytosis, the endocytic vesicles fuse with the punctured lysosomes and the substance is released to the cytosol.

An alternative to generation of singlet oxygen for puncturing liposomes is to use photocleavable lipids for constructing vesicle membranes (Chandra et al. 2006).

Many different kinds of molecule and molecular aggregates can be delivered to cells with liposomes in this way, and there are several variants of the method. One is to combine the molecule to be delivered in a liposome with a cationic peptide or cationic polyethyleneimine–amino acid combination. In this way, a faulty (mutated) gene can be replaced with a correct one and find its proper place in the nucleus (Ndoye et al. 2006).

An advantage of photochemical internalization is that it can be very specifically applied to individual cells or groups of cells, for instance, cancers, while a drug remains membrane enclosed and inactive in surrounding cells. Such specificity is achieved both by directing the membrane-puncturing light and by choosing sensitizers which are targeted to, for instance, cancer cells.

The other method for getting molecules where you want to have them in the cell is to attach them to a suitable carrier molecule. We have already mentioned the cell membrane-penetrating cationic peptides, but other ligands can be used for specific purposes. This so-called caged compound can then be set free by breaking the bond to the carrier molecule with light. An example is the delivery of oligonucleotide to the cell nucleus described by Ghosn et al. (2005). They attached the oligonucleotide to 1-(4,5-dimethoxy-2-nitrophenyl) ethyl ester (DMNPE). The DMNPE alters the charge and makes the molecule more lipophilic, so it can pass the membranes into the nucleus. As long as the oligonucleotide is attached to DMNPE, replication is blocked, but after breaking the attachment by irradiation with 365-nm UV-A radiation, the oligonucleotide becomes integrated into the genome. The authors used an optical technique (a so-called molecular beacon) to check whether hybridization took place or not. Alternatives to DMNPE have been investigated by Kim and Diamond (2006). Marriott et al. (2003) describe how proteins can be caged by use of bromomethyl-3,4-dimethoxy-2-nitrobenzene (BMDNB) attached to cysteine residues in the protein. An alternative approach for caging proteins is the introduction of unnatural amino acids through mutagenesis (Petersson et al. 2003).

Calcium ion is an important cellular messenger. The Ca^2+ concentration in the cytosol is usually near 0.1 μmolar. When it is caused to rise, a number of processes, dependent on the type of cell, are initiated. The Ca^2+ is released from organelles, the endoplasmic reticulum, or, in plants, the cell wall. To study these signaling pathways, it is desirable to be able to initiate experimentally a rise in cytosolic calcium concentration without having to activate the initial part of the signaling pathway. This can be done by supplying the cell with caged calcium ions, i.e., calcium ions in a cage of a chelator, which can be photochemically decomposed. Bacchi et al. (2003) describe a number of chelators that can be used in this way, nitrophenyl ethylene glycol-bis(2-aminoethyl) *N*,*N*,*N*′,*N*′-tetraacetic acid (NP-EGTA) being one example (Fig. 5.17).

5.14 Photogating of Membrane Channels and Related Techniques

For a long time, investigators of the nervous system have used electrodes to stimulate nerve cells and find out what kind of signals they conduct and what the result of their activity is. To this, new methods have now been added: photostimulation or photoinhibition.

There are basically three ways of making it possible for light to affect nerves:

1. Photodelivery of caged neurotransmitters. An example of this was provided by Callaway and Katz (1993). They bathed brain slices in a solution containing L-glutamic acid a-(4,5-dimethoxy-2-nitrobenzyl)ester. This compound in itself is inactive. When a brief (1 ms) pulse of ultraviolet radiation is delivered to the preparation, the neurotransmitter L-glutamic acid is released, and a spike of inward current can be recorded. The procedure can be repeated at least 30 times. Photorelease of caged compounds is treated more generally in the previous section.
2. Use of rhodopsins. Natural photogating of membrane channels takes place in our eyes with the help of rhodopsin in the membranes of outer segments of rods and cones. Also, in some microorganisms similar events occur, mediated by chromoproteins similar to our rhodopsins. Both vertebrate rhodopsin and so-called channelrhodopsin from a green alga have been used for artificial gating of other channels than their natural ones (Boyden et al. 2005; Li et al. 2005; Zhang et al. 2006). Genetic engineering is used to express the proteins in the desired tissues and couple them to the signaling pathways for the desired membrane channels. This is one aspect of "optogenetics." The definition of optogenetics varies, but according to Deisseroth (2011), it is "the combination of genetic and optical methods to achieve gain or loss of function of well-defined events in specific cells of living tissue." A general recent overview is provided by Packer et al. (2013).
3. Use of artificial pigments to regulate the channel. These methods can, in turn, be divided into two categories. A molecule that changes conformation upon illumination can be attached directly to the channel protein so that a part of it either blocks the channel or not, depending on the shape of the pigment molecule, or the pigment can be incorporated into the lipid of the membrane and change its conformation. The first method was pioneered by Lester et al. (1980), who chemically modified the nicotinic acetyl choline receptor to make it light sensitive. Banghart et al. (2004) used the method to regulate a potassium channel. They used a compound consisting of maleimide–azo group–quaternary amine. The maleimide reacted chemically with a cysteine sulfhydryl group in the channel protein, the azo group undergoes *cis–trans* isomerization upon absorption of light, and the nitrogen in the amine carries a positive charge, which, in the correct position, can prevent potassium ions from passing the channel. The arrangement is shown in Fig. 5.18. The *cis–trans* isomerization of the compound is photoreversible, and the photoequilibrium spectra (of same shape as action spectra) are shown in Fig. 5.19.

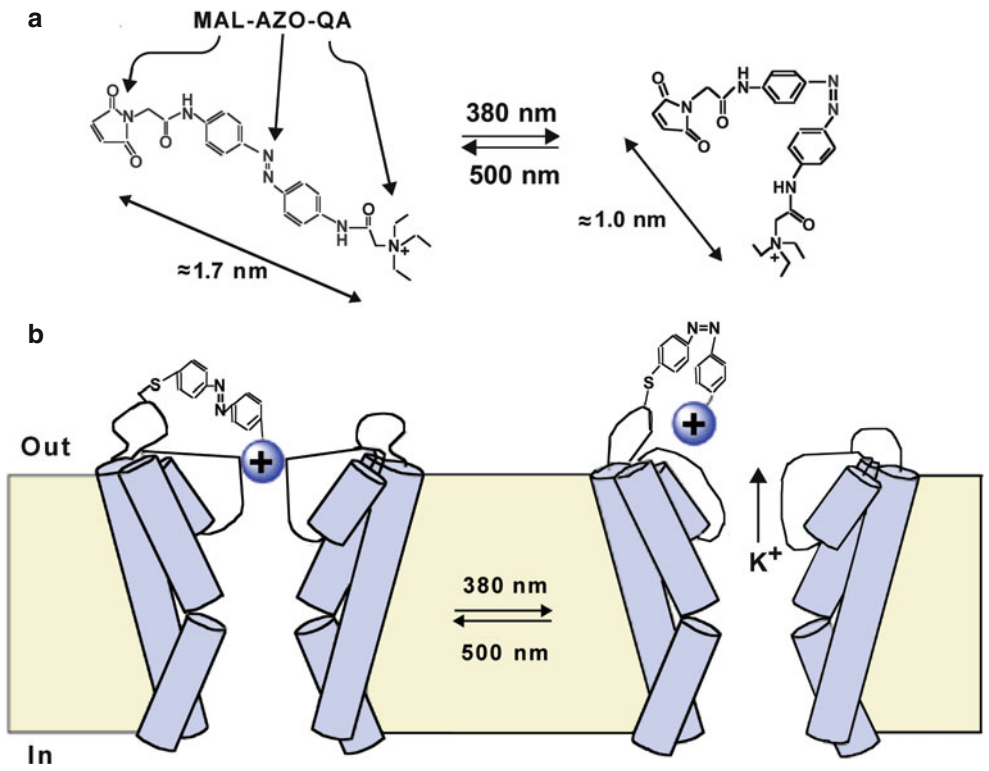

Fig. 5.18 (**a**) The reversibly photochromic chromophore consisting of a maleimide group (MAL), an azo group (AZO), and a quaternary ammonium nitrogen (QA). The latter is, in turn, attached to the potassium channel protein. When the chromophore absorbs 380-nm radiation, the distance between its ends decreases by 0.7 nm (7 Å). (**b**) The potassium channel is reversibly blocked by the positive charge on the chromophore by 500-nm light and opened again by 380-nm UV-A radiation (Reprinted by permission from Macmillan Publishers Ltd: *Nature Neurosci.* 12, 1381–1386 (Banghart et al. (2004), Copyright 2004)

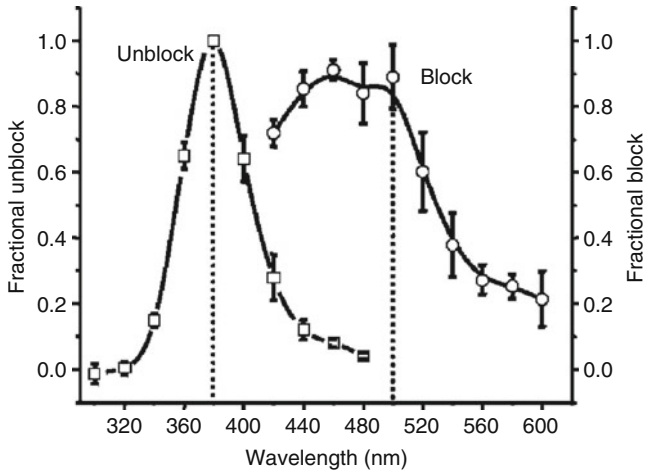

Fig. 5.19 Steady-state spectra for open and closed states of the potassium channel in Fig. 5.16. Steady-state spectra are action spectra normalized so that the sum of the ordinates of the curves is unity in the overlap region (From Banghart et al. (2004))

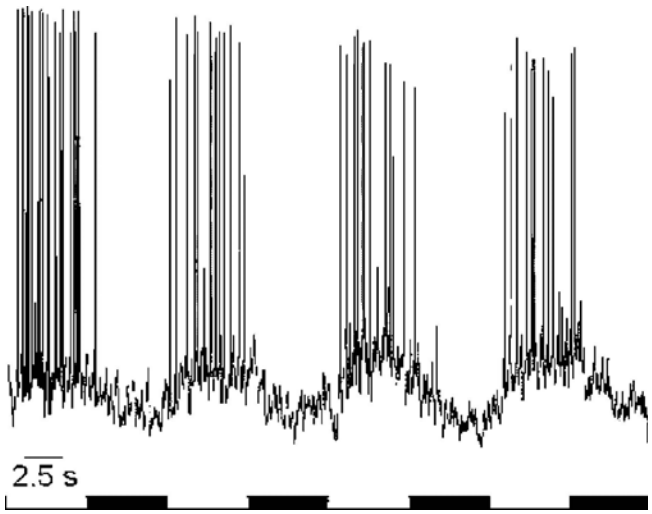

Fig. 5.20 The action potentials in a nerve cell are rapidly switched on by 390-nm radiation (*white bars*) acting on a modified membrane channel and equally rapidly switched off by 505-nm light (*black bars*) (From Chambers et al. (2006))

Membrane channel proteins can be stimulated electrically and in many cases also chemically. So what are the advantages and disadvantages of photoregulation? A particular cell can be probed with either an electrode or a light beam, while you can only use light to choose a particular kind of (modified) channel. The disadvantage with light is that you must modify the channel to make it light sensitive. With chemical stimulation, you can reach a particular channel type, but both spatial resolution and temporal resolution are extremely bad, especially compared to what can be achieved with light. As shown in Fig. 5.20, the switching of a channel on and off with light can be done very rapidly—within milliseconds.

Many of the experiments with photoregulation of membrane channels have been performed on nerve cells, and the results can be quite dramatic. Schroll et al. (2006) show how the behavior of fly larvae, in which neural cation channels have been amended with channel rhodopsin, can be altered just by illuminating the animals with blue light. Depending on what particular channel type has been modified, different behavioral changes result. Here we see another advantage of light stimulation over electrical stimulation: the animals can be completely unattached and free moving, and all the channels of a particular type can be immediately activated at once.

Folgering et al. (2004) show how a mechanosensitive channel can be regulated by light by incorporating a *cis–trans* photoreversible phospholipid-mimicking molecule into the lipid bilayer, so that the membrane can be photoreversibly distorted. So far, this has only been done in vitro in patch-clamp experiments, but it does not appear impossible to use a similar procedure with living organisms. Koçer et al. (2005) also made a mechanosensitive channel light switchable, but by a quite different method. By genetic engineering, they replaced a glycine residue in the channel protein by a cysteine residue. The sulfhydryl group of this cysteine, which was the only one in the protein, could then be reacted with a photochromic compound, by which the channel could be reversibly blocked by irradiation with visible light (λ>460 nm) and opened again by irradiation with UV radiation (366 nm).

Eisenman et al. (2007) have constructed a photoactivatable neurosteroid by which $GABA_A$ receptor function can be light regulated. It can be used for blocking neuron firing by 480-nm light.

Promising animal experiments for restoring vision in blind individuals have been done by many groups, including Doroudchi et al. (2011). These as several other researchers, used virus to introduce channelrhodopsin 2 into the defunct receptor cells. Channelrhodopsin 2 has the advantage of producing the required transport of sodium ions resulting in fast (within 50 ms) depolarization of the membrane in a more direct way than the natural system. The light effect is directly on the ion channel, while the natural system employs intermediate messengers. As long as only the natural channelrhodopsin 2 is used, vision is monochromatic with maximum sensitivity in the violet region. A recent thorough description of this field is provided by Natasha et al. (2013).

Chen et al. (2013) modified the plant UV-B receptor to create a system by which protein secretion can be controlled by UV-B and which can be used for studying protein trafficking in neurons.

5.15 Photocrosslinking and Photolabeling

It is of interest to know which molecules make contact with one another in the cells without forming strong and stable bonds. The three kinds of problem most often encountered

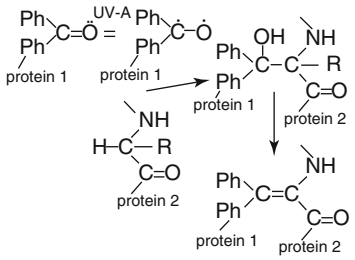

Fig. 5.21 Photocrosslinking two proteins using a protein (protein 1 in the figure) in which p-benzoylphenylalanine (pBpa) has been inserted. Ph stands for the phenyl group. Under irradiation with UV-A, the pBpa is converted to a diradical, which cross-links to an amino acid in protein 2. If R in this amino acid is hydrogen, dehydration takes place, resulting in the structure at the lower right. A more detailed diagram, showing intermediates and alternative reactions, is provided by Dormán and Prestwich (1994)

are elucidation of protein–protein contacts, protein–DNA contacts, and hormone–receptor contacts. Photocrosslinking and photolabeling are methods that have been used for this purpose for four decades. The older literature is reviewed by Brunner (1993), and emphasis here will be placed on specific recent developments.

For a couple of decades, it has been possible to incorporate unnatural amino acids into proteins in a site-specific way in vitro (Bain et al. 1989). A great leap was taken when Wang et al. (2001) designed a method for doing this in vivo. Soon thereafter (Chin et al. 2002), the method started to be used for incorporating photoreactive amino acids, which upon exposure to ultraviolet radiation form bonds to nearby protein molecules. In this way, the in vivo contact points between proteins can be determined. It would carry too far to describe the details of the method here, but up-to-date accounts are given by Xie and Schultz (2005, 2006). In brief, the function of the "amber" codon (UAG) is modified and its natural function suppressed and, using molecular components from Archaea, a translation system is engineered, which uses this codon to insert the desired amino acid. Later, the "opal" codon (UGA) was used for the same purpose. The first experiments dealt with insertion of the engineered systems into bacteria, but by now, researchers have succeeded in doing the same also with eukaryotic (including mammalian) cells. The types of unnatural amino acids that have been inserted now number over 30, and among them are three photoreactive ones, *p*-azidophenylalanine, *p-benzoylphenylalanine* (pBpa) (Fig. 5.21), and *p*-(3-trifluoromethyl-3H-diazirin-3-yl)-phenylalanine. Among these derivatives, pBpa is particularly useful, because it reacts to UV-A radiation (about 360-nm wavelength), which is not very destructive to cellular components and also gives greater penetration depth than the shorter-wavelength radiation necessary for the other photoreactive amino acids. A slight disadvantage to pBpa is that it has a preference for reacting with methionine. Therefore, it does not necessarily indicate the closest neighbor in an adjacent protein but one up to eight amino acid units away from it (Wittelsberger et al. 2006).

Results obtained by this method include elucidation of the contact between ATPase and a transport protein (Mori and Ito 2006), contacts between the components in dimeric enzymes (Blanck and Mehl 2006), and contacts between proteins in a signaling pathway (Hino et al. 2005).

When cells are irradiated with UV-C radiation, cross-links can develop between nucleic acids and adjacent proteins without any prior modification of either. These cross-links, however, are not very informative since they do not necessarily reflect closest neighbor relations. The use of UV-C also has drawbacks because of its destructive action and poor penetration in living matter. Therefore, Geyer et al. (2004) and others have developed more specific methods, which involve the addition of specific photoreactive groups that respond to UV-A radiation.

Also, some hormones can be photocrosslinked to their receptors without artificial photoreactants. Thus, the first photocrosslinking of a plant hormone, abscisic acid, was performed without prior modification (Hornberg and Weiler 1984). Also, steroid hormones containing unsaturated ketone groups can be photocrosslinked in the natural state (e.g., Gronemeyer and Pongs 1980; Schaltmann and Pongs 1982). If the hormone carries a label, such as a radioactive carbon atom, the hormone receptor is said to be *photoaffinity labeled.* But such experiments have later been complemented using hormones linked to artificial photocrosslinking groups (e.g., Todoroki et al. 2001), and for many other hormones, artificial photocrosslinkers are required (e.g., Beale et al. 1992; Swamy et al. 2000). To determine how RNA molecules contact ribosomal proteins, Demeshkina et al. (2003) used mRNA analogs containing a perfluoroarylazido group. Arylazido derivatives are highly reactive and can therefore be expected to react with and indicate close neighbors (not only amino acids in proteins but also bases in nucleic acids). The perfluoro group increases the lifetime of the excited singlet state and therefore also the reaction quantum yield.

5.16 Fluorescence-Aided DNA Sequencing

The Sanger method for DNA sequencing has enjoyed a remarkably long life in the rapidly developing field of molecular biology. However, the strong interest in DNA sequencing for phylogenetic research, forensic investigations, and other purposes has stimulated the search for cheaper and faster methods and methods allowing sequencing of single molecules. In the past few years, several methods using fluorescence techniques have been invented (Metzker 2005). Most of them are based either on the capillary electrophoresis introduced by Jorgenson and Lukacs (1981), or on

immobilizing DNA molecules on a substrate (Seo et al. 2005; Krieg et al. 2006), or on immobilizing an enzyme. Some of them can be used for sequencing single DNA molecules (Werner et al. 2003; Ramanathan et al. 2004; Bayley 2006). There are methods for labeling the bases in DNA with fluorophores with either absorption or emission spectra sufficiently different so that the bases can be distinguished by fluorescence (e.g., Lewis et al. 2005; Seo et al. 2005).

Another fluorescence method important in genomic research is fluorescence in situ hybridization (FISH) (see Jiang and Gill 2006 for a review on the application of the method to plants and references to other literature). In this method, a sequence-specific probe that is made to fluoresce is attached directly to DNA while it is still in the chromosome.

References

Ando R (2002) An optical marker based on the UV-induced green-to-red photoconversion of a fluorescent protein. Proc Natl Acad Sci U S A 99:12651–12656

Ashkin A (1970) Acceleration and trapping of particles by radiation pressure. Phys Rev Lett 24:156–159

Bacchi A, Carcelli M, Pelizzi C, Pelizzi G, Pelagatti P, Rogolino D, Tegoni M, Viappiani C (2003) Synthesis and spectroscopic and structural characterization of two novel photoactivatable Ca2+ compounds. Inorg Chem 42:5871–5879

Bain JD, Glabe CG, Dix TA, Chamberlin AR, Diala ES (1989) Biosynthetic site-specific incorporation of a non-natural amino acid into a polypeptide. J Am Chem Soc 111:8013–8014

Bakalova R, Zhelev Z, Jose R, Nagase T, Ohba H, Ishikawa M, Baba Y (2005) Role of free cadmium and selenium ions in the potential mechanism for the enhancement of photoluminescence of CdSe quantum dots under ultraviolet irradiation. J Nanosci Nanotechnol 5:887–894

Bakalova R, Zhelev Z, Aoki I, Ohba H, Imai Y, Kanno I (2006) Silica-shelled single quantum dot micelles as imaging probes with dual or multimodality. Anal Chem 78:5925–5932

Banghart M, Borges K, Isacoff E, Trauner D, Kramer RH (2004) Light-activated ion channels for remote control of neuronal firing. Nature Neurosci 12:1381–1386

Bayley H (2006) Sequencing single molecules of DNA. Curr Opin Chem Biol 10:628–637

Beale H, Hooley R, Smith SJ, Walker RP (1992) Photoaffinity probes for gibberellin-binding proteins. Phytochemistry 31:1459–1464

Berg K, Selbo K, Prasmickaite L, Tjelle TE, Sandvig K, Moan J, Gaudernack G, Fodstad Ø, Kjølsrud S, Anholt H, Rodal GH, Rodal SK, Høgset A (1999) Photochemical internalization: a novel technology for delivery of macromolecules into cytosol. Cancer Res 59:1180–1183

Betzig E, Chichester RJ (1992) Near-field optics: microscopy, spectroscopy, and surface modification beyond the diffraction limit. Science 257:189–195

Björn LO, Holmgren B (1996). Monitoring and modelling of the radiation climate. Abisko. Ecol. Bull. 45:204–209

Blanck SM, Mehl RA (2006) Systematic study of protein interfaces with genetically incorporated photocrosslinking amino acid, p-benzoylphenylalanine. Abstr Papers Am Chem Soc 231, 794

Boatman EM, Lisensky GC, Nordell KJ (2005) A safer, easier, faster synthesis for CdSe quantum dot nanocrystals. J Chem Educ 82:1697–1699

Bouldin KK, Menzel ER, Takatsu M, Murdock RH (2000) Diimide-enhanced fingerprint detection with photoluminescent CdS/dendrimer nanocomposites. J Forensic Sci 45:1239–1242

Boyden ES, Zhang F, Bamberg E, Nagel G, Deisseroth K (2005) Millisecond time-scale, genetically targeted optical control of neural activity. Nature Neurosci 8:1263–1268

Brunner J (1993) New photolabeling and crosslinking methods. Annu Rev Biochem 62:483–514

Brus LE (1984) Electron-electron and electron-hole interactions in small semiconductor crystallites: the size dependence of the lowest excited electronic state. J Chem Phys 80:4403–4409

Cademartiri L, Montanari E, Calestani G, Migliori A, Guagliardi A, Ozin GA (2006) Size-dependent extinction coefficients of PbS quantum dots. J Am Chem Soc 128:10337–10346

Callaway EM, Katz LC (1993) Photostimulation using caged glutamate reveals functional circuitry in living brain cells. Proc Natl Acad Sci U S A 90:7661–7665

Chalfie M, Tu Y, Euskirchen G, Ward WW, Prashier DC (1994) Green fluorescent protein as a marker for gene-expression. Science 263:802–805

Chambers JJ, Banghart MR, Trauner D, Kramer RH (2006) Light-induced depolarization of neurons using a modified shaker K^+ channel and a molecular photo- switch. J Neurophysiol 96:2792–2796

Chan PM, Yuen T, Ruf F, Gonzalez-Maeso J, Sealfon SC (2005) Method for multiplex cellular detection of mRNAs using quantum dot fluorescent in situ hybridization. Nucleic Acids Res 33:E161

Chandra B, Subramaniam R, Mallik S, Srivastava DK (2006) Formulation of photocleavable liposomes and the mechanism of their content release. Org Biomol Chem 4:1730–1740

Chandrasekhar, S. (1947) The transfer of radiation in stellar atmospheres. Bull. Amer. Math. Soc. 53, 641-711. Open access from http://projecteuclid.org/download/pdf_1/euclid.bams/1183510860

Chen D, Gibson ES, Kennedy MJ (2013) A light-triggered protein secretion system. J Cell Biol 201:631–640

Chin JW, Martin AB, King DS, Wang L, Schultz PG (2002) Addition of a photocrosslinking amino acid to the genetic code of *Escherichia coli*. Proc Natl Acad Sci U S A 99:11020–11024

Chu MQ, Song X, Cheng D, Liu SP, Zhu J (2006) Preparation of quantum dot-coated magnetic polystyrene nanospheres for cancer cell labelling and separation. Nanotechnology 17:3268–3273

Cotlet M, Goodwin PM, Waldo GS, Werner JH (2006) A comparison of the fluorescence dynamics of single molecules of a green fluorescent protein: one- versus two-photon excitation. Chem Phys Chem 7:250–260

Crut A, Géron-Landre B, Bonnet I, Bonneau S, Desbiolles P, Escude C (2005) Detection of single DNA molecules by multicolor quantum-dot end-labeling. Nucleic Acids Res 33:e98

Dacke M, Baird E, Byrne M, Scholtz, CH, Warrant EJ (2013) Dung beetles use the milky way for orientation. Curr Biol 23:298–300

Danuser G, Waterman-Storer CM (2006) Quantitative fluorescent speckle microscopy of cytoskeleton dynamics. Annu Rev Biophys Biomol Struct 35:361–387

Deisseroth K (2011) Optogenetics. Nat Methods 8:26–29

Demeshkina NA, Laletina ES, Meschaninova MI, Repkova MN, Ven'yaminova AG, Graifer DM, Karpova GG (2003) The mRNA codon environment at the P and E sites of human ribosomes deduced from photocrosslinking with pUUUGUU derivatives. Mol Biol 37:132–139 [Transl. from Molekulyarnaya Biologiya, Vol. 37, 147–155]

Deng D-W, Yu J-S, Pan Y (2006) Water-soluble CdSe and CdSe/CdS nanocrystals: a greener synthetic route. J Colloid Interface Sci 299:225–232

Derfus AM, Chan WCW, Bhatia SN (2004) Probing the cytotoxicity of semiconductor quantum dots. Nano Lett 4:11–18

Donega CD, Hickey SG, Wuister SF, Vanmaekelbergh D, Meijerink AJ (2003) Single-step synthesis to control the photoluminescence quantum yield and size dispersion of CdSe nanocrystals. Phys Chem B 2003(107):489–496

Donnert G, Keller K, Medda R, Andrei MA, Rizzoli SO, Lührmann R, Jahn R, Eggeling C, Hell SW (2006) Macromolecular-scale resolution in biological fluorescence microscopy. Proc Natl Acad Sci U S A 103:11440–11445

Dorman CJ (2007) Probing bacterial nucleoid structure with optical tweezers. BioEssays 29:212–216

Dormán G, Prestwich GD (1994) Benzophenone photophores in biochemistry. Biochemistry 33:5561–5673

Doroudchi MM, Greenberg KP, Liu J, Silka KA, Boyden ES, Lockridge JA, Arman AC, Janani R, Boye SE, Boye SL, Gordon GM, Matteo BC, Sampath AP, Hauswirth WW, Alan Horsager A (2011) Virally delivered channelrhodopsin-2 safely and effectively restores visual function in multiple mouse models of blindness. Molec Ther 19:1220–1229

Du W, Wang Y, Qingming Luo Q, Liu B-F (2006) Optical molecular imaging for systems biology: from molecule to organism. Anal Bioanal Chem 386:444–457

Eisenman LN, Shu H-J, Akk G, Wang C, Manion BD, Kress GJ, Evers AS, Steinbach JH, Covey DF, Zorumski CF, Mennerick S (2007) Anticonvulsant and anaesthetic effects of a fluorescent neurosteroid analog activated by visible light. Nature Neurosci 10:523–530

Elowitz MB, Surette MG, Wolf PE, Stock J, Leibler S (1997) Photoactivation turns green fluorescent protein red. Curr Biol 7:809–812

Folgering JHA, Kuiper JM, de Vries AH, Engberts JBFN, Poolman B (2004) Lipid-mediated light activation of a mechanosensitive channel of large conductance. Langmuir 20:6985–6987

Fricker M, Runions J, Moore I (2006) Quantitative fluorescence microscopy: from art to science. Annu Rev Plant Biol 57:79–107

Geyer H, Geyer R, Pingoud V (2004) A novel strategy for the identification of protein–DNA contacts by photocrosslinking and mass spectrometry. Nucleic Acids Res 32:e132

Ghosn B, Haselton FR, Gee KR, Monroe WT (2005) Control of DNA hybridization with photocleavable adducts. Photochem Photobiol 81:953–959

Grier DG, Roichman Y (2006) Holographic optical trapping. Appl Optics 45:880–887

Gronemeyer H, Pongs O (1980) Localization of ecdysterone on polytene chromosomes of *Drosophila melanogaster*. Proc Natl Acad Sci U S A 77:2108–2112

Habuchi S, Cotlet M, Gensch T, Bednarz T, Haber-Pohlmeier S, Rozenski J, Dirix G, Michiels J, Vanderleyden J, Heberle J, De Schryver FC, Hofkens J (2005) Evidence for the isomerization and decarboxylation in the photoconversion of the red fluorescent protein DsRed. J Am Chem Soc 127:8977–8984

Hammer NI, Early KT, Sill K, Odoi MY, Emrick T, Barnes MD (2006) Coverage-mediated suppression of blinking in solid state quantum dot conjugated organic composite nanostructures. J Phys Chem B 2006(110):14167–14171

Hardman R (2006) A toxicologic review of quantum dots: toxicity depends on physicochemical and environmental factors. Environ Health Perspect 114:165–172

Heim R (1994) Wavelength mutations and posttranslational autooxidation of green fluorescent protein. Proc Natl Acad Sci U S A 91:12501–12504

Hino M, Okazaki Y, Kobayashi T, Hayashi A, Sakamoto K, Yokoyama S (2005) Protein photo-crosslinking in mammalian cells by site-specific incorporation of a photo-active amino acid. Nat Methods 2:201–206

Høgset A, Prasmickaite L, Selbob P-K, Hellumb M, Engesæter BØ, Bonsted A, Berg K (2004) Photochemical internalisation in drug and gene delivery. Adv Drug Deliv Rev 56:95–115

Hornberg C, Weiler EW (1984) High-affinity binding-sites for abs*cis*ic acid on the plasmalemma of *Vicia faba* guard cells. Nature 310:321–324

Hoshino A, Fujioka K, Oku T, Nakamura S, Suga M, Yamaguchi Y, Suzuki K, Yashara M, Yamamoto K (2004) Quantum dots targeted to the assigned organelle in living cells. Micobiol Immunol 48:985–994

Hu FQ, Ran YL, Zhou ZA, Gao MY (2006) Preparation of bioconjugates of CdTe nanocrystals for cancer marker detection. Nanotechnology 17:2972–2977

Huang J, Xudong Wang X, Wang ZL (2006) Controlled replication of butterfly wings for achieving tunable photonic properties. Nano Lett 6:2325–2331

Jiang J, Gill BS (2006) Current status and the future of fluorescence in situ hybridization (FISH) in plant genome research. Genome 49:1057–1068

Jiang P, Yamauchi K, Yang M, Tsuji K, Xu MX, Maitra A, Bouvet M, Hoffman RM (2006) Tumor cells genetically labeled with GFP in the nucleus and RFP in the cytoplasm for imaging cellular dynamics. Cell Cycle 5:1198–1201

Jorgenson JW, Lukacs KD (1981) Zone electrophoresis in open-tubular glass capillaries. Anal Chem 53:1298–1302

Kim MS, Diamond SL (2006) Photocleavage of o-nitrobenzyl ether derivatives for rapid biomedical release applications. Bioorg Med Chem Lett 16:4007–4010

Kippeny T, Swafford LA, Rosenthal SJ (2002) Semiconductor nanocrystals: a powerful visual aid for introducing the particle in a box. J Chem Edu 79:1094–1100

Klostranec JM, Chan CW (2006) Quantum dots in biological and biomedical research: recent progress and present challenges. Adv Mater 2006(18):1953–1964

Koçer A, Walko M, Meijberg W, Feringa BL (2005) A light-actuated nanovalve derived from a channel protein. Science 309:755–758

Krieg A, Ruckstuhl T, Seeger S (2006) Towards single-molecule DNA sequencing: assays with low nonspecific adsorption. Anal Biochem 349:181–185

Krüger R, Kübler D, Pallissé R, Burkovski A, Lehmann WD (2006) Protein and proteome phosphorylation stoichiometry analysis by element mass spectrometry. Anal Chem 78:1987–1994

Lagerholm BC, Averett L, Weinreb GE, Jacobson K, Thompson NL (2006) Analysis method for measuring submicroscopic distances with blinking quantum dots. Biophys J 91:3050–3060

Lester HA, Krouse ME, Nass MM, Wassermann NH, Erlanger BF (1980) A covalently bound photoisomerizable agonist. Comparison with reversibly bound agonists at electrophorus electroplaques. J Gen Physiol 75:207–232

Lewis EK, Haaland WC, Nguyen F, Heller DA, Allen MJ, MacGregor RR, Berger CS, Willingham B, Burns LA, Scott GBI, Kittrell C, Johnson BR, Curl RF, Metzker ML (2005) Color-blind fluorescence detection for four-color DNA sequencing. Proc Natl Acad Sci U S A 102:5346–5351

Li X, Gutierrez DV, Hanson MG, Han J, Mark MD, Chiel H, Hegemann P, Landmesser LT, Herlitze S (2005) Fast noninvasive activation and inhibition of neural and network activity by vertebrate rhodopsin and green algae channelrhodopsin. Proc Natl Acad Sci U S A 102:17816–17821

Li ZH, Wang KM, Tan WH, Li J, Fu ZY, Ma CB, Li HM, He XX, Liu JB (2006) Immunofluorescent labeling of cancer cells with quantum dots synthesized in aqueous solution. Anal Biochem 354:169–174

Loudon R, Barnett SM (2006) Theory of the radiation pressure on dielectric slabs, prisms and single surfaces. Opt Express 14:11855–11869

Lukianova-Hleb EY, Volkov AN, Wu X, Lapotko DO (2013) Transient enhancement and spectral narrowing of the photothermal effect of plasmonic nanoparticles under pulsed excitation. Adv Mater 25:772–776

Lukianova-Hleb EY, Campbell KM, Constantinou PE, Braam J, Olson JS, Ware RE, Sullivan DJ Jr, Lapotko DO (2014) Hemozoin-generated vapor nanobubbles for transdermal reagent- and needle-free detection of malaria. Proc Natl Acad Sci U S A 111:900–905

Lukyanov KA, Chudakov DM, Lukyanov S, Verkhusha VV (2005) Photoactivable fluorescent proteins. Nat Rev Mol Cell Biol 6:885–891

Marriott G, Roy P, Jacobson K (2003) Preparation and light-directed activation of caged proteins. Meth Enzymol 360:274–288
Marshall P, Heudi O, Bains S, Freeman HN, Abou-Shakra F, Reardon, K (2002) The determination of protein phosphorylation on electrophoresis gel blots by laser ablation inductively coupled plasma-mass spectrometry. Analyst 2:459–461
McBride J, Treadway J, Feldman LC, Pennycook SJ, Rosenthal SJ (2006) Structural basis for near unity quantum yield core/shell nanostructures. Nano Lett 6:1496–1501
Medintz IL, Uyeda HT, Goldman ER, Mattoussi H (2005) Quantum dot bioconjugates for imaging, labelling and sensing. Nat Mater 4:435–446
Menzel ER, Savoy SM, Ulvick SJ, Cheng KH, Murdock RH, Sudduth MR (2000) Photoluminescent semiconductor nanocrystals for fingerprint detection. J Forens Sci 45:545–551
Metzker ML (2005) Emerging technologies in DNA sequencing. Genome Res 15:1767–1776
Michalet X, Pinaud FF, Bentolila LA, Tsay JM, Doose S, Li JJ, Sundaresan G, Wu AM, Gambhir SS, Weiss S (2005) Quantum dots for live cells, in vivo imaging, and diagnostics. Science 307:538–544
Moan J, Berg K (1991) The photodegradation of porphyrins in cells can be used to estimate the lifetime of singlet oxygen. Photochem Photobiol 53:549–553
Mori H, Ito K (2006) Different modes of SecY–SecA interactions revealed by site-directed photo-crosslinking in vivo. Proc Natl Acad Sci U S A 103:16159–16164
Natasha G, Tan A, Farhatnia Y, Rajadas J, Hamblin MR, Peng T, Khaw PT, Seifalian AM (2013) Channelrhodopsins: visual regeneration and neural activation by a light switch. New Biotechnol 30:461–474
Ndoye A, Dolivet G, Høgset A, Leroux A, Fifre A, Erbacher P, Berg K, Behró J-P, Guillemin F, Merlin J-L (2006) Eradication of p53-mutated head and neck squamous cell carcinoma xenografts using nonviral p53 gene therapy and photochemical internalization. Mol Ther 13:1156–1162
Nechyporuk-Zloy V, Stock C, Schillers H, Oberleithner H, Schwab A (2006) Single plasma membrane K^+channel detection by using dual-color quantum dot labeling. Am J Physiol Cell Physiol 291:266–269
Nelson T, Tausta SL, Gandotra N, Liu T (2006) Laser dissection of plant tissue: what you see is what you get. Annu Rev Plant Biol 57:181–201
Nida DL, Rahman MS, Carlson KD, Richards-Kortum R, Follen M (2005) Fluorescent nanocrystals for use in early cervical cancer detection. Gynecol Oncol 99(Suppl 1):S89–S94
O'Connell KMS, Rolig AS, Whitesell JD, Tamkun MM (2006) Kv2.1 Potassium channels are retained within dynamic cell surface microdomains that are defined by a perimeter fence. J Neurosci 26:9609–9618
Packer AM, Botond Roska B, Häusser M (2013) Targeting neurons and photons for optogenetics. Nature Neurosci 16:805–815
Paige JS, Nguyen-Duc T, Song W, Jaffrey SR (2012) Fluorescence imaging of cellular metabolites with RNA. Science 335:1194
Park TJ, Park JP, Seo GM, Chai YG, Lee SY (2006) Rapid and accurate detection of *Bacillus anthracis* spores using peptide-quantum dot conjugates. J Microbiol Biotechnol 16:1713–1719
Paterson L, Papagiakoumou E, Milne G, Garcés-Chávez V, Tatarkova SA, Sibbett W, Gunn-Moore FJ, Bryant PE, Riches AC, Dholakia K (2005) Light-induced cell separation in a tailored optical landscape. Appl Phys Lett 87:123901
Peterman EJG, Brasselet S, Moerner WE (1999) The fluorescence dynamics of single molecules of green fluorescent protein. J Phys Chem A 103:10553–10560
Peterson DS (2007) Matrix-free methods for laser desorption/ionization mass spectrometry. Mass Spectrom Rev 26:19–34
Petersson EJ, Brandt GS, Zacharias NM, Dougherty DA, Lester HA (2003) Caging proteins through unnatural amino acid mutagenesis. Meth Enzymol 360:258–273
Ramanathan A, Huff EJ, Lamers CC, Potamousis KD, Forrest DK, Schwartz DC (2004) An integrative approach for the optical sequencing of single DNA molecules. Anal Biochem 330:227–241
Raymond FR, Ho HA, Peytavi R, Bissonnette L, Boissinot M, Picard FJ, Leclerc M, Bergeron MG (2005) Detection of target DNA using fluorescent cationic polymer and peptide nucleic acid probes on solid support. BMC Biotechn 5, Art. No. 10
Rosetti R, Nakahara S, Brus LE (1982) Quantum size effects in the redox potentials, resonance Raman spectra, and electronic spectra of CdS crystallites in aqueous solution. J Chem Phys 79:1086–1088
Schaltmann K, Pongs O (1982) Identification and characterization of the ecdysterone receptor in *Drosophila melanogaster* by photoaffinity labeling. Proc Natl Acad Sci U S A 79:6–10
Schroll C, Riemensperger T, Bucher D, Ehmer J, Völler T, Erbguth K, Berber G, Hendel T, Nagel G, Buchner E, Fiala A (2006) Light-induced activation of distinct modulatory neurons triggers appetitive or aversive learning in *Drosophila* larvae. Curr Biol 16:1741–1747
Seo TS, Bai X, Kim DH, Meng Q, Shi S, Ruparel H, Li Z, Turro NJ, Ju J (2005) Four-color DNA sequencing by synthesis on a chip using photocleavable fluorescent nucleotides. Proc Natl Acad Sci U S A 102:5926–5931
Shkrob MA, Yanushevich YG, Chudakov DM, Gurskaya NG, Labas YA, Poponov SY, Mudrik NN, Lukyanov S, Lukyanov KA (2005) Far-red fluorescent proteins evolved from a blue chromoprotein from *Actinia equina*. Biochem J 392:649–654
Simpson GJ (2006) The diffraction barrier broken. Nature 440:879–880
So M-K, Xu C, Loening AM, Gambhir SS, Rao J (2006) Self-illuminating quantum dot conjugates for *in vivo* imaging. Nature Biotechnol 24:339–343
Stiller B, Karageirgiev P, Geue T, Morawetz K, Saphiannikova M, Mechau N, Neher D (2004) Optically induced mass transport studied by scanning near-field optical- and atomic force microscopy. Physics Low Dimens Struct 1–2:129–137
Swamy N, Addo JK, Ray R (2000) Development of an affinity-driven crosslinker: Isolation of a vitamin D receptor associated factor. Bioorg Med Chem Lett 10:361–364
Synge EH (1928) A suggested method for extending microscopic resolution into the ultra-microscopic region. Phil Mag 6:356–362
Todoroki Y, Tanaka T, Kisamori M, Hirai N (2001) 3-Azidoabscissic acid as a photoaffinity reagent for abscisic acid binding proteins. Bioorg Med Chem Lett 11:2381–2384
Torimoto T, Murakami S, Sakuraoka M, Iwasaki K, Okazaki K, Shibayama T, Ohtani B (2006) Photochemical fine-tuning of luminescent color of cadmium selenide nanoparticles: fabricating a single-source multicolor luminophore. J Phys Chem 110: 13314–13318
Tsien RY (1998) The green fluorescent protein. Annu Rev Biochem 67:509–544
Verkhusha VV, Lukyanov KA (2004) The molecular properties and applications of *Anthozoa* fluorescent proteins and chromoproteins. Nature Biotechnol 22:289–296
Viviani VR (1999) Cloning, sequence analysis, and expression of active *Phrixothrix* railroad-worms luciferases: relationship between bioluminescence spectra and primary structures. Biochemistry 38:8271–8279
Wang LV (2009) Multiscale photoacoustic microscopy and computed tomography. Nat Photonics 3:503–509
Wang LV, Hu S (2012) Photoacoustic tomography: In vivo imaging from organelles to organs. Science 335:1458–1462. doi:10.1126/science.1216210
Wang QB, Seo DK (2006) Synthesis of deep-red-emitting CdSe quantum dots and general non-inverse-square behavior of quantum confinement in CdSe quantum dots. Chem Mater 18:5764–5767
Wang L, Brock A, Herberich B, Schultz PG (2001) Expanding the genetic code of *Escherichia coli*. Science 292:498–500
Werner JH, Cai H, Jett JH, Reha-Krantz L, Keller RA, Goodwin PM (2003) Progress towards single-molecule DNA sequencing: a one color demonstration. J Biotechnol 102:1–14

Winkler LD, Arceo JF, Hughes WC, DeGraff BA, Augustine BH (2005) Quantum dots: an experiment for physical or materials chemistry. J Chem Educ 82:1700–1702

Wittelsberger A, Thomas BE, Mierke DF, Rosenblatt M (2006) Methionine acts as a "magnet" in photoaffinity crosslinking experiments. FEBS Lett 580:1872–1876

Xie J, Schultz PG (2005) Adding amino acids to the genetic repertoire. Curr Opin Chem Biol 9:548–554

Xie J, Schultz PG (2006) A chemical toolkit for proteins an expanded genetic code. Nature Rev Mol Cell Biol 7:775–782

Xu WB, Wang YX, Xu RH, Yin DZ (2006) Synthesis, modification and application in biology of quantum dots (in Chinese). J Inorg Mater 21:1031–1037

Yeh H-C, Ho Y-P, Shih I-M, Wang T-H (2006) Homogeneous point mutation detection by quantum dot-mediated two-color fluorescence coincidence analysis. Nucleic Acids Res 34:e35

Zhang F, Wang LP, Boyden ES, Deisseroth K (2006) Channelrhodopsin-2 and optical control of excitable cells. Nat Methods 3:785–792

Zheng J, Nicovich PR, Dickson RM (2007) Highly fluorescent noble-metal quantum dots. Annu Rev Phys Chem 58:409–431

Terrestrial Daylight

6

Lars Olof Björn

6.1 Introduction

Natural light at the surface of the Earth is almost synonymous with light from the sun. Light from other stars has, as far as is known, photobiological importance only for navigation by night-migrating birds and some beetles Dacke et al. (2013).

Moonlight, which originates in the sun, is important for the setting of some biological rhythms. A full moon may perturb the photoperiodism of some short-day plants and also synchronize rhythms in some marine animals.

However, the majority of photobiological phenomena are ruled by daylight, and we shall devote the remainder of this chapter to this topic. We shall treat the shortest wavelength components of daylight, UV-B radiation, at the end of this chapter, as special problems are involved with this wave band.

6.2 Principles for the Modification of Sunlight by the Earth's Atmosphere

As mentioned earlier, the radiation from the sun (Fig. 6.1) is spectrally very similar to blackbody radiation of 6,000 K (above 700 nm 5,777 K). There are, however, deviations both in the basic shape and due to reabsorption (Fraunhofer lines) of some light by gases in the higher, cooler layers of the sun.

The Earth's atmosphere reflects, refracts, scatters, and partially absorbs the radiation from the sun and thereby changes its spectral composition considerably. Part of the absorption and Rayleigh scattering is due to the main gases in the atmosphere, the concentration of which can be regarded as constant. Another part is due to ozone and water vapor (see Stomp et al. 2007), which occur in highly variable amounts. A third part is due to aerosol, which is also highly variable. The absorption causes loss of light, while scattering causes some light to be lost to space, while another part appears as diffuse light (skylight). Light is also reflected by clouds and thereby mostly lost to space, but this will not be considered in detail here. Light reflected from the ground is partly scattered downward or reflected from clouds and again appears at the surface as diffuse light, and for this reason, the ground reflectivity has some effect on skylight.

Daylight is also strongly dependent on the elevation of the sun above the horizon (90° minus the solar elevation is called the zenith angle of the sun and often symbolized by the Greek letter theta, θ), because the lower the sun, the more air the rays must pass before they reach the ground. Daylight can be considered as composed of two components—direct sunlight and scattered light. The scattered light is in most cases dominated by skylight, while some may reach the observer as scattered from the ground, trees, etc.

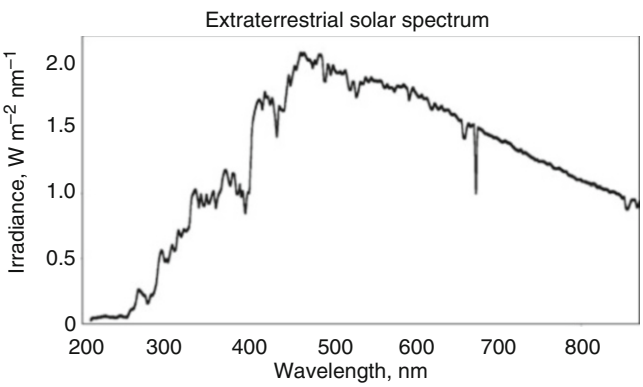

Fig. 6.1 The spectrum of sunlight on a plane perpendicular to the direction to the sun, outside the Earth's atmosphere

L.O. Björn
School of Life Science, South China Normal University, Guangzhou, China

Department of Biology, Lund University, Lund, Sweden
e-mail: Lars_Olof.Bjorn@biol.lu.se

L.O. Björn (ed.), *Photobiology: The Science of Light and Life*,
DOI 10.1007/978-1-4939-1468-5_6,

6.3 The UV-A, Visible, and Infrared Components of Daylight in the Open Terrestrial Environment Under Clear Skies

Accurate methods for computational modeling of daylight depart from the radiative transfer theory described by Chandrasekhar (1950). However, the fundamental formulas usually cannot be used directly; different approximations have to be used for various cases, and this is nothing for the average biologist to work with. However, as long as we are dealing with clear skies (no clouds) and relatively long wavelengths (near-infrared, visible, and UV-A radiations) and as long as we stay above water and vegetation, daylight can be well described by methods that are more easily handled.

A simple and for most purposes adequate procedure for this has been published by Bird and Riordan (1986). Their model, SPCTRAL2, has become very popular, and their paper had been cited over 340 times when this is being written. An alternative approach for part of the spectrum is that of Green and Chai (1988). We shall use the approach of Bird and Riordan (1986) here to show how the direct component (sunlight) and the component scattered by the atmosphere (skylight) vary with the solar elevation (i.e., with the zenith angle). The same algorithm can be used also for visualizing how other factors, such as air pressure, air humidity, aerosol, ozone column, and ground albedo, affect daylight. We show the result only from 300 to 800 nm, but the paper by Bird and Riordan (1986) can be used to model radiation up to 4 μm, i.e., 4,000 nm. Hulstrom et al. (1985) have published values for airmass 1.5 (i.e., a solar elevation of 41.8° above the horizon for a standard atmosphere).

Figure 6.2 shows three spectra, representing the direct sunlight, the skylight (diffuse radiation), and their sum, the so-called global radiation (the total daylight). Note that the skylight has its maximum moved toward shorter wavelengths compared to the direct sunlight. This corresponds to the fact that the sky appears blue in color and also to the fact that Rayleigh scattering is inversely proportional to the fourth power of the wavelength.

Figure 6.3 shows the irradiance on a horizontal plane and the one for the irradiance on a vertical plane in the compass direction (azimuth) toward the sun. These spectra are rather different. The sunset sunlight is of course much stronger in the horizontal direction (on a vertical plane). The scattered light is now not only skylight but also light scattered from the ground, and therefore, it contains much more long-wave components. Note also how deep the absorption bands for water vapor and oxygen have become, because the light must pass so much air when the sun is so low in the horizon. We can see from this that the concept "daylight spectrum" has no meaning if the geometry of measurement is not specified. We would get a third set of spectra for the fluence rate. The fluence rate can also be readily calculated using the algorithm of Bird and Riordan (1986), slightly modified: the diffuse component should be doubled, and the factor cosinus of incidence angle should be dropped in the expression for the direct component (sunlight).

The algorithm of Bird and Riordan (1986) assumes the skylight to come equally from all over the sky, or, in other words, the sky *radiance* is uniform. This is an approximation, and other more accurate descriptions exist. A model based on radiative transfer theory has been published by Liang and Lewis (1996), while the group of R. H. Grant (Grant and Heisler 1997; Grant et al. 1996a, b, 1997), based

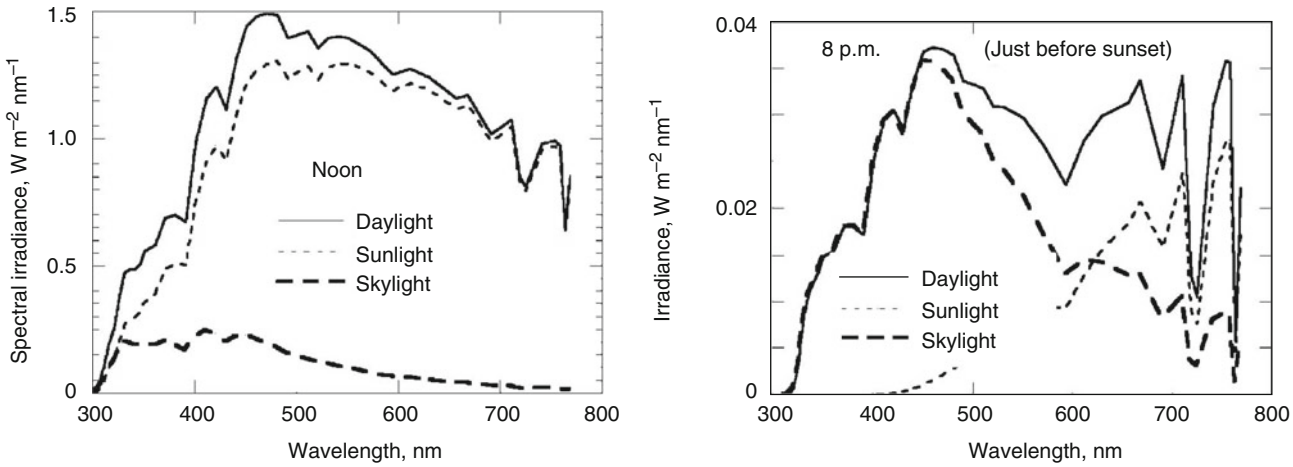

Fig. 6.2 Irradiance at noon (*left*) and just before sunset (*right*) from above on a horizontal plane in Lund (south Sweden, 55.7°N, 13.4°E) on July 15, 2002, as computed using the algorithm of Bird and Riordan (1986). The ozone column was assumed to be 300 Dobson units and the ground albedo 0.2, aerosol 0, and air pressure 1,000 mbar

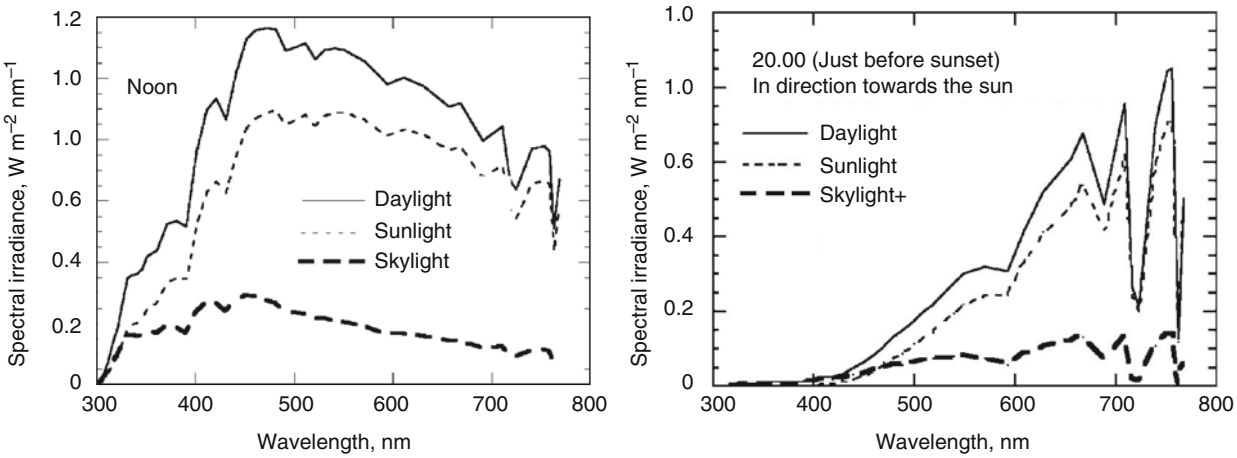

Fig. 6.3 Same as Fig. 6.2, except that the plane is vertical and pointed in the compass direction of the sun

on measurements, has developed a set of very simple models for various cloud conditions.

The paper by Bird and Riordan (1986), as stated in its title, deals only with clear skies. In modeling the diffuse skylight, it assumes the sky to have uniform (isotropic) radiance. This latter approximation works very well as long as we are interested only in the irradiance on a horizontal or nearly horizontal plane. For some other purposes, it may be of interest to model more exactly the variations in sky radiance, and how this can be done (in a relative sense also for cloudy conditions and for UV-B radiation) in a simple way has been described by Grant et al. (1996a, b, 1997) and Grant and Heisler (1997) in a series of papers, with a summary presently available at http://shadow.agry.purdue.edu/research.model.skyrad.html.

For direct sunlight, another method that is said to have some advantages (although not tested by the present author) has been published by Oke et al. (2010). In one test, under stable cloud-free conditions, it agreed well with the model of Bird and Riordan (1986), while in another, under frequently changing clouds test, it agreed much better with measured data than the older model did. This is not a pure calculation method, but requires for each occasion normalization against a pyrheliometer measurement, which explains the better agreement with spectroradiometer measurements under changing cloud conditions.

Sky radiance distribution, i.e., distribution of brightness across the sky, depends on several factors, including the position of the sun, cloudiness, and wavelength. The reader is referred to Román et al. (2012) for information about measurement and computer modeling of this.

Skylight is elliptically polarized (i.e., partly plane polarized), which is important for some animals who are able to determine the direction of polarization and use it for orientation (see, e.g., Labhart 1999). The degree of polarization can be approximated by $p = p_o \cdot \sin\mu/(1+\cos^2\mu)$, where μ is the angular distance from the sun. The value of p_o is never more than 94 %, usually lower, depending on aerosol in the air, reflection from the ground, etc. The direction of the major electrical vector is approximately along the circumference of "circles" on the sky with the sun in the center (e.g., Schwind and Horváth 1993). A few comments should be added to this simplified description (again, a more exact mathematical description can be obtained using the radiative transfer theory). Thus, the polarization is increased in the spectral bands where the terrestrial atmosphere absorbs strongly (Aben et al. 1999). When the sun is higher than about 20° above the horizon, there are two points within 20° of the sun, one above and one below, where polarization is zero. When the sun is less than about 20° above the horizon, one such point is located about 20° above the antisolar point (Bohren 1995, 2004).

6.4 Cloud Effects

Clouds usually decrease both the irradiance and the degree of polarization of daylight. However, under some circumstances, clouds can cause the irradiance above the values it would have had without clouds. This effect is particularly pronounced when most of the sky is overcast but the sun is not in clouds and when the ground is snow covered or otherwise highly reflecting.

6.5 Effects of Ground and Vegetation

Reflection from the ground is particularly important in the ultraviolet, since ultraviolet light reflected upward by the ground is partially scattered downward again by the atmosphere and the ground cover thus affects also downwelling radiation. The effect of reflection from the ground is greatest when it is covered by snow. Reflection from the ground can

be quite important for the visible spectrum and for plant growth, as shown by Hunt et al. (1985) and Kasperbauer and Hunt (1987).

Penetration of light into the ground is important for the germination of seeds. Soil transmission generally increases with increasing wavelength, thus giving buried seeds a far-red-biased environment (Kasperbauer and Hunt 1988).

Plant canopies absorb visible light and ultraviolet radiation but reflect and transmit far-red light and near-infrared radiation. Light in or under green vegetation is therefore strongly biased toward the longer wavelengths, a fact that is of paramount importance to the plants subjected to this regime. The plant-filtered light forces the phytochrome system to the Pr (inactive) state (Holmes and Smith 1977; Kasperbauer 1971, 1987; Smith 1986).

It is now possible to measure light *inside* plants and animals (Marijnissen and Star 1987; Star et al. 1987; Vogelmann 1986).

6.6 The UV-B Daylight Spectrum and Biological Action of UV-B

At the short-wavelength end of the daylight spectrum is the UV-B spectral band, 280–315 nm. This band is of particular interest because it is highly biologically active (mostly inhibitory). It is more difficult to measure than visible light and UV-A radiation because irradiance and fluence rate are lower. It is also more difficult to model than other daylight, because the spectral irradiance at ground surface is highly variable and dependent on other factors in addition to those influencing the longer wavelength components. The main factors influencing UV-B spectral irradiance at ground level are the elevation of the sun above the horizon and the amount of ozone in the atmosphere (Fig. 6.4).

A computer program to study the effects of these and other factors on the UV-B spectral irradiance and estimate the biological action was designed by Björn and Murphy (1985) based on Green (1983) and is further described by Björn (1989) and Björn and Teramura (1993). A more accurate code that can also be used for visible light and is based on radiative transfer theory is that of S. Madronich, presently available on the Internet (http://cprm.acd.ucar.edu/Models/TUV/).

UV-B is more highly scattered than longer daylight components, and even under clear skies, much of it reaches the ground as skylight rather than direct sunlight. Thus, the fluence rate can be appreciable even in shadow. If the ground is snow covered and especially if the snow is fresh, much radiation can reach the observer from snow. Snow also increases the ultraviolet component of skylight, because radiation reflected from the ground is to an appreciable extent scattered down again by the atmosphere.

Also, underwater ultraviolet radiation has its special measuring and modeling problems. In freshwater bodies and coastal water, the amount of UV-B-absorbing dissolved substances is usually so high that UV-B radiation does not penetrate very far. Exceptions are some Alpine lakes. But in clear ocean water, such as that in the Southern Ocean, UV-B radiation can be measured down to 60 m, and biological effects can be recorded at a depth of 20 m.

We shall return to UV-B radiation later, especially in Chaps. 21, 22, 23, 24, and 25.

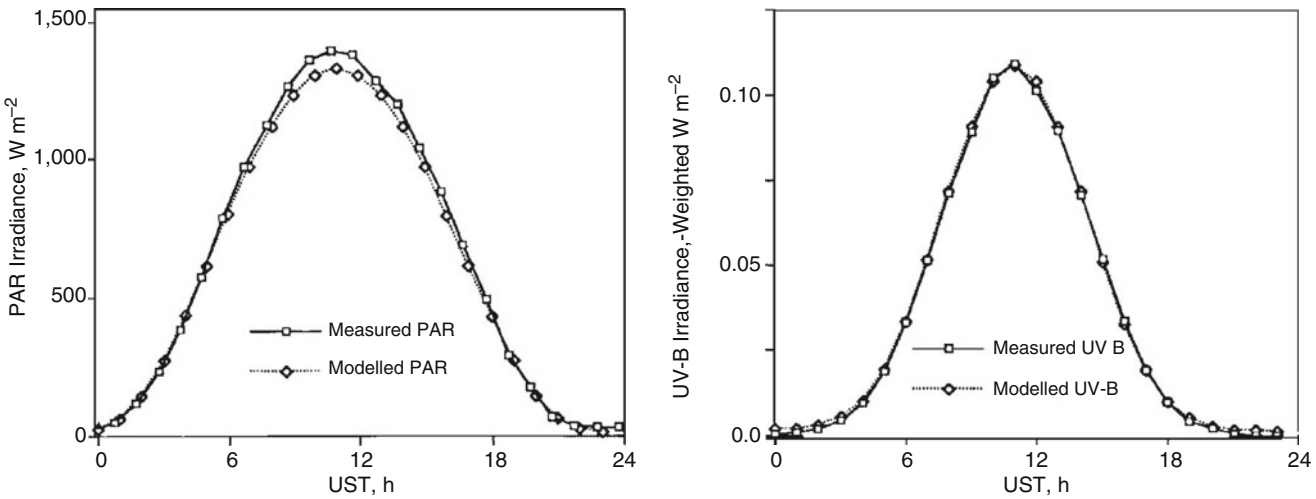

Fig. 6.4 The variation of daylight during a cloud-free day (July 5, 1994) at Abisko in northern Sweden (68.35°N, 18.82°E). The *left panel* shows photosynthetically active radiation (PAR, 400–700 nm), the *right panel* UV-B radiation. The UV-B radiation was weighted with a mathematical function to enhance the biologically more active shorter wavelength components. The *horizontal axis* shows Universal Standard Time. Note that the UV-B is more concentrated toward the middle of the day than is PAR (From Björn and Holmgren 1996)

References

Aben I, Helderman F, Stam DM, Stamnes P (1999) Spectral fine-structure in the polarisation of skylight. Geophys Res Lett 26:591–594

Bird RE, Riordan C (1986) Simple solar spectral model for direct and diffuse irradiance on horizontal and tilted planes at the earth's surface for cloudless atmospheres. J Clim Appl Meteorol 25:87–97

Björn LO (1989) Computer programs for estimating ultraviolet radiation in daylight. In: Diffey BL (ed) Radiation measurement in photobiology. Academic, London, pp 161–169

Björn LO, Holmgren B (1996) Monitoring and modelling of the radiation climate at Abisko. Ecol Bull 45:204–209

Björn LO, Murphy TM (1985) Computer calculation of solar ultraviolet radiation at ground level. Physiol Vég 23:555–561

Björn LO, Teramura AH (1993) Simulation of daylight ultraviolet radiation and effects of ozone depletion. In: Young AR, Björn LO, Moan J, Nultsch W (eds) UV Photobiology. Plenum Press, New York, pp 41–71

Bohren CF (1995) Optics, atmospheric. In: Trigg GL (ed) Encyclopedia of applied physics, vol 12. VCH Publishers, New York, pp 405–434

Bohren CF (2004) Atmospheric optics. In: Brown TG (ed) The optics encyclopedia: basic foundations and practical applications, vol 1. Wiley, Hoboken, pp 53–91

Chandrasekhar S (1950) Radiative transfer theory. Oxford University Press. Reprinted (1960) by Dover Publications, New York

Dacke M, Baird E, Byrne M, Scholtz, CH, Warrant EJ (2013) Dung beetles use the milky way for orientation. Curr Biol 23:298–300

Grant RH, Heisler GM (1997) Obscured overcast sky radiance distributions for UV and PAR wavebands. J Appl Meteorol 36: 1336–1345

Grant RH, Gao W, Heisler GM (1996a) Photosynthetically active radiation: sky radiance distributions under clear and overcast conditions. Agric For Meteorol 82:267–292

Grant RH, Heisler GM, Gao W (1996b) Clear sky radiance distributions in ultraviolet wavelength bands. Theor Appl Climatol 56:123–135

Grant RH, Gao W, Heisler GM (1997) Ultraviolet sky radiance distributions of translucent overcast skies. Theor Appl Climatol 3–4:129–139

Green AES (1983) The penetration of ultraviolet radiation to the ground. Physiol Plant 58:351–359

Green AES, Chai S-T (1988) Solar spectral irradiance in the visible and infrared regions. Photochem Photobiol 48:477–486

Holmes MG, Smith H (1977) Spectral distribution of light within plant canopies. In: Smith H (ed) Plants and the daylight spectrum. Academic, New York, pp 147–158

Hulstrom R, Bird R, Riordan C (1985) Spectral solar irradiance data sets for selected terrestrial conditions. Solar Cells 15:365–391

Hunt PG, Kasperbauer MJ, Matheny TA, Kasperbauer MJ (1985) Effect of soil surface color and *Rhizobium japonicum* strain on soybeen seedling growth and nodulation. Agron Abstr 85:157

Kasperbauer MJ (1971) Spectral distribution of light in a tobacco canopy and effects of end-of-day light quality on growth and development. Plant Physiol 47:775–778

Kasperbauer MJ (1987) Far red light reflection from green leaves and effects on phytochrome-mediated assimilate partitioning under field conditions. Plant Physiol 85:350–354

Kasperbauer MJ, Hunt PG (1987) Soil color and surface residue effects on seedling light environment. Plant Soil 97:295–298

Kasperbauer MJ, Hunt PG (1988) Biological and photometric measurement of light transmission through soils of various colors. Bot Gaz 149:361–364

Labhart T (1999) How polarization-sensitive interneurones of crickets see the polarization pattern of the sky: a field study with an opto-electronic model neurone. J Exp Biol 202:757–770

Liang SL, Lewis P (1996) A parametric radiative transfer model for sky radiance distribution. J Quant Spectrosc Radiat Transf 55: 181–189

Marijnissen JPA, Star WM (1987) Quantitative light dosimetry *in vitro* and *in vivo*. Lasers Med Sci 2:235–242

Oke S, Fukushige N, Kemmoku Y, Takikawa H, Sakakibara T, Araki K (2010) A new simple model of direct spectral irradiance with easily observable atmospheric parameters. IEEJ Trans 5:548–552

Román R, Antón M, Cazorla A, de Miguel A, Olmo FJ, Bilbao J, Alados-Arboledas L (2012) Calibration of an all-sky camera for obtaining sky radiance at three wavelengths. Atmos Meas Technol 5:2013–2024

Schwind R, Horváth G (1993) Reflection-polarization pattern at water surfaces and correction of a common representation of the polarization pattern of the sky. Naturwissenschaft 80:82–83

Smith H (1986) The perception of light quality. In: Kendrick RE, Kronenberg GMH (eds) Photomorphogenesis in plants. Martinus Nijhoff Publishers, Dordrecht, pp 187–217

Star WM, Marijnissen HPA, Jansen H, Keijzer M, van Gemert MJC (1987) Light dosimetry for photodynamic therapy by whole bladder wall irradiation. Photochem Photobiol 46:619–624

Stomp M, Huisman J, Stal LJ, Matthijs HCP (2007) Colorful niches of phototrophic microorganisms shaped by vibrations in the water molecule. ISME J 1:271–282

Vogelmann TC (1986) Light within the plant. In: Kendrick RE, Kronenberg GMH (eds) Photomorphogenesis in plants. Martinus Nijhoff Publishers, Dordrecht, pp 307–337

Underwater Light

7

Curtis D. Mobley

7.1 Introduction

The penetration of the sun's energy into natural waters (oceans, lakes, and rivers) is dependent upon the incident solar radiation, the state of the windblown surface, the bottom reflectance in shallow waters, and the absorbing and scattering properties of the water body. The absorbing and scattering properties are themselves determined by the type, concentration, and size distribution of the dissolved and particulate material within the water. The concentrations of water constituents such as phytoplankton, mineral particles, and dissolved substances vary by many orders of magnitude, and consequently so do absorption and scattering and the resulting measures of underwater light. This chapter introduces the terminology used to describe light and the medium through which it passes, and it illustrates the ranges of values found in natural waters. The emphasis is on the variability of light fields in natural waters.

The recent text by Johnsen (2012) gives an excellent introduction to light written with the needs of biologists in mind. Kirk (1994) discusses aquatic photosynthesis in detail. Mobley (1994) gives an overview of optical oceanography and the mathematics of radiative transfer theory as needed to compute underwater light fields. A good online resource is the Ocean Optics Web Book (www.oceanopticsbook.info).

The quantities needed to describe light and its interactions with water are grouped into three classes: radiometric variables, which describe the light itself; inherent optical properties, which describe material media; and apparent optical properties, which are a combination of the two. The next sections discuss each of these in turn.

C.D. Mobley
Sequoia Scientific, Inc., Bellevue, WA, USA
e-mail: curtis.mobley@sequoiasci.com

7.2 Radiometric Variables

All electromagnetic radiation—light in particular—is fully specified by the four-component Stokes vector, which relates the electric field of the propagating radiation to its state of polarization, spectral distribution of energy, and direction of travel. Many aquatic photobiological processes such as photosynthesis are assumed to be independent of the polarization state, although there may be exceptions such as the possible use of polarized light for navigation or visibility enhancement in searching for prey. This article ignores the complexities of polarization, in which case only the magnitude of the radiant energy is relevant. This is given by the first component of the Stokes vector, which is called the spectral radiance L. To a good approximation, water bodies are often horizontally homogeneous on scales of 100 m or less, in which case the radiance is a spatial function only of the depth z, the polar (θ) and azimuthal (ϕ) directions, and wavelength λ. With these assumptions, the radiance distribution $L(z, \theta, \phi, \lambda)$ gives a complete description of the light field. (Depth z is normally measured positive downward from 0 at the mean water surface; θ and ϕ refer to the direction the light is traveling, with $\theta = 0$ in the $+z$ direction.) Spectral radiance has units of watts of radiant power per unit area (perpendicular to the direction of travel) per unit steradian (of solid angle about direction θ, ϕ), per unit wavelength interval, or W m^{-2} sr^{-1} nm^{-1}. The directional information contained in the radiance is crucial for applications such as prediction of underwater visibility. However, this directional information is not needed for photobiology because absorption by randomly oriented phytoplankton and other water constituents does not depend on the direction of light travel. Thus, the radiometric variables most commonly measured and used for biology and thermodynamics (i.e., water heating) are various irradiances, which are integrals of the radiance over direction.

L.O. Björn (ed.), *Photobiology: The Science of Light and Life*,
DOI 10.1007/978-1-4939-1468-5_7,

Consider an instrument with a flat collecting surface, with each point of the surface being equally sensitive to light incident onto the surface from any direction seen by the detector. The detector is equipped with filters so that the incident power is measured as a function of wavelength. If such a detector has its collecting surface pointing upward, so as to collect light traveling downward, it measures the downwelling spectral plane irradiance $E_d(z, \lambda)$, which has units of W m^{-2} nm^{-1}. Note that the effective collection area of the detector as seen by radiance traveling in direction θ relative to the normal to the detector surface reduced by a factor of cosθ; such instruments are therefore called cosine detectors. If the radiance is known, $E_d(z, \lambda)$ is obtained by integrating the radiance over all downward directions, with the radiance weighted by cosθ to account for the sensor angular response:

$$E_{\mathrm{d}}(z,\lambda) = \int_0^{\pi/2}\int_0^{2\pi} L(z,\theta,\phi,\lambda)\cos\theta\sin\theta\,\mathrm{d}\theta\,\mathrm{d}\phi. \qquad (7.1)$$

Here $\sin\theta\,\mathrm{d}\theta\,\mathrm{d}\phi$ is the differential element of solid angle. If the same detector is pointing downward, it measures the upwelling plane irradiance $E_u(z, \lambda)$.

If the detector has a spherical collecting surface (think of a ping pong ball), it is equally able to detect light traveling in any direction. The measured quantity is then the scalar irradiance $E_0(z, \lambda)$, which is obtained from the radiance by integrating over all directions, but without the cosine weighting:

$$E_0(z,\lambda) = \int_0^{\pi}\int_0^{2\pi} L(z,\theta,\phi,\lambda)\sin\theta\,\mathrm{d}\theta\,\mathrm{d}\phi. \qquad (7.2)$$

Scalar irradiance (sometimes called fluence rate by biologists) is the measure of light energy available to drive photobiological processes, which do not depend on the direction of light propagation. Although the probability of a photon being absorbed by a chlorophyll molecule depends on wavelength, all photons, once absorbed, lead to the same photosynthetic reaction. Thus, it is the number of photons absorbed, not their individual energies, that is relevant to primary production calculations. The corresponding radiometric variable is the scalar irradiance converted from energy units (W m^{-2} nm^{-1}) to quantum units (photons s^{-1} m^{-2} nm^{-1}). A single photon contains energy hc/λ, where $h = 6.626\cdot10^{-34}$ J s is Planck's constant, $c = 2.998\cdot10^{8}$ m s^{-1} is the speed of light, and λ is the wavelength (here in meters).

Thus, the conversion from energy to quantum units is done by multiplying E_0 by λ/hc. A crude but commonly used measure of the total number of photons available for photosynthesis is the photosynthetically available radiation (PAR), defined by

$$\mathrm{PAR}(z) = \int_{400}^{700} E_0(z,\lambda)\frac{\lambda}{hc}\,\mathrm{d}\lambda. \qquad (7.3)$$

(Some researchers use 350 nm as the lower bound for the PAR range of wavelengths.) In aquatic systems PAR is often measured in μmol photons m^{-2} s^{-1}, where 1 mol is $6.023\cdot10^{23}$ photons. Note that PAR always refers to quantum units; it is not a synonym for broadband irradiance in energy units.

For studies concerned with the influence of ultraviolet (UV) radiation on aquatic organisms, other broadband quantities are of interest. UV-A is electromagnetic radiation with wavelengths in the 315–400 nm range, and UV-B is radiation in the 280–315 nm range. Thus, for example, the solar scalar irradiance penetrating to depth within the UV-B region of the spectrum, $E_{\mathrm{UV\text{-}B}}(z)$, is computed as

$$E_{\mathrm{UV\text{-}B}}(z) = \int_{280}^{315} E_0(z,\lambda)\,\mathrm{d}\lambda. \qquad (7.4)$$

There are other radiometric variables, but these give us what is needed.

7.3 Inherent Optical Properties

The optical properties of a material medium—here a water body—are specified by its inherent optical properties (IOPs). IOPs depend only on the medium, not on the light propagating through it. The two fundamental IOPs are the spectral absorption coefficient, $a(\lambda)$, and the volume scattering function $\beta(\psi, \lambda)$, where ψ is the scattering angle measured from 0 in the forward (unscattered) direction of light propagation. These two quantities fully specify (ignoring polarization) how light can interact with the medium.

Consider monochromatic light propagating in a particular direction through a water body. In going from location r to $r+\Delta r$ along the direction of propagation, some amount $\Delta\Phi(r)$ of the incident power $\Phi(r)$ is absorbed by the water. The fraction of power absorbed is the absorptance $A = \Delta\Pi(r)/\Pi(r)$. All quantities depend on wavelength, but not on the direction of propagation (in isotropic media such as water). The absorption coefficient $a(\lambda)$ is the absorptance per unit distance traveled, or conceptually

$$a = \lim_{\Delta r\to 0}\frac{\Delta\Phi(r)}{\Phi(r)\Delta r} = \frac{\mathrm{d}\ln\Phi(r)}{\mathrm{d}r}, \qquad (7.5)$$

with units of m^{-1}. Radiant energy absorbed at one wavelength is converted to chemical or thermal energy or is reemitted at another wavelength by fluorescence or other inelastic processes.

Rather than being absorbed, the radiant power may be scattered, i.e., the direction of propagation (elastic scattering) and or wavelength (inelastic scattering) may change through interaction with the water. The volume scattering function (VSF) is the fraction of incident power scattered into a unit solid angle centered on direction (ψ, α) per unit distance traveled. Here ψ is the polar scattering angle measured from zero in the direction of the unscattered beam, and α is the azimuthal angle of the scattering. If $\Delta\Phi_s$ is the power scattered into solid angle $\Delta\Omega$ as the light travels distance Δr, then the VSF is conceptually defined as

$$\beta(\psi,\alpha) = \lim_{\Delta r\to 0}\lim_{\Delta\Omega\to 0}\frac{\Delta\Phi_s(\psi,\alpha)}{\Phi\Delta r\Delta\Omega}, \qquad (7.6)$$

with units of m^{-1} sr^{-1}. For unpolarized light and isotropic media, as assumed here, scattering depends only on ψ.

Equations 7.5 and 7.6 are the definitions of these IOPs. Actual instruments of course have finite path lengths and solid angles. Moreover, the actual measurement of a and β are complicated by the fact that both absorption and scattering are always present, often in roughly equal amounts, in any water body. Thus, an instrument measuring the absorption coefficient must be corrected for losses from the incident beam due to scattering, which would otherwise appear as increased absorption. Likewise, a measurement of scattering must be corrected for absorption losses from the incident beam. A vicious circle thus results, which is the bane of IOP measurements in natural waters with both absorbing and scattering constituents.

IOPs are additive. That is, the total a and β are the sums of contributions by pure water, phytoplankton, mineral particles, dissolved substances, air bubbles, etc. This allows a and β for various water constituents to be measured or modeled separately. There are many such biogeochemical models for a and β for specific kinds of particles and dissolved substances. These models often parameterize the IOPs in terms of more easily measured quantities, e.g., absorption by phytoplankton is often modeled as a function of the chlorophyll concentration.

Just as for radiance, the angular scattering information contained in the VSF provides more information than is necessary for photobiological applications (although it is crucial for other applications such as remote sensing and visibility). The scattering coefficient b gives a measure of the total amount of scattering, without regard for the direction of the scattered radiance, and is obtained by integrating the VSF over all scattering directions (ψ, α):

$$b = \int_0^{2\pi}\int_0^{\pi}\beta(\psi,\alpha)\sin\psi\,d\psi\,d\alpha = 2\pi\int_0^{\pi}\beta(\psi)\sin\psi\,d\psi. \qquad (7.7)$$

b has units of m^{-1}. The 2π in the last term results from the assumption that the scattering is azimuthally symmetric so that the VSF is independent of α. The scattering phase function $\tilde{\beta}(\psi)$ is the VSF normalized by the total scattering coefficient:

$$\tilde{\beta}(\psi,\lambda) = \frac{\beta(\psi,\lambda)}{b(\lambda)}, \qquad (7.8)$$

which has units of sr^{-1}. The phase function thus shows the angular shape of the VSF without regard to the magnitude of the scattering.

The total loss of power from a collimated beam owing to both absorption and scattering out of the beam is given by the beam attenuation coefficient, $c = a + b$. The backscatter coefficient b_b is given by the VSF integrated over all scattering directions greater than 90°, i.e., over $\pi/2$ to π in Eq. 7.7. The ratio of b_b/a is a fundamental parameter for predicting how much radiance incident onto the sea surface is scattered back upward and returned to the sky without being absorbed. That water-leaving radiance is sunlight that has been transformed by interaction with the water column and thus carries information about the biogeochemical state of the water body. The backscatter fraction b_b/b is sensitive to particle size and index of refraction and thus carries information about the type of scattering particles in the water.

Case 1 waters are those in which the IOPs are determined predominately by phytoplankton and their covarying derivatives (detritus from dead cells and colored dissolved organic matter (CDOM) released by the cells). In such waters, absorption and scattering are correlated and can be parameterized by the chlorophyll concentration (albeit with large variability owing to phytoplankton physiological state and cell size for a given chlorophyll value). However, in general, absorption and scattering are uncorrelated and cannot be modeled by chlorophyll concentration alone. Consider, for example, coastal water containing high concentrations of CDOM from land runoff or sand from resuspended sediment. CDOM is strongly absorbing but almost nonscattering, whereas quartz sand is highly scattering but almost nonabsorbing. Such waters are called case 2. Both absorption and scattering are equally important in understanding underwater light, and both must be measured.

Figure 7.1 shows the range of absorption and scattering coefficients as a function of chlorophyll concentration in case 1 water according to the bio-optical models of Bricaud et al. (1998) for $a(\lambda)$ and Morel et al. (2002) for $b(\lambda)$. The left panel shows that the absorption coefficient varies by over two orders of magnitude at blue wavelengths over the range of the clearest ocean water (Chl = 0.01 mg m^{-3}) to extreme bloom conditions (Chl = 100 mg m^{-3}). The right panel shows that the scattering coefficient varies by five orders of magnitude for the same range of chlorophyll values. The actual

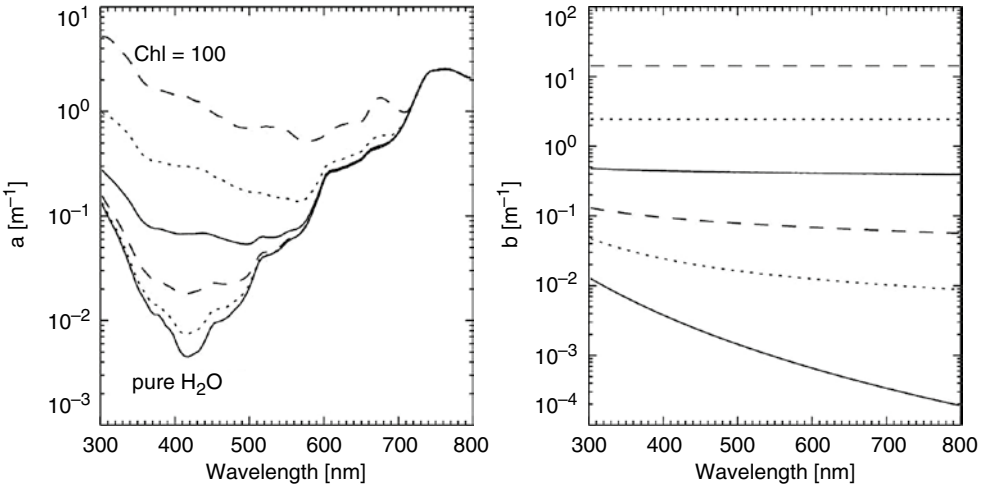

Fig. 7.1 Modeled variability of absorption and scattering coefficients in case 1 water as a function of chlorophyll concentration. The curves in each panel from bottom to top are for pure water, Chl = 0.01, 0.1, 1, 10, and 100 mg m^{-3}

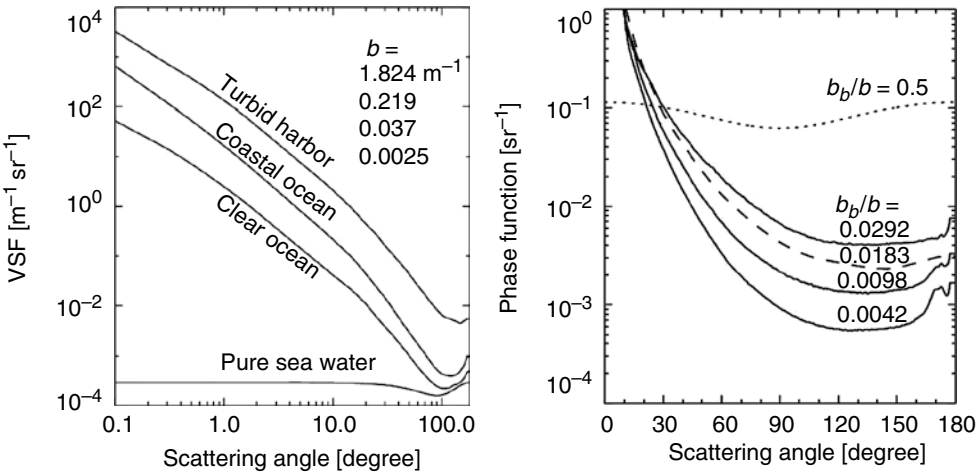

Fig. 7.2 Example variability in measured VSFs (*left panel*) and phase functions (*right panel*)

variability in both magnitude and spectral shape is much greater because of contributions by CDOM, mineral particles, microbubbles, and other water components that are often present in natural waters.

Variability in VSFs is just as great. The left panel of Fig. 7.2 shows three VSFs measured (Petzold 1972) at 514 nm (with an instrument with a 75 nm bandwidth) in clear Bahamas water, coastal California, USA, water, and the turbid harbor at San Diego, California, USA. There is a factor of 60 difference in the magnitudes of the clear versus turbid VSFs at small scattering angles, and each VSF has over five orders of magnitude difference between scattering angles of 0.1° and 180°. The corresponding total scattering coefficients vary by a factor of 50. The bottom curve of that figure shows the VSF for pure seawater. It is negligible in magnitude compared to the other VSFs, except at backscatter directions for the clearest ocean water. Backscatter by pure water becomes a significant part of the total backscatter in very clear waters.

The solid lines in the right panel of Fig. 7.2 show three phase functions $\tilde{\beta}(\lambda, 530\ \text{nm})$ measured in coastal New Jersey, USA, surface waters. These measurements were made within 1 day and a few kilometers of each other. Nevertheless, these phase functions differ by almost an order of magnitude in backscatter directions ($\psi > 90°$), and their backscatter fractions b_b/b vary by a factor of seven, from 0.42 % to almost 3 %. The dashed line in this panel shows the phase function for the Petzold San Diego harbor VSF, and the dotted line is the phase function for pure seawater. Pure seawater scatters symmetrically about $\psi = 90°$ and thus has a backscatter fraction of 0.5.

7.4 Apparent Optical Properties

As noted, the radiance distribution tells us everything there is to know about light, and the total IOPs $a(z, \lambda)$ and $b(\psi, z, \lambda)$ tell us everything about the optical properties of a water body. The behavior of radiance in a water body can be accu-

rately predicted by solving the radiative transfer equation (RTE), which expresses conservation of energy in terms of radiance. The inputs to the RTE are the total IOPs throughout the medium, the external radiance incident onto the water surface, the surface wave state (usually parameterized by the wind speed), and, for finitely deep water, the depth and reflectance of the bottom. The RTE is a very complicated integrodifferential equation and must be solved numerically. There are many techniques to do this (Mobley et al. 1993), and commercial software is available and widely used for solving the RTE in the aquatic setting (by the author and is a commercial product of Sequoia Scientific, Inc.; www.hydrolight.info). The RTE, hence light propagation in the ocean, depends only on the total IOPs. In other words, a photon only cares whether it is absorbed or scattered; what type of molecule does the absorption or scattering is irrelevant to the prediction of light propagation. Biologists, on the other hand, do care how much light is absorbed or scattered by each water column constituent; e.g., light absorbed by a mineral particle or water molecule is not available to be absorbed by a phytoplankton and thereby lead to photosynthesis.

However, as also noted, radiance and IOPs are difficult to measure and in many cases contain more information than is needed. This leads us to search for easily made optical measurements that can tell us something about the biogeochemical state of a water body, but without the need to measure the full radiance distribution or set of IOPs. Apparent optical properties (AOPs) satisfy this need. An ideal AOP depends strongly on the absorbing and scattering properties of the water body (i.e., on its biogeochemical state) but only weakly on external environmental conditions such as the incident solar radiance or surface wave state. Note that irradiance, for example, is not an AOP. It does depend on the water properties, but it is very sensitive to the external environment. For example, if the sun goes behind a cloud, the irradiance can change by an order of magnitude within seconds, even though the water body remains unchanged. An irradiance measurement thus tells us little about the water body itself.

AOPs are usually either ratios or normalized depth derivatives of radiometric variables. One of the most important AOPs is the remote-sensing reflectance, $R_{rs}(\lambda) = L_w(\text{air}, \lambda)/E_d(\text{air}, \lambda)$ with units of sr^{-1}. $L_w(\text{air}, \lambda)$ is the water-leaving radiance measured in air just above the sea surface, and $E_d(\text{air}, \lambda)$ is the incident sky and solar irradiance. L_w depends on the water properties because it is radiance that has passed into the water column, there to be modified by the water IOPs, and then been scattered back to the atmosphere. Its magnitude is sensitive to the external environment. However, the normalization of L_w by $E_d(\text{air}, \lambda)$ largely removes the effects of the external environment. For example, if E_d decreases by some factor when the sky goes from clear to cloudy, so does the radiance within the water body; hence, L_w decreases by the same factor, and the ratio L_w/E_d remains unchanged except for a small difference due to the different angular distributions of the incident radiance for the cloudy versus clear sky. Figure 7.3 illustrates the dependence of R_{rs} on water and sky conditions. The HydroLight radiative transfer code was used to solve the RTE using IOPs that were parameterized by chlorophyll and mineral particle concentrations for homogeneous water. R_{rs} was obtained from the computed radiance distribution $L(z, \theta, \phi, \lambda)$ using the definitions above. Four sets of IOPs were used: Chl = 0.1, 1, and 10 mg m^{-3} with no mineral particles and Chl = 1 mg m^{-3} with an additional 1 g mm^{-3} of red clay mineral particles. Three sky conditions were used: the sun at zenith angles of 0° and 50° in a clear sky and a heavily overcast sky. The figure shows that the R_{rs} spectra group nicely by water IOPs, with only a small variability caused by the sky condition. R_{rs} is thus a good AOP. Indeed, it is the basis for most satellite ocean color remote sensing, which has revolutionized our understanding of the oceans over the last half century.

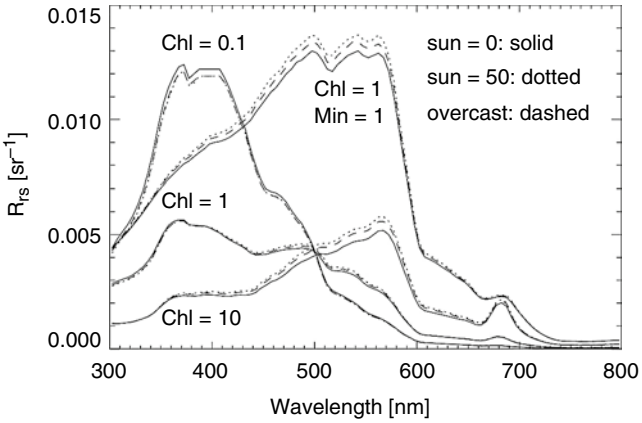

Fig. 7.3 Modeled example dependence of remote-sensing reflectance R_{rs} on water properties and sky conditions

Another reflectance AOP is the irradiance reflectance $R = E_u/E_d$. R_{rs} is less sensitive to sky conditions than is R and has thus replaced it as the reflectance most commonly used in remote sensing. R does, however, have the virtue of being measurable by just one instrument: the same cosine detector is used facing downward and then upward to measure E_u and E_d, respectively, which minimizes instrument calibration problems. Indeed, it is not even necessary that the plane irradiance sensor be calibrated to energy units; any multiplicative calibration factor cancels out.

Diffuse attenuation functions comprise another family of AOPs. These AOPs are normalized depth derivatives of radiometric variables. The diffuse attenuation function for downwelling plane irradiance E_d is defined by

$$K_d(z,\lambda) = -\frac{1}{E_d(z,\lambda)}\frac{dE_d(z,\lambda)}{dz} = -\frac{d\ln E_d(z,\lambda)}{dz}, \quad (7.9)$$

with units of m^{-1}. As with R, multiplicative factors on E_d resulting either from environmental changes or instrument calibration cancel. There is a K function for any radiometric variable; K_d, K_o, K_{Lu}, and K_{PAR} are the most commonly used. $L_u(z, \lambda)$ is the underwater radiance traveling toward the zenith. Equation 7.9 can be rewritten as

$$E_d(z,\lambda) = E_d(0,\lambda)\exp\left[-\int_0^z K_d(z',\lambda)\,dz'\right]. \quad (7.10)$$

Here $E_d(0, \lambda)$ is the irradiance just below the air-water surface. If K_d can be measured or modeled, E_d can be computed for a given surface irradiance value without solving the RTE. Similar equations hold for other K functions.

Near the sea surface, K functions depend on depth even in homogeneous water. This is because the angular distribution of the radiance distribution changes with depth as scattering redistributes the directional pattern of the incident sky radiance after it enters the water. However, in homogeneous water all K functions for a given set of IOPs approach a common value at great depth. This asymptotic K value, K_∞, is determined only by the IOPs. Other AOPs also approach asymptotic values and become IOPs at great depth. The asymptotic values can be computed from radiative transfer theory, given the IOPs. The rate at which AOPs approach their asymptotic values depends on the relative amount of absorption and scattering in the water. Higher scattering redistributes the angular pattern of the radiance quicker, so AOPs become asymptotic at shallower depths in highly scattering water than in highly absorbing water. These behaviors are illustrated in Fig. 7.4. HydroLight was again used to compute underwater radiances, from which K_d, K_{Lu}, and K_o were computed from their definitions. The simulations used IOPs for case 1 water with chlorophyll concentrations of Chl = 1 and 5 mg m^{-3} and clear sky conditions with solar zenith angles of 0° and 60°. For given IOP and sky conditions, the three K functions have different values near the sea surface, but they approach a common K_∞ value at depth. For a given chlorophyll value, the K functions near the surface depend on the sky condition. The K functions for the two different chlorophyll values separate at depth and become independent of sky condition. Note that the functions for the Chl = 5 mg m^{-3} approach their asymptotic value at a shallower depth than the curves for Chl = 1. This is because the higher scattering for the higher chlorophyll water redistributes the angular pattern of the radiance distribution more quickly with depth.

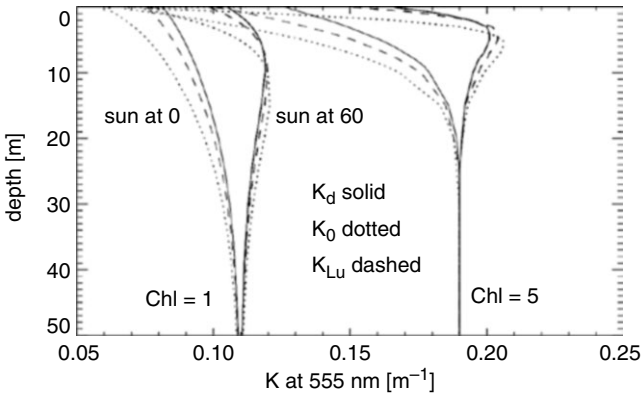

Fig. 7.4 Example dependence of diffuse attenuation functions at 555 nm on water and sky conditions. For each chlorophyll value, the three curves to the left near the surface are for the sun at the zenith, and the curves to the right are for a sun zenith angle of 60°. $K¥(\text{Chl}=1) = 0.11\ m^{-1}$ and $K¥(\text{Chl}=5) = 0.19\ m^{-1}$

IOPs do not depend on the ambient radiance and therefore can be measured on water samples. AOPs on the other hand do depend on the radiance and therefore must be measured in situ.

7.5 Variability of Underwater Irradiance

Natural waters vary enormously in composition. The clearest ocean or lake waters may have phytoplankton chlorophyll concentrations as low as 0.01 mg m^{-3}. At the other extreme, highly eutrophic lakes can have chlorophyll concentrations over 1,000 mg m^{-3}. Typical oceanic chlorophyll values are in the 0.1–10 range, with 0.5 being a rough global average. Water can contain almost no mineral particles, or a river can carry sediment loads of over 1 kg m^{-3}. Mineral particles can be highly absorbing, especially at blue wavelengths, or non-absorbing quartz or calcite particles. Scattering is strongly affected by the particle size distribution for a given type of particle. (As an analogy, think of the low visibility resulting from scattering by many small fog droplets versus much better visibility through fewer large rain drops, even though the water mass per cubic meter is the same.) The same variability holds for dissolved substances, not to mention pollutants. These wide ranges of water constituent types and concentrations produce an equally wide range in the magnitudes and spectral shapes underwater light fields.

Figure 7.5 shows HydroLight-computed examples of spectral scalar irradiance $E_o(z, \lambda)$ in quantum units in case 1 water for chlorophyll values of 0.01, 1, and 100 mg m^{-3}. Note that the wavelength of maximum light penetration shifts from deep blue at Chl = 0.01 to green at Chl = 1 to yellow at Chl = 100.

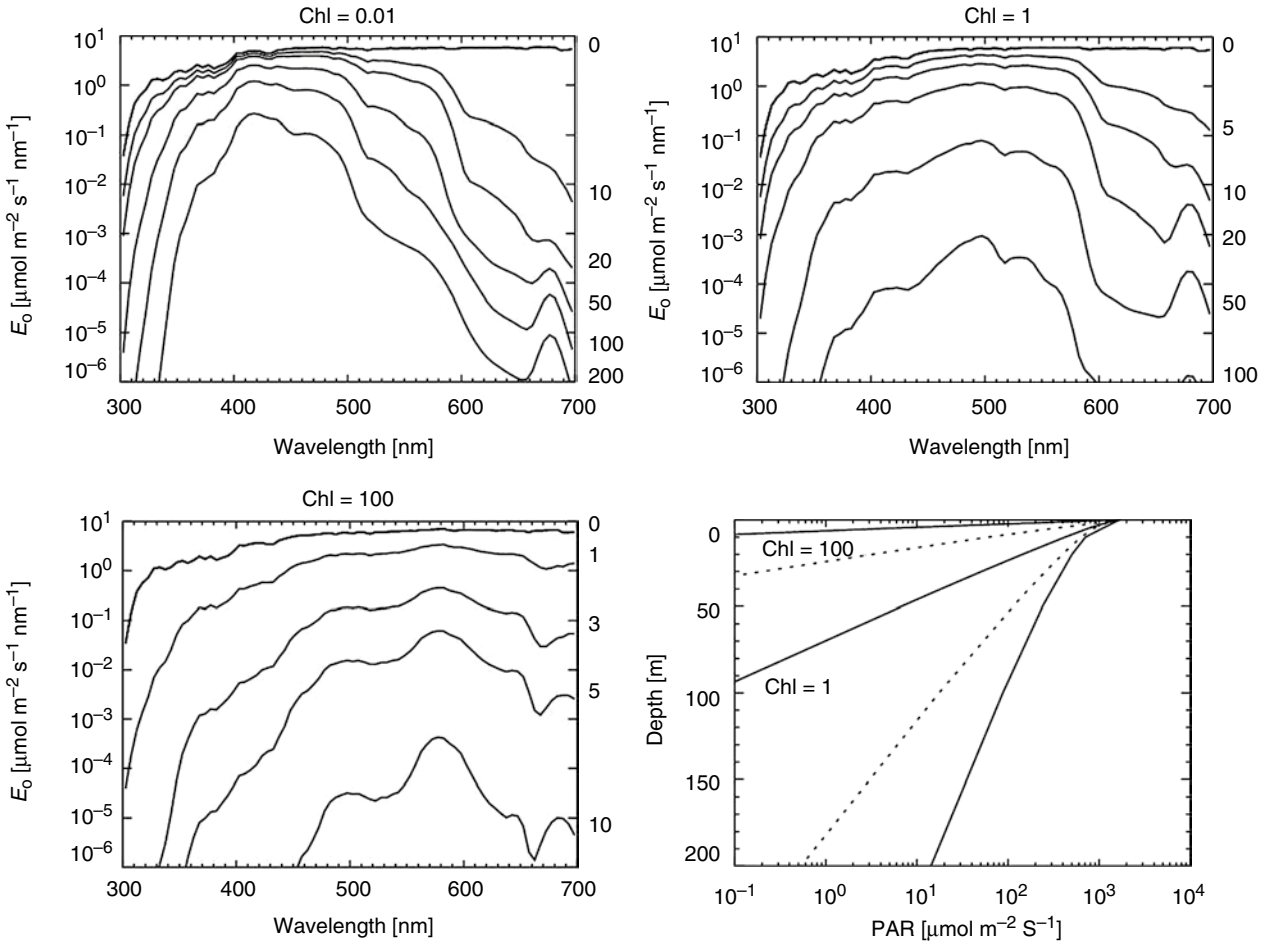

Fig. 7.5 Computed examples of spectral scalar irradiance E_0 in quantum units for chlorophyll values of 0.01, 1, and 100 mg m^{-3}. The numbers to the right of these plots show the depth in meters of the plotted spectra. The *solid lines* in the lower right panel shows the corresponding PAR values (computed from 400 to 700 nm); the *dashed lines* are for Chl = 0.1 and 10 mg m^{-3}

This wavelength dependence allows different species of phytoplankton, which have different pigment suites, to have a competitive advantage in different types of water. For this reason, the latest generation of ocean ecosystem models (Bissett et al. 1999) uses spectral irradiance rather than PAR to drive primary production calculations. The lower right panel of Fig. 7.5 shows the PAR values corresponding to the chlorophyll values of the other panels; dotted lines are for intermediate chlorophyll values. A rough rule of thumb says that photosynthesis can occur to PAR values as low as 1 µmol photons m^{-2} s^{-1}. This rule and these simulations indicate that photosynthesis occurs as deep as several hundred meters in the clearest water, but to only a few meters in very eutrophic water. The values in this figure were computed for the sun at a solar zenith angle of 50° in a clear sky; the values scale almost directly with changes in incident irradiance onto the sea surface for different sky conditions.

The simulations and data shown above only hint at the nature and variability of underwater light fields. The variety of water constituents is almost endless. Different species of phytoplankton have much different absorbing and scattering properties, which depend in complicated ways on the plankton light history and nutrient availability and thus show large variability even for the same species. The same holds for different types of mineral particles and dissolved substances. The types and concentrations of these components are often uncorrelated and vary widely with geographic location, time, and depth. The end result is that the underwater optical environment can be almost anything from the clearest of waters in which light penetrates hundreds of meters to almost opaque waters that become dark less than a meter below the surface. These differences in light environments are reflected in the much different biological communities in the world's waters.

Acknowledgments Writing this chapter was supported by HydroLight revenues. Emmanuel Boss of the University of Maine provided the New Jersey data used in Fig. 7.2.

References

Bissett WP, Carder KL, Walsh JJ, Dieterle DA (1999) Carbon cycling in the upper waters of the Sargasso Sea: II. Numerical simulation of apparent and inherent optical properties. Deep-Sea Res I 46:271–317

Bricaud A, Morel A, Babin M, Allali K, Claustre H (1998) Variations of light absorption by suspended particles with chlorophyll a concentration in oceanic (case 1) waters: analysis and implication for bio-optical models. J Geophys Res 103(C13):31033–31044

Johnsen S (2012) The optics of life: a biologist's guide to light in nature. Princeton University Press, Princeton

Kirk JTO (1994) Light and photosynthesis in aquatic ecosystems. Cambridge University Press, Cambridge

Mobley CD (1994) Light and water: radiative transfer in natural waters. Academic, San Diego (out of print but available on CD from the author or online at www.oceanopticsbook.info)

Mobley CD, Gentili B, Gordon HR, Jin Z, Kattawar GW, Morel A, Reinersman P, Stamnes K, Stavn R (1993) Comparison of numerical models for the computation of underwater light fields. Appl Optics 32(36):7484–7504

Morel A, Antoine D, Gentili B (2002) Bidirectional reflectance of oceanic waters: accounting for Raman emission and varying particle scattering phase function. Appl Optics 41(30):6289–6306

Petzold TJ (1972) Volume scattering functions for selected ocean waters. SIO Ref. 72–78, Scripps Inst. Oceanogr., 79 pages

Action Spectroscopy in Biology

8

Lars Olof Björn

8.1 Introduction

Action spectroscopy is a method for finding out what the initial step is in a photobiological or photochemical process. More exactly, the method serves to identify the kind of molecule absorbing the active light.

The basic principle of the method is the following: The more light that is absorbed, the greater its effect on the material systems under study. By comparing the effects of light having different wavelengths, a measure is obtained of the relative absorption at different wavelengths by the molecule directly affected by the light. This can then be compared to absorption spectra of various compounds. If everything works out, one can identify the compound absorbing the active light in the photoprocess under study.

A hypothetical example: molecule A, which is present in an organism, has the absorption spectrum shown in Fig. 8.1. Absorption of light by A causes a certain effect, say formation of anthocyanin in a plant. If a certain anthocyanin synthesis is obtained by irradiating for t minutes with N photons per m^2 and second of wavelength λ_1 (or λ_3), it ought to suffice with half as many photons of wavelength λ_2, since such light is absorbed twice as strongly. Or, conversely: if it is experimentally found that the two lights have the action described, this is an indication that molecule A is mediating the light effect. With only two wavelengths investigated, the conclusion is still very uncertain. If the agreement between efficiency of the light and the absorptive power of A is extended over a wider spectral region, the conclusion will be more firmly founded.

Figure 8.2 shows the result of a fictive experiment involving the pigment with the absorption spectrum in Fig. 8.1. The effect of various exposures to light of wavelengths l_1 and l_2 has been measured. The effect of the irradiation is plotted along the vertical axis versus some quantification of light on the horizontal axis (this can be either photon fluence or photon fluence rate or photon irradiance, depending on what is being studied).

Note that if we compare the effects of a certain amount of light or certain irradiance (such as that indicated by 1 or 2 in Fig. 8.2) for the two wavelengths, these effects do not (except in very special cases) have the same ratio (2) as the corresponding absorption coefficients in Fig. 8.1. Thus, we cannot construct an action spectrum just by comparing effects of a fixed exposure or irradiance. We must construct curves such as those in Fig. 8.2, so we can see how much light is needed for a specific effect to follow, which we choose as standard action.

The rest of this chapter will be more historical in character than other chapters. My experience is that action spectroscopy is better understood by studying several real examples of its use than theory alone. In addition, the papers cited here include some that can stand as good examples for young scientists. In some cases they reflect real scientific

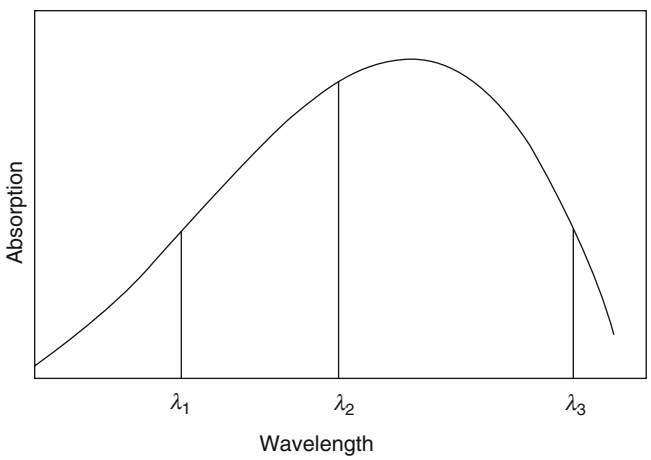

Fig. 8.1 The concept of action spectrum (see text)

L.O. Björn
School of Life Science, South China Normal University, Guangzhou, China

Department of Biology, Lund University, Lund, Sweden
e-mail: Lars_Olof.Bjorn@biol.lu.se

L.O. Björn (ed.), *Photobiology: The Science of Light and Life*,
DOI 10.1007/978-1-4939-1468-5_8, © Springer Science+Business Media New York 2015

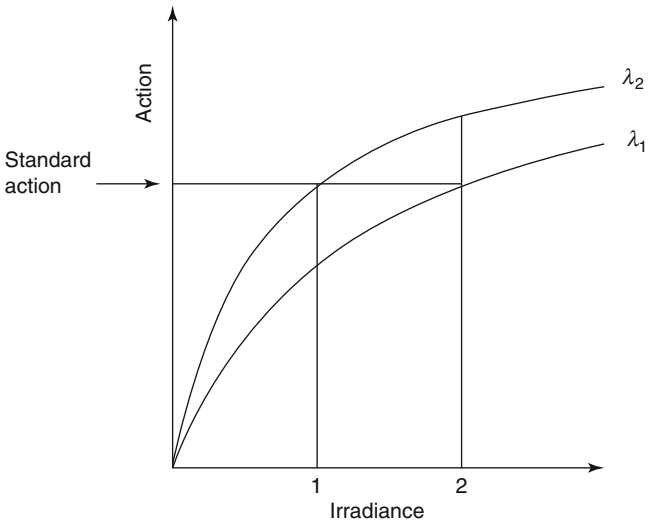

Fig. 8.2 The effect of different exposures of a sample (same system as in Fig. 8.1) on light of wavelengths λ_1 and λ_2. The effect or action of the light is plotted on the *vertical axis*. We compare in particular how much light is needed to achieve a certain action, which we choose as a standard action. We can see that twice as much is needed at wavelength λ_1 as at λ_2. From this we can deduce that light of wavelength λ_1 is absorbed by the active pigment only half as efficiently as light of wavelength λ_2

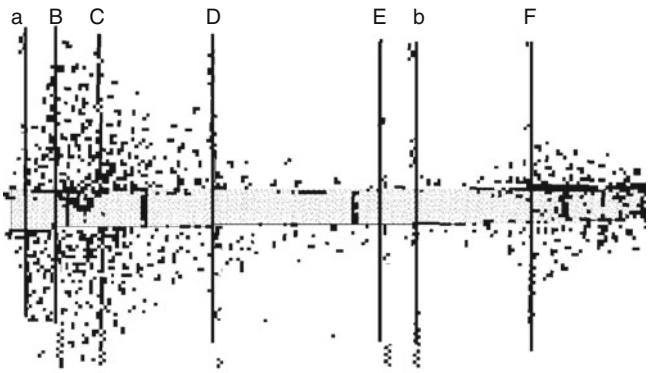

Fig. 8.3 A piece of a filamentous green alga (*Cladophora*, of which two whole cells and parts of two more cells are seen) with swimming bacteria in the sunlight spectrum projected in a microscope. The letters indicate the Fraunhofer lines in the solar spectrum, which are used for wavelength calibration: a = 718 nm, B = 687 nm, C = 656 nm, D = 589 nm, E = 527 nm, b = 518 nm, F = 486 nm. The accumulation of bacteria is greatest in the red region around 680 nm and in the blue region below 486 nm. These regions correspond to the main absorption bands of chlorophyll (From Engelmann (1882a))

ingenuity, and despite the rapid development of science, they have withstood the ravages of time remarkably well.

8.2 The Oldest History: Investigation of Photosynthesis by Means of Action Spectroscopy

Action spectroscopy may have its roots in Young's and von Helmholtz's theories about color vision. The first one, to my knowledge, to directly use action spectroscopy was T. W. Engelmann (1882a, b, 1884). He projected, under the microscope, spectra onto different algae and assayed the amounts of oxygen formed as a consequence of photosynthesis taking place in the algae. He estimated the relative amounts of oxygen by watching the accumulation of oxygen-loving (aerotactic) bacteria (Fig. 8.3).

Engelmann compared the oxygen-forming efficiency of different lights by reducing the light until the swimming movements of the algae stopped due to oxygen deficiency. In this way he could ascertain that in green algae it is chlorophyll that absorbs the light active in photosynthesis, while other pigments also participate in other kinds of algae. Figure 8.4 shows some of his comparisons between absorption spectra and action spectra. The chlorophyll present in red algae (as evident from their absorption spectra) does not show up in the action spectrum for their oxygen production. The cause of this surprising fact was not revealed until after World War II when Duysens, Emerson, and others discovered that two different photochemical systems cooperate in plant photosynthesis.

In addition to being an important step in the development of action spectroscopy and also in the history of photosynthesis research, Engelmann's experiments are important as early examples of a very sensitive "bioassay" of a chemical compound. The method of measuring oxygen by means of bacteria was so unconventional and the stated sensitivity in relation to other methods available at the time so remarkable that Engelmann was challenging the scientific authorities of his time. The algologist Pringsheim (1886) in Berlin as well as the Russian photosynthesis expert Timiriazeff (1885) found reason to criticize him using very harsh words.

Engelmann drew the correct conclusion that, in addition to chlorophyll, other pigments (colored substances) are able to absorb light and make it available to the photosynthesis process. He also understood (Engelmann 1882b) that there are other pigments in plant cells, which do not participate in photosynthesis but, on the contrary, "shadow" or "screen" the photosynthetically active pigments.

Engelmann's student Gaudikov studied chromatic adaptation (a designation in today's language, more consistent with the usual meanings of adaptation and acclimation, would be chromatic acclimation) in red algae and cyanobacteria, i.e. their acclimation to light of different colors. However, action spectra for this process were not determined until the 1960s by the Japanese Fujita and Hattori (1962) and in the 1970s, with greater precision, by the Americans J. Scheibe, S. Diakoff, and T. C. Vogelmann (see Diakoff and Scheibe 1973; Vogelmann and Scheibe 1978).

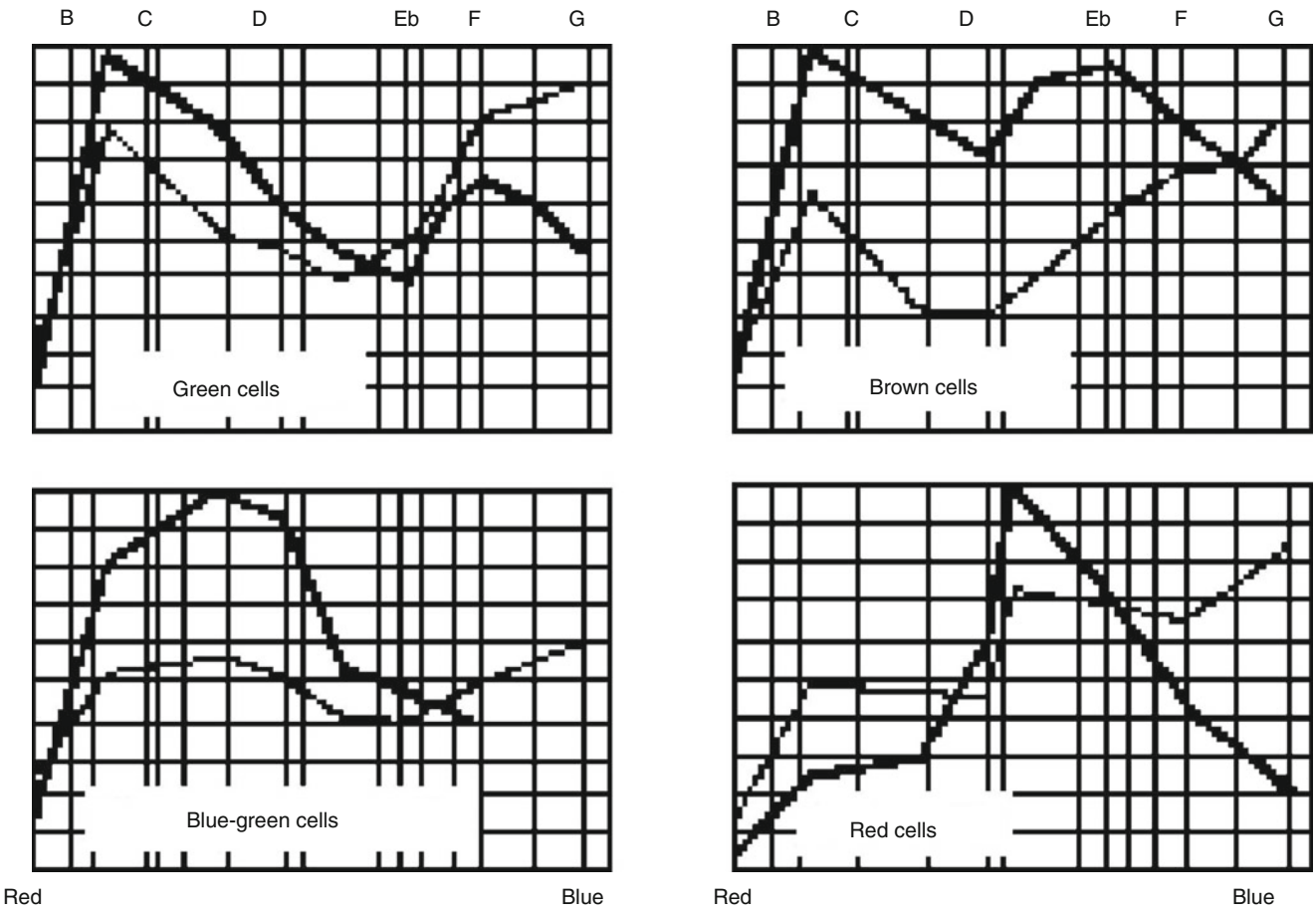

Fig. 8.4 Absorption spectra for algal cells (percent of incident light not penetrating the cells, *thin lines*) and action spectra for photosynthesis (*thick lines*). The high efficiency of light around 520 nm for photosynthesis by brown algae is due to light capture by the carotenoid fucoxanthin, the high efficiency around 620 nm in blue green algae to light capture by phycocyanin, and the high activity around 560 nm in red algae to light capture by phycoerythrin (From Engelmann (1884))

As for action spectra of photosynthesis, a few investigations were carried out during the intervening years, but real progress beyond Engelmann's results did not take place until the 1940s. For details of this development, the reader is referred to Haxo (1960). An early attempt was made also by Levring (1947) in Sweden to determine action spectra for photosynthesis in various algae, but he used wide spectral regions isolated with filters.

In this connection it is interesting to see how different scientists emphasized different aspects: Engelmann discussed in detail his method, spectral bandwidth, but lumped the algae together under the headings "green cells," "red cells," etc. Levring was less critical with regard to method but careful to state the species used and published separate spectra for closely related species.

It was above all the spectra measured by the Americans Haxo and Blinks (1950) by a polarographic method for oxygen measurement that was to yield results valid to this day (Fig. 8.5). Because of them, it became possible to do very careful comparisons between action spectra for photosynthesis and absorption spectra for various pigments in plants. Per Halldal brought this method to Sweden and improved it further (see Björn et al. 2007).

8.3 Investigation of Respiration Using Action Spectroscopy

The great Otto Warburg and his constant coworker Erwin Negelein (who, by the way, also determined action spectra for photosynthesis) over many years studied how the respiration of yeast cells is inhibited by carbon monoxide and how this inhibition can be removed by light (Fig. 8.6). They developed action spectroscopy to an accurate quantitative

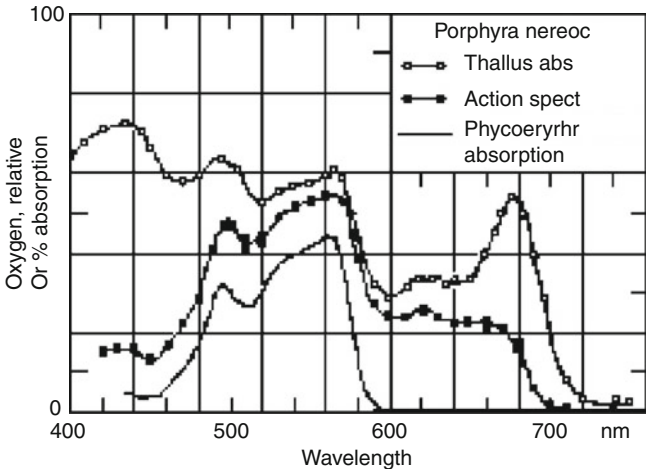

Fig. 8.5 The action spectrum for photosynthetic oxygen production in the red alga *Porphyra nereocystis* compared to the absorption spectrum of the same alga (Thallus abs.) and to the absorption spectrum of extracted phycoerythrin (From Haxo and Blinks (1950))

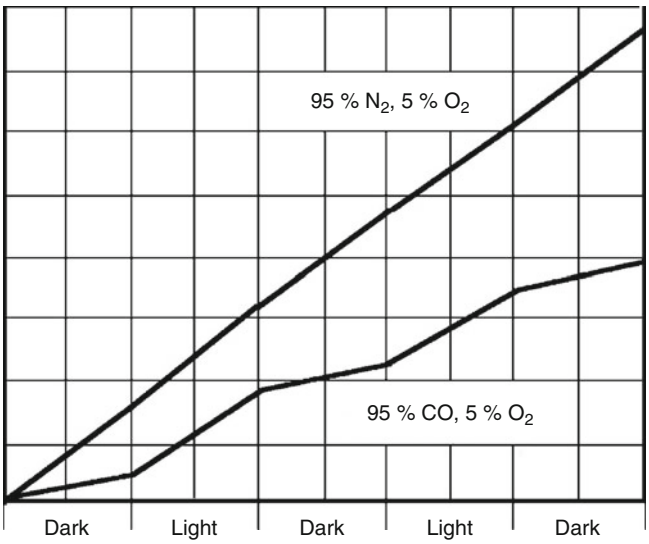

Fig. 8.6 The effect of light on oxygen uptake (respiration, *vertical axis*) in yeast in an atmosphere of 95 % nitrogen and 5 % oxygen (*straight line*) and in a mixture of 95 % carbon monoxide and 5 % oxygen. The horizontal coordinate is time, with alternating light and dark periods (From Warburg (1926))

method. As explicitly stated in one of their many papers, although they carried out the experiments together, it was Warburg who was the ingenious theoretician.

Their investigation led to the conclusion that the *Atmungsferment* (which we now call cytochrome *c* oxidase) is a protein to which iron-containing heme is bound and that the inactive complex formed with carbon monoxide is dissociated by light. The conclusion rests on the observation that the action spectrum for removing the inhibition of respiration by carbon monoxide agrees very well with the absorption spectrum for a complex between carbon monoxide and heme (Fig. 8.7). There is only a small shift in wavelength, which is explained by the binding to protein.

8.4 The DNA That Was Forgotten

At the beginning of the last century, Hertel (1905) in Jena had begun to study how microorganisms are affected by ultraviolet radiation. He managed to isolate nine different spectral lines from 210 to 558 nm and quantify the radiation using a thermopile. Considering the time, this was no small feat. Unfortunately, the evaluation of the biological effect was only semiquantitative. For constructing action spectra, he determined the irradiance that gave a just noticeable effect on the organism observable under the microscope. This effect could be stimulation of movement in *Paramecium* or contraction in rotifers. Unfortunately, he had no spectral line between 232 and 280 nm, and he therefore missed that region, which would later prove to be particularly interesting. Hertel's action spectra for ultraviolet damage to microorganisms are shown in Fig. 8.8. His experiments gave rise to a long-lived opinion that the deleterious action of ultraviolet radiation rises at an even rate toward shorter wavelength.

In the late 1920s, however, Gates (1928, 1930) found that the ability of ultraviolet radiation to kill bacteria varies with wavelength in the same way as does the ability of nucleic acid to absorb radiation (Fig. 8.9). This was the first indication of the fundamental importance of nucleic acid to life and a key experiment at the entrance to molecular biology.

At the same time as Gates' first report, another one was published, which was also on the road leading to the great revolution—Griffith's (1928) discovery of bacterial transformation. But it was not until after 1944 that the biological role of DNA became generally accepted by the demonstration of bacterial transformation by DNA (Avery et al. 1944).

One may wonder why Gates' experiments did not lead to a quicker development of DNA research. His work was in no way inferior to the transformation work. Perhaps an important reason was his way of publishing. In his first paper (1928) he does not show any convincing data. Despite this he clearly spelled out (although as we may think in retrospect, in a very cautious way) what was later proven to be essentially correct: "The close reciprocal correspondence between the curves of absorption of ultraviolet energy by these nuclear derivatives not only promotes the possibility that a single reaction is involved in the lethal action of ultraviolet light, but has a wider significance in pointing to these

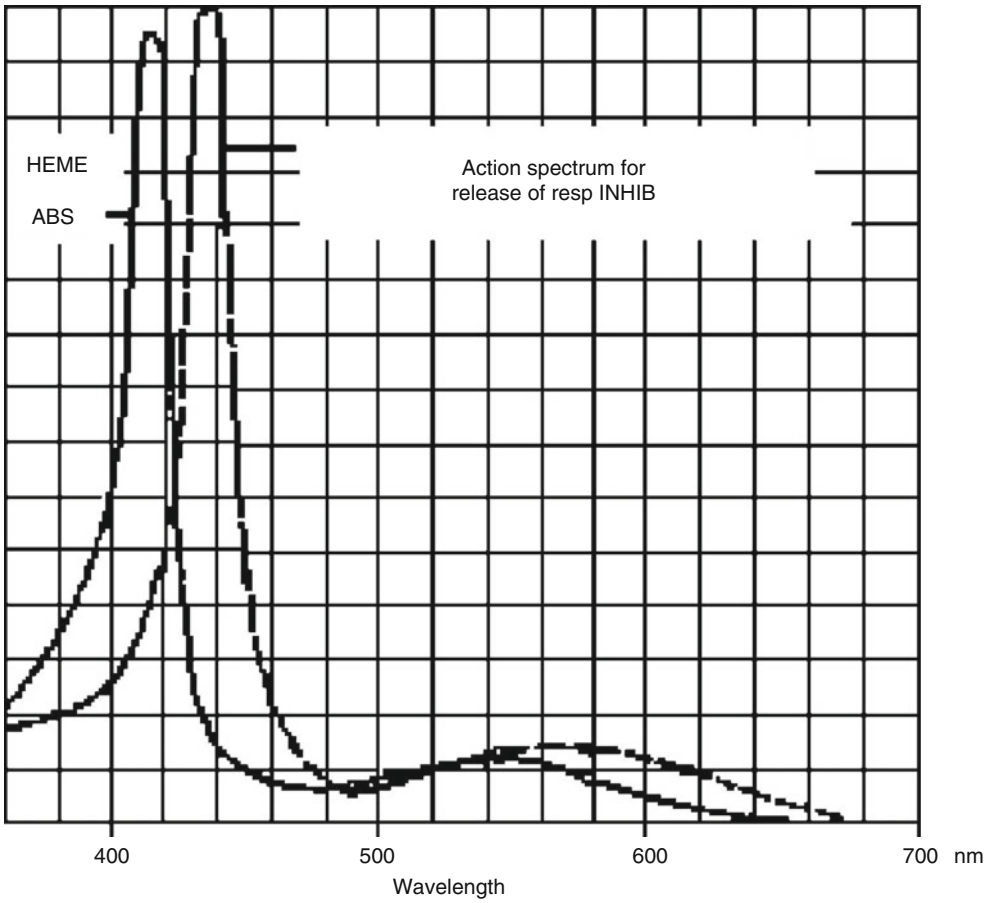

Fig. 8.7 Comparison between the absorption spectrum for heme and the action spectrum for release from CO inhibition of yeast respiration (From Warburg and Negelein (1929b); see also Warburg and Negelein (1929a))

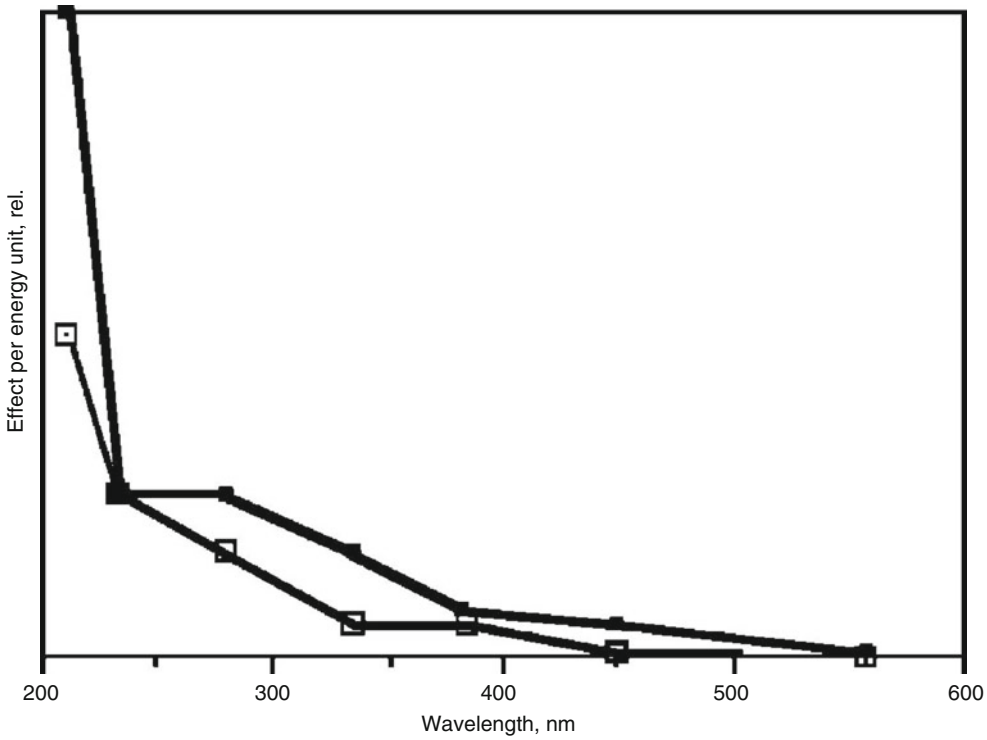

Fig. 8.8 Action spectra for induction of swimming movements in *Paramecium* (*top curve*) and for contraction in *Rotaria* (*curve with squares*) (Redrawn after Hertel (1905))

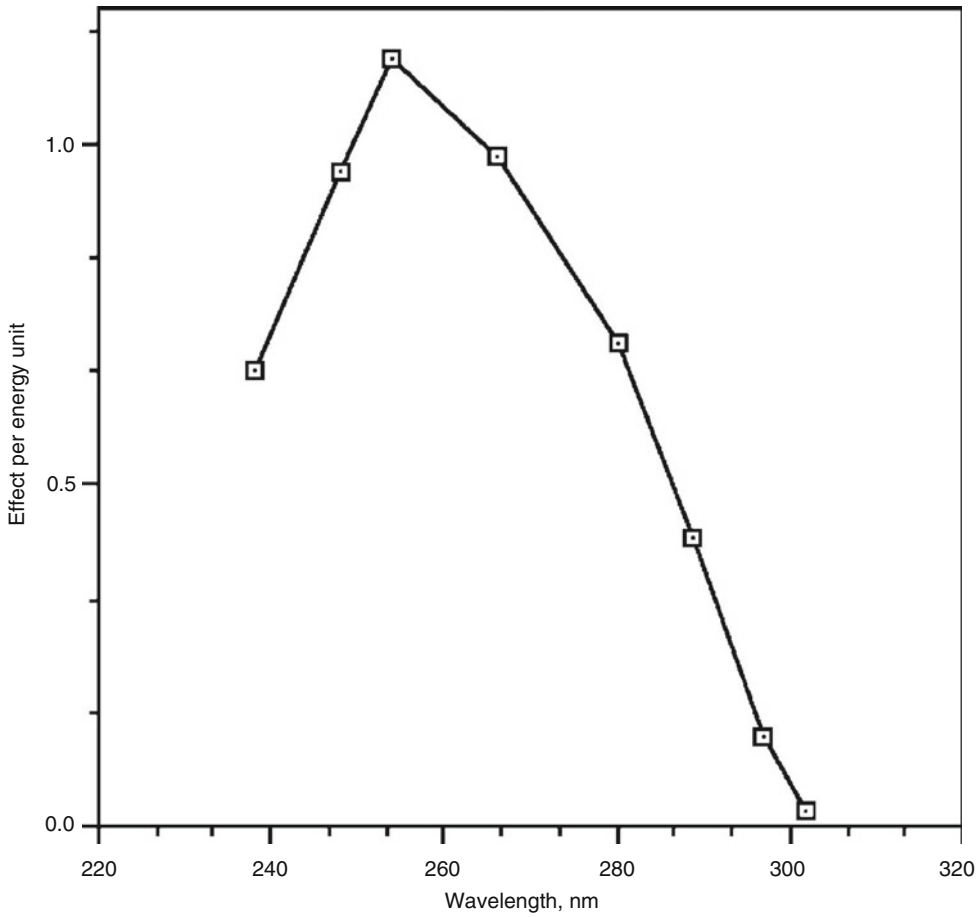

Fig. 8.9 Action spectrum for "killing" (inactivation of cell division) in the bacterium *Staphylococcus aureus*. The graph is similar to the absorption spectrum for DNA (Redrawn after Gates (1930))

substances as essential elements in growth and reproduction." After discussing some experiments done by others, which strengthened his views, he wrote: "Thus, while the relation of thymonucleic acid [i.e., DNA] to cell growth and reproduction remains a matter of conjecture, nevertheless the high concentration in the thymus gland and the coincidence of the evidence from these three independent series of experiments seem worthy of note, without further comment at present."

In the next paper Gates (1929) includes data for a bacterium, but the diagram is not drawn in such a way that it is easy to see the similarity to the DNA absorption spectrum, and DNA is mentioned neither in the discussion nor in the summary. In one more paper from 1930, the deleterious action of ultraviolet radiation is treated from another point of view. In one of his last publications, from 1931, Gates compares the action spectra for two bacterial species to the absorption spectra of the bacteria. About the critical substance, the destruction of which causes the death of the bacterial cells, Gates writes: "An examination of the evidence for its concentration in the cell nucleus, and the further search for evidence of its chemical character are reserved for the final paper of this series." Gates never got the opportunity to publish this final paper. He died on June 17, 1933. Although one paper was published posthumously, his followers obviously did not consider his ideas about DNA important, or even correct.

Contributing reasons to the fact that Gates' ideas never got the attention that their importance deserved were (1) that he was wrongly cited by later scientists (Hollaender and Claus 1936; e.g., "the maximum at 2499 A as reported by Gates"); (2), later scientists like Giese and Leighton (1935) went over to studying phenomena, e.g., swimming movements in *Paramecium*, which were very protein-dependent. Action spectra for such processes have maxima around 280 nm. This diverted the interest from nucleic acids to protein.

8.5 Plant Vision

One of the greatest triumphs of biological action spectroscopy is the discovery of the "vision pigment" of plants—phytochrome. However, at this point of the story, action spectroscopy is getting more complicated.

When the phytochrome saga opened, it was known that some effects of red light on plants could be canceled by exposing the plants to far-red light after the red. For instance,

some lettuce seeds do not germinate unless they are exposed to light after they have been allowed to take up water. Red light was found to be most efficient for this effect. Germination could be prevented by exposing the seeds to far-red light (720–740 nm) after the red.

Another example of red/far-red antagonism was the mode of growth of bean seedlings developing in darkness (Fig. 8.10). The tip of such a seedling is curved to a "plumular hook," but if the seedling receives just a minute of red light, the hook straightens out during subsequent growth (Fig. 8.10). Withrow et al. (1957) tackled the problem of quantifying the straightening effect of different kinds of light. For each of various fluences of light of different wavelengths, they measured by how many degrees the hooks of the bean plants were straightened out (Fig. 8.11).

They also quantified how efficient different kinds of lights were in counteracting the straightening effect of a previously administered saturating fluence of red light (Fig. 8.12). Based on the results, they were able to postulate the existence of a light-sensitive growth regulator, phytochrome. Phytochrome is formed in the plant in an inactive form (called P_r), which is transformable into the active form (P_{fr}) by red light.

The spectral curves that were obtained for the "straightening" and "bending" effects (Fig. 8.13) were postulated to correspond to absorption spectra for P_r and P_{fr}, respectively. It would never have been possible to isolate the phytochrome had not its "spectral signature" been determined beforehand in this way.

In Figs. 8.10 and 8.12, the lines for different wavelengths are not parallel. This means that the shape of the action spectra that are constructed from these lines will depend on the chosen level of action. That the curves are not parallel has to do with the fact that two photochemical reactions are involved to varying extents in all cases, i.e., the transformation of P_r to P_{fr} and the transformation of P_{fr} to P_r. The "most correct" shapes, i.e., those most closely corresponding to the absorption spectra of P_r and P_{fr} (Fig. 8.15), are obtained by investi-

Fig. 8.10 *Left*: Bean plants grown (*1*) in white light, (*2*) in darkness except for a few minutes of red light every day, and (*3*) in darkness except for a few minutes of far-red light every day

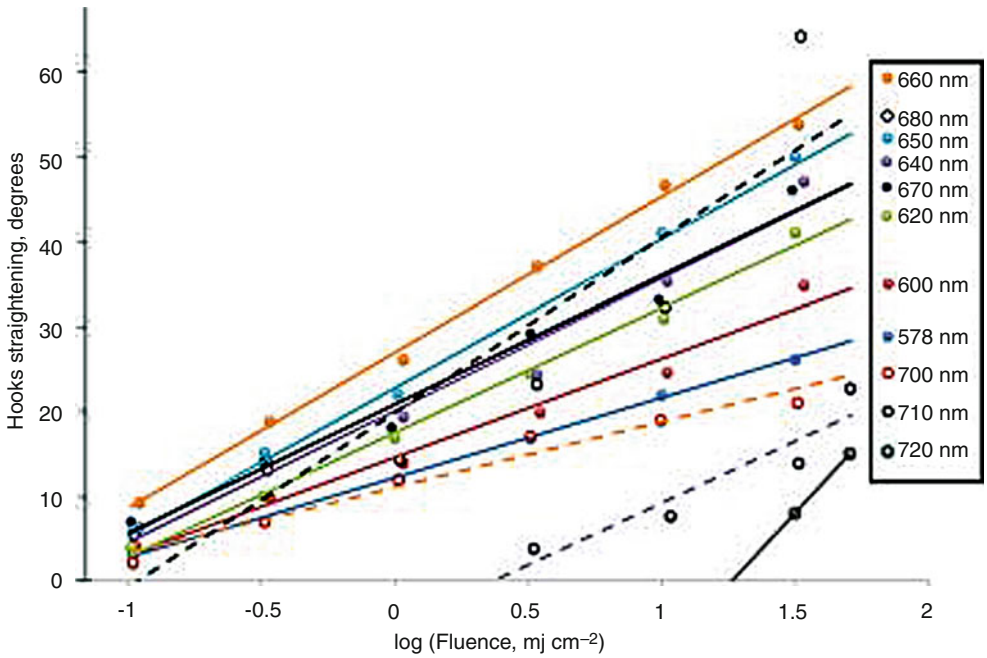

Fig. 8.11 The straightening effect on bean hooks of light of various wavelengths as a function of the energy fluence (Replotted from Withrow et al. (1957))

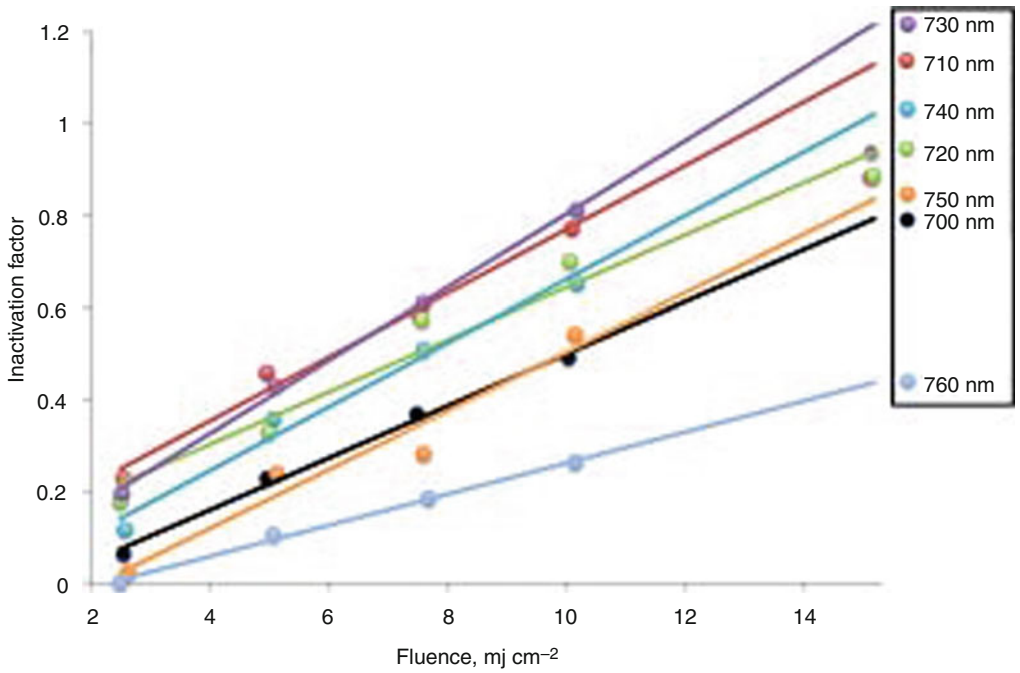

Fig. 8.12 Inactivation of red-induced hook straightening in bean plants by light of different wavelength as a function of fluence. In this case, a linear fluence scale was found to give better linearity of regression than the logarithmic scale in the previous graph (Redrawn from Withrow et al. (1957))

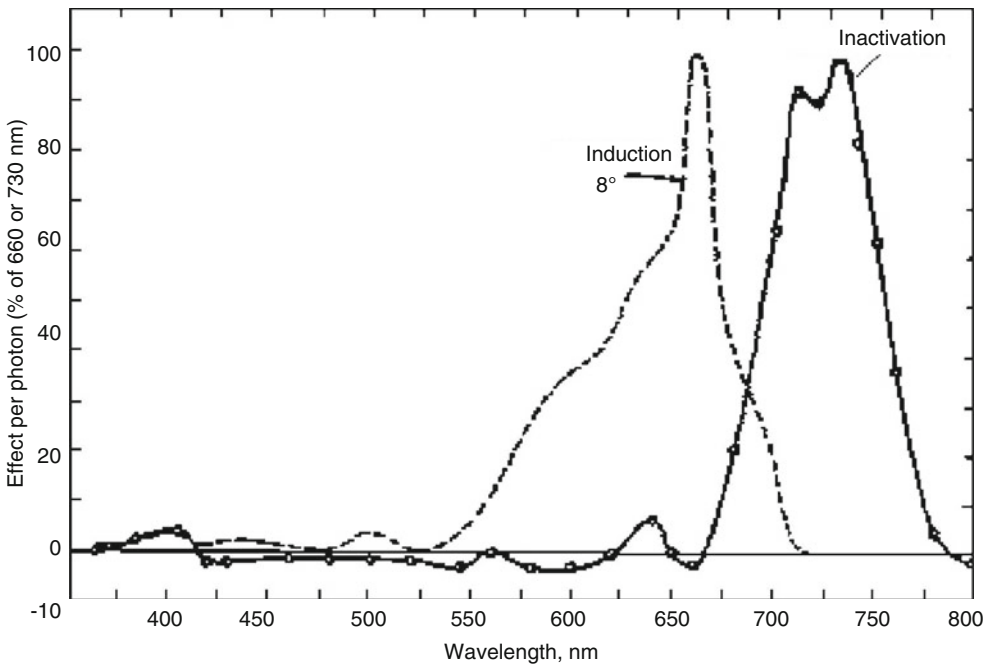

Fig. 8.13 Action spectra for straightening and for the inhibition of red-light-induced straightening of the bean hook, constructed from regression lines of the kind shown in Figs. 8.10 and 8.11 (Redrawn from Withrow et al. (1957))

gating the effects of very small fluences, resulting in small effects. Thus one has to find an appropriate compromise between this and the difficulty in measuring small effects accurately. In Fig. 8.14 a suitable level for recovering the action spectrum for $P_r ==> P_{fr}$ could be $P_{fr}/(P_r + P_{fr}) = 0.1$.

Let us see if we can make sense more in detail of the shapes and slopes of the graphs in Fig. 8.11. Consider the photoreversible system $P_r <==> P_{fr}$. It is now known that P_{fr} is the active form of phytochrome. Let us assume that monitored reaction (the straightening of the hook) is proportional to the amount of P_{fr}. This amount should be the difference between what is formed in the forward reaction $P_r ==> P_{fr}$ and that consumed in the back reaction $P_r <== P_{fr}$. The rate for each reaction is proportional to the product of fluence

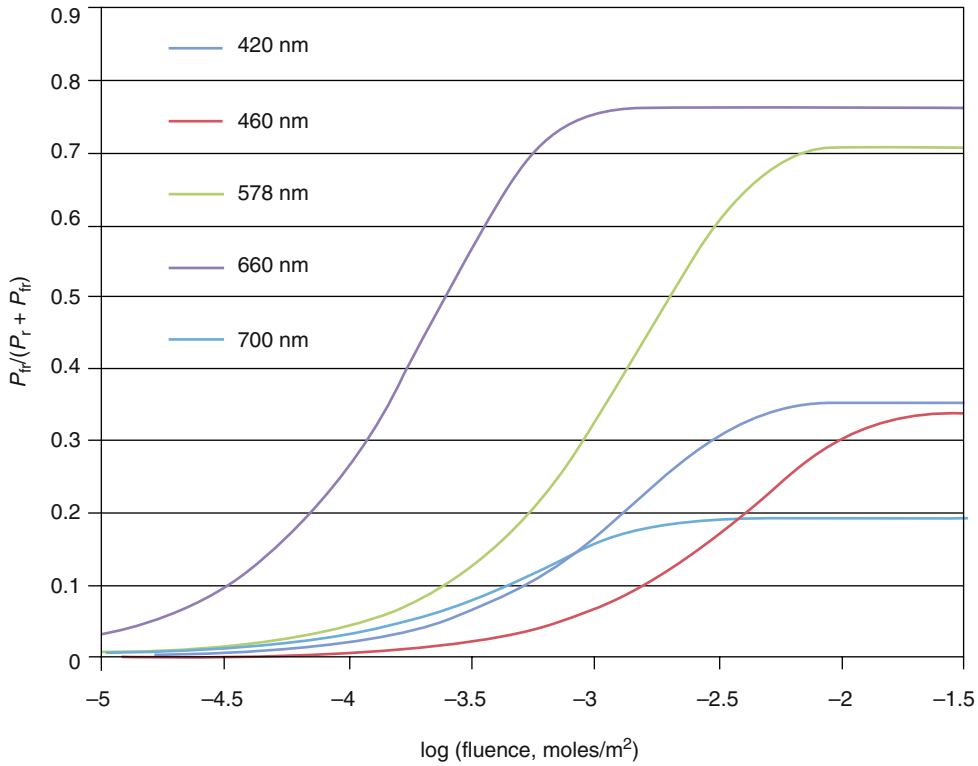

Fig. 8.14 Computed fraction of P_{fr} out of total phytochrome

rate and conversion cross section (the latter being the product of the absorption cross section and the quantum yield). So the net forward rate is $dP_{fr}/dt = I \times (P_r \times \sigma_r - P_{fr} \times \sigma_{fr}) = I \times ((P_t - P_{fr}) \times \sigma_r - P_{fr} \times \sigma_{fr}) = I \times (P_t \times \sigma_r - P_{fr} \times (\sigma_r + \sigma_{fr}))$. Here the sigmas stand for the conversion cross sections, the P for phytochrome concentration, r and fr for the red- and far-red-absorbing forms, and P_t for total phytochrome. We may for simplicity put $P_t = 1$ and express the other concentrations as fractions of this, which gives the simple form

$$dP_{fr} / dt = I \times \left(P_t \times \sigma_r - P_{fr} \times \left(\sigma_r + \sigma_{fr} \right) \right).$$

In integrated form this becomes

$$\sigma_r - \left(\sigma_r + \sigma_{fr} \right) \times P_{fr} = \sigma_r \times \exp\left(- \left(\sigma_r + \sigma_{fr} \right) \times I \times t \right).$$

or

$$P_{fr} = \left\{ 1 - \exp\left[- \left(\sigma_r + \sigma_{fr} \right) \times I \times t \right] \right\} / \left(1 + \sigma_{fr} / \sigma_r \right).$$

In Fig. 8.14 we have plotted P_{fr} according to this expression as a function of $\log(I \times t)$, i.e., log (fluence).

The complications of this light-sensitive system are well demonstrated by the action spectrum determined by Hartmann (1967) for the inhibiting effect of prolonged and relatively strong illumination on the extension growth of lettuce hypocotyls (Fig. 8.16). At first glance it does not seem to have anything to do with the shapes of the absorption spectra of the two phytochrome forms. But Hartmann showed that this phenomenon could be explained by phytochrome being the mediator of the light action. However, in this case one has to take into account not only the photochemical reactions, but also the fact that the physiologically active form of phytochrome, P_{fr}, is unstable and disappears if there is no P_r present from which P_{fr} can be continually reformed. It is for this reason that light gives the greatest physiological effect, which causes only a small part of the phytochrome to be continuously converted to P_{fr}. Light of longer wavelength has no effect because too little P_{fr} is formed. Light of too short a wavelength has no effect because P_{fr} is formed too quickly, and all phytochrome disappears before it can act for a sufficient amount of time. The inhibition of the growth of the lettuce hypocotyls is an example of a so-called high-intensity reaction (HIR).

8.6 Protochlorophyllide Photoreduction to Chlorophyllide *a*

The present author and many other researchers have studied the action spectra for synthesis of chlorophyll and formation of chlorophyll. Important early contributions were made by J. H. C. Smith at the Carnegie Institution, T. N. Godnev and A. A. Shlyk in Belorussia, and H. Virgin

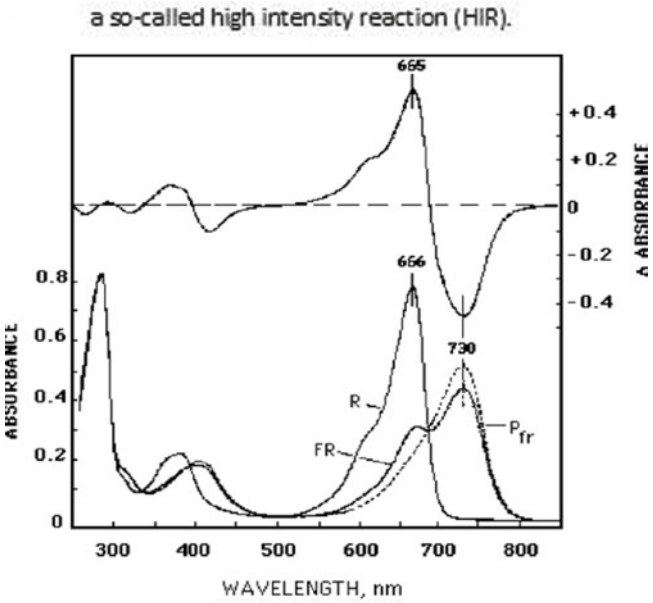

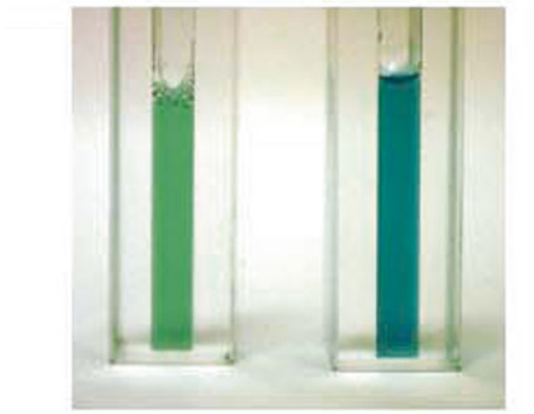

Fig. 8.15 *Top*: Absorption spectra of purified phytochrome from oats. The *curve marked R* is the measured absorption of far-red irradiated solution, containing almost only P_r. The *curve marked FR* is the measured absorption of red irradiated solution, containing mostly P_{fr} and some P_r. The *dotted curve marked* P_{fr} is the estimated spectrum of pure P_{fr}, which cannot be measured directly, since red light only partially converts P_r to P_{fr}. The *top curve* is a so-called difference spectrum showing the difference in absorption between far-red irradiated and red irradiated solutions. Since only the change due to irradiation shows up in this, almost the same difference spectrum can be obtained from plant tissue (After Vierstra and Quail (1983a, b)). *Bottom*: P_{fr} (*left*) and P_r (*right*) prepared from oat coleoptiles (Courtesy Gunvor Björn)

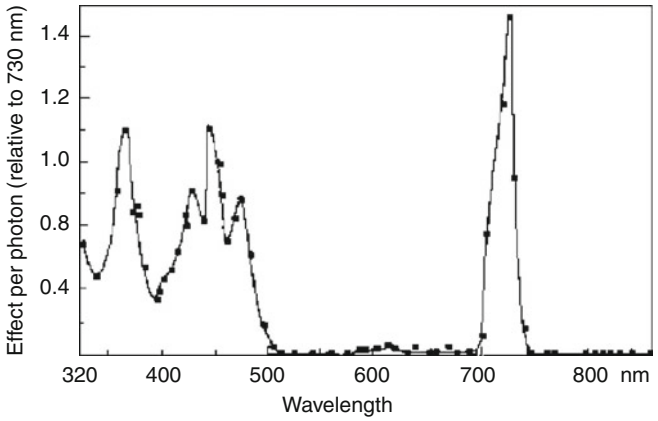

Fig. 8.16 Example of action spectrum for a high-intensity phytochrome reaction (HIR), the inhibition of lettuce hypocotyl longitudinal growth (Hartmann 1967). The sharp long-wavelength band is due to phytochrome, while a flavin-containing pigment is involved in the short-wavelength part

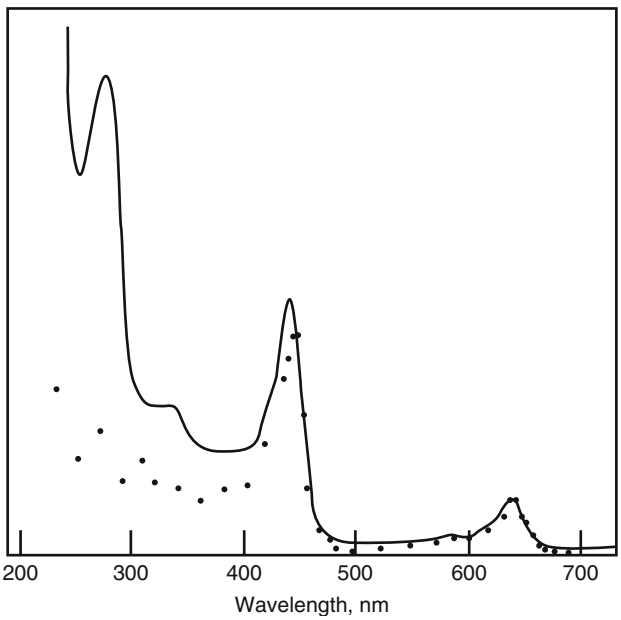

Fig. 8.17 The absorption spectrum of purified "protochlorophyll holochrome" (complex between protochlorophyllide, NADPH, and NADPH–protochlorophyllide photooxidoreductase) extracted from etiolated bean plants (Schopfer and Siegelman 1969) and the action spectrum for protochlorophyllide photoreduction to chlorophyllide *a* (Björn 1969a) (Redrawn from Björn (1969b))

in Sweden. Virgin's former students have continued this line of research in Göteborg (see Sundqvist and Björn 2007).

Chlorophyll formation is governed by several light-sensitive processes: conversion of protochlorophyllide to chlorophyllide with enzyme-bound protochlorophyllide as the light absorber, conversion of phytochrome, and action on the so-called blue light receptor.

One specific question in this context was whether radiation absorbed in the aromatic amino acids of the enzyme NADPH–protochlorophyllide photooxidoreductase would be able to cause the conversion of protochlorophyllide to chlorophyllide in the same way as does radiation absorbed in the protochlorophyllide itself. In Fig. 8.17 the absorption of the NADPH–protochlorophyllide photooxidoreductase complex with its substrates NADPH and protochlorophyllide is shown by the solid curve. In the visible region, the absorption is due to the protochlorophyllide. The high peak at 280 nm, on the other hand, is due to aromatic amino acids

in the protein. The action spectrum for protochlorophyllide photoreduction, shown by dots, has essentially the same features in the visible region but lacks the high peak at 280 nm. The conclusion is that energy absorbed in the aromatic amino acids cannot be used for photoreduction. There is also a small difference between absorption and action spectrum in the blue region (the so-called Soret peak of the spectra). This is probably because there are two fractions of protochlorophyll with slightly different spectra, of which only one can be converted by light (there may be no reductant, NADPH bound to the "inactive" complexes). There is also some blue-absorbing carotenoid contributing to the absorption spectrum.

8.7 Limitations of Action Spectroscopy: The Elusive Blue Light Receptor

Numerous "blue light phenomena" have been studied in plants and fungi: phototropism, chloroplast rearrangements, plastid differentiation, and nastic movements, to mention a few. The discussion about the possible nature of the molecule absorbing the active light in these processes has centered mainly on carotenoids and flavoproteins, because the action spectra are similar to absorption spectra of these compounds (which are so similar to each other and so variable with conditions and molecular details that a conclusion on action spectra alone seems impossible). As described in Chap. 11, it has been found that most blue light phenomena are mediated by flavoproteins but that some, e.g., stomatal movements, may be carotenoid-mediated. Because of the similarity of the absorption spectra for these two groups of compounds, action spectroscopy has not been able to distinguish between them. The questions have now mostly been solved, mainly by methods of molecular biology. However, action spectroscopy, after more than a hundred years, is a method still in use (e.g., Ziv et al 2007).

8.8 Another Use for Action Spectra

So far we have only discussed the use of action spectroscopy for identifying the molecules absorbing the light driving the various photoprocesses. I would like to point out one more important reason for determining action spectra. For this we shall go back to near the beginning of this chapter, to the damaging effect of ultraviolet radiation but look at it from another angle.

Over the past 35 years, there has been concern about the depletion of the stratospheric ozone layer (see Chap. 22). Such depletion results in increased levels of ultraviolet radiation at the surface of the Earth (unless other changes in the atmosphere were to compensate for the depletion in stratospheric ozone). Experiments have been carried out to forecast the biological effects of such changes in radiation. Ozone depletion has been simulated by exposing the organisms to be studied to artificial ultraviolet radiation. One problem has been that the artificial radiation cannot be given the same spectral composition as the additional solar radiation that would leak through a depleted ozone layer. Therefore, weighting functions have been needed to calculate how much artificial ultraviolet radiation that has to be administered to simulate certain ozone depletion, and for this, one has to determine action spectra for different ultraviolet effects. Initially, one relied on ordinary, "monochromatic" action spectra, determined as the other spectra in this chapter. However, since so many different ultraviolet effects with different action spectra are involved, it has turned out to be more realistic to determine "polychromatic action spectra." For this, one starts with a full spectrum and, for different samples, cuts away more and more of the short-wavelength part.

References

Avery OT, MacLeod CM, McCarty M (1944) Studies on the chemical nature of the substance inducing transformation of pneumococcal types. J Exp Med 79:137–157

Björn LO (1969a) Action spectra for transformation and fluorescence of protochlorophyll holochrome from bean leaves. Physiol Plant 22:1–17

Björn LO (1969b) Studies on the phototransformation and fluorescence of protochlorophyll holochrome in vitro. In: Metzner H (ed) Progress in photosynthesis research, vol 2. H. Laupp Jr, Tübingen, pp 618–629

Björn LO, Sundqvist C, Öquist G (2007) A tribute to Per Halldal (1922–1986), a Norwegian photobiologist in Sweden. Photosynth Res 92:7–11

Diakoff S, Scheibe J (1973) Action spectra for chromatic adaptation in *Tolypothrix tenuis*. Plant Physiol 51:382–385

Engelmann TW (1882a) Ueber Sauerstoffausscheidung von Pflanzenzellen im Mikrospektrum. Bot Ztg 40:419–426

Engelmann TW (1882b) Ueber Assimilation von *Haematococcus*. Bot Ztg 40:663–669

Engelmann TW (1884) Untersuchungen über die quantitativen Beziehungen zwischen Absorption des Lichtes und Assimilation in Pflanzenzellen. Bot Ztg 42:81–94, 97–106 and Tafel II

Fujita Y, Hattori A (1962) Photochemical interconversion between precursors of phycobilin chromoproteids in *Tolypothrix tenuis*. Plant Cell Physiol 3:209–220

Gates FL (1928) On nuclear derivatives and the lethal action of ultraviolet light. Science 68:479–480

Gates FL (1929) A study of the bactericidal action of ultra violet light. I. The reaction to monochromatic radiations. J Gen Physiol 14:31–42

Gates FL (1930) A study of the action of ultra violet light III. The absorption of ultra violet light by bacteria. J Gen Physiol 14:31–42

Giese AC, Leighton PA (1935) Quantitative studies on the photolethal effects of quartz ultra-violet radiation upon *Paramecium*. J Gen Physiol 18:557–571

Griffith F (1928) The significance of pneumococcal types. J Hyg 27: 113–159

Hartmann KM (1967) Ein Wirkungsspektrum der Photomorphogenese unter Hochenergiebedingungen und seine Interpretation auf der Basis des Phytochroms (Hypokotylwachstumshemmung bei *Lactuca sativa* L.). Z Naturforsch 22b:266–275

Haxo FT (1960) The wavelength dependence of photosynthesis and the role of accessory pigments. In: Allen MB (ed) Comparative biochemistry of photoreactive systems. Academic, New York, pp 339–376

Haxo FT, Blinks LR (1950) Photosynthetic action spectra of marine algae. J Gen Physiol 33:389–422

Hertel E (1905) Ueber physiologische Wirkung von Strahlen verschiedener Wellenlänge. Z Allg Physiol 5:95–122

Hollaender A, Claus WD (1936) The bactericidal effect of ultraviolet radiation on *Escherichia coli* in liquid suspensions. J Gen Physiol 19:753–765

Levring T (1947) Submarine daylight and the photosynthesis of marine algae. Göteborgs Kgl. Vetenskaps- och Vitterhets-samhälles Handl., 6:e följden, ser. B, band 5, nr 6. 90 s

Pringsheim N (1886) Zur Beurtheilung der Engelmann'schen Bakterienmethode in ihrer Brauchbarkeit zur quantitativen Bestimmung der Sauerstoffabgabe im Spektrum. Berl Deutsch Bot Ges 4:40–46

Schopfer P, Siegelman HW (1969) Purification of protochlorophyllide holochrome. In: Metzner H (ed) Progress in photosynthesis research, vol 2. H. Laupp Jr, Tübingen, pp 612–618

Sundqvist C, Björn LO (2007) A tribute to Hemming Virgin, a Swedish pioneer in plant photobiology. Photosynth Res 92:13–16

Timiriazeff C (1885) État actuel de nos conaissances sur la fonction chlorophyllienne. Ann. des Sc. Nat. Botanique (3) Tome II

Vierstra RD, Quail PH (1983a) Purification and initial characterization of 124-kilodalton phytochrome from *Avena*. Biochemistry 22: 2498–2505

Vierstra RD, Quail PH (1983b) Photochemistry of 124-kilodalton *Avena* phytochrome in vitro. Plant Physiol 72:264–267

Vogelmann TC, Scheibe J (1978) Action spectra for chromatic adaptation in the blue-green alga *Fremyella diplosiphon*. Planta 143:233–239

Warburg O (1926) Über die Wirkung des Kohlenoxyds auf den Stoffwechsel der Hefe. Biochem Z 177:471–486

Warburg O, Negelein E (1929a) Über die photochemische Dissoziation bei intermittierender Belichtung und das absolute Absorptionsspektrum des Atmungsferments. Biochem Z 202: 202–228

Warburg O, Negelein E (1929b) Absolutes Absorptionsspektrum des Atmungsferments. Biochem Z 204:495–499

Withrow RB, Klein WH, Elstad V (1957) Action spectra of photomorphogenetic induction and its inactivation. Plant Physiol 32:453–462

Ziv L, Tovin A, Strasser D, Gothilf Y (2007) Spectral sensitivity of melatonin suppression in the zebrafish pineal gland. Exp Eye Res 84:92–99

Spectral Tuning in Biology I: Pigments

9

Lars Olof Björn and Helen Ghiradella

9.1 Introduction

The justification for a book about photobiology rests partly on combination of various specialities for interdisciplinary comparisons. One topic suitable for comparisons is "spectral tuning." By this we mean the principles for how spectra of pigments, and factors that can modify their spectral responses, are adjusted to the needs of the organisms that produce them. A number of examples will be found in this chapter.

To pigments, substances that produce color by absorbing light of some wavelengths and reflecting or transmitting the rest, we must add a second class of color mechanism, *structural* colors. These are produced by the interaction of light with the detailed architecture of the material or structure on which it falls. We will begin with a discussion of biological pigments and in the next chapter move on to biological structural colors. We will also discuss some additional mechanisms by which organisms control their spectral presentation to the world.

Spectral tuning is relevant for vision (not only for color vision), photosynthesis, bioluminescence, flower colors, and adaptive coloration of animals, and especially for animals that move around among green plants, to increase contrast of edges. These processes are not independent. Flower colors are adapted to the vision of pollinators and as a contrast to photosynthetic pigments. Bioluminescence and vision have evolved together. Phytochrome has evolved to discriminate between direct daylight and light modified by chlorophyll absorption. The basis is the spectrum of the sun. To begin with, let us see what the relation is between the spectrum of the most important of all pigments, chlorophyll *a*, and the spectrum of the sun.

9.2 Why Are Plants Green?

Many people have discussed the spectrum of chlorophyll in relation to daylight. Some have come to the conclusion that they do not match well, as absorption "in the middle of the spectrum," i.e., the green band, is weak. A common idea is that an ideal pigment for photosynthetic energy conversion ought to be either black, absorbing all available radiation, or absorb most efficiently at the "peak" of daylight.

But what is the "peak" wavelength for daylight? The maximum of the daylight spectrum depends on how we plot it. For the present purpose, to simplify comparisons and calculations, we may represent the daylight spectrum by that of a 6,000 K blackbody radiator and thus apply Planck's radiation law (Chap. 1). We can then calculate that if we plot the spectrum as energy per uniform wavelength interval, the maximum is at 480 nm. But if we instead plot it as photons per uniform wavelength interval, the maximum is at 600 nm, and if we, following the habits of physicists, plot the spectrum as energy per uniform frequency interval, or photons per uniform frequency interval, the peak will be seen at frequencies corresponding to 800 nm and 1,200 nm, respectively.

Thus, the "maximum of the daylight spectrum" is an ambiguous concept, and we have to find another way of optimizing our pigment. As for the idea that an ideal pigment should absorb everything, we should remember that the better a substance absorbs, the better it emits, and the transformation of radiant energy into other energy forms is just the balance between absorption and reradiation. That total absorption is not an ideal is even more apparent in the case of color vision. Vertebrate cones, which are cells receiving light signals for color vision, are shorter than the rods involved in "noncolor night vision" (scotopic vision) and therefore absorb a smaller portion of the light and discriminate between wavelength bands better than they would if they were as long as rods.

L.O. Björn (✉)
School of Life Science, South China Normal University, Guangzhou, China

Department of Biology, Lund University, Lund, Sweden
e-mail: Lars_Olof.Bjorn@biol.lu.se

H. Ghiradella
Department of Biology, University at Albany, Albany, NY, USA
e-mail: hghff@albany.edu

L.O. Björn (ed.), *Photobiology: The Science of Light and Life*,
DOI 10.1007/978-1-4939-1468-5_9,

Photosynthesis depends on photochemistry, and photochemistry works particle to particle, photon to molecule. The useful energy storage can be regarded as the product of the number of reacting photons and the free energy that each converted photon contributes. Björn (1976) following this principle comes to the conclusion that the long-wave absorption band of a pigment giving maximum energy conversion in direct sunlight should be rather narrow and have a maximum at 707 nm. Furthermore, the pigment should be highly fluorescent (when not quenched by photochemistry). The maximum chemical potential difference that can be created by a one-step system is

$$\mu_o = kT \cdot \ln\left[\left(\Phi r^2 / 4R^2\right)\right] + h\nu_o\left(1 - T / T_S\right) - b^2\left[h^2/2\mathrm{k}\right]\left]T\left(1/T^2 - 1/T_s^2\right)\right.$$

where k = Boltzmann's constant, h Planck's constant, T ambient temperature, T_S the temperature of the radiating surface of the Sun, Φ the fluorescence yield, r the radius of the Sun, R the Earth-Sun distance, ν_o the frequency of the spectral peak of the absorption band, and b a parameter determining the width of the absorption band such that the half-band width is $2b\sqrt{(2\ln 2)} = 2.35b$. With numerical values inserted, this becomes $\mu_o = -0.342$ eV + (19/20) $h\nu_o$–$6.6.10^{-28}$b^{2}eV s^2 (eV stands for electron volts). The effective chemical potential difference under conditions of maximum energy conversion is 0.13 eV lower than that (just as the voltage of an electrical battery is lowered when power is drawn from it).

All this is for full sunlight. The optimum position of the absorption peak is lowered by 12 nm for every tenfold decrease of fluence rate, even if the spectrum of the daylight is not changed. Thus, it appears that the long-wavelength band of chlorophyll *a* in vivo is rather well matched to the conditions of our planet. The "blue" absorption band of chlorophyll (the Soret band) does not contribute to chemical potential, but leads to increased photon absorption and thus increased energy conversion, as do various accessory pigments.

Milo (2009) using partly different and refined arguments and seeking the optimum center wavelength of the reaction center for a system utilizing pigment antennae to feed the center with energy arrive at essentially the same result. The most refined analysis today of the reason that the spectra of photosynthetic systems have evolved to the properties that they have is that of Marosvölgyi and van Gorkom (2011). They have taken into account also the energetic cost of the construction of the pigments and can explain also the long-wavelength spectral band of chlorophyll *b* and the spectra of bacteriochlorophylls. By using real daylight spectra rather than a blackbody approximation of the solar spectrum, they also find that the optimum wavelengths are hardly dependent at all on photon fluence rate.

Mauzerall (1976) has speculated on how chlorophylls can have evolved from porphyrins along a path of increasing lipophilicity, making them suitable for incorporation into membranes. Björn et al. (2009) have concentrated their discussion specifically on the question of why chlorophyll *a* has been chosen as the key pigment for oxygenic photosynthesis. With the discovery that chlorophyll *d* can replace chlorophyll *a* not only in pigment antennae, but also in reaction centers, the latter has much of its uniqueness.

Various types of bacterial chlorophylls have absorption bands at longer wavelengths. They are not adapted to direct daylight, but to the light that penetrates down to the places (such as anoxic sediments below algae absorbing shorter-wavelength light) where these bacteria live. The record in long wavelengths is held by bacteriochlorophyll *b*. Its spectrum peaks at 1,020 nm, beyond two infrared absorption bands of water.

Kiang et al. (2007) and Stomp et al. (2007) have detailed how various photosynthetic pigments are adapted for different environments on Earth.

9.3 What Determines Spectra of Pigments?

Generally speaking, the absorption spectrum of a pigment is determined by (1) the structure of the chromophore(s) and (2) the environment of the chromophore.

The most important feature in chromophore structure is the arrangement of conjugated double bonds (alternating single and double bonds), i.e., the π electron clouds. The environment of the chromophore in many cases consists of, or is at least dominated by, a protein to which the chromophore is bound, but there are also important cases, such as vacuolar flower pigments, where the chromophore is not protein bound, and other factors are the main concern.

In general, the absorption peak with longest wavelength for a molecule with conjugated bonds increases with the length of the conjugated bond system. It depends, as we shall see, also very much on the shape of the conjugated system, whether it is straight or not and, in the case of macrocycles as in chlorophylls, on its symmetry. If conjugation is broken by single bonds and thus divided into two conjugated systems, the absorption spectrum is similar to the sum of the contributions from the two systems.

As a simple example of the effect of conjugated system length, let us consider a series of polyene hydrocarbons, $CH_2 = CH–(CH = CH)_{n-2}–CH = CH_2$, with n conjugated double bonds. Such a simple and regular system is fairly well understood. Energy levels for the ground state and the first excited state can be computed, and the wavelength of the long-wavelength absorption maximum corresponding to their difference determined. Two common approaches are the free electron (FE) theory and the linear combination of atomic orbitals (LCAO) method. In the former the Schrödinger

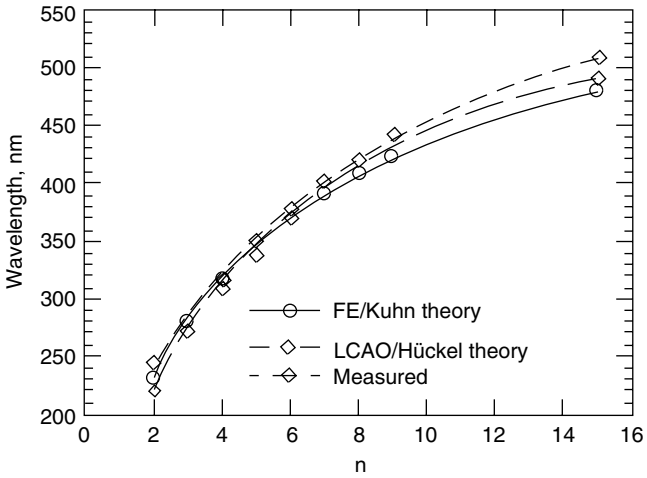

Fig. 9.1 The wavelength of the absorption maximum with longest wavelength for a series of polyenes with formula $CH_2 = CH–(CH = CH)_{n-2}–CH = CH_2$. The graph shows experimental values, as well as values calculated by two different methods, the Kuhn version of the free electron theory, and the Hückel version of the linear combination of atomic orbitals theory

equation is applied to a "gas" of π-electrons in a "box potential," i.e., a potential which is constant over an interval corresponding to the length of the conjugated system and zero outside of it. In the simplest version of this, the wavelength of the maximum would vary linearly with the length of the conjugated system, i.e., with n. However, one must consider that the length of the bonds between carbon atoms is not constant (every second bond is longer, and there are "edge effects"), and therefore, the potential is not constant in the "box"; and Kuhn has developed a method to allow for this, the result of which is shown in Fig. 9.1 (another complication, as we shall see later, is that the chain is not straight and may be folded in various ways). In the LCAO method, one starts by computing the orbitals of the individual atoms, and then sums up their wave functions. In a refined version due to Hückel, one allows for the variation in bond length. Both methods give quite good results for low values of n but underestimate the wavelength for large values of n. The reader interested in more information on these computational methods is referred to a textbook on electron spectra of organic molecules, such as that by Jensen and Bunker (2000) or the still very readable one by Murrell (1963).

The carotenoids, and the retinals of visual pigments, are biologically important molecules resembling polyenes. The principle of spectral tuning by variation of the conjugated bond system is beautifully exploited by plants in the regulation by the xanthophyll cycle of energy intake for photosynthesis (see Sect. 28.11). Also, the phycobiliproteins show a change in wavelength position related to the length of the conjugated system, but we shall see also that other factors are important for the tuning. A complication with simple polyenes and carotenoids is that the first excited state is "optically forbidden" or "dipole forbidden," i.e., cannot be reached from the ground state by light absorption (Schulten and Karplus 1972; see also Sect. 1.19). The absorption spectrum in the daylight region is due to transition to the second excited state (or, for carotenoids, the third excited state). The first excited state can still, for some carotenoids, participate in energy transfer to chlorophyll and make this very efficient (Thrash et al. 1979; Ritz et al. 2000), while for other carotenoids, it is too low (Polívka et al. 1999; but see Frank et al. 2000).

9.4 Relation Between the Absorption and Molecular Structure of Chlorophylls

Chlorophylls can be classified into three main groups, depending on whether the nucleus is that of porphin with 11 conjugated double bonds, dihydroporphin with 10, or tetrahydroporphin with 9 conjugated double bonds. In Fig. 9.2 it is shown which chlorophylls belong to each group, as well as the positions in organic solvent (in most cases ethyl ether) of their main absorption bands.

As is evident from Fig. 9.2, the long-wavelength transition, called Q_y, corresponds to a smaller energy change in the tetrahydroporphin type bacteriochlorophylls than in the dihydroporphin type pigments and to a smaller energy change in the dihydroporphin pigments than in the porphin pigments. Even in the porphin pigments, there is a certain asymmetry (not shown in Fig. 9.2) due to the side chains, so even in these one can distinguish between Q_x and Q_y transitions. Q_x and Q_y transitions can be distinguished through measurements of polarization of fluorescence excited by plane polarized light. Another way is to align the molecules in some way, for instance, in thin films, and study the absorption dichroism.

But the effects due to the chromophore environment are sometimes even larger than the effects of the differences in the conjugated double-bond system. Thus, the in vivo environment (mainly the bonding to protein) changes the Q_y band as shown in Table 9.1.

Those chlorophylls having the smallest energy gaps and the absorption bands at longest wavelengths are the reaction center special pairs (for exceptions, see Sect. 9.5). Their special absorption properties are due to formation of exciton complexes (see Chap. 1).

The reader who wishes to understand chlorophyll absorption spectra in more detail is referred to Linanto and Korppi-Tommola (2000). The theory of electronic spectra of organic molecules and the computational methods used to understand the spectra are treated in many books, e.g., Murrell (1963).

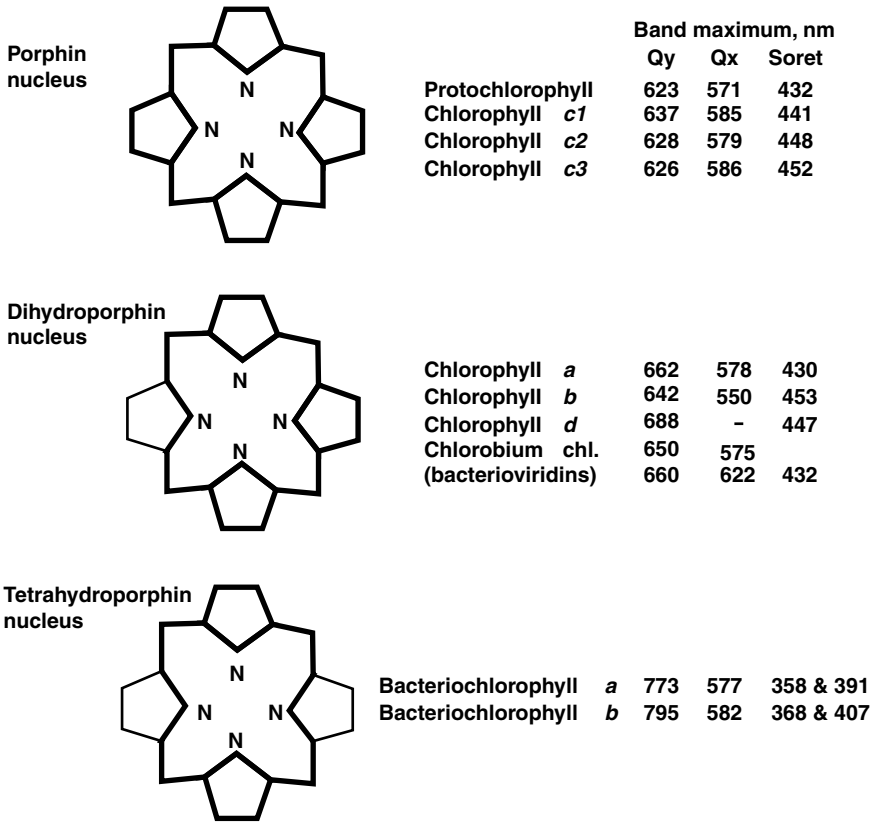

Fig. 9.2 The ring systems for the three main classes of chlorophylls. These ring systems are flat. The conjugated double-bond systems are indicated by heavy lines. While the conjugated system is rather isodiametric (approximating circular form) for the porphins, it is more elongated for the other two groups. The long axis of this elongated system is often referred to as the *y*-axis, and the transition moment for the so-called Q_y transition lies along this axis. The *x*-axis, and the direction of the Q_x transition, is almost perpendicular to this but also in the plane of the ring. The short-wavelength "Soret" band is complex with transitions along both axes. For instance, for bacteriochlorophyll *a* the 358 Soret component is in the *y*-direction and the 391 component in the *x*-direction

Table 9.1 Comparison of absorption spectra of chlorophyll pigments position of long-wavelength (Q_y) band (nm)

Pigment	In ethyl ether	In vivo
Protochlorophyll	624	630–650
Chlorophyll *a*	662	670–700
Chlorophyll *b*	644	650
Chlorophylls *c*	626–637	
Bacteriochlorophyll *a*	773	800–890
Bacteriochlorophyll *b*	795	1,020
Bacteriochlorophyll *c*		725–750

9.5 Tuning of Chlorophyll *a* and *b* Absorption Peaks by the Molecular Environment

Chlorophyll *a* is the key pigment in almost all organisms with oxygenic photosynthesis, i.e., cyanobacteria, algae, and plants. It functions in both reaction centers I and II and as antenna pigment in both photosystems. A great number of spectral forms can be distinguished in vivo and in thylakoid preparations.

In organic solvents the long-wavelength absorption peak of chlorophyll *a* lies at 662 nm (ethyl ether) to 663 nm (acetone), when the solution is dilute and the chlorophyll in a monomeric state. In vivo all chlorophyll a fractions are "red shifted," i.e., shifted to longer wavelengths compared to this. Some of the antenna chlorophylls in photosystem II (PSII) have the smallest shift, while a few molecules in photosystem I have the largest shift and, perhaps surprisingly, have peaks at even longer wavelength than photosystem I (PSI) reaction center chlorophyll (P700).

Cinque et al. (2000) were able to specify the spectra of two particular antenna chlorophyll chromophores in maize by comparing recombinant chlorophyll proteins lacking chromophores present in the wild type. They found that the long-wavelength (Q_y) peak of CP29 chlorophyll *a* is at 680 nm and that of LHC II chlorophyll *b* at 652 nm. Thus, the red shifts (bathochromic shifts) compared to solution in, e.g., ethyl ether are very different. However, the overall shapes of the two spectra are very similar in organic solution and protein environments.

Some chlorophyll species are extremely red shifted in vivo. Halldal (1968) discovered that the green alga *Ostreobium*, growing inside a coral on the Great Barrier Reef, contained unusually large amounts of such long-wavelength chlorophyll, "C_a720." It seemed to be an adaptation to the unusual environment of this organism. Other algae growing outside *Ostreobium* filtered away much of the daylight and left mostly far-red light for *Ostreobium* to use. Halldal asked his student Öquist to find out whether a more "ordinary" alga, *Chlorella*, would also be able to adapt to far-red light by forming more long-wavelength chlorophyll, and to some extent it could (Öquist 1969). But some

species of *Ostreobium* are exceptional and are still attracting the interest of scientists. Although most of the long-wavelength chlorophyll is associated to photosystem I, there seems also to be long-wavelength chlorophyll in photosystem II (Fuad et al. 1983; Zucchelli et al. 1990; Koehne et al. 1999). Investigators are puzzled by the fact that these pigament forms seem to be able to deliver energy to the reaction centers, which have absorption spectra peaking at shorter wavelengths and were thought to require higher energy quanta. The explanation may be, as in the case of dragonfish vision, that thermal quanta deliver the extra energy needed. This need not violate the second law of thermodynamics if the whole photosynthetic system is considered.

Some of the recent and detailed investigations have been done on cyanobacteria. It has been shown that also in this case the long-wavelength forms, at physiological temperatures (but not at very low temperature), can transfer absorbed energy to P700 (Pålsson et al. 1998). The main long-wavelength absorption peaks of these long-wavelength forms are variously given as 708 and 719 nm (Pålsson et al. 1998) and 705, 714, and 723 nm (Kochubey and Samokhval 2000), both for *Synechococcus elongatus*. For *Synechocystis* sp. PCC 6803, only a single long-wavelength form peaking at 710 nm was identified (Gill and Wittmershaus 1999), possibly due to methodological differences. The 719 nm form seems to arise from the 708 nm form when monomers of PSI are combined to the trimers present in vivo (Pålsson et al. 1998; Jordan et al. 2001). In a structural model (Jordan et al. 2001), for PSI the 710/719 nm chlorophyll is tentatively identified with the aC-A32/aC-B7 molecule pair, which seems to connect the monomers energetically. Thus, the long-wavelength band may arise by excimer splitting, just as in a long-wavelength spectral form of phycocyanobilin. However, Koehne et al. (1999) have obtained evidence that at least some long-wavelength forms in the eukaryotic alga *Oestrobium* have another origin.

To date the long-wavelength record for chlorophyll *a* tuning is held by the cyanobacterium *Spirulina platensis*, which has a form peaking at 738 nm (Shubin et al. 1991; Koehne and Trissl 1998; Karapetyan et al. 1997).

P700 of photosystem I as well as P680 of photosystem II are both dimers (within the photosystem monomer), with the tetrapyrrols closely stacked in a parallel manner and with tightly overlapping π orbitals, forming excimers. It is thus not difficult to understand that there is a large red shift from the absorption peak of chlorophyll *a* in dilute organic solution.

Carotenoids may be important for the spectral fine tuning of some other chlorophyll forms. Several of the carotenoids in PSI show extended overlap of their π orbitals with those of chlorophyll molecules (Jordan et al. 2001).

For cyanobacterial PSII a structural model has been published by Zouni et al. (2001). According to this model, $Chlz_{D1}$ and $Chlz_{D2}$ are identified with chlorophyll *a* bound to histidine in polypeptides D1 and D2. These chlorophylls have absorption peaks at 675 nm (Schelvis et al. 1994).

9.6 Phycobiliproteins and Phycobilisomes

In hardly any case is spectral tuning more important and critical than in photosynthetic antenna pigments. Light is absorbed by one chromophore and transferred over a series of other chromophores to photosynthetic reaction centers. The most common method for energy transfer is the Förster mechanism. For this to be efficient, the emission spectrum of the energy donor must in each step match the absorption spectrum of the receiver.

There are many kinds of antenna pigments in various organisms: chlorophylls, carotenoids, pteridines, and phycobiliproteins. We shall concentrate here on phycobiliproteins, which occur in cyanobacteria and several groups of algae, most important of which are the red algae. The description below will primarily reflect the conditions in cyanobacteria.

Cyanobacteria use several principles for spectral tuning, the first of which is variation of the structure of the chromophores (bilins). Different lengths of the conjugated bond system results in different transition energies: the greater the length, the lower the energy. The types of chromophores known are shown in Table 9.2 and their distribution among proteins in Table 9.3.

When the chromophores attach to proteins (which takes place via sulfur bridges at one or two points), two changes are immediately apparent: The absorption bands become sharper, and the intensity of the long-wavelength band increases in comparison to those at lower wavelengths. The sharpening of the bands takes place because the conformation of the chromophore, which in the free form is very

Table 9.2 Number of conjugated double bonds and absorption maxima for the phycobilins

Phycobilin	Number of conjugated double bonds	Absorption maximum in free form (nm)	Absorption maximum in phycobiliprotein
Phycourobilin (PUB)	5		495
Phycoerythrobilin (PEB)	6	530	545–565
Phycoviolobilin (PVB)	7		510–570
Phycocyanobilin (PCB)	8	600	610–671

Table 9.3 Occurrence of phycobilin chromophores among cyanobacterial phycobiliproteins and their *a* and *b* peptides

	On *a* peptide	On *b* peptide
Allophycocyanin	1 PCB	1 PCB
C-Phycocyanin	1 PCB	2 PCB
Phycoerythrocyanin	1 PVB	2 PCB
R-Phycocyanin II	1 PEB	2 PCB
Phycocyanin WH8501	1 PUB	2 PCB
C-Phycoerythrin	2 PEB	2 PEB
CU-Phycoerythrin (1)	3 PUB	1 PEB + 1 PUB
CU-Phycoerythrin (2)	1 PEB + 2 PUB	2 PEB
CU-Phycoerythrin (3)	3 PUB	2 PEB
CU-Phycoerythrin (4)	2 PEB + 1 PUB	2 PEB + 1 PUB

Source: After MacColl (1998), slightly simplified. For corresponding information for rhodophycean phycobiliproteins, see Table 1 of Holzwarth (1991), and for cryptophycean (cryptomonad) phycobiliproteins Glazer and Wedemayer (1995)

flexible and therefore distributed over a large number of conformational states, becomes restricted. The relative intensification of the long-wavelength band takes place because the chromophore becomes more straight, while in the free state, it is, on average, more circular, as one turn of a helix (Scheer and Kufer 1977; Knipp et al. 1998), with overlapping ends. The spectrum therefore is in this case more "porphyrin like," with a pronounced Soret-type band. Another effect of the binding to protein is that the position of the long-wavelength band is shifted, to very different extents in different cases which will be described below.

The chromophore is not fixed in the protein with complete rigidity. Of particular interest are cases in which the conformation of the chromophore can change under the influence of light, causing photochromicity of the chromoprotein, analogous to the behavior of phytochrome. The behavior was first noticed by Scheibe (1972) in an extract containing phycocyanin. The phenomenon was further examined in a number of papers by G.S. Björn, summarized by G.S. Björn (1980), L.O. Björn (1979), and Björn and Björn (1980). The experiments were mostly carried out on extracts, but in one case (G.S. Björn 1979), photoreversible photochromism was shown to occur also in vivo. In this case irradiation with light of 505 nm results in a decrease of absorption at this wavelength and an increase at 570 nm, while irradiation with 570 nm light reverses this effect, and the reaction can be repeated over and over again.

This particular case has been further explored by other researchers, in particular the group around H. Scheer in Germany (Zhao et al. 1995; Zhao and Scheer 1995; see also Ohad et al. 1979; Scharnagl and Fischer 1993). It has been found that the change in absorption spectrum is primarily due to rotation around a double bond between carbon atoms 15 and 16 in a phycoviolobilin chromophore in the a subunit of phycoerythrocyanin.

How rigidly the chromophore is held by the protein depends partly on the covalent (thioether) bonds between chromophore and protein. The bonds may go from either the A ring or the D ring, or both, and this affects the spectral properties. The extent to which the chromophore is stretched and kept rigid also affects another property of great importance for the function, namely, the excited state lifetime. A phycobilin chromophore which is not fixed in a protein has great flexibility, which gives greater possibilities for thermal relaxation, i.e., shorter lifetime and less efficient energy transfer and photochemical efficiency. This is in contrast to what is the case with chlorophylls, which are already in the free state rigid structures. The attachment to protein also favors a protonated state, which also lengthens the excited state life.

The ordered arrangement of chromophores in a protein matrix affects the chromophore spectrum by one more mechanism. It keeps certain chromophores in the close vicinity of one another, which results in the formation of exciplexes. As described in Sect. 1.17, this splits the energy levels of the isolated chromophores in a higher and a lower level, in turn splitting the absorption bands in a corresponding manner.

Thus, even though cyanobacterial phycocyanins and allophycocyanins all contain only a single type of chromophore, namely, phycocyanobilin, they exhibit a wide range of absorption bands, peaking from 620 nm in C-phycocyanin to 671 nm in allophycocyanin B and also in the "terminal linker polypeptide" in the center of the phycobilisomes, close to the chlorophyll in the thylakoid membranes.

Phytochromes constitute a quite different type of phycobiliproteins, which have a light-sensing function (Chaps. 11, 12, 13 and 19). Plant phytochromes, which are those studied in most detail and that contain phytochromobilin (closely related to phycocyanobilin) as chromophore, are interconvertible between two forms of which one has evolved to absorb maximally near the absorption maximum of chlorophyll, while the other one absorbs maximally just outside the chlorophyll absorption. Therefore, they are well suited for detecting the change in light spectrum caused by the presence of competing plants. Phytochromes of nonphotosynthetic bacteria, on the other hand (whose exact biological function is yet to be explored), contain a different type of phycobilin chromophore and absorb at longer wavelengths (Bhoo et al. 2001).

9.7 Spectral Tuning of Phycobilisomes: Chromatic Acclimation in Cyanobacteria

What we shall be dealing with in this chapter has traditionally been called chromatic adaptation, but in modern terminology, adaptation is hereditary and evolutionary adjustment to the environment. What we shall describe now is the nonhereditary adjustment to the spectrum of the surrounding light, and

this should for consistency be called chromatic acclimation. By this we mean, in a photosynthesis context, the ability of organisms to adjust their photosynthesis apparatus, and in particular the amounts of various light-harvesting pigments, to match the spectral composition of available light (Kehoe and Gutu 2006). (The term can also be used in vision science.) The phenomenon has been studied for a long time, but we shall focus here on recent developments.

Cyanobacteria have protein complexes called phycobilisomes attached to the outside of their photosynthetic membranes (thylakoid membranes). They are composed of phycobiloproteins serving to gather light energy that is efficiently channeled to the photosystems (mostly to photosystem II). There are several kinds of phycobiliproteins, but in the following, we shall focus on the blue (red-light-absorbing) phycocyanins and the red (green-light-absorbing) phycoerythrins of cyanobacteria. Light energy absorbed in phycoerythrin is transferred to phycocyanin and from there via another phycobiliprotein, allophycocyanin, to chlorophyll *a* in the thylakoid membrane.

Some other photosynthetic organisms are also capable of chromatic acclimation, but it is most dramatically obvious in some cyanobacteria. All cyanobacteria do not exhibit chromatic acclimation, but in all major phylogenetic groups of cyanobacteria, some members do. de Marsac (1977) divided cyanobacteria into three groups with respect to their ability in this respect:

Group I, not capable of chromatic acclimation

Group II, able to vary phycoerythrin content but not phycocyanin content

Group III, able to vary both phycoerythrin and phycocyanin contents

Gutu and Kehoe (2012) use the symbolism CA1, CA2, and CA3 for the corresponding variants of chromatic acclimation.

Of these, group III has, not surprisingly, attracted most interest from researchers (Fujita and Hattori 1962; Ohki and Fujita 1978), and during recent years, the mechanism has, to a large degree, been clarified for some cyanobacteria. However, it is also clear that the mechanism is not the same for all cyanobacteria. Cyanobacteria are well equipped with photoreceptors. In a single species there may be many different phytochrome-type proteins with GAF domains carrying bilin chromophores (Ma et al. 2012), but also rhodopsins can be involved in the regulation of photosynthetic pigment antennae (Irieda et al. 2012). We shall return to group III in the following, but first complete the picture with a couple of other kinds of chromatic acclimation discovered more recently.

Palenik (2001) found that at least some *Synechococcus* strains are able to increase their absorption of blue light when there is more of this available than light of longer wavelength. The effect was further studied by Shukla et al. (2012) and by them named CA4 (type 4 chromatic acclimation). These cells, when grown in blue light, increase their content of the chromophore phycourobilin at the expense of phycoerythrobilin, simply by isomerizing the latter to the former (Fig. 9.3) without changing the protein to which the chromophore is bound. This changes the absorption spectrum of the biliprotein. An isomerase, called MpeZ, catalyzing this reaction has also been found. The photoreceptor regulating the amount of isomerase is so far not characterized, but is likely to be a cyanobacteriochrome.

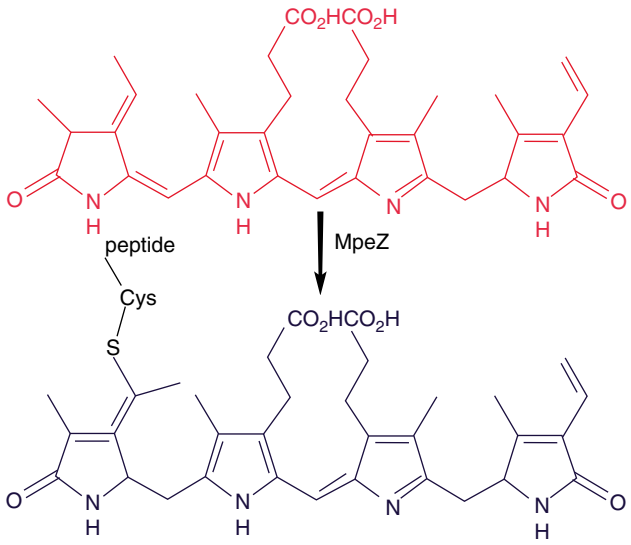

Fig. 9.3 The isomerization of phycoerythrobilin to phycourobilin. Note that the conjugated double-bond system is longer in phycoerythrobilin (*top*) (From Shukla et al. 2012)

Another type of chromatic acclimation that we can call type 5 (CA5) has been found by Duxbury et al. (2009). This is the ability of the strain of *Acaryochloris marina* (Chen et al. 2010; 2012; Chen and Blankenship 2013; Loughlin et al. 2013) to adjust the content of phycocyanobilin in relation to chlorophyll *d*, depending on the amount of orange or far-red light available.

We shall focus here on the best understood case, the type III acclimation of *Fremyella diplosiphon* (Fig. 9.6). Absorption spectra, visual appearances, and phycobilisome structures of this organism grown in red and green light are shown in Fig. 9.4. The photoreceptor that senses the light for this regulation is a cyanobacteriochrome called RcaE (Kehoe and Grossman 1996; Grossman and Baya 2001).

The photoreceptor for this regulation is a cyanobacteriochrome of the type that has only one cysteine link between the protein and the bilin (in this case phycocyanobilin). The switch between the two forms involves not only an isomerization around a double bond (15) from the 15Z configuration for the green-absorbing Pg form to the 15E configuration for the red-absorbing Pr form, but also a protonation when going from Pg to Pr. It is the protonation that causes most of the spectral change, not the isomerization. Pg is the active form,

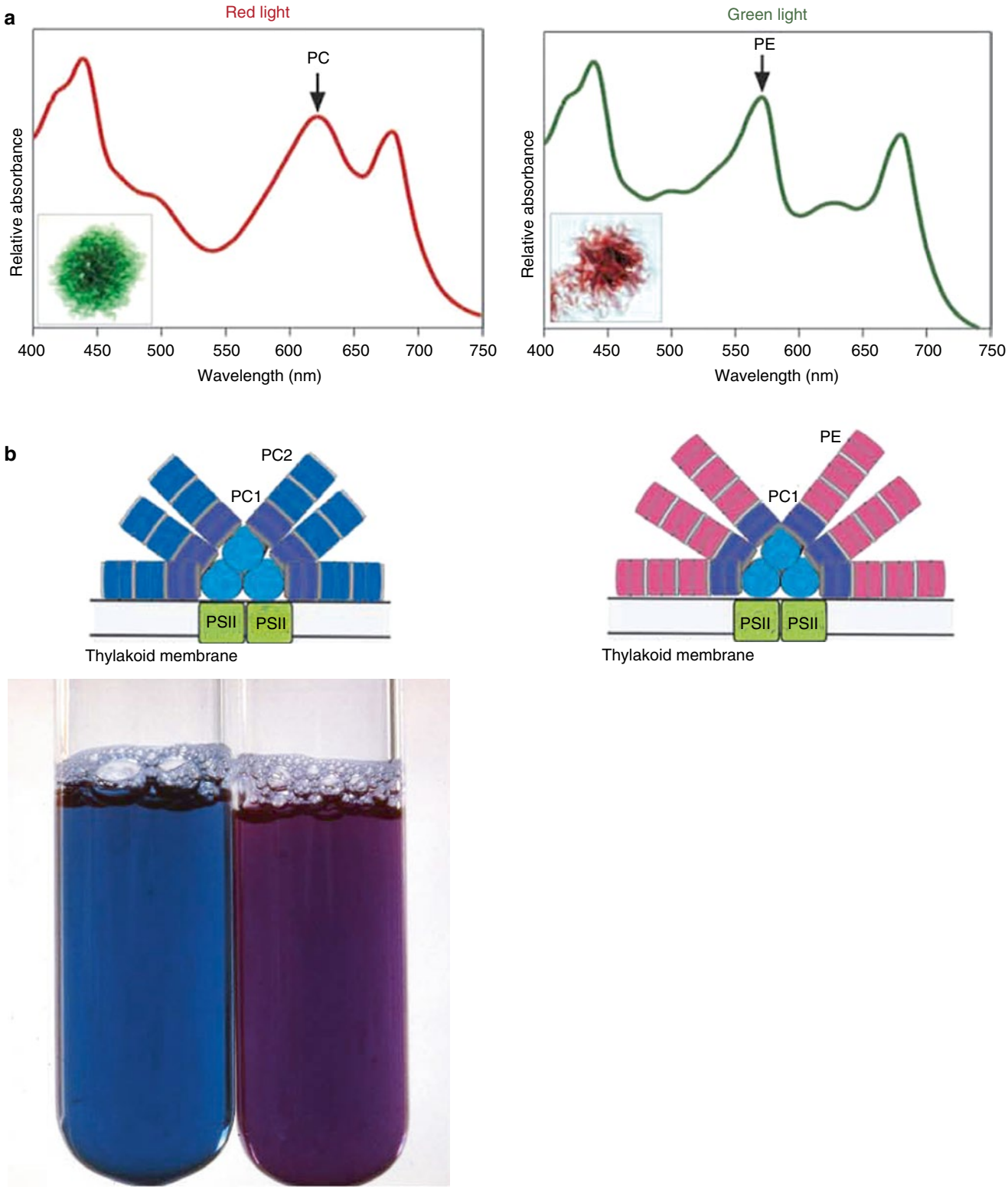

Fig. 9.4 (**a**) *Above*: Whole-cell absorption spectra of *Fremyella diplosiphon* grown in red (*left*) and green (*right*) light (*inset*, photos of the cultures). *Below*: Models of the corresponding phycobilisomes. PC1 and PC2, phycocyanins 1 and 2; PE, phycoerythrin; light blue, phycobilisome core with allophycocyanin; linker proteins not shown (From Gutu and Kehoe 2012). (**b**). Aqueous extracts of *Fremyella diplosiphon* grown in green (*left*) or red (*right*) light (Courtesy Gunvor Björn)

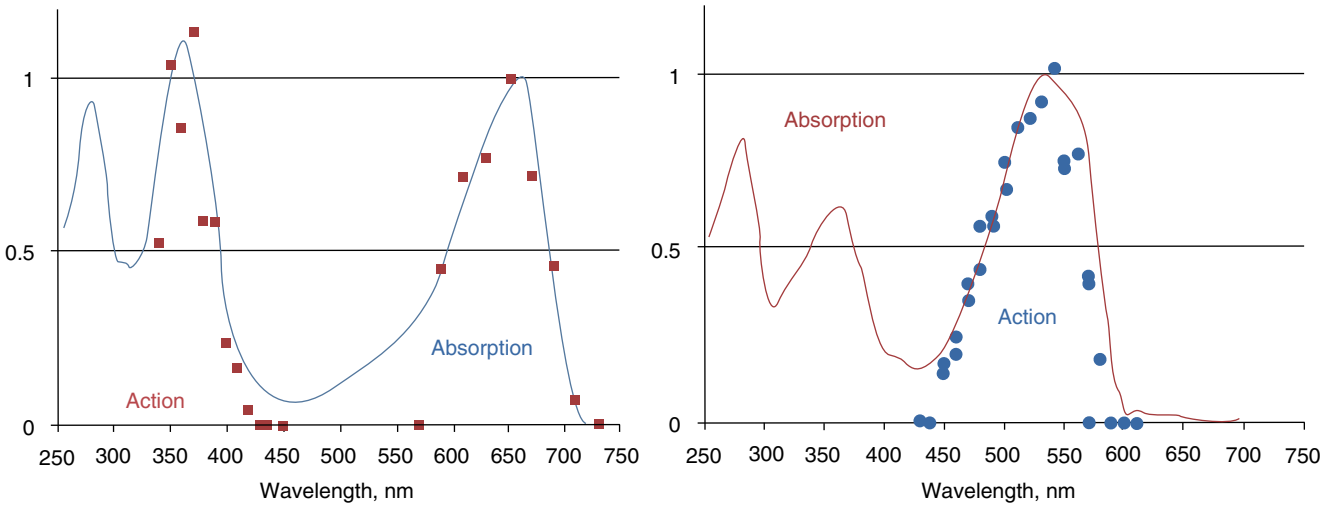

Fig. 9.5 The action spectrum for induction of phycoerythrin synthesis (*red squares*) and for its inhibition (*blue circles*) from Vogelmann and Scheibe (1978) compared to the Pr form (*left panel*, *blue line*) and the Pg form (*right panel*, *red line*) of RcaE (Hirose et al. 2013). All data are normalized to unity at the long-wavelength maximum

having histidine kinase activity (autophosphorylation in a first step, followed by transfer of a phosphate group to the protein RcaC via another one, RcaF). The phosphorylated form of RcaC inhibits transcription of phycoerythrin genes and increases transcription of phycocyanin genes (see detail in Gutu and Kehoe 2012). It is instructive to compare the action spectra for chromatic acclimation in *F. diplosiphon* (Vogelmann and Scheibe 1978) with the absorption spectrum for purified cyanobacteriochrome RcaE (Hirose et al. 2013) in Pr and Pg forms (Fig. 9.5).

We see from Fig. 9.5 that action and absorption spectra follow each other in the main bands around 350, 550, and 650 nm. However, between 420 and 570 nm, the action spectrum for induction of phycoerythrin synthesis drops to zero, while the corresponding absorption spectrum does not. This can be explained by the high rate of the reverse reaction in this spectral region. In the same way, one can understand that the action spectrum for inhibition of the induction drops to zero at short wavelengths, where the opposite reaction becomes important.

Let us try to express this a little more quantitatively. Since it is known now that it is the Pg form that is the active form, which inhibits phycoerythrin synthesis and promotes phycocyanin synthesis, let us try to model the effect of its formation.

Let us assume, based on Fig. 2 in Vogelmann and Scheibe (1978), that the span of PE/(PE + PC) after green-light treatment is from 0 to 0.6. Then halfway between is 0.3 and the corresponding log(fluence)/(J m^{-2}) ca 2.4 and thus the half-saturating 550 nm photon fluence ca 10^{-3} mol m^{-2}. This gives us the order of the action cross section as 1,000 m^2 mol^{-1}. The action cross section is the absorption cross-section times the quantum yield. The absorption cross section in turn is the absorption coefficient multiplied by ln(10), the latter factor coming from the fact that spectrophotometric absorption coefficients are based on decadic logarithms, while natural logarithms have to be used in kinetic computations.

From Fig. 3 in Vogelmann and Scheibe (1978), it appears that the reversal of PE induction saturates when there is still some PE synthesis remaining. The halfway saturation for 650 nm light is for a log(fluence) of about 1.8 (J m^{-2}), corresponding to a photon fluence of 3.4×10^{-4} mol m^{-2}. This gives us a rough value for the action cross section (σ) at 650 nm of 3,000 m^2 mol^{-1}. Thus, the action cross section of Pr at 650 nm appears to be about three times the size of the action cross section of Pg at 550 nm. Obviously estimated in a somewhat different way, Vogelmann and Scheibe (1978) arrive at a ratio of 7 instead of 3. Thus, these estimates are not very accurate, and in the calculations below, we have used the action cross sections 1,000 and 10,000 mol m^{-2} for the green-absorbing and the red-absorbing forms of the photoreceptor at their absorption maxima, i.e., a ratio of 10.

Let us now consider the reaction system

$$\mathrm{Pr} \leftrightarrow \mathrm{Pg}$$

where Pr and Pg are the red- and green-absorbing forms of photoreceptor pigment. With ε and ϕ standing for absorption cross sections and quantum yields, respectively, the rate of Pg formation is $\mathrm{d[Pg]/d}t = \mathrm{Frate}(\lambda)\{\varepsilon r(\lambda) \times \phi r \times [\mathrm{Pr}]$

$-\varepsilon g(\lambda)\times\phi g\times[\mathrm{Pg}]\}$, or with simpler notation $\mathrm{dPg/d}t=\mathrm{Frate}\times(\sigma r\times\mathrm{Pr}-\sigma g\times\mathrm{Pg})$, where t is time, Frate is photon fluence rate, σr and σg are wavelength-dependent action cross sections of the red- and green-absorbing forms of the photoreceptor, and Pr and Pg are the amounts of the two photoreceptor forms as fractions of the total. Considering that Pr = 1–Pg, and assuming that all photoreceptor is in the Pr form before irradiation with red light starts, this relationship can be integrated over time to yield

$\ln\{[\sigma r-(\sigma r+\sigma g)*\mathrm{Pg}]/\sigma r\}=-(\sigma r+\sigma g)\times\mathrm{Frate}\times t=-(\sigma r+\sigma g)\times F$, where $F=\mathrm{Frate}\times t$ is the fluence.

Thus, $\ln\{[\sigma r-(\sigma r+\sigma g)\times\mathrm{Pg}]\}/\sigma r]=-(\sigma r+\sigma g)\times F$ which can be rewritten as $1-(1+\sigma g/\sigma r)\times\mathrm{Pg}=\exp[-(\sigma r+\sigma g)\times F]$, i.e., $\mathrm{Pg}=\{1-\exp[-(\sigma r+\sigma g)\times F]\}/(1+\sigma g/\sigma r)$.

We have made the action cross sections for the green-absorbing and red-absorbing form 1,000 and 10,000 times the absorption coefficients with maxima normalized to 1, which we can call kr and kb, so we get

$$\mathrm{Pg}=\left\{1-\exp\left[-\left(10{,}000\times kr+1{,}000\times kg\right)\times F\right]\right\}/\left(1+0.1\times kg/kr\right)$$

We did not get a good fit with this. But by changing the factor 0.1 in the last parenthesis to 1, we obtained the violet curve marked "model" in Fig. 9.6, and by squaring it, we got a fit which is probably within experimental error.

Can we logically motivate the square relationship? We could get a square relationship if two parts of the phycoerythrin molecule (such as the protein part and the chromophore) were separately regulated by the photoreceptor.

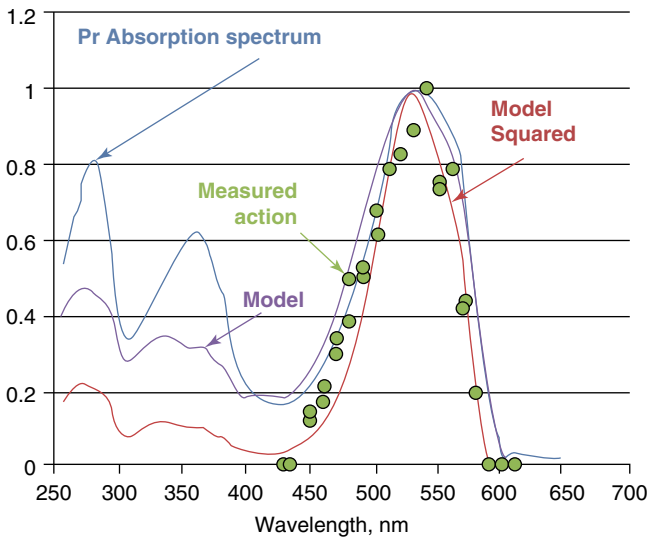

Fig 9.6 Measured action spectrum for phycoerythrin formation (Vogelmann and Scheibe 1975) compared to the Pr absorption spectrum (Hirose et al. 2013) and the modeled action spectrum as described in the text

9.8 Tuning of Phytochrome-Like Pigments

Since the publication of the second edition of this book, it has become obvious that there exist in many main groups of organisms pigments which are analogous to the plant photosensory pigments known as phytochromes (Rockwell and Lagarias 2010). Phytochrome-like pigments, or at least genes coding for such chromoproteins, have by now been found in various kinds of algae, fungi (Blumenstein et al. 2005; Rodriguez-Romero et al. 2010; Lamparter and Marwan 2001), Excavata (Bolige and Goto 2007), and in many major groups of bacteria: cyanobacteria (Rockwell et al. 2011), actinobacteria, α-proteobacteria, γ-proteobacteria, ∂-proteobacteria (White et al. 2008), Deinococcaceae, and Firmicutes. They have even been implicated in Archaea. The plant phytochromes have two main states with absorption peaks at about 660 and 730 nm, respectively. Their newly detected relatives in other organisms span over a very large spectral range, rivaling the spectral tuning of rhodopsin-type and chlorophyll-type pigments. This spectral variation is due to both chromophore modifications and protein interactions. The peaks of light sensitivity range from 382 nm (Song et al. 2011) for a *Synechocystis* pigment to 750 nm for a *Agrobacterium tumefaciens* pigment (Rottwinkel et al. 2010). In the latter case significant sensitivity extends above 800 nm.

The plant phytochromes and many of the related pigments in other groups have their open-chain tetrapyrrole (bilin-type) chromophore attached via a covalent bond to a cysteine in the apoprotein. The cyanobacteria exhibit a special richness and variability of phytochrome-like pigments. In a single cyanobacterial strain, *Nostoc* sp. PCC7120, seven different types have been found (Ma et al. 2012). In addition, this organism is equipped with a rhodopsin-type light sensor (Jung et al. 2003). More generally, there are two main types of phytochrome-like sensors in cyanobacteria, those which have their chromophore attached via a single cystein residue. These are appropriately called cyanobacterial phytochromes. An overview of this is given in the Introduction part of Anders et al. (2011). They exhibit red/far-red photoreversibility as plant phytochromes. The other types, called cyanobacteriochromes or cyanochromes, have two cysteine attachment points between chromophore and apoprotein. Their spectra are shifted to lower wavelengths, in an extreme case to 382 nm (Song et al. 2011).

Below we shall give some examples of the effect of chromophore and of protein environment on absorption (and sensitivity) spectra. It should be noted that in many cases described in the literature, chromoproteins have not been characterized after extraction from the original organism under investigation. Instead the corresponding gene, or even

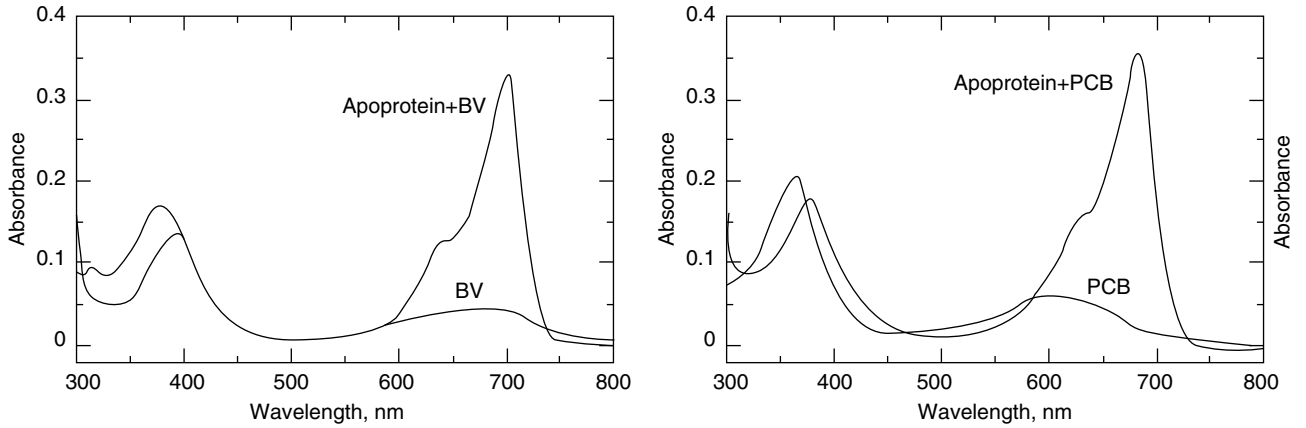

Fig. 9.7 Absorption spectra of biliverdin (*left*) and phycocyanobilin (*right*) in free form or combined with a phytochrome apoprotein (Agp1) from *Agrobacterium tumefaciens* (Lamparter et al. 2002). All pigments in unexcited dark state

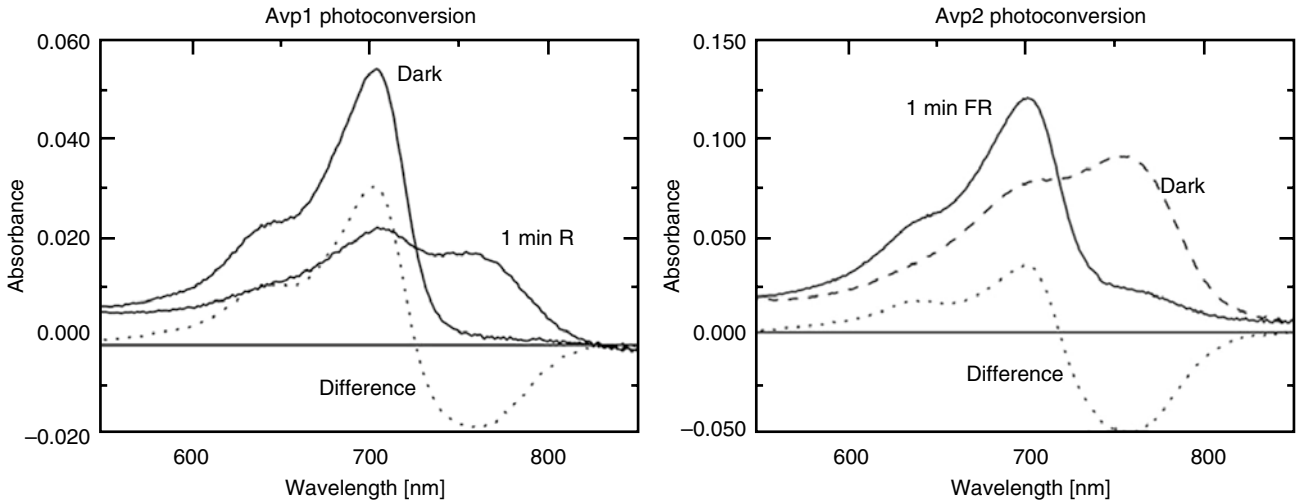

Fig. 9.8 Phototransformations of two phytochromes from *Agrobacterium vitis* according to Rottwinkel et al. (2010)

only part of it, has been cloned into another organism that has been able to produce the protein in sufficient amount for investigation.

From Fig. 9.7 we can learn several things: (1) The free forms of the bilins in solution have less sharp spectra because they are flexible, so the spectra are averaged over many conformations. The protein-bound forms, on the other hand, are fixed in a particular conformation. (2) The biliverdin chromoprotein has its absorption peak at longer wavelength (ca 703 nm) than the phycocyanobilin chromoprotein (ca 680 nm), because biliverdin has one double bond more.

Figure 9.8 shows the change of absorption spectra upon irradiation of two phytochromes prepared from genes of *Agrobacterium vitis*. Note that one of them changes towards longer wavelengths on irradiation with red light, in a way similar to the plant phytochrome. The other one, however, shifts to shorter wavelength upon irradiation. This type of phytochrome has been called bathyphytochrome (from Greek bathys, deep or low). As described in Fig. 12.14, these spectral changes are due to rotation of part of the bilin molecule around a double bond and changes in the protein that follow from this.

Figure 9.9 shows spectra of the other main type of photo sensory biliproteins, called cyanobacteriochromes (or cyanochromes), with two attachment points for the bilin via cysteine residues on the protein. One of these bonds is labile and may loosen in one of the spectral forms. The double attachment results in a very large shift to shorter wavelength (the chromophore in this case, as in others investigated, is phycocyanobilin). Irradiation with UV-A radiation results in the 534 nm form, while irradiation with green light produces the 382 nm form. By comparison with Fig. 9.7, we can see that the protein can modulate the phycocyanobilin absorption peak between 382 nm and 684 nm.

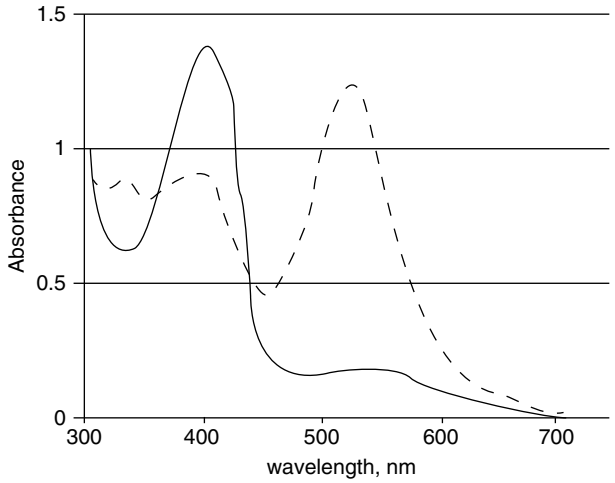

Fig. 9.9 *Green* irradiated (382 nm form), *solid line*, and UV-A irradiated (534 nm form), *dashed line*, of cyanobacteriochrome from *Synechocystis* sp. PCC 6803 (Redrawn from Song et al. 2011)

Further aspects of cyanobacterial chromatic acclimation are treated by Bussel and Kehoe (2014).

9.9 Visual Tuning

Visual pigments of animals span a spectral range of 300–700 nm (Marshall and Oberwinkler 1999), i.e., more than an octave of the electromagnetic spectrum. They are proteins with, in most cases, either 11-cis-retinal or 11-cis-3-dehydroretinal (Fig. 9.10: Makino et al. 1999) as chromophores. Proteins with 11-cis-retinal alone cover a range of absorption spectra with maxima from 360 to 635 nm (Kleinschmidt and Harosi 1992, Kochendoerfer et al. 1999). The term rhodopsin is somewhat ambiguous and sometimes covers all chromoproteins related to the human visual pigments, including light-sensitive proteins in algae, bacteria, and archaea, but sometimes visual pigments containing 11-cis-dehydroretinal (which are then termed porphyropsins) are excluded. The spectra of visual pigments to some extent depends on which chromophore they contain; dehydroretinal (also called *retinal*$_2$) with its longer conjugated double-bond system giving a red shift of 10–50 nm compared to 11-cis-retinal. Two other "primary chromophores" involved in animal vision are also known: 11-cis-4-hydroxyretinal has been found (as well as retinal and 3-dehydroretinal) in the eyes of the bioluminescent squid *Watasenia scintillans* (Matsui et al. 1988) and gives a blue shift compared to retinal. 3-Hydroxyretinal occurs in several insect orders (Vogt 1983; Vogt and Kirschfeld 1984; Tanimura et al. 1986; Seki and Vogt 1998), and different stereoisomers (3R and 3S enantiomers) of it occur, with different phylogenetic distributions (Seki and Vogt 1998). Many vertebrates, including humans, have a differentiation of light-sensitive cells in the retina between rods, specialized for "black-and-white vision" in weak light, and cones, specialized for color vision in stronger light.

In addition to these "primary chromophores," there are, in certain cases, "sensitizing chromophores" attached to the same proteins. These chromophores act in analogy to photosynthetic antenna pigments: they absorb light and transfer the energy to the primary chromophores. Only three such sensitizing chromophores have been detected so far: 11-cis-3-hydroxyretinol in Diptera (Vogt and Kirschfeld 1984) and defarnesylated *Chlorobium* pheophorbide methyl ester in bioluminescent dragonfish (Douglas et al. 1998, 1999) and chlorin e6 in salamander (Isayama et al. 2006). More about the dragonfish can be found in Chap. 26.

In addition to visual pigment structure, spectral filters in the form of colored oil drops contribute to spectral tuning of photoreceptor sensitivity in some animals, especially birds (Maier and Bowmaker 1993; Bowmaker et al. 1997; Vorobyev et al. 1998; Hart et al. 2000) and reptiles (Schneeweis and Green 1995). We also have filters in our own eyes, namely, in the yellow spot of the retina, macula lutea. This is the spot of highest visual acuity, devoid of blue-sensitive cones. Here the yellow pigment serves to prevent blue light to reach the green- and red-sensitive cones, for which it would degrade acuity by chromatic aberration.

However, most of the spectral tuning is achieved by variation of a few of the amino acids in the protein to which the chromophores are attached (Britt et al. 1993).

Humans use exclusively the 11-cis-retinal chromophore. In free form in methanol solution, 11-cis-retinal absorbs maximally at 380 nm (in protonated Schiff's base form, it absorbs maximally at 440 nm). Human rhodopsin, the protein-chromophore complex of rods, used in twilight vision, peaks at 493 nm (Wald and Brown 1958). The three human cone pigments, used in color vision, peak at 426, 530, and 552 nm (or 557 nm; all persons do not have exactly the same type). The human cone pigments are often referred to as SW (for short wavelength), MW, and LW pigments, respectively.

The effect of protein primary structure on spectral properties of visual pigments is studied (1) by comparing various naturally occurring pigments and (2) by site-directed mutagenesis experiments in which certain amino acids are changed.

An important determinant of the spectrum seems to be the negative charges on amino acids in proximity to the chromophore. We shall give two interesting examples of how this can work:

1. Ultraviolet vision has been demonstrated in many vertebrate (fish, amphibian, reptilian, avian, and mammal) species (Jacobs 1992). Yokoyama et al. (2000) have convincingly shown that ultraviolet-sensitive pigment in birds evolved from violet-sensitive pigments by a single

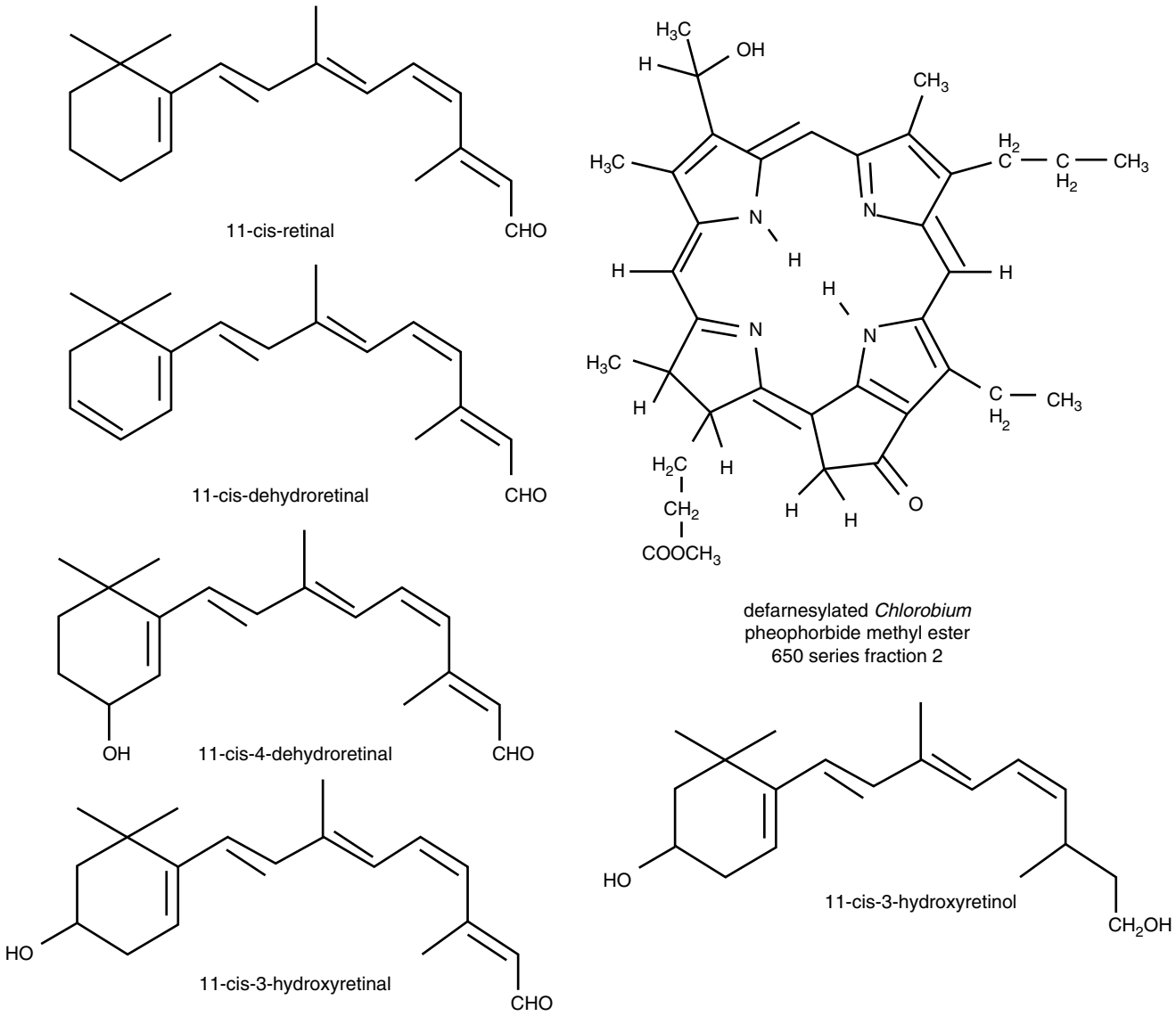

Fig. 9.10 Structures of five chromophores known from animal visual pigments. Several compounds related to the *Chlorobium* pheophorbide derivative also occur in dragonfish eyes. 11-cis-3-Hydroxyretinal occurs as two different enantiomers, with different phylogenetic distributions

amino acid substitution, namely, by a change of serine to cysteine at position 84. This shifts the absorption spectrum of the wild-type pigeon pigment with a maximum at 393 nm to one peaking at 358 nm. For the corresponding chicken pigment, the shift was from 415 to 369 nm. Conversely, the zebra finch UV pigment peaking at 359 nm could be shifted to 397 nm by a change at position 84 from cysteine to serine. It should be noted, however, that ultraviolet-absorbing pigments in other vertebrate groups have arisen independently and by other substitutions.

2. Human trichromatic color vision has arisen recently during evolution; most mammals have only dichromatic color vision and some, such as whales, do not have more than one type of cone pigment. Some New World monkeys also possess trichromatic color vision but that has arisen independently. The human type of trichromacy has arisen by gene duplication of a long-wavelength pigment and mutation of one of the gene copies to produce a middle-wavelength (MW) pigment. According to Neitz et al. (1991), the spectral differences between these pigments depend on three amino acid differences, and in addition there are several differences without spectral effect. Effects are detailed in Table 9.4 (values vary somewhat between investigators using different methods). In each case the change from a nonhydroxyl to a hydroxyl amino acid results in a "red shift," i.e., absorption at longer wavelengths.

Table 9.4 Spectral effects of amino acid (aa) substitutions in human cone pigments

Position	aa in MWP	aa in LWP	Δλ on change
180	Alanine	Serine	+6
277	Phenylalanine	Tyrosine	+9
285	Alanine	Threonine	+15

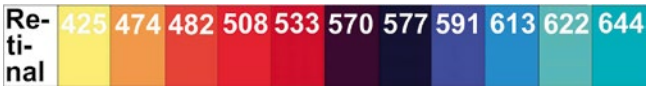

Fig. 9.11 Colors of the engineered rhodopsins produced by Wang et al. (2012). The numbers show the wavelengths of absorption maxima in nm. The free retinal (*far left*) is completely colorless

Those people who possess a 557 nm LW pigment have serine at position 180, while those with a 552 nm pigment have alanine. This position is also variable in the MW pigment but seems to produce a smaller spectral shift there, and investigations are not as thorough as for the LW pigment (see Sharpe et al. 1999 for details). The same person may, in fact, possess more than three different cone pigments (Neitz et al. 1993).

Fujimoto et al. (2005) have studied the spectral tuning of retinal proteins by quantum mechanical methods, while Nathans (1992) has discussed it in more general terms, easier to understand for the nonspecialist. Retinal undergoes a large decrease in dipole moment in going from the ground state to the photoexcited state: In the ground state, a positive charge is localized mainly to the Schiff's base nitrogen, and this charge is distributed more evenly throughout the π-electron system upon photoexcitation (Nathans 1990). A negative charge, such as from glutamate or aspartate, along the polyene chain of retinal would favor charge delocalization in the ground state and thus a smaller energy gap, i.e., a red shift. Polar groups along the polyene chain would favor or disfavor charge delocalization depending on orientation. Polarizable groups along the polyene chain would stabilize the excited state (produce a red shift) through compensatory charge movement. Twisting around single or double bonds would, respectively, decrease or increase charge delocalization. Moving the Schiff's base counterion further from the chromophore would decrease the effect of the ground state dipole moment and produce a red shift. A record shift for a single amino acid change (which has not been found in nature), from 500 to 380 nm, was produced experimentally by changing glutamic acid to glutamine at position 113 (references in Yokoyama 1997). Wang et al. (2012) performed systematic modifications of rhodopsin structure producing a whole range of rhodopsins with spectra peaking from 460 to 644 nm and having the colors in solution shown in Fig. 9.11.

It has been shown that in some cases the spectrum of a visual pigment can be modified even without change of amino acid in the protein and without change of chromophore, namely, by the concentration of chloride ions (Yamashita et al. 2013 and literature cited by them).

Returning to the human MW and LW pigments, one may wonder why their absorption spectra are not more different. Color vision would appear to be more efficient if they were. The difference between the LW (552 or 557 nm) absorption peak and that of the MW (530 nm) pigment is much smaller than between MW and SW (426 nm) pigment maxima. The difference between the human LW and MW pigments is much smaller than the difference between corresponding pigments in, e.g., the fruit fly *Drosophila* (in this animal the two pigments absorbing at longest wavelengths peak at 420 and 480 nm, respectively; in addition the fly has two pigments peaking in the ultraviolet). One explanation that has been proposed is that the image-forming optics of the human eye has a large chromatic aberration and the effect of this is minimized if the spectra are not too different. The perception of shapes and position depends mainly on the LW and MW cones, and the focusing of an image on the retina is adjusted for the average of their wavelengths. The blue color is mentally "painted" into the outlines formed by these receptors. In the part of the retina used for the sharpest vision, the luteum has very few SW receptors and contains a yellow pigment which absorbs blue light. The similarity of LW and MW spectra makes good focusing possible. On the other hand, the small difference in the human pigments may be just a consequence of the fact that the gene duplication has occurred so recently, and evolution has not had time to result in a bigger difference yet.

Insects have a completely different system for image generation (Chap. 15), without the chromatic aberration problems, but the visual acuity of the fruit fly eye is much lower than that of the human eye.

What are the evolutionary pressures causing visual pigment spectra to be tuned? Generally speaking, of course, color vision provides more information than monochromic vision. We prefer color television to black and white. According to Osorio and Vorobyev (1996) and Regan et al. (1998), the main importance of the differentiation into LW and MW pigments in primates has been to aid our forefathers in detecting fruits against a green background and judging the ripeness of fruits. This view has been questioned by Lucas et al. (1998) and Dominy and Lucas (2001), who provide evidence that trichromatic vision is important for the selection of leaves at an optimal developmental stage for consumption. As for ultraviolet vision in birds, one well-documented advantage for birds of prey is that UV vision allows them to see urine of rodents and thus to locate their whereabouts. Ultraviolet vision in birds is also important for recognition of plumage coloration of conspecifics and for detection and identification of edible berries (Siitari et al. 1999).

For insects depositing eggs on leaves, it is important to find the leaves and to judge their age and health status. It turns out that for this task *a red-light* receptor can be very important. Most insects do not have red-sensitive receptors,

but both sawflies (Peitsch et al. 1992) and moths (Kelber 1999) that oviposit (lay eggs) on leaves do. Excitation of green-sensitive photoreceptors gives an attractive signal, and the red-sensitive receptors provide a contrasting, repelling signal. In the case of moths, their ultraviolet-, violet-, and blue-sensitive receptors probably play a role in their orientation and choice of leaves (young leaves are preferred). On the other hand, in selecting green leaves, vision probably does not play an important role in the discrimination between plant species; for this, chemical cues are more important.

The daylight penetrating deepest into the ocean is in the blue-violet region, and consequently the vision of deepwater fish is tuned to this wavelength band (Lythgoe 1984), while surface-living fish and fish in shallow freshwater have a visual sensitivity peaking, like ours, in the green spectral region (although the span of pigments in fish is much wider than ours, with pigment absorption peaks spanning from the ultraviolet to the red). Although also several bioluminescent deepsea fishes have maximum sensitivity in the blue-violet region (Fernandez 1978), others, who use their bioluminescence for environmental illumination, show remarkable deviations from this rule (Douglas et al. 1998, 1999). Other aspects of the connection between bioluminescence and the vision of deepsea fishes have been treated by Warrant (2000).

Deep-diving whales have rod pigments peaking at 485 nm, while rod pigments of aquatic animals foraging closer to the surface (seals, manatees) peak near 500 nm. To the surprise of some investigators, none of six whale species and seven seal species possess SW cones (nor any LW cones), only MW cones (Peichl et al. 2001), with a pigment absorbing maximally around 524 nm (Fasick et al. 1998). It has been claimed that this means that they do not possess color vision (Peichl et al. 2001), but this may be jumping to a conclusion. Although color discrimination in whales has not been established, rods are saturated in strong light and cones useless in weak light; there may be intermediate depth and light levels where signals are obtained from both rods and cones and give whales and seals a dichromatic color vision (Fasick et al. 1998; Fasick and Robinson 2000). A corresponding phenomenon in humans was demonstrated many years ago through a very interesting experiment by John J. McCann and Jeanne L. Benton, described by Land (1964). They first illuminated a multicolored display with "monochromatic" (narrowband) light of 550 nm (500 nm would probably have worked as well), which was so weak that only the rods of a human observer were stimulated. Of course no colors could be discriminated under such circumstances. They then added a second narrowband beam of 656 nm wavelength. The irradiance of this second light was adjusted so that only the LW cones were stimulated. Thus, only the rods and the LW cones were operative. Nevertheless, the observer was able to give names to colors in the display almost as if it was illuminated by natural daylight and all three types of cones had been stimulated.

Color vision is not restricted to di-, tri-, and tetrachromatic versions. The mantis shrimp (Osorio et al. 1997; Marshall and Oberwinkler 1999; Cronin et al. 2001) may have up to 16 types of visual pigment, although this does not mean that it has a corresponding number of color channels. It also has the ability to further tune the sensitivity spectra of their receptors by color filters as required by the light environment they inhabit. These animals may live close to the water surface (in full daylight spectrum) or as deep as 30 m (in a restricted blue-light environment). All 16 types of light-sensitive pigments may not correspond to separate sensory input channels, but no doubt they provide polychromatic vision.

Rhodopsins are used not only for vision but also for energy collecting by microorganisms. Proteorhodopsins, a group of rhodopsins widely spread among many microorganisms, is particularly worth mentioning in this context. It is spectrally tuned to different habitats mainly by substitution at a single amino acid site (Man et al. 2003).

9.10 Tuning of Anthocyanins

Anthocyanins are the most common vacuolar pigments, giving color to many flowers, fruits, and autumn leaves. We may think of the cell sap of plant vacuoles as structureless and of interactions between anthocyanins and their environment as a dull subject, but if we do so, we are in error.

The great pioneer in the elucidation of chemical structures of plant compounds, Richard Willstätter, got a surprise when he compared the structures of the blue pigment of the cornflower (*Centaurea cyanus*) with that of the red pigment of a rose. He found that the pigments were chemically identical (he was not completely right, but that does not destroy the story). He thought that the difference in color came about from a difference in pH of the cell sap of the two plants. He was not right there either, but he got the main point—that anthocyanins can produce very different colors with practically identical chromophores.

The basic structure of an anthocyanin is shown in Fig. 9.12. The molecule consists of two fused six-membered rings connected to a third six-membered ring. A system of

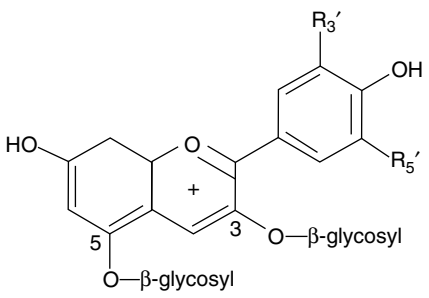

Fig. 9.12 The general structure of an anthocyanin in the flavylium cation form

conjugated double bonds extends over all rings. The fused rings carry three hydroxy groups, one or two of which form glycoside bonds with sugar molecules, often glucose. The sugar-free compound (the aglycon) is called anthocyanidin. The anthocyanidin of red rose flowers is cyanidin and that of cornflower succinyl-cyanidin (so they are indeed closely related, and the little difference does not explain the color difference). Pure cyanin (the glycosylated cyanidin) is red in acid solution, and if it is made alkaline, the color changes towards blue, so it is understandable that Willstätter ascribed the color difference between roses and cornflowers to a pH difference of the cell sap. However, the blue color acquired

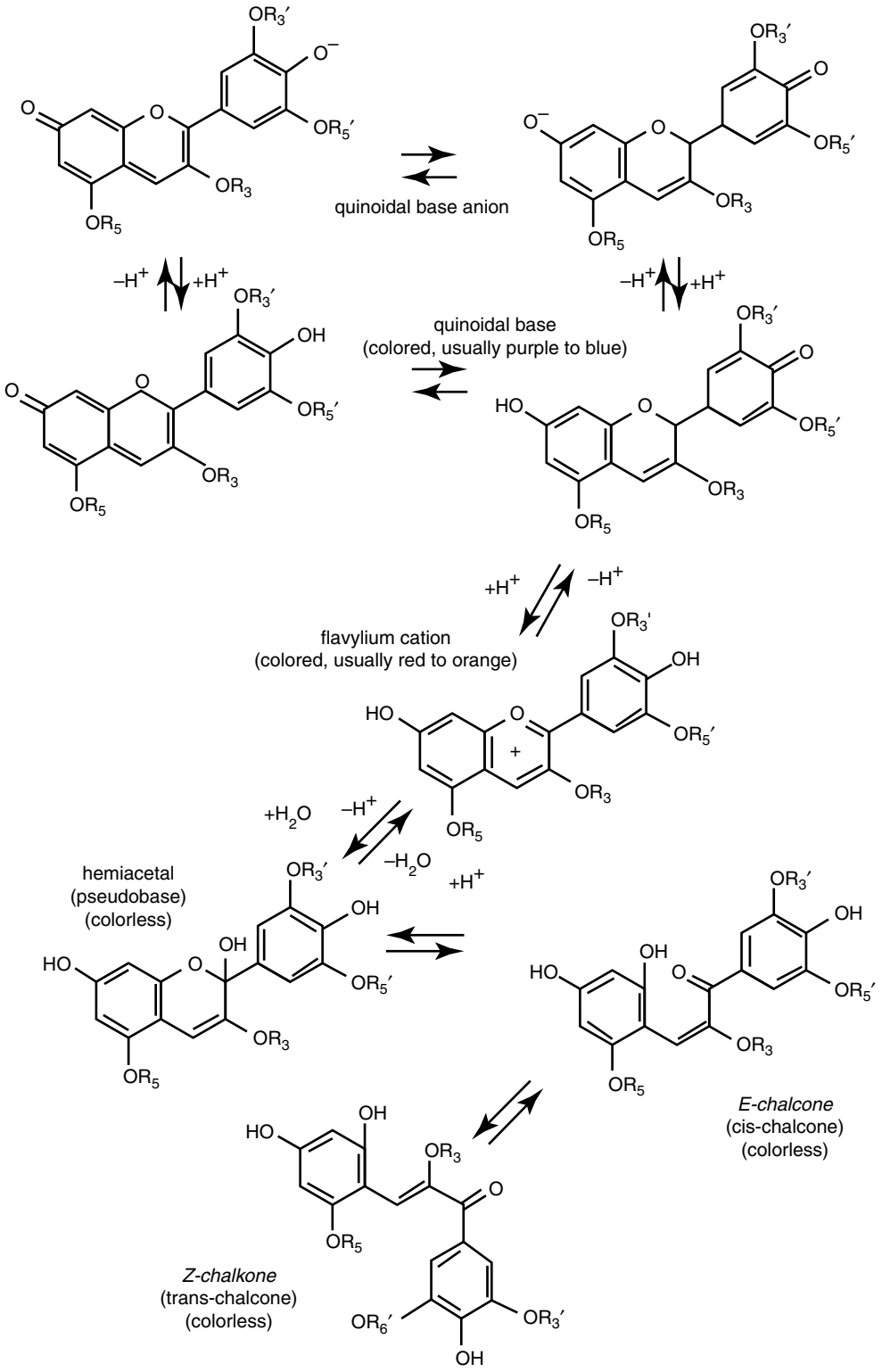

Fig. 9.13 An anthocyanin can exist in many different interconvertible molecular forms, as shown in this diagram: as different quinoidal bases anions or unionized quinonoidal bases, as flavylium cation, as hemiacetal (pseudo base), or as chalcone (E or Z form). Although hemiacetals and chalcones are colorless, they absorb ultraviolet radiation and can therefore appear colored to some animals. Their presence can also modify the hue of the colored forms

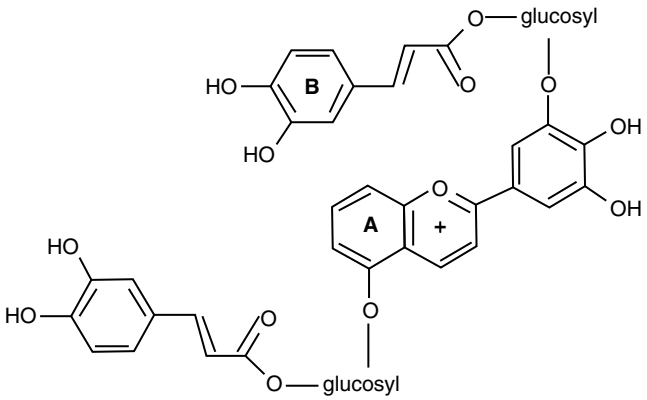

Fig. 9.14 The structure of gentiodelphin, schematic. In reality the molecule is more bent, so ring B closely overlaps the double ring A and the π orbitals of the ring systems fuse

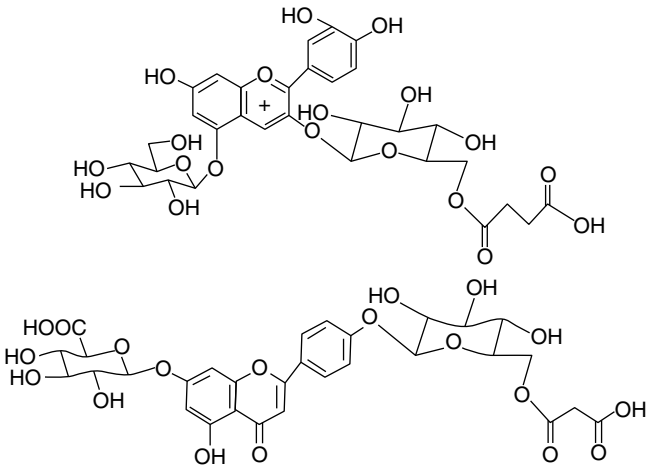

Fig. 9.15 According to Goto and Kondo (1991), the blue pigment of cornflower, protocyanin, is built up of six molecules each of the succinylcyanin cation (top) and the malonylflavone shown in the figure, plus one Fe and one Mg ion

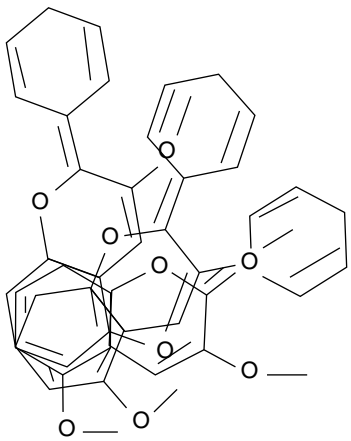

Fig. 9.16 An attempt to show the chiral stacking of delphin molecules. The sugar groups are omitted for clarity

upon alkalinization does not last long, the color fades away completely. This is because the molecule already, when the pH exceeds about 5, takes up water (Fig. 9.13). Furthermore, no plants are known with an alkaline cell sap, so the cornflower's blue color must be explained in another way.

The R-groups in Fig. 9.13 are numbered according to the conventional numbering of the carbon atoms to which they are bound. The groups can all be hydroxyl and can also be hydrogen; methoxyl; a chelated metal ion, such as Fe^{3+} or Al^{3+}; or a sugar or sugar derivative, while R_3 and R_5 can be a sugar or an acylated sugar. The equilibria between different forms depend on many things, such as the chelation with metal ions. In at least one case, it is also light dependent (Figueiredo et al. 1994).

The reason for the blue color of the cornflower rests in the phenomena of copigmentation and self-association. Copigmentation means that the color of the anthocyanin is influenced by other molecules in its environment. Self-association means that the anthocyanin molecule can associate with other anthocyanin molecules, and this also affects its color. Both self-association and associations between anthocyanins and uncolored phenolic compounds cause overlaps between the π-electron clouds of the individual molecules, and hence changes in the electron levels (Fig. 9.14). The concentration of anthocyanin in cell sap can exceed 20 m*M*, and this is more than sufficient for the molecules to associate to one another and sometimes form helical stacks through a combination of hydrophobic bonds between the rings and hydrophilic bonds between the sugar residues. These associations also prevent the formation of pseudo base, hence the bleaching of color that would otherwise take place at the pH prevalent in the cell sap.

Many different kinds of (uncolored) molecules and ions produce copigmentation effects with anthocyanins. The most important ones are some metal ions and colorless flavonoids (absorbing in the ultraviolet spectral region) and other phenolic compounds. In the case of the blue cornflower pigment (Fig. 9.15), Fe^{3+} and Mg^{2+} have been reported as copigmenting ions and a flavone as copigmenting phenol. Anthocyanins having two ortho-hydroxy groups at the B-ring (the leftmost ring in Fig. 9.15) form blue chelate complexes with trivalent metal ions such as iron(III) and aluminum(III), but not with magnesium. This latter ion is, however, very important in some other cases.

Goto and Kondo (1991) have written a very readable account of copigmentation, illustrated with color pictures. They describe structures of several more complex anthocyanins, with aromatic groups attached to the sugar residues, and a particularly interesting case of pigment complex, commelinin (rendering the blue color to *Commelina communis*). This consists of six molecules each of malonylawobanin (a complex anthocyanin) and flavocommelinin (a flavone glycoside) arranged around two magnesium ions. The intense blue color is partly due to exciton coupling between adjacent anthocyanin units. The molecular mass of this complex is nearly 1,000. Also chiral stacking (Fig. 9.16) can affect color.

The importance of the sugar groups in anthocyanins lies not in a direct effect on light absorption, but in their contribution to the folding and ordering of the chromophoric groups such that overlaps of π-electron clouds can take place.

The color of anthocyanins is affected not only by their chemical environment but also by physical factors: temperature and light. One summer day when one of the authors and his wife were having tea in their garden, she remarked that she had noticed how some flowers of a variety of *Phlox paniculata* had shifted color when they were reached by sunlight. He delivered a lecture on the psychology of color perception and the mistakes we can make, but she insisted. So we took the flowers to the lab and measured the reflection spectra after dark adaptation and after exposure to strong light for an hour (Björn et al. 1985). And indeed, the reflectance spectrum did change with light conditions. Color photos of the phenomenon have been published in Swedish journals (Björn 1985a, b). At the time we hypothesized that the color shift was caused by a light-activated proton pump in the tonoplast (the membrane surrounding the vacuole) which would change the pH of the cell sap. We attempted to show such a pH change using a white *Phlox* variety and artificial pH indicator dyes, but did not succeed. About a decade later, Figueiredo et al. (1994) demonstrated that the absorption spectrum of an artificial anthocyanin-like compound, 4′,7-dihydroxyflavylium chloride, could be reversibly affected, due to Z/E photoisomerization, by ultraviolet radiation (changing under irradiation from pale yellow to intense yellow), so it is possible that the color shift of our *Phlox* is due to an analogous phenomenon.

Thus, a number of factors can affect the color of anthocyanin-containing flower petals. Obviously the reason that plants have evolved colored flowers is that they attract pollinators. The pollinators also benefit from this, so a question naturally arises: To what extent have flowers adapted to pollinator vision, and to what extent has pollinator vision (and mental capacity, such as long-term and short-term memory) adapted to flower colors?

Chittka and coworkers (Chittka and Menzel 1992; Chittka 1996; Chittka et al. 1999; Chittka and Dornhous 1999) have studied this question. By comparison of color vision in various arthropod groups, they claim to be able to follow the evolution of color vision in insect pollinators. Photoreceptors among most Crustacea and Insecta fall into three rather distinct spectral classes: ultraviolet receptors with maxima around 350 nm, blue receptors with maxima at 400–460 nm, and green receptors with maxima from 470 to 550 nm. All these types seem to be very ancient. In addition, a few groups have red receptors with maxima around 600 nm. Chittka and coworkers see little evidence of insect adaptation to flower colors and believe that the main adjustment has been of flower colors to insect vision.

Only a minority of pollinators, such as hummingbirds and some butterflies, have red-sensitive photoreceptors. However, it must be borne in mind that pollinators without such receptors can see red flowers and distinguish them from other flowers and from green leaves.

The flowers of many plants vary in color with stage of development (Lunau 1996) and in this way signal to pollinators when a visit will be rewarded Lunau (2004). Of particular interest are flowers that change color during the year in synchronization with the availability of different pollinators.

Fig. 9.17 A flower of creeping tormentil, *Potentilla reptans* photographed in visible light (*left*) and in UV-A radiation (*right*) (Photo by L.O. Björn)

What has been described here for flower colors has, to some extent, a counterpart in the coloration of fruits of plants which depend on animals for seed dispersal.

The ultraviolet receptors of insects make it possible for them to see patterns invisible to us. Figure 9.17 shows an example of such a flower pattern due to ultraviolet-absorbing flavonoids.

References

Anders K, von Stetten D, Mailliet J, Kiontke S, Sineshchekov VA, Hildebrandt P, Hughes J, Essen L-O (2011) Spectroscopic and photochemical characterization of the red-light sensitive photosensory module of Cph2 from *Synechocystis* PCC 6803. Photochem Photobiol 87:160–173

Bhoo S-H, Davis SJ, Walker J, Baruch Karniol B, Vierstra RD (2001) Bacteriophytochromes are photochromic histidine kinases using a biliverdin chromophore. Nature 414:776–779

Björn LO (1976) Why are plants green? Relationships between pigment absorption and photosynthetic efficiency. Photosynthetica 19:121–129

Björn LO (1979) Photoreversibly photochromic pigments in organisms: properties and role in biological light perception. Quart Revs Biophys 12:1–23

Björn GS (1980) Phycochromes b and d: their occurrence in some phycoerythrocyanin-containing blue-green algae (cyanobacteria). Physiol Plant 48:483–485

Björn LO, Björn GS (1980) Yearly review: photochromic pigments and photoregulation in blue-green algae. Photochem Photobiol 32: 849–852

Björn GS, Braune W, Björn LO (1985) Light-induced, dark reversible colour shift in petals of *Phlox*. Physiol Plant 64:445–448

Björn LO, Papageorgiou GC, Blankenship RE, Govindjee (2009) A viewpoint: why chlorophyll *a*? Photosynth Res 99:85–98. doi:10.1007/s11120-008-9395-x

Blumenstein A, Vienken K, Tasler R, Purschwitz J, Veith D, Frankenberg-Dinkel N, Fischer R (2005) Curr Biol 15:1833–1838

Bolige A, Goto K (2007) Phytochrome-like responses in *euglena*: a low fluence response that reorganizes the spectral dependence of the high irradiance response in long-day photoperiodic induction of cell division. J Photochem Photobiol B Biology 86:97–108

Bowmaker JK, Heath LA, Wilkie SE, Hunt DM (1997) Visual pigments and oil droplets from six classes of photoreceptor in the retinas of birds. Vision Res 37:2183–2194

Britt SG, Feiler R, Kirschfeld K, Zuker CS (1993) Spectral tuning of rhodopsin and metarhodopsin in vivo. Neuron 11:29–39

Bussel AN, Kehoe DM (2014) Chromatic acclimation: a many-coloured mechanism for maximizing photosynthetic light harvesting efficiency. In: Flores E, Herrero A (eds) The cell biology of cyanobacteria. Caister Academic Press, Wymondham, UK. Ch. 6. ISBN 978-1-908230-38-6 (hardback), ISBN: 978-1-908230-92-8 (Ebook)

Chen M, Blankenship RE (2013) Expanding the solar spectrum used by photosynthesis. Trends Plant Sci 16:427–431

Chen M, Schliep M, Willows RD, Cai ZL, Neilan BA, Scheer H (2010) A red-shifted chlorophyll. Science 329:1318–1319

Chen M, Li YQ, Birch D, Willows RD (2012) A cyanobacterium that contains chlorophyll f —a red-absorbing photopigment. FEBS Lett 586:3249–3254

Chittka L (1996) Does bee color vision predate the evolution of flower color? Naturwissenschaft 83:136–138

Chittka L, Dornhaus A (1999) Comparisons in physiology and evolution, and why bees can do the things they do. http://www.ciencia.cl/CienciaAlDia/volumen2/numero2/articulos/articulo5-eng.html

Chittka L, Menzel R (1992) The evolutionary adaptation of flower colors and the insect pollinators' color vision. J Comp Physiol A 171:171–181

Chittka L, Thomson JD, Waser NM (1999) Flower constancy, insect psychology, and plant evolution. Naturwissenchaftliche 86:361–377

Cinque G, Croce R, Bassi R (2000) Absorption spectra of chlorophyll *a* and *b* in Lhcb protein environment. Photosynth Res 64:233–242

Cronin TW, Caldwell RL, Marshall J (2001) Sensory adaptation—tunable colour vision in a mantis shrimp. Nature 411:547–548

Dominy NJ, Lucas PW (2001) Ecological importance of trichromatic vision to primates. Nature 410:363–367

Douglas RH, Partridge JC, Dulai K, Hunt D, Mullineaux CW, Tauber AY, Hynninen PH (1998) Dragon fish see using chlorophyll. Nature 393:423–424

Douglas RH, Partridge JC, Dulai KS, Hunt DM, Mullineaux CW, Hynninen PH (1999) Enhanced retinal longwave sensitivity using a chlorophyll-derived photosensitiser in *Malacosteus niger*, a deep-sea dragon fish with far red bioluminescence. Vision Res 39:2817–2832

Duxbury Z, Schliep M, Ritchie RJ, Larkum AW, Chen M (2009) Chromatic photoacclimation extends utilisable photosynthetically active radiation in the chlorophyll d-containing cyanobacterium, *Acaryochloris marina*. Photosynth Res 101:69–75

Fasick JI, Robinson PR (1998) Mechanism of spectral tuning in the dolphin visual pigments. Biochemistry 37:433–438

Fasick JI, Robinson PR (2000) Spectral-tuning mechanisms of marine mammal rhodopsins and correlations with foraging depth. Vis Neurosci 17:781–788

Fasick JI, Cronin TW, Hunt DM, Robinson PR (1998) The visual pigments of the bottlenose dolphin (*Tursiops truncatus*). Vis Neurosci 15:643–651

Fernandez HRC (1978) Visual pigments of bioluminescent and nonbioluminescent deep-sea fishes. Vis Sci 19:589–592

Figueiredo P, Lima JC, Santos H, Wigand M-C, Brouillard M, Macanita AL, Pina F (1994) Photochromism of the synthetic 4′,7-dihydroxyflavylium chloride. J Am Chem Soc 116:1249–1254

Frank HA, Bautista JA, Josue J, Pendon Z, Hiller RG, Sharples FP, Gosztola D, Wasielewski MR (2000) Effect of the solvent environment on the spectroscopic properties and dynamics of the lowest excited states of carotenoids. J Phys Chem B 104:4569–4577

Fuad N, Day DA, Ryrie IJ, Thorne SW (1983) A photosystem II light-harvesting chlorophyll protein complex with a high fluorescence emission at 736 nm. Photobiochem Photobiophys 5:255–262

Fujimoto K, Hasegawa J, Hayashi S, Kato S, Nakatsuji H (2005) Mechanism of color tuning in retinal protein: SAC-CI and QM/MM study. Chem Phys Lett 414:239–242

Fujita Y, Hattori A (1962) Photochemical interconversion between precursors of phycobilin chromoprotein in *Tolypothrix tenuis*. Plant Cell Physiol 3:209–220

Gill EM, Wittmershaus BP (1999) Spectral resolution of low-energy chlorophylls in Photosystem I of *Synechocystis* sp. PCC 6803 through direct excitation. Photosynth Res 61:53–64

Glazer AN, Wedemayer GJ (1995) Cryptomonad biliproteins—an evolutionary perspective. Photosynth Res 46:93–105

Goto T, Kondo T (1991) Structure and molecular stacking of anthocyanins—flower color variation. Angew Chem Int Engl 30:17–33

Grossman AR, Bhaya D, He Q (2001) Tracking the light environment by cyanobacteria and the dynamic nature of light harvesting. J Biol Chem 276:11449–11452

Gutu A, Kehoe DM (2012) Emerging perspectives on the mechanisms, regulation, and distribution of light color acclimation in cyanobacteria. Mol Plant 5:1–13

Halldal P (1968) Photosyntheic capacities and photosynthetic action spectra of endozoic algae of the massive coral. Favia. Biol Bull 134:411–424

Hart NS, Partridge JC, Bennett ATD, Cuthill IC (2000) Visual pigments, cone oil droplets and ocular media in four species of estrildid finch. J Comp Physiol A 186:681–694

Hirose Y, Rockwell NC, Nishiyama K, Narikawa R, Ukaji Y, Inomata K, Lagarias JC, Ikeuchi M (2013) Green/red cyanobacteriochromes regulate complementary chromatic acclimation via a protochromic photocycle. Proc Natl Acad Sci U S A 110:4974–4979

Holzwarth AR (1991) Structure-function relationships and energy transfer in phycobiliprotein antennae. Physiol Plant 83:518–528

Irieda H, Morita T, Maki K, Homma M, Aiba H, Sudo Y (2012) Photo-induced regulation of the chromatic adaptive gene expression by *Anabaena* sensory rhodopsin. J Biol Chem 2012(287):32485–32493. doi:10.1074/jbc.M112.390864

Isayama T, Alexeev D, Makino CL, Washington I, Nakanishi K, Turro NJ (2006) An accessory chromophore in red vision. Nature 443:649

Jacobs GH (1992) Ultraviolet vision in vertebrates. Am Zool 32:544–554

Jensen P, Bunker PR (2000) Computational molecular spectroscopy. Wiley, Hoboken

Jordan P, Fromme P, Witt HT, Klukas O, Saenger W, Krauβ N (2001) Three-dimensional structure of cyanobacterial photosystem I at 2.5 nm resolution. Nature 411:909–917

Jung K-H, Trivedi VD, Spudich JL (2003) Demonstration of a sensory rhodopsin in eubacteria. Mol Microbiol 47:1513–1522

Karapetyan NV, Dorra D, Schweitzer G, Beszmertnaya IN, Holzwarth AR (1997) Fluorescence spectroscopy of the longwave chlorophylls in trimeric and monomeric photosystem I core complexes from the cyanobacterium *Spirulina platensis*. Biochemistry 36: 13830–13837

Kehoe DM, Grossman AR (1996) Similarity of a chromatic adaptation sensor to phytochrome and ethylene receptors. Science 273:1409–1412

Kehoe DM, Gutu A (2006) Responding to color: the regulation of complementary chromatic adaptation. Annu Rev Plant Biol 57:127–150

Kelber A (1999) Ovipositing butterflies use a red receptor to see green. J Exp Biol 202:2619–2630

Kiang NY, Siefert J, Govindjee, Blankenship RE (2007) Spectral signatures of photosynthesis. I. Review of Earth organisms. Astrobiology 7:252–274

Kleinschmidt J, Harosi F (1992) anion sensitivity and spectral tuning of cone visual pigments in situ. Proc Natl Acad Sci U S A 89:9181–9185

Knipp B, Müller M, Metzler-Nolte N, Balaban TS, Braslavsky SE, Schaffner K (1998) NMR verification of helical conformations of phycocyanobilin in organic solvents. Helv Chim Acta 81:881–888

Kochendoerfer GG, Lin SW, Sakmar TP, Mathies RA (1999) How color visual pigments are tuned. Trends Biochem Sci 24:300–305

Kochubey SM, Samokhval EG (2000) Long-wavelength chlorophyll forms in Photosystem I from pea thylakoids. Photosynth Res 63:281–290

Koehne B, Trissl HW (1998) The cyanobacterium *Spirulina platensis* contains a long wavelength-absorbing pigment C-738 (F-760(77 K)) at room temperature. Biochemistry 37:5494–5500

Koehne B, Elli G, Jennings RC, Wilhelm C, Trissl H-W (1999) Spectroscopic and molecular characterization of a long wavelength absorbing antenna of *Ostreobium sp*. Biochim Biophys Acta 1412:94–107

Lamparter T, Marwan W (2001) Spectroscopic detection of a phytochrome-like photoreceptor in the myxomycete *Physarum polycephalum* and the kinetic mechanism for the photocontrol of sporulation by Pfr. Photochem Photobiol 73:697–702

Lamparter T, Michael N, Mittmann F, Esteban B (2002) Phytochrome from *Agrobacterium tumefaciens* has unusual spectral properties and reveals an N-terminal chromophore attachment site. Proc Natl Acad Sci U S A 99:11628–11633

Land E (1964) The retinex theory of color vision. Sci Am 108–128

Linanto J, Korppi-Tommola J (2000) Spectroscopic properties of Mg-chlorin, Mg-porphin and chlorophylls a, b, c(1), c(2), c(3) and d studied by semi-empirical and ab initio MO/CI methods. Phys Chem Chem Phys 2:4962–4970

Loughlin P, Lin Y, Chen M (2013) Chlorophyll d and Acaryochloris marina: current status. Photosynth Res. doi:10.1007/s11120-013-9829-y

Lucas PW, Darvell B, Lee PKD, Yuen TDB, Choong MF (1998) Colour cues for leaf food selection by long-tailed macaques (*Macaca fascicularis*) with a new suggestion for the evolution of trichomatic colour vision. Folia Primatol 69:139–152

Lunau K (1996) Unidirectionality of floral colour changes. Plant Syst Evol 200:125–140

Lunau K (2004) Adaptive radiation and coevolution – pollination biology case studies. Org Divers Evol 4:207–224

Lythgoe JN (1984) Visual pigments and environmental light. Vis Sci 24:1539–1550

Ma Q, Hua H-H, Chen Y, Liu B-B, Krämer AL, Scheer H, Zhao K-H, Zhou M (2012) A rising tide of blue-absorbing biliprotein photoreceptors – characterization of seven such bilin-binding GAF domains in *Nostoc sp*. PCC7120. FEBS J 279:4095–4108

MacColl R (1998) Cyanobacterial phycobilisomes. J Struct Biol 124:311–334

Maier EJ, Bowmaker JK (1993) Color-vision in the passeriform bird, Leiothrix lutea—correlation of visual pigment absorbance and oil droplet transmission with spectral sensitivity. J Comp Physiol A 172:295–301

Makino CL, Groesbeek M, Lugtenburg J, Baylor DA (1999) Spectral tuning in salamander visual pigments studied with dehydroretinal chromophores. Biophys J 77:1024–1035

Man D, Wang W, Sabehi G, Arawind L, Post AF, Massana R, Spudich EN, Spudich JL, Béjà O (2003) Diversification and spectral tuning in marine proteorhodopsins. EMBO J 22:1726–1731

Marosvölgyi MA, van Gorkom HJ (2011) Cost and color of photosynthesis. Photosynth Res 103:105–109

Marshall J, Oberwinkler J (1999) The colourful world of the mantis shrimp. Nature 401:873–874

Matsui S, Seidou M, Uchiyama I, Sekiya N, Hiraki K, Yoshihara K, Kito Y (1988) 4-Hydroxyretinal, a new visual pigment chromophore found in the bioluminescent squid, *Watasenia scintillans*. Biochim Biophys Acta 966:370–374

Mauzerall D (1976) Chlorophyll and photosynthesis. Philos Trans Roy Soc Lond B 273:287–294

Milo R (2009) What governs the reaction center excitation wavelength of photosystems I and II? Photosynth Res 101:59–67

Murrell JN (1963) The theory of the electronic spectra of organic molecules. Methuen, London (German edition Elektronenspektren organischer Moleküle, Bibliographisches Institut Mannheim 1967)

Nathans J (1990) Determinants of visual pigment absorbance: Identification of the retinylidene Schiff's base counterion in bovine rhodopsin. Biochemistry 29:9746–9752

Nathans J (1992) Rhodopsin: structure, function, and genetics. Biochemistry 31:4923–4931

Neitz M, Neitz J, Jacobs GH (1991) Spectral tuning of pigments underlying red-green color vision. Science 252:971–974

Neitz J, Neitz M, Jacobs GH (1993) More than three different cone pigments among people with normal color vision. Vision Res 33:117–122

Ohad I, Clayton RK, Bogorad L (1979) Photoreversible absorbance changes in solutions of allophycocyanin purified from *Fremyella diplosiphon*: temperature dependence and quantum efficiency. Proc Natl Acad Sci U S A 76:5644–5659

Ohki K, Fujita Y (1978) Photocontrol of phycoerythrin formation in the blue-green alga *Tolypothrix tenuis* growing in the dark. Plant Cell Physiol 19:7–15

Öquist G (1969) Adaptations in pigment composition and photosynthesis by far red radiation in *Chlorella pyrenoidosa*. Physiol Plant 22:516–528

Osorio D, Vorobyev M (1996) Colour vision as an adaptation to frugivory in primates. Proc R Soc Lond B 263:593–599

Osorio D, Marshall NJ, Cronine TW (1997) Stomatopod photoreceptor spectral tuning as an adaptation for colour constancy in water. Vision Res 37:3299–3309

Palenik B (2001) Chromatic adaptation in marine *Synechococcus* strains. Appl Environ Microbiol 67:991–994

Pålsson LO, Flemming C, Gobels B, van Grondelle R, Dekker JP, Schlodder E (1998) Energy transfer and charge separation in photosystem I: P700 oxidation upon selective excitation of the long-wavelength antenna chlorophylls of *Synechococcus elongatus*. Biophys J 74:2611–2622

Peichl L, Behrmann G, Kröger HH (2001) For whales and seals the ocean is not blue: a visual pigment loss in marine mammals. Eur J Neurosci 13:1520–1528

Peitsch D, Fietz A, Hertel H, Desouza J, Ventura DF, Menzel R (1992) The spectral input systems of hymenopteran insects and their receptor-based color-vision. J Comp Physiol A Sens Neural Behav Physiol 170:23–40

Polívka T, Herek JL, Zigmantas D, Åkerlund HE, Sundström V (1999) Direct observation of the (forbidden) S-1 state in carotenoids. Proc Natl Acad Sci U S A 96:4914–4917

Regan BC, Julliot C, Simmen B, Viénot F, Charles-Dominique P, Mollon P (1998) Frugivory and colour vision in *Alouatta seniculus*, a trichromatic platyrrhine monkey. Vision Res 38:3321–3327

Ritz T, Damjanović A, Schulten K, Zhang JP, Koyama Y (2000) Efficient light harvesting through carotenoids. Photosynth Res 66:125–144

Rockwell NC, Lagarias JC (2010) A brief history of phytochromes. Chem Phys Chem 11:1172–1180

Rockwell NC, Martin SS, Feoktistova K, Lagarias JC (2011) Diverse two-cysteine photocycles in phytochromes and cyanobacteriochromes. Proc Natl Acad Sci U S A 108:11854–11859

Rodriguez-Romero J, Hedtke M, Kastner C, Müller S, Fischer R (2010) Fungi, hidden in soil or up in the air: light makes a difference. Annu Rev Microbiol 64:585–610

Rottwinkel G, Oberpichler I, Lamparter T (2010) Bathy phytochromes in rhizobial soil bacteria. J Bacteriol 192:5124–5133

Scharnagl C, Fischer SF (1993) Reversible photochemistry in the α-subunit of phycoerythrocyanin: characterisation of chromophore and protein by molecular dynamics and quantum chemical calculations. Photochem Photobiol 57:63–70

Scheer H, Kufer W (1977) Studies on plant bile pigments, IV: Conformational studies on C-phycocyanin from *Spirulina platensis*. Z Naturforsch 32c:513–519

Scheibe J (1972) Photoreversible pigment: occurrence in a blue-green alga. Science 176:1037–1039

Schelvis JPM, van Noort PI, Aartsma PI, van Gorkom HJ (1994) Energy transfer, charge separation and pigment arrangement in the reaction center of photo- system II. Biochim Biophys Acta 1184:242–250

Schneeweis DM, Green DG (1995) Spectral properties of turtle cones. Vis Neurosci 12:333–344

Schulten K, Karplus M (1972) On the origin of a low-lying forbidden transition in polyenes and related molecules. Chem Phys Lett 14:305–309

Seki T, Vogt K (1998) Evolutionary aspects of the diversity of visual pigment chromophores in the class Insecta. Comp Biochem Physiol B 119:53–64

Sharpe LT, Stockman A, Jägle H, Nathans J (1999) Opsin genes, cone photopigments, color vision, and color blindness. In: Gegenfurtner K, Sharpe LT (eds) Color vision: from genes to perception. Cambridge University Press, New York

Shubin VV, Murthy SDS, Karapetyan NV, Mohanty PS (1991) Origin of the 77-K variable fluorescence at 758 nm in the cyanobacterium *Spirulina platensis*. Biochim Biophys Acta 1060:28–36

Shukla A, Biswas A, Blot N, Partensky F, Karty JA, Hammad LA, Garczarek L, Gutu A, Schluchter WM, Kehoe DM (2012) Phycoerythrin-specific bilin lyase–isomerase controls blue-green chromatic acclimation in marine *Synechococcus*. Proc Natl Acad Sci U S A 109:20137–20141

Siitari H, Honkavaara J, Viitala J (1999) Ultraviolet reflection of berries attracts foraging birds. A laboratory study with redwings (*Turdus iliacus*) and bilberries (*Vaccinium myrtillus*). Proc R Soc Lond B 266:2125–2129

Song J-Y, Cho HS, Cho J-I, Jeon J-S, Lagarias JC, Park Y-I (2011) Near-UV cyanobacteriochrome signaling system elicits negative phototaxis in the cyanobacterium *Synechocystis sp*. PCC 6803. Proc Natl Acad Sci U S A 108:10780–10785

Stomp M, Huisman J, Stal LJ, Matthijs HCP (2007) Colorful niches of phototrophic microorganisms shaped by vibrations of the water molecule. ISME J 1:271–282

Tandeau de Marsac N (1977) Occurrence and nature of chromatic adaptation in cyanobacteria. J Bacteriol 130:82–91

Tanimura T, Isono K, Tsukahara Y (1986) 3-hydroxyretinal as a chromophore of *Drosophila melanogaster* visual pigment analyzed by high-pressure liquid- chromatography. Photochem Photobiol 43:225–228

Thrash RJ, Fang HL-B, Leroi GE (1979) On the role of forbidden low-lying excited states of light-harvesting carotenoids in energy transfer in photosynthesis. Photochem Photobiol 29:1049–1050

Vogelmann TC, Scheibe J (1978) Action spectra for chromatic adaptation in the blue-green alga *Fremyella diplosiphon*. Planta 143:233–239

Vogt K (1983) Is the fly visual pigment a rhodopsin? Zschr Naturforsch C 38:329–333

Vogt K, Kirschfeld K (1984) Chemical identity of the chromophores of fly visual pigment. Naturwissenchaftliche 71:211–213

Vorobyev M, Osorio D, Bennet ATD, Marshall NJ, Cuthill IC (1998) Tetrachromacy, oil droplets and bird plumage colours. J. Comp. Physiol. A – Sensory Neural Behav. Physiology 183:621–633

Wald G, Brown PK (1958) Human rhodopsin. Science 127:222–226

Wang W, Nossoni Z, Berbasova T, Watson CT, Yapici I, Sing K, Lee S, Vasileiou C, Geiger JH, Borhan B (2012) Tuning the electronic absorption of protein-embedded all-trans-retinal. Science 338:1340–1343

Warrant W (2000) The eyes of deep-sea fishes and the changing nature of visual scenes with depth. Phil Trans R Soc Lond B 355: 1155–1159

White D, Shropshire Jr W, Stephens K (1980) Photocontrol of development by Stigmatella aurantiaca. J Bacteriol 142:1023–1024

Yamashita T, Nakamura S, Tsutsui K, Morizum T, Shichid Y (2013) Chloride-dependent spectral tuning mechanism of L-group cone visual pigments. Biochemistry 52:1192–1197

Yokoyama S, Radlwimmer FB, Blow NS (2000) Ultraviolet pigments in birds evolved from violet pigments by a single amino acid change. Proc Natl Acad Sci U S A 97:7366–7271

Zhao K-H, Haessner R, Cmiel H, Scheer H (1995) Type I reversible photochemistry of phycoerythrocyanin involves Z/E-isomerization of a-84 phycoviolobilin chromophore. Biochimi Biophys Acta 1228:235–243

Zhao K-H, Scheer H (1995) Type I and type II reversible photochemistry of phycoerythrocyanin α-subunit from *Mastigocladus laminosus* both involve Z, E isomerization of phycoviolobilin chromophore and are controlled by sulfhydryls in apoprotein. Biochim Biophys Acta 1228:244–253

Zouni A, Witt H-T, Kern J, Fromme P, Krauss N, Saenger W, Orth P (2001) Crystal structure of photosystem II from *Synechococcus elongatus* at 3.8 Å resolution. Nature 409:739–743

Zuchelli G, Jennings RC, Garlaschi FM (1990) The presence of long-wavelength chlorophyll *a* spectral forms in the light-harvesting chlorophyll *a/b* protein complex II. J Photochem Photobiol B Biol 6:381–394

Spectral Tuning in Biology II: Structural Color

10

Shuichi Kinoshita, Helen Ghiradella, and Lars Olof Björn

10.1 Introduction

Structural colors are formed by the interaction of light with materials with very specific (and usually complex) micro- and nanoscale architecture; in biological systems, they are likely to occur in stiff, nonliving "biological materials." These nonliving materials include arthropod exoskeleton, bird feathers, fish scales, mollusk shells (particularly their inner linings), and the like.

Structural colors come in several basic types: let us begin here with a discussion of *iridescence*. Iridescence is defined as a category of color that changes with the illuminating and viewing angles; it is abundant in the animal kingdom as brilliant, often metallic, colors characteristic of many birds, fish, insects, marine annelids, and other invertebrates; it has more recently also been described in plants (Glover and Whitney 2010, Lee 2007).

Pioneering work on the subject was done by Mason (1923a, b, 1926, 1927a, b); since then, there has been an explosion of interest in these systems. Recent reviews include Fox (1976), Ghiradella (1991, 1998), Herring (1994, 2002), Parker (1998, 1999, 2000), Srinivasarao (1999), Vukusic and Sambles (2003), Kinoshita and Yoshioka (2005a, b), Kinoshita et al. (2008), Prum (2006), Berthier (2007), and Kinoshita (2008, 2013).

S. Kinoshita (✉)
Graduate School of Frontier Biosciences, Osaka University, Osaka, Japan
e-mail: skino@fbs.osaka-u.ac.jp

H. Ghiradella
Department of Biology, University at Albany, Albany, NY, USA
e-mail: hghff@albany.edu

L.O. Björn
School of Life Science, South China Normal University, Guangzhou, China

Department of Biology, Lund University, Lund, Sweden
e-mail: Lars_Olof.Bjorn@biol.lu.se

Let us start by focusing on a particular iridescent form, the biological mirror. As those readers who have driven on a country road at night know, many night-active wild animals have efficient reflectors in their eyes, as do our favorite pets, dogs and cats. These reflectors, located in the back of the eye behind the retina, double the sensitivity of the eyes to light. They do this by throwing photons that have escaped absorption by the light-sensitive pigments during their first passage through the retina, back through the retina again to give it a second chance to absorb them.

Some light-emitting organs of marine animals have reflectors like those behind the headlights of a car, which throw the light in a certain direction. Many fish scales act as "body mirrors" that reflect the downwelling daylight back towards the water surface, making it easier for their owners to avoid detection. There are even eyes that have mirrors as image-forming optical elements (Land and Nilsson 2002), somewhat analogous to astronomical reflecting telescopes.

These biological mirrors are built up of alternating layers of materials of high and low refractive index, forming a structure we call a "multilayer thin-film stack." We have previously (Chap. 1) treated reflection at a single boundary between media with different refractive indices. When several such boundaries are stacked upon one another, we cannot simply compute the reflectance at each of them using Fresnel's formulas (Section 1.9, in Chap. 1) nor compute the transmittance by taking their product for the following two reasons: (1) there will be multiple reflections of photons bouncing back and forth between the boundaries, and (2) there will be interference effects.

To understand how such complex mirrors function, we have to consider the phases of electromagnetic oscillations, which was not necessary for a single boundary. Phase and phase difference are usually expressed in angular measure (radians), where 2π radians (360°) correspond to a period of the electromagnetic oscillation. Reflection of light traveling from a medium of lower to one of higher refractive index differs in one important respect from reflection of light traveling in the other direction (Fig. 10.1): during reflection towards a

L.O. Björn (ed.), *Photobiology: The Science of Light and Life*,
DOI 10.1007/978-1-4939-1468-5_10,

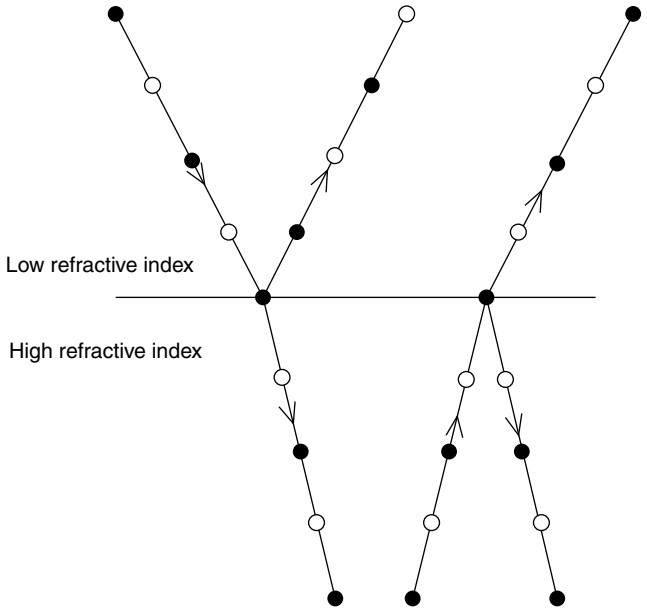

Fig. 10.1 Reflections at an interface between media of higher and lower refractive index. *Filled* and *empty circles* denote opposite phases (i.e., phases differing by π radians) of the electromagnetic waves

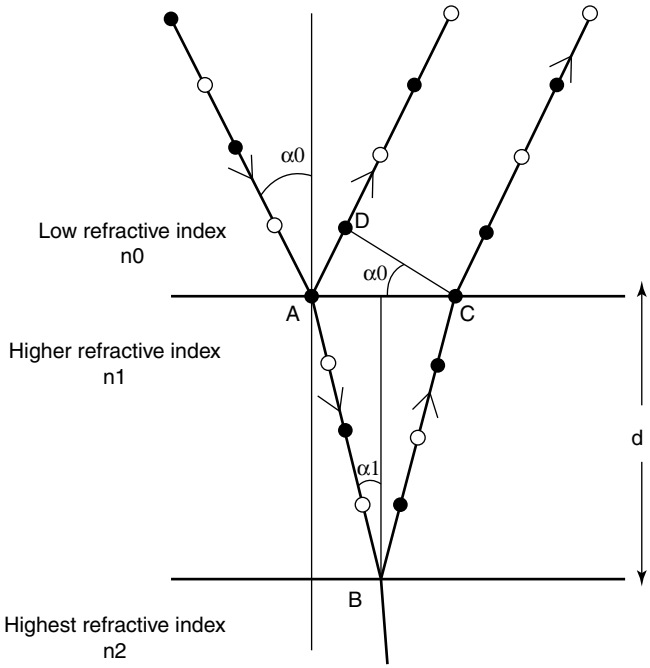

Fig. 10.2 Phase relations during reflection at two consecutive phase boundaries. The drawing is for the case $n_0 < n_1 < n_2$, corresponding to, e.g., the antireflective coating on a camera lens. In this case phase reversal takes place at both reflective surfaces, while with a soap film, the reversal takes place only at the first surface interacting with light

denser medium, the oscillation undergoes a phase change by π radians (180°). The detailed general treatment of reflection in multilayer stacks is complicated. We shall therefore focus here on some special cases, which are more easily understood and nevertheless demonstrate more general principles.

In addition to the multilayer stacks, we will describe some newly developing research, which is related to optical responses due to such completely different structures as regular arrangements of elements, on the one hand, and random ("spongy") structures on the other. The former correspond to so-called photonic crystals, whose study has been advanced in a surprisingly quick manner after the concept was established in the 1980s. However, in natural worlds, photonic crystals are found to be very common, appearing as the play of color in opal, brilliant wings in birds, and iridescent wings of butterflies and beetles, to name a few.

The spongy structural mode is related to a phenomenon called Tyndall blue or Rayleigh scattering and has long been believed to be the origin of non-iridescent blue colors of dragonflies and kingfishers. However, recent investigations have shown that even these colors are not due to simple light scattering processes, but are also related to the interference effect.

10.2 Reflection in a Single Thin Layer

Everyone is familiar with the reflections from soap films and knows that a range of colors can be produced by such reflection. In this case, we have a thin film of higher refractive index (approximately that of water) with the same medium (air) on both sides of the film. We can generalize this by considering a bulk medium of one refractive index, n_0, on one side, a thin film with a different refractive index, n_1, and on the other side a bulk medium with the third refractive index, n_2 (Fig. 10.2). We refer to these three media as being of orders 0, 1, and 2, respectively. For the soap film case, the relation between these indices is given as $n_0 = n_2 < n_1$. (A well-known example in which the relation $n_0 < n_1 < n_2$ holds is the antireflective coating on a camera lens.) As we shall see later, we can treat these and similar cases with the same set of equations.

We denote the incidence angle by α_0 and the angle of refraction in the film as α_1; Snell's law then gives the relationship $n_0 \sin\alpha_0 = n_1 \sin\alpha_1$, or $\sin\alpha_1 = n_0 \sin\alpha_0 / n_1$.

The ordinary Fresnel reflection factors for a single surface between bulk media 0 and 1 (Chap. 1) are given as

$$R_{01}^{p} = \left[\frac{n_1 \cos\alpha_0 - n_0 \cos\alpha_1}{n_1 \cos\alpha_0 + n_0 \cos\alpha_1}\right]^2,$$

$$R_{01}^{s} = \left[\frac{n_0 \cos\alpha_0 - n_1 \cos\alpha_1}{n_0 \cos\alpha_0 + n_1 \cos\alpha_1}\right]^2,$$

for light having the electric vector parallel to the plane of incidence (p-polarization) and perpendicular to it

(*s*-polarization), respectively. These give the reflection coefficients for power or intensity, and of course they are always represented by positive real numbers.

It turns out that for a thin film, due to the interference effect, not only these angle-dependent factors, but also another angle-dependent factor, has to be taken into account. This is a function also of the layer thickness (d), the vacuum wavelength (λ), and the refraction index (n_1) of the film. To compute this, we first calculate the phase difference between the rays reflected from the first and from the second surface (Fig. 10.2). This phase difference can be thought of as composed of four components. The first is due to the phase reversal at the first surface. The phase difference is π radians for $n_1 > n_0$, as with the soap film and the camera lens, but it is 0 for $n_1 < n_0$. The second is due to the longer distance (AB + BC) traveled inside the film with the refraction index of n_1 by the ray reflected from the second surface. Therefore, the phase difference results in $2n_1d(2\pi/\lambda)/\cos\ \alpha_1$ radians. The factor 2 at the front stems from the fact that the ray reflected from the second surface traverses the film twice, and n_1d is the "optical thickness" of the film, i.e., the geometrical thickness corrected for the shortening of the wavelength of light in proportion to the refraction index.

The third component of the phase difference is due to possible phase reversal during reflection at the second surface. It is 0 in the soap film case, because $n_1 > n_2$, and π radians in the camera lens case, because $n_1 < n_2$.

The fourth component of the phase difference is due to the shorter distance, AD, in Fig. 10.2, traveled in the n_0 medium. This phase difference is calculated as

$$\begin{aligned}
&\mathrm{AD}\cdot n_0(2\pi/\lambda) = \mathrm{AC}\cdot\sin\ \alpha_0\cdot n_0(2\pi/\lambda)\\
&\quad = 2d\tan\ \alpha_1\cdot\sin\ \alpha_0\cdot n_0(2\pi/\lambda)\\
&= 2d\left(\sin\ \alpha_1/\cos\ \alpha_1\right)\cdot n_1\sin\ \alpha_1(2\pi/\lambda)\\
&= 2n_1d\sin^2\alpha_1(2\pi/\lambda)/\cos\ \alpha_1\ (\text{radians}).
\end{aligned}$$

If we calculate the phase differences between these two pathways, we obtain

$$\begin{aligned}
&2n_1d(2\pi/\lambda)/\cos\ \alpha_1 - 2n_1d\sin^2\alpha_1(2\pi/\lambda)/\cos\ \alpha_1\\
&\quad = 2n_1d\left(1-\sin^2\alpha_1\right)(2\pi/\lambda)/\cos\ \alpha_1\\
&\quad = 2n_1d\cos^2\ \alpha_1(2\pi/\lambda)/\cos\ \alpha_1\\
&\quad = 2n_1d\ \cos\ \alpha_1(2\pi/\lambda)(\text{radians}),
\end{aligned}$$

which directly corresponds to the total phase difference in the case of $n_0 < n_1 < n_2$, because the phase reversal at each surface is canceled, while in case of $n_0 = n_2 < n_1$, we have to add π to the above formula, corresponding to the phase reversal at the first surface.

The Fresnel formulas given above, with expressions in squared brackets, represent intensity reflection coefficients. For many computations, however, it is advantageous to work with the corresponding unsquared expressions, so-called amplitude reflection coefficients, describing the change in amplitude of the electric wave upon reflection (the energy of the wave is proportional to the square of the amplitude). These coefficients, in contrast to the intensity reflection coefficients, can be either positive or negative (if light-absorbing materials are involved, the amplitude reflection coefficient is represented by a complex number, but we shall not consider this case here). A negative amplitude reflection coefficient means that the electric field changes direction during reflection, in other words, that we have a phase change of π radians. Therefore, when we do calculations based on the amplitude reflection coefficients, we do not have to worry about the phase changes of π radians during reflection, since they will come automatically with the sign of the amplitude reflection coefficient used.

The following QuickBasic program will compute the reflectance over a wavelength range of 0.3–1 μm for a thin film with refractive index n_1 between media with refractive indices n_0 (incidence side) and n_2 (output side), respectively. In reality, the multiple reflection within the film generally takes place and effectively influences the reflection intensity when the refractive index of the film is much higher or the output side is replaced by a metallic substance. However, we neglect this effect and take only the first and second reflections into account. Furthermore, the refractive indices will generally vary with wavelength, but this has also not been taken into account. Thus, the reflectance of the single thin layer is expressed as

$$R^{s,p} = \left(r_{01}^{s,p}\right)^2 + \left(r_{12}^{s,p}\right)^2 + 2r_{01}^{s,p}r_{12}^{s,p}\cos\ \delta,$$

where $r_{01}^{s,p}$ and $r_{12}^{s,p}$ are the Fresnel amplitude reflection coefficients corresponding to *s*- and *p*-polarizations for the interface between the bulk medium 0 and the film 1 and those between the film 1 and the bulk medium 2, respectively. δ is the phase difference described above and is expressed as $\delta = 2n_1d\cos\ \alpha_1(2\pi/\lambda)$. If we run on a Macintosh computer, the result will appear in the clipboard and can be transferred to other programs from there. If you wish to have the output in another form, line 200 should be modified accordingly, and for other computers and Basic dialects, modifications may have to be made.

```
INPUT "incidence angle in degrees =",
a0:pi = 3.14159: a0 = a0 * pi/180
INPUT "thickness of thin layer in micrometres =", d
```

```
INPUT "refractive index of medium 0=", n0
INPUT "refractive index of thin layer=", n1
INPUT "refractive index of medium 1=", n2
sina1 = n0 * SIN(a0)/n1: a1 = ATN(sina1/SQR(1-sina1 * sina1))
sina2 = n1 * sina1/n2: a2 = ATN(sina2/SQR(1-sina2 * sina2))
50 :PRINT "Enter p for parallel (p) polarization, s for perpendicular (s) polarization."
PRINT "Polarization directions are of electric vector relative to incidence plane."
INPUT "electric vector direction", polarization$
IF polarization$ = "p" THEN 150
IF polarization$ = "s" THEN 100
PRINT "Mistake! Try again!": GOTO 50
100 : r1 = (n0 * COS(a0)-n1 * COS(a1))/(n0 * COS(a0)+n1 * COS(a1))
r2 = (n1 * COS(a1)-n2 * COS(a2))/(n1 * COS(a1)+n2 * COS(a2)):GOTO 170
150 :r1 = (n1 * COS(a0)-n0 * COS(a1))/(n0 * COS(a1)+n1 * COS(a0))
r2 = (n2 * COS(a1)-n1 * COS(a2))/(n1 * COS(a2)+n2 * COS(a1)):GOTO 170
170 :OPEN "O",1,"clip:"
FOR L = .3 TO 1 STEP .01
delta=4*pi * n1 * d/L*COS(a1)
I = (r1 * r1+r2 * r2+2 * r1 * r2 * COS(delta))
I = I/(1+r1 * r1 * r2 * r2+2 * r1 * r2 * COS(delta))
200: PRINT#1, I: NEXT L: CLOSE 1: END
```

We show in Fig. 10.3 the output of this program for a soap film ($n_1=1.33$) of 0.33-μm thickness with $n_0=n_2=1$, both for normal incidence ($\alpha_0=0$) and for 45° incidence angle; in the latter case for both polarizations. This film would look yellow in a perpendicular direction and bluish green in a 45° direction. Note that the reflection spectrum shifts to a shorter wavelength with increasing incidence angle, that there are in each spectrum several peaks corresponding to phase shifts of integer multiples of 2π, and that for oblique angles, the *s*-polarized light is reflected better than the *p*-polarized light.

The wavelengths giving the maximum and minimum reflectance are easily obtained according to the value of $\cos\delta$ and the sign of the product $r_{01}^{s,p}\, r_{12}^{s,p}$ in the above formula. In the case of $n_0=n_2<n_1$, for example, the conditions for the maximum and minimum reflectance are given as $\cos\delta=-1$

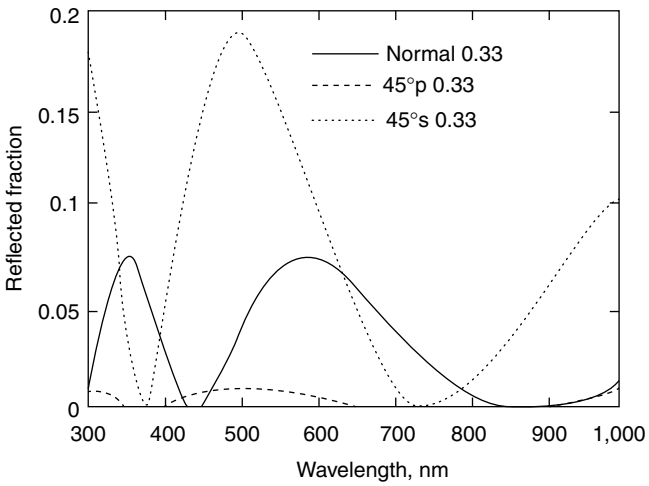

Fig. 10.3 Reflection in a soap film of 0.33-μm thickness and the refractive index of 1.33

and $\cos\delta=1$, because the sign of the product becomes negative, which result in $2n_1 d\cos\alpha_1(2\pi/\lambda)=(2m-1)\pi$ and $2n_1 d\cos\alpha_1(2\pi/\lambda)=2m\pi$, respectively. Thus, we obtain

$$\lambda_{\max}=\{4n_1 d/(2m-1)\}\cos\alpha_1=\{4n_1 d/(2m-1)\}\sqrt{1-(n_0/n_1)^2\sin^2\alpha_0},$$

$$\lambda_{\min}=\{4n_1 d/(2m)\}\cos\alpha_1=\{4n_1 d/(2m)\}\sqrt{1-(n_0/n_1)^2\sin^2\alpha_0},$$

where m denotes any positive integer and we have used the relation $\cos\alpha_1=\sqrt{1-(n_0/n_1)^2\sin^2\alpha_0}$.

Next we run the program for a typical camera lens antireflective coating with $n_0=1$, $n_1=1.38$ (corresponding to magnesium fluoride), and $n_2=1.89$ (heaviest flint glass). The optical thickness (thickness × refractive index) of the layer is adjusted to correspond to one quarter wavelength of yellow light (589 nm) in the layer, i.e., (0.589/4)/1.38 μm (Fig. 10.4). The wavelengths giving the maximum and minimum reflectance in this case are obtained by interchanging $\lambda_{\max}$ and $\lambda_{\min}$ in the above relations.

To obtain zero reflection with an antireflective coating on a lens, two conditions must be fulfilled: (1) the optical thickness of the coating film must be equal to one quarter of the wavelength of light (or this plus an integer multiple of the wavelength), which can be achieved only for a certain wavelength; and (2) the coating material must have a refraction index which is the square root of the product of the refractive indices of the outer medium (air) and the lens material (i.e., $n_1=\sqrt{n_0 n_2}$). In practice, compromises have to be made.

The reader might wonder what the construction of antireflective coating on a camera lens has to do with photobiology. The fact is that even some eyes, notably in the insect orders Lepidoptera and Diptera, have antireflective surfaces (Bernhard et al. 1965, 1968, 1970; Parker 1999, 2000; Yoshida

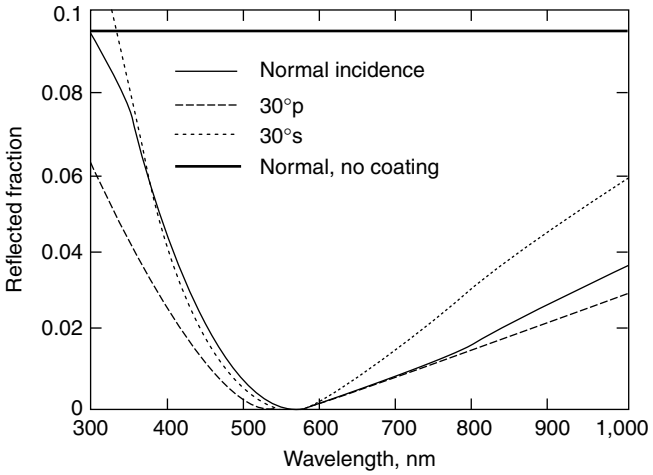

Fig. 10.4 Reflectance of a lens of heaviest flint glass ($n_1 = 1.89$) coated with a quarter-wave thickness (0.107 μm) of magnesium fluoride (MgF2, $n_1 = 1.38$). Reflected fraction of the incident light is shown for normal incidence and for 30° incidence angle with different polarizations. For comparison, the reflected ratio at normal incidence without coating is also shown. For oblique angles, even higher reflectance would be obtained without coating. The mixture of violet-blue and red reflected light gives such a lens a purple tint

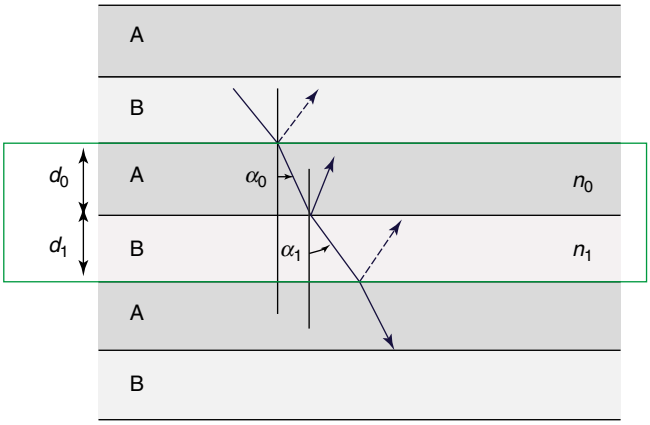

Fig. 10.5 Schematic illustration of multilayer stack. The dashed arrows indicate the phase reversal taking place during reflection. Complete constructive interference is obtained when the sum of (**A**) and (**B**) stacks is regarded as a film satisfying the thin-film interference condition for antireflective coating, while a single (**A**) or (B) layer satisfies the soap-bubble condition

et al. 1996; Yoshida 2002; Stavenga et al. 2006a). In this case, however, the antireflective surface is not obtained by addition of a layer of material of a different refractive index, but by finishing off the bulk material with tapering "nipples" smaller than the wavelength of the light, which effectively provide a gradual change in refractive index from that of the bulk material to that of air. The main biological advantage of the antireflective surface might be to make the bearer of the eyes less conspicuous by avoiding a shiny surface ("eyeshine") (Stavenga et al. 2006) and to some extent to improve vision.

This type of antireflective surface, usually called "moth-eye structure," has become one of the most advanced achievements of recently developing nanotechnology and has often been employed to reduce reflective loss at the surfaces of solar cells. The advantage of this "biological-inspired" antireflective coating lies in its extraordinarily wide angular and wavelength ranges, which cannot be achieved by simple film-type antireflective coatings, even when two or more layers are employed. (It is also an example of "biomimicry," an increasingly important technological approach to design, to which we will briefly return towards the end of this chapter.)

10.3 Reflection by Multilayer Stacks

We shall now come to a more complicated case of multilayer stacks forming efficient biological mirrors with nearly 100 % reflectance. The most important case is that of normal incidence. Eyes, for instance, are constructed such that light hits the retina, and therefore also the reflective backing of the retina, almost perpendicularly. However, using the computer program shown later, oblique incidence and both *s*- and *p*-polarizations can be handled.

Interference phenomena due to periodic multilayer stacks are qualitatively understood in terms of periodic piling of a pair of thin layers. Consider two layers designated as A and B with thickness d_0 and d_1 and refractive indices n_0 and n_1, respectively, as illustrated in Fig. 10.5. We will tentatively assume $n_0 > n_1$. If we consider a certain pair of AB layers, the phases of the reflected light at the upper and lower B-A interfaces both change by π radians, because the condition $n_0 > n_1$ holds. Thus, the relation similar to the antireflective coating described in the previous section is applicable. Taking into account that the present system consists of two layers, the wavelength of maximum reflectance will be given as

$$\lambda_{\max} = 2\{n_0 d_0 \cos \alpha_0 + n_1 d_1 \cos \alpha_1\}/m,$$

with the angles of refraction in the A and B layers as α_0 and α_1, respectively.

Furthermore, if we consider only the A layer within the AB layer, the phase of the reflected light does not change at the A-B interface, while it does change at the B-A interface. Thus, an interference condition corresponding to the soap film case can be applied:

$$\lambda_{\max} = 4n_0 d_0 \cos \alpha_0 / (2m' - 1),$$

where m' is a positive integer satisfying the condition $m' \leq m$. If the above two conditions are simultaneously satisfied at the same wavelength, the reflected light from the A-B interfaces adds to that from the B-A interfaces so that the multilayer will give the maximum reflectance. In particular,

the condition $m = 1$ and $m' = 1$ corresponds to the lowest-order reflection with the optical thicknesses of the A and B layers equal to each other. Land called this case "ideal stack" or "ideal multilayer" (Land 1972).

On the other hand, if the thicknesses of the A layers do not satisfy the latter relation, while the sum of the A and B layers satisfies the former one, the reflection at the A-B interface works more or less destructively so that the peak reflectance will decrease. This case is called a "non-ideal stack." An ideal stack is effective to increase the reflectance, whereas its reflection band width is also increased considerably. On the other hand, a non-ideal reflection band width can be suppressed, which is often effective to show the color more clearly.

The following computer program is based on the treatise by Huxley (1968) and is in agreement with the example treated by Land (1966).

```
pi = 3.14159
INPUT "refraction index of medium and spaces", na
INPUT "thickness of spaces, micrometres", da
INPUT "number of plates = ", p
INPUT "thickness of plates, micrometres", db
INPUT "refraction index of plates", nb
INPUT "incidence angle, degrees", aa:IF aa = 0 THEN aa = .001:aa = pi * aa/180
sinab = na * SIN(aa)/nb:ab = ATN(sinab/SQR(1-sinab * sinab))
27 : INPUT "choose polarization, p for parallel, s for perpendicular", pol$
IF pol$ = "s" THEN 29
IF pol$ = "p" THEN 30
PRINT "MISTAKE! Try again!"
28 : GOTO 27
29 :r = SIN(aa-ab)/SIN(aa+ab):GOTO 31
30 : r = -TAN(aa-ab)/TAN(aa+ab)
31 :OPEN "O",1,"clip:"
FOR L = .4 TO .85 STEP .001
fia = (2 * pi/L) * da * na * COS(aa):fib = (2 * pi/L) * db * nb * SQR(1-sinab * sinab)
kprim = -(COS(fia+fib)-r * r * COS(fia-fib))/(1-r * r)
k = (SIN(fia+fib)-r * r * SIN(fia-fib))/r/SIN(fib)/2
IF kprim * kprim<1 GOTO 100
REM In the following case mu is real
mu1 = kprim+SQR(kprim * kprim-1)
mu2 = kprim-SQR(kprim * kprim-1)
90 :murat = mu1/mu2:IF murat>1 THEN murat = 1/murat
```

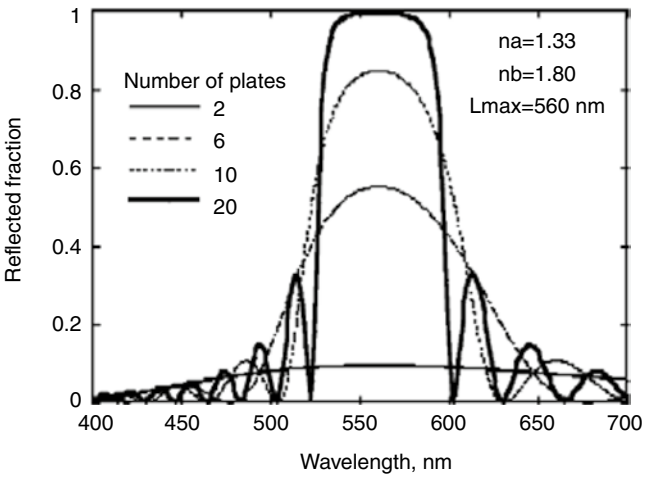

Fig. 10.6 Reflectance at normal incidence of a stack of guanine plates ($n = 1.80$) with spaces between the plates having a refractive index like that of seawater ($n = 1.34$). The thickness of plates and of spaces was chosen such that thickness times refractive index (optical path length) amounts to 140 nm. This leads to high reflection at 4 × 140 nm = 560 nm

```
95 :m2 = (murat)^ p
RR= 1/(1+4 * m2 * (1-k * k)/(1-m2)/(1-m2)):GOTO 200
100 :REM In the following case mu is complex
costheta = (COS(fia+fib)-r * r * COS(fia-fib))/(1-r * r)
theta = ATN(SQR(1-costheta * costheta)/costheta)
RR= 1/(1+(k * k-1)/SIN(p * theta)/SIN(p * theta))
200 :PSET(1000 * (L-.39),310-300 * RR):PRINT# 1,RR
300 :NEXT L:CLOSE 1
400 :FOR L = .4 TO .85 STEP .05
CALL MOVETO(1000 * (L-.39),310):CALL LINETO(1000 * (L-.39),320)
IF 10 * L<>INT(10 * L) THEN 500
CALL MOVETO(1000 * (L-.41),330): PRINT 1000 * L;"nm"
500 :NEXT L
END
```

Figure 10.6 shows examples of the output of this computer program. Within a certain wavelength range, about 100 nm, the reflectance reaches nearly 100 % for only 20 high index layers, i.e., 40 interfaces, while it is lower outside this region and oscillates with wavelength; the number of these oscillations increases with an increasing number of layers. In reality this results in shiny reflectance only within a certain wavelength range, which gives a colored appearance to the surface, as can be seen in, for instance, green and blue beetles.

Although Huxley's method of calculating the reflectance has the advantage of giving physical insight into such spectral features as the reflection band width and the oscillatory structures, it has an essential difficulty in freely changing such parameters as thicknesses and refractive indices of the layers. For this purpose, a transfer matrix (Born and Wolf 1959; Kinoshita 2013) and iterative methods (Kinoshita 2008) are often employed, which are applicable to multilayer stacks of any kind, even when the repetitive structure is absent and the refractive indices of the incidence and output media are different.

The hue of the metallic shine due to a multilayer stack also shows a typical iridescent nature: the color changes with incidence and/or viewing angles (Fig. 10.7; see also Fig. 10.4). Common examples where this effect can be seen in Europe are the heads of male mallards, which change between green and blue depending on from where they are seen. However, the angle-dependent color changes do not result only from the multilayer construction; there are also many examples where gratings (Chap. 3) produce the colorful effects (Pfaff and Reynders 1999; Srinivasarao 1999). Some of these latter include plants: for example, Glover and Whitney (2010) report that in several species of plants, epidermal cells are elongated and flat, with ridged cuticle that acts as a diffraction grating. In these cases, the iridescence often seems to be in the UV. In the rock dove, the color of the neck feather changes between green and purple, which is due to a single thin-layer mechanism at the outer cortex of the barbule (Yoshioka et al. 2007).

The structural color of the jewel beetle, *Chrysochroa fulguidissima*, is an excellent example of spectral tuning due to a multilayer stack. As shown in Fig. 10.8a, its elytra show shiny metallic green with copper-brown stripes on them. The peaks of the reflection spectra for green and copper-brown regions of the elytra were reported to be 550 nm and 750–950 nm, respectively (Hariyama et al. 2005). The electron microscopic observation showed that the epicuticle located just below the elytron surface was covered with several alternate layers of electron-dense and electron-lucent regions as shown in Fig. 10.8b. The reflection spectrum calculated using the wavelength-dependent refractive indices determined recently was actually in good agreement with that of the experiment (Yoshioka and Kinoshita 2011).

A tropical fish, the neon tetra, gives another interesting example. The *iridophores*, pigment cells containing multilayer stacks of guanine crystal plates, located under a blue stripe of a neon tetra have been extensively investigated since the 1970s (Lythgoe and Shand 1982; Nagaishi and Oshima 1992). It has been shown that a pair of stacks is present within each iridophore and in each stack are included many hexagonally shaped guanine platelets (see Fig. 10.9), which are enclosed by membranes and arranged regularly with a

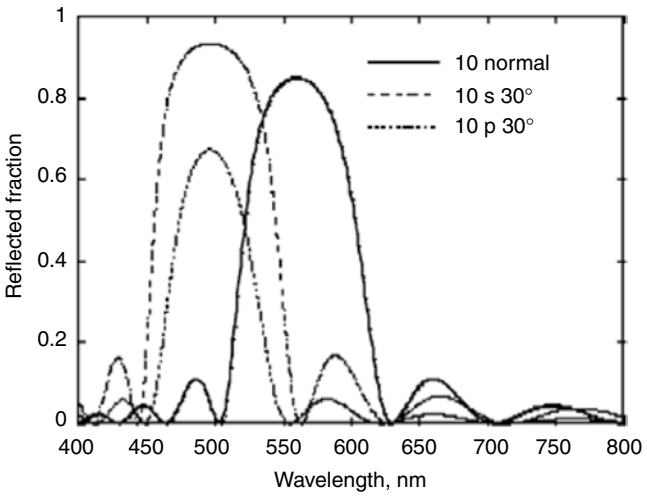

Fig. 10.7 Reflectance of a stack of 10 plates similar to those in Fig. 10.5 and with the same medium in between. Reflectance was computed for normal incidence and for an incidence angle of 30° and both polarizations

constant inclination angle to the surface. The inclination of the platelets may be effective to reflect light in a horizontal direction when illuminated from a dorsal direction. Thus, the color of the stripe is a typical case of multilayer interference.

The noteworthy point in this system is that its color changes from violet (under dark conditions) to yellow (under bright illumination) with the ambient light and also with the physiological conditions. Two major mechanisms have been proposed for this change: one is a change in the spacing between the platelets (Lythgoe and Shand 1982) and the other is a change in their inclination angle (Nagaishi and Oshima 1992) (see Fig. 10.9c). Recent experimentation has proved that the latter mechanism, called the "Venetian blind model," is more suitable to explain the experimental results (Yoshioka et al. 2011).

There exist other cases of "tunable" reflectors in the natural world. Hinton and Jarman (1972, 1973) describe beetles that can change color quickly by shifting between air and liquid in the cuticle; something similar is reported in the Panamanian tortoise beetle (Vigneron et al. 2007). Here there are within the elytra and elsewhere "chirped" layers of cuticle (see below) that have within them porous patches that can reversibly hold fluid. When the system is hydrated, it reflects a multilayer-based gold color, but when dehydrated, it becomes translucent and reveals an underlying red (non-structural) color. In other words, the system is reversibly deploying an iridescent screen.

A different mechanism, and one that is an exception to the rule of "nonliving materials" providing biological iridescent colors, is reported in the color-bearing iridocyte cells of certain squids (DeMartini et al. 2013). These cells have at their

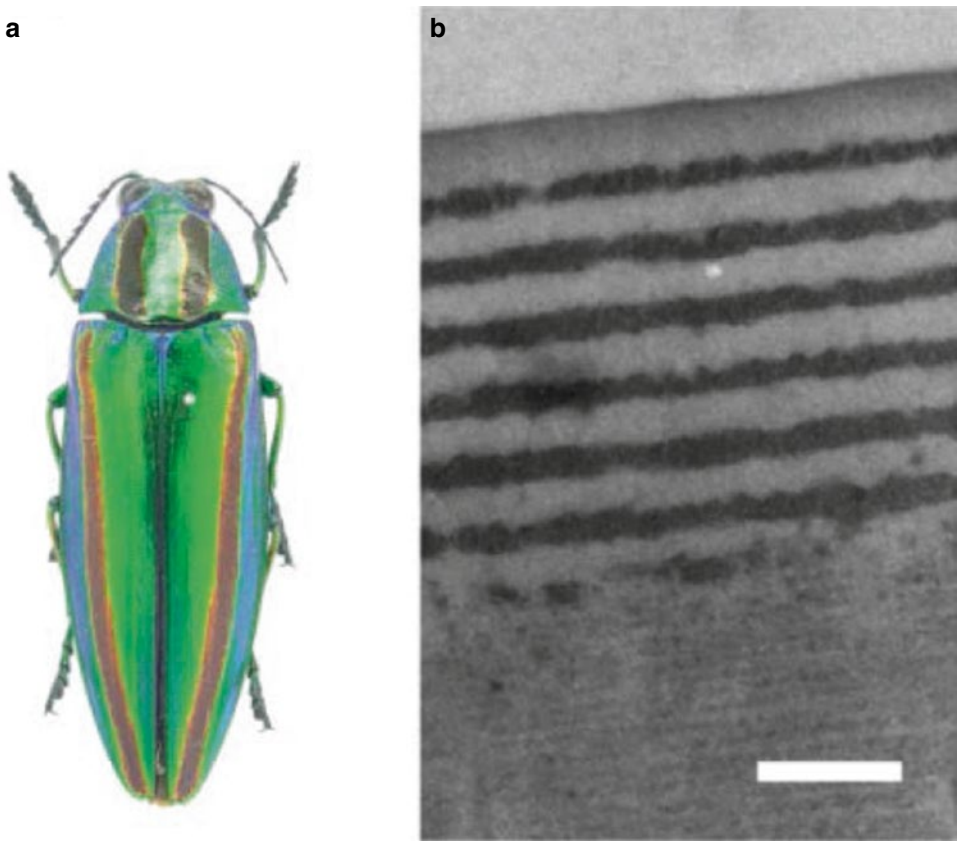

Fig. 10.8 (**a**) Jewel beetle, *Chrysochroa fulgidissima*, and (**b**) an electron micrograph of the multilayer system located beneath the elytron surface [the copper-brown striped part in (**a**)]. Scale bar: 500 nm (Reproduced from Yoshioka and Kinoshita 2011)

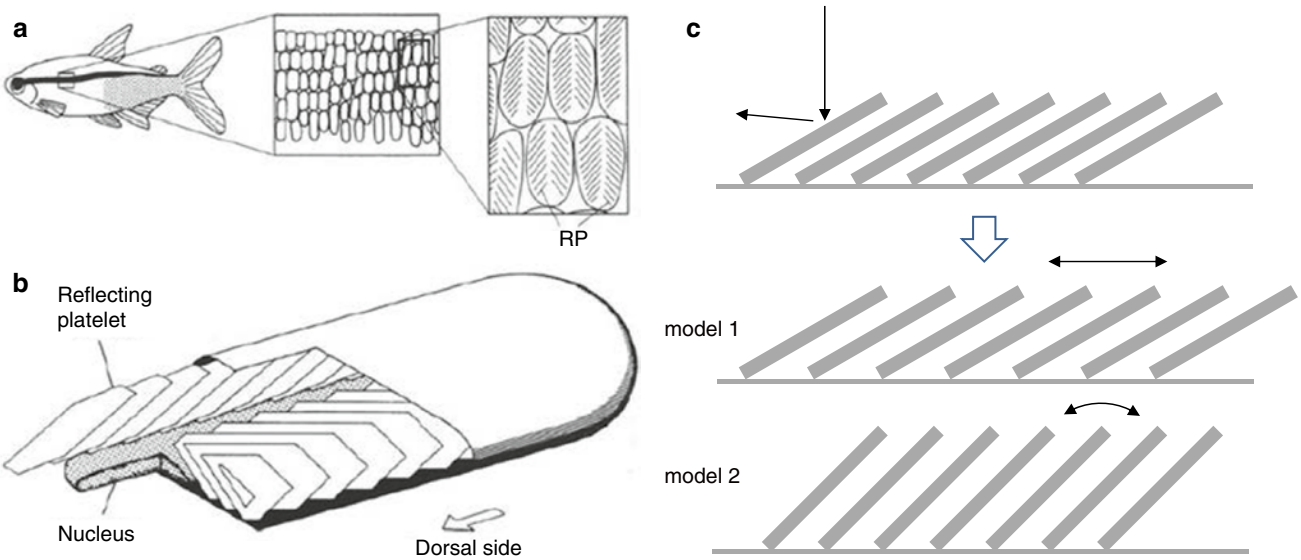

Fig. 10.9 Schematic illustrations of (**a**) a neon tetra and (**b**) its iridophore, which contains mainly two stacks of the thin light-reflecting platelets (RPs) (Reproduced from Nagaishi and Oshima (1992), with permission). (**c**) Two models for the color change due to the reflecting platelets are explained: model 1 represents the change of the spacing between platelets and model 2 that of the inclination angles

surfaces deep grooves that contain extracellular channels separating fingerlike cellular lamellae. By a reversible chemical cascade involving phosphorylation and condensing of reflecting proteins, the system can change lamella size and hence color from transparent through a spectrum from red to blue, or back again.

In those cases where high reflectance takes place over a wider wavelength range, such as often from the tapeta of eyes, this can be achieved in a number of ways. One mirror with high reflectance in one wavelength band (i.e., with one spacing and thickness of high index plates) can be positioned behind another with a different spectral tuning. Or the dimensions of the layers can be continuously varied from wide to narrow ("chirped layers") or have "chaotically" varying dimensions. An example of an animal in which layer thickness is varied in a way referred to as "doubly chirped" (thickest layers in the center) is the silverfish (Large et al. 2001). In the herring, neutral, silvery reflectance is obtained by a combination of different body surface scales reflecting red, green, and blue wavebands (Denton and Land 1971).

Chemical compounds employed for the layers of high and low refractive indices have a wide variety, depending on the organisms involved. For example, the combination of guanine and aqueous solution is generally used in animal eyes and also in skins of fish, lizards, and frogs; similarly, melanin and cuticle are used in beetle wings, cuticle and air in butterfly wings, and cellulose and aqueous solution in plants.

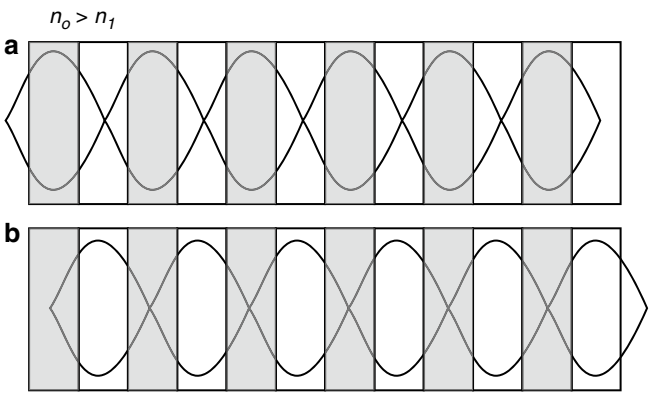

Fig. 10.10 Schematic illustration to explain the origin of the band gap. The light waves propagating to the right and left directions interfere with each other to form a standing wave. Consider a case where the wavelength of the light is twice the periodicity of the structure. (**a**) If the antinode of the standing wave is coincident with the high refractive index layer (n_0), the electromagnetic energy will be the highest, while (**b**) if it is coincident with the low refractive index layer (n_1), the energy will be the lowest; these together give the highest and lowest energy limits of the photonic band gap

10.4 Reflection Based on Photonic Crystals

We have been reviewing so far structural colors as more or less traditionally described, single thin-film or multilayer stacks, but in the 1980s, there appeared in the literature a new phrase, "photonic crystal," to describe many of the materials displaying structural color effects. As this concept was developed, these photonic crystal materials were classified as one, two, or three dimensional (1D, 2D or 3D); the multilayer thin-film stacks qualify as 1D photonic crystals, and despite the complexity of our optical treatment above, these are considered the optically simplest ones.

2D and 3D photonic crystals selectively reflect light within certain wavelength ranges ("photonic band gap") while transmitting others. Where one to punch a regular array of minute holes in a film, one would have a 2D photonic crystal. Biological examples of such iridescent 2D photonic crystals are found in marine polychaetes (Parker et al. 2001), barbules of bird feathers (Prum 2006), hairs of the comb rows of certain ctenophores (Welch et al. 2005), and butterfly scales (Vukusic and Hooper 2005). The ctenophores are especially interesting in that the comb bases rest above the light organs of the animals, and the hairs are apparently simultaneously producing reflected color from incident light and transmitting the bioluminescence from the light organs out into the environment.

3D photonic crystals abound in nature. The mineral opal consists of silica spheres that pack into a 3D face-centered cubic (fcc) lattice; their band gap structure produces their iridescent colors. Analogous structures show up in insect scales, notably in those of certain butterflies (Morris 1975; Ghiradella 1984a, 1985, 1989, 1998) and beetles (Ghiradella 1984b, 1998; Parker et al. 2003).

The origin of the photonic band gap is qualitatively explained, most simply by using a 1D photonic crystal as follows: when a light wave propagates within an alternately layered structure with different refractive indices, the light wave will be partially reflected and partially transmitted at the interfaces between these layers. The light waves thus generated will propagate to the right and left directions in Fig. 10.10 and will interfere with each other to form a standing wave. We consider a case where the wavelength of a light wave within the layers is equal to twice the period of the layers. If the antinode of the standing wave thus created coincides with a high refractive index part, the energy of electromagnetic wave will be the highest, while in the opposite case, it will be the lowest. Thus, for a single wavelength, at least two defining energy values, corresponding to the edge energies of the photonic band gap, will be realized.

When the thickness of one layer becomes narrower than that of the other, the overlap of the standing wave with the layered structure will be incomplete, so that the energy separation and hence the band gap width will be smaller. It is also expected that if the difference of the refractive indices becomes small, the band gap width will be smaller as well. Thus, a sufficient band gap for a visible effect is produced only when the refractive index contrast is large enough and the optical thicknesses of these two layer types are comparable.

The above idea can be used to qualitatively predict the presence of the photonic band gap in 2D and 3D photonic crystals. Consider a case where filled circles are located at

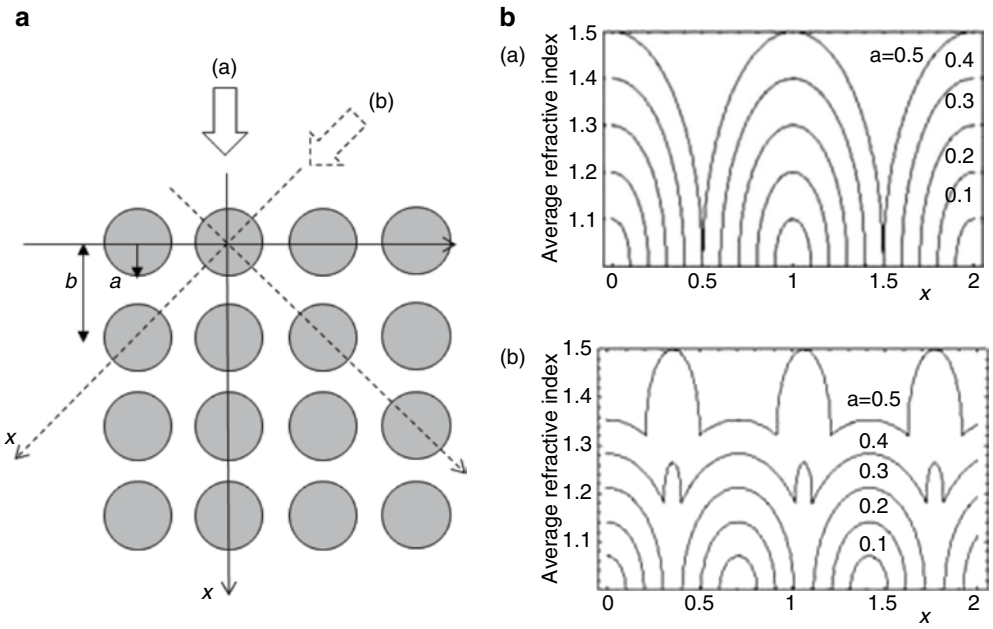

Fig. 10.11 Schematic illustration of a 2D photonic crystal in a square lattice. The average refractive indices are calculated when light is incident (**a**) normal and (**b**) obliquely to the lattice for $a = 0.1 \sim 0.5$, while a lattice constant b is kept constant at unity. The refractive index of the filled circle is set at 1.5, while that of the surrounding medium at 1.0

square lattice points as shown in Fig. 10.11a. When light is incident on the surface of this 2D photonic crystal from direction (a) or (b), the light wave experiences spatial variation of the refractive index during its propagation. The spatial average of the refractive index along the direction perpendicular to the propagation direction is easily calculated as shown in Figs. 10.11b (a) and (b), where the light is assumed to be incident (a) normally and (b) obliquely into the crystal lattice (here, we do not take the refraction at the surface of the photonic crystal into account). It is clear that the refractive index variation is distinct in case (a), particularly when $a = 0.3 \sim 0.5$, where a is the radius of the circle with the lattice constant b set at unity. In contrast, the variation is small in every radius for case (b). Thus, when the radius of the circle is sufficiently large, the refractive index contrast is strongly dependent on the direction of the light propagation. In fact, the band calculation for the refractive index of filled circles of $n = 1.5$, with n of the medium set at 1.0, shows that the photonic band gaps are open only in case (a) and not in case (b).

The band gap characteristics of 2D and 3D photonic crystals are of current interest to the communications industry, which seeks to develop hollow-core versions for more effective optical transmission fibers (another example of *biomimicry*). In such designs, the crystal cladding controls light leakage, while the air-filled core ($n = 1$) will transmit light faster than is now possible with glass fibers. Iridescent hollow-core photonic fibers are known from such biological systems as butterflies (Ghiradella 1994, 1998) and the sea mouse, *Aphrodite*, (Parker et al. (2001), among others.

We will first consider the barbules of the peacock, one of the most well-known avian species displaying structural colors. The colors of peacock feathers have attracted a great deal of scientific attention for more than 300 years and are now known as typical examples of biological photonic crystals. Since the early observations by Hooke (1665) and Newton (1704), it was in the twentieth century that more detailed observation was carried out by Mason (1923b) and then by Durrer (1962).

As shown in Fig. 10.12a, a feather barbule of peacock is somewhat curved along its long axis and slightly twisted from the root. Each barbule has the shape of connected segments of a typical size of 20–30 μm, the surfaces of which are smoothly curved like a saddle (Fig. 10.12b). The sophisticated color-producing structure in the peacock's feather (Fig. 10.12c) was first observed by Durrer (1962) using an electron microscope. It was found that below a cortex surface layer, a total of 3–11 layers of melanin rods (0.11–0.13 μm in diameter and ~0.7 μm in length) were arranged to form a 2D quasi-square lattice (Fig. 10.12c, d) (Zi et al. 2003). At the center of each lattice, a small air hole was present with increasing size towards the lower layers as shown in Fig. 10.12e. The medullary region of the barbule was filled with keratin with a small number of randomly distributed melanin rods and air holes. Durrer found that the rod-to-rod distance perpendicular to the surface correlated with the apparent color of a feather, while that parallel to the surface did not show such a correlation.

Natural photonic crystals are found in a more complete form in butterfly wings. We will explain a small lycaenid butterfly, *Callophrys rubi*, as an example. This butterfly is distributed widely in Eurasia and in North Africa and first

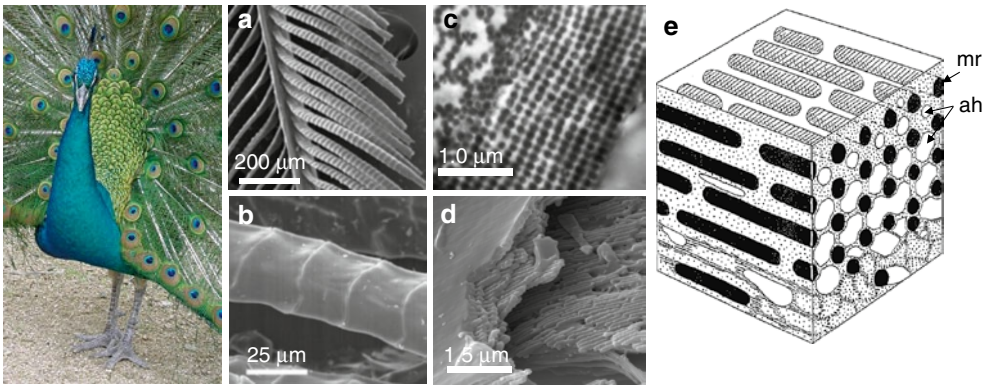

Fig. 10.12 Peacock, showing iridescent feathers. (**a**) part of feather barb, showing barbules, (**b**) segments of barbule, (**c**) cross section, and (**d**) fractured view of single barbule (Yoshioka and Kinoshita (2002); Kinoshita et al. 2008). (**e**) Schematic illustration of the internal architecture of the barbule with melanin rods (mr) and air holes (ah) (Reproduced from Durrer (1977), with permission)

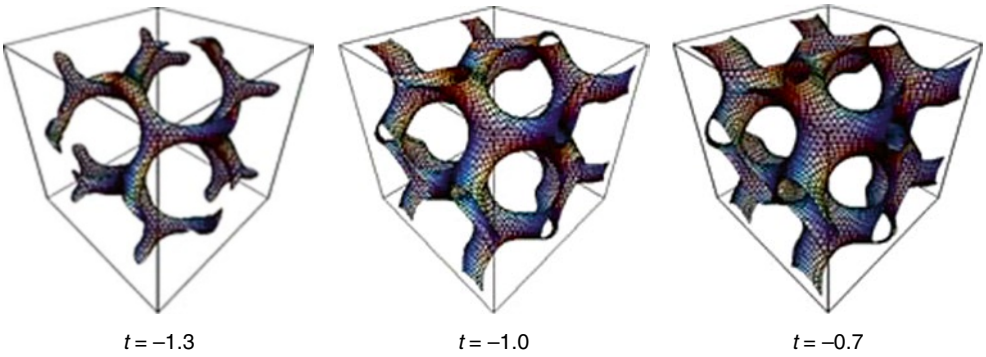

Fig. 10.13 Examples of gyroid structure for $t = -1.3$, -1.0, and -0.7

received attention by Onslow (1920, 1923). He noticed that a reflective scale of this butterfly showed irregular polygonal dark patches when observed under transillumination, hence the descriptor "mosaic scale" by Schmidt (1943). Afterward, the microstructure of this mosaic scale was investigated electron microscopically by Morris (1975). He observed that each polygonal grain, seen as a mosaic patch, was 5.4 μm in mean diameter and consisted of a simple cubic network with a lattice constant of 0.257 μm.

Ghiradella and Radigan (1976) also made an electron microscopic observation of the scale and observed a 3D photonic crystal that they interpreted as being cubic close packed, although it may in fact be a related form (see below). In any case, the elaborated structures in the interior of the *C. rubi* scales are now well known as typical examples of 3D biological photonic crystals, and the mosaic patches first observed within each scale about 100 years ago correspond to crystal domain structures having different lattice orientations.

Recently, it has been reported that these photonic structures can be expressed by a simple gyroid minimal surface, which is observed for block copolymer systems as a thermodynamically stable structure (Michielsen and Stavenga 2008; Saranathan et al. 2010). A gyroid is an infinitely connected 3D curved surface represented approximately by a mathematical expression

$$g(x, y, z) = t,$$

with

$$g(x, y, z) = \sin x \cos y + \sin y \cos z + \cos x \sin z,$$

which divides a 3D space into two according to a condition of $g(x, y, z) > t$ or $g(x, y, z) < t$ with t as a parameter. We show the examples of curved surface calculated for various t's in Fig. 10.13. If a space defined by $g(x, y, z) < t$ corresponds to a cuticle network, and that defined by $g(x, y, z) > t$ to a remaining air space, the photonic crystal structures found in the scales of various kinds of butterflies can be expressed fairly well by this formula. t in this case corresponds to a filling factor of cuticle network and it was reported that for *C. rubi*, t ranged $-1.4 < t < -1.0$, corresponding to the filling factor 0.16–0.26 (Michielsen and Stavenga 2008).

This proposal was experimentally confirmed by the comparison of calculated cross sections with TEM or SEM images (Michielsen and Stavenga 2008), by that of the reflection spectrum with the band calculation (Michielsen and Stavenga 2008; Poladian et al. 2009), by the finite-difference time-domain (FDTD) calculation (Michielsen et al. 2010), and also by the diffraction patterns obtained in small-angle X-ray scattering studies (Saranathan et al. 2010). Although these comparisons are not complete at the present

stage, they are expected to become clues to solving the problem of how these elaborate structures are formed during the pupal period of the butterflies.

10.5 Coloration Due to Random Structures

10.5.1 Rayleigh Scattering

The scattering of light does not in principle require regular structures to produce structural colors, and so it can be a most important source for colors with mechanisms completely different from those of thin-layer or photonic-crystal types. Light scattering is considered a light emission phenomenon due to an induced oscillating dipole under light illumination which emits light uniformly in different directions, so that it is basically non-iridescent; the color does not change with viewing angle. Thus, scattering has been thought of as a cause of bluish colors without directionality, which effect is generally found in a wide variety of random media. For example, the origin of the blue sky is explained as due to light scattering by atmospheric microparticles (Rayleigh 1871a, b), later called Rayleigh scattering. The pale bluish color of a suspension involving small colloidal particles is known as Tyndall blue. The blue or bluish color in these cases is based on the fact that scattering efficiency is proportional to the fourth power of light frequency and hence to an inverse of the fourth power of wavelength (inverse-fourth-power law).

Rayleigh scattering (see Chap. 1) is only applicable to a case where the particle size is sufficiently small as compared with the wavelength of light. When the particle size becomes larger, the deviation from the inverse-fourth-power law becomes remarkable and the light scattering in the visible region becomes enhanced. This is called Mie scattering, named after the research done by Mie (1908) on light scattering by metallic colloidal particles. With increasing particle size, the scattering direction largely changes from that of uniform Rayleigh scattering to that characterized by strong forward scattering (see Born and Wolf 1959).

In the past, Tyndall blue frequently appeared in the literatures as a typical example of a non-iridescent structural color. Mason (1923a, 1926) considered the colors of some birds and insects as due to Tyndall blue and used as examples the feather of a blue jay and the body/wing of a dragonfly. He proposed six necessary conditions for a medium to show the Tyndall blue: (1) inhomogeneities in the refractive index, (2) dimensions comparable to the wavelength of light, (3) blue scattering and red transmission, (4) size-dependent saturation of the blue color, (5) polarized scattering, and (6) inverse proportionality to the fourth power of wavelength.

Frank and Ruska (1939) applied the first commercially available electron microscope to investigate the feathers of the ivory-breasted pitta and the turquoise tanager, which were known to display Tyndall blue. Within barbs of the blue feathers, they found spongy structures consisting of keratin and air at the inner region of the medullary cell. Later, more detailed observation on the spongy structure was made by Schmidt and Ruska (1962) on several avian species. They reported that the spongy structure sometimes appeared to consist of numerous spherical or oval vacuoles, now called the *spherical type*, while at other times, they showed a network structure consisting of hard sticks and air holes, now called the *channel type* (Noh et al. 2010).

These spongy structures are now known to be widely distributed in avian species: kingfisher, parakeet, cotinga, jay, manakin, and bluebird are the well-known examples of this type. Until recently, however, it was generally believed that the Tyndall blue is the only cause for the blue colorations in these spongy structures. Yet, there were only a few reports to accurately measure the reflection spectrum, its angular dependence, and the polarization characteristics, which were the necessary conditions for Tyndall blue as proposed by Mason.

10.5.2 Coherent Scattering

However, it was gradually recognized that the light scattering was somehow modified and contributed effectively to animal colors. The first implication of the presence of interference phenomena on this problem was made by Raman (1934), who threw doubt on Tyndall scattering in the feather of an Indian roller. He found that the barb contained a series of cells whose colors varied from cell to cell. Further, he noticed that when the barb was fully damp, the dark blue changed into bright green and the light blue into light red. He compared these results with light scattering known for particles of various sizes and concluded light scattering does not suffice as explationation.

Dyck (1971) performed anatomical and optical investigations of the feathers of the rosy-faced love bird and plum-throated cotinga (*Cotinga maynana*). He found that the inner part of a barb was completely filled with a spongy structure, which consisted of a 3D network of connecting ca. 0.1-μm-wide keratin rods, which supported empty spaces ~0.1 μm in diameter. He investigated the spongy structures in various avian species and found that the widths of the rods and air spaces were strikingly uniform in size, while their orientations were definitely random. Furthermore, he found that the reflection spectrum showed a clear peak, which could not be explained in terms of the Rayleigh/Tyndall scattering (Fig. 10.14).

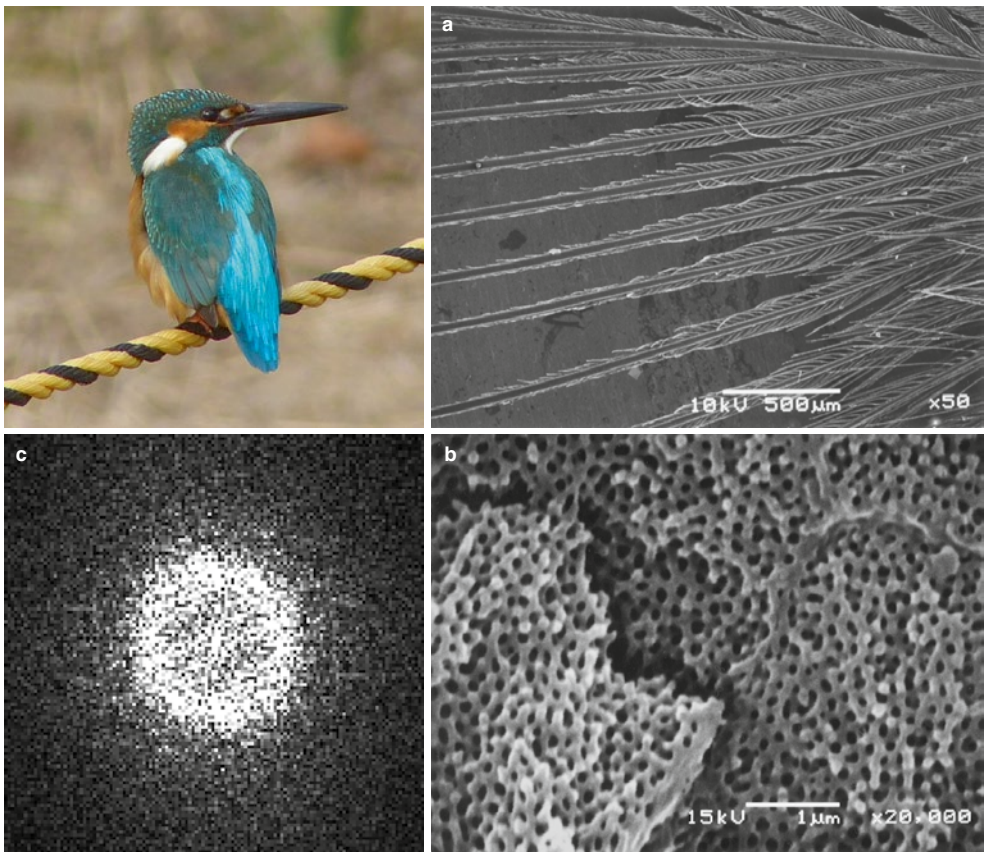

Fig. 10.14 (**a**) A common kingfisher, *Alcedo atthis*: (**a**) Barbs, (**b**) cross-section view of a fractured barb, (**c**) 2D Fourier image of the TEM image of its spongy structure (Reproduced from Kinoshita and Yoshioka 2005b)

Prum et al. (1998) played a decisive role in the solution of this problem. They employed a spatial Fourier transformation of a TEM image of the medullary spongy structure in the blue feather barbs of *C. maynana* and found a clear ring structure around the origin in wave vector space (see Fig. 10.14c for an example). If spongy structures with a wide variety of sizes are distributed, a Gaussian-like distribution would be obtained around the origin. The presence of a ring structure clearly indicates that a characteristic size of the network actually exists, which presumably corresponds to the reflection maximum.

Prum et al. (1998) simulated the reflection spectrum using the 2D Fourier power spectrum by averaging it radially and converting the radius of the ring into the peak position of the reflection spectrum, using the average refractive index. The result was in fairly good agreement with the experiment. They applied this method to the feathers of various other avian species (Prum et al. 1999a; Prum 2006) and to avian and mammalian skins (Prum et al. 1999b; Prum and Torres 2003, 2004), which appeared as quasi-ordered arrays of parallel collagen fibers, and found a similar spatial order.

Thus, it is now clear that the spongy structures generally possess a characteristic size which actually contributes to the generation of a well-defined reflection peak through constructive interference; Prum et al. (1998) called the light scattering of this type *coherent light scattering*. It also becomes clear that these structures are widely distributed in the animal kingdom, particularly in birds and insects. Their structural units appear sometimes in a form of a network and sometimes as randomly distributed spheres. These findings are quite important because the structure actually possesses short-range order, which induces the interference of light by enforcing reflection in a particular wavelength range.

Recently, Dufresne et al. (2009) employed small-angle X-ray scattering (SAXS) to analyze the spongy structures in various feather barbs and found similar ring structures both for channel and spherical types, as shown in Fig. 10.15. They found that the ring structure generally consisted of a definite ring, which was followed by a tail or a weak second ring outside the main ring (see Fig. 10.15c, d). Since the scattering efficiency of X-rays is very low, the structural information is directly obtainable without being disturbed by multiple scattering, which will thus be comparable with the Fourier analysis performed by Prum et al. (1998).

Further, Noh et al. (2010) measured the reflection spectra under various optical configurations and found that under directional lighting, the feather barbs were surprisingly iridescent, while under omni-directional illumination, they were actually non-iridescent: the reflection spectrum was evidently independent of the angle of incidence, if the refraction at the

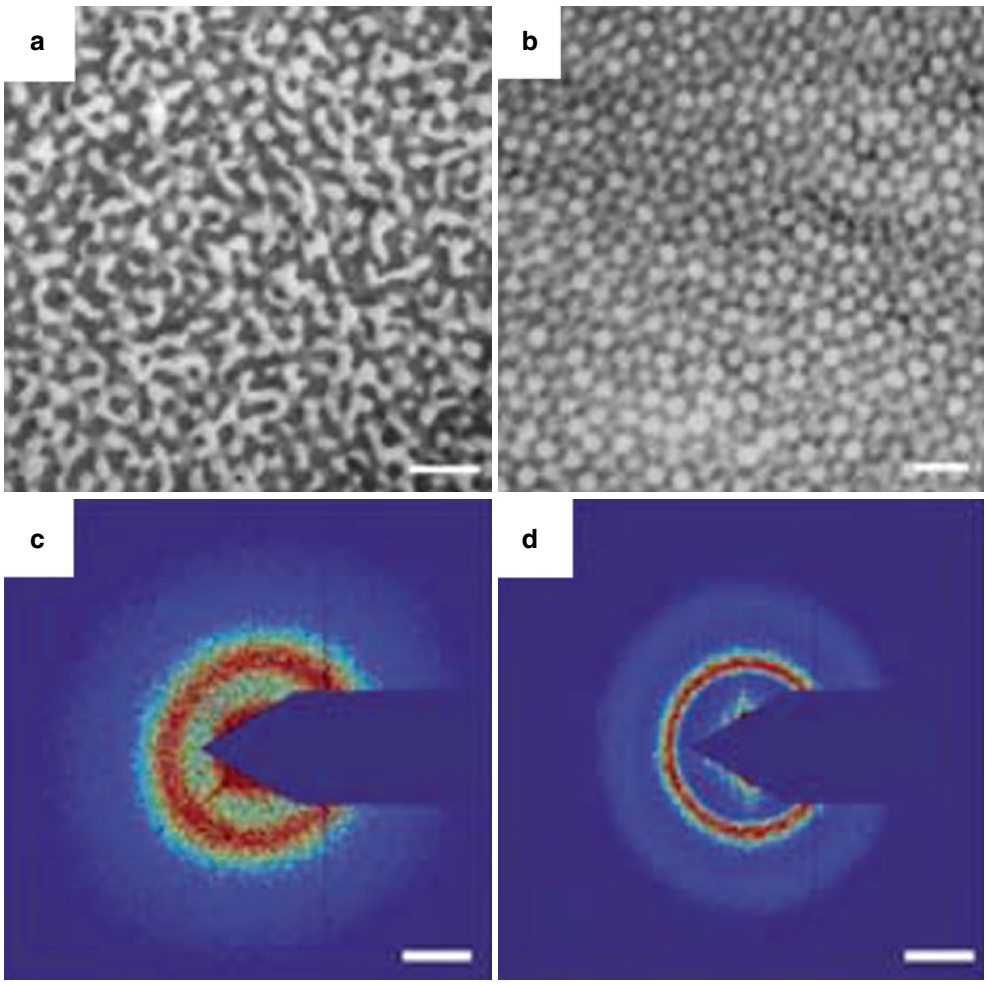

Fig. 10.15 Electron micrographs of feather barbs of (**a**) channel-type male eastern bluebird (*Sialia sialis*) and (**b**) sphere-type male plum-throated cotinga (*Cotinga maynana*), and the corresponding small-angle X-ray scattering patterns, (**c**) and (**d**). Scale bars are 500 nm for (**a**) and (**b**), and 0.025 cm^{-1} for (**c**) and (**d**) (Reproduced from Dufresne et al. (2009), with permission)

surface was properly corrected, and was dependent only on an angle between the directions of incidence and reflection. The authors attempted to reproduce the reflection spectrum from the SAXS pattern and obtained good agreement with respect to the main ring when the average refractive index was set at 1.25.

From the standpoint of spectral tuning, the spongy structure gives rather weak tuning capability, because its coloring mechanism is essentially based on random structure that is slightly modified by the presence of short-range order. However, it offers a special effect as compared to the ordinary interference-type structural color: the important point is that it is basically non-iridescent, so it does not show directionality, which eventually prevents the lustrous appearance. On the other hand, this rather passive mechanism results in the degradation of the reflection efficiency, which is, however, compensated for by placing dark pigments below the spongy structure. Thus, the interplay of pigmentary and structural colors is essential in this system, as it is in others, for example, the deep blue thin-film reflective scales of many of the *Morpho* butterflies (see below).

10.6 Diversity of Structural Colors

10.6.1 Morpho Butterflies

Very complicated structures, in which both multilayer interference and grating effects contribute to colors, have been often observed in nature, especially in the scales of butterfly wings (Ghiradella 1994, 1998). The most remarkable example is the *Morpho* butterfly inhabiting the New World from Central to South America. The wings of this butterfly display striking, even metallic, blue and have been attracting scientists' interest from the nineteenth century. Their surprisingly elaborate microstructures became clear just after the invention of electron microscope (Anderson and Richards 1942, Gentil 1942). The most remarkable features in the optical response of their wings are that while they strongly reflect the blue light, the reflection direction spreads widely but only within a plane nearly perpendicular to the ridge direction on the scale (the ridges are longitudinal folds projecting from the obverse surface of most butterfly scales) (Vukusic

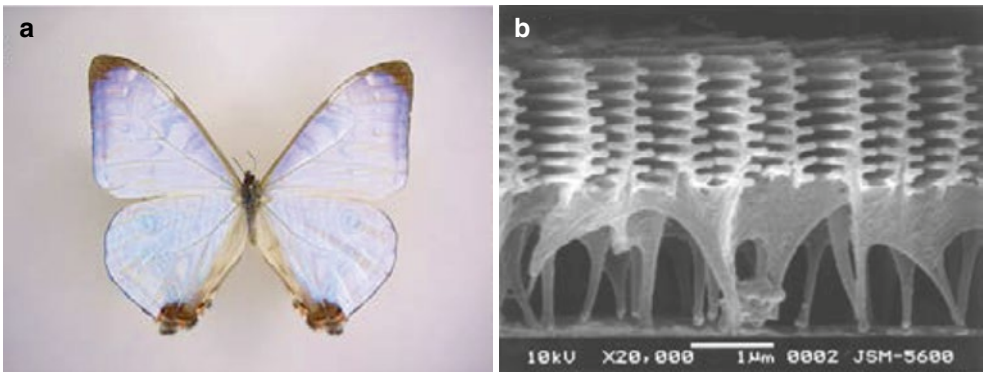

Fig. 10.16 (**a**) *Morpho sulkowskyi* and (**b**) scanning electron microscopic image of a cross section of a reflective scale

et al. 1999, Kinoshita et al. 2002a, b). Various models have been proposed so far and numerical calculations of diverse kinds have been performed to elucidate the mechanism of this blue reflection (Gralak et al. 2001; Kinoshita et al. 2002b; Plattner 2004; Zhu et al. 2009; Lee and Smith 2009).

It is now generally understood that the strongly blue and widely spreading reflections are caused by a unique scale ridge structure. As shown in Fig. 10.16b, the ridges are densely distributed at intervals of ~1 μm on a scale; they extend longitudinally for almost the full length of the scale. Each ridge has stacks of thin shelves, or *lamellae*, which project alternately from each side as shown in Fig. 10.16b; these and the air spaces between them form the mirror. This unique structure causes the miraculous balance of a multilayer interference and diffraction effect that is restricted to a plane perpendicular to the ridge direction (Kinoshita et al. 2002a, Kinoshita 2013). Further, the alternately configured lamellae can be regarded as obliquely inclining lamellae and enhance the backscattering when illuminated from oblique directions. This will make the blue wing more vivid without being disturbed by the specular reflection (Kambe et al. 2011). The color of the wing is largely affected by underlying melanin layers, which absorb the light other than blue, thereby ensuring the deep blue color. Lacking such underlying pigment, the scales are translucent and "pearlescent," with only a pale blue color (see Fig. 10.16a). Thus, plenty of architectural designs in addition to cooperation with pigment bestow such a beautiful color on this butterfly and on other reflective creatures.

10.6.2 Liquid Crystals

There exists in nature yet another class of structural color mechanism. Chemists have long known that certain liquid crystal molecules orient themselves in certain very specific fashions. One such is the so-called "helicoidal," "cholesteric," or "chiral" arrangement: the molecules are arrayed such that their orientation *precesses*, being in each layer slightly rotated with respect to those in the layer below. The thickness of the layers and the direction ("chirality") of the rotation can be tunable, and if tuned properly, they will produce structural colors that are analogous to multilayer stack colors.

Many thermometers using this type of liquid crystal are on the market; these work by reversibly changing their colors when the temperature is increased or decreased (thereby changing the thickness of the "layers" and hence the optical properties). A similar phenomenon occurs in biological systems; if collagen, chitin, or other biological fibrils are arranged in a regular helicoid fashion, the system can be tuned to produce color; this is the basis for the iridescent cuticles of many beetles, flies, and other insects (for reviews, see Neville 1993 and Srinivasarao 1999; see Lee 2007 for a discussion of this mechanism in plant coloration). The light reflected from these helicoid arrays is circularly polarized; the chirality of biological systems has seemed uniformly to reflect left-circularly polarized light, but at least one beetle has found a way to simultaneously reflect both left and right circularly polarized lights (Caveney 1971).

10.6.3 Interplay with Pigments

Let us bring the pigments back into play by noting that many organisms combine structural and pigmentary colors to get additional special effects. In birds, green plumage is often achieved by combining a structural blue color with a pigment yellow. As described above, in many, but not all, blue *Morpho* butterflies, a pigmentary "backing" intensifies the structural blue color by absorbing unwanted light entering the reflecting structures, because the wavelengths of such light are located in a range other than blue, are also likely to be out of phase with the "functional" light, and would dilute the purity of the interference color. In a species of *Morpho* butterflies, white spots on the wing are produced simply by removing the backing pigments in these areas, while the elaborate

microstructures are left untouched (Yoshioka and Kinoshita 2006). Since, after passing the reflecting structure, light of wavelengths other than blue is scattered by the underlying wing membrane and scales on the reverse side, it comes back to the obverse side without directionality and is perceived by the viewers as white spots on the wing.

10.6.4 Whiteness and Transparency

The biological world has a few additional ways of handling light. Scattering produces brilliant whites (Vukusic et al. 2007) and may yield more complex effects, especially if the combined optical behavior of all scales in a wing transect is taken into account (Stavenga et al. 2006b) or if structures and pigments interact to produce "emergent" optical effects (Rutkowski et al. 2005; Morehouse et al. 2007). And of course there is transparency, a highly effective technique for evading predators. We have already mentioned antireflective coatings, in particular the nipples that allow clearwing moths to become essentially invisible against any background (Yoshida et al. 1996; Yoshida 2002). But invisibility is best understood in the open seas (see Herring 2002, Wilson and Hastings 2013 for review), where there is no place to hide. Coelenterates and ctenophores may build bodies largely of transparent jelly, but arthropods and vertebrates must have muscles and skeletons. To some degree, these can be rendered transparent by arranging fibrous proteins so that they produce destructive interference in the predominantly blue light in their environment(s). But eyes must have pigment and gut contents quickly become opaque, even if they do not start that way. This may be the reason why so many fishes have instead evolved silvery mirrored sides to render themselves invisible.

10.6.5 Relation to Fluorescence

No discussion of spectral tuning would be complete without a brief mention of fluorescence, the process by which light of a relatively short wavelength is absorbed and reemitted at a longer wavelength (see Chap. 1). This has been reported to be widespread in spiders (Andrews et al. 2007), where it may have communication and possibly metabolic and other functions as well.

A particularly intriguing case is described in a *Papilio* butterfly (Vukusic and Hooper 2005); the reflective scales have 2D photonic crystals on their obverse surfaces; these collimate the light so that it is effectively emitted upward (or reflected with a help of a mirror lining the reverse surface) for the wavelengths of light at around 505 nm. This wavelength just matches a peak of a fluorescent pigment fused in the 2D photonic crystals as also does the central range of the animal's green visual pigment. Thus, the 2D photonic crystal in this case may be placed to successfully extract fluorescent light from the wing. A similar mechanism is now often used in light-emitting diodes to extract the light efficiently from the device, another example of biomimicry.

10.6.6 Biomimicry

In closing, we would like to revisit briefly some of the ideas and systems that we have discussed and present some additional information. First is biomimicry. We have alluded to the burgeoning interest in the field, even reaching into architectural design (Aldersey-Williams 2004). There has been particular interest in duplicating the *Morpho* iridescent scale system (e.g., Aryal et al. 2012), but other systems are being studied widely. Two books written for popular audiences are Benyus (2002) and Harman (2013); the latter considers some of the general economic and business concomitants of some of the systems.

In a related vein, scientists have realized that the highly structured *Morpho* wing might provide the design for a chemical sensor: gas molecules penetrating between the lamellae will change the refractive index of the air component and hence the reflectivity of the scale (Potyrailo et al. 2007). There is little question that more of these biological structures will have much to teach us about design.

10.6.7 Developmental Studies on Microstructures

One particularly intriguing question (actually allied to that of biomimicry) is how the organisms make these structures and materials in the first place. For many of those discussed above, the question remains to be investigated, but Ghiradella (1974, 1989) studied the development of the multilayer lamellae in the butterfly *Colias eurytheme* and of the 3D photonic crystals in another butterfly *Mitoura grynea*.

In the first case, it was possible to conjecture from the internal geometry (including the placement of actin bundles of the developing scale) that longitudinal tensile stress on the scale obverse epicuticular layer (the outer "envelope" of the nascent cuticle) may result in so-called elastic buckling, a common physical process that typically gives rise to regular and even folds. This has not been confirmed, but given the generality of regular folds in nonliving biological structures, it is almost certain that a common mechanism underlies this particular geometry.

The basis of the pattern formation is clearer with regard to the 3D photonic crystals; the smooth endoplasmic reticulum organizes itself into a 3D lattice; the cell then pulls in and weaves through the lattice space tubes of cell membrane

within which the cuticle is secreted, as cuticle always is, extracellularly. A variation of same system is obtained in striated muscle, in which the sarcoplasmic reticulum (the muscle cell's smooth endoplasmatic reticulum) organizes itself in such a way that the T-tubule invaginations of the cell membrane can carry the excitation from the nerve end plate deep into the contractile machinery.

References

Aldersley-Williams H (2004) Towards biomimetic architecture. Nat Mater 3:277–279

Anderson TF, Richards AG Jr (1942) An electron microscope study of some structural colors of insects. J Appl Phys 13:748–758

Andrews K, Reed SM, Masta SE (2007) Spiders fluoresce variably across many taxa. Biol Lett 3:265–267

Aryal M, Ko DH, Tumbleston JR, Gadisa A, Samulski ET, Lopez R (2012) Large area nanofabrication of butterfly wing's three dimensional ultrastructures. J Vac Sci Technol B 30:06182-1–06182-7

Benyus JM (2002) Biomimicry: innovation inspired by nature. Harper Collins, New York

Bernhard CG, Miller WH, Møller AR (1965) The insect corneal ripple array. A biological broad-band impedance transformer acts as an antireflection coating. Acta Physiol Scand 63(suppl 243):1–79

Bernhard CG, Gemne G, Møller AR (1968) Modification of specular reflexion and light transmission by biological surface structure – to see, to be seen or not to be seen. Quart Rev Biophys 1:89–105

Bernhard CG, Gemne G, Sällström J (1970) Comparative ultrastructure of corneal surface topography in insects with aspects on phylogenesis and function. Z Vergl Physiol 67:1–25

Berthier S (2007) Iridescences: the physical colors of insects. Springer, Berlin

Born M, Wolf E (1959) Principles of optics. Pergamon Press, London

Caveney S (1971) Cuticle reflectivity and optical activity in scarab beetles: the rôle of uric acid. Proc R Soc Lond B 178:205–225

DeMartini DG, Krogstad DV, Morse D (2013) Membrane invaginations facilitate reversible water flux driving tunable iridescence in a dynamic biophotonic system. Proc Natl Acad Sci U S A 110:2552–2556

Denton EJ, Land MF (1971) Mechanism of reflection in silvery layers of fish and cephalopods. Proc Roy Soc Lond A 178:43–61

Dufresne ER, Noh H, Saranathan V, Mochrie SGJ, Cao H, Prum RO (2009) Self-assembly of amorphous biophotonic nanostructures by phase separation. Soft Matter 5:1792–1795

Durrer H (1962) Schillerfarben beim Pfau (*Pavo cristatus* L.). Verhand Naturf Ges Basel 73:204–224

Durrer H (1977) Schillerfarben der Vogelfeder als Evolutionsproblem. Denkschr Schweiz Naturforsch Ges 91:1–127

Dyck J (1971) Structure and colour-production of the blue barbs of *Agapornis roseicollis* and *Cotinga maynana*. Z Zellforsch 115:17–29

Fox DL (1976) Animal biochromes and structural colours. University California Press, Berkeley

Frank F, Ruska H (1939) Übermikroskopische Untersuchung der Blaustruktur der Vogelfeder. Nature 27:229–230

Gentil K (1942) Elektronenmikroskopische Untersuchung des Feinbauses schillernder Leisten von Morpho-Schuppen. Z Morph Ökol Tiere 38:344–355

Ghiradella H (1974) Development of ultra-reflective butterfly scales: How to make an interference filter. J Morph 142:395–410

Ghiradella H (1984a) Development of ultraviolet reflecting butterfly scales: how to make an interference filter. J Morph 142:395–410

Ghiradella H (1984b) Structure of iridescent lepidopteran scales: variations on several themes. Ann Entomol Soc Am 77:637–645

Ghiradella H (1985) Structure and development of iridescent lepidopteran scales: the Papilionidae as a showcase family. Ann Entomol Soc Am 78:252–264

Ghiradella H (1989) Structure and development of iridescent butterfly scales: lattices and laminae. J Morph 202:69–88

Ghiradella H (1991) Light and color on the wing: structural colors in butterflies and moths. Appl Opt 30:3492–3500

Ghiradella H (1994) Structure of butterfly scales: patterning in an insect cuticle. Micr Res Tech 27:429–438

Ghiradella H (1998) Hairs, bristles and scales. In: Harrison FW, Locke M (eds) Microscopic anatomy of invertebrates, vol 11A, Insecta. Wiley-Liss, New York, pp 257–287

Ghiradella H, Radigan W (1976) Development of butterfly scales II. Struts, lattices and surface tension. J Morph 150:279–298

Glover BJ, Whitney HM (2010) Structural colour and iridescence in plants: the poorly studied relations of pigment colour. Ann Bot 105:505–511

Gralak B, Tayeb G, Enoch S (2001) Morpho butterfly wings color modeled with lamellar grating theory. Opt Exp 9:567–578

Hariyama T, Hironaka M, Horiguchi H, Stavenga DG (2005) The leaf beetle, the jewel beetle, and the damselfly: insects with a multilayered show case. In: Kinoshita S, Yoshioka S (eds) Structural colors in biological systems: principles and applications. Osaka University Press, Osaka, pp 153–176

Harman J (2013) The Shark's paintbrush. White Cloud Press, Ashland

Herring (1994) Reflective systems in aquatic animals. Comp Biochem Physiol 109A:513–546

Herring P (2002) The biology of the deep ocean. Oxford University Press, Oxford

Hinton HE, Jarman GM (1972) Physiological color change in the Hercules beetle. Nature 238:160–161

Hinton HE, Jarman GM (1973) Physiological color change in the elytra of the Hercules beetle. Dynastes hercules J Insect Physiol 19:533–549

Hooke R (1665) Micrographia: or same physiological descriptions of minute bodies made by magnifying glasses with observations and inquiries thereupon. Replicated by Dover Publication, New York

Huxley AF (1968) A theoretical treatment of the reflexion of light by multilayer structures. J Exp Biol 48:227–245

Kambe M, Zhu D, Kinoshita S (2011) Origin of retroreflection from a wing of the Morpho butterfly. J Phys Soc Jpn 80:054801-1–054801-10

Kinoshita S (2008) Structural colors in the realm of nature. World Scientific Publishing, Singapore

Kinoshita S (2013) Nanobiophotonics – an introductory textbook. Pan Stanford, Singapore

Kinoshita S, Yoshioka S (eds) (2005a) Structural colors in biological systems. Osaka University Press, Osaka

Kinoshita S, Yoshioka S (2005b) Structural colors in nature. A role of regularity and irregularity in the structure. ChemPhysChem 6:1443–1459

Kinoshita S, Yoshioka S, Kawagoe K (2002a) Mechanisms of structural color in the *Morpho* butterfly: cooperation of regularity and irregularity in an iridescent scale. Proc R Soc Lond B269:1417–1422

Kinoshita S, Yoshioka S, Fujii Y, Okamoto N (2002b) Photophysics of structural color in the *Morpho* butterflies. Forma 17:103–121

Kinoshita S, Yoshioka S, Miyazaki J (2008) Physics of structural colors. Rep Prog Phys 71:076401-1–076401-30

Land MF (1966) A multilayer interference reflector in the eye of the scallop, Pecten maximus. J Exp Biol 45:433–447

Land MF (1972) The physics and biology animal reflectors. Prog Biophys Mol Biol 24:77–106

Land MF, Nilsson D-E (2008) Animal eyes, 2nd ed. Oxford University Press, Oxford

Large MCJ, McKenzie DR, Parker AR, Steel BC, Ho K, Bosi SG, Nicorovici N, McPhedran RC (2001) The mechanism of light reflectance in silverfish. Proc R Soc Lond A 457:511–518

Lee D (2007) Nature's Palette: the science of plant color. University of Chicago Press, Chicago

Lee RT, Smith GS (2009) Detailed electromagnetic simulation for the structural color of butterfly wings. Appl Opt 48:4177–4190
Lythgoe JN, Shand J (1982) Changes in spectral reflexions from the iridophores of the neon tetra. J Physiol 325:23–34
Mason CW (1923a) Structural colors in feathers. I. J Phys Chem 27: 201–251
Mason CW (1923b) Structural colors in feathers. II. J Phys Chem 27:401–447
Mason CW (1926) Structural colors in insects. I. J Phys Chem 30:383–395
Mason CW (1927a) Structural colors in insects. II. J Phys Chem 31: 321–354
Mason CW (1927b) Structural colors in insects. III. J Phys Chem 31: 1856–1872
Michielsen K, Stavenga DG (2008) Gyroid cuticular structures in butterfly wing scales: biological photonic crystals. J R Soc Interface 5:85–94
Michielsen K, De Raedt H, Stavenga DG (2010) Reflectivity of the gyroid biophotonic crystals in the ventral wing scales of the green hairstreak butterfly. Callophyris rubi J R Soc Interface 7:765–771
Mie G (1908) Beiträge zur Optik trüber Meien, speziell kolloidaler Metallösungen. Annu Rev Plant Physiol Plant Mol Biol 330: 377–445
Morehouse NI, Vukusic P, Rutkowski R (2007) Pterin pigment granules are responsible for both broadband light scattering and wavelength selective absorption in the wing scales of pierid butterflies. Proc Roy Soc Lond B 274:359–366
Morris RB (1975) Iridescence from diffraction structures in the wing scales of *Callophrys rubi*, the Green Hairstreak. Proc R Soc Entomol A 48:149–154
Nagaishi H, Oshima N (1992) Ultrastructure of the motile iridophores of the neon tetra. Zool Sci 9:65–75
Neville AC (1993) Biology of fibrous composites. Cambridge University Press, Cambridge
Newton I (1704) Opticks: or a treatise of the reflections, refractions, inflections & colours of light. Republicated by Dover Publication, New York
Noh H, Liew SF, Saranathan V, Mochrie SGJ, Prum RO, Dufresne ER, Cao H (2010) How noniridescent colors are generated by quasi-ordered structures of bird feather. Adv Mater 22:2871–2880
Onslow H (1920) The iridescent colours of insects. II. Diffraction colours. Nature 106:181–183
Onslow H (1923) On a periodic structure in many insect scales, and the cause of their iridescent colours. Phil Trans 211:1–74
Parker AR (1998) The diversity and implications of animal structural colours. J Exp Biol 201:2343–2347
Parker AR (1999) Light-reflection strategies. Am Sci 87:248–255
Parker AR (2000) 515 million years of structural color. J Opt A Pure Appl Opt 2:R15–R28
Parker AR, McPhedran RC, McKenzie DR, Botten LC, Nicorovici N-AP (2001) Aphrodite's iridescence. Nature 409:36–37
Parker AR, Welch VL, Driver D, Martini N (2003) An opal analogue discovered in a weevil. Nature 426:786–787
Pfaff G, Reynders P (1999) Angle-dependent optical effects from submicron structures of films and pigments. Chem Rev 99:1963–1981
Plattner L (2004) Optical properties of the scales of *Morpho rhetenor* butterflies: theoretical and experimental investigation of the back-scattering of light in the visible spectrum. J R Soc Interface 1:49–59
Poladian L, Wichham S, Lee K, Large MCJ (2009) Iridescence from photonic crystals and its suppression in butterfly scales. J R Soc Interface 6:S233–S242
Potyrailo RA, Ghiradella H, Vertiatchikh A, Dovidenko K, Cournoyer JR, Olson E (2007) *Morpho* butterfly wing scales demonstrate highly selective vapour response. Nat Photonics 1:123–128
Prum RO (2006) Anatomy, physics and evolution of structural colors. In: Hill GE, McGraw KJ (eds) Bird coloration, vol 1, Mechanisms and measurements. Harvard University Press, Cambridge, MA, pp 295–353
Prum RO, Torres RH (2003) Structural colouration of avian skin: convergent evolution of coherently scattering dermal collagen arrays. J Exp Biol 206:2409–2429
Prum RO, Torres RH (2004) Structural colouration of mammalian skin: convergent evolution of coherently scattering dermal collagen arrays. J Exp Biol 207:2157–2172
Prum RO, Torres RH, Williamson S, Dyck J (1998) Coherent light scattering by blue feather barbs. Nature 396:28–29
Prum RO, Torres RH, Williamson S, Dick J (1999a) Two-dimensional fourier analysis of the spongy medullary keratin of structurally coloured feather barbs. Proc R Soc Lond B266:13–22
Prum RO, Torres RH, Kovach F, Williamson S, Goodman SM (1999b) Coherent light scattering by nanostructured collagen arrays in the caruncles of the *Malagasy asities* (Eurylaimidae: Aves). J Exp Biol 202:3507–3522
Raman CV (1934) The origin of the colours in the plumage of birds. Proc Ind Acad Sci A1:567–573
Rayleigh JWS (1871a) On the light from the sky, its polarization and colour. Phil Mag 41:107–120
Rayleigh JWS (1871b) On the scattering of light by small particles. Phil Mag 41:447–454
Rutkowski RL, Macedonia JM, Morehouse N, Taylor-Taft L (2005) Pterin pigments amplify iridescent ultraviolet signal in males of the orange sulphur butterfly, Colias eurytheme. Proc R Soc Lond B 272:2329–2335
Saranathan V, Osuji CO, Mochrie SGJ, Noh H, Narayanan S, Sandy A, Dufresne ER, Prum RO (2010) Structure, function, and self-assembly of single network gyroid (14_i32) photonic crystals in butterfly wing scales. Proc Natl Acad Sci 107:11676–11681
Schmidt WJ (1943) Die Mosaikschuppen des *Teinopalpus imperialis* Hope, ein neues Muster schillernder Schmetterlingsschuppen. Z Morph Ökol Tiere 39:176–216
Schmidt WJ, Ruska H (1962) Tyndallblau – Structur von Federn im Elektronenmikroskop. Z Zellforsch 56:693–708
Srinivasarao M (1999) Nano-optics in the biological world: beetles, butterflies, birds, and moths. Chem Rev 99:1935–1961
Stavenga DG, Foletti S, Palasantzas G, Arikawa K (2006a) Light on the moth-eye corneal nipple array of butterflies. Proc R Soc Lond B 273:661–667
Stavenga DG, Giraldo MA, Hoenders BJ (2006b) Reflectance and transmittance of light scattering scales stacked on the wings of pierid butterflies. Opt Exp 14:4880–4890
Vigneron JP, Pasteels JM, Windsor DM, Vértesy S, Rassart M, Seldrum T, Dumont J, Deparis O, Lousse V, Biró L, Ertz D, Welch V (2007) Switchable reflector in the Panamanian tortoise beetle, Charidotella egregia (Chrysomelidae: Cassinidae). Phys Rev E 76:031907-1–031907-10
Vukusic P, Hooper I (2005) Directionally controlled fluorescence emission in butterflies. Science 310:1151
Vukusic P, Sambles JR (2003) Photonic structures in biology. Nature 424:852–855
Vukusic P, Sambles JR, Lawrence CR, Wootton RJ (1999) Quantified interference and diffraction in single *Morpho* butterfly scales. Proc R Soc Lond B 266:1403–1411
Vukusic P, Hallam B, Noyes J (2007) Brilliant whiteness in ultrathin beetle scales. Science 315:348
Welch VL, Vigneron JP, Parker AR (2005) The cause of colouration in the ctenophore, *Beroë cucumis*. Curr Biol 15:R985–R986
Wilson T, Hastings JW (2013) Bioluminescence: living lights, lights for living. Harvard University Press, Cambridge, MA
Yoshida A (2002) Antireflection of butterfly and moth wings through microstructure. Forma 17:75–89

Yoshida A, Motoyama M, Kosaku A, Miyamoto K (1996) Nanoprotuberance array in the transparent wing of a hawkmoth, *Cephonodes Hylas*. Zool Sci 13:525–526

Yoshioka S, Kinoshita S (2002) Effect of macroscopic structure in iridescent color of the peacock feathers. Forma 17:169–181

Yoshioka S, Kinoshita S (2006) Structural or pigmentary? Origin of the distinctive white stripe on the blue wing of a Morpho butterfly. Proc R Soc Lond B273:129–134

Yoshioka S, Kinoshita S (2011) Direct determination of the refractive index of natural multilayer systems. Phys Rev E 83:051917-1–051917-7

Yoshioka S, Nakamura E, Kinoshita S (2007) Origin of two-color iridescence in rock dove's feather. J Phys Soc Jpn 76: 013801-1–013801-4

Yoshioka S, Matsuhana B, Tanaka S, Inouye Y, Oshima N, Kinoshita S (2011) Mechanism of variable structural colour in the neon tetra: quantitative evaluation of the Venetian blind model. J R Soc Interface 8:56–66

Zhu D, Kinoshita S, Cai D, Cole JB (2009) Investigation of structural colors in Morpho butterflies using the nonstandard-finite-difference time-domain method: Effects of alternately stacked shelves and ridge density. Phys Rev E 80:051924-1–051924-12

Zi J, Yu X, Li Y, Hu X, Xu C, Wang X, Liu X, Fu R (2003) Coloration strategies in peacock feathers. Proc Natl Acad Sci 100: 12576–12578

Photoactive Proteins

11

Lars Olof Björn

11.1 Introduction

Light is important for the biological function of a large number of proteins. We can group them as follows:

1. Photoenzymes
2. Light-activated and light-deactivated enzymes
3. Light-driven ion pumps
4. Light-regulated ion channels
5. Photosynthetic antenna proteins
6. Photoreceptors
7. Photoproteins and luciferases

These categories are not completely free from overlap. Many of the photoreceptor proteins also belong to group 2. They will be treated separately in Chap. 13. Photoproteins and luciferases (light-emitting proteins) will be treated in Chap. 26.

11.2 Photoenzymes and Light-Activated Enzymes

We shall in the following use the term *photoenzyme* for those enzymes which are "driven" by light, for which light can be regarded as one of the substrates in the enzyme-catalyzed reaction. For the reaction to proceed in these cases, light must be continuously applied. Occasionally the term has also been used for enzymes which become active after irradiation, but continue to be active at least for some time after irradiation has stopped. We shall treat these enzymes separately and use for them the term *light-activated enzymes*. Some enzymes can be reversibly activated or inactivated with different kinds of light. One enzyme, LPOR, belongs to both groups, photoenzymes and light-activated enzymes, because it needs light both for activation and for driving the catalytic reaction.

11.2.1 Photoenzymes

Photoenzymes have built-in chromophores which catch the light energy which is a necessary requirement for their function. Some very important photoenzymes are not often thought of as photoenzymes. They will be treated in other chapters, and we shall only mention them briefly here to point out that they are also, strictly speaking, photoenzymes. Photoenzymes have attracted attention not only for the particular processes that they catalyze but also more generally. Because they allow starting the catalytic reaction with a short flash of light, at the same time for all enzyme molecules in a sample, they allow detailed study of how enzymes function.

11.2.1.1 Plastocyanin: Ferredoxin Oxidoreductase

Plastocyanin: ferredoxin oxidoreductase is usually referred to as photosystem I. The main energy-catching chromophore is chlorophyll *a* and in some cases chlorophyll *d*. Some cyanobacteria preferentially use cytochrome c-553 as electron donor in place of plastocyanin (Ferreira and Straus 1994), while others switch between cytochrome c-553 and plastocyanin depending on the availability of iron and copper. In bacteria the corresponding photosystems use cytochromes and have various bacterial types of chlorophyll as chromophores (Azai et al. 2010; Sarrou et al. 2012).

11.2.1.2 Water: Plastoquinone Oxidoreductase

Water: plastoquinone oxidoreductase is usually referred to as photosystem II. Anoxygenic photosynthetic bacteria have related enzymes that oxidize various other substances in place of water. Energy-harvesting chromophores are various chlorophylls, carotenoids, and bilins.

L.O. Björn
School of Life Science, South China Normal University, Guangzhou, China

Department of Biology, Lund University, Lund, Sweden
e-mail: Lars_Olof.Bjorn@biol.lu.se

L.O. Björn (ed.), *Photobiology: The Science of Light and Life*,
DOI 10.1007/978-1-4939-1468-5_11,

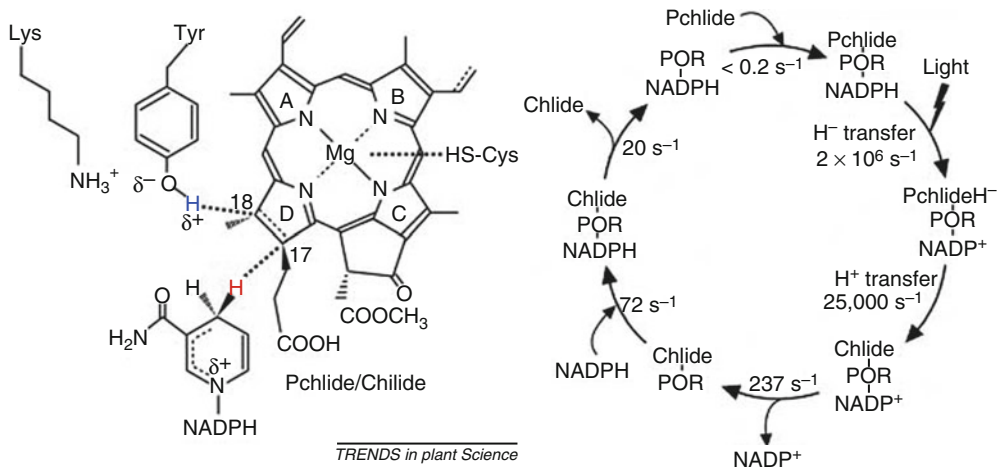

Fig. 11.1 *Left Panel*: Reduction of protochlorophyllide to chlorophyllide a by transfer of hydrogen as hydride ion from NADPH and as proton from tyrosine in LPOR (From Reinbothe et al. 2010). *Right panel*: The photocycle of LPOR according to Scrutton et al. (2012)

11.2.1.3 Light-Dependent NADPH: Protochlorophyllide Oxidoreductases (LPORs)

This is one type of enzyme that is able to reduce protochlorophyllide to chlorophyllide *a*; in angiosperms and some gymnosperms it is the only one. The other enzyme that can carry out this reaction, as well as the corresponding production of bacteriochlorophylls in bacteria, is DPOR, light-independent protochlorophyllide oxidoreductase. The two enzymes are not closely related, although some motifs are shared (Gabruk et al. 2012). DPOR is the only NADPH: protochlorophyllide reductase in anoxygenic bacteria, while many cyanobacteria and lower plants possess both (or one of them during part of the life cycle, and the other one during another phase). DPOR is thought to have, at least partly, evolved from nitrogenase (Bröcker et al. 2008, 2010). The phylogeny of LPOR among eukaryotic organisms has been studied by Yang and Cheng (2004). It is related to alcohol dehydrogenase (Masuda and Takamiya). In *Arabidopsis* there are three forms of LPOR, i.e., PORA, PORB, and PORC (Masuda and Takamiya 2004).

The light-dependent formation of chlorophyll (ide) *a* has been studied for a long time. Early researchers (Schmidt 1914; Frank 1946; Koski et al. 1951) determined action spectra in search of the light-gathering chromophore. Proof that this is protochlorophyllide was obtained by Smith and Kupke (1956), who managed to extract from dark-grown seedlings a protochlorophyllide-containing protein complex that they called protochlorophyll holochrome, which was converted to a chlorophyllide *a* protein complex upon exposure to light. Later much smaller active LPORs have been isolated, having about a tenth of the molecular weight of protochlorophyll holochrome. LPORs are unique among photoenzymes in that they require absorption of a photon to become active (Sytina et al. 2008, 2011). This photon changes the conformation of the protein to be more favorable for the catalytic reaction. If the enzyme is left in darkness after activation, it remains active for hours.

Reduction of protochlorophyllide to chlorophyllide *a* requires addition of two hydrogen atoms to a double bond between carbon atoms 17 and 18. The two hydrogens are transferred in quite different ways. First a hydride ion, i.e., a proton with two electrons, is transferred from NADPH bound to the enzyme. In a second step a proton is transferred from a tyrosine residue in the protein. Then the $NADP^+$ cation is exchanged for a new proton taken up from the environment (Fig. 11.1).

The photocycle of Scrutton et al. (2012) shown in Fig. 11.1 is not completely accepted by all. Much discussion has concerned a species named I675 (after the wavelength of its absorption maximum) not shown there, which is formed very quickly. By some it is regarded as an intermediate (e.g., Sytina et al. 2012), by others as being on a side track.

11.2.1.4 Aspartate Aminotransferase from *Escherichia coli*

Aspartate aminotransferase from *Escherichia coli* has a low activity in darkness, but irradiation with blue-violet light (410–430 nm) more than doubles the activity for the wild-type enzyme. The chromophore is pyridoxal 5′-phosphate, a form of vitamin B_6. In a mutant where a lysine residue has been changed to alanine, the activity is lower than that of the wild type in darkness, but increased several hundred times in light (Hill et al. 2010). The light dependence was for a while thought to be bi-photonic, but later investigations have shown that it is a single-photon process. The activity stimulation is due to photoenhanced deprotonation. Since the effect of light is rather modest for the wild type and can be so much increased by a substitution of a single amino acid, it is not likely that light plays a great biological role in this particular enzyme. But aspartate aminotransferase belongs to a very large group of enzymes with pyridoxal 5′-phosphate as coenzyme, and it is not unlikely that more interesting photoenzymes will be found among its members.

11.2.1.5 Photolyases

As described in Chap. 22 DNA can be damaged by ultraviolet radiation. Before the role of DNA was known, Hausser and v. Oehmcke (1933) discovered that discoloring of fruit peels due to exposure to ultraviolet radiation (UV) could be prevented if the fruits were exposed to strong visible light immediately after the UV treatment (Figs. 22.11, 28.8, and 28.9). Other early publications on the subject include Blum et al. (1949), Dulbecco (1949), and Kelner (1949). They all noted a remediation of UV damage to DNA by subsequent visible light. Rupert et al. (1958) were the first to carry out photoreactivation in vitro, and they showed that the photoreactivation catalyst had a dialyzable and a non-dialyzable part.

It is now known that some of the lesions in DNA molecules (likely reasons for all the UV effects described in the works cited above) can be repaired by photoenzymes referred to as photolyases (or photoreactivating enzymes). Some photolyases can repair cyclobutane-pyrimidine dimers (CPDs) and another type (6–4) photoproducts. If (6–4) photoproducts are left unrepaired, further irradiation with UV-A can convert them to Dewar photoproducts. For some time it was believed that Dewar photoproducts cannot be photorepaired. Recently, Fingerhut et al. (2012) found that (6–4) photolyase can repair Dewar photoproducts derived from T-C (6–4) photoproducts, but not those derived from and some (but not all) Dewar photoproducts formed from T-T (6–4) photoproducts (Fig. 11.2).

Photolyases are closely related to cryptochromes (see Chaps. 13 and 14), which have evolved from photolyases. Like these they contain an FAD cofactor (as $FADH^-$ in the dark state of the enzyme ready to receive light, see Liu et al. 2013) and another chromophore that can deliver absorbed light energy to the FAD. Also light absorbed directly in the FAD can drive the enzymatic DNA repair (Figs. 11.3, 11.4 and 11.5). At least some photolyases are phosphorylated (Teranishi et al. 2013).

When the pyrimidine bases in DNA are dimerized by the action of UV, they pop out of the central part of the DNA double helix into the aquatic environment, which makes it possible for the photolyase to recognize the lesion and attach to it. The FAD is held in a folded configuration with the adenine part folded back toward the flavin part, so that both parts are close to the DNA part to be repaired. While it is the flavin that donates an electron to the lesion, it is the adenine that conducts the returned electron back to the flavin (Fig. 11.4 and 11.7, left panel).

The full cycle of CPD photolyase action is depicted in Fig. 11.5. Note the unproductive back flow of electrons, which is here depicted as slow, and therefore not very important. Not all investigators agree that it is so slow and unimportant, but significantly decreases the quantum yield of the repair. We shall therefore have reason to discuss the quantum yield later.

The antenna chromophore varies between species and therefore also the action spectra for photolyase action. In most CPD photolyases it is methenyltetrahydrofolate (MTHF) or 8-hydroxy-5-deaza(ribo)flavin. The latter occurs in both some prokaryotes and eukaryotes. In some prokaryotes it is FMN or FAD. In (6–4) photoproduct photolyase from *Agrobacterium tumefaciens*, it was found to be 6,7-dimethyl-8-ribityllumazine (Zhang et al. 2013). In many cases the antenna chromophore is unknown. The CPD photolyase of *Bacillus firmus* (Malhotra et al. 1994) action spectrum shows a single peak at 410 nm and has a folate chromophore of some kind, but the action spectrum is different from those of MTHF-containing photolyases. Figure 11.6 shows some photolyase action spectra and one photolyase absorption spectrum. It is evident that spectra can be different even with the same chromophore, due to tuning influence of the protein. Nothing is known about the ecological or evolutionary significance of the spectral differences.

Data on quantum yields for photolyase repair varies among reports, from about 0.1 (Heelis and Sancar 1986) or about 0.2 (Byrdin et al 2010) to about 0.9 (Kim and Sancar 1991; Kao et al. 2005), even when the same photolyase, in

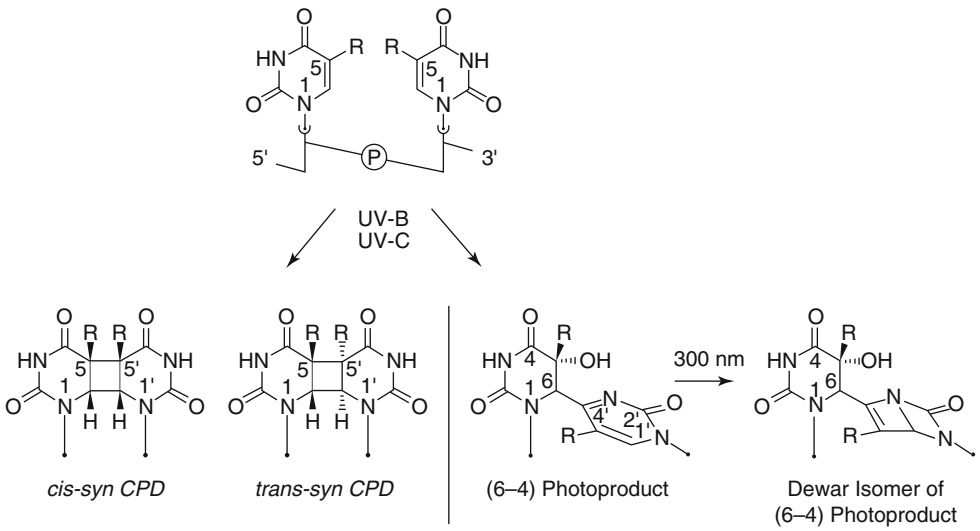

Fig. 11.2 Types of UV-induced lesions in DNA that can be repaired by photolyases (other kinds of damage that are less frequent need other systems for repair). Part of undamaged DNA-molecule on top. R denotes H in uracil (U) or CH3 in thymine (T). The cis–syn CPD is a diastereoisomer of the trans–syn CPD (From Weber (2005)

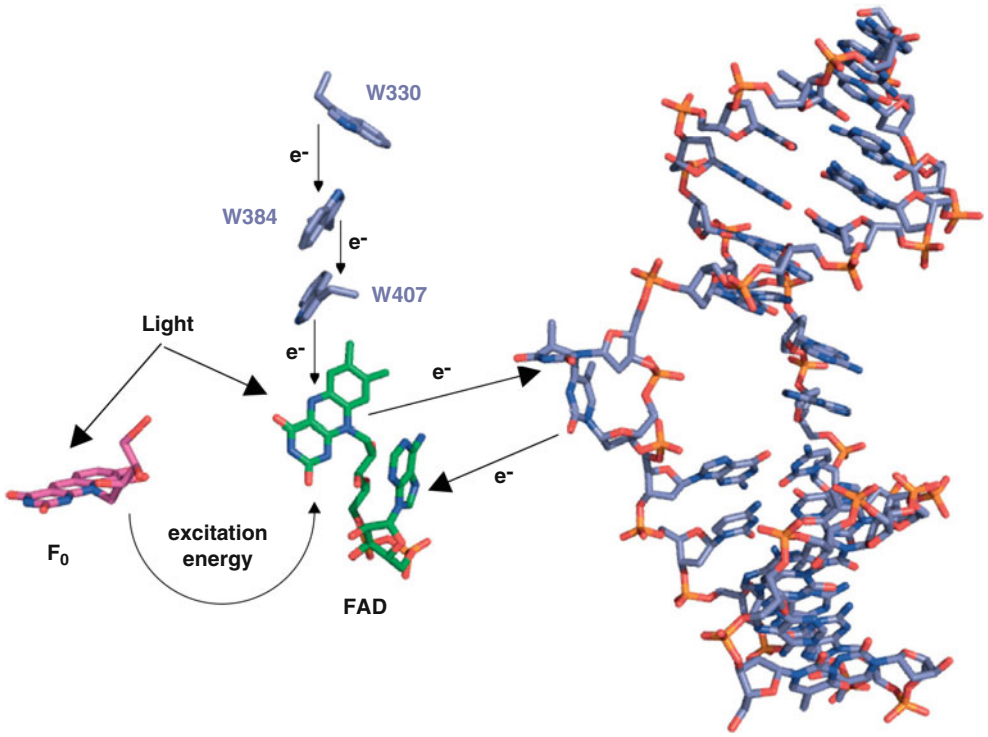

Fig. 11.3 The principle for remediation of a CPD lesion in DNA by a CPD photolyase. The structure to the right is the damaged DNA. Light is absorbed either in FAD or in the antenna chromophore. The excited FAD receives an electron from a tryptophan residue in the photolyase protein and is converted to $FAD^{-\bullet}$. The donating tryptophan regains an electron via a conductor of other tryptophan residues in the protein. The FAD semiquinone donates the odd electron to one bond in the CPD, but regains one from another bond. This results in splitting of the CPD to produce repaired DNA. Fo stands for the antenna chromophore, 8-hydroxy-5-deazariboflavin. From Benjdia (2012)

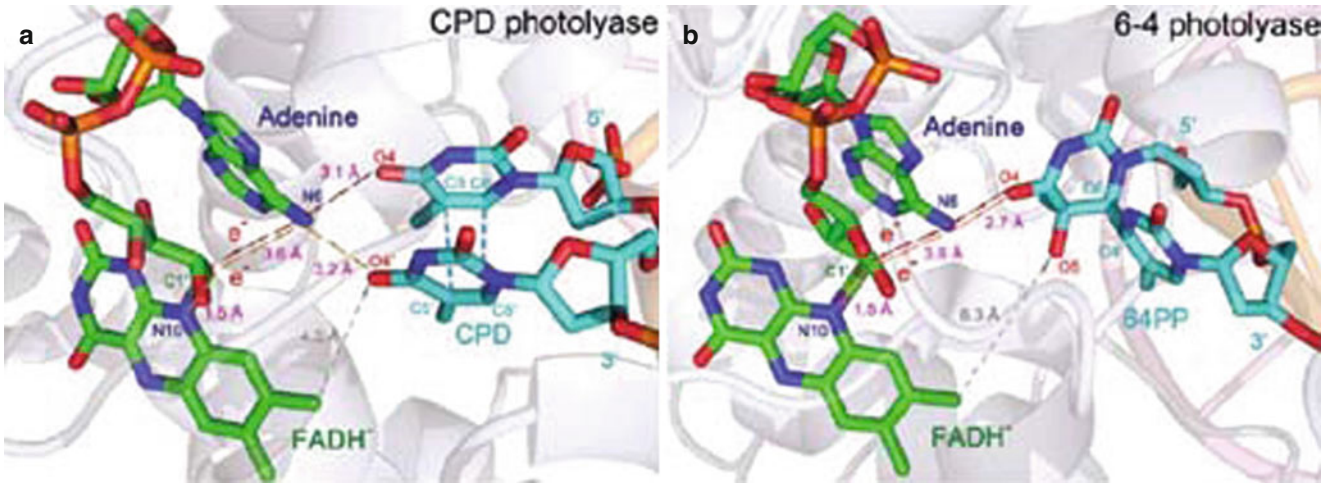

Fig. 11.4 Comparison of the enzyme structure around FAD in (**a**) CPD and (**b**) (6–4) photolyases (From Liu et al. 2011)

most cases CPD photolyase from *Escherichia coli*, is used. There can be various reasons for this. Not always is the substrate specified. Low yields can sometimes be explained by the use of an unnatural antenna chromophore. Thus Ramsey et al. (1992) obtained a quantum yield of 0.66 ± 0.03 for enzyme without antenna chromophore, 0.72 ± 0.04 for the intact enzyme with its natural 5,10-methenyltetrahydropteroylpolyglutamate cofactor, and only 0.34 ± 0.015 for the enzyme with the antenna chromophore without the polyglutamate part. The ratio between the two latter is in agreement with the finding by Lipman and Jorns (1992) that energy transfer from the antenna pigment is only half the native value if the polyglutamate part is omitted. In summary, it is likely that the quantum yield for the enzyme in the natural state is about 0.7. The structure of photolyase around the FAD chromophore is shown in Fig. 11.7. The expression of photolyase genes is often stimulated by ultraviolet radiation (e.g., Isely et al. 2009).

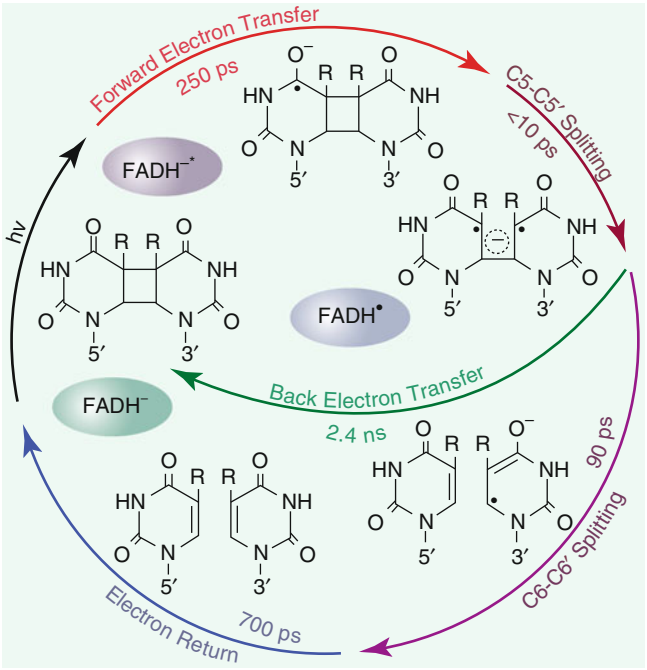

Fig. 11.5 Catalytic cycle of CPD photolyase (From Liu et al. 2011)

11.2.2 Type I Light-Activated Enzymes: Light-Induced Conformational Change

We have already mentioned above that LPOR belongs to this group, at the same time as it is a photoenzyme. The majority enzymes in this category, however, are not photoenzymes. Most of them function as photoreceptor proteins with bilin flavin chromophores.

11.2.2.1 Biliprotein Protein Kinases

Biliprotein protein kinases (phytochromes and related). These are photoreceptors and will be treated elsewhere (Chaps. 9 and 12–14).

11.2.2.2 BLUF Proteins

These will also be treated as photoreceptors (Chaps. 9 and 12–14).

11.2.3 Type II Light-Activated Enzymes: Photodissociation of Inhibitor

11.2.3.1 Urocanase

Urocanase (urocanate hydratase, EC 4.2.1.49) of *Pseudomonas putida* is an enzyme containing tightly bound NAD^+, which in the natural state is inhibited by sulfite in darkness. Irradiation with 11 W m^{-2} UV-A (ca 365 nm) dissociates off the sulfite and activates the enzyme (Hug and Roth 1971; Hug et al. 1972; Venema and Hug 1985). Experimentally the enzyme can also be activated in darkness by being brought in contact with triplet-excited indole-3-aldehyde, and light-activation can be counteracted by triplet quenchers (Venema et al. 1985). Thus it can be concluded that the photoactivation is due to triplet excitation of the NAD^+. No biological role for the light-dependency is known.

11.2.3.2 Nitrile Hydratase

Nagamune et al. (1990) found that when washed cells of *Rhodococcus sp*. N-771 were incubated in the cold (5°) and dark, their nitrile hydratase became gradually inactivated, but most of the activity could be recovered by illumination.

11.2.3.3 Cytochrome C Oxidase

This important enzyme does not need light for being active under normal conditions. But under some conditions it can be inactivated by endogenous nitric oxide, and this inhibition can be released by light. The complicated relations between the cytochrome c oxidase and nitric oxide are further treated in Chap. 26.

11.3 Light-Driven Ion Pumping by Rhodopsins

Rhodopsins acting as light-driven ion pumps occur in Archaea, Bacteria, and Eukarya. Organisms in the class Halobacteria (in the phylum Euryarchaeota in the domain Archaea) contain various rhodopsins, of which some transport ions and others have sensory functions. *Bacteriorhodopsins* transport protons (from the inside to outside the cells). The chromophore retinal is bound to a lysine residue in the protein via a protonated Schiff base. When the positively charged retinal absorbs a photon, it switches from all-trans to 13-cis configuration. This causes the pKa to drop (i.e., the dissociation constant increases) transiently, and the proton becomes less firmly bound and is released to the outside. Another proton is then taken up from the inside.

Halorhodopsin is a related light-driven pump (Schobert and Lanyi 1982) transporting chloride into cells. It undergoes a photocycle as depicted in Fig. 11.8. It has two chromophores, retinal and the carotenoid bacterioruberin. Contrary to the rhodopsin in our eyes, the retinal chromophore in the dark state is in the all-trans conformation and changes to the 13-cis form upon exposure to light. The first metastable state containing this 13-cis chromophore is called the K state, or HR_{600} (after its absorption spectrum). From this state the cycle proceeds forward to chloride transport or reverts to the original state. The HR_{600} state is a minimum energy state, so

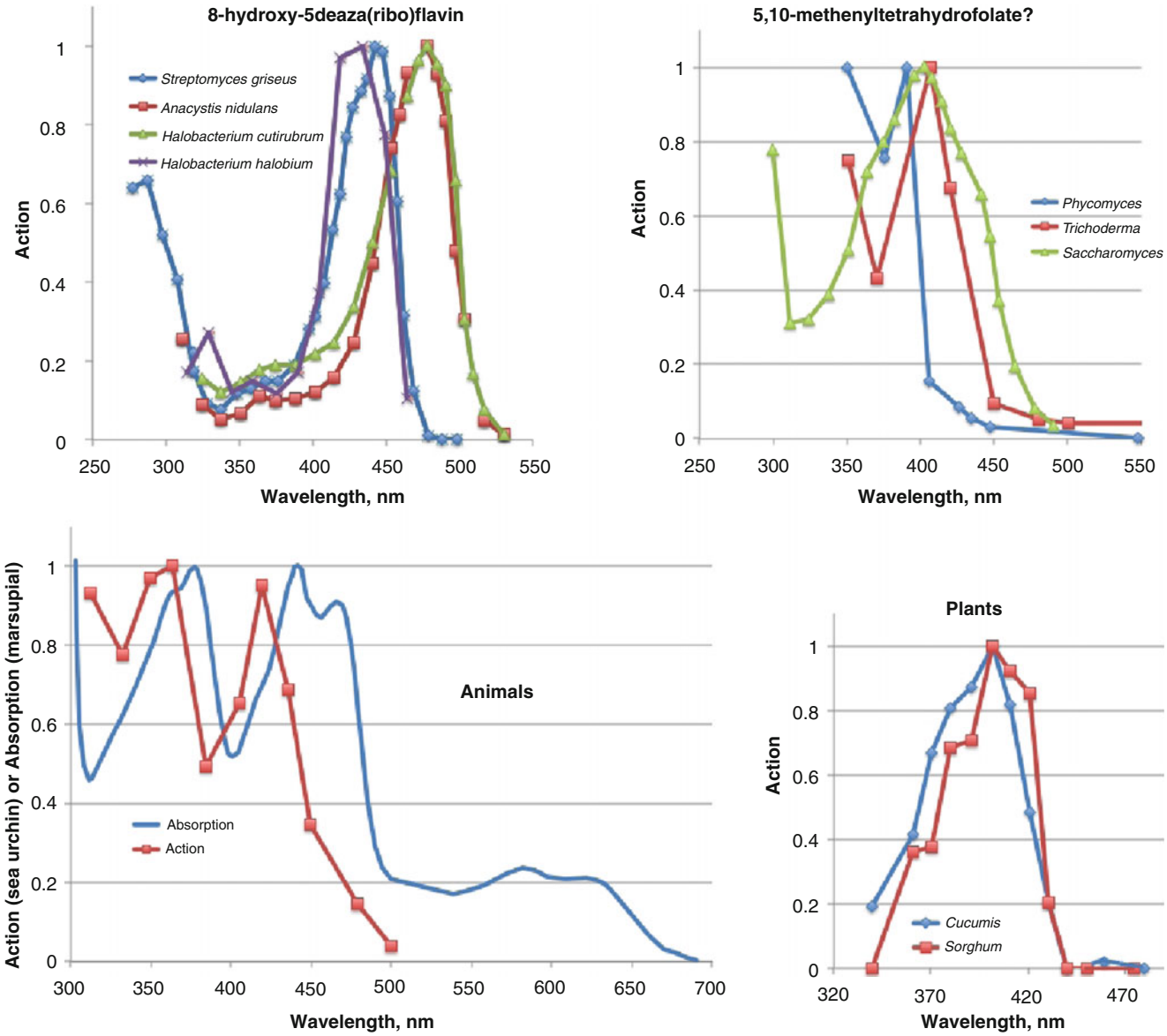

Fig. 11.6 Examples of spectra for photolyases, demonstrating the diversity. All are action spectra, except for the blue curve in the lover left panel, which is an absorption spectrum for purified photolyase. *Upper left* panel, photolyases using 8-hydroxy-5-deazaflavin or 8-hydroxy-5-deazariboflavin as antenna chromophore: *Streptomyces griseus* (bacterium, Eker et al. 1981), *Anacystis nidulans* (cyanobacterium, Eker et al. 1990), *Halobacterium cutirubrum* (archaeon, Eker et al. 1991), *Halobacterium halobium* (archaeon, Iwasa et al. 1988). *Upper right panel*, fungal photolyases probably using 5,10-methenyltetrahydrofolate as antenna chromophore: *Phycomyces blakesleeanus* (Zygomycota, Galland 1996), *Trichoderma harzianum* (Ascomycota, Sametz-Baron et al. 1997). *Lower left panel*, animal photolyases: Action spectrum for sea urchin eggs (*Hemicentrotus pulcherrimus*, Ejima et al. 1984), absorption spectrum of purified CPD photolyase from *Potorous tridactylis* (rat kangaroo, a marsupial, Yasui et al. 1994). The photolyases in this panel are thought to lack an antenna chromophore, and the active light is thus absorbed only in the FAD^- anion. *Lower right panel*, plant CPD photolyases: A dicotyledon (*Cucumis sativus*) and a monocotyledon (*Sorghum bicolor*), both from Hada et al. (2000). All spectra redrawn

proceeding from it either forward or backward in the cycle requires thermal energy. Pfisterer et al. have some interesting considerations concerning the optimal depth of the energy minimum associated with the HR_{600} state. If the energy is high in relation to the energy barrier in the forward direction, less thermal energy is needed, so the reaction is faster if the minimum energy is low. But then, on the other hand, the risk of backward reaction increases, so there is an optimum energy level for the HR_{600} state, and Pfisterer et al. find that this coincides with the energy level that the HR_{600} state actually has.

The difference between chloride pumps and proton pumps is very small. In fact, a proton pump can be converted to a chloride pump by substitution of a single amino acid (Sasaki et al. 1995). The pumping of chloride is best understood by first considering proton pumping. The retinal chromophore

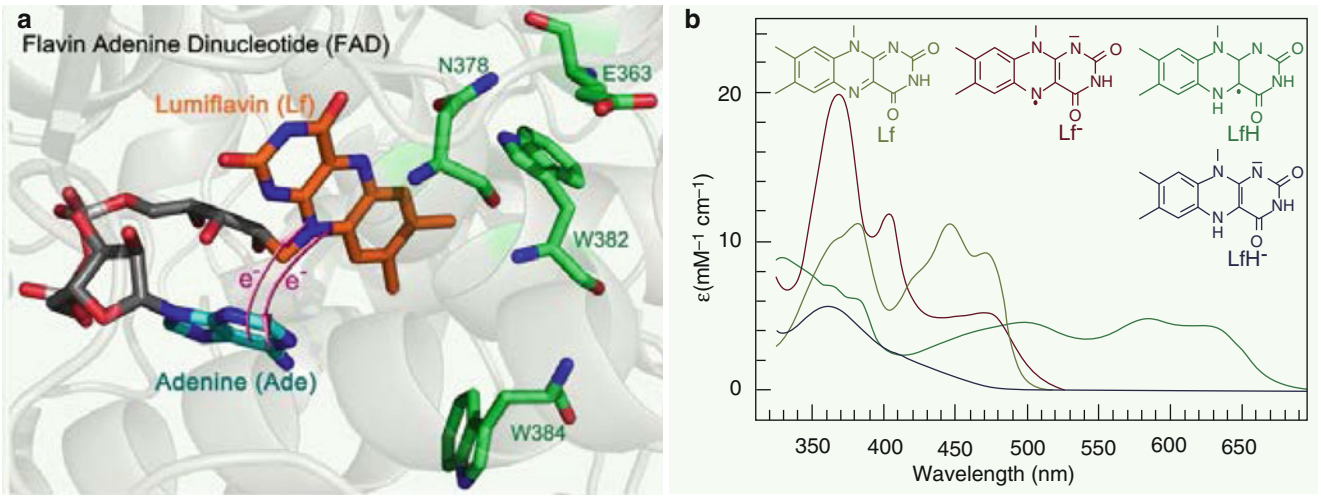

Fig. 11.7 *Left panel*: The adenine part of the FAD chromophore plays an important role in conducting electrons between the nucleotide bases in DNA and the flavin part of FAD. *Right panel*: absorption spectra for the different forms of flavin, i.e., neutral (*yellow-green*), anion (*red*), semiquinone (*green*), and protonated (*blue*). It is the anion form which is receiving light energy for repair, either directly or from the antenna chromophore (which is not shown here), and which therefore contributes to the action spectra (From Liu et al. 2013)

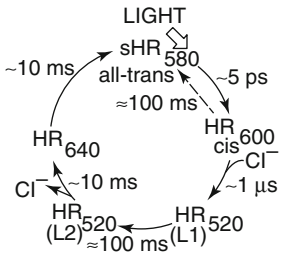

Fig. 11.8 The halorhodopsin (HR) photocycle. In darkness the halorhodopsin exists in the all-trans from shown on *top*. The trans-cis photoisomerization takes place at the 13-position. Note two different 520 nm forms (Modified after Pfisterer et al. 2009)

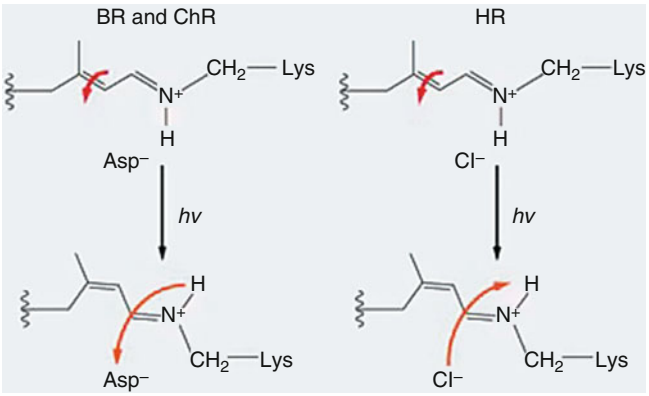

Fig. 11.9 Light-induced changes in proton-pumping (*left*) and chloride-pumping (*right*) rhodopsins. The light-induced trans-to-cis isomerization changes the position of a proton bound to the Schiff base nitrogen in such a way that it becomes less strongly bound and is transferred to an aspartate residue and from there via glutamate residues to the extracellular space. In the case of chloride pumping, the proton charge pulls the chloride along with it when the proton moves. The state after the initial isomerization corresponds to the HR_{600} state in Fig. 11.8, while the L1 state in Fig. 11.1 results from the chloride movement (From Zhang et al. 2011)

is attached to the protein via a so-called Schiff base linkage to a lysine residue (Fig. 11.9). When light absorption in the retinal chromophore causes its trans-to-cis isomerization, a proton bound to the lysine nitrogen comes into a new electric environment which allows it to be transferred to an aspartate residue in the protein. This in turn results in conformational change of the protein and transfer of the proton via glutamate residues to the space outside the cell.

The energy captured by light-induced proton or chloride pumping can be utilized for synthesis of ATP and also for driving other kinds of ion transport. Proton pumping rhodopsins have been found in halobacteria, eubacteria (Wang et al. 2012; Riedel et al. 2013), green algae (Wada et al. 2011), and fungi (Waschuk et al. 2005). *Proteorhodopsins* constitute a particularly widespread type of proton pump (Beja et al. 2000; de la Torre et al. 2003; Giovannoni et al. 2005; Frigaard et al. 2006; Bamann et al. 2013). Its operation in light has been shown to increase bacterial survival when organic carbon is scarce (Gomez-Consarnau et al. 2007, 2010; DeLong and Béjà 2010). Organisms living at different depths possess different spectral types of proteorhodopsin (Man et al. 2003). Also a kind of rhodopsin called *xanthorhodopsin* is quite widespread among different bacteria. Xanthorhodopsin is characterized by having a carotenoid (salinixanthin) antenna to collect extra light energy to the rhodopsin part (Lanyi and Balashov 2008). It sometimes occurs in the same organism together with other light-driven proton pumps (Kang et al. 2010; Riedel et al. 2013).

Recently a third kind of light-driven ion pump called KR2 (Fig. 11.10) has been discovered (Inoue et al. 2013). Under

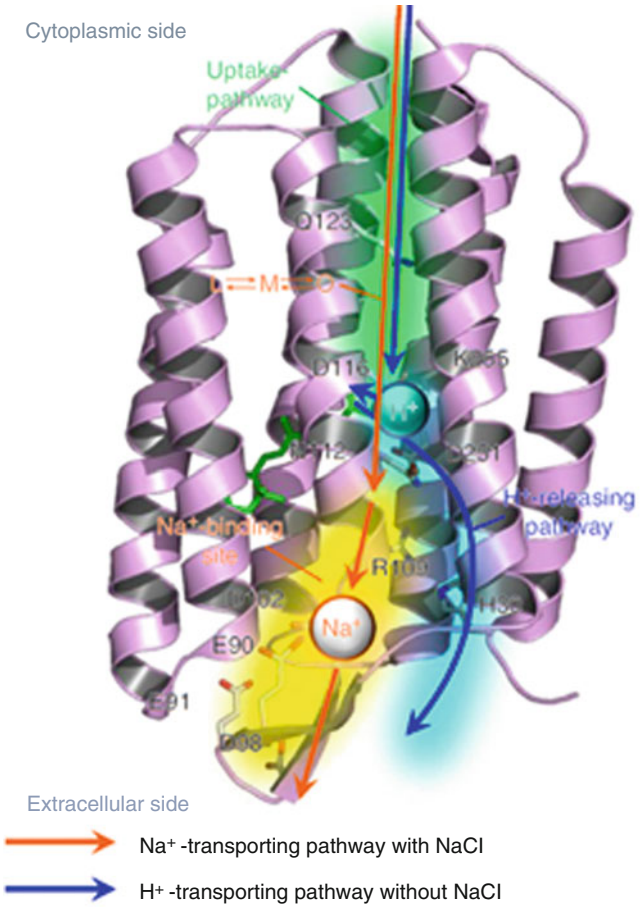

Fig. 11.10 Model of the light-driven sodium ion pump KR2 (From Inoue et al. (2013), with permission from Nature Publishing Group)

natural condition it transports sodium ions out of cells in the marine flavobacterium *Krokinobacter eikastus*. In the absence of its natural substrate sodium ions, the protein can pump the smaller lithium ions, but when presented only with larger cations like potassium, it switches to pumping protons.

For a time it was thought that a bacteriorhodopsin was a light-driven sodium pump (MacDonald et al. 1979), but later it has been clarified that the light-induced sodium ion transport observed was an indirect phenomenon: light-driven proton pumping followed by proton-sodium antiporting (Luisi et al. 1980).

11.4 Proton Pumping Using Bacteriochlorophyll-Based Photosystem

Also plants, algae, and various photoautotrophic bacteria pump protons across membranes using their photosystems. What is less known is the great importance of bacteria which are not photoautotrophic but pump protons using a very slimmed-down photosynthetic system that is easily transferred horizontally between bacterial strains. These bacteria, referred to as aerobic anoxygenic photoheterotrophic bacteria, are doing essentially the same as the organism pumping protons with rhodopsins (which strictly speaking are also aerobic anoxygenic photoheterotrophic bacteria), but are doing it using a different molecular machinery. Both kinds use the proton pumping for producing ATP and for helping in assimilating organic carbon from the environment. Aerobic anoxygenic photoheterotrophic bacteria are genetically very diverse (Richie and Johnson 2012). They were first discovered in the ocean but have later been found in the most diverse habitats exposed to sunlight, e.g., soil crusts (Csotonyi et al. 2010a, b) and high-altitude wetlands (Dorador et al. 2013) and saline lakes (Jiang et al. 2009). A particularly important group of aerobic anoxygenic photoheterotrophic bacteria is the so-called *Roseobacter* clade (Buchan et al. 2005).

11.5 Channelrhodopsins: Light-Gated Ion Channels

Kenneth Foster and coworkers were the first to realize that rhodopsins act as photoreceptors in green algae (Foster and Smyth 1980; Foster et al. 1984). *Channelrhodopsins* are type I (microbial type) rhodopsins that mediate phototaxis and other light-induced phenomena. Different types have been found in a large number of species (Yawo et al. 2013). The best investigated ones are the first discovered ones, channelrhodopsin 1 (ChR1, Nagel et al. 2002) and channelrhodopsin 2 (ChR2, Nagel et al. 2003) in *Chlamydomonas reinhardtii*. They differ not only spectrally (absorption and action peaks at 550 nm and 460 nm, respectively) but also in their ionic selectivity: ChR1 conducts exclusively protons, while ChR2 conducts small mono- and divalent metal and organic cations as well. In contrast to the rhodopsins dealt with in the previous section (light-driven ion pumps), they are light-gated cation channels.

Channelrhodopsins (as well as some of the proton-pumping rhodopsins) have found a practical application in "optogenetics" and related areas, i.e., techniques to manipulate neurons cells with light (Nagel et al. 2005; Dugué et al. 2012; Lin 2012).

11.6 Optogenetics

11.6.1 Introduction

The meaning of the term "optogenetics" has shifted over time (Dugué). We shall here follow Deisseroth (2011) and use it in the sense of "the combination of genetic and optical

methods to achieve gain or loss of function of well-defined events in specific cells of living tissue," but include in this chapter also some methods which do not fit into this definition.

11.6.2 Early Optical Methods for Recording Cell Processes

The first optical method for following what is going on in living cells was absorption spectrophotometry. Fortunately some of the molecules participating in respiration (cytochromes, cytochrome oxidase, flavoproteins, NAD) have prominent absorption spectra which change with oxidation level. This was exploited by pioneers as Keilin, Warburg, and Lundegårdh. Also for studies of the photosynthetic process, absorption spectrophotometry became important at an early date, but in vivo fluorescence, too, has provided crucial information.

In 1951 Strehler and Arnold (1951) attempted to demonstrate photophosphorylation in a suspension of chloroplast fragments by measuring light from added firefly extract containing luciferin and luciferase (Chap. 26). They failed to do that, but in the process discovered "delayed light emission," the light emitted by reversal of photosynthetic processes (Chap. 26). This in itself has become a valuable, noninvasive method for the study of photosynthesis. Later people have studied ATP generation cloning the luciferase gene into organisms and adding luciferin, but this method cannot be used while cells are still alive.

In 1985 the calcium indicating protein aequorin was cloned and expressed in a foreign organism (Inouye et al. 1985; Prasher et al. 1985). Aequorin is a protein from the jellyfish *Aequorea victoria* that emits light when it encounters calcium ions. Very quickly this was exploited for measurement of calcium release into the cytosol.

A dream for neurobiologists, and especially for scientists studying the function of the brain, has been to activate or inactivate specific neurons and groups of neurons. With the development of optogenetics this dream has come true. Although there are other methods, we shall focus here on those which employ natural or modified photoactive proteins.

Another opsin that has been used in optogenetics is channelrhodopsin 2 (Boyden et al. 2005; Li et al. 2005). It can be expressed in mammalian neurons and when irradiated with blue light (450–490 nm) causes depolarization. It reacts rapidly enough to cause individual spikes, reaching their maxima within a couple of milliseconds after the onset of light, and they do this in a very reproducible manner.

Channelrhodopsin 2 can also be used in the reverse way. Berglund et al. (2013) fused it to a luciferase in such a way that the luciferase part remained outside the cell when the channelrhodopsin was incorporated into the cell membrane. When the luciferin (called coelenterazine) for this particular luciferase appears in the external medium, the luciferin emits light.

11.6.3 Examples of Modern Developments

A recent general overview is provided by Packer et al. (2013).

11.6.3.1 Light Switch for Pain

Optovin is a small molecule containing the chromophore rhodanine. It can be attached specifically, via cysteine, to an ion channel called TrpA1 which mediates the sensation of pain in vertebrates. It allows the remote control of animal behavior by violet light (Kokel et al. 2013).

11.6.3.2 Restoration of Vision

Promising animal experiments for restoring vision in blind individuals have been done by many groups, including Doroudchi et al. (2011). These, as several other researchers, used virus to introduce channelrhodopsin 2 into the defunct receptor cells. Channelrhodopsin 2 has the advantage of producing the required transport of sodium ions resulting in fast (within 50 ms) depolarization of the membrane in a more direct way than the natural system. The light effect is directly on the ion channel, while the natural system employs intermediate messengers. As long as only the natural channelrhodopsin 2 is used, vision is monochromatic with maximum sensitivity in the violet region. A recent thorough description of this field is provided by Natasha et al. (2013).

11.6.3.3 UV-B-Triggered Protein Secretion

Chen et al. 2013 modified the plant UV-B receptor UVR8 to create a system by which protein secretion can be controlled by UV-B and which can be used for studying protein trafficking in neurons.

References

Azai C, Tsukatani Y, Itoh S, Oh-oka H (2010) C-type cytochromes in the photosynthetic electron transfer pathways in green sulfur bacteria and heliobacteria. Photosynth Res 104:189–199

Bamann C, Bamberg E, Wachtveitl J, Glaubitz C (2014) Proteorhodopsin. Biochim Biophys Acta 1837:614–625

Béjà O, Aravind L, Koonin EV, Suzuki MT, Hadd A, Nguyen LP, Jovanovich S, Gates CM, Feldman RA, Spudich JL, Spudich EN, DeLong EF (2000) Bacterial rhodopsin: evidence for a new type of phototrophy in the sea. Science 289:1902–1906

Benjdia A (2012) DNA photolyases and SP lyase: structure and mechanism of light-dependent and independent DNA lyases. Curr Opin Struct Biol 22:711–720

Berglund K, Birkner E, Augustine GJ, Hochgeschwender U (2013) Light-emitting channelrhodopsins for combined optogenetic and chemical-genetic control of neurons. PLoS One 8:e59759

Blum HF, Price JP, Robinson JC, Loos GM (1949) Effect of ultraviolet radiation on the rate of cell division of *Arbacia* eggs, and the enhancement of recovery by visible light. Anat Rec 105(3):524

Boyden ES, Zhang F, Bamberg E, Nagel G, Deisseroth K (2005) Millisecond time scale, genetically targeted optical control of neural activity. Nat Neurosci 8:1263–1268

Bröcker MJ, Virus S, Ganskow S, Heathcote P, Heinz DW, Schubert W-D, Jahn D, Moser J (2008) ATP-driven reduction by dark-operative protochlorophyllide oxidoreductase from *Chlorobium tepidum* mechanistically resembles nitrogenase catalysis. J Biol Chem 283:10559–10567

Bröcker MJ, Schomburg S, Heinz DW, Jahn D, Schubert W-D, Moser J (2010) Crystal structure of the nitrogenase-like dark operative protochlorophyllide oxidoreductase catalytic complex ChlN/ChlB)$_2$. J Biol Chem 285:27336–27345

Buchan A, González JM, Moran MA (2005) Overview of the marine Roseobacter lineage. Appl Environ Microbiol 71:5665–5677

Byrdin B, Lukacs A, Thiagarajan V, Eker APM, Brettel K, Vos MH (2010) Quantum yield measurements of short-lived photoactivation intermediates in DNA photolyase: toward a detailed understanding of the triple tryptophan electron transfer chain. J Phys Chem A 114:3207–3214

Chen D, Gibson ES, Kennedy MJ (2013) A light-triggered protein secretion system. J Cell Biol 201:631–640

Csotonyi JT, Swiderski J, Stackebrandt E, Yurkov V (2010a) Chapter 1: A new extreme environment for aerobic anoxygenic phototrophs: biological soil crusts. In: Hallenbeck PC (ed) Recent advances in phototrophic prokaryotes, Advances in experimental medicine and biology, vol 675. Springer Science + Business Media, New York

Csotonyi JT, Swiderski J, Stackebrandt E, Yurkov V (2010b) A new environment for aerobic anoxygenic phototrophic bacteria: biological soil crusts. Appl Environ Microbiol 2:651–656

de la Torre JR, Christianson LM, Béjà O, Suzuki MT, Karl DM et al (2003) Proteorhodopsin genes are distributed among divergent marine bacterial taxa. Proc Natl Acad Sci U S A 100:12830–12835

Deisseroth K (2011) Optogenetics. Nat Methods 8:26–29

DeLong EF, Béjà O (2010) The light-driven proton pump proteorhodopsin enhances bacterial survival during tough times. J Bacteriol 192:4798–4799

Dorador C, Vila I, Witzel K-P, Johannes F, Imhoff JF (2013) Bacterial and archaeal diversity in high altitude wetlands of the Chilean Altiplano. Fundam Appl Limnol 182(2):135–159

Doroudchi MM, Greenberg KP, Liu J, Silka KA, Boyden ES, Lockridge JA, Arman AC, Janani R, Boye SE, Boye SL, Gordon GM, Matteo BC, Sampath AP, Hauswirth WW, Alan Horsager A (2011) Virally delivered channelrhodopsin-2 safely and effectively restores visual function in multiple mouse models of blindness. Molec Therapy 19:1220–1229

Dugué GP, Akemann W, Knöpfel T (2012) Chapter 1: A comprehensive concept of optogenetics. In: Knöpfel T, Boyden E (eds) Progress in brain research, vol 196. Elsevier BV, Amsterdam

Dulbecco R (1949) Reactivation of ultraviolet-inactivated bacteriophage by visible light. Nature 163:949–950

Ejima Y, Ikenaga M, Shiroya T (1984) Action spectrum for photoreactivation of abnormality in sea urchin eggs. Photochem Photobiol 40:461–464

Eker APM, Dekker RH, Berends W (1981) Photoreactivation enzyme from Streptomyces griseus—IV. On the nature of the chromophoric cofactor in Streptomyces griseus photoreactivating enzyme. Photochem Photobiol 33:65–72

Eker APM, Kooiman P, Hessels JK, Yasui A (1990) DNA photoreactivating enzyme from the cyanobacterium *Anacystis nidulans*. J Biol Chem 265:8009–8015

Eker APM, Formenoy L, de Wit LEA (1991) Photoreactivation in the extreme halophilic archaebacterium *Halobacterium cutirubrum*. Photochem Photobiol 53:643–651

Ferreira F, Straus NA (1994) Iron deprivation in cyanobacteria. J Appl Phycol 6:199–210

Fingerhut BP, Heil K, EKaya E, Oesterling S, de Vivie-Riedle R, Carell T (2012) Mechanism of UV-induced Dewar lesion repair catalysed by DNA (6–4) photolyase. Chem Sci 3:1794–1797

Foster KW, Smyth RD (1980) The visual system of green algae – a forerunner of human vision. Fed Proc 39:2137

Foster KW, Saranak J, Patel N, Zarilli G, Okabe M, Kline T, Nakanishi K (1984) A rhodopsin is the functional photoreceptor for phototaxis in the unicellular eukaryote *Chlamydomonas*. Nature 311:756–759

Frank SJ (1946) The effectiveness of the spectrum in chlorophyll formation. J Gen Physiol 29:157–179

Frigaard NU, Martinez A, Mincer TJ, DeLong EF (2006) Proteorhodopsin lateral gene transfer between marine planktonic bacteria and archaea. Nature 439:847–850

Galland P (1996) Ultraviolet killing and photoreactivation of Phycomyces spores. Microbiol Res 151:9–17

Giovannoni RJ, Bibbs L, Cho J-C, Stapels MD, Desiderio R, Vergin KL, Rappé MS, Laney S, Wilhelm LJ, Tripp HJ, Eric J, Mathur EJ, Barofsky DF (2005) Proteorhodopsin in the ubiquitous marine bacterium SAR11. Nature 438:82–85

Gómez-Consarnau L, González JM, Coll-Lladó M, Gourdon P, Pascher T, Neutze R, Pedrós-Alió C, Pinhassi J (2007) Light stimulates growth of proteorhodopsin-containing marine flavobacteria. Nature 445:210–213. doi:10.1038/nature05381

Gomez-Consarnau L, Akram N, Lindell K, Pedersen A, Neutze R, Milton DL, Gonzalez JM, Pinhassi J (2010) Proteorhodopsin phototrophy promotes survival of marine bacteria during starvation. PLoS Biol 8:e1000358

Hada M, Iida Y, Yuichi Takeuchi Y (2000) Action spectra of DNA photolyases for photorepair of cyclobutane pyrimidine dimers in sorghum and cucumber. Plant Cell Physiol 41:644–648

Hausser KW, v. Oehmcke H (1933) Lichtbräunung an Fruchtschalen. Strahlentherapie 48:223–229

Heelis PF, Sancar S (1986) Photochemical properties of *Escherichia coli* DNA photolyase: a flash photolysis study. Biochemistry 25:8163–8166

Hill MP, Carroll EC, Vang MC, Addington TA, Toney MD, Larsen DS (2010) Light-enhanced catalysis by pyridoxal phosphate-dependent aspartate aminotransferase. J Am Chem Soc 132:16953–16961

Hug DH, Roth D (1971) Photoactivation of urocanase in Pseudomonas putida. Purification of inactive enzyme. Biochemistry (ACS) 10:1397–1402

Hug DH, Roth D, Hunter JK (1972) Light-driven periodic changes in urocanase activity of a heterotrophic bacterium. Arch Mikrobiol 86:83–90

Inoue K, Ono H, Abe-Yoshizumi R, Yoshizawa S, Ito H, Kogure K, Kandori H (2013) A light-driven sodium ion pump in marine bacteria. Nat Commun. 4:1678 (10 p). doi:10.1038/ncomms2689

Inouye S, Noguchi M et al (1985) Cloning and sequence analysis of cDNA for the luminescent protein aequorin. Proc Natl Acad Sci U S A 82:3154–3158

Isely N, Lamare M, Marshall C, Barker M (2009) Expression of the DNA repair enzyme, photolyase, in developmental tissues and larvae, and in response to ambient UV-R in the Antarctic sea urchin *Sterechinus neumayeri*. Photochem Photobiol 85:1168–1176

Iwasa T, Tokutomi S, Tokunaga F (1988) Photoreactivation of *Halobacterium halobium*: action spectrum and role of pigmentation. Photochem Photobiol 47:267–270

Jiang H, Dong D, Yu B, Lv G, Deng S, Wu Y, Dai M, Jiao N (2009) Abundance and diversity of aerobic anoxygenic phototrophic bacteria in saline lakes on the Tibetan plateau. FEMS Microbiol Ecol 67:268–278

Kang I, Oh H-M, Lim SI, Ferriera S, Giovannoni SJ, Cho JC (2010) Genome sequence of *Fulvimarina pelagi* HTCC2506 T, a Mn(II)-oxidizing alphaproteobacterium possessing an aerobic anoxygenic photosynthetic gene cluster and xanthorhodopsin. J Bacteriol 192:4798–4799

Kao T-T, Saxena C, Wang L, Sancar A, Zhong D (2005) Direct observation of thymine dimer repair in DNA by photolyase. Proc Natl Acad Sci U S A 102:16129–16132

Kelner A (1949) Effect of visible light on the recovery of *Streptomyces griseus* conidia from ultraviolet-injury. Proc Natl Acad Sci U S A 35:73–79

Kim ST, Sancar A (1991) Effect of base, pentose, and phosphodiester backbone structures on binding and repair of pyrimidine dimers by Escherichia coli DNA photolyase. Biochemistry (ACS) 30:8623–8630

Kokel D, Cheung CYJ, Mills R, Coutinho-Budd J, Huang L, Setola V, Sprague J, Jin S, Jin YN, Huang X-P, Bruni G, Woolf CJ, Roth BL, Hamblin MR, Zylka MJ, David J, Milan DJ, Peterson RT (2013) Photochemical activation of TRPA1 channels in neurons and animals. Nat Chem Biol 9:257–265

Lanyi JK, Balashov SP (2008) Xanthorhodopsin: a bacteriorhodopsin-like proton pump with a carotenoid antenna. Biochim Biophys Acta 1777:684–688

Li X, Gutierrez DV, Hanson MG, Han J, Mark MD et al (2005) Fast noninvasive activation and inhibition of neural and network activity by vertebrate rhodopsin and green algae channelrhodopsin. Proc Natl Acad Sci U S A 102:17816–17821

Lin JY (2012) Chapter 2: Optogenetic excitation of neurons with channelrhodopsins: light instrumentation, expression systems, and channelrhodopsin variants. In: Knöpfel T, Boyden E (eds) Progress in brain research, vol 196. Elsevier BV, Amsterdam

Lipman RSA, Schuman Jorns M (1992) Direct evidence for singlet-singlet energy transfer in *Escherichia coli* DNA photolyase. Biochemistry 31:787–791

Liu Z, Tan C, Guo X, Kao Y-T, Jiang Li J, Wang L, Sancar A, Zhong D (2011) Dynamics and mechanism of cyclobutane pyrimidine dimer repair by DNA photolyase. Proc Natl Acad Sci U S A 108:14831–14836

Liu Z, Zhang M, Guo X, Tan C, Li J, Lijuan Wang L, Sancar A, Zhong D (2013) Dynamic determination of the functional state in photolyase and the implication for cryptochrome. Proc Natl Acad Sci U S A 110:12972–12977

Luisi BF, Lanyi JK, Weber HJ (1980) Na^+ transport via Na+/H+ antiport in *Halobacterium halobium* envelope vesicles. FEBS Lett 117:354–358

MacDonald RE, Greene RV, Clark RD, Lindley EV (1979) Characterization of the light-driven sodium pump of *Halobacterium halobium*. J Biol Chem 254:11831–11838

Malhotra K, Kim S-T, Sancar A (1994) Characterization of a medium wavelength type DNA photolyase: purification and properties of photolyase from Bacillus firmus. Biochemistry (ACS) 33:8712–8718

Man D, Wang W, Sabehi G, Arawind L, Post AF, Massana R, Spudich EN, Spudich JL, Béjà O (2003) Diversification and spectral tuning in marine proteorhodopsins. EMBO J 22:1725–1731

Masuda T, Takamiya K-i (2004) Novel insights into the enzymology, regulation and physiological functions of light-dependent protochlorophyllide oxidoreductase in angiosperms. Photosynth Res 81:1–29

Nagamuna T, Kubata H, Hirata M, Honda J, Hirata A, Endo I (1990) Photosensitive phenomena of nitrile hydratase of Rhodococcus sp. N-771. Photochem Photobiol 51:87–90

Nagamune T, Kurata H, Hirata M, Honda J, Koike H, Masahiko Ikeuchi I, Inoue Y, Hirata A, Endo I (1990) Purification of inactivated photoresponsive nitrile hydratase. Biochem Biophys Res Commun 168:437–442

Nagel G, Ollig D, Fuhrmann M, Kateriya S, Musti AM, Bamberg E, Hegemann P (2002) Channelrhodopsin-1: a light-gated proton channel in green algae. Science 296:2395–2398

Nagel G, Szellas T, Huhn W, Kateriya S, Adeishvili N, Berthold P, Ollig D, Hegemann P, Bamberg E (2003) Channelrhodopsin-2, a directly light-gated cation-selective membrane channel. Proc Natl Acad Sci U S A 100:13940–13945

Nagel G, Brauner M, Liewald JF, Adeishvili N, Bamberg E, Gottschalk A (2005) Light activation of channelrhodopsin-2 in excitable cells of Caenorhabditis elegans triggers rapid behavioral responses. Curr Biol 15:2279–2284

Natasha G, Tan A, Farhatnia Y, Rajadas J, Hamblin MR, Peng T, Khaw P, Seifalian AM (2013) Channelrhodopsins: visual regeneration and neural activation by a light switch. New Biotechnol 30:461–474

Packer AM, Roska B, Häusser M (2013) Targeting neurons and photons for optogenetics. Nat Neurosci 16:805–815

Pfisterer C, Gruia A, Fischer S (2009) The mechanism of photo-energy storage in the halorhodopsin chloride pump. J Biol Chem 284:13562–13569

Prasher D, McCann RO et al (1985) Cloning and expression of the cDNA coding for aequorin, a bioluminescent calcium- binding protein. Biochem Biophys Res Comm 126:1259–1268

Ramsey AJ, Alderfer JL, Schuman Jorns M (1992) Energy transduction during catalysis by *Escherichia coli* DNA photolyase. Biochemistry 31:7134–7142

Reinbothe C, El Bakkouri M, Buhr F, Muraki N, Nomata J, Kurisu G, Fujita Y, Reinbothe S (2010) Chlorophyll biosynthesis: spotlight on protochlorophyllide reduction. Trends Plant Sci 15:614–624

Richie A, Johnson Z (2012) Abundance and genetic diversity of aerobic anoxygenic phototrophic bacteria of coastal regions of the Pacific Ocean. Appl Environ Microbiol 78:2858–2866

Riedel T, Gómez-Consarnau L, Tomasch J, Martin M, Jarek M, González JM, Spring S, Rohlfs M, Brinkhoff T, Cypionka H, Göker M, Fiebig A, Klein J, Goesmann A, Fuhrman JA, Wagner-Döbler I (2013) Genomics and physiology of a marine flavobacterium encoding a proteorhodopsin and a xanthorhodopsin-like protein. PLoS One 8(3):e57487. doi:10.1371/journal.pone.0057487

Rupert CS, Goodgal SH, Herriott RM (1958) Photoreactivation in vitro of ultraviolet inactivated *Haemophilus influenzae* transforming factor. J Gen Physiol 41:451–471

Sametz-Baron L, Berrocal TGM, Amit R, Herrera-Estrella A, Horwitz BA (1997) Photoreactivation of UV-inactivated spores of *Trichoderma harzianum*. Photochem Photobiol 65:849–854

Sarrou I, Khan Z, Cowgill J, Lin S, Brune D, Romberger S, Golbeck JH, Redding KE (2012) Purification of the photosynthetic reaction center from Heliobacterium modesticaldum. Photosynth Res 111:291–302

Sasaki J, Brown SLS, Chon Y-S, Kandori H, Maeda A, Needleman R, Lanyi JK (1995) Conversion of bacteriorhodopsin into a chloride ion pump. Science 269:73–75

Schmidt A (1914) Die Abhängigkeit der Chlorophyllbildung von der Wellenlänge des Lichtes. Beitr Biol Pflanz 12;269–296 (freely available at http://www.biodiversitylibrary.org/item/27490#page/294/mode/1up)

Schobert B, Lanyi JK (1982) Halorhodopsin is a light-driven chloride pump. J Biol Chem 257(17):10306–10313

Scrutton NS, Groot ML, Heyes DJ (2012) Excited state dynamics and catalytic mechanism of the light-driven enzyme protochlorophyllide oxidoreductase Phys. Chem Chem Phys 2012(14):8818–8824

Smith JHC, Kupke DW (1956) Some properties of extracted protochlorophyll holochrome. Nature 178:751–752

Strehler B, Arnold W (1951) Light production in green plants. J Gen Physiol 34:809–820

Sytina OA, Heyes DJ, Hunter CN, Alexandre MT, van Stokkum IHM, van Grondelle R, Louise Groot ML (2008) Conformational changes in an ultrafast light-driven enzyme determine catalytic activity. Nature 456:1001–1004

Sytina OA, Alexandre MT, Heyes DJ, Hunter CN, van Grondelle R, Groot ML (2011) Enzyme activation and catalysis: characterisation of the vibrational modes of substrate and product in protochlorophyllide oxidoreductase. Phys Chem Chem Phys 13:2307–2313

Sytina OA, van Stokkum IHM, Heyes DJ, Hunter CN, Groot ML (2012) Spectroscopic characterization of the first ultrafast catalytic intermediate in protochlorophyllide oxidoreductase. Phys Chem Chem Phys 14:616–625

Teranishi M, Nakamura K, Furukawa H, Hidema J (2013) Identification of a phosphorylation site in cyclobutane pyrimidine dimer photolyase of rice. Plant Physiol Biochem 63:24–29

Venema RC, Hug DH (1985) Activation of urocanase from Pseudomonas putida by electronically excited triplet species. J Biol Chem 260:12190–12193

Venema RC, Hunter JK, Hug DH (1985) In vivo role of sulfite in photocontrol of urocanase from Pseudomonas putida. Photochem Photobiol 41:77–81

Wada T, Shimono K, Kikukawa T, Hato M, Shinya N, Kim SY, Kimura-Someya T, Shirouzu M, Tamogami J, Miyauchi S, Jung K-H, Naoki Kamo N, Yokoyama S (2011) Crystal structure of the eukaryotic light-driven proton-pumping rhodopsin, *Acetabularia* rhodopsin II, from marine alga. J Mol Biol 411:986–998

Wang Z, O'Shaughnessy TJ, Soto CM, Rahbar AM, Robertson KL, Lebedev N, Vora GJ (2012) Function and Regulation of Vibrio campbellii Proteorhodopsin: Acquired phototrophy in a classical organoheterotroph. PLoS One 7(6):e38749. doi:10.1371/journal.pone.0038749

Waschuk SA, Bezerra AG Jr, Shi L, Leonid S, Brown LS (2005) Leptosphaeria Rhodopsin: bacteriorhodopsin-like proton pump from a eukaryote. Proc Natl Acad Sci U S A 102:6879–6883

Weber S (2005) Light-driven enzymatic catalysis of DNA repair: a review of recent biophysical studies on photolyase. Biochim Biophys Acta 1707:1–23

Yang J, Cheng Q (2004) Origin and evolution of the light-dependent protochlorophyllide oxidoreductase (LPOR) genes. Plant Biol (Stuttg) 6:537–544

Yasui A, Eker APM, Yasuhira S, Yajima H, Kobayashi T, Takao M, Oikawa A (1994) A new class of DNA photolyases present in various organisms including aplacental mammals. EMBO J 13:6143–6151

Yawo H, Asano T, Sakai S, Ishizuka T (2013) Optogenetic manipulation of neural and non-neural functions. Develop Growth Differ 55:474–490

Zhang F, Vierock J, Yizhar O, Fenno LE, Tsunoda S, Kianianmomeni A, Prigge M, Berndt A, Cushman J, Polle J, Magnuson J, Hegemann P, Deisseroth K (2011) The microbial opsin family of optogenetic tools. Cell 147:1446–1457

Zhang F, Scheerer P, Oberpichler I, Lamparter T, Krauß N (2013) Crystal structure of a prokaryotic (6–4) photolyase with an Fe-S cluster and a 6,7 dimethyl-8-ribityllumazine antenna chromophore. Proc Natl Acad Sci U S A 110:7217–7222

Molecules and Photochemical Reactions in Biological Light Perception and Regulation

12

Lars Olof Björn

12.1 Introduction

Many photochemical reactions involved in the sensing of and regulation by light and ultraviolet radiation by organisms consist of *cis–trans* (and *trans–cis*) isomerizations. We shall start with this class of photosensors and then go on to other mechanisms. There are many more known and unknown light-sensing molecular systems than those briefly described below, but (except for the first one) I have tried to concentrate on those more widespread. As examples of light-sensing pigments with a very limited distribution, one can mention stentorin and blepharismin of certain ciliates (Lenci et al. 2001).

The term "photoreceptor" means different things to different people. In zoology it refers to cells, which respond to light, such as the rods and cones of our eyes, but to plant scientists it means a pigment molecule, such as rhodopsin or phytochrome, which absorbs light at the start of a chain of events leading to light perception or regulation of a physiological process by light. We shall use the term here in this latter sense.

"Photoreceptor" in this sense is a concept related to "photoenzyme," i.e., an enzyme active only in light. A class of photoreceptors, the cryptochromes, are thought to have evolved from certain photolyases. Another photoenzyme, NADPH-protochlorophyllide oxidoreductase, can also be regarded as a photoreceptor, helping the plant to regulate chlorophyll synthesis and chloroplast development (Beale 1999).

L.O. Björn
Department of Biology, Lund University, Lund, Sweden

School of Life Science, South China Normal University, Guangzhou, China
e-mail: Lars_Olof.Bjorn@biol.lu.se

12.2 *Cis–Trans* and *Trans–Cis* Isomerization

Double bonds and conjugated double bond systems provide molecules with a certain rigidity. Molecular groups cannot rotate freely around double bonds or around single bonds in a continuous conjugation suite, as they can around isolated single bonds provided there is room enough. When a double bond is involved, there are two opposite torsion angles for which the energy has a minimum value and which thus represent stable conformations. Often the carbon atoms at the double bonds carry one hydrogen atom and one larger atomic group. These atoms then lie in the same plane, which is the same plane as the corresponding groups on the carbon atom at the other end of the double bond (in Fig. 12.1 this is the plane of the paper).

If the larger atomic groups are on the same side of the line through the double bond and the carbon atoms at its ends, the molecule is said to be in *cis*-configuration; if they are on opposite sides, the molecule has a *trans*-configuration. However, for larger molecules this designation may be difficult to apply, and another nomenclature has been introduced, i.e., Z- (for German *zusammen*, together) and E- (for German *entgegen*, opposite) configurations. In this system a priority is assigned for the atoms immediately attached to the double bond, such that higher priority is assigned to atoms of higher atomic number. Thus carbon atoms in the example in Fig. 12.1 have first priority, hydrogen atoms second priority.

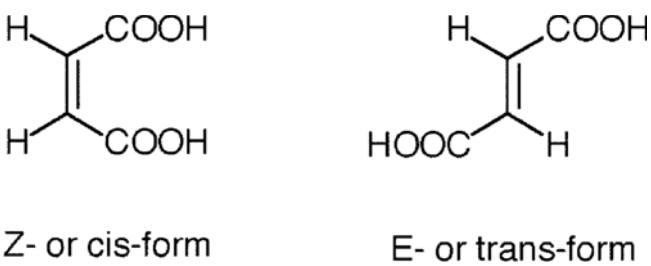

Fig. 12.1 A simple example of *cis–trans* isomerism

L.O. Björn (ed.), *Photobiology: The Science of Light and Life*,
DOI 10.1007/978-1-4939-1468-5_12, © Springer Science+Business Media New York 2015

When atoms of same priority are on the same side, we have a Z-configuration, otherwise an E-configuration.

By a very rough consideration, we can appreciate why *cis–trans* (E–Z) isomerizations are suitable for light sensing. A typical carbon–carbon single bond has a bond energy of 387 kJ per mole, while the typical double bond has a strength of about 610 kJ per mole. The difference is 263 kJ per mole. We can think of a rotation around a double bond to consist of the breaking of one of the bonds in the double bond, rotation around the remaining (single) bond, and reformation of a double bond. Thus one would need to add 263 kJ per mole (or 263,000/6.02 10^{23} J per molecule) to achieve the rotation. The energy of a photon is $h{\cdot}c/\lambda$ (see Chap. 1), and by equating the two energies, one obtains a typical wavelength for rotation of 455 nm, in the middle of the optical part of the electromagnetic spectrum to which the atmosphere is transparent. In rhodopsin of our rods the actual energy barrier for isomerization is 238 kJ/mol (Okada et al. 2001), but in different other photoreceptors based on *cis–trans* (or *trans–cis*) isomerization, the wavelength varies from the UV-B (for urocanic acid) to the near-infrared (for phytochrome) region. Some of the principles for this "tuning" are described in Chap. 9. In general the chromophores are bound to proteins, but we begin our account with *cis–trans* isomerization of a chromophore that is not bound to protein and is free to diffuse in the skin.

12.2.1 Simple Signaling Metabolites Undergoing *Cis–Trans* Isomerization

12.2.1.1 Urocanic Acid

Urocanic acid is present in the human skin, and photoisomerization from the *trans* to the *cis* form causes downregulation of the immune system (Chap. 24). This radiation-sensing reaction appears at first glance to be a very simple one: the pigment is structurally simple, of low molecular weight, and not protein bound. The isomerization seems to be a very simple reaction (Fig. 12.2).

But the simplicity is only apparent. The first indication of this is the fact that the action spectrum for photoisomerization is very different from the absorption spectrum of *trans-urocanic* acid. The absorption spectrum has a broadband peaking at about 280 nm, but radiation of this wavelength does not produce any photoisomerization, i.e., the quantum yield is zero at this wavelength. The quantum yield is maximal, 0.5, at 310 nm, where absorption is much weaker (also for the *cis* to *trans* isomerization, the quantum yield is about 0.5 at long wavelengths). Various theoretical explanations have been given for this strange behavior (Li et al. 1997; Hansson et al. 1997; Page et al. 2000; Ryan and Levy 2001), and the discussion is still going on. Urocanic acid is not the only substance which behaves in this way: cinnamic acid and related compounds have a quantum yield for *cis–trans*

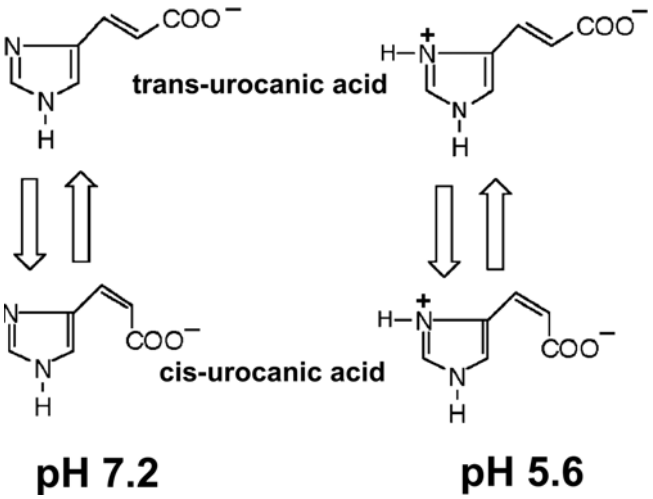

Fig. 12.2 Photoisomerizations of anionic and zwitterionic forms of urocanic acid. The *trans* form is also called E-urocanic acid, the *cis* form Z-urocanic acid

isomerization which is wavelength dependent (see the Sect. on 12.2.4 below).

Urocanic acid exists in several ionic forms depending on pH: at low pH as a cation, at slightly acidic pH in the skin as a zwitterion, and at neutral or higher pH as an anion. Spectra for both *trans* and *cis* forms peak near 280 nm in neutral solution, but near 270 nm at pH 5.6 (Morrison et al. 1980; Hansson et al. 1997; Li et al. 1997; Fig. 12.3).

Trans-urocanic acid is formed from histidine in the outermost layer of the skin, and after photoisomerization the *cis-urocanic* acid diffuses inward and acts on cells in deeper layers. The mechanism is uncertain. One view is that it interacts with a serotonin receptor (Walterscheid et al. 2006), a view that has been opposed by others (Prêle Finlay-Jone and Hart 2006).

Before we go on to proteins carrying chromophores that undergo *cis–trans* photoisomerization, a couple of other simple molecules should be mentioned.

12.2.1.2 Retinoic Acid

Retinoic acid occurs in the all-*trans* form as well as in a number of *cis*-stereoisomeric forms. All-*trans* retinoic acid binds more firmly to specific nuclear retinoic acid receptors (RARα, RARβ, RARγ) at low (nanomolar) concentrations and 13-*cis*-retinoic acid more weakly. Another group of nuclear receptors, retinoid-X receptors (RXRs), bind only to 9-*cis*-retinoic acid (Heyman et al. 1992; Teboul et al. 2008). Thus different stereoisomers can be expected to have different physiological effects, an expectation that has been experimentally confirmed. All-*trans* retinoic acid is involved in regulating the mammalian circadian clock and to influence the expression of a number of proteins within the "clock gene family" via RARα (e.g., Sherman et al. 2012), and RARα and RARγ exhibit circadian oscillation.

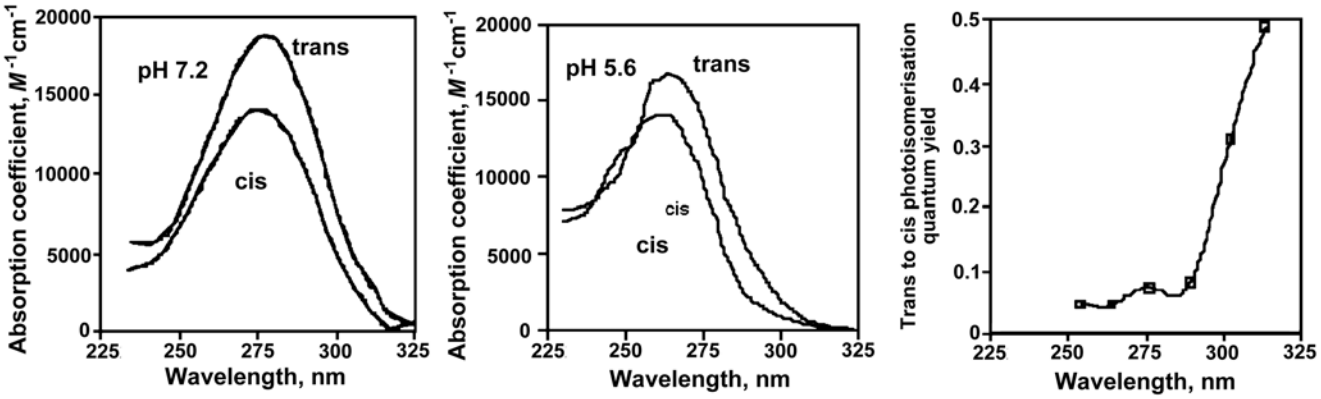

Fig. 12.3 Absorption spectra for *trans*- and *cis*-urocanic acid at pH 7.2 (redrawn after Hanson et al. 1997) and at pH 5.6 (redrawn after Morrison et al. 1980), as well as the quantum yield for *trans* to *cis* photoisomerization (from data of Morrison et al. 1984)

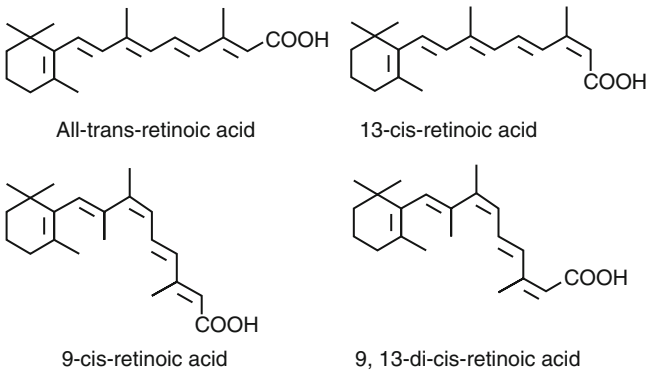

Fig. 12.4 Structures and absorption spectra of all-*trans*, 9-*cis*, and 13-*cis*-retinoic acids dissolved in methanol (Recalculated and drawn from data in Iole et al. (2005))

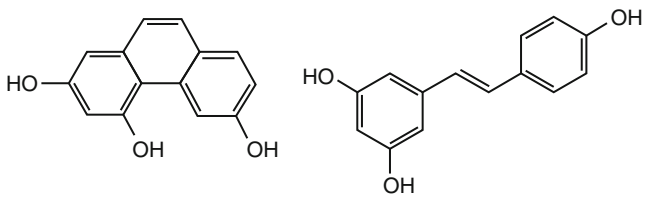

Fig. 12.5 *Cis*-resveratrol (*left*) and *trans*-resveratrol (*right*)

The different stereoisomers have different absorption spectra (Fig. 12.3), and therefore it is likely that the isomeric composition after irradiation with ultraviolet radiation depends on the spectrum of the radiation, but information about this available in the literature is very scant. Fu et al. (2003) report that irradiation of all-*trans* retinoic acid by fluorescent lamps resulted in five isomerization products (13-*cis*-RA, 11-*cis*-RA, 11,13-bis-*cis*-RA, 9-*cis*-RA, and 9,11-bis-*cis*-RA), all-*trans*-5,6-epoxyretinoic acid, and 13-*cis*-5,6-epoxyretinoic acid, see Fig. 12.4). Murayama et al. (1997) describe the light used only as 1200 lx white fluorescent light. They found that photoequilibrium in 10 mM ethanol solution is almost reached after 30 min with the following composition: all-*trans*-retinoic acid 25 %, 9-*cis*-retinoic acid 10 %, 11-*cis*-retinoic acid 10 %, 13-*cis*-retinoic acid 30 %, 9, 13-di-*cis*-retinoic acid 5 %, and unidentified compound 20 %. Several authors report that if oxygen is present, also photooxidation takes place. The situation in vivo is, however, more complicated, since retinoic acid occurs not only free but also bound to various other molecules, which probably affects phototransformation.

Ultraviolet radiation does not penetrate far into the human body, so phototransformation of retinoic acid can take place only in the skin and eyes (and in preparations containing retinoic acid applied to the skin; see Fu et al. 2003). Kunchala et al. (2000) as well as Hellmann-Regen et al. (2013), based on experiments with skin cell cultures, speculate that the light from traditional fluorescent lamps and especially compact fluorescent light bulbs may disrupt normal regulation by photoisomerization of all-*trans*- to mainly 13-*cis*-retinoic acid. As retinoic acid is applied for the treatment of acne, photoisomerization may have some effect in this context.

Retinoic acid is, however, used as a regulator throughout the animal world (Albalat 2009), and as in mammals different isomers perform different functions. Photoisomerization may have a great impact in small animals, such as sea urchin embryos (Maeng et al. 2012), hydrozoan larvae (Pennati et al. 2013), and insect larvae (Chen et al. 2010).

12.2.1.3 Resveratrol

Resveratrol is a stilbene derivative that can exist in *cis* or *trans* forms (Figs. 12.5 and 12.6). It is not synthesized by animals. Of the two stereoisomers of resveratrol, the *trans* isomer is the most stable one and the most abundant one in nature, but both coexist in different proportions in wine and foods (Álvarez Rodriguez et al. 2012) and especially in high amounts in red wine. It is considered to have a number of health-promoting effects in man (Kalantari and Das 2010). The *trans* form is in general more physiologically active, for

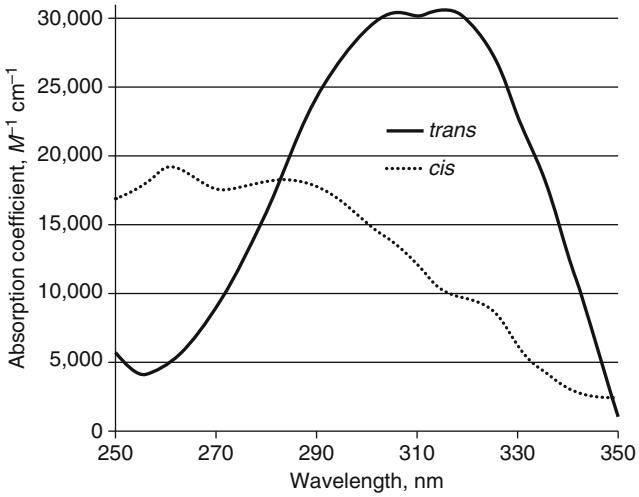

Fig. 12.6 Absorption spectra for *cis*- and *trans*-resveratrol. Calculated from data of Figueiras et al. 2011

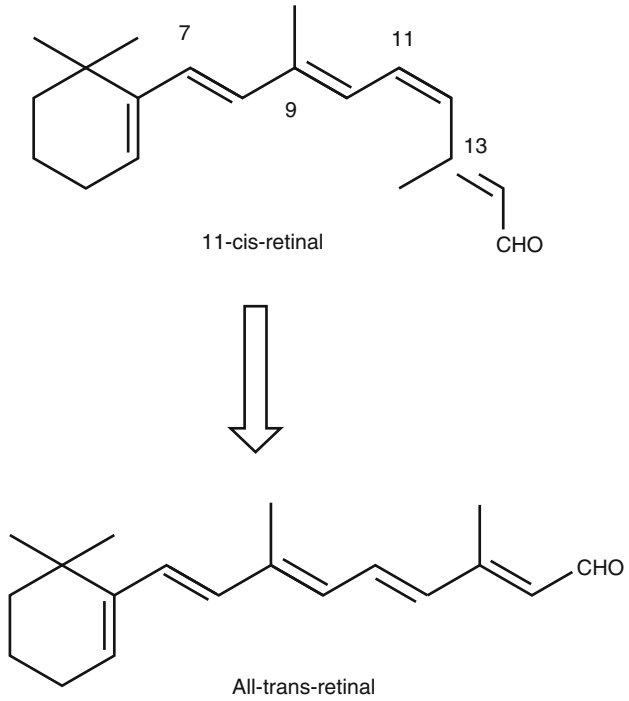

Fig. 12.7 Photoisomerization of the isolated retinal chromophore

instance, as an antiproliferative and antiinflammatory agent, than the *cis* form (Anisimova et al. 2011; Kim and Oh 2011; Rius et al. 2010), and is the form enzymatically synthesized in plants, but ultraviolet radiation partially converts it to the *cis* form (even in the plant) and so decreases the amount of the form active in the human body.

12.2.2 Eukaryotic Rhodopsin

When we see the word rhodopsin, our thoughts first go to the light-sensitive pigment of the rods in our own eyes. Very similar pigments, however, are present also in our cones and in the eyes of various insects, mollusks, and other animals. Recently it has been discovered that essentially the same type of pigment also occurs in various algae (Foster et al. 1984; Hegemann and Deininger 2001; Gualtieri 2001). Several types of archaea (archaebacteria) contain a kind of rhodopsin, but the latter is sufficiently different, both with respect to the chromophore and the protein structure, to warrant treatment in a separate section (Sect. 12.2.3). Both eukaryotic and archaean rhodopsins, however, are membrane bound and have seven membrane-spanning helices in the molecule. It should also be noted that there are eukaryotes which have proteins more similar to the archaean than to typically eukaryotic rhodopsin.

The chromophore of rhodopsin is retinal (in some animals dehydroretinal; see Chap. 9). We show it first in isolated form (Fig. 12.7) to display in a simple way the phototransformation from the 11-*cis* form to the all-*trans* form, corresponding to the primary process of vision. The side chain changes from a bent to a straight form. In rhodopsin the terminal carbon atom of retinal polyene chain is covalently tethered to a lysine side chain (lysine 296) of the protein (Fig. 12.7), forming a "Schiff base" in its protonated form. The counterion for the positive charge is formed by glutamine 113. The protein forms an antiparallel β-sheet in the vicinity of the chromophore, bringing the side chain of another amino acid (position 181) in close contact to the polyene chain of retinal. In our rod rhodopsin this amino acid is glutamine; in the red- and green-sensitive pigments of our cones, it is histidine.

When light isomerizes the rhodopsin-bound retinal from 11-*cis* to all-*trans*, the polyene chain cannot at once straighten out completely, because the straight chain does not fit in the protein pocket (see Okada et al. 2001 for a more detailed review of the events than the one given here). This restraint makes the retinal store energy, like a cocked spring. About two thirds of the photon energy is thus stored in the initial phase. Probably it is mainly the proximity of serine 186 that prevents the retinal from immediately reaching its *trans* equilibrium position. This intermediate stage is termed bathorhodopsin. Within microseconds the proton on the Schiff base is translocated to glutamine 113, whereby the attractive force between the two parts of the protein disappears and the protein helices can adjust their relative positions to allow the retinal to straighten out completely. This brings the rhodopsin to a low-energy state called metarhodopsin I. From this the rhodopsin, within a millisecond, changes to metarhodopsin II. This has higher energy than metarhodopsin I, and the transformation is made possible by a simultaneous increase in entropy: the forces between different parts of the

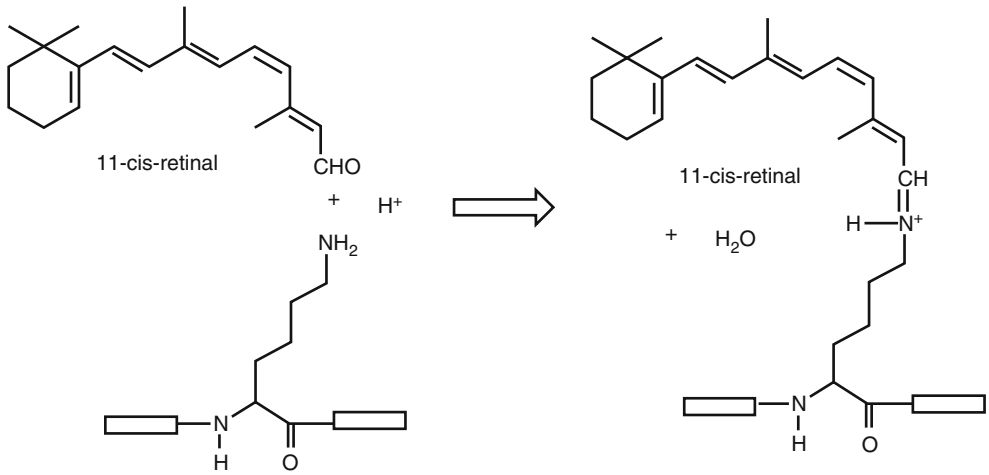

Fig. 12.8 The binding of retinal to a lysine side chain in the rhodopsin protein, forming a protonated Schiff base. Rectangles symbolize amino acids of the opsin

protein are decreased, and the different parts can move more freely with respect to each other. The process has some similarities to the melting of ice, and we may recall that the free energy change (ΔG) of a system consists of the change in total energy (enthalpy, ΔH) minus an entropy term, TΔS. In the transformation from metarhodopsin I to metarhodopsin II, the free energy is thus decreased even though the total energy increases. In this respect eukaryotic rhodopsin resembles photoactive yellow proteins (Sect. 12.2.4), but differs from archaean rhodopsins (Sect. 12.2.3). The transition also involves uptake of a proton (Fig. 12.8).

Metarhodopsin II is the "signaling state" of rhodopsin. By its formation groups are exposed which can interact with a protein called transducin, a so-called G protein, and thus make the transition from a biophysical to a biochemical phase of the signal transduction. The activated transducin activates phosphodiesterase which hydrolyzes cyclic guanosine monophosphate (cGMP). When the concentration of cGMP has fallen sufficiently, sodium ion channels in the membrane close, the electric membrane potential increases, and an electrical impulse is sent on to the nervous system.

Recently a new light-sensitive system has been discovered in vertebrates (Provencio et al. 1998; Barinaga 2002; Berson et al. 2002; Hattar et al. 2002). The start in this new development came with the study of how frogs can adjust their skin color by changing the size, shape, and position of the pigment-containing cells in their skin, the melanophores (Provencio et al. 1998). It turned out that the skin cells contained a light-sensitive pigment which was named melanopsin. The same pigment was found also in the frog's retina, as well as in mouse retinas. However, it is not in the rods (or cones), but in cells, retinal ganglion cells, inside (in the front of) the visual receptors. Some of these cells have nerve connections, not to the brain areas involved in vision, but to the suprachiasmatic nuclei where the main clock of the body (see Sect. 18.1.5) is thought to reside. The logical conclusion is that melanopsin is involved in the resetting of the biological clock by light. However, some of the melanopsin-containing retinal ganglion cells have connections to the part of the brain regulating pupil size in response to light. Melanopsin-containing cells, in contrast to the rods and cones, do not adjust their sensitivity in response to light level. They are therefore suited to record the light level, which is important, e.g., in photoperiodism and pupil size regulation. Although the melanopsins studied so far occur in vertebrates, their protein structure is more closely related to that of invertebrate opsins than to the vertebrate opsins of the rods and cones. Their photochemical reactions have so far not been studied in detail but are thought to be similar to those of rhodopsins.

12.2.3 Microbial Rhodopsins

Four types of archaean and bacterial rhodopsins are known. In contrast to the eukaryotic rhodopsins, they all contain all-trans retinal as the chromophore, and the photochemical step consists of its isomerization to 13-*cis* retinal. In some cases also the reverse reaction has some importance.

Many species within the Haloarchaea (the subdivision of Archaea formerly referred to as halobacteria) have been investigated, (Spudich 2001) but only four distinct types have been found, which are all present in species of the best investigated genus, *Halobacterium*. One of these rhodopsins, called bacteriorhodopsin (BR, Fig. 12.9), uses light energy to pump hydrogen ions out of the cells, and another one, called halorhodopsin (HR), pumps chloride ions into the cells. Both reactions contribute to making the inside of the cells negative, thus allowing the cells to accumulate cations at the expense of light energy. The light-driven export of protons also creates the proton motive force necessary for ATP synthesis and, indirectly, the free energy necessary for swimming and biochemical syntheses. BR and HR are induced only under low oxygen tension, while under high oxygen tension, the organisms can utilize oxygen for creation of the necessary free energy.

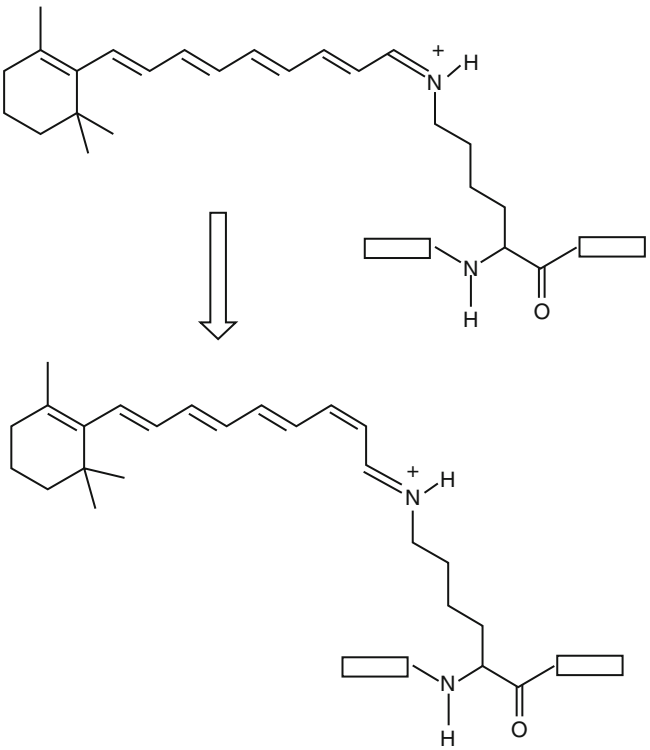

Fig. 12.9 The *trans–cis* isomerization of the chromophore in bacteriorhodopsin. As in Fig. 12.6, the *rectangles* symbolize amino acids of the opsin. The rapid *trans–cis* photoisomerization is followed by slower rearrangements of the opsin structure and movements of protons

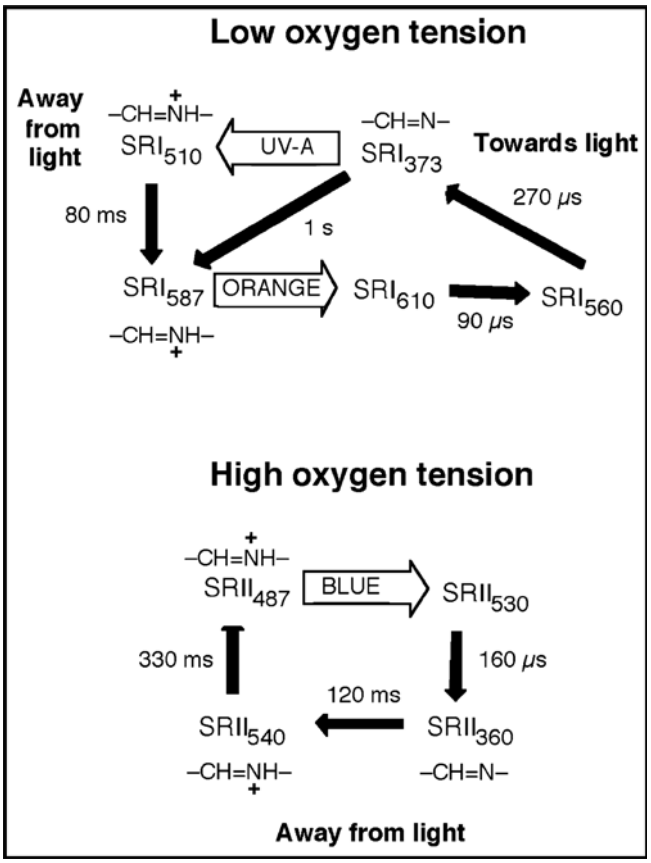

Fig. 12.10 The photocycles of sensory archaeal rhodopsins. Under low oxygen tension (*top*) *Halobacterium* and related organisms form bacteriorhodopsin and halorhodopsin, which pump ions, and sensory rhodopsin I (*SRI*). The latter is used to find a suitable light environment. As long as light is not very strong, the *orange light*-sensing reaction causes accumulation of the long-lived intermediate SRI373, which is a signaling state causing the organisms to move toward stronger light. If the UVA light becomes too strong, the UVA-sensing reaction causes conversion to SRI510, a signaling state which causes movement away from the strong light. In the presence of a high concentration of oxygen (*bottom*), only SRII is induced. The *blue-light*-sensitive reaction causes movement away from light. Like other nonoxygenic pigmented organisms, these are probably much more light sensitive in the presence of oxygen due to the possibility of formation of reactive oxygen species under illumination. As indicated in the figure, in some pigment forms the Schiff base is protonated, in other forms not (After Hoff et al. 1997, modified)

The two remaining archaerhodopsins, designated SRI and SRII (SR for sensory rhodopsin, Fig. 12.10), are used by the halobacteria to orient with respect to light. SRI is induced only under low oxygen conditions, SRII only under high.

SRI, formed under low oxygen conditions, has two signaling states. One, SRI_{373}, formed by the orange component of weak daylight, causes the cells to move toward stronger light. This is not due to direct sensing of light direction as in the topophototaxis of eukaryotic flagellates, but by modulation of the frequencies of spontaneous reversals of swimming direction. If the light becomes very strong, another signaling state, SRI_{510}, is formed under the action of the UVA component of daylight. This causes the cells to move toward weaker light.

Under high oxygen tension SRII, but not SRI (neither HR nor BR), is induced. SRI mediates only a light-avoiding signal.

SRI and SRII do not engage a signal-transmitting protein during only part of the photocycle (as eukaryotic rhodopsin engages transducin). Instead each one of them is permanently attached to its signal-transmitting protein, HtrI or HtrII, respectively. Obviously the conformational change in the rhodopsins caused by the photoisomerization of the chromophore is somehow transmitted to the signal-transmitting protein, but the details of this are not known.

12.2.4 Photoactive Yellow Proteins (PYPs, Xanthopsins)

Photoactive yellow proteins (PYPs) function as photoreceptors in purple bacteria, mediating negative phototaxis. One might think that this is too humble a function to warrant

treatment in a book like this one, but PYP happens to be one of the best-known photoreceptor pigments, and we can learn some more general principles from it. PYPs are also referred to as xanthopsins, although this term is misleading, since the proteins are not opsins. Three photoreactions shuttle the pigment between several forms, as shown in Fig. 12.11.

The PYP chromophore is *trans*-4-hydroxy cinnamic acid, and light causes photoisomerization to the *cis* form (Fig. 12.12). This initial reaction is followed by rotation of one half of the molecule with respect to the other around a single bond. Genick et al. (1997, 1998) have succeeded in following in detail the changes in the protein structure associated with these changes (Fig. 12.13). They managed to crystallize the protein and by time-resolved x-ray crystallography at low temperature captured the structure of the otherwise extremely short-lived (nanoseconds) intermediate.

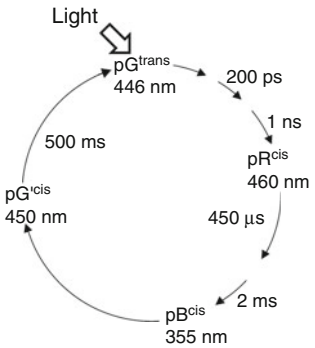

Fig. 12.11 The photocycle of PYP, simplified from Naseem et al. (2013) and other sources. There is no consensus regarding intermediates, transformation pathways, or reaction rates

By conversion to the signaling state, forces between different parts of the protein are weakened. It becomes more flexible, and the conversion can be likened to "melting," just as in the case of animal rhodopsin.

PYP is interesting also because it contains the prototype for a "PAS domain" (Pellequer et al. 1998). By this we mean a protein structure that occurs in many other signaling proteins (Taylor and Zhulin 1999), including some other photoreceptor proteins: phytochrome, phototropin (Salomon et al. 2000; Christie and Briggs 2001), and a blue-light receptor in the fungus *Neurospora* (Ballario and Macino 1997). PAS domains have been identified in proteins from all types of organisms: Archea, Bacteria, and Eucarya. It comprises a region of 100–120 amino acids. They seem to occur almost exclusively in sensors of two-component "phosphorelay" regulatory systems. The activation of a PAS protein, by either the photoconversion of a chromophore, binding of an external activator, or voltage sensing (as in some proteins regulating voltage-sensitive ion channeling), seems to involve the exposure of the PAS domain and initiation of protein kinase activity (either histidine kinase or, as in the case of phytochrome, serine/threonine kinase).

12.2.5 Phytochrome

The discovery of phytochrome is one of the classical detective stories of plant science (Butler 1980; Björn 1980b; Sage 1992). It started with the discovery that some effects of red light, such as the germination of seeds, photomorphogenesis of etiolated plants, and the inhibition of flowering in short-

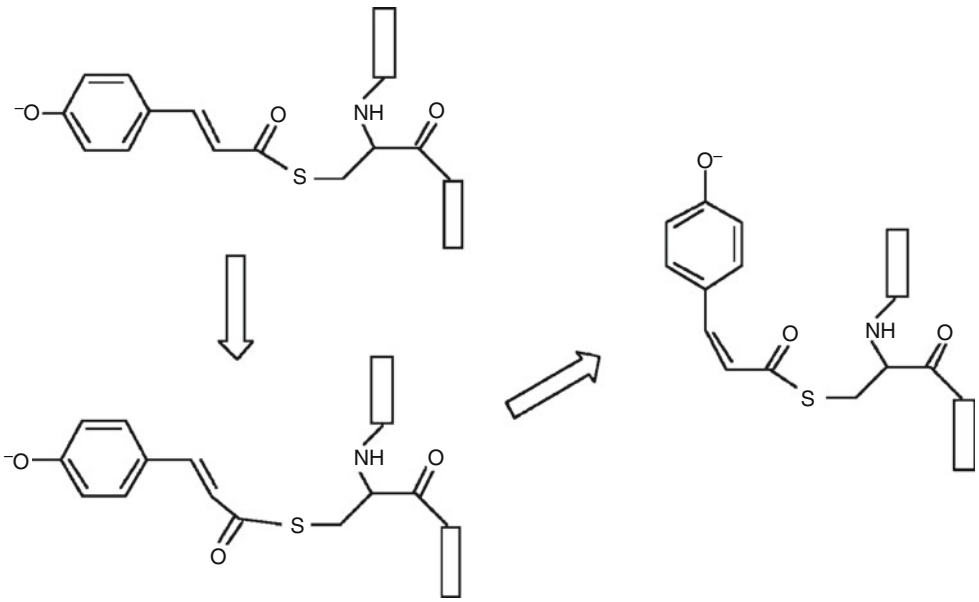

Fig. 12.12 A sketch of change of the PYP chromophore structure in two steps. The *rectangles* symbolize part of the protein. The cystine residue which forms a thioester linkage with the cinnamic acid is outlined. Only the first step requires photon absorption and at physiological temperature is complete in a few nanoseconds. The second step takes several milliseconds

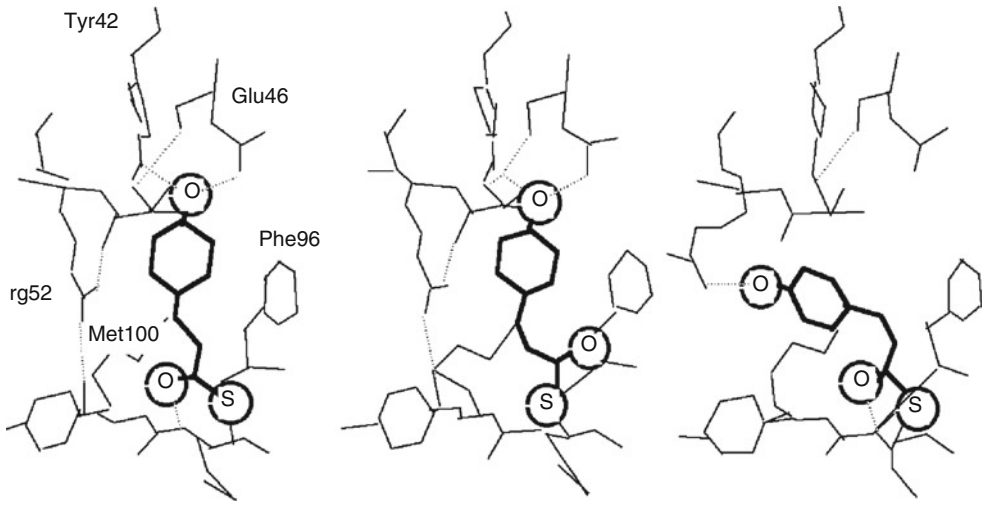

Fig. 12.13 Changes in PYP induced by light. Shown to the *left* is the region around the chromophore before light absorption. The chromophore skeleton is outlined in *bold*, with oxygen and sulfur atoms indicated. Amino acid skeletons are outlined with *thin lines. Dotted lines* stand for noncovalent interactions (hydrogen bonds). In the center is the intermediate structure a few nanoseconds after light absorption. The *trans–cis* isomerization of the chromophore has taken place, and its tail has flipped over, but the ring is still in its original position, with hydrogen bonds to the upper oxygen still intact. To the *right* is the "signaling state" reached after several milliseconds. The chromophore is still in its *cis* state, but the whole chromophore has changed position, broken the original hydrogen bonds to the ring-attached oxygen atom, and formed a new hydrogen bond. By these rearrangements both the chromophore and the PAS domain of the protein become accessible from the outside (Based on Genick et al. 1998)

day plants, could be reversed by irradiation with light of longer wavelength, the so-called far-red light (700–740 nm). By accurate action spectroscopy (see Sect. 8.5) the spectral properties of two different pigment forms were defined, and this made possible the detection in plants by absorption spectrophotometry and the subsequent purification of phytochrome.

It is now known that plants contain several phytochromes with different properties and regulatory roles. This is not the place to describe this in detail, and the reader is referred to chapters in this volume on photomorphogenesis and photoperiodism in plants (Chap. 19) and on the biological clock and its resetting by light (Chap. 18).

Phytochrome or phytochrome-like proteins have also been found in various algae, a myxomycete, cyanobacteria, and other photosynthetic and nonphotosynthetic bacteria (Schneider-Poetsch et al. 1998; Davis et al. 1999; Jiang et al. 1999; Herdman et al. 2000; Lamparter and Marwan 2001; Hubschmann et al. 2001; Bhoo et al. 2001).

Phytochrome is synthesized by the plant in the red-absorbing form, called Pr, and can be converted, via several intermediates, to the far-red-absorbing form by red light or direct daylight. It is the far-red-absorbing form that is considered to be the active (signaling) state, but in some cases one or several intermediates may be active. The reverse conversion (via another set of intermediate states) can take place under far-red light, under daylight filtered through vegetation or soil, or (with some phytochrome types and more slowly) in darkness. A pigment that changes its absorption spectrum in light (without being destroyed) is called photochromic; phytochrome is said to be photoreversibly photochromic, since the original state can be restored by another kind of light.

The chromophore in phytochrome has generally been believed to be an open-chain tetrapyrrole (see Fankhauser 2001), phytochromobilin (Fig. 12.14). Hanzawa et al. (2002) discuss other possibilities, such as the related phycocyanobilin, the same chromophore as is present in the photosynthetic antenna pigments phycocyanin and allophycocyanin of cyanobacteria and red algae. Phycocyanobilin is also the chromophore in cyanobacterial phytochrome, while those phytochromes of nonphotosynthetic bacteria that have been investigated so far have biliverdin as chromophore (Bhoo et al. 2001).

An interesting optical property of phytochrome is that conversion from Pr to Pfr or vice versa results in rotation of the transition moment corresponding to the long-wavelength absorption band with respect to the bulk of the protein. This was first shown by Etzold (1965) and Haupt (1970) by in vivo linear action dichroism and later confirmed by various methods (Sarkar and Song 1982; Kadota et al. 1982; Sundquist and Björn 1983a; b; Tokutomi and Mimuro 1989). At first it was believed that the rotation amounts to 90°, but the newer experiments and reinterpretation of the old in vivo experiments (Björn 1984) point to a smaller angle. Based on this and other evidence, Rospendowski et al. (1989) produced

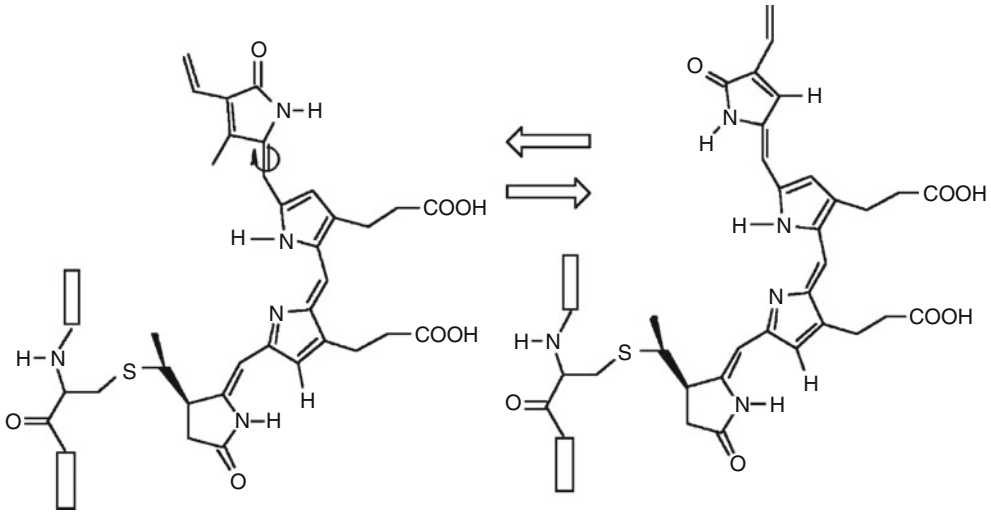

Fig. 12.14 The chromophore of higher plant phytochrome A (phytochromobilin) in the Pr (*left*) and Pfr (*right*) forms. The *rectangles* symbolize amino acid residues in the protein. The *circular arrow* indicates the double bond at which the pyrrole group to the right rotates during photoisomerization. Phytochrome B may contain the very similar phycocyanobilin as chromophore, in which the double bond and CH_2 group pointing straight up on top of the right-hand formula is replaced by a single bond and a CH_3 group, and phytochromes in nonphotosynthetic bacteria contain biliverdin

a drawing of how the chromophore moves in the protein during conversion.

Phytochrome in solution is a dimer (Jones and Quail 1986), and there is evidence that it is also dimeric in vivo. Like many other sensors it has a PAS domain (see Sect. 12.2.4.) and is an autophosphorylating protein kinase (Boylan and Quail 1996; Watson 2000).

12.2.6 Photosensor for Chromatic Adaptation of Cyanobacteria

Many cyanobacteria have the ability to adjust the amounts of the photosynthetic antenna pigments phycocyanin (red-absorbing) and phycoerythrin (green-absorbing) according to the spectrum of ambient light. This regulation process is known as chromatic adaptation, although with present-day definitions it would more appropriately be called chromatic acclimation. Long ago action spectroscopy revealed that the photoreceptor for chromatic adaptation in cyanobacteria must be a phycobiliprotein (Fujita and Hattori 1962; Lazaroff and Schiff 1962; Diakoff and Scheibe 1973; Vogelmann and Scheibe 1978), just like phytochrome. From cyanobacterial antenna pigments several photochromic chromopeptides can be prepared (Scheibe 1962; Björn 1980a; Fig. 12.15).

A new start on an old problem has been made from the other end at the Department of Plant Biology of the Carnegie Institution of Washington. The recent work has been reviewed by Grossman et al. (2001). Kehoe and Grossman (1996) found a gene, rcaE, coding for the protein RcaE, which is necessary for chromatic adaptation. RcaE binds a

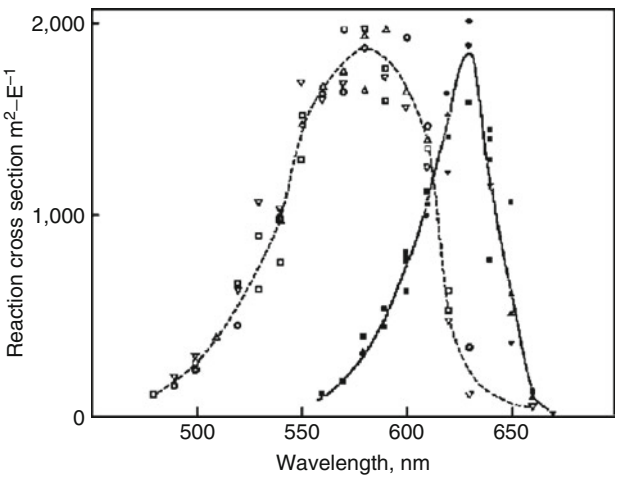

Fig. 12.15 Action spectra for conversions of phycochrome c to the short-wavelength form (*solid line* and filled symbols) and to the long-wavelength form (*dashed line*, empty symbols) (From Björn and Björn 1978). Somewhat similar action spectra were also obtained for phycochrome a, another polypeptide from phycocyanin (G.S. Björn 1980a)

tetrapyrrole chromophore covalently in a domain similar to that of phytochromes and also has a PAS domain typical for signal sensing proteins. It is believed that the chromophore is phycocyanobilin, which would fit well with the old spectral observations. According to the theory proposed by Grossman et al. (2001), there are, in addition to RcaE, two other proteins, RcaF and RcaC, involved in the signaling for chromatic adaptation. Under red light, RcaE autophosphorylates and transfers a phosphate group via RcaF to RcaC. In RcaC there are two sites that can be phosphorylated, and the one active

in this context is near the N-terminal (the role of the other site is unclear). This chain of events results in increased phycocyanin production. Green light, on the other hand, causes RcaE to change to the nonphosphorylating conformation, resulting in phycoerythrin synthesis. Kehoe and Gutu (2006) and Montgomery (2007) point out that chromatic adaptation in cyanobacteria is more complex than formerly believed and involves at least three signaling pathways: in addition to the phytochrome-type Rca system with separate effects of red and of green light, the Cgi ("controlled-by-green-light") system. Some cyanobacteria can acclimate to far-red light by a different mechanism (Gan et al. 2014).

12.2.7 Violaxanthin as a Blue-Light Sensor in Stomatal Regulation

Stomata are adjustable valves in the outer layer (epidermis) of leaves and other photosynthetic plant organs. They are designed to let sufficient carbon dioxide in from the external air without causing the plant to dry out due to outward diffusion of water vapor. Their regulatory system senses the water status, both directly in the leaves and indirectly in the rest of the plant body via the hormone abscisic acid. It also senses the internal carbon dioxide concentration. It senses light in several ways. One indirect way is via photosynthesis, since this causes the internal carbon dioxide concentration to fall. But the fastest and most dramatic light effect is blue-light specific, and there seems to be another light-sensing molecule involved than the cryptochromes and phototropins dealt with in the next section: the xanthophyll zeaxanthin (see Zeiger 2000 and Assman and Wang 2001 for reviews).

The strongest evidence for participation of zeaxanthin as a blue-light sensor of stomata is the fact that the stomata of an *Arabidopsis* mutant, npq1, which lacks a functional violaxanthin deepoxidase and therefore cannot accumulate zeaxanthin, does not show a blue-light-specific response (Frechilla et al. 1999). On the other hand, mutants defective in cryptochromes 1 or 2 or phototropin 1 have a normal response. However, there is also evidence of several independent blue-light channels for stomatal regulation (Lasceve et al. 1999) and that violaxanthin is only one of the sensors.

Violaxanthin has nine double bonds, so there are many possibilities for *cis–trans* isomerizations. Such a photoisomerization has not been directly shown, but postulated from kinetic experiments and the fact that the blue-light effect can be reversed by green light (Iino et al. 1985; Frechilla et al. 2000). The reversal spectrum has peaks at 490, 540, and 580 nm, similar to a wavelength-shifted zeaxanthin spectrum. We would like in this context to mention several experiments in the 1960s and 1970s in which blue-light effects in algae were reversed by light of longer wavelength (see Björn 1979 for a review).

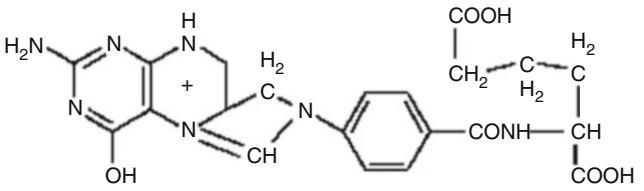

Fig. 12.16 N5, N10-methenyl-5,6,7,8-tetrahydrofolic acid, one of the chromophores in cryptochrome, probably acting as an antenna pigment for the other chromophore, FAD

12.3 Other Types of Photosensors

12.3.1 Cryptochromes

The term cryptochrome has been in use for a long time in plant physiology, as a name for the unknown blue-light photoreceptor. The name derives from the fact that it was hiding for such a long time (Björn 1980b). Now it is known that there are at least two quite different types of blue-light receptors in plants, called cryptochromes (cry1 and cry2) and phototropin. Thus the term has acquired a more restricted meaning than it used to have. On the other hand it has recently been discovered that chromoproteins similar to the plant cryptochromes are present also in other organisms than plants, including humans. These proteins are also called cryptochromes, but may have arisen independently during evolution (Todo et al. 1996). Recent reviews covering both cryptochromes and phototropins are provided by Lin (2000) and Christie and Briggs (2001). Regarding the effect of magnetic fields on cryptochromes, see Chap. 20 and Ahmad et al. (2007).

In plants cry2 represses phytochrome B action and plays a role in photoperiodism. cry1 regulates the period of the biological clock and is involved in the entrainment of the circadian oscillator (see Christie and Briggs 2001 for references).

Cryptochromes have two chromophores: 5,10-methenyltetrahydrofolic acid (Fig. 12.16) and flavin adenine dinucleotide (FAD). The latter is noncovalently bound to the protein. The role of the former is not known; probably it acts as an antenna pigment (in analogy with antenna pigments in photosynthesis) and transfers absorbed light energy to FAD, as is the case for the related photolyases.

The FAD part undergoes at least partial reduction upon illumination. The semiquinone formed by light action on cry1 has a long lifetime and seems to be able to act as a chromophore, too, giving the cryptochrome a sensitivity to green light under some circumstances. It has long been known that various blue-light effects in plants and fungi, in experiments designed to determine action spectra, are not parallel in log fluence vs. effect diagrams (see, e.g., Shropshire and Withrow (1958). The explanation may be this light sensitivity of the semiquinone or the participation

of several photoreceptors (such as the two cryptochromes, phototropin, and phytochrome) in the effects studied.

The signal transduction chains associated with cryptochromes have been difficult to elucidate, not only because more than one cryptochrome probably act in different ways but because plants have another blue-light receptor (phototropin) and because there are interactions with phytochrome. However, one signaling pathway proved surprisingly simple (Wang et al. 2001). In the dark, a protein called COP1 present in the nucleus prevents the activity of several genes by preventing the action of their transcription factors. After photoactivation of cryptochromes, their conformation is changed so they can bind to COP1 and prevent its action, thereby activating the genes.

Apart from their roles in the cell nucleus related to rhythmicity and gene regulation, cryptochromes seem to have direct effects on membranes. Thus cry1 activates an anion channel in the cell membrane and thereby influences the membrane potential. As for the mechanism of action, there is so far hardly more than speculation. Flavins are known to mediate light-driven electron transfer in other cases, but this has not been shown for cryptochromes. One indication for a role of electron transfer is the similarity between cryptochromes and photolyases. Merrow and Roenneberg (2001) speculate about relations between redox potential, cryptochromes, and the mechanism of the circadian oscillator.

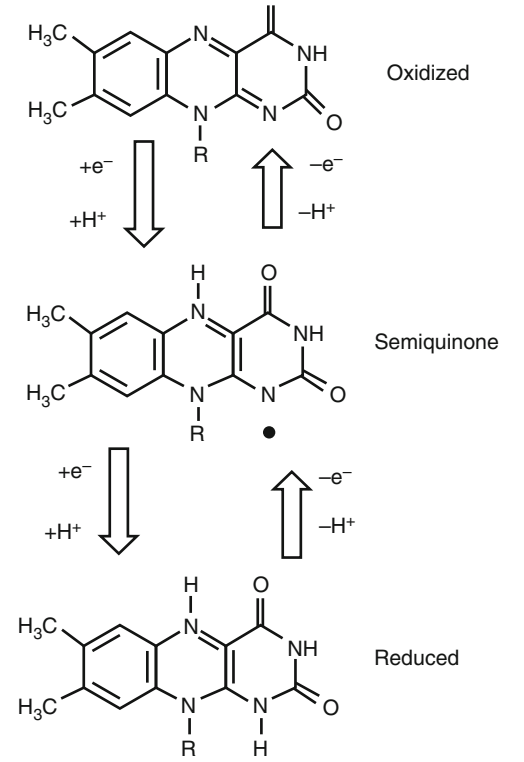

Fig. 12.17 The structures of FMN and FAD in oxidized and reduced forms and in the half-reduced (semiquinone) form

12.3.2 Phototropin

Phototropin is the photoreceptor primarily involved in plant phototropism, the phenomenon which, beginning with Darwin, has meant so much for stimulating interest in research in plant photobiology and about plant hormones. However, cryptochromes and phytochrome are also involved in the very complex phenomenon of phototropism (Galland 2001; Iino 2001). On the other hand, phototropin is involved in other blue-light reactions, such as high- and low-light-induced chloroplast movements (Sakai et al. 2001; Jarillo et al. 2001; Kagawa et al. 2001) and inhibition of hypocotyl extension growth (Folta and Spalding 2001). So far two main types of phototropin, phot1 and phot2 (Briggs et al. 2001), have been identified, of which phot1 acts primarily in phototropism, phot2 primarily in chloroplast photomovement.

Phototropin, like the cryptochromes, is a flavoprotein, and it also has two chromophores per molecule. In the phototropin, however, both chromophores consist of covalently bound flavine mononucleotide (FMN, Fig. 12.17). The protein part is quite different from that of the cryptochromes. The chromophore-binding regions are the so-called PAS domains, designated LOV1 and LOV2 (Salomon et al. 2000; Christie and Briggs 2001). (LOV stands for *l*ight, *o*xygen, or *v*oltage regulated.) The properties of these two domains can be investigated separately using molecular biology techniques. The absorption spectra of both show a striking (and expected) similarity to the action spectra for phototropism determined long ago (Fig. 12.18).

Upon illumination the chromophores, in both the LOV1 and LOV2 domains, undergo a spectral shift (Fig. 12.19); the absorbance in the blue region decreases, while that in the UVA part of the spectrum changes only little. Illumination also causes quenching of the fluorescence. In darkness both LOV1 and LOV2 return to the original state with halftimes at room temperature of 11.5 and 27 s, respectively. By amino acid substitution it has been made likely that the spectral change is caused by the formation of a bond between cystine (Cys39) and the FMN chromophore, with simultaneous reduction of the flavin (Fig. 12.20). This was confirmed by other methods (Crosson and Moffat 2001). The C-terminal end of phototropin is a serine/threonine kinase, which supposedly is activated by a conformational change resulting from the light-induced change in the chromophore region. The detailed structure of the LOV2 domain has now been determined and compared to other PAS domains (Crosson and Moffat 2001).

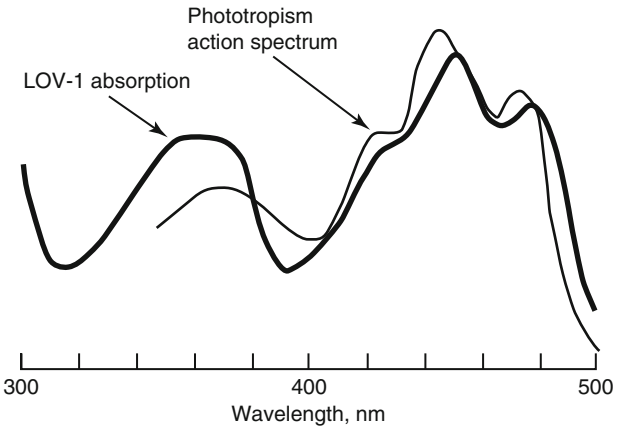

Fig. 12.18 Comparison of the action spectrum for phototropism of oat coleoptiles determined by Thimann and Curry (1961) with the absorption spectrum of the LOV1 protein domain of phototropin of an oat mutant determined by Salomon et al. (2000). The spectra for both LOV1 and LOV2 of the native oat are very similar, although not identical

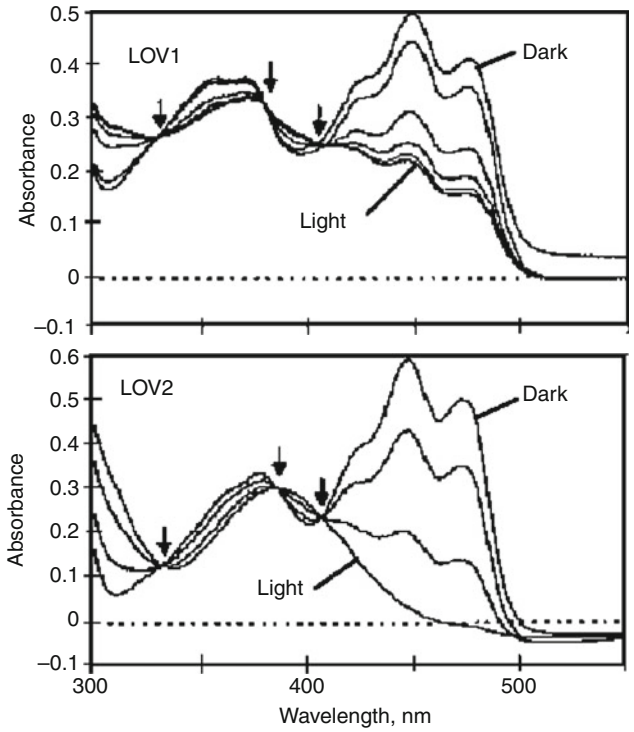

Fig. 12.19 Light-induced spectral changes taking place in the LOV1 and LOV2 domains of phototropin upon illumination. The *arrows* point to isosbestic points (wavelength positions with unchanged absorbance) (Reprinted, slightly modified, with permission from Salomon et al. 2000)

Red-light effects and blue-light effects in plants have traditionally been investigated by different sets of researchers, and there have been red-light meetings and blue-light meetings. It has become more and more difficult to uphold such a segregation as more and more interactions between the

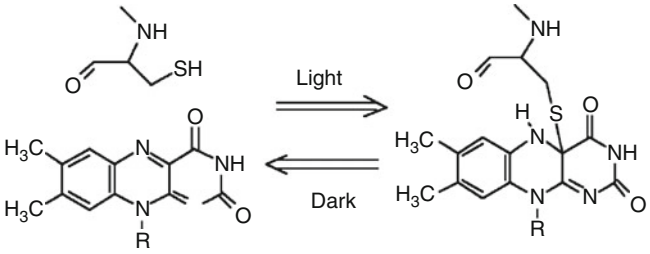

Fig. 12.20 The proposed light-induced, dark-reversible bonding between FMN and the cysteinyl residue in phototropin (Redrawn and simplified from (Crosson and Moffat 2001))

signaling channels have been discovered (Mohr 1994; Neff and Chory 1998; Parks et al. 2001). Nozue et al. (1998) even found a protein in a fern that possesses both phytochrome and phototropin properties.

12.3.3 The Plant UV-B Receptor UVR8

Ultraviolet B radiation (280–315 nm) affects plants and other organisms in many destructive and inhibitory ways (Chap. 22).

But plants also exhibit specific regulatory effects of UV-B radiation, and it has long been realized that plants possess a UV-B-specific photoreceptor, but only recently has it been characterized at the molecular level. This photoreceptor differs from all others enumerated above by having no non-amino acid chromatophore (Christie et al. 2012; Wu et al. 2012). The UV-B absorption is achieved by a large number of aromatic amino acids in the protein, of which several tryptophan residues are so closely positioned that the π-orbitals overlap. Absorption of UV-B radiation around 290 nm causes the protein to be monomerized from the dimeric state and translocated from the cytoplasm to the nucleus, where it interacts with a protein called COP1 and affects genes (O'Hara and Jenkins 2012). The photoreceptor is widespread among plants. The green alga *Chlamydomonas* has a similar protein (Christie et al. 2012) that probably has the same function. Related proteins with other functions occur in other organisms, including animals. One of these is RCC1, a regulator of DNA replication (Dasso et al. 1992; Dasso 1993) and mitosis. It thus appears that the UVR8 photoreceptor is specific for green plants, but has an ancient ancestry. Also some cyanobacteria have a receptor for UV-B radiation (Portwich and García-Pichel 2000).

The strong absorption band of UVR8 in the UV-B region (Fig. 12.21) is due mainly to 14 tryptophan and 10 tyrosine residues per monomer, with some contribution also from 8 phenylalanine residues. Of the tryptophan residues, 13 are located in the central core. Some of the tryptophan residues are so close that their pi orbitals overlap. Three of them (W233, W285, and W337), close to the monomer surface

interacting with the other monomer in dimer formation, are particularly important for the function, and W285 is indispensable.

The UVR8 dimer is kept together by electrostatic interactions between positively charged arginine and negatively charged amino acids on the opposite monomer (Fig. 12.22). Interactions occur also between arginine and the pi electron clouds of the tryptophan residues. When UV-B radiation is absorbed, these pi electron orbitals are altered, and the interactions are no longer strong enough to keep the monomers together.

Recently Wu et al. (2014) have performed calculations that indicate that the primary reaction initiated by UV-B radiation is a transfer of electrons from tryptophan 233 via tryptophan 285 to arginine 338 coupled to proton transfer from tryptophan 233 to aspartic acid 129, leading to disruption of salt bridges, starting at arginine 338.

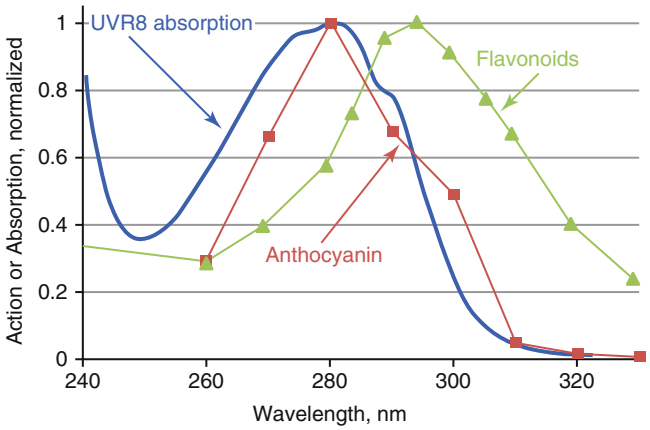

Fig. 12.21 Examples of action spectra for processes thought to be mediated by a special UV-B receptor: (induction of flavonoid synthesis (Beggs and Wellmann 1995) and of anthocyanin synthesis (Takeda and Abe 1992) compared to the absorption spectrum for UVR8 (Christie et al. 2012)

12.3.4 The Orange Carotenoid Protein, ORP

The orange carotenoid protein (OCP) is a cyanobacterial photoactive protein binding a keto-carotenoid molecule (Fig. 12.23). Its role is to adjust the photosynthetic apparatus to the fluence rate and protect the organism against excessive light. Plants, algae, and cyanobacteria have various mechanisms for protection against excess light which may cause damage by the so-called non-photochemical quenching (NPQ). In plants and algae the lowering of pH inside the thylakoids caused by strong light triggers this photoprotection. But the OCP functions in a completely different way, independently of changes in pH or redox potential (Berera et al. 2013). The same protein acts as light sensor, signal propagator, and quencher of excess energy. It is most

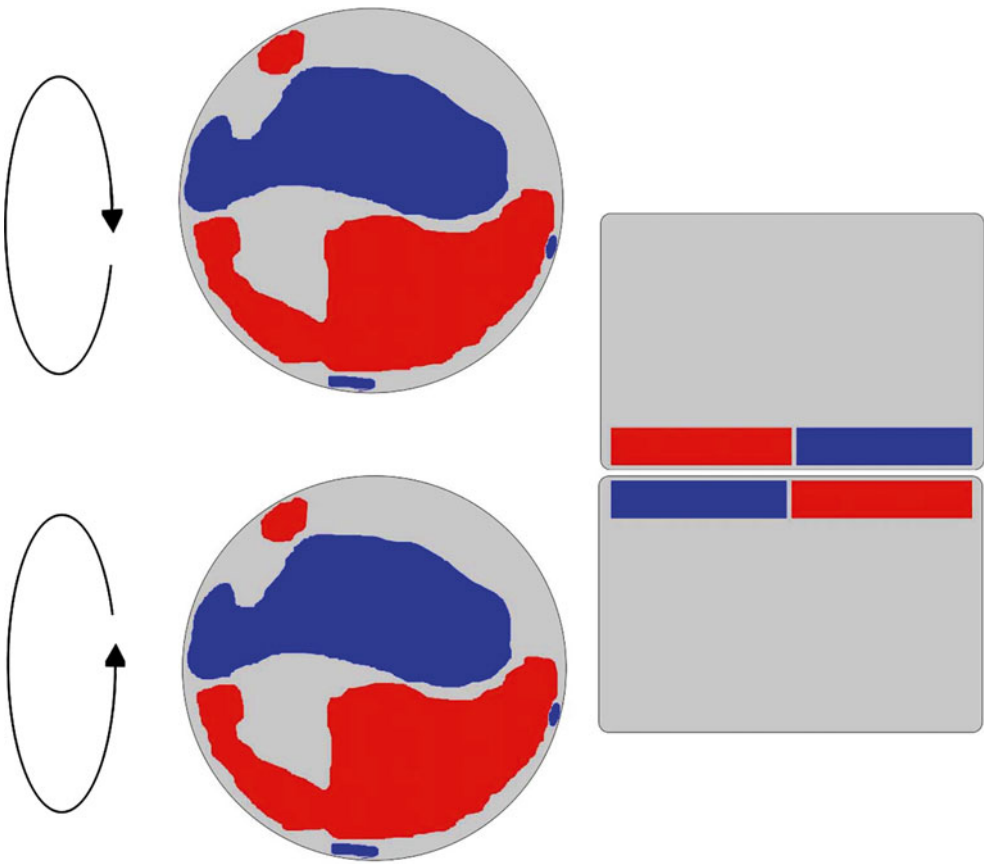

Fig. 12.22 Sketch of UVR8 monomers (*left*) with positive charges indicated by *blue* and negative charges by *red* and a dimer (*right*) showing how opposite charges hold the dimer together

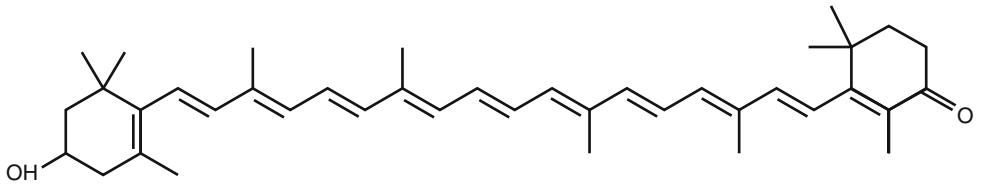

Fig. 12.23 The xanthophyll 3′-hydroxyechinenone present in OCP

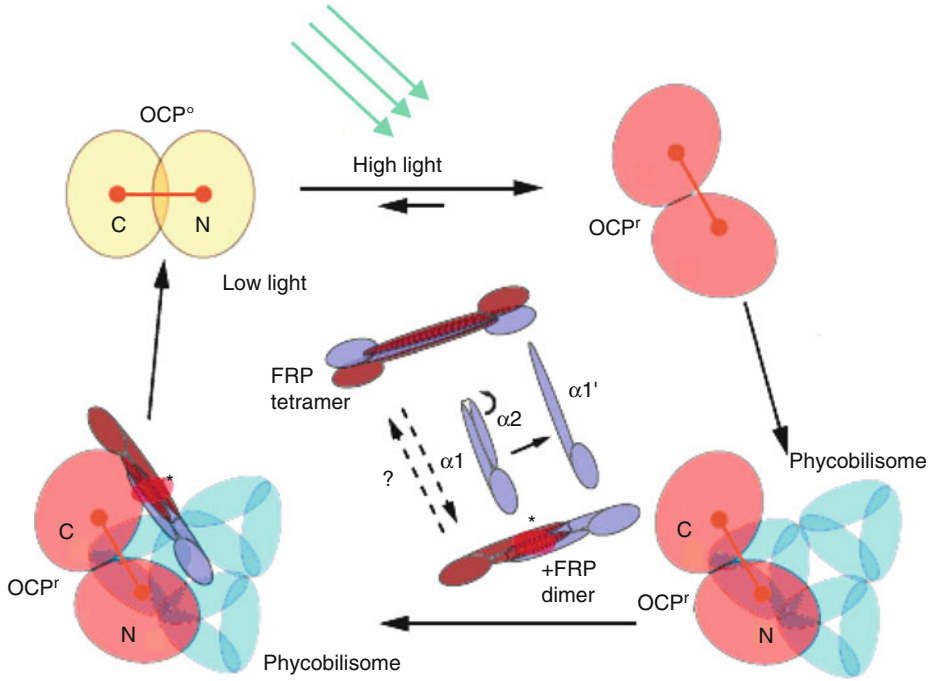

Fig. 12.24 Light-induced transformation of OCP from the OCP° (*low light*) state to the OCP^r (*high light*) state and following attachment to phycobilisomes, and FRP detatchment and return to the OCP° state in low light. From Sutter et al. (2013)

sensitive to blue-green light. When it is isolated from the organism, it has an orange color in its weak-light state, but shifts to red upon irradiation with strong light. In the organism, it is free in solution in its dark form. Upon exposure to strong light, it undergoes a large conformational change and attaches to phycobilisomes (cyanobacterial light-harvesting protein complexes on the thylakoid membranes, Fig. 12.24). Excess energy is channeled from the phycobilisomes to the OCP and is then degraded to heat. When energy in this way is channeled away from the phycobilisome, its fluorescence decreases, which provides a convenient way to monitor the changes in its energy state.

The quantum yield for change of the OCP from its low-light state to the protective state is only about 0.03 (Wilson et al. 2008), which makes sense, since it is only in strong light that excitation energy should be degraded to heat. When light is absorbed in the carotenoid molecule, there is a redistribution of charges which affects the interactions with the protein, so that the latter changes conformation. This exposes new parts of the molecule that have affinity for the phycobilisome. A second protein, called FRP (for "Fluorescence Recovery Protein) is required to release it again when incident fluence decreases.

Gwizdala et al. (2011) showed that it is necessary for the OCP to have contact with the central part (the core) of the phycobilisome to be able to channel energy away. OCP has no effect on the peripheral parts (the rods).

Although all cyanobacteria do not possess OCP, it is represented in all major morphological subsections and phylogenetic clades (Kirilovsky and Kerfeld 2013; Kerfeld and Kirilovsky 2013).

References

Ahmad M, Galland P, Ritz T, Wiltschko R, Wiltschko W (2007) Magnetic intensity affects cryptochrome-dependent responses in Arabidopsis thaliana. Planta 225:615–624

Albalat A (2009) The retinoic acid machinery in invertebrates: ancestral elements and vertebrate innovations. Mol Cell Endocrinol 313:23–35

Álvarez Rodríguez R, Lahoz IR, Faza OA, Cid MM, Silva Lopez C (2012) Theoretical and experimental exploration of the

photochemistry of resveratrol: beyond the simple double bond isomerization. Org Biomol Chem 10:9175–9182
Anisimova N Yu, Kiselevsky MV, Sosnov AV, Sadovnikov SV, Stankov IN, Gakh AA (2011) Trans-, cis-, and dihydro-resveratrol: a comparative study. Chem Central J 5:88 (6 pp)
Assmann SM, Wang XQ (2001) From milliseconds to millions of years: guard cells and environmental responses. Curr Opin Plant Biol 4:421–428
Ballario P, Macino G (1997) White-collar proteins: PASsing the light signal in Neurospora crassa. Trends Microbiol 5:458–462
Barinaga M (2002) How the brain's clock gets daily enlightenment. Science 295:955–957
Beale SI (1999) Enzymes of chlorophyll biosynthesis. Photosynth Res 60:43–73
Beggs CJ, Wellmann E (1995) Photocontrol of flavonoid synthesis. In Kendrick RE, Kronenberg GHM (eds) Photomorphogenis in plants, 2nd ed. Kluwer Academic Publishers, The Netherlands, pp. 733–751
Berera R, Gwizdala M, van Stokkum IHM, Kirilovsky D, van Grondelle R (2013) Excited states of the inactive and active forms of the orange carotenoid protein. J Phys Chem B 117:9121–9128
Berson DM, Dunn FA, Takao M (2002) Phototransduction by retinal ganglion cells that set the circadian clock. Science 295:1070–1073
Bhoo SH, Davis SD, Walker J, Karniol B, Vierstra RD (2001) Bacteriophytochromes are photochromic histidine kinases using a biliverdin chromophore. Nature 414:776–779
Björn LO (1979) Photoreversibly photochromic pigments in organisms: properties and role in biological light perception. Q Rev Biophys 12:1–23
Björn GS (1980a) Photoreversibly photochromic pigments from blue-green algae. Diss. Lund University. LUNBDS/(NBFB-1009/1-28/(1980)
Björn LO (1980b) The history of phyto-photo-science (not to be left in skoto toto and silence. In: De Greef J (ed) Photoreceptors and plant development. Antwerp University Press, Antwerp, pp 9–13, Proc. Annu. Europ. Photomorphogenesis Symp
Björn LO (1984) Light-induced linear dichroism in photoreversibly photochromic sensor pigments. V. Reinterpretation of the experiments on in vivo action dichroism of phytochrome. Physiol Plant 60:369–372
Björn GS, Björn LO (1978) Action spectra for conversions of phycochrome c from *Nostoc muscorum*. Physiol Plantarum 43: 195–200
Boylan MT, Quail PH (1996) Are the phytochromes protein kinases? Protoplasma 195:12–17
Briggs WR, Beck CF, Cashmore AR et al (2001) The phototropin family of photoreceptors. Plant Cell 13:993–997, 17 authors
Butler WL (1980) Remembrances of phytochrome twenty years ago. In: De Greef J (ed) Photoreceptors and plant development. Antwerp University Press, Antwerp, pp 3–7, Proc. Annu. Europ. Photomorphogenesis Symp
Chen J, Gai Q, Lv Z, Chen J, Nie Z (2010) All-trans retinoic acid affects subcellular localization of a novel BmNIF3l protein: functional deduce and tissue distribution of NIF3l gene from silkworm (Bombyx mori). Arch Insect Biochem Physiol 74:217–231
Christie JM, Briggs WR (2001) Blue light sensing in higher plants. J Biol Chem 276:11457–11460
Christie JM, Arvai AS, Baxter KJ, Heilmann M, Ashley J, Pratt AJ, O'Hara A, Kelly SM, Hothorn M, Smith BO, Hitomi K, Jenkins GI, Getzoff ED (2012) Plant UVR8 photoreceptor senses UV-B by tryptophan-mediated disruption of cross-dimer salt bridges. Science 335:1492–1496
Crosson S, Moffat K (2001) Structure of a flavin-binding plant photoreceptor domain: insights into light mediated signal transduction. Proc Natl Acad Sci U S A 98:2995–3000
Dasso M (1993) RCC1 in the cell-cycle – the regulator of chromosome condensation takes on new roles. Trends Biochem Sci 18:96–101
Dasso M, Nishitani H, Kornbluth S, Nishimoto T, Newport JW (1992) RCC1, a regulator of mitosis, is essential for DNA replication. Mol Cell Biol 12:3337–3345
Davis SJ, Vener AV, Vierstra RD (1999) Bacteriophytochromes: phytochrome-like photoreceptors from nonphotosynthetic eubacteria. Science 286:2517–2520
Diakoff S, Scheibe J (1973) Action spectra for chromatic adaptation in tolypothrix tenuis. Plant Physiol 51:382–385
Etzold H (1965) Der polarotropismus und phototropismus der chloronemen von dryopteris filix-mas (L.) Schott. Planta 64:254–280
Fankhauser C (2001) The phytochromes, a family of Red/Far-red absorbing photoreceptors. J Biol Chem 276:11453–11456
Figuereiras TS, Neves-Petersen MT, Petersen SB (2011) Activation energy of light induced isomerization of resveratrol. J Fluoresc 21:1897–1906
Folta KM, Spalding EP (2001) Unexpected roles for cryptochrome2 and phototropin revealed by high-resolution analysis of blue light-mediated hypocotyl growth inhibition. Plant J 26:471–478
Foster KW, Saranak J, Patel N, Zarilli G, Okabe M, Kline T, Nakashini K (1984) A rhodopsin is the functioning photoreceptor for phototaxis in the unicellular eukaryote Chlamydomonas. Nature 311:756–759
Frechilla S, Zhu JX, Talbott LD, Zeiger E (1999) Stomata from npq1, a zeaxanthin-less Arabidopsis mutant lacking a specific response to blue light. Plant Cell Physiol 40:949–954
Frechilla S, Talbott LD, Bogomolni RA, Zeiger E (2000) Reversal of a blue-light stimulated stomatal opening by green light. Plant Cell Physiol 41:171–176
Fu PP, Cheng SH, Coop L, Xia Q, Culp SJ, Tolleson WH, Wamer WG, Howard PC (2003) Photoreaction, phototoxicity, and photocarcinogenicity of retinoids. J Environ Sci Health 21(2):165–197
Fujita Y, Hattori A (1962) Photochemical interconversion between precursors of phycobilin chromoprotein in Tolypothrix tenuis. Plant Cell Physiol 3:209–220
Galland P (2001) Phototropism in phycomyces. In: Häder DP, Lebert M (eds) Photomovement. Elsevier, Amsterdam, pp 621–657
Gan F, Zhang S, Rockwell NC, Martin SS, Lagarias JC, Bryant DA (2014) Extensive remodeling of a cyanobacterial photosynthetic apparatus in far-red light. Science 345:1312–1317
Genick UK, Borgstrahl GEO, Kingman N, Ren Z, Pradervand C, Burke PM, Srajer V, Teng TY, Schildkamp W, McRee DE, Moffat K, Getzoff ED (1997) Structure of a protein cycle intermediate by millisecond time-resolved crystallography. Science 275:1471–1475
Genick UK, Soltis SM, Kuhn P, Canestrelli IL, Getzoff ED (1998) Structure at 0.85 Å resolution of an early protein photocycle intermediate. Nature 392:206–209
Grossman AR, Bhaya D, He Q (2001) Tracking the light environment by cyanobacteria and the dynamic nature of light harvesting. J Biol Chem 276:11449–11452
Gualtieri P (2001) Rhodopsin-like proteins: light detection pigments in leptolyngbya, euglena, ochromonas, pelvetia. In: Häder DP, Lebert M (eds) Photomovement. Elsevier, Amsterdam, pp 281–295
Gwizdala M, Wilson A, Kirilovsky D (2011) In vitro reconstitution of the cyanobacterial photoprotective mechanism mediated by the orange carotenoid protein in Synechocystis PCC 6803. Plant Cell 23:2631–2643
Hansson KM, Li B, Simon JD (1997) A spectroscopic study of the epidermal ultraviolet chromophore trans-urocanic acid. J Am Chem Soc 119:2715–2721
Hanzawa H, Shinomura T, Inomata K, Kakiuchi T, Kinoshita H, Wada K, Furuya M (2002) Structural requirements of bilin chromophore for the photosensory specificity of phytochromes A and B. Proc Natl Acad Sci U S A 99:4725–4729
Hattar S, Liao HW, Takao M, Berson DM, Yau KW (2002) Melanopsin containing retinal ganglion cells: architecture, projections, and intrinsic photosensitivity. Science 295:1065–1070

Haupt W (1970) Localization of phytochrome in the cell. Physiol Veg 8:551–563
Hegemann P, Deininger W (2001) Algal eyes and their rhodopsin photoreceptors. In: Häder DP, Lebert M (eds) Photomovement. Elsevier, Amsterdam, pp 475–503
Hellmann-Regen J, Heuser I, Regen F (2013) UV-A emission from fluorescent energy-saving light bulbs alters local retinoic acid homeostasis. Photochem Photobiol. doi:10.1039/c3pp50206f, in press
Herdman M, Coursin T, Rippka R, Houmard J, Tandeau de Marsac N (2000) A new appraisal of the prokaryotic origin on eukaryotic phytochromes. J Mol Evol 51:205–213
Heyman RA, Mangelsdorf DJ, Dyck JA, Stein R, Eichele G, Evans RM, Thallers C (1992) 9-cis retinoic acid is a high affinity ligand for the retinoid X receptor. Cell 66:397–406
Hoff WD, Jung KH, Spudich (1997) Molecular mechanism of photosignaling by archaeal sensory rhodopsins. Annu Rev Biophys Biomol Struct 26:223–258
Hubschmann T, Borner T, Hartmann E, Lamparter T (2001) Characterization of the Cph1 holo-phytochrome from Synechocystis sp. PCC 6803. Eur J Biochem 268:2055–2063
Iino M (2001) Phototropism in higher plants. In: Häder DP, Lebert M (eds) Photomovement. Elsevier, Amsterdam, pp 659–812
Iino M, Ogawa T, Zeiger E (1985) Kinetic properties of the blue-light response of stomata. Proc Natl Acad Sci U S A 82:8019–8023
Ioele G, Cione E, Risoli A, Genchi G, Ragno G (2005) Int J Pharm 293:251–260
Jarillo JA, Gabrys H, Capel J, Alonso JM, Ecker JR, Cashmore AR (2001) Phototropin-related NPL1 controls chloroplast relocation induced by blue light. Nature 410:952–954
Jiang ZY, Swem LR, Rushing BG, Devanathan S, Tollin G, Bauer CE (1999) Bacterial photoreceptor with similarity to photoactive yellow protein and plant phytochromes. Science 285:406–409
Jones AM, Quail P (1986) Quaternary structure of 124-kilodalton phytochrome from Avena sativa L. Biochemistry 25:2987–2995
Kadota A, Wada M, Furuya M (1982) Phytochrome-mediated phototropism and different dichroic orientation of Pr and Pfr in protonemata of the fern Adiantum capillus-veneris. Photochem Photobiol 35:533–536
Kagawa T, Sakai T, Suetsugu N, Oikawa K, Ishiguru S, Kato T, Tabata S, Okada K, Wada M (2001) Arabidopsis NPL1: a phototropin homolog controlling the chloroplast high-light avoidance response. Science 291:2138–2141
Kalantari H, Das DK (2010) Physiological effects of resveratrol. Biofactors 36:401–406
Kehoe DM, Grossman AR (1996) Similarity of a chromatic adaptation sensor to phytochrome and ethylene receptors. Science 273:1409–1412
Kehoe DM, Gutu A (2006) Responding to color: the regulation of complementary chromatic adaptation. Annu Rev Plant Biol 57:127–150
Kerfeld CA, Kirilovsky D (2013) Structural, mechanistic and genomic insights into OCP-mediated photoprotection. Adv Bot Res 65:1–26
Kim H, Oh S-J, Liu Y, Lee M-Y (2011) A comparative study of the antiplatelet effects of cis- and trans-resveratrol. Biomol Ther 19:201–205
Kirilovsky D, Kerfeld CA (2013) The Orange carotenoid protein: a blue-green light photoactive protein. Photochem Photobiol Sci 12:1135–1143
Kunchala SR, Suzuki T, Murayama A (2000) Photoisomerization of retinoic acid and its influence on regulation of human keratinocyte growth and differentiation. Indian J Biochem Biophys 37:71–76
Lamparter T, Marwan W (2001) Spectroscopic detection of a phytochrome-like photoreceptor in the myxomycete Physarum polycephalum and the kinetic mechanism for the photocontrol of sporulation by Pfr. Photochem Photobiol 73:697–702
Lasceve G, Leymarie J, Olney MA, Liscum E, Christie JM, Briggs WR (1999) *Arabidopsis* contains at least four independent blue-light-activated signal transduction pathways. Plant Physiol 120:605–614
Lazaroff N, Schiff J (1962) Action spectrum for developmental photoinduction of the blue-green alga Nostoc muscorum. Science 137:603–604
Lenci F, Ghetti F, Song PS (2001) Photomovement in ciliates. In: Häder DP, Lebert M (eds) Photomovement. Elsevier, Amsterdam, pp 281–295
Li B, Hanson KM, Simon JD (1997) Primary processes of the electronic excited states of trans-urocanic acid. Phys Chem A 101:969–972
Lin C (2000) Plant blue-light receptors. Trends Plant Sci 5:337–342
Maeng S, Kim GJ, Choi EJ, Yang HO, Lee DS, Sohn YC (2012) 9-cis-retinoic acid induces growth inhibition in retinoid-sensitive breast cancer and sea urchin embryonic cells via retinoid X receptor and replication factor C3. Mol Endocrinol 26:1821–1835
Merrow M, Roenneberg T (2001) Circadian clocks: running on redox. Cell 106:141–143
Mohr H (1994) Coaction between pigment systems. In: Kendrick RE, Kronenberg GHM (eds) Photomorphogenesis in plants, 2nd edn. Kluwer Acad. Publ, Dordrecht, pp 545–564
Montgomery BL (2007) Sensing the light: photoreceptive systems and signal transduction in cyanobacteria. Mol Microbiol 64:16–27
Morrison H, Avnir D, Bernasconi C, Fagan G (1980) Z/E photoisomerization of urocanic acid. Photochem Photobiol 32:711–714
Morrison H, Bernasconi C, Pandey G (1984) A wavelength effect on urocanic acid E/Z photoisomerization. Photochem Photobiol 40:549–550
Murayama A, Suzuki T, Matsui M (1997) Photoisomerization of retinoic acids in ethanol under room light: A warning for cell biological study of geometrical isomers of retinoids. J Nutr Sci Vitaminol 43:167–176
Naseem S, Laurent AD, Carroll EC, Vengris M, Kumauchi M, Hoff WD, Krylov AI, Larsen DS (2013) Photo-isomerization upshifts the pKa of the Photoactive Yellow Protein chromophore to contribute to photocycle propagation. J Photochem Photobiol A Chem 270:43–52
Neff MM, Chory J (1998) Genetic interactions between phytochrome A, phytochrome B, and cryptochrome 1 during Arabidopsis development. Plant Physiol 118:27–35
Nozue K, Kanegae T, Imaizumi T, Fukuda S, Okamoto H, Yeah KC, Lagarias JC, Wada M (1998) A phytochrome from the fern Adiantum with features of the putative photoreceptor NPH1. Proc Natl Acad Sci U S A 95:15826–15830
O'Hara A, Jenkins GI (2012) In vivo function of tryptophans in the Arabidopsis UV-B photoreceptor UVR8. Plant Cell 24: 3755–3766
Okada T, Ernst OP, Palczewski K, Hofmann KP (2001) Activation of rhodopsin: new insights from structural and biochemical studies. Trends Biochem Sci 26:318–324
Page CS, Olivucci M, Merchán M (2000) A theoretical study of the low-lying states of the anionic and protonated forms of urocanic acid. J Phys Chem A 104:8796–8805
Parks BM, Folta KM, Spaldin EP (2001) Photocontrol of stem growth. Curr Opin Plant Biol 2001:436–440
Pellequeler JL, Wagner-Smith KA, Kay SA, Getzoff ED (1998) Photoactive yellow protein: a structural prototype for the three-dimensional fold o the PAS domain superfamily. Proc Natl Acad Sci U S A 95:5884–5890
Pennati R, Dell'Anna A, Zega G, De Bernardi F, Piraino S (2013) Retinoic acid influences antero-posterior positioning of peptidergic neurons in the planula larva of the hydrozoan Clava multicornis. Mar Ecol 34(Suppl 1):143–152
Portwich A, Garcia-Pichel F (2000) A novel prokaryotic UVB photoreceptor in the cyanobacterium Chlorogloeopsis PCC 6912. Photochem Photobiol 71:493–498
Prêle CM, Finlay-Jone JJ, Hart PH (2006) The receptor for cis-urocanic acid remains elusive. J Investig Dermatol 126:1191–1193

Provencio I, Jiang G, De Grip WJ, Hayes WP, Rollag MD (1998) Melanopsin: an opsin in melanophores, brain, and eye. Proc Natl Acad Sci U S A 95:340–345

Rius C, Abu-Taha M, Hermenegildo C, Piqueras L, Cerda-Nicolas J-M, Issekutz AC, Estañ L, Cortijo J, Morcillo EJ, Orallo F, Sanz M-J (2010) Trans- but not cis-resveratrol impairs angiotensin-II-mediated vascular inflammation through inhibition of NF-κB activation and peroxisome proliferator-activated receptor-γ upregulation. J Immunol 2010;185:3718–3727

Rospendowski BN, Farrens DL, Cotton TM, Song PS (1989) Surface enhanced resonance Raman scattering (SERRS) as a probe of the structural differences between the Pr and Pfr forms of phytochrome. FEBS Lett 258:1–4

Ryan W, Levy DH (2001) Electronic spectroscopy and photoisomerization of trans-urocanic acid in a supersonic jet. J Am Chem Soc 123:961–966

Sage LC (1992) Pigment of the imagination: a history of phytochrome research. Academic, San Diego

Sakai T, Kagawa T, Kasahara M, Swartz TE, Christie JM, Briggs WR, Wada M, Okada K (2001) Arabidopsis nph1 and npl1: blue-light receptors that mediate both phototropism and chloroplast relocation. Proc Natl Acad Sci U S A 98:6969–6974

Salomon M, Christie JM, Knieb E, Lempert U, Briggs WR (2000) Photochemical and mutational analysis of the FMN-binding domains of the plant blue light receptor, phototropin. Biochemistry 39:9401–9410

Sarkar HK, Song PS (1982) Nature of phototransformation of phytochrome as probed by intrinsic tryptophan residues. Biochemistry 21:1967–1972

Scheibe J (1962) Photoreversible pigment: occurrence in a blue-green alga. Science 176:1037–1039

Schneider-Poetsch HAW, Kolukisaoglu U, Clapham DH, Hughes J, Lamparter T (1998) Non-angiosperm phytochromes and the evolution of vascular plants. Physiol Plant 102:612–622

Sherman H, Gutman R, Chapnik N, Meylan J, le Coutre J, Froy O (2012) All-trans retinoic acid modifies the expression of clock and disease marker genes. J Nutrit Biochem 23:209–217

Shropshire W, Withrow RB (1958) Action spectrum of phototropic tip-curvature of Avena. Plant Physiol 33:360–366

Spudich JL (2001) Color-sensitive vision by halobacteria. In: Häder DP, Lebert M (eds) Photomovement. Elsevier, Amsterdam, pp 151–178

Sundqvist D, Björn LO (1983a) Light-induced linear dichroism in photoreversibly photochromic sensor pigments. II. Chromophore rotation in immobilized phytochrome. Photochem Photobiol 37: 69–75

Sundqvist D, Björn LO (1983b) Light-induced linear dichroism in photoreversibly photochromic sensor pigments. III. Chromophore rotation estimated by polarized light reversal of dichroism. Physiol Plant 59:263–269

Sutter M, Wilson A, Leverenz RL, Lopez-Igualb R, Thurotte A, Salmeena AE, Kirilovsky D, Kerfeld CA (2013) Crystal structure of the FRP and identification of the active site for modulation of OCP-mediated photoprotection in cyanobacteria. Proc Natl Acad Sci U S A 110:10022–10027

Takeda J, Abe S (1992) Light-induced synthesis of anthocyanin in carrot cells in suspension – IV. The action spectrum. Photochem Photobiol 56:69–74

Taylor RR, Zhulin IB (1999) PAS domains: internal sensors of oxygen, redox potential, and light. Microbiol Mol Biol 63:479–506

Teboul M, Guillaumond F, Grechez-Cassiau A, Delaunay F (2008) The nuclear hormone receptor family round the clock. Mol Endocrinol 22:2573–2782

Thimann KV, Curry GM (1961) Phototropism. In: McElroy WD, Glass B (eds) Light and life. Johns Hopkins Press, Baltimore, pp 646–672

Todo T, Ryo H, Yamamoto K, Toh H, Inui T, Ayaki H, Nomura T, Ikenaga M (1996) Drosophila (6–4)photolyase, a human photolyase homolog, and the blue-light photoreceptor family. Science 272:109–112

Tokutomi S, Mimuro M (1989) Orientation of the chromophore transition moment in the 4-leaved shape model for pea phytochrome molecule in red-light absorbing form and its rotation induced by the phototransformation to the far-red-light absorbing form. FEBS Lett 255:350–353

Vogelmann TC, Scheibe J (1978) Action spectra for chromatic adaptation in blue-green Fremyella diplosiphon. Planta 143:233–239

Walterscheid JP, Nghiem DX, Kazimi N, Nutt LK, McConkey DJ, Norval M, Ullrich SE (2006) Cis-urocanic acid, a sunlight-induced immunosuppressive factor, activates immune suppression via the 2A 5-HT receptor. Proc Natl Acad Sci U S A 103:17420–17425

Wang H, Ma LG, Li JM, Zhao HY, Deng WW (2001) Direct interaction of Arabidopsis cryptochromes with COP1 in mediation of photomorphogenic development. Science 294:154–158

Watson JC (2000) Light and protein kinases. Adv Bot Res Inc Adv Plant Pathol 32:149–184

Wilson A, Punginelli C, Gall A, Bonetti C, Alexandre M, Routaboul J-M, van Kerfeld CA, Grondelle R, Robert B, Kennis JTM, Kirilovsky D (2008) A photoactive carotenoid protein acting as light intensity sensor. Proc Natl Acad Sci U S A 110:10022–10027

Wu D, Hu Q, Yan Z, Chen W, Yan C, Huang X, Zhang J, Yang P, Deng H, Wang J, Deng XW, Shi Y (2012) Structural basis of ultraviolet-B perception by UVR8. Nature 484:215–220

Wu M, Eriksson LA, Strid Å (2014) The photochemical reaction mechanism of UV-B-induced monomerization of UVR8 dimers as the first signaling event in UV-B-regulated gene expression in plants. J Phys Chem 118:951–965

Zeiger E (2000) Sensory transduction of blue light in guard cells. Trends Plant Sci 5:183–185

Photoreceptive Proteins and Their Evolution

13

Lars Olof Björn

13.1 Introduction

Many of the photoreceptor molecules have two main parts: one light-sensing part and another part transmitting the signal, often by transfer of a phosphate group. These two parts may have different evolutionary histories and have been united at a later stage in evolution. Thus the signaling parts of two different photoreceptors, such as two protein domains acting as kinases, may be related, while the light-sensing parts may be unrelated. This makes it impossible to compose completely correct evolutionary relationships in the form of "trees."

In his book *In the Blink of an Eye*, Parker (2004) vividly describes how the "invention" of vision triggered the so-called Cambrian explosion, the rapid evolution by which all the animal phyla of the present-day fauna emerged within only a few million years (see also Parker 2011; Alvarez 2008). But long before the Cambrian explosion organisms were able to use light for gathering information about the world around them, and light has had an impact on evolution since the origin of life.

In a distant past, when our earliest ancestors inhabited the planet, there were no continents. An ocean covered all of the young Earth's surface except for volcanoes here and there. The ocean volume was probably about twice the present, and plate tectonics had not yet sculpted the Earth with high mountains and great ocean depths (Flament et al. 2008; Arndt and Nisbet 2012). Water transmits best light of short wavelength, from UV-A to blue. It is therefore not surprising that the earliest light-recording pigments had their absorption bands in this spectral region. Specializing at light of very high wavelength, as plant phytochromes or the vision of some fishes, is of more recent date. Even in the phytochrome superfamily of proteins, which we often regard as typical long-wavelength sensors, there are bacterial members that tune the bilin absorption to the blue-violet region of the spectrum (Narikawa et al. 2008), so this may be the original wavelength region for this photoreceptor family as well.

13.2 Problems with the Classification of Photoreceptors

Photoreceptors can be classified in various ways, according to:

1. Function, e.g., photoperiodism, stomata regulation, vision, phototaxis
2. Spectral coverage, e.g., ultraviolet-B, blue light, red light
3. Type of chromophore, e.g., flavine, retinal, bilin
4. Occurence in the cell, e.g., cell membrane, other membrane, cytosol, nucleus
5. Domain (e.g., PAS (Möglich et al. (2009), GAF, BLUF, LOV, EAL) structure (domain architecture) of the protein part
6. Overall tertiary and quaternary structure of the protein
7. Signal output, e.g., phosphorylation, reduction, or oxidation

To a certain degree some of these classifications are correlated, but the correlation is not strict. There are, for instance, photoreceptors with the same chromophore, but with completely different proteins. Cryptochromes and BLUF domain blue light sensors (Gomelsky and Klug 2002) both contain FAD as chromophore. Members of two families of rhodopsins without any sequence similarity have retinal as chromophore. The same protein may have two different functions, e.g., serve both as cryptochrome (light-sensing protein) and photolyase (repair enzyme) (Bayram et al. 2008). The amino acid sequence may be unrelated, but the overall protein structure related, as in the two families of rhodopsins. Proteins containing flavin (FMN or FAD) as chromophore are mostly active in the UV-A to blue spectral band, but in some cases in the green (Bouly et al. 2007; Wang et al.

L.O. Björn
School of Life Science,
South China Normal University, Guangzhou, China

Department of Biology, Lund University, Lund, Sweden
e-mail: Lars_Olof.Bjorn@biol.lu.se

L.O. Björn (ed.), *Photobiology: The Science of Light and Life*,
DOI 10.1007/978-1-4939-1468-5_13,

2013) or even red (Beel et al. 2012) parts of the spectrum. Finally, there are sensor proteins which have more than one chromophore. Thus Jiang et al. (1999) described a xanthopsin-phytochrome combination, and phototropin-phytochrome combinations (neochromes) have arisen at least twice during evolution (Suetsugo et al. 2005).

For these reasons and others it is difficult to find a completely logical and still useful classification of chromophores. We have chosen to divide the sensor proteins into eight major groups mainly based on type of chromophore and try to follow a phylogenetic classification within each of these main groups. We will use the following classification:
Cryptochromes
Rhodopsins
Xanthopsins (PYPs)
Phytochromes and phytochrome-like photosensors
Light, oxygen, voltage (LOV) domain-containing proteins
Sensor of blue light using FAD (BLUF) domain-containing proteins
Ciliate photoreceptors (stentorin-related)
Ultraviolet-resistance locus eight family (UVR8)

13.3 Photolyases/Cryptochromes

The function of the earliest representatives of this group seems to have been to act as photolyases, i.e., to repair damaged DNA by a light-dependent process. Only later did some members of the group acquire a role as photoreceptor pigments, and this switch of function has taken place more than once during evolution. Some of the proteins can function both as photolyase and as photoreceptor, such as one in the fungus *Aspergillus niger* (Bayram et al. 2008) [and one in *Trichoderma harzianum* (Berrocal-Tito et al. 2000)] so the distinction between photolyase and cryptochrome is diffuse. All members of this class contain an FAD chromophore that is involved in photochemistry, and most of them also contain a secondary chromophore that acts as an "antenna" that can collect light energy and transfer it to the FAD (Müller and Carell (2009). The antenna chromophore is in some cases 5,10-methenyl tetrahydrofolate (MTHF) (Öztürk et al. 2008). but can also be FMN, FAD, 8-hydroxy-5-deazaflavin, or 6,7-dimethyl-8-ribityl-lumazine (Geisselbrecht et al. 2012). The cryptochrome found in *Rhodobacter sphaeroides*, which carries the 6,7-dimethyl-8-ribityl-lumazine antenna chromophore, is special also because it has, in addition to FAD, an iron-sulfur cluster at the catalytic site Oberpichler et al. (2011).

The photolyase/cryptochrome superfamily has representatives in all three domains of life (Archaea, Eubacteria, and Eukaryota) and thus seems to have been present in the last common ancestor of present-day organisms, "LUCA." An alternative could be horizontal (lateral) gene transfer. Photolyase genes occur in virus (*Entomopoxvirinae*) that have been involved in horizontal transfer of photolyase genes among insects (Afonso et al. 1999; Nalcacioglu 2010; Biernat et al. 2011). Photolyase genes occur also in baculovirus (van Oers et al. (2004), in *Chordopoxvirinae* that infect vertebrates (Afonso et al. 2000), and in marine *Cafeteria roenbergensis* giant virus (Fischer et al. 2010) that infects zooplankton; researchers do not seem to think that lateral gene transfer has been important in the macroevolution and spread of these proteins.

There is no complete consensus regarding the phylogenetic relationships between the major classes of photolyases/cryptochromes, and different phylogenetic trees have been published (e.g., Lucas-Lledó and Lynch 2009; Rivera et al. 2012; Oberpichler et al. 2011; Kiontke et al. 2011; Asimgil and Kavakli 2012). Different authors also use different names for the various groups, which makes the literature somewhat confusing. We follow here, with simplification, the scheme from Rivera et al. (2012) (CPD and (6–4) refer to different kinds of DNA damage that are described in Chap. 22.):

1. Class 1 CPD photolyases
2.
   - 2.1. Class 2 CPD photolyases
   - 2.2. Plant cryptochromes (probably evolved from early form of 2.1)
3.
   - 3.1. Single DNA strand photolyases/DASH cryptochromes
   - 3.2.
     - 3.2.1. (6–4) photolyases
     - 3.2.2. Animal cryptochromes
       - 3.2.2.1. Insect type 1 + sponge + Cnidaria cryptochrome
       - 3.2.2.2. Insect type 2 + vertebrate cryptochrome

The above scheme indicates that cryptochromes have evolved from photolyases at least three times, i.e., plant cryptochromes from CPD photolyases, DASH cryptochromes from single strand DNA photolyases, and animal cryptochromes from (6–4) photolyases. The strange name DASH comes from the four genera in which representatives for the group were first found: *Drosophila*, *Arabidopsis*, *Synechocystis*, *Homo* (Brudler et al. (2003). As the name indicates, these proteins are widely distributed among eukaryotes, but there are also representatives from Eubacteria. Most of the proteins in category 3.1 above are probably only photolyases. One member with cryptochrome activity is *Fusarium fujikuroi* CryD DASH cryptochrome (Castrillo et al. 2013).

Essen (2006) points to the similarities between function in DNA repair and in photoreception. In both functions light-induced electron transfer is involved. So it is not surprising that some enzymes can carry out both functions, and a plant

photolyase may acquire cryptochrome function by substitution of a single amino acid (Burney et al. 2012). The separation between single-strand DNA photolyases and DASH cytochromes is not clear. Some authors regard these as two names for the same proteins rather than two groups of proteins.

From the above one could get the impression that the only roles for proteins in this superfamily are DNA repair and photoreception. However, many cryptochromes, including the human ones, serve other functions, especially as parts of circadian oscillators (Chap. 18) and as photo-magnets in animal orientation (Chap. 20).

Both the photolyase repair function and the cryptochrome light-sensing function depend on the light-induced electron transfer. For cryptochrome also blue-light-induced proton transfer, phosphorylation (Zuo et al. 2012) and conformational change (Kondoh et al. 2011) of the protein have been observed. The signaling state contains the FAD chromophore in the semiquinone state (Banerjee et al. 2007), but the signaling mechanism is not established (Chaves et al. 2011) and may differ between different kinds of cryptochrome. The downstream signaling of plant cryptochrome 2 involves at least two pathways (Liu et al. 2011).

13.4 Rhodopsins

Based on their structure, rhodopsins can be divided into two main groups, i.e., microbial (type 1) and animal (type 2) rhodopsins. Type 1 rhodopsins occur mainly in archaeans and fungi but also in some bacteria (Hoff et al. 1995; Jung et al. 2003) and some algae (see Ruiz-González and Marín 2004). Rhodopsins can also be classified according to function as ion-transporting, sensory, and others. The two classifications divide the rhodopsins in quite different ways. Rhodopsins that are structurally closely related can be found in organisms that are only very distantly related, indicating the occurrence of lateral (horizontal) gene transfer. Therefore it is not surprising that rhodopsin genes can also be found in viruses (Yutin and Koonin 2013). Furthermore, very different types of rhodopsin can be found in closely related organisms (or even within the same organism). This has contributed to making the elucidation of rhodopsin evolutionary history a difficult task.

Type 1 and type 2 rhodopsins share almost no amino acid sequences (Taylor and Agarwal 1993; Soppa 1994). However, all type 1 rhodopsins are clearly related as are all type 2 rhodopsins. From this one could draw the conclusion that they have independent origins, but by applying a method based on the probabilities of nucleotide replacement in DNA (Fitch 1970), Shen et al. (2013) could trace a distant relationship, and the theory of a common origin has been strengthened by the finding of Devine et al. (2013) that the structural

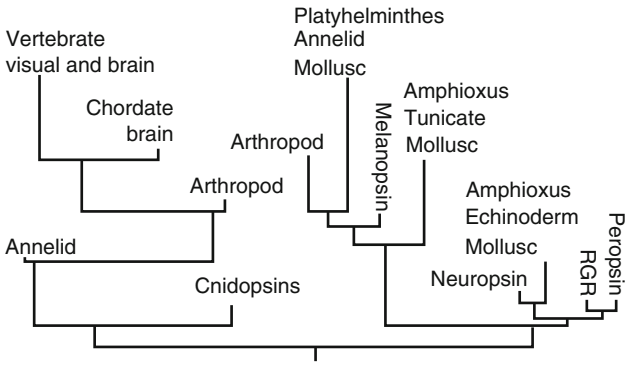

Fig. 13.1 Evolutionary tree of type 2 rhodopsins (Redrawn and simplified after Porter et al. 2012)

similarity cannot be explained by functional constraint. The retinal chromophore is attached to a lysine residue in both clades, but in different conformations. Shen et al. (2013) speculate that at some point during evolution the function as light sensors and the attachment of a chromophore have been abandoned, releasing the conservation of the chromophore-binding structure of the protein. The split between type 1 and type 2 rhodopsins must have taken place at least 1.5 billion years ago (Taylor and Agarwal 1993).

Of the rhodopsins in fungi some are of type 1 and others of type 2 (Novikov et al. 2012). Those of type 1 are rather different from those present in Archaea (Brown 2004; Washuk et al. 2005; Fan et al. 2011; Ito et al. 2012), while those of type 2 fall among the metazoan ones. Rhodopsins usually have one (as the human ones) or two photoactive states (and either the 11-cis or the all trans form or both can be photoactive), but one kind of type 1 rhodopsin has been shown to possess a complicated photocycle with three photoactive states (Sudo et al. 2011; Inoue et al. 2012). The evolution of type 1 rhodopsins is further discussed by Ruiz-González and Marín (2004) and Zhang et al. (2011).

The origin of type 2 rhodopsins (Fig. 13.1), also called GPCR, can be traced back to the ancestor of opisthokonts (1100 MYA) (Krishnan et al. 2012).

Type 2 rhodopsins can be phylogenetically divided into seven subfamilies, and only one of them is involved in imaging vision. According to Feuda et al. (2012) the first group to branch off from the path that leads to human rhodopsins is the one that contains melanopsin and placopsin. Placopsin is a pigment present in placozoans, a kind of primitive eyeless animal, possibly on the first evolutionary track branching off from the path leading to other Metazoa (Osigus et al. 2013). Melanopsin is involved in the setting of the biological clock by light (Chap. 18) in many different kinds of animal. This phylogeny differs from that of other authors, such as Terakita (2005) who regard the so-called rhabdomeric rhodopsins as splitting off together with the melanopsins.

13.5 Photoactive Yellow Proteins (PYPs, Xanthopsins)

The first photoactive yellow protein (PYP) was discovered in 1985 (Meyer 1985) in the purple photosynthetic bacterium *Ectothiorhodospira halophila* (later renamed *Halorhodospira halophila*). Soon thereafter it was found to exhibit light-induced changes reminiscent of rhodopsin (Meyer et al. 1987). Now 140 related gene sequences are known from a variety of bacteria, but the corresponding proteins have not been characterized in all cases. No PYP genes are known from Archaea or Eukaryota.

PYP genes can be classified into eight main groups based on base sequences. This classification is completely different from the classification of the bacteria in which the proteins occur (Kumauchi et al. 2008; Meyer et al. 2012), indicating widespread horizontal transmission of the PYP genes. Thus the distribution of the eight PYP groups of Meyer et al. (2012) among bacterial taxa is as follows:

I. α-, γ-, and δ-Proteobacteria
II. α- and γ-Proteobacteria
III. Bacteroides and Spirochaetes
IV. α-Proteobacteria
V. Bacteroides, β-, γ-, and δ-Proteobacteria
VI. δ-Proteobacteria
VII. γ-Proteobacteria
VIII. α–Proteobacteria

The PYPs are involved in a great number of functions, and within a single one of the groups above there may be representatives having different functions. The chromophore is p-hydroxy-cinnamic acid, which is bleached by a trans-cis isomerization upon exposure to light and quickly reverses in the dark (Meyer et al. 2012). It is thought that signal transmission occurs by association of some protein with the PYP in the bleached state.

Most PYPs occur in proteobacteria, but there are also two *Bacterioides* species and one spirochaete known to contain PYP. They appear sometimes to be involved in phototaxis, but in *Rhodospirillum centenum* it regulates a polyketide synthase gene.

Some proteins contain both a PYP part and a bacteriophytochrome domain (Kyndt et al. 2007, 2010).

13.6 Phytochrome-Like Photoreceptor Proteins

Phytochromes were first discovered in land plants and then also in green algae. These first discovered members of the superfamily are receptors specialized for red and far-red light. Now we know that this type of protein occurs in all domains of life and that, in general, they are tuned (spectrally adapted) to shorter wavelengths.

Phytochromes are photochromic, i.e., change absorption spectrum when they are exposed to light, and do this in a reversible way, such that they can change in one way under one kind of light, and in the opposite way under another kind of light. More about this in Chap. 11. They are proteins having an open-chain tetrapyrrole as chromophore. This chromophore is slightly different in different kinds of phytochromes. Bacteria utilize biliverdin, while cyanobacteria and plants use phycocyanobilin or phytochromobilin. The wavelength of the main absorption peak of the ground ("dark") state varies from 400 nm to 754 nm depending on species (Auldridge and Forest 2011), so the tuning range is comparable to that of rhodopsins. In most cases the active form absorbs at longer wavelength than the inactive form, but the reverse is found in some cases.

One hypothesis concerning the origin of this superfamily of photoreceptors is that the proteins originated as bilin sensors (and, indirectly, as sensors of molecular oxygen). The bilin requires oxygen for its formation, so this type of sensor is likely to have originated later than oxygenic photosynthesis.

The superfamily consists of two main groups of photoreceptors (also some non-photoreceptor proteins are closely related):

1. Cyanobacteriochromes
2. Phytochromes
   2.1. Bacteriophytochromes
   2.2. Cyanobacterial phytochromes
   2.3. Fungal phytochromes
   2.4. Plant phytochromes
   2.5. Phytochrome-like proteins

As many other photoreceptor proteins, phytochromes can be clearly divided into a light-sensing ("signal input") part on the N-terminal side and one "signal output" part on the C-terminal side. The latter, in the active form, has kinase activity. All phytochrome-like proteins contain two typical domains, a PHY domain and a GAF domain. GAF stands for cyclic guanosine monophosphate phosphodiesterase/adenylate cyclase/formate hydrogen lyase. The GAF domain is of very ancient origin and occurs in many other proteins, too (Aravind and Ponting 1997; Anantharaman et al. 2001). As the name implies it binds cyclic guanosine monophosphate (cGMP). Although there is no sequence homology, some GAF domains have an unexpected structural similarity to some PAS domains (Ho et al. 2000). Although the light-sensing part of plant phytochromes is derived from the corresponding in cyanobacteria, the output part (the kinase)

probably is not. Plant phytochromes thus are, in a sense, chimeric.

The cyanobacteriochromes (at least those in the DXCF-cyanobacteriochrome subfamily) differ from the phytochromes by forming a photolabile thioether linkage between the chromophore (in this case phycoviolobilin) and a cysteine in the apoprotein in addition to the stable cysteine-chromophore linkage common for all proteins in the superfamily (Burgie et al. 2013).

The sensor proteins in this category signal by transphosphorylation. The prokaryotic versions are histidine kinases, while the plant phytochromes phosphorylate serine and threonine. More about this in Sect. 12.2.5.

13.7 BLUF Photoreceptors

BLUF stands for **B**lue **L**ight photoreceptor **U**sing **F**AD, but the concept does not include the likewise FAD-containing cryptochromes. They are defined by a typical amino acid sequence in the FAD-binding BLUF domain. This type of photoreceptor is one of those which (as also the plant UV-B receptor UVR8) long evaded discovery. BLUF receptors were first reported almost simultaneously in a prokaryote, the proteobacterium *Rhodobacter sphaeroides* (Braatsch et al. 2002; Masuda and Bauer 2002), and in a eukaryote, *Euglena gracilis* (Iseki et al. 2002). After this BLUF domains have been identified in ca 10 % of all fully sequenced bacteria. A BLUF photoreceptor is involved in the regulation of photosynthesis in *Rhodobacter sphaeroides*, in phototaxis in the cyanobacterium *Synechocystis sp*. PCC6803 and in *Euglena gracilis*, and in the latter it also mediates light-induction of adenylyl cyclase activity. Otherwise the functions are so far unknown. Mandalari et al. (2013) have constructed a BLUF phylogeny showing a few major clades containing several members, while many other BLUF domains remain as isolated single-member clades.

13.8 LOV Domain Photoreceptors

The workings of this type of photoreceptor have been observed as long as people have noticed the ability of plants to grow toward light, an ability described in more detail by Darwin and Darwin (1881). But the nature of the photoreceptor for this ability was long debated. Both flavin compounds and carotenes have absorption spectra that approximately match the action spectrum for phototropism. Finally the mystery was solved by a research team lead by Winslow Briggs at the Carnegie Institution of Washington (Huala et al. 1997; Christie et al. 1998) who identified the receptor as a novel type of flavoprotein, later named phototropin 1 and found to be a member of a widespread family called LOV domain proteins, distributed over all three domains of life (Krauss et al. 2009). The chromophore is flavin mononucleotide (FMN), in contrast to the redox-active chromophore (FAD) in cryptochromes.

In plants and algae there are three types of LOV domain photoreceptors, namely, phototropin, Zeitlupe, and aureochrome (Wada and Suetsugu 2013), and other types occur in bacteria (Losi 2004). Unlike phytochrome and cryptochrome, phototropins characteristically localize to the plasma membrane (Christie 2007). Kinetically LOV proteins are divided into two groups, i.e., slow-cycling and fast-cycling.

Eukaryotic LOV domains are divided into six clades: PHOT LOV1, PHOT LOV2, AUREO LOV, PASLOV PAS, PASLOV LOV, and Hap LOV (Ishikawa et al. 2009). AUREO LOV is subdivided into clades 1, 2, and 3 based on bZIP domain sequences.

13.9 Ciliate Photoreceptors

Some ciliates within the order Heterotrichida exhibit photoresponses which are mediated by any of the main classes of photoreceptors described above. They contain proteins having chromophores related to the well-known plant compound hypericin (Fig. 13.2). The latter is produced by *Hypericum* species and has been used for medical purposes. The ciliates most thoroughly investigated with respect to their photoreactions and photoreceptors are those belonging to genera *Stentor, Maristentor*, and *Blepharisma*. Only for these genera it has been established that the photoreactions are associated with the ciliate-specific photoreceptors described below, while the situation in other cases is at present uncertain, since the organisms contain also rhodopsins and flavin compounds (reviewed by Cadetti et al. 2000). For *Stentor*, action spectroscopy shows stentorin to be the active chromophore for photophobic response (Wood 1976), and for *Blepharisma*, blepharismin (Matsuoka et al. 1992). Another evidence supports the latter conclusion (Matsuoka et al. 1995). The proteins to which the chromophores are attached have so far not been well characterized. The stentorin chromophore is linked to a 50 kDa apoprotein. Several substances have been proposed as parts of a signal transduction chain, but the information so far is very scanty. Because the phylogenetic distribution of this type of photoreceptor is so limited, it is probably of rather late origin compared to other photoreceptors.

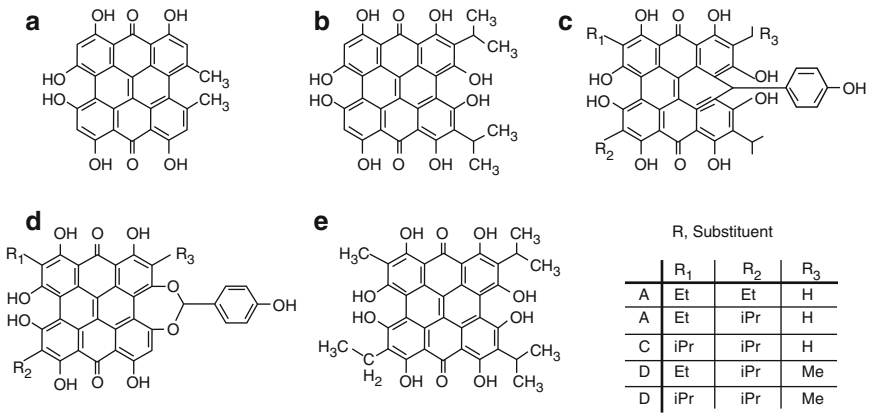

Fig. 13.2 Structures of (**a**) hypericin, (**b**) stentorin, (**c**) blepharismin, (**d**) oxyblepharismin, and (**e**) plausible formula for maristentorin (From Mukherjee et al. 2006)

13.10 The Plant UV-B Receptor, UVR8

It has long been realized that plants possess a UV-B-specific photoreceptor, but only recently has it been characterized on the molecular level. This photoreceptor differs from all others enumerated above by having no non-amino acid chromatophore (Christie et al. 2012; Wu et al. 2012). The UV-B absorption is achieved by a large number of aromatic amino acids in the protein, of which several tryptophan residues are so closely positioned that the π-orbitals overlap. Absorption of UV-B radiation around 290 nm causes the protein to be monomerized from the dimeric state and translocated from the cytoplasm to the nucleus, where it interacts with other proteins and affects gene transcription (see Chap. 11). The photoreceptor is widespread among plants. The green alga *Chlamydomonas* has a similar protein (Christie et al. 2012) that probably has the same function. Related proteins with other functions occur in other organisms, including animals. One of these is RCC1, a regulator of DNA replication (Dasso et al. 1992; Dasso 1993) and mitosis. It thus appears that the UVR8 photoreceptor is specific for green plants, but has an ancient ancestry.

References

Afonso CL, Tulman ER, Lu Z, Oma E, Kutish GF, Rock DL (1999) The Genome of *Melanoplus sanguinipes* Entomopoxvirus. J Virol 73:533–552

Afonso CL, Tulman ER, Lu Z, Zsak L, Kutish GF, Rock D (2000) The genome of fowlpox virus. J Virol 74:3815–3831

Alvarez CE (2008) On the origins of arrestin and rhodopsin. BMC Evol Biol 8:222. doi:10.1186/1471-2148-8-222, 2008

Anantharaman V, Koonin EV, Aravind L (2001) Regulatory potential, phyletic distribution and evolution of ancient, intracellular small-molecule binding domains. J Mol Biol 307:1271–1292

Aravind L, Ponting CP (1997) The GAF domain: an evolutionary link between diverse phototransducing proteins. Trends Biochem Sci 22(12):458–459. doi:10.1016/S0968-0004(97)01148-1

Arndt NT, Nisbet EG (2012) Processes on the young earth and the habitats of early life. Annu Rev Earth Planet Sci 40:521–549

Asimgil H, Kavakli IH (2012) Purification and characterization of five members of photolyase/cryptochrome family from *Cyanidioschyzon merolae*. Plant Sci 185–186:190–198

Auldridge ME, Forest KT (2011) Bacterial phytochromes: more than meets the light. Crit Revs Biochem Molec Biol 46:67–88

Banerjee R, Schleicher E, Meier S, Muñoz Viana R, Pokorny R, Ahmad M, Bittl R, Batschauer A (2007) The signaling state of *Arabidopsis* cryptochrome 2 contains flavin semiquinone. J Biol Chem 282:14916–14922

Bayram Ö, Biesemann C, Krappmann S, Galland P, Braus GH (2008) More than a repair enzyme: *Aspergillus nidulans* photolyase-like CryA is a regulator of sexual development. Molec Biol Cell 19:3254–3262

Beel B, Prager K, Spexard M, Sasso S, Weiss D, Müller N, Heinnickel M, Dewez D, Ikoma D, Grossman AR, Kottke T, Mittag M (2012) A flavin binding cryptochrome photoreceptor responds to both blue and red light in *Chlamydomonas reinhardtii* W. Plant Cell 24:2992–3008

Berrocal-Tito GM, Rosales-Saavedra T, Herrera-Estrella A, Horwitz BA (2000) Characterization of blue-light and developmental regulation of the photolyase gene *phr1* in *Trichoderma harzianum*. Photochem Photobiol 71:662–668

Biernat MA, Ros VID, Vlak JM, van Oers MM (2011) Baculovirus cyclobutane pyrimidine dimer photolyases show a close relationship with lepidopteran host homologues. Insect Mol Biol 20:457–464

Bouly J-P, Schleicher E, Dionisio-Sese M, Vandenbussche F, Van Der Straeten D, Bakrim N, Meier S, Batschauer A, Galland P, Bittl R, Ahmad M (2007) Cryptochrome blue light photoreceptors are activated through interconversion of flavin redox states. J Biol Chem 282:9383–9391

Braatsch S, Gomelsky M, Kuphal S, Klug G (2002) A single flavoprotein, AppA, integrates both redox and light signals in *Rhodobacter sphaeroides*. Mol Microbiol 45:827–836

Brown LS (2004) Fungal rhodopsins and opsin-related proteins: eukaryotic homologues of bacteriorhodopsin with unknown functions. Photochem Photobiol Sci 3:555–565

Brudler R, Hitomi K, Hiromi Daiyasu H, Toh H, Kucho K-i, Masahiro Ishiura M, Kanehisa M, Victoria A, Roberts VA, Todo T, Tainer JA, Getzoff ED (2003) Identification of a new cryptochrome class: structure, function, and evolution. Mol Cell 11:59–67

Burgie ES, Walker JM, Phillips GN Jr, Vierstra RD (2013) A photolabile thioether linkage to phycoviolobilin provides the foundation for the blue/green photocycles in DXCF-cyanobacteriochromes. Structure 21:88–97

Burney S, Wenzel R, Kottke T, Roussel T, Hoang N, Bouly J-P, Bittl R, Heberle J, Ahmad M (2012) Single amino acid substitution reveals latent photolyase activity in *Arabidopsis* cry1. Angew Chem Int Ed 51:9356–9360

Cadetti L, Marroni F, Marangoni R, Kuhlmannc H-W, Gioffré D, Colombetti G (2000) Phototaxis in the ciliated protozoan ophryoglena flava: dose–effect curves and action spectrum determination. J Photochem Photobiol B: Biol 57:41–50

Castrillo M, García-Martínez J, Avalos J (2013) Light-dependent functions of the Fusarium fujikuroi CryD DASH cryptochrome in development and secondary metabolism. Appl Environ Microbiol 79:2777

Chaves I, Pokorny R, Byrdin M, Hoang N, Ritz T, Brettel K, Essen L-O, van der Horst GTJ, Batschauer A, Ahmad M (2011) The cryptochromes: blue light photoreceptors in plants and animals. Annu Rev Plant Biol 62:335–364

Christie JM (2007) Phototropin blue-light receptors. Annu Rev Plant Biol 58:21–45

Christie JM, Reymond P, Powell GK, Bernasconi P, Raibekas AA, Liscum E, Briggs WR (1998) *Arabidopsis* NPH1: a flavoprotein with the properties of a photoreceptor for phototropism. Science 282:1698–1701

Christie JM, Arvai AS, Baxter KJ, Heilmann M, Pratt AJ, O'Hara A, Kelly SM, Hothorn M, Smith BO, Hitomi K, Jenkins GI, Getzoff ED (2012) Plant UVR8 photoreceptor senses UV-B by tryptophan-mediated disruption of cross-dimer salt bridges. Science 335:1492–1496

Darwin C, Darwin F (1881) The power of movement in plants. D. Appleton & Co., New York

Dasso M (1993) RCC1 in the cell-cycle – the regulator of chromosome condensation takes on new roles. Trends Biochem Sci 18:96–101

Dasso M, Nishitani H, Kornbluth S, Nishimoto T, Newport JW (1992) RCC1, a regulator of mitosis, is essential for DNA replication. Mol Cell Biol 12:3337–3345

Devine EL, Oprian DD, Theobald DL (2013) Relocating the active-site lysine in rhodopsin and implications for evolution of retinylidene proteins. Proc Natl Acad Sci U S A 110:13351–13355

Essen L-O (2006) Photolyases and cryptochromes: common mechanisms of DNA repair and light-driven signaling? Curr Opin Struct Biol 16:51–59

Fan Y, Solomon P, Oliver RP, Brown LS (2011) Photochemical characterization of a novel fungal rhodopsin from *Phaeosphaeria nodorum*. Biochim Biophys Acta 1807:1457–1466

Feuda R, Hamilton SC, McInerney JO, Pisani D (2012) Metazoan opsin evolution reveals a simple route to animal vision. Proc Natl Acad Sci U S A 109:18868–18872

Fischer MG, Allen MJ, Wilson WH, Suttle CA (2010) Giant virus with a remarkable complement of genes infects marine zooplankton. Proc Natl Acad Sci USA 107:19508–19513

Fitch Q (1970) Distinguishing homologous from analogous proteins. Syst Zool 19:99–113

Flament N, Coltice N, Rey PF (2008) A case for late-Archaean continental emergence from thermal evolution models and hypsometry. Earth Planet Sci Lett 275:326–336

Geisselbrecht Y, Frühwirth S, Schroeder C, Pierik AJ, Gabriele Klug G, Essen L-O (2012) CryB from *Rhodobacter sphaeroides*: a unique class of cryptochromes with new cofactors. EMBO Rep 13:223–229

Gomelsky M, Klug G (2002) BLUF: a novel FAD-binding domain involved in sensory transduction in microorganisms. Trends Biochem Sci 27:497–500

Ho Y-SJ, Burden LM, Hurley JH (2000) Structure of the GAF domain, a ubiquitous signaling motif and a new class of cyclic GMP receptor. EMBO J 19:5288–5299

Hoff WD, Matthijs HCP, Schubert H, Crielaard W, Hellingwerf KJ (1995) Rhodopsin(s) in eubacteria. Biophys Chem 56:193–199

Huala E, Oeller PW, Liscum E, Han IS, Larsen E, Briggs WR (1997) *Arabidopsis* NPH1: a protein kinase with a putative redox-sensing domain. Science 278:2120–2123

Inoue K, Reissig L, Sakai M, Kobayashi K, Homma M, Fujii M, Kandori H, Sudo Y (2012) Absorption spectra and photochemical reactions in a unique photoactive protein, middle rhodopsin MR. J Phys Chem B 116:5888–5899

Iseki M, Matsunaga S, Murakami A, Ohno K, Shiga K, Yoshida K et al (2002) A blue-light-activated adenylyl cyclase mediates photoavoidance in *Euglena gracilis*. Nature 415:1047–1051

Ishikawa M, Takahashi F, Nozaki H, Nagasato C, Motomura T, Kataoka H (2009) Distribution and phylogeny of the blue light receptors aureochromes in eukaryotes. Planta 230:543–552. doi:10.1007/s00425-009-0967-6

Ito H, Sumii M, Kawanabe A, Fan Y, Furutani Y, Brown LS, Hideki Kandori H (2012) Comparative FTIR study of a new fungal rhodopsin. J Phys Chem B 116:11881–11889

Jiang ZY, Swem LR, Rushing B-G, Devanathan S, Tollinand G, Bauer CE (1999) Bacterial photoreceptor with similarity to photoactive yellow protein and plant phytochromes. Science 285:406–409

Jung K-H, Trivedi VD, Spudich JL (2003) Sensory rhodopsin in eubacteria. Mol Microbiol 47:1513–1522

Kiontke S, Geisselbrecht Y, Pokorny R, Carell T, Batschauer A, Essen L-A (2011) Crystal structures of an archaeal class II DNA photolyase and its complex with UV-damaged duplex DNA. EMBO J 30:4437–4449

Kondoh M, Shiraishi C, Müller P, Ahmad M, Hitomi K, Getzoff ED, Terazima M (2011) Light-induced conformational changes in full-length *Arabidopsis thaliana* cryptochrome. J Mol Biol 413:128–137

Krauss U, Minh BQ, Losi A, Gärtner W, Eggert T, von Haeseler A, Jaeger K-E (2009) Distribution and phylogeny of light-oxygen-voltage-blue-light-signaling proteins in the three kingdoms of life. J Bacteriol 191:7234–7242

Krishnan A, Sällman Almén M, Fredriksson R, Schiöth HB (2012) The origin of GPCRs: identification of mammalian like rhodopsin, adhesion, glutamate and frizzled GPCRs in fungi. PLoS ONE 7:e29817, 15 pp

Kumauchi M, Hara MT, Stalcup P, Xie A, Hoff WD (2008) Identification of six new photoactive yellow proteins – diversity and structure-function relationships in a bacterial blue light photoreceptor. Photochem Photobiol 84:956–969

Kyndt JA, Fitch JC, Meyer TE, Cusanovich MA (2007) The photoactivated PYP domain of *Rhodospirillum centenum* Ppr accelerates the recovery of the bacteriophytochrome domain after white light illumination. Biochemistry 46:8256–8262

Kyndt JA, Fitch JC, Seibeck S, Borucki B, Heyn MP, Meyer TE, Cusanovich MA (2010) Regulation of the Pprhistidinekinase by light-induced interactions between its photoactive yellow protein and bacteriophytochromedomains. Biochemistry 2010, 1744–1754

Liu H, Liu B, Zhao C, Pepper M, Lin C (2011) The action mechanisms of plant cryptochromes. Trends Plant Sci 16:684–691

Losi A (2004) The bacterial counterparts of plant phototropins. Photochem Photobiol Sci 3:566–574

Lucas-Lledó JI, Lynch M (2009) Evolution of mutation rates: phylogenomic analysis of the photolyase/cryptochrome family. Mol Biol Evol 26:1143–1153

Mandalari C, Losi A, Gärtner W (2013) Distance-tree analysis, distribution and co-presence of bilin-and flavin-binding prokaryotic photoreceptors for visible light. Photochem Photobiol Sci 12:1144–1157

Masuda S, Bauer CE (2002) AppA is a blue light photoreceptor that antirepresses photosynthesis gene expression in *Rhodobacter sphaeroides*. Cell 110:613–616

Matsuoka T, Matsuoka S, Yamaoka Y, Kuriu T, Watanabe Y, Takayanagi M, Kato Y, Taneda K (1992) Action spectra for step-up photophobic response in *Blepharisma*. J Protozool 39:498–502

Matsuoka T, Watanabe Y, Sagara Y, Takayanagi M, Kato Y (1995) Additional evidence for blepharismin photoreceptor pigment mediating step-up photophobic response of unicellular organism *Blepharisma*. Photochem Photobiol 62:190–193

Meyer T (1985) Isolation and characterization of soluble cytochromes, ferredoxin and other chromophoric proteins from the halophile

phototrophic bacterium *Ectothiorhodospira halophila*. Biochim Biophys Acta 806:175–183
Meyer TA, Kyndt JA, Memmi S, Moser T, Colón-Acevedo B, Devreese B, Van Beeumen JJ (2012) The growing family of photoactive yellow proteins and their presumed functional roles. Photochem Photobiol Sci 11:1495–1514
Meyer TE, Yakali E, Cusanovich MA, Tollin G (1987) Properties of a water-soluble, yellow protein isolated from a halophilic phototrophic bacterium that has photochemical activity analogous to sensory rhodopsin. Biochemistry 26:418–423
Möglich AA, Ayers R, Moffat K (2009) Structure and signaling mechanism of Per-ARNT-Sim domains. Structure 17:1282–1294
Mukherjee P, Fulton DB, Halder M, Han X, Armstrong DW, Petrich JW, Lobban CS (2006) Maristentorin, a novel pigment from the positively phototactic marine ciliate *Maristentor dinoferus*, is structurally related to hypericin and stentorin. J Phys Chem B 2006(110):6359–6364
Müller M, Carell T (2009) Structural biology of DNA photolyases and cryptochromes. Curr Opin Struct Biol 19:277–285
Nalcacioglu R, Dizman YA, Vlak JM, Demirbag Z, van Oers MM (2010) Amsacta moorei entomopoxvirus encodes a functional DNA photolyase (AMV025). J Invertebr Pathol 105:363–365
Narikawa R, Kohchib T, Ikeuchia M (2008) Characterization of the photoactive GAF domain of the CikA homolog (SyCikA, Slr 1969) of the cyanobacterium Synechocystis sp. PCC 6803. Photochem Photobiol Sci 7:1253–1259
Novikov GV, Sivozhelezov VS, Shebanova AS, Shaitan KV (2012) Classification of rhodopsin structures by modern methods of structural bioinformatics. Biochemistry (Mosc) 77:435–443 (Biokhimiya 77: 544–554)
Oberpichler I, Pierik AJ, Wesslowski J, Pokorny R, Rosen R, Vugman M, Zhang F, Neubauer O, Ron EZ, Batschauer A, Lamparter T (2011) A photolyase-like protein from *Agrobacterium tumefaciens* with an iron-sulfur cluster. PLoS ONE 6:e26775. doi:10.1371/journal.pone.0026775
Osigus H-J, Eitel M, Schierwater B (2013) Chasing the urmetazoon: striking a blow for quality data? Mol Phylogenet Evol 66:551–557
Öztürk N, Kao Y-T, Selby CP, Kavakl IH, Partch CL, Zhong D, Sancar A (2008) Purification and characterization of a type III photolyase from *Caulobacter crescentus*. Biochemistry 47:10255–10261
Parker A (2004) In the blink of an eye: how vision kick-started the big bang of evolution. Simon & Schuster, London. ISBN 0-7432-5733-2
Parker AR (2011) On the origin of optics. Optics & Laser Technol. 43, 323–329
Porter ML, Blasic JR, Bok MJ, Cameron EG, Pringle T, Cronin TW, Robinson PR (2012) Shedding new light on opsin evolution. Proc R Soc B 279:3–14
Rivera AS, Ozturk N, Fahey B, Plachetzki DC, Degnan BM, Aziz Sancar A, Oakley TH (2012) Blue-light-receptive cryptochrome is expressed in a sponge eye lacking neurons and opsin. J Exp Biol 215:1278–1286
Ruiz-González RX, Marin M (2004) New insights into the evolutionary history of type 1 rhodopsins. J Mol Evol 58:348–358
Shen L, Chen C, Zheng H, Jin L (2013) The evolutionary relationship between microbial rhodopsins and metazoan rhodopsins. Sci World J Article ID 435651, 10 p
Soppa J (1994) Sequence comparison does not support an evolutionary link between halobacterial retinal proteins including bacteriorhodopsin and eukaryotic G-protein-coupled receptors. FEBS Lett 342:7–11
Sudo Y, Ihara K, Kobayashi S, Suzuki D, Irieda H, Kikukawa T, Kandori H, Homma MJ (2011) A microbial rhodopsin with a unique retinal composition shows both sensory rhodopsin II and bacteriorhodopsin-like properties. Biol Chem 286:5967–5976
Suetsugo N, Kong S-G, Kasahara M, Wada M (2013) Both LOV1 and LOV2 domains of phototropin2 function as the photosensory domain for hypocotyl phototropic responses in *Arabidopsis thaliana* (Brassicaceae). Am J Bot 100:60–69
Taylor EW, Agarwal A (1993) Sequence homology between bacteriorhodopsin and G-protein coupled receptors: exon shuffling or evolution by duplication? FEBS Lett 325:161–166
Terakita A (2005) The opsins. Genome Biol 6:213 (9 p)
van Oers MM, Herniou EA, Usmany M, Messelink GJ, Vlak JM (2004) Identification and characterization of a DNA photolyase containing baculovirus from *Chrysodeixis chalcites*. Virology 330: 460–470
Wada M, Suetsugu N (2013) Evolution of three LOV blue light receptor families in green plants and photosynthetic stramenopiles: phototropin, ZTL/FKF1/LKP2 and aureochrome. Plant Cell Physiol 54:8–23. doi:10.1093/pcp/pcs165
Wang Y, Maruhnich SA, Mageroy MH, Justice JR, Folta KM (2013) Phototropin 1 and cryptochrome action in response to green light in combination with other wavelengths. Planta 237:225–237
Waschuk SA, Bezerra AG Jr, Shi L, Brown LS (2005) *Leptosphaeria* rhodopsin: bacteriorhodopsin-like proton pump from a eukaryote. Proc Natl Acad Sci USA 102:6879–6883
Wood DC (1976) Action spectrum and electrophysiological responses correlated with the photophobic response of *Stentor coeruleus*. Photochem Photobiol 24:261–266
Wu D, Hu Q, Yan Z, Chen W, Yan C, Huang X, Zhang J, Yang P, Deng H, Wang J, Deng XW, Shi Y (2012) Structural basis of ultraviolet-B perception by UVR8. Nature 484:215–220
Yutin N, Koonin EV (2013) Proteorhodopsin genes in giant viruses. Biol Direct 7:34, 2012
Zhang F, Vierock J, Yizhar O, Fenno LE, Tsunoda S, Kianianmomeni A, Prigge M, Berndt A, Cushman J, Polle J, Magnuson J, Hegemann P, Deisseroth K (2011) The microbial opsin family of optogenetic tools. Cell 147:1446–1457
Zuo ZC, Meng Y-Y, Yu X-H, Zhang Z-L, Feng D-S, Sun S-F, Liua B, Lin C-T (2012) A study of the blue-light-dependent phosphorylation, degradation, and photobody formation of *Arabidopsis* CRY2. Mol Plant 5:726–733

Signaling Cross Talk Under the Control of Plant Photoreceptors

14

Lei Jiang and Shaoshan Li

14.1 Introduction

Plants have evolved the capacity to sense and interpret diverse light signals to modulate their development. In the extensively studied plant *Arabidopsis thaliana*, four distinct families of photoreceptors (phytochromes, cryptochromes, phototropins, and UV-B photoreceptor) have been well characterized. In this chapter, we give a general description on molecular mechanism of photoreceptors and basic structures of different light signaling. We then dedicate to the signaling cross talk under the control of various kinds of photoreceptors, including (1) signaling interaction between light and UV-B; (2) physical interactions among phytochrome, phototropin, and cryptochrome; and (3) signaling integration of phytochrome and cryptochrome.

14.2 Photoreceptor Regulation and Activity: An Overview

Photoreceptors have the ability to sense and distinguish light of different spectral composition, delivering the signal to the downstream components, initiating transcription of various genes. This finally results in multiple developmental processes, including seed germination, seedling photomorphogenesis, phototropism, gravitropism, chloroplast movement, shade avoidance, circadian rhythms, and flower induction (Quail 2002). Therefore, the photoreceptors play the central role in plant life. After germination, seedlings follow one of two developmental patterns. Skotomorphogenesis (or etiolation) in the dark is characterized by long hypocotyl, closed cotyledons in *Arabidopsis*, and the development of proplastids into etioplasts. By contrast, growth in the light leads to photomorphogenesis (or de-etiolation) characterized by short hypocotyls, expanded open cotyledons, and the development of mature chloroplasts (Jiao et al. 2007). A wide spectrum of light can induce photomorphogenesis; however, for clarification, we here define the far red-, red-, blue-, and UV-A-induced photomorphogenesis as light photomorphogenesis, while UV-B-induced one as UV-B photomorphogenesis. In *Arabidopsis*, there are five phytochromes (PHYA to PHYE) that perceive red/far-red light, three cryptochromes (CRY1 to CRY3) and two phototropins (PHOT1 and PHOT2) that sense blue/UV-A light, and one known UV-B photoreceptor (UVR8) that senses UV-B (280-215 nm).

Phytochromes (phys) are homodimeric photoreceptors of approximately 120 kDa monomers that bear a single linear tetrapyrrole chromophore, which exists in two photoconvertible forms: Pr (red light-absorbing phy) and Pfr (far-red light-absorbing phy) (Vierstra and Zhang 2011). The photoconversion results in their translocation from the cytoplasm into the nucleus (Quail 2002). This translocation is caused by the phosphorylation of PHYs, which leads to alter its stability and affinity toward downstream signal components (Kim et al. 2004; Ryu et al. 2005). Photoactivated phytochrome has kinase activity, inducing phosphorylation of PIF3 (PHYTOCHROME-INTERACTING PROTEIN 3) and PKS1, initiating the *downstream signaling* (Al-Sady et al. 2006; Fankhauser et al. 1999) (Fig. 14.1).

Cryptochromes (crys) are photolyase-like blue light/UV-A receptors that bind a flavin adenine dinucleotide chromophore (Yu et al. 2010). *Arabidopsis* has three members of this family, CRY1, CRY2, and CRY3, which show significant homology to microbial photolyase, but lack photorepair activity. CRY1 is nuclear localized in the dark but largely cytoplasmic under light, while CRY2 is constitutively nuclear (Lin and Shalitin 2003). A more divergent CRY3 does not have the photolyase-related (PHR) domain and less conserved DAS domain (CCT), which are present in CRY1 and CRY2 Partch et al. 2005). However, CRY3 has a dual function in regulating its transport to chloroplast and mitochondria (Kim et al. 2004). Light can induce the

L. Jiang (✉) • S. Li
School of Life Science, South China Normal University, Guangzhou, China
e-mail: leoi.jiang@gmail.com; lishsh@scnu.edu.cn

L.O. Björn (ed.), *Photobiology: The Science of Light and Life*,
DOI 10.1007/978-1-4939-1468-5_14, © Springer Science+Business Media New York 2015

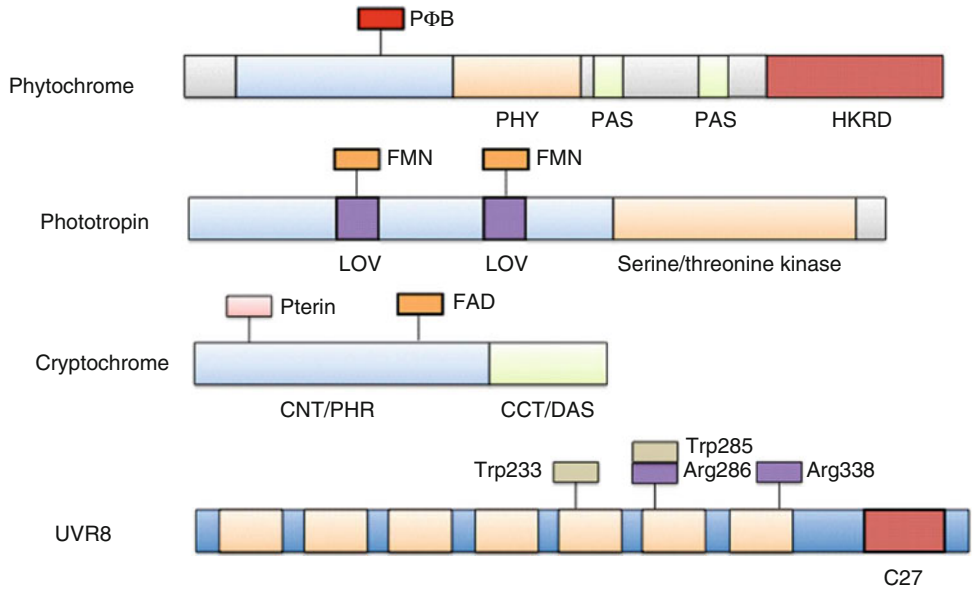

Fig. 14.1 The structure of various kinds of photoreceptors. The phytochromes are dimeric chromoproteins. Each polypeptide consists of an N-terminal photosensory domain that covalently binds a single bilin chromophore (PΦB), followed by a C-terminal domain. Phototropins have a photosensory N-terminal half and a C-terminal half with serine/threonine kinase function. The N terminus contains two flavin mononucleotide (FMN) chromophore-binding LOV domains (LOV1 and LOV2). Cryptochromes 1 and 2 have an N-terminal photolyase-related (PHR) domain (CNT) and a less conserved, intrinsically unstructured C-terminal DAS domain (CCT), which is not present in CRY3. The PHR domain noncovalently binds to two chromophores, a flavin adenine dinucleotide (FAD), and a pterin. UVR8 is a seven-bladed β-propeller protein. Arginine (Arg) residues at positions 286 and 338 facilitate hydrogen bonds that hold the homodimer together, while tryptophan (Trp) residues at positions 285 and 233 serve as chromophores. C27 is a protein interaction domain, which is responsible for the interaction with RUPs and COP1

autophosphorylation of CRY1 and CRY2, resulting from the conformational change in the C-terminus CCT domain by the activation of the N-terminus CNT domain. Phosphorylated CRYs can be dimerized and possibly interact with downstream factors (Sang et al. 2005).

Phototropins (phots) are the plant-specific blue light receptors with serine/threonine protein kinase activity. They bear two LOV domains that bind flavin mononucleotide chromophores (Christie 2007). Several transient developments, including phototropism, chloroplast movement, and stomatal opening, are controlled by them. *Arabidopsis* PHOT1 and PHOT2 are mainly associated with the plasma membrane, but only a fraction of PHOT1 is relocated to the cytoplasm (Christie 2007). Blue light triggers the autophosphorylation of PHOT1 and PHOT2, initiating the transduction of the light signal (Christie 2007).

UV-B Photoreceptor: UVR8 (UV RESISTANCE LOCUS 8) is the recently identified UV-B-specific photoreceptor, with two tryptophans (W233 and W285) as the chromophores. In the absence of UV-B radiation, dimeric UVR8 is localized in the cytoplasm. Upon exposure to UV-B, it monomerizes and migrates to the nucleus. This change is essential for the following signaling transduction.

14.3 Simplified Light and UV-B Signaling

14.3.1 Introduction

Light signaling is one of the most well-elucidated pathways in *Arabidopsis*, which more than a hundred regulators have been found to play a role in response to light. Several reviews have been published to summarize the complicated signaling (Quail 2002; Jiao et al. 2007), and here we give a simplified signaling model in regard of seedling morphogenesis and will focus on the interconnections shortly.

14.3.2 Light Signaling Pathway

In the dark, a seedling undergoes skotomorphogenesis, in the absence of photoreceptor activation. In this process, there are two groups of proteins, namely, COP/DET/FUS (CONSTITUTIVE PHOTOMORPHOGENIC/DE-ETIOLATED/FUSCA) and PIFs, to maintain the status of skotomorphogenesis. The COP/DET/FUS complex is a member of the ubiquitin system, which is responsible for

protein degradation (Sullivan et al. 2003). Because they work in concert to degrade a number of photomorphogenesis-promoting transcription factors, such as HY5 (LONG HYPOCOTYL 5), COP/DET/FUS are the central repressors of photomorphogenesis (Saijo et al. 2003; Osterlund et al. 2000). COP1 is one of the proteins in the complex and has the activity of Ub E3 ligase by interacting with many of the photomorphogenesis-promoting transcription factors. It has been shown that the ubiquitination is promoted by SPA (SUPPRESSOR OF PHYA-105) family proteins (Osterlund et al. 2000; Laubinger et al. 2004). After light illumination, the activated photoreceptors (PHYA, PHYB, CRY1, and CRY2) suppress COP1 function by translocating from nucleus to cytoplasm, resulting in the photomorphogenesis-promoting transcription factors, which initiate the expression of a large number of light-responsive genes to promote photomorphogenesis (Osterlund et al. 2000).

Contrasting to the repressed function of COP/DET/FUS by inactivate photomorphogenesis-promoting transcription factors, another group of proteins called PIFs directly regulate gene expression to promote skotomorphogenesis (Leivar et al. 2008). PIFs, the basic helix-loop-helix (bHLH) transcription factors, include PIF1/PIL5 (PIF3-LIKE 5), PIF3, PIF4, PIF5/PIL6, and PIF6/PIL2, and they physically interact with phytochromes (Castillon et al. 2007). In the dark, PIFs activate skotomorphogenesis-promoted genes (Leivar et al. 2008), but they are inactivated by light resulting in repression of photomorphogenesis. This inactivation is due to the phosphorylation by photoactivated Pfr form of phytochromes. The phosphorylated PIFs are subsequently degraded by proteasome, and its stability is dependent on COP1 and SPA protein (Al-Sady et al. 2006; Shen et al. 2007). Briefly, the complicated signaling pathway downstream of light photoreceptors is mainly classified into two above branches, COP1-HY5 and PIFs pathways, and recently research revealed that these key components play an important role in light signaling cross talk (Fig. 14.2).

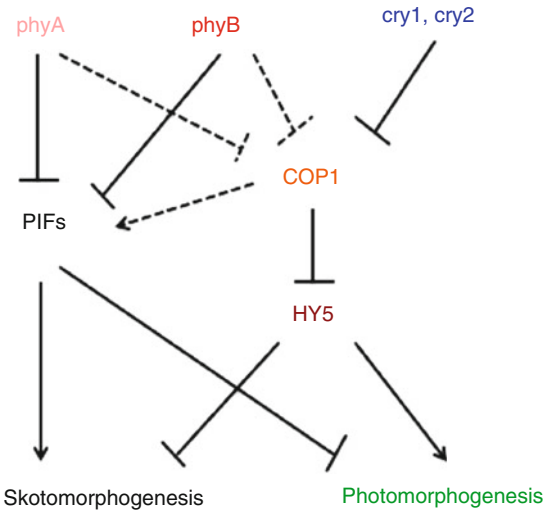

Fig. 14.2 A simplified light signaling pathway in *Arabidopsis*. Under light, the photoreceptors suppress two main branches of light signaling, COP1-HY5 and PIFs. COP1, which is repressed by phytochromes and cryptochromes, is an ubiquitin E3 ligase, and it directly targets HY5 for degradation. HY5 is a bZIP transcription factor that promotes photomorphogenesis in all light conditions (Fig. 14.1). PIFs are bHLH transcription factors that are required for skotomorphogenesis. Phytochromes directly interact with PIFs, resulting in PIFs' degradation, while COP1 positively affects PIF's protein level. Note: between two proteins, *solid lines* indicate a direct effect, while *dotted lines* represent an indirect regulation

14.3.3 UV-B Signaling Pathway

Compared to the complicated signaling pathways in light responses, the pathways activated by UV-B radiation is much simpler to chart. With the recently identified UV-B receptor UVR8, this signaling pathway can be structurally described. Upon UV-B irradiation, UVR8 is activated by converting from dimers to monomers (Rizzini et al. 2011). The monomerized UVR8 further interacts with COP1 to promote its accumulation (Favory et al 2009). COP1 then stabilizes the central transcription factors HY5 and its homolog, HYH, resulting in the initiation of UV-B-responsive genes to promote UV-B photomorphogenesis (Ulm et al. 2004). However, not all of these genes are UVR8 dependent. To fine-tune this linear pathway, several components have been identified to form feedback regulations. STO/BBX24 (SALT TOLERANCE/B-BOX DOMAIN PROTEIN 24) interacts with both HY5 and COP1 to involve in a negative feedback loop by impinging on HY5 (Jiang et al. 2012). FHY3 (FAR-RED ELONGATED HYPOCOTYL 3) and HY5 work together to modulate the expression of COP1 as the members of a positive feedback loop (Huang et al. 2012). RUP1/2 (REPRESSOR UV-B PHOTOMORPHOGENESIS 1/2) belong to the WD40-repeat protein superfamily, interacting both with COP1 and UVR8 to act as negative feedback regulators (Gruber et al. 2010). It has been reported that RUP1/2 mediate the redimerization of UVR8, leading to the disruption of UVR8-COP1 interaction to attenuate the signaling, and this regulation is independent of COP1 (Heijde and Ulm 2013). For the detailed information on UV-B signaling, please refer to the reviews by Jenkins (2009), Heijde and Ulm (2012), Jiang et al. (2012) and Tilbrook et al. (2013) (Fig. 14.3).

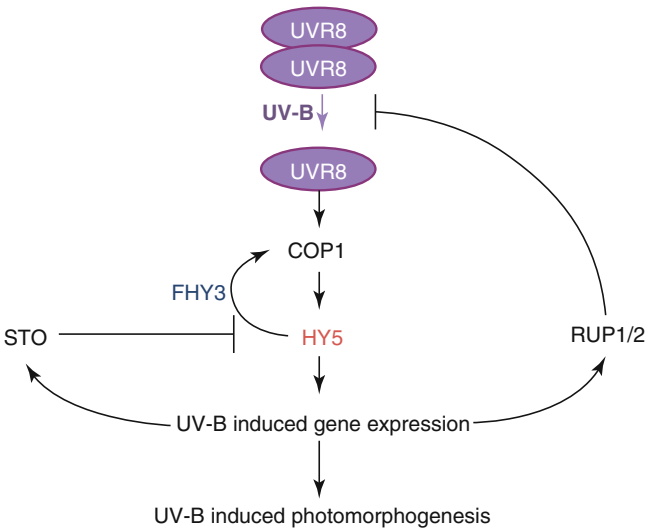

Fig. 14.3 UV-B signaling pathway in *Arabidopsis*. The UV-B radiation is specifically perceived by the UV-B photoreceptor UVR8, resulting in the rapid accumulation of COP1 and its interaction with UVR8. COP1-UVR8 interaction presumably stabilizes and activates HY5 for its transcriptional activity, leading to UV-B-regulated gene expression and photomorphogenesis (Fig. 14.3). This UV-B signaling cascade is feedback regulated by a few negative regulators, including BBX24 and RUP1/RUP2. While RUP1/RUP2 negatively regulates UV-B signaling by interacting with UVR8, the BBX24 protein fine-tunes the UV-B responses by impinging on HY5. FHY3 and HY5 have the ability to bind to COP1 promoter to control the expression of *COP1*

14.4 Signaling Cross Talk Between Light and UV-B

14.4.1 Introduction

Before the identification of UVR8, many attempts have been made in pursuit of the distinct UV-B signal transduction pathway. The light-induced CHS gene is found to be upregulated by all kinds of light and controlled by photoreceptors. For instance, UV-A and blue light-induced CHS expression is modulated by cry1, but cry1 is not required for UV-B-induced expression. In addition, UV-A and blue light each act synergistically with UV-B to stimulate CHS, and this synergism is retained in cry1-deficient mutant (Fuglevand et al. 1996). These results support the notion that there might be a considerable complexity in both photoreception and signal transduction in regulating CHS by UV-B and UV-A/blue light in *Arabidopsis*.

Stomatal opening is one of many physiological responses of plants regulated by blue light receptors, PHOT1 and PHOT2 (Kinoshita et al. 2001; Boccalandro et al. 2012), but it can also be modulated by UV-B (Eisinger et al. 2000). The blue light- and UV-B-induced stomatal opening is reversed by green light (Eisinger et al. 2003). However, phot1/phot2 double mutants show normal stomatal opening in response to UV-B, and green light fails to antagonize this process (Eisinger et al. 2003), indicating that phot1 and phot2 are required for the inhibition of UV-B effects by green light. The UV-B bending response of *Arabidopsis* hypocotyls during phototropism appears to be mediated by phototropins (Eisinger et al. 2003). The above evidence give a clear picture that UV-B is governed by a distinct photoreceptor and deeply cross-talked with other light photoreceptors. However, the above phenotypes are difficult to identify in large genetic screening. The phenotypes with shorter hypocotyl and higher pigment accumulation under low-fluence rate of UV-B are easier to screen by the eyes. Thus, all the regulators in UV-B signaling are identified by these two phenotypes. Moreover, hypocotyl growth inhibition and pigment accumulation are also featured in light photomorphogenesis. With the identification of UVR8, several main regulators in UV-B signaling have been revealed. Not surprisingly, most of them have other functions in other light signaling.

14.4.2 COP1: A Negative Factor in Light Signaling but a Positive Factor in UV-B Signaling

COP1 encodes a RING finger E3 ubiquitin ligase, which consists of three functional domains: a RING finger required for ligase activity, a coiled-coil domain for dimerization, and a WD40-repeat domain for target binding (Yi and Deng 2005). In the dark, COP1 function as an E3 ligase to target the light-responsive transcription factors (such as HY5) to repress the light photomorphogenesis. While, in the presence of light, COP1 is inactivated, resulting in the stabilization of HY5 to unleash the light responses (Osterlund et al. 2000). It is believed that early inactivation of COP1 by visible light occurs through direct interaction with phytochromes and cryptochromes (Wang et al. 2001; Seo et al. 2004), and the nuclear exclusion of COP1 is a rate-limiting step for photomorphogenic development (Subramanian et al. 2004). Moreover, the E3 ligase activity requires plant-specific SPA proteins, which is physically interacting with COP1 through the coiled-coil domain (Laubinger et al. 2004).

The *cop1* mutants display light-grown phenotypes even in darkness, including short hypocotyls, open cotyledons, and elevated pigment levels. These constitutive light and UV-B photomorphogenic phenotypes make them very difficult to investigate under UV-B, but after prolonged UV-B treatment, cop1–4 mutant shows chlorosis, suggesting COP1 may plant a positive role in UV-B responses (Oravecz et al. 2006). Surprisingly, a large number of UV-B-responsive genes are inactivated in the cop1–4 mutant (Oravecz et al. 2006). In contrast to the relocation to cytoplasm in light, COP1 is stabilized and accumulates in the nucleus (Oravecz et al. 2006). This accumulation is caused by direct gene upregulation by

UV-B (Huang et al. 2012). The rapid interaction of UVR8 and COP1 is believed to account for the stabilization (Favory et al. 2009), but the molecular mechanism is still unknown. COP1 is also crucial to UV-B-induced HY5 activation, and they both accumulate in the nucleus in response to UV-B (Oravecz et al. 2006). This indicates that COP1 may not have an E3 ligase activity in UV-B signaling, and the notion is further supported by the evidence that SPA is not required for the proper function of COP1 in response to UV-B (Oravecz et al. 2006). Thus this protein has dual opposite functions in response to two different spectra of light. One might ask what the function is under solar light, which contains both UV-B and visible light. Is COP1 located in the cytoplasm or in the nucleus? Is the amount of COP1 decreased or increased? These are questions to be elucidated in the field condition.

14.4.3 HY5 Has the Leading Role in Both Light and UV-B Signaling

Distinct light qualities, which are mediated through different photoreceptors, have similar effects on the transcriptomes during photomorphogenesis (Ma et al. 2001). Therefore, it is reasonable to suggest that one or more integration points exist for light signaling. A few light-induced transcription factors have been identified as key regulators during seedling morphogenesis. One of them is HY5, which is a target of COP1 for 26S proteasome-mediated degradation (Osterlund et al. 2000).

HY5 encodes a bZIP (basic leucine zipper) transcription factor, which could be the most important transcription factor that not only controls photomorphogenesis (Osterlund et al. 2000) but also governs other kinds of development, such as plant hormone responses (Lau and Deng 2010). Genome-enabled high-throughput analysis of immunoprecipitated chromatin (ChIP-chip or ChIP-seq) have revealed that HY5 binds directly to the promoter regions of light-responsive genes (Lee et al. 2007) and controls ~20 % of the light-regulated genes in *Arabidopsis* (Ma et al. 2002). Meanwhile, HY5 also guides the posttranscriptional regulation systems. For example, HY5 regulates eight miRNA (micro RNA) genes that in turn control the transcript abundance of specific target genes. Overexpressing HY5-targeted miR408 resulted in phenotypes that are opposite to the hy5 mutants (Zhang et al. 2011). Therefore, HY5 is likely to play a hierarchical role in photomorphogenesis. Recently developed large-scale analysis tools have enabled us to gain more insight into the mechanisms of how HY5 functions as a central transcription factor. More than 10,000 genes are found to be regulated by HY5 (Zhang et al. 2011), which is three times larger than previously reported (Lee et al. 2007), owing to the development of the resolution of ChIP-seq. As a transcription factor, HY5 has its own binding characters, which is aimed at 1 kb upstream of the transcription start site (TSS) and 5′ untranslated regions (UTRs) (Zhang et al. 2011). Three binding motifs, G-box, C-box, and hybrid CG-boxes, have been found to occur at a higher frequency in the identified HY5-binding regions (Zhang et al. 2011). Most surprisingly, histone modification is involved in HY5-mediated gene regulation. Comparing the pattern between wild-type and *hy5* seedlings revealed that the level of permissive H3 histone modifications (acetylated H3K9 and trimethylated H3K4) was increased, while that of the inhibitory histone H3 modification (di-methylated H3K9) was substantially decreased in HY5-bound regions for genes positively regulated by HY5 (Zhang et al. 2011). Another important feature is that HY5 can be a candidate in a feedback regulation loop, and we will talk about this later.

The *hy5* mutant shows aberrant light-mediated phenotypes in *Arabidopsis*, including an elongated hypocotyl and reduced chlorophyll/anthocyanin accumulation (Oyama et al. 1997). But this kind of disturbance is slightly reduced by photomorphogenic UV-B radiation (Ulm et al. 2004), and the hypersensitive phenotype is further extended to UV-B stress (Brown et al. 2005). Genome-wide expression analysis reveals that a large number of UV-B-inducible genes are regulated by HY5, including the genes involved in UV protection (Ulm et al. 2004). Therefore, similar to the role in light signaling, HY5 is also a central transcription factor in UV-B-responsive pathway. However, the function of HY5 in UV-B signaling is under the control of UVR8, rather than other photoreceptors, because UV-B-induced upregulation of HY5 does not show any changes in various photoreceptor mutants (Ulm et al. 2004). UV-B-induced HY5-dependent genes have a large overlap with UVR8- and COP1-dependent genes, suggesting these three components work together to control the UV-B responses (Brown and Jenkins 2008; Oravecz et al. 2006). Interestingly, UVR8 itself is proposed to associate with chromatin in the vicinity of the HY5 genomic locus regardless of UV-B (Brown et al. 2005), but this is not the mechanism that UV-B-induced HY5 expression is tightly regulated by UVR8. In contrast to the COP1-mediated degradation of HY5 in darkness, COP1 is required for the HY5 expression under UV-B (Oravecz et al. 2006). In turn, HY5 is found to bind to the ACGT-containing elements (ACEs) within the COP1 promoter to upregulate COP1 (Huang et al. 2012). Thus, HY5 is involved in a positive feedback loop to fine-tune the UV-B responses.

14.4.4 BBX24/STO Negatively Modulates Light and UV-B Signaling

STO is a B-box-type zinc finger protein with sequence similarities to CONSTANS (Griffiths et al. 2003). It was identified

through a screening from a series of yeast calcineurin mutants, where STO protein can rescue the yeast salt-sensitive phenotype caused by the deficient of the catalytic subunit genes (cna1cna2) or the regulatory subunit gene (cnb1) (Lippuner et al. 1996). However, *Arabidopsis* overexpressed with STO has not shown typical salt tolerance phenotypes, and STO gene itself cannot be regulated by salt treatment (Nagaoka and Takano 2003). Even more surprisingly, STO is found to have a negative role in light signaling (Indorf et al. 2007). STO also called BBX24 according to the nomenclature for the B-box transcription factors (Khanna et al. 2009).

Despite the ambiguous phenotypes in salt treatment and sto/bbx24 mutant and its overexpression, *Arabidopsis* have the obvious responses to red, far-red, and blue lights. Mutant has a shorter hypocotyl length under these light conditions, indicating STO/BBX24 is a negative regulator in light pathways (Indorf et al. 2007). The transcript is also controlled by lights and circadian clock, which is supported by the evidence that the regulation is through PHYA and PHYB, not PHOTs or CRYs (Indorf et al. 2007). STO/BBX24 interacts with COP1 in a yeast two-hybrid system (Holm et al. 2001), and both of them are co-localized in vivo in darkness (Indorf et al. 2007; Yan et al. 2011). It is assumed that COP1 is responsible for the degradation of STO/BBX24 in darkness and the proper function in light (Indorf et al. 2007; Yan et al. 2011). After accumulation of STO/BBX24 in light, it negatively modulates the light-responsive genes, such as CHS (Indorf et al. 2007).

A recent study has also extended the negative function of STO/BBX24 to the UV-B signaling, which is in agreement with the hypersensitive phenotypes under UV-B, such as short hypocotyls and enhanced anthocyanin accumulation (Jiang et al. 2012). Both as a negative factor in two kinds of signaling, is there any difference on the mechanism? STO/BBX24 can interact with COP1 and HY5 in vivo, and the interaction with COP1 is dependent on the presence of UV-B (Jiang et al. 2012). This interaction bears the most different mechanism involved in these two signaling, where COP1 functions as an E3 ligase to degrade STO/BBX24 in dark, and COP1 disarms the interaction to stabilize STO/BBX24 in light (Indorf et al. 2007; Yan et al. 2011), while COP1 is required for the accumulation of STO/BBX24 under UV-B (Jiang et al. 2012). This indicates STO/BBX24 acts downstream of UVR8, because UVR8-COP1 interaction is the prerequisite for the stabilization of COP1 under UV-B. However, no evidence shows that STO/BBX24 has a direct physical interaction with UVR8 (Jiang et al. 2012). As a central transcription factor in both light and UV-B signaling, HY5-STO/BBX24 interaction seems essential to the negative function of STO/BBX24. The UV-B-induced accumulation of HY5 is reduced by STO/BBX24, and even the transcriptional activity of HY5 is also repressed by STO/BBX24, resulting in the downregulation of most of the UV-B-responsive genes (Jiang et al. 2012). Interestingly, HY5-STO/BBX24 interaction seems reduced by UV-B (Jiang et al. 2012). It is not clear whether the negative function of STO/BBX24 in light signaling achieves through HY5, but one should keep in mind that STO/BBX24 is also a transcription factor. The targets of STO/BBX24 remain to be further elucidated.

14.4.5 FHY3: A Dual Function in Light and UV-B Signaling

As we mentioned before that phytochrome is activated to a Pfr form by red and far-red light, and this activation results in the translocation from cytoplasm and nucleus. Genetic studies have identified two pairs of homologous genes essential for PHYA signaling: FHY1 (FAR-RED ELONGATED HYPOCOTYL 1) and FHL (FHY1-LIKE), and FAR1 (FAR-RED-IMPAIRED RESPONSE 1) and FHY3 (FAR-RED ELONGATED HYPOCOTYL 3) (Hiltbrunner et al. 2005, 2006; Lin et al. 2007). FHY1 and FHL are essential for light-regulated PHYA nuclear accumulation and subsequent light responses (Hiltbrunner et al. 2005, 2006; Rosler et al. 2007). However, the expression of FHY1/FHL is activated by FAR1/FHY3, transposase-derived transcription factors, through directly binding to the promoter region of FHY1/FHL (Lin et al. 2007). Meanwhile, the expression of FAR/FHY3 is in turn negatively regulated by PHYA signaling (Lin et al. 2007). Thus, FAR/FHY3 act at a focal point of a feedback loop that maintains the homeostasis of PHYA signaling. However, this feedback regulation does not act alone, because HY5 is reported to bind to the FHY1/FHL promoters and the binding region is very near to the FAR/FHY3 binding region (Li et al. 2010). Further, it is found that HY5 interferes with FHY3 for binding to the FHY1 promoter (Li et al. 2010). Moreover, HY5 has a physical interaction with FAR/FHY3, but HY5 is a repressor for FHY1/FHL, while FAR/FHY3 is an activator (Li et al. 2010). These provide a complicated mechanism that HY5 works together with other cofactors to fine-tune the PHYA signaling.

Surprisingly, FHY3 shows a positive function in UV-B signaling (Huang et al. 2012). FHY3 is repressed by far-red light (Li et al. 2010) but is activated by UV-B and is believed to be regulated at a posttranscriptional level as the protein level is eventual downregulated under UV-B (Huang et al. 2012). FHY3 also has the ability to bind to COP1 promoter to further positively regulate UV-B signaling (Huang et al. 2012). But its homolog, FAR, which has a function in PHYA signaling, is not essential in photomorphogenic UV-B response, and FHY1, a target of FHY3 in PHYA signaling, shows no transcriptional response to UV-B (Huang et al. 2012). The different transcriptional behaviors of FHY3, FAR, and FHY1 indicate a fine-tuning of light signals that

distinguish the PHYA signaling from UV-B pathway. UV-B can attenuate the interaction of HY5 with FHY3 (Huang et al. 2012), which is very similar to the HY5-STO/BBX24 interaction. As mentioned before, HY5 can also bind to COP1 promoter (Huang et al. 2012), suggesting HY5-FHY3 interaction modulates the UV-B-induced COP1 expression in concert. Therefore, the working model of HY5-FHY3 interaction is absolutely contrasting from PHYA signaling to UV-B signaling, where HY5 and FHY3 work antagonistically to bind to FHY1/FHL to regulate PHYA activities in far-red light, but they function synergistically to bind to COP1 to modulate UV-B responses.

The main regulators described above are all involved in both light and UV-B signaling, despite two negative factors, RUP1 and RUP2. Expression of both RUP1 and RUP2 is induced by UV-B in a UVR8-, COP1-, and HY5-dependent manner (Gruber et al. 2010). RUPs interact with UVR8 resulting in modulating UVR8 redimerization (Heijde and Ulm 2013). Therefore, RUPs play an important role in a negative feedback regulation. Interestingly, in another study that described RUP1 and RUP2 as EFO1 and EFO2 (EARLY FLOWERING BY OVEREXPRESSION 1 and 2), RUP1/EFO1 and RUP2/EFO2 expression is seen to be gated by the circadian clock, with expression levels peaking at daybreak and gradually subsiding to their lowest level at the onset of the night period (Wang et al. 2011). However, UV-B-induced RUPs are not likely to have the rhythmical expression type, but UV-B is indeed entertaining signal for circadian clock. The expression of select clock genes is UV-B responsive, indicating that UV-B entrains the plant clock via transcriptional activation. Moreover, UV-B induction of clock gene expression is gated by the clock. UVR8 and COP1 are essential to this biological process, and HY5 and HYH are dispensable (Feher et al. 2011). However, like RUPs, UV-B-dependent induction of HY5 expression does not follow a circadian rhythm (Feher et al. 2011). It can be deduced that temporal restriction of UV-B-specific responses by the clock may limit metabolic energy costs without compromising UV-B protection. However, the exact role of clock-regulated UV-B gene expression induction is still unknown.

14.5 Physical Interaction Between Photoreceptors

14.5.1 Introduction

With the identification of UVR8 as a UV-B receptor, the photomorphogenic UV-B signaling is getting better to be understood. But UVR8 is likely the "strangest" photoreceptor when compared with others (i.e., intrinsic tryptophan vs. bounded cofactor as a chromophore, dimer to monomer vs. monomer to dimer, or phosphorylation to activation). Meanwhile, UVR8 is not evidenced to physically interact with other photoreceptors, suggesting UVR8-mediated UV-B signaling is independent of other photoreceptors, though the critical regulators are mostly shared by others. In this section, we will focus on the physical interaction between PHYs, CRYs, and PHOTs.

14.5.2 Phytochrome-Phototropin Interaction

In higher plants, phytochrome is believed to enter the nucleus upon light activation and regulate transcription, whereas phototropins are considered to be member associated. These two kinds of photoreceptors govern almost different developmental processes, suggesting they are not associated together. However, some evidence is challenging this notion. *Arabidopsis* fhl/fhy1 mutants do not show light-dependent phyA nuclear translocation, but phyA-mediated responses still can be found, implying that a cytoplasmic signal also exists (Rosler et al. 2007). Phytochrome is surprisingly associated with the plasma membrane as derived from a fluorescence correlation microscopy study in moss *Ceratodon*, implying that phytochrome assembled with phycoerythrobilin is less mobile at the cell periphery than in the cytoplasm (Böse et al. 2004). After all, this challenging evidence is difficult to understand unless the finding of neochrome in ferns and algae. Neochrome is a chimeric molecular that is capable of phytochrome function in a phototropin (Nozue et al. 1998; Suetsugu et al. 2005). Further, a finding suggests that phytochrome is associated physically with phototropin at the plasma membrane in moss *Physcomitrella patens* (Jaedicke et al. 2012).

Phytochrome 4 (Pp.phy4) is the predominate photoreceptor responsible for vectorial light sensing in Physcomitrella (Mittmann et al. 2004). By using various kinds of protein interaction assay, such as yeast two hybrid, bimolecular fluorescence complementation, and co-immunoprecipitation, Pp.phy4 is confirmed to be physically associated with phototropins at the plasma membrane, and light has no effect on their association (Mittmann et al. 2004). Meanwhile, *Arabidopsis* phyA and phot1 also interact at the plasma membrane in onion epidermis cells, but only a small fraction of the phytochrome is associated with phototropin (Mittmann et al. 2004). This is in agreement with the evidence that a small proportion of phyA always retains in the cytoplasm irrespective of the light conditions (Hisada et al. 2000). However, *Arabidopsis* phyA-phot1 interaction cannot be detectable in a yeast two-hybrid assay (Hisada et al. 2000), probably because of lack of some important factors, such as PKS1. All these indicate that there might be a phytochrome cytoplasmic signaling, suggesting signals from plant photoreceptors do not always end up in transcriptional changes.

And the downregulation of protochlorophyllide oxidoreductase A (PORA) by phytochrome is controlled via cytoplasmic Pfr (Paik et al. 2012).

14.5.3 Phytochrome-Cryptochrome Interaction

Pretreatment of plant tissue with red light (which specifically activates the phytochrome photoreceptor) can significantly enhance cryptochrome-dependent responses to blue light, whereas far-red light (which converts phytochrome to the inactive Pr form) reduces responsiveness to blue light (Mohr 1994). Genetic experiments with severely phytochrome-deficient single and double mutants demonstrate that a minimal level of active phytochrome is necessary for full cryptochrome activity; *Arabidopsis* phyA/phyB double mutant is impaired in cry1-mediated inhibition of hypocotyl elongation and anthocyanin accumulation (Casal and Boccalandro 1995; Ahmad and Cashmore 1997). It seems that phytochrome is required for the full activity of cryptochrome. As mentioned before, the photoactivated phytochrome has the kinase activity, and surprisingly cryptochromes are its target (Ahmad et al. 1998). In vitro kinase assay demonstrated that cry1 is phosphorylated in a phytochrome-dependent manner, but red or blue light does not affect this in vitro phosphorylation. However, in vivo assay exhibits that the phosphorylation of cry1 is enhanced by red light but compromised by supplemental with far-red light (Ahmad et al. 1998). Meanwhile, phytochrome is mainly targeting the C-terminal of cry1 (Ahmad et al. 1998). The phyA-cry1 interaction is further confirmed in the yeast two-hybrid assay, where both photoreceptors form a better conformational activity than in vitro purification (Ahmad et al. 1998).

Loss of cry1 activity in turn impairs the phytochrome responses. The time to flowering under short-day conditions is dramatically reduced in phyB mutant (Goto et al. 1991), lacking the phyB signal transduction pathway (Ahmad and Cashmore 1996). However, hy4 mutant, deficient in cry1 protein and showing reduced responsiveness to red light, flowered significantly earlier than the wild-type parent (Ahmad and Cashmore 1996). This result indicates a direct interaction of the mutant alleles of CRY1 with phyB resulting in impaired function.

14.6 Phytochrome and Cryptochrome Signal Integration

To date, there is no evidence showing cryptochromes could interact with phototropins or UVR8 could associate with other photoreceptors. Different light colors that selectively activate different photoreceptors activate a highly overlapping set of genes. Therefore, the signaling responded to different spectrum of light is sharing some components downstream from the photoreceptors. These include the negative regulator of the DET/COP/FUS class and the positive regulator HY5 (Quail 2002), which are already discussed above. In particular, COP1 is responsible for the degradation of phyA, cry2, and HY5 (Holm et al. 2001; Seo et al. 2004; Shalitin et al. 2002). In this section, we are going to discuss three signaling components which act downstream of both phyA and cryptochrome and are required for a subset of light responses.

OBP3 (OBF4-binding protein 3) belongs to a Dof (DNA binding with one finger) transcription factor (Kang and Singh 2000), and the function in light signaling is identified through an activation-tagging mutagenesis of phyB (Ward et al. 2005). A gain-of-function mutant, sob1-D (suppressor of phyB-4 dominant), suppresses the long hypocotyl phenotype of phyB, which is caused by the overexpression of OBP3 (Ward et al. 2005). OBP3-RNAi transgenic lines show reduced responsive to red light in terms of hypocotyl length, and this aberrant phenotype requires functional phyB, indicating OBP3 is a positive regulator of phyB-mediated inhibition of hypocotyl elongation (Ward et al. 2005). Furthermore, OBP3-RNAi lines are found to have larger cotyledons and reach the most dramatic size under blue light. The OBP3-mediated cotyledon expansion requires cry1 in blue light. These suggest that OBP3 is a negative regulator of cry1-mediated cotyledon expansion (Ward et al. 2005). Thus, OBP3 is a component in phyB and cry1 signaling pathway, acting as a positive and negative role, respectively. Ward et al. suggest that OBP3 might also work as a general inhibitor of tissue expansion with phyB and cry1. But these provide the solid evidence that OBP3 represents a connection between phyB and cry1 signal transduction.

HFR1 (long hypocotyl in far-red 1) is a bHLH transcription factor, which is a positive regulator of phyA-mediated light responses (Fairchild et al. 2000). phyA/hfr1 double mutant shows enhanced hypocotyl growth phenotype and each of the single parental mutant, indicating HFR1 has the function independent of phyA (Fairchild et al. 2000). When grown in blue light, however, hfr1 mutants exhibit reduced de-etiolation responses, including hypocotyl growth, cotyledon opening, and anthocyanin accumulation (Duek and Fankhauser 2003). Moreover, the functional cry1, not cry2, is required for the hyposensitive to blue light, but HFR1 is not important for the normal accumulation of cry1 (Duek and Fankhauser 2003). Genetic analysis further reveals that HFR1 is downstream of phyA and cry1 (Duek and Fankhauser 2003), providing a model that HFR1 is a positive integrator for both phyA and cry1 signaling.

SUB1 (short under blue light 1), encoding a Ca2+-binding protein, is first identified by exaggerative short hypocotyl

under blue light but later is found to have the same response to far-red not to red light (Guo et al. 2001). sub1 is epistatic to cry2 in blue light, and phyA is epistatic to sub1 in both far-red and blue light, suggesting SUB1 functions both in phyA and cry2 signal transduction pathways (Guo et al. 2001). Moreover, blue- and far-red-induced CHS and CHI are significantly enhanced in sub1 mutant, and this enhancement is also observed in light-induced HY5 protein accumulation (Guo et al. 2001). Therefore, SUB1 defines a point of cross talk between cryptochrome and PHYA signaling.

At molecular level, it has been shown that the interaction between phytochromes and cryptochromes occurs at the level of photoreceptor. With the advanced of technique, especially the large scale of expression analysis, the presence of multiple levels of signal integration has been suggested. HY5 and COP1 represent two typical integrators, which master the signal transduction under all photoreceptors. More specifically, here we discussed three components integrating the phytochrome and cryptochrome signaling. OBP3 has a dual function, HFR1 is a positive regulator, and SUB1 negatively modulates both phytochrome and cryptochrome responses. However, there is evidence that phototropin signaling is cross-talked with phytochrome or cryptochrome. For instance, phototropism and chloroplast movement are primarily controlled by phototropin, but the amplitude of the response is modulated by both phytochrome and cryptochrome (DeBlasio et al. 2003; Ohgishi et al. 2004). To date, the underlying molecular mechanisms are still unknown.

References

Ahmad M, Cashmore AR (1996) The *pef* mutants of *Arabidopsis thaliana* define lesions early in the phytochrome signaling pathway. Plant J 10:1103–1110

Ahmad M, Cashmore AR (1997) The blue-light receptor cryptochrome 1 shows functional dependence on phytochrome A or phytochrome B in *Arabidopsis thaliana*. Plant J 11:421–427

Ahmad M, Jarillo JA, Smirnova O, Cashmore AR (1998) The CRY1 blue light photoreceptor of *Arabidopsis* interacts with phytochrome A *in vitro*. Mol Cell 1:939–948

Al-Sady B, Ni W, Kircher S, Schäfer E, Quail PH (2006) Photoactivated phytochrome induces rapid PIF3 phosphorylation prior to proteasome-mediated degradation. Mol Cell 23:439–446

Boccalandro HE, Giordano CV, Ploschuk EL, Piccoli PN, Bottini R, Casal JJ (2012) Phototropins but not cryptochromes mediate the blue light-specific promotion of stomatal conductance, while both enhance photosynthesis and transpiration under full sunlight. Plant Physiol 158:1475–1484

Böse G, Schwille P, Lamparter T (2004) The mobility of phytochrome within protonemal tip cells of the moss *Ceratodon purpureus*, monitored by fluorescence correlation spectroscopy. Biophys J 87:2013–2021

Brown BA, Jenkins GI (2008) UV-B signaling pathways with different fluence-rate response profiles are distinguished in mature *Arabidopsis* leaf tissue by requirement for UVR8, HY5, and HYH. Plant Physiol 146:576–588

Brown BA, Cloix C, Jiang GH, Kaiserli E, Herzyk P, Kliebenstein DJ, Jenkins GI (2005) A UV-B-specific signaling component orchestrates plant UV protection. Proc Natl Acad Sci U S A 102: 18225–18230

Casal JJ, Boccalandro H (1995) Co-action between phytochrome B and HY4 in *Arabidopsis thaliana*. Planta 197:213–218

Castillon A, Shen H, Huq E (2007) Phytochrome interacting factors: central players in phytochrome-mediated light signaling networks. Trends Plant Sci 12:514–521

Christie JM (2007) Phototropin blue-light receptors. Annu Rev Plant Biol 58:21–45

DeBlasio SL, Mullen JL, Luesse DR, Hangarter RP (2003) Phytochrome modulation of blue light-induced chloroplast movements in *Arabidopsis*. Plant Physiol 133:1471–1479

Duek PD, Fankhauser C (2003) HFR1, a putative bHLH transcription factor, mediates both phytochrome A and cryptochrome signaling. Plant J 34:827–836

Eisinger W, Swartz T, Bogonolni R, Taiz L (2000) The ultraviolet action spectrum for stomatal opening in broad bean. Plant Physiol 122:99–105

Eisinger WR, Bogomolni RA, Taiz L (2003) Interactions between a blue-green reversible photoreceptor and a separate UV-B receptor in stomatal guard cells. Am J Bot. 90:1560–1566

Fairchild CD, Schumaker MA, Quail PH (2000) HFR1 encodes an atypical bHLH protein that acts in phytochrome A signal transduction. Genes Dev 14:2377–2391

Fankhauser C, Yeh K-C, Lagarias JC, Zhang H, Elich TD, Chory J (1999) PKS1, a substrate phosphorylated by phytochrome that modulates light signaling in *Arabidopsis*. Science 284: 1539–1541

Favory JJ, Stec A, Gruber H, Rizzini L, Oravecz A, Funk M (2009) Interaction of COP1 and UVR8 regulates UV-B induced photomorphogenesis and stress acclimation in *Arabidopsis*. EMBO J 28:591–601

Feher B, Kozma-Bognar L, Kevei E, Hajdu A, Binkert M, Davis SJ, Schäfer E, Ulm R, Nagy F (2011) Functional interaction of the circadian clock and UV RESISTANCE LOCUS 8-controlled UV-B signaling pathways in *Arabidopsis thaliana*. Plant J 67:37–48

Fuglevand G, Jackson JA, Jenkins GI (1996) UV-B, UV-A, and blue light signal transduction pathways interact synergistically to regulate chalcone synthase gene expression in *Arabidopsis*. Plant Cell 8:2347–2357

Goto N, Kumagai T, Koornneef M (1991) Flowering responses to light-breaks in photomorphogenic mutants of *Arabidopsis thaliana*. Physiol Plant 83:209–215

Griffiths S, Dunford RP, Coupland G, Laurie DA (2003) The evolution of CONSTANS-like gene families in barley, rice, and *Arabidopsis*. Plant Physiol 131:1855–1867

Gruber H, Heijde M, Heller W, Albert A, Seidlitz HK, Ulm R (2010) Negative feedback regulation of UV-B-induced photomorphogenesis and stress acclimation in *Arabidopsis*. Proc Natl Acad Sci U S A 107:20132–20137

Guo HW, Mockler T, Duong H, Lin C (2001) SUB1, an *Arabidopsis* Ca^{2+}-binding protein involved in cryptochrome and phytochrome coaction. Science 291:487–490

Heijde M, Ulm R (2012) UV-B photoreceptor-mediated signaling in plants. Trends Plant Sci 17:230–237

Heijde M, Ulm R (2013) Reversion of the *Arabidopsis* UV-B photoreceptor UVR8 to the homodimeric ground state. Proc Natl Acad Sci U S A 110:1113–1118

Hiltbrunner A, Tscheuschler A, Viczian A, Kunkel T, Kircher S, Toth R, Honsberger A, Nagy F, Fankhauser C, Schäfer E (2005) Nuclear accumulation of the phytochrome A photoreceptor requires FHY1. Curr Biol 15:2125–2130

Hiltbrunner A, Tscheuschler A, Viczian A, Kunkel T, Kircher S, Schäfer E (2006) FHY1 and FHL act together to mediate nuclear

accumulation of the phytochrome A photoreceptor. Plant Cell Physiol 47:1023–1034

Hisada A, Hanzawa H, Weller JL, Nagatani A, Reid JB, Furuya M (2000) Light-induced nuclear translocation of endogenous pea phytochrome A visualized by immunocytochemical procedures. Plant Cell 12(7):1063–1078

Holm M, Hardtke CS, Gaudet R, Deng XW (2001) Identification of a structural motif that confers specific interaction with the WD40 repeat domain of *Arabidopsis* COP1. EMBO J 20:118–127

Huang X, Ouyang X, Yang P, Lau OS, Li G, Li J, Chen H, Deng XW (2012) *Arabidopsis* FHY3 and HY5 positively mediate induction of COP1 transcription in response to photomorphogenic UV-B light. Plant Cell 24:4590–4606

Indorf M, Cordero J, Neuhaus G, Rodriuez-Franco M (2007) Salt tolerance (STO), a stress-related protein, has a major role in light signalling. Plant J 51:563–574

Jaedicke K, Lichtenthaler AL, Meyberg R, Zeidler M, Hughes J (2012) A phytochrome-phototropin light signaling complex at the plasma membrane. Proc Natl Acad Sci U S A 109:12231–12236

Jenkins G (2009) Signal transduction in response to UV-B radiation. Annu Rev Plant Biol 60:407–431

Jiang L, Wang Y, Björn LO, He JX, Li SS (2012) Sensing of UV-B radiation by plants. Plant Sig Behav 7:1–5

Jiao Y, Lau OS, Deng XW (2007) Light-regulated transcriptional networks in higher plants. Nat Rev Genet 8:217–230

Kang HG, Singh KB (2000) Characterization of salicylic acid-responsive, *Arabidopsis* Dof domain proteins: Overexpression of OBP3 leads to growth defects. Plant J 21:329–339

Khanna R, Kronmiller B, Maszle DR, Coupland G, Holm M, Mizuno T, Wu SH (2009) The *Arabidopsis* B-Box Zinc Finger Family. Plant Cell 21:3416–3420

Kim JI, Shen Y, Han YJ, Park JE, Kirchenbauer D, Soh MS, Nagy F, Schafer E, Song PS (2004) Phytochrome phosphorylation modulates light signaling by influencing the protein-protein interaction. Plant Cell 16:2629–2640.

Kinoshita T, Doi M, Suetsugu N, Kagawa T, Wada M, Shimazaki K (2001) Phot1 and phot2 mediate blue light regulation of stomatal opening. Nature 414:656–660

Lau OS, Deng XW (2010) Plant hormone signaling lightens up: integrators of light and hormones. Curr Opin Plant Biol 13:571–577

Laubinger S, Fittinghoff K, Hoecker U (2004) The SPA quartet: a family of WD-repeat proteins with a central role in suppression of photomorphogenesis in *Arabidopsis*. Plant Cell 16: 2293–2306

Lee J, He K, Stolc V, Lee H, Figueroa P, Gao Y, Tongprasit W, Zhao H, Lee I, Deng XW (2007) Analysis of transcription factor HY5 genomic binding sites revealed its hierarchical role in light regulation of development. Plant Cell 19:731–749

Leivar P, Monte E, Oka Y, Liu T, Carle C, Castillon A, Huq E, Quail PH (2008) Multiple phytochrome-interacting bHLH transcription factors repress premature seedling photomorphogenesis in darkness. Curr Biol 18:1815–1823

Li J, Li G, Gao S, Martinez C, He G, Zhou Z, Huang X, Lee J-H, Zhang H, Shen Y, Wang H, Deng XW (2010) *Arabidopsis* transcription factor ELONGATED HYPOCOTYL5 plays a role in feedback regulation of phytochrome A signaling. Plant Cell 22:3634–3649

Lin C, Shalitin D (2003) Cryptochrome structure and signal transduction. Annu Rev Plant Biol. 54:469–496

Lin R, Ding L, Casola C, Ripoll DR, Feschotte C, Wang H (2007) Transposase-derived transcription factors regulate light signaling in *Arabidopsis*. Science 318:1302–1305

Lippuner V, Cyert MS, Gasser CS (1996) Two classes of plant cDNA clones differentially complement yeast calcineurin mutants and increase salt tolerance of wild-type yeast. J Biol Chem 271:12859–12866

Ma L, Li J, Qu L, Hager J, Chen Z, Zhao H, Deng XW (2001) Light control of *Arabidopsis* development entails coordinated regulation of genome expression and cellular pathways. Plant Cell 13: 2589–2607

Ma L, Gao Y, Qu L, Chen Z, Li J, Zhao H, Deng XW (2002) Genomic evidence for COP1 as a repressor of light-regulated gene expression and development in *Arabidopsis*. Plant Cell 14:2383–2398

Mittmann F, Brückern G, Zeidler M, Repp A, Abts T, Hartmann E, Hughes J (2004) Targeted knockout in *Physcomitrella* reveals direct actions of phytochrome in the cytoplasm. Proc Natl Acad Sci U S A 101:13939–13944

Mohr H (1994) Coaction between pigment systems. In: Kendrick RE, Kronenberg GHM (eds) Photomorphogenesis in plants, 2nd edn. Kluwer Academic Publishers, Dordrecht, pp 353–372

Nagaoka S, Takano T (2003) Salt tolerance-related protein STO binds to a Myb transcription factor homologue and confers salt tolerance in *Arabidopsis*. J Exp Bot 54:2231–2237

Nozue K, Kanegae T, Imaizumi T, Fukuda S, Okamoto H, Yeh KC, Lagarias JC, Wada M (1998) A phytochrome from the fern *Adiantum* with features of the putative photoreceptor NPH1. Proc Natl Acad Sci U S A 95:15826–15830

Ohgishi M, Saji K, Okada K, Sakai T (2004) Functional analysis of each blue light receptor, cry1, cry2, phot1, and phot2, by using combinatorial multiple mutants in *Arabidopsis*. Proc Natl Acad Sci U S A 101:2223–2228

Oravecz A, Baumann A, Máté Z, Brzezinska A, Molinier J, Oakeley EJ, Adam E, Schäfer E, Nagy F, Ulm R (2006) CONSTITUTIVELY PHOTOMORPHOGENIC1 is required for the UV-B response in *Arabidopsis*. Plant Cell 18:1975–1990

Osterlund MT, Hardtke CS, Wei N, Deng XW (2000) Target destabilization of HY5 during light-regulated development of *Arabidopsis*. Nature 405:462–466

Oyama T, Shimura Y, Okada K (1997) The *Arabidopsis* HY5 gene encodes a bZIP protein that regulates stimulus-induced development of root and hypocotyl. Genes Dev 11:2983–2995

Paik I, Yang S, Choi G (2012) Phytochrome regulates translation of mRNA in the cytosol. Proc Natl Acad Sci U S A 109:1335–1340

Partch CL, Sancar A (2005) Photochemistry and photobiology of cryptochrome blue-light photopigments: the search for a photocycle. Photochem Photobiol. 81:1291–1304

Quail PH (2002) Phytochrome photosensory signalling networks. Nat Rev Mol Cell Biol 3:85–93

Rizzini L, Favory JJ, Cloix C, Faggionato D, O'Hara A, Kaiserli E, Baumeister R, Schäfer E, Nagy F, Jenkins GI, Ulm R (2011) Perception of UV-B by the *Arabidopsis* UVR8 protein. Science 332:103–106

Rosler J, Klein I, Zeidler M (2007) *Arabidopsis* fhl/fhy1 double mutant reveals a distinct cytoplasmic action of phytochrome A. Proc Natl Acad Sci U S A 104:10737–10742

Ryu JS, Kim JI, Kunkel T, Kim BC, Cho DS, Hong SH, Kim SH, Fernández AP, Kim Y, Alonso JM, Ecker JR, Nagy F, Lim PO, Song PS, Schäfer E, Nam HG (2005) Phytochrome-specific type 5 phosphatase controls light signal flux by enhancing phytochrome stability and affinity for a signal transducer. Cell 120:395–406

Saijo Y, Sullivan JA, Wang H, Yang J, Shen Y, Rubio V, Ma L, Hoecker U, Deng XW (2003) The COP1-SPA1 interaction defines a critical step in phytochrome A-mediated regulation of HY5 activity. Genes Dev 17:2642–2647

Sang Y, Li QH, Rubio V, Zhang YC, Mao J, Deng XW, Yang HQ (2005) N-terminal domain-mediated homodimerization is required for photoreceptor activity of Arabidopsis CRYPTOCHROME 1. Plant Cell 17:1569–1584

Seo HS, Watanabe E, Tokutomi S, Nagatani A, Chua NH (2004) Photoreceptor ubiquitination by COP1 E3 ligase desensitizes phytochrome A signaling. Genes Dev 18:617–622

Shalitin D, Yang H, Mockler TC, Maymon M, Guo H, Whitelam GC, Lin C (2002) Regulation of *Arabidopsis* cryptochrome 2 by blue-light-dependent phosphorylation. Nature 417:763–767

Shen Y, Khanna R, Carle CM, Quail PH (2007) Phytochrome induces rapid PIF5 phosphorylation and degradation in response to red-light activation. Plant Physiol 145:1043–1051

Subramanian C, Kin BH, Lyssenko NN, Xu X, Johnson CH, von Arnim AG (2004) The *Arabidopsis* repressor of light signaling, COP1, is regulated by nuclear exclusion: Mutational analysis by bioluminescence resonance energy transfer. Proc Natl Acad Sci U S A 101:6798–6802

Suetsugu N, Mittmann F, Wagner G, Hughes J, Wada M (2005) A chimeric photoreceptor gene, NEOCHROME, has arisen twice during plant evolution. Proc Natl Acad Sci U S A 102:13705–13709

Sullivan JA, Shirasu K, Deng XW (2003) The diverse roles of ubiquitin and the 26S proteasome in the life of plants. Nat Rev Genet 4:948–958

Tilbrook K, Arongaus AB, Binkert M, Heijde M, Yin R, Ulm R (2013) The UVR8 UV-B photoreceptor, perception, signaling and response. Arabidopsis Book 11:e0164

Ulm R, Baumann A, Oravecz A, Mate Z, Adam E, Oakeley EJ, Schäfer E, Nagy F (2004) Genome-wide analysis of gene expression reveals function of the bZIP transcription factor HY5 in the UV-B response of *Arabidopsis*. Proc Natl Acad Sci U S A 101:1397–1402

Vierstra RD, Zhang J (2011) Phytochrome signaling: solving the Gordian knot with microbial relatives. Trends Plant Sci 16:417–426

Wang H, Ma LG, Li JM, Zhao HY, Deng XW (2001) Direct interaction of *Arabidopsis* cryptochromes with COP1 in light control development. Science 294:154–158

Wang W, Yang D, Feldmann KA (2011) EFO1 and EFO2, encoding putative WD-domain proteins, have overlapping and distinct roles in the regulation of vegetative development and flowering of *Arabidopsis*. J Exp Bot 62:1077–1088

Ward JM, Cufr CA, Denzel MA, Neff MM (2005) The Dof transcription factor OBP3 modulates phytochrome and cryptochrome signaling in *Arabidopsis*. Plant Cell 17:475–485

Yan H, Marquardt K, Indorf M, Jutt D, Kircher S, Neuhaus G, Rodriguez-Franco M (2011) Nuclear localization and interaction with COP1 are required for STO/BBX24 function during photomorphogenesis. Plant Physiol 156:1772–1782

Yi C, Deng XW (2005) COP1 – From plant photomorphogenesis to mammalian tumorigenesis. Trends Plant Sci 15:618–625

Yu X, Liu H, Klejnot J, Lin C (2010) The cryptochrome blue light receptors. Arabidopsis Book 8:e0135

Zhang H, He H, Wang X, Wang X, Yang X, Li L, Deng XW (2011) Genome-wide mapping of the HY5-mediated gene networks in *Arabidopsis* that involve both transcriptional and post-transcriptional regulation. Plant J 65:346–358

The Diversity of Eye Optics

15

Lars Olof Björn

15.1 Introduction

In this review of the different solutions of the optical problems of eye designs encountered in the animal kingdom, we shall not follow the course of evolution. Instead we shall start with our own eyes, as this is what the readers in general are likely to be most familiar with. The emphasis will thus first be on "camera-type" eyes, and later we will deal with compound and other types of eyes. The evolution of vision has recently been treated by Nilsson (2013) and Backfisch et al. (2013), and comprehensive accounts of animal eyes are provided by Land and Nilsson (2012).

15.2 The Human Eye

We assume that the reader has a basic knowledge of the structure of the human eye. It is probably a common misconception that the refraction of light necessary for the projection of an image on the retina is mainly due to the lens. In fact, 80 % of the refractive power is due to the curved external surface of the eye, at the outer surface of the cornea, because the difference in refractive index between the cornea and air is much greater than that between the lens and its surrounding media (aqueous humor in front, vitreous humor behind) (Fig. 15.1).

To understand how the optical components of the eye function, and why evolution of eye design in different environments has given the results it has, we shall start with how light is refracted in spherical interface.

From the formula derived in the legend of Fig. 15.2, we can see that:

1. For fixed n_1, n_2, and R, the smaller is a, the larger is b.
2. For fixed a, n_1, and n_2, the smaller is R, the smaller is b.
3. For fixed a and R, the larger is the difference between n_2 and n_1, the smaller is b.
4. For infinitely large a, i.e., point A at infinite distance, $n_2/b = (n_2 - n_1)/R$, or $b = R \cdot n_2/(n_2 - n_1)$. In this case, b is the focal distance of the refracting interface. The inverse value of b is called the refractive power or dioptric power of the interface. With b expressed in m, the refractive power will be expressed in diopters (= $m - 1$). Since the radius of the outer surface of the cornea is over 7 mm and the radius of the pupil less than 4 mm (in bright light much less), we can use the formula from Fig. 15.2 as a first approximation to judge the refractive power P_1 of the outer external surface of the eye using the dimensions in Table 15.1: $P_1 = (n_2 - n_1)/(n_2 R) = (1.3777 - 1)/0.00777$ $m^{-1} = 48.52$ m^{-1} (or 48.52 diopters or 48.52 D). As we can see in Fig. 15.1, the inner surface of the cornea is

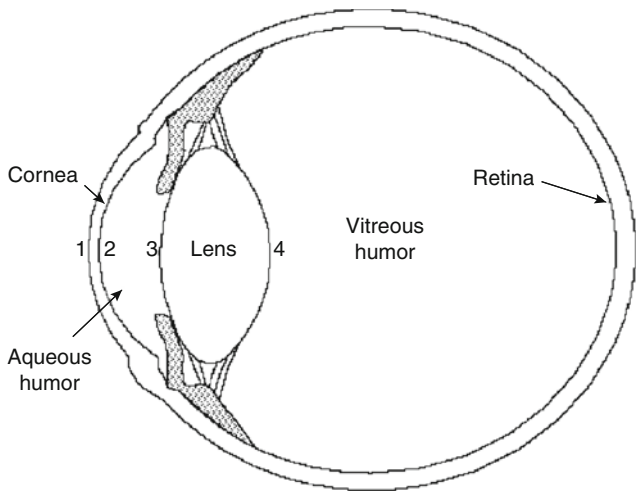

Fig. 15.1 Longitudinal section of a human eye (*schematic*). The numbers indicate the numbering of interfaces used in the calculations in the text

L.O. Björn
School of Life Science, South China Normal University, Guangzhou, China

Department of Biology, Lund University, Lund, Sweden
e-mail: Lars_Olof.Bjorn@biol.lu.se

L.O. Björn (ed.), *Photobiology: The Science of Light and Life*,
DOI 10.1007/978-1-4939-1468-5_15, © Springer Science+Business Media New York 2015

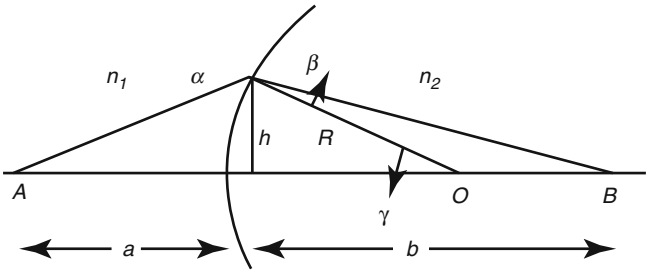

Fig. 15.2 Refraction of light at a spherical interface between media with different refractive indices, n_1 and n_2. The radius of curvature is R, the center of the sphere O. A ray from A to B is refracted in the surface at a distance h from the line from A to B. The angle of incidence is α, the angle of refraction β. The shortest distance of A from the interface is a; that of B is b. For small values of h we have the following relations: $h/R = \sin(\gamma) \approx \gamma$; $h/a = \tan(\alpha - \gamma) \approx \alpha - \gamma$; $h/b = \tan(\gamma - \beta) \approx \gamma - \beta$. From this follows that $h/R + h/a \approx \alpha \approx \sin(\alpha)$ and $h/R + h/b \approx \beta \approx \sin(\beta)$. Since, according to Snell's law (see Chap. 1), $n_1 \sin(\alpha) = n_2 \sin(\beta)$, it follows that $n_1(h/R + h/a) = n_2(h/R + h/b)$, i.e., $n_1(1/R + 1/a) = n_2(1/R + 1/b)$ (independently of h as long as h is small compared to R), or $n_1/a + n_2/b = (n_2 - n_1)/R$

Table 15.1 Properties of eye components

Eye component	Distal R	Proximal R	Thickness	Refractive index
1. Cornea	7.77	6.40	0.50	1.3777
2. Aqueous humor	3.16			1.3371
3. Lens	12.40	−8.10	4.02	1.4000
4. Vitreous humor	16.4			1.3377

The refractive index is for green light (*center of visible range*). The refractive index for the lens is for a portion near the center of the lens. Sources: Liou and Brennan (1997); Liu et al. (2005); Navarro et al. (1985)

slightly more curved than the external surface, and the medium inside the cornea has a slightly lower refractive index, giving a negative contribution to the refractive power. Using the same formula again, we can calculate that the contribution from this interface is $P_2 = -6.34\ \mathrm{m}^{-1}$.

To get the total refractive power from these two interfaces, we would make no big error by just adding them: $48.52 - 6.34\ \mathrm{m}^{-1} = 42.18\ \mathrm{m}^{-1}$. But a more correct calculation is to take the distance between them, $d_{1,2} = 0.5\ \mathrm{mm} = 0.0005\ \mathrm{m}$, into account using the formula $P_{1,2} = P_1 + P_2 - P_1 \cdot P_2 \cdot d_{1,2}/n_{1,2} = 48.52 - 6.34 + 48.52 \cdot 6.34 \cdot 0.0005/1.3777\ \mathrm{m}^{-1} = 42.29\ \mathrm{m}^{-1}$. Here $d_{1,2}$ stands for the distance between the interfaces and $n_{1,2}$ for the refractive index of the medium between them. When we come to the lens below, the correction term is more important, because the thickness of the lens is greater than that of the cornea.

In analogy with the above, we can calculate the refractive power of the front surface of the lens to be $P_3 = (1.4000 - 1.3371)/(12.40 \cdot 0.001)\ \mathrm{m}^{-1} = 5.31\ \mathrm{m}^{-1}$ and that of the back surface $P_4 = (1.3377 - 1.4000)/(-8.10 \cdot 0.001)\ \mathrm{m}^{-1} = 7.69\ \mathrm{m}^{-1}$. Note that in the latter case, we use a negative value for the radius, since the center of the curvature is now in the direction from which the light is coming. The total refracting power of the lens is $P_{3,4} = 5.31 + 7.69 - 5.31 \cdot 7.69 \cdot 4.02 \cdot 0.001/1.4000\ \mathrm{m}^{-1} = 12.88\ \mathrm{m}^{-1}$. We see that the refracting power of the lens is only about one quarter of that of the cornea. This is for an eye adjusted for vision at a distance. It is, as we shall see, different for an eye adjusted (accommodated) for vision at short distance and even more so for eyes of aquatic animals.

We can also make an estimate of the total refractive power of the eye: $P_{\mathrm{eye}} = P_{1,2} + P_{3,4} - P_{1,2} \cdot P_{3,4} \cdot 16.4 \cdot 0.001/1.3371\ \mathrm{m}^{-1} = 48.49$. This is just enough to focus light from a distant object on the retina in the back of the eye.

We must remember that all these calculations are a bit approximative, since they all depend on the approximations $\tan(\alpha) \approx \alpha \approx \sin(\alpha)$. The further we go from the optical axis, the less valid are these approximations. Furthermore, the refractive index of the lens is not constant, it is higher in the center than in the periphery, it varies with wavelength, and the interfaces where refractions occur are not perfectly spherical.

In Sect. 15.3, we shall come to a case where we cannot use the approximations used here and have to explore the function of an eye in another way.

The lens is elastic and has a tendency to contract radially and extend along the optical axis of the eye, i.e., increase the curvature of its refractive interfaces. This tendency is counteracted by the fibers in which it is suspended, which are stretched by the elasticity of the outer tissue of the eye. This in turn can be counteracted by the contraction of the ciliary muscle. So by the contraction of the ciliary muscle, the refractive power of the lens is increased. This regulation is called accommodation. In Fig. 15.3, we see a comparison of the shape of the lens when it is adjusted for distance vision and for near vision. Birds and reptiles also accommodate by changing the shape of the lens, although with different mechanical systems (Ott 2006). Amphibians and fishes accommodate in an entirely different way by moving the lens, and we shall soon understand why.

15.3 An Eye in Water: The Problem

For a fish living in water, the refractive index of the water in front of the cornea is about 1.33, i.e., close to that of the optical elements in the eye in Fig. 15.1, with the exception of the lens. The materials of which a fish eye is built do not differ much from the corresponding materials of a human eye. This means that the outer surface of the cornea has almost no refractive power and the demands on the lens are much greater than for a terrestrial animal. Lens surfaces must be much more curved, and in general the lens of a fish eye has a spherical shape. This accentuates another problem: spherical aberration. To understand this, let us study the behavior of light passing through a sphere; we can take a glass sphere in air as example (Fig. 15.4).

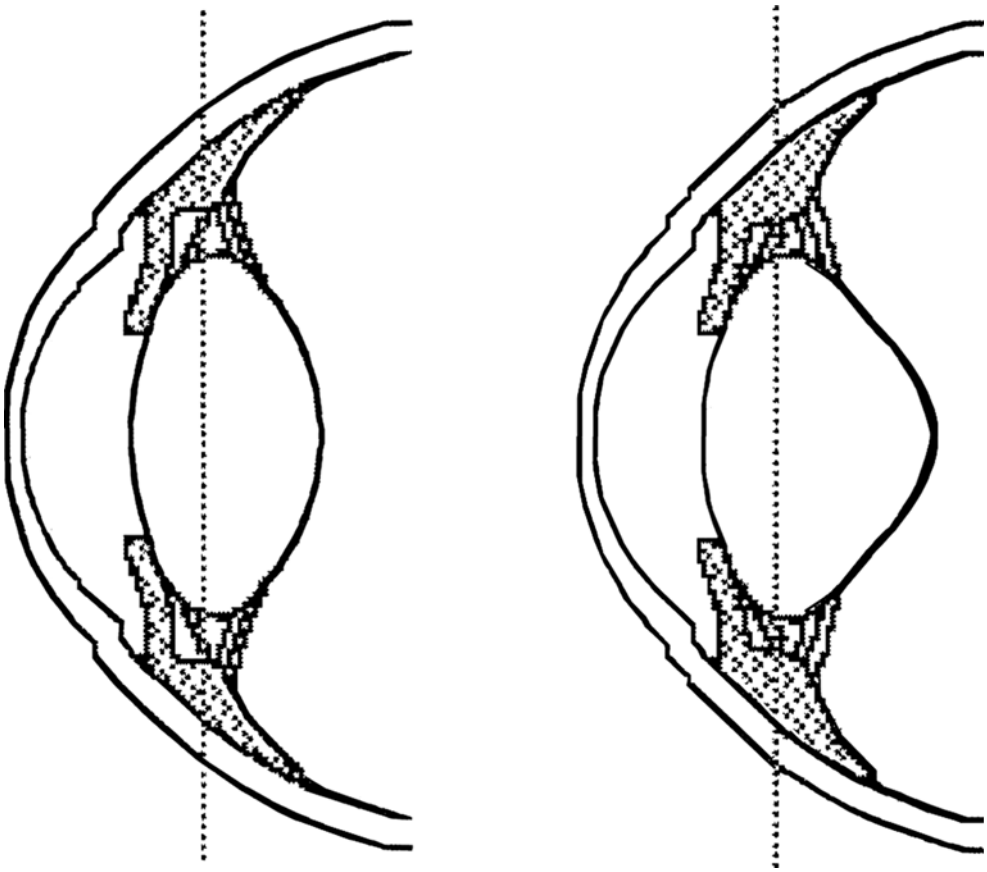

Fig. 15.3 The shape of the human lens in an eye adjusted for vision at a distance (*left*) and on a nearby object (*right*)

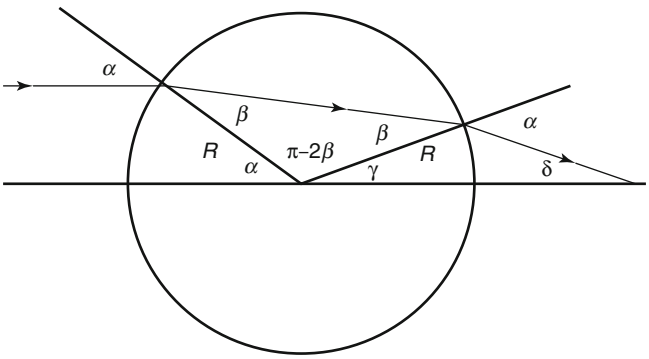

Fig. 15.4 Refraction of light in a homogeneous sphere

In Fig. 15.4, we see a ray of light entering from a medium with refractive index n_1 into a sphere of refractive index n_2 and exiting on the other side into the medium of refractive index n_1. We have drawn the incident ray as parallel to the horizontal optical axis, but this is not a special case. Because of the spherical symmetry, any direction can be chosen for the optic axis. We have also drawn the two radii of the sphere and continued their directions outside the sphere to show the incidence and refraction angles α and β. For the first refraction the angle of incidence is α and the angle of refraction β, since the radius is perpendicular to the sphere's surface at the point of intersection. The relation between α and β, according to Snell's law, is $n_1 \sin(\alpha) = n_2 \sin(\beta)$. Because two sides of the triangle between the center of the sphere are equal (= R), it is clear that the angle of incidence at the other refraction is β, and so the angle of refraction there must be α, again according to Snell's law. Since the sum of angles in a triangle is π, the third angle in the isosceles triangle just referred to is $\pi - 2\beta$, and the angle γ is $\pi - \alpha - (\pi - 2\beta) = 2\beta - \alpha$. We express the angles in radians here and in the following calculations. The angle δ is π–γ–(the top angle in the triangle containing γ and δ). This angle, as can easily be seen in Fig. 15.3, is $2\pi - \alpha - \beta$, and it follows that $\delta = \pi - \gamma - (2\pi - \pi - \beta) = \pi - (2\beta - \alpha) - (2\pi - \alpha - \beta) = 2\alpha - \beta - \pi$.

We can now calculate the distance between the focal point and the center of the sphere as $R \cdot \cos(\gamma) + R \cdot \sin(\gamma)/\tan(\delta)$. Using the other relationships we have derived, this can be expressed in terms of R, α, n_1, and n_2. If the glass sphere were to act as a good lens, this distance should be independent of the distance of the incident rays from the optical axis, but it turns out that this is not at all the case. In Fig. 15.5, we have traced the rays through a glass sphere of refractive index 1.538 immersed in water of refractive index 1.336. The further from the optical axis the rays impinge on the sphere, the shorter is the distance at which the rays intersect the optical

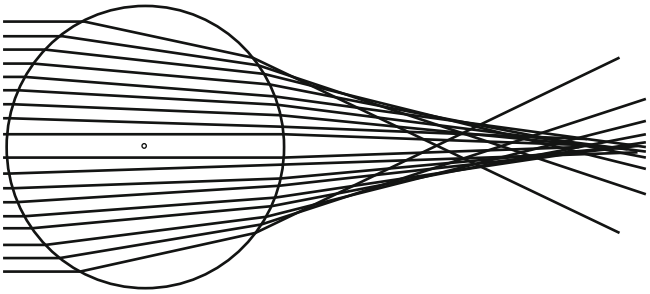

Fig. 15.5 Propagation of light through a glass sphere with refractive index 1.538, immersed in water with refractive index 1.336. The inability of such a lens to focus sharply is a phenomenon known as spherical aberration

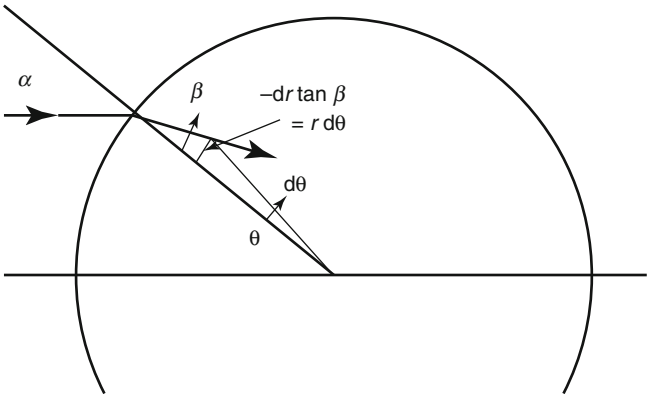

Fig. 15.6 Tracing of a light ray through a sphere with variable refractive index

axis. It is this deviation from good focusing that is called spherical aberration.

15.4 An Eye in Water: The Solution

The solution to this problem used by most fishes and many other aquatic animals is to develop a lens with a variable refractive index. We have seen that in a sphere with a uniform refractive index, the rays far from the optical axis are deflected too much to be focused at the same point as the more central rays. Thus, we can understand that to correct this, we have to have a lens which has a lower refractive index in the periphery.

It turns out that it is possible to have a good lens with this property and still retain spherical symmetry. The pattern of refractive index decrease from the center to periphery in the eye lens has now been measured for a number of aquatic animals. If we know the refractive index as a function of the distance from the sphere center, to trace the ray through the sphere, we need to keep track of how far we are from the center, and of course of the ray's direction, to be able to compute how the light progresses from one point to another.

This is easiest to do if we use polar coordinates (Fig. 15.6), with the center of the sphere as origin and the angle θ between the optic axis and the point as one variable and the distance r from the point and the center of the sphere as the other variable.

The position of the tip of the advancing ray at any time is therefore described with the coordinates θ, r. We further use the following variables: n_0, n_{cort}, and n_{core} – the refractive index of the external medium, that of the peripheral part of the sphere, and that of the center of the sphere. The angle of incidence at the external surface of the sphere is α, and the refraction angle at this refraction is β. The relation between them is the usual Snell's formula: $n_0 \cdot \sin(\alpha) = n_{\text{cort}} \cdot \sin(\beta)$. We can then see from Fig. 15.6 that, as we follow the ray a short bit into the sphere and θ is increased by a small amount, dθ (much smaller than in the drawing), then r decreases by the amount $\mathrm{d}r = r \cdot \mathrm{d}\theta/\tan(\beta)$. When we know the decrease in r, we can compute the increase in refractive index, dnr, and then we know how much the light is refracted and can compute a new direction of the ray. In this way, we can continue to trace the course of the light through the sphere. This has been done in Fig. 15.7.

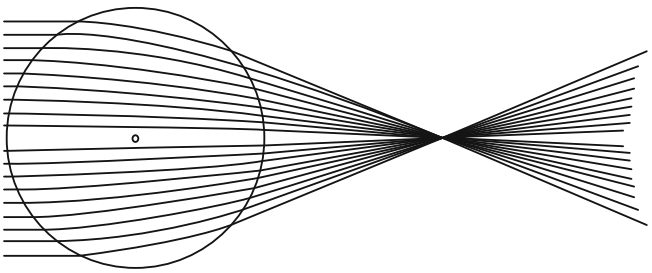

Fig. 15.7 Light traversing a sphere with variable refractive index, highest in the center

The refractive index data for Fig. 15.7 is for a rainbow trout and has been taken from Jagger and Sands (1996). In this paper, the refractive index n_r is given as the following function of the refractive index n_{core} in the center of the lens and n_{cort} in the periphery, radial distance r from the center of the lens, and $K = (n_{\text{cort}}/n_{\text{core}}) - 1$, the latter of course not being an independent variable, but introduced as an abbreviation.

To use this formula in a convenient way in a computer program, to know how much we have to change the refractive index for each small change dr in radial position, we differentiate the expression:

Note that this expression is negative, because K is negative, but we get an increase in n_r as we proceed inward in the lens, because then also dr is negative. Eventually both dr and dn_r will turn positive, as the light starts to approach the surface of the sphere again.

Those readers who are interested in computing should now be able to implement a program for plotting figures such

as Fig. 15.7 on their own computers. For other eyes there are various formulas like the one for n_r above. See, for instance, one for the octopus lens in Jagger and Sands (1999) or a number of lenses in Jagger (1992). The cephalopod eyes and lenses, like that of octopus, although evolved along a different path, are in principle very similar to fish eyes and lenses (Jagger and Sands 1996) and are often referred to as an example of convergent evolution. Convergent evolution is a phenomenon encountered over and over in the study of eyes.

As we shall learn in the next section, the sphere is only an approximation of the lens shape in fishes. Nature is more sophisticated than that.

15.5 Another Problem: Chromatic Aberration

The refractive index of all substances varies with wavelength (a phenomenon known as dispersion), and except in the vicinity of absorption bands, it increases with decreasing wavelength. The refractive powers of the cornea and lens can therefore not be optimal for all wavelengths at the same time. For some wavelength regions we get imaging errors collectively known as chromatic aberration. We distinguish between longitudinal chromatic aberration, which means that the image is projected at the wrong distance in relation to the retina, and lateral (or transverse) chromatic aberration, meaning that the projected image has different size for different wavelength regions. We humans overcome this problem by having sharp vision over a wide wavelength range only in the fovea, a small area of the retina close to the optic axis of the eye, where the chromatic aberration has minimal effect. We also have no ultraviolet-sensitive cells as fishes (and many other animals) do; we even have few blue-sensitive cones in the area for sharpest vision, and the yellow pigment there decreases blur from blue and violet light. Finally, we have small pupils when the things we are looking at are well illuminated, so then we use only the central parts of the cornea and lens, further limiting chromatic aberration.

For fishes the chromatic aberration constitutes a more severe problem. Generally they cannot restrict the pupil, so it is large even in strong light. A spherical shape of the lens is much worse from the viewpoint of chromatic aberration than our "lens-shaped" lens, and many fishes have ultraviolet vision (some are also sensitive to light of longer wavelength than we are). But fishes have their tricks, too. Kröger and Campbell (1996) found that the longitudinal chromatic aberration was less than predicted from lens dispersion in several fishes. The reason for this was found (Jagger 1997; Kröger et al. 1999) to be that, for a fixed wavelength, different zones of the lens have different refractive powers, by having slightly different radii of curvature. This makes light from at least one zone produce a sharp image for each spectral band (although some blurring will be produced from the other zones). Another structural finesse which counteracts (longitudinal) chromatic aberration is that the light-sensitive outer segments of retinal cells tuned to different wavelengths are positioned at different depths in the retina, corresponding to the depths where the spectral bands to which they are tuned are focused.

The trick to have the lens divided into zones with different refractive powers would not work well for us, since our eyes are equipped with an iris that contracts in strong light. Thus, in strong light we use only the central part of the lens. But if you look into the eyes of a cat, you will see that it has a pupil which is not circular like ours but forming a vertical slit, which even when it closes lets the eye use peripheral parts of the lens. A goat, on the other hand, has pupils which are horizontal slits, with the same consequence.

Nautilus, the mollusk with beautiful spiral shells, has a pinhole camera-type eye that has problems with neither spherical nor chromatic aberration, since its eye lacks lens as well as cornea. On the other hand, the visual acuity is low, especially in dim light when the pinhole in the iris has to open up to let more light in.

15.6 Problems and Solutions for Amphibious Animals

Terrestrial and aquatic animals each have their specific optical problems to solve in the adaptation of their eyes to their environments. What then about animals who live both in air and water? There are many such animals: penguins and wingborne sea birds, such marine mammals as whales and seals, as well as many reptiles and even fishes. One can imagine that their problems must be much greater than those of animals who have to adapt to a single external medium. We can just think of how blurred our own vision is when we go underwater without goggles.

For birds diving for fish, it can be assumed that it would be of great advantage to be able to see the fish clearly both from the air and immediately after the dive through the water surface. Can they do this? The question has been tested for some birds. Katzir and Howland (2003) found that cormorants accommodate within 40–80 ms upon immersion in water. The cormorant has relatively low visual acuity in air relative to birds of the same body and eye size adapted to air vision only, and underwater its acuity is comparable to the higher values reported for fishes and marine mammals (Strod et al. 2004). On the other hand, cormorants are able to fish in darkness during the long arctic night (Grémillet et al. 2005), so perhaps there has been no strong evolutionary pressure for sharp air vision in their case. Martin (1998) studied the eyes of albatross, which forage only in light. Albatross eyes have

a flat cornea, which minimizes the change in refractive power of the eye upon immersion in water.

The bottlenose dolphin has a completely different eye, with a curved cornea and a spherical lens without accommodation capability (Litwiler and Cronin 2001), but a special shape of the pupil makes it possible for the dolphin to have almost the same visual acuity in air as in water (Herman et al. 1975). Herman et al. (1975) cite older literature about visual acuity for many other marine mammals. The harbor seal (Hanke et al. 2006) also has a largely curved cornea, but this has a central vertical strip that is flat and a pupil which closes to a vertical slit, so in sufficiently strong light, the seal has the same visual acuity in air and water.

Crocodiles, which have good distance focus in air (Fleishman et al. 1988), as well as some semiaquatic snakes (Schaeffel and Mathis 1991) surprisingly do not focus underwater, although they hunt underwater. On the contrary, some other snakes, even from the same genus (*Natrix*), possess an enormous accommodation ability. They can change the refractive power of the lens by over 100 diopters when they go from air to water, compared to some 15 diopters of accommodation in a human infant and a mere 1–2 diopters for the author at the age of 71.

The Atlantic flying fish seems to be able to select a suitable landing site among seaweed by means of vision. Instead of a smoothly curved cornea like those of most fishes, it has a pyramid-shaped one with three flat "windows." Measurements show that this allows it to see reasonably well at a distance during its flight (Baylor 1967; Fig. 15.8).

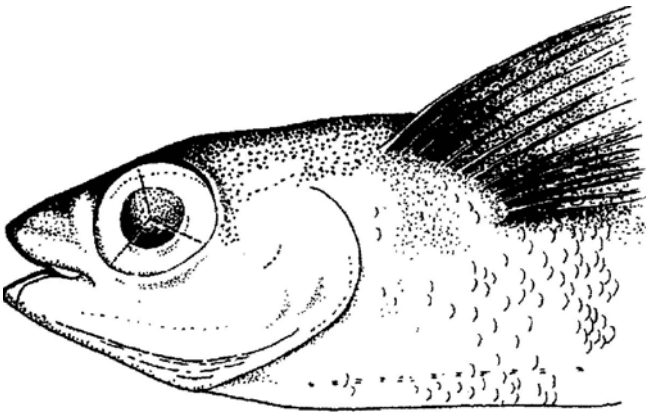

Fig. 15.8 The Atlantic flying fish has a pyramid-shaped cornea with three flat "windows" (From Baylor 1967)

A somewhat similar arrangement, but with two flat windows, is present in another fish, *Mnierpes macrocephalus*, living in the intertidal region (Graham and Rosenblatt 1970), and also in *Coryephoblennius galerita*, a fish living on rocky shores, which frequently makes excursions out of the water (Jermann and Senn 1992). The latter has one flat cornea window pointing up and a curved one pointing down. The most interesting is the "four-eyed fish," *Anableps anableps* (Fig. 15.9). It is a minnow living in freshwater pools in Central and South America and catching prey both in the

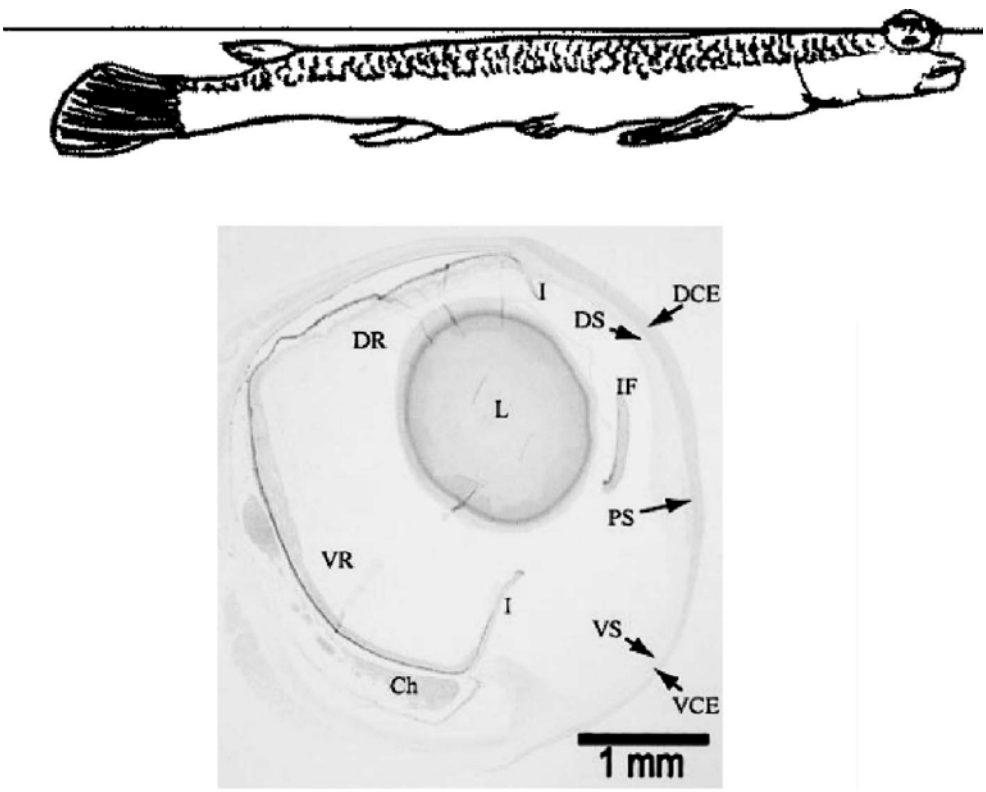

Fig. 15.9 (*Top*) *Anableps* swimming at the water surface (After Saidel and Fabiane 1998). (*Bottom*) Light micrograph of longitudinal section through eye of *Anableps*. *DR* dorsal retina, for looking up into the air, *VS* and *VCE* layers of the corresponding ventral cornea, *VR* ventral retina for looking into the water, *DS* and *DCE* layers of the corresponding dorsal cornea. Note that the lens is flatter in the direction for looking in the air than in the direction for looking in the water (From Swamynathan et al. 2003)

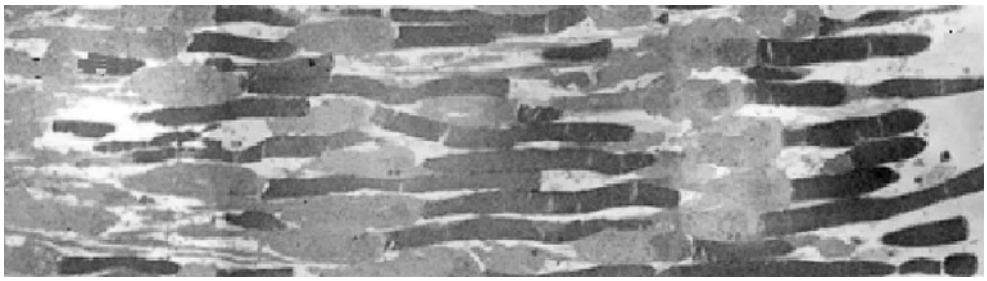

Fig. 15.10 Part of the retina of an oilbird with multiple layers of rods (From Martin et al. 2004)

water and above it. It swims with the eye exactly at the water surface. The eye has separate retinae for looking in the water and looking in the air but uses the same oblong lens for both retinae.

Some crustaceans, and at least one mollusk (Land 2000), also have separate optical systems for different purposes, but in most cases both systems are then below the water's surface.

15.7 Feedback Regulation During Eye Development

How come everything fits together so well in an eye? The cones (or rhabdomeres in the arthropod eyes to be described later) with different spectral sensitivities must be properly connected to the correct brain cells, otherwise the animal could not distinguish blue from green. The lens must focus the image sharply on the retina. We have seen that eyes can accommodate by moving the lens or changing its shape, but that can only be done to a degree. And what causes the lens to have the proper refraction index gradient? A fish can grow from almost microscopic size to become bigger than a human, and throughout this development the eye must be able to produce sharp images to remain useful.

The answer can to a large extent be summarized in one word: feedback. The eye sends signals to the brain, and if the brain finds that the image is not good enough, it sends signals back to the eye to correct the situation. Accommodation is, of course, one result of such feedback, but the brain feeds back also to developmental processes. The refractive index gradient can be affected (Kröger et al. 2001), as well as the size of the eye (Kröger and Wagner 1996).

If animals are reared in red light, the kind of visible light refracted least by the eye, the eye will develop in such a way that if the animals are transferred to blue light, the image will be projected in front of the retina. Conversely, if they are reared in blue light and then transferred to red light, the red light will be too weakly refracted, and the image will be projected behind the retina (Kröger and Fernald 1994).

The most dramatic experiments have been carried out with chicks supplied with eyeglasses with positive or negative lenses. In such experiments, it has been shown that the growth rate of the eye components is affected in a matter of hours by the distorted vision (Zhu et al. 2005).

15.8 Eyes with Extreme Light Sensitivity

We have probably all noticed how night-active animals reflect the light from the car's headlights with their eyes. They have a reflective tapetum, a mirror, behind the light-sensitive cells, which directs any light that has escaped being caught in the first pass back through the light-sensitive layer.

The oilbird, *Steatornis caripensis*, lives in caves in Venezuela and Trinidad and flies out only at night to pick fruits in the forests in Venezuela. Thus, it never experiences light stronger than full moonlight. In the cave, it also echolocates like bats, but vision is an important sense, as one can see from the construction of its retina (Martin et al. 2004; Fig. 15.10). In the human eye, the ratio between the diameter of the fully dilated pupil and the length of the eye is approximately 0.3. In the oilbird eye it is 0.56, which means that the irradiance of the retina can be made 3.5 times that of the human eye for the same ambient lighting. The retina is packed with rods (the most light-sensitive kind of cell in vertebrates) and has only few cones. There are a million rods per square millimeter of retinal surface, as compared to a maximum of about 160,000 in the human retina. The high density of rods is possible in part because the rods are thin, but in addition they are packed three tiers thick. Light that penetrates the first layer may therefore be absorbed in the second or third. Surprisingly, though, the oilbird seems to lack a reflective tapetum. Also many deep-sea fishes have a tiered or, as the term of the trade goes, a "multibank" retina (Wagner et al. 1998).

15.9 Compound Eyes

As far as we know, the first sophisticated eyes to evolve were compound eyes. Of these early eyes, those of trilobites (Fig. 15.11) are best preserved (some for more than half a billion years), partly because they had lenses made of calcite. Some of them are thought to have had bifocal lenses, so they could be used to see both nearby and more distant objects

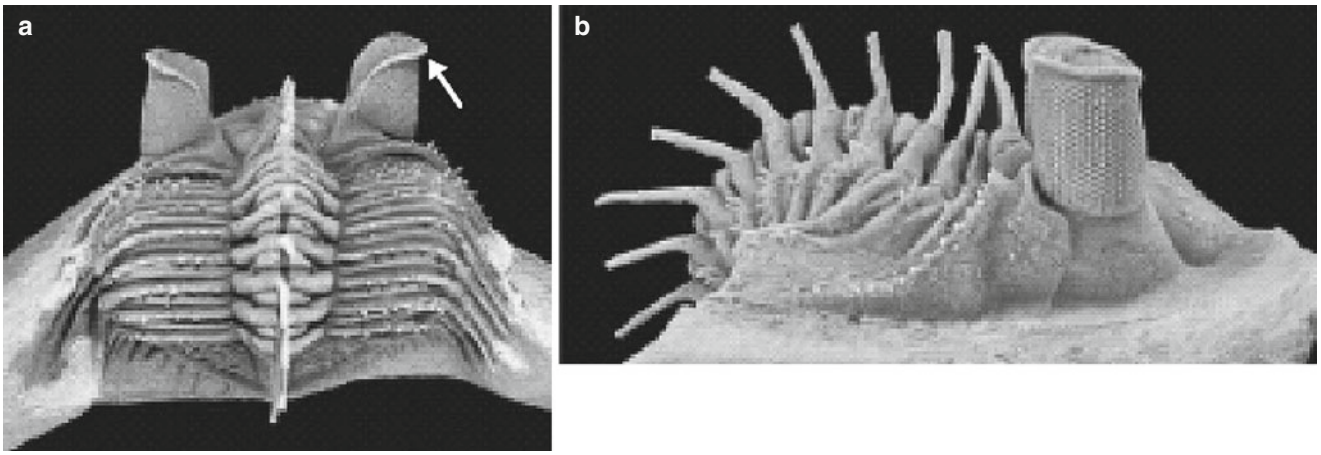

Fig. 15.11 The Devonian trilobite *Erbenochile erbeni* (see Fortey and Chatterton 2003) from the back (**a**) and side (**b**). This animal could see in all horizontal directions at once and had an eyeshade (*arrow*) above each eye to protect from light from the water surface. In the Devonian, there were no birds in the sky to worry about (Copyright the Natural History Museum, London. Reproduced with permission)

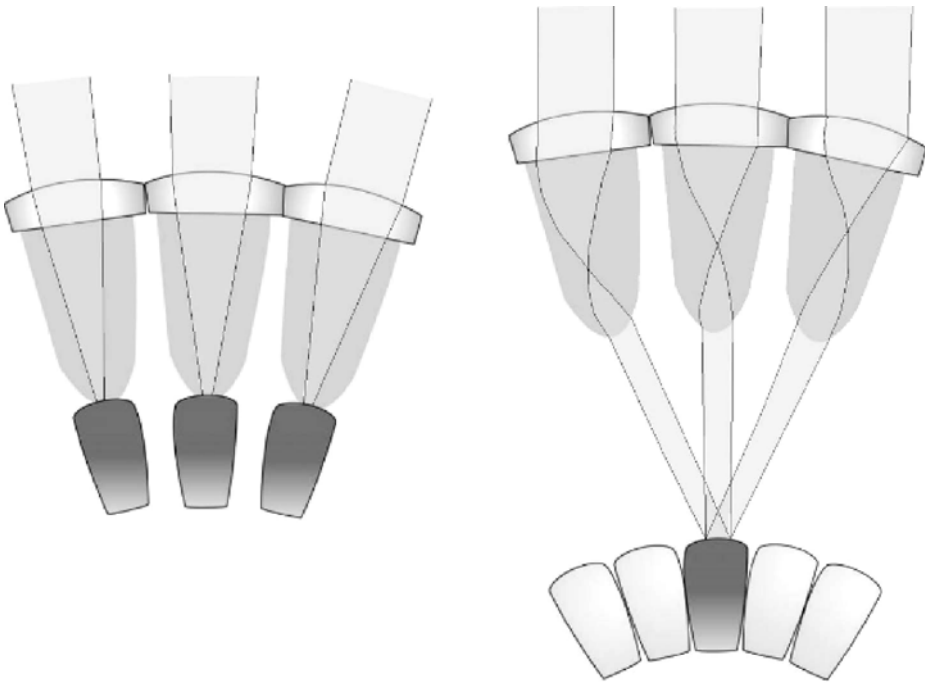

Fig. 15.12 In an apposition eye (*left*) composed of several ommatidia, each ommatidium separately receives light from one direction. In a superposition eye (*right*), light from one direction is, via the lenses of several ommatidia, focused on the light-sensitive part (*rhabdom*) of one ommatidium. The superposition eye shown here works by refraction optics, but there exist also those with reflection optics (e.g., Gaten 1994; see also section 15.11 on mirror optics below) and those with a combination of refraction and reflection optics

(Gál et al. 2000). A survey of the different types of trilobite eyes is given by Thomas (2005).

Compound eyes in extant animals are known mainly from crustaceans and insects but are present also in some other animals, such as horseshoe crabs. They can be broadly classified into apposition and superposition eyes (Fig. 15.12), and both these categories are present in both crustaceans and insects. Excellent reviews have been published by Horridge (2012) and by Land and Nilsson (2002), and compound eyes are treated also by Horridge (2005) and in a book edited by Warrant and Nilsson (2006). Here only a brief introduction will be given.

The optical system of a superposition eye is so constructed that an erect image is formed on the array of rhabdoms (the retina), not an inverted image as in our eyes. In general, animals adapted to strong light have apposition eyes, those adapted to dim light have superposition eyes, but some dim-light-adapted animals have rather light-sensitive apposition eyes, and some adapted to strong light have superposition eyes (e.g., Belušič et al. 2013). Acclimation to different light conditions can be achieved by the movement of pigment grains.

A compound eye in a small animal cannot attain the resolutions provided by good camera-type eyes. As one of the

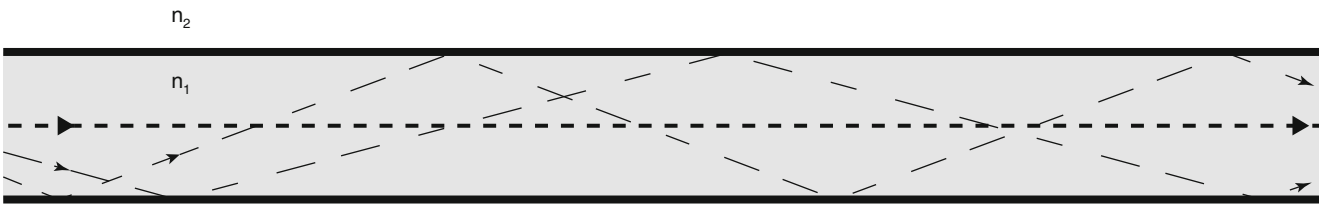

Fig. 15.13 Light propagating along an internally reflecting cylinder according to ray optics

pioneers (Mallock 1894) in the study of this subject put it: "The best of the [compound] eyes… would give a picture about as good as if executed in rather coarse wool-work and viewed at a distance of a foot." But recent research has revealed that some eyes are a little better than previously thought (see below). The spatial or angular resolution of eyes can be measured and expressed in different ways, and distinguishing two bright points from one another is not the same as being able to resolve a pattern of equally sized parallel white and black lines. Applying the latter, most commonly used, criterion, we can say that even the best compound eyes seldom resolve better than 1–2°. Only the largest eyes of dragonflies and praying mantis are about four times better than that, while we can resolve about 1 s of arc, and raptors such as eagles can do even better (see Gaffney and Hodos 2003 for a table of visual acuity for different birds).

Because of the small dimensions of the components of compound eyes, their function cannot always be analyzed with the kind of optics ("ray optics" or "geometrical optics"; Fig. 15.13), which we used for camera-type eyes above. Instead one must for insects with very thin rhabdoms use "physical optics," in which the electromagnetic wave nature of light is taken into account. To fully appreciate the following treatise, the reader is advised to first read Sect. 1.2 in Chap. 1.

One aspect of physical optics often encountered when dealing with the function of compound eyes is "propagation mode theory." This is a very complicated topic and is easily misunderstood. For one thing, the term "mode" has several meanings, which are often confused. The propagation mode we shall be dealing with here is different from cavity mode or some other terms used when dealing with laser technology, but we shall just call it "mode" in the following. Considerable simplification of the full mode theory can be used when variations of refractive index are as small as in complex eyes (Snyder 1969), but even the simplified theory is something for the real experts (as can be understood from just reading the title of Snyder's treatment in the reference list below), and here I shall give only a nonquantitative account, with only very simple mathematics, to give the reader a feeling of what mode theory is about.

In an object ("light conductor") consisting of a light-transmitting medium for which some dimensions are of about the same size as the wavelength of light, light cannot propagate in as many ways as in a larger space. Such a light conductor can be a thin fiber used to transmit telephone signals, but it can also be an ommatidium in a complex eye (actually the rods and cones in our own eyes also behave in such a way, and an accurate treatment of their optics also requires physical optics and mode theory). A mode is a set of guided electromagnetic waves in the light conductor. We shall assume in the following that the light conductor is approximately cylindrical and that the radius of the cylinder is not larger than the wavelength of the light it conducts. (Some light-conducting structures in real eyes are, it is true, far from cylindrical, but the cylinder approximation will be enough to get a qualitative understanding.) The cylindrical space itself has a higher refractive index than the surrounding, so the cylinder is delimited by the boundary between two media with different refractive indices.

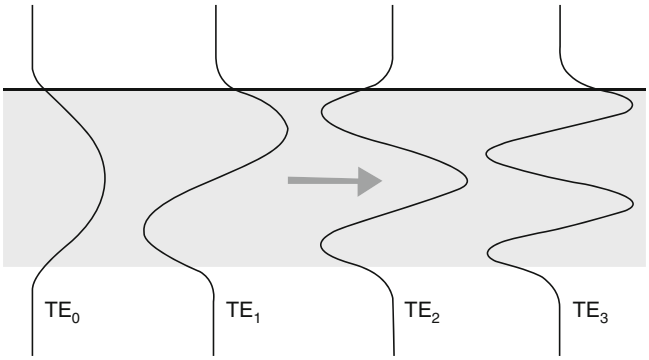

Fig. 15.14 Electric fields of modes propagating in a cylindrical light guide. The *arrow* shows the direction of light propagation and also the direction in which field strength is plotted. Note that with increasing mode number, more and more of the electrical field, and thus the electromagnetic energy (which is proportional to the square of the field strength), appears outside the fiber

Taking only ray optics into account, light rays can be described as bouncing in any way between the walls of the cylinder, as long as angles of incidence exceed the critical angle (Fig. 15.13) and equal the angles of reflection. But according to mode optics, only certain modes can travel along the conductor, namely, those for which the wavelength has a certain relation to the diameter of the light conductor (Fig. 15.14).

In geometrical optics, we treat light as if it is exactly restricted to a certain space, as there exists, for instance, in

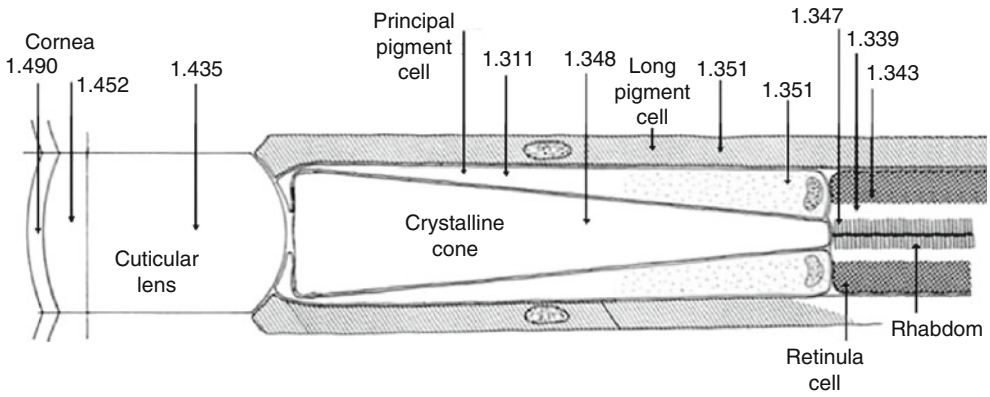

Fig. 15.15 Outer part of an ommatidium in the apposition eye of the honeybee, *Apis mellifera*. To the right is the outermost part of the light-sensitive structure, the rhabdom (*all of the rhabdom not shown*). It has a cross section of 1 μm (1,000 nm) (Adapted from Varela and Wiitanen 1970)

front of a mirror, but not at all inside a mirror. But as we have already seen in the treatment of near-field microscopy in Chap. 5, this no longer holds exactly when we go to very great detail and small dimensions. We have something called the "near-field," a part of the electromagnetic field which goes a little bit outside the limits set by geometrical optics. Therefore we shall not be surprised that the waves representing the modes in Fig. 15.14 extend a little beyond the boundary between regions of different refractive indices. The higher the mode order, the further outside the border does the mode penetrate, and the higher is the probability that light will escape to the external medium.

To compute how many modes that can propagate in a light conductor, it is convenient to introduce the concept of normalized frequency, V (also referred to as the waveguide parameter or V number). This is a dimensionless number: Here a is the diameter of the conductor. If V is below 4.810, only one mode can propagate. From this it can be understood that in animal body structures, where the differences in refractive indices are small, not many modes can propagate. The number of modes is dependent on the refractive indices, so for a proper analysis, these must be very accurately determined. Note that

$(n_{21}\text{-}n_{22})=(n_1\text{-}n_2) \bullet (n_1+n_2)$

we can use the formula to make a quick estimate of how light (we assume a wavelength of 500 nm) propagates in the ommatidium of a compound eye of a honeybee. The rhabdom, the light-sensitive structure to the right in 15.15, has a diameter of 4,000 nm and a refractive index (n_1) of 1.347, as compared to the refractive index of the surrounding substance (n_2), 1.339.

Thus, $V=2\pi(1000/500)\cdot(1.347^2-1.339^2)^{1/2}=2\pi\cdot 2\cdot(0.008\cdot 2.686)^{1/2}=1.84$, and in this structure only one mode can propagate. The crystalline cone (to the left of it in the diagram), as the name implies, has a conical shape rather than a cylindrical one, but since most of it has a diameter much larger than the rhabdom, and the refractive index difference at the boundary to neighboring cells is 3.7 times larger, we can guess that more than one mode can propagate in it. As we shall see below, interesting things can happen in the junction between the crystalline cone and rhabdom. Different modes are associated with different energy distributions in the cross section of the conductor (and in the near field outside it). The total energy distribution of all the modes is not obtained by adding the energy distributions but by adding the electromagnetic fields of the modes and squaring the sum, provided that the modes are coherent (in step with one another, in analogy with the famous Young's double-slit experiment).

As an example of where the mode theory can lead us, I shall try to explain a discovery which also illustrates what was said above: "recent research has revealed that some eyes are a little better than previously thought." Nilsson et al. (1984) and van Hateren and Nilsson (1987) found that the vision of certain butterflies with apposition eyes is sharper than what could be explained with simple-minded optics. The lens projects a bright point in the environment as an Airy disk into the crystalline cone (Fig. 15.15). This Airy disk is wider than the rhabdom in that particular ommatidium, and consequently one might think that the neighboring rhabdoms would be affected by light from the bright point.

However, in this case the dimensions of the rhabdom are such that two modes can propagate in it (can "be excited," as the jargon goes). The cross-sectional pattern of the electromagnetic field of the sum of these modes corresponds very well to the pattern of the Airy disk, with the consequence that the light from the bright point is conducted into only one rhabdom and the image in the butterfly brain will be sharper than it would otherwise be.

15.10 Nipple Arrays on Insect Eyes

As was briefly mentioned in Chap. 1, some insect eyes carry tiny structures on their lenses that decrease reflection of light from them (Fig. 15.16). The biological advantage is probably not primarily to gain more light for vision, but to decrease the risk of being spotted by enemies.

During an electron microscopic work on photoreceptor structures in a night moth, Bernhard and Miller (1962)

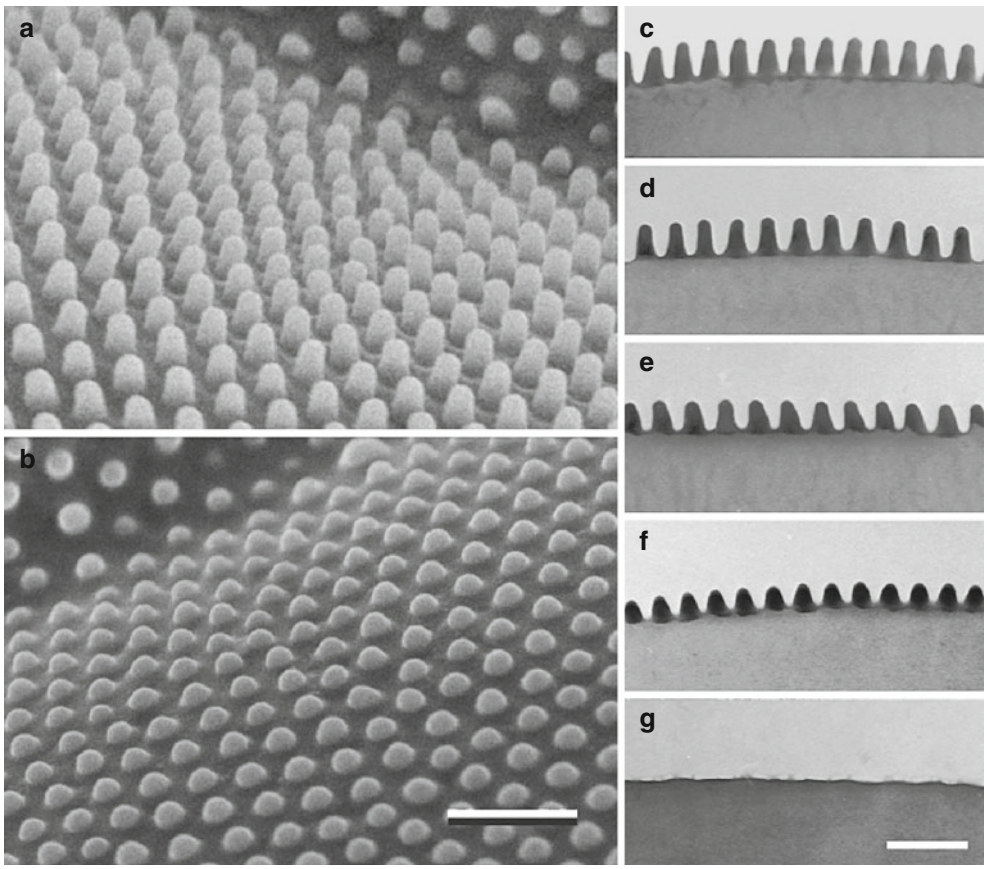

Fig. 15.16 *Left*, in surface view: corneal nipple arrays in the nymphalid *Polygonia c-aureum* (**a**) and the lycaenid *Pseudozizeeria maha* (**b**), showing differences in nipple height and shape. The bar is 500 nm. *Right*, in longitudinal section: corneal nipple arrays in the nymphalids *Bicyclus anynana* and *Polygonia c-aureum* (**c**, **d**), the pierid *Pieris rapae* (**e**), the lycaenid *Pseudozizeeria maha* (**f**), and the papilionid *Papilio xuthus* (**g**). Bars are 500 nm (From Stavenga et al. 2006)

discovered that the corneal surface carried cone-shaped protuberances termed nipples, about 200 nm in height and arranged in a hexagonal array. The antireflective effect of the nipple array was shown in microwave experiments on lens models scaled to the frequency of the microwaves (Bernhard et al. 1963, 1965) as well as in comparative spectrophotometric measurements on corneal fragments from insects with nippled and non-nippled facets (Miller et al. 1966).

Recently interest in and study of these structures have increased, partly due to the possibility of technical applications. A detailed analysis of the corneal nipple arrays of several moth and butterfly species has been carried out by Stavenga and coworkers (Stavenga et al. 2006). They modeled the reflectance from dimensions and optical theory. It was found that the reflectance of the eyes decreases with increasing nipple height. Nipples with a paraboloid shape and height 250 nm, touching each other at the base, almost completely eliminate the reflectance for normally incident light.

Nipples and similar antireflective structures do not occur only in the order Lepidoptera but also in Trichoptera and, although with smaller height, in some Diptera (Bernhard et al. 1970). In a very small moth with tiny eyes, instead of nipples, the cornea has a system of regular, radial ridges, spaced about 250 nm apart. For such eyes, operating near the diffraction limit, this was judged to be a better arrangement (Meyer-Rochow and Stringer 1993).

15.11 Eyes with Mirror Optics

The eyes treated so far have refraction optics, but (as is the case with telescopes and some other man-made instruments) eyes can also have mirror (reflection) optics or a combination of refraction and reflection optics. How biological mirrors themselves are constructed and function is described in Chap. 10, so we will skip this subject here. One place for reflectors in eyes has already been touched upon, namely, those in the tapetum behind the light-sensitive cells, which let light pass a second time through them and thus increase the light sensitivity.

Only a couple of examples of reflection optics will be described here, and the reader is referred to Land (2000) for details and further examples.

One eye that combines refractive and reflective elements for projecting an image on the retina is that of a scallop. It has a lens like a normal camera-type eye, but the lens alone has no enough refracting power to produce a sharp image at the retina; it would fall far inside the eye. But the curved surface of the eye bottom reflects the rays

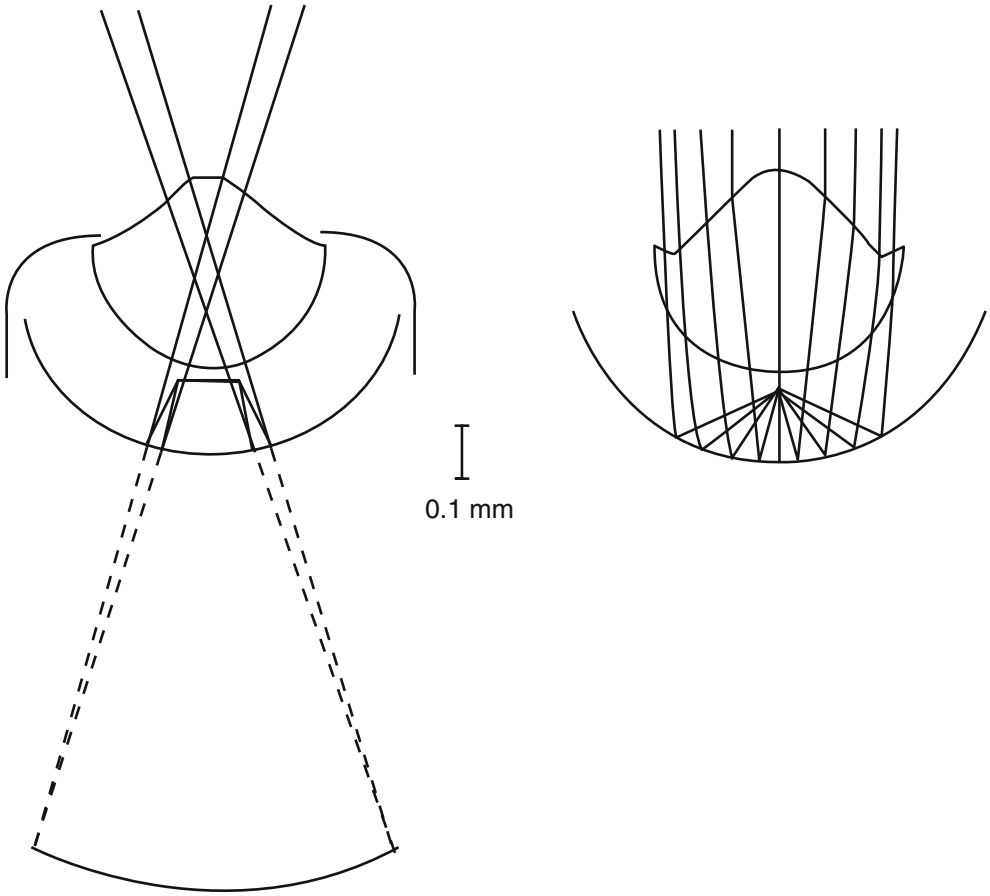

Fig. 15.17 Scallop eye, schematic (Modified after Land 2000). The sketch to the left shows where the image would fall if formed by the lens alone (*dash-dot rays*) and where it actually is projected after reflection at the bottom of the eye (*solid line rays*). The sketch to the right shows more in detail how a beam of light parallel to the optical axis is focused

back to converge on the retina in front of it from behind (Fig. 15.17).

For some time it was unknown how decapod crustaceans like crayfish, lobsters, shrimp, and prawns can see, until Vogt (1975, 1977) discovered that their compound superposition eyes have reflection optics. The principle is shown in Fig. 15.18. Note that the corneas are flat. The material below them does not have a refractive index so that it can produce an image. It is instead the reflective walls of the ommatidia that direct the light to the rhabdoms. The diagram shows the ommatidia in a light-adapted state, where pigment grains (gray) separate the ommatidia optically from one another. In a dark-adapted eye, the pigment grains are positioned in such a way that they do not separate the rhabdoms. In the upper center is a tangential section of the eye near the surface, and it can be seen that the ommatidia are square in cross section, not hexagonal as most ommatidia in insects.

It is interesting that a description of the reflection optics in compound eyes in a popular science magazine (Land 1978) inspired a design of an x-ray telescope for astronomy (Angel 1979; Lee and Szema 2005). X-rays cannot be deflected by ordinary lenses, and one must use either reflecting optics or so-called zone plates, based on diffraction, somewhat resembling transmission gratings, but with circular geometry.

15.12 Scanning Eyes

Both camera-type eyes, like ours, and compound eyes view a large solid angle "in one bite." This is different from a television camera, which scans the visual field point by point. We have examples of this way of imaging in the animal world, most pronounced in small crustaceans belonging to the copepods. The best studied genera are *Copilia* (Figs. 15.19 and 15.20) and *Sapphirina*. These animals have two eyes, each with a very large (in relation to the body size) lens in front of the body, and deep in the body a smaller lens and a very tiny retina. The retina is so small that almost only one point at a time can be projected upon it. But the retinae of the two eyes oscillate sideways at a rate of up to 5 s^{-1} min, getting alternatingly closer and further apart. In this way, they scan a thin strip of the visual field.

Copilia and *Sapphirina* can be regarded as extreme cases of a common theme. They can image only two points at a time (one with each eye) and over a short time almost only a line. But scanning eye movements are common, not only in other crustaceans like *Daphnia* (Frost 1975) and crabs (Sandeman 1978) but also in spiders, mollusks (Land 1982), and other animals. In these cases, the retina is not quite as small as in *Copilia* and *Sapphirina*, but nevertheless the eye

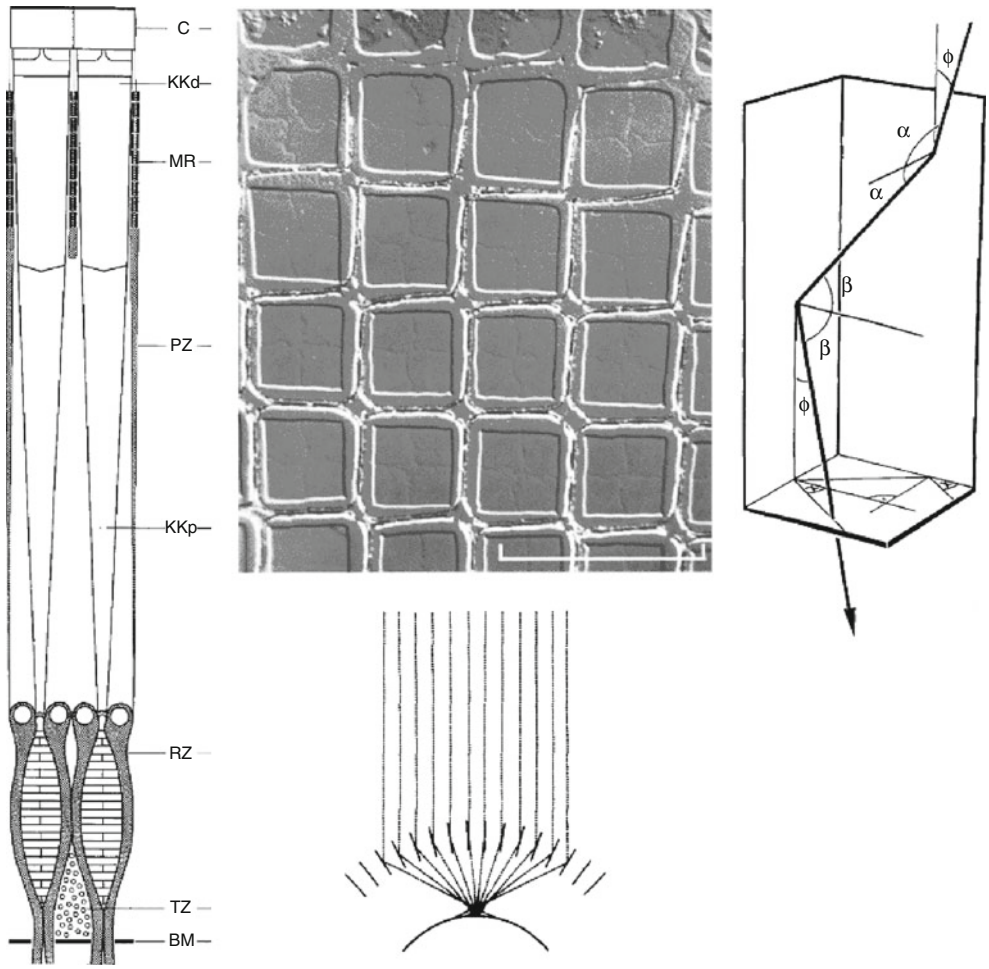

Fig. 15.18 Crayfish eye (From Vogt 1980). To the *left* are two ommatidia from the compound superposition eye. To the *right* is a diagram showing how a light ray is reflected against the walls of an ommatidium on its way to the rhabdom, and at *lower center* one which shows the ray tracing in the whole eye for light from a distant point. The *upper center* is a surface view of the eye showing the square facets

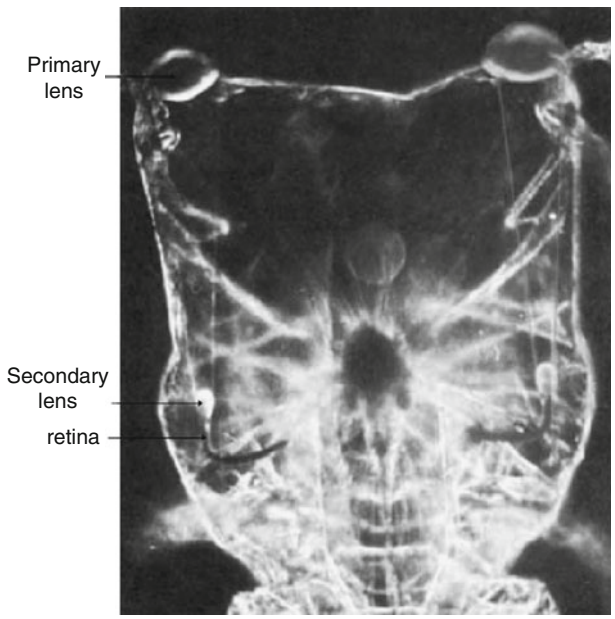

Fig. 15.19 The front part of the body of *Copilia quadrata*. The width is about 1 mm. The approximately 2-mm-long tail is not visible (From Gregory et al. 1964)

movements expand the visual field. Even unicellular organisms like *Euglena* or dinoflagellates, which rotate during their swim and thereby let a shadow from a pigment spot intermittently fall on the light sensor and thereby determine the light direction, can be said to use a related principle.

In fact, we ourselves carry out small unconscious eye movements called saccades all the time, but these have a different function. In our case, it is thought that these eye movements counteract a shutdown of the signals from the retina, which would be the case if the same stimulus was maintained on the same spot over a long time. It is thought that the jerky flight of some insects with fixed eyes serves the same purpose.

The tiny eyes of arthropods and other invertebrates have fascinated and inspired people from ancient times, over the years when magnifying glasses and primitive microscopes (Fig. 15.21) opened a new world, to our days. It has already been mentioned how the elucidation of the function of crayfish and lobster eyes helped astronomers to improved x-ray telescopes. The nipple arrays have been copied in solar energy collectors to help light get in but also in light-emitting diodes to help light get out (Iwaya et al. 2006). There are

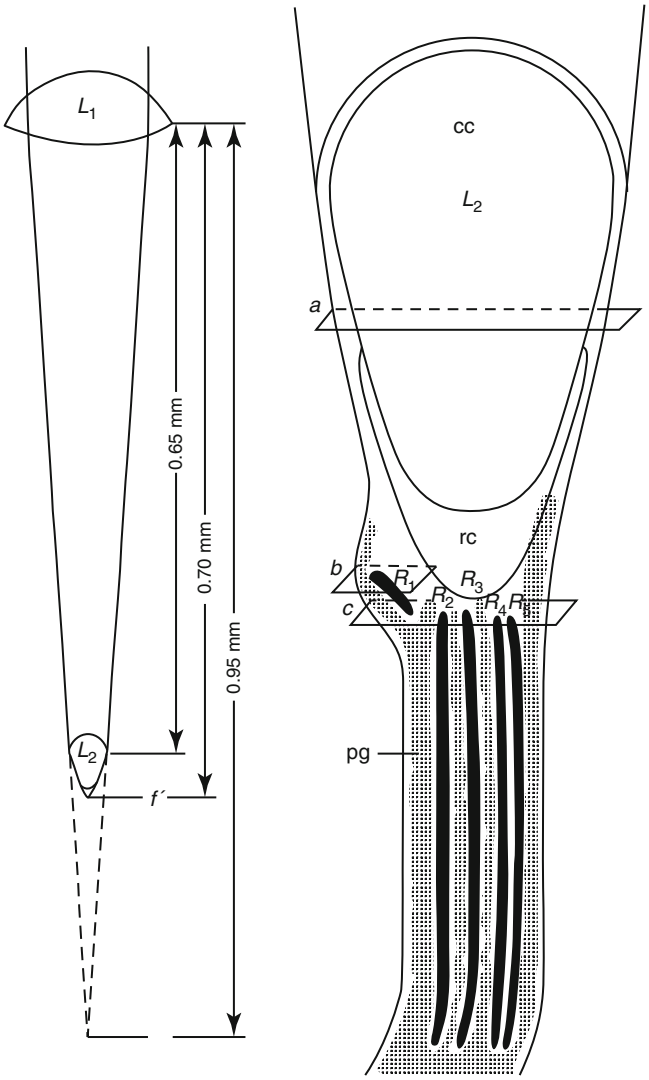

Fig. 15.20 Sketch of a *Copilia* eye (*left*) and detail of the inner part (*right*) (From Wolken and Florida 1969)

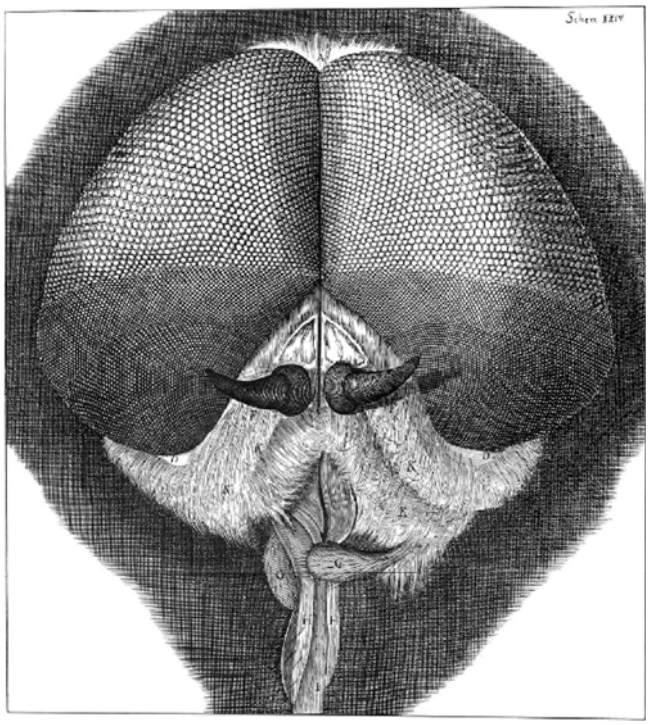

Fig. 15.21 Robert Hooke's (1665) drawing of the head of gray drone fly

many more examples of how eyes have inspired technology (Lee and Szema 2005; Duparré and Wippermann 2006).

This shows the importance of interdisciplinary communication, something which is also an aim of this book.

15.13 Evolution of Eyes

Most organisms have some way to sense the light, and many can also sense the direction of light. But we shall restrict the term eye to a structure which can sense the direction of light rather well and produce a kind of "picture" of the external world, but not necessarily as a projection on a retina. Although many pigments are employed as light sensors (see Chap. 13), only a group of chromoproteins collectively known as rhodopsins are used as sensors in eyes. The chromophores, which together with the protein moieties, the opsins, form the rhodopsins, are all closely related terpenoids known as retinals, although it has recently been found that in special cases chlorophyll derivatives are also involved in vision (Douglas et al. 1998, 1999; Isayama et al. 2006) and archaean rhodopsin can have a carotenoid as antenna chromophore (Balashov et al. 2005).

Rhodopsins occur throughout the three domains of life: Archaea, Bacteria, and Eukarya. The rhodopsins in Archaea are of a type, also occurring in Bacteria and Eukarya, which seems not to be involved in imaging vision and in the eyes, although they may act in light sensing (while some use light to pump ions in or out of cells). The type of rhodopsin involved in vision, having amino acid sequences quite different from those of "archaean" or "type 1" rhodopsins, occurs only within Bacteria and Eukarya. Both main types of rhodopsin may occur in the same bacterium, in which case the type 1 rhodopsins have probably been acquired by gene transfer from archaeans (Mongodin et al. 2005). Both main types of rhodopsin may have a distant common evolutionary relationship despite differences in amino acid sequence, since they share a seven-helix transmembrane structure (although some helices have been lost in some of them). There are also opsins which do not combine with the retinal and are not used for vision (Terakita 2005).

From this it seems likely that all eyes have evolved from a common light-sensing structure. Opinions about the later evolution differ among experts. Some believe that imaging

eyes have evolved independently more than 40 (or even more than 60) times in different animal groups (von Salvini-Plawen and Mayr 1961, as cited by Gehring 2005), while Gehring (2005) argues strongly for monophyly, and Fernald (2000) can be said to take an intermediate position. There seems to be a deep evolutionary split between ciliary photoreceptors (as the rods and cones in our eyes) and rhabdomeric photoreceptors (as the ones in simple and compound eyes of arthropods). But Arendt et al. (2004) found both ciliary and rhabdomeric photoreceptors in the same animal species, a rag worm.

At least in part the differences between "monophylogenists" and advocates of convergent evolution are to some extent due to terminology confusion. "A has evolved from B" or "A is homologous with B" was clear as long as scientists had only visible morphological characters to consider. When molecular phylogeny emerged, the terminology for a while became blurred but is now beginning to clear up again. As Nielsen and Martinez (2003) point out, "homologous structures in two or more taxa are structures derived from the same structure in their latest common ancestor." In that sense, all parts of all eyes are certainly not homologous. On the other hand, it has been clearly demonstrated that several of the genes and signaling systems for the development of eyes are related between animals as different as insects and vertebrates. The most dramatic has been the demonstration (Gehring 2005) that eyes can be induced on the antenna of a fruit fly by transfer of a mouse gene (Pax6) which induces eye formation in that animal or a similar gene from a fruit fly that induces eye formation in a toad (Onuma et al. 2002). It should be pointed out that Pax6 has other functions, too, and perhaps this and related genes are more generally involved in the organization of sense organs and nerve systems rather than specific eye organizers. A single Pax-type gene is present in the box jellies (cubozoans), where it is expressed both in parts of the eyes (retina and lens) and in the balance organs (Kozmik et al. 2003). Oakley (2003 a, b) contemplates the question of monophyly or polyphyly specifically for compound eyes. He presents evidence that the compound eyes of insects and crustaceans are homologous. But the group among crustaceans with compound eyes that he has particularly studied, myococopid ostracods, seems to have no close relatives or ancestors with compound eyes, so it seems that compound eyes have evolved again on that line. Oakley (2003b) suggests the possibility that "complex structures like eyes might not evolve de novo every time and many of the steps toward origin need not be repeated… genes or even whole developmental pathways may be retained during evolution, even in the absence of the morphological features where those genes were once expressed." As a classic example, the existence of a latent developmental program was proposed to explain the experimental induction of teeth in chickens (Kollar and Fisher 1980; Gould 1983; Chen et al. 2000). In a more recent example, Whiting et al. (2003) suggested, based on phylogenetic distribution, that insect wings may be evolving by "switchback evolution." This appears to me to be a very reasonable standpoint, and Harris et al. (2006) can now be added to the list of citations as an even more striking illustration.

Although the opsin part of rhodopsins are all related (with the exception of the archaeal type), and the chromophores are also related, there are differences in the details, not only in the opsin proteins, but also in the chromophores (Chap. 9) and in their biosynthesis. In eukaryotes, the retinal is formed by the oxygenation of β-carotene but in the cyanobacterium *Synechocystis* by oxygenation of a β-apocarotenal (Ruch et al. 2005). For the formation of 3-hydroxyretinal and 3-hydroxyretinol from the retinal in insects, one or, respectively, two more oxygenation steps are required, each using specific enzymes (Seki et al. 1998; Ahmad et al. 2006). All these oxygenations require molecular oxygen, and the pathways could not have evolved prior to the oxygenation of the environment. As in eukaryotes, the retinal in halobacteria is formed by oxygenation of β-carotene (Peck et al. 2001). Since the split between eukaryotes and archaeans is thought to be older than environmental oxygen, this indicates either parallel evolution or horizontal gene transfer, a question that could perhaps be solved by a comparison of the sequences of the various oxygenases.

The materials of the lenses have no common origin. The main proteins in vertebrate lenses, the crystallins (see Piatigorsky 2006), have nothing in common with the lens material in arthropods or mollusks, and lenses in some animals like trilobites (Thomas 2005) and brittle stars (Aizenberg et al. 2001) were or are made, wholly or in part, from an inorganic material, calcite.

One cannot but marvel when realizing how sophisticated the eyes or other light-recording structures are in some at first glance very "simple" animals, like the brittle stars (Aizenberg et al. 2001) or box jellies (Martin 2004; Nilsson et al. 2005), or even some unicellular organisms. Gehring (2005) shows pictures of various dinoflagellates having eye-like structures with lenses, light-sensitive regions, and pigmented areas within a single cell. Francis (1967) estimated the refractive index of the presumed lens of such an organism to be around 1.5, i.e., much higher than that of a human lens, which makes it even more likely that it really has an optical function. However, it is to go too far to speculate, as Gehring (2005) does, that a dinoflagellate structure could be an eye precursor, since the rather advanced eyes of trilobites probably evolved before dinoflagellates.

The lenses of brittle stars (Aizenberg et al. 2001) and of box jellies (Nilsson et al. 2005) have a surprisingly advanced construction, being able to produce images supposedly too sharp for the nervous systems of these animals to take full advantage of. In both cases, they have refractive index

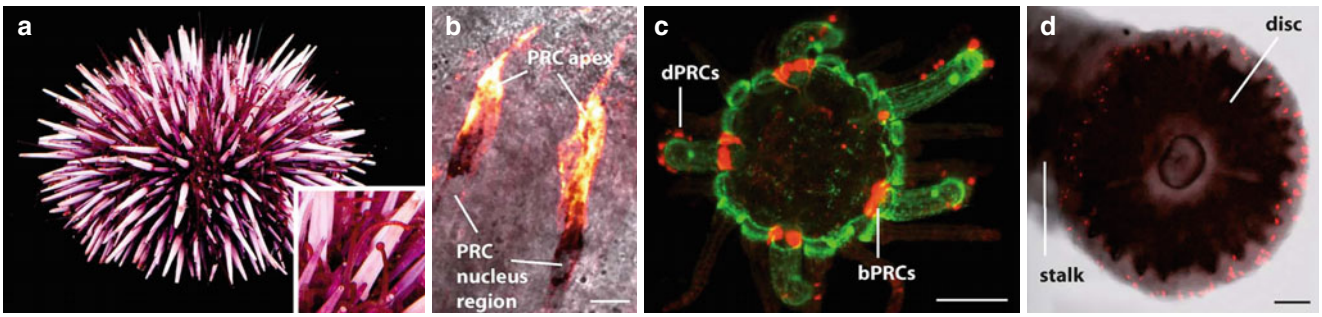

Fig. 15.22 Tube foot expression of r-opsin in *S. purpuratus*. (**a**) Adult specimen. (*Inset*) Tube feet extended between spines. (**b**) Sp-opsin4 RNA probe (*black*) and antibody (*yellow*) clearly colocalize in disk photoreceptive cells. (**c**) Sp-opsin4-positive photoreceptive cells (*red*) at base (*bPRCs*) and disk (*dPRCs*) of primary podia in an early juvenile counterstained with anti-synaptotagmin B (green), a general echinoderm nervous system marker. (**d**) Disk photoreceptive cells arranged around the rim of an adult tube foot disk. Sp-opsin4 antibody labeling (*red*) (From Ullrich-Lüter et al. 2011)

gradients of the same type as described above for the lenses in fish and octopus eyes. Also other echinoderms and cnidarians are sensitive to light. Some other members in these groups possess what can be described as crude vision. Sea urchins have been investigated in most detail (Ullrich-Lüter et al. (2011). Between their spines they have tube feet which have photoreceptive cells both at their bases and in their distal disks (Fig. 15.22). Depending on how many spines they have, their visual acuity varies between ca 30° (0.07 sr) for *Echinometra* species (Blevins and Jonsen 2004) to 10° (0.024 sr) for *Strongylocentrotus purpuratus* (Jackson and Johnsen 2011).

A review of the dermal light sense that many animals possess is provided by Ramirez et al. (2011).

References

Ahmad ST, Joyce MV, Boggess B, O'Tousa JE (2006) The role of Drosophila ninaG oxidoreductase in visual pigment chromophore biogenesis. J Biol Chem 281:9205–9209

Aizenberg J, Tkachenko A, Weiner S, Addadi L, Hendler G (2001) Calcitic microlenses as part of the photoreceptor system in brittlestars. Nature 412:819–822

Angel JRP (1979) Lobster eyes as x-ray telescopes. Astrophys J 233: 364–373

Arendt D, Tessmar-Raible K, Snyman H, Dorresteijn AW, Wittbrodt J (2004) Ciliary photoreceptors with a vertebrate-type opsin in an invertebrate brain. Science 306:869–871

Backfisch B, Rajan VBV, Fischer RM, Lohs C, Arboleda E, Tessmar-Raible K, Raible F (2013) Stable transgenesis in the marine annelid *Platynereis dumerilii* sheds new light on photoreceptor evolution. Proc Natl Acad Sci USA 110:193–198

Balashov SP, Imasheva ES, Boichenko VA, Antón J, Wang JM, Lanyi JK (2005) Xanthorhodopsin: a proton pump with a light-harvesting carotenoid antenna. Science 309:2061–2064

Baylor ER (1967) Air and water vision of the Atlantic flying fish, Cypselurus heterurus. Nature 214:307–308

Belušič G, Pirih P, Stavenga DG (2013) A cute and highly contrast-sensitive superposition eye – the diurnal owlfly *Libelloides macaronius*. J Exp Biol 216:2081–2088

Bernhard CG, Miller WH (1962) A corneal nipple pattern in insect compound eyes. Acta Physiol Scand 56:385–386

Bernhard CG, Møller AR, Miller WH (1963) Function of corneal nipples in compound eyes of insects. Acta Physiol Scand 58:381–382

Bernhard CG, Miller WH, Møller AR (1965) Insect corneal nipple array—a biological broad-band impedance transformer that acts as an antireflection coating. Acta Physiol Scand S 63(5- Suppl):243

Bernhard CG, Gemne G, Sällström J (1970) Comparative ultrastructure of corneal surface topography in insects with aspects on phylogenesis and function. Zschr Vergl Physiol 67:1–25

Blevins E, Johnsen S (2004) Spatial vision in the echinoid genus Echinometra. J Exp Biol 207:4249–4253

Chen Y, Zhang Y, Jiang TX, Barlow AJ, St Amand TR, Hu Y, Heaney S, Francis-West P, Chuong CM, Maas R (2000) Conservation of early odontogenic signaling pathways in Aves. Proc Natl Acad Sci USA 97:10044–10049

Douglas RH, Partridge JC, Dulai K, Hunt D, Mullineaux CW, Tauber AY, Hynninen PH (1998) Dragon fish see using chlorophyll. Nature 393(6684):423–424

Douglas RH, Partridge JC, Dulai KS, Hunt DM, Mullineaux CW, Hynninen PH (1999) Enhanced retinal longwave sensitivity using a chlorophyll-derived photosensitiser in Malacosteus niger, a deep-sea dragon fish with far red bioluminescence. Vision Res 39:2817–2832

Duparré JW, Wippermann FC (2006) Micro-optical artificial compound eyes. Bioinsp Biomim 1:R1–R16

Fernald RD (2000) Evolution of eyes. Curr Opin Neurobiol 10: 444–450

Fleishman LJ, Howland HC, Howland MJ, Rand RS, Davenport ML (1988) Crocodiles don't focus underwater. J Comp Physiol A 163: 441–443

Fortey R, Chatterton B (2003) A Devonian trilobite with an eyeshade. Science 301:1689

Francis D (1967) On the eyespot of the dinoflagellate Nematodinium. J Exp Biol 47:495–501

Frost BJ (1975) Eye movements in Daphnia pulex (De Geer). J Exp Biol 62:175–187

Gaffney MF, Hodos W (2003) The visual acuity and refractive state of the American kestrel (Falco sparverius). Vision Res 43: 2053–2093

Gál J, Horváth G, Clarkson ENK, Haiman O (2000) Image formation by bifocal lenses in a trilobite eye? Vision Res 40:843–853

Gaten E (1994) Geometrical optics of a galatheid compound eye. J Comp Physiol A 175:749–759

Gehring WJ (2005) New perspectives on eye development and the evolution of eyes and photoreceptors. J Hered 96:171–184

Gould SJ (1983) Hen's teeth and horse's toes. W.W. Norton, New York

Graham JB, Rosenblatt RH (1970) Aerial vision: unique adaptation in an intertidal fish. Science 168:586–588

Gregory RL, Ross HE, Moray N (1964) The curious eye of Copilia. Nature 201:1166–1168

Grémillet D, Kuntz G, Gilbert C, Woakes AJ, Butler PJ, le Maho Y (2005) Cormorants dive through the polar night. Biol Lett 1:469–471

Hanke FD, Dehnhardt G, Schaeffel F, Hanke W (2006) Corneal topography, refractive state, and accommodation in harbor seals (Phoca vitulina). Vision Res 46:837–847

Harris MP, Hasso SM, Ferguson MWJ, Fallon JF (2006) The development of archosaurian first-generation teeth in a chicken mutant. Curr Biol 16:371–377

Herman LM, Peacock MF, Ynkeer MP, Madsen CJ (1975) Bottlenosed dolphin: double-slit pupil yields equivalent aerial and underwater diurnal acuity. Science 189:650–652

Hooke R (1665) Micrographia: or, some physiological descriptions of minute bodies made by magnifying glasses with observations and inquiries thereupon. J. Martyn and J. Allestry, London

Horridge GA (2002) The design of the compound eye depends on the physics of light. In: Björn LO (ed) Photobiology: the science of light and life. Kluwer Academic Publishers, Dordrecht, pp 181–218

Horridge GA (2005) The spatial resolutions of the apposition compound eye and its neurosensory feature detectors: observation versus theory. J Insect Physiol 51:243–266

Isayama T, Alexeev D, Makino CL, Washington I, Nakanishi K, Turro NJ (2006) An accessory chromophore in red vision. Nature 443:649

Iwaya M, Kasugai H, Kawashima T, Iida K, Honshio A, Miyake Y, Kamiyama S, Amano H, Akasaki I (2006) Improvement in light extraction efficiency in group III nitride-based light-emitting diodes using moth-eye structure. Thin Solid Films 515:768–770

Jackson E, Johnsen S (2011) Orientation to objects in the sea urchin Strongylocentrotus purpuratus depends on apparent and not actual object size. Biol Bull 220:86–88

Jagger WS (1992) The optics of the spherical fish lens. Vision Res 32:1271–1284

Jagger WS (1997) Chromatic and monochromatic optical resolution in the rainbow trout. Vision Res 37:1249–1254

Jagger WS, Sands PJ (1996) A wide-angle gradient index optical model of the crystalline lens and eye of the rainbow trout. Vision Res 36:2623–2639

Jagger WS, Sands PJ (1999) A wide-angle gradient index optical model of the crystalline lens and eye of the octopus. Vision Res 39: 2841–2853

Jermann T, Senn DG (1992) Amphibious vision in Coryphoblennius galerita L. (Perciformes). Experientia 48:217–218

Katzir G, Howland HC (2003) Corneal power and underwater accommodation in great cormorants (Phalacrocorax carbo sinensis). J Exp Biol 206:833–841

Kollar EJ, Fisher C (1980) Tooth induction in chick epithelium: expression of quiescent genes for enamel synthesis. Science 207:993–995

Kozmik Z, Daube M, Frei E, Norman B, Kos L, Dishaw LJ, Noll M, Piatigorsky J (2003) Role of Pax genes in eye evolution: a cnidarian PaxB gene uniting Pax2 and Pax6 functions. Dev Cell 5:773–785

Kröger RHH, Campbell MCW (1996) Dispersion and longitudinal chromatic aberration of the crystalline lens of the African cichlid fish Haplochromis burtoni. J Opt Soc Am A 13:2341–2347

Kröger RHH, Fernald RD (1994) Regulation of eye growth in the African cichlid fish Haplochromis burtoni. Vision Res 34:1807–1814

Kröger RHH, Wagner HJ (1996) The eye of the blue acara (Aequidens pulcher, Cichlidae) grows to compensate for defocus due to chromatic aberration. J Comp Physiol A 179:837–842

Kröger RHH, Campbell MCW, Fernald RD, Wagner HJ (1999) Multifocal lenses compensate for chromatic defocus in vertebrate eyes. J Comp Physiol A 184:361–369

Kröger RHH, Campbell MCW, Fernald RD (2001) The development of the crystalline lens is sensitive to visual input in the African cichlid fish, Haplochromis burtoni. Vision Res 41:549–559

Land MF (1978) Animal eyes with mirror optics. Sci Am 239: 126–134

Land MF (1982) Scanning eye movements in a heteropod mollusc. J Exp Biol 96:427–430

Land MF (2000) Eyes with mirror optics. J Opt A Pure Appl Opt 2:R44–R50

Land MF, Nilsson DE (2012) Animal eyes (2nd ed.). Oxford University Press, Oxford, p 271. ISBN 978-0-19-958114-6

Lee LP, Szema R (2005) Inspirations from biological optics for advanced photonic systems. Science 18:1148–1150

Liou HL, Brennan NA (1997) Anatomically accurate, finite model eye for optical modeling. J Opt Soc Am A 14:1684–1695

Litwiler TL, Cronin TW (2001) No evidence of accommodation in the eyes of the bottlenose dolphin, Tursiops truncatus. Mar Mamm Sci 17:508–525

Liu YJ, Wang ZQ, Song LP, Mu GG (2005) An anatomically accurate eye model with a shell-structure lens. Optik 116:241–246

Mallock A (1894) Insect sight and the defining power of compound eyes. Proc R Soc Lond B 55:85–90

Martin GR (1998) Eye structure and amphibious foraging in albatrosses. Proc R Soc Lond B.265:665–671

Martin VJ (2004) Photoreceptors of cubozoan jellyfish. Hydrobiologia 530–531:135–144

Martin G, Rojas LM, Ramírez Y, McNeil R (2004) The eyes of oilbirds (Steatornis caripensis): pushing at the limits of sensitivity. Naturwiss 91:26–29

Meyer-Rochow VB, Stringer IA (1993) A system of regular ridges instead of nipples on a compound eye that has to operate near the diffraction limit. Vision Res 33:2645–2647

Miller WH, Møller AR, Bernhard CG (1966) The corneal nipple array. In: Bernhard CG (ed) The functional organization of the compound eye. Pergamon Press, London, pp 21–33

Mongodin EF, Nelson KE, Daugherty S, DeBoy RT, Wister J, Khouri JH, Weidman J, Walsh DA, Papke RT, Sanchez Perez G, Sharma AK, Nesbø CL, MacLeod D, Bapteste E, Doolittle WF, Charlebois RL, Legault B, Rodriguez-Valera F (2005) The genome of Salinibacter ruber: convergence and gene exchange among hyperhalophilic bacteria and archaea. Proc Natl Acad Sci USA 102:18147–18152

Navarro R, Santamaría J, Bescós J (1985) Accommodation-dependent model of the human eye with aspherics. J Opt Soc Am A 8: 1273–1281

Nielsen C, Martinez P (2003) Patterns of gene expression: homology or homocrazy? Dev Genes Evol 2013:149–154

Nilsson DE (2013) Eye evolution and its functional basis. Vis Neurosci 30:5–20

Nilsson DE, Kelber A (2007) A functional analysis of compound eye evolution. Arthropod Struct Dev 36:373–385

Nilsson DE, Land MF, Howard J (1984) Afocal apposition optics in butterfly eyes. Nature 312:561–563

Nilsson DE, Gislen L, Coates MM, Skogh C, Garm A (2005) Advanced optics in a jellyfish eye. Nature 435:201–205

Oakley TH (2003a) The eye as a replicating and diverging, modular developmental unit. Trends Ecol Evol 18:623–627

Oakley TH (2003b) On homology of arthropod compound eyes. Integr Comp Biol 43:522–530

Onuma Y, Takahashi S, Asashima M, Kurata S, Gehring WJ (2002) Conservation of Pax-6 function and upstream activation by Notch signaling in eye development of frogs and flies. Proc Natl Acad Sci USA 99:2020–2025

Ott M (2006) Visual accommodation in vertebrates: mechanisms, physiological response, and stimuli. J Comp Physiol A 192:97–111

Peck RF, Echavarri-Erasun C, Eric A, Johnson EA, Wailap Victor Ngi WV, Kennedy SP, Hoodi L, DasSarma S, Krebs MP (2001) brp and blh are required for synthesis of the retinal cofactor of bacteriorhodopsin in Halobacterium salinarum. J Biol Chem 23:5739–5744

Piatigorsky J (2006) Seeing the light: the role of inherited developmental cascades in the origins of vertebrate lenses and their crystallins. Heredity 96:275–277

Ramirez MD, Speiser DI, Pankey S, Oakley TH (2011) Understanding the dermal light sense in the context of integrative photoreceptor cell biology. Vis Neurosci 28:265–279

Ruch S, Beyer P, Ernst H, Al-Babili S (2005) Retinal biosynthesis in Eubacteria: in vitro characterization of a novel carotenoid oxygenase from Synechocystis sp. PCC6803. Mol Microbiol 55:1015–1024

Saidel WM, Fabiane RS (1998) Optomotor response of Anableps anableps depends on the field of view. Vision Res 38:2001–2006

Salvini-Plawen LV, Mayr E (1977) On the evolution of photoreceptors and eyes. J Evol Biol 10:207–263

Sandeman DC (1978) Eye-scanning during walking in the crab Leptograpsus variegatus. J Comp Physiol 124:249–257

Schaeffel F, Mathis U (1991) Underwater vision in semi-aquatic European snakes. Naturwissenschaften 78:373–375

Seki T, Isono K, Ozaki K, Tsukahara Y, Shibata-Katsuta Y, Ito M, Irie T, Katagir M (1998) The metabolic pathway of visual pigment chromophore formation in Drosophila melanogaster. All-trans (3S)-3-hydroxyretinal is formed from all-trans retinal via (3R)-3-hydroxyretinal in the dark. Eur J Biochem 257:522–527

Snyder AW (1969) Asymptotic expressions for eigenfunctions and eigenvalues of a dielelectric or optical waveguide. IEEE Trans Microw Theory Techn MIT-17:1130–1138

Stavenga DG, Foletti S, Palasantzas G, Arikawa K (2006) Light on the moth-eye corneal nipple array of butterflies. Proc Roy Soc B 273:661–667

Strod T, Arnd Z, Izhaki I, Katzir G (2004) Cormorants keep their power: visual resolution in a pursuit-diving bird under amphibious and turbid conditions. Curr Biol 14:R376–R377

Swamynathan SK, Crawford MA, Robison WG, Kanungo J, Platigorsky J (2003) Adaptive differences in the structure and macromolecular compositions of the air and water corneas of the "four-eyed" fish (Anableps anableps). FASEB J 17:1996–2005

Terakita A (2005) The opsins. Genome Biol 6:213

Thomas AT (2005) Developmental palaeobiology of trilobite eyes and its evolutionary significance. Earth Sci Rev 71:77–93

Ullrich-Lüter EM, Dupont S, Arboleda E, Hausen H, Maria Ina Arnone MI (2011) Unique system of photoreceptors in sea urchin tube feet. Proc Natl Acad Sci USA 108:8367–8372

van Hateren JH, Nilsson DE (1987) Butterfly optics exceed the theoretical limits of conventional apposition eyes. Biol Cybern 57:159–168

Varela FG, Wiitanen W (1970) The optics of the compound eye of the honeybee. J Gen Physiol 55:336–358

Vogt K (1975) Zur Optik des Flusskrebsauges. Z Naturforsch 30: 691–691

Vogt K (1977) Ray path and reflection mechanisms in crayfish eyes. Z Naturforsch 32:466–468

Vogt K (1980) Die Spiegeloptik des Flusskrebsauges. (The optical system of the crayfish eye.). J Comp Physiol A 135:1–19

von Salvini-Plawen L, Mayr E (1961). In: Hecht MK, Steere WC, Wallace B (eds), Evolutionary biology, vol. 10. Plenum Press, New York, pp 207–263

Wagner HJ, Fröhlich E, Negishi K, Collin SP (1998) The eyes of deep-sea fish II. Functional morphology of the retina. Progr Retin Eye Res 17:637–685

Warrant E, Nilsson DE (eds) (2006) Invertebrate vision. Cambridge University Press, Cambridge

Whiting MF, Bradler S, Maxwell T (2003) Loss and recovery of wings in stick insects. Nature 421:264–267

Wolken JJ, Florida RG (1969) The eye structure and the optical system in the crustacean copepod Copilia. J Cell Biol 40:279–286

Zhu XY, Park TW, Winawer J, Wallman J (2005) In a matter of minutes, the eye can know which way to grow. Invest Ophthalmol Vis Sci 46:2238–2241

The Evolution of Photosynthesis and Its Environmental Impact

16

Lars Olof Björn and Govindjee

16.1 Introduction

The earth began to form about 4.6 Ga (gigayears, billion years) ago. Thirty million years later a core had formed (Yin et al. 2002; Kleine et al. 2002), and as early as 4.4 Ga ago, there may have been a continental crust and an ocean (Wilde et al. 2001). Land probably started to emerge from the ocean 3.4 Ga ago (Flament 2013). Between 4.2 and 3.7 Ga ago, the earth was subjected to "the late heavy bombardment" (Gomes et al. 2005), which is by many thought to have wiped out any life that might have existed at that time. The oldest known fossils are 3.34 Ga old (Fliegel et al. 2010). The first organisms emerging after that cataclysm may not have been able to carry out photosynthesis, but relied on conversion of energy for their life processes by reducing carbon dioxide to methane, using hydrogen as reductant (see Thauer et al. 2008 for further information). Photosynthetic life is likely as ancient as the currently earliest fossils, probably at least 3.3–3.4 Ga (Blankenship 1992; Tice and Lowe 2004, 2006; Westall et al. 2011). The earliest photosynthesis differed from the process taking place in plants now, but there are likely to be some features that may be traced all the way back to the earliest form of photosynthesis.

L.O. Björn (✉)
School of Life Science, South China Normal University, Guangzhou, China

Department of Biology, Lund University, Lund, Sweden
e-mail: Lars_Olof.Bjorn@biol.lu.se

Govindjee
Biochemistry, Biophysics and Plant Biology, Department of Plant Biology, University of Illinois, Urbana, IL, USA
e-mail: gov@life.uiuc.edu

16.2 A Brief Review of Oxygenic Photosynthesis

Oxygenic photosynthesis consists of the oxidation of water to molecular oxygen and reduction of carbon dioxide to organic matter, primarily carbohydrate. It takes place in chloroplasts, with one set of reactions in the pigment-rich thylakoid membranes and another set of reactions in the stroma (Figs. 16.1 and 16.2).

In the thylakoid membranes the following takes place: Light is absorbed by chlorophyll *a* and other pigment molecules. The absorbed energy is transferred to reaction centers (RC). There are two kinds of reaction center-containing pigment-protein complexes, photosystem I (PSI) and photosystem II (PSII) (see Figs. 16.3 and 16.4). They can be regarded as light-powered "electron pumps" that move electrons between electron carriers, and thereby chemically stabilize the energy, originally contained in absorbed photons. These pumps are connected in series by another protein complex (the cytochrome b/f complex) and two smaller, mobile electron carriers, plastoquinone, and plastocyanin. The "electron pumps" lift electrons from an energy-poor state in water to an energy-rich state in NADPH. What remains of the two water molecules from which electrons have been removed is free oxygen (molecular oxygen, O_2) and hydrogen ions (protons). As a consequence of the electron transfer process, protons are pumped from the stroma into the interior of the thylakoids. This proton concentration difference between the inside of the thylakoid and the outside (stroma) is then used to produce energy-rich phosphate, ATP by the ATP synthase. The process outlined above is, in essence, the chemiosmotic theory of Peter Mitchell for which he received the Nobel Prize in 1978. In the stroma, reduced ferredoxin and ATP and protons are used to reduce carbon dioxide to carbohydrate. This is a very brief description of the essential steps of oxygenic photosynthesis. For further details on the photosynthetic

L.O. Björn (ed.), *Photobiology: The Science of Light and Life*,
DOI 10.1007/978-1-4939-1468-5_16,

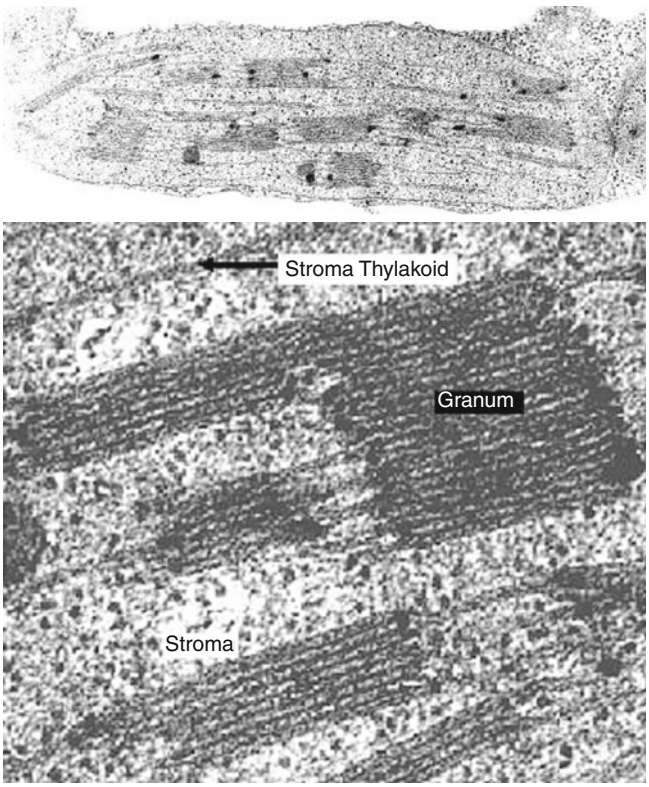

Fig. 16.1 An electron micrograph of a section of a chloroplast from tobacco leaf (*top*) and the same at a higher magnification (*bottom*) showing details of grana and thylakoids. The stroma thylakoids (*stroma lamellae*) run through the stroma between the grana (Courtesy of Professor Claes Weibull, Lund University)

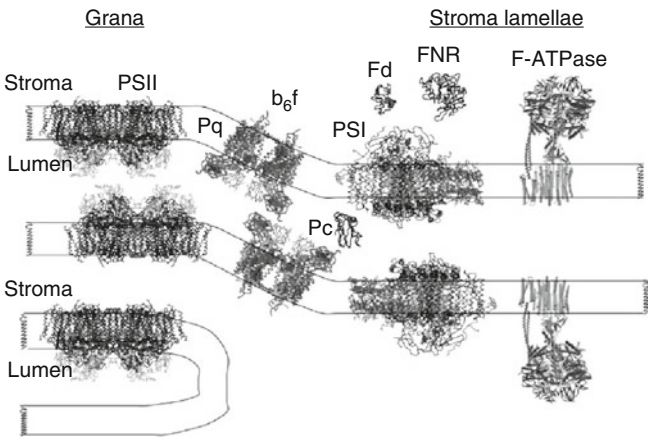

Fig. 16.2 Arrangement of molecules participating in photosynthesis in a green plant. Of the large protein complexes, photosystem II (*PSII*) is located predominantly in the grana lamellae (parts of thylakoid membranes forming grana) and photosystem I (*PSI*) and F-ATPase (ATP synthase) mainly in the stroma lamellae. In PSII, electrons are transferred from water to the cytochrome b6f complex via plastoquinone (*Pq*), and from there, they are transferred to PSI via plastocyanin (*Pc*). Electrons from PSI go via ferredoxin (*Fd*) and ferredoxin-NADP reductase (*FNR*) to NADP. The resulting NADPH is used as a reductant in carbon dioxide assimilation, which takes place in the stroma. Coupled to the electron transport is a translocation of protons from the stroma to the lumen of the thylakoid membrane. Protons flowing back to the stroma via the ATP synthase drive the synthesis of ATP, which is also used in carbon dioxide assimilation. Variations of this scheme occur, and cyanobacteria and algae on the red line of evolution differ in several respects (see Sects. 16.7 and 16.8) (From Nelson and Ben-Shem 2002)

process, see Ke (2001), Blankenship (2014), Nelson and Ben-Shem (2005), Golbeck (2006) for PSI, and Wydrzynski and Satoh (2005) and Rutherford and Faller (2003) for PSII. Oxygenic photosynthesis is carried out by plants, algae and cyanobacteria. In contrast, a large number of photosynthetic bacteria carry out anoxygenic photosynthesis where water is not oxidized, and oxygen is not evolved (see Section 16.5; for details, and chapters in Blankenship et al. 1995, and Hunter et al. 2009).

16.3 The Domains of Life

The living world is subdivided into three "domains" or main organismal groups, i.e., Archaea (formerly called archaebacteria), Bacteria (eubacteria, or just bacteria), and Eukarya (eukaryotes) (Woese 2005).

Photosynthesis is only found in the domain Bacteria (as such or when they became parts of certain Eukarya). That plants can carry out photosynthesis is because the precursors of plant cells had combined with a photosynthetic bacterium in endosymbiotic events (see Sect. 16.8)

16.4 Predecessors of the First Photosynthetic Organisms

As already mentioned, oxygenic photosynthesis can be divided into two processes: (1) oxidation of water and transport of electrons and protons in the thylakoids, with ensuing synthesis of ATP, and (2) reduction of carbon dioxide, taking place in the stroma. Of these, the reduction of carbon dioxide may be a much more ancient process than the oxidation of water. One type of light-independent carbon dioxide reduction is its reduction to methane with hydrogen as a reductant. Light-independent reduction of carbon dioxide in early organisms may be more ancient than that driven by the thylakoids (Battistuzzi et al. 2004). It is possible that one of these early light-independent carbon reduction pathways is the ancestor of the carbon fixation taking place in the stroma of chloroplasts. Plants use the enzyme RuBisCO (ribulose-1, 5-bisphosphate carboxylase/oxygenase) to bind carbon dioxide; further, some nonphotosynthetic bacteria also use this enzyme.

RuBisCO has similarities to other enzymes with other functions in bacteria, which do not fix carbon dioxide, such as 2,3-diketo-5-methylthiopentyl-1-phosphate enolase in

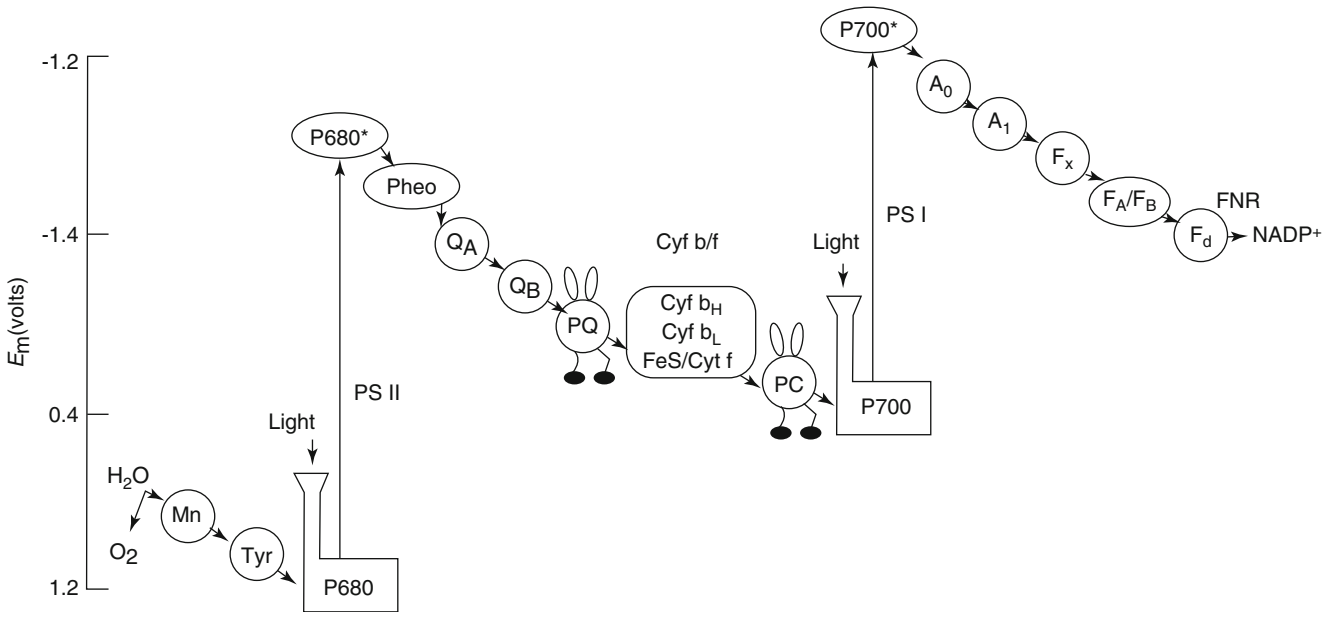

Fig. 16.3 Drawing of electron transport (the so-called Z-scheme) in oxygenic photosynthesis in plants, algae, and cyanobacteria. Light is collected by antennas pigments, symbolized as funnels and transferred to reaction center pigments (P680 in PS II and P700 in PS I, in both cases chlorophyll a). Electrons are "sucked" from water via the manganese complex (made up of 4 Mn and 1 Ca) in the water-splitting enzyme and a specific tyrosine residue in a PS II peptide. Using energy from light, photosystems "lift" the electrons to a higher energy (more negative redox potential). They leave the reaction center chlorophylls, which temporarily become positively charged, and flow over a chain of electron carriers. Of these, Pheo (pheophytin), Q_A and Q_B (both quinones), as well as A_0 (chlorophyll), A_1 (vitamin K), F_x and F_A, and F_B (iron–sulfur centers) are membrane bound, while PQ is plastoquinone that diffuses in the membrane lipid, PC is plastocyanin, a small copper protein that diffuses in the aqueous lumen space, and Fd (ferredoxin) and $NADP^+$ (nicotinamide dinucleotide phosphate) diffuse in the stroma. FNR stands for the enzyme ferredoxin-$NADP^+$ reductase. The feet and rabbit ears on PQ and PC symbolize that they are mobile. Between them is the large cytochrome b6/f complex with several electron carriers. When $NADP^+$ takes up two electrons and one proton, it becomes NADPH, which is used for carbon dioxide reduction (From Govindjee 2000). What is missing in the diagram is a bicarbonate ion, bound on a non-heme iron, between Q^A and Q^B, nd required for the reduction of Q^B. An account of the research that has led to the Z-scheme is given by Govindjee and Björn (2012)

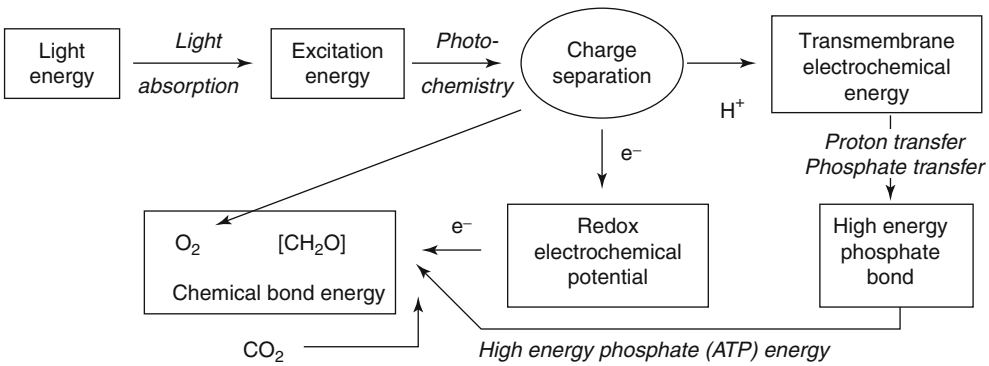

Fig. 16.4 Energy transformation in photosynthesis. Light energy absorbed by antennas pigments is transferred to reaction centers where charge separation takes place. The positive charges are transferred to water, which splits into hydrogen ions (H^+) and molecular oxygen (O_2). The nonequilibrium distribution of hydrogen ions ultimately results in energy trapped in ATP, while the energy gained by the nicotinamide adenine dinucleotide ($NADP^+$) as it is reduced to NADPH makes it possible for it to act as a reductant for carbon dioxide, aided by the energy from ATP

Bacillus subtilis (Ashida et al. 2003, 2005), and it may have evolved from a protein involved in sulfur metabolism.

When the first photosynthetic organisms appeared, they inherited many useful biochemical components from their nonphotosynthetic predecessors, including soluble components present in the chloroplast stroma and the electron transporters in the thylakoid membranes.

Iron–sulfur proteins are thought to have an ancestry that reaches back to life's beginnings, with their active centers being derived from inorganic iron sulfide. Eck and Dayhoff

(1966) suggested that the protein part of ferredoxin has evolved from a peptide with only four amino acids. Other types of electron transporters in the thylakoids with very ancient origins are quinones and cytochromes. According to one view (Schoepp-Cothenet et al. 2013) the last universal common ancestor (LUCA) was equipped with quinones and cytochromes, but reasons for a different view have also been presented (Sousa et al. 2013b; Xiong and Bauer 2002). The most important of the thylakoid pigments, chlorophyll *a*, is derived from the same biosynthetic pathway that leads to heme, the central part of cytochromes. During chlorophyll biosynthesis, there are steps that convert protochlorophyllide to chlorophyllide; interestingly, the genes for the enzyme reducing protochlorophyllide to chlorophyllide *a* in the dark (DPOR) is thought to have been derived from genes for another enzyme, nitrogenase, which is used by organisms to fix N_2 (Armstrong 1998; Chew et al. 2007).

Photosystems I and II are possibly descendants of cytochrome *b*, as structural similarities between the cytochrome b6/f-and photosystems have been presented by Xiong and Bauer (2002); further, the cytochrome complex also contains one molecule of chlorophyll *a* per monomer (Baldet al. 1992; Huang et al. 1994; Pierre et al. 1997; Stroebel et al. 2003; Kurisu et al. 2003; Dashdori et al. 2005). Another line of evidence for an ancient relationship between cytochromes and reaction centers comes from the finding that cytochromes *b* from various sources, as well as other heme compounds, can be photoreduced using light absorbed in the heme (Pierre et al. 1982; Asard et al. 1989; Gu et al. 1993; Rubinstein 1993; Zhang et al. 2005; Löwenich et al. 2008).

16.5 The First Photosynthesis

The first photosynthetic organisms did not have two types of photosystems in series, as the present-day cyanobacteria, algae, and plants do, but contained a single type of photosystem. The very first photosynthetic organisms could not oxidize water to molecular oxygen—thus far, the researchers agree, but not further. Extant photosynthesizing bacteria can, with regard to photosystems, be divided into three main groups. (1) Cyanobacteria (formerly referred to as blue-green algae) with two photosystems (PSI and PSII) connected in series, and evolving oxygen; we shall return to them later; (2) green sulfur bacteria, heliobacteria, and acidobacteria, with only a single photosystem resembling PSI of plants and cyanobacteria; (3 purple bacteria and filamentous anoxygenic phototrophs (also known as green non-sulfur bacteria), also with single photosystem resembling the PSII core in plants and cyanobacteria, but without water oxidizing machinery (see Hu et al. 2002). All photosystems, PSI-like as well as PSII-like, have important similarities so that there is no doubt that they all derive from the same ancestral photosystem.

Where is the origin of this first photosynthesizer? Nisbet et al. (1995) suggested that the ability to photosynthesize would have evolved from a system involved in orientation (e.g., phototaxis) in bacteria living deep in the sea near hydrothermal vents, which were able to sense heat radiation from the vents. Björn (1995) suggested that it would not have been possible to drive photosynthesis by the heat radiation from those vents. However, Beatty et al. (2005) showed that photoautotrophic bacteria are present in the vicinity of thermal vents. White et al. (2000, 2002a, b) have shown that the vents radiate not only heat radiation but also visible light which probably originates from oxidation of sulfide (Tapley et al. 1999).

Hirabayashi et al. (2004) have cultivated a photosynthetic bacterium, *Chlorobium phaeobacteroides*, in very weak light (less than 3 μmol photons m^{-2} s^{-1} of photosynthetically active radiation). After theoretical considerations, Raven et al. (2000) suggested that a photosynthetic organism might be able to live even with a daily average of only 4 nmol photons m^{-2} s^{-1}.

The most ancient evidence for photosynthesis, accepted by a majority of scientists, is found in a 3.416-Ga-old chert in South Africa (Tice and Lowe 2004, 2006). Even more ancient evidence for photosynthesis is present in the carbon isotope composition of a 3.8-Ga-old graphite in Greenland (Olson 2006). The organisms performing this ancient photosynthesis may have used molecular hydrogen as a reductant. Later, electron donors such as divalent iron (Fru et al. 2013) or hydrogen sulfide were utilized. Fossils attributed to photosynthetic organisms based on morphological features have been described by Awramik (1992) and Fru et al. (2013).

Green sulfur bacteria, heliobacteria, and photosynthetic acidobacteria, which have the same type of PSI-like photosynthetic reaction center, are not closely related, as judged by other characteristics. Nor all the bacteria having PSII-like photosystems are closely related. *Chloroflexus aurantiacus*, with a photosystem of type II, has about the same pigment complement as *Chlorobium tepidum* with a photosystem of type I. These apparent "inconsistencies" are explainable by "horizontal" or "lateral" gene transfer, meaning that a gene can be transferred from one unrelated organism to another (Raymond and Blankenship 2003; Raymond et al. 2003a, b). During the enormous time span of bacterial evolution, there must have been sufficient occasion for transfer of all the genes required for the formation of photosystems.

Although anoxygenic photosynthesis is thought by most to have preceded the more complicated oxygenic photosynthesis (see Björn and Govindjee 2009), there has been disagreement about whether the use of chlorophyll *a* as light-harvesting and reaction-center pigment, as is the case in most extant oxygenic organisms, or some version of bacteriochlorophyll came first. Granick (1957) reasoned that, since chlorophyll *a* precedes bacteriochlorophyll in the biosynthetic pathway of modern organisms, chloro-

phyll *a*-based photosynthesis must have preceded bacteriochlorophyll-based photosynthesis in evolution. Olson and Pierson (1987) further speculated that the first photosynthesis was mediated by a pigment, a couple of steps further back in the biosynthetic path, namely, protoporphyrin IX. The absorption coefficient of this compound at its long-wavelength absorption maximum is 7,000 M^{-1} cm^{-1} (in ethyl ether), as compared to 22,000 for protochlorophyll and 90,000 for chlorophyll *a*. Therefore it seems that the additional steps within the prolongation of the biosynthetic path way brought with it considerable improvement in absorption power. The addition of the a light-harvesting antennas to the reaction center led to more photosynthesis and, thus, growth, since more photons could be harvested (see Sect. 1.18).

Further, Olson and Pierson (1987) drew up a scheme, in which a reaction center of type 1 evolved before type 2. In a primitive organism with this single reaction center and only one type of photoreaction, a gene duplication took place which led to an organism with both type 1 and type 2 reaction centers, as in the present-day cyanobacteria. Bacteria having only type 2 reaction centers then evolved by deletion of the genes for type 1 reaction centers. With increase in sequenced bacterial genomes, it has become possible to test these ideas. Mulkidjanian and Galperin (2013) arrived at largely the same evolutionary scenario as did Olson and Pierson (1987) (Fig. 16.5), but with additional details.

A final step in the evolution of anoxygenic photosynthesis would have been the replacement of chlorophyll *a* with various forms of bacteriochlorophyll. Gupta (2013) provides evidence that genes in the terminal steps of bacteriochlorophyll (or more specifically bacteriochlorophyll *a*) synthesis are derived from the corresponding genes for chlorophyll *a* synthesis.

Chlorine reductase is found in anoxygenic photosynthetic bacteria, but not in cyanobacteria. Gupta (2013) points out that conserved insertions or deletions in the NifH, BchX, and BchL proteins provide evidence that BchX homologues originated prior to the BchL homologues and that a conserved indel in the BchL protein provides evidence that BchL homologues from Heliobacteriaceae are primitive in comparison to sequences from other phototrophs. Several researchers (including Radhey S. Gupta) have come to the conclusion that photosynthesis originated in Heliobacteriaceae; further, they find it likely that either Chloroflexi or Cyanobacteria were the earliest recipients of the genes for photosynthesis from Heliobacteriaceae. The latter might well also be a common ancestor for both Chloroflexi and Cyanobacteria. This view differs from that of Mulkidjanian et al. (2006) and Mulkidjanian and Galperin (2013), who regard photosynthesis to have originated in a hypothetical Procyanobacteria, which would have given rise to all other photosynthetic bacteria.

The scheme of Mulkidjanian and Galperin (2013) is largely in agreement with the one by Olson and Pierson (1987) focusing on the evolution of photosynthetic pigments. Olson and Pierson find it likely that the first photosynthesis pigment was protoporphyrin IX, the precursor of protochlorophyllide. The primitive reaction center would in addition have contained FeS as primary electron acceptor. A quinone could have been added later and allowed proton transport across a membrane. They assume that cytochrome would have been added later.

16.6 Photoheterotrophy in the Ocean: Light Harvesting on the Loose

16.6.1 Energy-Harvesting Systems on the Run I: Proteorhodopsin

As mentioned above, it has been difficult to define how the evolution of photosynthesis has taken place among organisms; this is because of the widespread horizontal transfer of photosynthesis genes. Two fundamentally different photoconverters are present in today's organisms. One type uses rhodopsin as the light absorbing pigment to mediate proton translocation across a membrane. The other type uses chlorophylls to convert light energy into redox energy, which is stored in electron carriers, the mean theme of this chapter.

Microbial rhodopsin was first known from halorhodopsin in *Halobacterium*. A variant of this rhodopsin, known as proteorhodopsin, is found not only among α- (Stingl et al. 2007), β-, and γ-proteobacteria, such as the classical organoheterotroph *Vibrio campbellii* (Wang et al. 2012), but also among Bacteriodetes (Gómez-Consarnau et al. 2007, 2011, González et al. 2008; Riedel et al. 2010), Archaea (Frigaard et al. 2006), and eukaryotes (Janke et al. 2013). Although proteorhodopsin is related to halorhodopsin and other "microbial" (type I) rhodopsins, it forms a very distinct clade (McCarren and DeLong 2007; Fig. 16.6).

We have little doubt that viruses harboring proteorhodopsin genes have contributed to their widespread distribution (Yutin and Koonin 2012). The proteorhodopsin-containing organisms are not able to carry out carbon dioxide assimilation, but the light-driven proton translocation across a membrane provides them, via a membrane-bound ATP-synthase, with ATP. This kind of light harvesting has been found in many taxa, despite the lower absorption cross section of proteorhodopsin as compared to absorption cross sections of (bacterio-)chlorophyll-based photosystems (Bryant and Frigaard 2006). It has been experimentally shown that rhodopsins can help bacteria grow in a low organic carbon environment to gather carbon compounds from their environment and, thus, increase growth (Gómez-Consarnau et al. 2007; Steindler et al. 2011).

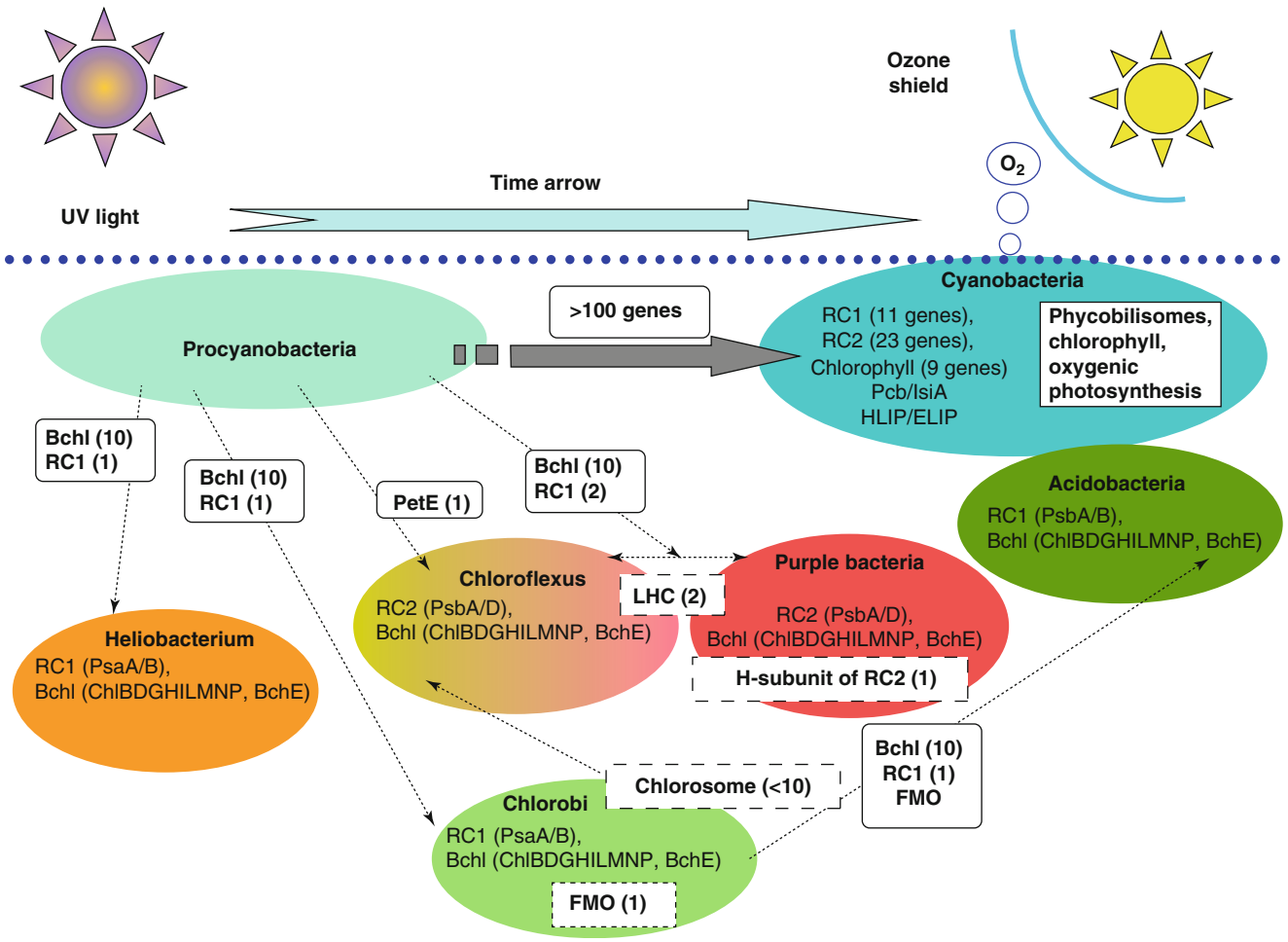

Fig. 16.5 Evolution of bacterial reaction centers according to Mulkidjanian and Galperin (2013). Gupta (2013) arrived at a slightly different relationship, with primitive photosynthesis having arisen in Heliobacteriaceae and from there spreading first to either Cyanobacteria or Chloroflexi. He regards Chlorobi as descendents of Chloroflexi, despite the differences in the reaction center type they have *BChl*, bacteriochlorophyll; *Chl*, chlorophyll; *ELIP*, early light-stress protein; *FMO*, Fenna-Matthews-Olson complex; *IsiA*, a photoprotective protein; *LHC*, light-harvesting complex: *HLIP*, high light-induced protein; *Pcb*, prochlorophyte chlorophyll binding protein; *Psa* and *Psb*, reaction center polypeptides; *RC*, reaction center; (Copyright 2013 © National Academy of Sciences USA; reproduced with permission)

16.6.2 Energy-Harvesting Systems on the Run II: Roseobacter

The other "photoconverter on the run" that deserves special mention is the chlorophyll-based photoconverter found in aerobic anoxygenic type of photosynthesis common within the "Roseobacter clade," which has many genera and is exclusively marine or hypersaline, with isolates which require salt and/or are tolerant to it (Wagner and Bibl 2006). Like the proteorhodopsin system, it produces ATP, but there is only transitory photoreduction in the system. Holert et al. (2011) have shown that in *Dinoroseobacter shibae*, light-driven reactions contribute to chemiosmotic energy conservation. The genes for this kind of "photosynthesis" are transmitted between bacteria by plasmids (Petersen et al. 2012, 2013; Yutin and Koonin 2012). Not all members of the *Roseobacter* clade carry out light harvesting, but those who do are found in many marine habitats, both as free-living bacteria and as symbionts in dinoflagellates, and other organisms (Allgaier et al. 2003).

Kirchman and Hanson (2013) have compared the energy economy of organisms for harvesting energy, those that use proteorhodopsin, with those that use a chlorophyll-type photosystem, as in the *Roseobacter* (Fig. 16.7); further, Kirshman and Hansen found that the *Roseobacter* system is more efficient, even after they had taken into account the lower maintenance cost for the proteorhodopsin system. This is simply because *Roseobacter* has a large antennas system per reaction center. A higher ratio of light-harvesting pigments to protein gives a better energy-gathering capability with respect to the maintenance cost.

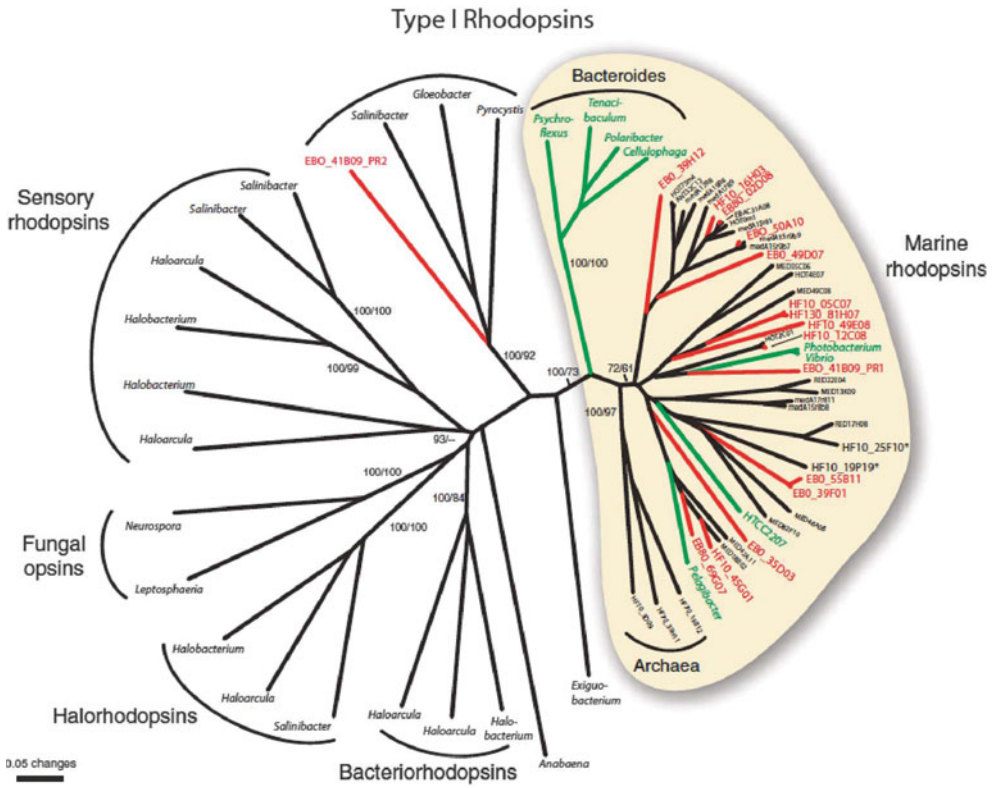

Fig. 16.6 Phylogenetic relationship among "microbial" (type I) rhodopsins. What is designated above as "marine rhodopsins" is what is usually referred to as proteorhodopsins (from McCarren and DeLong 2007)

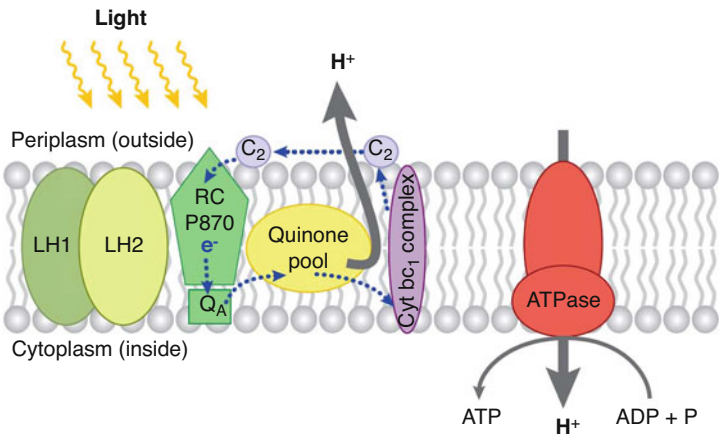

Fig. 16.7 The energy harvesting system of Roseobacter and related bacteria (from Wagner-Döbler and Bibl 2006)

16.7 Appearance of Oxygenic Photosynthesis

In contrast to cyanobacteria that have PSII, anoxygenic photosynthetic bacteria lack the water-oxidizing (oxygen-evolving) complex, even if they possess a photosystem of type II. The type II photosystem of these bacteria differs also in some other respects from the PSII of plants, algae, and cyanobacteria. The oxygenic PSII-type reaction center contains six separated pigment molecules instead of the "special pair"-type chlorophyll molecules, arranged as a tightly coupled pair in most anoxygenic autotrophs and in PSI. The "special pair" arrangement gives a lower-lying first excited state than a single molecule would have. As long as not very large quanta are needed for the electron transfer, this is an advantage since it allows the use of a wider part of the daylight spectrum. For the stepwise oxidation of water, more energy is required than for the electron transport processes mediated by most anoxygenic photosystems. Rutherford and Faller (2003) postulated that this is the main reason for the special chlorophyll characteristics of PSII

compared to special pair bacteriochlorophyll arrangement found in anoxygenic photosystems.

Dismukes et al. (2001) have speculated on how the water-oxidizing system could have evolved via a bicarbonate-oxidizing and oxygen-evolving intermediate stage. The interesting finding of Warburg et al. (1965) that oxygen evolution is stimulated by carbon dioxide may have been the first indication of this concept. Clausen et al. (2005a, b) have shown that *free* carbon dioxide is not an intermediate in oxygen evolution. Bicarbonate has been shown to function on both the electron acceptor and donor sides of PS II (see reviews by Van Rensen et al. 1999; Shevela et al. 2012). Further, in the crystal structure of PS II, Ferreira et al. (2004) have modeled one bicarbonate anion near the nonheme iron on the acceptor side and another one on the electron donor side. However, Umena et al. (2011) do not see any bound bicarbonate on the donor side. This does not mean that there is no effect of bicarbonate on the donor side of PSII; it may be involved in protonation reactions during water oxidation, without it being bound on that side (see Shevela et al. 2013).

Johnson et al. (2013) provide geologic indications that manganese may have served as an electron donor for photosynthesis before a system for its re-reduction by water evolved. By isotopic analysis of drill cores, they established that the oxidative branch of the Mn cycle predates rise of oxygen. Blankenship and Hartman (1998) point to hydrogen peroxide as a possible reductant before water.

There are different opinions about how organisms evolved from having one photosystem to two photosystems as in cyanobacteria, algae, and plants. One can imagine that from the first photosynthetic organism evolution took place along two lines, but with a single photosystem in each case. One line led to bacteria having photosystems of type I and the other to bacteria with type II photosystem. The two kinds of bacteria then entered into a symbiosis, which became more and more intimate, until the result was an integrated organism, which evolved into the first cyanobacterium. (We note, however, that this is not enough without the origin of the oxygen evolving complex, which by itself remains quite a mystery.) Another possibility is that gene transfer took place from one organism to another without complete fusion of the two lines of evolution. There is also a third possibility that was suggested by Allen (2005); we describe it below.

Much of the evidence for the views of how the early evolution of photosynthesis took place is based on comparison between extant organisms. But there is also reliable geological evidence for it. Morphological features of bacteria preserved in fossils do not give much guidance in clarifying the nature of the first photosynthetic bacteria, except that the occurrence of heterocyst-like structures strengthens the view that both cyanobacteria and an oxygen-containing atmosphere are of great antiquity (Tomitani et al. 2006). There are also chemical and physical characteristics of fossils to support this view, even if their interpretation is often debated. Perhaps, 2-α-methyl hopane is a reliable signature of the presence of cyanobacteria (Summons et al. 1999); it has been indeed found in 2.7-Ga-old rocks (Brocks et al. 2003). However, similar compounds have also been traced to be related to anaerobic bacteria (Härtner et al. 2005) and, in particular, those carrying out photosynthesis with Fe^{2+} as electron donor (Eickhoff et al. 2013). One opinion is that the oldest proof for the existence of cyanobacteria dates to about 2.15 Ga ago (Hofmann 1976; Tomitani et al. 2006; Rasmussen et al. 2008), but oxygen production had taken place earlier than that (Crowe et al. 2013). Sometimes a certain carbon isotope ratio has been seen as a sign that the carbon has been assimilated by RuBisCO or to indicate the existence of a certain kind of assimilating organism. Farquhar et al. (2011) provide a thorough and critical discussion of various proxies for the oxygenation of the oceans and the atmosphere during the Great Oxygenation Event (2.45–2.32 Ga ago) and the first oxygenic photosynthesis taking place about 200 Ma before that. Anbar et al. (2007) present evidence for "a whiff of oxygen" 2.501 ± 0.008 Ga ago. Crowe et al. (2013) argue for at least transient oxygenation already about 3 Ga ago.

Banded iron formations (BIFs) have been interpreted in many different ways (see Krapež et al. 2003, for further information). It is thought that the formation of at least some of them has been mediated by photosynthetic bacteria, which have oxidized divalent to trivalent iron, instead of oxidizing water as cyanobacteria do (Kappler et al. 2005).

The type of photosynthesis carried out by cyanobacteria requires a very complicated machinery with cooperation between the two photosystems in series and an enzyme which collects four oxidation equivalents for the 4-step oxidation of water. Many researchers believe that the evolution of this complex machinery from the first primitive chlorophyll-based photoconverter(s) required a vast expanse of time. Contrary to this view, Rosing and Frei (2004) have arrived at the conclusion that such photosynthesis took place already 3.7 Ga ago. This opinion rests on the observation of changing ratios between thorium and uranium in old sediments. Under reducing conditions both elements are insoluble, and therefore, the ratio between their concentrations should not change during sedimentation. But in fact, the ratio between the concentrations has changed, and, thus, some kind of fractionation must have taken place. This can happen in the presence of oxygen, when uranium is oxidized to soluble uranyl complexes. Thorium, on the contrary, remains insoluble under such conditions. Thus, a changed ratio is taken as evidence for the presence of oxygen 3.7 Ga ago. However, objections have been voiced for interpreting geological features in terms of the involvement of biological activity (e.g., Brasier et al. 2005; Moorbath 2005).

Small amount of hydrogen peroxide could have formed abiotically in the Archaean age by the action of ultraviolet radiation on pyrite, and there have been speculations that

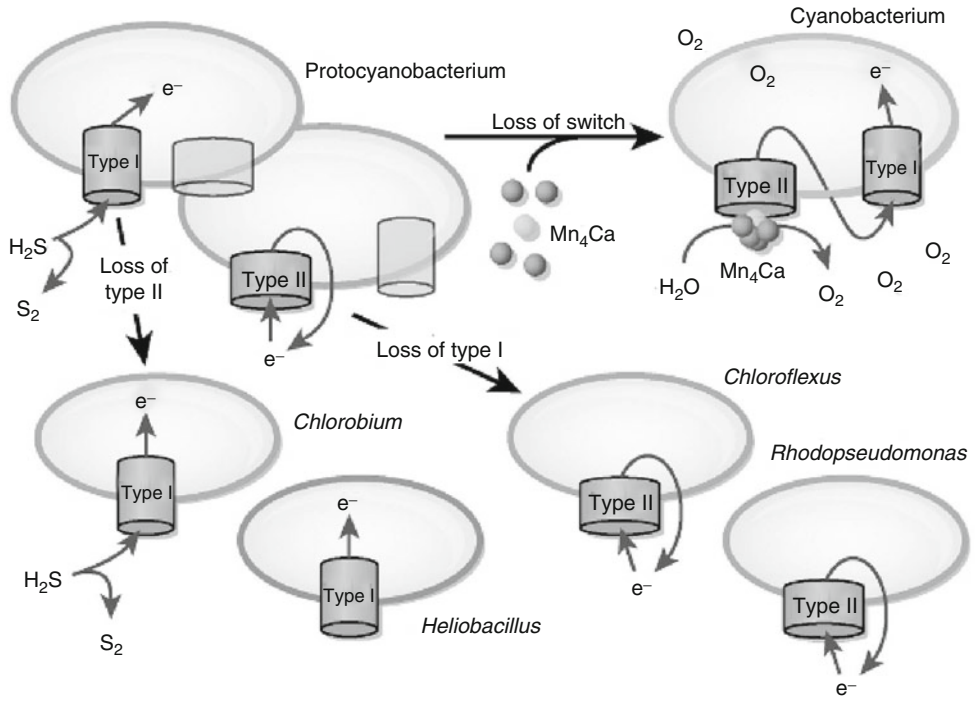

Fig. 16.8 An early photosynthesizer having two photosystems and a switch to select expression of the gene for one or the other (*upper left*) could, during evolution, lose one or the other of the genes and turn into one of several types of nonoxygenic photosynthetic bacteria (either as *Chlorobium* or *Heliobacillus* with a type I photosystem or as *Chloroflexus* or *Rhodopseudomonas* with a type II photosystem). Alternatively it could, under appropriate environmental conditions, lose the switch and evolve into an organism constitutively equipped with two photosystems and then evolve into a cyanobacterium with oxygenic photosynthesis (from Allen and Martin 2007; reprinted by permission from Macmillan Publishers Ltd: *Nature* 445, 610–612, copyright 2007)

oxygenic photosynthesis evolved from a pathway for detoxification of hydrogen peroxide (Borda et al. 2001) (see also Blankenship and Hartman 1998 and references therein; Rutherford and Nitschke 1996; Bader 1994; Samuilov et al. 2001 concerning the possibility of peroxide as an electron donor). In our opinion, the structure of the oxygen-evolving complex, which has little similarity to other manganese-containing hydrogen peroxide utilizing enzymes with known structure, does not support such a theory.

The structure of the oxygen-evolving complex (Yano et al. 2006; Umena et al. 2011) has similarities to some manganese minerals; it is possible that it may have inherited its structure from these compounds (Sauer and Yachandra 2002). Photochemical oxidation of manganese driven by ultraviolet radiation may have taken place early in the earth's history and could have been the starting point for the evolution of the oxygen-evolving mechanism in oxygenic photosynthesis (Anbar and Holland 1992; Allen and Martin 2007). Related to this is the finding that UV inhibits PSII in present-day organisms partly by UV absorption by manganese (Hakala et al. 2005, 2006).

According to a hypothesis of Allen (2005) and elaborated by Allen and Martin (2007) and Sousa et al. (2013a, b), organisms having two types of photosystems are older than oxygenic photosynthesis. Arguments have been made that the ancestral photosystem was probably more similar to PSI than to PSII (Baymann et al. 2001; Mulkidjanian et al. 2006). After gene duplication of this PSI-like photosystem, a PSII-like photosystem evolved within the same organism that had no oxygen evolution capability (Fig. 16.8). The evolution pressure for the change in properties of the new, PSII-like, photosystem could have been the changing environmental conditions, in particular changing redox conditions. Because of the variability of the environment, it would have been advantageous for the organism to keep genes for both photosystems, and a regulatory switch must have evolved that made it possible for the organism to transcribe the gene that was most appropriate for the changed environment. One scenario for the acquisition of oxygen-evolving capacity is that the PSII-like system evolved toward a state where it could connect to a manganese compound that was already able to be photooxidized by ultraviolet radiation, but could from now on be oxidized through PSII by light of longer wavelengths. The mechanism for switching between transcription of one or the other photosystem gene then became superfluous and disappeared. The first cyanobacterium had evolved.

Evolution of a bacterial type 2 photosystem required, in addition to the addition of an oxygen evolving center, also an adaptation that would protect the system from the damaging effects of oxygen. The two parts of the originally homodimeric photosystem became gradually more differentiated. The electron transfer chain became concentrated on one of

the monomers, and mechanisms developed for rapid exchange of the easily damaged peptide that supported it.

Once the cyanobacteria emerged and started to produce oxygen, several hundred million years elapsed before oxygen started to accumulate in the atmosphere. The earliest evidence that water was used as the hydrogen source in photosynthesis is found in 2.97-Ga (billion years)-old South African rocks (Crowe et al. 2013), while the so-called Great Oxidation Event (GOE) took place 2.45–3.32 Ga ago (Bekker et al. 2004; Kump 2008; Sessions et al. 2009). There are several explanations for the lag in oxygenation of the atmosphere. One is that that there were many reducing substances (hydrogen, divalent iron, reduced sulfur, probably also methane) that had to be oxidized first (Zahnle et al. 2013). Holland (2009) points to a probable change in volcanic gases that would have favored oxygen accumulation at this time and reproduction of cyanobacteria might also have been hampered by ultraviolet radiation, since no protection by ozone would have existed before oxygenation of the atmosphere. A prerequisite for oxygen accumulation was prevention, by burial, of reoxidation of assimilated carbon (Karhu and Holland 1996; Fennel et al. 2005). From time to time reoxidation seems to have occurred (Kump et al. 2011) resulting in fluctuations in the oxygen content (Canfield et al. 2013; Partin et al. 2013). It took an even longer time before the deep strata of the ocean became oxidized, and this led to chemical problems, which delayed full oxygenation (see below). But once the oxygen started to accumulate, it poisoned many life-forms. Never before or after has any other form of life dominated the planet so completely for such a long time as cyanobacteria did—about a billion years. This domination is also due to the offspring of cyanobacteria that are present as chloroplasts in plants and algae.

16.8 From Cyanobacteria to Chloroplasts

> Let us imagine a palm tree, growing peacefully near a spring, and a lion hiding in the bush nearby, all of its muscles taut, with blood thirsty eyes, prepared to jump upon an antelope and to strangle it. The symbiotic theory, and it alone, lays bare the deepest mysteries of this scene, unravels and illuminates the fundamental principle that could bring forth two such utterly different entities as a palm tree and a lion. The palm behaves so peacefully, so passively, because it is a symbiosis, because it contains a plethora of little workers, green slaves (chromatophores) that work for it and nourish it. The lion must nourish itself. Let us imagine each cell of the lion filled with chromatophores, and I have no doubt that it would immediately lie down peacefully next to the palm, feeling full, or needing at most some water with mineral salts.
>
> Constantin Sergeevich Mereschkowsky (1905) in Über Natur und Ursprung der Chromatophoren im Pflanzenreiche. Biol. Centralbl. 25, 593–604. Annotated English translation by W. Martin and K.V. Kowallik (1999) Eur. J. Phycol. 34, 287–295

The theory that chloroplasts are derived from cyanobacteria, which were long ago taken up by nonphotosynthetic organisms, is more than 100 years old. However, the overwhelming support that this theory is correct has been obtained from molecular biology. By comparison of DNA sequences, the cyanobacterial ancestry of chloroplasts has been established, just as it is now certain that mitochondria are descendants of another bacterial clade.

Among chloroplasts, there are, in addition to a couple of smaller branches, two main developmental lines. According to Rogers et al. (2007) we have the "green line" (in green algae and plants) and the "red line" (in red algae and most other algae). Even if some researchers still remain open to the idea that these two lines started with two separate endosymbiotic events, the following view prevails: All chloroplasts are derived from one cyanobacterium that was incorporated in one eukaryotic cell. It is a little surprising that it is so, since we have so many other examples of very intimate symbiotic relationships between a number of algae and a number of other organisms. For example, a new type of chloroplast that is the result of a more recent endosymbiotic event has been observed: Marin et al. (2005) have found an amoeba containing a plastid with a different cyanobacterial origin; see also Rogers et al. (2007). However, this does not detract from the fact that chloroplasts of all major groups had been derived from a single endosymbiotic event. The chloroplasts of green algae, glaucophytes, land plants, and red algae are directly derived in such a way, while other chloroplasts in the red line are derived by secondary endosymbiosis, in which certain organisms engulfed red algae. Chloroplasts of some groups, especially some dinoflagellates, have an even more complicated evolutionary history (see, e.g., Stoebe and Maier 2002; Bhattcharaya et al. 2003).

Many cyanobacteria have phycoerythrin (red) and phycocyanin (blue), and a small amount of another protein, allophycocyanin (also blue) as light-collecting pigments. They are assembled into complexes known as phycobilisomes, which are located on the external side of the thylakoid membranes which house the two photosystems (PSI and PSII). The most primitive cyanobacteria do not have any thylakoids, but carry out photosynthesis by their outer cell membrane, but they do have phycobilisomes (Gutiérrez-Cirlos et al. 2006). Red algae have the same pigment arrangement. One type of cyanobacterium, referred to as prochlorophytes (after *Prochloron*, the genus first discovered), does not use phycocyanin and phycoerythrin as its main light-harvesting system–sometimes not at all, but instead chlorophyll *a* and chlorophyll *b*, as green algae and plants do.

It was once thought that the green and the red evolutionary lines each arose from two different types of cyanobacteria. Later, a cyanobacterium (*Prochlorococcus marinus*) was discovered which utilizes chlorophyll *a* and chlorophyll *b*,

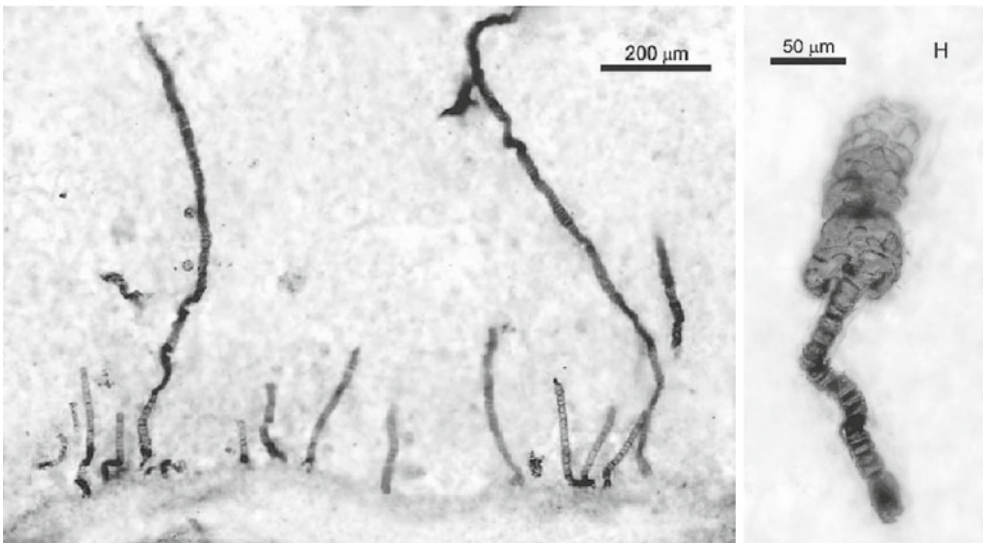

Fig. 16.9 1,200-Ma-old fossils of the red alga Bangiomorpha pubescens (from Butterfield 2000)

and phycobilins for light harvesting (Hess et al. 1996). Most researchers, therefore, now believe that the first chloroplast was derived from a cyanobacterium having both phycobilisomes and chlorophyll *b*. In each of the developmental lines, one of the pigment sets would have been lost later. The common origin of the chloroplasts in both lines is strengthened by the fact that the protein import machinery is very similar. These import systems must have evolved during early stages of interfacing the incorporated cyanobacteria with its host, Also genes transferred from the cyanobacteria to the nucleus of their host on the "red line" and "green line" are in general so similar that it is difficult to argue that they are the consequence of endosymbiosis in very different organisms.

Fossils of red algae have been found which date back to 1.2 Ga (Butterfield 2000; Fig. 16.9). These are the oldest organisms for which one has been able to infer sexuality. Other algae on the red line, for instance, cryptophytes, diatoms, brown algae, and yellow-green algae, have evolved by uptake of red algae into a nonphotosynthetic organism (or possibly already photosynthetic organism that had lost its original photosystems), and also this may have taken place only once. One reason to believe that these different algal chloroplasts have resulted from a single secondary endosymbiotic event is the surprising fact that they all have the same type of phosphoribulokinase (an enzyme of the Calvin–Benson–cycle) as organisms on the green line of chloroplast evolution, a type very different from the type present in red algae (Petersen et al. 2006). The most probable interpretation of this is that soon after the secondary endosymbiotic event, a lateral gene transfer from the green line took place, and the phosphoribulokinase from the red alga was lost. In a later publication, some of the same authors present evidence that cryptophytes, haptophytes, and stramenopiles have acquired their chloroplasts through separate secondary symbiotic events (Baurain et al. 2010).

Plastocyanin, a copper protein that is an electron carrier in the chloroplast, is missing in chloroplasts of the entire red line of evolution (and also in some cyanobacteria); here, electrons from cytochrome b6/f complex are, instead, carried to PSI by a small soluble cytochrome, cytochrome c6 (Raven et al. 1999). The use of plastocyanin as an electron carrier was probably established after the emergence of oxygenic photosynthesis, as copper may have been tied up in insoluble sulfide during a period of Earth's history (see below). On the other hand, iron is less accessible now than it was before the oxygenation of the atmosphere.

16.9 Evolution of Photosynthetic Pigments and Chloroplast Structure

Forms of chlorophyll typical for extant photosynthetic bacteria, which do not evolve oxygen, are collectively referred to as bacteriochlorophyll. Chlorophyll *a* is a biochemical precursor to these chlorophyll forms (Chew and Bryant 2007; Masuda and Fujita 2008). For this reason, Granick (1957) postulated that bacteria, with bacteriochlorophyll as photosynthetic pigment, have evolved from those which had chlorophyll *a*. But those present-day bacteria which have bacteriochlorophyll (and only one photosystem) seem to be more primitive and carry out a simpler kind of photosynthesis than cyanobacteria, which are the only extant bacteria with chlorophyll *a*. The solution to this apparent paradox

could be that there had existed now extinct nonoxygenic organisms having only one photosystem, with chlorophyll *a*.

The reasons that chlorophyll is a suitable pigment for photosynthesis are discussed in Chap. 9, Sect. 9.2 and by Kiang et al. (2007) from a spectral perspective, and by Mauzerall (1976) from a chemical perspective, while Björn et al. (2009a) have traced the possible reasons for the uniqueness of Chl *a* for its use in the primary photochemistry. This is due to its physicochemical properties as affected by its protein environment; Chl *a* in vivo is capable of generating a radical cation or a radical anion or remaining completely redox silent, all depending on the protein environment. Many authors, e.g., Björn et al. (2009b) have speculated about what kind of photosynthesis might take place on other planets.

When cyanobacteria had turned into chloroplasts, further evolution along the "green" line (green algae and plants) began to differ from that along the "red" line (red algae, diatoms, and brown algae). We know that cyanobacteria were, and are, equipped with very sophisticated light-collecting antennas in the form of phycobilisomes. These can be regarded as a kind of energy transformer, which collects all kinds of light and adapts the excitation energy so the quanta correspond to the energy levels of chlorophyll. The red algae inherited these structures rather unchanged. Cryptophytes have the same kinds of red and blue pigments arranged in a slightly different way. But why have these exquisite light transformers disappeared from the rest of the "red" line and never appeared on the line leading to land plants?

We probably have a good explanation for this now. We shall recount here in essence an explanation given by Anderson (1999) that relies on different light environments to which the organisms have adapted. In order to streamline our discussion, we shall limit ourselves to a comparison between red algae and land plants. Red algae live in water, often deeper than other algae. The light reaching them has been filtered through water, which absorbs long-wavelength light more strongly than other visible (and photosynthetically active) light. Therefore, a deficiency in photons absorbed by PSI relative to PSII could easily develop. To avoid this, it is suggested that some excitation energy is transferred from PSII to PSI. Red algae collect energy mainly via their phycobilisomes, and this energy can be used both by PS II and by PS I.

For land plants, the situation is different. The first land plants were small beach organisms living without competition from larger plants, exposed to full sunlight; their forerunners, the green algae, lived in very exposed habitats. Therefore, the challenge for the first land plants was not lack of light energy, and thus, they did not have much use for phycobilisomes. With time, plants developed a complex light-harvesting system, and the chloroplast became more and more shaded by other chloroplasts. The light hitting the chloroplast became, during the evolution of plants and ecosystems, more and more depleted in shortwave light, while the long-wave light (the long-wave edge of the chlorophyll absorption spectrum) was not attenuated to the same extent. The spectral situation was opposite to that for chloroplasts found in red algae. Now the imbalance between the photosystems could not be adjusted by energy transfer from PSII to PSI, since PSII had enough energy for its own needs only. Rather PSI and PSII had to be separated to prevent excess energy transfer from PSII to PSI; otherwise, PSII would be even more depleted of energy. Evolution has succeeded in this by the development of grana in the chloroplasts of land plants (see Figs. 16.1 and 16.2).

Grana are regions in the chloroplasts where thylakoid membranes are closely stacked on top of one another and are enriched in PSII. The stacking of membranes and the absence of PSI gives room for larger pigment antennas, not in the form of phycobilisomes, but in the form of chlorophyll *a* and chlorophyll *b*-containing light-harvesting complexes located within the thylakoid membrane. PSI is located in the less stacked membrane regions. This is advantageous because PSI delivers reducing equivalents via ferredoxin to NADP, which is then used for the reduction of carbon dioxide in the stroma.

The structure of chloroplasts, and in particular the proximity of membranes to one other, is not static, but it constantly adjusts to the available light. During evolution more and more sophisticated regulation systems have appeared, as have various mechanisms for protection against excess light (Demmig-Adams et al. 2006). One of the most important of these mechanisms is the so-called xanthophyll cycle, giving protection against strong light while allowing efficient use of weak light. Remarkably, it exists in essentially the same form while exploiting different kinds of xanthophylls, both in the "red" and the "green" line of evolution. It is left for future researchers to find out whether this is an example of convergent evolution or due to common descent. The reader is referred to Demmig-Adams, Adams, and Mattoo (Eds) (2006) and Demmig-Adams, Garab, Adams, and Govindjee (Eds) (2014) for details about the topic of photoprotection.

Yoshi (2006) has traced the evolution of carotenoids on the "green line." The most primitive living algae on this line have carotenoids that absorb maximally in the violet part of the spectrum, while more modern types have carotenoids with absorption peaks at longer wavelengths. Y. Yoshi speculates that this may reflect the high ultraviolet radiation conditions under which the algae have evolved. Those ancient algae living before a protecting ozone layer had developed (and preserved as "living fossils" today) would have had to live at a depth where they were protected from ultraviolet radiation. The spectrum of light is filtered by water to enhance the shortwave part of photosynthetically active radiation. More modern algae would have evolved near the water surface, in a light regime that is enriched with longer wavelength photons. A difficulty with Yoshi's interpretation is that an ozone layer most likely evolved long before the appearance of eukaryotic algae.

16.10 Many Systems for the Assimilation of Carbon Dioxide Have Been Tried in the Course of Evolution

Assimilation of carbon dioxide is not necessarily coupled to photosynthesis. The ability to take up carbon dioxide and assimilate carbon into organic substance is older than the ability to photosynthesize. It takes place in both Archaea and Bacteria. This ability has evolved either before the two domains had separated or one of these groups of organisms has acquired it from the other group by horizontal (lateral) gene transfer. Since many enzymes are involved, the former possibility is the most likely one.

Apart from the first two enzymes, enzymes listed in Table 16.1 and their assimilation pathways (Fig. 16.10) are present only in Bacteria and Archaea. But the typical carbon-binding enzyme of plants, algae and cyanobacteria, RuBisCO, occurs also in some Archaea, even though the complete Calvin–Benson cycle has not been demonstrated in them.

The first alternative to the Calvin–Benson cycle detected was a cycle discovered by Evans et al. (1966) (see also Buchanan and Arnon 1990). The acetyl-CoA pathway is present in some acetate-forming bacteria, some sulfate-reducing bacteria, and some hydrogen-oxidizing Archaea.

The 3-hydroxypropionate pathway is present in green nonsulfur bacteria, some hydrogen-oxidizing bacteria, and some sulfur-reducing Archaea. Thus, every type of carbon dioxide assimilation occurs in taxonomically quite different types of microorganisms. Selesi et al. (2005) have detected a large set of RuBisCO types in soil microorganisms, of which only a minor part is derived from photosynthetic organisms.

It is clear that RuBisCO is a very ancient enzyme, which was "designed" under conditions quite different from the present ones. The most important differences are that oxygen was absent from the primordial environment and the concentration of carbon dioxide was much higher than in the contemporary environment. Therefore, the properties of RuBisCO are not optimal for the present environment. It binds carbon dioxide only weakly (i.e., it has a low affinity and a high Michaelis constant for carbon dioxide). This was not a problem as long as the concentration of carbon dioxide was very high. RuBisCO reacts also with oxygen, in addition to carbon dioxide, and when this happens, a product, phosphoglycolic acid, is formed. There are indications that the ability to metabolize phosphoglycolic acid evolved very early, even before oxygen had accumulated outside the cyanobacterial cell (Eisenhut et al. 2008).

To compensate for the poor properties of RuBisCO, different photosynthesizers have evolved different strategies. A common one is to produce large amounts of the enzyme to compensate for its slowness, and this has made it the most ubiquitous protein molecule on earth. Various systems for concentrating carbon dioxide in proximity to the RuBisCO have also evolved, so carbon dioxide can compete efficiently with oxygen for the common binding site. There is also the view that photorespiration is essential for plants that have evolved it. Carbon concentrating mechanisms of cyanobacteria and algae have been described by Badger and Price (2003); Giordano et al. (2005); and Keeley and Rundel (2003). Here we shall limit ourselves to alternative pathways that rely on a spatial and temporal separation of light energy conversion and carbon fixation that provide advantages, the so-called C4 metabolism and CAM.

Table 16.1 Pathways and Enzymes for CO_2 Assimilation

CO_2-binding enzyme	Pathway for CO_2 assimilation
Ribulose-1,5-bisphosphate-carboxylase-oxygenase (RuBisCO, rubisco)	Calvin–Benson cycle
Phosphoenol pyruvate carboxylase (PEPC)	C4 and CAM cycles
Formate dehydrogenase	Acetyl-CoA pathway
Carbon monoxide dehydrogenase	Acetyl-CoA pathway
Pyruvate:ferredoxin oxidoreductase	Arnon–Buchanan cycle (reductive TCA cycle)
2-Oxoglutarate: ferredoxin oxidoreductase	Arnon–Buchanan cycle
Isocitrate dehydrogenase	Arnon–Buchanan cycle
Pyruvate carboxylase	Arnon–Buchanan cycle
Acetyl-CoA carboxylase	3-Hydroxypropionate cycle
Propionyl-CoA carboxylase	3-Hydroxypropionate cycle

16.11 C4 Metabolism

About half of this planet's photosynthetic production takes place on land and the other half in water (Geider et al. 2001; Falkowski and Raven 2007) According to Sage (2004) the mere 3 % of the terrestrial plants having C4 metabolism carry out about half of CO_2 fixation on land. C4 metabolism is present in about 7,500 species of seed plants (3 % of the species of terrestrial plants), of which 4,500 are grasses, 1,500 sedges, and 1,200 dicots (Sage 2005). C4 plants occur primarily in warm and dry countries and among epiphytes. It is well-known that C4 metabolism has evolved many times in different locations.

C4 plants have evolved at least 45 times in 19 families of higher plants (Sage 2004). From this we understand that there has been a very strong evolution pressure toward this kind of metabolism. An important component in this evolution pressure has been the decrease in carbon dioxide pressure that took place between 30 and 40 Ma ago (Retallack 2002). Another component has been the drying of the environment that was an even more recent event (Osborne and Beerling 2006; Strömberg and McInerney 2011). C4 metabolism (Fig. 16.11) became a significant component of the carbon cycle as recently as 10 Ma ago.

In C4 metabolism carbon dioxide is not initially bound to RuBisCO, as is the case in C3 plants. Instead bicarbonate ions (formed from carbon dioxide and water with the aid of

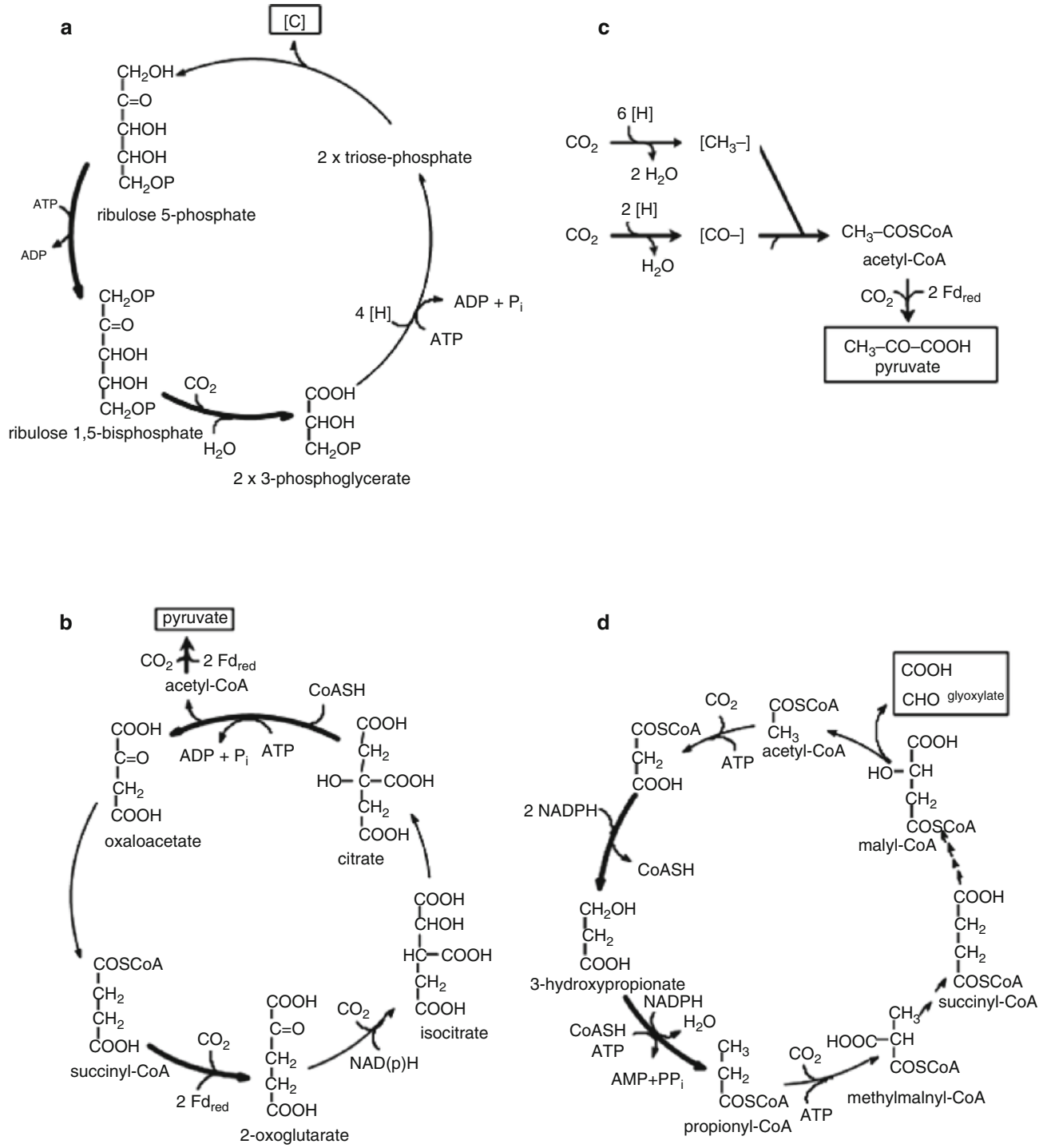

Fig. 16.10 Metabolic cycles for assimilation of carbon dioxide present in various prokaryotes: (**a**) the Calvin–Benson cycle, (**b**) the reductive TCA (TriCarboxylic Acid) cycle (Arnon–Buchanan cycle), (**c**) the reductive acetyl-CoA pathway, and (**d**) the 3-hydroxpropionate cycle. Of these only the Calvin–Benson cycle is present in photosynthetic eukaryotes (cyanobacteria, algae, and plants). C: assimilated carbon, [H]: reducing equivalents, Fdred: reduced ferredoxin, P or P in a circle: phosphate groups, CH_3–: enzyme-bound methyl group, CO–: enzyme-bound carbon monoxide (from Hügler et al. 2003)

the enzyme carbonic anhydrase) is bound by the enzyme phosphoenolpyruvate carboxylase (PEPC; see Table 16.1 and Fig. 16.11) and when it combines with phosphoenol-pyruvate (PEP) malate is formed. Malate has four carbon atoms, hence the designation C4 metabolism. In C3 metabolism, the first stable product is 3-phosphoglyceric acid, which has three carbon atoms. C4 metabolism is more efficient at a low concentrations of carbon dioxide, because

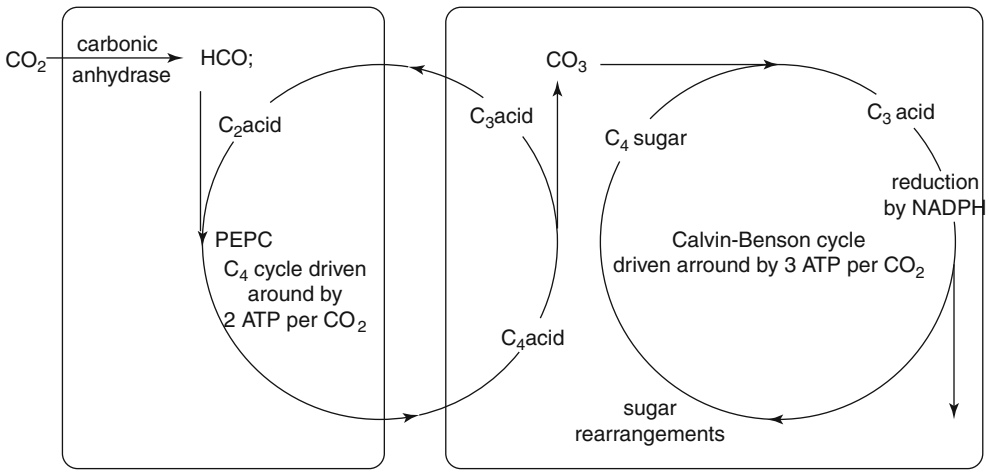

Fig. 16.11 Carbon dioxide assimilation in C4 plants. The first cycle (see the *left box*) concentrates carbon dioxide at the rubisco, and the assimilation itself proceeds as in C3 plants (see the *right box*)

PEPC binds bicarbonate very tightly and lowers the relative binding of oxygen.

C4 carbon fixation is also more efficient under dry conditions since plants can conserve water by keeping their stomata only slightly open. This causes a lowering of the inner carbon dioxide concentration in the plants, but this can be compensated by the increased CO_2 utilization efficiency of C4 metabolism. C4 metabolism is also more efficient than C3 metabolism at high temperatures. In C3 plants, photorespiration, due to competition by oxygen for RuBisCO makes carbon dioxide uptake inefficient at high temperatures. Under other conditions, like low light, C4 metabolism is less efficient than C3 metabolism, because it uses up more ATP (5 molecules per molecule of CO_2 assimilated, compared to 3 for C3 plants).

One fascinating fact about C4 metabolism is that it has evolved within a relatively short time and independently within many groups of plants. C4 metabolism occurs primarily among seed plants, but has been found also elsewhere, even among diatoms (Reinfelder et al. 2000, 2004).

Since oxygen concentration during the Carboniferous (370–300 Ma ago) was even higher and the carbon dioxide concentration even lower than today (Fig. 12.9), one would have expected the C4 metabolism to have evolved by then. But all the plant fossils from that time for which the isotopic composition of the carbon has been investigated have a C3-like signature, $\partial^{13}C \approx -20$ ‰ (Beerling et al. 2002; Bocherens et al. 1993).

One enigmatic circumstance is that CAM plants which also use PEPC (phosphoenol pyruvate carboxylase, discussed below) were present earlier. So why do we have only C3-type isotope discrimination from that time? Perhaps CAM plants did not contribute much to biomass production. The corresponding $\partial^{13}C$ value for C4 plants is about −13 ‰ (e.g., Hattersley 1982). There is some suspicion that some C4 plants could have evolved during the Carboniferous, but remained low in number (Osborne and Beerling 2006). A possible reason that more C4 plants did not evolve during this period is that the temperature was low.

We refer to Andrew Benson (pp. 793–813) and James A. Bassham (pp. 815–832) for the stories behind the discovery of the Calvin–Benson pathway and to M. D. Hatch (pp. 875–880) for C4 metabolism (Govindjee et al. 2005). For further details on C4 photosynthesis, see Raghavendra and Sage (2011).

16.12 Crassulacean Acid Metabolism

Another way of using PEPC to complement the assimilation by RuBisCO is shown by plants possessing crassulacean acid metabolism (CAM). As the name implies, this kind of metabolism was first found in the family Crassulaceae. CAM plants have the ability to take up carbon dioxide during the night when the stomata are open and binding it to PEP with the help of PEPC. The carbon fixation by the Calvin–Benson cycle is carried out during the day, when the stomata are closed. By keeping stomata open only during the night, CAM plants conserve water.

CAM is more ancient than C4 metabolism, and it has been driven by water stress (Keeley and Rundel 2003). It is known only to exist in vascular plants, and it is present in species of clubmosses, ferns, the unusual gymnosperm *Welwitschia mirabilis*, the cycad *Dioon edule*, some monocots, and some dicots. Among the dicots, the following families, among others have CAM: Aizoaceae, Cactaceae, Portulaceae, Crassulaceae, Euphorbiaceae, Asclepiadaceae, and Asteraceae. Among the monocots, we have Bromeliaceae and Orchidaceae. Like C4 metabolism, CAM has evolved several times within various plant groups as an adaptation to water deficiency, mainly among desert plants and plants living on stones or as epiphytes on other plants (see Keeley and Rundel 2003). However, there

are also aquatic CAM plants, but the reason for this is not clear. Among aquatic plants, the large and primitive genus *Isoëtes* deserves special mention. All of its members seem to be CAM plants (although only about one third of the approximate 125 species have been investigated). Since this genus existed already during the early Triassic, more than 200 Ma ago, it must be assumed that CAM existed then (Keeley and Rundel 2003). Dekker and de Wit (2006) have provided further evidence for the early evolution of CAM. See Black and Osmond (pp. 881–893) in Govindjee et al. (2005) for the description of the discovery of CAM.

16.13 Evolution of ATP-Synthesizing Enzymes

The use of proton gradients for the synthesis of ATP occurs in all three domains of life—Archaea, Bacteria, and Eukarya—and the last common ancestor of all organisms is likely to have made use of this. The ancestry of the ATP-synthesizing enzyme of chloroplasts, F-ATPase, has been described by Zhaxybayeva et al. (2005). This enzyme consists of several subunits that are conserved across Bacteria and Archaea.

16.14 The Journey onto Land

Photosynthetic organisms are thought to have been present on land as early as 1.2 Ga ago, based on carbon isotope ratios (see Horodyski and Knauth 1994). These organisms were probably cyanobacteria forming crusts as can still be found in deserts. The oldest lichen-like fossils containing what has been interpreted as cyanobacteria are about 600 Ma old (Yuan et al. 2005). Stronger evidence, both morphological (Taylor et al. 2004) and chemical (Jahren 2003) for lichens, is found from the early Devonian, approximately 400 Ma ago. However, based on the "molecular clock," Heckman et al. (2001) estimated that terrestrial fungi existed prior to 900 Ma ago, and these first terrestrial fungi might well have been living in lichen-like associations. While land plants now account for about half of the planet's photosynthesis, the contribution of these early pioneers was perhaps almost negligible compared to that of the ocean.

A great increase in the amount of photosynthetic production came with the evolution of the embryophytes. Their closest relatives are the Charales (stoneworts), a type of green algae (Karol et al. 2001). Spores that are suspected to stem from liverwort-like plants have been found that are from the mid-Ordovician, 475 Ma ago (Wellman et al. 2003), but bryophyte fossils that can be identified with more certainty are younger, from late Silurian, 425 Ma ago. "Molecular clock" evidence points to a much earlier separation of the terrestrial-plant line from the algal line of evolution (Heckman et al. 2001). In the early Devonian (approximately 410 Ma ago) plants (e.g., *Eophyllophyton bellum*) had evolved that had leaves and roots (Hao et al. 2003). Their leaves seem to have been adapted to a dry climate and high carbon dioxide concentration. In the late Devonian (370 Ma ago), as the atmospheric concentration of carbon dioxide fell (Fig. 16.13), larger leaves, megaphylls, evolved, which were more efficient in collecting both carbon dioxide and light, as well as in transpiration of water vapor (Beerling et al. 2001 Mercer-Smith and Mauzerall 1981).

In the terrestrial environment, the weight of the plant body cannot be supported by buoyancy as in the water. To be able to stretch toward the light among competitors, plants had to improve their rigidity. An important means for this was to strengthen the cell walls with lignin. Such strengthening was also required for the water conduits to withstand the pressure difference. Lignin synthesis requires molecular oxygen and could thus not commence until the oxygen concentration had risen to a sufficient level. Lignin synthesis builds on the phenylpropanoid pathway, which can be traced back to the characeans: Flavonoids have been found in *Nitella* (Markham and Porter 1969). The "molecular clock" indicates that the line leading to terrestrial plants diverged from the charophytes about 1 Ga ago (Heckman et al. 2001), so this pathway can be assumed to have at least this age.

Throughout their evolution land plants maintained a close association with fungi. A majority of extant plants have mycorrhiza, and many have endophytic fungi also in the shoots and, of course, fungi on the leaf surfaces. The combination of rooted plants and mycorrhizal fungi increased the weathering of the continental rocks enormously. This, in turn, meant a positive feedback on photosynthesis by providing more nutrients, also for marine organisms.

Aquatic organisms do not require protection from desiccating evaporation, but when plants colonized land, protection mechanisms were necessary for them to conserve water. Therefore, land plants developed cuticle and cutinized external cell walls and sometimes wax coatings. All this is an obstacle to gas exchange, and so sophisticated gas valves evolved which we refer to as stomata. Stomata are adjustable openings, which are regulated to allow an optimal balance between the loss of water and access to carbon dioxide. Water and carbon dioxide conditions are sensed directly in the leaf for short-term regulation, but water availability is sensed also in the roots and hormonal signals (in the form of abscisic acid) sent to the stomata for long-term regulation. In addition, several light-sensing systems affect the stomatal aperture. In addition to regulation of the individual stomata, there is also a developmental regulation to achieve an optimal number and size distribution of stomata. The higher the atmospheric concentration of carbon dioxide, the more sparsely stomata develop on the leaf surface. Studying the stomata density on fossil leaves provides a method for

estimating past carbon dioxide concentrations (McElwain 1998; McElwain et al. 1995, 2002; Haworth et al. 2005).

After having adapted to the terrestrial environment, some plants returned to water and had to cope with new challenges (Rascio 2002). It was not simply a reversal of the adaptation to dry land; some researchers believe that our modern charophytes have also made a transient visit to terra firma. On the land, plants had become larger and needed to develop aerenchyma (air-conducting tissue) to provide all living cells with sufficient oxygen. If roots or rhizomes were to be maintained in anoxic muddy ground, diffusive oxygen transport may not be sufficient. Also the provision with carbon dioxide could be a problem, and this explains the evolution of various mechanisms for its concentration, including a kind of C4 metabolism.

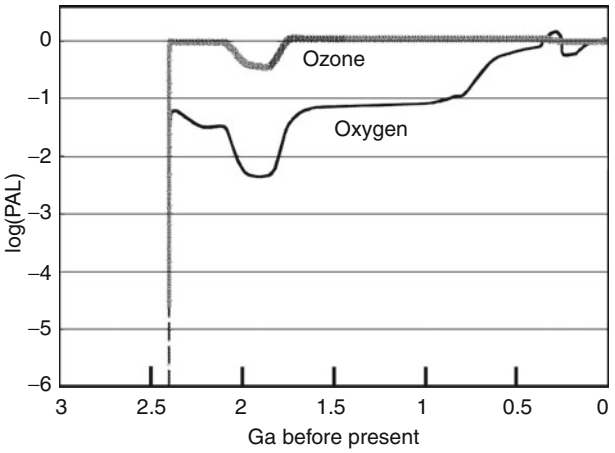

Fig. 16.12 Evolution of the earth's atmosphere. Ozone and oxygen, on a logarithmic scale, as fraction of the present atmospheric level (PAL), during the past three billion years (based on Beerling et al. 2002; Berner 2006; Canfield 2005; Falkowski et al. 2005; Huey and Ward 2005; Segura et al. 2003, and other sources)

16.15 Impact of Photosynthesis on the Biospheric Environment

When we think about how photosynthesis has affected our environment, we may first remember that it has produced the oxygen we breathe and (directly or indirectly) the food we eat. But the impact of photosynthesis is much wider. The oxygen produced by photosynthesis has also given rise to the ozone layer, which protects the biosphere from the UV-B radiation from the sun (Chap. 22). Fossil fuel, on which we have now become dependent, has been produced by photosynthesis in times past. The sequestration of carbon from the atmosphere has given us a human-friendly climate, which, unfortunately, we are now destroying. But perhaps photosynthesis, as an environmental-friendly way of energy transformation, can help us to draw up a blueprint for a solution to the conflict between our hunger for energy and the necessity to maintain an environment that can sustain humanity.

However, we must be aware that photosynthesis has not always resulted in a good environment for the inhabitants of our planet. Free oxygen is still a hazard for our own cells and even for the chloroplasts that produce it.

Photosynthesis has not always had a friendly, Gaia-like (Lovelock 1979) influence on inhabitants of the earth. When oxygen first started to accumulate, it almost certainly killed off a large part of the earth's population by direct poisoning. It was even a hurdle to the producers themselves. Many of the cyanobacteria (as many other bacteria as well as Archaea) carry out nitrogen fixation using nitrogenase. Nitrogenase is extremely sensitive to oxygen and easily inhibited by it, and organisms had to invent various methods for protecting nitrogen-fixing enzymes from oxygen. Some of the filamentous cyanobacterial forms developed special cells (heterocysts) and compartmentalized photosystems to fix nitrogen. Heterocysts contain only PSI and do not fix carbon dioxide or contain oxygen-producing PSII and therefore provide an oxygen-free environment. From morphological fossils it has been deduced that this arrangement is 1.5 Ga old. No ancient and convincing fossil of heterocysts themselves has been found, so the existence of ancient heterocysts (Golubic and Seong-Joo 1999) rests on the presence of akinetes, a kind of resting cell. In modern cyanobacteria there is a strict correlation between the occurrence of heterocysts and akinetes.

Before cyanobacteria evolved, the oxygen content of the atmosphere was less than 10^{-5} times the present value (Fig. 16.12). The initial effects of photosynthetic oxygen production on climate were disastrous. Before the oxygenation of the atmosphere, the earth was kept comfortably warm (too warm for the humans) not only by a high atmospheric content of carbon dioxide but also by another greenhouse gas, methane. When oxygen arrived, methane was first oxidized to carbon dioxide by an emerging new group of microorganisms. Then the concentration of carbon dioxide was drastically lowered by cyanobacterial assimilation. This led to a sharp temperature decrease and a glaciation, which lasted for about 100 Ma, between 2.3 and 2.2 Ga ago (Liang et al. 2006). Since traces from this time of glaciation (the Makganyene glaciation) are found near the ancient equator, some scientists believe that the whole globe became covered with ice and snow during at least part of this time. During this "Snowball Earth" (Kirschvink et al. 2000) an ice cover prevented silicate weathering, a process that consumes carbon dioxide; see Kopp et al. (2005). Gradually volcanism increased the carbon dioxide content and this eventually put an end to the long ice age. In the meantime the hydrothermal vents at the bottom of the sea had spewed out nutrients at a rate, which could not be matched by its consumption by organisms under the ice surface. Therefore, many nutrients were abundant at the end of the glaciation, but probably not all. See also Sekin et al. (2011)

for the relation between glaciation/deglaciation and oxygen production Hannah et al. (2004) and Canfield et al. (2013).

Contributing to the severity of this glaciation may have been that the sun emitted less energy than it does today (e.g., Gough 1981; Fig. 16.14), but not all scientists believe in this "faint young sun" theory. Neither is the "snowball" scenario unquestionable. An alternative explanation for glaciation in the equatorial region is that the "tilt" (the inclination) of the earth's axis was greater in the past (Williams et al. 1998; but see Levrard and Laskar 2003).

One way of constraining the timing of oxygenation of the atmosphere comes from studies of the isotopic sulfur composition of pyrite. Most chemical and physical processes lead to a fractionation of isotopes of elements, which depends on atomic weight. Photochemical processes can lead to deviations from this, i.e., to mass-independent fractionation. As long as the atmosphere remains reducing, hydrogen sulfide emitted from volcanoes remains in the atmosphere long enough for photochemical processes to imprint their special signature on the pyrite that is eventually formed. In pyrites which, by use of osmium isotope ratios, could be accurately dated to 2,316 ± 7 Ma ago, the sulfur isotope ratio indicates an oxidizing atmosphere; thus, this is taken as a minimum age for the oxic atmosphere (Hannah et al. 2004; Bekker and Holland 2012). The oxygen concentration at that time was, of course, much lower than today.

Campbell and Allen (2008) have pointed out that the oxygen content of the atmosphere has risen in steps, and every step has been associated with the formation of supercontinents. The explanation for this is that in connection with the collision between the continents, new mountains emerged and erosion increased and consequently also the input of nutrients to the sea (Lenton 2001). This increased not only photosynthesis and the production of molecular oxygen but also the burial under sediments of oxidizable material (organic carbon and pyrite), so that the newly formed oxygen was not consumed again (Fennel et al. 2005). It has been suggested that the last large increase of atmospheric oxygen, from 10 % of the present to above the present level during the Carboniferous and Permian, around 300 Ma ago (Figs. 16.13 and 16.14), is due to the emergence and spread of land plants and burial of the produced organic material in swamps.

The protein complexes involved in the electron transport chain in the thylakoids contain a variety of metals. In addition to the magnesium atoms of chlorophyll, there are 12 Fe in PSI, six Fe in the cytochrome b6/f complex, and two Fe, four Mn, and one Ca in PSII. The electron transfer chain contains additional soluble metal-containing proteins: iron containing ferredoxin and either copper containing plastocyanin or iron containing cytochrome c_6. These metals can sometimes be difficult to obtain, depending on, for instance, the redox potential of the environment and the presence of hydrogen sulfide. PSI contains more iron than the other

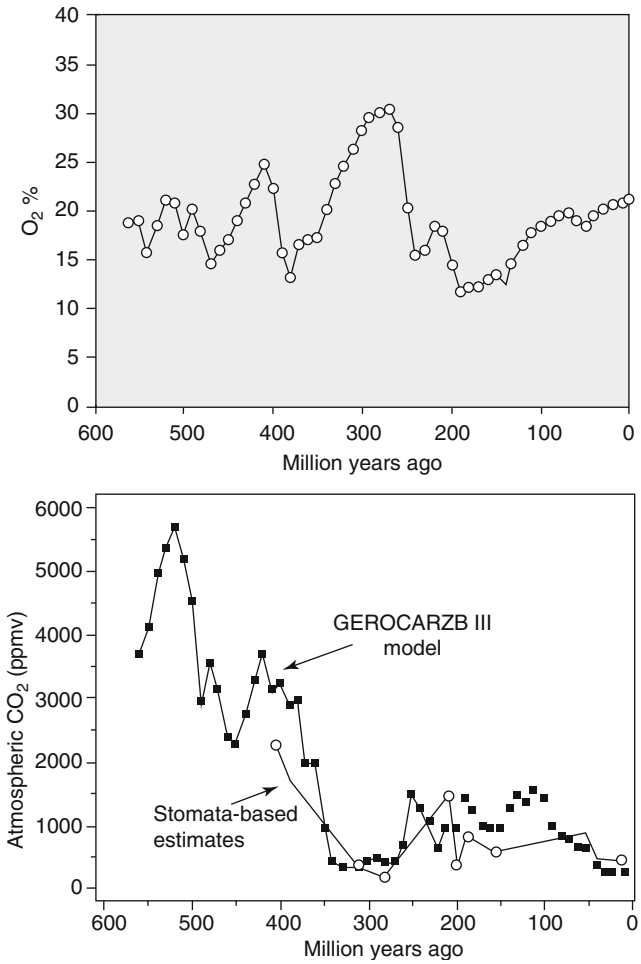

Fig. 16.13 Atmospheric changes over the Phanerozoic. *Upper panel*: The atmospheric oxygen content in percent according to the GEOCARBSULF model (redrawn from Berner 2006). *Lower panel*: The carbon dioxide content according to the GEOCARBSULF model compared to estimates based on stomata from various sources. In general the carbon dioxide decreases when the oxygen content increases

complexes, and Strzepek and Harrison (2004) have noted that diatoms adapted to coastal regions, where iron is more available, have a lower PSII/PSI ratio (around 3) compared to diatoms adapted to oceanic regions (around 9), where available iron is often a limiting factor for growth. Presumably the PSI of oceanic diatoms have larger light-collecting pigment antennas to compensate for the lower number of reaction centers. Furthermore, the coastal diatom *Thalassiosira weissflogii* uses cytochrome c_6 (Inda et al. 1999; Strzepek and Harrison 2004), another iron-containing protein, while the marine diatom *Thalassiosira oceanica* uses plastocyanin for electron transfer to PSI (Peers and Price 2006). Many cyanobacteria and eukaryotic algae still retain their capacity to synthesize both plastocyanin and cytochrome c_6 to adapt their metabolism to changing aqueous environments (Hervás et al. 2003). For historical accounts on the structure and function of PSI, see Fromme

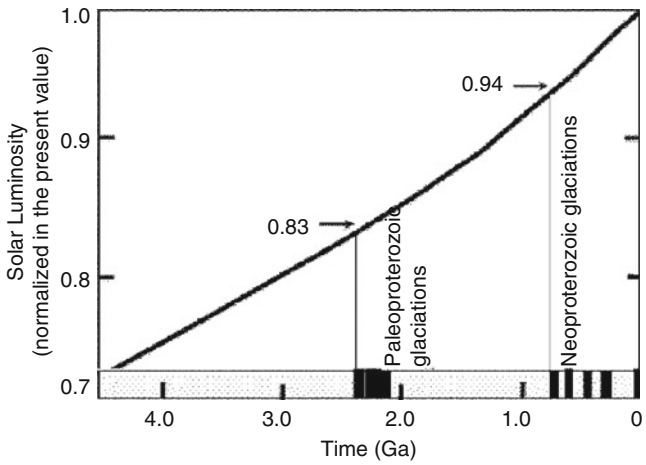

Fig. 16.14 The relative power radiated by the sun during earth history, and the timing of glaciations (From Tajika 2003, based on Gough 1981.) Not all scientists (see Sackmann and Boothroyd 2003) believe in this "faint young sun" scenario, the main argument being the documented presence of liquid water on Mars ≈3.8 Ga (gigayears) ago

and Mathis (pp. 311–326) and Witt (pp. 237–259) in Govindjee et al. (2005).

During a period after the emergence of cyanobacteria and oxygen-evolving photosynthesis, hydrogen sulfide was available only in the depths of the oceans (Canfield 1998). One can imagine that the cyanobacteria present at that time adapted their photosynthetic machinery to economize with iron, because much of this metal was tied up as sulfide. The closest present-day analog to this ancient ocean is the Black Sea. According to Anbar and Knoll (2002), sulfidic conditions in the deep sea prevailed most of the time between 2,500 and 543 Ma ago, although the ocean surface where photosynthesis could take place was oxygenated. Still, the sulfidic depth caused a deficiency of several important metals, such as iron and, even more so, molybdenum. Lack of molybdenum may have been the cause for the evolution of molybdenum-free nitrogenases (using vanadium and iron, Berman-Frank et al. 2003). According to Canfield et al. (2007) the increase of deep ocean oxygen over a critical point spurred the rapid evolution of animal life.

Conclusions

Photosynthesis is a very ancient process on our planet. It has had profound impact on the biosphere, the chemical composition of Earth's surface and Earth's atmosphere, and on climate, including radiation in the environment. It is difficult to imagine what this planet would have been like had photosynthesis (and especially the oxygenic variant) not evolved. In any case we would not have been here to find out.

Acknowledgement The authors are grateful to George C. Papageorgiou for careful reading of the manuscript and many valuable suggestions. Govindjee thanks B.C. Tripathy, P.K. Mohapatra, S.K. Nayak, and P.K. Jena for their hospitality, while he was a Visiting Professor in Botany at Ravenshaw University, Cuttack, Odisha, India, during January–March, 2014.

References

Allen JF (2005) A redox switch hypothesis for the origin of two light reactions in photosynthesis. FEBS Lett 579:963–968

Allen JF, Martin W (2007) Out of thin air. Nature 445:61–612

Allgaier M, Uphoff H, Felske A, Wagner-Döbler I (2003) Aerobic anoxygenic photosynthesis in Roseobacter clade bacteria from diverse marine habitats. Appl Environ Microbiol 69:5051–5059. doi:10.1128/AEM.69.9.5051-5059.2003

Anbar AD, Holland HD (1992) The photochemistry of manganese and the origin of banded iron formations. Geochim Cosmochim Acta 56:2595–2603

Anbar AD, Knoll AH (2002) Proterozoic ocean chemistry and evolution: a bioinorganic bridge. Science 297:1137–1142

Anbar AD, Duan Y, Lyons TW, Arnold GL, Kendall B, Creaser RA, Kaufman AJ, Gordon GW, Scott C, Garvin J, Buick R (2007) A whiff of oxygen before the great oxidation event? Science 317:1903–1906

Anderson JM (1999) Insights into the consequences of grana stacking of thylakoid membranes in vascular plants: a personal perspective. Aust J Plant Physiol 26:625–639

Armstrong GA (1998) Greening in the dark: light-independent chlorophyll biosynthesis from anoxygenic photosynthetic bacteria to gymnosperms. J Photochem Photobiol B Biol 43:87–100

Asard H, Venken M, Caubergs R, Reijnders W, Oltmann FL, De Greef JA (1989) b-Type cytochromes in higher plant plasma membranes. Plant Physiol 90:1077–1083

Ashida H, Saito Y, Kojima C, Kobayashi K, Ogasawara N, Yokota A (2003) A functional link between RuBisCO-like protein of Bacillus and photosynthetic RuBisCO. Science 302:287–290

Ashida H, Danchin A, Yokota A (2005) Was photosynthetic RuBisCO recruited by acquisitive evolution from RuBisCO-like proteins involved in sulfur metabolism? Res Microbiol 156:611–618

Awramik SM (1992) The oldest records of photosynthesis. Photosynth Res 33:75–89

Bader KP (1994) Physiological and evolutionary aspects of the O_2/H_2O_2 cycle in cyanobacteria. Biochim Biophys Acta 1188:213–219

Badger MR, Price GD (2003) CO2-concentrating mechanisms in cyanobacteria: molecular components, their diversity and evolution. J Exp Bot 54:609–622

Bald D, Kruip J, Boekema EJ, Rögner M (1992) Structural investigations on cyt b6 f complex and PS I complex from the cyanobacterium Synechocystis PCC6803. In: Murata N (ed) Photosynthesis: from light to biosphere, Part I. Kluwer Academic Publishers, Dordrecht, pp 629–633

Battistuzzi FU, Andreia Feijao A, Blair Hedges SB (2004) A genomic timescale of prokaryote evolution: insights into the origin of methanogenesis, phototrophy, and the colonization of land. BMC Evolut Biol 4:44, 14 pp

Baurain D, Brinkmann H, Petersen J, Rodríguez-Ezpeleta N, Stechmann A, Demoulin V, Roger AJ, Burger G, Lang BJ, Philippe H (2010) Phylogenomic evidence for separate acquisition of plastids in cryptophytes, haptophytes, and stramenopiles. Mol Biol Evol 27: 1698–1709

Baymann F, Brugna M, Muhlenhoff U, Nitschke W (2001) Daddy, where did (PS)I come from? Biochim Biophys Acta 1507:291–310

Beatty JT, Overmann J, Lince MT, Manske AK, Lang AS, Blankenship RE, Van Dover CL, Martinson TA, Plumley GF (2005) An obligately

photosynthetic bacterial anaerobe from a deep-sea hydrothermal vent. Proc Natl Acad Sci U S A 102:9306–9310
Beerling DJ, Osborne CP, Chaloner WG (2001) Evolution of leaf-form in land plants linked to atmospheric CO2 decline in the Late Palaeozoic era. Nature 410:352–354
Beerling DJ, Lake JA, Berner RA, Hickey JJ, Taylor DW, Royer DL (2002) Carbon isotope evidence implying high O2/CO2 ratios in the Permo-Carboniferous atmosphere. Geochim Cosmochim Acta 66:3757–3767
Bekker A, Holland HD (2012) Oxygen overshoot and recovery during the early Paleoproterozoic. Earth Planetary Sci Lett 317–318: 295–304
Bekker A, Holland HD, Wang P-L, Rumble D III, Stein HJ, Hannah JL, Coetzee LL, Beukes NJ (2004) Dating the rise of atmospheric oxygen. Nature 427:117–120
Berman-Frank I, Lundgren P, Falkowski P (2003) Nitrogen fixation and oxygen evolution in cyanobacteria. Res Microbiol 154:157–164
Berner RA (2006) GEOCARBSULF: a combined model for Phanerozoic atmospheric O2 and CO2. Geochim Cosmochim Acta 70:5653–5664
Bhattcharaya D, Yoon HS, Hackett JD (2003) Photosynthetic eukaryotes unite: endosymbiosis connects dots. Bioessays 26:50–60
Björn LO (1995) Origins of photosynthesis. Nature 376:25–26
Björn LO, Ekelund NGA (2005) Dinoflagellater—hopplock från livets smörgåsbord. Svensk Bot Tidskr 99:7–16
Björn LO, Govindjee (2009) The evolution of photosynthesis and chloroplasts. Curr Sci 96:1466–1474
Björn LO, Papageorgiou GC, Blankenship RE, Govindjee (2009a) A viewpoint: why chlorophyll a? Photosynth Res 99:85–98
Björn LO, Papageorgiou GC, Dravins D, Govindjee (2009b) Detectability of life on exoplanets. Curr Sci 96:1171–1175
Blankenship RE (1992) Origin and early evolution of photosynthesis. Photosynth Res 33:91–100
Blankenship RE (2014) Molecular mechanisms of photosynthesis. 2nd Edition, Wiley-Blackwell, Hoboken, NJ
Blankenship RE, Hartman H (1998) The origin and evolution of oxygenic photosynthesis. Trends Biochem Sci 23:94–97
Blankenship RE, Madigan MT, Bauer CE (eds.) (1995) Anoxygenic Photosynthetic Bacteria, Advances in Photosynthesis and Respiration, vol. 3, Springer, Dordrecht
Bocherens H, Friis EM, Mariotti A, Pedersen KR (1993) Carbon isotopic abundances in Mesozoic and Cenozoic fossil plants—paleoecological implications. Lethaia 26:347–358
Borda MJ, Elsetinow AR, Schoonen MA, Strongin DR (2001) Pyrite-induced hydrogen peroxide formation as a driving force in the evolution of photosynthetic organisms on an early Earth. Astrobiology 1:283–288
Brasier MD, Green OR, Lindsay JF, McLoughlin N, Steele A, Stoakes C (2005) Precambrian Res 140:55–102
Brocks JJ, Buick R, Summons RE, Logan GA (2003) A reconstruction of Archean biological diversity based on molecular fossils from the 2.78 to 2.45 billion-year-old Mount Bruce Supergroups, Hamersley Basin, Western Australia. Beochim Cosmochim Acta 67:4321–4335
Bryant DA, Frigaard N-U (2006) Prokaryotic photosynthesis and phototrophy illuminated. Trends Microbiol 18:488–496
Buchanan BB, Arnon DI (1990) A reverse Krebs cycle in photosynthesis: consensus at last. Photosynth Res 24:47–53
Butterfield NJ (2000) Bangiomorpha pubescens n. gen., n. sp.: implications for the evolution of sex, multicellularity, and the Mesoproterozoic/Neoproterozoic radiation of eukaryotes. Paleobiology 26:386–404
Campbell IH, Allen CM (2008) Formation of supercontinents linked to increases in atmospheric oxygen. Nat Geosci 1:554–558
Canfield DE (1998) A new model for proterozoic ocean chemistry. Nature 396:450–453
Canfield DE (2005) The early history of atmospheric oxygen: Homage to R.M. Garrels. Annu Rev Earth Planet Sci 33:1–36
Canfield DE, Poulton SW, Narbonne GM (2007) Late Neo-Proterozoic deep-ocean oxygenation and the rise of animal life. Science 315:92–95
Canfield DE, Ngombi-Pemba L, Hammarlund EU, Bengtson S, Chaussidon M, Gauthier-Lafaye F, Meunier A, Riboulleau A, Rollion-Bard C, Rouxel O, Dan Asael D, Pierson-Wickmann A-C, El Albani A (2013) Oxygen dynamics in the aftermath of the Great Oxidation of Earth's atmosphere. Proc Natl Acad Sci U S A 110:16736–16741
Chew AGM, Bryant DA (2007) Chlorophyll biosynthesis in bacteria: the origins of structural and functional diversity. Annu Rev Microbiol 61:113–129
Clausen J, Beckmann K, Junge W, Messinger J (2005a) Evidence that bicarbonate is not the substrate in photosynthetic oxygen evolution. Plant Physiol 139:1444–1450
Clausen J, Junge W, Dau H, Haumann M (2005b) Photosynthetic water oxidation at high O2 backpressure monitored by delayed chlorophyll fluorescence. Biochemistry 44:12775–12779
Crowe SE, Døssing LA, Beukes NJ, Bau M, Kruger SJ, Frei R, Canfield DE (2013) Atmospheric oxygenation three billion years ago. Nature 501:535–539
Dashdori N, Zhang H, Kim H, Yan J, Cramer WA, Savikhin S (2005) The single chlorophyll a molecule in the cytochrome b6 f complex, unusual optical properties protect the complex against singlet oxygen. Biophys J 88:4178–4187
Decker JE, de Wit MJ (2006) Carbon isotope evidence for CAM photosynthesis in the Mesozoic. Terra Nova 18:9–17
Demmig-Adams B, Adams WW III, Mattoo A (eds) (2006) Photoprotection, photoinhibition, gene regulation, and environment. Springer, New York
Demmig-Adams S, Garab G, Adams W III, Govindjee (eds) (2014) Non-photochemical quenching and energy dissipation in plants, algae and cyanobacteria, vol 40, Advances in photosynthesis and respiration. Springer, Dordrecht
Dismukes GC, Klimo VV, Baranov SV, Kozlov YN, DasGupta J, Tyryshkin A (2001) The origin of atmospheric oxygen on Earth: the innovation of oxygenic photosynthesis. Proc Natl Acad Sci U S A 98:2170–2175
Eck RV, Dayhoff MO (1966) Evolution of the structure of ferredoxin based on living relics of primitive amino acid sequences. Science (NS) 152:363–366
Eickhoff M, Birgel D, Talbot HM, Peckmann J, Kappler A (2013) Oxidation of Fe(II) leads to increased C-2 methylation of pentacyclic triterpenoids in the anoxygenic phototrophic bacterium Rhodopseudomonas palustris strain TIE-1. Geobiology 11:268–278
Eisenhut M, Ruth W, Haimovich M, Bauwe H, Kaplan A, Hagemann M (2008) The photorespiratory glycolate metabolism is essential for cyanobacteria and might have been conveyed endosymbiontically to plants. Proc Natl Acad Sci U S A 105:17199–17204
Evans MC, Buchanan BB, Arnon DI (1966) A new ferredoxin dependent carbon reduction cycle in a photosynthetic bacterium. Proc Natl Acad Sci U S A 55:928–934
Falkowski PG, Raven JA (2007) Aquatic Photosynthesis. Princeton University Press, Princeton
Falkowski PG, Katz ME, Milligan AJ, Fennel K, Cramer BS, Aubry MP, Berner RA, Novacek MJ, Zapol WM (2005) The rise of oxygen over the past 205 million years and the evolution of large placental mammals. Science 309:2202–2204
Farquhar J, Zerkle AL, Bekker A (2011) Geological constraints on the origin of oxygenic photosynthesis. Photosynth Res 107:11–36
Fennel K, Follows M, Falkowski PG (2005) The co-evolution of the nitrogen, carbon and oxygen cycles in the Proterozoic ocean. Am J Sci 305:526–545

Ferreira KN, Iverson TM, Maghlaoui K, Barber J, Iwata S (2004) Architecture of the photosynthetic oxygen-evolving center. Nature 303:1831–1837

Flament N, Coltice N, Rey PF (2013) The evolution of the 87Sr/86Sr of marine carbonates does not constrain continental growth. Precamb Res 229:177–188

Fliegel D, Kosler J, McLoughlin N, Simonetti A, de Wit MJ, Wirth R, Furnes H (2010) In-situ dating of the Earth's oldest trace fossil at 3.34 Ga. Earth Planet Sci Lett 299:290–298

Frigaard N-U, Martinez A, Mincer TJ, DeLong EF (2006) Proteorhodopsin lateral gene transfer between marine planktonic Bacteria and Archaea. Nature 439:847–850

Fru EC, Ivarsson M, Kilias SP, Bengtson S, Belivanova V, Marone F, Fortin D, Broman C, Stampanoni M (2013) Fossilized iron bacteria reveal a pathway to the biological origin of banded iron formation. Nat Comm 4(2050):7

Geider RJ, Delucia EH, Falkowski GD et al (2001) Primary productivity of planet earth: biological determinants and physical constraints in terrestrial and aquatic habitats. Glob Chang Biol 7:849–882

Giordano M, Beardall J, Raven JA (2005) CO_2 concentrating mechanisms in algae: mechanisms, environmental modulation, and evolution. Annu Rev Plant Physiol 56:99–131

Golbeck JH (ed) (2006) Photosystem I: the light-driven plastocyanin: ferredoxin oxidoreductase. Springer, New York

Golubic S, Seong-Joo L (1999) Early cyanobacterial fossil record: preservation, palaeoenvironments and identification. Eur J Phycol 34:339–348

Gomes R, Levison HF, Tsiganis K, Morbidelli A (2005) Origin of the cataclysmic Late Heavy Bombardment period of the terrestrial planets. Nature 435:466–469

Gómez-Consarnau L, Akram N, Lindell K, Pedersen A, Neutze R, Milton DL, González JM, Pinhassi J (2011) Proteorhodopsin phototrophy promotes survival of marine bacteria during starvation. PLoS Biol 8:e1000358

Gómez-Consarnau L, González JM, Coll-Llado M, Gourdon P, Pascher T, Richard Neutze R, Pedrós-Alió C, Pinhassi J (2007) Light stimulates growth of proteorhodopsin-containing marine Flavobacteria. Nature 445:210–213

González JM, Fernandez-Gomez B, Fernandez-Guerra A, Gómez-Consarnau L, Sanchez O, Coll-Llado M, del Campo J, Escudero L, Rodriguez-Martinez R, Alonso-Saez L, Latasa M, Paulsen I, Nedashkovskaya O, Lekunberri I, Pinhassi J, Pedros-Alio C (2008) Genome analysis of the proteorhodopsin-containing marine bacterium Polaribacter sp.MED152 (Flavobacteria). Proc Natl Acad Sci U S A 105:8724–8729

Gough DO (1981) Solar interior structure and luminosity variations. Solar Physics 74:21–34

Govindjee (2000) Milestones in photosynthesis research. In: Yunus M, Pathre U, Mohanty P (eds) Probing photosynthesis: mechanisms, regulation and adaptation. Taylor & Francis, London, pp 9–39

Govindjee, Björn LO (2012) Dissecting oxygenic photosynthesis: the evolution of the "Z"-scheme for thylakoid reactions. Chapter 1. In: Shigeru I, Prasanna M, Guruprasad KN (eds) Photosynthesis: overviews on recent progress & future perspective. IK International Publishing House Pvt. Ltd, New Delhi, pp 1–27

Govindjee, Beatty JT, Gest H, Allen JF (eds) (2005) Discoveries in photosynthesis. Springer, Dordrecht

Granick S (1957) Speculations on the origins and evolution of photosynthesis. Ann NY Acad Sci 69:292–308

Gu Y, Li P, Sage JT, Champion PM (1993) Photoreduction of heme proteins: spectroscopic studies and cross-section measurements. J Am Chem Soc 115:4993–5004

Gupta RS (2013) Molecular markers for photosynthetic bacteria and insights into the origin and spread of photosynthesis. Adv Bot Res 66:37–65

Gutiérrez-Cirlos EB, Pérez-Gómez B, Krogmann DW, Gómez-Lojero C (2006) The phycocyanin-associated rod linker proteins of the phycobilisome of Gloeobacter violaceus PCC 7421 contain unusually located rod-capping domains. Biochim Biophys Acta 1757: 130–134

Hakala M, Tuominen I, Keränen M, Tyystjärvi T, Tyystjärvi E (2005) Evidence for the role of the oxygen-evolving manganese complex in photoinhibition of Photosystem II. Biochim Biophys Acta 1706:68–80

Hakala M, Rantamäki S, Puputti E-M, Tyystjärvi T, Tyystjärvi E (2006) Photoinhibition of manganese enzymes: insights into the mechanism of photosystem II photoinhibition. J Exp Bot 57:1809–1816

Hannah JL, Bekker A, Stein HJ, Markey RJ, Holland HD (2004) Primitive Os and 2316 Ma age for marine shale: implications for Paleoproterozoic glacial events and the rise of atmospheric oxygen. Earth Planetary Sci Lett 225:43–52

Hao SG, Beck CB, Wang DM (2003) Structure of the earliest leaves: adaptations to high concentrations of atmospheric CO2. Intern J Plant Sci 164:71–75

Härtner T, Straub KL, Kannenberg E (2005) Occurrence of hopanoid lipids in anaerobic Geobacter species. FEMS Microbiol Lett 243:59–64

Hattersley PW (1982) 13C values of C4 types in grasses. Aust J Plant Physiol 9:139–154

Haworth M, Hesselbo SP, McElwain JC, Robinson SA, Brunt J (2005) Mid- Cretaceous pCO2 based on stomata of the extinct conifer Pseudofrenelopsis (Cheirolepidiaceae). Geology 33:749–752

Heckman DS, Geiser DM, Eidell BR, Stauffer RL, Kardos NL, Hedges SB (2001) Molecular evidence for the early colonization of land by fungi and plants. Science 293:1129–1133

Hervás M, Navarro JA, de la Rosa MA (2003) Electron transfer between membrane complexes and soluble proteins in photosynthesis. Acc Chem Res 36:798–805

Hess WR, Partensky F, van der Staay GWM, Garcia Fernandez JM, Borner T, Vaulot D (1996) Coexistence of phycoerythrin and a chlorophyll a/b antenna in a marine prokaryote. Proc Natl Acad Sci U S A 93:11126–11130

Hirabayashi H, Ishii T, Takaichi S, Inoue K, Uehara K (2004) The role of carotenoids in the photoadaptation of the brown-colored sulfur bacterium Chlorobium phaeobacteroides. Photochem Photobiol 79:280–285

Hofmann HJ (1976) Precambrian microflora, Belcher Islands, Canada: significance and systematics. J Paleontol 50:1040–1073

Holert J, Hahnke S, Cypionka H (2011) Influence of light and anoxia on chemiosmotic energy conservation in Dinoroseobacter shibae. Environ Microbiol Rep 3:136–141

Holland HH (2009) Why the atmosphere became oxygenated: a proposal. Geochim Cosmochim Acta 73:5241–5255

Horodyski RJ, Knauth LP (1994) Life on land in the Precambrian. Science 263:494–498

Hu X, Ritz T, Damjanovic A, Felix Autenrieth F, Schulten K (2002) Photosynthetic apparatus of purple bacteria. Quart Revs Biophys 35:1–62

Huang D, Everly RM, Cheng RH, Heymann JB, Schagger H, Sled V, Ohnishi T, Baker TS, Cramer WA (1994) Characterization of the chloroplast cytochrome b f complex as a structural and functional dimer. Biochemistry 33:4401–4409

Huey RB, Ward PD (2005) Hypoxia, global warming, and terrestrial late Permian extinctions. Science 308:398–401

Hügler M, Hüber H, Stetter KO, Fuchs G (2003) Autotrophic CO2 fixation pathways in archaea (Crenarchaeota). Arch Microbiol 179: 160–173

Hunter CN, Daldal F, Thurnauer MC, Beatty J.T(Eds.) (2009) The Purple Phototrophic Bacteria. Advances in Photosynthesis and Respiration, vol. 28, Springer, Dordrecht

Inda LA, Erdner DL, Peleato ML, Anderson DM (1999) Cytochrome c6 isolated from the marine diatom Thalassiosira weissflogii. Phytochemistry 51:1–4

Jahren AH, Porter S, Kuglitsch JJ (2003) Lichen metabolism identified in early Devonian terrestrial organisms. Geology 31:99–102

Janke C, Scholz F, Becker-Baldus J, Glaubitz C, Wood PG, Bamberg E, Wachtveitl J, Bamann C (2013) Photocycle and vectorial proton transfer in a rhodopsin from the eukaryote Oxyrrhis marina. Biochemistry 52:2750–2763. http://dx.doi.org/10.1021/bi301412n

Johnson JE, Webb SM, Thomas K, Ono S, Kirschwink JL, Fischer WW (2013) Manganese-oxidizing photosynthesis before the rise of cyanobacteria. Proc Natl Acad Sci U S A 110:11238–11243

Kappler A, Pasquero C, Konhauser KO, Newman DK (2005) Deposition of banded iron formations by anoxygenic phototrophic Fe(II)-oxidizing bacteria. Geology 33:865–868

Karhu JA, Holland HD (1996) Carbon isotopes and the rise of atmospheric oxygen. Geology 24:867–870

Karol KG, McCourt RM, Cimino MT, Delwiche CF (2001) The closest living relatives of land plants. Science 294:2351–2353

Ke B (2001) Photosynthesis: photobiochemistry and photobiophysics. Springer, Dordrecht

Keeley JE, Rundel PW (2003) Evolution of CAM and C4 carbon-concentrating mechanisms. Int J Plant Sci 164(3 Suppl):S55–S77

Kiang NY, Siefert J, Govindjee, Blankenship RE (2007) Spectral signatures of photosynthesis I review of earth organisms. Astrobiology 7:252–274

Kirchman DL, Hanson TE (2013) Bioenergetics of photoheterotrophic bacteria in the oceans. Environ Microbiol Rep 5:188–199

Kirschvink JL, Gaidos EJ, Bertani LE, Beukes NJ, Gutzmer J, Maepa LN, Steinberger RE (2000) Paleoproterozoic snowball earth: extreme climatic and geochemical global change and its biological consquences. Proc Natl Acad Sci U S A 97:1400–1405

Kleine T, Münker C, Mezger K, Palmer H (2002) Rapid accretion and early core formation on asteroids and the terrestrial planets from Hf–W chronometry. Nature 952–955

Kopp RE, Kirschwink J-L, Hilburn IA, Nash CZ (2005) The Paleoproterozoic snowball Earth: a climate disaster triggered by the evolution of oxygenic photosynthesis. Proc Natl Acad Sci U S A 102:11131–11136

Krapež B, Barley MA, Pickard AL (2003) Hydrothermal and resedimented origins of the precursor sediments to banded iron formation: sedimentological evidence from the early Palaeoproterozoic Brockman supersequence of Western Australia. Sedimentology 50:979–1011

Kump LR (2008) The rise of atmospheric oxygen. Nature 451: 277–278

Kump LR, Junium C, Arthur MA, Brasier A, Fallick A, Melezhik V, Lepland A, Crne AE, Luo G (2011) Isotopic evidence for massive oxidation of organic matter following the Great Oxidation Event. Science 334:1694–1696

Kurisu G, Zhang H, Smith JL, Cramer WA (2003) Structure of the cytochrome b f complex of oxygenic photosynthesis: tuning the cavity. Science 302:1009–1014

Lenton T (2001) The role of land plants, phosphorus weathering and fire in the rise and regulation of atmospheric oxygen. Glob Chang Biol 7:613–629

Levrard B, Laskar J (2003) Climate friction and the earth's obliquity. Geophys J 154:970–990

Liang M-C, Hartman H, Kopp RE, Kirschvink JL, Yung YL (2006) Production of hydrogen peroxide in the atmosphere of a snowball Earth and the origin of oxygenic photosynthesis. Proc Natl Acad Sci U S A 103:18896–18899

Lovelock JE (1979) Gaia: a new look at life on Earth. Oxford University Press, New York, p xi+157

Löwenich D, Kleinermanns K, Karunakaran V, Kovalenko SA (2008) Transient and stationary spectroscopy of cytochrome c: ultrafast internal conversion controls photoreduction. Photochem Photobiol 84:193–201

Marin B, Nowack ECM, Melkonian M (2005) A plastid in the making: evidence for a second primary endosymbiosis. Protist 156:425–432

Markham KR, Porter LJ (1969) Flavonoids in the green algae (Chlorophyta). Phytochemistry 8:1777–1781

Masuda T, Fujita Y (2008) Regulation and evolution of chlorophyll metabolism. Photochem Photobiol Sci 7:1131–1149

Mauzerall D (1976) Chlorophyll and photosynthesis. Philos Trans R Soc Lond B Biol Sci 273:287–294

McCarren J, DeLong EF (2007) Proteorhodopsin photosystem gene clusters exhibit co-evolutionary trends and shared ancestry among diverse marine microbial phyla. Envir Microbiol 9:846–858

McElwain JC (1998) Do fossil plants signal palaeatmospheric CO2 concentration in the geological past? Philos Trans R Soc Lond B Biol Sci 353:83–96

McElwain JC, Mitchell FJG, Jones MB (1995) Relationship of stomatal density and index of Salix cinerea to atmospheric carbon dioxide concentrations in the Holocene. The Holocene 5:539–570

McElwain JC, Mayle FE, Beerling DJ (2002) Stomatal evidence for a decline in atmospheric CO concentration during the Younger Dryas stadial: a comparison with Antarctic ice core records. J Quat Sci 17:21–29

Mercer-Smith JA, Mauzerall D (1981) Molecular hydrogen production by uroporphyrin and coproporphyrin: a model for the origin of photosynthetic function. Photochem Photobiol 34:407–410

Moorbath S (2005) Palaebiology: dating the earliest life. Nature 434:155

Mulkidjanian AY, Galperin MY (2013) A time to scatter genes and a time to gather them: evolution of photosynthesis genes in bacteria. Adv Bot Res 66:1–35

Mulkidjanian AY, Koonin EV, Makarova KS, Mekhedov SL, Sorokin A, Wolf YI, Dufresne A, Partensky F, Burd H, Kaznadzey D, Haselkorn R, Galperin MY (2006) The cyanobacterial genome core and the origin of photosynthesis. Proc Natl Acad Sci U S A 103:13126–13131

Nelson N, Ben-Shem A (2002) Photosystem I reaction center: past and future. Photosynth Res 73:193–206

Nelson N, Ben-Shem A (2005) The structure of photosystem I and evolution of photosynthesis. Bioessays 27:914–922

Nisbet EG, Cann JR, van Dover C (1995) Origins of photosynthesis. Nature 373:479–480

Olson JM (2006) Photosynthesis in the Archean era. Photosynth Res 88:109–117

Olson JM, Pierson BK (1987) Origin and evolution of photosynthetic reaction centers. Orig Life 17:419–430

Osborne CP, Beerling DJ (2006) Nature's green revolution: the remarkable evolutionary rise of C4 plants. Philos Trans Roy Soc B Biol Sci 361:173–194

Partin C-A, Bekker A, Planavsky NJ, Scott CT, Gill BC, Li C, Podkovyrov V, Maslov A, Konhauser KO, Lalonde SV, Love GD, Poulton SW, Lyons TW (2013) Large-scale fluctuations in Precambrian atmospheric and oceanic oxygen levels from the record of U in shales. Earth Planet Sci Lett 369–370:284–293

Peers G, Price NM (2006) Copper-containing plastocyanin used for electron transport by an oceanic diatom. Nature 441:341–344

Petersen J, Teich R, Brinkmann H, Cerff R (2006) A "green" phosphoribulokinase in complex algae with red plastids: evidence from a single secondary endosymbiosis leading to haptophytes, cryptophytes, heterokonts, and dinoflagellates. J Mol Evol 23:1109–1118

Petersen J, Brinkmann H, Bunk B, Michael V, Päuker O, Pradella S (2012) Think pink: photosynthesis, plasmids and the Roseobacter clade. Environ Microbiol 14:2661–2672

Petersen J, Frank O, Göker M, Pradella S (2013) Extrachromosomal, extraordinary and essential—the plasmids of the Roseobacter clade. Appl Microbiol Biotechnol 97:2805–2815. doi:10.1007/s00253-013-4746-8

Pierre J, Bazin M, Debey P, Santus R (1982) One-electron photoreduction of bacterial cytochrome P450 by ultraviolet light. 1. Steady-state measurements. Eur J Biochem 124:533–537
Pierre Y, Breyton C, Lemoine Y, Robert B, Vernotte C, Popot J-L (1997) On the presence and role of a molecule of chlorophyll a in the cytochrome b f complex. J Biol Chem 272:21901–21908
Raghavendra AS, Sage R (eds.) (2011) C4 photosynthesis and related CO_2 concentrating mechanisms. Advances in Photosynthesis and Respiration, Vol. 32, Springer, Dordrecht
Rascio N (2002) The underwater life of secondarily aquatic plants: some problems and solutions. Crit Rev Plant Sci 21:401–427
Rasmussen B, Fletcher IR, Brocks JJ, Kilburn RR (2008) Reassessing the first appearance of eukaryotes and cyanobacteria. Nature 455:1101–1104
Raven JA, Evans MCW, Korb RE (1999) The role of trace metals in photosynthetic electron transport in O2-evolving organisms. Photosynth Res 60:111–149
Raven JA, Kübler JE, Beardall J (2000) Put out the light and then put out the light. J Mar Biol Ass UK 80:1–25
Raymond J, Blankenship RE (2003) Horizontal gene transfer in eukaryotic algal evolution. Proc Natl Acad Sci U S A 100:7419–7420
Raymond J, Zhaxybayeva O, Gogarten JP, Blankenship RE (2003a) Evolution of photosynthetic prokaryotes: a maximum-likelihood mapping approach. Philos Trans R Soc Lond B Biol Sci 358: 223–230
Raymond J, Siefert JL, Staples CR, Blankenship RE (2003b) The natural history of nitrogen fixation. Mol Biol Evol 21:541–554
Reinfelder JR, Kraepiel AML, Morel FMM (2000) Unicellular C4 photosynthesis in a marine diatom. Nature 407:996–999
Reinfelder JR, Milligan AJ, Morel FMM (2004) The role of C4 photosynthesis in carbon accumulation and fixation in a marine diatom. Plant Physiol 135:2106–2111
Retallack GJ (2002) Carbon dioxide and climate over the past 300 Myr. Philos Trans R Soc Lond B Biol Sci 360:659–673
Riedel T, Tomasch J, Buchholz I, Jacobs J, Kollenberg M et al (2010) The proteorhodopsin gene is expressed constitutively by a Flavobacterium representative of the proteorhodopsin carrying microbial community in the North Sea. Appl Environ Microbiol 76:3187–3197
Rogers MB, Gilson PR, Su V, McFadden GI, Keeling PJ (2007) The complete chloroplast genome of the chlorarachniophyte Bigelowiella natans: evidence for independent origins of Chlorarachniophyte and Euglenid secondary endosymbionts. Mol Biol Evol 24:54–62
Rosing MT, Frei R (2004) U-rich Archaean sea-floor sediments from Greenland— indications of >3700 Ma oxygenic photosynthesis. Earth Planet Sci Lett 217:237–244
Rubinstein B (1993) Plasma membrane redox processes: components and role in plant processes. Annu Rev Plant Physiol Plant Mol Biol 44:131–155
Rutherford AW, Faller P (2003) Photosystem II: evolutionary perspectives. Philos Trans R Soc Lond B Biol Sci 358:245–253
Rutherford AW, Nitschke W (1996) Photosystem II and the quinone-iron-consisting reaction centers: comparisons and evolutionary perspectives. In: Baltscheffsky H (ed) Origin and evolution of biological energy conversion. Wiley-VCH, New York, pp 143–175
Sackmann IJ, Boothroyd AI (2003) Our Sun. V. A bright young Sun consistent with helioseismology and warm temperatures on ancient earth and mars. Astrophys J 583:1024–1039
Sage RF (2004) The evolution of C4 photosynthesis. New Phytol 161:341–370
Samuilov VD, Bezryadnov DB, Gusev MV, Kitasov AV, Fedorenko TA (2001) Hydrogen peroxide inhibits photosynthetic electron transport in cells of cyanobacteria. Biochemistry (Mosc) 66:640–645
Sauer K, Yachandra VK (2002) A possible evolutionary origin for the Mn-4 cluster of the photosynthetic water oxidation complex from natural MnO2 precipitates in the early ocean. Proc Natl Acad Sci U S A 99:8631–8636
Schoepp-Cothenet B, van Lis R, Atteia A, Baymann F, Capowiez L, Ducluzeau A-L, Duval S, ten Brink F, Russell MJ, Wolfgang Nitschke W (2013) On the universal core of bioenergetics. Biochim Biophys Acta 1827:79–93
Segura A, Krelove K, Kasting JF, Sommerlatt D, Meadows V, Crisp D, Cohen M, Mlawer E (2003) Ozone concentrations and ultraviolet fluxes on earth-like planets around other stars. Astrobiology 3:689–708
Sekine Y, Suzuki K, Senda R, Goto KT, Tajika E, Tada R, Goto K, Yamamoto S, Ohkouchi N, Ogawa NO, Maruoka T (2011) Osmium evidence for synchronicity between a rise in atmospheric oxygen and Palaeoproterozoic deglaciation. Nat Comm 2:1–5
Selesi D, Schmid M, Hartmann A (2005) Diversity of green-like and red-like ribulose-1,5-bisphosphate carboxylase/oxygenase large-subunit genes (cbbL) in differently managed agricultural soils. Appl Environ Microbiol 71:175–184
Sessions AL, Doughty DM, Welander PV, Summons RE, Newman DK (2009) The continuing puzzle of the great oxidation event. Curr Biol 19:R567–R574
Shevela D, Eaton-Rye JJ, Shen J-R, Govindjee (2012) Photosystem II and unique role of bicarbonate: a historical perspective. Biochim Biophys Acta 1817:1134–1151
Shevela D, Nöring B, Koroidov S, Shutova T, Samuelsson G, Messinger J (2013) Efficiency of photosynthetic water oxidation at ambient and depleted levels of inorganic carbon. Photosynth Res 117:401–412
Sousa FL, Shavit-Grievink L, Allen JF, Martin WF (2013a) Chlorophyll biosynthesis gene evolution indicates photosystem gene duplication, not photosystem merger, at the origin of oxygenic photosynthesis. Genome Biol Evol 5:200–216
Sousa FL, Thiergart T, Landan G, Nelson-Sathi S, Pereira IAC, Allen JF, Lane N, Martin WF (2013b) Early bioenergetic evolution. Philos Trans R Soc B 368:20130088
Steindler L, Schwalbach MS, Smith DP, Chan F, Giovannoni SJ (2011) Energy starved Candidatus Pelagibacter ubique substitutes light-mediated ATP production for endogenous carbon respiration. PLoS One 6:e19725. doi:10.1371/journal.pone.0019725
Stingl U, Desiderio RA, Cho JC, Vergin KL, Giovannoni SJ (2007) The SAR92 clade: an abundant coastal clade of culturable marine bacteria possessing proteorhodopsin. Appl Environ Microbiol 73:2290–2296
Stoebe B, Maier U-G (2002) One, two, three: nature's tool box for building plastids. Protoplasma 219:123–130
Stroebel D, Choquet Y, Popot J-L, Picot D (2003) An atypical haem in the cytochrome b6 f complex. Nature 426:413–418
Strömberg CAE, McInerney FA (2011) The Neogene transition from C3 to C4 grasslands in North America: assemblage analysis of fossil phytoliths. Paleobiology 37:50–71
Strzepek RF, Harrison PJ (2004) Photosynthetic architecture differs in coastal and oceanic diatoms. Nature 431:689–692
Summons RE, Jahnke LL, Hope JM, Logan GA (1999) 2-Methylhopanoids as biomarkers for cyanobacterial oxygenic photosynthesis. Nature 400:554–557
Tajika E (2003) Faint young sun and the carbon cycle: implication for the Proterozoic global glaciations. Earth Planet Sci Lett 214:443–453
Tapley DW, Buettner GR, Shick JM (1999) Free radicals and chemiluminescence as products of the spontaneous oxidation of sulfide in seawater, and their biological implications. Biol Bull 196:52–56
Taylor WA, Free C, Boyce C, Helgemo R, Ochoada J (2004) SEM analysis of Spongiophyton interpreted as a fossil lichen. Int J Plant Sci 165:875–881
Thauer RK, Kaster A-C, Seedorf H, Buckel W, Hedderich R (2008) Methanogenic archaea: ecologically relevant differences in energy conservation. Nat Revs Microbiol 6:579–591
Tice MM, Lowe DR (2004) Photosynthetic microbial mats in the 3,416 Myr-old ocean. Nature 431:549–552

Tice MM, Lowe DR (2006) Hydrogen-based carbon fixation in the earliest known photosynthetic organisms. Geology 34: 37–40

Tomitani A, Knoll AH, Cavanaugh CM, Ohno T (2006) The evolutionary diversification of cyanobacteria: molecular-phylogenetic and paleontological perspectives. Proc Natl Acad Sci U S A 103: 5442–5447

Umena Y, Kawakami K, Shen J-R, Kamiya N (2011) Crystal structure of oxygen-evolving photosystem II at a resolution of 1.9 Å. Nature 473:55–60

Van Rensen JJS, Xu C, Govindjee (1999) Role of bicarbonate in Photosystem II, the water—plastoquinone oxido-reductase of plant photosynthesis. Physiol Plant 105:585–592

Wagner-Döbler I, Biebl H (2006) Environmental Biology of the marine Roseobacter lineage. Annu Rev Microbiol 60:255–280

Wang Z, O'Shaughnessy TJ, Soto CM, Rahbar AM, Robertson KL, Lebedev N, Vora GJ (2012) Function and regulation of Vibrio campbellii proteorhodopsin: acquired phototrophy in a classical organoheterotroph. PLoS One 7:e38749. doi:10.1371/journal.pone.0038749

Warburg O, Krippahl G, Jetschma C (1965) Widerlegung der Photolyse des Wassers und Beweis der Photolyse der Kohlensäure nach Versuchen mit lebender Chlorella und den Hill-Reagentien Nitrat und K Fe(Cn). Z Naturforsch B B20:993–996

Wellman CH, Osterloff PL, Mohiuddin U (2003) Fragments of the earliest land plants. Nature 425:282–285

Westall F, Cavalazzi B, Lemelle L, Marrocchi Y, Rouzaud J-N, Simionovici A, Salomé M, Mostefaoui S, Andreazza C, Foucher F, Toporski J, Jauss A, Thiel V, Southam G, MacLean L, Wirick S, Hofmann A, Meibom A, Robert F, Défarge C (2011) Implications of in situ calcification for photosynthesis in a ~3.3 Ga-old microbial biofilm from the Barberton greenstone belt, South Africa. Earth Planet Sci Lett 310:468–479

White SN, Chave AD, Reynolds GT, Gaidos EJ, Tyson JA, Van Dover CL (2000) Variations in ambient light emission from black smokers and flange pools on the Juan de Fuca Ridge. Geophys Res Lett 27:1151–1154

White SN, Chave AD, Reynolds GT (2002) Investigations of ambient light emission at deep-sea hydrothermal vents. J Geophys Res Solid Earth 107 (B1), Art. No. 2001

White SN, Chave AD, Reynolds GT, Van Dover CL (2002) Ambient light emission from hydrothermal vents on the. Mid-Atlantic Ridge. Geophys Res Lett 29, Art. No. 1744

Wilde SA, Valley JW, Peck WH, Graham CM (2001) Evidence from detrital zircons for the existence of continental crust and oceans on the earth 4.4 Gyr ago. Nature 409:175–178

Williams DM, Kasting JF, Frakes LA (1998) Low-latitude glaciation and rapid changes in the Earth's obliquity explained by obliquity-oblateness feedback. Nature 396:453–455

Woese CR (2005) The archaeal concept and the world it lives in: a retrospective. In: Govindjee, Beatty JT, Gest H, Allen JF (eds) Discoveries in photosynthesis. Springer, Dordrecht, pp 1109–1120

Wydrzynski TJ, Satoh K (eds) (2005) Photosystem II — the light-driven water: plastoquinone oxidoreductase (advances in photosynthesis and respiration 22). Springer, Dordrecht

Xiong J, Bauer CE (2002a) A cytochrome b origin of photosynthetic reaction centers: an evolutionary link betweeen respiration and photosynthesis. J Mol Biol 322:1025–1037

Xiong J, Bauer CE (2002b) Complex evolution of photosynthesis. Annu Rev Plant Biol 53:503–521

Yano J, Kern J, Sauer K, Latimer MJ, Pushkar Y, Biesiadka J, Loll B, Saenger W, Messinger J, Zouni A, Yachandra VK (2006) Where water is oxidized to dioxygen: structure of the photosynthetic Mn4 Ca cluster. Science 314:821–825

Yin Q, Jacobsen SB, Yamashita K, Blichert-Toft J, Télouk P, Albarède F (2002) A short timescale for terrestrial planet formation from Hf-W chronometry of meteorites. Nature 418:949–952

Yoshi Y (2006) Diversity and evolution of photosynthetic antenna systems in green plants. Phycol Res 54:220–229

Yuan X, Xiao S, Taylor TN (2005) Lichen-like symbiosis 600 million years ago. Science 308:1017–1020

Yutin N, Koonin EV (2012) Proteorhodopsin genes in giant viruses. Biol Direct 7(34):6

Zahnle KJ, Catling DC, Claire MW (2013) The rise of oxygen and the hydrogen hourglass. Chem Ecol 362:26–34

Zhang BP, Janicke MT, Woodruff WH, Bailey JA (2005) Photoreduction of a heme peptide encapsulated in nanostructured materials. J Phys Chem B 109:19547–19549

Zhaxybayeva O, Lapierre P, Gogarten JP (2005) Ancient gene duplications and the root(s) of the tree of life. Protoplasma 227:53–64

Photosynthetic Light Harvesting

17

Tihana Mirkovic and Gregory D. Scholes

17.1 Introduction

A prominent example of photobiology is light-initiated energy conversion—the process of photosynthesis. The photochemical energy transduction of photosynthesis starts with photoinitiated electron transfer reactions that occur on picosecond and longer time scales. Here we will focus on the photoinitiation process, which is called light harvesting. Sunlight is absorbed by chromophores such as chlorophyll bound at high concentration in proteins. Electronic energy transfer (EET) transmits the excitation energy to reaction centers wherein the electron transfer reactions are initiated. We recommend specialist reviews (Green and Parson 2003; Sundström et al. 1999; van Grondelle and Novoderezhkin 2006; Novoderezhkin and van Grondelle 2010; Scholes et al. 2011; Renger and Müh 2013; Cheng and Fleming 2009; Fassioli et al. 2014) for more detailed information on the biophysics of light harvesting. Here we will provide an introductory account in the context of photobiology.

Light-harvesting complexes are comprised of chromophores, light-absorbing molecules, usually bound into a protein scaffold. Photosynthesis is initiated by the absorption of light by the chromophores, which excites a molecule from the ground state to an electronic excited state. The excited state of a molecule like chlorophyll is short lived compared to usual biological processes, relaxing to the ground state with a time constant of about 4 ns in vivo (Connolly et al. 1982; Mullineaux et al. 1993). Before the molecule can return to its ground electronic state, the electronic excitation must be "harvested." That is, the excitation is transferred through space among the chromophores until it eventually reaches a reaction center where it initiates charge separation. That is the process of EET.

A map of the organization of light-harvesting complexes around reaction centers in a thylakoid membrane representative of higher plants or green algae (Croce and van Amerongen 2011) is shown in Fig. 17.1a. We show the reaction center from photosystem II, stripped of the protein scaffold in the lower part of Fig. 17.1a. Surrounding the reaction centers are major and minor chlorophyll-containing antenna complexes that bind, in total, about 200 chlorophylls per reaction center. Light harvesting involves the absorption of sunlight by any of these chlorophyll chromophores and subsequent transfer through space of that electronic excitation to the special pair of a reaction center. This process effectively concentrates the excitation at reaction centers so they can be cycled significantly more frequently than would be possible by direct excitation in sunlight—that is, the so-called antenna effect.

Light-harvesting complexes are not restricted to this particular design. Indeed, there is a wide variety of light-harvesting antenna structures in nature (Fig. 17.1b). They differ in the arrangements of chromophores as well as chromophore types. In addition to the various chlorophylls, other chromophores such as bilins and carotenoids tune the absorption spectra so that light can be harvested from the blue wavelengths all the way to the near-infrared, depending on the organism. All antenna complexes are able to convert the photogenerated excitations to charge separation with high efficiency (Blankenship 2002). Quantum efficiencies—the probability of converting an absorbed photon into a charge separated state—depend on antenna size, light conditions, and the organism. They are documented to be in the range 50–90 %, for example, the light harvesting to charge separation efficiency is in the range 84–90 % for photosystem II of higher plants (Jursinic and Govindjee 1977; Wientjes et al. 2013).

T. Mirkovic
Department of Chemistry, University of Toronto,
Toronto, ON, Canada
e-mail: tmirkovi@chem.utoronto.ca

G.D. Scholes (✉)
Department of Chemistry, University of Toronto,
Toronto, ON, Canada

Department of Chemistry, Princeton University,
Washington Rd., Princeton, NJ 08544, USA
e-mail: greg.scholes@utoronto.ca, gscholes@princeton.edu

L.O. Björn (ed.), *Photobiology: The Science of Light and Life*,
DOI 10.1007/978-1-4939-1468-5_17, © Springer Science+Business Media New York 2015

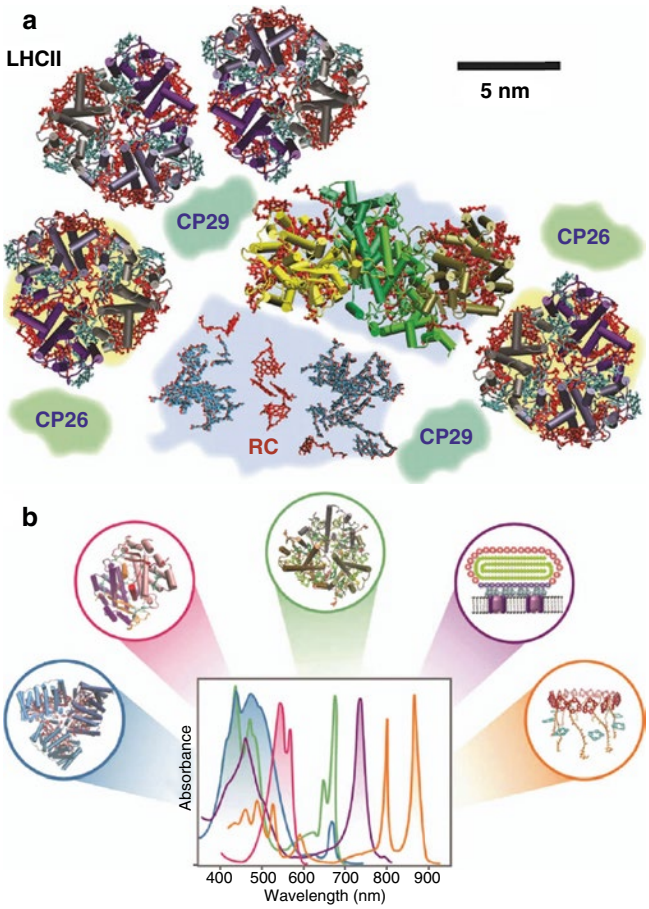

Fig. 17.1 (**a**) Structural organization of light-harvesting complexes and reaction centers in higher plants and green algae. Excitation energy captured by the LHCII and the minor peripheral light-harvesting complexes is transferred, via core light-harvesting complexes CP43 and CP47, to the reaction center where charge separation is initiated (Adapted from Scholes et al. (2011)). (**b**) Variation in light-harvesting antennae commonly encountered in photosynthetic organisms, which vary widely in their protein structure and the number and arrangement of pigments utilized. The molecular structures (with parent organisms in brackets) from left to right are peridinin-chlorophyll-protein or PCP (of *Amphidinium carterae*), phycoerythrin 545 (of *Rhodomonas* CS24), light-harvesting complex LHCII (of *Spinacia olearia*), schematic representation of a chlorosome (of *Chloroflexus aurantiacus*), and light-harvesting complex LH2 (of *Rhodopseudomonas acidophila*). Their respective absorption spectra, shown in matching colors, illustrate how different organisms have evolved to optimize their light-harvesting capabilities in different regions of the visible spectrum (Adapted from Scholes et al. (2012))

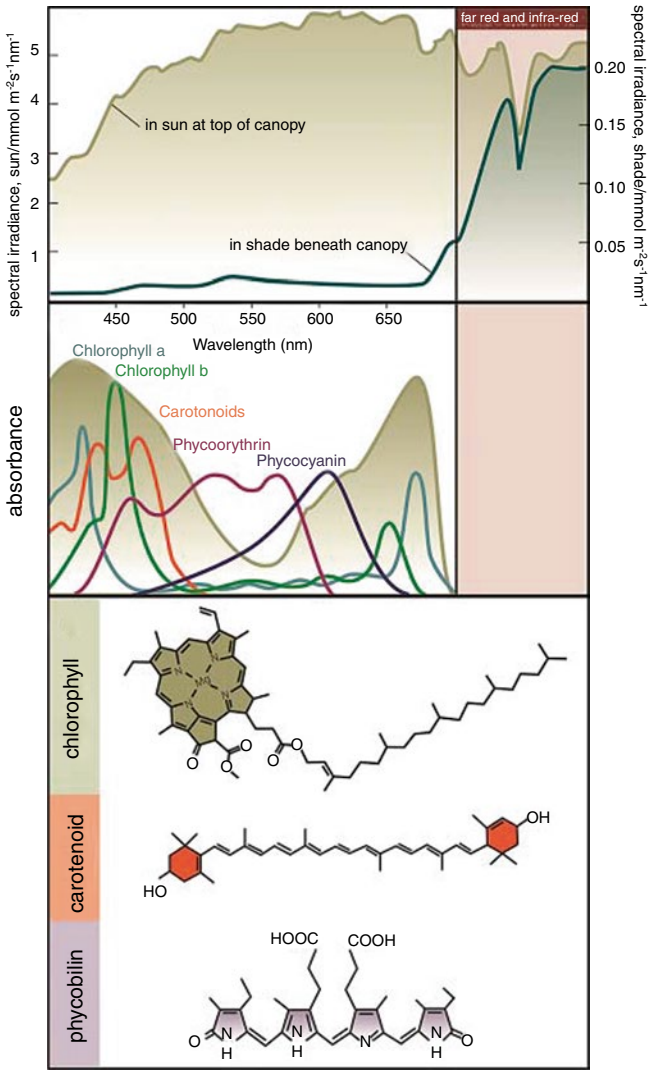

Fig. 17.2 (**a**) Spectral distribution of sunlight at the top of plant canopy and in the shade beneath it. (**b**) Action spectrum (illustrated as shaded spectrum) of photosynthesis for a higher plant (spectrum adapted from Campbell and Reece 2005) and absorption spectra of pigments involved in photosynthetic light-harvesting. (**c**) Schematic illustration of chlorophyll, carotenoid, and phycobilin structures

17.2 Light Quality and Pigments

The variation in the quality of light, or spectral composition, and the varying light intensity in different environments are vast, yet photosynthetic organisms have adapted to thrive in diverse conditions. The fluence rate at the top of the plant canopy can be over 100 times higher than in the shade beneath the canopy, when comparing in the visible part of the spectrum (Fig. 17.2a). Water provides a particularly interesting stratified environment based on available light. Blue light penetrates significantly deeper than red light in clear water (see Chap. 7).

An additional consideration is that not all wavelengths of light can support photosynthesis with the same efficiency, which is illustrated in the photosynthetic action spectrum (Fig. 17.2b; cf. Chap. 8). The action spectrum shows the yield of photosynthesis (e.g., oxygen production) as a function of excitation wavelength. It can be thought of as the relative effectiveness of different photon energies at generating electrons. The action spectrum reveals clearly the spectral cross section of light harvesting. Thriving in various light conditions requires diversification of light-harvesting complexes as well as nimble adaptation to prevailing conditions.

In all photosynthetic organisms, initial light absorption is performed by special organic pigments, which chemically and structurally can be broadly subdivided into three major groups: chlorophylls (Sects. 9.2, 9.3, 9.4, and 9.5), carotenoids, and phycobilins (Fig. 17.2b, c and Sects. 9.6 and 9.7). In green plants, for example, the action spectrum is in close agreement with the absorption spectrum of chlorophylls and carotenoids with prominent bands in the violet-blue and red region of the spectrum. The middle of the visible spectrum is reflected and transmitted, giving leaves their green color. So, why would plants evolve to reflect green light (Kiang et al. 2007)? Suggestions have been made that chlorophyll absorption is exactly complementary to bacteriorhodopsin, a purple pigment which was utilized in the earliest photosynthetic aquatic bacteria. It is believed that organisms that subsequently optimized their photosynthetic machinery relied on chlorophyll systems to capture available light after sunlight was filtered by bacteriorhodopsin. Reviews (Björn et al. 2009; Mauzerall 1973) have highlighted that biosynthetic pathways for metal porphyrins, which were utilized in electron transport, already existed prior to photosynthesis, and implementation of the existing precursor for the production of chlorins via porphyrins was a clear evolutionary advantage. Björn (1976) also suggested that the optimal absorption position for the light-harvesting pigment would be around 700 nm, as evidenced by the exclusive dominance of chlorophylls which use only the excitation energy from the red part of the spectrum to drive water-splitting and ferredoxin-reducing photochemistry. It is believed that this ability to efficiently absorb red light was the evolutionary driving force to select Chl *a* as the most abundant pigment in photosynthesis (Granick 1965; Björn et al. 2009). Later, as light did not present a limiting resource for photosynthesis in plants, lack of evolutionary pressure did not result in innovation of novel light-harvesting machineries which would utilize a wider part of the solar spectrum, and the family of chlorophyll pigments remains the most abundant in photosynthesis today.

Blue-green light is absorbed by phycobilins (Fig. 17.2b) and coincides with the action spectrum of red algae and cyanobacteria. These organisms can live in deeper waters where the longer wavelength light used by green plants is already filtered out. Owing to the high nitrogen content of phycobiliproteins, their production can be very costly whenever nitrogen is limiting. Thus, in the interest of energy conservation, higher plants, which are exposed to an abundance of light when growing on land, do not utilize phycobiliproteins for the capture of green light (Björn et al. 2009).

Considering the enormous variety of photosynthetic organisms, the diversity of chromophores utilized for light harvesting is not that large. There are certainly far fewer chromophore types than LHC "designs." So what structural and functional characteristics have led to the optimization of these classes of pigments? The basic structure of a chlorophyll molecule is similar to the heme part of hemoglobin, containing a porphyrin-like ring structure, coordinated to a central magnesium atom (Fig. 17.2c). The structural variation among the different chlorophylls originates from the differences in side-chain substitutions on the ring, which ultimately affect the absorption characteristics of the different pigments. The yellow-orange carotenoid chromophores, which display a triple peak in the 400–500 nm region, coinciding with chlorophyll Soret band absorption, are bicyclic and based either on α-carotene (one β and one ε ring) or β-carotene (two β rings). The open-chain tetrapyrrole bilins resemble a split porphyrin structure that has been twisted into a linear conformation.

All the pigments are based on π-electron systems, cyclic or linear, and they are all characterized by exceptionally high molar extinction coefficients, typically on the order of 1×10^5 M^{-1} cm^{-1}. In linear conjugated molecules, such as carotenoids and π-conjugated polymers, scaling laws predict that the dipole strength of the lowest allowed electronic transition will be correlated to the length squared (Tretiak et al. 1999). However, conformation disorder manifest as bond twists and conjugation interruptions is expected at normal temperatures, leading to the plateauing of the scaling at lengths corresponding to 10–15 double bonds (Scholes and Rumbles 2006).

We have so far only considered pigments as separate entities whose primary attribute is absorption strength, but as we are going to find out in the next sections, pigments are only pieces to a big puzzle. The construction of artificial light-harvesting model systems has been hindered by both the development of suitable pigments and the formation of the scaffolding that would circumvent the challenges of organizing large numbers of constituent chromophores. Recent advances have explored the path of developing an architectural platform of multichromophore biohybrid complexes that synergistically combines the bioinspired as well as synthetic building blocks for the formation of versatile assemblies for light harvesting (Reddy et al. 2013; Yang et al. 2013). The rationale behind the design of these biohybrid architectures is that synthesis of the framework structure to accommodate a large number of chromophores in an organized manner is extremely challenging. These limitations are overcome, as the bioconjugate utilizes the framework created by the analogue of a native photosynthetic light-harvesting peptide. The native chromophores, bacteriochlorophylls and their derivatives, on the other hand, have often limited synthetic malleability, but recently developed bacteriochlorins (Yang et al. 2013) are very stable towards diverse reaction conditions and can be tailored in a variety of ways, allowing for wavelength tuning, overcoming limitation that natural systems face in terms of a reduced coverage of the solar spectrum. It was also shown that these oligomeric biohybrid architectures that contain such bacteriochlorins exhibit energy

transfer yields to the native-like BChl *a* target sites on the order of 90 % (Reddy et al. 2013). Key advances in the field of artificial photosynthetic model systems will depend on the realization that in these large molecular assemblies, the role of constituent chromophores expands from primary energy absorbers to efficient energy conduits. Synergetic interactions between parts of light-harvesting assemblies will further dictate the desirable spectral features of participating chromophores. Some aspects of the photophysics governing these constraints will be discussed in the following sections.

17.3 Physical Principles of Antenna Architecture

There is a remarkable variation in antenna structures (Hohmann-Marriott and Blankenship 2011) (Figs. 17.3 and 17.4), but they show some basic principles in common with regard to the architectural assembly of chromophores (Fig. 17.4). Most antenna complexes are realized through pigment-protein associations, where the protein backbone allows for chromophores to be held in precise positions, predetermining the separation and relative orientation of these light-harvesting molecules. The advantage of a three-dimensional arrangement compared to a simple one-dimensional model is illustrated in Fig. 17.3. The efficiency of transferring excitation energy between two remote pigments, assuming equal ratio of donors and traps, in 1D is much smaller, compared to higher dimensional systems owing to the properties of random walks. This statistical problem has been researched in the 1960s, where the model consisted of an infinite lattice of unit cells defined with N points of which $(N-1)$ are occupied by a chlorophyll molecule, while one is represented by a trap (Pearlstein 1966, 1967; Robinson 1967; Montroll 1969). Calculations by Montroll (1969) assumed equal probability of excitation at any nontrapping chlorophyll, and steps were taken to near-neighbor lattice points only. For the limit of $N \to \infty$, the number of steps, n, required to reach the trap was evaluated as follows:

$$\langle n \rangle = \begin{cases} \dfrac{N^2}{6} & \text{linear chain} \\ \pi^{-1} N \log N & \text{square lattice} \\ 1.5164 N & \text{single cubic lattice} \end{cases} \tag{17.1}$$

A downhill energetic ordering of chromophores greatly biases the random walk. This principle is often referred to as an energy funnel, Fig. 17.3c, illustrating how high-energy pigments funnel excitation to energetically lower lying chromophores. In this downhill energy transfer model, excitation moves from the periphery towards the reaction center, and each step is associated with a small loss of energy as heat. The energy cost of the built-in irreversibility in the process is

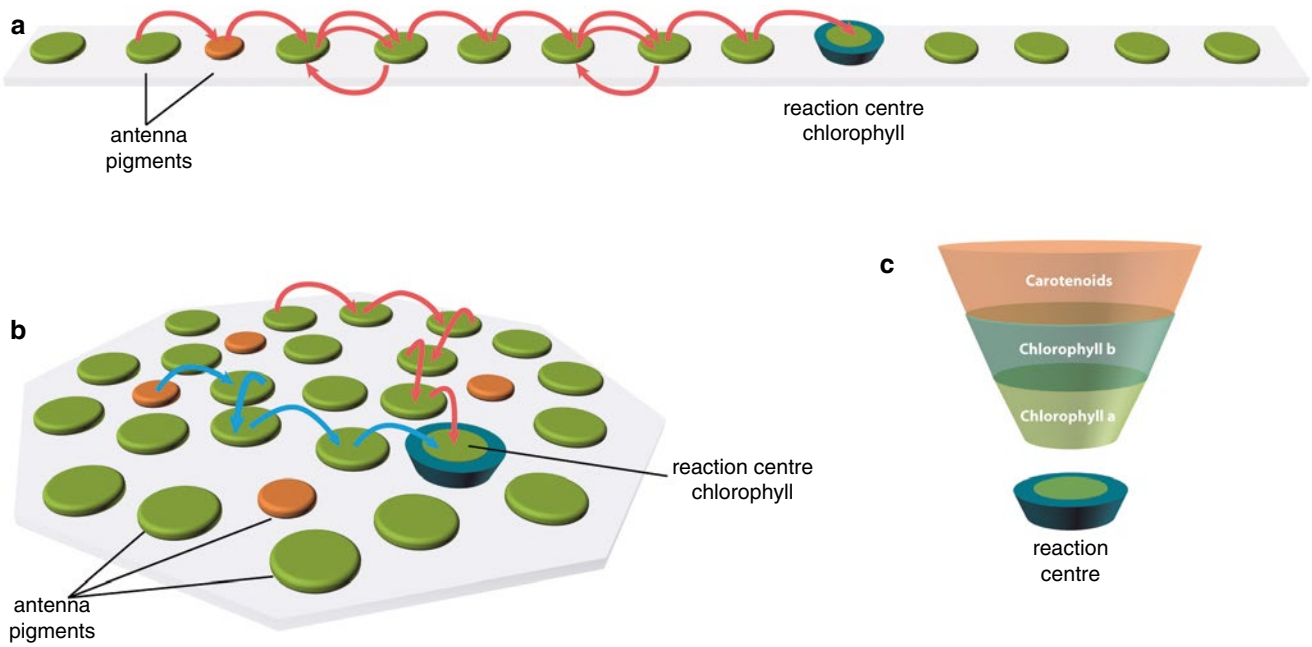

Fig. 17.3 Schematic illustration of excitation transfer paths taken in an inefficient one-dimensional arrangement model (**a**), where far more steps are necessary for the shuttling of the energy to the reaction center, as compared to when the light-harvesting chromophores rely on a three-dimensional spatial distribution (**b**). The funnel analogy of a photosynthetic antenna, where higher-energy pigments at the periphery are excited first and subsequently deliver the excitation energy to red-absorbing chromophores in the proximity of the reaction center

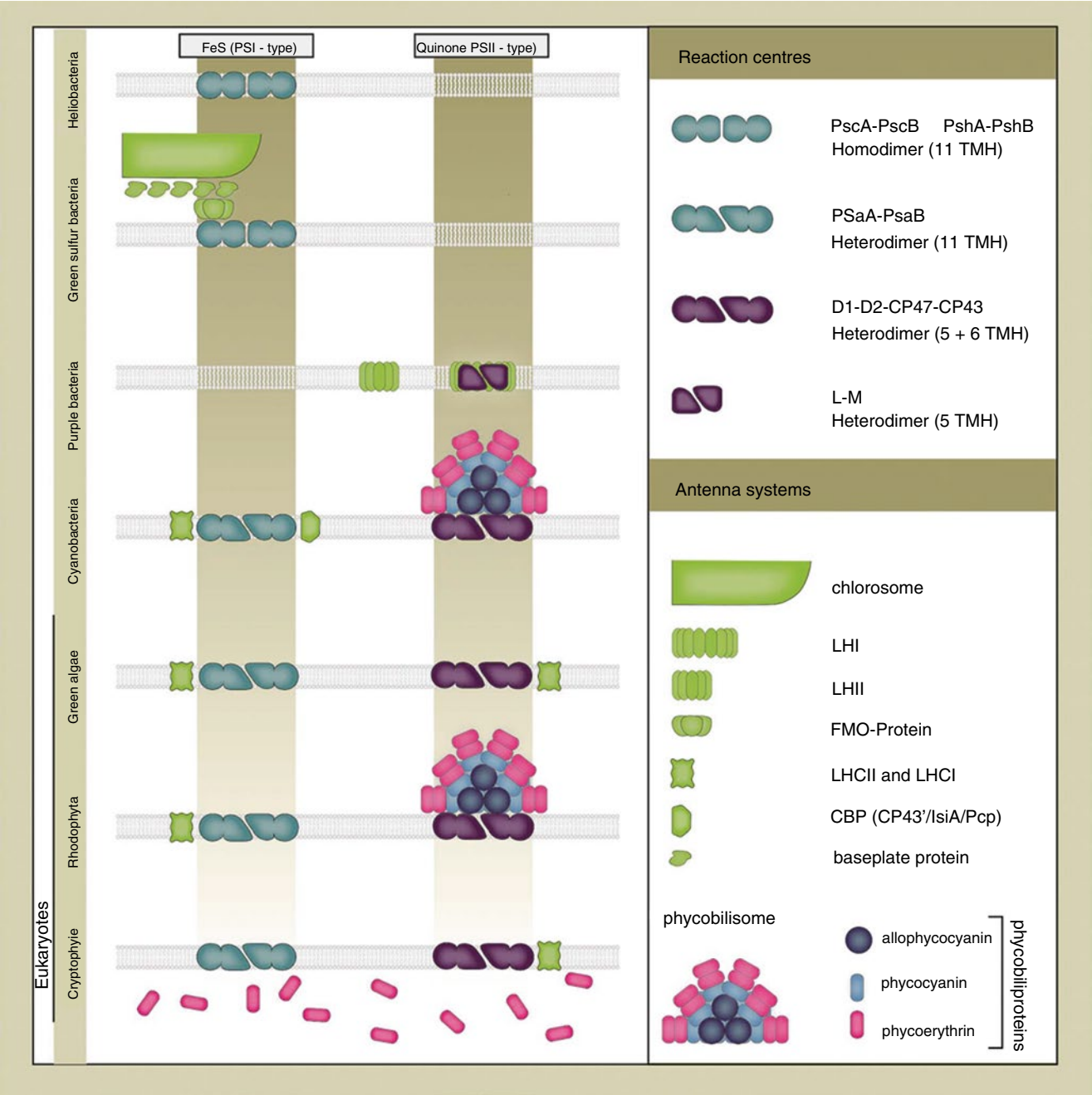

Fig. 17.4 Light-harvesting machinery of some photosynthetic organisms. Abbreviations: *TMH* transmembrane, *LH* light harvesting, *LHC* light-harvesting complex, *CPB* chlorophyll-binding protein

justified, as the net outcome is the concentration of the excitation energy at the reaction center.

Photosynthetic cells generally contain hundreds of thousands of reaction centers and tens of millions of antenna pigment molecules. Often, we think of an elementary unit, a photosynthetic unit (PSU), mentioned above, which represents a set of antenna associated with a particular reaction center, defined by a stoichiometric ratio between the total number of those two components. Theoretical treatments of membranes have focused on either treating all pigments individually, relying on a random walk process, or by grouping them in pools and only treating the interactions between the elementary units. On a microscopic level, describing the interaction among N pigments in a light-harvesting complex would require precise knowledge of the structural details, including the position, orientation, and relative distances. The kinetic properties would have to be evaluated by solving the rate matrix for the system of N coupled states.

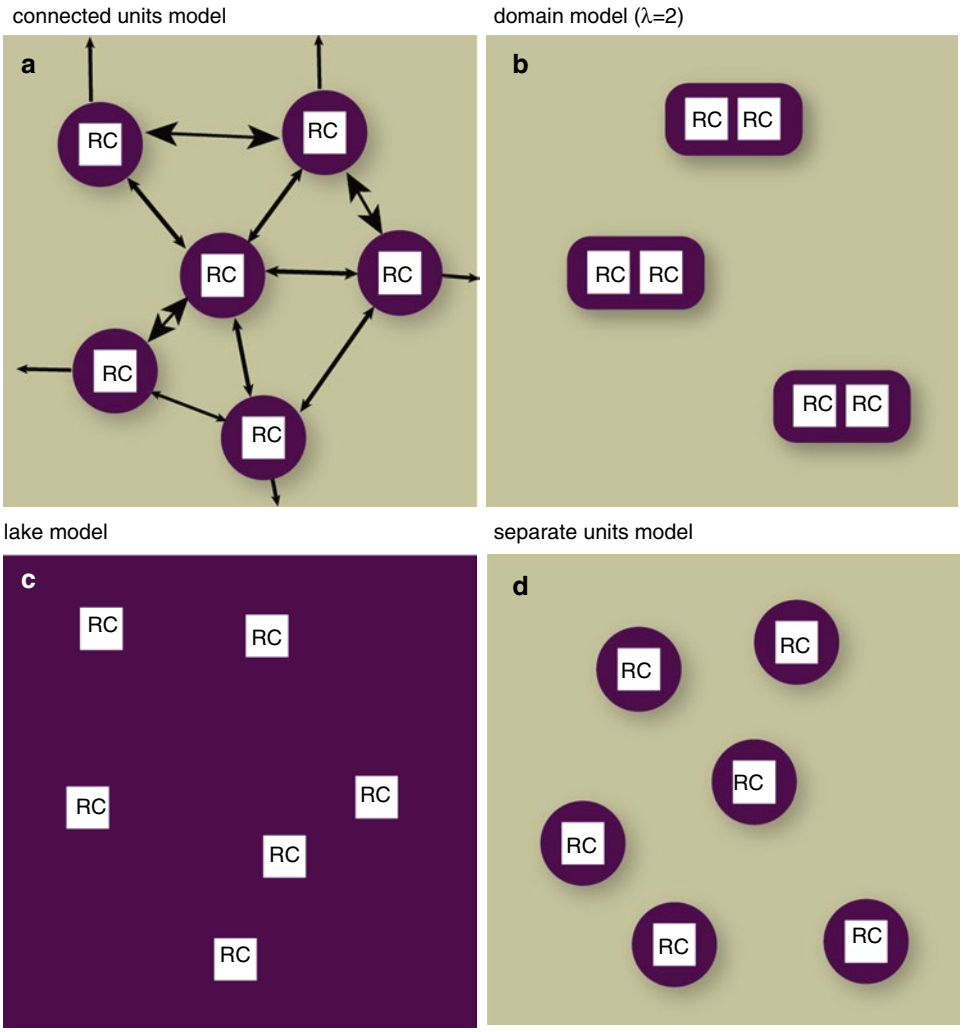

Fig. 17.5 Models of antenna organization. (**a**) Connected units, (**b**) Domain model. In the extreme cases of the separate units (puddle) model (**d**), antenna pigments are associated exclusively with a single RC, whereas in the lake model (**c**) energy absorbed by individual antenna pigments is equally likely to be transferred to any RC (Adapted from Bernhardt and Trissl (1999))

The sophistication and complexity of microscopic models can be circumvented by resorting to simplifying assumptions (e.g., energy transfer within the elementary unit is infinitely fast or the pigments are isoenergetic). That sort of global approach has previously been discussed by Bernhardt and Trissl (1999) by contrasting the "puddle" and the "lake" arrangement (Fig. 17.5). The separate units in the "puddle" model are completely isolated from one another, and their excitons are localized to that specific PSU. The other extreme is illustrated by the "lake" model, where reaction centers are embedded in a matrix of antenna pigments where excitons are free to visit any of the reaction centers. Upon encountering a reaction center that is closed to photochemistry, the energy could be transferred to a reaction center that is open, eventually leading to trapping. This model is applicable to many purple bacteria (Blankenship 2002).

A couple of variations of the intermediate case also exist, where exchange of excitons can occur between different PSUs to a certain degree. In the connected units model, developed by Joliot and Joliot (1964), the puddles are interconnected to a certain degree, but the degree of energy transfer between pigments in different puddles is less probable than between chromophores within the same puddle. In the domain model (Paillotin et al. 1979; Den Hollander et al. 1983), which is mathematically more sophisticated, a group of PSUs with a specific number of RCs are localized in a puddle (mini-lake). This scenario seems to be more obvious for dimeric aggregation of RCs, something observed in green photosynthetic bacteria, where more than one RC associates with a single chlorosome antenna complex well separated from other peripheral antennae (Blankenship 2002).

Fluorescence techniques have been developed to further elucidate these statistical models of PSU organizations. Relationships between the photochemical and fluorescence yields with respect to the fraction of open/closed reaction centers may distinguish between the extremes of a lake and puddle arrangement. Closure of a trap results in the removal of one of the decay pathways, prompting the increase in the fluorescence yield. In the puddle arrangement, the fluorescence intensity linearly increases with the fraction of traps that are

closed, but the relationship in the lake model is a bit more complicated, demonstrating a nonlinear increase of emission as the traps are progressively closed. This shows that in the lake model the diffusion of excitation is strongly facilitated with the final goal of the capture of that energy by an open trap, leading to comparatively lower emission yields in the lake arrangement as compared to the puddle architecture.

Today, our view of the PSU has become considerably more sophisticated, as detailed biochemical and biophysical information on specific complexes have become available. This has enabled the elucidation of the energy transfer events that occur within the PSU. High-resolution crystal structures have been elucidated for several light-harvesting complexes and that has inspired sophisticated models for energy transfer (van Grondelle and Novoderezhkin 2006; Cheng and Fleming 2009; Scholes and Fleming 2006; Renger and Müh 2013). Most recently, models that even include atomistic details of the protein environment have been reported (Olbrich and Kleinekathöfer 2010; Olbrich et al. 2011; Shim et al. 2012; Curutchet et al. 2011).

17.4 Energy Transfer Mechanism

Perrin in 1927 noted the phenomenon of energy transfer while undertaking fluorescence quenching experiments. Observations suggested that interactions between molecules in solution occurred over distances greater than their diameters and in the absence of collisions. It was realized that these interactions that lead to transfer of electronic excitation energy were derived from the Coulombic coupling between transition dipole moments of the molecules. Dipole-dipole coupling has an inverse distance-cubed dependence ($1/R^3$, where R is the center-to-center separation of donor and acceptor chromophores), so it can act to transfer energy between molecules separated by up to several nanometers.

The model was further clarified with the vision of Theodor Förster who realized that in solution, excited molecules undergo multiple collisions with the surrounding matrix, leading to phase decoherence before incoherent energy transfer can occur (Förster 1946). What this means is that spectral lines are quite broad for molecules in solution (or similar condensed phases) and therefore energy is conserved even when transferred between two chromophores with different spectra as long as the fluorescence spectrum of the donor overlaps to some extent with the absorption spectrum of the acceptor chromophore; see the shaded gray region in Fig. 17.6a. We now have a much better understanding of the origins of spectral line broadening; see Sect. 2 of Oh et al. (2011) and references cited therein. These details are significant in more sophisticated theories for energy transfer, but we will not cover that subject here.

Spectral overlap is much less probable for molecules in the gas phase at low temperature because the vibronic transitions are sharp lines, not broad bands. Nevertheless, the gas phase vibronic transitions of donor and acceptor chromophores can be an important ingredient in Förster theory. That is, vibronic progressions in the donor fluorescence spectrum and acceptor absorption provide an important contribution to the spectral overlap (energy conservation during energy transfer), especially when the two chromophores are different. For example, energy transfer from a green- to a red-absorbing molecule is enabled because of the donor fluorescence transitions to vibrations in its ground electronic state and/or acceptor absorption transitions to vibronic levels in the acceptor excited state. The Förster spectral overlap sums over all the ways these energy-conserving coupled transitions can happen.

Förster's interest in the topic of energy transfer was sparked by realizing that energy capture in photosynthesis was much more efficient than would be predicted assuming that photons were directly absorbed by the reaction centers. The highly efficient energy transfer between closely spaced chromophores was described in terms of a "hopping process," where excitation migrates through an antenna complex in a random walk fashion and each step is promoted by weak electronic coupling between the transition dipole moments of the light-harvesting chromophores.

Förster summarized his theory in an expression for the energy transfer rate from the donor to the acceptor, which is dependent on the center-to-center separation R, expressed in units of cm; the relative orientation of their transition dipoles (κ) (Fig. 17.5c); and the Förster spectral overlap integral, J_F (Fig. 17.6b). The rate is (Braslavsky et al. 2008):

$$k^{\text{Förster}} = \frac{1}{\tau_D} \frac{9{,}000(\ln 10) k^2 \phi_D J_F}{128\pi^5 N_A n^4} \frac{1}{R^6} \qquad (17.2)$$

where ϕ_D is the donor quantum yield, τ_D the excited state lifetime of the donor (in same units as $1/k$), n is the refractive index of the surrounding medium, and N_A (in units of mol^{-1}) is Avogadro's number. The Förster spectral overlap (J_F), which has the units of $M^{-1}\,\text{cm}^3$ or $M^{-1}\,\text{cm}^{-1}\,\text{nm}^4$, is derived from the overlap of the area-normalized donor emission spectrum ($F_D(\lambda)$) and the absorption spectrum of the acceptor expressed in extinction coefficients, $\varepsilon_A(\lambda)$ [$M^{-1}\,\text{cm}^{-1}$]. The expression for the Förster spectral overlap integral J_F is as follows:

$$J_F = \int_0^\infty F_D(\lambda)\varepsilon_A(\lambda)\lambda^4 \mathrm{d}\lambda \qquad (17.3)$$

An example calculation for the overlap integral J_F has been illustrated in Fig. 17.6b for the case of phycoerythrin 545 (PE545) (donor) and chlorophyll *a* (acceptor). Note that

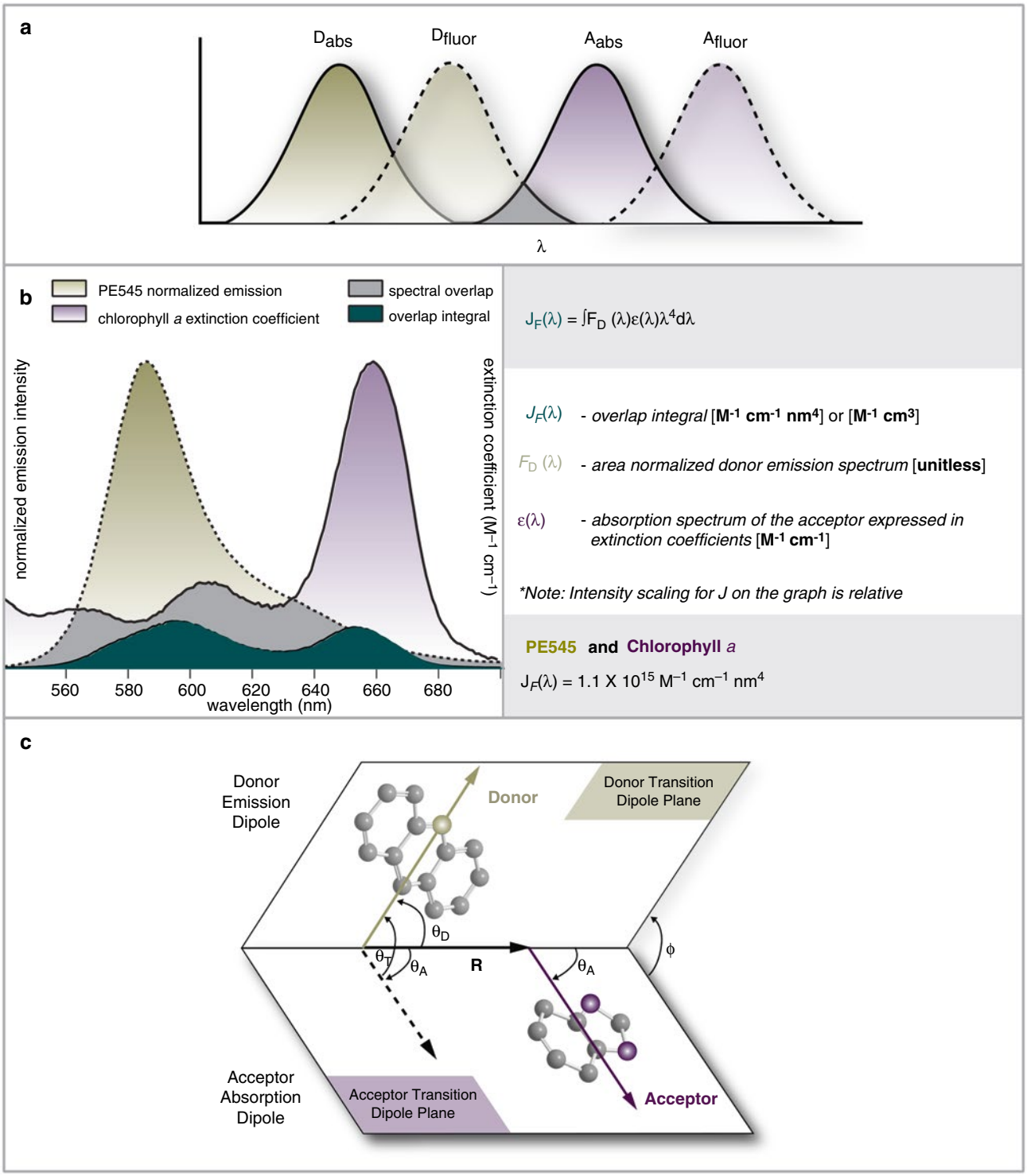

Fig. 17.6 (**a**) Spectral overlap of the donor emission and acceptor absorption required for Förster resonance energy transfer. (**b**) Calculated overlap integral between the emission of phycoerythrin 545 (PE545) and chlorophyll *a*. (**c**) Schematic representation of the angles used for calculating the orientation factor between two dipoles

the scaling for J_F on the graph is arbitrary, as the two *y*-axes are used for the donor and acceptor spectral intensities.

The other key ingredient in Förster theory, indeed all theories for energy transfer, is the electronic coupling. As mentioned above, in Förster theory the electronic coupling is assumed to be a transition dipole-dipole coupling, so it depends on $1/R^3$ and the orientation factor, κ:

$$\kappa = \hat{\mu}_D \cdot \hat{\mu}_A - 3\left(\hat{\mu}_D \cdot \hat{R}\right)\left(\hat{\mu}_A \cdot \hat{R}\right) \qquad (17.4)$$

where $\hat{\mu}_D$ and $\hat{\mu}_A$ represent transition dipole moment unit vectors of the donor and the acceptor, respectively, whereas $\hat{R}$ is the unit vector of the centre-to-centre separation of the transition dipole moments. The vectors and angles used to define the orientational factor are illustrated in (Fig. 17.6c), and the geometric graphic of κ^2 is summarized in the following expression:

$$\begin{aligned}\kappa^2 &= \left(\cos\theta_T - 3\cos\theta_D \cos\theta_A\right)^2 \\ &= \left(\sin\theta_D \sin\theta_A \cos\phi - 2\cos\theta_D \cos\theta_A\right)^2\end{aligned} \tag{17.5}$$

Despite the general success of Förster theory, numerous studies employing high-resolution structural models, ultrafast spectroscopy, and quantum chemical calculations indicate that only a few cases of energy transfer within photosynthetic light-harvesting complexes can be correctly characterized by conventional Förster theory. Chromophores in light-harvesting systems are generally found at very high concentration (up to 0.6 M in pigment-protein complexes), with a high degree of architectural organization. Even though pigment distances have been optimized to minimize electron transfer, which requires overlap of molecular wave functions, it is expected that the interaction energies of neighboring chlorophylls, located 0.5–2 nm apart, would vary widely and that the variation in the coupling strength would have a direct impact on the quantum mechanical characteristics of energy transfer kinetics. That has motivated developments that extend the original Förster theory (Beljonne et al. 2009; van Grondelle and Novoderezhkin 2006; Ishizaki and Fleming 2012; Cheng and Fleming 2009).

There are three principle ways that energy transfer theories need modification to predict energy transfer in light-harvesting complexes. First, electronic coupling must be calculated without invoking the dipole approximation, because of the close intermolecular separation described above. Second, the presence and role of molecular exciton states as excitation donors and acceptors need to be considered. That is usually done using generalized Förster theory (GFT) (Scholes and Fleming 2000; Mukai et al. 1999; Jang et al. 2004) or modified Redfield theory (Yang and Fleming 2002; van Grondelle and Novoderezhkin 2006). Third, solvent screening of the electron coupling should be considered (Scholes et al. 2007; Curutchet et al. 2011). More subtle, yet highly interesting, corrections are needed to account for dynamical effects of coherence (Scholes 2010; Ishizaki and Fleming 2012; Lambert et al. 2013).

The electronic coupling between the donor and acceptor chromophores, which promotes electronic energy transfer processes in photosynthetic light harvesting, can be partitioned into a long-range coulombic contribution (sometimes also referred to as electrodynamic interaction), V^{ed}, and a short-range term, V^{ioo}, which is dependent on interchromophore orbital overlap (Scholes 2003; Olaya-Castro and Scholes 2011) and becomes very significant below 5 Å. The coupling term, V^{total}, at all separations can be expressed as the sum of the two contributions:

$$V^{total} = V^{ed} + V^{ioo} \tag{17.6}$$

In Förster theory, the weakly coupled chromophores are assumed to be well separated compared to their size, so that the short-range term V^{ioo} is neglected, and the Coulombic coupling can be approximated as a point dipole-dipole interaction. This model that centers on the localized donor-acceptor states is, for example, applicable to the weakly coupled B800 ring of purple bacterial LH2 (Krueger et al. 1998). The main problem with the dipole-dipole approximation is that it works well only when the separation between chromophores is large compared to the size of those molecules (or if the molecules and their arrangement are symmetric, like a "sandwich" dimer of anthracene molecules). When the dipole approximation fails, we need to account more realistically for the shape of the transition densities of the chromophores when we calculate the Coulombic coupling between them. A straightforward approach is to use the transition density cube (TDC) method developed by Krueger and co-workers (Krueger et al. 1998). How and why this is useful is reviewed elsewhere (Scholes 2003; Scholes and Fleming 2006).

Interchromophore orbital overlap effects V^{ioo} influence the electronic coupling when molecules are very close. The main case where they matter is when the transitions on the molecules—de-excitation of the donor and excitation of the acceptor—are spin forbidden (Andrews et al. 2011). Triplet-triplet energy transfer and the closely related energy transfer from triplet chlorophyll to sensitize singlet oxygen are processes in photosynthesis mediated by V^{ioo}.

17.5 Summary and Further Reading

We recommend specialist reviews for more detailed information on the biophysics of light harvesting (Green and Parson 2003; Sundström et al. 1999; van Grondelle and Novoderezhkin 2006; Novoderezhkin and van Grondelle 2010; Scholes et al. 2011; Renger and Müh 2013; Cheng and Fleming 2009; Fassioli et al. 2014). One of the topics that has generated great interest recently is the question of coherence in light harvesting. In other words, is the incoherent hopping model, where excitation energy jumps randomly from molecule to molecule, sufficiently accurate to capture the details of light harvesting? It is clear this model does not work when chromophores are relatively strongly electronically coupled. We suggest the interested reader to refer to these reviews—and references cited therein—for more information (Fassioli et al. 2014; Scholes et al. 2011, 2012; Cheng and Fleming 2009; Ishizaki and Fleming 2012; Huelga and Plenio 2013).

Acknowledgments This work was supported by DARPA under the QuBE program, the United States Air Force Office of Scientific Research (FA9550-13-1-0005), and the Natural Sciences and Engineering Research Council of Canada (G.D.S.).

References

Andrews DL, Curutchet C, Scholes GD (2011) Resonance energy transfer: beyond the limits. Laser Photonics Rev 5:114–123

Beljonne D, Curutchet C, Scholes GD, Silbey RJ (2009) Beyond Forster resonance energy transfer in biological nanoscale systems. J Phys Chem B 113:6583–6599

Bernhardt K, Trissl HW (1999) Theories for kinetics and yields of fluorescence and photochemistry: how, if at all, can different models of antenna organization be distinguished experimentally? Biochim Biophys Acta 1409:125–142

Björn LO (1976) Why are plants green? Photosynthetica 10:121–129

Björn LO, Papageorgiou GC, Blankenship RE, Govindjee (2009) A view point: why chlorophyll a? Photosynth Res 99:85–98

Blankenship RE (2002) Molecular mechanisms of photosynthesis. Backwell Science, Malden

Braslavsky SE, Fron E, Rodriguez HB, Roma ES, Scholes GD, Schweitzer G, Valeur B, Wirz J (2008) Pitfalls and limitations in the practical use of Forster's theory of resonance energy transfer. Photochem Photobiol Sci 7:1444–1448

Campbell NA, Reece JB (2005) Biology, 7th edn. Pearson Benjamin Cummings, San Francisco

Cheng Y-C, Fleming GR (2009) Dynamics of light harvesting in photosynthesis. Annu Rev Phys Chem 6:241–262

Connolly JS, Janzen AF, Samuel EB (1982) Fluorescence lifetimes of chlorophyll a: solvent, concentration and oxygen dependence. Photochem Photobiol 36:559–563

Croce R, van Amerongen H (2011) Light-harvesting and structural organization of photosystem II: from individual complexes to thylakoid membrane. J Photochem Photobiol B 104:142–153

Curutchet C, Kongsted J, Munoz-Losa A, Hossein-Nejad H, Scholes GD, Mennucci B (2011) Photosynthetic light-harvesting is tuned by the heterogeneous polarizable environment of the protein. J Am Chem Soc 133:3078–3084

Den Hollander WTF, Bakker JGC, van Grondelle R (1983) Trapping, loss and annihilation of excitations in a photosynthetic system. I. Theoretical aspects. Biochim Biophys Acta 725:492–507

Fassioli F, Dinshaw R, Arpin PC, Scholes GD (2014) Photosynthetic light harvesting: excitons and coherence. J R Soc Interface 11:20130901

Förster T (1946) Energiewanderung und Fluoreszenz. Naturwissenschaften 6:166–175

Granick S (1965) Evolution of heme and chlorophyll. In: Bryson V, Vogel HJ (eds) Evolving genes and proteins. Academic, New York, pp 67–88

Green BR, Parson WW (2003) Light-harvesting antennas in photosynthesis. Kluwer, Dordrecht

Hohmann-Marriott MF, Blankenship RE (2011) Evolution of photosynthesis. Annu Rev Plant Biol 62:515–548

Huelga SF, Plenio MB (2013) Vibrations, quanta and biology. Contemp Phys 54:181–207

Ishizaki A, Fleming GR (2012) Quantum coherence in photosynthetic light harvesting. Annu Rev Condens Matter Phys 3:333–361

Jang S, Newton MR, Silbey RJ (2004) Multichromophoric Förster Resonance Energy Transfer. Phys Rev Lett 92:218301-1-218301-4

Joliot P, Joliot A (1964) Etude cinetique de la reaction photochemique liberant loxygene au cours de la photosynthese. C R Acad Sci Paris 258:4622–4625

Jursinic P, Govindjee (1977) Temperature dependence of delayed light emission in the 6 to 340 microsecond range after a single flash in chloroplasts. Photochem Photobiol 26:617–628

Kiang NY, Segura A, Tinetti G, Blankenship RE, Govindjee, Cohen M, Siefert J, Crisp D, Meadows VS (2007) Spectral signatures of photosynthesis: coevolution with other stars and the atmosphere on extrasolar worlds. Astrobiology 7:486–487

Krueger BP, Scholes GD, Jimenez R, Fleming GR (1998) Electronic excitation transfer from carotenoid to bacteriochlorophyll in the purple bacterium *Rhodopseudomonas acidophila*. J Phys Chem B 102:2284–2292

Lambert N, Chen Y-N, Cheng Y-C, Li C-M, Chen G-Y, Nori F (2013) Quantum biology. Nat Phys 9:10–18

Mauzerall D (1973) Why chlorophyll? Ann N Y Acad Sci 206: 483–494

Montroll EW (1969) Random walks on lattices. III. Calculation of first-passage times with application to exciton trapping on photosynthetic units. J Math Phys 10:753–765

Mukai K, Abe S, Sumi H (1999) Theory of rapid excitation-energy transfer from B800 to optically-forbidden exciton states of B850 in the antenna system LH2 of photosynthetic purple bacteria. J Phys Chem B 103:6096–6102

Mullineaux CW, Pascal AA, Horton P, Holzwarth AR (1993) Excitation-energy quenching in aggregates of the LHC II chlorophyll-protein complex: a time-resolved fluorescence study. Biochim Biophys Acta Bioenerg 1141:23–28

Novoderezhkin VI, van Grondelle R (2010) Physical origins and models of energy transfer in photosynthetic light-harvesting. Phys Chem Chem Phys 12:7352–7365

Oh MHJ, Salvador MR, Wong CY, Scholes GD (2011) Three-pulse photon-echo peak shift spectroscopy and its application for the study of solvation and nanoscale excitons. Chem Phys Chem 12:88–100

Olaya-Castro A, Scholes GD (2011) Energy transfer from Förster-Dexter theory to quantum coherent light-harvesting. Int Rev Phys Chem 1:49–77

Olbrich C, Kleinekathöfer C (2010) Time-dependent atomistic view on the electronic relaxation in light-harvesting system II. J Phys Chem B 114:12427–12437

Olbrich C, Jansen TLC, Kleinekathöfer C (2011) Quest for spatially correlated fluctuations in the FMO light-harvesting complex. J Phys Chem B 115:758–764

Paillotin G, Swenberg CE, Breton J, Geacintov NE (1979) Analysis of picosecond laser induced fluorescence phenomena in photosynthetic membranes utilizing a master equation approach. Biophys J 25:513–533

Pearlstein RM (1966) Migration and trapping of excitation quanta in photosynthetic units. PhD thesis. University of Maryland, College Park, Maryland

Pearlstein RM (1967) Migration and trapping of excitation quanta in photosynthetic units. Brookhaven Symp Biol 19:8–15

Perrin J (1927) Fluorescence and molecular induction by resonance. C R Acad Sci (Paris) 184:1097–1100

Reddy KR, Jian J, Krayer M, Harris MA, Springer JW, Yang E, Jiao J, Niedzwiedzki DM, Pandithavidana D, Parkes-Loach PS, Kirmaier C, Loach PA, Bocian DF, Holten D (2013) Palette of lipophilic bioconjugatable bacteriochlorins for construction of biohybrid light-harvesting architectures. Chem Sci 4:2036–2053

Renger T, Müh F (2013) Understanding photosynthetic light-harvesting: a bottom up theoretical approach. Phys Chem Chem Phys 15:3348–3371

Robinson GW (1967) Excitation transfer and trapping in photosynthesis. Brookhaven Symp Biol 19:16–48

Scholes GD, Fleming GR (2000) On the mechanism of light harvesting in photosynthetic purple bacteria: B800 to B850 energy transfer. J Phys Chem B 104:1854–1868

Scholes GD (2003) Long-range resonance energy transfer in molecular systems. Annu Rev Phys Chem 54:57–87
Scholes GD, Rumbles G (2006) Excitons in nanoscale systems. Nat Mater 5:683–696
Scholes GD, Fleming GR (2006) Energy transfer and photosynthetic light harvesting. Adv Chem Phys 132:57–130
Scholes GD, Curutchet C, Mennucci B, Cammi R, Tomasi J (2007) How solvent controls electronic energy transfer and light harvesting. J Phys Chem B 111:6978–6982
Scholes GD (2010) Quantum-coherent electronic energy transfer: did Nature think of it first? J Phys Chem Lett 1:2–8
Scholes GD, Fleming GR, Olaya-Castro A, van Grondelle R (2011) Lessons from nature about solar light harvesting. Nat Chem 3:763–774
Scholes GD, Mirkovic T, Turner DB, Fassioli F, Buchleitner A (2012) Solar light harvesting by energy transfer: from ecology to coherence. Energy Environ Sci 11:9374–9393
Shim S, Rebentrost P, Valleau S, Aspuru-Guzik A (2012) Atomistic study of the long-lived quantum coherences in the Fenna-Metthews-Olson complex. Biophys J 102:649–660
Sundström V, Pullerits T, van Grondelle R (1999) Photosynthetic light-harvesting: reconciling dynamics and structure of purple bacterial LH2 reveals function of photosynthetic unit. J Phys Chem B 103:2327–2346
Tretiak S, Zhang WM, Chernyak V, Mukamel S (1999) Excitonic couplings and electronic coherence in bridged naphthalene dimers. Proc Natl Acad Sci U S A 96:13003–13008
van Grondelle R, Novoderezhkin VI (2006) Energy transfer in photosynthesis: experimental insights and quantitative models. Phys Chem Chem Phys 14:793–807
Wientjes E, van Amerongen H, Croce R (2013) Quantum yield of charge separation in photosystem II: functional effect of changes in the antenna size upon light acclimation. J Phys Chem B. doi:10.1021/jp401663w
Yang E, Ruzie C, Krayer M, Diers JR, Niedzwiedzki KC, Lindsey JS, Bocian DF, Holten D (2013) Photophysical properties and electronic structure of bacteriochlorin– chalcones with extended near-infrared absorption. Photochem Photobiol 89:586–604
Yang M, Fleming GR (2002) Influence of phonons on exciton transfer dynamics: comparison of the Redfield, Förster, and modified Redfield equations. Chem Phys 275:355–372

How Light Resets Circadian Clocks

18

Anders Johnsson, Charlotte Helfrich-Förster,
and Wolfgang Engelmann

18.1 Biological Clocks

The daily revolutions of the earth around its axis are responsible for day and night and its annual orbit around the sun for the seasons with their fluctuations in day length. Most organisms have adapted to these diurnal and annual cycles. The strategies and mechanisms used are quite delicate and complicated.

It came as a surprise that photosynthesis and many other processes are, however, *additionally controlled by internal clocks*. Thus, photosynthesis fluctuates not only during the daily light-dark cycle (=LD; see the List of Abbreviations and http://www.circadian.org/dictionary.html) but also when the plants are kept under LL and constant temperature (Hennessey and Field 1991). However, the period length (period for short) of this rhythmic event then deviates from exactly 24 h and is therefore called *circadian* (from Latin circa, about, and dies, day). If in the absence of LD and temperature cycles other 24 h time cues (also called zeitgeber, German for time giver) would control the rhythm, it should show an exact 24 h rhythm. This is not the case, demonstrating the endogenous nature of a clock that is locked to light signals (see Fig. 18.1).

18.1.1 Spectrum of Rhythms

Endogenous rhythms of organisms are not only tuned to the daily cycle of 24 h. The range of rhythms found in organisms covers *ultradian* (with periods of several hours to very short ones), *circadian*, and *annual* (with periods of about a year) rhythms. Other rhythms such as tidal, 14-day, and monthly ones cope with influences of the moon on the earth, mainly on the water movements of the oceans, and they are therefore found in organisms at the coasts and in the sea. Annual rhythms interact with the day-length changes during the year (see below). There are furthermore rhythms with periods covering *several* years. The following discussion of a "biological clock" is restricted to circadian rhythms. Even they are often not just composed of one clock type but form a "circadian system" consisting of two or more clocks with different properties which are or are not coupled mutually (Rosbash 2009; Bell-Pedersen et al. 2005; Panda and Hogenesch 2004).

18.1.2 Function of Circadian Clocks

The term "clock" usually implies a time-measuring device or function. For instance, the day length (or night length) can be determined by an organism. Since day length is a function of the time of the year (long days in summer, short days in winter), it can be used to time certain events such as flowering or tuber formation of a plant or breeding of birds and mammals during the most appropriate season. These processes are denoted photoperiodism (see Chap. 19).

However, a clock can also be used to set a certain temporal order. For instance, the circadian control of our sleep-wake cycle ensures that we rise in the morning and fall asleep in the evening at a preferred time. Food intake and digestion are likewise controlled by this clock and gated to certain times of the day (Silver et al. 2011; Duguay and Cermakian 2009; Forsgren 1935). *The circadian clock will time these events also under constant conditions*.

Furthermore, circadian clocks can serve as alarm clocks. They tell the organism important times of the day. For instance, the alarm clocks of insects such as bees allow them to visit the flowers of a plant at the time they offer nectar and/or pollen. From the standpoint of the plant, attracting certain insects is

A. Johnsson
Department of Physics, Norwegian University of Science and Technology (NTNU), Trondheim, Norway
e-mail: anders.johnsson@ntnu.no

C. Helfrich-Förster
Lehrstuhl für Neurobiologie und Genetik, Biozentrum Universität Würzburg, Würzburg, Germany
e-mail: charlotte.foerster@biozentrum.uni-wuerzburg.de

W. Engelmann (✉)
Department of Botany,
University of Tübingen, Tübingen, Germany
e-mail: engelmann@uni-tuebingen.de

L.O. Björn (ed.), *Photobiology: The Science of Light and Life*,
DOI 10.1007/978-1-4939-1468-5_18,

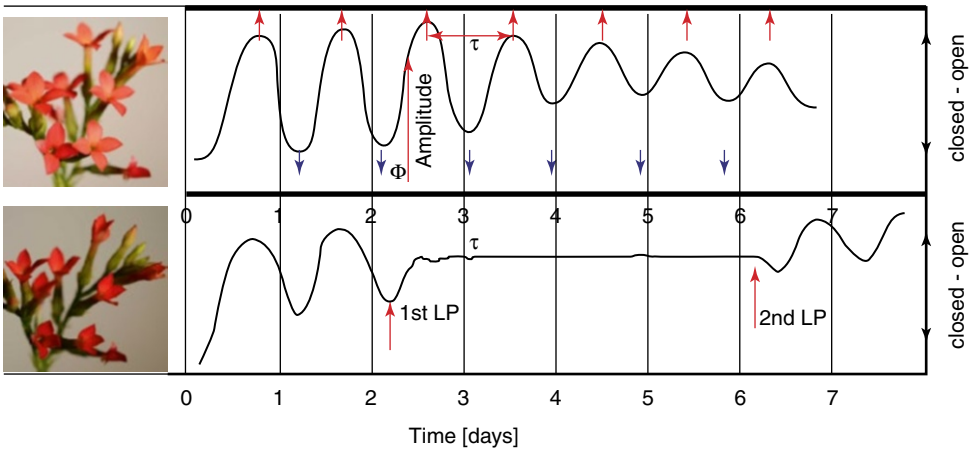

Fig. 18.1 *Top*: petal movement of a single flower of *Kalanchoe blossfeldiana* released from 12:12 h LD cycles in DD for 7 days shows free run of 22 h (whereas in LD the period is 24 h, not shown). Maximal (*short red arrows*) and minimal (*short blue arrows*) opening of flowers, period length τ (*red double-headed arrow*), phase Φ and amplitude (*vertical red line*) are indicated. Second diagram: rhythm annihilating light pulse (1st LP, *red arrow*), which, if given at the proper time (in minimum) and strength, induces arrhythmicity. A second LP (2nd LP, *red arrow*) starts the oscillation again. Insets show open and closed petals of flowers; see also a time-lapse movie (links: http://nbn-resolving.de/urn:nbn:de:bsz:21-opus-66695 and http://nbnresolving.de/urn:nbn:de:bsz:21-opus-66709)

more efficient if timed to their active period. If flowers open at night, pollination by moths or bats is facilitated. Evolution has worked on the plant and the pollinator to bring about this delicate interplay controlled by circadian clocks. This phenomenon is often termed synchronization to the environment.

Alarm clocks might also exist in man. Some humans are able to wake up at a certain time of the night without external help by relying on a "head clock" (Clauser 1954). Although not tested yet, this alarm device might be based on a circadian clock.

Circadian clocks can also be used by insects (Heinze and Reppert 2012; Homberg et al. 2011; Merlin et al. 2011; Reppert et al. 2010; Collett 2008), birds (Muheim 2011), lizards (Foà et al. 2009), fishes (Leis et al. 2011), bats (Holland et al. 2010), and other animals (Ugolini et al. 2007) for navigation and orientation using the direction of the sun. These animals have to take the changing position of the sun or the polarization pattern of the sky during the day into account, and the circadian clock is used as an internal time reference for this sun compass orientation (Able 1995; Schmidt-Koenig 1975). Some birds fly at night and orient by using a star compass, whereby the changing night sky is compensated for (Dacke et al. 2011; Ugolini et al. 2005).

18.1.3 Properties and Formal Structure of the Circadian System

Besides being found in almost all living beings, from prokaryotes to higher organisms, circadian clocks possess a number of formal properties. The clocks:

- Have a period of roughly 24 h (about 18 and 28 h in extreme cases) under constant conditions
- Are synchronized by time cues (mainly daily light and temperature changes) to 24 h function on the cellular level and are heritable
- Are of advantage to the clock bearer
- Have a period that is only slightly dependent on temperature (if constant)

If, for instance, the plant *Kalanchoe blossfeldiana* is kept under constant weak green light conditions, the period of the opening and closing of the four petals of the flowers amounts to 22 h at a temperature of 22 °C (Fig. 18.1). If exposed to an LD 12:12, the flowers open during the light period and close during the dark period. The period of the cycle is now exactly 24 h. Under constant conditions the "free-run" period is 21.9 h at 15 °C, 22.3 h at 20 °C, and 21.3 h at 25 °C (Oltmanns 1960). The differences in period are quite small compared to the influence temperature normally has on chemical and biochemical reactions.

Mutants of organisms are known which differ in clock properties. For instance, the locomotor activity rhythm of the *Drosophila* mutant pers has a period of 19.5 h compared to 24.4 h for the wild type, and the period of the mutant perl amounts to 28.6 h. Another mutant (*per0*) is arrhythmic.

Any useful model of a circadian system has to take the general properties above into account and has to offer mechanisms which lead to the circadian period of about 24 h, to the low temperature dependence of period, to ways of synchronizing the rhythms to the 24 h time cues, etc. We will first discuss modeling of a circadian system (see Sect. 18.1.4) and then focus on some features of the light action on the clocks (see Sect. 18.1.5). Clocks in different organisms will be treated in subsequent sections.

18.1.4 Modeling Circadian Clocks

Published models of circadian systems are of different kinds. Some are purely mathematical ones, describing the variables in, usually, differential equations; others are presented as block diagrams based on concepts from control theory. They often use numerical methods to simulate the circadian behavior. A third form of models describes reactions in words and figures without deriving or attempting quantitative relations (see the selected examples in Sects. 18.2, 18.3, 18.4, 18.5, 18.6, and 18.7).

Ultimately, the models should give precise qualitative and quantitative descriptions and predictions at the molecular, the cellular, and the organism level.

It is important to model not only the circadian system proper but also the inputs particularly the light pathways – and also the outputs of the clock.

The Light Input to the Clock The detailed way in which light affects a circadian system is important for a model. Light signals from the environment are perceived in photoreceptor molecules and organs which might differ widely between organisms. These photoreceptors have to be identified for each system. After photons are absorbed, the excitation energy affects the clock via a signal chain. The details of these pathways have to be known and the way in which the transformed light signal enters the clock has to be determined. Modeling requires specific knowledge for each circadian system under study.

The Circadian System and the Feedback Concept In models for circadian systems, the concepts of positive and negative *feedback* and of time *delay* are frequently used. *Feedback* simply means that a signal in the system is fed back to one or several points in the system and affects the production or the destruction of the signal itself. Control theory tells that feedback in a system might lead to oscillations, in particular if the signal in the feedback loop is delayed in a suitable way.

In several relevant models the feedback links can easily be visualized: often this "circular process" is denoted TTFL (for transcription-translation feedback loop) in the present context. The time delays which exist in the system could be due to transcription, translation, transport, and production or decomposition of clock-related components (see Sects. 18.2, 18.3, 18.4, 18.5, 18.6, and 18.7).

A simple description of a feedback oscillator is as follows: let $c(t)$ represent the concentration of an oscillating central variable in the clock (e.g., the protein FRQ). In a feedback model the signal $c(t)$ in the loop is delayed in a suitable way before feeding back to reinforce (amplify) an already existing signal and induce oscillations. If we assume that the substance is produced at time t according to the concentration of the same substance $c(t)$ at a certain earlier time $c(t-t_0)$, we have a simple feedback system with delay t_0. The situation can be expressed as

$$\left(\text{Production of substance at time } t\right) = -K \times \left(\text{concentration of substance at time} \left(t - t_0\right)\right)$$

Here K is a positive constant and the negative sign indicates that production is decreased if the concentration was high t_0 hours earlier, while it is increased if concentration was low t_0 hours earlier (inhibition occurs if concentration was high, activation occurs if concentration was low at some time units earlier).

The approach can describe sustained oscillations in the variable c if the delay t_0 and the feedback signal are large enough (i.e., if K is large enough). Furthermore, the period of the oscillations will be about four times the delay time introduced. Circadian oscillations would thus need a delay of about 6 h in the example in order to end up with a 24 h period. Interestingly, experimental results pointing at an explicit delay of about 6 h in a molecular feedback chain of the clock in *Drosophila* has recently been published (see page 39 and Meyer et al. 2006).

Simple models based on explicit feedback and time delay concepts (but using nonlinearities that are always present in biological systems and needed to create sustained and limited concentrations in the systems) have been used to simulate features of circadian rhythms (*Kalanchoe* petal rhythm, Johnsson et al. 1973; Karlsson and Johnsson 1972), photoperiodic flowering in *Chenopodium* (Bollig et al. 1976), and activity rhythm in the New Zealand *weta* (Lewis 1999). The specifications of the TTFL began later with the mechanisms of interaction between mRNA and protein levels (Hardin et al. 1990), and several molecular models have been published (Leloup and Goldbeter 2008; Dunlap et al. 2007; Loros et al. 2007; Mackey 2007; Lema and Auerbach 2006).

Many models of the circadian clockwork have been published, emphasizing different aspects of the oscillating system (Dalchau 2012; Beersma 2005) and different approaches such as used in systems biology (Hogenesch and Ueda 2011; Yamada and Forger 2010; Ukai and Ueda 2010; Hubbard et al. 2009). For the history see Tyson et al. (2008) and Roenneberg et al. (2008).

Output Signals from the Clock It is also important to model reaction sequences downstream of the clock. The period of the circadian system will be reflected in the reactions driven by the clock. Amplitude and phase of the driven reactions might change, but the final reactions that are

observable – the *hands of the clock* – have the same period as the clock. This is stressed since environmental light signals might affect the downstream reactions directly, thereby changing, for instance, their amplitude. Such changes should not be mistakenly ascribed to light effects on the circadian system itself.

The photoreception can be clock controlled by feedback links that change the properties of light receptor systems (for instance, control of the iris muscle in mammals, Fig. 18.10, and leaf position in plants). In addition, light adaptation and other changes of sensitivity to light might increase the level of complexity in modeling the light-induced effects on the circadian clock. Detailed modeling of the light reactions relies of course on experimental investigations of the light perception and transduction of the various organisms.

Posttranscriptional feedback loops (PTFL) have acquired much interest in recent studies, e.g., with respect to KaiC phosphorylation, Sect. 18.2, and also protein oxidation processes (Brown et al. 2012). In such a system the parameters of the overall system will then be dependent on the PTFL and more complex output signals can be found.

Single and Multi-oscillator Models Several important features of circadian systems are modeled on the assumption that one single oscillator controls the clock. A one-oscillator model does not preclude the presence of many cellular oscillators. It only assumes that they are so strongly coupled to each other that they (in most cases) behave as one single unit (a "lumped" model).

However, in multi-oscillator models the circadian system can have new features that are not explainable under the assumption that the system consists of one single oscillator. The circadian system of humans is an example which is often modeled by two interacting oscillators. One of them is then assumed to have its strongest influence on (among other rhythms) the activity rhythm and the other one on (among others) the body temperature rhythm. Usually the two oscillators are coupled and oscillate in phase, but the dual nature of the system can show up in, for example, isolation experiments (without time cues) where the rhythms might display different periods (Oishi et al. 2001; Kronauer et al. 1982; Wever 1979).

Modeling often starts with a simple one-oscillator assumption, an approach that eventually turns out to be too simple. Many circadian systems should be modeled as multi-oscillatory systems, even on a single cell level (Daan et al. 2001; Roenneberg and Mittag 1996). In the case of *Drosophila*, several oscillators are nowadays implicated in more detailed modeling (see Sect. 18.6.3).

It is interesting that after a period of intensive experimental studies of the molecular mechanisms that underlie circadian rhythms, formal modeling of circadian rhythms and their light reactions has gained impact. Many models of the circadian clockwork have been published, emphasizing different aspects of the oscillating system. Not all of them focus on the light perception and the light reactions. We, therefore, do not mention all models here but refer to some papers (Beersma 2005; Ruoff and Rensing 2004; Leloup and Goldbeter 1999; Forger et al. 1999; Lakin-Thomas and Johnson 1999; Jewett et al. 1999a, b; Leloup and Goldbeter 1998; Deacon and Arendt 1996; Goldbeter 1995; Diez-Noguera 1994).

18.1.5 Comments on Light, Photoreceptors, and Circadian Models

As has been emphasized, light is the most important input signal to a circadian system, and there are several general features that must be handled by models such as:

- *Entrainment*: Repetitive light pulses entrain the circadian rhythm ("entrainment," "synchonization," "phase locking"). The external light cycle will function as a synchronizer. This general property of circadian systems has also to be simulated by models of circadian systems. The range of entrainment can be used to test models. Besides light, temperature changes are also entraining circadian rhythms. At the same time, the speed of the circadian clock is only marginally affected by the environmental temperature, because they are "temperature compensated." Models should take care of both facts (see, e.g., Ruoff and Rensing 2004, 1996).
- *Single light pulses*: Single light pulses given to an organism during free-run phase shift, the rhythm and a phase response curve describes its time course. A model should handle this and the light signal pathway into the clock in detail.
- *Acclimation*: Photoreceptors function over a huge range of light intensities. As an example, the human eye covers nine orders of magnitude. Still, the eye senses a contrast ratio of only 1,000. The reason is that the eye adapts to a light level that is interpreted as darkness. It can shift across six orders of magnitude. It takes 20–30 min to adapt from bright sunlight to complete darkness and about 5 min to adapt to bright sunlight from darkness.
- *Masking*: Masking is an immediate response to stimuli such as light and other environmental influences that overrides the influence of the circadian system on behavior and physiology of an organism. Masking effects differ from entrainment of the clock, and techniques can be used to distinguish between both (Rietveld et al. 1993). Nocturnal animals respond to *darkness* by becoming more active (positive masking) and to *light* by becoming less active (negative masking). Diurnal animals show the opposite response (Pendergast and Yamazaki 2011). In fruit flies (Kempinger et al. 2009) and primates (Erkert et al. 2006), nocturnal light can shift the circadian clock and increase nocturnal activity independent of the clock.

- *Damping*: Circadian rhythms might damp out under certain environmental conditions such as LL and/or DD or at too high or too low temperatures. There is apparently a permissive range allowing circadian rhythms to occur.
- *Stopping the clock* by light pulses: In many models phase shifts and amplitude changes brought about by light pulses are concomitant features. Under certain conditions an external light pulse can reduce the amplitude completely, thus stopping the oscillation, and models must cope with this feature. Arrythmicity was indeed found (see Winfree 1970) for certain combinations of irradiance and pulse durations in *Drosophila* (Chandrashekaran and Engelmann 1973), modeled by Leloup and Goldbeter (2001), in *Culex* mosquito (Peterson 1981a, b), and in *Kalanchoe* (Engelmann et al. 1978). The phase at which such an arrhythmicity can be induced was fairly restricted (subjective midnight point; the strength of the pulse has to be such that it is just between evoking a strong or a weak phase response curve). A mathematically and biologically interesting question arises: will a circadian system start oscillating spontaneously again after having been sent into the nonoscillatory state or is it stable? The so-called singularities, limit cycles, etc., have attracted interest with respect to the mathematical structure of the circadian systems. An interesting case of arrhythmicity in the Siberian hamster was reported by Steinlechner et al. (2002) (see page 51).

The necessary synchronization of a circadian clock to the environmental cycle is most frequently achieved by using the LD cycle as time cue, but temperature rises or temperature drops can also function as zeitgeber. In animals non-photic zeitgeber such as feeding, social cues, and other signals can entrain (Silver et al. 2011; Honma and Honma 2009; Satoh et al. 2006; Mistlberger and Skene 2005; Stephan 2002).

If a *Kalanchoe* plant is kept for some days in an air-conditioned chamber with 12:12 h LD and after the last 12 h of light transferred to DD, the circadian opening and closing of the flowers will continue to run with its characteristic period going through subjective day and night cycles. A light pulse would shift this rhythm or not, depending on the phase of the clock at which the pulse is applied. If given before the subjective midnight point, the rhythm will be delayed, if given after this point, the rhythm will be advanced. During the subjective day period, there is normally a "dead zone" where a light pulse is without effect on the rhythm. These phase shifts can be plotted with respect to magnitude and direction by a *phase response curve*. They are based on experiments with light pulses administered at different phases (see Fig. 18.2).

The dominant role of light in this entrainment might be due to the high reliability of light as zeitgeber, whereas temperature changes during day and night are less reliable. However, the beginning of the light period and correspondingly of the dark period does not occur at the same time of the day during the course of the year. During the summer the light period is longer than during the winter, which is quite obvious at higher latitudes. This fact has to be taken into account by the organisms if light is the entraining agent.

Photoperiodic Induction The Bünning hypothesis, according to which the circadian clock is used by organisms to measure day (night) length and initiate photoperiodic events accordingly (Bünning 1936), has been modeled. LD conditions in combination with variations of the circadian clock could be used to predict, e.g., flower induction and hibernation. The modeling thus involves the proper treatment of the light perception for the induction of the photoperiodic events *and* the light perception for the phasing and entrainment of the clock. The two perception mechanisms can of course be unified – only experiments can verify the models proposed. Even simple approaches can in some cases model photoperiodic events fairly precisely, e.g., flower induction in *Chenopodium* as described by Bollig et al. (1976).

Photoreceptors Depending on the organism the photopigments and photoreceptors for resetting the clocks can be quite diverse (Collin et al. 2009; Cermakian and Boivin 2009; Foster et al. 2007 and Table 18.1). In many unicellulars, such as yeast or most algae such as *Ostreococcus* (Sect. 18.3), no special receptor structures have been found (Gotow and Nishi 2008). Instead pigment molecules in the cells are changed by light and a transduction chain finally resets the clock. In animals specialized light receptive organs are used such as the vertebrate eyes or the compound eyes in insects. But often extraretinal photoreceptors serve to perceive the synchronizing light either in addition to or instead of the usual eyes. For instance, in birds the pineal organ is light sensitive and synchronizes the circadian rhythm if the eyes are obscured or denervated or removed. In *Drosophila* flies, the circadian clock neurons in the brain are light sensitive on their own via the blue-light pigment cryptochrome. Furthermore the Hofbauer-Buchner eyelets are extraretinal structures in the brain and serve as additional devices for synchronization (Sect. 18.6).

There are several reasons why organisms use multiple photopigments and photoreceptors (Foster and Helfrich-Förster 2001; Roenneberg and Foster 1997); see also page 39, among them:

- Natural LD cycles do not simply consist of light steps. Instead, light is increasing and decreasing slowly during the twilight of the day.
- If organisms use certain light intensities during twilight as the onset, respectively, end of the day, the day length can be measured accurately and reliably and independently of daily weather conditions.

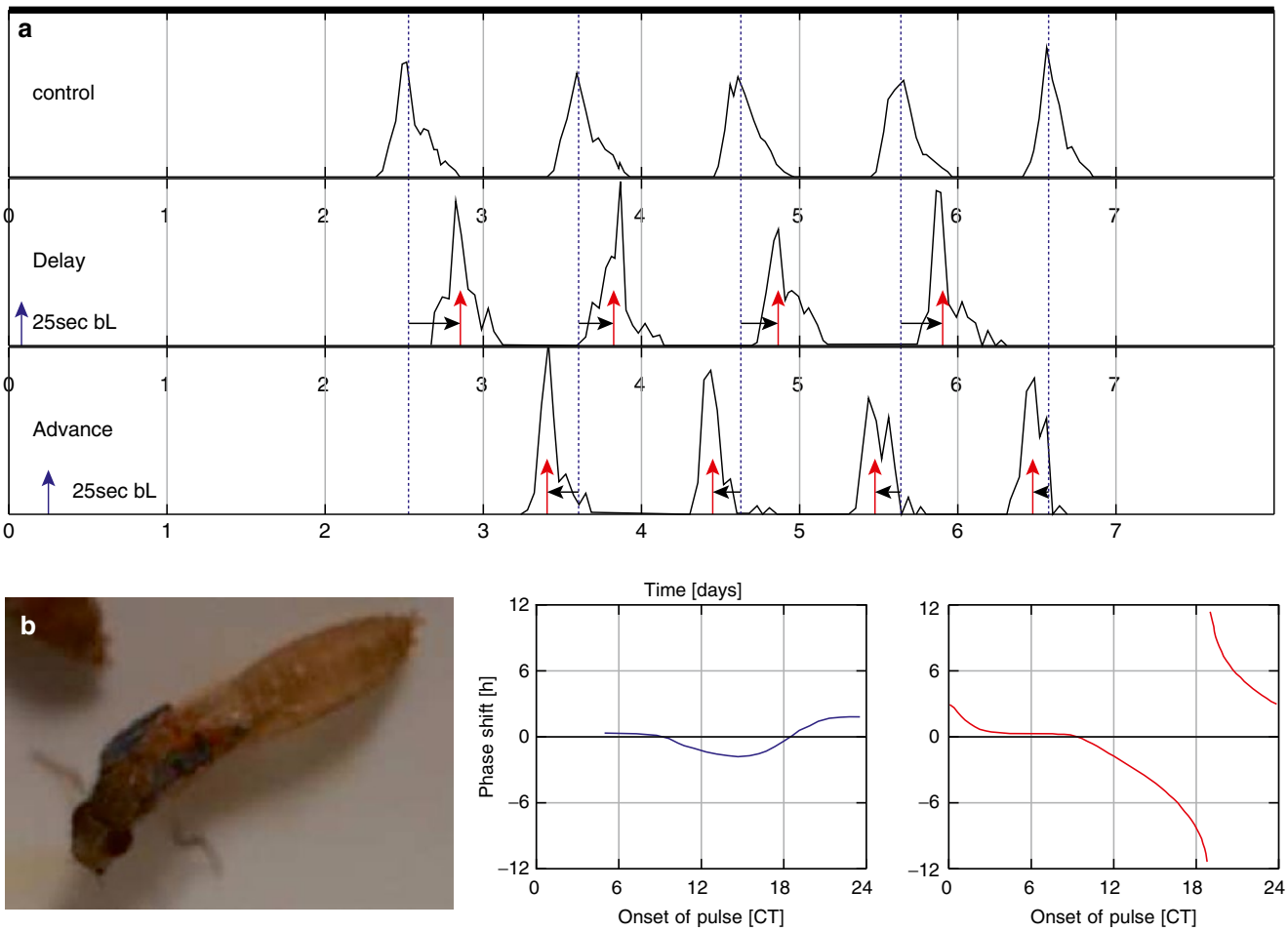

Fig. 18.2 (**a**) Eclosion rhythm of *Drosophila pseudoobscura*. Pupae kept in LD 12:12 h and released in DD at time 0 on first day. *Curves* in upper part show eclosion rate of a control population, the phase-shifting effect of a 25 sec *blue*-light exposure at two different phases (2 and 6 h after onset of DD, marked by *blue vertical arrow*) leading to a delay (→) and an advance (←), respectively (differences between the time of maximal eclosions of control (*blue vertical dashed lines*) and eclosion peaks of light-treated groups (*red arrows*). (**b**) A phase response *curve* plots the magnitude and direction (−values, delay; +values, advance) of the phase shifts against the phase at which the pupae were illuminated. *Left curve* (*blue*) for weak phase responses, *right curve* (*red*) for strong responses. CT is circadian time, CT 0 is the time at which the light period would begin if the LD12:12 would have continued. Inset shows a fly eclosing from the puparium (see also the time-lapse movies, links: [http://nbn-resolving.de/urn:nbn:de:bsz:21-opus-66660] and [http://nbn-resolving.de/urn:nbn:de:bsz:21-opus-66676])

Table 18.1 Chromophores overview of photopigments in various groups in this chapter. See list of abbreviations

Group	Genus	Photopigment (spectral range) → effects	See page
Cyanobacteria	*Synechococcus*	Chlorophyll → energy state of cell	15
Algae	*Ostreococcus*	LOV-HK, Rhod-HK, CRY-photolyase family CPF1, CPF2	20
Algae	*Chlamydomonas*	CRYs, phototropin NPH1	22
Plants	*Arabidopsis*	CRYs, ZTL, phototropins (UV-A) and UVR (UV-B), PHY	26
Fungi	*Neurospora*	WC-1 (FAD/LOV), flavin-binding VVD receptor	32
Insects	*Drosophila*	CRY (LNv), rhodopsin (compound eye, ocelli, HB eyelet)	39
Mammals	Mammals	Melanopsin (ipRGC), rhodopsins (rods, cones)	50

- During twilight at dusk and dawn, not only the intensity of light changes but also its spectral composition. Different qualities of the environmental light can be used by a set of different photoreceptors.
- Entrainment by dawn and dusk is more effective than lights on/off programs in all animals tested so far including man Fleissner and Fleissner (2001).
- The signal-to-noise ratio is reduced if several inputs are used. Photopigments like PHY (Auldridge and Forest 2011), CRY (Chaves et al. 2011), opsins (Foster et al. 2007), and others synchronize circadian rhythms. Properties and functions of relevant pigments are described under the examples for organisms with circadian rhythms (Sects. 18.2, 18.3, 18.4, 18.5, 18.6, and 18.7). Depending on the kind of photoreceptor, different spectral wavelengths are more or less effective in resetting the circadian clock. Using varying fluence rates of colored light, action spectra can be obtained (see Chap. 8) which tell us how many photons of the different wavelengths are needed in order to evoke the same effect (see page 35). The effect of light depends, however, not only on the wavelength and the fluence rate but also on the phase of the circadian clock at which the light was given (see Sect. 18.1.5) and on the duration and shape of the pulses.

18.1.6 Adaptive Significance and Evolutionary Aspects of Circadian Clocks

The adaptive significance of possessing a circadian clock (Johnson 2005) has been demonstrated in cyanobacteria by using mutants with different periods in competition with each other and with the wild strain (Woelfle et al. 2004; Gonze et al. 2002; Johnson and Golden 1999; Ouyang et al. 1998): see also page 15, in *Arabidopsis* (Hut and Beersma 2011; Yerushalmi et al. 2011; Michael et al. 2003; Green et al. 2002), in *Drosophila* (Xu et al. 2011; Rosato and Kyriacou 2011; Kumar et al. 2005; Beaver et al. 2002; Fleury 2000; Klarsfeld and Rouyer 1998), and in mammals (Daan et al. 2011; Tauber et al. 2004; Sharma 2003; Hurd and Ralph 1998; DeCoursey and Krulas 1998).

The different functions of circadian clocks just mentioned are surely not the only reasons why they evolved. Winfree (1986) and others have discussed that early in evolution circadian clocks might have served to protect organisms from adverse effects of light. Circadian timing and light reception might have coevolved and even preceded the evolution of specialized photoreceptors and eyes. Homologies between pacemaking molecules and ancient photopigments from fungi to mammals suggest an evolutionary link between modern clock proteins and ancient light sensing proteins (Tauber et al. 2004; Sharma 2003; Crosthwaite et al. 1997). However, this link is difficult to prove. An interesting example is CRY, which is used as a clock protein in mammals but as a photopigment in *Drosophila*'s clock neurons in the brain. In peripheral clocks of *Drosophila*, CRY appears to fulfill both roles. Furthermore, in higher animals (vertebrates, insects) the retina is not only a photoreceptor organ but harbors at the same time (peripheral) clocks (see Sect. 18.7.4). It would be interesting to know whether primitive eyes (for instance, eye spots) contain circadian clock cells. Among vertebrates, retinal clocks seem to be quite ancient (lamprey Menaker et al. 1997).

Vertebrates show a wide evolutionary variety in their circadian system. They possess a so-called circadian axis (retina, pineal, suprachiasmatic nucleus) with circadian oscillators. In mammals, the pineal as part of this axis does not contain a circadian oscillator. Mammals also lack extraretinal circadian photoreceptors (in the pineal) in contrast to other vertebrates (Bertolucci and Foà 2004). A "nocturnal bottleneck" that could have led to the evolution of mammals and their exceptional circadian system is discussed by Menaker et al. (1997).

18.1.7 Current Concepts and Caveats

To understand how circadian clocks are synchronized by light and other time cues, the mechanisms of circadian oscillators have to be known, as well as the photoreceptors and pigments involved in the entrainment. The clock mechanisms are currently intensively studied (see Sect. 18.2 and the following ones). The prevailing opinion is *that feedback loops* (*TTFLs*) *between clock gene products acting on the promoters of their genes are at the heart of these clocks* (Hardin 2005). Transcription and translation are thus involved in modeling the clock.

However, the picture is probably more complicated, and cautions have been raised (Lakin-Thomas 2006). For instance, these TTFLs might not be the core clocks, but elements between the environmental inputs and the clock mechanism proper (Merrow et al. 1999). Other cases have been reported which make it difficult to accept the presently favored concept of a circadian clock mechanism as a general one. Enucleated *Acetabularia* still has a circadian rhythm of oxygen production (Karakashian and Schweiger 1976), dry seeds of bean plants show circadian rhythms in respiration (Bryant 1972), and some enzymes of human erythrocytes

fluctuate in a circadian way (O'Neill and Reddy 2011; Ashkenazi et al. 1975). What is common to the two last mentioned systems is the complete lack of nucleic acid metabolism. This is an important issue, since several of the recently proposed models of circadian systems use feedback systems in transcriptional and translational events. It might therefore be wise to keep an open eye on alternative mechanisms underlying the circadian oscillators. Of course, there is no guarantee that all circadian clocks use the same mechanism, although their properties are often quite similar.

Proteins could, for instance, be involved in timing mechanisms. We refer to the circadian clock mechanism in *Synechococcus* in Sect. 18.2, to *Ostreococcus* in Sect. 18.3, and to a report of Meyer et al. (2006) on the *Drosophila* clock (page 39). Another interesting case is the diapause of embryos in the eggs of silk moths (*Bombyx mori*), which is broken by exposure to low temperature. The duration of the chilling period is measured by esterase A4 complexing with another enzyme, PIN. After 14 days it dissociates from PIN, the conformation of the esterase A4 changes, and it becomes suddenly active. This enzyme is thus a kind of molecular timer (although here not on a 24 h basis, Kai et al. 1999).

Membranes and electrical activities might also be involved in the clock mechanism. Colwell suggested that neural activities in the suprachiasmatic nucleus (SCN) are required to generate rhythms in gene expression (Colwell 2011); see also results of Nitabach et al. (2005) in *Drosophila*.

Even if TTFLs are not at the heart of all clock mechanisms, it is still possible to build models on the general concept of feedback as discussed on page 6 – the delays and the molecular mechanisms have then to be found among other cellular reactions.

Photic phase response curves are similar in all organisms and this is true for mammals, nocturnal as well as diurnal, including man. However, the amplitude and duration of the advance and delay portion and the presence and length of a dead zone (see page 10) might vary in different species (Rusak and Zucker 1979). This allows for adjustment of the phase and period of the circadian clock to the 24 h day.

We will now discuss the circadian clocks and photoreceptors in selected examples.

18.2 Clocks and Light in Cyanobacteria

The simplest organisms known to possess a circadian clock are cyanobacteria. These prokaryotes are among the smallest, albeit most abundant, organisms on earth and were for a long time not thought to possess a circadian clock. It was assumed that a cell dividing several times per day (e.g., *Synechococcus elongatus* once every 5–6 h, Mori et al. 1996) would have no use for a circadian timing mechanism and that a nucleus is needed.

However, Stal and Krumbein (1985a, b) observed in cyanobacteria a circadian nitrogenase activity in reducing atmospheric nitrogen to ammonia. This enzyme is inhibited by oxygen and has therefore to be protected against oxygen produced during the day by photosynthesis. Evolution solved this dilemma in two ways, by either separating the processes in space or in time (Mitsui et al. 1986). Later it turned out that gene expression, metabolism, and cell division are all driven by a circadian clock (Johnson 2010). Besides *Synechococcus* (Mackey et al. 2011), the circadian rhythms of other cyanobacteria such as *Synechocystis* (Layana and Diambra 2011), *Cyanothece* (McDermott et al. 2011; Bradley and Reddy 1997), and *Prochlorococcus* (Mullineaux and Stanewsky 2009; Axmann et al. 2009; Zinser et al. 2009) were also studied. *Synechococcus* and *Prochlorococcus* dominate the picophytoplankton of the oceans, the latter being probably the most abundant photosynthetic organism on earth. In the following the main properties of the circadian clock, clock-driven processes, and the present view of the molecular clockwork and its light resetting in cyanobacteria are presented. How circadian clocks in cyanobacteria might have evolved is discussed by Johnson et al. (2011), Hut and Beersma (2011), and Simons (2009).

The necessary temperature independence of the period length (Sect. 18.1.5) was indeed found, even in the thermophilic cyanobacterium *Thermosynechococcus elongatus* tested in a temperature range between 35 and 55 °C (Onai et al. 2004). Since chemical reactions are usually temperature dependent with a Q_{10} often around two to three, meaning that the reaction is twice or three times as fast at a temperature 10 °C higher, mechanisms are needed to compensate the temperature effects (proposals; see Hatakeyama and Kaneko 2012; Akiyama 2012; Murakami et al. 2008; Kotov et al. 2007).

The circadian clock should be accurate despite a noisy environment inside and outside the cell. The individual oscillators in cyanobacteria are indeed quite stable. The stability in a population could be due to intercellular coupling, but this has been shown to be negligible theoretically and experimentally (Amdaoud et al. 2007). The high stability of individual oscillators in cyanobacteria must therefore be based on genetical and metabolic grounds.

In spite of the high precision of the clock, it has to be synchronized with the 24 h environment. The main environmental time cues are light and temperature. Lin et al. (1999) showed for *Synechococcus* that temperature pulses in addition to light entrain the circadian clock, but light was the most efficient time cue under the experimental conditions chosen. The rhythm continues if the cultures are transferred to LL or DD conditions, but as in other *diurnal* (i.e., day active versus *nocturnal*) organisms, the circadian period is shorter at higher light intensities and longer under lower intensities (25 h in DD, 22.6 h in LL, Aoki et al. 1997; Kondo et al. 1993).

Light phase shifts the rhythm (Golden et al. 2007), and a preliminary action spectrum has been determined (Inouye et al. 1998). It resembles the absorption spectrum of chlorophyll, indicating that photosynthesis in the thylakoids is responsible for the entrainment and phase shifting of the rhythm. At least, no other photoreceptor as an essential input pathway has been found in screens for phase-resetting mutants, although seven blue-light candidates have been predicted (Mackey et al. 2009). Instead, the phase of the clock seems to depend directly on the energy state of the cell, and the metabolic changes (caused by light) synchronize the clock (Mackey et al. 2011). This was tested by changing the ATP/(ADP + ATP) ratio in an oscillating in vitro system consisting of KaiA, KaiB, and KaiC. The metabolic effects of darkness were simulated by adding ADP to reduce the ratio of ATP/(ADP + ATP). To simulate the return to light, pyruvate kinase was added to convert the ADP to ATP. Phase shifts in the phosphorylation rhythm resulted, and the phase response curve obtained in vitro was similar to the one in vivo (Rust et al. 2011). A model by Rust et al. (2007) mimicked the phase response curve obtained from in vitro experiments. There seems to be a direct sensing of the electron flow by electron carriers of photosynthesis and respiration which synchronize the clock by affecting the ATP/ADP ratio and the oxidative state of the plastochinon pool (see Fig. 18.3 and its legend).

The clock mechanism has been studied intensively, and the results are reviewed in a number of papers, such as Johnson et al. (2011), Mackey et al. (2011), Dong et al. (2010a), Loza-Correa et al. (2010), Taniguchi et al. (2010), Brunner et al. (2008), and Iwasaki and Kondo (2004). In the following we will briefly sketch it and its properties and the inputs and outputs.

The circadian system of cyanobacteria was supposed to consist of a negative feedback loop where the products of a gene cluster of three open reading frames KaiA, KaiB, and KaiC influence the transcription of their genes (Ishiura et al. 1998). It turned out, however, that these Kai proteins form a basic timing process of the circadian clock which, in contrast to the circadian clock mechanisms in eukaryotic organisms, persists even without transcription and translation (Nakajima et al. 2005).

The properties of the circadian rhythm are not ascribed to the Kai *promoters*, but to the Kai *proteins*. Specific regulation of the KaiBC promoter is not essential for the oscillation; even an *Escherichia coli*-derived promoter could do, provided the promoter supports sufficient RNA polymerase activity. A functional clock can be assembled from the KaiA, KaiB, and KaiC proteins in the presence of ATP in a test tube and exhibit its regular circadian period without damping for at least three cycles autonomously. The in vitro rhythm is furthermore temperature compensated, and it reflects the period if proteins from mutations affecting period length are used. The in vivo phase-resetting effect of light can be mimicked in vitro by adding ATP. The KaiABC clock has been studied biochemically, biophysically, and structurally (Murayama et al. 2011; Johnson et al. 2011).

How this protein clockworks is depicted in Fig. 18.3, which has been simplified by concentrating on the mechanisms which are used for the light entrainment of the clock (Kim et al. 2012). For details of the KaiC loop and its phosphorylation and dephosphorylation, see Qin et al. (2010). The players are the KaiC, KaiB, and KaiA proteins. KaiC consists of six monomers of two duplicated domains, CI (=N-terminal ring) and CII (=C-terminal ring). They form a homohexamer, which can be observed under the electron microscope (Mori et al. 2002). Twelve ATP molecules bound between its N- and C-terminal domains. Both domains possess ATPase activity, and the interfaces between CII domains are sites of phosphotransferase activities (Egli et al. 2012). KaiA enhances phosphorylation of KaiC, and KaiB inhibits it. The histidine kinase SasA interacts with KaiC and is necessary for a robust circadian rhythm (Iwasaki et al. 2000). KaiC contains two ATP-/GTP-binding domains which play an important role in the rhythm generation (Nishiwaki et al. 2000).

KaiC phosphorylation is the molecular timer for the circadian rhythm in *Synechococcus*. The energy consumed per day amounts to 15 ATPs only (net, the absolute numbers of ATP molecules hydrolyzed and synthesized over the daily cycle are unknown). The period is mainly determined by the KaiC, since period mutations (ranging from 14 to 60 h (Kondo et al. 1994)) consist of single amino acid substitutions in the KaiC protein.

How this chemical clock could work has been discussed by Naef (2005), and models have been proposed by Kurosawa et al. (2006). Since no distinct phase element was found, the question is, how this timing mechanism enables global circadian gene expression. Apparently, the clock regulates the compaction (condensation or super-coiling status) of the chromosome and in this way controls the access to promoter elements and expression of genes globally, leading to circadian oscillation in many parts of metabolism and physiology (Woelfle and Johnson 2006; Cervený and Nedbal 2009; Nakahira et al. 2004; Smith and Williams 2006; Mackey et al. 2011) and this has been modeled (e.g., Miyoshi et al. 2007). There are at least two classes of clock-regulated genes: about 80 % of the assayed promoters are active during the day with a maximum near the end of day. In the smaller group expression has an opposite phase and is maximal at dawn and at night when the chromosome is compacted and minimal at dusk. These genes may encode, for instance, oxygen-sensitive enzymes, and they perform best at night, when photosynthesis is absent. Chromosome dynamics or DNA topology may thus be phase determining (Min et al. 2004). The global modulation of promoter activity as a result of circadian changes in the topology of chromosomes was termed oscillating nucleoid or oscilloid model (Woelfle et al. 2004).

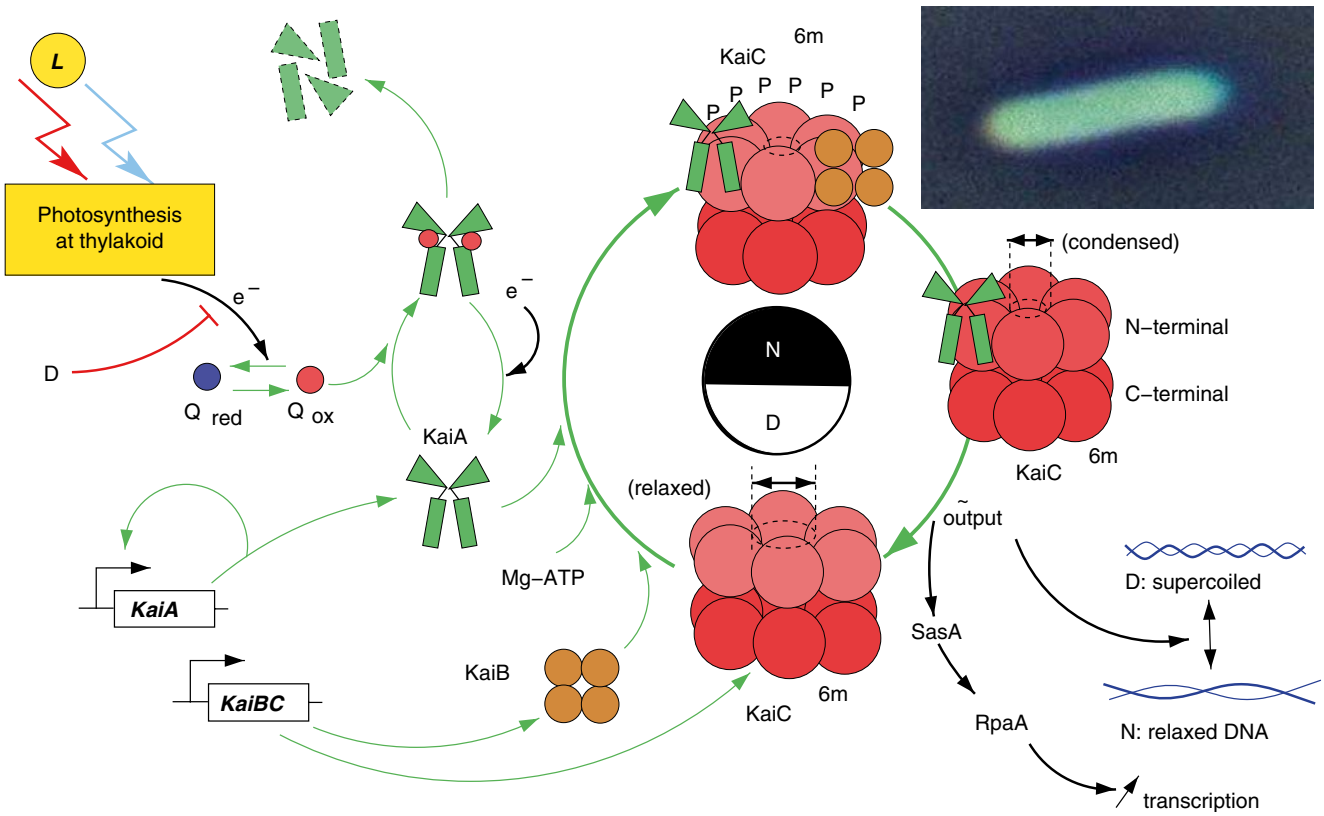

Fig. 18.3 Model of the circadian clock of the cyanobacterium *Synechococcus elongatus* (inset, kindly supplied by Kondo: A cell). The hexameric KaiC protein ($KaiC^{6m}$, *red*) consists of 6 monomeric KaiC proteins ($KaiC^{1m}$ with N- and C-terminal domains at very right) and undergoes during the course of a day (*thick green arrows*, night and day indicated by N and D in *black circle*) conformational changes (*top* and *right*, condensed as indicated by *small dashed ovals*; *bottom*, relaxed with *wider dashed ovals*, both with *double-headed arrow* indicating the width). The cycling of this loop is governed by Mg-ATP phosphorylation during the day due to the KaiA protein (*green* structure; genes in italics). Mg-ATP competes with the hexameric KaiB ($KaiB^{4m}$, *brown circles*) for KaiC. Later the phosphorylated (P's) KaiC becomes dephosphorylated, and the KaiB and KaiA are dissociated by mid-morning (relaxed conformation). Still later, under the influence of KaiA, assembly begins again and a new cycle starts. A rhythmic output (*~bottom right*, *upper black arrow*) pathway transduces temporal information from the oscillator to the genome by switching the coiling structure of the chromosome DNA (*blue waves*) from supercoiled (*top*, day) to relaxed (*bottom*, night): this affects metabolism via high and low amplitude expressing genes. There is furthermore an increase (→) in transcription via SasA and RpaA (*~bottom right*, *lower black arrows*). *Red* and *blue* light (flashes, *top left*) is absorbed by chlorophyll a in the thylakoid membrane (as in the following figures light is an L in a *yellow circle* and its absorption indicated in *yellow*). The photosynthetic electron transport and the respiratory electrons determine the plastoquinone ratio between the reduced (*blue circle* Qred) and oxidized (*red circle* Qox) form. Oxidized plastoquinone binds to KaiA (*green* structure), which aggregate (not shown) and degrade (*light green oval*, broken border) (After Mutoh et al. (2013), Kim et al. (2012), Mackey et al. (2011), Johnson et al. (2011), Qin et al. (2010))

This simple protein clock explains, also, why and how a circadian timing mechanism can function in cyanobacteria with generation times of 8 h or less (Kondo et al. 1997) and how division can still be gated by the circadian clock (Mori et al. 1996).

Using a bacterial luciferase gene as a reporter of clock-regulated promoter activity allowed continuous video recording of the amount of emitted light from many clones on a medium in Petri dishes (Kondo et al. 1993). First, the promoter for the psbAI gene (one of three psbA genes encoding a critical photosystem II reaction center protein, D1) was found to be controlled by the circadian clock. Then it was discovered that virtually all promoters in the genome are regulated by the circadian system. Most of them are activated during subjective day; some, such as the *purF* promoter (purF synthesis), are activated during the night. Division is also controlled by the circadian clock, even if occurring faster than 24 h (Johnson 2010; Dong et al. 2010b).

With low-light-level microscopy, the rhythm in single *Synechococcus* cells could be monitored (Mihalcescu et al. 2004), and recently confocal fluorescence correlation spectroscopy was used to study the dynamics of underlying processes (Goda et al. 2012).

How are all the outputs mentioned coupled to the circadian clock? The temporal information is transmitted from the Kai oscillator to RpaA via the SasA-dependent positive pathway. A further pathway is the LabA-dependent negative pathway. It is responsible for feedback regulation of KaiC. However, the *labA*/*sasA* double mutant has still a circadian *kaiBC* expression rhythm. That indicates a third circadian output pathway, which is CikA dependent. It acts as a negative regulator of *kaiBC* expression independent of the LabA-dependent pathway. The *labA*/*sasA*/*cikA* triple mutant is almost arrhythmic, in spite of a preserved circadian KaiC phosphorylation rhythm. A model was proposed in which temporal information from the Kai oscillator is transmitted to gene expression through these three separate output pathways (Taniguchi et al. 2010).

18.3 Algal Clocks: From Simple to Complex

Circadian rhythms are also found in eukaryotic algae such as *Euglena* (Mittag 2001), *Chlamydomonas* (Schulze et al. 2010), *Acetabularia* (Yang and de Groot 1992), and *Lingulodinium* (Wagner et al. 2005). As an example, we will select an extreme, the smallest known, eukaryote *Ostreococcus tauri* and mention additionally the more complicated and 30 times larger *Chlamydomonas*.

Ostreococcus tauri belongs to the Chlorophyta (class Prasinophyceae) and was discovered in 1994 in the picoplankton of the Thau lagoon in Southern France by Courties and Chretiennot-Dinet (1994). The coccoid cells are haplonts, only about 1 µm small, and the ultrastructure is very simple: they lack a cell wall and contain only a single chloroplast, mitochondrion, and Golgi body besides the nucleus. Other *Ostreococcus* species live in many oceanic regions. High-light and low-light adapted ecotypes of *Ostreococcus* in the Pacific Ocean and the subtropical and tropical North Atlantic have been described by Demir-Hilton et al. (2011). In the marine environment the long wavelengths are absorbed within the first meters of the water. Therefore, specific blue-light receptors such as aureochromes are used to absorb the short wavelengths (Djouani-Tahri et al. 2011a).

The genome has been completely sequenced and annotated (which means that after identification of the elements on the genome, biological information has attached to the sequences). For further information, see also link [http://www.geneontology.org/GO.evidence.shtml||geneontology] and Corellou et al. (2009). It is tiny (13 Mb) and about 20 chromosomes are densely packed (Grimsley et al. 2010; Keeling 2007) containing only ~8,000 genes. A genome-wide analysis of gene expression was conducted under LD conditions by Monnier et al. (2010) and showed that almost all were rhythmic. Transcriptional regulation of the main processes in the nucleus and the organelles, such as DNA replication, mitosis, and photosynthesis, was found to a high extent. Genes involved in handling oxidative stress and DNA repair allow *Ostreococcus tauri* to grow under a wide range of light intensities.

Ostreococcus can be manipulated and propagated easily. Transcriptional and translational luciferase reporter lines are available and allow to record the expression of individual clock genes in vivo and to differentiate between effects on transcriptional and posttranscriptional processes (Djouani-Tahri et al. 2011b; Corellou et al. 2009).

Work by Thommen et al. (2010) and Corellou et al. (2009) suggests that its circadian clock is a simplified *Arabidopsis* clock (see Sect. 18.4.1 and Fig. 18.5). Models with *only one feedback loop* were proposed by Pfeuty et al. (2012) and Troein et al. (2011) to describe the *Ostreococcus* clock (see Fig. 18.4). The reason for using such a simple model is the finding that this alga possesses only two of the clock genes known in land plants such as *Arabidopsis thaliana* (which expresses five homologues of TOC1 and eight of CCA1; see Fig. 18.5). The model is based on a negative transcriptional feedback loop between TOC1and CCA1. The time delay is brought about by the timing of the expression of TOC1 and CCA1. CCA1 represses TOC1 expression during most of the day except during a couple of h before dusk by binding to an evening element sequence (EE) in the TOC1 promoter (Morant et al. 2010). It afterward induces CCA1 transcription, so that CCA1 is expressed in the night and early morning (Corellou et al. 2009; Harmer et al. 2000).

With this model light responses like those resulting from changing the light period from 2 to 22 h in a 24 h day, or skeleton photoperiods (a short light pulse at the beginning and at the end simulates the LD period; see Pittendrigh 1964), have been successfully simulated (Troein et al. 2011; Thommen et al. 2012).

The *Ostreococcus* clock is insensitive to fluctuations in light intensities (clouds, different depths in the water). This is due to the phase response curve (see Sect. 18.1.5), which possesses a broad dead zone in which light does not shift the phase of the rhythm. Only when light hits the oscillator outside the dead zone, it is sensed and re-entrains the oscillator. While synchronized with the LD cycle, the oscillator is blind to light. The light intensities might fluctuate considerably without affecting the clock (Pfeuty et al. 2012).

In *Ostreococcus tauri* a histidine kinase LOV-HK was found as a new class of eukaryotic blue-light receptor (Djouani-Tahri et al. 2011a). It is related to the large family of LOV-histidine kinases found in prokaryotes. It senses blue light and is under circadian control. But it is also important

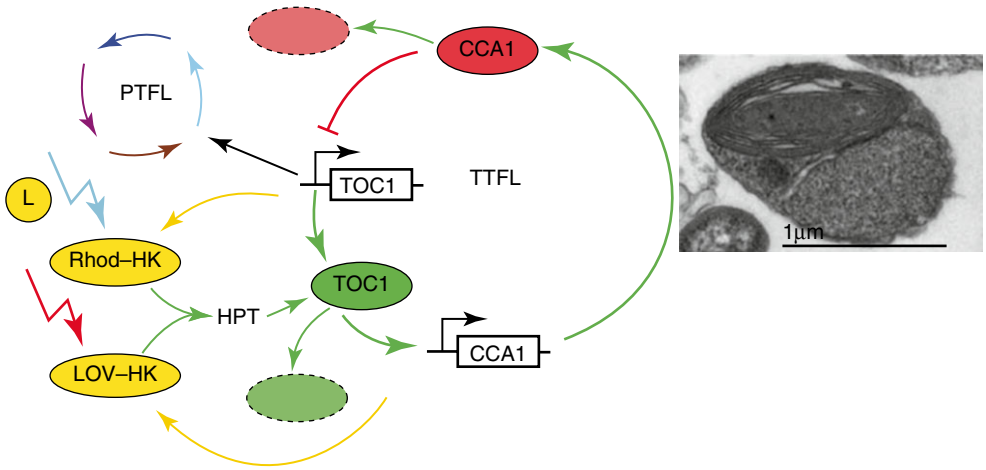

Fig. 18.4 *Ostreococcus tauri* cell (inset) and molecular model of its circadian clock and light inputs. The clock consists of a negative transcriptional/translational feedback loop (*TTFL*) between TOC1 and CCA1. Transcription and translation of TOC1 (*green oval*) activates (*thick green arrows*) transcription of the CCA1 protein which represses (*thick red* – I) TOC1 expression. CCA1 is degraded by proteasomes (*red oval*, broken border) with a maximum during the day. Degradation of TOC1 (*green oval*, broken border) by proteasomes peaks in the dark and is diurnally regulated. This transcription/translation feedback loop (TTFL, *thick arrows/lines*) drives a posttranslational circadian feedback loop (PTFL, ring of differently *colored arrows*, mechanism unknown) and an output of it is seen in the circadian rhythm of the redox state of peroxiredoxin (PRX, not shown). Normally the TTFL and PTFL are coupled, but in DD transcription ceases and the TTFL stops. However, the PRX rhythm persists, because it is driven by the PTFL. Long- (*red flash*) and short-wavelength (*blue flash*) light (L in *yellow circle*) are absorbed by a rhodopsin histidine kinase (Rhod-HK, *oval*), respectively, LOV histidine kinase (LOV-HK, oval) and affect via histidine phosphotransfer (HPT) TOC1. There is furthermore a feedback (*yellow arrows*) from the TTFL to the photoreceptors (After Pfeuty et al. (2012), McClung (2011) and Troein et al. (2011). Inset courtesy of François-Yves Bouget and Marc Lefranc)

for the function of the circadian clock under blue light independent of its blue-light-sensing property. Another histidine kinase, rhodopsin-HK (Rhod-HK), probably senses longer wavelengths than LOV-HK (Pfeuty et al. 2012). Using long- and short-wavelength photoreceptors (see Fig. 18.4) allows the cells to discriminate light variations due to depth changes from those due to the day/night cycling.

Cryptochromes are further blue-light receptors in *Ostreococcus*. Five genes of the Cry/photolyase family (CPF) were identified by Heijde et al. (2010). All five CPF members are regulated by light, and CPF1 and CPF2 display photolyase activity. CPF1 is furthermore involved in the maintenance of the *Ostreococcus* circadian clock.

The molecular basis of light-dependent control of cell division in *Ostreococcus* was studied by Moulager et al. (2010, 2007). They found that the clock regulates directly cell division independently of the metabolism. The transcription of the main cell cycle genes such as cyclins and kinases was under circadian control.

Studies by van Ooijen et al. (2011) and O'Neill et al. (2011) in animals and plants revealed that posttranslational events such as rhythmic protein modifications are also involved in circadian timing. Non-transcriptional mechanisms are able to sustain circadian timing in *Ostreococcus*, although normally it functions together with transcriptional components. Targeted protein degradation in the circadian mechanism seems to play a central role. It was proposed that the oldest oscillator components are non-transcriptional, as in cyanobacteria, and conserved across the plant and animal kingdoms.

Another much studied unicellular green alga is *Chlamydomonas reinhardtii* (Chlorophyta > Chlorophyceae > Volvocales > Chlamydomonadaceae). It is of 14–22 µm size and found worldwide in freshwater but also in the soil. It is used as a model organism for molecular biology; for studies of flagellar motility, chloroplast dynamics, biogenesis, and genetics; and also for its circadian clock. Phototactic movement (swimming towards light) is driven by the flagellae and controlled by a circadian clock (Bruce 1972; Gaskill et al. 2010). This clock furthermore controls UV sensitivity (Nikaido and Johnson 2000), chemotaxis (Byrne et al. 1992), adherence to glass, cell division (Goto and Johnson 1995; Bruce 1970), and starch and nitrogen metabolism. The period length is temperature compensated, as in all circadian rhythms.

Light pulses with a certain fluence rate and wavelength at the breakpoint between delay shifts and advance shifts reduce the amplitude of the rhythm to such a degree that the clock stops its oscillation and reaches a "singularity." The results are interpreted in the context of limit cycle models of circadian clocks and are used to suggest new strategies for measuring action spectra of light-induced clock resetting (Johnson et al. 1992).

The phase-shifting effect of light pulses was studied by Johnson et al. (1991) and Kondo et al. (1991). Blue and red light resets the circadian clock. PHY homologues of higher

plants are not present, but homologues of cyanobacterial PHY (CHLAMYOPSIN5 and MIXED LINEAGE PROTEIN KINASE) and the cyanobacterial kinase CikA and two CRYs with significant homology to the CRYs from plants and animals were found (Mittag et al. 2005). Whether photoreceptor proteins ChR-1 and ChR-2 in the eyespot of *Chlamydomonas reinhardtii* at the outer chloroplast envelope are involved in the phase shift is not known (Hegemann 2008).

The genome of *Chlamydomonas reinhardtii* is entirely sequenced (Matsuo and Ishiura 2011). Subproteome and phosphoproteome analysis were and are used for finding photoreceptors (Boesger et al. 2009). Much work is devoted to the clock network and to clarify how clock-related factors are interconnected. System biology approaches are used for this means, metabalance (May et al. 2009; Manichaikul et al. 2009) and functional proteomics (Wagner and Mittag 2009). Based on elementary flux mode analysis, Schäuble et al. (2011) combined sequence information with metabolic pathway analysis and included circadian regulation. They are able to predict changes in the metabolic state and hypothesize on the physiological role of circadian control in nitrogen metabolism. Review articles of the circadian rhythm of *Chlamydomonas* are by Schulze et al. (2010), Brunner et al. (2008), Mittag and Wagner (2003), Werner (2002), Suzuki and Johnson (2002), and Mittag (2001), and for modeling the *Chlamydomonas* clock, see Jacobshagen et al. (2008), Matsuo and Ishiura (2011), and Breton and Kay (2006).

The germination efficiency of zygospores of *Chlamydomonas reinhardtii* depends on the photoperiod and is higher in long days and lower in short days (Mittag et al. 2005; Suzuki and Johnson 2002). A CO homologous gene (see Sect. 18.4.3) is influenced by day length and by the circadian clock, being more expressed in short photoperiods. Under these conditions algae accumulate more starch and express genes which coordinate cell growth and division (Romero and Valverde 2009). CO orthologs might represent ancient regulators of photoperiodic events. They arose early in the evolutionary lineage leading to flowering plants (Serrano et al. 2009).

18.4 Light Effects on Circadian Clocks in Plants: *Arabidopsis*

To grow and develop successfully, it is essential for plants to synchronize metabolism and physiology with the environment and the seasonal changes. Quite a number of plants can also synchronize the opening of their petals with the activity of visiting insects such as bees and butterflies, which in 1751 led Linnaeus to construct a flower clock: various plants are planted as a kind of clock circle in a round garden bed in such a way that their flowers open or close at the corresponding day- and nighttime. A circadian clock is often responsible for it, and this clock allows also to measure day length to anticipate changes in the surrounding, be it daily or seasonal ones. In both cases, light signals are the main pathways to transfer these transitions to the plant.

Many processes in plants are directly affected by light such as photosynthesis (Chaps. 16 and 17), photomorphogenesis, and photoperiodism (Chap. 19) and stomatal movements. The biological clock processes do not immediately show their light dependence but are synchronizing the plants to the external light program and its period (or rhythm). In general, multiple photoreceptors sense the quality and quantity of light in the environment (Chaps. 12, 13, and 14). Red light is sensed by phytochromes (PHYs), blue light by cryptochromes (CRYs) and ZTL of the ZTL family (ZTL and FKF1). Furthermore phototropins (absorbing in the UV-A/blue, Heijde and Ulm 2012) and UVR8 absorbing in UV-B (Rizzini et al. 2011) are used by plants. This system of different photoreceptors with partially antagonistic functions and overlapping action spectra detects radiation of different wavelengths over a wide spectral range. The PHY and CRY photoreceptors interact with each other and respond at different expression levels and localizations, allowing a simultaneous response to two or more environmental parameters (van Zanten et al. 2012; Kami et al. 2010).

Arabidopsis thaliana plants are well suited for studying the influence of light on circadian clocks, since many biochemical, physiological, and developmental events are under their control. Furthermore, numerous mutants are known, among them quite a number which affect the clockwork, clock inputs, and clock outputs. Besides mutants in which the function of the photoreceptors is affected, others are known, in which the transfer of the light-induced signals is changed (Strasser et al. 2010; Yanovsky et al. 2001).

For continuous recording it has been of much advantage to use a construct of the firefly luciferase gene with a promoter of the cab2 gene which is under control of the circadian clock. The method allows monitoring of circadian rhythms in whole plants but also in different tissues of the plant by recording the bioluminescence with a sensitive camera. It also makes screening of mutations in the clock easy by looking for aberrant temporal patterns of luciferase expression (Millar et al. 1995).

Plants contain circadian clocks in each cell. The clock components consist of interwoven feedback loops, outputs to the clock-controlled genes and driven processes, and inputs from the synchronizing time cues such as light (Fig. 18.5 and Sect. 18.4.1). In addition, posttranscriptional and posttranslational events contribute to the generation and maintenance of the rhythms (McWatters and Devlin 2011; Harmer 2009). Multiple photoreceptors are used by the plants to synchronize the circadian clock. The transduction pathways from light perception to the clock are apparently quite closely linked to the clock mechanism.

Whereas in animals a hierarchy of clock units with circadian centers is the rule, in plants cellular circadian clocks run autonomously in the different tissues and organs and are synchronized by the LD environment. Plant hormones might coordinate these local clocks. More details will be presented in Sect. 18.4.2.

Temperature compensation and the mechanism, by which the circadian clock of *Arabidopsis* avoids changes in period length under different environmental temperatures, has been discussed by Troncoso-Ponce and Mas (2012), Salomé et al. (2010), and Portolés and Más (2010); see also Hatakeyama and Kaneko (2012), Bodenstein et al. (2011), and Eckardt (2010).

18.4.1 Clock Mechanism and Clock-Controlled Genes

The *Arabidopsis* clock is a multi-feedback system with various coupled loops, which receives external inputs such as light and dark signals and possesses output pathways to control transcription, translation, and many physiological and metabolic processes in the plant. The interlocked loops are thought to make the clock more robust, more accurate, and less affected by disturbances of the environment but allow also more flexible inputs in different climates (Harmer 2009; Michael et al. 2003). Figure 18.5 shows a model of the clock (Pokhilko et al. 2012; Lu et al. 2011; Nakamichi 2011) including light inputs (Kolmos et al. 2011; Kim et al. 2007). From the various outputs of the clock (Kami et al. 2010), only the pathway to flowering and hypocotyl growth are indicated (Lu et al. 2012; Kunihiro et al. 2010).

The central loop consists of the clock genes *CCA1* and *LHY* and their products CCA1 and LHY and the clock gene *TOC1* and its product TOC1, a DNA-binding transcription factor. CCA1 and LHY are expressed with peaks shortly after dawn and repress TOC1 expression by binding to the evening element in its promoter. This is the morning oscillator. TOC1 is a DNA-binding transcription factor which peaks at dusk (Gendron et al. 2012). It represses (not activates, as shown by Pokhilko et al. 2012) *CCA1* and *LHY*.

The *ELF3*, *ELF4*, and *LUX* genes and their products ELF3, ELF4, and LUX, forming the evening complex EC, regulate clock gene expression at night. LUX binds directly to the promoters of the target genes *CCA1* and *LHY*, but ELF3 and ELF4 proteins are important for the function of the EC complex. The CCA1 and LHY proteins inhibit the expression of the *ELF3*, *ELF4*, and *LUX* genes thus closing the loop (Chow et al. 2012; Herrero et al. 2012; Nakamichi et al. 2012; Troncoso-Ponce and Mas 2012).

In a third loop, EC is also connected to the morning genes *PRR7* and *PRR9* by repressing them. PRR7 and PRR9 inhibit the expression of *CCA1* and *LHY* by binding to their promoters. CCA1 and LHY in turn regulate *PRR7* and *PRR9* positively.

In a fourth loop, GI induces TOC1 in the evening and is negatively regulated by TOC1, CCA1, and LHY. TOC1 is rhythmically and light dependent degraded by combining with GI and ZTL, and ZTL serves as a light receptor. There is also a dark-dependent protein degradation (Adams and Carré 2011).

A fifth loop was proposed based on the finding that about 90 % of the transcripts of *Arabidopsis* do cycle. This large number is supposed to be due to a dynamic chromatin remodeling by the circadian clock via jumonji C (JmjC), a domain-containing protein, acting as histone demethylase (Lu and Tobin 2011).

The various clock genes, their products, and their interactions are studied intensively, and a final model has not yet been gained. Furthermore, the molecular composition of circadian clocks can differ between various cell and organ types. Thus, PRR3 modulates TOC1 stability in vasculature cell types, but not in others; CCA1 and LHY are not able to inhibit TOC1 expression in dark-grown roots (further examples in Harmer 2010; Hotta et al. 2008).

A circadian clock provides evolutionary advantage by increasing fitness and adaptation. This is shown in *Arabidopsis thaliana* plants which are arrhythmic (by overexpressing CCA1) by a reduced viability under extreme short days (Green et al. 2002) and a higher susceptibility to pathogen infections (Wang et al. 2011). Furthermore, the *ztl* mutant with a longer period and the *toc1* mutant with a shorter period than the wild type contain more chlorophyll and produce more carbohydrates and biomass when grown under LD matching the length of their circadian period (Dodd et al. 2005).

18.4.2 Light as the Main Time Cue of the Circadian Clock

Whereas photoreceptors and the light-regulated responses including gene expression have been intensively studied, the signal transduction components are much less known. A large number of signaling components must exist, which are affected by external and internal factors. Both genetical and biochemical approaches are used to clarify these transduction pathways and modes.

Light is the most important time cue for synchronizing the circadian clock of *Arabidopsis* with the environmental 24 h day. The phase of the clock can be shifted by applying short light pulses in plants kept under constant conditions. The rhythm is delayed, if the light is applied in the first part of the subjective night, and is advanced, if the light is applied in the second part. The phase shifts can be plotted as a phase response curve (Covington et al. 2001). In a similar way, LD

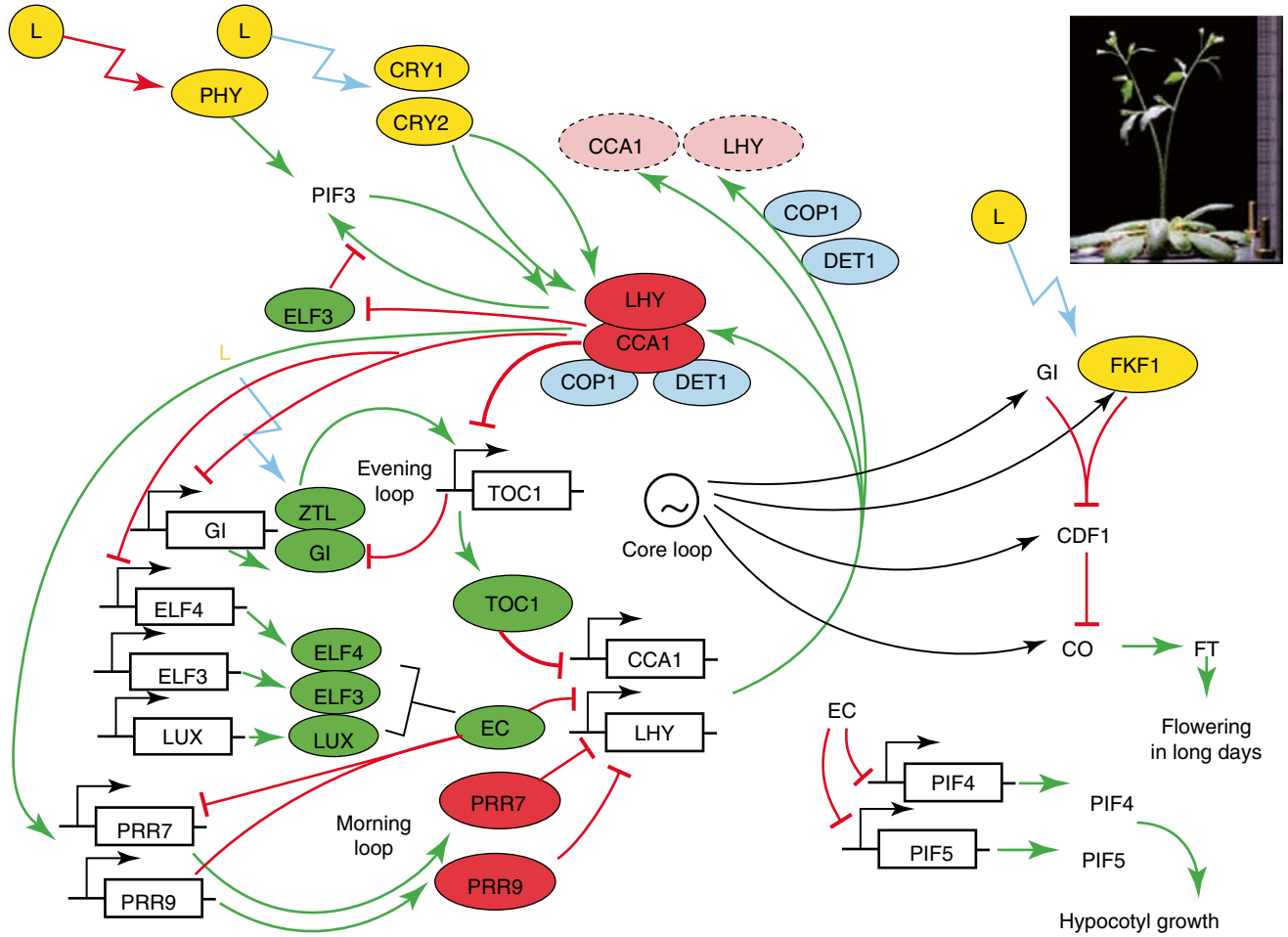

Fig. 18.5 *Arabidopsis* clock and light resetting: *Red* light (*red flash*) is absorbed by PHY, and PIF3 links the light signal to the transcription factors CCA1 (*red oval*) and LHY (*red oval*). *Blue* light (*blue flash*) is absorbed by CRY1 and CRY2, which interact with CCA1 and LHY. In the photoperiodic induction of flowering (*right* part of figure), blue light is absorbed by FKF1 which, together with GI, degrades CDF1 thereby releasing under long day conditions the inhibiting effect of CO. Long days are recognized by a coincidence mechanism based on clock regulation and leads to the formation of the flower hormone FT and flowering. Another clock output, the regulation of the hypocotyl growth via the evening complex EC and its inhibition of the PIF4 and 5 transcription is shown at *bottom right*. Central loop (*thick green arrows* and *thick red* – I) consists of clock genes *CCA1* and *LHY* (*black boxes* with *dented arrows*, TAIR nomenclature for *Arabidopsis*), their products CCA1 and LHY (*red* – I), and the clock gene *TOC1* and its product TOC1 (*green oval*). TOC1 represses (*thick red* a) *CCA1* and *LHY*. The products (*small green ovals*) of *ELF3*, *ELF4*, and *LUX* form the evening complex EC and are the major elements of the evening loop. In a third loop EC represses the morning genes *PRR7* and *PRR9* (*red ovals*). Their products PRR7 and PRR9 inhibit the expression of *CCA1* and *LHY*, and they regulate *PRR7* and *PRR9* positively. In a fourth loop GI (*small green oval*) induces TOC1 in the evening and is negatively regulated by TOC1, CCA1, and LHY. A fifth loop links the circadian clock to the dynamic chromatin remodeling via JMT30 (not shown). Inset shows an *Arabidopsis thaliana* plant exposed at two different times in a space experiment (Johnsson et al. 2009) (After Brown et al. (2012), Pokhilko et al. (2012), Sawa et al. (2007))

cycles synchronize the clock by phase shifting. Red and blue light are most effective, suggesting that PHY and CRY photoreceptors are involved, as indicated by the flashes in Fig. 18.5.

In addition to resetting the phase, light modulates also the period of the clock. Under LL conditions, but not under DD, *phy* and *cry* mutants have a longer period. This indicates that they are within the light input pathway and not part of the central oscillator itself. Otherwise the longer period should also show up under DD. The same applies for mutations in PRR7 and PRR9, where only LL causes a long period, apparently by affecting pathways. However, the *ztl* mutant has a longer period both under LL and DD, which suggests that ZTL plays a role within the central clock. Phototropin1 mutants do not affect the circadian rhythm.

Light signals can also entrain or reset the circadian clock at several points at the transcriptional, posttranscriptional, and posttranslational levels in the various clock loops by affecting the expression, activity, stability, or localization of oscillator components (Kozma-Bognár and Káldi 2008). Transcription of the clock genes LHY, CCA1, PRR7, PRR9, and GI is upregulated by red, far-red, and blue light. However, the corresponding mRNAs of LHY and CCA1 are degraded

by light. In this way timing and entrainment are improved (Jones 2009; Yakir et al. 2007). Translation of LHY is induced by light, and its level depends on the available mRNA, which peaks at dawn. Cyclic removal of clock proteins is crucial for oscillator function, as mentioned before. Thus, proteolysis plays an important role and preferentially takes place in the dark. TOC1 degradation is controlled by the F-box protein ZTL, which binds to it light independent, but the degradation rate is increased in the dark. The mechanism of GI degradation is still unclear.

Which intermediate factors link these photoreceptors with the circadian components and how they do it is not well understood. For instance, the TOC1 protein in the first FBL is stabilized by light and degraded in darkness by an ubiquitin ligase complex, which is regulated by PRR3 and GI. The accumulation of ZTL over the day decreases TOC1 protein levels at the onset of night and increases the robustness of the transcriptional feedback loops of TOC1. Likewise, PRR5 protein accumulates in the evening before it is degraded by ZTL. It is suggested that PRR5, TOC1, GI, and ZTL form a functional unit in the evening loop (see Fig. 18.5, Harmer 2010; Jones 2009). Other candidates for light inputs are ELF3 and ELF4 in one of the feedback loops.

Many questions concerning the *Arabidopsis* clock and how it interacts with light are still open. For instance, most components of the clock act in the nucleus as transcriptional regulators and are together with light-signaling proteins colocalized in nuclear foci (figure 4 in Herrero and Davis 2012) generating rhythmic transcript accumulation. Further information and references can be found in Jones (2009) and Harmer (2010).

Output of the circadian system affects gene expressions, but gene expression is also directly affected by light and not only via the clock (*immediate light effects*). The clock output can furthermore gate the light input according to the phase of the clock by, e.g., affecting the *phy* and *cry* genes at the level of transcription (Toth et al. 2001) or by other types of rhythmic regulation such as the regulation of leaf position. This feature has been termed "Zeitnehmer" (German for time taker, in contrast to "zeitgeber," time giver or time cue).

Under natural conditions the changing day lengths during the course of the year has to be taken into account. That is, neither dawn nor dusk drive the rhythm, but at least two signals must be used. For more information see Chap. 19 and Sect. 18.4.3.

Non-photic time cues are also used by the plant. Temperature cycles entrain the clock. Imbibition of *Arabidopsis* seeds sets a circadian clock which is insensitive to light during the first 60 h. From the 36th hour onward, light initiates a second rhythm which runs independently of the imbibition rhythm (i.e., the output, namely, CAB2 and CAT2, shows the two rhythms superimposed). Light applied after the 60th hour synchronizes the two rhythms (Kolar et al. 1998).

18.4.3 Photoperiodism

Many plants use the seasonal change in day length as a signal for growth (Niwa et al. 2009) and flowering (Millar 1999). In contrast to the effect of light on the circadian clock of *Arabidopsis*, the mechanism of photoperiodic induction of flowering in this plant is known in considerable detail (Srikanth and Schmid 2011; Amasino 2010; Imaizumi 2010; de Montaigu et al. 2010; Michaels 2009).

Plants measure day length in the leaves by a circadian clock. Depending on the type (long-day, short-day, long-short-day, short-long-day plant), the photoperiodic effect occurs under long days; short days; first long days, then short days; or first short day, then long days, respectively. In this way, a developmental switch from the vegetative to the reproductive stage is activated.

Day-length sensing in *Arabidopsis* occurs by an external coincidence mechanism, as predicted already in 1936 by Bünning (1936). It operates by the circadian and light regulation of CO in the leaves, which under appropriate day length induces FT expression, the long-searched florigen (see Fig. 18.5). It is transported to the apical meristem in the shoot, where it promotes flowering. FT combines at the apex with FD, which is present there, but inactive without FT. The FT-FD complex initiates reproductive development (flower evocation). Flower meristem identity genes are activated and flowers are induced according to the ABC (DE) model (Litt and Kramer 2010). Both CO and FT expressions are controlled by a group of transcription factors with overlapping functions (Lu et al. 2012; Imaizumi 2010).

A further prerequisite for flowering of some plants is *vernalization*, by which a prolonged cold period results in meristem competence to flower through the epigenetic repression of the floral repressor FLOWERING LOCUS C (Michaels 2009).

The CO-FT interaction is conserved among plants (Srikanth and Schmid 2011). The photoperiodic responses are conferred by the same genetic pathway in the long-day plant *Arabidopsis thaliana* and the short-day plant rice *Oryza sativa*. But the functions differ (Hayama and Coupland 2003).

18.5 Fungal Clocks and Light Resetting: *Neurospora*

Neurospora crassa (fungi: *Ascomycota*, *Ascomycetes*, *Sordariales*, *Sordariaceae*) was originally thought to be a tropical fungus (see page 34) but is nowadays found all over the world. It is a model organism for genetic and physiological studies, because it is easy to grow and has a haploid life cycle, which facilitates analysis of genetic

recombination. The genome of the seven chromosomes is entirely sequenced (43 megabases long, includes approximately 10,000 genes), and strains of knockouts are available for most identified genes (see Colot et al. 2006 and link: [http://www.fgsc.net/]). A large collection of mutants is available and continuously updated (for further information see link: [http://www.fgsc.net/2000compendium/NewCompend.html‖Collectionofmutants]). Transformation methods are routinely used, and molecular genetics methods such as the use of an inducible promoter for dosage control and RNAi for gene silencing are available (Ziv and Yarden 2010). Imaging techniques are applied (Larrondo et al. 2012; Castro-Longoria et al. 2010; Gooch et al. 2008) including the use of luciferase, GFP, and mCherry. For an overview of modern molecular biological approaches used in *Neurospora* studies, see Jinhu and Yi (2010) and Dunlap and Loros (2005).

Neurospora crassa was used already since the 1950s for studying circadian rhythms (Pittendrigh et al. 1959). The formation of aerial hyphae and asexual macroconidia (generation cycle in *Neurospora*; see Springer 1993) is under circadian control but manifested in many other functions. Rhythmic conidiation shows up in bands which are formed while the mycelium grows over the agar surface in "running tubes" (see link: http://geiselmed.dartmouth.edu/dunlaploros/research/media.php). The period and phase shifts can be determined simply by using a ruler and time markings at the growth front, but more accurate and elaborate imaging methods are also applied (Hogenesch and Ueda 2011; Dunlap and Loros 2005; Morgan et al. 2003).

About 20 % of the genes of *Neurospora* are clock controlled (Smith et al. 2010). This allows modulation of numerous biochemical and physiological processes in a circadian fashion. Pharmacological and genetical approaches have been used in order to unravel the circadian system which underlies overt rhythms such as conidiation (Lakin-Thomas et al. 1990). By the way, in *Neurospora* cytoplasm and nuclei stream through the colony (called syncytium) and the circadian rhythm stays in synchrony.

In the following the circadian system of *Neurospora* and its constituents will be described first (see Sect. 18.5.1 and Baker et al. 2012 for a recent review and a historical account, further reviews by Lakin-Thomas et al. 2011, Jinhu and Yi 2010, Brunner and Káldi 2008, de Paula et al. 2007, Dunlap et al. 2007, Loros et al. 2007). Thereafter (Sect. 18.5.2) it is shown how the circadian system is entrained (Merrow and Roenneberg 2007) by temperature (Brunner and Schafmeier 2006; Diernfellner et al. 2005) and light (Schafmeier and Diernfellner 2011; Price-Lloyd et al. 2005; Kozma-Bognár and Káldi 2008) and which photoreceptors are used (Chen et al. 2010). The outputs of the clock are described (Sect. 18.5.3) and finally a photoperiodic reaction of *Neurospora* is briefly mentioned (Sect. 18.5.4).

18.5.1 The Circadian System of Neurospora and Models

The circadian system of *Neurospora* consists of interwoven negative and positive feedback loops made up by a complicated interplay of various factors which affect the expression and function of the core clock components transcriptionally and posttranscriptionally. Phosphorylations and dephosphorylations of clock components ensure the robustness, precision, and entrainment of the circadian system and account for the complexities in rhythmic behavior (Baker et al. 2012; Schafmeier and Diernfellner 2011; Lakin-Thomas et al. 2011), modeling: Tseng et al. (2012).

A *transcription-translation oscillator* (TTO) has been proposed which possesses all the formal properties of a true circadian oscillator with light entrainment and temperature compensation. The molecular mechanism has been studied intensively (review: Vitalini et al. 2010; Dunlap et al. 2007; Loros et al. 2007). The gene *frq*, its mRNA, and product FRQ are essential components and belong to a negative limb of a feedback loop. In this loop *frq* expression is inhibited by the transcription factor WCC (white color complex). Details are given in Fig. 18.6 and a time line of the clock events in figure 4 of Baker et al. (2012).

In addition to the FRQ-WCC oscillator, there might be a *FRQ-less oscillator* (FLO) which is independent of FRQ and WCC (Lakin-Thomas et al. 2011) and coupled to the feedback loop shown in Fig. 18.6. Strains lacking FRQ (frq^0) or lacking WC-1 (*wc0*) still exhibit circadian rhythms in a choline-requiring strain depleted of choline. The same has been reported for nitrate reductase activity under DD or LL conditions. Apparently in both cases an FLO is the cause for this nutritionally induced rhythm in the absence of an intact FRQ protein.

Furthermore, a *FRQ-less oscillator which requires WC* (WFLO) but is independent of FRQ was proposed by de Paula et al. (2006) and Correa and Bell-Pedersen (2002). This oscillator requires WC-1 and WC-2 for activity. The WC-1 level is rhythmic in the absence of FRQ, indicating that this WFLO generates the rhythm of WC-1. The rhythm can be observed under DD and LL conditions. In contrast to the FRQ-WCC oscillator, its rhythm is apparently not inhibited by high or low light levels. This oscillator and the FRQ-WCC oscillator may interact with each other through their common WC proteins.

How to integrate these diverse oscillators that do not fit the TTO mechanism? This has been discussed in the context of the circadian system by Lakin-Thomas et al. (2011) (see their figure 3.2). FLOs might represent more than a dozen metabolic oscillators, which are not connected to the circadian system. Or, according to de Paula et al. (2007), there are multiple FLOs, which together with the FRQ/WCC oscillator form a network of coupled oscillators. But individual FLOs may drive a particular output. The FLOs may also

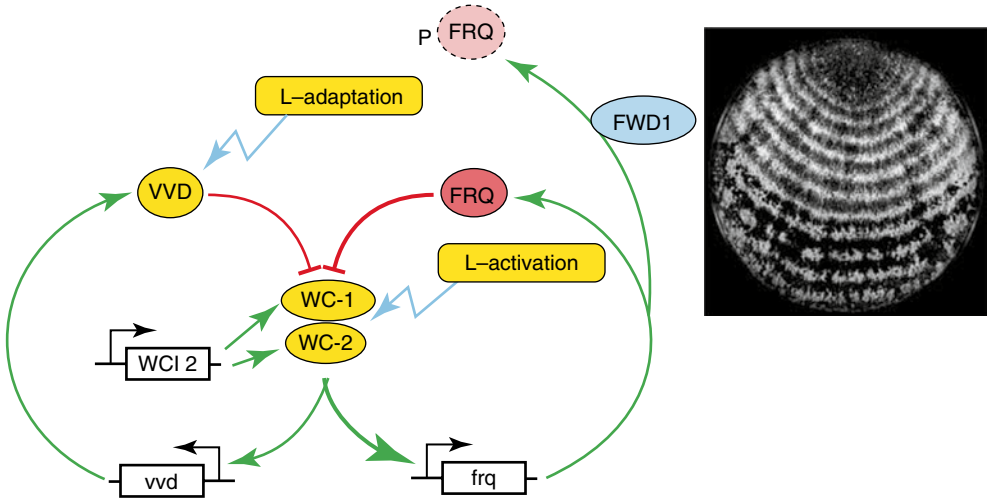

Fig. 18.6 Model of the biochemical and molecular processes of the *Neurospora* clock. The main feedback loop (*thick lines*) consists of *frq* (*black box* with *dented arrow* indicating transcription) which expresses FRQ (*red oval*) in the late night and early morning while activated by a WCC transcription factor (consisting of WC-1 and WC-2, *yellow ovals*). This is the positive arm in the feedback loop. In the negative arm FRQ dimerizes and forms a complex with FRH (a RNA helicase, not shown), which inhibits WCC (*thick red* – I). From noon to evening kinases phosphorylate WCC thereby inactivating it in the early night (not shown). In the late night FRQ interacts with ubiquitin ligase FWD-1 (*blue oval*) and is degraded (*light red oval* with *dashed border*) in proteasomes. Now the frq promoter can transcribe again being reactivated by newly synthesized WCC. In a second feedback loop (*thin lines*) VVD expressed by *vvd* inhibits (*thin red* – I) WCC. This feedback loop is responsible for adaptation under longer *blue*-light exposure (L-adaptation). Phase shifting of the circadian rhythm by light pulses and other light effects (e.g., carotenoid formation) occur via the *blue-light* receptor WCC (L-activation) (Modified from Brown et al. (2012))

function upstream or downstream of the FRQ/WCC oscillator. They need to bypass FRQ/WCC to drive the conidiation rhythm and biochemical rhythms when FRQ and WCC are disabled (Roenneberg and Merrow 1998). Or a single FLO is the central rhythm generator, which is mutually coupled to the FRQ/WCC, supplying stability, period control, and rhythmic input (Li and Lakin-Thomas 2010).

Brody et al. (2010) proposed that the many conditions and mutations leading to FLOs may converge on a pathway that includes ROS and the activation of a RAS-cAMP protein kinase. A cAMP pathway and metabolic regulation is involved also in other organisms (Bass and Takahashi 2010).

These findings suggest that the FRQ/WCC oscillation is not independent of the FLOs, which should be taken into account with respect to the TTO shown in Fig. 18.6, where FLO and WFLO are omitted.

Another question is how typical the molecular composition of the *Neurospora* clock is among the fungi. Whereas WC-1 and WC-2 are conserved, FRQ is less so, and other proteins might replace it as a negative element but work in a similar manner (Salichos and Rokas 2010; Dunlap and Loros 2006).

18.5.2 Entrainment and Photoreceptors of the Circadian System

The clock components described above can explain the molecular bases of the inputs and outputs. Temperature changes and light pulses or LD cycles are able to entrain the clock. We will concentrate on light but mention briefly temperature effects.

Moderate temperature changes of 1–2 °C are already sufficient for entrainment (Liu et al. 1998). The amount of FRQ depends on the phase of the oscillator and on the environmental temperature. Changing temperature corresponds to shifts in clock time, because the amount of FRQ is immediately changed within the clock mechanism.

As is usual in circadian rhythms, the period is only slightly dependent on a constant environmental temperature. This temperature compensation is valid in *Neurospora* between 30 and 36 °C. Many different gene products influence temperature compensation, but *frq* plays a major role: FRQ stability is involved, and CK2 by its phosphorylation of FRQ. Other kinases and phosphatases of the clockwork are not involved (Mehra et al. 2009). The temperature compensation is seen at the posttranslational level and due to the ratio and abundance of a small and a large isoform of FRQ, which are expressed in a temperature-dependent fashion. At lower temperatures (20 °C) the small and large isoforms are equal, at higher temperatures (28 °C) more of the large isoform as well as more FRQ is present (Diernfellner et al. 2007).

WC-1 is not only a clock component but also a blue-light photoreceptor: it is responsible for all light responses in *Neurospora*. There are three types of light-induced circadian responses observed: first, LL suppresses the circadian

modulation of conidiation. Instead, conidia are formed all the time. In DD or safelight such as red, conidiation occurs in a circadian pattern (period length 22 h). Second, a single brief pulse of light applied in DD phase shifts the conidiation rhythm either by advancing or by delaying it. An action spectrum of light which phase shifts the rhythm shows maximal effects at 465 nm (Dharmananda 1980). A light pulse applied at late subjective day and early subjective night delays the rhythm; a light pulse at late subjective night and early subjective morning advances the rhythm. Third, LD cycles (or periodic light pulses) entrain the circadian clock. Below it will be shown how these effects of light – the rhythm annihilating one of LL, the phase shifting one of pulses, and the entraining one – are related in terms of molecular events. The light input pathways are also well understood.

In contrast to plants, *Neurospora* is sensitive to the blue range only and is blind to light beyond 520 nm. Light activates hundreds of genomic regions, about 20 % of all genes (Schafmeier and Diernfellner 2011; Smith et al. 2010). At least 3 % of the genes of *Neurospora* are light inducible, shown by microarray analysis (Lewis et al. 2002). WCC controls the expression of 24 transcription factor genes including those of the circadian oscillator.

Blue light induces *frq*, and *wc-1* and *wc-2* are required for it (the double mutant white color *wc-1* and *wc-2* is blind for light). The light is received by the FAD-associated LOV domain of WC-1 and changes its conformation allowing WCC to bind to LREs in promoters of immediate light-induced genes, i.e., induction begins in no more than 5 min (Lewis et al. 2002). The WCC-LRE complex enhances the capacity of WCC to activate transcription. Two different WC-1/WC-2 complexes are formed, a smaller one which binds to LREs in the dark and activates *frq* expression in the dark (and light exposure reduces its binding) and a larger one which replaces the smaller one after light exposure. The larger one is responsible for the light-induced activation of *frq* transcription.

This light-induced WC/LRE binding corresponds to the light-induced entrainment of the clock and phase resetting (Baker et al. 2012; Crosthwaite et al. 1997). Since *frq* expression cycles, the effect of light on the oscillator depends on the phase: when FRQ levels are low or rising before subjective dawn, a light pulse increases *frq* mRNA and advances the clock phases with highest *frq* expression in the later morning. If FRQ levels decrease, light will again increase *frq* mRNA, which will now delay the phase.

The blue-light chromophore that mediates binding of the larger WCC to *frq* LREs is FAD (and not FMN, discussed in Liu 2003). A mutant in which the LOV domain is removed does not show light responses anymore (He et al. 2002) and is arrhythmic in LD cycles and in DD. The circadian clock of this mutant cannot be entrained by light, but temperature cycles do entrain it. Deleting the WC-1 LOV domain has thus separated the light and dark function of WC-1.

VVD is another photoreceptor in *Neurospora* (Belozerskaya et al. 2012; Zoltowski et al. 2007). It is not essential for clock function, but modulates all its light responses. In *vvd* mutants light-induced gene expression is elevated (leading to, e.g., higher carotenoid synthesis and giving the mutant a vivid orange color), the phase of the circadian clock altered, and light adaptation partially lost. Furthermore, circadian gating of light induction of gene expression is affected in vvd (induction is higher in the subjective morning).

VVD is responsible for photoadaptation in *Neurospora* by reverting the elevated levels of light-induced gene transcription within 2–4 h to preinduction levels. In this way *Neurospora* can detect changes in light intensity and not just lights on or lights off (Schwerdtfeger 2003). VVD interacts in the nucleus with the WC-1 in the WCC and reduces its ability to activate transcription. Increasing light yields more VVD and stronger inactivation of the newly activated WCC (Chen et al. 2010; Hunt et al. 2010). The expression of vvd is clock controlled and it gates the input to the clock (Zeitnehmer). VVD allows the clock to take phase cues from dusk (Elvin et al. 2005), to avoid any WCC induction by moonlight (Malzahn et al. 2010), and it contributes to temperature compensation of the clock (Hunt et al. 2007).

There might be further photoreceptors as suggested by the genome sequence of *Neurospora* (Belozerskaya et al. 2012). It indicates a putative *cry* gene, two *phy*-like genes, and two genes of the Archean rhodopsin. Their functions are unknown. The finding of Dragovic (2002) that under certain circumstances (high light intensities) the conidiation of *wc-2* mutants is still driven by the LDcycle suggests the existence of a wc-independent photoreceptor.

18.5.3 Outputs of the Circadian System

How the time information of the clock is used to regulate the various metabolic, physiological, and developmental overt rhythms in the cell is not yet well understood at the molecular level (Vitalini et al. 2006). The central clock affects numerous genes, which are not part of the clock, but controlled by it (clock-controlled genes, Loros et al. 2007). Primary clock-controlled genes are directly regulated by the WCC, and secondary clock-controlled genes are further downstream from the clock. An additional regulation can occur at the mRNA level through message stability rather than production (Guo et al. 2010). Chromatin remodeling, posttranscriptional, translational, and posttranslational mechanisms could provide further control of circadian rhythmicity.

Neurospora as a pioneer organism for biochemical investigations offers much information on metabolic pathways (Davis 2000), and chronobiologists take advantage of it by

studying the circadian influences (Bass and Takahashi 2010; Harrisingh and Nitabach 2008; Hastings et al. 2008). They are using a systems biology approach to monitor rhythmicity in RNA, proteins, and the metabolism (for transcriptome, proteome, and metabolome, see Dong et al. 2008) under different lighting conditions and under specific genetic backgrounds. Further circadian outputs concern development (e.g., cell cycle and conidiation, Correa and Bell-Pedersen 2002), organelles, transport and signaling pathways (Baker et al. 2012), and osmotic stress (Vitalini et al. 2007).

Screens for clock-controlled genes were performed in *Neurospora crassa* and so far over 400 (Dong and Golden 2008; Correa et al. 2003; for functional categories see table 1 in Dunlap and Loros 2004) have been found by using different methods (review Bell- Pedersen 2000). They are being characterized at the molecular level (Lakin-Thomas et al. 2011). As much as 25 % of the *Neurospora* transcriptome is under clock control. Most of the *ccg* expression peaks just before dawn, but there are others which show maximal expression at other phases of the day (Correa et al. 2003).

If each of the 24 transcription factors regulates about 20 downstream genes and if WCC directly binds to regulate rhythms in about 180 additional morning-specific targets, the various phases of all of the known clock-controlled genes would be taken care of.

The outputs of the clock can feed back to input pathways, as exemplified by the clock-controlled component VVD on light input (Elvin et al. 2005). Such output to input loops can provide certain time-of-day-specific gates.

18.5.4 Photoperiodism

The circadian system seems to control also photoperiodic propagation and reproduction (conidiation, protoperithecia formation) of *Neurospora crassa* (Rémi et al. 2010; Tan et al. 2004; Roenneberg and Merrow 2001). Without FRQ photoperiod cannot be measured, indicating the role of the circadian system in the photoperiodic time measurement. The strains of *Neurospora crassa* have been isolated mainly from tropical areas. The survival vale of photoperiodic reactions in such strains is doubtful. However, Jacobson et al. (2004) found strains as far north as Alaska. A temporal segregation of asexual and sexual reproduction with conidiation in March and perithecia in July was described by Pandit and Maheshwari (1994).

18.6 How Light Affects *Drosophila's* Circadian System

We are now coming to animals, which differ fundamentally from the examples treated so far. They possess a central nervous system that controls behavior and central circadian clocks brain. If light is going to synchronize these clocks, it either has to reach the clocks directly in translucent specimens or indirectly via specialized photoreceptor organs or via both pathways.

The fruit fly *Drosophila* is an example of an insect using both pathways. It has many advantages as an experimental animal such as easy rearing and a short generation time. It is well known genetically and a large number of mutants is available. *Drosophila* is amenable to genetic and molecular methods. For these and other reasons, this insect was and is used also for studying circadian rhythms, especially eclosion of the flies out of the puparium (a case produced in the last larval stage, in which metamorphosis from the larva to the fly takes place) and locomotor activity of the adults. Many mutations affecting the circadian clock, the photoreceptors, and the photoreception are known. Therefore, the effects of light on the circadian system could be studied intensively and successfully.

General reviews on the circadian clocks of *Drosophila* (Allada and Chung 2010; Tomioka and Matsumoto 2010), their genetics (Hardin 2011), molecular mechanism (Duvall and Taghert 2011; Hardin 2011; Weber et al. 2011), and their location and neurobiology (Yoshii et al. 2010, 2012; Hermann et al. 2012; Rieger et al. 2009) are available. Special reviews on the effect of light on the circadian rhythm and the pathways to the circadian system are by Peschel and Helfrich-Förster (2011), Barth et al. (2010), and Choi and Nitabach (2010). The output pathways of *Drosophila*'s circadian system are reviewed by Tomioka et al. (2012), Helfrich-Förster et al. (2011), and Frenkel and Ceriani (2011).

18.6.1 Circadian Eclosion

After completing several larval stages, *Drosophila* forms a puparium in which pupation and metamorphosis into the adult stage takes place. Eclosion from the puparium occurs under the daily LD cycles in a restricted time window (*gate*) only during the early morning hours. A fly which is not yet ready to eclose uses the next gate on the following day. If a culture of *Drosophila* flies is transferred into constant conditions of darkness, eclosion occurs still rhythmically. This shows that eclosion in a population of flies is not just the response to the onset of light, but under control of a circadian clock.

The eclosion rhythm can be entrained by an LD cycle and phase shifted by a single light pulse. Therefore, photoreceptors must exist which transfer the signal evoked by light to the oscillator controlling eclosion. An action spectrum for phase shifting the eclosion rhythm with a single light pulse shows a broad maximum in the blue (457 nm) and further maxima at 375, 435, and 473 nm. Light of wavelengths above 540 nm is ineffective (Klemm and Ninnemann 1976).

The responsible photoreceptors for eclosion are (1) the larval eyes (a pair of Bolwig organs close to the mouth hook, each consisting of 12 light sensitive cells which are retained in the adult eyelet) using rhodopsin (Malpel et al. 2002) and (2) lateral neurons (LNs) using CRY (Kaneko et al. 2000). Eclosion of mutants which lack extraretinal photoreception but possess functional larval eyes is still entrained. Mutants lacking CRY and the visual system cannot be entrained by light, but temperature cycles do entrain, demonstrating a functional oscillator system (Malpel et al. 2004).

Whereas the visual sensitivity of the compound eyes of flies reared on a carotenoid-free diet is decreased by three orders of magnitude, the photosensitivity of the circadian eclosion rhythm is not affected. Furthermore, the eclosion rhythm of mutants lacking compound eyes was still synchronized by light. The compound eyes in the metamorphosed fly in the puparium are thus not needed to phase shift and entrain the eclosion rhythm.

How the circadian signals which control eclosion arise and reach their targets is reviewed by Helfrich-Förster (2005a, b). Recently, experiments were performed which try to simulate more natural conditions such as an LD pattern with gradually changing light intensities and varying day lengths. Under these conditions the eclosion rhythm of *Drosophila* seems to be more robust and shows seasonal variations (De et al. 2012).

18.6.2 Locomotor Activity and Sleep Are Controlled by Several Circadian Oscillators

Drosophila flies, like other animals, possess a multi-oscillatory system to control different events in a circadian way (Stanewsky et al. 1997). Circadian oscillators seem to be widespread throughout the different tissues and cells: using a construct in which the luciferase gene *luc* is fused to the regulatory upstream region of per (which is under circadian control), luminescence rhythms of the whole fly, of parts of the fly, and of cultured tissue can be monitored. Even the rhythms of cultured body parts are synchronized by LD cycles (Plautz et al. 1997), showing that the underlying peripheral oscillators are cell autonomous and photo responsive. Light entrains these oscillators directly, probably via CRY (Ivanchenko et al. 2001; Ito et al. 2008) (see Sect. 18.6.4).

However, behavior such as eclosion of the flies out of the puparium, adult locomotor activity, and sleep is driven by circadian centers in the brain. Adult activity rhythms can already be entrained by light applied in the first larval stage. The clock is apparently running at that time and throughout larval and pupal development and is resettable by light (Sehgal et al. 1992).

In an LD cycle, the flies are mainly active during the light period and sleep during the night. Sleep is defined as a quiescent state with reduced responsiveness to external stimuli (Bushey and Cirelli 2011). In order to sleep flies retreat to a preferred location, become immobile for periods up to 2.5 h, and do hardly respond to stimuli. Sleep is more abundant in young flies than in old ones and can be modulated by stimulants and hypnotics as in other animals (Hendricks et al. 2000; Shaw et al. 2000). Preventing sleep experimentally leads to a sleep rebound on the following night or day. During the day flies usually take a nap during midday. As a consequence, most activity occurs during the morning and evening. In DD the bimodal activity patterns are less pronounced, because morning and evening activity bouts come closer together and sometimes merge into one main activity bout. This is different under LL of low fluence rate, where both activity bouts are separated by a pronounced time of inactivity (nap) (Bachleitner et al. 2007; Yoshii et al. 2012). LL of low fluence rate does furthermore lengthen the free-running period of the flies in a dose-dependent manner (Konopka et al. 2007). At higher light intensities the flies become arrhythmic.

The clocks timing activity and sleep reside in about 150 clock neurons in the brain consisting of seven major groups, namely, three groups of dorsal neurons DNs ($DN_{1–3}$) and of four groups of LNs (LN_d, l-LN_v, s-LN_v, LPN) expressing different peptides/proteins (see Peschel and Helfrich-Förster 2011 and Fig. 18.7). Based on cell-specific ablation (Stoleru et al. 2004), respectively, targeted expression of PER (Grima et al. 2004), it was suggested that the ventral subset of the small LN cells (sLNs) is responsible for the morning activity, and the dorsal set of LNs (LNds) for the evening activity, thus providing a neuronal basis for morning and evening oscillators. The two oscillators were thought to be functionally coupled. Two oscillators could allow the fly to adapt to the seasonal changes of day length. A model of Pittendrigh and Daan (1976) predicts that the period of the morning oscillator M is shortened and that of the evening oscillator E is lengthened by light. As a consequence, M and E activity bouts are close together under short days and DD, but far apart under long days and under LL of low fluence rate. With increasing fluence rate of LL, the two activity bouts are predicted to free run with short and long periods, respectively, until the flies finally become arrhythmic (Daan et al. 2001).

This was indeed found (Rieger et al. 2006). However, it is more complicated than expected. First, the blue-light photopigment CRY has to be knocked out to clearly see the internal desynchronization into the two free-running components. Second, the activity component with a short period did not only start from the M activity bout but in addition from the E activity bout, suggesting that the M cells may also control aspects of the E activity. The same is true for the E cells that can provoke M activity under certain conditions

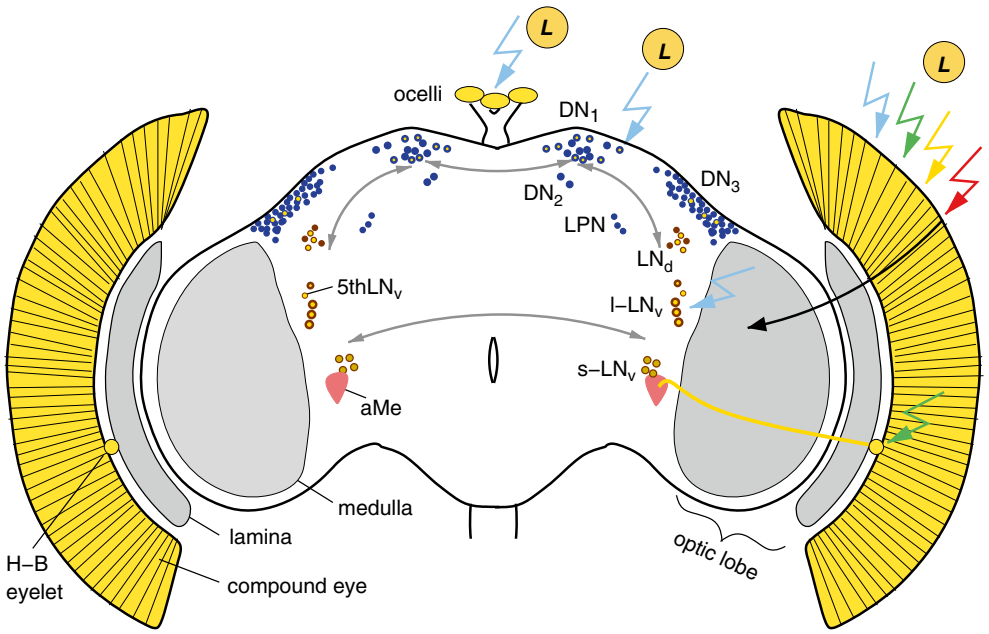

Fig. 18.7 Photoreceptors and neuronal clockwork of *Drosophila melanogaster*: looking toward the front of the brain from anterior, rhythm-relevant neurons and photoreceptors are shown. Light (L in *yellow circle*) for synchronization is received by the compound eye, the Hofbauer-Buchner (*H-B*) eyelets, ocelli, and via cryptochrome by some clock neurons themselves (each marked by a *yellow point*). The clock neurons consist of lateral neurons, LN (4 l-LN_v, 4 s-LN_v, one 5th s-LN_v, 6 LN_d, and 3 LPN), and of dorsal Nneurons (~15 DN_1, 2 DN_2, 30 DN_3). Clock neurons marked in *red* are located in the anterior brain, the ones marked in *blue* in the posterior brain. Lateral and dorsal neurons as well as the clock neurons of the two brain hemispheres are connected with each other (*gray arrows*) and the majority of them project into the accessory medulla (*aMe*) – a small neuropil at the base of the medulla (*pink area*) that was first described in cockroaches as the site of the circadian clock (Homberg et al. 2003). The compound eyes express five different rhodopsins (see text) and are sensitive to *blue*, *green*, *yellow*, and *red* light (colored flashes). They transfer light information via the optic lobe (here visible: lamina and medulla) to the central brain (*black arrow*). The ocelli express only rhodopsin 2, which is *blue-light* sensitive. The H-B eyelets consist of four photoreceptor cells expressing rhodopsin 6, which has its absorption maximum in the *green* but responds also to *red* light. The H-B eyelets project toward the LNs. Direct synaptic contact was shown between the precursors of the H-B eyelets and the larval s-LN_v (Wegener et al. 2004) but may exist also for the adult LNs and perhaps also for the DNs that project into the aMe. Cryptochrome in the clock neurons themselves is maximally responsive to *blue* light. The s-LN_v (except the fifth) and l-LNv express the neuropeptide pigment-dispersing factor, *PDF*, that seems to be released in a rhythmic manner and is an important communication signal within the clock network. The l-LN_v appears to play a special role in the light input pathway to the clock as well as in arousal and sleep (details see text) (After Peschel and Helfrich-Förster (2011), and Helfrich-Förster (2005a, b))

(Rieger et al. 2009; Sheeba et al. 2010). Third, the original simple assumption that the s-LN_v controls the M component and the LN_d controls the E component had to be refined. The two activity components are most likely controlled by variable subsets of DN and LN that interact in a complex manner depending on the environmental light and temperature conditions (reviewed by Yoshii et al. 2012). In spite of this obvious complexity, it is quite convincing that the brain clock of *Drosophila* is composed of M and E clock neurons that respond differently to light (and temperature) and control different aspects of behavior. M and E components are also involved in the circadian system of mammals (see Sect. 18.7.1).

Sleep occurring during the midday nap and the night appears to be controlled by the s-LN_v (that are neither M nor E oscillators) and by sleep centers in the midbrain of the fly (Shaw et al. 2000). During neuronal activity the l-LNv promotes arousal. They are activated by the neuromodulators dopamine and octopamine and by light and inhibited by GABA. GABAergic inhibition of the l-LNv is important for sleep (McCarthy et al. 2011; Chung et al. 2009; Lear et al. 2009; Agosto et al. 2008; Parisky et al. 2008).

18.6.3 Molecular Mechanisms of Circadian Clock

The circadian oscillators which control activity and eclosion are supposed to consist of one main molecular feedback loop plus additional ones (Tomioka et al. 2012; Duvall and Taghert 2011; Hardin 2011). These are generated by interactions of several clock genes, the products of which activate or repress transcription, alter the stability of proteins or degrade them, and change subcellular localization. Transcription is activated by the transcription factors CLK, CYC, and PDP1#. Transcription is repressed by PER, TIM, and VRI. Protein stability and subcellular localization depends on the kinase DBT, CK2, SGG, and PP2a. SLIMB targets phosphorylated

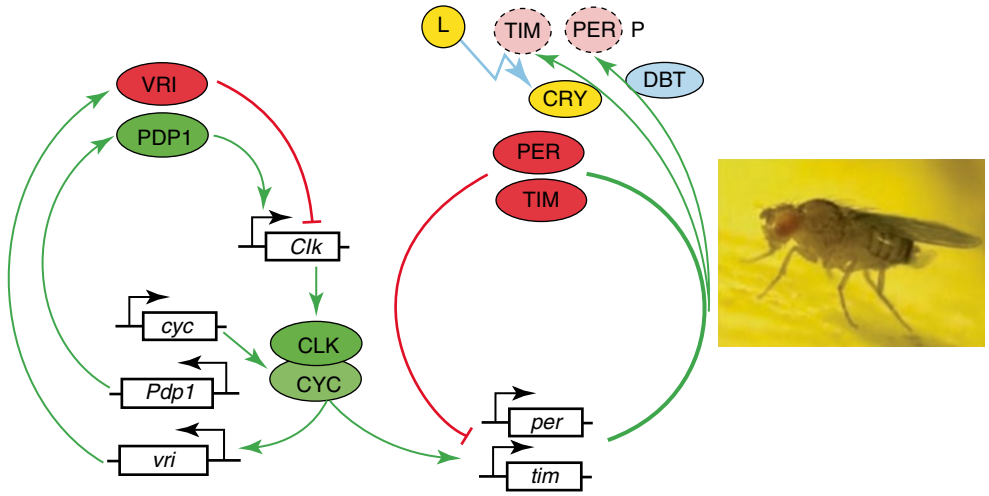

Fig. 18.8 Model of the circadian *Drosophila* clock based on a feedback loop involving transcriptional and translational events in the clock cells. The feedback loop has the following structure: CLK and CYC are transcription factors. They form heterodimers and bind to an E-box in the promoters of *per* and *tim* (and clock-controlled genes *ccg*) in the *nucleus* activating the transcription of *per* and *tim*. mRNA levels increase until they reach high levels early in the evening. The proteins PER and TIM reach maximal levels with a lag in late evening. Degradation of PER by DBT is counteracted by rapid binding of PER and TIM in the cytoplasm and accumulation in foci. After 6 h the complexes abruptly dissociate, PER and TIM move rapidly into the nucleus. DBT and SGG (not shown) in the *cytoplasm* interact with nuclear entrance or phosphorylate PER and destabilizes it. In the *nucleus* PER and TIM repress their own transcription by directly interacting with CLK-CYC transcriptional activators. TIM and PER are phosphorylated and degraded. This stops transcriptional repression at the end of the circadian cycle. Due to the lag between mRNAs and proteins, and due to a 6 h timer in the PER:TIM complex, this negative feedback results in a stable cycling in *per* and *tim* mRNA and protein levels. Entrainment of the clock by light (L in *yellow circle*) functions by affecting (*blue flash*) the blue-sensitive CRY. It stimulates CRY:TIM interaction, which triggers TIM degradation and prevents PER:TIM binding. TIM is phosphorylated, ubiquinated, and degraded in proteasomes. Other photoreceptors (rhodopsin, see text) and their interaction with the molecular gears of the clock are not shown (After Hardin (2005), Cyran et al. (2005). Insert by Dennis Pauls and ChristianWegener, Würzburg)

PER for degradation in the proteasome. Which role these components may play in each circadian oscillator cell of *Drosophila* is shown in Fig. 18.8.

Results (Meyer et al. 2006; Cyran et al. 2005) from experiments in which the FRET signals of PER and TIM (tagged with two different fluorescent proteins) were measured in S2 cells (Schneider 2 cells, derived from a culture of late stage of *Drosophila melanogaster* embryos) show that PER and TIM bind rapidly in the cytoplasm and accumulate in foci. After 6 h the complexes abruptly dissociate, PER and TIM move independently and rapidly into the nucleus. This speaks in favor of a timer in the foci, perhaps similar to the circadian timing in Cyanophyceae (Sect. 18.2).

In this connection, it should also be mentioned that in many insects PER is not found in the nucleus and thus cycling of per mRNA might not always be necessary for PER cycling. Instead posttranscriptional mechanisms might be involved and the negative feedback of clock proteins on their own expression could be optional (Helfrich-Förster 2005a, b).

18.6.4 Photoreceptors of the Clock

Drosophila uses multiple photoreceptors for entraining its circadian system (for reasons see page 10). The rhythm of activity in adult flies can be entrained by (1) the compound eyes and (2) ocelli as external photoreceptors and by the (3) Hofbauer-Buchner eyelets behind the compound eyes (Veleri et al. 2007; Helfrich-Förster et al. 2002) and (4) LN_v and DN neurons in the brain as internal photoreceptors (see Fig. 18.7 and reviews by Rieger et al. 2003; Helfrich-Förster et al. 1998). Whereas in (1), (2), and (3), rhodopsins serve as photopigments, in (4) this is CRY (Klarsfeld et al. 2004). Only when all photoreceptors are eliminated, fruit flies are unable to entrain their activity and sleep rhythm to LD cycles (Helfrich-Förster et al. 2001), suggesting that the multiple photoreceptors fulfill partially redundasnt roles and each single one is capable to reset the molecular feedback loop.

The following basic light effects must be explained:

1. Phase shifting by light pulses
2. Entrainment by LD cycles
3. Attenuation of the rhythm by LL of high fluence rate
4. Internal desynchronization (period lengthening/shortening in subpopulations) by LL of low fluence rate
5. Adaptation of the activity pattern to different day lengths

According to the model (Fig. 18.8), all these effects are achieved through light-dependent degradation of TIM. Because TIM is not light sensitive by itself, the light signal must be transduced to TIM. As indicated in Fig. 18.7, this occurs via the blue-light-absorbing photopigment

CRY. Photochemical changes in its flavin chromophore allow CRY to interact with TIM in the cytoplasm and the nucleus. This leads to TIM phosphorylation and its subsequent degradation in the proteasome (Naidoo et al. 1999) preventing the PER/TIM complex from participating in the negative feedback loop (Ceriani et al. 1999).

If a light pulse hits during the phases of the rising TIM concentration, TIM is reduced before it enters the nucleus and builds up again after the end of the pulse. The following peaks in TIM concentration are thus delayed (see Fig. 18.8). Because cytoplasmic PER is degraded if not protected by TIM, the PER peak is also delayed. If the light pulse hits at peaking TIM concentrations or afterward, nuclear TIM (bound in the PER/TIM complex) is degraded earlier, followed by PER degradation. As a consequence per and tim transcription starts earlier and the subsequent buildup of TIM and PER is also advanced. Thus, the following peaks in TIM and PER are advanced. This explains point 1.

The entrainment by LD cycles is the result of advancing and delaying phase shifts. These will keep the circadian oscillation in a certain phase relationship to the LD cycle. This explains point 2. LL of high fluence rate keeps the TIM level permanently extremely low (close to zero). As a consequence also PER cannot accumulate, *per* and *tim* mRNA remain at an intermediate level, and finally the clock genes and proteins stop to oscillate. This explains point 3.

LL of low fluence rate slows down the accumulation of TIM, but does not prevent it. As a consequence TIM and PER accumulation is permanently delayed, and this results in a period lengthening. This explains the first part of point 4.

The period shortening of some clock neurons under dim LL is more difficult to explain by the model, and the same is true for adaptation of the activity pattern to different day lengths since this includes a phase advance (period shortening) of the M oscillators (see page 37).

Thus, the model can explain the first three light effects mentioned as well as period lengthening (point 4). There is also experimental evidence: TIM degradation induced by light pulses can be measured in the LNs (see Fig. 18.7). It correlates well with the amount of phase shifts of the activity rhythm elicited by light pulses. Furthermore, the spectral response curves for TIM degradation and for phase shifts of the activity rhythm display a maximum between 400 and 450 nm, and this matches the absorption spectrum of CRY (Berndt et al. 2007), clearly indicating that these events are causally related.

Most interestingly, CRY levels are light controlled: CRY levels are maximal in the early morning and decrease over the course of the day reaching a minimum in the early night before they increase again during the night (Emery et al. 1998). This fact explains why the circadian clock is most sensitive to light pulses of low fluence rate in the early morning (about 3 h before lights on), when CRY level is maximal (Emery et al. 1998). Nevertheless, CRY is not the only factor that mediates phase shifts and entrains the clock to LD cycles:

(a) Not all clock neurons contain CRY (Yoshii et al. 2008; Benito et al. 2008)
(b) Entrainment of the molecular feedback loop upon light does also occur in mutants without functional CRY, at least in some clock neurons (Helfrich-Förster et al. 2001)
(c) CRY-less flies can still entrain their sleep/wake rhythms to LD cycles and respond with phase shifts to light pulses, although with strongly reduced magnitude (Kistenpfennig et al. 2012)
(d) Wild-type flies show a more pronounced phase-delay zone than advance zone in their PRC, although CRY is at its minimum during the early night when phase delays occur
(e) The activity of wild-type flies can still be entrained by red light (600 nm), although CRY does not respond to light of wavelengths above 540 nm. The clock of eyeless flies lacks sensitivity to long wavelengths completely (Helfrich-Förster et al. 2002) and is much less sensitive to light of all wavelengths as compared to wild-type flies (1 by a magnitude of 1,000 (Hirsh et al. 2010) and not 10, as wrongly stated in Helfrich-Förster et al. 2002 due to a calculation error of the wild-type sensitivity).

This all emphasizes that CRY-independent pathways contribute to the light responses of the fruit fly's clock.

Indeed, the still missing points of the basic light effects can only be explained by photoreception via the compound eyes and perhaps the H-B eyelets (point 4, period shortening during internal desynchronization under LL of low fluence rate; point 5, adaptation of the activity pattern to different day lengths). Only flies that lack these photoreceptor organs are unable to shorten period under LL and to adapt to different photoperiods (Rieger et al. 2006, 2003).

The most difficult point to explain is the period shortening of some clock neurons in response to LL. According to the model in Fig. 18.8, permanent TIM degradation can only slow down the feedback loop and finally stop it but hardly accelerate it. This implies that the input via the photoreceptor organs to the clock neurons does not lead to TIM degradation. This is in agreement with the fact that flies that retain the compound eyes and H-B eyelets but lack functional CRY do not become arrhythmic under LL, not even at high fluence rates (Stanewsky et al. 1998; Emery et al. 2000; Helfrich-Förster et al. 2001; Yoshii et al. 2004; Rieger et al. 2003). Moreover, the PER/TIM feedback loop runs with high amplitude in these flies under LL conditions without any sign for permanent TIM reduction (Rieger et al. 2006).

So far, it is completely unknown by which transduction cascade the light signal from the photoreceptor organs is transferred to the molecular clock and whether there are

parallels to the mammalian system, where light input via the retinohypothalamic tract results in an increase of Ca^{2+} and cAMP in certain clock neurons finally leading to the activation of cAMP-responsive binding element (CREB). CREB binds to CREs in the promoters of *per1* and *per2* genes and activates their transcription. It is not yet established whether there are functional CRE sequences in the *Drosophila* per upstream region, but it was shown that mutations in the *Drosophila* CREB gene affect per expression (Belvin et al. 1999). Alternatively, per expression may be affected indirectly, for example, by the CREB-binding protein (CBP) that influences the transcriptional activity of the CLK/CYC heterodimer (Lim et al. 2007; Hung et al. 2007).

Although not yet proven, it is imaginable that activation of *per* transcription by light can provoke period shortening under LL conditions in some neurons as was observed by Rieger et al. (2006). Another possibility is that the period of some neurons is shortened via neuronal communication within the clock network.

The l-LN_v neurons, which are responsible for arousal and sleep (see above), seem to play a crucial role in transferring the light information from the compound eyes to the network of clock neurons. Upon light the LN_v increases neuronal activity (Sheeba et al. 2008b), releases the pigment-dispersing factor PDF, and increases arousal of the flies (Sheeba et al. 2008a; Shang et al. 2008).

But PDF acts also on the clock neurons themselves. Most clock neurons express the PDF receptor (Im and Taghert 2010), and they respond to PDF either by shortening or lengthening the period of their molecular clock (Yoshii et al. 2009). An increase of PDF in the dorsal brain does lead to internal desynchronization of the free-running activity rhythm into two components as does LL (Helfrich-Förster et al. 2000; Wülbeck et al. 2008). Furthermore, the same clock neurons seem to free run with a short and long periods, respectively, as observed under LL (Yoshii et al. 2009). This suggests that PDF is the factor that accelerates the speed of the M cells and decelerates the speed of the E cells.

Most interestingly, a recent study suggests that M and E clock cells express different adenylate cyclases, which may enable the two types to respond differentially to PDF (Duvall and Taghert 2012). In accordance with this, neither did *pdf-null* mutants show internal desynchronization upon light nor are they able to adapt M and E peaks to different photoperiods – very similar to eyeless mutants (Yoshii et al. 2009, 2012).

Several rhodopsins may be responsible for the observed light effects on the circadian clock: Rh1, Rh3, Rh4, and Rh5 which are expressed in the compound eyes, Rh6 which is expressed in the compound eyes and in the H-B eyelets, and Rh2 which is found in the ocelli (summarized in Szular et al. 2012). Among these Rh1 and Rh6 have been shown to be responsible for entraining fruit flies to red light (Hanai et al. 2008), whereas Rh1, Rh5, and Rh6 (plus CRY) are essential for entrainment to green and yellow light (Hanai and Ishida 2009).

In summary, the fly has at least two principle light-input pathways to the clock – one working via CRY on TIM degradation directly in the clock neurons and the other working via the photoreceptor organs and the neuropeptide PDF. The CRY pathway enables the fly clock to respond quickly and strongly to light. The photoreceptor input pathway seems to be more subtle but necessary for adapting the flies activity to different day lengths.

18.7 Light and Circadian Clocks in Mammals

Among vertebrates, the circadian clocks of mammals are the best studied. For experimental reasons, rodents are favored and among these mice (Ripperger et al. 2011) and rats, because they can be reared easily, are small and have a short generation time. However, most rodents used are night active, which has to be taken into account, if connections to the human circadian system are made. Day-active rodents are, e.g., the sand rat *Psammomys obesus* and the Nile grass rat *Arvicanthis niloticus*.

During the night diurnal and nocturnal species are sensitive to light at the same time. The molecular mechanisms of light resetting are also comparable. But animals in LL exposed to darkness would reset the SCN clock during their resting period, that is, at night in diurnal and during the day in nocturnal species. Arousal-independent cues (melatonin and GABA) shift the clock in day- and night-active animals at the same circadian time. Arousal-dependent zeitgeber (serotonin: its cerebral levels follow activity pattern) phase shift only during resting and have thus opposite effects in diurnal and nocturnal species (Challet 2007).

Several hands of the clock can be recorded such as locomotor activity, body temperature, melatonin secretion (see Sect. 18.7.6), or expression of clock genes or clock-driven genes. The locomotor activity is measured by running wheels or by infrared light beams (Jud et al. 2005). The records are used to construct actograms which allow to determine period and phase shifting of the rhythm.

Further advantages of using mice are that the genome was mapped and sequenced (see Müller and Grossniklaus 2010 for historical aspects), that many mutants are available, and that genetic and molecular biological methods are applicable. However, among the vertebrates mammals are special in several respects. Thus, peripheral clocks of mammals are not directly entrainable by light, and the pineal is not photoreceptive in contrast to most other vertebrates. In zebrafish, for instance, peripheral clocks are directly entrained by light, which resembles the situation in *Drosophila*, and the pineal

is photoreceptive and contains a circadian oscillator as the central clock (see Sect. 18.7.6). These pineal cells are specialized photoreceptor cells resembling structurally and functionally retinal photoreceptors. They synthesize rhythmically the hormone melatonin with high levels at night and low levels during the day (Idda et al. 2012).

In the following we discuss the clock centers in the SCN and its network (Sect. 18.7.1), the clock mechanism driving these rhythms (Sect. 18.7.2), the circadian photoreceptors in the eye and the inputs to the SCN (Sect. 18.7.3), the circadian clocks in the eyes (Sect. 18.7.4), peripheral clocks (Sect. 18.7.5), and the function of the pineal organ (Sect. 18.7.6).

18.7.1 SCN and Its Network

The paired SCN is a center of circadian timing in mammals. It is situated in the anterior part of the hypothalamus at the ventral part of the third ventricle just above the optic chiasma (Fig. 18.10; Mohawk and Takahashi 2011; Welsh et al. 2010) and each SCN in a *Rhesus* monkey consists of about 10,000 neuron cells and additionally 15,000 glia cells (Roberts et al. 2012). Reorganization of neuron-astrocyte interactions and synaptic connectivity within the SCN is discussed by Jackson (2011), Marpegan et al. (2011), Ng et al. (2011), and Girardet et al. (2010). The SCN consists of a dorsomedial shell (dmSCN) and a ventrolateral core (vlSCN) with diverse afferents and efferents. Their neurons use different neuropeptides: in the shell VIP, GRP, and GABA, in the core AVP and PK2 (Mohawk and Takahashi 2011). For further details of structure and function of the SCN, see Tonsfeldt and Chappell (2012), Lowrey and Takahashi (2011), Dibner et al. (2010), Golombek and Rosenstein (2010), and Welsh et al. (2010); for the genetics of the SCN oscillators, its transcriptional loops, and how epigenetic mechanisms contribute to the control of circadian gene expression, see, e.g., Lowrey and Takahashi (2011), Colwell (2011), Kwon et al. (2011), Ripperger and Merrow (2011), and Bellet and Sassone-Corsi (2010).

The SCN is a circadian center and not just a place that transfers information of the LD cycle from the eye to an oscillator situated somewhere else. If this were the case, the various circadian rhythms would not disappear upon destruction of the SCN, but would not be synchronized anymore and would free run. However, the animals became arrhythmic.

There is further evidence for the SCN being a master oscillator: in organotypic slice cultures, in which the dorsal/ventral architecture is preserved (Silver and Schwartz 2005), metabolism, electrophysiological, and molecular events are still rhythmic. A particular strong evidence is that neural grafts of fetal SCN reestablish the circadian rhythms in SCN lesioned and thus arrhythmic recipients with the characteristic circadian properties of the donor.

To work properly as coordinated clocks, the oscillations must be coupled and form a network. Coupling of the neurons increases strength and precision of the rhythms, they resist better perturbations, and the range of entrainment is narrowed (Abraham et al. 2010). The overall period of the SCN is the average of the periods of the single cells. However, the intercellular coupling has to reach a certain strength, which is not present in dispersed SCN cell cultures.

The SCN oscillators must furthermore be synchronized with the 24 h environment. This occurs mainly by retinal inputs which generate action potentials. These travel along the retinohypothalamic tract (RHT) to the core of the SCN. There they activate the firing rate in the SCN neurons (see Sect. 18.7.3).

Since the core receives retinal inputs directly, the molecular oscillators respond immediately to the retinal inputs. The information from the core to the shell is transmitted in a so far unknown way and occurs delayed, so that the shell neurons react more slowly.

About 60–70 % of the SCN neurons show a circadian rhythm in action potentials which can last in single neurons for 4–6 h. The neurons switch between a hyperpolarized downstate during the night when they are silent and a depolarized upstate during the day when they are active. In this active state they respond to synaptic inputs that reduce their firing, but are not responsive to excitatory signals. During the night they are silent but respond to stimulation. How the change from day to night states occurs is unknown. The molecular oscillators in the SCN neurons influence the membranes and ion channels of the neuronal cells by a second messenger system which leads to circadian firing. It is highest during the day in diurnal as well as in nocturnal animals (Colwell 2011).

Under LL the rhythm of the locomotor activity of mammals can occasionally show a *bimodal rhythm* with a phase difference between the two components (Watanabe et al. 2007, 2006) or *splitting* with different periods (Butler et al. 2012; Indic et al. 2008; Helfrich-Förster 2004). Splitting is caused by the left and right halves of the SCN which oscillate in antiphase to each other (Mendoza et al. 2009; Tavakoli-Nezhad and Schwartz 2005). Arrhythmicity results, if the neurons within the SCN decouple from each other. The rhythmicity of individual cells remains, however, intact.

Internal desynchronization by non-24 h LD cycles (e.g., 11:11 h, called forced desynchrony protocol) can dissociate the molecular rhythms in the shell and core. The core stays entrained to the LD, but the shell is entrained for certain periods only. In between the rhythm free runs. As a result, two components of the locomotor activity, the body temperature and the slow-wave sleep, are displayed with different period lengths.

Splitting, internal desynchronization, and arrhythmicity are simulated by two groups of oscillators which are weakly

coupled mutually but strongly coupled inside the group (Schroder et al. 2012). Light increases transcription of clock genes, which alters the circadian properties of individual cells. In DD weak coupling in the groups leads to oscillations with a single bout of activity per day. In LL, synchrony in a group occurs only under strong coupling. With increasing light intensity the rhythms of the two groups are in antiphase, which shows up as bimodal activity. At high light intensity arrhythmicity is found (Butler et al. 2012). Another model based on the Goodwin oscillator describes also splitting (Gu et al. 2011).

Many core neurons terminate on shell cells and their interplay leads to the circadian output to other hypothalamic regions. VIP modulates light-induced phase shifting and shifts the locomotor activity. If applied to the SCN in vitro, it shifts also the phase. Loss of VIP signaling leads to desynchrony among SCN neurons. Other neurotransmitters such as GRP and GABA phase shift the oscillations in SCN and the locomotor activity rhythm and synchronize asynchronous SCN neurons. Ca^{2+} signaling and cAMP activation, and perhaps other neuropeptides, are involved in synchronization by VIP.

Even in the intact SCN, the oscillations are not completely in synchrony, but their phase shows wavelike gradients at the various axes (shown by imaging, figure 3 in Mohawk et al. 2012), and the structure and synaptic connections of the SCN neurons and glia cells can change within a few hours. In order to find out how this occurs, various electrophysiological techniques were applied to individual SCN neurons and to SCN *slices* (Schaap et al. 2003). They allow monitoring of SCN neurons for longer periods. In organotypic slices from transgenic mice in which a luciferase reporter (Yamaguchi et al. 2003) or a fluorescent protein reporter (Quintero et al. 2003) drives a clock gene promoter, time-lapse imaging showed in horizontally cut slices two oscillating components, which might reflect the activity of *morning* and *evening oscillators* (de la Iglesia et al. 2004; Jagota et al. 2000). They had been inferred already earlier from behavioral studies (Pittendrigh and Daan 1976).

In photoperiodic reactions such evening and morning oscillators are supposed to measure day length (Jagota et al. 2000) (see Sect. 18.7.6). The photoperiod (day length) changes the pattern of the clock gene expression: long days broaden the clock gene expression of the SCN and lengthen the time of its neuronal activity in the dmSCN and along the rostral-caudal axis of the SCN (see also Sect. 18.4.3).

Outputs of the SCN: Intercellular communications in the mammalian clock system are not restricted to the clock cells in the SCN. Primary targets of the SCN outputs are predominantly located in the hypothalamus and the thalamus (see Fig. 18.10 and references in Li et al. (2012)). How does the circadian information of the SCN reach the other brain areas?

The signals of the SCN are spread as synchronized nerve impulses to central parasympathetic nuclei (e.g., the dorsal motor nucleus of the vagus, which innervates gastrointestinal and respiratory organs) and central sympathetic nuclei (e.g., intermediolateral cell column of the spinal cord). Sympathetic signals to the adrenal gland are converted to hormonal (glucocorticoid) signals. They are released into the bloodstream and bind to glucocorticoid receptors of peripheral organs, activate the mammalian *Per1* gene in systemic cells, and reset clocks all over the body (Tonsfeldt and Chappell 2012; Okamura 2007).

Locomotor activity is driven by cyclic releasing factors acting on receptors in the hypothalamus at the wall of the third ventricle. Circadian signaling factors are PK2, AVP, and CLC. They influence also other behavioral and physiological rhythms (Li et al. 2012; Dibner et al. 2010; Klein et al. 1991) such as thermal regulation (Kräuchi et al. 2006; Ruby et al. 2002), sleep-wake cycle, functions of the circulatory and gastrointestinal system (Bass and Takahashi 2010; Green et al. 2008; Gachon et al. 2004), and endocrine events (Vollrath 2002). The synthesis and secretion of melatonin is also controlled by the SCN (see Sect. 18.7.6 and Simonneaux and Ribelayga 2003).

If the SCNs are destroyed, the circadian control of these functions disappears. The close connection between SCN and metabolism shows how the circadian system is integrated with physiology (Hardie et al. 2012; Froy 2011; Bellet and Sassone-Corsi 2010). AMP-activated protein kinase (AMPK) is an energy sensor of the cell. It is activated, if the energy status falls, promotes ATP production, and conserves ATP by switching off biosynthetic pathways. It furthermore regulates the energy balance of the body via the hypothalamus that promotes also metabolism and feeding behavior. Circadian rhythms and metabolism are closely linked via the activating (CLOCK-BMAL1) and repressive (REV-ERB-a-REV-ERB-b) transcriptional complexes, the coordinate actions of which generate rhythmic gene expression (Cho et al. 2012).

18.7.2 Mechanism of the Mammalian Clock

The molecular basis of the mammalian master clock in the SCN has been studied intensively using various methods, among them systems biology which is used to identify the circadian system and its components, to analyse and measure them, to control the system, and to put it together from its parts (Hogenesch and Ueda 2011; Ukai and Ueda 2010; Baggs and Hogenesch 2010). The clock mechanism presently known involves three basic helix-loop-helix transcription factors (Clock, Npas2, and Bmal1), two period genes (*Per1* and *Per2*), two cryptochrome genes (*Cry1* and *Cry2*), CKIε and δ, and two orphan nuclear hormone receptors (RevErbα and Rorα). Gene expression is regulated by transcriptional factors (Dbp, Tef, Hfl, and Nfl3; Bmal2, Bhlhb2,

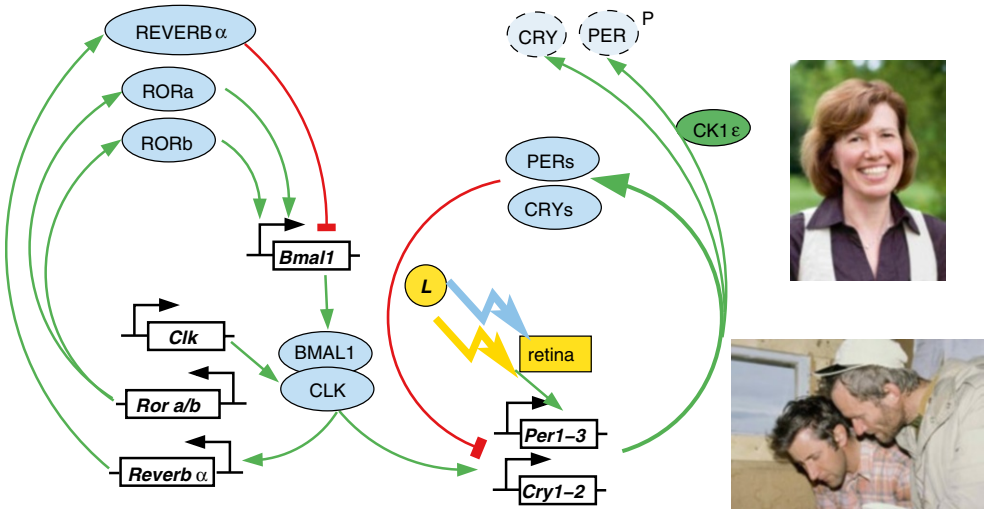

Fig. 18.9 The circadian clock of mammals consists of a main feedback loop in which the products (PERs and CRYs, *thick green arrows*) of the *Per1*, *Per2*, and *Per3* genes and of the *Cry1* and *Cry2* genes inhibit (*thick red – I*) the expression of their genes (*Per1–3* and *Cry1–2*). A kinase (CK1ε) is responsible for the destruction of the PERs and CRYs (*blue ovals* with broken borders). Further feedback loops (*REVERBa*, *RORa*, and *RORb*) interact with *Bmal1* which via BMAL1/CLK affects the *Per* and *Cry* genes. Light (*L* and *yellow* and *blue flash*) affects the *Per* and *Cry* genes (After Kim et al. (2012)). Insets: The female author of this chapter and her coauthors during a circadian experiment in Spitsbergen (see link: http://nbn-resolving.de/urn:nbn:de:bsz:21-opus-53405)

and Bhlhb3; one period-related gene *Per3*; RevErbβ, Rorβ, and Rorγ Ukai and Ueda 2010).

How the clock genes and clock-related genes interact with each other is at least partly clarified (see Fig. 18.9 and 18.10). CLOCK and BMAL1 dimerize and activate transcription of *Per* and *Cry* through E-box elements. The PER and CRY proteins accumulate in the cytosol, are phosphorylated, and then are translocated into the nucleus. There they inhibit the activity of *Clock* and *BMal1*. After the turnover of PER and CRY, a new cycle of activation by CLOCK and BMAL1 begins. This clock oscillator influences physiological and metabolic processes.

The rhythmic expression of *Bmal1* mRNA is also clock regulated. The *Bmal1* promoter contains RRE instead of an E-box, and its activities are controlled by the rhythmically expressed transcriptional repressor REVERBα and the activator RORα. CRY inhibits by feedback the CLOCK/BMAL1 complex and is responsible for the functioning of the mammalian clock. Critical for the function is also the E-box-mediated transcriptional/posttranscriptional loop.

The circadian clock of mammals possesses also posttranscriptional regulation. Using newer technologies, several protein kinase, adenylate cyclase, and proteasome inhibitors were found which lengthen the period of the clock. The decisive step seems to be the *CKIε*/*δ*-dependent phosphorylation of PER2.

Circadian clocks must be protected against fluctuations in the environment such as temperature and food. They are therefore temperature compensated. Theoretical studies of Isojima et al. (2009) show that the effect of *CKIε* and *CKIδ* activity on PER2 determines period and is temperature insensitive. Circadian oscillators of mammals are also resistant against fluctuations of the transcription rate (Dibner et al. 2009).

It was mentioned already on page 9 that a special light pulse at a critical phase of the circadian oscillator might lead to arrhythmicity. This feature has been used by Ukai and Ueda (2010) and Pulivarthy et al. (2007) to find out whether the arrhythmicity is due to a stop of the oscillators in a singular state or whether the oscillators continue to oscillate but desynchronized to each other. In mammalian cell cultures made photo responsive by coupling αρ protein to melanopsin, it was shown that desynchronization of the cellular clocks and not arrhythmicity was responsible (Ukai and Ueda 2010; Pulivarthy et al. 2007). In light-responsive immortalized fibroblasts of mice, such a critical light pulse reduces the amplitude of the rhythm by 40 % but desynchronizes simultaneously the cells (Pulivarthy et al. 2007). In rats it was shown in vivo that desynchronization is responsible for the low amplitude of the locomotor activity after such a critical light pulse (Ukai et al. 2007).

Using a tunable oscillator (see Tigges et al. 2009) in mammalian cells, it could be clarified how the phases of expression of oscillating genes are determined by the three CCEs (E/E-box, D-box, and RRE). The transcriptional activator DBP activates gene expression via the D-box; the E4BP4 represses gene expression. Dbp is regulated by the E-box, the morning control element. E4bp4, however, is regulated by the RRE, the nighttime control element. RRE activators are expressed during the day phase through the D-box. The RRE repressors are influenced by a morning element (E-box). A daytime activator and a morning repressor determine the nighttime transcription through the RRE

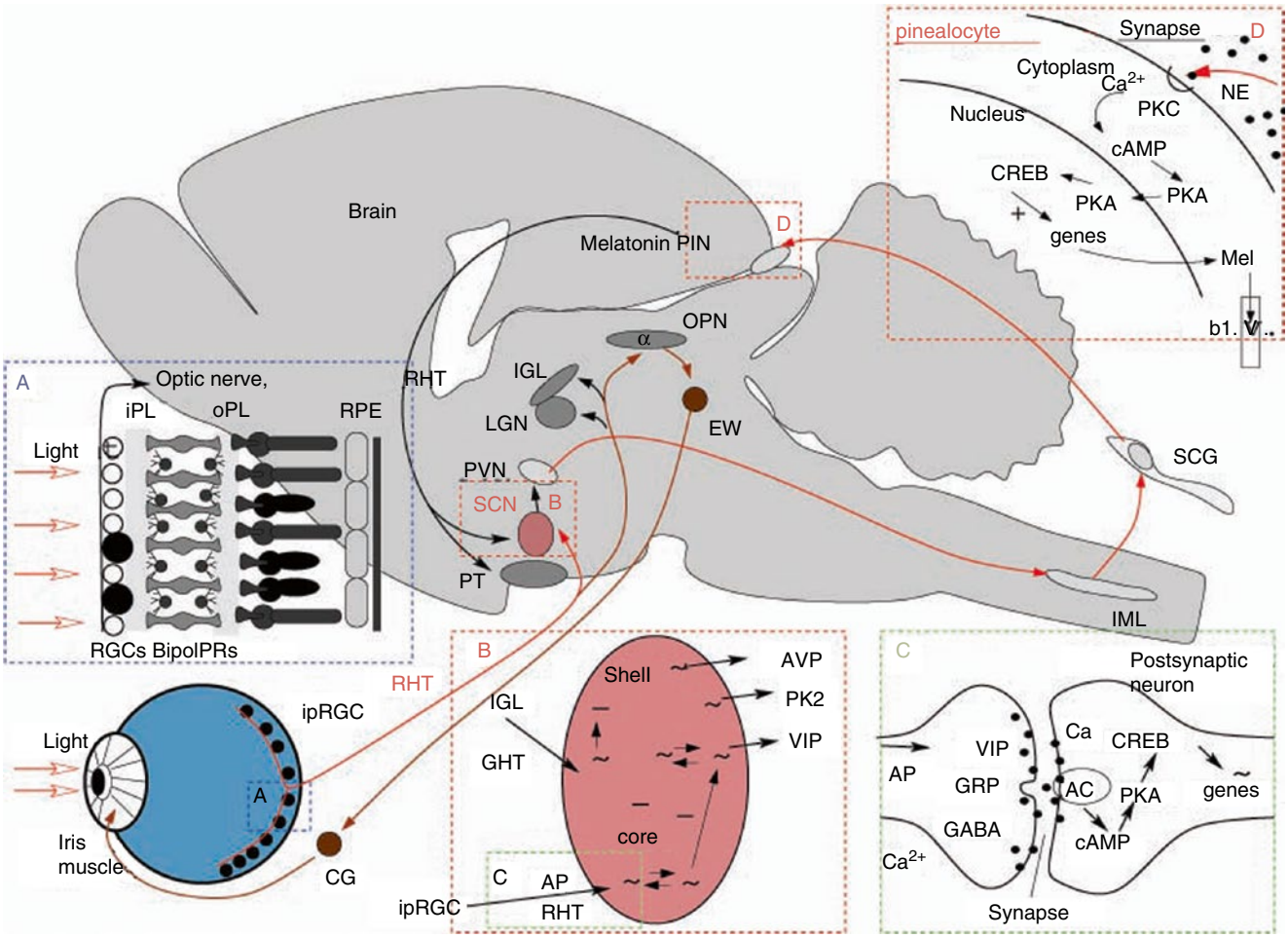

Fig. 18.10 Circadian centers of mammals and their pathways: the environmental L/D is received by the retina (*bottom left* and insert A) in ipRGC (*dark blobs* in A) and in the rods (PRs, short structures) and cones (long structures) and reach via action potentials (AP, insert C) in the RHT the SCN (insert B). The APs (insert C) open Ca^{2+} channels (Ca) which leads to discharge of neurotransmitters VIP, GRP, and GABA from the presynaptic neurons into the synapse and clock gene activation in the postsynaptic neurons via receptors (only AC shown), cAMP, PKA, and CREB. The signals are received by clock neurons cells (*circles* with ~, insert B) in the core of the SCN, which are entrained by them and by mutual interactions (⇌). They in turn synchronize clock cells in the shell of the SCN which interact with each other (⇌) and with other cells (*circles* with -). They communicate with target tissue/organs via neurotransmitters like AVP, PK2, VIP. Signals from the SCN reach the pineal (PIN) via sympathetic innervation with synapses in the PVN, IML, and SCG. Insert D shows part of a pinealocyte where the signals trigger via norepinephrine (NE) the release of melatonin (Mel) into the blood vessels (bl.v.) of the brain. The signal cascade involves Ca^{2+} and PKC which increase cAMP. PKA phosphorylates CREB in the nucleus, activating genes involved in melatonin synthesis. Melatonin reaches via the blood different targets, among them SCN cells and cells of the pars tuberalis (PT; main figure), both of which contain numerous melatonin receptors. The PT controls photoperiodic events. Another direct target of the ipRGC in the retina is the olivary pretectal nucleus (OPN) linking the pupillary light reflex via EW, CG, and the iris muscles (After Berson (2003), Hastings and Herzog (2004), Meijer and Schwartz (2003), Lincoln (2006), Pévet et al. (2006), Welsh et al. (2010), Dibner et al. (2010), and Schmidt et al. (2011))

(Ukai-Tadenuma et al. 2008). Rhythms did not have a strong amplitude, if only the morning activator or only the night repressor was expressed. Morning activation and night repression are responsible for the control during the day. Various combinations of transcriptional regulators with CCEs for the three basic circadian phases (morning, day, and night) result in other phases and show that transcriptional regulation of upstream transcription factors can determine the phase of the downstream output. The period length of the clock is largely determined by posttranscriptional circuits.

18.7.3 Circadian Photoreceptors in the Eye

As mentioned, the SCN of mammals is only synchronized by light perceived via the eyes: enucleated animals free run in LD cycles (Meijer et al. 1996).

Whereas the rods and cones of the outer retina are responsible for normal vision and communicate with the brain via the optic nerve, a small subset of intrinsically photosensitive retinal ganglion cells (ipRGCs; see Fig. 18.9) in the inner nuclear layer of the retina controls the circadian rhythm in the

SCN. These cells regulate also masking effects of the light, the immediate melatonin suppression, and the pupil reflexes (Hughes et al. 2012; Lucas et al. 2012). They occur in small numbers only (in humans 0.2–0.8 % of all ganglion cells in the retina) but spread widely as a network across the entire retina (Moore et al. 1995) and are strongly arborized (Hannibal et al. 2002). They detect the average illuminance of the day and integrate it over long intervals (Do and Yau 2010; Pickard and Sollars 2010; Husain 2005; Warren et al. 2003). In addition they receive input from the rod/cone circuitry. Plachetzki et al. (2005) provide a historical overview.

There are five types of ipRGCs, M1–M5, which differ in connection and function. The Brn3b-negative M1 cells innervate the SCN and entrain the clock cells, and the Brn3b-positive M1 cells innervate the shell of the OPN. From there the pupillary light response is controlled. The other M cells innervate the core of the OPN, the SC, the dLGN, and other regions, but their specific functions are not yet known (Hughes et al. 2012).

The LD cycles of the environment are sensed by the Brn3b-negative M1 ipRGCs and transferred as electrical signals via their monosynaptic axons in the RHT to the SCN. Melanopsin serves as the photopigment. G protein is activated, thereafter PLC and finally an influx of Ca^{2+} leads to action potentials. As a result, Glu and PACAP are released postsynaptically at the SCN neurons. Ca^{2+} influx activates protein kinases and CREB is phosphorylated (Golombek and Rosenstein 2010). It binds to CREs in promoters of many clock genes such as the *Per1* and *Per2* genes and activates transcription. Depending on the time at night at which light occurred, the increased PER advances or delays the locomotor activity rhythm.

The transduction cascade of the melanopsin-expressing ipRGCs differs fundamentally from the one of the rod and cone photoreceptors, since a different G protein is involved and melanopsin activation results in membrane depolarization rather than hyperpolarization as in rods and cones. It thus resembles more closely the phototransduction cascade of invertebrates (Palczewski 2012; Bailes and Lucas 2010). Whereas mammals have just one melanopsin (Opn4m), fish, birds, and amphibians possess two, Opn4m and Opn4x (Bellingham et al. 2006).

All inputs of the accessory light perception use the rod-cone and the melanopsin system (Hattar et al. 2003). However, the quality of the information differs. Cones signal rapid changes in light intensity, and rods and melanopsin gradual modulations during the day at dim and brighter intensities. Mice possess a small population of short-wavelength-sensitive S-cones which could explain the UV sensitivity (Provencio and Foster 1995). The SCN is thus able to encode environmental light over a wide range of intensities and temporal frequencies (Lucas et al. 2012).

After the light has been absorbed in the retina and the signals have reached the SCN, *immediate early genes* for transcription regulator proteins and furthermore nitrogen monoxide come into action. The latter is required for light-induced phase shifts of behavioral rhythms (reviewed by Rea 1998).

Under DD, circadian rhythms are maintained by the clock cells of the SCN. But the eyes, which also contain autonomous circadian clocks (see Sect. 18.7.4), can also modulate circadian rhythms in the SCN even in the absence of light. Removal of the eyes abolishes circadian rhythms in some cells of the SCN; they were apparently driven by inputs from the eyes. However, removal of the eyes can also amplify a normally dampened circadian rhythm in other cells of the SCN (Beaule and Amir 2003).

18.7.4 Retinal Clocks in the Eye

After presenting the circadian photoreceptors in the retina (Sect. 18.7.3), we have to point out that the retina of the eye contains circadian clocks itself. The retina, its cells and tissues, and their interactions are well studied. It consists of several tissue layers with five classes of neurons (photoreceptors, horizontal cells, bipolar cells, amacrine cells, and ganglion cells) and glia (Guido et al. 2010; Tosini et al. 2008). There are three nuclear layers (outer and inner nuclear layer, ganglion cell layer; see inset A in Fig. 18.9). Light has to pass through these layers and their neurons before reaching the photoreceptors.

The outer segments of rods and cones absorb light with various opsin photopigments in stacked discs. The disks are shed at the tip of the segments, phagocytosed and digested in the retinal pigment epithelium (Bobu and Hicks 2009; Strauss 2005; Grace et al. 1999; Young 1976). At the base the segments are renewed by forming new disks. This *internal* renewal is important for the functional integrity of rods and cones, because they cannot be replaced by new cells. The shedding of the outer disks occurs in the rods in the morning and in the cones in the evening, that is, at times, when they are not used anymore.

Several photopigments with diverse functions are found in the various cell layers (Peirson et al. 2009). They synchronize the circadian rhythms (Iuvone et al. 2005; Green and Besharse 2004; Devlin 2002).

Circadian clocks in the mammalian eye were predicted by Reme et al. (1991). They have later been found in the retinas of all classes of vertebrates. The retina contains besides the normal visual system a *circadian* system with receptors for synchronizing light and with many mutually coupled clocks (Ruan et al. 2006). Different aspects of retinal physiology such as sensitivity to light (differences of more than six orders

of magnitude), neurohormone synthesis, rod disk shedding, intracellular signaling, and gene expression are controlled by these clocks (Green and Besharse 2004; Tosini and Fukuhara 2002; Tosini and Menaker 1996). The retinal clock cells control also the circadian melatonin expression in the eye and are partly responsible difference in the sensitivity to light.

There are indications that in the retina two or more oscillator types control the local physiology. Melatonin and dopamine in the ganglion cells of the inner retina and a part of the inner nuclear layer and/or the photoreceptors are regulated in antiphase (Thompson et al. 2003; Hattar et al. 2003).

This close connection between circadian clocks and photoreceptors is known also from invertebrates and *Neurospora*.

The molecular components and genetic basis of the retinal and other peripheral clocks of the body are the same as the one in the SCN cells (Yamazaki et al. 2000), and they possess the same properties such as shorter periods in corresponding mutants. These shorter periods show up also in the output of the eye clocks (Grace et al. 1996). There are, however, variations in molecular detail (Steenhard and Besharse 2000).

The retinal clock cells control the local physiology and are responsible also for a circadian output of melatonin in the eye. This changes the sensitivity of the retina to light, covering a range of more than six orders of magnitude.

Similarities and differences in the molecular mechanisms of the retinal versus the SCN oscillators are discussed by Green and Besharse (2004). They also examined the interactions between the retinal and the SCN clocks. Light and dopamine phase shift the retinal clock (Steenhard and Besharse 2000). The circadian release of melatonin in the eye is responsible for the rhythmic adaptation of phototransduction, for the recycling of biochemical components in the retina, and for other aspects of the retinal physiology. Other rhythmic events in the eye such as visual resolution (Tassi et al. 2000), ERG, intraocular pressure (Nickla et al. 1998), cats: Sole et al. (2007), choroid thickening, and eye growth might be or are also under circadian control.

18.7.5 Peripheral Clocks and Their Entrainment

In the brain, clock genes are not only expressed in the SCN but also in other parts of the central nervous system (e.g., cerebellum, hippocampus, arcuate nuclei, paraventricular hypothalamic nuclei, piriform and cerebral cortices, olfactory bulbs, amygdala, retina Guilding and Piggins 2007). Furthermore, rhythms of clock gene and/or protein expression have been observed in peripheral tissues and organs such as liver, pancreas, fat tissue, gut, lung, and heart (references, also for the following, in Pévet and Challet 2011); Bass and Takahashi (2010). These rhythms persist in culture, that is, without the influence of the SCN cells. However, they dampen after a few cycles. Imaging has shown that individual cells continue to express rhythms, but are not synchronized anymore. In contrast to the SCN, they do not react to external time cues such as the LD cycle of the environment and cannot communicate with and entrain each other. Peripheral oscillators can be entrained by temperature cycles as exhibited in core body temperature. Thus, rhythmic gene expression can be driven by both local intracellular clocks and by extracellular systemic cues.

Metabolism is linked with the circadian system not only via the SCN but also via peripheral tissues, endocrine, and local signals. Feeding time and certain drug treatments can generate behavioral rhythms in the absence of the SCN (Honma and Honma 2009). The liver clock is reset by feeding, and the clock genes and protein expression shift their phase accordingly (references in Mohawk et al. 2012).

18.7.6 Pineal Organ, Melatonin, and Photoperiodism

The pineal resembles a tiny *pine* cone and is an endocrine gland in the center of the vertebrate brain between the hemispheres (see Fig. 18.9). It is a part of the "photoneuroendocrine system" (retina, suprachiasmatic nucleus, pineal) and consists mainly of pinealocytes, which produce and secrete melatonin. In lower vertebrates, they contain functional circadian oscillators, but in mammals they do not (Falcón et al. 2009). Furthermore, mammals lack extraretinal circadian photoreceptors in the pineal (Bertolucci and Foà 2004). Instead, light is perceived in photoreceptors of the rods, cones, and melanopsin-expressing retinal ganglion cells (for the exceptional circadian system of mammals and its evolution, see Menaker et al. 1997; Heesy and Hall 2010; Davies et al. 2012). The light signals are converted to electric signals in this photoneuroendocrine system (Do and Yau 2010). The electric signals are propagated via the RHT neurons to the SCN. From the SCN the light signaling is conveyed to the pineal via the paraventricular nuclei (PVN) of the hypothalamus, the sympathetic preganglionic neurons of the intermediolateral cell column of the spinal cord (IML), and noradrenergic sympathetic neurons to the superior cervical ganglion (SCG) (see Fig. 18.9 and Pévet and Challet 2011 for the neurotransmitters involved). The SCN output stimulating the PVN derives from two populations of SCN neurons, one active during daytime and the other during nighttime.

The pinealocytes in the pineal synthesize melatonin (=N-acetyl-5-methoxytryptamine Reiter et al. 2010) during the night upon release of noradrenaline from sympathetic pineal nerve terminals (for the neurotransmitters used in the

pineal, see Stehle et al. 2011). Melatonin is immediately released into the blood circulation but also into the cerebrospinal fluid and rapidly degraded in the liver. Therefore, its plasma concentration precisely reflects its synthesis.

Central and local mechanisms regulate amplitude and rhythmic timing of melatonin synthesis from serotonin. Although the pinealocytes possess – like most cell types – the basic clock machinery, they are not able to produce a melatonin rhythm. Instead the rhythm is controlled by the SCN and without its sympathetic input there is no rhythm (Borjigin et al. 2012).

Melatonin transfers the temporal cues received from the SCN to the structures within the brain or the periphery that express melatonin receptors (Pévet and Challet 2011) (but note that circadian information can be sent from the SCN also via nervous or other hormonal signals). In some of them such as the *pars tuberalis* of the hypophysis, the melatonin signals drive rhythms; in other targets they synchronize peripheral oscillators, such as in the fetal adrenal gland. Some of these sites may not be involved in circadian control, but instead in photoperiodic responses (see page 56 and Chap. 19).

Besides melatonin, the pineal secretes also N-acetylserotonin (NAS) rhythmically. At night the levels are even higher than those of melatonin. NAS as an antioxidant is even more effective than melatonin. It may thus not only serve as the precursor of melatonin (Jang et al. 2010).

The rhythm of pineal melatonin is a very reliable marker of the circadian clock. But the phase of melatonin secretion varies widely between individuals and strains, as shown in rats. This wide variation of melatonin onset in an animal model is paralleled by a wide range of circadian chronotypes in humans.

Light affects melatonin synthesis not only by its resetting effect on the circadian system but has also an immediate effect ("masking") if applied at night. One lux is already sufficient in golden hamster to inhibit melatonin synthesis (Brainard et al. 1983). For humans, a fluence response curve for immediate inhibition by blue light, which is most effective, was determined by Brainard et al. (2008).

Melatonin is produced not only in the pineal but also in the Harderian gland, the gastrointestinal tract, and the retina but is there only of local importance (see Sect. 18.7.4 and Hardeland et al. 2011). It is found not only in animals but also in bacteria, unicellular eukaryotes, and plants serving various tasks (Dibner et al. 2010).

Melatonin acts at the central level as well as at the periphery: it does not only affect the gonads and other centrally controlled events but also other tissues of the body and the brain (Pévet et al. 2006). Being a small molecule, melatonin can pass the placenta and convey circadian and seasonal information to the fetus (Stehle et al. 2011).

Melatonin modulates sleep propensity (Cajochen et al. 2010; Pandi-Perumal et al. 2006; Turek 2005; Gillette and Abbott 2005), vascular tone, immune function, controls seasonal reproduction (Sellix and Menaker 2011; Reiter et al. 2010; Revel et al. 2009), seasonal thermoregulation including torpor and hibernation (Saarela and Reiter 1994; Heldmaier and Steinlechner 1981; Chap. 12 in Heldmaier and Werner 2004), metabolism, energy balance (body weight regulation!), and immune responses (references in Barrenetxe et al. 2004).

Phase shifting of the SCN clockwork is the central and best characterized effect of melatonin (Shimomura et al. 2010). Treatment with exogenous melatonin can synchronize the SCN (Pévet and Challet 2011). Orally or injected melatonin pulses advance or delay the circadian rhythm depending on the phase of application. The phase response curve to melatonin pulses is similar to that of light pulses but displaced by 180° (Lewy et al. 1996). Therefore, melatonin can be used in a similar way as light pulses – if properly phased, to shift the circadian system. Circadian phase disorders can be treated in this way (Lewy and Sack 1997).

Melatonin shows connections to human diseases as discussed in Sects. 18.8.3, 18.8.4, and 18.8.5 and by Hardeland et al. (2012) and Pandi-Perumal et al. (2013). It is used to cure sleep disturbances and insomnia (for instance, in elderly people, Fiorentino and Martin 2010), depression, jet lag, and shift-work-related sleep cycle disorders (see Sect. 18.8). The antioxidant properties of melatonin (Reiter et al. 1999; Pandi-Perumal et al. 2012) might protect the skin against UV (Reiter et al. 2004).

In seasonally breeding mammals the melatonin production in the pineal plays a decisive role (reviews Ikegami and Yoshimura 2012; Hut and Beersma 2011; Walton et al. 2011; Revel et al. 2009; Morgan and Hazlerigg 2008). The duration and magnitude of the melatonin secretion depends on the length of the night, which changes during the year especially in higher latitudes. In this way seasonal changes are sensed by photoperiodically responsive mammals and control reproduction (stimulating or inhibiting, depending on the species (Stehle et al. (2001), Hoffmann (1981)) and pelage color, among others. The length of the night is coded by the duration of the nocturnal peak of melatonin (Revel et al. 2009; Morgan and Hazlerigg 2008). Clock genes in calendar cells of the *pars tuberalis* of the hypophysis, where melatonin receptors are strongly expressed, regulate prolactin release (Johnston et al. 2006; Lincoln et al. 2003). These cells contain circadian clocks, and the phase relationship between the expression of the clock genes *Cry* and *Per1* is set by melatonin at dusk, respectively, dawn.

Whereas the photoperiodic timing in the SCN for the melatonin secretion in the pineal uses *external* coincidence, the timing in the *pars tuberalis* seems to follow an *internal* coin-

cidence (see Sect. 18.4.3). As a consequence the transcription of downstream genes (prolactin releasing factor?) leads to either a long-day cell state or a short-day cell state (Lincoln et al. 2002).

Pinealectomy abolishes the photoperiodic response.

18.8 Light and the Human Circadian System

The effect of light on the circadian system of mammals has been discussed already in Sect. 18.7. A few peculiarities of the human circadian system and its responses to light are mentioned in the following.

The circadian system governs not only the sleep-wake cycle, body temperature, alertness, and efficiency but also many other metabolic, physiological, and behavioral events such as enzymatic activities in organs, hormonal secretion, and so on. There is a long list of circadian clock-driven events in man (Minors and Waterhouse 1981).

The sleep/wake cycle (Dijk and von Schantz 2005), body temperature, and urine amount and its composition can be monitored easily and have therefore often been used as hands of the circadian system. Melatonin concentration in the blood is a particularly useful measure because it is not much disturbed by activities, in contrast to the body temperature rhythm. Light has, however, an immediate suppressing effect on melatonin concentration (Pévet and Challet 2011; Reiter et al. 2010).

The circadian system shows up clearly under isolation from external time cues. In a cave or in an isolation facility, a person who has no information of the outside time will sleep and wake according to its internal circadian clock. By continuously measuring the body temperature, the sleep time, and the locomotor activity, the period length of these parameters can be determined under the light conditions given (see, e.g., Johnsson et al. 1979).

However, the design of the recording conditions has to be taken into account. Wever (1979) and others (e.g., Weitzman et al. 1981; Siffre 1975; Mills 1964) determined an average "free run" of about 25 h, but this estimate was too high, as discussed by Czeisler and Gooley (2007): the subjects were able to self-select their LD cycle. They exposed themselves to light during most of the *delay* portion of the phase response curve during wakefulness and to darkness during most of the phase-*advance* portion. As a result of this and due to the light intensities used, the free-running periods were overestimated (Khalsa et al. 2003; Honma et al. 2003; Klerman et al. 1996). Using other protocols such as "forced desynchrony," which had been used already in 1938 by Kleitman (1963), period could be measured without the influence of the self-selected LD cycles (Duffy and Wright 2005; Czeisler et al. 1999) and turned out to be much closer to 24 h, namely, 24.2 h as an average. To entrain the circadian clock of a person with such a period to the 24 h day, the rhythm has to be advanced daily by about 0.2 h (12 min). The period of about 25 % of tested persons is less than 24.0 h, requiring a daily delay, whereas in the remaining individuals period is longer, thus requiring a daily advance of the rhythm. The interindividual variation in period length in humans is much smaller than assumed before (0.55 % instead of 30 %, references in Czeisler and Gooley 2007) and corresponds now more to the values of other mammals such as hamster and mouse. Entrainment thus requires daily shifts of less than 1 h.

In the forced desynchrony protocols, the LD cycles used were outside of the range of entrainment (e.g., an LD cycle of 28 h). If non-24 h cycles inside the range of entrainment are used, the observed period length shows a so-called after-effect, which depends on the imposed cycle length. Subjects after a 24.65 h cycle displayed a longer period than subjects after entrainment by a 23.5 h cycle and demonstrate the plasticity of the human circadian system (Scheer et al. 2007). Blind individuals exhibit a free-run period closer to 24.5 h, and the shorter period in sighted subjects might represent an aftereffect of the entrained life to 24 h.

18.8.1 Light Synchronizes the Human Circadian System

Which time cues synchronize the human circadian system? The free-running rhythm of humans can be synchronized to the 24 h day by knowing the time of day and by external time cues such as light, temperature, noise, or social contact (for entrainment by non-photic signals, see Mistlberger and Skene 2005). Light plays a much more important role in humans than claimed by, e.g., Wever (1979) in earlier studies, and shorter exposures (Laakso et al. 1993) and lower intensities than assumed before are able to entrain the human circadian system (Wright et al. 2001).

In man, as in other mammals, the eyes seem to be the only places harboring photoreceptors which are able to synchronize or phase shift the circadian rhythms in the SCN, the master clock in vertebrates. Findings of Campbell and Murphy (1998) that extraretinal photoreception can phase shift the circadian rhythm of body temperature and melatonin concentration by illuminating the backside of the knees could not be verified in later experiments; see Rüger et al. (2003) with further references. Recently, Timonen et al. (2012) claimed to have influenced the circadian clock by light administered via the ear. This needs to be confirmed. That the eyes are the only sites for the photoreception is supported by the following:

All humans with bilateral enucleation and 20 % of the remaining blind people exhibit free-running circadian rhythms ("blind free runners," Emens et al. 2005). In the rest either the blindness affects only normal vision of images, but not the *circadian* vision based on the ipRGCs, or other time cues are used for synchronization (Mistlberger and Skene 2005). Occasionally, free run is observed even in people with intact vision living in a normal environment (Giedke et al. 1983; Miles et al. 1977). It is not known why light (and other time cues) are ineffective in these people.

As in other mammals, single light pulses are able to phase shift circadian rhythms in humans. The phase response curve is of the strong or weak type (see page 10), depending on the strength and length of the light exposure (Khalsa et al. 2003; Minors et al. 1991) (questioned, however, by Duffy and Wright 2005 with further references). The human circadian system is responsive to light throughout the daytime (and of course much more during the nighttime, but under normal conditions the daytime light exposure synchronizes the human circadian system) without a "dead zone" (see page 10 and Jewett et al. 1997). A dose-response curve for phase shifting the melatonin rhythm by white light exists. Exposure to a light intensity of 2,000 lx for 1–3 h increased the magnitude of light-induced delays, whereas shorter exposures with higher intensities (4,000 and 8,000 lx) do not increase the shift further (Dewan et al. 2011). Light exposures of as low as 1.5 lx are sufficient to keep the circadian rhythm entrained (Czeisler and Gooley 2007). Phase shifting the rhythm by intermittent light is more effective than is a continuously applied light pulse.

Besides phase the amplitude of the rhythm is an important parameter. A first light pulse has been claimed to reduce the amplitude of the circadian rhythm in man, which would render the system more sensitive toward the phase-shifting effect of a second light pulse (Czeisler et al. 1989). A light pulse of a critical strength applied at a critical phase point (subjective midnight) induces arrhythmicity by pushing the clock into a singular point (references in Czeisler and Gooley (2007); see also page 9).

In order to find out which wavelengths are effective in shifting the phase of the circadian rhythm in man, action spectra (see Chap. 8) were determined by using the suppression of plasma melatonin. The results of those experiments are compiled and discussed by Brainard and Hanifin (2005). Light in the short-wavelength range (459–484 nm) is most effective. This differs from the spectral sensitivity of the visual system and points to special circadian photoreceptors as discussed in Sect. 18.7.3. The circadian rhythms of some people completely blind for vision are still entrained, and this applies also for suppressing melatonin by light. Responsible are the retinal ganglion cells which project directly to the SCN. Rods and cones are apparently dispensable but serve additionally for entrainment. Longer wavelengths are effective in resetting especially at low light intensities. The issue of photoreception and circadian entrainment has been discussed in Sect. 18.7.4 (for humans see also Kronauer et al. 1999). A detailed action spectrum which could help to identify the photoreceptors is still missing. Spectral sensitivity of the retinal ganglion cells to light seems to change during the night (Figueiro et al. 2005). The background light and the history of previous illumination affect the resetting properties of light, but this issue needs more studies.

18.8.2 Significance of Light and the Circadian Clock in Shift Work and Jet Lag

The circadian rhythm of modern man is often delayed with respect to the natural LD cycle. He uses electric light and can therefore stay up during the winter time much longer than natural daylight would otherwise permit (Cardinali 1998). This independence or even insulation from the natural light easily leads to permanent sleep deprivation. In addition, modern society expects full range services throughout the 24 h. Traffic, economy, health service, and security have to rely on shift work or night work by a considerable part of the workers (about 20 % in the industrialized nations, half of them on night or rotating shifts).

Normally the circadian clock is in synchrony with the daily cycling of external 24 h cycles, and the body can adapt to the cyclic demands. Night work and shift work clashes with our circadian clock and disrupts this synchrony. The internal coherence among oscillations is lost and problems may arise. Sleep disturbances and effects on health (Reed 2011; Erren et al. 2010) and on safety of workers and drivers (Philip and Akerstedt 2006; Barger et al. 2005) are due to shift work (Kecklund et al. 2012; Saksvik et al. 2011; Arendt 2010; Folkard 2008) and jet lag (Arendt 2009; Auger and Morgenthaler 2009; Coste and Lagarde 2009).

About 10 % of shift workers suffer from shift work disorder. The resulting internal desynchrony brings behavioral, hormonal, and metabolic rhythms out of phase and increases the risk of gastrointestinal problems, cancer, depression, heart disease, sleep disturbances, and accidents; it furthermore affects reproductive cycles, menstruation, and pregnancy (Mahoney 2010; Su et al. 2008) and decreases productivity (Roth 2012).

The synchronizing effect of light on the circadian system of man is one of the problems of shift work (Monk 2000). For instance, the high fluence rate of outdoor light in the morning after a night shift prevents the phase shift of the circadian system needed for optimal adjustment of the night workers clock (Horowitz et al. 2001). Wearing dark goggles is advisable in this case (Eastman et al. 1994). On the other hand, light can be used also for adjusting the clock to the

shift work schedule, if properly applied (Turek 2005; Crowley et al. 2003). Models are used successfully for constructing LD cycles which phase shift the rhythm in such a way that they align better with shift work and day sleep schedules (Jewett et al. 1999b; Martin and Eastman 1998). More empirical data from shift work effects on the circadian rhythms are, however, needed for detailed simulations of this kind (Åkerstedt 1998). Other counteractions consist of light exposures at certain times of the circadian cycle (Boivin and James 2005) and of using chronobiotics such as melatonin (see Sect. 18.7.6 and Arendt (2005)). In using combinations of light and melatonin, it should be taken into account that the phase-shifting effect of light pulses and melatonin pulses is 180° out of phase (Skene 2003).

Whether the internal desynchrony occurs at a peripheral or at a central level has been studied by Salgado-Delgado et al. (2008) in a rat model. Working and feeding during the sleeping period uncouples metabolic functions from the biological clock which remains fixed to the LD cycle. The data suggest that in night workers the combination of work and eating during working hours may cause internal desynchronization. In this connection the quality of sleep and the cognitive performance of shift workers and workers with day shift only were studied in offshore fleet workers (Hansen et al. 2010). Morning types (for testing the chronobiological phase type, see link [http://nbn-resolving.de/urn:nbn:de:bsz:21-opus-37910] ‖Chronobiological phase type, page 97) are under higher health risk even if treated with bright light (Griefahn and Robens 2010).

This internal desynchrony occurs already at the level of the first output from the SCN, namely, relaying nuclei of the hypothalamus such as the arcuate and dorsomedial nucleus, both associated with metabolism and regulation of the sleep/wake cycle. They transmit temporal signals to other brain areas and to the periphery. The SCN itself and the paraventricular nucleus stay, however, locked to the LD cycle (Salgado-Delgado et al. 2010). Desynchronization between clock and the LD cycle is thus unfavorable or even increases mortality (Park et al. 2012).

Jet lag is another problem. The circadian clock cannot rapidly adapt to a new LD cycle and this leads to desynchrony. Overviews and practical considerations are provided by Kolla and Auger (2011), Arendt (2009), Auger and Morgenthaler (2009), Coste and Lagarde (2009), and Revell and Eastman (2005). Symptoms can be reduced by proper avoidance or exposure to light (Zee and Goldstein 2010). Based on the human phase response curve to light pulses, one should avoid morning light and expose oneself to evening light in flying westward but expose oneself to morning light and avoid evening light in flying eastward (however, flight time and duration influence also adaptation to the new time zone). Chronobiotics (melatonin) and behavioral therapies are alternatives (Srinivasan et al. 2008; Touitou and Bogdan 2007). A discrepancy between biological and social timing leads to chronic sleep shortage and jet lag symptoms (*social jet lag*). It contributes to weight-related pathologies such as obesity (Roenneberg et al. 2012).

18.8.3 Light, Sleep, and Sleep Disorders

The sleep/wake cycle and its influence on performance is an interplay of the external LD and social cycles and of internal oscillators, namely, a circadian clock and a homeostatic oscillator. Sleep homeostasis implies that sleep deficit increases the intensity and duration of sleep and excessive sleep reduces sleep propensity. The circadian system determines sleep propensity, timing of sleep, and sleep structure and consolidates sleep and wakefulness, but the homeostatic oscillator contributes also to sleep timing and duration, to REM and slow-wave sleep, and furthermore to performance parameters such as attention and memory (Dijk and von Schantz 2005). The homeostatic oscillator interacts with the clock or its outputs according to the circadian principle *the longer we are awake*, *the shorter we sleep* and according to the homeostatic regulation of sleep *the longer we are awake*, *the deeper our sleep* (Bjorvatn and Pallesen 2009).

The circadian clock gates sleep and wakefulness in such a way, that it occurs in synchrony with the LD cycle of the environment. The clock stops the production of melatonin and increases cortisol secretion and heart rate 2–3 h prior to waking up (Cajochen et al. 2010).

The effects of light on sleep have been reviewed by Sadeghniiat-Haghighi et al. (2011), Zamanian et al. (2010), and Czeisler and Gooley (2007), and various treatments of sleep disorders are discussed by Thorpy (2011), Dodson and Zee (2010), Bjorvatn and Pallesen (2009), and Blythe et al. (2009).

Common sleep disorders are (Reid et al. 2011; Barion and Zee 2007; Fahey and Zee 2006):

- The rapid time zone change syndrome (jet lag) with excessive sleepiness and a reduced alertness during daytime in people who travel across time zones (Auger and Morgenthaler 2009; Dean et al. 2009).
- The shift work sleep disorder in people who frequently rotate shifts or work at night (Kolla and Auger 2011).
- The delayed sleep phase syndrome; affected people (typically adults) fall asleep at very late times and have difficulties in waking up in time (Rahman et al. 2009; Okawa and Uchiyama 2007).
- The advanced sleep phase syndrome, in which sleep is advanced (frequent in the elderly); affected people are sleepy in the evening; sleep onset and waking up is early (Caruso and Hitchcock 2010). This syndrome is associated with a mutation in Per2, a clock gene (Xu et al. 2005; Toh et al. 2001).

- The non-24 h sleep-wake disorder, in which an individual has a normal sleep pattern but a period deviating from 24 h (Okawa and Uchiyama 2007). This syndrome might be caused by weakened or missing stimuli. In blind people, this disorder is more frequently found (Skene and Arendt 2007; Das et al. 2006). Timed melatonin or Zopiclone treatment and/or bright light treatment was successful in this syndrome but is often not used (fewer than 15 % of the 3,000 blind and visually impaired New Zealanders have been prescribed melatonin Warman et al. 2011).
- Irregular sleep-wake rhythm disorder, in which a circadian pattern is lacking. It occurs in aging and with neurodegenerative diseases, such as Alzheimer's disease, but also in traumatic brain injury and in mentally retarded persons (Zee and Vitiello 2009). Causes are degeneration or decreased neuronal activity of SCN neurons, decreased response of the clock to zeitgeber such as light and activity, too weak exposure to bright light, lack of social contact and physical activity during the day. This disorder is treated by consolidating sleep during the night and wakefulness during the day mainly by restoring or enhancing SCN zeitgeber. Pharmacologic treatments were negative or inconsistent,
- Sleep disturbance in psychiatric disorders (Harvey et al. 2011). Clock genes and dopamin/serotonin have been linked to a range of disorders.

Sleep protection and sleep hygiene are important for the well being of adults, children and babies including premature newborns. For the development of the latter and a relaxed condition and good clinical conditions, oral feeding and a close parent-infant relationship are important. A correct sleeping-awaking pattern is a key factor for the development of the brain. To protect sleep of newborns, the environment has to be modified in such a way, that the noise level is reduced, a dark (or at least a semi-dark) period is offered and the face of the infant protected from direct light (Colombo and Bon 2011).

According to Bruni and Novelli (2010) about 20–30 % of young children are affected by sleep disorders (problems getting to sleep = dyssomnias, sleep terrors and sleepwalking = parasomnias). Besides medication such as melatonin, light therapy and scheduled waking is used as a safe and protective intervention for parasomnias (Montgomery and Dunne 2007).

Gradisar et al. (2011) point to the high incidence of sleep disturbance in the youth and in adults (period 1999–2010 reviewed). Sleep onset is delayed in school students, and this delay increases with age of students, which shortens night sleep and increases daytime sleepiness. Begin of weekend sleep is 2 h later and longer. A worldwide delayed sleep-wake behavior pattern exists and delayed sleep phase disorder is wide spread. A fixed advanced sleep/wake schedule with morning blue-light exposure advances circadian phase (Sharkey et al. 2011). How important short-wavelength light in the morning is has been shown by Figueiro and Rea (2010) and is relevant to lighting practice in schools. Wolfson and Carskadon (2003) discuss the effects of advanced sleep disorder on performance and schoolwork. Kohyama (2011) reports that more than 50 % of interviewed Japanese children complained of daytime sleepiness, 25 % of insomnia, and some of both. It is due to asynchronization, brought about by a combination of nighttime light exposure disturbing the clock and decreased melatonin secretion, and a lack of morning light exposure, which prevents synchronization of the clock to the 24 h cycle and reduces the activity of the serotonergic system. An early phase of asynchronization results from inadequate sleep hygiene. It can easily be resolved by a regular sleep-wake cycle. Without adequate intervention the symptoms worsen and become chronic.

Sleep disorders are common in millions of older adults, which might be partly due to the aging processes of the eye lens. As a result the transmission of blue light to the retina is reduced. The entrainment of the circadian clock is hampered and the risk of sleep disturbances increases. Kessel et al. (2011) showed a positive correlation between lens aging and sleep disorders and propose that this results from a disturbed entrainment.

Additionally, environmental and physiological conditions weaken synchronization in the aged. A regular 24 h LD cycle promotes synchronization. Evening light exposure benefits older adults with early evening sleepiness and does not influence the quality of the subsequent sleep (Münch et al. 2011); low irradiances and 90 min exposure are already sufficient (Figueiro et al. 2011). Further studies are needed (Schmoll et al. 2011; Figueiro et al. 2009; Gammack 2008).

In treating sleep disorders, shiftwork and jet lag, light therapy and melatonin administration are effectively used, whereby the timing of the light exposure are important (Gooley 2008; Lack and Wright 2007; Dagan and Borodkin 2005); for practical advices see Dumont and Beaulieu (2007).

Subjects in polar regions, where suboptimal light conditions prevail during the dark part of the year were studied by Arendt (2012). Their health is affected, and the same is true for people in temperate zones with insufficient light exposure. If the intensity of light exposure was increased, circadian phase advanced and sleep improved. Light rich in blue is more effective than white light. In polar regions at the south base personnel adapt their circadian system to night work within a week, whereas in temperate zones this rarely occurs. The same was found on high-latitude North Sea oil installations. In both cases conflicts with the environmental light are absent, which could explain the faster adaptation.

18.8.4 Shift Work and Cancer

Shift work has increased worldwide and was classified as a potential cancer risk by the International Agency for Research on Cancer in 2007; for background and practical information, see Erren et al. (2010) and Erren (2010). Sufficient evidence from animal experiments exist that light exposure during the biologic night increases tumor growth. There is some evidence that night-shift work causes breast cancer (Hansen and Stevens 2011), for which the light exposure during the night could be responsible by reducing melatonin production (Reed 2011).

If night-shift work should indeed increase breast cancer rate, blindness should lower the risk and nighttime illumination in communities should increase it. This was confirmed by studies (Stevens 2009b). Furthermore, clock genes have been related to breast cancer risk, particularly a *Per3* mutation. The same mutation predicts a chronobiological morning type and shorter sleep duration. Epigenetic influences on clock genes might be caused by night light (Stevens 2009a).

However, phase shift of the circadian rhythm, sleep disruption, lifestyle factors such as diet, less physical activity and a high BMI and lower vitamin D as well as endocrine influences due to a disturbed clock (Fritschi et al. 2011; Costa et al. 2010) could be additional factors increasing cancer risk (Humble 2010; Bertone-Johnson 2009). Independent of melatonin there is an interaction between sleep and the immune system: Sleep disturbances can suppress the immune system and increase cancer-stimulatory cytokines. However, the causes of cancer are complex and manyfold. An undisturbed and good sleep without light interruption could be a way of reducing the cancer risk (Blask 2009).

18.8.5 Affective Disorders, Endogenous Depressions

Circadian rhythms are not influenced by jet lag, shift work and sleep disorders only, but also by several psychiatric disorders. They include affective disorders, in which the amplitude and phase of several rhythms are altered. It has therefore been suggested that the clock is changed or its sensitivity to zeitgeber such as light or social cues. Non-pharmacological (light therapy, sleep deprivation) and pharmacological (lithium, antidepressants, agomelatine, vitamin D) (Parker and Brotchie 2011, and Chapter 23) therapies of affective disorders influence circadian rhythms, which might indicate that they play a role in these disorders (Schulz and Steimer 2009).

There are several connections between endogenous depression and circadian rhythms (Chellappa et al. 2009; Germain and Kupfer 2008; Lamont et al. 2007; McClung 2007), the causes of which are not well understood. Animal models could help here (Kronfeld-Schor and Einat 2012; Workman and Nelson 2011; Ashkenazy et al. 2009a, b). In depressed patients the phase relationship of the circadian rhythm to the light sensitivity could be anomalous due to some defect in the retina (Steiner et al. 1987). Treatments which affect the circadian rhythms and the sensitivity of the retina to light have a therapeutic effect (Even et al. 2008; Terman and Terman 1999).

A number of disorders in humans are caused by circadian desynchrony as a result of improper light schedules. The physiological responses are discussed by Antle et al. (2009). Clinical aspects of human circadian rhythms are described by Klerman (2005) and practical aspects of chronotherapeutics and chronopharmacological aspects by Wirz- Justice and Terman (2012), Ohdo et al. (2011), Levi and Schibler (2007), and Benedetti et al. (2007).

Four subtypes of depression can be self-treated using agents without prescription: *neuroticism* with *Hypericum perforatum* and antihistamines, *malaise* (fatigue, aching, etc.) in cases of an activated immune system with analgesics, *demotivation* with energizing agents, and *SAD* with bright morning light. *Melancholia*, however, cannot be self-treated and requires hospitalization, if severe (Charlton 2009).

18.8.5.1 SAD: A Recurrent Depression

A special type of depression is the seasonal affective disorder (SAD). It was described by Rosenthal et al. (1984), and his book (Rosenthal 2006) is a standard introduction. Patients show typical symptoms of major depressive disorder, but the depressive episodes occur at a characteristic time of the year. It affects 0.4–2.9 % of the US population. The figures vary between different studies (Howland 2009a; Westrin and Lam 2007a; Winkler et al. 2006), countries, and cultures (Kasof 2009). SAD is found also in children (Giedd et al. 1998), but not as commonly as in young adults, and is more frequent in women. SAD occurs at various latitudes (Kegel et al. 2009; Hansen et al. 2008; Mersch et al. 1999) and in both hemispheres (Brancaleoni et al. 2009; Teng et al. 1995). In polar regions SAD is rare, but a milder form is reported (Magnusson and Partonen 2005).

SAD occurs usually during fall or winter (Madsen et al. 2012). The cognitive and emotional symptoms are as in other types of depression, but the vegetative symptoms are reversed, namely, longer sleep and increased appetite. During spring the symptoms disappear due to the daylight or a light therapy. The latter is effective both in seasonal and in non-seasonal depression (Fischer et al. 2012; Pail et al. 2011; Howland 2009b; Shirani and Louis 2009; Prasko 2008; Even et al. 2008; Terman 2007; Michalak et al. 2007; Levitan 2005 and Golden et al. 2005), but it has, however, to be continued during the winter. It is recommended against SAD in Canadian, American, and international clinical guidelines.

Bright light is more effective than dim light (Rastad et al. 2011), although room light does work in mild cases (Rastad et al. 2008). An exposure of 10 min is already sufficient (Tanaka et al. 2011) and even the light of light-emitting diodes of a "litebook" screen (Desan et al. 2007). Effective doses depend on the individual and range from 10,000 lx for 30 min/day for 8 weeks to 3,000 lx for 2 h/day for 5 weeks. Patients sit comfortably in front of the light box and glance occasionally at it. The amount of light and the wavelength was studied by Anderson et al. (2009). Blue light (Gordijn et al. 2012; Pail et al. 2011; Strong et al. 2009) or blue-light-enriched white light (Meesters et al. 2011) is more effective than standard treatment and red light (Gagné et al. 2011).

Light therapy works for 20–50 % of SAD patients only (Terman et al. 1996). Therefore, alternatives or additional methods are used such as cognitive-behavioral therapy (Rohan et al. 2009), negative air ions (Flory et al. 2010), and pharmacological treatments using antidepressants (Westrin and Lam 2007b; Winkler et al. 2006). Second-generation antidepressants (fluoxetine, escitalopram, duloxetine, reboxetine) are, however, not effective (Thaler et al. 2011). An alternative way of applying light for SAD treatment via the ear canal was used by Timonen et al. (2012). Predictors of response to light therapy were studied by Privitera et al. (2010). Light might exert its effect via the retina of SAD patients, but this has not been verified yet (Lavoie et al. 2009).

According to the phase shift hypothesis, SAD patients become depressed, because the circadian clock is delayed with respect to the sleep/wake cycle. The severity of symptoms does indeed correlate with the degree of misalignment. As a therapy, light exposure in the morning phase advances the clock and restores the correct phase relationship. An alternative treatment is afternoon/evening low-dose melatonin application.

A subgroup of SAD patients is phase advanced, and light should be administered in the evening and melatonin in the morning, but the other type is predominant (Lewy et al. 2006a, b, 2007, 2009).

The duration of melatonin secretion may be influenced in SAD (Salva et al. 2011; Srinivasan et al. 2006), and therefore, melatonin might work as a therapy (Lewy 2007; Lewy et al. 2006a, b). The binding of monoaminergic ligands in the brain changes seasonally, and brain monoamine transmission is involved in many psychiatric disorders. Seen from a phylogenetic standpoint, monoamines adapt the organisms and cells to seasonal changes in the environment such as light, temperature, and energy resources (Praschak-Rieder and Willeit 2012; Ciarleglio et al. 2011; Willeit et al. 2008).

In this connection it has been discussed, whether SAD might reflect some kind of photoperiodic reaction in humans (Howland 2009b; Levitan 2007; Bronson 2004; Wehr 2001; Roenneberg and Aschoff 1990). Photoperiodism in primates is well known (Cayetanot et al. 2005; Oster et al. 2002; Wehr 2001; Di Bitetti and Janson 2000). Sleep, body weight, mood, and behavior in humans are under seasonal control (Cizza et al. 2011). However, the influence of temperature fluctuations and day length is nowadays much lower due to temperature control and the use of artificial light. Sleep has shortened, more food is consumed, and the long-term weight has increased. Especially in women, who are more predisposed to seasonality, SAD might be analogous to hibernation. It is characterized by depressed mood, hypersomnia, weight gain, and carbohydrate craving during the winter.

Hereditary factors seem also to be involved in SAD, as evidenced by family history, twin studies, and molecular genetics studies (Howland 2009a). The mutated gene expressing melanopsin is supposed to increase the risk of SAD (Roecklein et al. 2009), reactions of the hypothalamus to light might be abnormal (Vandewalle et al. 2011), and clock genes might be involved in mental disorders (Lamont et al. 2007; McClung 2007).

There are many questions unanswered, before the light/SAD/clock relations are settled (Klerman 2005). General (Partonen and Magnusson 2001) and special literature on SAD are by Praschak-Rieder and Willeit (2012), Lewy et al. (2006a, b), and two articles in Touitou (1998), and for management of SAD, see Author (2009) and Lam and Levitan (2000).

18.9 Final Remarks and Acknowledgements

In this chapter, we tried to give an overview of circadian rhythms and their entrainment by light by selecting examples from various organisms. The choices are subjective but cover the widespread occurrence of these rhythms ranging from cyanobacteria to human beings.

The reader will have noticed that the field is a wide one and developing fast, for instance, by comparing the present edition of the book with the second (2008) and first one (2008). It is not easy to keep up with new results and sometimes difficult to judge in cases of controversial findings and opinions. We have tried to cover results published in a large number of papers (more than 700 cited). To restrict the number of references, we have preferred to cite reviews and relatively recent papers. If more detailed references are needed, contact the third author at engelmann@uni-tuebingen.de.

We acknowledge help of many colleagues providing literature, information, and critique, especially Lars Olof Björn, Jonathan Emens, Susan Golden, Carl Johnson, Patricia Lakin-Thomas, Stephan Michel, Takao Kondo, Peter Ruoff, Ueli Schibler, Dorothea Staiger, Stephan Steinlechner, Michael Young, Hinrich Lüning, Påvel Nicklasson, François-Yves Bouget, and Marc Lefranc and Dennis Pauls and Christian Wegener, Würzburg.

References

Able KP (1995) Orientation and navigation: a perspective on fifty years of research. Condor 97:592–604

Abraham U, Granada AE, Westermark PO, Heine M, Kramer A, Herzel H (2010) Coupling governs entrainment range of circadian clocks. Mol Syst Biol 6:438

Adams S, Carré IA (2011) Downstream of the plant circadian clock: output pathways for the control of physiology and development. Essays Biochem 49:53–69

Agosto J, Choi JC, Parisky KM, Stilwell G, Rosbash M, Griffith LC (2008) Modulation of GABAA receptor desensitization uncouples sleep onset and maintenance in *Drosophila*. Nat Neurosci 11:354–359

Åkerstedt T (1998) Is there an optimal sleep-wake pattern in shift work? Scand J Work Environ Health 24(Suppl 3):18–27

Akiyama S (2012) Structural and dynamic aspects of protein clocks: how can they be so slow and stable? Cell Mol Life Sci 69:2147–2160

Allada R, Chung BY (2010) Circadian organization of behavior and physiology in *Drosophila*. Annu Rev Physiol 72:605–624

Amasino R (2010) Seasonal and developmental timing of flowering. Plant J 61:1001–1013

Amdaoud M, Vallade M, Weiss-Schaber C, Mihalcescu I (2007) Cyanobacterial clock, a stable phase oscillator with negligible intercellular coupling. Proc Natl Acad Sci U S A 104:7051–7056

Anderson JL, Glod CA, Dai J, Cao Y, Lockley SW (2009) Lux vs. wavelength in light treatment of seasonal affective disorder. Acta Psychiatr Scand 120:203–212

Antle MC, Smith VM, Sterniczuk R, Yamakawa GR, Rakai BD (2009) Physiological responses of the circadian clock to acute light exposure at night. Rev Endocr Metab Disord 10:279–291

Aoki S, Kondo T, Wada H, Ishiura M (1997) Circadian rhythm of the cyanobacterium *Synechocystis sp*. strain PCC 6803 in the dark. J Bacteriol 179:5751–5755

Arendt J (2005) Melatonin: characteristics, concerns, and prospects. J Biol Rhythms 20:291–303

Arendt J (2009) Managing jet lag: some of the problems and possible new solutions. Sleep Med Rev 13:249–256

Arendt J (2010) Shift work: coping with the biological clock. Occup Med 60:10–20

Arendt J (2012) Biological rhythms during residence in polar regions. Chronobiol Int 29:379–394

Ashkenazi I, Hartman H, Strulovitz B, Dar O (1975) Activity rhythms of enzymes in human red blood cell suspension. J Interdisc Cycle Res 6:291–301

Ashkenazy T, Einat H, Kronfeld-Schor N (2009a) Effects of bright light treatment on depression- and anxiety-like behaviors of diurnal rodents maintained on a short daylight schedule. Behav Brain Res 201:343–346

Ashkenazy T, Einat H, Kronfeld-Schor N (2009b) We are in the dark here: induction of depression- and anxiety-like behaviours in the diurnal fat sand rat, by short daylight or melatonin injections. Int J Neuropsychopharmacol 12:83–93

Auger RR, Morgenthaler TI (2009) Jet lag and other sleep disorders relevant to the traveler. Travel Med Infect Dis 7:60–68

Auldridge ME, Forest KT (2011) Bacterial phytochromes: more than meets the light. Crit Rev Biochem Mol Biol 46:67–88

Anonymous (2009) Management of seasonal affective disorder. Drug Ther Bull 47:128–132

Axmann IM, Dühring U, Seeliger L, Arnold A, Vanselow JT, Kramer A, Wilde A (2009) Biochemical evidence for a timing mechanism in *Prochlorococcus*. J Bacteriol 191:5342–5347

Bachleitner W, Kempinger L, Wülbeck C, Rieger D, Helfrich-Förster C (2007) Moonlight shifts the endogenous clock of *Drosophila melanogaster*. Proc Natl Acad Sci U S A 104:3538–3543

Baggs JE, Hogenesch JB (2010) Genomics and systems approaches in the mammalian circadian clock. Curr Opin Genet Dev 20:581–587

Bailes HJ, Lucas RJ (2010) Melanopsin and inner retinal photoreception. Cell Mol Life Sci 67:99–111

Baker CL, Loros JJ, Dunlap JC (2012) The circadian clock of *Neurospora crassa*. FEMS Microbiol Rev 36:95–110

Barger LK, Cade BE, Ayas NT, Cronin JW, Rosner B, Speizer FE, Czeisler CA (2005) Extended work shifts and the risk of motor vehicle crashes among interns. N Engl J Med 352:125–134

Barion A, Zee PC (2007) A clinical approach to circadian rhythm sleep disorders. Sleep Med 8:566–577

Barrenetxe J, Delagrange P, Martinez JA (2004) Physiological and metabolic functions of melatonin. J Physiol Biochem 60:61–72

Barth M, Schultze M, Schuster CM, Strauss R (2010) Circadian plasticity in photoreceptor cells controls visual coding efficiency in *Drosophila melanogaster*. PLoS One 5:e9217

Bass J, Takahashi JS (2010) Circadian integration of metabolism and energetics. Science 330:1349–1354

Beaule C, Amir S (2003) The eyes suppress a circadian rhythm of fos expression in the suprachiasmatic nucleus in the absence of light. Neuroscience 121:253–257

Beaver LM, Gvakharia BO, Vollintine TS, Hege DM, Stanewsky R, Giebultowicz JM (2002) Loss of circadian clock function decreases reproductive fitness in males of *Drosophila melanogaster*. Proc Natl Acad Sci USA 19:2134–2139

Beersma DGM (2005) Why and how do we model circadian rhythms? J Biol Rhythms 20:304–313

Bell-Pedersen D (2000) Understanding circadian rhythmicity in *Neurospora crassa*: from behavior to genes and back again. Fungal Genet Biol 29:1–18

Bell-Pedersen D, Cassone V, Earnest D, Golden S, Hardin P, Thomas T, Zoran M (2005) Circadian rhythms from multiple oscillators: lessons from diverse organisms. Nat Rev Genet 6:544–556

Bellet MM, Sassone-Corsi P (2010) Mammalian circadian clock and metabolism - the epigenetic link. J Cell Sci 123:3837–3848

Bellingham J, Chaurasia S, Melyan Z, Liu C, Cameron M, Tarttelin E, Iuvone P, Hankins M, Tosini G, Lucas R (2006) Evolution of melanopsin photoreceptors: discovery and characterization of a new melanopsin in nonmammalian vertebrates. PLoS Biol 4:e254

Belozerskaya TA, Gessler NN, Isakova EP, Deryabina YI (2012) *Neurospora crassa* light signal transduction is affected by ROS. J Signal Transduct 2012:791963

Belvin MP, Zhou H, Yin JC (1999) The *Drosophila* dCREB2 gene affects the circadian clock. Neuron 22:777–787

Benedetti B, Barbini B, Colombo C, Smeraldi E (2007) Chronotherapeutics in a psychiatric ward. Sleep Med Rev 11:509–522

Benito J, Houl JH, Roman GW, Hardin PE (2008) The blue-light photoreceptor cryptochrome is expressed in a subset of circadian oscillator neurons in the *Drosophila* cns. J Biol Rhythms 23:296–307

Berndt A, Kottke T, Breitkreuz H, Dvorsky R, Hennig S, Alexander M, Wolf E (2007) A novel photoreaction mechanism for the circadian blue light photoreceptor *Drosophila* cryptochrome. J Biol Chem 282:13011–13021

Berson DM (2003) Strange vision: ganglion cells as circadian photoreceptor. Trends Neurosci 26:314–320

Bertolucci C, Foà A (2004) Extraocular photoreception and circadian entrainment in nonmammalian vertebrates. Chronobiol Int 21:501–519

Bertone-Johnson ER (2009) Vitamin D and the occurrence of depression: causal association or circumstantial evidence? Nutr Rev 67:481–492

Di Bitetti MS, Janson CH (2000) When will the stork arrive? Patterns of birth seasonality in neotropical primates. Am J Primatol 50:109–130

Bjorvatn B, Pallesen S (2009) A practical approach to circadian rhythm sleep disorders. Sleep Med Rev 13:47–60

Blask DE (2009) Melatonin, sleep disturbance and cancer risk. Sleep Med Rev 13:257–264
Blythe J, Doghramji PP, Jungquist CR, Landau MB, Valerio TD, Ancoli-Israel S, Auerbach SH (2009) Screening & treating patients with sleep/wake disorders. JAAPA Suppl Sleep, 1–17; quiz 19
Bobu C, Hicks D (2009) Regulation of retinal photoreceptor phagocytosis in a diurnal mammal by circadian clocks and ambient lighting. Invest Ophthalmol Vis Sci 50:3495–3502
Bodenstein C, Heiland I, Schuster S (2011) Calculating activation energies for temperature compensation in circadian rhythms. Phys Biol 8:056007
Boesger J, Wagner V, Weisheit W, Mittag M (2009) Analysis of flagellar phosphoproteins from *Chlamydomonas reinhardtii*. Eukaryot Cell 8:922–932
Boivin DB, James FO (2005) Light treatment and circadian adaptation to shift work. Ind Health 43:34–48
Bollig I, Chandrashekaran M, Engelmann W, Johnsson A (1976) Photoperiodism in *Chenopodium rubrum* – an explicit version of the Bünning hypothesis. Int J Chronobiol 4:83–96
Borjigin J, Zhang LS, Calinescu AA (2012) Circadian regulation of pineal gland rhythmicity. Mol Cell Endocrinol 349:13–19
Bradley RL, Reddy KJ (1997) Cloning, sequencing, and regulation of the global nitrogen regulator gene ntca in the unicellular diazotrophic cyanobacterium *Cyanothece* sp. strain BH68K. J Bacteriol 179:4407–4410
Brainard GC, Hanifin JP (2005) Photons, clocks, and consciousness. J Biol Rhythms 20:314–325
Brainard GC, Richardson BA, King TS, Matthews SA, Reiter RJ (1983) The suppression of pineal melatonin content and N-acetyltransferase activity by different light irradiances in the Syrian hamster: a dose-response relationship. Endocrinology 113:293–296
Brainard GC, Sliney G, Hanifin JP, Glickman G, Byrne B, Greeson JM, Jasser S, Gerner E, Rollag MD (2008) Sensitivity of the human circadian system to short-wavelength (420-nm) light. J Biol Rhythms 23:379–386
Brancaleoni G, Nikitenkova E, Grassi L, Hansen V (2009) Seasonal affective disorder and latitude of living. Epidemiol Psichiatr Soc 18:336–343
Breton G, Kay SA (2006) Circadian rhythms lit up in *Chlamydomonas*. Genome Biol 7:215
Brody S, Oelhafen K, Schneider K, Perrino S, Goetz A, Wang C, English C (2010) Circadian rhythms in *Neurospora crassa*: downstream effectors. Fungal Genet Biol 47:159–168
Bronson FH (2004) Are humans seasonally photoperiodic? J Biol Rhythms 19:180–192
Brown SA, Kowalska E, Dallmann R (2012) (Re)inventing the circadian feedback loop. Dev Cell 22:477–487
Bruce VG (1970) The biological clock in *Chlamydomonas reinhardi*. J Protozool 17:328–334
Bruce VG (1972) Mutants of the biological clock in *Chlamydomonas reinhardi*. Genetics 70:537–548
Bruni O, Novelli L (2010) Sleep disorders in children. Clin Evid (Online)
Brunner M, Káldi K (2008) Interlocked feedback loops of the circadian clock of *Neurospora crassa*. Mol Microbiol 68:255–262
Brunner M, Schafmeier T (2006) Transcriptional and post-transcriptional regulation of the circadian clock of cyanobacteria and *Neurospora*. Genes Dev 20:1061–1074
Brunner M, Simons MJP, Merrow M (2008) Lego clocks: building a clock from parts. Genes Dev 22:1422–1426
Bryant TR (1972) Gas exchange in dry seeds: circadian rhythmicity in the absence of DNA replication, transcription, and translation. Science 178:634–636
Bushey D, Cirelli C (2011) From genetics to structure to function: exploring sleep in *Drosophila*. Int Rev Neurobiol 99:213–244
Butler MP, Rainbow MN, Rodriguez E, Lyon SM, Silver R (2012) Twelve-hour days in the brain and behavior of split hamsters. Eur J Neurosci 36:2556–2566
Byrne TE, Wells MR, Johnson CH (1992) Circadian rhythms of chemotaxis to ammonium and of methylammonium uptake in *Chlamydomonas*. Plant Physiol 98:879–886
Bünning E (1936) Die endonome Tagesrhythmik als Grundlage der photoperiodischen Reaktion. Ber Deut Bot Ges 54:590–607
Cajochen C, Chellappa S, Schmidt C (2010) What keeps us awake? The role of clocks and hourglasses, light, and melatonin. Int Rev Neurobiol 93:57–90
Campbell SS, Murphy PJ (1998) Extraocular circadian phototransduction in humans. Science 279:396–399
Cardinali D (1998) The human body circadian: how the biological clock influences sleep and emotion. Cienc Cult 50:172–177
Caruso CC, Hitchcock EM (2010) Strategies for nurses to prevent sleep-related injuries and errors. Rehabil Nurs 35:192–197
Castro-Longoria E, Ferry M, Bartnicki-Garcia S, Hasty J, Brody S (2010) Circadian rhythms in *Neurospora crassa*: dynamics of the clock component frequency visualized using a fluorescent reporter. Fungal Genet Biol 47:332–341
Cayetanot F, van Someren EJW, Perret M, Aujard F (2005) Shortened seasonal photoperiodic cycles accelerate aging of the diurnal and circadian locomotor activity rhythms in a primate. J Biol Rhythms 20:461–469
Ceriani M, Darlington T, Staknis D, Mas P, Petti A, Weitz C, Kay S (1999) Light-dependent sequestration of TIMELESS by CRYPTOCHROME. Science 285:553–568
Cermakian N, Boivin DB (2009) The regulation of central and peripheral circadian clocks in humans. Obes Rev 10(Suppl 2):25–36
Cervený J, Nedbal L (2009) Metabolic rhythms of the cyanobacterium Cyanothece sp. ATCC 51142 correlate with modeled dynamics of circadian clock. J Biol Rhythms 24:295–303
Challet E (2007) Minireview: entrainment of the suprachiasmatic clockwork in diurnal and nocturnal mammals. Endocrinology 148:5648–5655
Chandrashekaran MK, Engelmann W (1973) Early and late subjective night phase of the *Drosophila* rhythm require different energies of blue light for phase shifting. Z Naturforsch 28c:750–753
Charlton BG (2009) A model for self-treatment of four sub-types of symptomatic 'depression' using non-prescription agents: neuroticism (anxiety and emotional instability); malaise (fatigue and painful symptoms); demotivation (anhedonia) and seasonal affective disorder 'SAD'. Med Hypotheses 72:1–7
Chaves I, Pokorny R, Byrdin M, Hoang N, Ritz T, Brettel K, Essen L-O, van der Horst GTJ, Batschauer A, Ahmad M (2011) The cryptochromes: blue light photoreceptors in plants and animals. Annu Rev Plant Biol 62:335–364
Chellappa SL, Schröder C, Cajochen C (2009) Chronobiology, excessive daytime sleepiness and depression: is there a link? Sleep Med 10:505–514
Chen CH, Dunlap JC, Loros JJ (2010) Neurospora illuminates fungal photoreception. Fungal Genet Biol 47:922–929
Cho H, Zhao X, Hatori M, Yu RT, Barish GD, Lam MT, Chong L-W, Di- Tacchio L, Atkins AR, Glass CK, Liddle C, Auwerx J, Downes M, Panda S, Evans RM (2012) Regulation of circadian behaviour and metabolism by REV-ERB-a and REV-ERB-b. Nature 485:123–127
Choi C, Nitabach MN (2010) Circadian biology: environmental regulation of a multioscillator network. Curr Biol 20:R322–R324
Chow BY, Helfer A, Nusinow DA, Kay SA (2012) ELF3 recruitment to the PRR9 promoter requires other evening complex members in the *Arabidopsis* circadian clock. Plant Signal Behav 7:170–173
Chung BY, Kilman VL, Keath JR, Pitman JL, Allada R (2009) The GABA(A) receptor RDL acts in peptidergic PDF neurons to promote sleep in Drosophila. Curr Biol 19:386–390

Ciarleglio CM, Resuehr HES, McMahon DG (2011) Interactions of the serotonin and circadian systems: nature and nurture in rhythms and blues. Neuroscience 197:8–16
Cizza G, Requena M, Galli G, de Jonge L (2011) Chronic sleep deprivation and seasonality: implications for the obesity epidemic. J Endocrinol Invest 34:793–800
Clauser C (1954) Die Kopfuhr. Ferdinand Enke, Stuttgart
Collett TS (2008) Insect navigation: visual panoramas and the sky compass. Curr Biol 18:R1058–R1061
Collin SP, Davies WL, Hart NS, Hunt DM (2009) The evolution of early vertebrate photoreceptors. Philos Trans R Soc Lond B Biol Sci 364:2925–2940
Colombo G, Bon GD (2011) Strategies to protect sleep. J Matern Fetal Neonatal Med 24(Suppl 1):30–31
Colot HV, Park G, Turner GE, Ringelberg C, Crew CM, Litvinkova L, Weiss RL, Borkovich KA, Dunlap JC (2006) A high-throughput gene knockout procedure for *Neurospora* reveals functions for multiple transcription factors. Proc Natl Acad Sci U S A 103: 10352–10357
Colwell CS (2011) Linking neural activity and molecular oscillations in the SCN. Nat Rev Neurosci 12:553–569
Corellou F, Schwartz C, Motta J-P, Djouani-Tahri EB, Sanchez F, Bouget F-Y (2009) Clocks in the green lineage: comparative functional analysis of the circadian architecture of the picoeukaryote *Ostreococcus*. Plant Cell 21:3436–3449
Correa A, Bell-Pedersen D (2002) Distinct signaling pathways from the circadian clock participate in regulation of rhythmic conidiospore development in *Neurospora crassa*. Eukaryot Cell 1:273–280
Correa A, Lewis ZA, Greene AV, March IJ, Gomer RH, Bell-Pedersen D (2003) Multiple oscillators regulate circadian gene expression in *Neurospora*. Proc Natl Acad Sci U S A 100:13597–13602
Costa G, Haus E, Stevens R (2010) Shift work and cancer – considerations on rationale, mechanisms, and epidemiology. Scand J Work Environ Health 36:163–179
Coste O, Lagarde D (2009) Clinical management of jet lag: what can be proposed when performance is critical? Travel Med Infect Dis 7:82–87
Courties C, Chretiennot-Dinet MJ (1994) Smallest eukaryotic organism. Nature 370:255
Covington MF, Pandab S, Liu XL, Strayer CA, Wagner DR, Kay SA (2001) ELF3 modulates resetting of the circadian clock in *Arabidopsis*. Plant Cell 13:1305–1316
Crosthwaite SK, Dunlap JC, Loros JJ (1997) Neurospora wc-1 and wc-2: transcription, photoresponses, and the origins of circadian rhythmicity. Science 276:763–769
Crowley SJ, Lee C, Tseng CY, Fogg LF, Eastman CI (2003) Combinations of bright light, scheduled dark, sunglasses, and melatonin to facilitate circadian entrainment to night shift work. J Biol Rhythms 18:513–523
Cyran S, Yiannoulos G, Buchsbaum A, Saez L, Young M, Blau J (2005) The double-time protein kinase regulates the subcellular localization of the *Drosophila* clock protein period. J Neurosci 25:5430–5437
Czeisler CA, Gooley JJ (2007) Sleep and circadian rhythms in humans. Cold Spring Harb Symp Quant Biol 72:579–597
Czeisler C, Kronauer R, Allan J, Duffy J, Jewett M, Brown E, Ronda J (1989) Bright light induction of strong (type 0) resetting of the human circadian pacemaker. Science 244:1328–1333
Czeisler CA, Duffy JF, Shanahan TL, Brown EN, Mitchell JF, Rimmer DW, Ronda JM, Silva EJ, Allan JS, Emens JS, Dijk DJ, Kronauer RE (1999) Stability, precision, and near-24-hour period of the human circadian pacemaker. Science 284:2177–2181
Daan S, Spoelstra K, Albrecht U, Schmutz I, Daan M, Daan B, Rienks F, Poletaeva I, dell'Omo G, Vyssotski A, Lipp HP (2011) Lab mice in the field: unorthodox daily activity and effects of a dysfunctional circadian clock allele. J Biol Rhythms 26:118–129
Daan SA, Albrecht U, van der Horst GTJ, Illnerova H, Roenneberg T, Wehr TA, Schwartz WJ (2001) Assembling a clock for all seasons: are there M and E oscillators in the genes? J Biol Rhythms 16:105–116
Dacke M, Byrne MJ, Baird E, Scholtz CH, Warrant EJ (2011) How dim is dim? Precision of the celestial compass in moonlight and sunlight. Philos Trans R Soc Lond B Biol Sci 366:697–702
Dagan Y, Borodkin K (2005) Behavioral and psychiatric consequences of sleep-wake schedule disorders. Dialogues Clin Neurosci 7:357–365
Dalchau N (2012) Understanding biological timing using mechanistic and black-box models. New Phytol 193:852–858
Das A, Sasmal NK, Deb RK, Bera NK, Sanyal D, Chatterjee SS, Bhaduri G (2006) A study of sleeping disorders in blind patients. J Indian Med Assoc 104:619–621, 626
Davies WIL, Collin SP, Hunt DM (2012) Molecular ecology and adaptation of visual photopigments in craniates. Mol Ecol 21:3121–3158
Davis RH (2000) *Neurospora*: contributions of a model organism. Oxford University Press, Oxford
De J, Varma V, Sharma VK (2012) Adult emergence rhythm of fruit flies *Drosophila melanogaster* under seminatural conditions. J Biol Rhythms 27:280–286
Deacon S, Arendt J (1996) Adapting to phase shifts. I. An experimental model for jet lag and shift work. Physiol Behav 59:665–673
Dean DA, Forger DB, Klerman EB (2009) Taking the lag out of jet lag through model-based schedule design. PLoS Comput Biol 5:e1000418
DeCoursey P, Krulas J (1998) Behavior of SCN-lesioned chipmunks in a natural habitat: a pilot study. J Biol Rhythms 13:229–244
Demir-Hilton E, Sudek S, Cuvelier ML, Gentemann CL, Zehr JP, Worden AZ (2011) Global distribution patterns of distinct clades of the photosynthetic picoeukaryote *Ostreococcus*. ISME J 5:1095–1107
Desan PH, Weinstein AJ, Michalak EE, Tam EM, Meesters Y, Ruiter MJ, Horn E, Telner J, Iskandar H, Boivin DB, Lam RW (2007) A controlled trial of the litebook light-emitting diode (LED) light therapy device for treatment of seasonal affective disorder (SAD). BMC Psychiatry 7:38
Devlin PF (2002) Signs of the time: environmental input to the circadian clock. J Exp Bot 53:1535–1550
Dewan K, Benloucif S, Reid K, Wolfe LF, Zee PC (2011) Light-induced changes of the circadian clock of humans: increasing duration is more effective than increasing light intensity. Sleep 34:593–599
Dharmananda S (1980) Studies on the circadian clock of *Neurospora crassa*: lightinduced phase shifting. Ph.D. thesis, University of California, Santa Cruz
Dibner C, Sage D, Unser M, Bauer C, d'Eysmond T, Naef F, Schibler U (2009) Circadian gene expression is resilient to large fluctuations in overall transcription rates. EMBO J 28:123–134
Dibner C, Schibler U, Albrecht U (2010) The mammalian circadian timing system: organization and coordination of central and peripheral clocks. Annu Rev Physiol 72:517–549
Diernfellner AC, Schafmeier T, Merrow MW, Brunner M (2005) Molecular mechanism of temperature sensing by the circadian clock of *Neurospora crassa*. Genes Dev 19:1968–1973
Diernfellner A, Colot HV, Dintsis O, Loros JJ, Dunlap JC, Brunner M (2007) Long and short isoforms of neurospora clock protein frq support temperature compensated circadian rhythms. FEBS Lett 581:5759–5764
Diez-Noguera A (1994) A functional model of the circadian system based on the degree of intercommunication in a complex system. Am J Physiol 267:1118–1135
Dijk D-J, von Schantz M (2005) Timing and consolidation of human sleep, wakefullness, and performance by a symphony of oscillators. J Biol Rhythms 20:279–290

Djouani-Tahri E-B, Christie JM, Sanchez-Ferandin S, Sanchez F, Bouget F-Y, Corellou F (2011a) A eukaryotic LOV-histidine kinase with circadian clock function in the picoalga *Ostreococcus*. Plant J 65:578–588

Djouani-Tahri EB, Sanchez F, Lozano J-C, Bouget F-Y (2011b) A phosphate regulated promoter for fine-tuned and reversible overexpression in *Ostreococcus*: application to circadian clock functional analysis. PLoS One 6:e28471

Do MTH, Yau K-W (2010) Intrinsically photosensitive retinal ganglion cells. Physiol Rev 90:1547–1581

Dodd AN, Salathia N, Hall A, Kévei E, Tóth R, Nagy F, Hibberd JM, Millar AJ, Webb AAR (2005) Plant circadian clocks increase photosynthesis, growth, survival, and competitive advantage. Science 309:630–633

Dodson ER, Zee PC (2010) Therapeutics for circadian rhythm sleep disorders. Sleep Med Clin 5:701–715

Dong G, Golden SS (2008) How a cyanobacterium tells time. Curr Opin Microbiol 11:541–546

Dong G, Kim Y-I, Golden SS (2010a) Simplicity and complexity in the cyanobacterial circadian clock mechanism. Curr Opin Genet Dev 20:619–625

Dong G, Yang Q, Wang Q, Kim Y-I, Wood TL, Osteryoung KW, van Oudenaarden A, Golden SS (2010b) Elevated ATPase activity of KaiC applies a circadian checkpoint on cell division in *Synechococcus elongatus*. Cell 140:529–539

Dong W, Tang X, Yu Y, Nilsen R, Kim R, Griffith J, Arnold J, Schüttler H-B (2008) Systems biology of the clock in neurospora crassa. PLoS One 3:e3105

Dragovic Z (2002) Light reception and circadian behavior in 'blind' and 'clock-less' mutants of *Neurospora crassa*. EMBO J 21: 3643–3651

Duffy JF, Wright KP (2005) Entrainment of the human circadian system by light. J Biol Rhythms 20:326–338

Duguay D, Cermakian N (2009) The crosstalk between physiology and circadian clock proteins. Chronobiol Int 26:1479–1513

Dumont M, Beaulieu C (2007) Light exposure in the natural environment: relevance to mood and sleep disorders. Sleep Med 8:557–565

Dunlap J, Loros J (2004) The *Neurospora* circadian system. J Biol Rhythms 19:414–424

Dunlap J, Loros J (2005) Analysis of circadian rhythms in *Neurospora*: overview of assays and genetic and molecular biological manipulation. Methods Enzymol 393:3–22

Dunlap JC, Loros JJ (2006) How fungi keep time: circadian system in Neurospora and other fungi. Curr Opin Microbiol 9:579–587

Dunlap JC, Loros JJ, Colot HV, Mehra A, Belden WJ, Shi M, Hong CI, Larrondo LF, Baker CL, Chen C-H, Schwerdtfeger C, Collopy PD, Gamsby JJ, Lambreghts R (2007) A circadian clock in *Neurospora*: how genes and proteins cooperate to produce a sustained, entrainable, and compensated biological oscillator with a period of about a day. Cold Spring Harb Symp Quant Biol 72:57–68

Duvall LB, Taghert PH (2011) Circadian rhythms: biological clocks work in phospho-time. Curr Biol 21:R305–R307

Duvall LB, Taghert PH (2012) The circadian neuropeptide PDF signals preferentially through a specific adenylate cyclase isoform AC3 in M pacemakers of *Drosophila*. PLoS Biol 10:e1001337

Eastman CI, Stewart KT, Mahoney MP, Liu L, Fogg LF (1994) Dark goggles and bright light improve circadian rhythm adaptation to night-shift work. Sleep 17:535–543

Eckardt NA (2010) Temperature compensation of the circadian clock: a role for the morning loop. Plant Cell 22:3506

Egli M, Mori T, Pattanayek R, Xu Y, Qin X, Johnson CH (2012) Dephosphorylation of the core clock protein KaiC in the cyanobacterial KaiABC circadian oscillator proceeds via an ATP synthase mechanism. Biochemistry 51:1547–1558

Elvin M, Loros JJ, Dunlap JC, Heintzen C (2005) The PAS/LOV protein VIVID supports a rapidly dampened daytime oscillator that facilitates entrainment of the *Neurospora* circadian clock. Genes Dev 19:2593–2605

Emens JS, Lewy AJ, Lefler BJ, Sack RL (2005) Relative coordination to unknown 'weak zeitgebers' in free-running blind individuals. J Biol Rhythms 20:159–167

Emery P, So W, Kaneko M, Hall J, Rosbash M (1998) CRY, a Drosophila clock and light-regulated cryptochrome, is a major contributor to circadian rhythm resetting and photosensitivity. Cell 95:669–679

Emery P, Stanewsky R, Hall J, Rosbash M (2000) *Drosophila* cryptochrome – a unique circadian-rhythm photoreceptor. Nature 404:456–457

Engelmann W, Johnsson A, Kobler H, Schimmel M (1978) Attenuation of the petal movement rhythm of *Kalanchoe* with light pulses. Physiol Behav 43:68–76

Erkert HG, Gburek V, Scheideler A (2006) Photic entrainment and masking of prosimian circadian rhythms (*Otolemur garnettii*, primates). Physiol Behav 88:39–46

Erren TC (2010) Shift work, cancer and "white-box" epidemiology: association and causation. Epidemiol Perspect Innov 7:11

Erren TC, Falaturi P, Morfeld P, Knauth P, Reiter RJ, Piekarski C (2010) Shift work and cancer: the evidence and the challenge. Dtsch Arztebl Int 107:657–662

Even C, Schröder CM, Friedman S, Rouillon F (2008) Efficacy of light therapy in nonseasonal depression: a systematic review. J Affect Disord 108:11–23

Fahey CD, Zee PC (2006) Circadian rhythm sleep disorders and phototherapy. Psychiatr Clin N Am 29:989–1007; abstract ix

Falcón J, Besseau L, Fuentès M, Sauzet S, Magnanou E, Boeuf G (2009) Structural and functional evolution of the pineal melatonin system in vertebrates. Ann N Y Acad Sci 1163:101–111

Figueiro MG, Rea MS (2010) Lack of short-wavelength light during the school day delays dim light melatonin onset (DLMO) in middle school students. Neuro Endocrinol Lett 31:92–96

Figueiro MG, Bullough JD, Parsons RH, Rea MS (2005) Preliminary evidence for a change in spectral sensitivity of the circadian system at night. J Circadian Rhythm 3:14

Figueiro MG, Bierman A, Bullough JD, Rea MS (2009) A personal light-treatment device for improving sleep quality in the elderly: dynamics of nocturnal melatonin suppression at two exposure levels. Chronobiol Int 26:726–739

Figueiro MG, Lesniak NZ, Rea MS (2011) Implications of controlled short wavelength light exposure for sleep in older adults. BMC Res Notes 4:334

Fiorentino L, Martin JL (2010) Awake at 4 AM: treatment of insomnia with early morning awakenings among older adults. J Clin Psychol 66:1161–1174

Fischer R, Kasper S, Pjrek E, Winkler D (2012) On the application of light therapy in German-speaking countries. Eur Arch Psychiatry Clin Neurosci 262:501–505

Fleissner G, Fleissner G (2001) Perception of natural Zeitgeber signals. In: Kumar V (ed) Biological rhythms. Narosa Publishing House, New Delhi

Fleury F (2000) Adaptive significance of a circadian clock: temporal segregation of activities reduces intrinsic competitive inferiority in Drosophila parasitoids. Proc Biol Sci 267:1005–1010

Flory R, Ametepe J, Bowers B (2010) A randomized, placebo-controlled trial of bright light and high-density negative air ions for treatment of seasonal affective disorder. Psychiatry Res 177:101–108

Folkard S (2008) Do permanent night workers show circadian adjustment? a review based on the endogenous melatonin rhythm. Chronobiol Int 25:215–224

Forger D, Jewett M, Kronauer R (1999) A simpler model of the human circadian pacemaker. J Biol Rhythms 14:532–537

Forsgren E (1935) Über die Rhythmik der Leberfunktion, des Stoffwechsels und des Schlafes. Gumperts Bokhandel, Göteborg
Foster R, Helfrich-Förster C (2001) Photoreceptors for circadian clocks in mice and fruit flies. Philos Trans R Soc Lond B Biol Sci 356 B:1779–1789
Foster RG, Hankins MW, Peirson SN (2007) Light, photoreceptors, and circadian clocks. Methods Mol Biol 362:3–28
Foà A, Basaglia F, Beltrami G, Carnacina M, Moretto E, Bertolucci C (2009) Orientation of lizards in a Morris water-maze: roles of the sun compass and the parietal eye. J Exp Biol 212: 2918–2924
Frenkel L, Ceriani MF (2011) Circadian plasticity: from structure to behavior. Int Rev Neurobiol 99:107–138
Fritschi L, Glass DC, Heyworth JS, Aronson K, Girschik J, Boyle T, Grundy A, Erren TC (2011) Hypotheses for mechanisms linking shiftwork and cancer. Med Hypotheses 77:430–436
Froy O (2011) The circadian clock and metabolism. Clin Sci (Lond) 120:65–72
Gachon F, Nagoshi E, Brown SA, Ripperger J, Schibler U (2004) The mammalian circadian timing system: from gene expression to physiology. Chromosoma 113:103–112
Gagné A-M, Lévesque F, Gagné P, Hébert M (2011) Impact of blue vs red light on retinal response of patients with seasonal affective disorder and healthy controls. Prog Neuropsychopharmacol Biol Psychiatry 35:227–231
Gammack JK (2008) Light therapy for insomnia in older adults. Clin Geriatr Med 24:139–149, viii
Gaskill C, Forbes-Stovall J, Kessler B, Young M, Rinehart CA, Jacobshagen S (2010) Improved automated monitoring and new analysis algorithm for circadian phototaxis rhythms in Chlamydomonas. Plant Physiol Biochem 48:239–246
Gendron JM, Pruneda-Paz JL, Doherty CJ, Gross AM, Kang SE, Kay SA (2012) Arabidopsis circadian clock protein, TOC1, is a DNA-binding transcription factor. Proc Natl Acad Sci U S A 109: 3167–3172
Germain A, Kupfer DJ (2008) Circadian rhythm disturbances in depression. Hum Psychopharmacol 23:571–585
Giedd JN, Swedo SE, Lowe CH, Rosenthal NE (1998) Case series: pediatric seasonal affective disorder. A follow-up report. J Am Acad Child Adolesc Psychiatry 37:218–220
Giedke H, Engelmann W, Reinhard P (1983) Free running circadian rest-activity cycle in normal environment. A case study. Sleep Res 12:365
Gillette M, Abbott S (2005) Basic mechanisms of circadian rhythms and their relation to the sleep/wake cycle. In: Cardinali DP, Perumal SR (eds) Neuroendocrine correlates of sleep/wakefullness. Springer, New York
Girardet C, Becquet D, Blanchard M-P, François-Bellan A-M, Bosler O (2010) Neuroglial and synaptic rearrangements associated with photic entrainment of the circadian clock in the suprachiasmatic nucleus. Eur J Neurosci 32:2133–2142
Goda K, Ito H, Kondo T, Oyama T (2012) Fluorescence correlation spectroscopy to monitor Kai protein-based circadian oscillations in real time. J Biol Chem 287:3241–3248
Goldbeter A (1995) A model for circadian oscillations in the *Drosophila* period protein (PER). Proc Biol Sci 261:319–324
Golden RN, Gaynes BN, Ekstrom RD, Hamer RM, Jacobsen FM, Suppes T, Wisner KL, Nemeroff CB (2005) The efficacy of light therapy in the treatment of mood disorders: a review and meta-analysis of the evidence. Am J Psychiatry 162:656–662
Golden SS, Cassone VM, LiWang A (2007) Shifting nanoscopic clock gears. Nat Struct Mol Biol 14:362–363
Golombek DA, Rosenstein RE (2010) Physiology of circadian entrainment. Physiol Rev 90:1063–1102
Gonze D, Roussel MR, Goldbeter A (2002) A model for the enhancement of fitness in Cyanobacteria based on resonance of a circadian oscillator with the external lightdark cycle. J Theor Biol 214:577–597
Gooch VD, Mehra A, Larrondo LF, Fox J, Touroutoutoudis M, Loros JJ, Dunlap JC (2008) Fully codon-optimized luciferase uncovers novel temperature characteristics of the *Neurospora* clock. Eukaryot Cell 7:28–37
Gooley JJ (2008) Treatment of circadian rhythm sleep disorders with light. Ann Acad Med Singapore 37:669–676
Gordijn MCM, t Mannetje D, Meesters Y (2012) The effects of blue-enriched light treatment compared to standard light treatment in seasonal affective disorder. J Affect Disord 136:72–80
Goto K, Johnson CH (1995) Is the cell division cycle gated by a circadian clock? The case of *Chlamydomonas reinhardtii*. J Cell Biol 129:1061–1069
Gotow T, Nishi T (2008) Simple photoreceptors in some invertebrates: physiological properties of a new photosensory modality. Brain Res 1225:3–16
Grace MS, Wang LA, Pickard GE, Besharse JC, Menaker M (1996) The tau mutation shortens the period of rhythmic photoreceptor outer segment disk shedding in the hamster. Brain Res 735:93–100
Grace MS, Chiba A, Menaker M (1999) Circadian control of photoreceptor outer segment membrane turnover in mice genetically incapable of melatonin synthesis. Vis Neurosci 16:909–918
Gradisar M, Gardner G, Dohnt H (2011) Recent worldwide sleep patterns and problems during adolescence: a review and meta-analysis of age, region, and sleep. Sleep Med 12:110–118
Green CB, Besharse JC (2004) Retinal circadian clocks and control of retinal physiology. J Biol Rhythms 19:91–102
Green CB, Takahashi JS, Bass J (2008) The meter of metabolism. Cell 134:728–742
Green RM, Tingay S, Wang ZY, Tobin EM (2002) Circadian rhythms confer a higher level of fitness to *Arabidopsis* plants. Plant Physiol 129:576–584
Griefahn B, Robens S (2010) Alterations of the cortisol quiescent period after experimental night work with enforced adaptation by bright light and its relation to morningness. Eur J Appl Physiol 108:719–726
Grima B, Chelot E, Xia R, Rouyer F (2004) Morning and evening peaks of activity rely on different clock neurons of the *Drosophila* brain. Nature 431:869–873
Grimsley N, Péquin B, Bachy C, Moreau H, Piganeau G (2010) Cryptic sex in the smallest eukaryotic marine green alga. Mol Biol Evol 27:47–54
Grone BP, Chang D, Bourgin P, Cao V, Fernald RD, Heller HC, Ruby NF (2011) Acute light exposure suppresses circadian rhythms in clock gene expression. J Biol Rhythms 26:78–81
Gu C, Wang J, Wang J, Liu Z (2011) Mechanism of phase splitting in two coupled groups of suprachiasmatic-nucleus neurons. Phys Rev E Stat Nonlin Soft Matter Phys 83:046224
Guido ME, Garbarino-Pico E, Contin MA, Valdez DJ, Nieto PS, Verra DM, Acosta-Rodriguez VA, de Zavalía N, Rosenstein RE (2010) Inner retinal circadian clocks and non-visual photoreceptors: novel players in the circadian system. Prog Neurobiol 92: 484–504
Guilding C, Piggins HD (2007) Challenging the omnipotence of the suprachiasmatic timekeeper: are circadian oscillators present throughout the mammalian brain? Eur J Neurosci 25:3195–3216
Guo J, Cheng P, Liu Y (2010) Functional significance of FRH in regulating the phosphorylation and stability of *Neurospora crassa* circadian clock protein FRQ. J Biol Chem 285:11508–11515
Hanai S, Ishida N (2009) Entrainment of drosophila circadian clock to green and yellow light by rh1, rh5, rh6 and cry. Neuroreport 20:755–758
Hanai S, Hamasaka Y, Ishida N (2008) Circadian entrainment to red light in *Drosophila*: requirement of rhodopsin 1 and rhodopsin 6. Neuroreport 19:1441–1444

Hannibal J, Hindersson P, Knudsen SM, Georg B, Fahrenkrug J (2002) Melanopsin is expressed in PACAP-containing retinal ganglion cells of the human retinohypothalamic tract. Invest Ophthalmol Vis Sci 45:4202–4209

Hansen J, Stevens RG (2012) Case-control study of shift-work and breast cancer risk in Danish nurses: impact of shift systems. Eur J Cancer 48:1722–1729

Hansen JH, Geving IH, Reinertsen RE (2010) Offshore fleet workers and the circadian adaptation of core body temperature, blood pressure and heart rate to 12-h shifts: a field study. Int J Occup Saf Ergon 16:487–496

Hansen V, Skre I, Lund E (2008) What is this thing called "SAD"? a critique of the concept of seasonal affective disorder. Epidemiol Psichiatr Soc 17:120–127

Hardeland R, Cardinali DP, Srinivasan V, Spence DW, Brown GM, Pandi- Perumal SR (2011) Melatonin–a pleiotropic, orchestrating regulator molecule. Prog Neurobiol 93:350–384

Hardeland R, Madrid JA, Tan D-X, Reiter RJ (2012) Melatonin, the circadian multioscillator system and health: the need for detailed analyses of peripheral melatonin signaling. J Pineal Res 52:139–166

Hardie DG, Ross FA, Hawley SA (2012) AMPK: a nutrient and energy sensor that maintains energy homeostasis. Nat Rev Mol Cell Biol 13:251–262

Hardin PE (2005) The circadian timekeeping system of Drosophila. Curr Biol 15:R714–R722

Hardin PE (2011) Molecular genetic analysis of circadian timekeeping in *Drosophila*. Adv Genet 74:141–173

Hardin PE, Hall JC, Rosbash M (1990) Feedback of the Drosophila period gene product on circadian cycling of its messenger RNA levels. Nature 343:536–540

Harmer SL (2009) The circadian system in higher plants. Annu Rev Plant Biol 60:357–377

Harmer S (2010) Plant biology in the fourth dimension. Plant Physiol 154:467–470

Harmer S, Hogenesch L, Straume M, Chang H, Han B, Zhu T, Wang X, Kreps J, Kay S (2000) Orchestrated transcription of key pathways in *Arabidopsis* by the circadian clock. Science 290:2110–2113

Harrisingh MC, Nitabach MN (2008) Circadian rhythms. Integrating circadian timekeeping with cellular physiology. Science 320:879–880

Harvey AG, Murray G, Chandler RA, Soehner A (2011) Sleep disturbance as transdiagnostic: consideration of neurobiological mechanisms. Clin Psychol Rev 31:225–235

Hastings MH, Herzog ED (2004) Clock genes, oscillators, and cellular networks in the suprachiasmatic nuclei. J Biol Rhythms 19: 400–413

Hastings MH, Maywood ES, O'Neill JS (2008) Cellular circadian pacemaking and the role of cytosolic rhythms. Curr Biol 18:R805–R815

Hatakeyama TS, Kaneko K (2012) Generic temperature compensation of biological clocks by autonomous regulation of catalyst concentration. Proc Natl Acad Sci U S A 109:8109–8114

Hattar S, Lucas RJ, Mrosovsky N, Thompson S, Douglas RH, Hankins MW, Lem J, Biel M, Hofman F, Foster RG (2003) Melanopsin and rod-cone photoreceptive systems account for all major accessory visual functions in mice. Nature 424:75–81

Hayama R, Coupland G (2003) Shedding light on the circadian clock and the photoperiodic control of flowering. Curr Opin Plant Biol 6:13–19

He Q, Cheng P, Yang Y, Wang L, Gardner K, Liu Y (2002) White collar-1, a DNA binding transcription factor and a light sensor. Science 297:840–843

Heesy CP, Hall MI (2010) The nocturnal bottleneck and the evolution of mammalian vision. Brain Behav Evol 75:195–203

Hegemann P (2008) Algal sensory photoreceptors. Annu Rev Plant Biol 59:167–189

Heijde M, Ulm R (2012) UV-B photoreceptor-mediated signalling in plants. Trends Plant Sci 17:230–237

Heijde M, Zabulon G, Corellou F, Ishikawa T, Brazard J, Usman A, Sanchez F, Plaza P, Martin M, Falciatore A, Todo T, Bouget F-Y, Bowler C (2010) Characterization of two members of the cryptochrome/photolyase family *from Ostreococcus tauri* provides insights into the origin and evolution of cryptochromes. Plant Cell Environ 33:1614–1626

Heinze S, Reppert SM (2012) Anatomical basis of sun compass navigation i: the general layout of the monarch butterfly brain. J Comp Neurol 520:1599–1628

Heldmaier G, Steinlechner S (1981) Seasonal control of energy requirements for thermoregulation in the Djungarian hamster (*Phodopus sungorus*), living in natural photoperiod. J Comp Physiol B 142:429–437

Heldmaier G, Werner D (2004) Environmental signal processing and adaptation, vol 110. Blackwell Synergy

Helfrich-Förster C (2005a) Neurobiology of the fruit fly's circadian clock. Genes Brain Behav 4:65–76

Helfrich-Förster C, Stengl M, Homberg U (1998) Organization of the circadian system in insects. Chronobiol Int 15:567–594

Helfrich-Förster C, Winter C, Hofbauer A, Hall J, Stanewsky R (2001) The circadian clock of fruit flies is blind after elimination of all known photoreceptors. Neuron 30:249–261

Helfrich-Förster C, Edwards T, Yasuyama K, Schneuwly S, Meinertzhagen I, Hofbauer A (2002) The extraretinal eyelet of Drosophila: development, ultrastructure and putative circadian function. J Neurosci 22:9255–9266

Helfrich-Förster C (2004) The circadian clock in the brain: a structural and functional comparison between mammals and insects. J Comp Physiol A 190:601–613

Helfrich-Förster C (2005b) Organization of endogenous clocks in insects. Biochem Soc Trans 33:957–961

Helfrich-Förster C, Täuber M, Park JH, Mühlig-Versen M, Schneuwly S, Hofbauer A (2000) Ectopic expression of the neuropeptide pigment-dispersing factor alters behavioral rhythms in *Drosophila melanogaster*. J Neurosci 20:3339–3353

Helfrich-Förster C, Nitabach MN, Holmes TC (2011) Insect circadian clock outputs. Essays Biochem 49:87–101

Hendricks JC, Finn SM, Panckeri KA, Chavkin J, Williams JA, Sehgal A, Pack AI (2000) Rest in *Drosophila* is a sleep-like state. Neuron 25:129–138

Hennessey TL, Field CB (1991) Circadian rhythms in photosynthesis. Plant Physiol 96:831–836

Hermann C, Yoshii T, Dusik V, Helfrich-Förster C (2012) Neuropeptide F immunoreactive clock neurons modify evening locomotor activity and free-running period in *Drosophila melanogaster*. J Comp Neurol 520:970–987

Herrero E, Davis SJ (2012) Time for a nuclear meeting: protein trafficking and chromatin dynamics intersect in the plant circadian system. Mol Plant 5:554–565

Herrero E, Kolmos E, Bujdoso N, Yuan Y, Wang M, Berns MC, Uhlworm H, Coupland G, Saini R, Jaskolski M, Webb A, Gonçalves J, Davis SJ (2012) EARLY FLOWERING4 recruitment of EARLY FLOWERING3 in the nucleus sustains the *Arabidopsis* circadian clock. Plant Cell 24:428–443

Hirsh J, Riemensperger T, Coulom H, Iché M, Coupar J, Birman S (2010) Roles of dopamine in circadian rhythmicity and extreme light sensitivity of circadian entrainment. Curr Biol 20:209–214

Hoffmann K (1981) The role of the pineal gland in the photoperiodic control of seasonal cycles in hamsters. In: Follett D, Follett B (eds) Biological clocks in seasonal reproductive cycles. Wright, Bristol, pp 237–250

Hogenesch JB, Ueda HR (2011) Understanding systems-level properties: timely stories from the study of clocks. Nat Rev Genet 12:407–416

Holland RA, Borissov I, Siemers BM (2010) A nocturnal mammal, the greater mouse-eared bat, calibrates a magnetic compass by the sun. Proc Natl Acad Sci U S A 107:6941–6945

Homberg U, Reischig T, Stengl M (2003) Neural organization of the circadian system of the cockroach *Leucophaea maderae*. Chronobiol Int 20(4):577–591

Homberg U, Heinze S, Pfeiffer K, Kinoshita M, el Jundi B (2011) Central neural coding of sky polarization in insects. Philos Trans R Soc Lond B Biol Sci 366:680–687

Honma KI, Honma S (2009) The SCN-independent clocks, methamphetamine and food restriction. Eur J Neurosci 30:1707–1717

Honma S, Hashimoto S, Nakao M, Kato Y, Honma K-I (2003) Period and phase adjustments of human circadian rhythms in the real world. J Biol Rhythms 18:261–270

Horowitz T, Cade B, Wolfe J, Czeisler C (2001) Efficacy of bright light and sleep/darkness scheduling in alleviating circadian maladaptation to night work. Am J Physiol 281:384–391

Hotta CT, Xu X, Xie Q, Dodd AN, Johnson CH, Webb AA (2008) Are there multiple circadian clocks in plants? Plant Signal Behav 3:342–344

Howland RH (2009a) An overview of seasonal affective disorder and its treatment options. Phys Sportsmed 37:104–115

Howland RH (2009b) Somatic therapies for seasonal affective disorder. J Psychosoc Nurs Ment Health Serv 47:17–20

Hubbard KE, Robertson FC, Dalchau N, Webb AAR (2009) Systems analyses of circadian networks. Mol Biosyst 5:1502–1511

Hughes S, Hankins MW, Foster RG, Peirson SN (2012) Melanopsin phototransduction: slowly emerging from the dark. Prog Brain Res 199:19–40

Humble MB (2010) Vitamin D, light and mental health. J Photochem Photobiol B 101:142–149

Hung H-C, Maurer C, Kay SA, Weber F (2007) Circadian transcription depends on limiting amounts of the transcription co-activator nejire/cbp. J Biol Chem 282:31349–31357

Hunt SM, Elvin M, Crosthwaite SK, Heintzen C (2007) The PAS/LOV protein VIVID controls temperature compensation of circadian clock phase and development in *Neurospora crassa*. Genes Dev 21:1964–1974

Hunt SM, Thompson S, Elvin M, Heintzen C (2010) VIVID interacts with the WHITE COLLAR complex and FREQUENCY-interacting RNA helicase to alter light and clock responses in *Neurospora*. Proc Natl Acad Sci U S A 107:16709–16714

Hurd MW, Ralph MR (1998) The significance of circadian organization for longevity in the golden hamster. J Biol Rhythms 13:430–436

Husain M (2005) The neural retina: three channels of light detection. Adv Clin Neurosci Rehabil 5:22–23

Hut RA, Beersma DGM (2011) Evolution of time-keeping mechanisms: early emergence and adaptation to photoperiod. Philos Trans R Soc Lond B Biol Sci 366:2141–2154

Idda ML, Bertolucci C, Vallone D, Gothilf Y, Sánchez-Vázquez FJ, Foulkes NS (2012) Circadian clocks: lessons from fish. Prog Brain Res 199:41–57

de la Iglesia HO, Cambras T, Schwartz WJ, Diez-Noguera A (2004) Forced desynchronization of dual circadian oscillators within the rat suprachiasmatic nucleus. Curr Biol 14:796–800

Ikegami K, Yoshimura T (2012) Circadian clocks and the measurement of daylength in seasonal reproduction. Mol Cell Endocrinol 349:76–81

Im SH, Taghert PH (2010) PDF receptor expression reveals direct interactions between circadian oscillators in *Drosophila*. J Comp Neurol 518:1925–1945

Imaizumi T (2010) *Arabidopsis* circadian clock and photoperiodism: time to think about location. Curr Opin Plant Biol 13:83–89

Indic P, Schwartz WJ, Paydarfar D (2008) Design principles for phase-splitting behaviour of coupled cellular oscillators: clues from hamsters with 'split' circadian rhythms. J R Soc Interface 5:873–883

Inouye C, Okamoto K, Ishiura M, Kondo T (1998) The action spectrum of phase shift by light signal in the circadian rhythm in cyanobacterium. Plant Cell Physiol 39(Suppl):S82

Ishiura M, Kutsuna S, Aoki S, Iwasaki H, Andersson C, Tanabe A, Golden S, Johnson C, Kondo T (1998) Expression of a gene cluster kaiABC as a circadian feedback process in cyanobacteria. Science 281:1519–1523

Isojima Y, Nakajima M, Ukai H, Fujishima H, Yamada RG, Masumoto KH, Kiuchi R, Ishida M, Ukai-Tadenuma M, Minami Y, Kito R, Nakao K, Kishimoto W, Yoo S-H, Shimomura K, Takao T, Takano A, Kojima T, Nagai K, Sakaki Y, Takahashi JS, Ueda HR (2009) CKiepsilon/delta-dependent phosphorylation is a temperature-insensitive, period-determining process in the mammalian circadian clock. Proc Natl Acad Sci U S A 106:15744–15749

Ito C, Goto SG, Shiga S, Tomioka K, Numata H (2008) Peripheral circadian clock for the cuticle deposition rhythm in *Drosophila melanogaster*. Proc Natl Acad Sci U S A 105:8446–8451

Iuvone PM, Tosini G, Pozdeyev N, Haque R, Klein DC, Chaurasia SS (2005) Circadian clocks, clock networks, arylalkylamine n-acetyltransferase, and melatonin in the retina. Prog Retin Eye Res 24:433–456

Ivanchenko M, Stanewsky R, Giebultowicz JM (2001) Circadian photoreception in *Drosophila*: functions of cryptochrome in peripheral and central clocks. J Biol Rhythms 16:205–215

Iwasaki H, Kondo T (2004) Circadian timing mechanism in the prokaryotic clock system of cyanobacteria. J Biol Rhythms 19:436–444

Iwasaki H, Williams S, Kitayama Y, Ishiura M, Golden S, Kondo T (2000) A kaiC-interacting sensory histidine kinase, SasA, necessary to sustain robust circadian oscillation in cyanobacteria. Cell 101:223–233

Jackson FR (2011) Glial cell modulation of circadian rhythms. Glia 59:1341–1350

Jacobshagen S, Kessler B, Rinehart CA (2008) At least four distinct circadian regulatory mechanisms are required for all phases of rhythms in mrna amount. J Biol Rhythms 23:511–524

Jacobson D, Powell A, Dettman J, Saenz G, Barton M, Hiltz M, Dvorachek W Jr, Glass N, Taylor J, Natvig D (2004) *Neurospora* in temperate forests of western North America. Mycologia 96:66–74

Jagota A, de la Iglesia H, Schwartz W (2000) Morning and evening circadian oscillations in the suprachiasmatic nucleus in vitro. Nat Neurosci 3:372–376

Jang S-W, Liu X, Pradoldej S, Tosini G, Chang Q, Iuvone PM, Ye K (2010) Nacetylserotonin activates TrkB receptor in a circadian rhythm. Proc Natl Acad Sci U S A 107:3876–3881

Jewett M, Rimmer D, Duffy J, Klerman E, Kronauer R, Czeisler C (1997) Human circadian pacemaker is sensitive to light throughout subjective day without evidence of transients. Am J Physiol 273:R1800–R1809

Jewett M, Borbely A, Czeisler C (1999a) Special issue: proceedings workshop on biomathematical models of circadian rhythmicity, sleep regulation and neurobehavioral function in humans, May 18–21 1999 Dedham, Mass. J Biol Rhythm 14

Jewett M, Kronauer R, Megan E (1999b) Interactive mathematical models of subjective alertness and cognitive throughput in humans. J Biol Rhythms 14:588–597

Jinhu G, Yi L (2010) Molecular mechanism of the Neurospora circadian oscillator. Protein Cell 1:331–341

Johnson CH (2005) Testing the adaptive value of circadian systems. Methods Enzymol 393:818–837

Johnson CH (2010) Circadian clocks and cell division: what's the pacemaker? Cell Cycle 9:3864–3873

Johnson CH, Golden SS (1999) Circadian programs in Cyanobacteria: adaptiveness and mechanism. Annu Rev Microbiol 53:389–409

Johnson CH, Kondo T, Hastings JW (1991) Action spectrum for resetting the circadian phototaxis rhythm in the CW15 strain of

Chlamydomonas: II. Illuminated cells. Plant Physiol 97: 1122–1129

Johnson CH, Kondo T, Goto K (1992) Circadian rhythms in Chlamydomonas. In: Honma K, Honma S, Hiroshige T (eds) Circadian clocks from cell to human: proc Fourth Sapporo symp biol rhythms. Hokkaido Univ. Hokkaido University Press, Sapporo, pp 139–155

Johnson CH, Stewart PL, Egli M (2011) The cyanobacterial circadian system: from biophysics to bioevolution. Annu Rev Biophys 40:143–167

Johnsson A, Karlsson H, Engelmann W (1973) Phase shifts in the *Kalanchoe* petal rhythm, caused by light pulses of different duration. A theoretical and experimental study. J Chronobiol 1:147–156

Johnsson A, Engelmann W, Klemke W, Ekse AT (1979) Free-running human circadian rhythms in Svalbard. Z Naturforsch C 34C:470–473

Johnsson A, Solheim BGB, Iversen T-H (2009) Gravity amplifies and microgravity decreases circumnutations in *Arabidopsis thaliana* stems: results from a space experiment. New Phytol 182:621–629

Johnston J, Tournier B, Andersson H, Masson-Pevet M, Lincoln G, Hazlerigg D (2006) Multiple effects of melatonin on rhythmic clock gene expression in the mammalian *Pars tuberalis*. Endocrinology 147:959–965

Jones MA (2009) Entrainment of the Arabidopsis circadian clock. J Plant Biol 52:202–209

Jud C, Schmutz I, Hampp G, Oster H, Albrecht U (2005) A guideline for analyzing circadian wheel-running behavior in rodents under different lighting conditions. Biol Proced Online 7:101–116

Kai H, Arai T, Yasuda F (1999) Accomplishment of time-interval activation of esterase A4 by simple removal of pin fraction. Chronobiol Int 16:51–58

Kami C, Lorrain S, Hornitschek P, Fankhauser C (2010) Light-regulated plant growth and development. Curr Top Dev Biol 91:29–66

Kaneko M, Hamblen M, Hall J (2000) Involvement of the period gene in developmental time-memory: effect of the per short mutation on phase shifts induced by light pulses delivered to Drosophila larvae. J Biol Rhythms 15:13–30

Karakashian M, Schweiger H (1976) Circadian properties of the rhythmic system in individual nucleated and enucleated cells of *Acetabularia mediterranea*. Exp Cell Res 97:366–377

Karlsson H, Johnsson A (1972) A feedback model for biological rhythms. II. Comparisons with experimental results, especially on the petal rhythm of Kalanchoe. J Theor Biol 36:175–194

Kasof J (2009) Cultural variation in seasonal depression: cross-national differences in winter versus summer patterns of seasonal affective disorder. J Affect Disord 115:79–86

Kecklund G, Milia LD, Axelsson J, Lowden A, Akerstedt T (2012) 20th International symposium on shiftwork and working time: biological mechanisms, recovery, and risk management in the 24-h society. Chronobiol Int 29:531–536

Keeling PJ (2007) *Ostreococcus tauri*: seeing through the genes to the genome. Trends Genet 23:151–154

Kegel M, Dam H, Ali F, Bjerregaard P (2009) The prevalence of seasonal affective disorder (SAD) in Greenland is related to latitude. Nord J Psychiatry 63:331–335

Kempinger L, Dittmann R, Rieger D, Helfrich-Forster C (2009) The nocturnal activity of fruit flies exposed to artificial moonlight is partly caused by direct light effects on the activity level that bypass the endogenous clock. Chronobiol Int 26:151–166

Kessel L, Siganos G, Jørgensen T, Larsen M (2011) Sleep disturbances are related to decreased transmission of blue light to the retina caused by lens yellowing. Sleep 34:1215–1219

Khalsa S, Jewett M, Cajochen C, Czeisler C (2003) A phase response curve to single bright light pulses in human subjects. J Physiol 549:945–952

Kim W-Y, Fujiwara S, Suh S-S, Kim J, Kim Y, Han L, David K, Putterill J, Nam HG, Somers DE (2007) ZEITLUPE is a circadian photoreceptor stabilized by GIGANTEA in blue light. Nature 449:356–360

Kim Y-I, Vinyard DJ, Ananyev GM, Dismukes GC, Golden SS (2012) Oxidized quinones signal onset of darkness directly to the cyanobacterial circadian oscillator. Proc Natl Acad Sci U S A 109:17765–17769

Kistenpfennig C, Hirsh J, Yoshii T, Helfrich-Förster C (2012) Phase-shifting the fruit fly clock without cryptochrome. J Biol Rhythms 27:117–125

Klarsfeld A, Rouyer F (1998) Effects of circadian mutations and LD periodicity on the life span of *Drosophila melanogaster*. J Biol Rhythms 13:471–478

Klarsfeld A, Malpel S, Michard-Vanhee C, Picot M, Chelot E, Rouyer F (2004) Novel features of cryptochrome-mediated photoreception in the brain circadian clock of *Drosophila*. J Neurosci 24:1468–1477

Klein D, Moore R, Reppert S (1991) Suprachiasmatic nucleus: the mind's clock. Oxford University Press, New York

Kleitman L (1963) Sleep and wakefulness. University of Chicago Press, Chicago

Klemm E, Ninnemann H (1976) Detailed action spectrum for the delay shift in pupae emergence of *Drosophila pseudoobscura*. Photochem Photobiol 24:369–371

Klerman EB (2005) Clinical aspects of human circadian rhythms. J Biol Rhythms 20:375–386

Klerman EB, Dijk DJ, Kronauer RE, Czeisler CA (1996) Simulations of light effects on the human circadian pacemaker: implications for assessment of intrinsic period. Am J Physiol 270: R271–R282

Kohyama J (2011) Sleep health and asynchronization. Brain Dev 33:252–259

Kolar C, Fejes E, Adam E, Schaefer E, Kay S, Nagy F (1998) Transcription of *Arabidopsis* and wheat Cab genes in single tobacco transgenic seedlings exhibits independent rhythms in a developmentally regulated fashion. Plant J 13:563–569

Kolla BP, Auger RR (2011) Jet lag and shift work sleep disorders: how to help reset the internal clock. Cleve Clin J Med 78:675–684

Kolmos E, Herrero E, Bujdoso N, Millar AJ, Tóth R, Gyula P, Nagy F, Davis SJ (2011) A reduced-function allele reveals that EARLY FLOWERING3 repressive action on the circadian clock is modulated by phytochrome signals in *Arabidopsis*. Plant Cell 23:3230–3246

Kondo T, Johnson C, Hastings J (1991) Action spectrum for resetting the circadian phototaxis rhythm in the CW15 strain I: cells in darkness. Plant Physiol 95:197–205

Kondo T, Strayer C, Kulkarni R, Taylor W, Ishiura M, Golden S, Johnson C (1993) Circadian rhythms in prokaryotes: luciferase as a reporter of circadian gene expression in cyanobacteria. Proc Natl Acad Sci U S A 90:5672–5676

Kondo T, Tsinoremas N, Golden S, Johnson C, Kutsuna S, Ishiura M (1994) Circadian clock mutants of cyanobacteria. Science 266:1233–1236

Kondo T, Mori T, Lebedeva NV, Aoki S, Ishiura M, Golden SS (1997) Circadian rhythms in rapidly dividing cyanobacteria. Science 275:224–227

Konopka RJ, Pittendrigh C, Orr D (2007) Reciprocal behaviour associated with altered homeostasis and photosensitivity of *Drosophila* clock mutants. J Neurogenet 21:243–252

Kotov NV, Baker RE, Dawidov DA, Platov KV, Valeyev NV, Skorinkin AI, Maini PK (2007) A study of the temperature dependence of bienzyme systems and enzymatic chains. Comput Math Methods Method 8:93–112

Kozma-Bognár L, Káldi K (2008) Synchronization of the fungal and the plant circadian clock by light. Chembiochem 9:2565–2573

Kräuchi K, Cajochen C, Pache M, Flammer J, Wirz-Justice A (2006) Thermoregulatory effects of melatonin in relation to sleepiness. Chronobiol Int 23:475–484

Kronauer RE, Czeisler CA, Pilato SF, Moore-Ede MC, Weitzman ED (1982) Mathematical model of the human circadian system with two interacting oscillators. Am J Physiol 242:3–17

Kronauer RE, Forger DB, Jewett ME (1999) Quantifying human circadian pacemaker response to brief, extended, and repeated light stimuli over the phototopic range. J Biol Rhythms 14:500–515

Kronfeld-Schor N, Einat H (2012) Circadian rhythms and depression: human psychopathology and animal models. Neuropharmacology 62:101–114

Kumar S, Mohan A, Sharma V (2005) Circadian dysfunction reduces lifespan in *Drosophila melanogaster*. Chronobiol Int 22:641–653

Kunihiro A, Yamashino T, Mizuno T (2010) PHYTOCHROME-INTERACTING FACTORS PIF4 and PIF5 are implicated in the regulation of hypocotyl elongation in response to blue light in *Arabidopsis thaliana*. Biosci Biotechnol Biochem 74:2538–2541

Kurosawa G, Aihara K, Iwasa Y (2006) A model for the circadian rhythm of cyanobacteria that maintains oscillation without gene expression. Biophys J 91:2015

Kwon I, Choe HK, Son GH, Kim K (2011) Mammalian molecular clocks. Exp Neurobiol 20:18–28

Laakso M, Hätönen T, Stenberg D, Alila A, Smith S (1993) The human circadian response to light -strong and weak resetting. J Biol Rhythms 8:351–360

Lack LC, Wright HR (2007) Treating chronobiological components of chronic insomnia. Sleep Med 8(6):637–644

Lakin-Thomas PL (2006) Transcriptional feedback oscillators: maybe, maybe not. J Biol Rhythms 21:83–92

Lakin-Thomas P, Johnson H (1999) Commentary: molecular and cellular models of circadian systems. J Biol Rhythms 14:486–489

Lakin-Thomas P, Cote G, Brody S (1990) Circadian rhythms in Neurospora crassa: biochemistry and genetics. Crit Rev Microbiol 17:365–416

Lakin-Thomas PL, Bell-Pedersen D, Brody S (2011) The genetics of circadian rhythms in Neurospora. Adv Genet 74:55–103

Lam R, Levitan R (2000) Pathophysiology of seasonal affective disorder: a review. J Psychiatr Neurosci 25:469–480

Lamont EW, Harbour VL, Barry-Shaw J, Diaz LR, Robinson B, Stewart J, Amir S (2007) Restricted access to food, but not sucrose, saccharine, or salt, synchronizes the expression of Period2 protein in the limbic forebrain. Neuroscience 144:402–411

Larrondo LF, Loros JJ, Dunlap JC (2012) High-resolution spatiotemporal analysis of gene expression in real time: in vivo analysis of circadian rhythms in *Neurospora crassa* using a FREQUENCY-luciferase translational reporter. Fungal Genet Biol 49:681–683

Lavoie M-P, Lam RW, Bouchard G, Sasseville A, Charron M-C, Gagné A-M, Tremblay P, Filteau M-J, Hébert M (2009) Evidence of a biological effect of light therapy on the retina of patients with seasonal affective disorder. Biol Psychiatry 66:253–258

Layana C, Diambra L (2011) Time-course analysis of cyanobacterium transcriptome: detecting oscillatory genes. PLoS One 6:e26291

Lear BC, Zhang L, Allada R (2009) The neuropeptide PDF acts directly on evening pacemaker neurons to regulate multiple features of circadian behavior. PLoS Biol 7:e1000154

Leis JM, Siebeck U, Dixson DL (2011) How Nemo finds home: the neuroecology of dispersal and of population connectivity in larvae of marine fishes. Integr Comp Biol 51:826–843

Leloup JC, Goldbeter A (1998) A model for circadian rhythms in *Drosophila* incorporating the formation of a complex between the PER and TIM proteins. J Biol Rhythms 13:70–87

Leloup JC, Goldbeter A (1999) Chaos and biorhythmicity in a model for circadian oscillations of the PER and TIM proteins in Drosophila. J Theor Biol 198:445–459

Leloup JC, Goldbeter A (2001) A molecular explanation for the long-term suppression of circadian rhythms by a single light pulse. Am J Physiol 280:1206–1212

Leloup J-C, Goldbeter A (2008) Modeling the circadian clock: from molecular mechanism to physiological disorders. Bioessays 30:590–600

Lema G, Auerbach A (2006) Modes and models of GABA A receptor gating. J Physiol 572:183

Levi F, Schibler U (2007) Circadian rhythms: mechanisms and therapeutic implications. Annu Rev Pharmacol Toxicol 47:593–628

Levitan RD (2005) What is the optimal implementation of bright light therapy for seasonal affective disorder (SAD)? J Psychiatry Neurosci 30:72

Levitan RD (2007) The chronobiology and neurobiology of winter seasonal affective disorder. Dialogues Clin Neurosci 9:315–324

Lewis R (1999) Control system models for the circadian clock of the New Zealand Weta, *Hemideina thoracica* (Orthoptera: Stenopelmatidae). J Biol Rhythms 14:480–485

Lewis ZA, Correa A, Schwerdtfeger C, Link K, Xie X, Gomer R, Thomas T, Ebbole D, Bell-Pedersen D (2002) Overexpression of White Collar-1(WC-1) activates circadian clock-associated genes, but is not sufficient to induce most light-regulated gene expression in *Neurospora crassa*. Mol Microbiol 45:917–931

Lewy A, Sack R (1997) Exogenous melatonin's phase-shifting effects on the endogenous melatonin profile in sighted humans: a brief review and critique of the literature. J Biol Rhythms 12:588–594

Lewy AJ (2007) Melatonin and human chronobiology. Cold Spring Harb Symp Quant Biol 72:623–636

Lewy AJ, Ahmed S, Sack RL (1996) Phase shifting the human circadian clock using melatonin. Behav Brain Res 73:131–134

Lewy AJ, Emens J, Jackman A, Yuhas K (2006a) Circadian uses of melatonin in humans. Chronobiol Int 23:403–412

Lewy AJ, Lefler BJ, Emens JS, Bauer VK (2006b) The circadian basis of winter depression. Proc Natl Acad Sci U S A 103:7414–7419

Lewy AJ, Rough JN, Songer JB, Mishra N, Yuhas K, Emens JS (2007) The phase shift hypothesis for the circadian component of winter depression. Dialogues Clin Neurosci 9:291–300

Lewy AJ, Emens JS, Songer JB, Sims N, Laurie AL, Fiala SC, Buti AL (2009) Winter depression: integrating mood, circadian rhythms, and the sleep/wake and light/dark cycles into a bio-psycho-social-environmental model. Sleep Med Clin 4:285–299

Li J-D, Hu W-P, Zhou Q-Y (2012) The circadian output signals from the suprachiasmatic nuclei. Prog Brain Res 199:119–127

Li S, Lakin-Thomas P (2010) Effects of prd circadian clock mutations on FRQ-less rhythms in *Neurospora*. J Biol Rhythms 25:71–80

Lim C, Lee J, Choi C, Kim J, Doh E, Choe J (2007) Functional role of creb-binding protein in the circadian clock system of *Drosophila melanogaster*. Mol Cell Biol 27:4876–4890

Lin R, Chou H, Huang T (1999) Priority of light/dark entrainment over temperature in setting the circadian rhythms of the prokaryote *Synechococcus* RF-1. Planta 209:202–206

Lincoln GA (2006) Melatonin entrainment of circannual rhythms. Chronobiol Int 23:301–306

Lincoln GA, Messager S, Andersson H, Hazlerigg D (2002) Temporal expression of seven clock genes in the suprachiasmatic nucleus and the pars tuberalis of the sheep: evidence for an internal coincidence timer. Proc Natl Acad Sci U S A 99:13890–13895

Lincoln GA, Andersson H, Loudon A (2003) Clock genes in calendar cells as the basis of annual timekeeping in mammals–a unifying hypothesis. J Endocrinol 179:1–13

Litt A, Kramer EM (2010) The ABC model and the diversification of floral organ identity. Semin Cell Dev Biol 21:129–137

Liu Y (2003) Molecular mechanisms of entrainment in the Neurospora circadian clock. J Biol Rhythms 18:195–205

Liu Y, Merrow M, Loros J, Dunlap J (1998) How temperature changes reset a circadian oscillator. Science 281:825–829

Loros JJ, Dunlap JC, Larrondo LF, Shi M, Belden WJ, Gooch VD, Chen C-H, Baker CL, Mehra A, Colot HV, Schwerdtfeger C, Lambreghts R, Collopy PD, Gamsby JJ, Hong CI (2007) Circadian output, input, and intracellular oscillators: insights into the circadian systems of single cells. Cold Spring Harb Symp Quant Biol 72:201–214

Lowrey PL, Takahashi JS (2011) Genetics of circadian rhythms in mammalian model organisms. Adv Genet 74:175–230

Loza-Correa M, Gomez-Valero L, Buchrieser C (2010) Circadian clock proteins in prokaryotes: hidden rhythms? Front Microbiol 1:130

Lu SX, Tobin EM (2011) Chromatin remodeling and the circadian clock: jumonji C-domain containing proteins. Plant Signal Behav 6:810–814

Lu SX, Knowles SM, Webb CJ, Celaya RB, Cha C, Siu JP, Tobin EM (2011) The Jumonji C domain-containing protein JMJ30 regulates period length in the *Arabidopsis* circadian clock. Plant Physiol 155:906–915

Lu SX, Webb CJ, Knowles SM, Kim SHJ, Wang Z, Tobin EM (2012) CCA1 and ELF3 interact in the control of hypocotyl length and flowering time in *Arabidopsis*. Plant Physiol 158:1079–1088

Lucas RJ, Lall GS, Allen AE, Brown TM (2012) How rod, cone, and melanopsin photoreceptors come together to enlighten the mammalian circadian clock. Prog Brain Res 199:1–18

Mackey SR (2007) Biological rhythms workshop IA: molecular basis of rhythms generation. Cold Spring Harb Symp Quant Biol 72:7–19

Mackey SR, Ditty JL, Zeidner G, Chen Y, Golden SS (2009) Mechanisms for entraining the cyanobacterial circadian clock system with the environment. In: Ditty JL, Mackey SR, Johnson C (eds) Bacterial circadian programs. Springer, Berlin, pp 141–156

Mackey SR, Golden SS, Ditty JL (2011) The itty-bitty time machine genetics of the cyanobacterial circadian clock. Adv Genet 74:13–53

Madsen H, Dam H, Hageman I (2012) Study protocol: a cross-sectional survey of seasonal affective disorder in Danish populations with and without severe visual impairments. BMJ Open 2:e001020

Magnusson A, Partonen T (2005) The diagnosis, symptomatology, and epidemiology of seasonal affective disorder. CNS Spectr 10:625–634; quiz 1–14

Mahoney MM (2010) Shift work, jet lag, and female reproduction. Int J Endocrinol 2010:813764

Malpel S, Klarsfeld A, Rouyer F (2002) Larval optic nerve and adult extra-retinal photoreceptors sequentially associate with clock neurons during *Drosophila* brain development. Development 129:1443–1453

Malpel S, Klarsfeld A, Rouyer F (2004) Circadian synchronization and rhythmicity in larval photoperception-defective mutants of Drosophila. J Biol Rhythms 19:10–21

Malzahn E, Ciprianidis S, Káldi K, Schafmeier T, Brunner M (2010) Photoadaptation in *Neurospora* by competitive interaction of activating and inhibitory LOV domains. Cell 142:762–772

Manichaikul A, Ghamsari L, Hom EFY, Lin C, Murray RR, Chang RL, Balaji S, Hao T, Shen Y, Chavali AK, Thiele I, Yang X, Fan C, Mello E, Hill DE, Vidal M, Salehi-Ashtiani K, Papin JA (2009) Metabolic network analysis integrated with transcript verification for sequenced genomes. Nat Methods 6:589–592

Marpegan L, Swanstrom AE, Chung K, Simon T, Haydon PG, Khan SK, Liu AC, Herzog ED, Beaulé C (2011) Circadian regulation of ATP release in astrocytes. J Neurosci 31:8342–8350

Martin SK, Eastman CI (1998) Medium-intensity light produces circadian rhythm adaptation to simulated night-shift work. Sleep 21:154–165

Matsuo T, Ishiura M (2011) *Chlamydomonas reinhardtii* as a new model system for studying the molecular basis of the circadian clock. FEBS Lett 585:1495–1502

May P, Christian J-O, Kempa S, Walther D (2009) Chlamycyc: an integrative systems biology database and web-portal for *Chlamydomonas reinhardtii*. BMC Genomics 10:209

McCarthy EV, Wu Y, Decarvalho T, Brandt C, Cao G, Nitabach MN (2011) Synchronized bilateral synaptic inputs to *Drosophila melanogaster* neuropeptidergic rest/arousal neurons. J Neurosci 31:8181–8193

McClung CA (2007) Circadian genes, rhythms and the biology of mood disorders. Pharmacol Ther 114:222–232

McClung CA (2011) Circadian rhythms: lost in post-translation. Curr Biol 21:R400–R402

McDermott JE, Oehmen CS, McCue LA, Hill E, Choi DM, Stöckel J, Liberton M, Pakrasi HB, Sherman LA (2011) A model of cyclic transcriptomic behavior in the cyanobacterium *Cyanothece sp*. ATCC 51142. Mol Biosyst 7:2407–2418

McWatters HG, Devlin PF (2011) Timing in plants–a rhythmic arrangement. FEBS Lett 585:1474–1484

Meesters Y, Dekker V, Schlangen LJM, Bos EH, Ruiter MJ (2011) Low-intensity blue-enriched white light (750 lux) and standard bright light (10,000 lux) are equally effective in treating SAD. A randomized controlled study. BMC Psychiatry 11:17

Mehra A, Baker CL, Loros JJ, Dunlap JC (2009) Post-translational modifications in circadian rhythms. Trends Biochem Sci 34:483–490

Meijer J, Watanabe K, Detari L, deVries M, Albus H, Treep J, Schaap J, Rietveld W (1996) Light entrainment of the mammalian biological clock. Prog Brain Res 111:175–190

Meijer JH, Schwartz WJ (2003) In search of the pathways for light-induced pacemaker resetting in the suprachiasmatic nucleus. J Biol Rhythms 18:235–249

Menaker M, Moreira L, Tosini G (1997) Evolution of circadian organization in vertebrates. Braz J Med Biol Res 30:305–313

Mendoza J, Pévet P, Challet E (2009) Entrainment and coupling of the hamster suprachiasmatic clock by daily dark pulses. J Neurosci Res 87:758–765

Merlin C, Heinze S, Reppert SM (2011) Unraveling navigational strategies in migratory insects. Curr Opin Neurobiol 22(2):353–361

Merrow M, Roenneberg T (2007) Circadian entrainment of *Neurospora crassa*. Cold Spring Harb Symp Quant Biol 72:279–285

Merrow M, Brunner M, Roenneberg T (1999) Assignment of circadian function for the *Neurospora* clock gene frequency. Nature 399:584–586

Mersch P, Middendorp H, Bouhuys A, Beersma D, van den Hoofdakker R (1999) Seasonal affective disorder and latitude: a review of the literature. J Affect Disord 53:35–48

Meyer P, Saez L, Young M (2006) PER-TIM interactions in living *Drosophila* cells: an interval timer for the circadian clock. Science 311:226–229

Michael TP, Salome PA, Yu HJ, Spencer TR, Sharp EL, McPeek MA, Alonso JM, Exker JR, McClung CR (2003) Enhanced fitness conferred by naturally occurring variations in the circadian clock. Science 302:1049–1053

Michaels SD (2009) Flowering time regulation produces much fruit. Curr Opin Plant Biol 12:75–80

Michalak EE, Murray G, Wilkinson C, Dowrick C, Lam RW (2007) A pilot study of adherence with light treatment for seasonal affective disorder. Psychiatry Res 149:315–320

Mihalcescu I, Hsing W, Leibler S (2004) Resilient circadian oscillator revealed in individual cyanobacteria. Nature 430:81–85

Miles L, Raynal D, Wilson M (1977) Blind man living in normal society has circadian rhythm of 24.9 hours. Science 198:421–423

Millar AJ (1999) Tansley review no. 103 – biological clocks in Arabidopsis thaliana. New Phytol 141:175–197

Millar AJ, Carre IA, Strayer CA, Chua N-H, Kay AS (1995) Circadian clock mutants in *Arabidopsis* identified by luciferase imaging. Science 267:1161–1163

Mills JN (1964) Circadian rhythms during and after three months in solitude underground. J Physiol 174:217–231

Min H, Johnson CH, Golden SS (2004) Phase determination of circadian gene expression in *Synechococcus elongatus* PCC 7942. J Biol Rhythms 19:103–112

Minors DS, Waterhouse J (1981) Circadian rhythms and the human. Wright, Bristol
Minors D, Waterhouse J, Wirz-Justice A (1991) A human phase response curve to light. Neurosci Lett 133:36–40
Mistlberger RE, Skene DJ (2005) Nonphotic entrainment in humans? J Biol Rhythms 20:339–352
Mitsui A, Kumazawa S, Takahashi A, Ikemoto H, Cao S, Arai T (1986) Strategy by which nitrogen-fixing unicellular cyanobacteria grow photoautotrophically. Nature 323:720–722
Mittag M (2001) Circadian rhythms in microalgae. Int Rev Cytol 206:213–247
Mittag M, Wagner V (2003) The circadian clock of the unicellular eukaryotic model organism Chlamydomonas reinhardtii. Biol Chem 384:689–695
Mittag M, Kiaulehn S, Johnson CH (2005) The circadian clock in *Chlamydomonas reinhardtii*. What is it for? What is it similar to? Plant Physiol 137:399–409
Miyoshi F, Nakayama Y, Kaizu K, Iwasaki H, Tomita M (2007) A mathematical model for the kai-protein-based chemical oscillator and clock gene expression rhythms in cyanobacteria. J Biol Rhythms 22:69
Mohawk JA, Takahashi JS (2011) Cell autonomy and synchrony of suprachiasmatic nucleus circadian oscillators. Trends Neurosci 34:349–358
Mohawk JA, Green CB, Takahashi JS (2012) Central and peripheral circadian clocks in mammals. Annu Rev Neurosci 35:445–462
Monk TH (2000) What can the chronobiologist do to help the shift worker? J Biol Rhythms 15:86–94
Monnier A, Liverani S, Bouvet R, Jesson B, Smith JQ, Mosser J, Corellou F, Bouget F-Y (2010) Orchestrated transcription of biological processes in the marine picoeukaryote *Ostreococcus* exposed to light/dark cycles. BMC Genomics 11:192
de Montaigu A, Tóth R, Coupland G (2010) Plant development goes like clockwork. Trends Genet 26:296–306
Montgomery P, Dunne D (2007) Sleep disorders in children. Clin Evid (Online) 2007:pii
Moore R, Speh J, Card J (1995) The rhd originates from a distinct subset of retinal ganglion cells. J Comp Neurol 352:351–366
Morant P-E, Thommen Q, Pfeuty B, Vandermoere C, Corellou F, Bouget F-Y, Lefranc M (2010) A robust two-gene oscillator at the core of *Ostreococcus tauri* circadian clock. Chaos 20:045108
Morgan L, Greene A, Bell-Pedersen D (2003) Circadian and light-induced expression of luciferase in *Neurospora crassa*. Fungal Genet Biol 38:327–332
Morgan PJ, Hazlerigg DG (2008) Photoperiodic signalling through the melatonin receptor turns full circle. J Neuroendocrinol 20:820–826
Mori T, Binder B, Johnson C (1996) Circadian gating of cell division in Cyanobacteria growing with average doubling times of less than 24 hours. Proc Natl Acad Sci U S A 93:10183–10188
Mori T, Saveliev S, Xu Y, Stafford W, Cox M, Inman R, Johnson C (2002) Circadian clock protein KaiC forms ATP-dependent hexameric rings and binds DNA. Proc Natl Acad Sci U S A 99:17203–17208
Moulager M, Monnier A, Jesson B, Bouvet R, Mosser J, Schwartz C, Garnier L, Corellou F, Bouget F-Y (2007) Light-dependent regulation of cell division in *Ostreococcus*: evidence for a major transcriptional input. Plant Physiol 144:1360–1369
Moulager M, Corellou F, Vergé V, Escande M-L, Bouget F-Y (2010) Integration of light signals by the retinoblastoma pathway in the control of s phase entry in the picophytoplanktonic cell *Ostreococcu*s. PLoS Genet 6:e1000957
Muheim R (2011) Behavioural and physiological mechanisms of polarized light sensitivity in birds. Philos Trans R Soc Lond B Biol Sci 366:763–771
Mullineaux CW, Stanewsky R (2009) The rolex and the hourglass: a simplified circadian clock in *Prochlorococcus*? J Bacteriol 191:5333–5335
Murakami R, Miyake A, Iwase R, Hayashi F, Uzumaki T, Ishiura M (2008) ATPase activity and its temperature compensation of the cyanobacterial clock protein KaiC. Genes Cells 13:387–395
Murayama Y, Mukaiyama A, Imai K, Onoue Y, Tsunoda A, Nohara A, Ishida T, Maéda Y, Terauchi K, Kondo T, Akiyama S (2011) Tracking and visualizing the circadian ticking of the cyanobacterial clock protein kaic in solution. EMBO J 30:68–78
Mutoh R, Nishimura A, Yasui S, Onai K, Ishiura M (2013) The ATP-mediated regulation of KaiB-KaiC interaction in the cyanobacterial circadian clock. PLoS One 8:e80200
Müller B, Grossniklaus U (2010) Model organisms–a historical perspective. J Proteomics 73:2054–2063
Münch M, Scheuermaier KD, Zhang R, Dunne SP, Guzik AM, Silva EJ, Ronda JM, Duffy JF (2011) Effects on subjective and objective alertness and sleep in response to evening light exposure in older subjects. Behav Brain Res 224:272–278
Naef F (2005) Circadian clocks go in vitro: purely post-translational oscillators in cyanobacteria. Mol Syst Biol 1:2005.0019
Naidoo N, Song W, Hunter-Ensor M, Seghal A (1999) A role for the proteasome in the light response of the timeless clock protein. Science 285:1737–1741
Nakahira Y, Katayama M, Miyashita H, Kutsuna S, Iwasaki H, Oyama T, Kondo T (2004) Global gene repression by KaiC as a master process of prokaryotic circadian system. Proc Natl Acad Sci U S A 101:881–885
Nakajima M, Imai K, Ito H, Nishiwaki T, Murayama Y, Iwasaki H, Oyama T, Kondo T (2005) Reconstitution of circadian oscillation of cyanobacterial KaiC phosphorylation in vitro. Science 308:414–415
Nakamichi N (2011) Molecular mechanisms underlying the *Arabidopsis* circadian clock. Plant Cell Physiol 52:1709–1718
Nakamichi N, Kiba T, Kamioka M, Suzuki T, Yamashino T, Higashiyama T, Sakakibara H, Mizuno T (2012) Transcriptional repressor prr5 directly regulates clock-output pathways. Proc Natl Acad Sci U S A 109:17123–17128
Ng FS, Tangredi MM, Jackson FR (2011) Glial cells physiologically modulate clock neurons and circadian behavior in a calcium-dependent manner. Curr Biol 21:625–634
Nickla D, Wildsoet C, Wallman J (1998) Visual influences on diurnal rhythms in ocular length and choroidal thickness in chick eyes. Exp Eye Res 66:163–181
Nikaido SS, Johnson CH (2000) Daily and circadian variation in survival from ultraviolet radiation in *Chlamydomonas reinhardtii*. Photochem Photobiol 71:758–765
Nishiwaki T, Iwasaki H, Ishiura M, Kondo T (2000) Nucleotide binding and autophosphorylation of the clock protein KaiC as a circadian timing process of cyanobacteria. Proc Natl Acad Sci U S A 97:495–499
Nitabach MN, Sheeba V, Vera DA, Blau J, Holmes TC (2005) Membrane electrical excitability is necessary for the free-running larval *Drosophila* circadian clock. J Neurobiol 62:1–13
Niwa Y, Yamashino T, Mizuno T (2009) The circadian clock regulates the photoperiodic response of hypocotyl elongation through a coincidence mechanism in *Arabidopsis thaliana*. Plant Cell Physiol 50:838–854
Ohdo S, Koyanagi S, Matsunaga N, Hamdan A (2011) Molecular basis of chronopharmaceutics. J Pharm Sci 100:3560–3576
Oishi T, Yamao M, Kondo C, Haida Y, Masuda A, Tamotsu S (2001) Multiphotoreceptor and multioscillator system in avian circadian organization. Microsc Res Tech 53:43–47
Okamura H (2007) Suprachiasmatic nucleus clock time in the mammalian circadian system. Cold Spring Harb Symp Quant Biol 72:551–556
Okawa M, Uchiyama M (2007) Circadian rhythm sleep disorders: characteristics and entrainment pathology in delayed sleep phase and non-24-h sleep-wake syndrome. Sleep Med Rev 11:485–496
Oltmanns O (1960) Über den Einfluss der Temperatur auf die endogene Tagesrhythmik und die Blühinduktion bei der Kurztagpflanze *Kalanchoe blossfeldiana*. Planta 54:233–264

Onai K, Morishita M, Itoh S, Okamoto K, Ishiura M (2004) Circadian rhythms in the thermophilic cyanobacterium *Thermosynechococcus elongatus*: compensation of period length over a wide temperature range. J Bacteriol 186:4972–4977

O'Neill JS, Reddy AB (2011) Circadian clocks in human red blood cells. Nature 469:498–503

O'Neill JS, van Ooijen G, Dixon LE, Troein C, Corellou F, Bouget F-Y, Reddy AB, Millar AJ (2011) Circadian rhythms persist without transcription in a eukaryote. Nature 469:554–558

van Ooijen G, Dixon LE, Troein C, Millar AJ (2011) Proteasome function is required for biological timing throughout the twenty-four hour cycle. Curr Biol 21:869–875

Oster H, Maronde E, Albrecht U (2002) The circadian clock as a molecular calendar. Chronobiol Int 19:507–516

Ouyang Y, Andersson C, Kondo T, Golden S, Johnson C (1998) Resonating circadian clocks enhance fitness in Cyanobacteria. Proc Natl Acad Sci U S A 95:8660–8664

Pail G, Huf W, Pjrek E, Winkler D, Willeit M, Praschak-Rieder N, Kasper S (2011) Bright-light therapy in the treatment of mood disorders. Neuropsychobiology 64:152–162

Palczewski K (2012) Chemistry and biology of vision. J Biol Chem 287:1612–1619

Panda S, Hogenesch JB (2004) It's all in the timing: many clocks, many outputs. J Biol Rhythms 19:374–387

Pandi-Perumal SR, Srinivasan V, Maestroni GJM, Cardinali DP, Poeggeler B, Hardeland R (2006) Melatonin: nature's most versatile biological signal? FEBS J 273:2813–2838

Pandi-Perumal SR, Bahammam AS, Brown GM, Spence DW, Bharti VK, Kaur C, Hardeland R, Cardinali DP (2013) Melatonin antioxidative defense: therapeutical implications for aging and neurodegenerative processes. Neurotox Res 23:267–300

Pandit A, Maheshwari R (1994) Sexual reproduction by Neurospora in nature. Fungal Genet Newsl 41:67–68

Parisky KM, Agosto J, Pulver SR, Shang Y, Kuklin E, Hodge JJL, Kang K, Kang K, Liu X, Garrity PA, Rosbash M, Griffith LC (2008) PDF cells are a GABA-responsive wake-promoting component of the *Drosophila* sleep circuit. Neuron 60:672–682

Park N, Cheon S, Son GH, Cho S, Kim K (2012) Chronic circadian disturbance by a shortened light-dark cycle increases mortality. Neurobiol Aging 33:1122.e11–1122.e22

Parker G, Brotchie H (2011) 'D' for depression: any role for vitamin D? 'Food for Thought' ii. Acta Psychiatr Scand 124:243–249

Partonen T, Magnusson A (2001) Seasonal affective disorder: practice and research. Oxford University Press, Oxford

de Paula RM, Lewis ZA, Greene AV, Seo K, Morgan L, Vitalini M, Bennett L, Gomer R, Bell-Pedersen D (2006) Two circadian timing circuits in *Neurospora crassa* cells share components and regulate distinct rhythmic processes. J Biol Rhythms 21:159–168

de Paula RM, Vitalini MW, Gomer RH, Bell-Pedersen D (2007) Complexity of the *Neurospora crassa* circadian clock system: multiple loops and oscillators. Cold Spring Harb Symp Quant Biol 72:345–351

Peirson SN, Halford S, Foster RG (2009) The evolution of irradiance detection: melanopsin and the non-visual opsins. Philos Trans R Soc Lond B Biol Sci 364:2849–2865

Pendergast JS, Yamazaki S (2011) Masking responses to light in period mutant mice. Chronobiol Int 28:657–663

Peschel N, Helfrich-Förster C (2011) Setting the clock–by nature: circadian rhythm in the fruitfly *Drosophila melanogaster*. FEBS Lett 585:1435–1442

Peterson E (1981a) Dynamic response of a circadian pacemaker. I. Recovery from extended light exposure. Biol Cybern 40:171–179

Peterson E (1981b) Dynamic response of a circadian pacemaker. II. Recovery from light pulse perturbations. Biol Cybern 40:181–194

Pévet P, Challet E (2011) Melatonin: both master clock output and internal time-giver in the circadian clocks network. J Physiol Paris 105:170–182

Pévet P, Agez L, Bothorel B, Saboureau M, Gauer F, Laurent V, Masson-Pévet M (2006) Melatonin in the multi-oscillatory mammalian circadian world. Chronobiol Int 23:39–51

Pfeuty B, Thommen Q, Corellou F, Djouani-Tahri EB, Bouget F-Y, Lefranc M (2012) Circadian clocks in changing weather and seasons: lessons from the picoalga *Ostreococcus tauri*. Bioessays 34:781–790

Philip P, Akerstedt T (2006) Transport and industrial safety, how are they affected by sleepiness and sleep restriction? Sleep Med Rev 10:347–356

Pickard GE, Sollars PJ (2010) Intrinsically photosensitive retinal ganglion cells. Sci China Life Sci 53:58–67

Pittendrigh CS (1964) The entrainment of circadian oscillations by skeleton photoperiods. Science 144:565

Pittendrigh C, Daan S (1976) A functional analysis of circadian pacemakers in nocturnal rodents. J Comp Physiol A106:333–355

Pittendrigh CS, Bruce BG, Rosensweig NS, Rubin ML (1959) Growth patterns in *Neurospora*. Nature 184:169–170

Plachetzki D, Serb J, Oakley T (2005) New insights into the evolutionary history of photoreceptor cells. Trends Ecol Evol 20:465–467

Plautz J, Kaneko M, Hall J, Kay S (1997) Independent photoreceptive circadian clocks throughout *Drosophila*. Science 278:1632–1635

Pokhilko A, Fernández AP, Edwards KD, Southern MM, Halliday KJ, Millar AJ (2012) The clock gene circuit in Arabidopsis includes a repressilator with additional feedback loops. Mol Syst Biol 8:574

Portolés S, Más P (2010) The functional interplay between protein kinase CK2 and CCA1 transcriptional activity is essential for clock temperature compensation in *Arabidopsis*. PLoS Genet 6:e1001201

Praschak-Rieder N, Willeit M (2012) Imaging of seasonal affective disorder and seasonality effects on serotonin and dopamine function in the human brain. Curr Top Behav Neurosci 11:149–167

Prasko J (2008) Bright light therapy. Neuro Endocrinol Lett 29(Suppl 1):33–64

Price-Lloyd N, Elvin M, Heintzen C (2005) Synchronizing the *Neurospora crassa* circadian clock with the rhythmic environment. Biochem Soc Trans 33:949–952

Privitera MR, Moynihan J, Tang W, Khan A (2010) Light therapy for seasonal affective disorder in a clinical office setting. J Psychiatr Pract 16:387–393

Provencio I, Foster RG (1995) Circadian rhythms in mice can be regulated by photoreceptors with cone-like characteristics. Brain Res 694:183–190

Pulivarthy SR, Tanaka N, Welsh DK, Haro LD, Verma IM, Panda S (2007) Reciprocity between phase shifts and amplitude changes in the mammalian circadian clock. Proc Natl Acad Sci U S A 104:20356–20361

Qin X, Byrne M, Xu Y, Mori T, Johnson CH (2010) Coupling of a core posttranslational pacemaker to a slave transcription/translation feedback loop in a circadian system. PLoS Biol 8:e1000394

Quintero J, Kuhlman S, McMahon D (2003) The biological clock nucleus: a multiphasic oscillator network regulated by light. J Neurosci 23:8070–8076

Rahman SA, Kayumov L, Tchmoutina EA, Shapiro CM (2009) Clinical efficacy of dim light melatonin onset testing in diagnosing delayed sleep phase syndrome. Sleep Med 10:549–555

Rastad C, Ulfberg J, Lindberg P (2008) Light room therapy effective in mild forms of seasonal affective disorder–a randomised controlled study. J Affect Disord 108:291–296

Rastad C, Ulfberg J, Lindberg P (2011) Improvement in fatigue, sleepiness, and health-related quality of life with bright light treatment in persons with seasonal affective disorder and subsyndromal SAD. Depress Res Treat 2011:543906

Rea M (1998) Photic entrainment of circadian rhythms in rodents. Chronobiol Int 15:395–423

Reed VA (2011) Shift work, light at night, and the risk of breast cancer. AAOHN J 59:37–45; quiz 46

Reid KJ, McGee-Koch LL, Zee PC (2011) Cognition in circadian rhythm sleep disorders. Prog Brain Res 190:3–20
Reiter RJ, Tan DX, Cabrera J, D'Arpa D, Sainz R, Mayo J, Ramos S (1999) The oxidant/antioxidant network: role of melatonin. Biol Signals Recept 8:56–63
Reiter RJ, Tan DX, Herman TS, Thomas CR (2004) Melatonin as a radioprotective agent: a review. Int J Radiat Oncol Biol Phys 59:639–653
Reiter RJ, Tan DX, Fuentes-Broto L (2010) Melatonin: a multitasking molecule. Prog Brain Res 181:127–151
Reme C, Wirz-Justice A, Terman M (1991) The visual input stage of the mammalian circadian pacemaking system: I. Is there a clock in the mammalian eye? J Biol Rhythms 6:5–29
Reppert SM, Gegear RJ, Merlin C (2010) Navigational mechanisms of migrating monarch butterflies. Trends Neurosci 33:399–406
Revel FG, Masson-Pévet M, Pévet P, Mikkelsen JD, Simonneaux V (2009) Melatonin controls seasonal breeding by a network of hypothalamic targets. Neuroendocrinology 90:1–14
Revell VL, Eastman CI (2005) How to trick mother nature into letting you fly around or stay up all night. J Biol Rhythms 20:353–365
Rieger D, Stanewsky R, Helfrich-Forster C (2003) Cryptochrome, compound eyes, Hofbauer-Buchner eyelets, and ocelli play different roles in the entrainment and masking pathway of the locomotor activity rhythm in the fruit fly *Drosophila melanogaster*. J Biol Rhythms 18:377–391
Rieger D, Shafer OT, Tomioka K, Helfrich-Forster C (2006) Functional analysis of circadian pacemaker neurons in *Drosophila melanogaster*. J Neurosci 26:2531–2543
Rieger D, Wülbeck C, Rouyer F, Helfrich-Förster C (2009) Period gene expression in four neurons is sufficient for rhythmic activity of *Drosophila melanogaster* under dim light conditions. J Biol Rhythms 24:271–282
Rietveld WJ, Minors DS, Waterhouse JM (1993) Circadian rhythms and masking: an overview. Chronobiol Int 10:306–312
Ripperger JA, Merrow M (2011) Perfect timing: epigenetic regulation of the circadian clock. FEBS Lett 585:1406–1411
Ripperger JA, Jud C, Albrecht U (2011) The daily rhythm of mice. FEBS Lett 585:1384–1392
Rizzini L, Favory J-J, Cloix C, Faggionato D, O'Hara A, Kaiserli E, Baumeister R, Schäfer E, Nagy F, Jenkins GI, Ulm R (2011) Perception of UV-B by the *Arabidopsis* uvr8 protein. Science 332:103–106
Roberts DE, Killiany RJ, Rosene DL (2012) Neuron numbers in the hypothalamus of the normal aging Rhesus monkey: stability across the adult lifespan and between the sexes. J Comp Neurol 520:1181–1197
Roecklein KA, Rohan KJ, Duncan WC, Rollag MD, Rosenthal NE, Lipsky RH, Provencio I (2009) A missense variant (P10L) of the melanopsin (OPN4) gene in seasonal affective disorder. J Affect Disord 114:279–285
Roenneberg T, Aschoff J (1990) Annual rhythm of human reproduction II: environmental correlations. J Biol Rhythms 5:217–240
Roenneberg T, Foster R (1997) Twilight times: light and the circadian system. Photochem Photobiol 66:549–561
Roenneberg T, Merrow M (1998) Molecular circadian oscillators: an alternative hypothesis. J Biol Rhythms 13:167–179
Roenneberg T, Merrow M (2001) Seasonality and photoperiodism in fungi. J Biol Rhythms 16:403–414
Roenneberg T, Mittag M (1996) The circadian program of algae. Semin Cell Dev Biol 7:753–763
Roenneberg T, Chua EJ, Bernardo R, Mendoza E (2008) Modelling biological rhythms. Curr Biol 18:R826–R835
Roenneberg T, Allebrandt KV, Merrow M, Vetter C (2012) Social jetlag and obesity. Curr Biol 22:939–943
Rohan KJ, Roecklein KA, Lacy TJ, Vacek PM (2009) Winter depression recurrence one year after cognitive-behavioral therapy, light therapy, or combination treatment. Behav Ther 40:225–238
Romero JM, Valverde F (2009) Evolutionarily conserved photoperiod mechanisms in plants: when did plant photoperiodic signaling appear? Plant Signal Behav 4:642–644
Rosato E, Kyriacou CP (2011) The role of natural selection in circadian behaviour: a molecular-genetic approach. Essays Biochem 49:71–85
Rosbash M (2009) The implications of multiple circadian clock origins. PLoS Biol 7:e62
Rosenthal NE (2006) Winter blues. Guilford Press, New York
Rosenthal NE, Sack DA, Gillin JC, Lewy AJ, Goodwin FK, Davenport Y, Mueller PS, Newsome DA, Wehr TA (1984) Seasonal affective disorder. A description of the syndrome and preliminary findings with light therapy. Arch Gen Psychiatry 41:72–80
Roth T (2012) Shift work disorder: overview and diagnosis. J Clin Psychiatry 73:e09
Ruan GX, Zhang DQ, Zhou T, Yamazaki S, McMahon DG (2006) Circadian organization of the mammalian retina. Proc Natl Acad Sci U S A 20:9703–9708
Ruby N, Dark J, Burns D, Heller H, Zucker I (2002) The suprachiasmatic nucleus is essential for circadian body temperature rhythms in hibernating ground squirrels. J Neurosci 22:357–364
Rüger M, Gordijn MCM, Beersma DGM, de Vries B, Daan S (2003) Acute and phase-shifting effects of ocular and extraocular light in human circadian physiology. J Biol Rhythms 18:409–419
Ruoff P, Rensing L (1996) The temperature-compensated goodwin model simulates many circadian clock properties. J Theor Biol 179:275–285
Ruoff P, Rensing L (2004) Temperature effects on circadian clocks. J Theor Biol 29:445–456
Rusak B, Zucker I (1979) Neural regulation of circadian rhythms. Physiol Rev 59:449–526
Rust MJ, Markson JS, Lane WS, Fisher DS, O'Shea EK (2007) Ordered phosphorylation governs oscillation of a three-protein circadian clock. Science 318:809–812
Rust MJ, Golden SS, O'Shea EK (2011) Light-driven changes in energy metabolism directly entrain the cyanobacterial circadian oscillator. Science 331:220–223
Rémi J, Merrow M, Roenneberg T (2010) A circadian surface of entrainment: varying T, t, and photoperiod in *Neurospora crassa*. J Biol Rhythms 25:318–328
Saarela S, Reiter R (1994) Function of melatonin in thermoregulatory processes. Life Sci 54:295–311
Sadeghniiat-Haghighi K, Yazdi Z, Jahanihashemi H, Aminian O (2011) The effect of bright light on sleepiness among rapid-rotating 12-hour shift workers. Scand J Work Environ Health 37:77–79
Saksvik IB, Bjorvatn B, Hetland H, Sandal GM, Pallesen S (2011) Individual differences in tolerance to shift work–a systematic review. Sleep Med Rev 15:221–235
Salgado-Delgado R, Angeles-Castellanos M, Buijs MR, Escobar C (2008) Internal desynchronization in a model of night-work by forced activity in rats. Neuroscience 154:922–931
Salgado-Delgado R, Nadia S, Angeles-Castellanos M, Buijs RM, Escobar C (2010) In a rat model of night work, activity during the normal resting phase produces desynchrony in the hypothalamus. J Biol Rhythms 25:421–431
Salichos L, Rokas A (2010) The diversity and evolution of circadian clock proteins in fungi. Mycologia 102:269–278
Salomé PA, Weigel D, McClung CR (2010) The role of the *Arabidopsis* morning loop components CCA1, LHY, PRR7, and PRR9 in temperature compensation. Plant Cell 22:3650–3661
Salva MAQ, Hartley S, Barbot F, Alvarez JC, Lofaso F, Guilleminault C (2011) Circadian rhythms, melatonin and depression. Curr Pharm Des 17:1459–1470
Satoh Y, Kawai H, Kudo N, Kawashima Y, Mitsumoto A (2006) Time-restricted feeding entrains daily rhythms of energy metabolism in mice. Am J Physiol Regul Integr Comp Physiol 290:R1276–R1283

Sawa M, Nusinow DA, Kay SA, Imaizumi T (2007) FKF1 and GIGANTEA complex formation is required for day-length measurement in Arabidopsis. Science 318:261–265
Schaap J, Albus H, VanderLeest H, Eilers P, Detari L, Meijer J (2003) Heterogeneity of rhythmic suprachiasmatic nucleus neurons: implications for circadian waveform and photoperiodic encoding. Proc Natl Acad Sci U S A 100:15994–15999
Schafmeier T, Diernfellner ACR (2011) Light input and processing in the circadian clock of *Neurospora*. FEBS Lett 585:1467–1473
Scheer FAJL, Wright KP, Kronauer RE, Czeisler CA (2007) Plasticity of the intrinsic period of the human circadian timing system. PLoS One 2:e721
Schmidt TM, Chen S-K, Hattar S (2011) Intrinsically photosensitive retinal ganglion cells: many subtypes, diverse functions. Trends Neurosci 34:572–580
Schmidt-Koenig K (1975) Migration and homing in animals. Springer, Berlin/Heidelberg
Schmoll C, Lascaratos G, Dhillon B, Skene D, Riha RL (2011) The role of retinal regulation of sleep in health and disease. Sleep Med Rev 15:107–113
Schroder S, Herzog ED, Kiss IZ (2012) Transcription-based oscillator model for light-induced splitting as antiphase circadian gene expression in the suprachiasmatic nuclei. J Biol Rhythms 27:79–90
Schulz P, Steimer T (2009) Neurobiology of circadian systems. CNS Drugs 23(Suppl 2):3–13
Schulze T, Prager K, Dathe H, Kelm J, Kiessling P, Mittag M (2010) How the green alga *Chlamydomonas reinhardtii* keeps time. Protoplasma 244:3–14
Schwerdtfeger C (2003) Vivid is a flavoprotein and serves as a fungal blue light photoreceptor for photoadaptation. EMBO J 22:4846–4855
Schäuble S, Heiland I, Voytsekh O, Mittag M, Schuster S (2011) Predicting the physiological role of circadian metabolic regulation in the green alga *Chlamydomonas reinhardtii*. PLoS One 6:e23026
Sehgal A, Price J, Young MW (1992) Ontogeny of a biological clock in *Drosophila melanogaster*. Proc Natl Acad Sci U S A 89:1423–1427
Sellix MT, Menaker M (2011) Circadian clocks in mammalian reproductive physiology: effects of the "other" biological clock on fertility. Discov Med 11:273–281
Serrano G, Herrera-Palau R, Romero JM, Serrano A, Coupland G, Valverde F (2009) *Chlamydomonas* CONSTANS and the evolution of plant photoperiodic signaling. Curr Biol 19:359–368
Shang Y, Griffith LC, Rosbash M (2008) Light-arousal and circadian photoreception circuits intersect at the large PDF cells of the *Drosophila* brain. Proc Natl Acad Sci U S A 105:19587–19594
Sharkey KM, Carskadon MA, Figueiro MG, Zhu Y, Rea MS (2011) Effects of an advanced sleep schedule and morning short wavelength light exposure on circadian phase in young adults with late sleep schedules. Sleep Med 12:685–692
Sharma V (2003) Adaptive significance of circadian clocks. Chronobiol Int 20:901–919
Shaw PJ, Cirelli C, Greenspan RJ, Tononi G (2000) Correlates of sleep and waking in *Drosophila melanogaster*. Science 287:1834–1837
Sheeba V, Fogle KJ, Kaneko M, Rashid S, Chou Y-T, Sharma VK, Holmes TC (2008a) Large ventral lateral neurons modulate arousal and sleep in *Drosophila*. Curr Biol 18:1537–1545
Sheeba V, Gu H, Sharma VK, O'Dowd DK, Holmes TC (2008b) Circadian- and light-dependent regulation of resting membrane potential and spontaneous action potential firing of *Drosophila* circadian pacemaker neurons. J Neurophysiol 99:976–988
Sheeba V, Fogle KJ, Holmes TC (2010) Persistence of morning anticipation behavior and high amplitude morning startle response following functional loss of small ventral lateral neurons in *Drosophila*. PLoS One 5:e11628
Shimomura K, Lowrey PL, Vitaterna MH, Buhr ED, Kumar V, Hanna P, Omura C, Izumo M, Low SS, Barrett RK, LaRue SI, Green CB, Takahashi JS (2010) Genetic suppression of the circadian clock mutation by the melatonin biosynthesis pathway. Proc Natl Acad Sci U S A 107:8399–8403
Shirani A, Louis EKS (2009) Illuminating rationale and uses for light therapy. J Clin Sleep Med 5:155–163
Siffre M (1975) Six months alone in a cave. Natl Geogr Mag 147:426
Silver R, Schwartz W (2005) The suprachiasmatic nucleus is a functionally heterogeneous timekeeping organ. Methods Enzymol 393:451–465
Silver R, Balsam PD, Butler MP, LeSauter J (2011) Food anticipation depends on oscillators and memories in both body and brain. Physiol Behav 104:562–571
Simonneaux V, Ribelayga C (2003) Generation of the melatonin endocrine message in mammals: a review of the complex regulation of melatonin synthesis by norepinephrine, peptides, and other pineal transmitters. Pharmacol Rev 55:325–395
Simons MJP (2009) The evolution of the cyanobacterial posttranslational clock from a primitive "phoscillator". J Biol Rhythms 24:175–182
Skene D (2003) Optimization of light and melatonin to phase-shift human circadian rhythms. J Neuroendocrinol 15:438–441
Skene DJ, Arendt J (2007) Circadian rhythm sleep disorders in the blind and their treatment with melatonin. Sleep Med 8:651–655
Smith RM, Williams SB (2006) Circadian rhythms in gene transcription imparted by chromosome compaction in the cyanobacterium *Synechococcus elongatus*. Proc Natl Acad Sci U S A 103:8564–8569
Smith KM, Sancar G, Dekhang R, Sullivan CM, Li S, Tag AG, Sancar C, Bredeweg EL, Priest HD, McCormick RF, Thomas TL, Carrington JC, Stajich JE, Bell-Pedersen D, Brunner M, Freitag M (2010) Transcription factors in light and circadian clock signaling networks revealed by genomewide mapping of direct targets for *Neurospora* white collar complex. Eukaryot Cell 9:1549–1556
Sole MJD, Sande PH, Bernades JM, Aba MA, Rosenstein RE (2007) Circadian rhythm of intraocular pressure in cats. Vet Ophthalmol 10:155–161
Springer M (1993) Genetic control of fungal differentiation: the three sporulation pathways of *Neurospora crassa*. Bioessays 15:365–374
Srikanth A, Schmid M (2011) Regulation of flowering time: all roads lead to Rome. Cell Mol Life Sci 68:2013–2037
Srinivasan V, Smits M, Spence W, Lowe AD, Kayumov L, Pandi-Perumal SR, Parry B, Cardinali DP (2006) Melatonin in mood disorders. World J Biol Psychiatry 7:138–151
Srinivasan V, Spence DW, Pandi-Perumal SR, Trakht I, Cardinali DP (2008) Jet lag: therapeutic use of melatonin and possible application of melatonin analogs. Travel Med Infect Dis 6:17–28
Stal LJ, Krumbein M (1985a) Nitrogenase activity in the non-heterocystous cyanobacterium *Oscillatoria* sp. grown under alternating light-dark cycles. Arch Microbiol 143:67–71
Stal LJ, Krumbein M (1985b) Oxygen protection of nitrogenase in the aerobically nitrogen fixing non-heterocystous cyanobacterium Oscillatoria sp. Arch Microbiol 143:72–76
Stanewsky R, Jamison C, Plautz J, Kay S, Hall J (1997) Multiple circadian-regulated elements contribute to cycling period gene expression in *Drosophila*. EMBO J 16:5006–5018
Stanewsky R, Kaneko M, Emery P, Beretta B, Wager-Smith K, Kay SA, Rosbash M, Hall JC (1998) The cryb mutation identifies cryptochrome as a circadian photoreceptor in *Drosophila*. Cell 95:681–692
Steenhard BM, Besharse JC (2000) Phase shifting the retinal circadian clock: xPer2 mRNA induction by light and dopamine. J Neurosci 20:8572–8577
Stehle JH, von Gall C, Schomerus C, Korf H (2001) Of rodents and ungulates and melatonin: creating a uniform code for darkness by different signaling mechanisms. J Biol Rhythms 16:312–325
Stehle JH, Saade A, Rawashdeh O, Ackermann K, Jilg A, Sebestény T, Maronde E (2011) A survey of molecular details in the human

pineal gland in the light of phylogeny, structure, function and chronobiological diseases. J Pineal Res 51:17–43
Steiner M, Werstiuk E, Seggie J (1987) Dysregulation of neuroendocrine crossroads: depression, circadian rhythms and the retina–a hypothesis. Prog Neuropsychopharmacol Biol Psychiatry 11:267–278
Steinlechner S, Stieglitz A, Ruf T (2002) Djungarian hamsters: a species with a labile circadian pacemaker? Arrhythmicity under a light-dark cycle induced by short light pulses. J Biol Rhythms 17:248–258
Stephan FK (2002) The "other" circadian system: food as a Zeitgeber. J Biol Rhythms 17:284–292
Stevens RG (2009a) Light-at-night, circadian disruption and breast cancer: assessment of existing evidence. Int J Epidemiol 38:963–970
Stevens RG (2009b) Working against our endogenous circadian clock: breast cancer and electric lighting in the modern world. Mutat Res 680:106–108
Stoleru D, Peng Y, Agosto J, Rosbash M (2004) Coupled oscillators control morning and evening locomotor behaviour of Drosophila. Nature 431:862–868
Strasser B, Sánchez-Lamas M, Yanovsky MJ, Casal JJ, Cerdán PD (2010) *Arabidopsis thaliana* life without phytochromes. Proc Natl Acad Sci U S A 107:4776–4781
Strauss O (2005) The retinal pigment epithelium in visual function. Physiol Rev 85:845–881
Strong RE, Marchant BK, Reimherr FW, Williams E, Soni P, Mestas R (2009) Narrow-band blue-light treatment of seasonal affective disorder in adults and the influence of additional nonseasonal symptoms. Depress Anxiety 26:273–278
Su S-B, Lu C-W, Kao Y-Y, Guo H-R (2008) Effects of 12-hour rotating shifts on menstrual cycles of photoelectronic workers in Taiwan. Chronobiol Int 25:237–248
Suzuki L, Johnson CH (2002) Photoperiodic control of germination in the unicell *Chlamydomonas*. Naturwissenschaften 89:214–220
Szular J, Sehadova H, Gentile C, Szabo G, Chou W-H, Britt SG, Stanewsky R (2012) Rhodopsin 5- and rhodopsin 6-mediated clock synchronization in drosophila melanogaster is independent of retinal phospholipase c-? signaling. J Biol Rhythms 27:25–36
Tan Y, Merrow M, Roenneberg T (2004) Photoperiodism in *Neurospora crassa*. J Biol Rhythms 19:135–143
Tanaka K, Takahashi M, Tanaka M, Takanao T, Nishinoue N, Kaku A, Kato N, Tagaya H, Miyaoka H (2011) Brief morning exposure to bright light improves subjective symptoms and performance in nurses with rapidly rotating shifts. J Occup Health 53:258–266
Taniguchi Y, Takai N, Katayama M, Kondo T, Oyama T (2010) Three major output pathways from the kaiabc-based oscillator cooperate to generate robust circadian kaibc expression in cyanobacteria. Proc Natl Acad Sci U S A 107:3263–3268
Tassi P, Pellerin N, Moessinger M, Hoeft A, Muzet A (2000) Visual resolution in humans fluctuates over the 24h period. Chronobiol Int 17:187–195
Tauber E, Last K, Olive P, Kyriacou C (2004) Clock gene evolution and functional divergence. J Biol Rhythms 19:445–458
Tavakoli-Nezhad M, Schwartz WJ (2005) c-Fos expression in the brains of behaviorally 'split' hamsters in constant light: calling attention to a dorsolateral region of the suprachiasmatic nucleus and the medial division of the lateral habenula. J Biol Rhythms 20:419–429
Teng C, Akerman D, Cordas T, Kasper S, Vieira A (1995) Seasonal affective disorder in a tropical country: a case report. Psychiatry Res 56:11–15
Terman M (2007) Evolving applications of light therapy. Sleep Med Rev 11:497–507
Terman J, Terman M (1999) Photopic and scotopic light detection in patients with seasonal affective disorder and control subjects. Biol Psychiatry 46:1642–1648
Terman M, Amira L, Terman J, Ross D (1996) Predictors of response and nonresponse to light treatment for winter depression. Am J Psychiatry 153:1423–1429
Thaler K, Delivuk M, Chapman A, Gaynes BN, Kaminski A, Gartlehner G (2011) Second-generation antidepressants for seasonal affective disorder. Cochrane Database Syst Rev 12:CD008591
Thommen Q, Pfeuty B, Morant P-E, Corellou F, Bouget F-Y, Lefranc M (2010) Robustness of circadian clocks to daylight fluctuations: hints from the picoeucaryote *Ostreococcus tauri*. PLoS Comput Biol 6:e1000990
Thommen Q, Pfeuty B, Corellou F, Bouget F-Y, Lefranc M (2012) Robust and flexible response of the *Ostreococcus tauri* circadian clock to light/dark cycles of varying photoperiod. FEBS J 279:3432–3448
Thompson CL, Rickman CB, Shaw SJ, Ebright JN, Kelly U, Sancar A, Rickman DW (2003) Expression of the blue-light receptor cryptochrome in the human retina. Invest Ophthalmol Vis Sci 44:4515–4521
Thorpy MJ (2011) Understanding and diagnosing shift work disorder. Postgrad Med 123:96–105
Tigges M, Marquez-Lago TT, Stelling J, Fussenegger M (2009) A tunable synthetic mammalian oscillator. Nature 457:309–312
Timonen M, Nissilä J, Liettu A, Jokelainen J, Jurvelin H, Aunio A, Räsänen P, Takala T (2012) Can transcranial brain-targeted bright light treatment via ear canals be effective in relieving symptoms in seasonal affective disorder? A pilot study. Med Hypotheses 78:511–515
Toh KI, Jones R, He Y, Eide EJ, Hinz WA, Virshup DM, Ptácek LJ, Fu YH (2001) An hper2 phosphorylation site mutation in familial advanced sleep phase syndrome. Science 291:1040–1043
Tomioka K, Matsumoto A (2010) A comparative view of insect circadian clock systems. Cell Mol Life Sci 67:1397–1406
Tomioka K, Uryu O, Kamae Y, Umezaki Y, Yoshii T (2012) Peripheral circadian rhythms and their regulatory mechanism in insects and some other arthropods: a review. J Comp Physiol B 182(6):729–740
Tonsfeldt KJ, Chappell PE (2012) Clocks on top: the role of the circadian clock in the hypothalamic and pituitary regulation of endocrine physiology. Mol Cell Endocrinol 349:3–12
Tosches MA, Bucher D, Vopalensky P, Arendt D (2014) Melatonin signaling controls circadian swimming behavior in marine zooplankton. Cell 159:46–57
Tosini G, Fukuhara C (2002) The mammalian retina as a clock. Cell Tissue Res 309:119–126
Tosini G, Menaker M (1996) Circadian rhythms in cultured mammalian retina. Science 272:419–421
Tosini G, Pozdeyev N, Sakamoto K, Iuvone PM (2008) The circadian clock system in the mammalian retina. Bioessays 30:624–633
Toth R, Kevei E, Hall A, Millar AJ, Nagy F, Kozma-Bognar L (2001) Circadian clock-regulated expression of phytochrome and cryptochrome genes in *Arabidopsis*. Plant Physiol 127:1607–1616
Touitou Y (1998) Biological clocks: mechanisms and applications, Proc Internat Congr Chronobiol Paris 7–11 September 1997. Elsevier, Amsterdam
Touitou Y, Bogdan A (2007) Promoting adjustment of the sleep-wake cycle by chronobiotics. Physiol Behav 90:294–300
Troein C, Corellou F, Dixon LE, van Ooijen G, O'Neill JS, Bouget F-Y, Millar AJ (2011) Multiple light inputs to a simple clock circuit allow complex biological rhythms. Plant J 66:375–385
Troncoso-Ponce MA, Mas P (2012) Newly described components and regulatory mechanisms of circadian clock function in *Arabidopsis thaliana*. Mol Plant 5:545–553
Tseng Y-Y, Hunt SM, Heintzen C, Crosthwaite SK, Schwartz J-M (2012) Comprehensive modelling of the Neurospora circadian clock and its temperature compensation. PLoS Comput Biol 8:e1002437

Turek FW (2005) Role of light in circadian entrainment and treating sleep disorders–and more. Sleep 28:548–549
Tyson JJ, Albert R, Goldbeter A, Ruoff P, Sible J (2008) Biological switches and clocks. J R Soc Interface 5(Suppl 1):S1–S8
Ugolini A, Boddi V, Mercatelli L, Castellini C (2005) Moon orientation in adult and young sandhoppers under artificial light. Proc Biol Sci 272:2189–2194
Ugolini A, Somigli S, Pasquali V, Renzi P (2007) Locomotor activity rhythm and sun compass orientation in the sandhopper Talitrus saltator are related. J Comp Physiol A 193:1259–1263
Ukai H, Ueda HR (2010) Systems biology of mammalian circadian clocks. Annu Rev Physiol 72:579–603
Ukai H, Kobayashi TJ, Nagano M, Masumoto KH, Sujino M, Kondo T, Yagita K, Shigeyoshi Y, Ueda HR (2007) Melanopsin-dependent photo-perturbation reveals desynchronization underlying the singularity of mammalian circadian clocks. Nat Cell Biol 9:1327–1334
Ukai-Tadenuma M, Kasukawa T, Ueda HR (2008) Proof-by-synthesis of the transcriptional logic of mammalian circadian clocks. Nat Cell Biol 10:1154–1163
Vandewalle G, Hébert M, Beaulieu C, Richard L, Daneault V, Garon M-L, Leblanc J, Grandjean D, Maquet P, Schwartz S, Dumont M, Doyon J, Carrier J (2011) Abnormal hypothalamic response to light in seasonal affective disorder. Biol Psychiatry 70:954–961
Veleri S, Rieger D, Helfrich-Förster C, Stanewsky R (2007) Hofbauer-Buchner eyelet affects circadian photosensitivity and coordinates TIM and PER expression in *Drosophila* clock neurons. J Biol Rhythms 22:29–42
Vijayan V, Zuzow R, O'Shea EK (2009) Oscillations in supercoiling drive circadian gene expression in cyanobacteria. Proc Natl Acad Sci U S A 106:22,564–22,568
Vitalini MW, de Paula RM, Park WD, Bell-Pedersen D (2006) The rhythms of life: circadian output pathways in Neurospora. J Biol Rhythms 21:432–444
Vitalini MW, de Paula RM, Goldsmith CS, Jones CA, Borkovich KA, Bell- Pedersen D (2007) Circadian rhythmicity mediated by temporal regulation of the activity of p38 MAPK. Proc Natl Acad Sci U S A 104:18223–18228
Vitalini MW, Dunlap J, Heintzen C, Liu Y, Loros J, Bell-Pedersen D (2010) Circadian rhythms. In: Borkovich KA, Ebbole DJ (eds) Cellular and molecular biology of filamentous fungi. ASM Press, Washington, DC, pp 442–466
Vollrath L (2002) Chronoendokrinologia- quo vadis? Ann Anat 184:583–593
Wagner V, Mittag M (2009) Probing circadian rhythms in Chlamydomonas rheinhardtii by functional proteomics. Methods Mol Biol 479:173–188
Wagner V, Gessner G, Mittag M (2005) Functional proteomics: a promising approach to find novel components of the circadian system. Chronobiol Int 22:403–415
Walton JC, Weil ZM, Nelson RJ (2011) Influence of photoperiod on hormones, behavior, and immune function. Front Neuroendocrinol 32:303–319
Wang W, Barnaby JY, Tada Y, Li H, Tör M, Caldelari D, Lee DU, Fu X-D, Dong X (2011) Timing of plant immune responses by a central circadian regulator. Nature 470:110–114
Warman GR, Pawley MDM, Bolton C, Cheeseman JF, Fernando AT, Arendt J, Wirz-Justice A (2011) Circadian-related sleep disorders and sleep medication use in the New Zealand blind population: an observational prevalence survey. PLoS One 6:e22073
Warren E, Allen C, Brown R, Robinson D (2003) Intrinsic light responses of retinal ganglion cells projecting to the circadian system. Eur J Neurosci 17:1727–1735
Watanabe T, Kojima M, Tomida S, Nakamura TJ, Yamamura T, Nakao N, Yasuo S, Yoshimura T, Ebihara S (2006) Peripheral clock gene expression in CS mice with bimodal locomotor rhythms. Neurosci Res 54:295–301
Watanabe T, Naito E, Nakao N, Tei H, Yoshimura T, Ebihara S (2007) Bimodal clock gene expression in mouse suprachiasmatic nucleus and peripheral tissues under a 7-hour light and 5-hour dark schedule. J Biol Rhythms 22:58–68
Weber F, Zorn D, Rademacher C, Hung H-C (2011) Post-translational timing mechanisms of the *Drosophila* circadian clock. FEBS Lett 585:1443–1449
Wegener C, Hamasaka Y, Nässel DR (2004) Acetylcholine increases intracellular Ca^{2+} via nicotinic receptors in cultured pdf-containing clock neurons of drosophila. J Neurophysiol 91:912–923
Wehr TA (2001) Photoperiodism in humans and other primates: evidence and implications. J Biol Rhythms 16:348–364
Weitzman ED, Czeisler CA, Zimmerman JC, Moore-Ede MC (1981) Biological rhythms in man: relationship of sleep-wake, cortisol, growth hormone, and temperature during temporal isolation. Adv Biochem Psychopharmacol 28:475–499
Welsh DK, Takahashi JS, Kay SA (2010) Suprachiasmatic nucleus: cell autonomy and network properties. Annu Rev Physiol 72:551–577
Werner R (2002) *Chlamydomonas reinhardtii* as a unicellular model for circadian rhythm analysis. Chronobiol Int 19:325–343
Westrin A, Lam RW (2007a) Long-term and preventative treatment for seasonal affective disorder. CNS Drugs 21:901–909
Westrin A, Lam RW (2007b) Seasonal affective disorder: a clinical update. Ann Clin Psychiatry 19:239–246
Wever RA (1979) The circadian system of man. Springer, New York
Willeit M, Sitte HH, Thierry N, Michalek K, Praschak-Rieder N, Zill P, Winkler D, Brannath W, Fischer MB, Bondy B, Kasper S, Singer EA (2008) Enhanced serotonin transporter function during depression in seasonal affective disorder. Neuropsychopharmacology 33:1503–1513
Winfree A (1970) Integrated view of resetting a circadian clock. J Comp Physiol A 28:327–374
Winfree AT (1986) The timing of biological clocks. Scientific American Books, Inc., New York
Winkler D, Pjrek E, Iwaki R, Kasper S (2006) Treatment of seasonal affective disorder. Expert Rev Neurother 6:1039–1048
Wirz-Justice A, Terman M (2012) Chronotherapeutics (light and wake therapy) as a class of interventions for affective disorders. Handb Clin Neurol 106:697–713
Woelfle M, Johnson C (2006) No promoter left behind: global circadian gene expression in cyanobacteria. J Biol Rhythms 21:419
Woelfle MA, Ouyang Y, Phanvijhitsiri K, Johnson CH (2004) The adaptive value of circadian clocks: an experimental assessment in Cyanobacteria. Curr Biol 14:1481–1486
Wolfson AR, Carskadon MA (2003) Understanding adolescents' sleep patterns and school performance: a critical appraisal. Sleep Med Rev 7:491–506
Workman JL, Nelson RJ (2011) Potential animal models of seasonal affective disorder. Neurosci Biobehav Rev 35:669–679
Wright KP, Hughes RJ, kronauer RE, Dijk DJ, Czeisler CA (2001) Intrinsic near-24-hour pacemaker period determines limits of circadian entrainment to a weak synchronizer in humans. Proc Natl Acad Sci U S A 98:14027–14032
Wülbeck C, Grieshaber E, Helfrich-Förster C (2008) Pigment-dispersing factor (pdf) has different effects on *Drosophila*'s circadian clocks in the accessory medulla and in the dorsal brain. J Biol Rhythms 23:409–424
Xu Y, Padiath QS, Shapiro RE, Jones CR, Wu SC, Saigoh N, Saigoh K, Ptacek LJ, Fu YH (2005) Functional consequences of a CKIdelta mutation causing familial advanced sleep phase syndrome. Nature 434:640–644

Xu K, DiAngelo JR, Hughes ME, Hogenesch JB, Sehgal A (2011) The circadian clock interacts with metabolic physiology to influence reproductive fitness. Cell Metab 13:639–654

Yakir E, Hilman D, Harir Y, Green RM (2007) Regulation of output from the plant circadian clock. FEBS J 274:335–345

Yamada Y, Forger D (2010) Multiscale complexity in the mammalian circadian clock. Curr Opin Genet Dev 20:626–633

Yamaguchi S, Isejima H, Matsuo T, Okura R, Yagita K, Kobayashi M, Okamura H (2003) Synchronization of cellular clocks in the suprachiasmatic nucleus. Science 302:1408–1412

Yamazaki S, Numano R, Abe M, Hida A, Takahashi R, Ueda M, Block GD, Sakaki Y, Menaker M, Tei H (2000) Resetting central and peripheral circadian oscillators in transgenic rats. Science 288:682–685

Yang XP, de Groot EJ (1992) Identification of two clock proteins in Acetabularia cliftonii and construction of cdna libraries from *Acetabularia cliftonii* and *Acetabularia mediterranea*. Int J Biochem 24:1141–1150

Yanovsky MJ, Mazzella MA, Whitelam GC, Casal JJ (2001) Resetting of the circadian clock by phytochromes and cryptochromes in Arabidopsis. J Biol Rhythms 16:523–530

Yerushalmi S, Yakir E, Green RM (2011) Circadian clocks and adaptation in *Arabidopsis*. Mol Ecol 20:1155–1165

Yoshii T, Funada Y, Ibuki-Ishibashi T, Matsumoto A, Tanimura T, Tomioka K (2004) Drosophila cryb mutation reveals two circadian clocks that drive locomotor rhythm and have different responsiveness to light. J Insect Physiol 50:479–488

Yoshii T, Todo T, Wülbeck C, Stanewsky R, Helfrich-Förster C (2008) Cryptochrome is present in the compound eyes and a subset of *Drosophila*'s clock neurons. J Comp Neurol 508:952–966

Yoshii T, Wülbeck C, Sehadova H, Veleri S, Bichler D, Stanewsky R, Helfrich-Förster C (2009) The neuropeptide pigment-dispersing factor adjusts period and phase of *Drosophila*'s clock. J Neurosci 29:2597–2610

Yoshii T, Hermann C, Helfrich-Förster C (2010) Cryptochrome-positive and – negative clock neurons in *Drosophila* entrain differentially to light and temperature. J Biol Rhythms 25: 387–398

Yoshii T, Rieger D, Helfrich-Förster C (2012) Two clocks in the brain: an update of the morning and evening oscillator model in Drosophila. Prog Brain Res 199:59–82

Young R (1976) Visual cells and the concept of renewal. Invest Ophthalmol Vis Sci 15:700–725

Zamanian Z, Kakooei H, Ayattollahi SMT, Dehghani M (2010) Effect of bright light on shift work nurses in hospitals. Pak J Biol Sci 13:431–436

van Zanten M, Tessadori F, Peeters AJM, Fransz P (2012) Shedding light on large scale chromatin reorganization in *Arabidopsis thaliana*. Mol Plant 5:583–590

Zee PC, Goldstein CA (2010) Treatment of shift work disorder and jet lag. Curr Treat Options Neurol 12:396–411

Zee PC, Vitiello MV (2009) Circadian rhythm sleep disorder: irregular sleep wake rhythm type. Sleep Med Clin 4:213–218

Zhdanova I, Reebs S (2006) Circadian rhythms in fish. In: Sloman K, Wilson R, Balshine S (eds) Behavior and physiology of fish, vol 24, Fish physiology. Elsevier, Amsterdam, pp 197–238

Zinser ER, Lindell D, Johnson ZI, Futschik ME, Steglich C, Coleman ML, Wright MA, Rector T, Steen R, McNulty N, Thompson LR, Chisholm SW (2009) Choreography of the transcriptome, photophysiology, and cell cycle of a minimal photoautotroph, *Prochlorococcus*. PLoS One 4:e5135

Ziv C, Yarden O (2010) Gene silencing for functional analysis: assessing RNAi as a tool for manipulation of gene expression. Methods Mol Biol 638:77–100

Zoltowski BD, Schwerdtfeger C, Widom J, Loros JJ, Bilwes AM, Dunlap JC, Crane BR (2007) Conformational switching in the fungal light sensor Vivid. Science 316:1054–1057

Photomorphogenesis and Photoperiodism in Plants

19

James L. Weller and Richard E. Kendrick

19.1 Introduction

It has long been observed that light affects the way plants grow. Effects of light can be observed on processes and phenomena throughout the plant life cycle, including seed germination, apical hook opening, stem elongation, leaf expansion, the synthesis of photosynthetic and protective pigments, stomatal regulation, lateral branching, bud dormancy and flowering. The vast majority of these effects are unrelated to the use of light for photosynthesis and are mediated through a specialised system of photoreceptors that informs the plant about its surroundings and directs it to develop appropriately.

Photomorphogenesis is a general term encompassing all responses to light that affect plant form. Two specific classes of photomorphogenic response are sometimes distinguished. *Phototropic* responses involve the reorientation of plant organs with respect to an asymmetry in the incident light, as in the case of shoot tips bending to grow towards the light. *Photoperiodic* responses are those in which various aspects of development are modified in response to changes in the daily light/dark cycle and involve a circadian timing mechanism. Developmental features commonly subject to photoperiodic control include flowering, bud dormancy and leaf senescence.

This chapter will give an overview of our current knowledge about the way in which these different responses are achieved. We will discuss the discovery and nature of the photoreceptors involved in these phenomena, their physiological roles as determined in the laboratory and their possible significance in the natural environment. Although lower plants also show clear photomorphogenic responses, they have in general been less intensively studied, and we will restrict this discussion to higher plants.

J.L. Weller (✉)
School of Plant Science, University of Tasmania, Hobart, Tasmania, Australia
e-mail: jim.weller@utas.edu.au

R.E. Kendrick
Department of Plant Science, Wageningen University, Wageningen, The Netherlands

19.2 Photomorphogenetic Photoreceptors

As with other photobiological responses, an initial step in the investigation of photomorphogenic responses was the determination of action spectra. Early measurements identified the blue (BL), red (R) and far-red (FR) regions of the spectrum as being particularly important for the control of plant growth (e.g. Went 1941; Parker et al. 1949) and formed the point of departure in the search for specific photoreceptor pigments for light in these wavebands. Relatively rapid progress was made in biochemical characterisation of the photoreceptor responsible for R and FR responses (Sage 1992). In contrast, progress towards identification of a specific BL photoreceptor was limited due to the large number of different BL-absorbing compounds in the plant with the potential to serve as a photoreceptor chromophore and to the lack of a distinctive photophysiological assay.

However, the advent of molecular genetic approach from around 1990 brought rapid developments in our understanding of the nature, diversity and functions of the photoreceptor pigments involved in informational light sensing. Five classes of higher plant photoreceptors have now been characterised in detail; the *phytochrome* family of R- and FR-absorbing photoreceptors, three different photoreceptor families mediating responses in the BL and UV-A regions of the spectrum (*cryptochrome*, *phototropin* and *ZTL/FKF1* families) and the UV-B photoreceptor UVR8 (Fig. 19.1). We will discuss each of these in turn.

L.O. Björn (ed.), *Photobiology: The Science of Light and Life*,
DOI 10.1007/978-1-4939-1468-5_19, © Springer Science+Business Media New York 2015

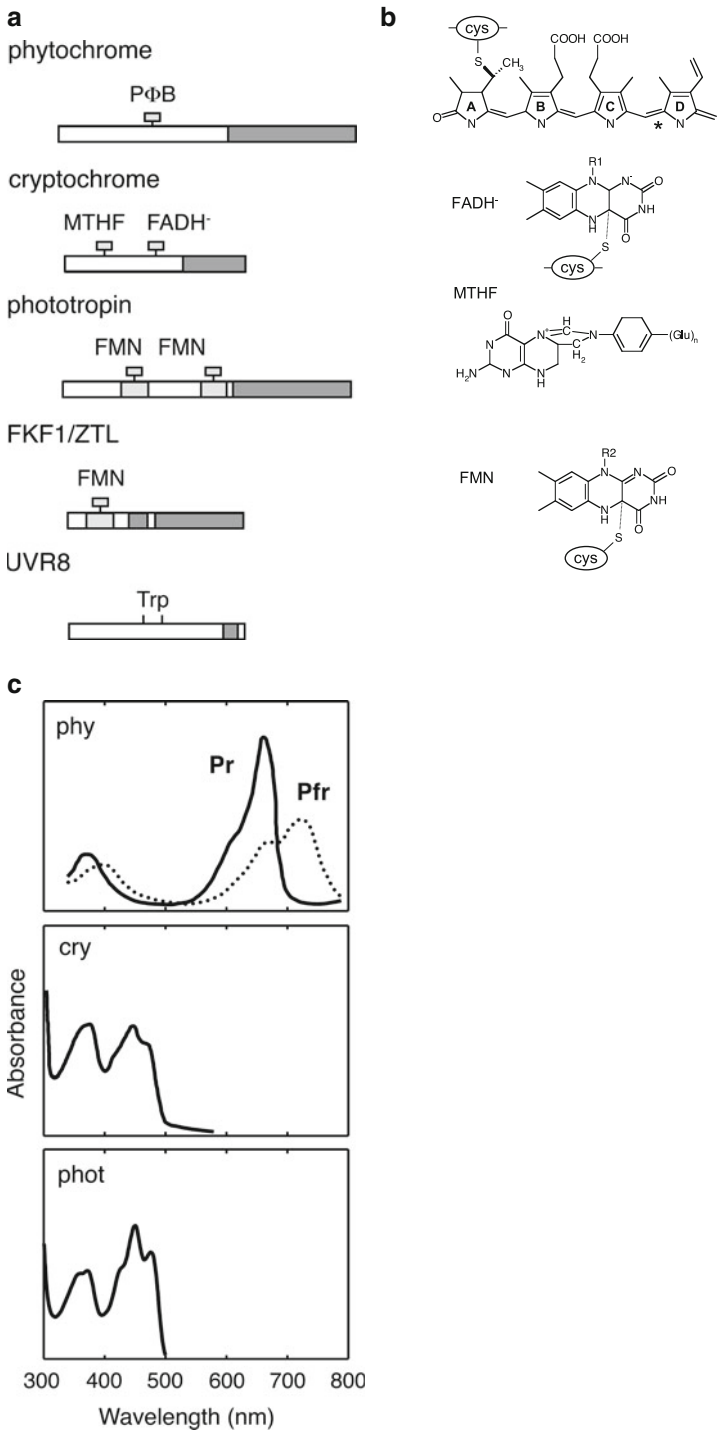

Fig. 19.1 Characteristics of plant photoreceptors. (**a**) Illustrates protein domain structures for the five classes of photoreceptor proteins. (**b**) Shows the structures and approximate attachment sites of chromophores for each class of photoreceptor, except UVR8. The asterix indicates the double bond involved in photoisomerization of the phytochrome chromophore. (**c**) Shows *in vitro* absorption spectra for phytochrome, cryptochrome and phototropin redrawn from Butler et al. (1964), Lin et al. (1995) and Christie et al (1999)

19.2.1 Phytochromes

19.2.1.1 Isolation

The main impetus in the early search for photoreceptors came from observations that the inductive effects of R on several aspects of plant development could be reversed by irradiation with FR. The fact that this R/FR reversibility occurred for diverse responses suggested that it might be a property of a single photoreceptor (Withrow et al. 1957). This was proven by the purification of a protein that exhibited R-/FR-reversible absorption changes. The protein was named *phytochrome*, a name derived from the Greek words for *plant* and *colour*. The two forms of phytochrome are characterised by absorption peaks at around 660 and 730 nm and are referred to as Pr and Pfr, respectively (Fig. 19.1). Both Pr and Pfr also have secondary absorption peaks in the BL region of the spectrum but

can to some extent absorb light across the visible and near UV spectrum. These two forms of phytochrome can be repeatedly interconverted by light pulses, and continuous light establishes a dynamic equilibrium between them that depends on the composition of the light.

19.2.1.2 Genes and Gene Family

The first phytochrome-encoding gene was identified from oat seedlings in 1984 by expression screening (Hershey et al. 1984), and phytochrome genes have been subsequently identified in many other flowering plants, as well as gymnosperms, ferns, mosses and algae (Mathews 2006). Phytochrome-related sequences have also been found in a wide range of microbes, including cyanobacteria, fungi and diatoms, suggesting a very ancient origin (Kehoe and Grossman 1996; Davis et al. 1999; Karniol et al. 2005). In higher plants, phytochromes are encoded by a small gene family. Three ancient branches, phyA, phyB and phyC, date back to the origin of flowering plants and possibly as far back as the origin of seed plants (Mathews 2010). Within angiosperms an additional duplication within the phyB lineage giving rise to phyE seems to be relatively ancient and widespread, and independent duplications within the phyA and phyB subfamilies have occurred within various taxa (Sharrock and Mathews 2006). In other cases such as poplar and some legumes, the phyC and phyE lineages subsequently appear to have been lost (Howe et al. 1998; Platten et al. 2005a). Nevertheless, the control of photomorphogenesis appears to be dominated by phyA and phyB in most species that have been studied in detail, and it is possible that additional phytochromes merely refine this basic programme.

19.2.1.3 Gene/Protein Structure

The generic phytochrome apoprotein has a molecular mass of around 125 kDa and consists of two domains; an N-terminal domain of 75 kDa that binds the chromophore and a C-terminal domain of 55 kDa that consists of two regions with homology to histidine kinases (Fig. 19.1) (Rockwell et al. 2006). The first of these C-terminal regions contains two PAS domains, which are implicated in protein-protein interactions. This region also contains a small domain that is essential for the regulatory activity of the molecule. Gene and protein structure are in general highly conserved across the phytochrome family, with the most notable difference being small poorly conserved N- and C-terminal extensions in phyB-type phytochromes (Sharrock and Mathews 2006). Phytochromes are synthesised in cytosol in the red-light-absorbing (Pr) configuration and form dimers in vivo. Deletion and point mutation studies have given some indication of areas of importance for determination of the absorption spectrum, photochromicity, dimerisation and signal transduction for both phyA and phyB (Rockwell et al. 2006).

19.2.1.4 Chromophore

The phytochrome chromophore, phytochromobilin (PΦB), is an open-chain bilitriene (Fig. 19.1), similar to the chromophore for the photosynthetic pigment C-phycocyanin in cyanobacteria. Feeding studies combined with analysis of chromophore-deficient mutants have shown that phytochromobilin is formed in plastids by a pathway which branches from the pathway for chlorophyll synthesis with the chelation of Fe^{2+} rather than Mg^{2+} to protoporphyrin IX (Rockwell et al. 2006; Davis 2006). Heme is then oxygenised to biliverdin resulting in the opening of the tetrapyrrole ring. This is followed by reduction of the A-ring to form PΦB. Free PΦB assembles autocatalytically to the phytochrome apoprotein and attaches at its C3 position to a cysteine residue in the middle of the N-terminal domain via a thioether linkage (Rockwell et al. 2006). Photoreversibility of the phytochrome holoprotein derives from isomerisation of bound PΦB about the double bond between rings C and D. It is worth noting that the absorption peaks of the Pr and Pfr are red shifted 35 and 100 nm, respectively, relative to that of free phytochromobilin conformers. This illustrates the importance of the protein environment for the light-absorbing properties of the chromophore and hence for the spectral characteristics of the photoreceptor. PΦB-deficient mutants have been isolated in a range of species and shown to carry mutations in structural genes for enzymes in PΦB biosynthesis (Muramoto et al. 1999; Kohchi et al. 2001). As a consequence of PΦB deficiency, these mutants have reduced levels of spectrally active phytochrome and exhibit strong defects in responses to light that are attributable to reduced activity of multiple members of the phytochrome family (Parks and Quail 1991; Weller et al. 1997b). All *Arabidopsis* phy apoproteins can assemble with PΦB in vitro (Eichenberg et al. 2000), and it is assumed that all higher plant phytochromes utilise PΦB as their sole chromophore in vivo. Some lower plant phytochromes may use a related bilin phycocyanobilin (PCB), and microbial phy also utilise a wider range of chromophores including biliverdin (bacteria) and PCB (cyanobacteria) (Rockwell and Lagarias 2010; Ulijasz and Vierstra 2011).

19.2.2 Cryptochromes

The contribution of a BL-specific photoreceptor system to de-etiolation was first inferred from observations that BL could promote de-etiolation, even in plants grown under continuous red light (i.e. under conditions which are saturating for phytochrome activity). In addition, mutants strongly deficient in phytochrome chromophore synthesis (and hence in the activities of all phytochromes) were shown to retain substantial responsiveness to BL (Briggs 2006). The unidentified BL photoreceptor was often referred to as *cryptochrome*,

from the Greek words for *hidden* and *colour*, reflecting its elusive nature. The primary BL photoreceptor in de-etiolation was finally identified in 1994, after cloning of the defective gene in an *Arabidopsis* mutant (*hy4*) specifically impaired in de-etiolation under BL (Ahmad and Cashmore 1994). This photoreceptor is now known as cryptochrome 1 (cry1). A second member of the cryptochrome family, cryptochrome 2 (cry2), was identified by its homology to cry1 (Lin et al. 1998). As in the case of the phytochromes, these two cryptochrome subfamilies have undergone independent duplication in certain taxa (Perrotta et al. 2000; Platten et al. 2005a; Hirose et al. 2006).

The CRY1 and CRY2 apoproteins are around 75 kDa in molecular mass and have two distinct parts (Fig. 19.1). The N-terminal half shows similarity to enzymes called photolyases, which are activated by BL and UV light to repair certain kinds of damage to DNA. In contrast, the C-terminal halves of cry1 and cry2 show only a very low degree of similarity to each other and to other known proteins. When expressed in *E. coli*, the photolyase-like domain binds the same two chromophores as photolyases (Fig. 19.1) – a flavin (flavin adenine dinucleotide) and a pterin (methenyltetrahydrofolate) (Lin et al. 1995; Malhotra et al. 1995) – although it has yet to be confirmed that the latter chromophore is utilised in planta. It has been speculated that the pterin chromophore may serve as a kind of antenna and may predominantly determine the UV-A/BL-absorbing properties of the molecule, while the flavin chromophore may be essential to the initial signalling reaction (Chaves et al. 2011). The FAD chromophore is thought to undergo a light-driven redox cycle between the oxidised form, which absorbs BL most effectively, and a reduced form, which characteristically absorbs green light (GL) (Liu et al. 2011). This interpretation is consistent with observations that GL can antagonise some cryptochrome-dependent responses to BL (Chaves et al. 2011).

19.2.3 Phototropin

Despite the substantial problems encountered in the biochemical search for a BL photoreceptor, this approach did prove successful in the identification of the photoreceptor for BL-induced phototropism. Work in the lab of Winslow Briggs identified a 120 kDa membrane protein that underwent autophosphorylation after irradiation with BL. The action spectrum and various kinetic aspects of this reaction showed a close correlation to those for phototropism, suggesting that the protein itself might function as a photoreceptor (Briggs 2006). The physiological significance of the protein was confirmed by its absence in aphototropic *nph1* mutants of *Arabidopsis* (Liscum and Briggs 1995), and cloning of the *NPH1* gene in 1997 subsequently revealed a protein with clear characteristics of a BL receptor (Huala et al. 1997). This protein is now known as phototropin 1 (phot1). A second *NPH1*-like gene (*NPL1*) was also identified and subsequently also shown to encode an active phototropin photoreceptor (phot2) that functions together with phot1 in the BL regulation of phototropism, chloroplast movement, stomatal opening and leaf expansion (Kagawa et al. 2001; Kinoshita et al. 2001; Sakai et al. 2001; Sakamoto and Briggs 2002). Phot2 is present in all plants, whereas phot1 appears restricted to spermatophytes (Galvan-Ampudia and Offringa 2007).

The phot molecules consist of two distinct halves; a C-terminal domain with clear homology to classical serine/threonine kinases, and an N-terminal half containing two domains that each bind a flavin mononucleotide (FMN) chromophore (Fig. 19.1). These domains have been termed LOV domains for their presence in a range of proteins involved in the sensing of *l*ight, *o*xygen or *v*oltage (Christie et al. 1999). Both FMN chromophores undergo a photocycle that involves formation of a cysteinyl adduct and loss of BL absorption upon BL exposure. Mutational studies have shown that the majority of phot activity depends on the photochemical activity of the LOV2 domain, while the role of LOV1 domain is less clear (Christie and Murphy 2013).

19.2.4 Other LOV-Domain Blue-Light Photoreceptors

Following the isolation of phototropins, sequence homologies and forward genetics identified a second small family of LOV-domain proteins encoded in the *Arabidopsis* genome (Nelson et al. 2000; Somers et al. 2000). However, outside their single LOV domain, these proteins show no similarity with the phototropins, but instead incorporate an F-box domain (implicated in protein-protein interactions) and a kelch repeat domain (Fig. 19.1). Most higher plants have a basic complement of two such proteins (ZTL and FKF1) although *Arabidopsis* itself has an additional protein (LKP2) more closely related to ZTL (Schultz et al. 2001). It has subsequently been shown that LOV domains from these proteins attach FMN chromophore, and they are now known to act as photoreceptors regulating light-dependent protein turnover in photoperiodic and circadian regulation (see Sect. 19.5.2.1 below).

19.2.5 UV-B Photoreceptors

In addition to the effects of BL and UV-A mediated by the phytochrome and cryptochrome families, shorter wavelength UV (UV-B) also affects plant growth. At high irradiances this is due to the effects of DNA damage, but at low irradiances photomorphogenic effects are also observed (Kim

et al. 1998). Although phytochromes and cryptochromes can contribute to these low-irradiance effects, in some cases they have been shown to be independent of known photoreceptors, suggesting the existence of a distinct photoreceptor for UV-B (Ulm 2006). However, it is only recently that this photoreceptor was identified (Rizzini et al. 2011) as UVR8, a beta-propeller protein with homology to the mammalian guanine nucleotide exchange factor RCC1.

UVR8 was first identified in screens for *Arabidopsis* mutants showing increased sensitivity to UV-B damage and shown to be absolutely required for developmental responses to UV-B under conditions that exclude contribution from other known photoreceptors (Kliebenstein et al. 2002; Favory et al. 2009). UVR8 exists as a dimer in the absence of UV-B light but reversibly dissociates into monomers after light absorption. UVR8 expression does not show conspicuous regulation by light, but it does become enriched in the nucleus in response to UV-B (Kaiserli and Jenkins 2007; Favory et al. 2009).

Unlike many other photoreceptors, UVR8 does not appear to require a covalently bound chromophore, and the primary perception mechanism seems instead to depend on UV absorbance by certain tryptophan residues in the protein itself, which are clustered at the dimerisation interface (Christie et al. 2012). Mutational studies have established that substitution of three specific tryptophans is sufficient to confer constitutive dimerisation and loss of signalling interactions, but only partial loss of biological activity, suggesting that momomerisation alone is not sufficient for function (O'Hara and Jenkins 2012).

19.3 Physiological Roles of Photoreceptors

Considering the number and nature of plant photoreceptors, it is easy to see how early attempts to interpret physiological observations of photomorphogenesis were hampered by the diversity and functional overlap of the photoreceptors involved. The identification of photoreceptor-specific mutants has been essential for the characterisation of the functions and interactions of the photoreceptors, and mutants continue to be an important tool in dissection of signalling pathways. Null mutants have now been identified for each of the 13 known photoreceptors in *Arabidopsis*, and photoreceptor-specific mutants have also been identified in other higher plant species, notably tomato, rice and pea. These have been useful in testing generalisations about photoreceptor function and in studying processes not easily studied in *Arabidopsis*. Sense and antisense transgenic lines expressing altered levels of specific photoreceptors have also been of use in exploring photoreceptor functions where no mutants have been available and in species not convenient for mutant analysis. In recent years the availability of genome scale approaches has also facilitated analysis of photoreceptor involvement in natural variation.

As the number of known plant photoreceptors has grown, it is becoming clear that many light-regulated processes are controlled by multiple photoreceptors, which may interact in different ways in different developmental contexts (Casal 2006, 2013). The following sections present an overview of what is known about the photocontrol of several of the better-studied processes in higher plants. The exception is flowering, which is dealt with in Sect. 19.5.

19.3.1 Germination

In species that exhibit seed dormancy, germination can often be induced by a light treatment given to imbibed seed. In general, small-seeded species are more responsive than large-seeded ones. In a classic study on lettuce seed germination in the 1930s, Flint and MacAlister found that R was particularly effective at inducing germination, while FR and BL were inhibitory (Sage 1992). It was shown subsequently that the effect of R could be reversed by FR. In some highly sensitive seeds, including *Arabidopsis*, a distinct non-FR-reversible phase can be identified. Three hours after imbibition, germination of *Arabidopsis* seeds can be induced by R in a fully FR-reversible manner, and this response is absent in the *phyB* mutant (Shinomura et al. 1996). After longer periods of imbibition, the sensitivity to light increases and, at 48 h germination, can be induced by very small amounts of light, including FR, and is therefore no longer FR reversible. This second phase is absent in the *phyA* mutant (Shinomura et al. 1996).

These two responses illustrate some more general features of phyA and phyB function. PhyB controls responses which can be induced by low-fluence R in the order of 1–1,000 μmol m^{-2} and which are reversible by FR. These are called low-fluence responses (LFR) and are a function of the amount of phyB in the Pfr form (Fig. 19.2). PhyA-mediated responses are much more sensitive to light and have a range in threshold fluence approximately four orders of magnitude lower than LFR (0.1–100 nmol m^{-2}). These very-low-fluence responses (VLFR) require only a very small proportion of phyA (<0.1 %) to be converted to the Pfr form. They can therefore be induced by light of any wavelength from 300 to 750 nm and are not reversible by FR (Fig. 19.2). The molecular basis for the difference between these two forms of response is not yet understood.

19.3.2 Seedling Establishment

The development of the germinating seedling and its establishment as a fully autotrophic plant require the coordination

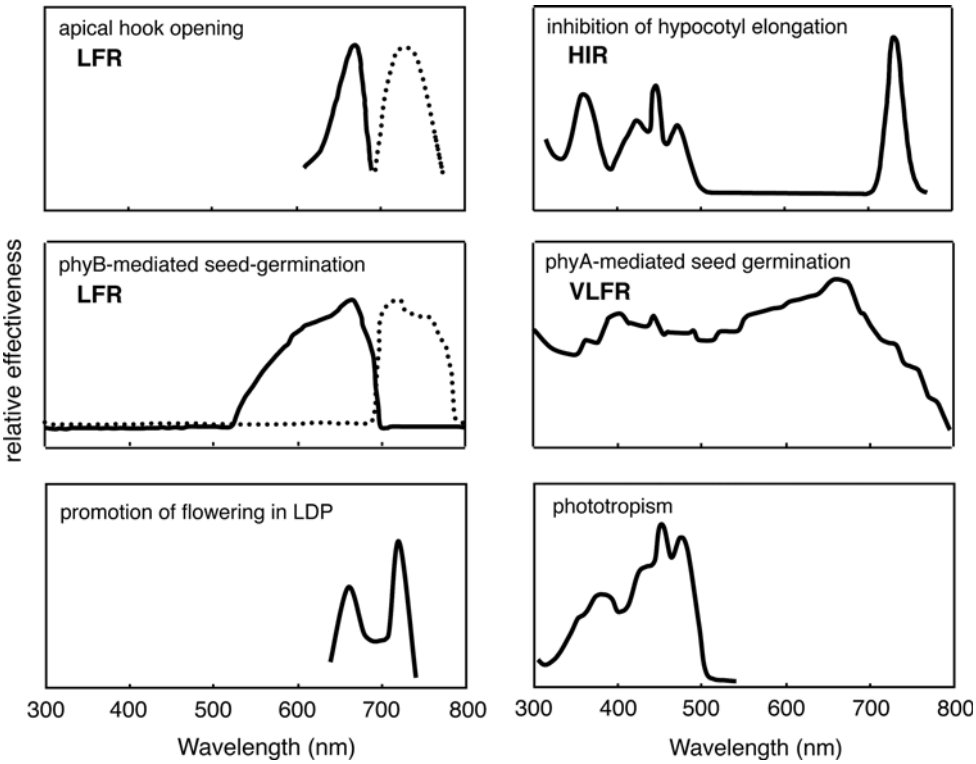

Fig. 19.2 Action spectra for representative photomorphogenic responses. *LFR*-low-fluence response, *HIR*, high-irradiance response, *VLFR*, very-low-fluence response. Broken lines represent reversal of response (Redrawn from Withrow et al. 1957; Hartmann 1967; Baskin and Iino 1987; Carr-Smith et al. 1989; Shinomura et al. 1996)

of several different light-regulated processes. These include inhibition of stem or hypocotyl elongation, apical hook opening, opening and expansion of cotyledons and leaves and the induction of accumulation of photosynthetic and protective pigments. The regulation of these processes by light, which is often termed *de-etiolation*, can be dramatically demonstrated by the exposure of etiolated (dark-grown) seedlings to brief R pulses. Experiments of this kind show roles for phyA and phyB that are generally consistent with the LFR and VLFR response modes identified in the control of germination. These responses also manifest in coordinated changes in the expression of many different genes, both nuclear and plastidic (Tepperman et al. 2001, 2004).

Light responses during seedling establishment are more commonly studied by growing plants under different irradiances of continuous monochromatic light. The responses induced under these conditions are often stronger than those observed in response to a single light pulse and are termed high-irradiance responses (HIRs). HIRs to continuous BL, R and FR have all been reported. The FR-HIR is in most cases controlled entirely by phyA, whereas the R-HIR is controlled mainly by the phyB-type phytochromes (Fig. 19.3) (Franklin et al. 2003). The exception is in rice, where phyC may also contribute to de-etiolation in response to continuous FR (Takano et al. 2005). PhyA can also act under continuous R, but its contribution can often only be seen at lower irradiances, where the phyB-type phytochromes are not active (Kerckhoffs et al. 1997; Mazzella et al. 1997).

The HIRs can be considered as a series of responses to pulses of light, and the fundamental photoreactions have been explored by replacing the continuous irradiation with intermittent pulses. R-HIR can be effectively induced by an R pulse every 4 h in an FR-reversible manner, suggesting that the R-HIR is effectively a continuous activation of LFR. In contrast, the FR-HIR can be replaced only by FR pulses given every 3 min. Under this regime, the effect of the FR pulses is reversible by R (Shinomura et al. 2000). The FR-HIR is therefore distinct from the phyA-mediated VLFR and operates by a mechanism fundamentally different from phyB-mediated LFR. The molecular basis for these differences is not yet understood, although recent results suggest that the dynamics of degradation and intracellular transport play an important role (see Sect. 19.4.1).

De-etiolation can also be induced by BL. Under high-irradiance continuous BL, cry1 is the main photoreceptor for de-etiolation responses, with a threshold for activity of around 5 $\mu mol \cdot m^{-2} \cdot s^{-1}$, whereas at lower irradiances, phyA becomes the predominant BL photoreceptor (Fig. 19.3). PhyB-type phytochromes also make a minor contribution under high-irradiance BL that becomes more evident in the absence of phyA and cry1 (Poppe et al. 1998; Weller et al. 2001b; Platten et al. 2005b). In *Arabidopsis*, the second cryptochrome, cry2, is also reported to have a minor role in

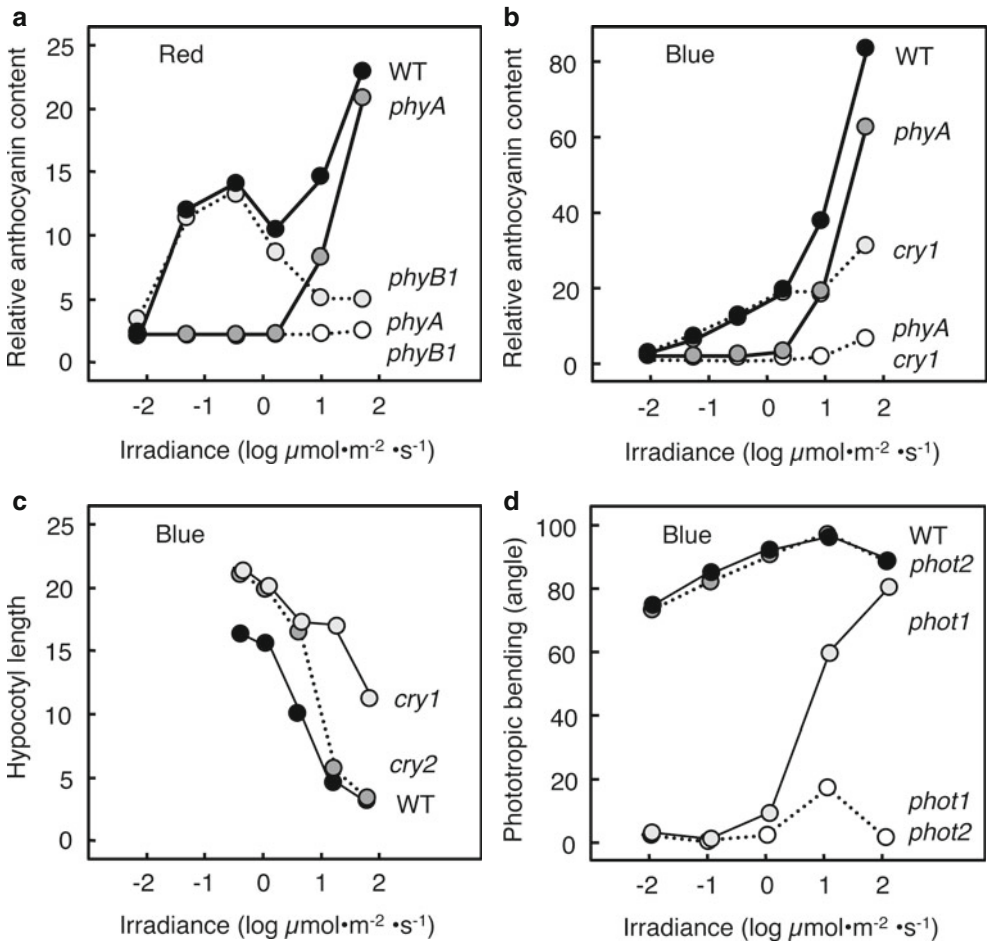

Fig. 19.3 Irradiance dependence for various photomorphogenic responses in wild-type and photoreceptor mutant seedlings of tomato (**a**, **b**) and Arabidopsis (**c**, **d**), exposed for 24 h to monochromatic red or blue light. (Redrawn from Kerckhoffs et al. 1997, Weller et al. 2001b, Guo et al. 1998, Sakai et al. 2001)

the control of seedling light responses under lower-irradiance BL (Fig. 19.3) (Lin et al. 1998).

Temporal differences in the action of different photoreceptors are also observed. Immediately following exposure of etiolated seedlings to R, phyA is the main photoreceptor controlling inhibition of hypocotyl elongation, and phyB only becomes predominant after several hours of exposure (Parks and Spalding 1999). This functional separation is similar to the temporal phases observed for phyA- and phyB-mediated germination and may be due in part to phyA degradation. Similar analyses have shown that inhibition of elongation in response to blue light is mediated initially by phot1 for the first 30 min following exposure and then subsequently by cry1 and cry2 (Folta and Spalding 2001).

19.3.3 Phototropism

Detailed action spectra indicated that the photoreceptor responsible for seedling phototropism has an absorption peak in the UV-A and a 3-component peak in the BL region of the spectrum. Fluence-response curves for induction of phototropism by BL pulses resolved two components (Liscum and Stowe-Evans 2000). The "first-positive" component can be induced by fluences of 0.1–500 μmol m^{-2} and shows reciprocity within a certain fluence range. The "second-positive" component has a similar fluence threshold but is also time dependent, with a minimum time requirement of around 10 min. *phot1* mutants lack the first-positive response and are completely aphototropic under low irradiances of continuous BL, suggesting that they are also deficient in the second-positive response. However, under continuous BL of higher irradiance (>10 μmol m^{-2} s^{-1}), *phot1* mutants show a normal phototropic response (Sakai et al. 2000), implying the action of another photoreceptor, subsequently shown to be phot2 (*NPL1*) (Fig. 19.3) (Sakai et al. 2001). The function of phototropin in the control of hypocotyl elongation was initially thought to be restricted to the perception of unilateral B, because *nph1* plants exhibit grossly normal de-etiolation responses (Liscum and Briggs 1995). However, more detailed analyses have shown that phototropins can mediate a more general inhibition of elongation in response to B (Folta and Spalding 2001; Sakamoto and Briggs 2002).

Although phyA, phyB, cry1 and cry2 have all been proposed to contribute to the B phototropic response, it is now clear that these photoreceptors are neither necessary nor sufficient for directional light sensing, at least in *Arabidopsis* hypocotyls. Nevertheless they can modulate expression of the phototropic response, by increasing its amplitude or speeding up its development. In addition, absorption of R by phytochrome can enhance the subsequent phototropin-mediated response to unilateral B (Parks et al. 1996). One suggestion is that this may an indirect effect resulting from phytochrome suppression of gravitropism (Lariguet and Fankhauser 2004).

19.3.4 Shade Avoidance

Light responses in established, fully autotrophic seedlings are often referred to as shade-avoidance responses. In response to shading, stem elongation increases, development of lateral organs such as leaves and branches is suppressed, and flowering is accelerated (Casal 2013). Vegetational shading involves changes in both irradiance and spectral quality of the light reaching the plant. The main difference in spectral quality is an effective enrichment for FR, which is due to the fact that leaves transmit FR but absorb BL and R. The term shade avoidance as applied to laboratory experiments refers specifically to responses induced by manipulation of the FR content against a constant background of photosynthetically active radiation (Fig. 19.4).

Once again, the availability of multiple photoreceptor mutants has allowed the control of shade-avoidance responses to be dissected in detail. These analyses show that phyB/(E)-type phytochromes dominate the response, with mutants deficient in these phytochromes appearing as strongly shade-avoiding plants even when grown under high-irradiance light of high R:FR (Devlin et al. 1998, 1999; Weller et al. 2000). This indicates that these phytochromes act as a simple developmental switch in which Pfr formed under light of high R:FR actively initiates photomorphogenic responses and this activation is proportionately reduced as the photoequilibrium is shifted back towards the Pr form by increasing FR supplementation.

It was initially assumed that phyA was unlikely to be important for shade avoidance, as phyA-deficient mutants show no substantial difference from WT seedlings when grown in white light (Whitelam et al. 1993, Weller et al. 1997a). However, phyA can in fact oppose the phyB-mediated shade-avoidance response by inhibiting stem elongation under light of low R:FR ratio (Smith et al. 1997; Weller et al. 1997a), and it is clear that the balance of phyA to phyB is therefore important in determining the degree of responsiveness to changes in R:FR.

In addition to changes in R:FR, canopy shade also clearly represents a reduction in overall irradiance. This is thought to act through both phytochrome and cryptochrome systems (Keller et al. 2011).

Fig. 19.4 Shade-avoidance response of wild-type tomato seedlings simulated by addition of high irradiance far-red light to the white light source, lowering the ratio of red to far-red light from 6.3 to 0.1

19.3.5 Chloroplast Movement

One important physiological mechanism for short-term acclimation to altered light levels is the relocation of chloroplasts within mesophyll tissues. Under high irradiances, chloroplasts move towards anticlinal cell walls thus reducing the amount of intercepted light, whereas under low irradiances, they accumulate along the periclinal walls to maximise light absorption. These "avoidance" and "accumulation" responses occur within 2 h of a change in light conditions. In angiosperms these movements are primarily responses to the BL spectral region and are mediated exclusively by phototropins but can be modified or enhanced by phytochromes (DeBlasio et al. 2003; Luesse et al. 2010). Interestingly, whereas both phot1 and phot2 contribute to the accumulation response, the avoidance response is controlled only by phot2 (Sakai et al. 2001).

19.3.6 Stomatal Opening

In general plant stomata tend to be closed in darkness and open in response to light, particularly light in the blue region of the spectrum. This means that CO_2 uptake and fixation

occur while energy from the light reactions of photosynthesis is available Both phototropins and cryptochromes appear to contribute independently to this response with phototropins functioning across a wide irradiance range and cryptochromes mainly at higher irradiances (Kinoshita et al. 2001; Mao et al. 2005).

19.4 Photoreceptor Regulation and Early Signalling

Most of the classical photomorphogenic responses listed above are whole-plant responses and occur on a scale of hours to days after first exposure to the light stimulus. Recent molecular and genetic dissections are revealing shorter-term cellular and molecular and hormonal events underlying these responses. While each photoreceptor and photoreceptor group participates in distinct signalling networks, it is clear that transcriptional regulation, sub-cellular partitioning and control of protein stability are common themes across these networks. Details of specific components within light signalling networks are covered in Chap. 14. Here we will restrict our discussion to regulation of photoreceptor expression and early events in photoreceptor signalling.

19.4.1 Phytochrome

Two features considered characteristic of phytochrome in early studies were its presence at much higher levels in dark-grown than in light-grown seedlings and its rapid disappearance after exposure to light. These features are now known to mainly reflect the properties of phyA. PhyA accumulates as Pr in the cytosol and conversion to Pfr after light exposure initiates both a rapid proteasome-mediated degradation of the protein and a rapid downregulation of *PHYA* transcription (Rockwell et al. 2006; Hennig 2006). PhyA degradation is mainly dependent on the CUL1-RING ubiquitin ligase pathway (Debrieux et al. 2013). Other phytochromes are expressed at a much lower level than phyA in dark-grown seedlings and are not strongly light regulated. In light-grown plants, phytochrome genes are widely expressed around the plant at generally similar level across different tissues (Goosey et al. 1997; Hauser et al. 1997) and show regulation by the circadian clock (Toth et al. 2001).

Both phyA and phyB are synthesised in the cytosol in darkness and show light-dependent nuclear transport, with response modes typical of VFLR and FR-HIR for phyA and LFR for phyB (Kircher et al. 1999, 2002; Hisada et al. 2000; Gil et al. 2000). This implies a major role in transcriptional regulation, and indeed, major genome-wide changes in transcription occur within an hour of phytochrome activation (Tepperman et al. 2001, 2004). Other phytochrome responses, such as osmotic changes leading to organ movement and cell growth, occur much more rapidly, indicating a role for phytochrome in the cytoplasm (Hughes 2013).

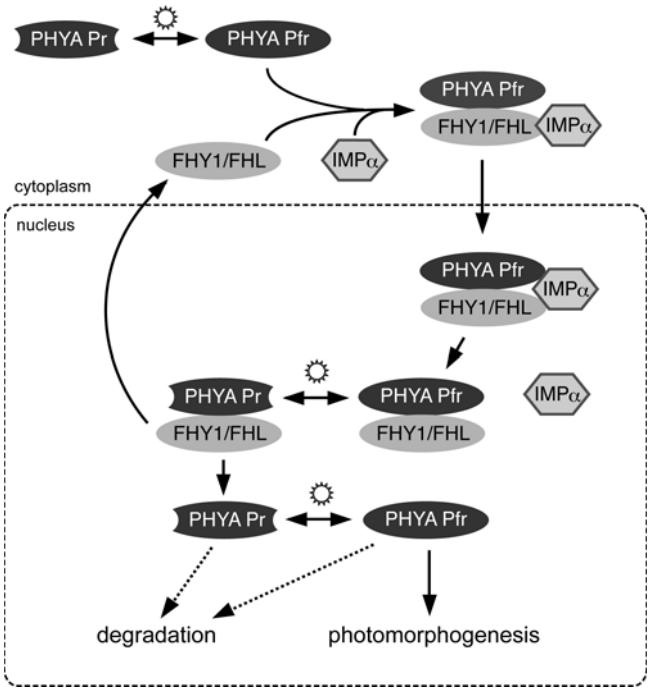

Fig. 19.5 Model for light-induced nuclear transport of phyA, (Adapted from Kircher et al. 2011; Rausenberger et al. 2011). Following irradiation, phyA in the cytoplasm is converted to the Pfr form and interacts with FHY1/FHL proteins. These proteins in turn interact with importin α, which facilitates the transport of the complex into the nucleus. In the nucleus the complex dissociates, and an equilibrium between photoconversion and degradation is established that depends on the spectral quality of the light. The highest levels of the active Pfr form are thought to occur under far-red wavelengths, due to the fact that these conditions minimize overall phyA degradation by protecting it in the inactive but more stable Pr form

Differences in the dynamics of intracellular transport are thought to be a key factor explaining how phytochromes with very similar absorbance properties can mediate responses with quite different spectral sensitivities. In recent years it has become clear that phytochrome nuclear transport is facilitated by interaction with proteins that themselves possess a nuclear localisation signal (Pfeiffer et al. 2012). PhyB-type phytochromes undergo relatively slow nuclear import, which is facilitated by the PIF family of bHLH transcription factors (Pfeiffer et al. 2012), which also act in phytochrome signalling (Leivar and Quail 2010; see Chap. 14). In contrast, phyA is much more rapidly imported after light exposure. This import depends on two related proteins, FHY1 and FHL, which physically interact with phyA and can shuttle it in both directions across the nuclear membrane (Fig. 19.5). These two proteins are indispensible for phyA nuclear import and for the HIR mode of phyA action (Hiltbrunner et al. 2006; Genoud et al. 2008; Kircher et al.

2011). The most advanced explanation for the distinct action spectrum of phyA HIR has invoked an interaction between facilitated transport, photoconversion and degradation that leads to accumulation of phyA in the nucleus under continuous FR but not continuous R (Rausenberger et al. 2011).

In addition to their roles in nuclear import of phyA, the FHY1 and FHL proteins may guide nuclear phyA into signalling complexes involving a number of transcription factors, including LAF1 (Myb type) and HFR1 (bHLH type) (Yang et al. 2009). The retention of certain responses to FR in a *phy1 fhl* double mutant, which is unable to import phyA to the nucleus, has provided additional evidence that phyA can also act in the cytoplasm (Rösler et al. 2007).

Despite homology of phytochrome C-terminal domains to histidine kinases, and the histidine kinase activity of prokaryotic phytochromes (Rockwell et al. 2006), plant phytochromes instead show light-dependent autophosphorylation characteristic of ser/thr kinase activity (Yeh and Lagarias 1998), although functionally significant tyrosine phosphorylation has also recently been reported (Nito et al. 2013). A range of functions have been ascribed to phytochrome autophosphorylation. For example, phyA autophosphorylation in the N-terminal region impedes the degradation of phyA (Han et al. 2010), while phosphorylation of one particular residue in *Arabidopsis* phyB may influence signalling by increasing the rate at which the active Pfr form reverts to the inactive Pr form (Medzihradszky et al. 2013).

Other studies have identified targets of phytochrome phosphorylation. Some of these target proteins have also been shown to interact physically with phy (Ahmad et al. 1998; Fankhauser et al. 1999; Choi et al. 1999; Colon-Carmona et al. 2000), but in most cases, evidence is still lacking about whether this phosphorylation is direct and whether it is functionally significant (Quail 2006). Two exceptions may be the PIF family of transcription factors (Leivar and Quail 2011; see Chap. 14) and FHY1 (Chen et al. 2012).

19.4.2 Cryptochrome

CRY transcription is regulated by the circadian clock (Toth et al. 2001; Platten et al. 2005b; Zhang et al. 2008), and in some species, a strong repression by light has also been reported (Platten et al. 2005b). The *Arabidopsis* cry2 protein differs from cry1 in being unstable under high-irradiance BL (Lin et al. 1998). This is reminiscent of the rapid light-induced degradation of phyA but, in contrast, depends mainly on the COP1 ubiquitin ligase pathway (see Chap. 14; Lau and Deng 2012; Weidler et al. 2012). Both cry1 and cry2 have been shown to localise to the nucleus (Kleiner et al. 1999; Matsumoto et al. 2003), although studies of a number of BL-induced phenomena involving changes in ion fluxes across cell membranes (e.g. Spalding 2000) suggest that cryptochromes could also be involved in light-driven redox reactions outside the nucleus.

To date, there is little known about the primary reactions of cryptochromes. Autophosphorylation occurs rapidly in response to light exposure (Shalitin et al. 2003), and the prevailing interpretation of the primary light reaction is that light absorption initiates electron transport from the FAD chromophore to ATP, which is bound in an adjacent pocket (Brautigam et al. 2004), and this then facilitates phosphotransfer to residues in the C-terminal domain. This phosphorylation may be supplemented by other protein kinases and causes a change in conformation of the molecule such that the C-terminal domain becomes exposed to interaction with signalling partners, one of which is COP1 (Wang et al. 2001; Zhang et al. 2006; Lau and Deng 2012; see Chap. 14).

19.4.3 Phototropin

In etiolated seedlings, phot1 is much more abundant than phot2 and is downregulated by light, whereas phot2 levels increase (Christie and Murphy 2013). This may explain the greater photosensitivity of phot1 relative to phot2 inferred from mutant analyses (Sakai et al. 2001). Both phot1 and phot2 are predominantly associated with the plasma membrane in dark-grown epidermal and subepidermal cells of the hypocotyl and in guard cells (Sakamoto and Briggs 2002; Harada et al. 2003) and partially relocalise to the cytosol in response to light (Aihara et al. 2008; Wan et al. 2008). Localisation of phot2 to the Golgi apparatus has also been reported (Kong et al. 2006), but the significance of this is not clear. *PHOT1* gene expression shows circadian regulation in *Arabidopsis* and in several other species is strongly downregulated in response to light (Kanegae et al. 2000).

The primary structure of the phototropin C-terminal domain clearly identifies it as a classical ser/thr kinase, and single substitutions at a number of conserved residues indicate that autophosphorylation in the kinase activation loop is essential for phot function (Inoue et al. 2008a, 2011; Sullivan et al. 2010). As in the case of cryptochromes, the activity of the C-terminal domain of the photoreceptor is constrained in darkness by the light-sensing N-terminal half. In darkness the phototropin FMN chromophore is bound in a non-covalent manner in a hydrophobic pocket of the LOV domain but upon light exposure forms a covalent bond with an adjacent cysteine residue (Salomon et al. 2000). This causes a conformational change within the LOV domain, which disrupts its interaction with an adjacent alpha-helical region and releases activity of the kinase domain (Harper et al. 2003). Autophosphorylation is implicated in the binding of phototropin to several interacting proteins, and several targets of transphosphorylation have also been identified that may

variously act to modulate phototropism (Demarsy et al. 2012) or mediate phototropin control of stomatal opening (Takemiya et al. 2013).

19.5 Photoperiodism

The importance of the duration of the daily photoperiod for plant development was first noted over 90 years ago. Using changes in day length, plants can monitor the time of year and predict seasonal change in other environmental variables. A number of processes exhibit photoperiodic regulation, including the induction of flowering, the formation of storage organs such as bulbs and tubers and the onset of bud dormancy. Of these, it is the induction of flowering that has been studied most intensively. Clear differences in photoperiodic responsiveness were first documented by Garner and Allard (1920), who classified plants according to whether flowering was preferentially induced under long days (long-day plants (LDP)) or short days (short-day plants (SDP)) (Fig. 19.6). Other early observations indicated that flowering responses could be dramatically altered by low irradiances or short exposures to light. This suggested that the light served as a source of information rather than of energy and showed photoperiodism to be a truly photomorphogenic phenomenon.

19.5.1 Light and the Circadian Clock

Endogenous rhythms have been observed in plants for more than 200 years. However, the importance of an endogenous circadian rhythm for the timekeeping aspect of photoperiodism was first suggested in the 1930s by Erwin Bünning (1964). In fact, photoperiodism can be thought of as the adaptation of circadian timekeeping to the measurement of day length. As such it must involve interaction of light signalling ("input") and specific flower induction ("output") pathways with a circadian oscillator or "clock". One characteristic feature of circadian rhythms is that they show a free-running period that is close to but not exactly 24 h. However, under daily light/dark (L/D) cycles, the rhythmic outputs become synchronised or *entrained* to a period of 24 h exactly.

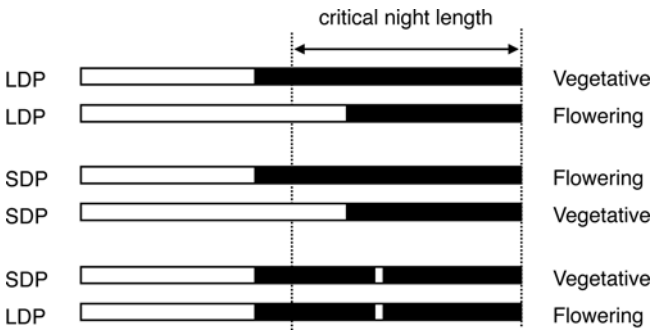

Fig. 19.6 Summary of differences in flowering responses of short day plants (*SDP*) and long-day plants (*LDP*). Open and filled bars represent light and dark periods, respectively

There are generally considered to be two basic models for the way in which light might interact with the clock (Thomas and Vince-Prue 1997). In the *internal coincidence* model, photoperiodic induction results from the increasing overlap in phase of two distinct circadian output rhythms. Light interacts with the induction process solely by controlling the phase and/or period (i.e. entrainment) of the two rhythms. In the *external coincidence* model, developed from ideas first proposed by Bünning, the circadian clock generates an output rhythm in light sensitivity and photoperiodic induction results from the coincidence of an inductive light signal with the light-sensitive phase of this rhythm. In this model, light has two roles: entrainment of the clock and direct interaction with downstream components necessary for the response. A third effect of light in photoperiodism may be to influence output responses directly, without the involvement of a timing component. The challenge is to understand how the plant is able to integrate these signals and generate the appropriate response.

19.5.1.1 Physiological Approaches

Detailed physiological investigations of the relationship between light and the circadian clock have been performed across a wide variety of different species, both SDP and LDP (see Thomas and Vince-Prue 1997). These studies have generated a large amount of complex and often contradictory literature. However, there is reasonable agreement on some of the more general conclusions, and these are summarised below.

Short-Day Plants

In a fixed daily cycle, it is clear that changes in day length could in theory be detected either as changes in length of the light period or of the dark period. It has been established that for many SDP it is mainly the length of the night that is measured, suggesting that processes necessary for floral induction can only take place if the night is longer than a certain *critical night length*. Interruption of an inductive long night with a short-light treatment prevents its effect and delays flowering. In many species, this night-break (NB) response is relatively sensitive and has thus been amenable to pulse experiments and a detailed photobiological analysis (Thomas and Vince-Prue 1997).

NB responses in SDP show action spectra typical of phytochrome-mediated LFR, for which R is inhibitory to flowering and subsequent FR cancels this inhibition. In this response, phytochrome in its Pfr form is clearly acting to inhibit flowering. In addition to the light quality of the NB, its timing can also be important, and several different SDP species show circadian rhythmicity in the responsiveness to

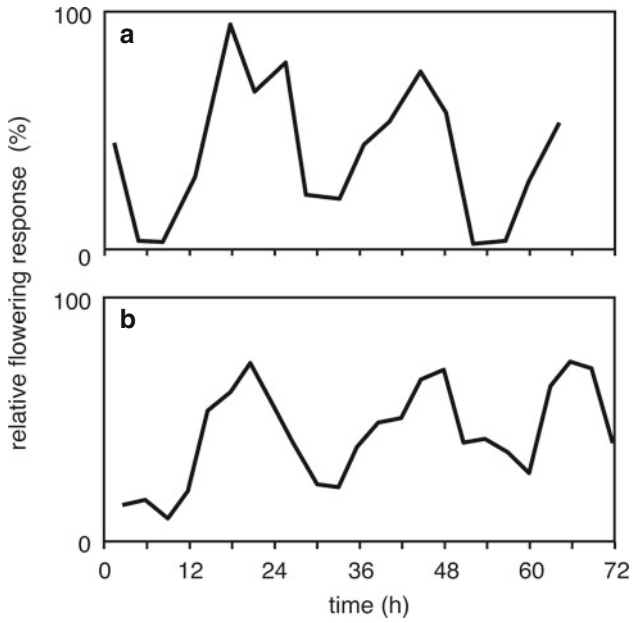

Fig. 19.7 Circadian rhythms in flowering responses to light treatments in SDP and LDP. (**a**) Rhythmic response of the SDP *Glycine max* (soybean) to a 4 h night-break with white light given at various times during an extended night following an 8-h photoperiod (redrawn from Coulter and Hamner, 1964). (**b**) Rhythmic response of the LDP *Hordeum vulgare* (barley) to 6 h of far-red light added at various times during an extended photoperiod of continuous white light (redrawn from Deitzer et al. 1982)

a NB (Fig. 19.7), consistent with the external coincidence model (Thomas and Vince-Prue 1997). Other light treatments can reset the phase of this rhythm. In some cases, the phase-setting effects of light were shown to occur independently of effects on flower induction, and R was also the most effective wavelength for inducing phase shifts. Phase shifting has generally been found to require longer exposures to light than the NB response. With even longer periods of light exposure (>6 h), the phase of the rhythm is no longer shifted but suspended and only released approximately 9 h after transfer to darkness (Thomas and Vince-Prue 1997).

Other studies have shown that in addition to the strong inhibitory effect of R shown in the NB response, FR is also effective for inhibition of flowering when given at the end of the day or early in the dark period. This clearly suggests the action of a second phytochrome, which promotes flowering in its Pfr form. This response does not affect the timing of NB sensitivity.

Long-Day Plants

Until recently, less was known about light requirements in LDP photoperiodism. As for SDP, light reactions governing flowering in LDP occur in both light and dark periods, although one or the other may predominate in any one species. The concept of a critical night length is again relevant, but for LDP, nights must be shorter than the critical length for plants to flower. In some LDP, R NB is effective for promotion of flowering. Their effectiveness varies during the night, and the response can be partially reversed by FR. However, unlike in SDP, a clear rhythmicity in responsiveness is not observed, and in general, longer periods of light are required to elicit a response (Thomas and Vince-Prue 1997).

Light reactions during the photoperiod have also been demonstrated in LDP. For example, FR added to a photoperiod of R or white light (WL) can promote flowering, with rhythmic variation in effectiveness (Fig. 19.7). Although phase-shifting experiments are much more difficult to perform in LDP and less conclusive, light-induced changes in phase of the rhythm of FR responsiveness have been reported (e.g. Deitzer et al. 1982).

Photoperiodic responses in LDP have more often been investigated using extensions of a short, non-inductive photoperiod. Action spectra for the promotion of flowering by photoperiod extensions most commonly show peaks at around 710–720 nm, well above the absorbance peak of Pr and clearly below that of Pfr (Thomas and Vince-Prue 1997). This peak is similar to that seen for the FR-HIR in seedling de-etiolation, suggesting the involvement of phyA. However, in other species, action spectra with peaks in both R and FR have also been reported (Carr-Smith et al. 1989), indicating that a second phytochrome is probably involved (Fig. 19.2). In some species, notably crucifers, BL is also effective as a day extension.

19.5.1.2 Genetic Approaches

The most detailed understanding of photoperiod response has come from studies in *Arabidopsis* (a LDP) and rice (a SDP). A number of flowering mutants or genetic variants have also been characterised in other photoperiodic species, including the LDP wheat, barley and garden pea and the SDP soybean and potato. Not surprisingly, studies of photoperiod response mutants and other genetic variants have identified photoreceptor, light signalling and circadian clock-related genes, as well as a number of other genes that integrate the light and clock inputs through output pathways for photoperiodic flower induction. Molecular and physiological analyses of these mutants are providing invaluable information about molecular components important for photoperiodic responsiveness.

Photoreceptor Mutants

Early flowering is also a well-known feature of shade-avoidance responses, suggesting that low R:FR acts to deactivate a phytochrome normally acting to inhibit flowering under high R:FR. Mutants for *phyB*-like genes in both SDP and LDP species show early flowering under both SD and LD, suggesting that these photoreceptors confer general inhibition of flowering in their Pfr form (Devlin et al. 1998,

1999; Weller et al. 2001a; Takano et al. 2005). The fact that relatively long periods of light are necessary for promotion of flowering in LDP, and the similarity of action spectra for this promotion to that seen for the FR-HIR in seedling de-etiolation, has for some time suggested that phyA might have a significant flower-promoting role in LDP. This has been confirmed in *phyA* mutants of *Arabidopsis* and pea (Weller et al. 2001a; Yanovsky and Kay 2002). In the SDP rice and soybean, phyA mutants instead confer early flowering (Takano et al. 2005; Liu et al. 2008).

As a generalisation, it thus appears that phyA is associated with photoperiod sensing and has opposite effects in SDP and LDP. In contrast, phyB acts to inhibit flowering in both LDP and SDP and under natural conditions is not directly involved in time measurement, with a role instead in sensing shade.

In *Arabidopsis*, an important role in the photoperiodic control of flowering has also been demonstrated for the cryptochrome photoreceptor family. Cry2, despite a relatively minor effect on seedling photomorphogenic responses, has a strong promotive effect on flowering under LD (Guo et al. 1998) that is dependent on the activation of phyB (Mockler et al. 2003). This suggests that the perception of day length has become the dominant function of this photoreceptor in *Arabidopsis*. However, in general, relatively few species show strong control of flowering by BL, and the importance of cry2 in photoperiodism may not be widespread.

Finally, the ZTL/FKF1 photoreceptors are also intimately involved in photoperiod sensing through light-dependent regulation of core circadian clock and output components (see below). Although this mechanism has primarily been elucidated in *Arabidopsis*, it seems likely to be conserved, and recent evidence in potato does point to a conserved role for FKF1 in photoperiod sensing (Kloosterman et al. 2013).

Photoreceptor Mutants and the Circadian Rhythm

Studies of circadian clock properties in photoreceptor mutants have shown that multiple photoreceptors contribute to the control the circadian period in a manner that closely parallels their roles in the control of de-etiolation. In *Arabidopsis*, phyB-type phytochromes are responsible for period shortening under high-irradiance R, while phyA acts under low-irradiance R and BL. Cry1 and cry2 act redundantly to shorten the circadian period under BL across a wide irradiance range (Somers et al. 1998). These results suggest that all of these photoreceptors may have the ability to contribute to entrainment of the clock under certain circumstances. However, the significance of this for plants growing under high WL irradiances is unclear. Under such conditions, phyB and cry1 would be expected to be the predominant photoreceptors controlling clock period, although a quadruple mutant lacking phyA, phyB, cry1 and cry2 can entrain normally to WL/D cycles (Yanovsky et al. 2000a).

Circadian Rhythm Mutants

Numerous genes essential for correct maintenance of circadian rhythms under light/dark cycles have now been identified in *Arabidopsis* (Nagel and Kay 2012), and many of these were first isolated in mutant screens for altered flowering time, emphasising the importance of normal circadian regulation for photoperiodism. The key feature of these genes is that they affect multiple clock outputs, including rhythmic control of gene expression and leaf movement.

The *Arabidopsis* circadian clock was initially envisaged as a simple transcriptional feedback loop involving three components: the closely related myb transcription factors *LHY* and *CCA1* and the pseudo-response regulator (PRR) homologue *TOC1* (Alabadi et al. 2002; Mizoguchi et al. 2002). Other genes have subsequently been identified that are also necessary for circadian rhythmicity under constant conditions, including *LUX*, *GI*, *ELF3*, *ELF4* and other *PRR* genes (e.g. Park et al. 1999; Fowler et al. 1999; Hazen et al. 2005; Farré et al. 2005; Nakamichi et al. 2005; McWatters et al. 2000). Inclusion of these genes has necessitated a gradual shift to a more complex model involving multiple interlocking negative feedback loops (Nagel and Kay 2012) and multiple points for light input. Interestingly these components have also been identified in other species by virtue of their effects on photoperiod response (Turner et al. 2005; Hecht et al. 2007; Liew et al. 2009; Watanabe et al. 2011; Faure et al. 2012; Matsubara et al. 2012; Weller et al. 2012).

As described above, light influences the clock in a number of different ways. Some of the mechanisms by which this occurs are now known. For example, the *LHY* and *CCA1* genes both identified as early targets of phytochrome action in transcript profiling of seedling responses to R and FR (Martinez-Garcia et al. 2000). Both genes contain G-box light-regulated elements in their promoters and are transcriptionally activated by the binding of phytochrome and PIF3. Three positive factors in light signalling, FHY3, FAR1 and HY5, bind to the promoter of *ELF4* and activate its expression (Li et al. 2011). Phytochrome-dependent light input to the clock may also occur through ELF3, a multifunctional protein with a role in control of light signalling to the clock (McWatters et al. 2000; Kolmos et al. 2011): potentially by direct physical interaction of phytochromes with ELF3 (Liu et al. 2001). In a third example, the ZTL and FKF1 blue-light receptors have been shown to regulate the stability of TOC1 by targeting it for proteasome-dependent degradation (Mas et al. 2003; Baudry et al. 2010).

19.5.2 Signalling in Photoperiodism

19.5.2.1 Long-Distance Signalling in Evocation of Photoperiod Responses

The sensitivity to flower-inducing light signals varies tremendously among different species. In many cases the site at

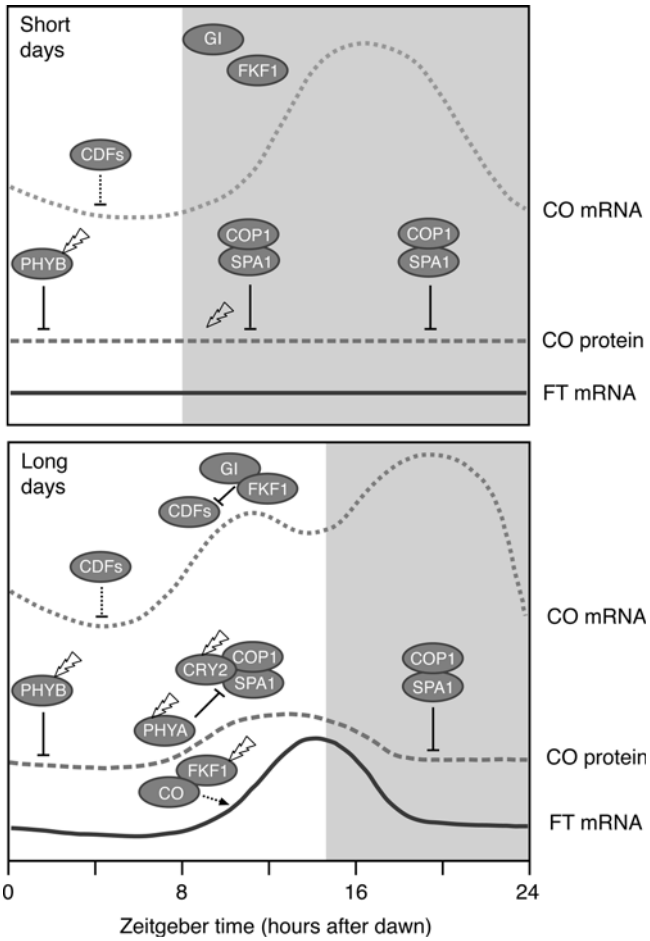

Fig. 19.8 Model depicting the molecular basis for the photoperiod response in Arabidopsis. Light influences the rhythmic induction of FT through transcriptional and post-translational regulation of CONSTANS. At least four photoreceptors play a significant role in this regulation (Redrawn from Andres and Coupland (2012))

which light is perceived can be separated from the eventual site of flower formation, indicating the existence of some form of long-distance communication. This has been studied in classic physiological experiments involving grafting, leaf-removal and differential exposure of different parts of the plant and more recently through transgenic approaches to drive gene expression in specific tissues. Experiments of this kind have provided evidence for a promoter of flowering (often called "florigen") as the main long-distance signal in the photoperiod response, although a role for inhibitory signals has not been definitively excluded.

Speculations about the nature of the floral regulators have considered known plant hormones (gibberellins, cytokinins), various metabolites (sugars, polyamines) and, more recently, specific RNA molecules and proteins. Over recent years, numerous detailed studies have identified a major role for genes in the *FT* family as integrators of multiple external and internal signals controlling flowering, including photoperiod. *FT* genes encode small proteins with homology to mammalian phosphatidylethanolamine-binding proteins, and in *Arabidopsis* and rice, it has been conclusively established that FT proteins act as florigens (Andres and Coupland 2012; Brambilla and Fornara 2013). In *Arabidopsis*, *FT* transcription is low under SD but is activated in vascular bundles under LD, and FT protein is translocated from phloem companion cells to the shoot apex, where it enters the shoot apical meristem (Corbesier et al. 2007; Jaeger and Wigge 2007; Mathieu et al. 2007). In rice, two distinct *FT*-like genes, *Hd3a* and *RFT1*, are, respectively, activated under inductive SD and non-inductive LD and encode SD- and LD-specific florigens (Tamaki et al. 2007; Komiya et al. 2009; Tsuji et al. 2011).

In both *Arabidopsis* and rice, FT proteins reaching the SAM enter the nucleus and bind to the bZIP transcription factor FD to induce expression of inflorescence identity genes in the MADS-domain family (Abe et al. 2005; Wigge et al. 2005; Taoka et al. 2011). In rice, a more detailed picture has recently emerged in which FT proteins after entering cells in the SAM first bind to 14-3-3 proteins in the cytoplasm before moving to the nucleus and forming a ternary complex with FD (Taoka et al. 2011).

19.5.2.2 Genetic Analysis of the Photoperiod Response Mechanism Measurement

Over the past 10 years, there has also been intense interest in the mechanisms by which photoperiod regulates *FT* genes and, in particular, how light and the circadian clock may interact. These mechanisms have been elucidated in two species, rice and *Arabidopsis*, and this comparison provides the first detailed molecular understanding of how plants can respond in an opposite manner to photoperiod cues. However, the taxonomic distance between these two species for the moment gives only limited insight into how these different mechanisms may have evolved.

Arabidopsis

In *Arabidopsis*, attention has focused mainly on *CONSTANS*, a nuclear protein with motifs suggestive of a role in regulation of transcription and/or protein-protein interaction. CO is a potent promoter of flowering, and its direct and major regulatory target is *FT* itself (Samach et al. 2000; Wigge et al. 2005). CO protein binds to the *FT* promoter in association with other transcription factors (Song et al. 2012a; Kumimoto et al. 2010; Tiwari et al. 2010) and is therefore likely to activate *FT* expression directly. A series of studies have provided evidence that a high level of CO protein is necessary for activation of *FT* expression and only occurs when high levels of *CO* expression coincide with light, which in turn occurs only in the afternoon of LD photoperiods, and is thought to explain the LD flowering response of *Arabidopsis* (Fig. 19.8).

It is now known that both transcriptional and post-transcriptional mechanisms contribute to the regulation of

CO protein level. *CO* transcription is controlled by the circadian clock, with a peak around dusk in LD and early in the night in SD, and consistent with this, *CO* transcript levels and/or rhythms are altered in many of the clock mutants described above. In addition, the FKF1 photoreceptor promotes *CO* expression in the afternoon through blue-light-dependent degradation of CDF proteins, which are Dof-type transcription factors that bind to the *CO* promoter and inhibit *CO* transcription (Fig. 19.8) (Imaizumi et al. 2005). Several other proteins that regulate *CO* transcription have been described, but their function is not yet well understood (Morris et al. 2010; Ito et al. 2012).

Other studies have shown that post-transcriptional regulation of CO is also important for the photoperiod response (Valverde et al. 2004; Zuo et al. 2011). In the middle of a LD photoperiod, a phyB-dependent mechanism promotes the proteasome-dependent degradation of CO protein, but in the evening this degradation is opposed by light through the action of phyA and cry2, stabilising CO and allowing the activation of *FT* (Fig. 19.8). While the mechanism by which phytochromes regulate CO stability is not yet clear, two mechanisms for BL-dependent stabilisation of CO have been outlined. Cry2 antagonises the dark-dependent degradation of CO by the COP1/SPA E3 ubiquitin ligase complex (Zuo et al. 2011, Chap. 14), while the FKF1 photoreceptor stabilises CO through a direct interaction (Song et al. 2012b). As both FKF1 and CRY2 proteins are most abundant in the afternoon under LD, both of these mechanisms contribute to maintaining a high level of CO protein specifically under LD.

The photoperiod response in *Arabidopsis* therefore depends on circadian regulation of CO expression, and on complex interactions between multiple photoreceptor inputs, that act to entrain the circadian clock (phyA, phyB, cry1, cry2), to otherwise regulate clock components (ZTL), to activate CO transcription (FKF1) and to regulate CO protein stability (phyA, phyB, cry2, FKF1).

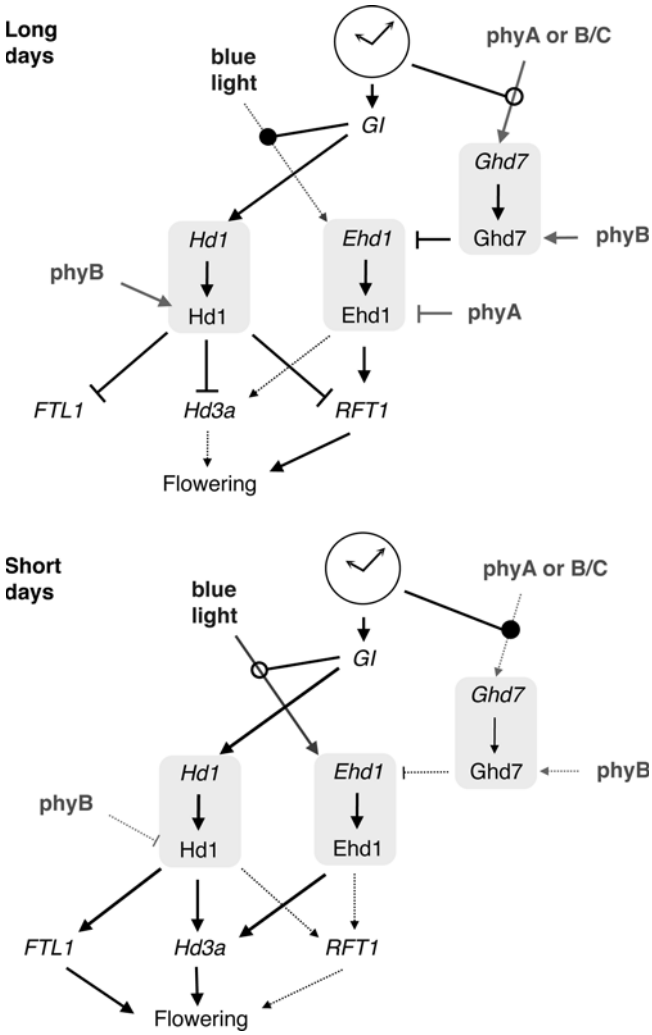

Fig. 19.9 Genetic model depicting the network controlling photoperiod-responsive flowering in rice (Redrawn from Itoh and Izawa 2013; Brambilla and Fornara 2013). Weak and strong effects are indicated by dashed and solid lines respectively. Circles indicate gating of light signals by the circadian clock

Rice

In rice, the *CO*-like gene *Hd1* has also been shown to be important for photoperiod responsiveness. However, in contrast to *Arabidopsis* CO, Hd1 has a dual role, contributing to upregulation of *Hd3a* and induction of flowering under SD but also acting to repress *Hd3a* and inhibit flowering under non-inductive LD (Hayama et al. 2002). *Hd1* expression shows a diurnal expression rhythm, but in contrast to *Arabidopsis CO*, the coincidence of light and *Hd1* expression that occurs under LD represses rather than promotes flowering (Fig. 19.9). *Hd1* expression during the light phase in SD can be increased, and flowering delayed by overexpression of the rice *GI* ortholog (Hayama et al. 2003; Ishikawa et al. 2011), suggesting a conserved role for *GI* and clock regulation of *Hd1*. Interestingly, Hd1 requires phyB to inhibit flowering, but the nature of this interaction is not yet clear (Ishikawa et al. 2011).

In addition to this *Hd1*-dependent pathway, the photoperiod response in rice also involves an Hd1-independent pathway. This pathway features two other genes not conserved in *Arabidopsis*: *Ehd1*, a B-type response regulator that promotes flowering and *Hd3a*/*RFT1* expression in SD, and *Ghd7*, a CCT-domain protein that represses *Ehd1* expression in LD (Fig. 19.9). In SD, *Ehd1* is upregulated in the morning through a BL-dependent mechanism involving *GI* (Itoh et al. 2010), whereas in LD, *Ehd1* is repressed in the morning by phytochrome-dependent induction of *Ghd7*. A shift in the sensitive phase for phytochrome induction of *Ghd7* from morning in LD to midnight in SD explains both the SD-specific *Ehd1* expression and the ability of a short night break to repress this expression and promote flowering (Itoh et al. 2013).

The photoperiodic control of flowering in rice thus essentially consists of two linked external coincidence mechanisms

and at least two photoreceptor systems. Given the importance of diurnal expression rhythms in these mechanisms, it is not surprising that roles for other clock components such as *ELF3* are also beginning to emerge (Saito et al. 2012).

It is clear that powerful molecular genetic studies combined with careful physiological studies have enabled substantial recent progress in answering several of the long-standing questions in higher plant photoperiodism: the molecular mechanisms underlying the photoperiod response, the basis for the difference between LDP and SDP responses, and nature of mobile signalling in photoperiodism. We can look forward to continued rapid progress on all three fronts.

19.6 Photomorphogenesis and Phototropism in the Natural Environment

In discussing the significance of photomorphogenesis in the natural environment, several things must be kept in mind. We need to consider the changes that may occur in the properties of light reaching the plant, the kind of information plants may extract from these changes, and the way in which this information might be converted into an appropriate developmental response.

Most plants have adopted a sedentary habit and are therefore committed to adapt to changes in their environment by developmental plasticity. Natural selection is therefore likely to have favoured modifications of development that maximise energy capture or that improve the ability of the plant to resist detrimental effects of light. In addition, correlation between changes in light environment and other environmental variables such as cold or drought are also likely to have favoured crosstalk between light signalling and other signalling pathways and the exploitation of light information as a predictive signal. Conditions of continuous selection would also result in pressure to extract increasing amounts of information from light, through an ability to monitor more subtle changes. This in turn could conceivably have supported the evolution of multiple photoreceptors with diverse light-sensing properties.

Speculations about the importance of photoreceptors in the natural environment have been largely based on studies of mutants and transgenic lines grown as single plants in controlled-environment conditions, combined with an intuitive appreciation for the developmental predicament of the plant. However, they have recently begun to receive solid support from experiments conducted under natural and/or competitive conditions (Ballare 1999).

19.6.1 Improving Energy Capture

In general, higher plants have two strategies to increase their capture of energy. They can either gain access to more energy by extending their growth into areas of stronger light, or they can more efficiently capture the energy already reaching them.

Measurements of light quality in the natural environment have shown that changes in the amount of light due to cloud cover or the time of day are accompanied by relatively small changes in its spectral distribution (Franklin and Whitelam 2005). In contrast, chlorophyll-containing tissues absorb efficiently in the R and B region of the spectrum but transmit and reflect a substantial proportion of light in the FR waveband. Thus, the presence of plants affects the local light environment by causing a measurable decrease in the ratio of R to FR light energy. This may occur by the filtering out of R and/or by increased lateral reflection of FR. However, it is particularly significant that increases in lateral reflection of FR from neighbouring plants occur prior to any reduction in the amount of photosynthetically active R and BL wavelengths (Ballare et al. 1990). An increase in the amount of FR is thus an unambiguous signal to the plant that potential competitors are growing nearby. Where this signal is unidirectional, the appropriate response of the plant is obviously to redirect its growth away from the other plants. In a denser population, the gradient in FR will not be as great, and the response may also include an increase in overall growth rate. Although the horizontal and lateral components of the response to shading are often treated separately as phototropism and shade avoidance, it is more appropriate to consider both responses as aspects of a strategy in which the plant is actively "foraging" for light (Ballare et al. 1997).

A negative phototropism in response to increases in lateral FR reflected from neighbouring plants has been demonstrated in cucumber. This response is completely lacking in a phyB-deficient mutant, indicating that in addition to its role in shade avoidance, phyB is also important for the detection of non-shading neighbours (Ballare et al. 1992). The existence of additional phyB-type phytochromes with differing roles at different stages of development suggests that plants are still evolving to fine-tune their capacity for shade avoidance and neighbour detection and emphasises the importance of these responses for the plant.

As the canopy closes or population density increases, increases in the leaf area index also occur, and as a result the light energy in the R and BL wavebands decreases. Under such circumstances, a plant may also be exposed to a lateral gradient in BL and show a positive phototropic response. The phyB-deficient mutant of cucumber retains the ability to respond to such a gradient (Ballare et al. 1991), implying the action of a BL photoreceptor, which is most probably phototropin, under conditions of deep shade, where it is likely that the observed growth responses result from a reduction in activity of several photoreceptors including the phyB-type phytochromes, cry1 and phototropin (Ballare 1999). Without phyA however, seedlings cannot sense the FR transmitted through the canopy and do not de-etiolate, indicating that

phyA may be essential for maintaining a degree of de-etiolation in highly competitive situations (Yanovsky et al. 1995).

Under shade conditions many plants may also increase their efficiency of light capture, by modifying various features of their photosynthetic organs. Depending on the species, this may include modification of light harvesting complex composition, chloroplast organisation, orientation or position and leaf shape, size or thickness (Terashima and Hikosaka 1995; Vogelmann et al. 1996; Mullineaux and Karpinski 2002). Acclimation to shade is therefore a complex phenomenon but does at least in some cases involve responses that can be considered photomorphogenic such as leaf reorientation (Inoue et al. 2008b). The fact that phototropins control chloroplast orientation and stomatal aperture also clearly implies an important role in the regulation of photosynthesis (Boccalandro et al. 2012). However, in general the contribution of photomorphogenic photoreceptors to photosynthetic acclimation is not yet well understood.

19.6.2 Light and the Seed Habit

Other adaptive responses to light seem to have arisen with the development of the seed habit. Control of seed germination is important to allow seedling to develop in favourable light environment. Particularly for small-seeded species germinating under the soil surface, seedlings must be able to emerge into full light before the seed energy reserves are exhausted. The extremely low fluences of light needed to induce germination of some species can be understood as a signal to the seed that it is near the soil surface before making the irreversible commitment to germinate. In other species, the higher light requirement and R/FR reversibility of germination may reflect a strategy to preferentially promote germination under gaps in the canopy (Casal and Sanchez 1998).

Investment of energy in the seed has allowed a period of time in which seedlings can develop independently of the need to photosynthesise. In effect this provides a longer period of time over which the seedling can integrate information about its light environment and adjust its development appropriately. In combination with the seed habit, many species have developed a growth strategy of etiolation in which they are able to suppress normal light-regulated leaf development and elongate rapidly growing in darkness. This could conceivably have been favoured in evolution because it increases the efficiency with which the plant uses stored seed reserves but also because its rapid emergence into the light after germination will maximise competitive advantage. However, along with this strategy comes the need for anticipation of imminent emergence into the light environment, and a rapid response immediately following emergence. PhyA does appear to serve this purpose under natural conditions, and it is conceivable that some of the distinct features of phyA could have arisen in response to this pressure (Mathews 2006).

19.6.3 Avoidance or Survival of Unfavourable Conditions

In addition to useful light for photosynthesis, sunlight also contains potentially damaging UV wavelengths. Various phenylpropanoid pigments including sinapates and flavonoids absorb UV and reduce its damaging effects on the plant (Bieza and Lois 2001). The production of these pigments in many cases is strongly induced by light as a result of increased expression of certain genes in phenylpropanoid metabolism (Shirley 1996; Ryan et al. 2001). In many cases, this induction is strongest in young seedlings and immature leaves, which are more susceptible to UV damage.

It is also possible that light can also serve as an indirect signal of other adverse aspects of the environment. For example, the fact that in some species light can act to inhibit germination can be understood in terms of the need for a damp environment and a correlation between reduced water availability near the soil surface and increased light levels. A similar association could explain the negative phototropism of some roots, and experimental evidence supporting this has recently been reported (Galen et al. 2007). The action of phot1 allows roots near the surface to reorient and grow downwards into the soil, with consequences for the availability of water to those roots and performance under drought conditions (Galen et al. 2007).

A more complicated kind of correlative selection may underlie many seasonal responses. Factors such as temperature and water availability can clearly become limiting at certain times of year in some environments, and many plants are able to avoid the deleterious effects of these seasonal extremes through suppression of normal growth and the adoption of various survival strategies. These include seed and bud dormancy, formation of storage organs and initiation of flowering, which can be timed so as to allow the reproductive cycle to be completed before unfavourable conditions return. Changes in limiting factors of temperature and water availability can act directly as triggers for these changes (as seen in cold temperature requirements for germination or flowering). However, although seasonal, these factors are also subject to irregular short-term variation, whereas change in day length is a much more constant and reliable indicator of season from year to year. In general, the degree of photoperiod responsiveness is an important aspect of adaptation to growth at a given latitude (Thomas and Vince-Prue 1997).

As the molecular basis for light and photoperiod responses has become better understood, increasing numbers of studies are turning towards an investigation of the ecological

significance of observed genetic variation or the genetic basis for natural variation in plant responses. Notable recent examples include demonstrations of the contribution of the phyC photoreceptor to natural variation in *Arabidopsis* flowering time (Balasubramanian et al. 2006), the role of *FT* homologues in latitudinal variation in seasonal dormancy in poplar (Böhlenius et al. 2006) and the fitness consequences of genetic variation in *Arabidopsis* circadian clock function (Michael et al. 2003).

19.7 Concluding Remarks

Considering that plants are fixed in one place and dependent on light as an energy source, it is not surprising that sophisticated mechanisms have evolved enabling them to modify their development in response to light and thus to better compete with their neighbours. Persistent selective pressures for extracting more subtle information from the light environment have favoured the evolution of several distinct photoreceptor systems. For the most part, these systems act synergistically, increasing the general sensitivity of the plant to light. However, some photoreceptors have developed discrete light-sensing abilities, which may be linked to specific physiological and ecological roles.

The past 30 years have seen major advances in our understanding of the photoreceptors involved in photomorphogenesis and the definitive identification of some of the molecular and cellular processes required for expression of light responses. We still do not fully understand the complexities of signal transduction or the network of interactions between light, plant hormones and other factors. Nevertheless, the genetic and molecular tools are now available to enable a thorough analysis of these aspects of photomorphogenesis over the coming years. Greater understanding of photomorphogenesis will bring an increased ability to manipulate plant light responses for practical purposes, such as in the control of density-dependent shading, flowering and yield in horticultural and crop plants. It will also help us to better understand the origins and adaptive significance of natural variation in growth habit and flowering phenology.

References

Abe M, Kobayashi Y, Yamamoto S, Daimon Y, Yamaguchi A, Ikeda Y, Ichinoki H, Notaguchi M, Goto K, Araki T (2005) FD, a bZIP protein mediating signals from the floral pathway integrator FT at the shoot apex. Science 309:1052–1056

Ahmad M, Cashmore AR (1994) HY4 gene of Arabidopsis thaliana encodes a protein with characteristics of a blue-light photoreceptor. Nature 366:162–166

Ahmad M, Jarillo JA, Smirnova O, Cashmore AR (1998) The CRY1 blue light photoreceptor of Arabidopsis interacts with phytochrome A in vitro. Mol Cell 1:939–948

Aihara Y, Tabata R, Suzuki T, Shimazaki K, Nagatani A (2008) Molecular basis of the functional specificities of phototropin 1 and 2. Plant J 56:364–375

Alabadí D, Yanovsky MJ, Mas P, Harmer SL, Kay SA (2002) Critical role for CCA1 and LHY in maintaining circadian rhythmicity in Arabidopsis. Curr Biol 12:757–761

Andrés F, Coupland G (2012) The genetic basis of flowering responses to seasonal cues. Nat Rev Genet 13:627–639

Balasubramanian S, Sureshkumar S, Agrawal M, Michael TP, Wessinger C, Maloof JN, Clark R, Warthmann N, Chory J, Weigel D (2006) The PHYTOCHROME C photoreceptor gene mediates natural variation in flowering and growth responses of Arabidopsis thaliana. Nat Genet 38:711–715

Ballare CL, Casal JJ, Kendrick RE (1991) Responses of light-grown wild-type and long-hypocotyl mutant cucumber seedlings to natural and simulated shade light. Photochem Photobiol 54:819–826

Ballare CL (1999) Keeping up with the neighbours: phytochrome sensing and other signalling mechanisms. Trends Plant Sci 4:97–102

Ballare CL, Scopel AL, Sanchez RA (1990) Far-red irradiation reflected from adjacent leaves: an early signal of competition in plant canopies. Science 247:329–332

Ballare CL, Scopel AL, Sanchez RA (1997) Foraging for light – photosensory ecology and agricultural implications. Plant Cell Environ 20:820–825

Ballare CL, Scopel AL, Radosevich SR, Kendrick RE (1992) Phytochrome-mediated phototropism in de-etiolated seedlings. Occurrence and ecological significance. Plant Physiol 100:170–177

Baskin TI, Iino M (1987) An action spectrum in the blue and ultraviolet for phototropism in alfalfa. Photochem Photobiol 46:127–136

Baudry A, Ito S, Song YH, Strait AA, Kiba T, Lu S, Henriques R, Pruneda-Paz JL, Chua NH, Tobin EM, Kay SA, Imaizumi T (2010) F-box proteins FKF1 and LKP2 act in concert with ZEITLUPE to control Arabidopsis clock progression. Plant Cell 22:606–622

Bieza K, Lois R (2001) An Arabidopsis mutant tolerant to lethal ultraviolet-B levels shows contsitutively elevated accumulation of flavonoids and other phenolics. Plant Physiol 126:1105–1115

Boccalandro HE, Giordano CV, Ploschuk EL, Piccoli PN, Bottini R, Casal JJ (2012) Phototropins but not cryptochromes mediate the blue light-specific promotion of stomatal conductance, while both enhance photosynthesis and transpiration under full sunlight. Plant Physiol 158:1475–1484

Böhlenius H, Huang T, Charbonnel-Campaa L, Brunner AM, Jansson S, Strauss SH, Nilsson O (2006) CO/FT regulatory module controls timing of flowering and seasonal growth cessation in trees. Science 312:1040–1043

Brambilla V, Fornara F (2013) Molecular control of flowering in response to day length in rice. J Integr Plant Biol 55:410–418

Brautigam CA, Smith BS, Ma Z, Palnitkar M, Tomchick DR, Machius M, Deisenhofer J (2004) Structure of the photolyase-like domain of cryptochrome 1 from Arabidopsis thaliana. Proc Natl Acad Sci U S A 101:12142–12147

Briggs WR (2006) Blue/UV-A photoreceptors: historical overview. In: Schäfer E, Nagy F (eds) Photomorphogenesis in plants and bacteria, 3rd edn. Springer, Dordrecht, pp 171–198

Bünning E (1964) The physiological clock. Springer, Berlin

Butler WL, Hendricks SB, Siegelman HW (1964) Action spectra of phytochrome in vitro. Photochem Photobiol 3:521–528

Carr-Smith HD, Thomas B, Johnson CB (1989) An action spectrum for the effect of continuous light on flowering in wheat. Planta 179:428–432

Casal JJ (2006) The photoreceptor interaction network. In: Schäfer E, Nagy F (eds) Photomorphogenesis in plants and bacteria, 3rd edn. Springer, Dordrecht, pp 407–438. (2000)

Casal JJ (2013) Photoreceptor signaling networks in plant responses to shade. Annu Rev Plant Biol 64:403–427

Casal JJ, Sanchez RA (1998) Phytochromes and seed germination. Seed Sci Res 8:317–329

Chaves I, Pokorny R, Byrdin M, Hoang N, Ritz T, Brettel K, Essen LO, van der Horst GT, Batschauer A, Ahmad M (2011) The cryptochromes: blue light photoreceptors in plants and animals. Annu Rev Plant Biol 62:335–364

Chen F, Shi X, Chen L, Dai M, Zhou Z, Shen Y, Li J, Li G, Wei N, Deng XW (2012) Phosphorylation of FAR-RED ELONGATED HYPOCOTYL1 is a key mechanism defining signaling dynamics of phytochrome A under red and far-red light in Arabidopsis. Plant Cell 24:1907–1920

Choi G, Yi H, Lee J, Kwon YK, Soh MS, Shin B, Luka Z, Hahn TR, Song PS (1999) Phytochrome signalling is mediated through nucleoside diphosphate kinase 2. Nature 401:610–613

Christie JM, Murphy AS (2013) Shoot phototropism in higher plants: new light through old concepts. Am J Bot 100:35–46

Christie JM, Salomon M, Nozue K, Wada M, Briggs WR (1999) LOV (light, oxygen, or voltage) domains of the blue-light photoreceptor phototropin (nph1): binding sites for the chromophore flavin mononucleotide. Proc Nat Acad Sci USA 96:8779–8783

Christie JM, Arvai AS, Baxter KJ, Heilmann M, Pratt AJ, O'Hara A, Kelly SM, Hothorn M, Smith BO, Hitomi K, Jenkins GI, Getzoff ED (2012) Plant UVR8 photoreceptor senses UV-B by tryptophan-mediated disruption of cross-dimer salt bridges. Science 335:1492–1496

Colon-Carmona A, Chen DL, Yeh KC, Abel S (2000) Aux/IAA proteins are phosphorylated by phytochrome in vitro. Plant Physiol 124:1728–1738

Corbesier L, Vincent C, Jang S, Fornara F, Fan Q, Searle I, Giakountis A, Farrona S, Gissot L, Turnbull C, Coupland G (2007) FT protein movement contributes to long-distance signaling in floral induction of Arabidopsis. Science 316:1030–1033

Coulter MW, Hamner KC (1964) Photoperiodic flowering response of Biloxi soybean in 72-hour cycles. Plant Physiol 39:846–856

Davis SJ (2006) The phytochrome chromophore. In: Schäfer E, Nagy F (eds) Photomorphogenesis in plants and bacteria, 3rd edn. Springer, Dordrecht, pp 41–64

Davis SJ, Vener AV, Vierstra RD (1999) Bacteriophytochromes: phytochrome-like photoreceptors from nonphotosynthetic eubacteria. Science 286:2517–2520

DeBlasio SL, Mullen JL, Luesse DR, Hangarter RP (2003) Phytochrome modulation of blue light-induced chloroplast movements in Arabidopsis. Plant Physiol 133:1471–1479

Debrieux D, Trevisan M, Fankhauser C (2013) Conditional involvement of constitutive photomorphogenic1 in the degradation of phytochrome A. Plant Physiol 161:2136–2145

Deitzer GF, Hayes R, Jabben M (1982) Phase shift in the circadian rhythm of floral promotion by far-red light in Hordeum vulgare L. Plant Physiol 69:597–601

Demarsy E, Schepens I, Okajima K, Hersch M, Bergmann S, Christie J, Shimazaki K, Tokutomi S, Fankhauser C (2012) Phytochrome kinase substrate 4 is phosphorylated by the phototropin 1 photoreceptor. EMBO J 31:3457–3467

Devlin PF, Patel SR, Whitelam GC (1998) Phytochrome E influences internode elongation and flowering time in Arabidopsis. Plant Cell 10:1479–1488

Devlin PF, Robson PRH, Patel SR, Goosey L, Sharrock RA, Whitelam GC (1999) Phytochrome D acts in the shade-avoidance syndrome in Arabidopsis by controlling elongation growth and flowering time. Plant Physiol 119:909–915

Eichenberg K, Baurle I, Paulo N, Sharrock RA, Rudiger W, Schafer E (2000) Arabidopsis phytochromes C and E have different spectral characteristics from those of phytochromes A and B. FEBS Lett 470:107–112

Fankhauser C, Yeh KC, Lagarias JC, Zhang H, Elich TD, Chory J (1999) PKS1, a substrate phosphorylated by phytochrome that modulates light signaling in Arabidopsis. Science 284:1539–1541

Farre EM, Harmer SL, Harmon FG, Yanovsky MJ, Kay SA (2005) Overlapping and distinct roles of PRR7 and PRR9 in the Arabidopsis circadian clock. Curr Biol 15:47–54

Faure S, Turner AS, Gruszka D, Christodoulou V, Davis SJ, von Korff M, Laurie DA (2012) Mutation at the circadian clock gene EARLY MATURITY 8 adapts domesticated barley (Hordeum vulgare) to short growing seasons. Proc Natl Acad Sci U S A 109:8328–8333

Favory JJ, Stec A, Gruber H, Rizzini L, Oravecz A, Funk M, Albert A, Cloix C, Jenkins GI, Oakeley EJ, Seidlitz HK, Nagy F, Ulm R (2009) Interaction of COP1 and UVR8 regulates UV-B-induced photomorphogenesis and stress acclimation in Arabidopsis. EMBO J 28:591–601

Folta KM, Spalding EP (2001) Unexpected roles for cryptochrome 2 and phototropin revealed by high-resolution analysis of blue light-mediated hypocotyl growth inhibition. Plant J 26:471–478

Fowler S, Lee K, Onouchi H, Samach A, Richardson K, Morris B, Coupland G, Putterill J (1999) GIGANTEA: a circadian clock-controlled gene that regulates photoperiodic flowering in Arabidopsis and encodes a protein with several possible membrane-spanning domains. EMBO J 18:4679–4688

Franklin KA, Praekelt U, Stoddart WM, Billingham OE, Halliday KJ, Whitelam GC (2003) Phytochromes B, D, and E act redundantly to control multiple physiological responses in Arabidopsis. Plant Physiol 131:1340–1346

Franklin KA, Whitelam GC (2005) Phytochromes and shade-avoidance responses in plants. Ann Bot 96:169–175

Galen C, Rabenold JJ, Liscum E (2007) Functional ecology of a blue light photoreceptor: effects of phototropin-1 on root growth enhance drought tolerance in Arabidopsis thaliana. New Phytol 173:91–99

Galván-Ampudia CS, Offringa R (2007) Plant evolution: AGC kinases tell the auxin tale. Trends Plant Sci 12:541–547

Garner WW, Allard AH (1920) Effect of the relative length of day and night and other factors of the environment on growth and reproduction in plants. J Agric Res 18:553–606

Genoud T, Schweizer F, Tscheuschler A, Debrieux D, Casal JJ, Schäfer E, Hiltbrunner A, Fankhauser C (2008) FHY1 mediates nuclear import of the light-activated phytochrome A photoreceptor. PLoS Genet 4(8):e1000143. doi:10.1371/journal.pgen.1000143

Gil P, Kircher S, Adam E, Bury E, Kozma-Bognar L, Schafer E, Nagy F (2000) Photocontrol of subcellular partitioning of phytochrome-B:GFP fusion protein in tobacco seedlings. Plant J 22:135–145

Goosey L, Palecanda L, Sharrock RA (1997) Differential patterns of expression of the arabidopsis PHYB, PHYD, and PHYE phytochrome genes. Plant Physiol 115:959–969

Guo HW, Yang WY, Mockler TC, Lin CT (1998) Regulation of flowering time by Arabidopsis photoreceptors. Science 279:1360–1363

Han YJ, Kim HS, Kim YM, Shin AY, Lee SS, Bhoo SH, Song PS, Kim JI (2010) Functional characterization of phytochrome autophosphorylation in plant light signaling. Plant Cell Physiol 51: 596–609

Harada A, Sakai T, Okada K (2003) Phot1 and phot2 mediate blue light-induced transient increases in cytosolic Ca^{2+} differently in Arabidopsis leaves. Proc Natl Acad Sci U S A 100:8583–8588

Harper SM, Neil LC, Gardner KH (2003) Structural basis of a phototropin light switch. Science 301:1541–1544

Hartmann KM (1967) Ein Wirkungspectrum der Photomorphogenese unter Hochenergiebe-dingungen und seine Interpretation auf der Basis der Phytochroms (Hypokotylwachstumshemmung bei *Lactuca sativa* L.). Z Naturforsch 22b:1172–1175

Hauser BA, Pratt LH, Cordonnier-Pratt MM (1997) Absolute quantification of five phytochrome transcripts in seedlings and mature plants of tomato (Solanum lycopersicum L.). Planta 201:379–387

Hayama R, Yokoi S, Tamaki S, Yano M, Shimamoto K (2003) Adaptation of photoperiodic control pathways produces short-day flowering in rice. Nature 422:719–722

Hazen SP, Schultz TF, Pruneda-Paz JL, Borevitz JO, Ecker JR, Kay SA (2005) LUX ARRHYTHMO encodes a Myb domain protein essential for circadian rhythms. Proc Natl Acad Sci U S A 102: 10387–10392

Hecht V, Knowles CL, Vander Schoor JK, Liew LC, Jones SE, Lambert MJ, Weller JL (2007) Pea LATE BLOOMER1 is a GIGANTEA ortholog with roles in photoperiodic flowering, deetiolation, and transcriptional regulation of circadian clock gene homologs. Plant Physiol 144:648–661

Hennig L (2006) Phytochrome degradation and dark reversion. In: Schäfer E, Nagy F (eds) Photomorphogenesis in plants and bacteria, 3rd edn. Springer, Dordrecht, pp 131–154

Hershey HP, Colbert JT, Lissemore JL, Barker RF, Quail PH (1984) Molecular cloning of cDNA for Avena phytochrome. Proc Natl Acad Sci U S A 81:2332–2336

Hiltbrunner A, Tscheuschler A, Viczián A, Kunkel T, Kircher S, Schäfer E (2006) FHY1 and FHL act together to mediate nuclear accumulation of the phytochrome A photoreceptor. Plant Cell Physiol 47:1023–1034

Hirose F, Shinomura T, Tanabata T, Shimada H, Takano M (2006) Involvement of rice cryptochromes in de-etiolation responses and flowering. Plant Cell Physiol 47:915–925

Hisada A, Hanzawa H, Weller JL, Nagatani A, Reid JB, Furuya M (2000) Light-induced nuclear translocation of endogenous pea phytochrome A visualized by immunocytochemical procedures. Plant Cell 12:1063–1078

Howe GT, Bucciaglia PA, Hackett WP, Furnier GR, Cordonnier-Pratt MM, Gardner G (1998) Evidence that the phytochrome gene family in black cottonwood has one PHYA locus and two PHYB loci but lacks members of the PHYC/F and PHYE subfamilies. Mol Biol Evol 15:160–175

Huala E, Oeller PW, Liscum E, Han IS, Larsen E, Briggs WR (1997) Arabidopsis NPH1 – a protein kinase with a putative redox-sensing domain. Science 278:2120–2123

Hughes J (2013) Phytochrome cytoplasmic signaling. Annu Rev Plant Biol 64:377–402

Imaizumi T, Schultz TF, Harmon FG, Ho LA, Kay SA (2005) FKF1 F-box protein mediates cyclic degradation of a repressor of CONSTANS in Arabidopsis. Science 309:293–297

Inoue S, Kinoshita T, Matsumoto M, Nakayama KI, Doi M, Shimazaki K (2008a) Blue light-induced autophosphorylation of phototropin is a primary step for signalling. Proc Natl Acad Sci U S A 105:5626–5631

Inoue S, Kinoshita T, Takemiya A, Doi M, Shimazaki K (2008b) Leaf positioning of Arabidopsis in response to blue light. Mol Plant 1:15–26

Inoue S, Matsushita T, Tomokiyo Y, Matsumoto M, Nakayama KI, Kinoshita T, Shimazaki K (2011) Functional analyses of the activation loop of phototropin2 in Arabidopsis. Plant Physiol 156:117–128

Ishikawa R, Aoki M, Kurotani K, Yokoi S, Shinomura T, Takano M, Shimamoto K (2011) Phytochrome B regulates heading date 1 (Hd1)-mediated expression of rice florigen Hd3a and critical day length in rice. Mol Genet Genomics 285:461–470

Ito S, Song YH, Josephson-Day AR, Miller RJ, Breton G, Olmstead RG, Imaizumi T (2012) FLOWERING BHLH transcriptional activators control expression of the photoperiodic flowering regulator CONSTANS in Arabidopsis. Proc Natl Acad Sci U S A 109:3582–3587

Itoh H, Izawa T (2013) The coincidence of critical day length recognition for florigen gene expression and floral transition under long-day conditions in rice. Mol Plant 6:635–649

Itoh H, Nonoue Y, Yano M, Izawa T (2010) A pair of floral regulators sets critical day length for Hd3a florigen expression in rice. Nat Genet 42:635–638

Jaeger KE, Wigge PA (2007) FT protein acts as a long-range signal in Arabidopsis. Curr Biol 17:1050–1054

Kagawa T, Sakai T, Suetsugu N, Oikawa K, Ishiguro S, Kato T, Tabata S, Okada K, Wada M (2001) Arabidopsis NPL1: a phototropin homolog controlling the chloroplast high-light avoidance response. Science 291:2138–2141

Kaiserli E, Jenkins GI (2007) UV-B promotes rapid nuclear translocation of the Arabidopsis UV-B specific signaling component UVR8 and activates its function in the nucleus. Plant Cell 19:2662–2673

Kanegae H, Tahir M, Savazzini F, Yamamoto K, Yano M, Sasaki T, Kanegae T, Wada M, Takano M (2000) Rice NPH1 homologues, OsNPN1a and OsNPN1b, are differently photoregulated. Plant Cell Physiol 41:415–423

Karniol B, Wagner JR, Walker JM, Vierstra RD (2005) Phylogenetic analysis of the phytochrome superfamily reveals distinct microbial subfamilies of photoreceptors. Biochem J 392:103–116

Kehoe DM, Grossman AR (1996) Similarity of a chromatic adaptation sensor to phytochrome and ethylene receptors. Science 273: 1409–1412

Keller MM, Jaillais Y, Pedmale UV, Moreno JE, Chory J, Ballaré CL (2011) Cryptochrome 1 and phytochrome B control shade-avoidance responses in Arabidopsis via partially independent hormonal cascades. Plant J 67:195–207

Kerckhoffs LHJ, Schreuder MEL, van Tuinen A, Koornneef M, Kendrick RE (1997) Phytochrome control of anthocyanin biosynthesis in tomato seedlings – analysis using photomorphogenic mutants. Photochem Photobiol 65:374–381

Kim BC, Tennessen DJ, Last RL (1998) UV-B-induced photomorphogenesis in Arabidopsis thaliana. Plant J 15:667–674

Kinoshita T, Doi M, Suetsugu N, Kagawa T, Wada M, Shimazaki K (2001) phot1 and phot2 mediate blue light regulation of stomatal opening. Nature 414:656–660

Kircher S, Gil P, Kozma-Bognar L, Fejes E, Speth V, Husselstein-Muller T, Bauer D, Adam E, Schafer E, Nagy F (2002) Nucleocytoplasmic partitioning of the plant photoreceptors phytochrome A, B, C, D, and E is regulated differentially by light and exhibits a diurnal rhythm. Plant Cell 14:1541–1555

Kircher S, Terecskei K, Wolf I, Sipos M, Adam E (2011) Phytochrome A-specific signaling in Arabidopsis thaliana. Plant Signal Behav 6:1714–1719

Kircher S, Kozma-Bognar L, Kim L, Adam E, Harter K, Schafer E, Nagy F (1999) Light quality-dependent nuclear import of the plant photoreceptors phytochrome A and B. Plant Cell 11:1445–1456

Kleiner O, Kircher S, Harter K, Batschauer A (1999) Nuclear localization of the Arabidopsis blue light receptor cryptochrome 2. Plant J 19:289–296

Kliebenstein DJ, Lim JE, Landry LG, Last RL (2002) Arabidopsis UVR8 regulates ultraviolet-B signal transduction and tolerance and contains sequence similarity to human regulator of chromatin condensation 1. Plant Physiol 130:234–243

Kloosterman B, Abelenda JA, Gomez Mdel M, Oortwijn M, de Boer JM, Kowitwanich K, Horvath BM, van Eck HJ, Smaczniak C, Prat S, Visser RG, Bachem CW (2013) Naturally occurring allele diversity allows potato cultivation in northern latitudes. Nature 495:246–250

Kohchi T, Mukougawa K, Frankenberg N, Masuda M, Yokota A, Lagarias JC (2001) The Arabidopsis HY2 gene encodes phytochromobilin synthase, a ferredoxin-dependent biliverdin reductase. Plant Cell 13:425–436

Kolmos E, Herrero E, Bujdoso N, Millar AJ, Tóth R, Gyula P, Nagy F, Davis SJ (2011) A reduced-function allele reveals that EARLY FLOWERING3 repressive action on the circadian clock is modulated by phytochrome signals in Arabidopsis. Plant Cell 23:3230–3246

Komiya R, Yokoi S, Shimamoto K (2009) A gene network for long-day flowering activates RFT1 encoding a mobile flowering signal in rice. Development 136:3443–3450

Kong SG, Suzuki T, Tamura K, Mochizuki N, Hara-Nishimura I, Nagatani A (2006) Blue light-induced association of phototropin 2 with the Golgi apparatus. Plant J 45:994–1005

Kumimoto RW, Zhang Y, Siefers N, Holt BF 3rd (2010) NF-YC3, NF-YC4 and NF-YC9 are required for CONSTANS-mediated,

photoperiod-dependent flowering in Arabidopsis thaliana. Plant J 63:379–391
Lariguet P, Fankhauser C (2004) Hypocotyl growth orientation in blue light is determined by phytochrome A inhibition of gravitropism and phototropin promotion of phototropism. Plant J 40:826–834
Lau OS, Deng XW (2012) The photomorphogenic repressors COP1 and DET1: 20 years later. Trends Plant Sci 17:584–593
Leivar P, Quail PH (2011) PIFs: pivotal components in a cellular signaling hub. Trends Plant Sci 16:19–28
Li G, Siddiqui H, Teng Y, Lin R, Wan XY, Li J, Lau OS, Ouyang X, Dai M, Wan J, Devlin PF, Deng XW, Wang H (2011) Coordinated transcriptional regulation underlying the circadian clock in Arabidopsis. Nat Cell Biol 13:616–622
Liew LC, Hecht V, Laurie RE, Knowles CL, Vander Schoor JK, Macknight RC, Weller JL (2009) DIE NEUTRALIS and LATE BLOOMER 1 contribute to regulation of the pea circadian clock. Plant Cell 10:3198–3211
Lin C, Robertson DE, Ahmad M, Raibekas AA, Jorns MS, Dutton PL, Cashmore AR (1995) Association of flavin adenine dinucleotide with the Arabidopsis blue light receptor cry1. Science 269:968–970
Lin C, Yang HY, Guo HW, Mockler T, Chen J, Cashmore AR (1998) Enhancement of blue-light sensitivity of Arabidopsis seedlings by a blue light receptor cryptochrome 2. Proc Natl Acad Sci U S A 95:2686–2690
Liscum E, Briggs WR (1995) Mutations in the nph1 locus of Arabidopsis disrupt the perception of phototropic stimuli. Plant Cell 7:473–485
Liscum E, Stowe-Evans EL (2000) Phototropism: "A simple" physiological response modulated by multiple interacting photosensory-response pathways. Photochem Photobiol 72:273–282
Liu XL, Covington MF, Fankhauser C, Chory J, Wagner DR (2001) ELF3 encodes a circadian clock-regulated nuclear protein that functions in an Arabidopsis PHYB signal transduction pathway. Plant Cell 13:1293–1304
Liu B, Kanazawa A, Matsumura H, Takahashi R, Harada K, Abe J (2008) Genetic redundancy in soybean photoresponses associated with duplication of the phytochrome A gene. Genetics 180:995–1007
Liu H, Liu B, Zhao C, Pepper M, Lin C (2011) The action mechanisms of plant cryptochromes. Trends Plant Sci 16:684–691
Luesse DR, DeBlasio SL, Hangarter RP (2010) Integration of Phot1, Phot2, and PhyB signalling in light-induced chloroplast movements. J Exp Bot 61:4387–4397
Malhotra K, Kim ST, Batschauer A, Dawut L, Sancar A (1995) Putative blue-light photoreceptors from Arabidopsis thaliana and Sinapis alba with a high degree of sequence homology to DNA photolyase contain the two photolyase cofactors but lack DNA repair activity. Biochem 34:6892–6899
Mao J, Zhang YC, Sang Y, Li QH, Yang HQ (2005) A role for Arabidopsis cryptochromes and COP1 in the regulation of stomatal opening. Proc Natl Acad Sci U S A 102:12270–12275
Martinez-Garcia JF, Huq E, Quail PH (2000) Direct targeting of light signals to a promoter element-bound transcription factor. Science 288:859–863
Mas P, Kim WY, Somers DE, Kay SA (2003) Targeted degradation of TOC1 by ZTL modulates circadian function in Arabidopsis thaliana. Nature 426:567–570
Mathews S (2006) Phytochrome-mediated development in land plants: red light sensing evolves to meet the challenges of changing light environments. Mol Ecol 15:3483–3503
Mathews S (2010) Evolutionary studies illuminate the structural-functional model of plant phytochromes. Plant Cell 22:4–16
Mathieu J, Warthmann N, Küttner F, Schmid M (2007) Export of FT protein from phloem companion cells is sufficient for floral induction in Arabidopsis. Curr Biol 17:1055–1060
Matsubara K, Ogiso-Tanaka E, Hori K, Ebana K, Ando T, Yano M (2012) Natural variation in Hd17, a homolog of Arabidopsis ELF3 that is involved in rice photoperiodic flowering. Plant Cell Physiol 53:709–716
Matsumoto N, Hirano T, Iwasaki T, Yamamoto N (2003) Functional analysis and intracellular localization of rice cryptochromes. Plant Physiol 133:1494–1503
Mazzella MA, Magliano TMA, Casal JJ (1997) Dual effect of phytochrome A on hypocotyl growth under continuous red light. Plant Cell Environ 20:261–267
McWatters HG, Bastow RM, Hall A, Millar AJ (2000) The ELF3 zeitnehmer regulates light signalling to the circadian clock. Nature 408:716–720
Medzihradszky M, Bindics J, Ádám É, Viczián A, Klement É, Lorrain S, Gyula P, Mérai Z, Fankhauser C, Medzihradszky KF, Kunkel T, Schäfer E, Nagy F (2013) Phosphorylation of phytochrome B inhibits light-induced signaling via accelerated dark reversion in Arabidopsis. Plant Cell 25:535–544
Michael TP, Salome PA, Yu HJ, Spencer TR, Sharp EL, McPeek MA, Alonso JM, Ecker JR, McClung CR (2003) Enhanced fitness conferred by naturally occurring variation in the circadian clock. Science 302:1049–1053
Mizoguchi T, Wheatley K, Hanzawa Y, Wright L, Mizoguchi M, Song HR, Carre IA, Coupland G (2002) LHY and CCA1 are partially redundant genes required to maintain circadian rhythms in Arabidopsis. Dev Cell 2:629–641
Mockler T, Yang H, Yu X, Parikh D, Cheng YC, Dolan S, Lin C (2003) Regulation of photoperiodic flowering by Arabidopsis photoreceptors. Proc Natl Acad Sci U S A 100:2140–2145
Morris K, Thornber S, Codrai L, Richardson C, Craig A, Sadanandom A, Thomas B, Jackson S (2010) DAY NEUTRAL FLOWERING represses CONSTANS to prevent Arabidopsis flowering early in short days. Plant Cell 22:1118–1128
Mullineaux P, Karpinski S (2002) Signal transduction in response to excess light: getting out of the chloroplast. Curr Opin Plant Biol 5:43–48
Muramoto T, Kohchi T, Yokota A, Hwang IH, Goodman HM (1999) The Arabidopsis photomorphogenic mutant hy1 is deficient in phytochrome chromophore biosynthesis as a result of a mutation in a plastid heme oxygenase. Plant Cell 11:335–347
Nagel DH, Kay SA (2012) Complexity in the wiring and regulation of plant circadian networks. Curr Biol 22:R648–R657
Nakamichi N, Kita M, Ito S, Yamashino T, Mizuno T (2005) PSEUDO-RESPONSE REGULATORS, PRR9, PRR7 and PRR5, together play essential roles close to the circadian clock of Arabidopsis thaliana. Plant Cell Physiol 46:686–698
Nelson DC, Lasswell J, Rogg LE, Cohen MA, Bartel B (2000) FKF1, a clock-controlled gene that regulates the transition to flowering in Arabidopsis. Cell 101:331–340
Nito K, Wong CC, Yates JR 3rd, Chory J (2013) Tyrosine phosphorylation regulates the activity of phytochrome photoreceptors. Cell Rep 3:1970–1979
O'Hara A, Jenkins GI (2012) In vivo function of tryptophans in the Arabidopsis UV-B photoreceptor UVR8. Plant Cell 24:3755–3766
Park DH, Somers DE, Kim YS, Choy YH, Lim HK, Soh MS, Kim HJ, Kay SA, Nam HG (1999) Control of circadian rhythms and photoperiodic flowering by the Arabidopsis GIGANTEA gene. Science 285:1579–1582
Parker MW, Hendricks SB, Borthwick HA, Went FW (1949) Spectral sensitivities for stem and leaf growth of etiolated pea seedlings and their similarity to action spectra for photoperiodism. Am J Bot 36:194–204
Parks BM, Spalding EP (1999) Sequential and coordinated action of phytochromes A and B during Arabidopsis stem growth revealed by kinetic analysis. Proc Natl Acad Sci U S A 96:14142–14146
Parks BM, Quail PH (1991) Phytochrome-deficient hy1 and hy2 long hypocotyl mutants of Arabidopsis are defective in phytochrome chromophore biosynthesis. Plant Cell 3:1177–1186

Parks BM, Quail PH, Hangarter RP (1996) Phytochrome A regulates red-light induction of phototropic enhancement in Arabidopsis. Plant Physiol 110:155–162

Perrotta G, Ninu L, Flamma F, Weller JL, Kendrick RE, Nebuloso E, Giuliano G (2000) Tomato contains homologues of Arabidopsis cryptochromes 1 and 2. Plant Mol Biol 42:765–773

Pfeiffer A, Nagel MK, Popp C, Wüst F, Bindics J, Viczián A, Hiltbrunner A, Nagy F, Kunkel T, Schäfer E (2012) Interaction with plant transcription factors can mediate nuclear import of phytochrome B. Proc Natl Acad Sci U S A 109:5892–5897

Platten JD, Foo E, Elliott RC, Hecht V, Reid JB, Weller JL (2005a) Cryptochrome 1 contributes to blue-light sensing in pea. Plant Physiol 139:1472–1482

Platten JD, Foo E, Foucher F, Hecht V, Reid JB, Weller JL (2005b) The cryptochrome gene family in pea includes two differentially expressed CRY2 genes. Plant Mol Biol 59:683–696

Poppe C, Sweere U, Drumm-Herrel H, Schäfer E (1998) The blue light receptor cryptochrome 1 can act independently of phytochrome A and B in Arabidopsis thaliana. Plant J 16:465–471

Quail PH (2006) Phytochrome signal transduction network. In: Schäfer E, Nagy F (eds) Photomorphogenesis in plants and bacteria, 3rd edn. Springer, Dordrecht, pp 335–356

Rausenberger J, Tscheuschler A, Nordmeier W, Wüst F, Timmer J, Schäfer E, Fleck C, Hiltbrunner A (2011) Photoconversion and nuclear trafficking cycles determine phytochrome A's response profile to far-red light. Cell 146:813–825

Rizzini L, Favory JJ, Cloix C, Faggionato D, O'Hara A, Kaiserli E, Baumeister R, Schäfer E, Nagy F, Jenkins GI, Ulm R (2011) Perception of UV-B by the Arabidopsis UVR8 protein. Science 332:103–106

Rockwell NC, Lagarias JC (2010) A brief history of phytochromes. ChemPhysChem 11:1172–1180

Rockwell NC, Su YS, Lagarias JC (2006) Phytochrome structure and signaling mechanisms. Annu Rev Plant Biol 57:837–858

Rösler J, Klein I, Zeidler M (2007) Arabidopsis fhl/fhy1 double mutant reveals a distinct cytoplasmic action of phytochrome A. Proc Natl Acad Sci U S A 104:10737–10742

Ryan KG, Swinny EE, Winefield C, Markham KR (2001) Flavonoids and UV photoprotection in Arabidopsis mutants. Z Naturforsch 56:745–754

Sage LC (1992) Pigment of the imagination: a history of phytochrome research. Academic, New York

Saito H, Ogiso-Tanaka E, Okumoto Y, Yoshitake Y, Izumi H, Yokoo T, Matsubara K, Hori K, Yano M, Inoue H, Tanisaka T (2012) Ef7 encodes an ELF3-like protein and promotes rice flowering by negatively regulating the floral repressor gene Ghd 7 under both short- and long-day conditions. Plant Cell Physiol 53:717–728

Sakai T, Wada T, Ishiguro S, Okada K (2000) RPT2: a signal transducer of the phototropic response in Arabidopsis. Plant Cell 12:225–236

Sakai T, Kagawa T, Kasahara M, Swartz TE, Christie JM, Briggs WR, Wada M, Okada K (2001) Arabidopsis nph1 and npl1: blue light receptors that mediate both phototropism and chloroplast relocation. Proc Natl Acad Sci U S A 98:6969–6974

Sakamoto K, Briggs WR (2002) Cellular and subcellular localization of phototropin 1. Plant Cell 14:1723–1735

Salomon M, Christie JM, Knieb E, Lempert U, Briggs WR (2000) Photochemical and mutational analysis of the FMN-binding domains of the plant blue light receptor phototropin. Biochemistry 39:9401–9410

Samach A, Onouchi H, Gold SE, Ditta GS, Schwarz-Sommer Z, Yanofsky MF, Coupland G (2000) Distinct roles of CONSTANS target genes in reproductive development of Arabidopsis. Science 288:1613–1616

Schultz TF, Kiyosue T, Yanovsky M, Wada M, Kay SA (2001) A role for LKP2 in the circadian clock of Arabidopsis. Plant Cell 13:2659–2670

Shalitin D, Yu X, Maymon M, Mockler T, Lin C (2003) Blue light-dependent in vivo and in vitro phosphorylation of Arabidopsis cryptochrome 1. Plant Cell 15:2421–2429

Sharrock RA, Mathews S (2006) Phytochrome genes in higher plants. In: Schäfer E, Nagy F (eds) Photomorphogenesis in plants and bacteria, 3rd edn. Springer, Dordrecht, pp 99–130

Shinomura T, Nagatani A, Hanzawa H, Kubota M, Watanabe M, Furuya M (1996) Action spectra for phytochrome A- and B-specific photoinduction of seed germination in Arabidopsis thaliana. Proc Natl Acad Sci U S A 93:8129–8133

Shinomura T, Uchida K, Furuya M (2000) Elementary processes of photoperception by phytochrome A for high-irradiance response of hypocotyl elongation in Arabidopsis. Plant Physiol 122:147–156

Shirley BW (1996) Flavonoid biosynthesis – new functions for an old pathway. Trends Plant Sci 1:377–382

Smith H, Xu Y, Quail PH (1997) Antagonistic but complementary actions of phytochromes A and B allow seedling de-etiolation. Plant Physiol 114:637–641

Somers DE, Devlin PF, Kay SA (1998) Phytochromes and cryptochromes in the entrainment of the Arabidopsis circadian clock. Science 282:1488–1490

Somers DE, Schultz TF, Milnamow M, Kay SA (2000) ZEITLUPE encodes a novel clock-associated PAS protein from Arabidopsis. Cell 101:319–329

Song YH, Lee I, Lee SY, Imaizumi T, Hong JC (2012a) CONSTANS and ASYMMETRIC LEAVES 1 complex is involved in the induction of FLOWERING LOCUS T in photoperiodic flowering in Arabidopsis. Plant J 69:332–342

Song YH, Smith RW, To BJ, Millar AJ, Imaizumi T (2012b) FKF1 conveys timing information for CONSTANS stabilization in photoperiodic flowering. Science 336:1045–1049

Spalding EP (2000) Ion channels and the transduction of light signals. Plant Cell Environ 23:665–674

Sullivan S, Kaiserli E, Tseng TS, Christie JM (2010) Subcellular localization and turnover of Arabidopsis phototropin 1. Plant Signal Behav 5:184–186

Takano M, Inagaki N, Xie X, Yuzurihara N, Hihara F, Ishizuka T, Yano M, Nishimura M, Miyao A, Hirochika H, Shinomura T (2005) Distinct and cooperative functions of phytochromes A, B, and C in the control of deetiolation and flowering in rice. Plant Cell 17:3311–3325

Takemiya A, Sugiyama N, Fujimoto H, Tsutsumi T, Yamauchi S, Hiyama A, Tada Y, Christie JM, Shimazaki K (2013) Phosphorylation of BLUS1 kinase by phototropins is a primary step in stomatal opening. Nat Commun 4:2094. doi:10.1038/ncomms3094

Tamaki S, Matsuo S, Wong HL, Yokoi S, Shimamoto K (2007) Hd3a protein is a mobile flowering signal in rice. Science 316:1033–1036

Taoka K, Ohki I, Tsuji H, Furuita K, Hayashi K, Yanase T, Yamaguchi M, Nakashima C, Purwestri YA, Tamaki S, Ogaki Y, Shimada C, Nakagawa A, Kojima C, Shimamoto K (2011) 14-3-3 proteins act as intracellular receptors for rice Hd3a florigen. Nature 476:332–335

Tepperman JM, Hudson ME, Khanna R, Zhu T, Chang SH, Wang X, Quail PH (2004) Expression profiling of phyB mutant demonstrates substantial contribution of other phytochromes to red-light-regulated gene expression during seedling de-etiolation. Plant J 38:725–739

Tepperman JM, Zhu T, Chang HS, Wang X, Quail PH (2001) Multiple transcription-factor genes are early targets of phytochrome A signaling. Proc Natl Acad Sci U S A 98:9437–9442

Terashima I, Hikosaka K (1995) Comparative ecophysiology of leaf and canopy photosynthesis. Plant Cell Environ 18:1111–1128

Thomas B, Vince-Prue D (1997) Photoperiodism in plants, 2nd edn. Academic, London

Tiwari SB, Shen Y, Chang HC, Hou Y, Harris A, Ma SF, McPartland M, Hymus GJ, Adam L, Marion C, Belachew A, Repetti PP, Reuber TL, Ratcliffe OJ (2010) The flowering time regulator CONSTANS is

recruited to the FLOWERING LOCUS T promoter via a unique cis-element. New Phytol 187:57–66
Toth R, Kevei E, Hall A, Millar AJ, Nagy F, Kozma-Bognar L (2001) Circadian clock-regulated expression of phytochrome and cryptochrome genes in Arabidopsis. Plant Physiol 127:1607–1616
Tsuji H, Taoka K, Shimamoto K (2011) Regulation of flowering in rice: two florigen genes, a complex gene network, and natural variation. Curr Opin Plant Biol 14:45–52
Turner A, Beales J, Faure S, Dunford RP, Laurie DA (2005) The pseudo-response regulator Ppd-H1 provides adaptation to photoperiod in barley. Science 310:1031–1034
Ulijasz AT, Vierstra RD (2011) Phytochrome structure and photochemistry: recent advances toward a complete molecular picture. Curr Opin Plant Biol 14:498–506
Ulm R (2006) UV-B perception and signalling in higher plants. In: Schäfer E, Nagy F (eds) Photomorphogenesis in plants and bacteria, 3rd edn. Springer, Dordrecht, pp 279–304
Valverde F, Mouradov A, Soppe W, Ravenscroft D, Samach A, Coupland G (2004) Photoreceptor regulation of CONSTANS protein in photoperiodic flowering. Science 303:1003–1006
Vogelmann TC, Nishio JN, Smith WK (1996) Leaves and light capture – light propagation and gradients of carbon fixation within leaves. Trends Plant Sci 1:65–70
Wan YL, Eisinger W, Ehrhardt D, Kubitscheck U, Baluska F, Briggs W (2008) The subcellular localization and blue-light-induced movement of phototropin 1-GFP in etiolated seedlings of Arabidopsis thaliana. Mol Plant 1:103–117
Wang HY, Ma LG, Li JM, Zhao HY, Deng XW (2001) Direct interaction of Arabidopsis cryptochromes with COP1 in light control development. Science 294:154–158
Watanabe S, Xia Z, Hideshima R, Tsubokura Y, Sato S, Yamanaka N, Takahashi R, Anai T, Tabata S, Kitamura K, Harada K (2011) A map-based cloning strategy employing a residual heterozygous line reveals that the GIGANTEA gene is involved in soybean maturity and flowering. Genetics 188:395–407
Weidler G, Zur Oven-Krockhaus S, Heunemann M, Orth C, Schleifenbaum F, Harter K, Hoecker U, Batschauer A (2012) Degradation of Arabidopsis CRY2 is regulated by SPA proteins and phytochrome A. Plant Cell 24:2610–2623
Weller JL, Beauchamp N, Kerckhoffs LHJ, Platten JD, Reid JB (2001a) Interaction of phytochromes A and B in the control of de-etiolation and flowering in pea. Plant J 26:283–294
Weller JL, Liew LC, Hecht VF, Rajandran V, Laurie RE, Ridge S, Wenden B, Vander Schoor JK, Jaminon O, Blassiau C, Dalmais M, Rameau C, Bendahmane A, Macknight RC, Lejeune-Hénaut I (2012) A conserved molecular basis for photoperiod adaptation in two temperate legumes. Proc Natl Acad Sci U S A 109: 21158–21163
Weller JL, Murfet IC, Reid JB (1997a) Pea mutants with reduced sensitivity to far-red light define an important role for phytochrome a in day-length detection. Plant Physiol 114:1225–1236
Weller JL, Perrotta G, Schreuder MEL, van Tuinen A, Koornneef M, Giuliano G, Kendrick RE (2001b) Genetic dissection of blue-light sensing in tomato using mutants deficient in cryptochrome 1 and phytochromes A, B1 and B2. Plant J 25:427–440
Weller JL, Terry MJ, Reid JB, Kendrick RE (1997b) The phytochrome-deficient pcd2 mutant of pea is unable to convert biliverdin IXα to 3(Z)-phytochromobilin. Plant J 11:1177–1186
Went FW (1941) Effects of light on stem and leaf growth. Am J Bot 28:83–95
Whitelam GC, Johnson E, Peng J, Carol P, Anderson ML, Cowl JS, Harberd NP (1993) Phytochrome A null mutants of Arabidopsis display a wild-type phenotype in white light. Plant Cell 5:757–768
Wigge PA, Kim MC, Jaeger KE, Busch W, Schmid M, Lohmann JU, Weigel D (2005) Integration of spatial and temporal information during floral induction in *Arabidopsis*. Science 309: 1056–1059
Withrow RB, Klein WH, Elstad V (1957) Action spectra of photomorphogenic induction and its inactivation. Plant Physiol 32: 453–462
Yang SW, Jang IC, Henriques R, Chua NH (2009) FAR-RED ELONGATED HYPOCOTYL1 and FHY1-LIKE associate with the Arabidopsis transcription factors LAF1 and HFR1 to transmit phytochrome A signals for inhibition of hypocotyl elongation. Plant Cell 21:1341–1359
Yanovsky MJ, Casal JJ, Whitelam GC (1995) Phytochrome A, phytochrome B and HY4 are involved in hypocotyl growth responses to natural radiation in Arabidopsis – weak de-etiolation of the phyA mutant under dense canopies. Plant Cell Environ 18:788–794
Yanovsky MJ, Kay SA (2002) Molecular basis of seasonal time measurement in Arabidopsis. Nature 419:308–312
Yanovsky MJ, Mazzella MA, Casal JJ (2000) A quadruple photoreceptor mutant still keeps track of time. Curr Biol 10:1013–1015
Yeh KC, Lagarias JC (1998) Eukaryotic phytochromes – light-regulated serine/threonine protein kinases with histidine kinase ancestry. Proc Natl Acad Sci U S A 95:13976–13981
Zhang Q, Li H, Li R, Hu R, Fan C, Chen F, Wang Z, Liu X, Fu Y, Lin C (2008) Association of the circadian rhythmic expression of GmCRY1a with a latitudinal cline in photoperiodic flowering of soybean. Proc Natl Acad Sci U S A 105:21028–21033
Zhang YC, Gong SF, Li QH, Sang Y, Yang HQ (2006) Functional and signaling mechanism analysis of rice CRYPTOCHROME 1. Plant J 46:971–983
Zuo Z, Liu H, Liu B, Liu X, Lin C (2011) Blue light-dependent interaction of CRY2 with SPA1 regulates COP1 activity and floral initiation in Arabidopsis. Curr Biol 21:841–847

The Light-Dependent Magnetic Compass

20

Rachel Muheim and Miriam Liedvogel

20.1 Introduction

The use of directional information from the Earth's magnetic field for compass orientation has been demonstrated in a large variety of animals across different taxa. Behavioral and physiological evidence suggests two possible mechanisms that could independently allow the detection of magnetic properties (for reviews see Wiltschko and Wiltschko 1995, 2005; Freake et al. 2006; Johnsen and Lohmann 2008): (1) a light-dependent biochemical process detecting the axial alignment and inclination angle of the geomagnetic field lines, providing the animals with directional magnetic information for magnetic compass orientation (inclination compass), and (2) a magnetite-mediated process, providing magnetic map information from spatial variation in the intensity and/or inclination of the geomagnetic field (map or signpost sense). The functional properties of the magnetic compass of most animals studied to date can be assigned to either one of the two groups, consistent with either a light-dependent mechanism or a non-light-dependent, magnetite-based mechanism. This chapter focuses on the light-dependent process of magnetoreception, summarizing the state of the art of behavioral, physiological, neurobiological, and biophysical evidence supporting the involvement of light in magnetic compass orientation.

20.2 Behavioral Evidence for Light-Dependent Magnetoreception

Behavioral experiments have conclusively identified light to be a key prerequisite for the primary magnetoreception process in a growing number of organisms including birds, amphibians, and some insects (Phillips and Borland 1992a; Phillips and Sayeed 1993; Wiltschko et al. 1993, 2010; Deutschlander et al. 1999b; Muheim et al. 2002; Vacha and Soukopova 2004; Phillips et al. 2010a). In addition, there is strong (albeit indirect) evidence that also C57BL/6J mice have a light-dependent magnetic compass (Muheim et al. 2006). Magnetic compass orientation independent of light has only been shown in a few exceptions, like the subterranean mole rats (Marhold et al. 1997) and sea turtles (Lohmann and Lohmann 1993). In the case of the mole rats, magnetic compass information has been shown to be mediated by a magnetite-based mechanism (Thalau et al. 2006). It is well possible that these exceptional cases are the result of an adaptation to the specific lifestyles of these organisms. As a general conclusion drawn from recent knowledge, animals need access to light of a specific wavelength range and intensities to be able to perceive magnetic compass information.

20.2.1 Light-Dependent Magnetic Compass Orientation in Insects

Magnetic compass orientation in adult and larval *Drosophila* and mealworm beetles (*Tenebrio* spp.) depends on the wavelength of light: animals trained towards a light gradient under UV light orient towards the trained magnetic direction of the light gradient when tested in a uniform arena under short-wavelength light (<450 nm). When tested under long-wavelength light (>450 nm), they shift their orientation by ~90° relative to the trained magnetic direction (Phillips and Sayeed 1993; Dommer et al. 2008; Vacha et al. 2008). This suggests that these insects possess a light-dependent magnetic compass with antagonistic short- and long-wavelength inputs. The spectral dependencies of magnetic compass orientation in both *Drosophila* and *Tenebrio* are compatible with a cryptochrome-based mechanism in which the magnetic field has antagonistic effects on short- and long-wavelength photo-signaling pathways (see below; reviewed by Phillips et al. 2010a).

R. Muheim (✉)
Department of Biology, Lund University, Lund, Sweden
e-mail: rachel.muheim@biol.lu.se

M. Liedvogel
Max-Planck-Institute for Evolutionary Biology,
Ploen, Germany
e-mail: liedvogel@evolbio.mpg.de

L.O. Björn (ed.), *Photobiology: The Science of Light and Life*,
DOI 10.1007/978-1-4939-1468-5_20,

20.2.2 Antagonistic Spectral Mechanism Mediating Magnetic Compass Orientation in Amphibians

Similar 90° shifts in orientation under longer wavelengths have also been described in newts and frog and toad tadpoles (Phillips and Borland 1992b; Freake and Phillips 2005; Diego-Rasilla et al. 2010, 2013; reviewed by Phillips et al. 2001, 2010a). The shoreward orientation of North American Eastern red-spotted newts trained to learn the magnetic alignment of an artificial shore is mediated by a magnetic inclination compass that depends on the wavelength of the ambient light. Magnetic orientation of newts tested under long-wavelength light (>500 nm) is rotated by 90° from the trained shoreward directions shown under short-wavelength light (400–450 nm; Phillips and Borland 1992a, b). Newts tested under an intermediate wavelength of 475 nm are disoriented. It is highly unlikely that this abrupt shift from oriented behavior to complete disorientation is caused by a gradual decrease in sensitivity of one spectral mechanism alone. This led to the suggestion that two antagonistic spectral mechanisms might be involved (Phillips and Borland 1992b; Deutschlander et al. 1999b): one high-sensitive, short-wavelength mechanism mediating oriented behavior in the trained direction of the artificial shore (Fig. 20.1a) and a second low-irradiance, long-wavelength mechanism shifting orientation by 90° relative to the shore (Fig. 20.1b). In the intermediate-wavelength condition, both mechanisms are equally excited, which leads to disorientation (Fig. 20.1c). Complete elimination of magnetic compass orientation in newts tested under near-infrared light (>715 nm) adds additional support for the hypothetical involvement of two discrete spectral mechanisms (Phillips and Borland 1992c).

20.2.3 Magnetic Compass Orientation of Birds Depends on the Presence, Wavelength, and Irradiance of Light

First evidence for the importance of light for magnetic compass orientation in birds came from homing experiments with pigeons. Young, inexperienced homing pigeons were disoriented after displacement in complete darkness or under 660 nm red light but oriented towards the home direction when transported to the release site under 565 nm green or full-spectrum light (Wiltschko and Wiltschko 1981, 1998). Orientation experiments with passerine migrants in orientation funnels illuminated with monochromatic light gave further support for the involvement of a wavelength-dependent, light-sensitive magnetoreception process. Night-migratory songbirds, like European robins (*Erithacus rubecula*), Australian silvereyes (*Zosterops lateralis*), and garden warblers (*Sylvia borin*), showed well-oriented behavior into the seasonally expected migratory directions when tested under monochromatic light of peak wavelengths between 373 nm (UV) and 565 nm (green), comparable to the responses shown under full-spectrum light (Rappl et al. 2000; Wiltschko and Wiltschko 2001; Wiltschko et al. 2010; Fig. 20.2). However, when tested under longer-wavelength spectra, the birds became disoriented (Wiltschko et al. 1993; Wiltschko and Wiltschko 1999; Fig. 20.2). These results indicate that light-dependent magnetoreception becomes critical under light of peak wavelengths longer than 565 nm.

In a series of experiments with European robins tested under narrowband (9–11 nm half bandwidth) green (560.5 nm) and green-yellow (567.5 nm) light, Muheim et al. (2002) showed that the transition from oriented magnetic compass behavior under 560.5 nm to disorientation under 567.5 nm happens very abruptly (Fig. 20.3). The authors concluded that at least two spectral mechanisms are underlying light-dependent magnetic compass orientation in birds (Muheim et al. 2002) and proposed an antagonistic mechanism similar to that found in amphibians and insects.

Light-dependent magnetoreception varies in birds not only with wavelength but also with photon irradiance (light intensity) at the same wavelength. Night-migratory birds tested under low-light regimes (~0.5–21×10^{15} quanta s^{-1} m^{-2}), similar to light levels experienced under a starry sky, are well oriented towards the migratory direction. Birds tested under higher photon irradiances (~29–54×10^{15} quanta s^{-1} m^{-2}) are disoriented or show shifts in orientation deviating from the expected migratory direction (e.g., Wiltschko and Wiltschko (2001); Muheim et al. (2002); Wiltschko et al. (2010)). At such irradiances, birds do not seem to be able to use their inclination compass, that is, they do not react to an inversion of the vertical component of the magnetic field (Wiltschko et al. 2003a) and their magnetic compass orientation performance cannot be disrupted by radio-frequency electromagnetic fields (Wiltschko et al. 2005). Instead, the birds show a reaction to shifts of the horizontal component of the magnetic field vector, indicating the use of a polarity compass or an alignment along a magnetic direction.

There is general consensus on the involvement of at least two magnetoreception mechanisms, which are used under different wavelength scenarios. However, there is a vivid debate over the underlying mechanisms and putative interaction of these receptor types. Based on the parallels between the findings in behavioral experiments on birds, insects, and newts, Muheim and coworkers suggested the presence of two antagonistically interacting spectral mechanisms, with a high-sensitive short-wavelength mechanism leading to oriented behavior and a low-sensitive long-wavelength mechanism leading to shifted orientation (Muheim et al. 2002). Similar to the behavior observed in newts, the disorientation found in migratory birds under the intermediate wavelengths could be explained by an equal excitation of both magnetoreceptor types (Phillips

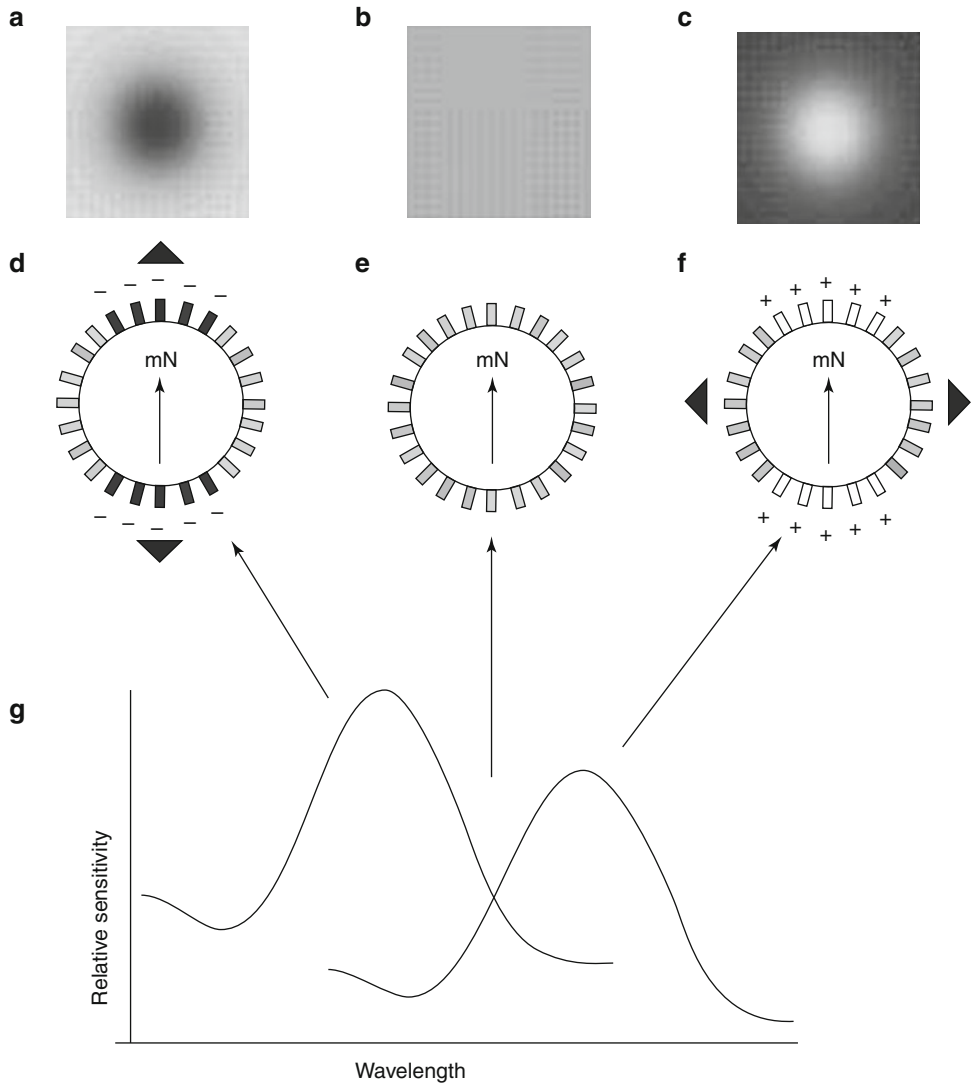

Fig. 20.1 Illustration of the hypothetical antagonistic spectral mechanism proposed to mediate the light-dependent array of axially sensitive receptors. (**a**–**c**) Magnetic modulation patterns as suggested to be perceived by an animal looking parallel along the magnetic field vector (for more details, see Fig. 20.4). (**d**–**f**) Alignment of putative receptors (*small rectangles*) along the magnetic axis in a spherical receptor organ, like the eyes or pineal organ. (**g**) Putative spectral sensitivity curves for two hypothetical antagonistic inputs to the light-dependent magnetic compass with a short- and a long-wavelength mechanism. Under short-wavelength light (**a**–**d**), the receptors aligned along the magnetic axis show a decrease in response (*dark rectangles* labeled "–"), while receptors aligned perpendicular to the magnetic field (*gray rectangles*) remain unaffected. Under long-wavelength light (**c**–**e**), the receptors aligned along the magnetic axis show an increase in response (*white rectangles* labeled "+"), resulting in a "reversed" magnetic modulation pattern. *Arrowheads* at the edge of the circular array indicate the axes with the lowest level of response, which differ by 90° in (**a**–**d**) and (**c**–**e**). (**b**–**d**) Under intermediate wavelengths of light, both mechanisms are activated equally and the directional response is eliminated (Adapted from Phillips et al. (2010a))

et al. 2010a). Alternatively, over-excitation of both mechanisms could make the perceived magnetic pattern unrecognizable; thus, the birds would not be able to use the vision-mediated inclination compass any longer and would need to resort to a light-independent magnetite-based receptor. However, this hypothesis is opposed by the view that the observed 90° shifts under red are no true 90° shifts, but instead "fixed" orientations (absolute geographic 90° shifts during autumn and spring both turned to the same geographic direction and thus not relative to the natural migratory direction). This would reject the assumed similarity of the magnetoreception system in birds and newts (Wiltschko et al. 2004a). Instead, it has been suggested that the shifted orientation responses observed under high light irradiances are the results of a third, yet unspecified, novel type of light-dependent magnetoreceptor. This receptor would not be based on a light-mediated radical-pair mechanism nor a magnetite-based process, since the "fixed" orientation responses under such conditions differ between wavelengths and are not mediated by the inclination compass any longer (Wiltschko et al. 2005).

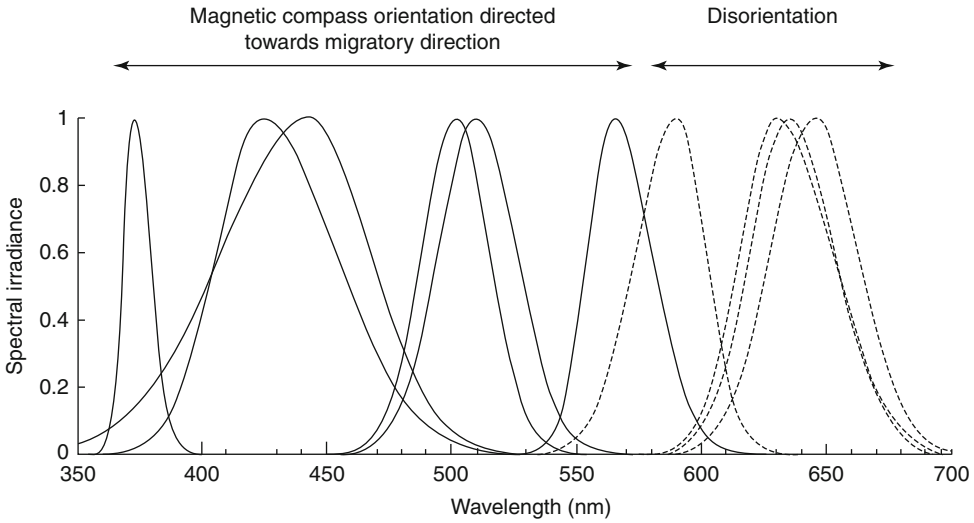

Fig. 20.2 Spectral curves under which migratory songbirds have been tested for magnetic compass orientation. The birds are well oriented when tested under low irradiance ($0.5–21 \times 10^{15}$ quanta s^{-1} m^{-2}) to *green* light (*solid spectral curves*) but become disoriented under longer-wavelength light (*dotted spectral curves*)

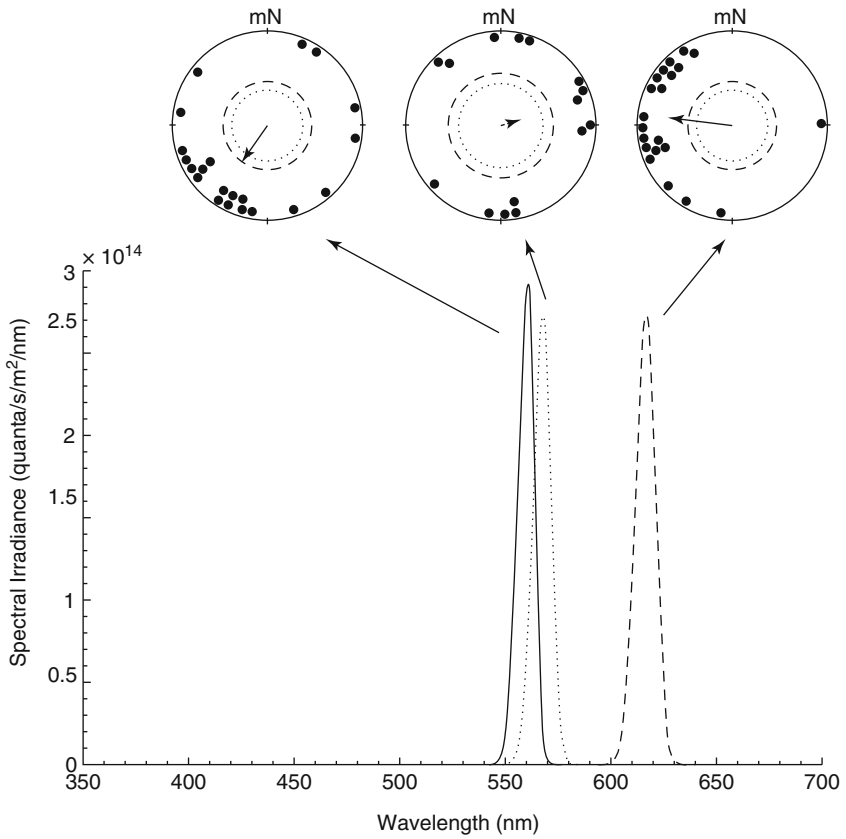

Fig. 20.3 Magnetic orientation of European robins tested during autumn migration under narrowbanded light. Birds are well oriented under 560.5 nm *green* light (*left*) and totally disoriented under 567.5 nm *green-yellow* light (*middle*) and showed a 90° shift in orientation under 617 nm *red* light (*right*) (Adapted from Muheim et al. (2002))

20.3 Mechanisms of Light-Dependent Magnetoreception

The behavioral data presented above imply that the light-mediated magnetic information necessary for compass orientation has to meet the following requirements: (1) The nature of magnetic information used for compass orientation has to be axial rather than polar, that is, sensing the alignment of the magnetic field lines in space but not the polarity of flux. (2) The functional range of the magnetic compass has to be reasonably plastic in order to adapt to different magnetic field intensities outside to locally experienced intensity range. This was shown in European robins that were disoriented when tested in artificial magnetic fields with intensities weaker (4–34 μT) or stronger (60–105 μT) than the local magnetic field at the testing locality (47 μT; Wiltschko 1968, 1978; Wiltschko et al. 2006; Winklhofer et al. 2013). However, after preexposure to such unnatural, and never before experienced, magnetic fields for

just a few hours, the very same birds were able to orient using their magnetic compass perfectly fine in subsequent experiments. Birds thus seem to be able to learn or adapt to changing properties of the ambient magnetic field, that is, they can learn to orient under novel magnetic conditions. In other words, the functional range of their magnetic compass is flexible and allows adjustment to previously not experienced magnetic conditions, allowing magnetic compass orientation as long as the magnetic field provides directional information.

20.3.1 Chemical Magnetoreception Based on a Radical-Pair Mechanism

Various biophysical mechanisms have been suggested to explain light-dependent magnetoreception in animals. The currently most discussed model was first proposed by a physicist, Klaus Schulten. He suggested that the yield of a biochemical reaction proceeding via a radical pair might be dependent to the orientation of an external magnetic field and could thus be used for compass orientation (Schulten et al. 1978; Schulten 1982). The proposed mechanism involves a light-induced electron transfer between an electron donor and an acceptor molecule. The electron transfer results in the generation of a transient radical-pair intermediate that can exist in a singlet or a triplet excited state, and the transient radicals will subsequently decay in chemically different singlet or triplet products. Theoretical calculations and in vitro experiments have shown that the ratio between singlet and triplet products from radical-pair reactions is sensitive to and can thus be modulated by an Earth-strength magnetic field, thereby theoretically providing the basis for a magnetic compass (Henbest et al. 2008; Maeda et al. 2008, 2012; Rodgers and Hore 2009). This idea was revived in 2000 by Klaus Schulten together with Thorsten Ritz. The physicists proposed that the retina with its almost perfect half-ball shape would be well suited as an ordered structure and that the radical-pair intermediate could be involved in the visual reception system, for example, by altering the photosensitivity of the photoreceptor molecule (Ritz et al. 2000). Ritz further proposed cryptochromes as likely photoreceptor molecules. According to this hypothesis, the reaction yield anisotropy of the receptor radical pair governs the directional response. Magnetosensitive photoreceptors arranged in an ordered array in photosensory organs, such as the retina or the pineal, would respond differently, depending on their alignment relative to the magnetic field. Consequently, the effect on the visual perception process would be dependent on the alignment of the photoreceptor to the geomagnetic field and thus allow the animals to derive a directional heading by literally "seeing" the magnetic field lines (Fig. 20.4). In such a light-sensitive magnetoreception system, the animals could perceive the magnetic field as a three-dimensional pattern of light irradiance or color variation in their visual field (Fig. 20.4; for recent reviews, see Rodgers and Hore 2009; Ritz et al. 2010; Solov'yov et al. 2010; Phillips et al. 2010b).

The general feasibility of radical-pair-based magnetoreception has recently been demonstrated by spectroscopic observations of an artificially designed molecule system as model magnetoreceptor: these data clearly show that the radical-pair reaction process is sensitive to geomagnetic field strengths and the lifetime of a light-induced transient radical pair is long enough to be altered by Earth-strength magnetic fields. The model receptor molecule provides further insight into the structural and dynamic design that is required to detect directional information of the Earth's magnetic field necessary to facilitate magnetic compass orientation (Maeda et al. 2008).

20.3.2 Behavioral Evidence for a Radical-Pair-Based Magnetoreceptor

The radical-pair model meets all the necessary criteria to be a likely candidate for the light-dependent magnetic compass receptor (Ritz et al. 2002, 2010; Liedvogel and Mouritsen 2010; Phillips et al. 2010a; Mouritsen and Hore 2012): (1) the putative visual image perceived by the animal has axial properties, thus does not allow determination of the polarity of the field lines and is in line with an inclination compass and (2) the singlet-triplet yield and, consequently, the visual pattern perceived by the animal depends on the intensity of the magnetic field; thus, exposure to magnetic field intensities never experienced before can lead to disorientation, followed by a slow adaptation to the "new" pattern (cf. Wiltschko 1968, 1978; Wiltschko et al. 2006; Winklhofer et al. 2013). Adaptation has also been suggested as explanation for the ability of birds to orient under monochromatic red light after preexposure to the same light for one hour before the start of the orientation experiments (Wiltschko et al. 2004b).

The most convincing evidence for the involvement of a radical-pair mechanism in light-dependent magnetoreception comes from experiment using low-intensity oscillating radio-frequency magnetic fields (RF fields) in the lower MHz range (0.1–100 MHz). This treatment serves as a diagnostic tool that allows testing whether a radical-pair mechanism is involved in the primary magnetoreception process of an orientation response (Henbest et al. 2004; Ritz et al. 2004). The reasoning for this is that high-frequency oscillatory fields should be oscillating too fast and be too low in intensity to affect a magnetite crystal receptor (Steiner and Ulbricht 1989; Kirschvink 1996). However, they should interfere with the electrons, which are involved in the radical-pair forming process. These properties make the application of RF fields a unique tool to study the involvement of a

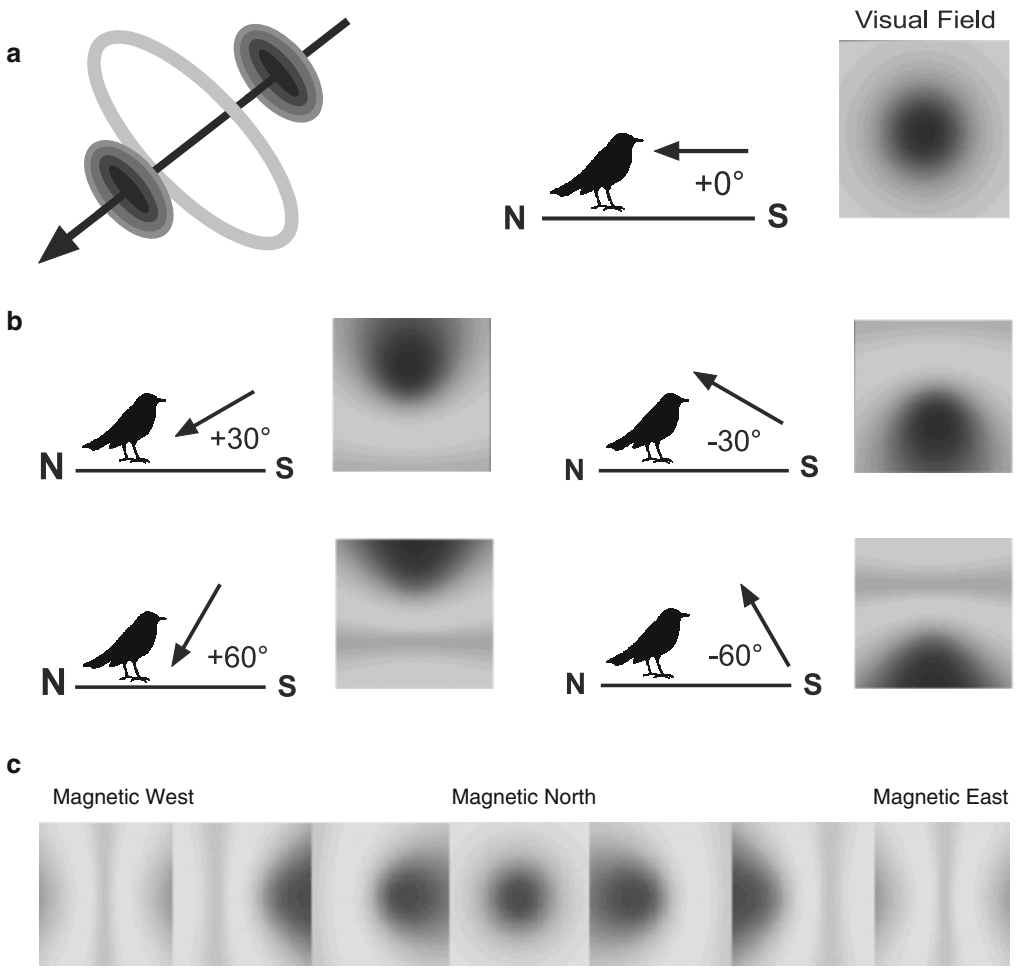

Fig. 20.4 Illustration of hypothetical light-dependent magnetic compass perception through magnetosensitive photoreceptors. (**a** *left*) Three-dimensional pattern of the magnetic field vector consisting of a dark area on each side of the magnetic field axis and a ring in the center. (**a** *right*) Magnetic modulation pattern perceived by an animal (bird) looking parallel along the magnetic field vector (*arrow*). (**b**) Magnetic modulation patterns at different latitudes (i.e., different magnetic field inclinations) in the Northern and Southern Hemisphere. (**c**) Magnetic modulation patterns perceived by animals facing different directions relative to the alignment of the magnetic field during a head scan from west to east (After Ritz et al. 2000)

radical-pair mechanism in magnetoreception. Thus, if RF disturbance leads to a behavioral response – either resulting in disorientation or a directional shift in magnetic orientation behavior – this treatment proves that whatever is involved in the process of magnetic orientation does involve a radical-pair forming process. In contrast, if magnetic compass orientation is solely based on a magnetite-based process, magnetic compass orientation should remain unchanged by the RF treatment.

RF interference has been applied to test the magnetic compass orientation performance of birds and mole rats: European robins and zebra finches exposed to RF fields aligned nonparallel to the geomagnetic field vector became disoriented when tested under either a broadband RF field or distinct single frequencies of 1.375 or 7 MHz (Ritz et al. 2004; Thalau et al. 2005; Keary et al. 2009). On the other hand, the orientation of mole rats, which is supposed to be mediated by a non-light-dependent magnetoreceptor, was not impaired by a RF field, supporting previous indications that their magnetic compass is light independent and based on magnetite (Thalau et al. 2006). These data provide the so far strongest, albeit indirect, support of a radical-pair-based magnetoreceptor mechanism in birds.

20.3.3 Involvement of Cryptochromes in Magnetosensitive Photoreception

A photoreceptor molecule involved in the primary magnetoreception process mediated by a light-dependent radical-pair mechanism as described above needs to meet a number of criteria. The putative receptor molecule needs to form radical pairs that persist long enough so that the radical-pair yields can be modified by an Earth-strength magnetic field

and localization in a spatially fixed relationship relative to each other (reviewed by Rodgers and Hore 2009; Liedvogel and Mouritsen 2010; Phillips et al. 2010a; Mouritsen and Hore 2012). The classical photopigments, like the opsins, do not possess the biochemical properties to form radical pairs and thus are unlikely to be involved in magnetoreception. In contrast, there are strong indications that cryptochromes are the thought-after candidates for the magnetoreception molecule. Cryptochromes are blue-green light photopigments, mainly known for their role in the animal circadian clock (e.g., Emery et al. 1998; Cashmore et al. 1999; Partch and Sancar 2005; Chaves et al. 2011). They are the only currently known vertebrate photoreceptor molecules that have the potential to form radical pairs upon excitation by light. The ancestral forms of cryptochromes, the photolyases, have been demonstrated to form radical-pair intermediates that persist long enough for magnetic field effects to occur (Weber et al. 2002; Giovani et al. 2003). More recently, also cryptochromes have been shown to produce persistent, spin-correlated radical pairs upon photoexcitation in several taxa of the animal kingdom, including insects, amphibians, and birds (Liedvogel et al. 2007b; Biskup et al. 2009; Schleicher et al. 2009).

Cryptochromes are ubiquitous and have been demonstrated in a large variety of organisms, including bacteria, plants, and animals, both invertebrates and vertebrates, including humans (for a review, see Chaves et al. 2011). In species known to use a magnetic compass, cryptochromes have been reported in *Drosophila melanogaster* (Emery et al. 1998), bullfrogs (Eun and Kang 2003), laboratory mice (Van der Horst et al. 1999), mole rats (Avivi et al. 2004), and birds. To date, cryptochrome expression has been reported in the retinae of two migratory bird species, European robins and garden warblers, and several nonmigratory species, including chicken (*Gallus gallus*) and zebra finches (*Taeniopygia guttatta;* Möller et al. 2004; Mouritsen et al. 2004; Niessner et al. 2011; reviewed by Liedvogel and Mouritsen 2010). A detailed neurohistological study of cryptochrome expression in robins and chicken recently revealed that the outer segments of the avian UV/V cones are most likely the primary sites of the light-dependent magnetoreceptor (Niessner et al. 2011). Niessner and colleagues found cryptochrome expression in virtually every cone across the entire retina, which is one of the requirements for the radical-pair model to work.

Recent studies with *Drosophila melanogaster* convincingly showed that cryptochromes are involved in light-dependent magnetoreception. Gegear and coworkers found that adult *Drosophila* are able to discriminate a magnetic field that is about ten times the intensity of the Earth's magnetic field (Gegear et al. 2008). This ability requires both a functional cryptochrome gene and broadband illumination that includes short-wavelength ($\lambda < 420$ nm) light. Also, cryptochrome-mediated effects of blue light on the circadian rhythm in *Drosophila* were shown to be influenced by magnetic fields (Yoshii et al. 2009). It has even been shown that the human variant of the cryptochrome can rescue light-dependent magnetosensitivity in a *Drosophila* mutant lacking *Drosophila* cryptochrome (Foley et al. 2011). Together, these findings suggest that magnetic field detection may be an intrinsic property of cryptochrome-based photo-signaling systems, from which light-dependent magnetoreception might have evolved (Phillips et al. 2010a). Still, more research – especially within naturally occurring field strengths – is needed to unambiguously separate observations of cryptochrome expression as a result of circadian rhythmicity and magnetoreception.

20.3.4 Is There a Common, Cryptochrome-Based Mechanism Underlying Light-Dependent Magnetoreception in Insects, Amphibians, and Birds?

Magnetic compass orientation in newts shows an abrupt transition from normal to 90° shifted orientation at about 475 nm, which has been suggested to be mediated by an antagonistic interaction of short- and long-wavelength inputs (Phillips and Borland 1992b; Deutschlander et al. 1999a; Phillips et al. 2001). In aquatic vertebrates, <480 nm light converts the fully oxidized form of the cryptochrome flavin chromophore (FAD_{ox}) into the radical, flavo-semiquinone form (FADH•), which in turn is excited by light between 480 and 650 nm (Zikihara et al. 2008; Biskup et al. 2009; Fig. 20.5a–c). This nicely corresponds with the spectral properties of magnetic compass orientation in newts, which made Phillips and coworkers propose that the fully oxidized and flavo-semiquinone forms of cryptochrome could provide the short- and long-wavelength inputs to the light-dependent magnetic compass, that is, providing antagonistic magnetically sensitive inputs (Phillips et al. 2010a). In view of the observation that amphibian cryptochromes can form spin-correlated radical pairs (Biskup et al. 2009), it makes cryptochrome molecules suitable candidates for an involvement in a radical-pair mechanism.

The behavioral and neurophysiological responses of insects to magnetic stimuli under UV and visible light are also consistent with the action spectra of photo-signaling pathways involving different redox forms of insect cryptochromes (Phillips et al. 2010a; Fig. 20.5b). Here, FAD is reduced to the anion radical $FAD^{\bullet -}$ upon blue-light excitation, which has been suggested to be the ground state (Ozturk et al. 2009). Exposure to darkness leads to a complete reoxidation. In addition, a *s*pectral antagonism has been shown to be involved in cryptochrome photo-signaling systems in vivo in both plants (Folta and Maruhnich 2007) and *Drosophila*

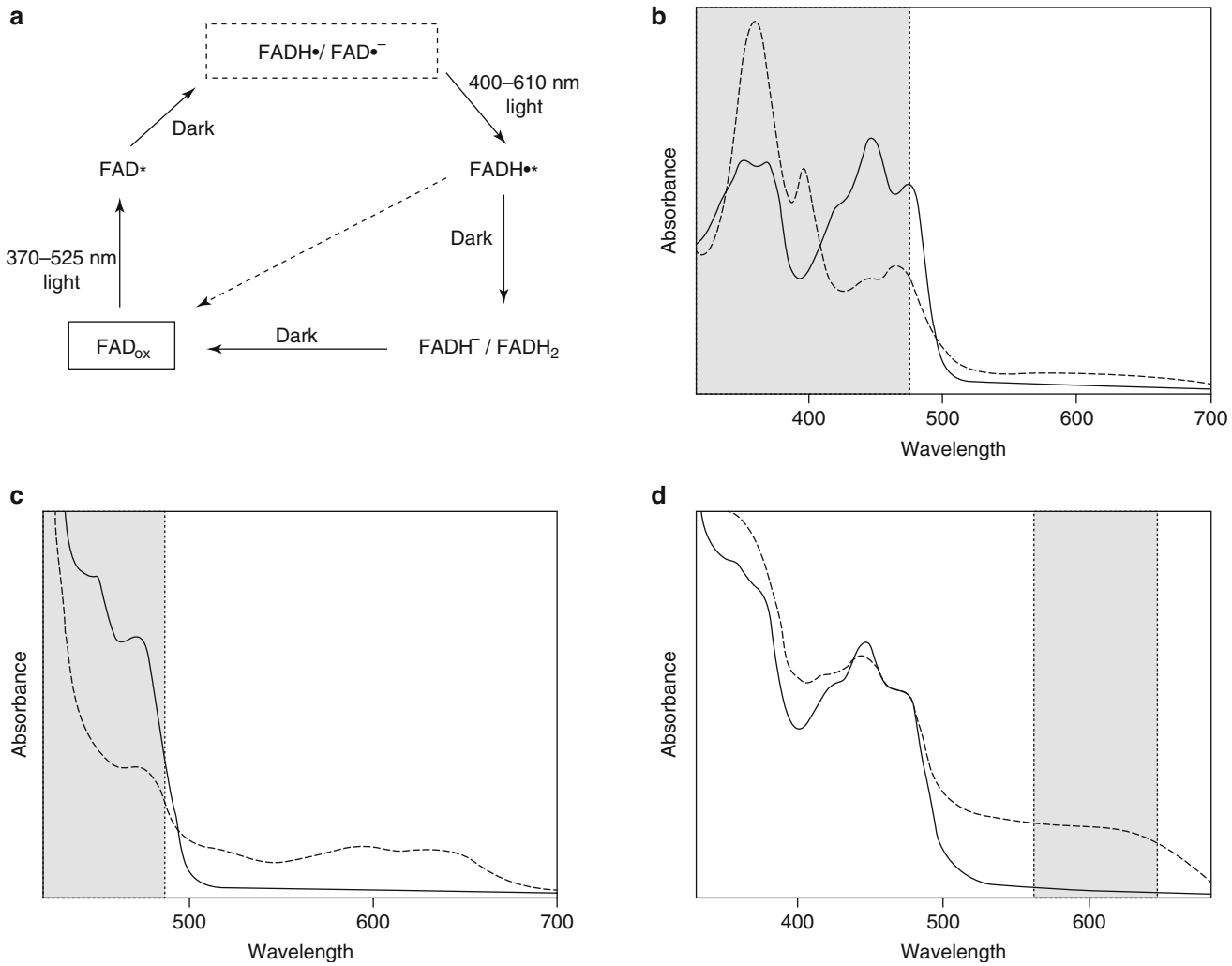

Fig. 20.5 (**a**) Interconversion of the three redox states of the flavin chromophore in a typical cryptochrome photosystem. The fully oxidized flavin chromophore (FAD_{ox}) is reduced by ~370–525 nm light to the partially reduced flavo-semiquinone radical ($FAD^{\bullet-}$ or FADH•) via a transient FAD*. Upon illumination by ~400–610 nm light, the flavo-semiquinone radicals can either convert to the fully reduced form (FADH- or $FADH_2$) or alternatively be reverted back to the fully oxidized form (FAD_{ox}). A magnetic field effect on photoreduction of the fully oxidized flavin chromophore (FAD_{ox}) has been generally accepted to be involved in the light-dependent magnetic compass. The photoreduction of the flavo-semiquinone radical ($FAD^{\bullet-}$ or FADH•) to the fully reduced form has been proposed to be involved in the antagonistic effect of the magnetic field on the response of the magnetic compass under long-wavelength light in amphibians and some insects (Phillips et al. 2010a). (**b**–**d**) Absorption of (**b**) insect cryptochrome (*Drosophila* DmCRY1; Berndt et al. 2007), (**c**) zebra fish cryptochrome (ZfCRY-DASH; Zikihara et al. 2008), and (**d**) chicken cryptochrome (GgCRY4; Ozturk et al. 2009). The *solid lines* give the absorption of the fully oxidized state (FAD_{ox}) and the *dotted lines* the absorption of the partially reduced form of the flavo-semiquinone radical ($FAD^{\bullet-}$ or FADH•). The *gray* highlighted wavelength ranges indicate changes in magnetic orientation behavior found in insects (**b**), amphibians (**c**), and birds (**d**) (Simplified after Phillips et al. (2010a))

(Hoang et al. 2008). In these systems, the short-wavelength-dependent responses are presumed to reflect a signaling pathway involving photoreduction of the fully oxidized to the radical form, while the antagonistic effects of long-wavelength light is suggested to further photoreduce the radical form to the fully reduced form, which is subsequently converted back into the fully oxidized form in the dark (Berndt et al. 2007; Hoang et al. 2008).

Still, it remains to be shown whether the long-wavelength-dependent photoreduction of the cryptochrome radical to the fully reduced form would be antagonistic to its effect on the initial photoreduction reaction, that is, whether the magnetic field would produce inverse or complementary patterns of response (Phillips et al. 2010a; Fig. 20.5).

In birds, an involvement of cryptochrome is less well clear. The well-oriented behavior under UV to 565 nm green light, abrupt transition to disorientation under 568 nm green-yellow light, and 90° shifted orientation or disorientation under longer wavelengths (Muheim et al. 2002; Wiltschko et al. 2010) fit the cry absorption spectrum only to a limited degree (Figs. 20.5d). Most cryptochromes in their fully oxidized form are insensitive above 500 nm (Liedvogel et al.

2007b), while birds are well oriented towards the migratory direction also under 565 nm green light (Muheim et al. 2002; Wiltschko et al. 2010). Also the change in orientation shown by birds around 565–570 nm is not reflected by the transition between neither of the known redox forms of bird cryptochromes (Liedvogel et al. 2007b; Ozturk et al. 2009). Thus, it remains unclear how the magnetic compass responses of birds under different light spectra can be explained by a cryptochrome-based magnetic compass.

20.4 Localization of the Light-Dependent Magnetoreceptor

Where in the animals are the light-dependent magnetoreceptors located, by which neuronal pathway is the information transmitted from the receptor to the brain, and where in the brain is the information processed? Magnetic fields can transmit through any type of organic matter; thus, magnetoreceptors can be located just about anywhere in animals' bodies. However, as outlined above, behavioral experiments clearly show that light is necessary for light-dependent magnetic orientation to function; thus, the receptors have to be located at a peripheral site of the animals that can be reached by light.

20.4.1 Extraretinal Receptor Sites for Light-Dependent Magnetoreceptor in Amphibians

In animals that have special photoreceptors-containing structures apart from the eyes, like the parietal eyes of reptiles or the pineal complex of fish, some reptiles, and the frontal organ of amphibians, light-dependent photoreception may take place in extraretinal photoreceptors (for review, see Phillips et al. 2010a). This has been elegantly demonstrated in Eastern red-spotted newts. Light-dependent magnetoreception of the shoreward orientation of newts takes place in photosensitive, extraocular photoreceptors in the pineal complex or hypothalamus (Deutschlander et al. 1999a). Newts trained to learn the magnetic alignment of the artificial shore in the training tank with the top of their head, but not their eyes, covered with a red-light filter demonstrate the same 90° shifted response shown by newts tested completely illuminated by red light (Deutschlander et al. 1999a). Thus, the light-sensitive-magnetosensitive receptors mediating shoreward orientation in newts are most likely located in extraocular photoreceptors in the pineal complex or hypothalamus. In anuran amphibians and lizards, photoreceptors with two antagonistic photoreception mechanisms, like those proposed to underlie the light-dependent magnetic compass in newts, have been found in the pineal complex (Eldred and Nolte 1978; Solessio and Engbretson 1993).

20.4.2 The Eyes as Sites for Light-Dependent Magnetoreception in Birds and Mammals

In birds, and also mammals, the only locations where light can reach specialized photoreceptors are the eyes. Unlike in newts, an involvement of the avian pineal in magnetoreception is very unlikely, despite of responsive cells in the avian pineal to magnetic field inversions (Semm 1983; Demaine and Semm 1985). Homing pigeons homed successfully after pinealectomy, while pinealectomized pied flycatchers (*Ficedula hypoleuca*) showed seasonally appropriate orientation as long as they received daily injections of melatonin, suggesting no crucially dependent involvement of the pineal in magnetoreception (Maffei et al. 1983; Schneider et al. 1994).

Extracellular electrophysiological recordings provided first evidence for the involvement of the visual center in light-dependent magnetoreception. Cells in the nucleus of the basal optic root (nBOR) and in the optic tectum showed magnetic responsiveness to changes in the direction of a magnetic field and to slow inversions of the vertical component of the magnetic field, with peak responses under wavelengths of 503 nm and 582 nm (Semm et al. 1984; Semm and Demaine 1986). The nBOR receives direct input from the contralateral retina, thus supporting the hypothesis that light-dependent magnetoreception takes place at locations innervated by the optic nerve, with the eyes as likely candidates. Unfortunately, these studies have been proven difficult to replicate; thus, any conclusions drawn from these findings have to be taken with caution.

Still, recent research on the neural basis of magnetoreception has largely substantiated these findings and provided new insights into the neural pathways and brain areas involved in information transfer and processing in both birds and mammals (e.g., Nemec et al. 2001, 2005; Heyers et al. 2007). A brain structure in the visual Wulst, named "Cluster N," connected to the retina via the thalamofugal pathway, has recently been identified and suggested to be involved in the processing of light-dependent magnetic information in migratory birds during nighttime (Mouritsen et al. 2005; Heyers et al. 2007; Zapka et al. 2010). Migratory birds with a (chemically) lesioned Cluster N were shown to be disoriented when tested for magnetic compass orientation, while their sunset and star compass remained intact and functional for orientation. These results strongly indicate that Cluster N is involved in processing magnetic compass information at nighttime under low light levels (Zapka et al. 2009).

As there is almost complete crossover of the fibers of the optic nerves, the left brain hemisphere gets its visual input almost exclusively from the right eye and vice versa. To test whether magnetic compass orientation is also lateralized, either one of the experimental birds' eyes is unilaterally covered with light-tight eye cops prohibiting any stimulus being perceived via this respective eye, and the birds are then tested

for magnetic compass orientation. Such lateralization experiments initially suggested that magnetic compass information is laterally processed with a dominance of the right eye and left brain hemisphere (Wiltschko et al. 2002, 2003b). However, follow-up experiments could not replicate these findings, neither on the receptor level nor on the level of higher integration areas in the brain, but rather suggest that both garden warblers and European robins have a magnetic compass in both eyes (Liedvogel et al. 2007a; Hein et al. 2010; Engels et al. 2012).

20.5 Outlook

During the past decade, new techniques and highly interdisciplinary research approaches have led to significant advances in our understanding of the biophysical and molecular mechanisms of light-dependent magnetoreception. The use of inducible transcription factors to study neuronal activity during magnetoreception, the search for cryptochrome expression at potential sites of magnetoreception, and the study of orientation behavior under RF fields all have provided valuable, but nevertheless indirect, evidence for the location, type, and biochemical and molecular mechanism of the magnetoreceptor.

With the development of reliable magnetic compass assays in model organisms such as *Drosophila melanogaster* (Phillips and Sayeed 1993; Dommer et al. 2008; Painter et al. 2013), zebra finches (Voss et al. 2007; Keary et al. 2009), and laboratory mice (Muheim et al. 2006), access to cryptochrome-deficient model animals has opened up another new and promising avenue in magnetoreception research, allowing direct tests of the involvement of cryptochromes or other molecules involved in the primary magnetoreception process.

To understand the type of magnetic stimulus and exact functionality of candidate brain regions that are involved in magnetic orientation, carefully controlled electrophysiological experiments are needed. Electrophysiology is extremely hard to carry out (and prone to artifacts) with magnetic stimuli involved, and all data reported to date have been proven difficult to repeat. However, these approaches will be key to (1) definitively prove the involvement of candidate brain areas in integrating magnetic information, (2) identify and characterize the exact type of (magnetic) stimulus that these brain areas most sensitively respond to (it could be a sudden change or a gradual variation of the azimuth, that is, the horizontal direction, of the resulting magnetic vector, or it could be an inversion of the inclination angle of the magnetic field vector), (3) understand the nature of (inhibitory/excitatory) neuronal responses (so far, nothing is known about the intrinsic neuronal dynamics of, for example, Cluster N), and (4) provide insight into the temporal scale of the putative response (pattern) after stimulus onset.

Acknowledgments We are grateful to John Phillips for inspiring discussions on magnetic compass orientation and magnetoreception. We thank the Swedish Research Council (RM), a Feodor Lynen Fellowship, Alexander von Humboldt Foundation (ML), and the Center for Animal Movement Research (CAnMove) at Lund University for the support.

References

Avivi A, Oster H, Joel A et al (2004) Circadian genes in a blind subterranean mammal III: molecular cloning and circadian regulation of cryptochrome genes in the blind subterranean mole rat, *Spalax ehrenbergi*_,_ _superspecies. J Biol Rhythms 19:22–34

Berndt A, Kottke T, Breitkreuz H et al (2007) A novel photoreaction mechanism for the circadian blue light photoreceptor Drosophila cryptochrome. J Biol Chem 282:13011–13021

Biskup T, Schleicher E, Okafuji A et al (2009) Direct observation of a photoinduced radical pair in a cryptochrome blue-light photoreceptor. Angew Chem Int Ed 48:404–407. doi:10.1002/anie.200803102

Cashmore AR, Jarillo JA, Wu Y-J, Liu D (1999) Cryptochromes: blue light receptors for plants and animals. Science 284:760–765

Chaves I, Pokorny R, Byrdin M et al (2011) The cryptochromes: blue light photoreceptors in plants and animals. Annu Rev Plant Biol 62:335–364. doi:10.1146/annurev-arplant-042110-103759

Demaine C, Semm P (1985) The avian pineal gland as an independent magnetic sensor. Neurosci Lett 62:119–122

Deutschlander ME, Borland SC, Phillips JB (1999a) Extraocular magnetic compass in newts. Nature 400:324–325

Deutschlander ME, Phillips JB, Borland SC (1999b) The case for light-dependent magnetic orientation in animals. J Exp Biol 202:891–908

Diego-Rasilla FJ, Luengo RM, Phillips JB (2013) Use of a light-dependent magnetic compass for y-axis orientation in European common frog (*Rana temporaria*) tadpoles. J Comp Physiol 199:619–628. doi:10.1007/s00359-013-0811-0

Diego-Rasilla FJ, Luengo RM, Phillips JB (2010) Light-dependent magnetic compass in Iberian green frog tadpoles. Naturwissenschaften 97:1077–1088. doi:10.1007/s00114-010-0730-7

Dommer DH, Gazzolo PJ, Painter MS, Phillips JB (2008) Magnetic compass orientation by larval Drosophila melanogaster. J Insect Physiol 54:719–726

Eldred WD, Nolte J (1978) Pineal photoreceptors: evidence for a vertebrate visual pigment with two physiologically active states. Vision Res 18:29–32

Emery P, So WV, Kaneko M et al (1998) CRY, a Drosophila clock and light-regulated cryptochrome, is a major contributor to circadian rhythm resetting and photosensitivity. Cell 95:669–679. doi:10.1016/S0092-8674(00)81637-2

Engels S, Hein CM, Lefeldt N et al (2012) Night-migratory songbirds possess a magnetic compass in both eyes. PLoS ONE 7:e43271. doi:10.1371/journal.pone.0043271

Eun BK, Kang HM (2003) Cloning and expression of cryptochrome2 in the bullfrog, _Rana catesbeiana_. Mol Cells 16:239–244

Foley LE, Gegear RJ, Reppert SM (2011) Human cryptochrome exhibits light-dependent magnetosensitivity. Nat Commun 2:356. doi:10.1038/ncomms1364

Folta KM, Maruhnich SA (2007) Green light: a signal to slow down or stop. J Exp Bot 130. doi:10.1093/jxb/erm130

Freake MJ, Muheim R, Phillips JB (2006) Magnetic maps in animals: a theory comes of age? Q Rev Biol 81:327–347. doi:10.1086/511528

Freake MJ, Phillips JB (2005) Light-dependent shift in bullfrog tadpole magnetic compass orientation: evidence for a common magnetoreception mechanism in anuran and urodele amphibians. Ethology 111:241–254

Gegear RJ, Casselman A, Waddell S, Reppert SM (2008) Cryptochrome mediates light-dependent magnetosensitivity in *Drosophila*. Nature 454:1014–1018. doi:10.1038/nature07183

Giovani B, Byrdin M, Ahmad M, Brettel K (2003) Light-induced electron-transfer in a cryptochrome blue-light photoreceptor. Nat Struct Biol 10:489–490

Hein CM, Zapka M, Heyers D et al (2010) Night-migratory garden warblers can orient with their magnetic compass using the left, the right or both eyes. J R Soc Interface 7:S227–S233. doi:10.1098/rsif.2009.0376.focus

Henbest KB, Maeda K, Hore PJ et al (2008) Magnetic-field effect on the photoactivation reaction of Escherichia coli DNA photolyase. Proc Natl Acad Sci 105:14395–14399. doi:10.1073/pnas.0803620105

Henbest KB, Rodgers CT, Hore PJ, Timmel CR (2004) Radio frequency magnetic field effects on a radical recombination reaction: a diagnostic test for the radical pair mechanism. J Am Chem Soc 126:8102–8103

Heyers D, Manns M, Luksch H et al (2007) A visual pathway links brain structures active during magnetic compass orientation in migratory birds. PLoS ONE 2:e937. doi:10.1371/journal.pone.0000937

Hoang N, Schleicher E, Kacprzak S et al (2008) Human and Drosophila cryptochromes are light activated by flavin photoreduction in living cells. PLoS Biol 6:e160. doi:10.1371/journal.pbio.0060160

Van der Horst GTJ, Muijtjens M, Kobayashi K et al (1999) Mammalian Cry1 and Cry2 are essential for maintenance of circadian rhythms. Nature 398:627–630

Johnsen S, Lohmann KJ (2008) Magnetoreception in animals. Phys Today 61:29. doi:10.1063/1.2897947

Keary N, Ruploh T, Voss J et al (2009) Oscillating magnetic field disrupts magnetic orientation in Zebra finches, *Taeniopygia guttata*. Front Zool 6:25. doi:10.1186/1742-9994-6-25

Kirschvink JL (1996) Microwave absorption by magnetite: a possible mechanism for coupling nonthermal levels of radiation to biological systems. Bioelectromagnetics 17:187–194

Liedvogel M, Feenders G, Wada K et al (2007a) Lateralized activation of Cluster N in the brains of migratory songbirds. Eur J Neurosci 25:1166–1173. doi:10.1111/j.1460-9568.2007.05350.x

Liedvogel M, Maeda K, Henbest K et al (2007b) Chemical magnetoreception: bird cryptochrome 1a is excited by blue light and forms long-lived radical-pairs. PLoS ONE 2:e1106. doi:10.1371/journal.pone.0001106

Liedvogel M, Mouritsen H (2010) Cryptochromes—a potential magnetoreceptor: what do we know and what do we want to know? J R Soc Interface 7:S147–S162. doi:10.1098/rsif.2009.0411.focus

Lohmann KJ, Lohmann CM (1993) A light-independent magnetic compass in the leatherback sea turtle. Biol Bull 185:149–151

Maeda K, Henbest KB, Cintolesi F et al (2008) Chemical compass model of avian magnetoreception. Nature 453:387–390. doi:10.1038/nature06834

Maeda K, Robinson AJ, Henbest KB et al (2012) Magnetically sensitive light-induced reactions in cryptochrome are consistent with its proposed role as a magnetoreceptor. Proc Natl Acad Sci 109:4774–4779. doi:10.1073/pnas.1118959109

Maffei L, Meschini E, Papi F (1983) Pineal body and magnetic sensitivity: homing in pinealectomized pigeons under overcast skies. Z Für Tierpsychol 62:151–156

Marhold S, Wiltschko W, Burda H (1997) A magnetic polarity compass for direction finding in a subterranean mammal. Naturwissenschaften 84:421–423

Möller A, Sagasser S, Schierwater B, Wiltschko W (2004) Retinal cryptochrome in a migratory bird: a possible transducer for the avian magnetic compass. Naturwissenschaften 91:585–588

Mouritsen H, Feenders G, Liedvogel M et al (2005) Night-vision brain area in migratory songbirds. Proc Natl Acad Sci U S A 102:8339–8344

Mouritsen H, Hore P (2012) The magnetic retina: light-dependent and trigeminal magnetoreception in migratory birds. Curr Opin Neurobiol 22:343–352. doi:10.1016/j.conb.2012.01.005

Mouritsen H, Janssen-Bienhold U, Liedvogel M et al (2004) Cryptochromes and neuronal-activity markers colocalize in the retina of migratory birds during magnetic orientation. Proc Natl Acad Sci U S A 101:14294–14299. doi:10.1073/pnas.0405968101

Muheim R, Bäckman J, Åkesson S (2002) Magnetic compass orientation in European robins is dependent on both wavelength and intensity of light. J Exp Biol 205:3845–3856

Muheim R, Edgar NM, Sloan KA, Phillips JB (2006) Magnetic compass orientation in C57BL/6J mice. Learn Behav 34:366–373

Nemec P, Altmann J, Marhold S et al (2001) Neuroanatomy of magnetoreception: the superior colliculus involved in magnetic orientation in a mammal. Science 294:366–368

Nemec P, Burda H, Oelschläger HA (2005) Towards the neural basis of magnetoreception: a neuroanatomical approach. Naturwissenschaften 92:151–157

Niessner C, Denzau S, Gross JC et al (2011) Avian ultraviolet/violet cones identified as probable magnetoreceptors. PLoS ONE 6:e20091. doi:10.1371/journal.pone.0020091

Ozturk N, Selby CP, Song S-H et al (2009) Comparative photochemistry of animal type 1 and type 4 cryptochromes. Biochemistry 48:8585–8593. doi:10.1021/bi901043s

Painter MS, Dommer DH, Altizer WW et al (2013) Spontaneous magnetic orientation in larval Drosophila shares properties with learned magnetic compass responses in adult flies and mice. J Exp Biol 216:1307–1316. doi:10.1242/jeb.077404

Partch CL, Sancar A (2005) Photochemistry and photobiology of cryptochrome blue-light photopigments: the search for a photocycle. Photochem Photobiol 81:1291–1304

Phillips JB, Borland SC (1992a) Wavelength-specific effects of light on magnetic compass orientation of the Eastern red-spotted newt, *Notophthalmus viridescens*. Ethol Ecol Evol 4:33–42

Phillips JB, Borland SC (1992b) Behavioural evidence for use of light-dependent magnetoreception mechanism by a vertebrate. Nature 359:142–144

Phillips JB, Borland SC (1992c) Magnetic compass orientation is eliminated under near-infrared light in the Eastern red-spotted newt, *Notophthalmus viridescens*. Anim Behav 44:796–797

Phillips JB, Deutschlander ME, Freake MJ, Borland SC (2001) The role of extraocular photoreceptors in newt magnetic compass orientation: parallels between light-dependent magnetoreception and polarized light detection. J Exp Biol 204:2543–2552

Phillips JB, Jorge PE, Muheim R (2010a) Light-dependent magnetic compass orientation in amphibians and insects: candidate receptors and candidate molecular mechanisms. J R Soc Interface R Soc 7:S241–S256. doi:10.1098/rsif.2009.0459.focus

Phillips JB, Muheim R, Jorge PE (2010b) A behavioral perspective on the biophysics of the light-dependent magnetic compass: a link between directional and spatial perception? J Exp Biol 213:3247–3255. doi:10.1242/jeb.020792

Phillips JB, Sayeed O (1993) Wavelength-dependent effects of light on magnetic compass orientation in *Drosophila melanogaster*. J Comp Physiol 172:303–308

Rappl R, Wiltschko R, Weindler P et al (2000) Orientation behaviour of garden warblers, *Sylvia borin*, under monochromatic light of various wavelengths. Auk 117:256–260

Ritz T, Adem S, Schulten K (2000) A model for photoreceptor-based magnetoreception in birds. Biophys J 78:707–718. doi:10.1016/S0006-3495(00)76629-X

Ritz T, Ahmad M, Mouritsen H et al (2010) Photoreceptor-based magnetoreception: optimal design of receptor molecules, cells, and neuronal processing. J R Soc Interface 7:S135–S146. doi:10.1098/rsif.2009.0456.focus

Ritz T, Dommer DH, Phillips JB (2002) Shedding light on vertebrate magnetoreception. Neuron 34:503–506

Ritz T, Thalau P, Phillips JB et al (2004) Resonance effects indicate a radical-pair mechanism for avian magnetic compass. Nature 429:177–180. doi:10.1038/nature02534

Rodgers CT, Hore PJ (2009) Chemical magnetoreception in birds: the radical pair mechanism. Proc Natl Acad Sci U S A 106:353–360. doi:10.1073/pnas.0711968106

Schleicher E, Bittl R, Weber S (2009) New roles of flavoproteins in molecular cell biology: blue-light active flavoproteins studied by electron paramagnetic resonance. FEBS J 276:4290–4303. doi:10.1111/j.1742-4658.2009.07141.x

Schneider T, Thalau HP, Semm P, Wiltschko W (1994) Melatonin is crucial for the migratory orientation of pied flycatchers, *Ficedula hypoleuca*. J Exp Biol 194:255–262

Schulten K (1982) Magnetic field effects in chemistry and biology. Adv Solid State Phys 22:61–83

Schulten K, Swenberg CE, Weller A (1978) A biomagnetic sensory mechanism based on magnetic field modulated coherent electron spin motion. Z für Phys Chem 111:1–5. doi:10.1524/zpch.1978.111.1.001

Semm P (1983) Neurobiological investigations on the magnetic sensitivity of the pineal gland in rodents and pigeons. Comp Biochem Physiol 76:683–689

Semm P, Demaine C (1986) Effects of earth-strength magnetic stimuli on the pineal gland and central nervous neurons. A short review. Biophys. Eff. Steady Magn. Fields. Springer Verlag, Berlin, pp 117–119

Semm P, Nohr D, Demaine C, Wiltschko W (1984) Neural basis of the magnetic compass: interactions of visual, magnetic and vestibular inputs in the pigeon's brain. J Comp Physiol 155:283–288

Solessio E, Engbretson GA (1993) Antagonistic chromatic mechanisms in photoreceptors of the parietal eye of lizards. Nature 364:442–445

Solov'yov IA, Mouritsen H, Schulten K (2010) Acuity of a cryptochrome and vision-based magnetoreception system in birds. Biophys J 99:40–49. doi:10.1016/j.bpj.2010.03.053

Steiner UE, Ulbricht (1989) Magnetic field effects in chemical kinetics and related phenomena. Chem Rev 89:51–147

Thalau P, Ritz T, Burda H et al (2006) The magnetic compass mechanisms of birds and rodents are based on different physical principles. J R Soc Interface 3:583–587. doi:10.1098/rsif.2006.0130

Thalau P, Ritz T, Stapput K et al (2005) Magnetic compass orientation of migratory birds in the presence of a 1.315 MHz oscillating field. Naturwissenschaften 92:86–90

Vacha M, Půžová T, Drštková D (2008) Effect of light wavelength spectrum on magnetic compass orientation in Tenebrio molitor. J Comp Physiol A Neuroethol Sens Neural Behav Physiol 194:853–859. doi:10.1007/s00359-008-0356-9

Vacha M, Soukopova H (2004) Magnetic orientation in the mealworm beetle *Tenebrio* and the effect of light. J Exp Biol 207:1241–1248

Voss J, Keary N, Bischof H-J (2007) The use of the geomagnetic field for short distance orientation in zebra finches. NeuroReport 18:1053–1057. doi:10.1097/WNR.0b013e32818b2a21

Weber S, Kay CWM, Mogling H et al (2002) Photoactivation of the flavin cofactor in Xenopus laevis (6–4) photolyase: observation of a transient tyrosyl radical by time-resolved electron paramagnetic resonance. Proc Natl Acad Sci 99:1319–1322

Wiltschko R, Ritz T, Stapput K et al (2005) Two different types of light-dependent responses to magnetic fields in birds. Curr Biol 15:1518–1523

Wiltschko R, Stapput K, Thalau P, Wiltschko W (2010) Directional orientation of birds by the magnetic field under different light conditions. J R Soc Interface 7:S163–S177. doi:10.1098/rsif.2009.0367.focus

Wiltschko R, Wiltschko W (1995) Magnetic orientation in animals. Springer, Berlin

Wiltschko R, Wiltschko W (1998) Pigeon homing: effect of various wavelengths of light during displacement. Naturwissenschaften 85:164–167

Wiltschko W (1968) Über den Einfluss statischer Magnetfelder auf die Zugorientierung der Rotkehlchen, _Erithacus rubecula_. Z Für Tierpsychol 25:537–558

Wiltschko W (1978) Further analysis of the magnetic compass of migratory birds. Anim. Migr. Navig. Homing. Springer, Berlin, pp 301–310

Wiltschko W, Gesson M, Stapput K, Wiltschko R (2004a) Light-dependent magnetoreception in birds: interaction of at least two different receptors. Naturwissenschaften 91:130–134

Wiltschko W, Moller A, Gesson M et al (2004b) Light-dependent magnetoreception in birds: analysis of the behaviour under red light after pre-exposure to red light. J Exp Biol 207:1193–1202. doi:10.1242/jeb.00873

Wiltschko W, Munro U, Ford H, Wiltschko R (1993) Red light disrupts magnetic orientation of migratory birds. Nature 364:525–527

Wiltschko W, Munro U, Ford H, Wiltschko R (2003a) Magnetic orientation in birds: non-compass responses under monochromatic light of increased intensity. Proc R Soc Lond Ser B Biol Sci 270:2133–2140

Wiltschko W, Munro U, Ford H, Wiltschko R (2003b) Lateralization of magnetic compass orientation in silvereyes, *Zosterops l. lateralis*. Aust J Zool 51:597–602

Wiltschko W, Stapput K, Thalau P, Wiltschko R (2006) Avian magnetic compass: fast adjustment to intensities outside the normal functional window. Naturwissenschaften 93:300–304

Wiltschko W, Traudt J, Güntürkün O et al (2002) Lateralization of magnetic compass orientation in a migratory bird. Nature 419:467–470

Wiltschko W, Wiltschko R (2005) Magnetic orientation and magnetoreception in birds and other animals. J Comp Physiol 191:675–693

Wiltschko W, Wiltschko R (1981) Disorientation of inexperienced young pigeons after transportation in total darkness. Nature 291:433–434

Wiltschko W, Wiltschko R (2001) Light-dependent magnetoreception in birds: the behaviour of European robins, *Erithacus rubecula*, under monochromatic light of various wavelengths and intensities. J Exp Biol 204:3295–3302

Wiltschko W, Wiltschko R (1999) The effect of yellow and blue light on magnetic compass orientation in European robins, *Erithacus rubecula*. J Comp Physiol A Neuroethol Sens Neural Behav Physiol 184:295–299. doi:10.1007/s003590050327

Winklhofer M, Dylda E, Thalau P et al (2013) Avian magnetic compass can be tuned to anomalously low magnetic intensities. Proc R Soc B Biol Sci. doi:10.1098/rspb.2013.0853

Yoshii T, Ahmad M, Helfrich-Förster C (2009) Cryptochrome mediates light-dependent magnetosensitivity of Drosophila's circadian clock. PLoS Biol 7:e1000086. doi:10.1371/journal.pbio.1000086

Zapka M, Heyers D, Hein CM et al (2009) Visual but not trigeminal mediation of magnetic compass information in a migratory bird. Nature 461:1274–1277. doi:10.1038/nature08528

Zapka M, Heyers D, Liedvogel M et al (2010) Night-time neuronal activation of Cluster N in a day- and night-migrating songbird. Eur J Neurosci 32:619–624. doi:10.1111/j.1460-9568.2010.07311.x

Zikihara K, Ishikawa T, Todo T, Tokutomi S (2008) Involvement of electron transfer in the photoreaction of Zebrafish cryptochrome-DASH. Photochem Photobiol 84:1016–1023. doi:10.1111/j.1751-1097.2007.00364.x

Phototoxicity

21

Lars Olof Björn and Pirjo Huovinen

21.1 Introduction

Phototoxicity means that something which is not toxic in itself is converted into a toxin or produces a toxin by the action of light. We can divide phototoxicity into several classes:

Type I phototoxicity arises when a pigment, after absorption of light and acquiring an excited state, either combines directly with an important cell constituent (Fig. 21.1) or transfers electrons or hydrogen atoms. The transfer may take place from or to another molecule, which then becomes a toxic radical or radical ion or produces toxins in subsequent reactions. As an example of the action of a type I phototoxin, we show in Fig. 21.1 how 8-methoxypsoralen (MOPS in medical jargon) combines with thymine residues in DNA.

Type II phototoxicity arises when a pigment (photosensitizer) after absorption of light goes from the excited singlet state to a triplet state, and then reacts with molecular oxygen and produces singlet excited oxygen (see Chap. 1), which is highly toxic.

In some cases, a pigment molecule excited by light absorption transfers an electron to molecular oxygen, thereby producing superoxide anion (see Fig. 21.2). According to the above definitions, this is type I phototoxicity, but in the literature it has also been designated type II phototoxicity, because in practice it is easier to distinguish between oxygen-independent and oxygen-dependent phototoxicity. The main cellular targets of both type I and II phototoxins are DNA, membrane lipids, and membrane proteins. A wide variety of organisms (except those having special protection systems) can be poisoned by most of the substances; that is, they are rather unspecific with regard to poisoned organism.

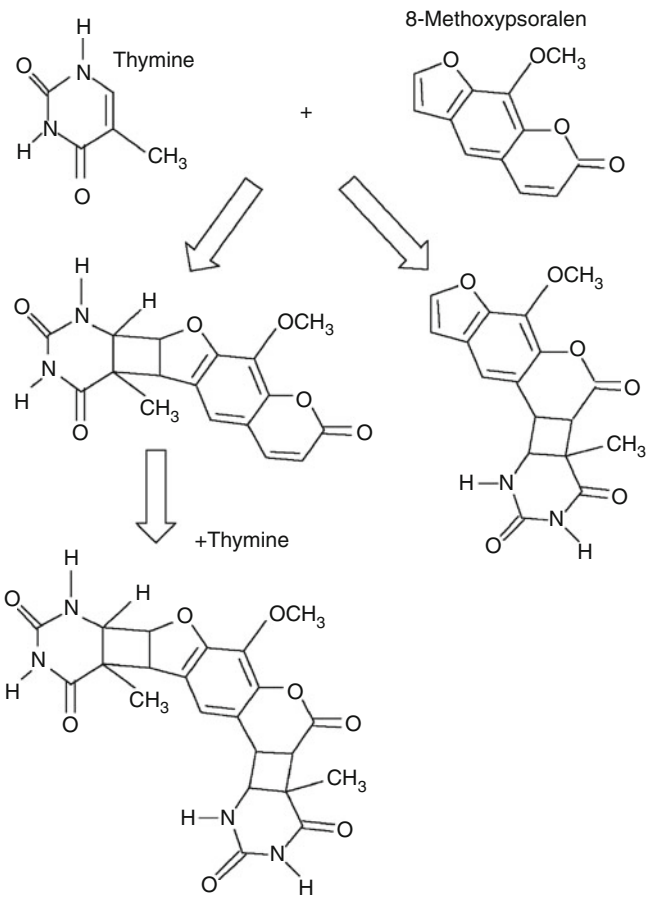

Fig. 21.1 Formation of photoadduct between 8-methoxypsoralen and thymine residues in DNA. The thymine is shown for simplicity as free molecules, but is in reality part of a DNA molecule. One 8-methoxypsoralen molecule can combine with two thymine residues, and if they are bound to opposite DNA strands, cross-bridges can form between the strands. Although "phototoxicity" sounds dangerous, this and other similar reactions are also exploited in phototherapy of certain diseases

L.O. Björn (✉)
School of Life Science, South China Normal University, Guangzhou, China

Department of Biology, Lund University, Lund, Sweden
e-mail: Lars_Olof.Bjorn@biol.lu.se

P. Huovinen
Universidad Austral de Chile, Instituto de Ciencias Marinas y Limnológicas, Valdivia, Chile
e-mail: pirjo.huovinen@uach.cl

L.O. Björn (ed.), *Photobiology: The Science of Light and Life*,
DOI 10.1007/978-1-4939-1468-5_21, © Springer Science+Business Media New York 2015

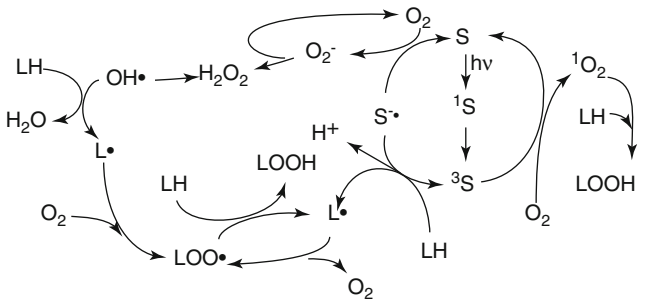

Fig. 21.2 Diagram showing how a pigment (S), excited by light (hυ) via an excited singlet state (^{1}S) to an excited triplet state (^{3}S), can damage a membrane lipid (LH) in several ways (note that the lipid molecules enter the reactions at four points in the diagram). (*1*) Type II reaction (*right part* of the diagram): the triplet pigment may react with triplet (ground state) oxygen (O_2) to form singlet oxygen ($^1O_2$), which can directly convert the lipid to a lipid peroxide (LOOH). (*2*) Classical type I reaction (*lower part* of the diagram): the triplet pigment abstracts a hydrogen atom from the lipid, creating a lipid radical (L•), which combines with triplet oxygen to form a lipid peroxy radical (LOO•). The latter abstracts a hydrogen atom from another lipid molecule to form a lipid peroxide. In this way a new lipid radical is formed, and a chain reaction is created. (*3*) Oxygen-dependent hydrogen abstraction (*upper part* of the diagram): an electron is donated to triplet oxygen, creating superoxide anion, which via formation of hydrogen peroxide and hydroxide radical abstracts hydrogen from the lipid. Also in this case the lipid is degraded to lipid peroxide, and a chain reaction is initiated

As a third type of phototoxicity, we can categorize those cases when a substance is converted into a toxin by a photochemical reaction which does not fall into any of the above categories.

As an example in which several mechanisms contribute to the photodestructive action, we show in Fig. 21.2 a schematic description of how membrane lipids are peroxidized by a photoexcited pigment (see Samadi et al. 2001).

An interesting consequence of lipid peroxidation is that a weak light (ultraweak luminescence) is emitted during the reaction. Lipid peroxidative chain reactions can be initiated also in ways other than through phototoxic action.

In our disposition of the topic "phototoxicity," we shall not follow the categorization into types I and II, but rather subdivide into the different contexts in which phototoxicity has been observed. We shall not include photoallergic reactions here, which, as they involve the immune system, are of a different character. Photoallergy will be treated in Chap. 24.

21.2 Phototoxicity in Plant Defense

The most important defenses of plants against parasites and grazers are of a chemical nature, and among chemical defenses phototoxicity plays an important role, especially among flowering plants. The phototoxic substances employed by plants can also affect people when they appear in food, perfumes, and other cosmetic products and even if we just touch certain plants.

Downum (1992) estimates that 75–100 different phototoxic molecules have been isolated from flowering plants. Phototoxins or phototoxic activity has been reported for about 40 of more than 100 angiosperm families, representing all subclasses except Alismatidae and Arecidae. Many plants have several phototoxic substances. From *Ammi majus* as well as from *Angelica archangelica*, the following ones are reported: angelicin, bergapten, 8-methoxypsoralen, and pimpinellin—from the former one, in addition, furocoumarin and from the latter, one psoralen. The plant family Apiaceae (former name Umbelliferae) dominates the most important cases of phototoxicity of to humans.

The phototoxins affect bacteria, fungi, nematodes, insects, and other organisms. This wide spectrum is due to the fact that the toxins attack cellular constituents common to all cells. DNA is a major target for type I acting chemicals, such as acetophenones, coumarins, furanochromones, furanoquinolines, pterocarpans, and sesquiterpenes. Examples of type II acting compounds are isoquinolines and thiophenes.

Photosensitizers generally have many double bonds, that is, many π-electrons, and most of them are polycyclic. The most common types in plants are acetylenes and furanocoumarins, but many other types also occur.

Since absorption of ultraviolet radiation is a common feature of organic compounds, and absorption for polycyclic systems and acetylenes with conjugated triple bonds (compounds with many π-electrons) extends into the UV-A region, it is not surprising that UV-A (of which there is much more in daylight than of UV-B) in most cases is the most important spectral region for inflicting phototoxicity. However, there are exceptions, and hypericin (present in *Hypericum*, St. John's wort) with its many fused phenyl rings absorbs and is excited to phototoxicity even by yellow and orange light, while some other substances require UV-B radiation. Detailed information on action spectra is still lacking in most cases. Guesses made based on absorption spectra are not reliable, since cases are known in which the phototoxic action takes place with radiation of longer wavelength than that absorbed by the pure substance. The reason for this is probably that the spectrum is shifted when the substance binds to cellular components.

The mode of action of hypericin has been debated, but it has now been established (Delaey et al. 2000) that it required oxygen for phototoxicity. Like several other phototoxic compounds from plants (e.g., psoralen, 8-methoxypsoralen), it has been used in the phototherapy of diseases. Hypericin

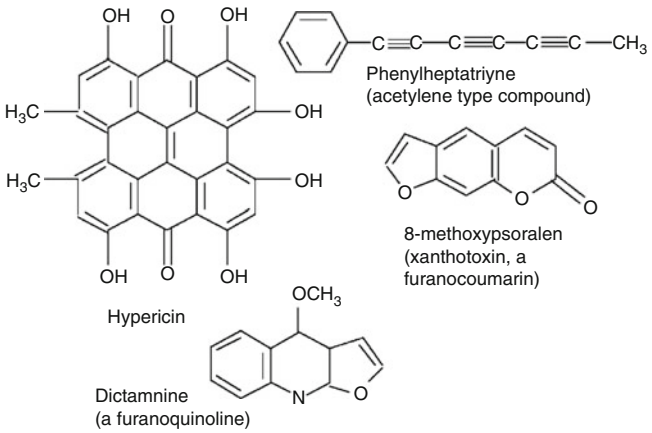

Fig. 21.3 Examples of phototoxic substances from plants

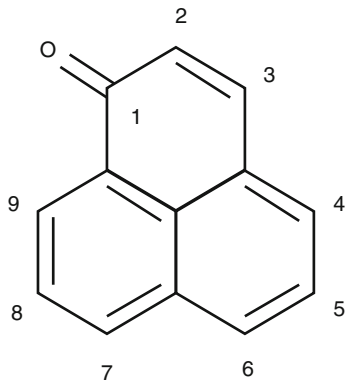

Fig 21.4 Structure of phenalenone in benzene solution

may be particularly dangerous for the lens of the eye (Ehrenshaft et al. 2013).

Specific plant species causing problems for humans and domestic animals naturally vary among countries, but the following are worth mentioning here:

Fig, *Ficus carica*. Fig can be troublesome only for those involved in picking and handling them professionally. One source speculates that fig could have caused trouble for Adam and Eve!

Angelica, *Angelica archangelica*. This and other *Angelica* species are used as traditional medicine from Korea to Lapland and also in drinks. They have caused problems for growers and collectors.

Buckwheat, *Fagopyrum esculentum*. Causes trouble mainly in grazing cattle.

Celery, *Apium graveolens*. Has caused burns when ingested before visiting suntan parlor. Contains 5-methoxypsoralen, 8-methoxypsoralen (xanthotoxin), and 4,5′,8-trimethylpsoralen. Of special interest is that this plant can contain tenfold increased contents of psoralen derivatives after infection with a fungus, *Sclerotinia sclerotium* (pink rot disease). Persons handling celery professionally are at risk. Disease-resistant celery contains increased levels of furocoumarins (Fig. 21.3).

Hogweed (*Heracleum*), especially Russian hogweed (*Heracleum mantegazzianum*). Light produces severe blisters in skin that has been in touch with the plant. The plant has spread over large areas of Europe and North America. *Heracleum* species contain angelicin, bergapten, pimpinellin, 5-methoxypsoralen, and other related substances.

Spring parsley (also erroneously called wild carrot), *Cymopterus watsonii*, growing in Oregon, Nevada, and western Utah. Problems with grazing sheep and cattle. Newborn lambs and calves die because mothers become so touch sensitive that they refuse nursing. The plant contains furocoumarins, 8-methoxypsoralen (xanthotoxin), and bergapten.

Lei flowers, especially *Pelea anisata*. Leis are the greeting wreaths that visitors receive on their arrival to Hawaii.

Burning bush of Moses (also called gas plant), *Dictamnus albus*. The plant grows wild in Europe and Asia and is used as a garden plant also in other parts of the world. It belongs to the family Rutaceae, which harbors also other plants with some phototoxicity, among them *Citrus* species and *Ruta graveolens*, garden rue.

St. John's wort. *Hypericum* species contain hypericin and can cause trouble both to grazing animals and to persons who consume drinks based on *Hypericum* extracts and are exposed to light afterwards.

Some of the phytophototoxins are used for medical treatments. The most noteworthy example is treatment of vitiligo and psoriasis with 8-methoxypsoralen and related substances. In fact, the juice of the Egyptian plant *Ammi majus* has been used for this purpose since 2000 B.C. (Pathak and Fitzpatrick 1992). We can only give some examples of detailed mechanisms of action in phototoxicity. For further information on phototoxic plants and plant phototoxins, see Pathak (1986), Downum (1992), Lovell (1993), and the following Internet sites: (1) http://telemedicine.org/Botanica/Bot5.htm and (2) http://www.ars-grin.gov/cgi-bin/duke/chemical_activity.pl.

Flors and Nonell (2006) have described phototoxic phytoalexins (phytoalexins are toxins that are induced and not present in unstressed plants) having a phenalenone group (Fig. 21.4) in their molecular structure. They produce singlet oxygen upon irradiation with UV-A to blue light and are toxic to fungi. They were first found in Haemodoraceae and Musaceae (Cooke and Edwards 1981), but subsequently found to be common not only in members of these families but also in Strelitziaceae. They were so long overlooked because they do not occur in unstressed plants. Related substances are present also in species of Annonaceae, Lauraceae, Magnoliaceae, Fumariaceae, Menispermaceae, and Papaveraceae (Flors and Nonell 2006).

21.3 Phototoxins of Fungal Plant Parasites

Phototoxins are not used only for plant defense but also for attack on plants by parasitic fungi. So far only one case has been thoroughly researched, but a number of plant pathogenic fungi produce photosensitizing substances. A review of the subject (Daub and Ehrenshaft 2000) has recently appeared.

The best known example of a plant parasite using a phototoxin to weaken its host is the genus *Cercospora*. About 500 parasitic *Cercospora* species are known and cause, for example, leaf spot of sugar beet, gray leaf spot of corn, purple seed stain of soybean, frogeye leaf spot of tobacco, and brown eye spot of coffee. For sugar beet the active pigment, cercosporin (Fig. 21.5), has been isolated from 34 *Cercospora* species grown in culture, while other species do not produce cercosporin and still can parasitize plants.

Cercosporin is a type II phototoxin. After reaching its triplet state during illumination, it reacts with oxygen to form singlet oxygen. The singlet oxygen destroys the cell membrane of host cells, which leads to leakage of nutrients to the fungus.

Of course, the fungus has cell membranes which could be damaged by cercosporin, so it must have some defense against its own toxin. In culture, they can accumulate up to millimolar toxin in the medium without observable toxic effects. In fact, it defends itself in two ways:

1. As long as the cercosporin is inside the hyphae, it is kept in a reduced form, which in light produces only a small amount of singlet oxygen. After secretion to the environment, it is oxidized to the highly active form. The two forms can be easily distinguished under the microscope, since the reduced form has a green fluorescence and the oxidized one a red fluorescence.
2. In addition, the fungus is extraordinarily well equipped with a set of triplet and singlet oxygen quenchers. That they are efficient is shown by the fact that *Cercospora* is resistant also to the effects of other singlet oxygen–producing phototoxins. Among the quenchers of singlet oxygen pyridoxine is thought to be particularly important for *Cercospora*.

Interestingly, *Cercospora* does not produce cercosporin in darkness (when it would be of no use); its synthesis is triggered by light.

Pigments having structures related to cercosporin (perylenequinones, see Fig. 25.1), and presumably having a corresponding function, are produced by a number of other fungi: by *Cladosporium* species, by the bamboo pathogens *Shiraia bambusicola* and *Hypocrella bambusae*, and by *Stemphylium botryosum* and some *Alternaria* and *Elsinoe* species. Also, light-requiring fungal toxins of other types are known, produced by *Cercospora* species and *Dothistroma pini* (Jalal et al. 1992; Stoessl et al. 1990).

21.4 Phototoxic Drugs and Cosmetics

Many phototoxic drugs are either antibiotics or medications for blood pressure and heart disease, but there are also others. In combination with light, they may cause extreme sunburn, vesicles, hives, and edema. Among antibiotics, photosensitivity reactions have more commonly been noted after administration of the following: doxycycline ("Vibramycin," etc.), demeclocycline, tetracycline (Fig. 21.6), nalidixic acid, and lomefloxacin. For blood pressure and heart medications, a similar short list includes

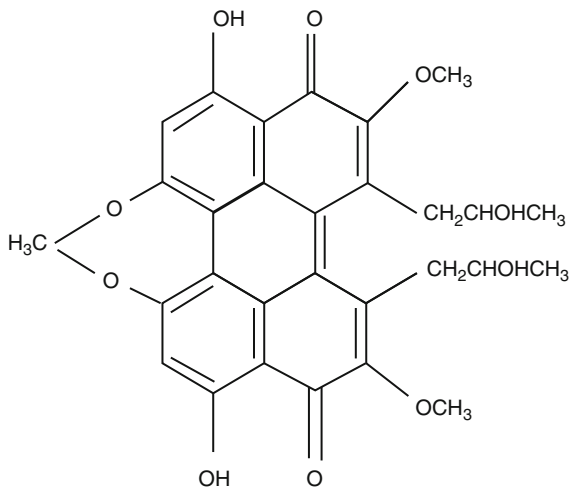

Fig. 21.5 Cercosporin, the phototoxin of the parasitic fungus *Cercospora*

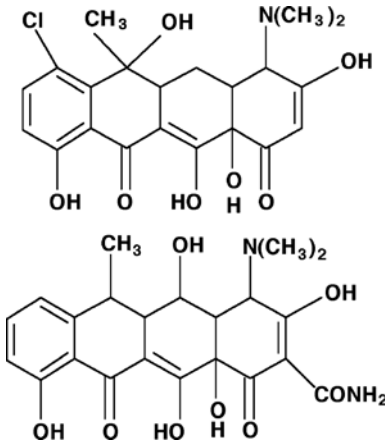

Fig. 21.6 (*Top*) Chlortetracycline, the first tetracycline, introduced in 1948. Tetracycline itself (introduced in 1952) has the same structure, with hydrogen in place of chlorine. (*Bottom*) Doxycycline, introduced in 1968, is one of the most potent photosensitizers among the tetracyclines

hydrochlorothiazide (occurs as an ingredient in a large number of formulations), chlorothiazide, furosemide, and amiodarone. Amiodarone is responsible for an unusually high number of cases. Among other drugs causing photosensitivity reactions, chlorpromazine and other phenothiazines and birth control pills containing estrogens may be mentioned.

Somewhat surprising is the fact that also sun lotions containing para-aminobenzoic acid (PABA) or esters of it, which are sold to protect from the sun, are also a common cause of photosensitivity. These substances were selected for their ability to absorb UV-B radiation (daylight with wavelength below 315 nm), since formerly this radiation was supposed to be the only threat from sunlight. At the long-wavelength edge of their absorption band, they let radiation through to depths where they can cause the photosensitivity reactions.

It is well known that use of perfumes in combination with sunlight is unwise, because many perfumes are phototoxic or at least discolor the skin when exposed to sunlight. This is, of course, because many, if not most of them, are based on plant extracts and often contain substances mentioned in the section on phototoxins in plant defense. Freund (1916) described skin discolorations, which he attributed to eau de cologne containing bergamot oil, although he did not clearly understand the role of sunlight. Bergamot orange, *Citrus bergamia*, like many other *Citrus* species, was later found to contain photosensitizing substances.

21.5 Metabolic Disturbances Leading to Phototoxic Effects of Porphyrins or Related Compounds

A number of different disturbances in both humans and animals lead to the appearance in the skin of phototoxic compounds such as uro- and coproporphyrinogens (porphyrin precursors), protoporphyrin IX (the immediate precursor of heme, Fig. 21.7), and phylloerythrin (a breakdown product of chlorophyll, Fig. 21.8). These substances are phototoxins of type II, generating singlet oxygen in light.

In human patients, a variety of diseases have been described which go under the common designation of porphyria. With the exception of a type called acute intermittent porphyria, they lead to photosensitivity of the skin: variegate porphyria (Frank and Christiano 1998) and hereditary coproporphyria (acute porphyrias with increased levels of both porphyrin precursors and porphyrins) and porphyria cutanea tarda, erythropoietic protoporphyria, and congenital porphyria (nonacute porphyrias with increased levels of porphyrins). Porphyria is due to a disturbance in either the liver (hepatic porphyria or protoporphyria) or the red blood cells

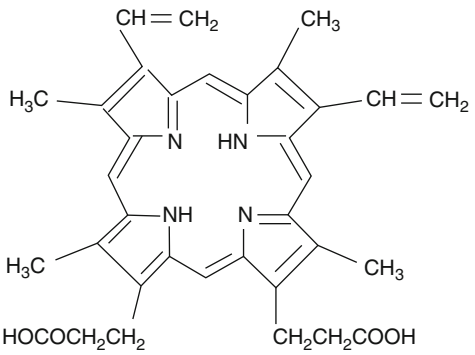

Fig. 21.7 Protoporphyrin IX, the immediate precursor of heme, which accumulates in protoporphyria due to lack of ferrochelatase (or inhibition of the enzyme due to, e.g., lead poisoning)

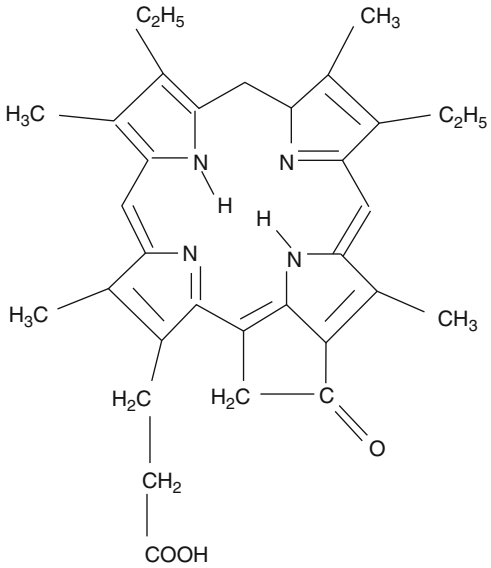

Fig. 21.8 Phylloerythrin, which causes phototoxicity in animals due to malfunctioning of the liver. In healthy animals, the substance is broken down in the liver

(erythropoietic porphyria or protoporphyria). To complicate things further, an erythrohepatic porphyria has recently been described (Gauer et al. 1995), and erythropoietic porphyria may lead to secondary damage to the liver.

Porphyria may be inherited or acquired, and even in cases when it is caused by environment, lifestyle, alcohol (Doss et al. 1999), lead poisoning, liver transplantation (Sheth et al. 1994), etc., inherited predisposition may play a role. Gross et al. (2000) remark in a review: "The molecular genetics of the porphyrias is very heterogenous. Nearly every family has its own mutation." Correct treatment of porphyria is therefore not easy and requires very careful examination. Porphyria cannot be cured, but symptoms can often be ameliorated in other ways than avoidance of light. There are prospects for a future cure of the erythropoietic

protoporphyria. In this condition, the enzyme ferrochelatase is lacking in the red blood cells, causing accumulation of protoporphyrin IX. It may become possible to cure this by retroviral-mediated gene transfer to the bone marrow (Todd 1994). At present the symptoms can be alleviated using β-carotene, interestingly the same compound as used by plants to quench triplet chlorophyll.

In ruminants, another group of diseases with names such as geeldikkop ("yellow head") and alveld is important. Geeldikkop, affecting sheep in South Africa, is the best studied of these. It is caused by saponins in the plant *Tribulus terrestris* (puncture vine or calthrops of the family Zygophyllaceae) grazed upon by sheep (Miles et al. 1994; Wilkins et al. 1996). Liver damage caused by these saponins prevents breakdown of phylloerythrin, a substance produced from chlorophyll by acid in the stomach and rumen bacteria. The phylloerythrin is circulated to skin capillaries, where it can be exposed to light. In other parts of the world, *Panicum* species such as kleingrass or bambatsi grass, *P. coloratum* (Muchiri et al. 1980; Bridges et al. 1987; Regnault 1990), and switchgrass, *P. virgatum* (Puoli et al. 1992), cause the same disease in sheep and in horses (Cornick et al. 1988).

Similar symptoms were induced by *Myoporum laetum* in calves (Raposo et al. 1998), and buttercup (*Ranunculus bulbosus*) has been suspected as a cause in cattle (Kelch et al. 1992). Mold fungi in hay and fungi in pasture can cause similar problems (Scruggs et al. 1994; Casteel et al. 1995). Finally, it has been known for a long time that cyanobacterial toxins in drinking water can cause liver damage with associated photosensitivity in cattle. In the case of the fungus *Pithomyces chartarum* in lamb pasture (Hansen et al. 1994), it is not clear whether the photosensitivity is due to primary photosensitization or liver damage.

21.6 Polycyclic Aromatic Hydrocarbons as Phototoxic Contaminants in Aquatic Environments

21.6.1 Nature and Occurrence of PAHs

Some compounds have a potential to become toxic or acquire increased toxicity when they interact with natural or simulated sunlight. Such compounds with a possible environmental relevance include photoactive insecticides, such as naturally occurring α-terthienyl (Kagan et al. 1984, 1987) and some photodynamic dyes (Larson and Berenbaum 1988); a carbamate insecticide (Zaga et al. 1998), trinitrotoluene (TNT, an explosive), and some related compounds (Davenport et al. 1994); photoreactive nanomaterials (e.g., TiO_2 nanoparticles) used in a wide range of products (Ma et al. 2012); and many polycyclic aromatic hydrocarbons (PAHs) (Newsted and Giesy 1987; Arfsten et al. 1996; Diamond 2003). PAHs, composed of multiple aromatic rings (Fig. 21.9) and present in coal and petroleum products, are widespread organic environmental contaminants, some having carcinogenic potential. PAHs can be introduced into the environment, for example, through incomplete combustion of organic matter. In aquatic environments oil spills, surface runoff from land, and industrial and domestic wastewaters are among the possible sources of PAH contamination, as well as airborne PAHs entering aquatic systems through dry fallout and rainfall (Neff 1979, 1985; Latimer and Zheng 2003). Photoenhanced toxicity of petroleum products (Pelletier et al. 1997; Wernersson 2003) and creosote (Schirmer et al. 1999) has been related to phototoxicity of PAHs present. Furthermore, liquid-phase elutriates of petroleum-containing sediments (Davenport and Spacie 1991), urban stormwater runoff (Ireland et al. 1996), as well as PAH-contaminated sediments (Ankley et al. 1994; Monson et al. 1995) contain phototoxic components, suggesting the role of PAHs. Interaction with solar radiation has also been shown to increase the toxicity of weathered oil (Cleveland et al. 2000; Little et al. 2000; Barron et al. 2003).

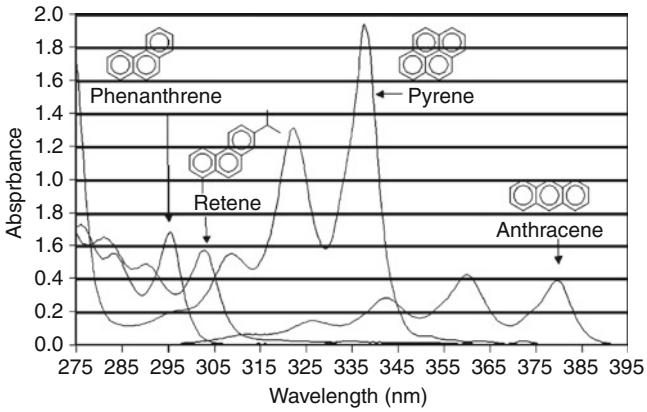

Fig. 21.9 Absorption spectra of anthracene, pyrene, phenanthrene, and retene (7-isopropyl-1-methylphenanthrene) (10 mg^{-1} in dimethyl sulfoxide) (Modified from Huovinen et al. (2001), with permission from Elsevier Science)

Although generally considered relatively acutely non-toxic under normal laboratory lighting, numerous PAHs, such as anthracene, benzo[a]pyrene (3,4-benzopyrene, benzo[d,e,f]chrysene), fluoranthene, and pyrene, have a potential to become highly toxic in the presence of UV radiation, and a risk that PAHs constitute through this photoenhanced toxicity to aquatic organisms has been recognized (reviewed by Landrum et al. 1987; Arfsten et al. 1996; Ankley et al. 2003; Diamond 2003; Pelletier et al. 2006). Since bioassays used to test the toxicity of chemicals are commonly carried out in the laboratory under artificial lighting not including UV radiation, the risk related to photoactive compounds in natural conditions can be underestimated with traditional toxicity testing. On the other hand, the

ecological relevance of PAH phototoxicity evaluations and their use in risk assessment has been criticized (McDonald and Chapman 2002) as often experimental approaches cannot be considered representative of natural environmental conditions where a suite of factors interact.

21.6.2 Mechanisms of PAH Phototoxicity

Because of their chemical structure, many PAHs absorb energy in the UV waveband (Newsted and Giesy 1987; Huang et al. 1993; Diamond et al. 2000; Huovinen et al. 2001) (Fig. 21.9). According to the quantitative structure/activity relationship (QSAR) model, the phototoxicity of PAHs can be related to the HOMO-LUMO gap (i.e., energy difference between the highest occupied molecular orbital and the lowest unoccupied molecular orbital), which has been suggested as a suitable ground state index of the electronic structure relating to absorbed energy and molecular stability (Mekenyan et al. 1994). However, the comparison of the phototoxic potency of PAHs is complicated because it is also related to the bioaccumulation potential of each compound (Boese et al. 1998). Contaminated environments generally contain a mixture of numerous PAHs, and phototoxicity of PAH mixtures has been regarded as somewhat additive (Swartz et al. 1997; Boese et al. 1999; Erickson et al. 1999). Co-exposure with other contaminants, for example, methyl tertiary-butyl ether or piperonyl butoxide, has been shown to increase bioconcentration and photoinduced toxicity of some PAHs (Cho et al. 2003; Weinstein and Garner 2008). Also, substituted PAHs can contribute to phototoxicity (Boese et al. 1998; Kosian et al. 1998). With some exceptions, phototoxicity is likely in a substituted PAH only if the aromatic structure of its parent compound is phototoxic (Veith et al. 1995).

Phototoxicity of PAHs is reported to occur mainly via photosensitization and/or photomodification reactions. The role of PAHs as active photosensitizers is related to their capability of forming triplet states and transferring their triplet energy to oxygen, potentially resulting in the formation of biologically damaging singlet oxygen (Foote 1987; Larson and Berenbaum 1988; see Chap. 1). Photosensitization reactions of bioaccumulated PAHs in biological matrices are regarded as important mechanisms for phototoxicity, which is supported by studies demonstrating enhanced toxicity when bioaccumulation of PAHs in aquatic organisms is followed by exposure to UV radiation in clean uncontaminated water (Bowling et al. 1983; Allred and Giesy 1985; Ankley et al. 1994, 1997; Boese et al. 1997; Monson et al. 1999; Huovinen et al. 2001). Phototoxicity via photosensitization is considered a function of both PAH dose in tissue and UV intensity (Ankley et al. 1995; Huovinen et al. 2001).

In addition to photodegradation (Neff 1979, 1985), PAHs may be photomodified into more toxic forms, for example, via photooxidation (McConkey et al. 1997; Mallakin et al. 1999; Lampi et al. 2006). Photomodification of PAH can result in a complex mixture of products (Mallakin et al. 1999). The enhanced toxicity of many photoproducts can probably be attributed to increased aqueous solubility and thus potentially increased bioavailability, as well as increased bioactivity (Duxbury et al. 1997; McConkey et al. 1997). Although many photomodified PAHs are toxic as such, they can be phototoxic as well (Huang et al. 1993; Mallakin et al. 1999). According to model predictions, photosensitization and photomodification contribute additively to phototoxicity (Huang et al. 1997; Krylov et al. 1997; Mezey et al. 1998; El-Alawi et al. 2002).

21.6.3 Factors Affecting Exposure to Phototoxicity of PAHs in Aquatic Systems

Due to their hydrophobic nature, PAHs tend to accumulate in sediments and organic particles (Neff 1979, 1985), resulting in a decrease in their bioavailability to organisms. However, disturbance of contaminated sediment, for example, during a storm or dredging, may result in mobilization and resuspension of PAHs in the water, increasing the risk of phototoxicity (Davenport and Spacie 1991; Ireland et al. 1996). On the other hand, because of their lipophilic nature, PAHs also tend to bioaccumulate in organisms. In addition to waterborne PAHs, possible routes of exposure to PAHs are their bioaccumulation from contaminated sediments (Ankley et al. 1994; Boese et al. 1998), through maternal transfer (Hall and Oris 1991; Pelletier et al. 2000), via ingested food and potentially also via the food chain. Factors related to PAH bioavailability and bioaccumulation, defining finally the body burden (together with metabolism) (reviewed by Burgess et al. 2003), form the basis for the photosensitization-based phototoxicity risk.

The potential for UV exposure varies in different types of waters. UV-B penetration depths can range from a few centimeters in highly humic lakes (Lean 1998; Huovinen et al. 2003; Kirk 2011), few meters in costal marine waters (Huovinen and Gómez 2011), to dozens of meters in clear oceanic waters (Smith et al. 1992; Kirk 2011). The spectra of underwater UV irradiance change with depth, as penetration decreases with decreasing wavelength (Lean 1998; Huovinen et al. 2003; Kirk 2011). This spectral variation among natural waters affect the potential for phototoxicity (Barron et al. 2000), since the phototoxic response is related to the UV absorption characteristics of a compound (Newsted and Giesy 1987; Diamond et al. 2000; Huovinen et al. 2001; Lampi et al. 2006) (Fig. 21.9). Aquatic biota in PAH-contaminated areas (particularly in clear, shallow waters and littoral areas, which often provide habitats for various aquatic

organisms during reproduction and early development) may be at risk. UV exposure and thus phototoxicity can also be increased, for example, during low flow (Ireland et al. 1996) or when organisms move up in the water column. Other factors, such as increased turbidity, which reduce the penetration of UV radiation in the water column, can attenuate phototoxicity as well (Ireland et al. 1996).

In addition to strongly contributing to attenuation of UV radiation, humic substances have a complex role in aquatic systems in potentially affecting the phototoxicity of PAHs. Dissolved humic material may mitigate the potential for photoinduced toxicity (Gensemer et al. 1998, 1999) by reducing the bioaccumulation of PAHs to organisms (Oris et al. 1990; Weinstein and Oris 1999). On the other hand, the risk for phototoxicity may be increased as a result of higher UV penetration in aquatic ecosystems due to decrease of dissolved organic carbon content induced by UV radiation (Morris and Hargreaves 1997), acidification, and climate warming (Schindler et al. 1996). Humic substances as potential photosensitizers (Larson and Berenbaum 1988) play a role in photodegradation of aquatic contaminants via formation of reactive oxygen species by UV radiation (Boule et al. 1999).

In all, a variety of factors affecting the exposure of organisms to PAHs and to UV radiation, as well as interactions between multiple environmental factors and stressors present in natural conditions, complicate the risk assessment for phototoxicity. Currently ecotoxicological risk assessment is facing new challenges under global climate change scenarios, also influencing photoactivated toxicity as both PAH and UV exposure can potentially be altered by climate change in several ways (Gouin et al. 2013; Hooper et al. 2013).

21.6.4 Phototoxicity of PAHs to Aquatic Biota

Since the early evidence of a potential risk of co-exposure to PAHs and UV radiation to aquatic organisms and environments (e.g., Bowling et al. 1983; Oris and Giesy 1985), information on the mechanisms of phototoxicity and the effects on aquatic biota have been increasing over the last decades. Phototoxicity of PAHs has been demonstrated in a variety of aquatic organisms, including bacteria, phytoplankton, aquatic macrophytes, zooplankton, benthic invertebrates, insect larvae, amphibians, bivalves, and fish, with responses in biota ranging from acute lethality to chronic effects, such as reproductive impairment (reviewed by Landrum et al. 1987; Arfsten et al. 1996; Ankley et al. 2003; Diamond 2003; Pelletier et al. 2006; Barron 2007).

Species vary in their sensitivity to the phototoxicity of PAHs (Boese et. al. 1997; Hatch and Burton 1998; Spehar et al. 1999), which could be related to behavioral (Hatch and Burton 1999) and potentially to metabolic and morphological differences. Translucent early life stages are expected to be more vulnerable to phototoxicity than pigmented juvenile and adult stages (Barron et al. 2005). Also previous exposure of organisms to UV radiation can lead to development of protective mechanisms (e.g., pigmentation) reducing their sensitivity (Boese et al. 1997; Gevertz et al. 2012). Defense mechanisms against oxidative stress, for example, carotenoid pigments, could mitigate the effects of PAH phototoxicity by quenching singlet oxygen generated from PAH photosensitization (Gala and Giesy 1993). Xanthophyll cycling, which has traditionally been associated with photochemical reactions to excess solar radiation, has been suggested also as an energy dissipative response to photoinduced PAH toxicity in microalgae (Southerland and Lewitus 2004). Photoprotective UV-absorbing compounds, such as mycosporine-like amino acids reported in various aquatic organisms or phenolic compounds (phlorotannins) of brown algae, might affect phototoxic potential by providing protection against UV exposure and possibly via their antioxidant activity (Dunlap and Yamamoto 1995; Huovinen et al. 2010). Furthermore, a possibility for repair of phototoxic effects has been demonstrated (Oris and Giesy 1986).

Although phototoxicity potential of numerous PAHs is well known, attention should be paid to the ecological relevance of especially laboratory-based results when using them in risk evaluations (McDonald and Chapman 2002). Overall, the importance of incorporating phototoxicity in water and sediment quality evaluations has been recognized, and recently conceptual frameworks (the adverse outcome pathway) have been proposed to improve predictive approaches and support ecotoxicological risk assessment (Ankley et al. 2010).

References

Allred PM, Giesy JP (1985) Solar radiation-induced toxicity of anthracene to *Daphnia pulex*. Environ Toxicol Chem 4:219–226

Ankley GT, Collyard SA, Monson PD, Kosian PA (1994) Influence of ultraviolet light on the toxicity of sediments contaminated with polycyclic aromatic hydrocarbons. Environ Toxicol Chem 13:1791–1796

Ankley GT, Erickson RJ, Phipps GL, Mattson VR, Kosian PA, Sheedy BR, Cox JS (1995) Effects of light intensity on the phototoxicity of fluoranthene to a benthic macroinvertebrate. Environ Sci Technol 29:2828–2833

Ankley GT, Erickson RJ, Sheedy BR, Kosian PA, Mattson VR, Cox JS (1997) Evaluation of models for predicting the phototoxic potency of polycyclic aromatic hydrocarbons. Aquat Toxicol 37:37–50

Ankley GT, Burkhard LP, Cook PM, Diamond SA, Erickson RJ, Mount DR (2003) Assessing risks from photoactivated toxicity of PAHs to aquatic organisms. In: Douben PET (ed) PAHs: an ecotoxicological perspective. Wiley, Chichester, pp 275–296

Ankley GT, Bennett RS, Erickson RJ, Hoff DJ, Hornung MW, Johnson RD, Mount DR, Nichols JW, Russom CL, Schmieder PK, Serrano JA, Tietge JE, Villenueve DL (2010) Adverse outcome pathways: a conceptual framework to support ecotoxicology research and risk assessment. Environ Toxicol Chem 29:730–741

Arfsten DP, Schaeffer DJ, Mulveny DC (1996) The effects of near ultraviolet radiation on the toxic effects of polycyclic aromatic hydrocarbons in animals and plants: a review. Ecotoxicol Environ Saf 33:1–24

Barron MG (2007) Sediment-associated phototoxicity to aquatic organisms. Hum Ecol Risk Assess 13:317–321

Barron MG, Little EE, Calfee R, Diamond S (2000) Quantifying solar spectral irradiance in aquatic habitats for the assessment of photoenhanced toxicity. Environ Toxicol Chem 19:920–925

Barron MG, Carls MG, Short JW, Rice SD (2003) Photoenhanced toxicity of aqueous phase and chemically dispersed weathered Alaska North Slope crude oil to Pacific herring eggs and larvae. Environ Toxicol Chem 22:650–660

Barron MC, Carls MG, Short JW, Rice SD, Heintz RA, Rau M, DiGiulio R (2005) Assessment of the phototoxicity of weathered Alaska North Slope crude oil to juvenile pink salmon. Chemosphere 60: 105–110

Boese BL, Lamberson JO, Swartz RC, Ozretich RJ (1997) Photoinduced toxicity of fluoranthene to seven marine benthic crustaceans. Arch Environ Contam Toxicol 32:389–393

Boese BL, Lamberson JO, Swartz RC, Ozretich R, Cole F (1998) Photoinduced toxicity of PAHs and alkylated PAHs to a marine infaunal amphipod (*Rhepoxynius abronius*). Arch Environ Contam Toxicol 34:235–240

Boese BL, Ozretich RJ, Lamberson JO, Swartz RC, Cole FA, Pelletier J, Jones J (1999) Toxicity and phototoxicity of mixtures of highly lipophilic PAH compounds in marine sediment: can the ∑PAH model be extrapolated? Arch Environ Contam Toxicol 36:270–280

Boule P, Bolte M, Richard C (1999) Phototransformations induced in aquatic media by NO_3^-/NO_2^-, Fe^{III} and humic substances. In: Boule P (ed) The handbook of environmental chemistry, vol 2, Part I. Environmental photochemistry. Springer, Berlin, pp 181–215

Bowling JW, Leversee GJ, Landrum PF, Giesy JP (1983) Acute mortality of anthracene-contaminated fish exposed to sunlight. Aquat Toxicol 3:79–90

Bridges DH, Camp BJ, Liningston CW, Bailey EM (1987) Kleingrass (*Panicum coloratum* L.) poisoning in sheep. Vet Pathol 24:525–531

Burgess RM, Ahrens MJ, Hickey CW, den Besten PJ, ten Hulscher D, van Hattum B, Meador JP, Douben PET (2003) An overview of the partitioning and bioavailability of PAHs in sediments and soils. In: Douben PET (ed) PAHs: an ecotoxicological perspective. Wiley, Chichester, pp 99–126

Casteel SW, Rottinghaus GE, Hohson GC, Wicklow DT (1995) Liver disease in cattle induced by consumption of moldy hay. Vet Hum Toxicol 37:248–251

Cho EA, Bailer AJ, Oris JT (2003) Effect of methyl tert-butyl ether on the bioconcentration and photoinduced toxicity of fluoranthene in fathead minnow larvae (*Pimephales promelas*). Environ Sci Technol 37:1306–1310

Cleveland L, Little EE, Calfee RD, Barron MG (2000) Photoenhanced toxicity of weathered oil to *Mysidopsis bahia*. Aquat Toxicol 49:63–76

Cornick JL, Carter GK, Bridges CH (1988) Kleingrass-associated hepatoxicosis in horses. J Am Vet Med Assoc 193:932–935

Cooke RG, Edwards JM (1981) Naturally occuring phenalenones and related compounds. In Cadby PA et al. (eds) Progress in the chemistry of organic natural products, Springer-Verlag, Vienna, pp. 153–190

Daub ME, Ehrenshaft M (2000) The photoactivated *Cercospora* toxin cercosporin: contributions to plant disease and fundamental biology. Annu Rev Phytopathol 38:461–490

Davenport R, Spacie A (1991) Acute phototoxicity of harbor and tributary sediments from lower Lake Michigan. J G Lakes Res 17: 51–56

Davenport R, Johnson LR, Schaeffer DJ, Balbach H (1994) Phototoxicology. 1. Light-enhanced toxicity of TNT and some related compounds to *Daphnia magna* and *Lytechinus variegatus* embryos. Ecotoxicol Environ Saf 27:14–22

Delaey E, Vandenbougaerde A, Merlevede W, de Witte P (2000) Photocytotoxicity of hypericin in nomroxic and hypoxic conditions. J Photochem Photobiol B: Biol 56:19–24

Diamond SA (2003) Photoactivated toxicity in aquatic environments. In: Helbling EW, Zagarese H (eds) UV effects in aquatic organisms and ecosystems. The Royal Society of Chemistry, Cambridge, pp 219–250

Diamond SA, Mount DR, Burkhard LP, Ankley GT, Makynen EA, Leonard EN (2000) Effect of irradiance spectra on the photoinduced toxicity of three polycyclic aromatic hydrocarbons. Environ Toxicol Chem 19:1389–1396

Doss MO, Kuhnel A, Gross U, Sieg I (1999) Hepatic porphyrias and alcohol. Med Klin 94:314–328

Downmum KR (1992) Light-activated plant defence. New Phytol 122:401–420

Dunlap WC, Yamamoto Y (1995) Small-molecule antioxidants in marine organisms: antioxidant activity of mycosporine-glycine. Comp Biochem Physiol 112B:105–114

Duxbury CL, Dixon DG, Greenberg BM (1997) Effects of simulated solar radiation on the bioaccumulation of polycyclic aromatic hydrocarbons by the duckweed *Lemna gibba*. Environ Toxicol Chem 16:1739–1748

Ehrenshaft M, Roberts JE, Mason RP (2013) Hypericin-mediated photooxidative damage of α-crystallin in human lens epithelial cells. Free Radic Biol Med 60:347–354

El-Alawi YS, Huang X-D, Dixon DG, Greenberg BM (2002) Quantitative structure-activity relationship for the photoinduced toxicity of polycyclic aromatic hydrocarbons to the luminescent bacteria *Vibrio fischeri*. Environ Toxicol Chem 21:2225–2232

Erickson RJ, Ankley GT, DeFoe DL, Kosian PA, Makynen EA (1999) Additive toxicity of binary mixtures of phototoxic polycyclic aromatic hydrocarbons to the oligochaete *Lumbriculus variegatus*. Toxicol Appl Pharmacol 154:97–105

Flors C, Nonell S (2006) Light and singlet oxygen in plant defense against pathogens: phototoxic phenalenone phytoalexins. Acc Chem Res 39:293–300

Foote, CS (1987) Type I and type II mechanisms of photodynamic action. In: Heitz JR, Downum KR (eds) Light-activated pesticides. ACS Symposium Series 339. American Chemical Society, Washington, DC, pp 22–38

Frank J, Christiano AM (1998) Variegate porphyria: past, present and future. Skin Pharmacol Appl Skin Physiol 11:310–320

Freund E (1916) Über bisher noch nicht beschriebene kunstliche Hautverfarbungen. Dermatol Wochenschr 63:931–933

Gala WR, Giesy JP (1993) Using the carotenoid biosynthesis inhibiting herbicide, fluridone, to investigate the ability of carotenoid pigments to protect algae from the photoinduced toxicity of anthracene. Aquat Toxicol 27:61–70

Gauer EB, Doss MO, Riemann JF (1995) Erythrohepatic protoporphyria, a rare cause in the differential-diagnosis of parenchymatous jaundice. Deut Med Wochenschr 120:713–717

Gensemer RW, Dixon DG, Greenberg BM (1998) Amelioration of the photo-induced toxicity of polycyclic aromatic hydrocarbons by a commercial humic acid. Ecotoxicol Environ Saf 39:57–64

Gensemer RW, Dixon DG, Greenberg BM (1999) Using chlorophyll *a* fluorescence to detect the onset of anthracene photoinduced toxicity in *Lemna gibba*, and the mitigating effects of a commercial humic acid. Limnol Oceanogr 44:878–888

Gevertz AK, Tucker AJ, Bowling AM, Williamson GE, Oris JT (2012) Differential tolerance of native and nonnative fish exposed to ultraviolet radiation and fluoranthene in Lake Tahoe (California/ Nevada), USA. Env Toxicol Chem 31:1129–1135

Gouin T, Armitage JM, Cousins IT, Muir DCG, Ng CA, Reid L, Tao S (2013) Influence of global climate change on chemical fate and

bioaccumulation: the role of multimedia models. Environ Toxicol Chem 32:20–31

Gross U, Hoffmann GF, Doss MO (2000) Erythropoi9etic and hepatic porphyrias. J Inherit Metab Dis 23:641–661

Hall AT, Oris JT (1991) Anthracene reduces reproductive potential and is maternally transferred during long-term exposure in fathead minnows. Aquat Toxicol 19:249–264

Hansen DE, McCoy RD, Hedstrom OR, Snyder SP, Ballerstedt PB (1994) Photosensitization associated with exposure to *Pithomyces chartarum* in lambs. J Vet Med Assoc 204:1668–1671

Hatch AC, Burton GA Jr (1998) Effects of photoinduced toxicity of fluoranthene on amphibian embryos and larvae. Environ Toxicol Chem 17:1777–1785

Hatch AC, Burton GA Jr (1999) Photo-induced toxicity of PAHs to *Hyalella azteca* and *Chironomus tentans*: effects of mixtures and behavior. Environ Pollut 106:157–167

Hooper MJ, Ankley GT Cristol DA, Maryoung LA, Noyes PD, Pinkerton, KE (2013) Interactions between chemical and climate stressors: a role for mechanistic toxicology in assessing climate change risks. Env Toxicol Chem 32:32–48

Huang X-D, Dixon DG, Greenberg BM (1993) Impacts of UV radiation and photomodification on the toxicity of PAHs to the higher plant *Lemna gibba* (duckweed). Environ Toxicol Chem 12:1067–1077

Huang X-D, Krylov SN, Ren L, McConkey BJ, Dixon DG, Greenberg BM (1997) Mechanistic quantitative structure-activity relationship model for the photoinduced toxicity of polycyclic aromatic hydrocarbons. II. An empirical model for the toxicity of 16 polycyclic aromatic hydrocarbons to the duckweed *Lemna gibba* L. G-3. Environ Toxicol Chem 16:2296–2303

Huovinen P, Leal P, Gómez I (2010) Interacating effects of copper, nitrogen and ultraviolet radiation on the physiology of three south Pacific kelps. Mar Freshw Res 61:330–341

Huovinen P, Gómez I (2011) Spectral attenuation of solar radiation in Patagonian fjord and coastal waters and implications for algal photobiology. Cont Shelf Res 31:254–259

Huovinen PS, Soimasuo MR, Oikari AOJ (2001) Photoinduced toxicity of retene to *Daphnia magna* under enhanced UV-B radiation. Chemosphere 45:683–691

Huovinen PS, Penttilä H, Soimasuo MR (2003) Spectral attenuation of solar ultraviolet radiation in humic lakes in Central Finland. Chemosphere 51:205–214

Ireland DS, Burton GA Jr, Hess GG (1996) *In situ* toxicity evaluations of turbidity and photoinduction of polycyclic aromatic hydrocarbons. Environ Toxicol Chem 15:574–581

Jalal MAF, Hossain MB, Robeson DI, van der Helm D (1992) *Cercospora beticola* phytotoxins: cebetins that are photoactive, Mg^{2+}-binding, chlorinated anthraquinone-xanthone conjugates. J Am Chem Soc 114:5967–5971

Kagan J, Kagan PA, Buhse HE Jr (1984) Light-dependent toxicity of α-terthienyl and anthracene toward late embryonic stages of *Rana pipiens*. J Chem Ecol 10:1115–1122

Kagan J, Bennett WJ, Kagan ED, Maas JL, Sweeney SA, Kagan IA, Seigneurie E, Bindokas V (1987) α-Terthienyl as a photoactive insecticide: toxic effects on nontarget organisms. In: Heitz JR, Downum KR (eds) Light-activated pesticides. ACS Symposium Series 339. American Chemical Society, Washington, DC, pp 176–191

Kelch WR, Kerr IA, Adair HS, Boyd GD (1992) Suspected buttercup (*Ranunculus bulbosus*) toxicosis with secondary photosensitization in Charolais heifer. Vet Hum Toxicol 34:238–239

Kirk JTO (2011) Light and photosynthesis in aquatic ecosystems, 3rd edn. Cambridge University Press, Cambridge

Kosian PA, Makynen EA, Monson PD, Mount DR, Spacie A, Mekenyan OG, Ankley GT (1998) Application of toxicity-based fractionation techniques and structure-activity relationship models for the identification of phototoxic polycyclic aromatic hydrocarbons in sediment pore water. Environ Toxicol Chem 17:1021–1033

Krylov SN, Huang X-D, Zeiler LF, Dixon DG, Greenberg BM (1997) Mechanistic quantitative structure-activity relationship model for the photoinduced toxicity of polycyclic aromatic hydrocarbons: I. Physical model based on chemical kinetics in a two-compartment system. Environ Toxicol Chem 16:2283–2295

Lampi MA, Gurska J, McDonald KIC, Xie F, Huang X-D, Dixon DG, Greenberg BM (2006) Photoinduced toxicity of polycyclic aromatic hydrocarbons to *Daphnia magna*: Ultraviolet-mediated effects and the toxicity of polycyclic aromatic hydrocarbon photoproducts. Environ Toxicol Chem 25:1079–1087

Landrum PF, Giesy JP, Oris JT, Allred PM (1987) Photoinduced toxicity of polycyclic aromatic hydrocarbons to aquatic organisms. In: Vandermeulen JH, Hrudey SE (eds) Oil in freshwater: chemistry, biology, countermeasure technology. Proc. Symp. Oil Pollution in Freshwater, Edmonton, Alberta, Canada. Pergamon Press, New York, pp 304–318

Larson RA, Berenbaum MR (1988) Environmental phototoxicity. Solar ultraviolet radiation affects the toxicity of natural and man-made chemicals. Environ Sci Technol 22:354–360

Latimer JS, Zheng J (2003) The sources, transport, and fate of PAHs in the marine environment. In: Douben PET (ed) PAHs: an ecotoxicological perspective. Wiley, Chichester, pp 9–33

Lean D (1998) Attenuation of solar radiation in humic waters. In: Hessen DO, Tranvik LJ (eds) Aquatic humic substances. Ecology and biogeochemistry, vol 133, Ecol. Studies. Springer, Berlin, pp 109–124

Little EE, Cleveland L, Calfee R, Barron MG (2000) Assessment of the photoenhanced toxicity of a weathered oil to the tidewater silverside. Environ Toxicol Chem 19:926–932

Lovell CR (1993) Plants and the skin. Blackwell Scientific Publishing, Oxford

Ma H, Brennan A, Diamond SA (2012) Phototoxicity of TiO_2 nanoparticles under solar radiation to two aquatic species: *Daphnia magna* and Japanese medaka. Environ Toxicol Chem 31:1621–1629

Mallakin A, McConkey BJ, Miao G, McKibben B, Snieckus V, Dickson DG, Greenberg BM (1999) Impacts of structural photomodification on the toxicity of environmental contaminants: anthracene photooxidation products. Ecotoxicol Environ Saf 43:204–212

McConkey BJ, Duxbury CL, Dixon DG, Greenberg BM (1997) Toxicity of a PAH photooxidation product to the bacteria *Photobacterium phosphoreum* and the duckweed *Lemna gibba*: effects of phenanthrene and its primary photoproduct, phenanthrenequinone. Environ Toxicol Chem 16:892–899

McDonald BG, Chapman PM (2002) PAH phototoxicity—an ecologically irrelevant phenomenon? Mar Pollut Bull 44:1321–1326

Mekenyan OG, Ankley GT, Veith GD, Call DJ (1994) QSARs for photoinduced toxicity: I. Acute lethality of polycyclic aromatic hydrocarbons to Daphnia magna. Chemosphere 28:567–582

Mezey PG, Zimpel Z, Warburton P, Walker PD, Irvine DG, Huang X-D, Dixon DG, Greenberg BM (1998) Use of quantitative shape-activity relationships to model the photoinduced toxicity of polycyclic aromatic hydrocarbons: electron density shape features accurately predict toxicity. Environ Toxicol Chem 17:1207–1215

Miles CO, Wilkins AL, Erasmus GL, Kellerman TS, Coetzer J (1994) Photosensitivity in South Africa. 7. Chemical composition of biliary crystals from a sheep with experimentally induced geeldikkop. Onderstepoort J Vet Res 61:215–222

Monson PD, Ankley GT, Kosian PA (1995) Phototoxic response of *Lumbriculus variegatus* to sediments contaminated by polycyclic aromatic hydrocarbons. Environ Toxicol Chem 14:891–894

Monson PD, Call DJ, Cox DA, Liber K, Ankley GT (1999) Photoinduced toxicity of fluoranthene to northern leopard frogs (*Rana pipiens*). Environ Toxicol Chem 18:308–312

Morris DP, Hargreaves BR (1997) The role of photochemical degradation of dissolved organic carbon in regulating the UV transparency of three lakes on the Pocono Plateau. Limnol Oceanogr 42: 239–249

Muchiri DJ, Bridges CH, Ueckert DN, Bailey EM (1980) Photosensitization of sheep on kleingrass pasture. J Am Vet Sci Assoc 177:353–354

Neff JM (1979) Polycyclic aromatic hydrocarbons in the aquatic environment. Sources, fates and biological effects. Applied Science Publishers Ltd, London

Neff JM (1985) Polycyclic aromatic hydrocarbons. In: Rand GM, Petrocelli SR (eds) Fundamentals of aquatic toxicology. Methods and applications. Hemisphere Publishing Corporation, New York, pp 416–454

Newsted JL, Giesy JP (1987) Predictive models for photoinduced acute toxicity of polycyclic aromatic hydrocarbons to *Daphnia magna*, Strauss (Cladocera, Crustacea). Environ Toxicol Chem 6:445–461

Oris JT, Giesy JP Jr (1985) The photoenhanced toxicity of anthracene to juvenile sunfish (*Lepomis* spp.). Aquat Toxicol 6:133–146

Oris JT, Giesy JP Jr (1986) Photoinduced toxicity of anthracene to juvenile bluegill sunfish (*Lepomis macrochirus* Rafinesque): photoperiod effects and predictive hazard evaluation. Environ Toxicol Chem 5:761–768

Oris JT, Hall AT, Tylka JD (1990) Humic acids reduce the photoinduced toxicity of anthracene to fish and daphnia. Environ Toxicol Chem 9:575–583

Pathak MA (1986) Phytodermatitis. Clin Dermatol 4:102–121

Pathak MA, Fitzpatrick TB (1992) The evolution of photochemotherapy with psoralens and UVA (PUVA): 2000 BC to 1992 AD. J Photochem Photobiol B: Biol 14:3–22

Pelletier MC, Burgess RM, Ho KT, Kuhn A, McKinney RA, Ryba SA (1997) Phototoxicity of individual polycyclic aromatic hydrocarbons and petroleum to marine invertebrate larvae and juveniles. Environ Toxicol Chem 16:2190–2199

Pelletier MC, Burgess RM, Cantwell MG, Serbst JR, Ho KT, Ryba SA (2000) Importance of maternal transfer of the photoreactive polycyclic aromatic hydrocarbon fluoranthene from benthic adult bivalves to their pelagic larvae. Environ Toxicol Chem 19:2691–2698

Pelletier E, Sargian P, Demers S (2006) Ecotoxicological effects of combined UVB and organic contaminants in coastal waters: a review. Photochem Photobiol 82:981–993

Puoli JR, Reid RI, Belesky DP (1992) Photosensitization in lambs grazing switchgrass. Agron J 84:1077–1080

Raposo JB, Mendez MC, de Adrade BB, Riet-Correa F (1998) Experimental intoxication by *Myoporum kaetyn* in cattle. Vet Hum Toxicol 40:275–277

Regnault TRH (1990) Secondary photosensitization of sheep grazing bambatsi grass (Panicum coloratum var. makarikariense). Aust Vet J 67:419

Samadi A, Martinez LA, Miranda MA, Morera IM (2001) Mechanism of lipid peroxidation photosensitized by tiaprofenic acid: Product studies using linoleic acid and 1,4-cyclohexadienes as model substrates. Photochem Photobiol 73:359–365

Schindler, DW, Curtis PJ, Parker B, Stainton MP (1996) Consequences of climate warming and lake acidification for UV-B penetration in North American boreal lakes. Nature 379:705–708

Schirmer K, Herbrick J-AS, Greenberg BM, Dixon DG, Bols NC (1999) Use of fish gill cells in culture to evaluate the cytotoxicity and photocytotoxicity of intact and photomodified creosote. Environ Toxicol Chem 18:1277–1288

Scruggs DW, Blue GK (1994) Toxic hepatopathy and photosensitization in cattle fed moldy alfalfa hay. J Am Vet Med Assoc 204:264–266

Sheth AP, Esterly NB, Rabinowitz IG, Poh-Fitzpatrick MB (1994) Cutaneous porphyria-like photosensitivity after liver transplantation. Arch Dermatol 130:614–617

Smith RC, Prézelin BB, Baker KS, Bidigare RR, Boucher NP, Coley T, Karentz D, MacIntyre S, Matlick HA, Menzies D, Ondrusek M, Wan Z, Waters KJ (1992) Ozone depletion: ultraviolet radiation and phytoplankton biology in Antarctic waters. Science 255: 952–959

Southerland HA, Lewitus AJ (2004) Physiological responses of estuarine phytoplankton to ultraviolet light-induced fluoranthene toxicity. J Exp Mar Biol Ecol 298:303–322

Spehar RL, Poucher S, Brooke LT, Hansen DJ, Champlin D, Cox DA (1999) Comparative toxicity of fluoranthene to freshwater and saltwater species under fluorescent and ultraviolet light. Arch Environ Contam Toxicol 37:496–502

Stoessl A, Abramowski Z, Lester HH, Rock GL, Towers GHN (1990) Further toxic properties of the fungal metabolite dothistromin. Mycopathologia 112:179–186

Swartz RC, Ferraro SP, Lamberson JO, Cole FA, Ozretich RJ, Boese BL, Schults DW, Behrenfeld M, Ankley GT (1997) Photoactivation and toxicity of mixtures of polycyclic aromatic hydrocarbon compounds in marine sediment. Environ Toxicol Chem 16:2151–2157

Todd DJ (1994) Erythropoietic protoporphyria. Br J Dermatol 131: 751–766

Veith GD, Mekenyan OG, Ankley GT, Call DJ (1995) A QSAR analysis of substituent effects on the photoinduced acute toxicity of PAHs. Chemosphere 30:2129–2142

Weinstein JE, Oris JT (1999) Humic acids reduce the bioaccumulation and photoinduced toxicity of fluoranthene to fish. Environ Toxicol Chem 18:2087–2094

Weinstein JE, Garner TR (2008) Piperonyl butoxide enhances the bioconcentration and photoinduced toxicity of fluoranthene and benzo[a]pyrene to larvae of the grass shrimp (Palaemonetes pugio). Aquat Toxicol 87:28–36

Wernersson A-S (2003) Predicting petroleum phototoxicity. Ecotoxicol Environ Saf 54:355–365

Wilkins AL, Miles CO, DeKock WT, Erasmus GL, Basson AT, Kellerman TS (1996) Photosensitivity in South Africa. 9. Structure elucidation of a α-glucosidase-treated saponin from *Tribulus terrestris*, and the identification of saponin chemotypes of South African *T. terrestris*. Onderstepoort J Vet Res 63:327–334

Zaga A, Little EE, Rabeni CF, Ellersieck MR (1998) Photoenhanced toxicity of a carbamate insecticide to early life stage anuran amphibians. Environ Toxicol Chem 17:2543–2553

Ozone Depletion and the Effects of Ultraviolet Radiation

22

Lars Olof Björn and Richard L. McKenzie

22.1 Introduction: What's Up Down Under? The Ozone Layer's Gone Asunder!

The fear of increased ultraviolet radiation at the Earth's surface in connection with depletion of stratospheric ozone caused by human activities has spurred not only diplomatic activity and political action but also the investigation of ultraviolet radiation effects on biological systems, from cells to the biosphere as a whole. What has emerged is also a greatly increased understanding of daylight ultraviolet radiation as an ecological and health factor under natural conditions.

A great number of reviews and special volumes of books and journals on this subject have seen the light in recent years, such as Young et al. (1993), Lumsden (1997), Rozema (1999), and Rozema et al. (1997a, 2001). In the fulfillment of the Montreal Protocol, the United Nations Environmental Protection Programme (UNEP) regularly evaluates the biological consequences of ozone depletion, and some of the reports from these evaluations are now available as special journal issues van der Leun et al. (1995, 1999, 2003, 2007), UNEP (2011), and Williamson et al. (2014). Several popular science books deal with the subject, e.g., Nilsson (1996). The field has even been considered interesting enough for scientists dealing with the sociology of the scientific process (Nolin 1995) and has resulted in an account of the negotiations involved in saving the ozone layer by one of the main actors (Benedick 1991, 1998). In recent years, there has been increasing attention on the interactions between ozone depletion and climate change. It has been shown that the Montreal Protocol has been important also for climate protection (UNEP 2011) (Daniel et al. 2010; Velders et al. 2009, 2012; Xu et al. 2013).

After a few words about ozone and ozone depletion and how it affects ultraviolet radiation, we shall start with a short account of some effects of ultraviolet radiation at the molecular level and go on to higher levels of biological organization.

22.2 The Ozone Layer

Ozone, O_3, is formed from oxygen, O_2, by the action of ultraviolet-C (UV-C) radiation in the 175–242-nm band in the stratosphere. The high-energy UV-C photons first split some of the oxygen molecules into free oxygen atoms, O, which then combine with oxygen to form ozone. Ozone is also destroyed by photochemical reactions, which depend on altitude. Most of the ozone is present at an altitude of 20–30 km, with concentrations decreasing above and below that level. Even at its peak near 25 km, its concentration rarely exceeds 3 ppm. Troposphere concentrations are typically only 20–50 parts per billion. In polluted regions, reactions in photochemical smog can increase ozone concentrations to levels that are dangerous to human health. In some cities (e.g., Los Angeles), health warnings are issued when concentrations exceed 100 parts per billion (which is still a much lower concentration of ozone than occurs at 25 km). The ozone molecules very efficiently absorb UV-B radiation (of much higher fluence rate than the UV-C) and are thereby split again into free oxygen molecules. The strong absorption of UV-B radiation in ozone molecules causes heating of the air, and layers higher up in the stratosphere, where the radiation is stronger, are heated more than the lower layers. This results in a lower density of the upper layers and is the reason that the stratosphere, in contrast to the lower atmosphere (troposphere), is stratified, with very little vertical movement of air.

L.O. Björn (✉)
School of Life Science, South China Normal University, Guangzhou, China

Department of Biology, Lund University, Lund, Sweden
e-mail: Lars_Olof.Bjorn@biol.lu.se

R.L. McKenzie
National Institute of Water and Atmospheric Research, (NIWA), Omakau, Central Otago, New Zealand
e-mail: richard.mckenzie@niwa.co.nz

L.O. Björn (ed.), *Photobiology: The Science of Light and Life*,
DOI 10.1007/978-1-4939-1468-5_22,

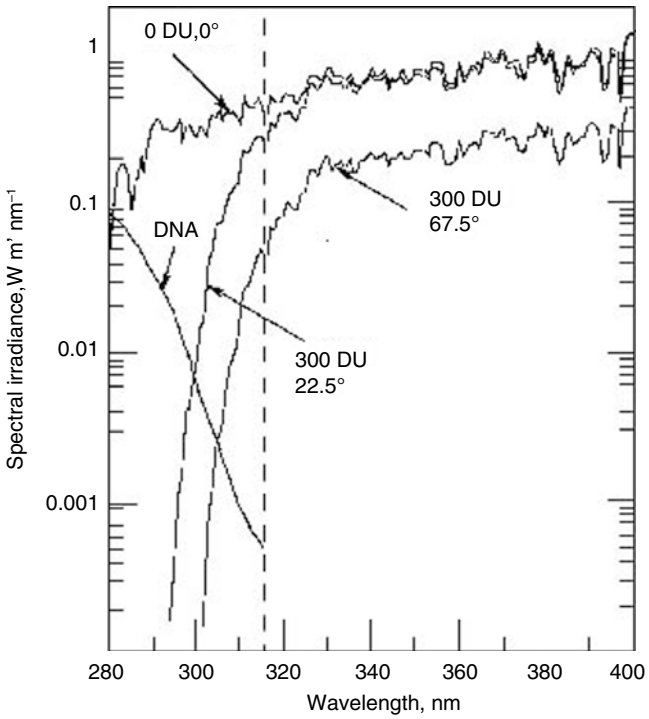

Fig. 22.1 Spectrum of UV spectral irradiance for several observing conditions. Note the logarithmic scale. 300 DU (Dobson units) of ozone is an amount corresponding to a 3-mm-thick layer of pure ozone at a pressure of 1 bar and a temperature of 0 °C. The *dashed vertical line* marks the limit between UV-A radiation (315–400 nm) and UV-B radiation (280–315 nm). Ozone has appreciable absorption in the UV-B band but only a small effect on UV-A radiation. Therefore, the difference between the curves in the UV-A band corresponds mainly to the dependence on solar zenith angle (SZA). SZA's 22.5 and 67.5 correspond to noon at the summer and winter solstices, respectively, at latitude 45°. Note that in the UV-B region, the latter values are an order of magnitude less than the former

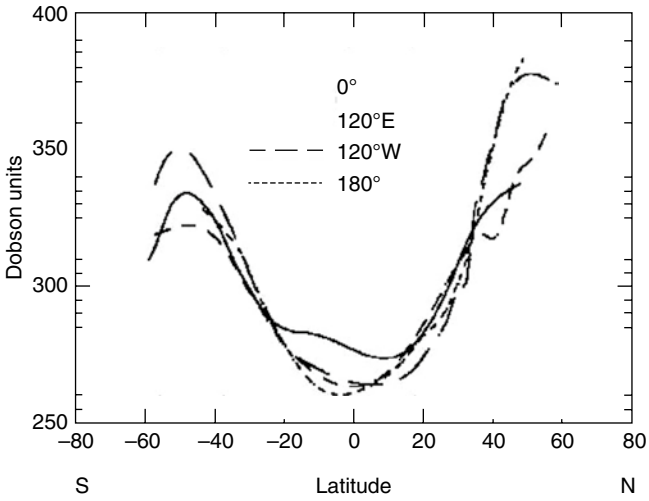

Fig. 22.2 The latitudinal distribution of average ozone at three different longitudes (Data from Labitzke and van Loon (1997)). The values are averaged for all seasons over the years 1979–1993. Ozone formed near the equator is transported to higher latitudes, resulting in high values there, but at the highest latitudes, anthropogenic depletion lowers the values. The ozone layer is subject to natural annual variations, as well as to anthropogenic and natural long-term changes

The absorption maximum of ozone is at practically the same wavelength as that of DNA, and ozone protects DNA very efficiently from the radiation from the sun (Fig. 22.1).

It is only at UV-B wavelengths longer than about 290 nm that sufficient radiation leaks through to interact with the long-wavelength edge of the DNA absorption band, as well as with other cell constituents. There is generally[1] more ozone at mid to high latitudes than near the equator (Fig. 22.2). The average solar zenith angle is also greater at high latitudes (i.e., the average solar elevation above the horizon during the day is lower), and both of these circumstances contribute to a much lower yearly UV-B exposure at high latitudes compared to the tropics (Fig. 22.3).

The ozone column (the total amount of ozone from ground level to space) varies over the year, and both amplitude and phase are latitude dependent. In the northern hemisphere, the variation can be described by:

$$\begin{aligned}&(\text{ozone column} - \text{yearly average})\\&= 0.07\cdot(\text{La}+10)/90\cdot\cos\left((\text{Dn}-90-(44-\text{La})\cdot 3.1)\cdot 2\cdot\pi/365.25\right)\end{aligned}$$

Dobson units (DU) for latitudes lower than 44°N and

$$\begin{aligned}&(\text{ozone column} - \text{yearly average})\\&= 0.07\times(\text{La}+10)/90\times\cos\left((\text{Dn}-90)\times 2\times\pi/365.25\right)\end{aligned}$$

DU for La >44°N, where La is the latitude in degrees and Dn the day number (January 1 = 1). These equations can be used to estimate the expected column (total) ozone once you know the yearly average (Fig. 22.2) but does not take recent changes into account. For values before 2013, go to NASA's website "Ozone over your house" http://toms.gsfc.nasa.gov/teacher/ozone_overhead_v8.html. For current values of ozone, go to http://www.temis.nl/protocols/O3global.html and get approximate values from maps there. Values of erythemal radiation can be obtained from maps at http://www.temis.nl/uvradiation/UVindex.html. If you want spectral values of ultraviolet radiation, or values weighted in another

[1] Apart from polar regions in the spring time, where heterogeneous reactions on the surfaces of ice crystals can efficiently destroy ozone, leading to column ozone amounts less than 100 DU in Antarctica and less than 150 DU in the Arctic (Kuttipurath et al. 2012).

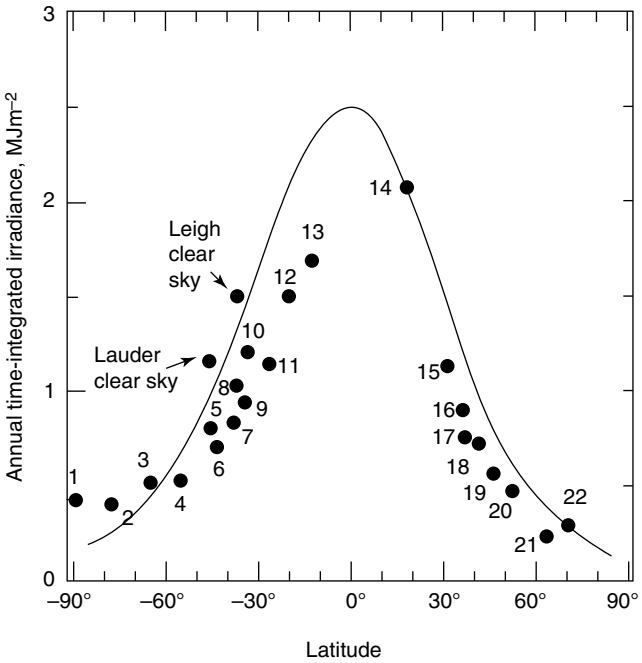

Fig. 22.3 Latitude and cloud dependence of daylight UV-B radiation. The diagram shows (*solid line*) the annual erythemally active radiation (time-integrated irradiance) for various latitudes calculated for cloud-free conditions and (numbered symbols) the actually measured values at different locations. The difference is mainly due to clouds. Note that clouds can increase the irradiance under certain conditions, which is particularly evident at high southern latitudes. For Lauder and Leigh, clear-sky values were also estimated from measurements on cloud-free days. The numbers represent the following locations: *1* South Pole, *2* McMurdo, *3* Palmer, *4* Ushuaia (Tierra del Fuego), *5* Lauder (New Zealand), *6* Hobart (Tasmania), *7* Melbourne, *8* Leigh (New Zealand), *9* Sydney, *10* Perth, *11* Brisbane, *12* Alice Springs, *13* Darwin, *14* Mauna Loa (Hawaii), *15* San Diego, *16* Kos (Greece), *17* Athens (Greece), *18* Thessaloniki, *19* Garmisch-Partenkirchen, *20* Oxford (England), *21* Reykjavik, and *22* Barrow (Alaska)

way than erythemal, use the ozone values in combination with the "Quick TUV Calculator" at http://cprm.acd.ucar.edu/Models/TUV/Interactive_TUV/.

The ozone column is also affected by the rhythms of the sun. The changes due to the 11-year cycle are rather small, about 1.5–2 % (Reid 1999). Although the sun radiates more ultraviolet radiation at a sunspot maximum than when the sun is "quiet," the change is much larger in the ozone-forming UV-C band than in the UV-B band, and therefore the net effect is to make the UV-B fluence rate at ground level slightly less at a "solar maximum." The effects due to changes in ozone transport are larger than the direct effect (Labitzke and van Loon 1997). Larger changes are likely to take place over longer solar cycles (Lean and Rind 1999). From the viewpoint of UV-B conditions at ground level, the variations in cloudiness brought about by solar influence on the terrestrial magnetosphere and thus on cosmic ray flux are probably more important than the ozone variations in both 11-year and long-term perspectives, but as yet they are largely unexplored. Concerning the ozone layer and UV radiation in the past, see Björn and McKenzie (2007).

22.3 Ozone Depletion

As noted above, ozone is continuously formed by UV-C radiation and decomposed again by UV-B radiation. There are also other processes involved in the natural dynamics of the ozone layer, leading to the observed seasonal and latitudinal variabilities in ozone. Generally, the highest concentration of ozone occurs during the spring, and lowest amounts occur in the autumn (but see footnote on previous page). But this situation has been disturbed by emission of artificially generated substances, mainly organic halogen compounds and nitrogen oxides.

Many organic halogen compounds, such as the chlorofluorocarbons (CFCs), are very inert substances as long as they stay in the troposphere, but when they eventually reach sufficient altitude in the stratosphere, they are decomposed by the UV-C radiation there and produce free halogen atoms. Of these, fluorine atoms are of minor interest, but both chlorine and bromine react with "odd oxygen" (O as well as O_3) and form monoxides: $Cl + O == > ClO$ and $Cl + O_3 == > ClO + O_2$. Nitrogen monoxide functions in an analogous way: $NO + O == > NO_2$; $NO + O_3 == > NO_2 + O_2$. These substances thus both destroy ozone already present and prevent formation of new ozone by sweeping up the free oxygen atoms. Still, this would not be catastrophic in itself if the ozone-depleting substances would themselves be depleted by the process. However, the following reactions also take place: $ClO + O == > Cl + O_2$; $NO_2 + O == > NO + O_2$. In other words, through reactions which further deplete the stratosphere of ozone-forming free oxygen, the ozone-destroying substances are regenerated; a chain reaction results. It has been estimated that a single halogen atom may destroy thousands of ozone molecules before it finally undergoes a chain-ending reaction of some kind. When we remember that the amount of ozone is so small, corresponding to about 3 mm of the whole atmosphere (or 6 g out of the 10 tons of air on a square meter), it is understandable that the effect is serious. The ozone hole over Antarctica, which started to develop in the early 1970s and appears every antarctic spring, is well known, but it is less well known that depletion has taken place everywhere in the world except near the equator and that it has, at times, been quite significant even in some populated parts of the world.

22.4 The World Avoided by the Montreal Protocol

After scientists had realized that pollution of the atmosphere with nitrogen oxides (Crutzen 1970) and organic halogen compounds (Rowland and Molina 1974; Molina and Rowland 1974) threatens the ozone layer, they started trying to convince companies, politicians, and the public that emissions of these substances must be limited. The resistance was very strong, since large economic interests were involved. Finally, however, they succeeded, and an international treaty, called the Montreal Protocol, was signed and later followed up, in steps, by amendments when it was found that the original agreement was not sufficient.

The importance of the Montreal Protocol and follow-up agreements, by which the emission of ozone-depleting substances has been limited, can hardly be overestimated. Figures 22.4, 22.5a, b, and 22.6 show how biologically destructive ultraviolet radiation would have increased and the ozone layer would have decreased under "business as usual" conditions, compared to the situation under agreed Montreal limitations.

One of the consequences of increased ultraviolet radiation at ground level is increased risk of skin cancer. Figure 22.7 depicts the number of new skin cancer cases expected each year to 2100 and the number that would have been expected in year 2030 without implementation of the Montreal Protocol.

The Montreal Protocol has also contributed to lowering the rate of increase in greenhouse gases, in fact more than the Kyoto protocol has (UNEP 2011; Daniel et al. 2010; Morgenstern et al. 2008; Velders et al. 2007, 2009; 2012; Xu et al. 2013).

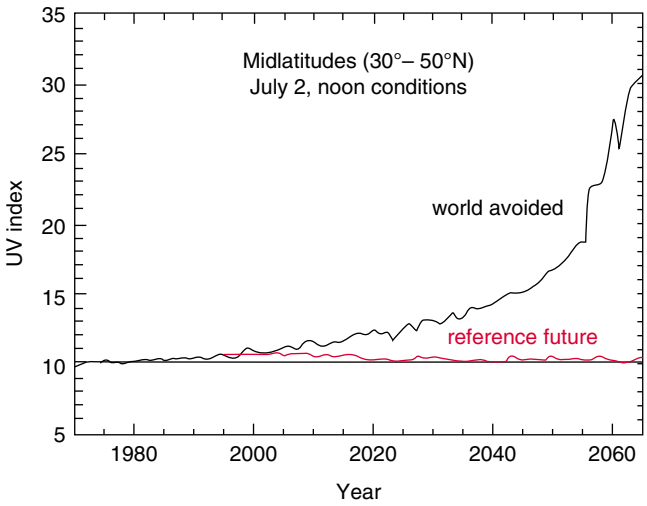

Fig. 22.4 The UV index (erythemally weighted irradiance in W m^{-2} multiplied by 40) at mid-latitudes in the summer calculated to have taken place with "business as usual" (*black line*) and with adherence to the emission internationally agreed rules (*red line*) (From McKenzie et al. (2011) based on Newman et al. (2009))

In 1992, when the future of the ozone layer was still very uncertain, one of us (LOB) summarized the situation thus:

The roof on our living room
Our planet is unique, it is blue.
It has pulled a space-suit on, for me and you,
for all the members living here
in the biosphere.

Despite its tiny mass
the fragile shield of ozone gas
did not permit the rays of death to pass.
A billion years to make it,
ten or so for man to break it.

A hole has opened in the southern sky.
The question is no longer why:
It was the vicious CFC
that set the chlorine atoms free
and caused the thinning of O_3.

Pinatubo coughed,
and set dust aloft,
contributing to a hole
also near the northern pole.

Leaky roof on living room
early sign of coming doom,
of the final cataclysm
killing every organism.

Men and women carry on.
Making more of self is fun.
But before all world is gone
something drastic must be done.
Is there still a little chance
of putting an end to the doomsday dance?

The adherence to the Montreal Protocol has prevented immediate catastrophe. The negative effects on crop production and ecosystems are judged to have been small (Wargent and Jordan 2013). It is estimated that the number of new skin cancer cases appearing during the year 2030 will be two million fewer due to the Montreal Protocol, and the number of cases avoided will be ever greater thereafter. However, in a long-term perspective, the future of the ozone layer is still uncertain, due to interactions between ozone and climate (Dameris 2010; IPCC 2005). Increases in greenhouse gases lead not only to increased surface temperatures but also to decreased stratospheric temperatures, and this affects the ozone layer. In addition to forecasting the future of the ozone layer, attempts have been made to probe its distant past (Björn and McKenzie 2007).

22.5 Molecular Effects of UV-B Radiation

We shall describe the most important effects on the molecular level. As an example of the large number of effects, Fig. 22.8 gives an overview of UV-B effects on plants. Some of these effects are common to all organisms, while others are specific to plants. Some of the effects of special relevance to man are dealt with in Chaps. 23 and 24.

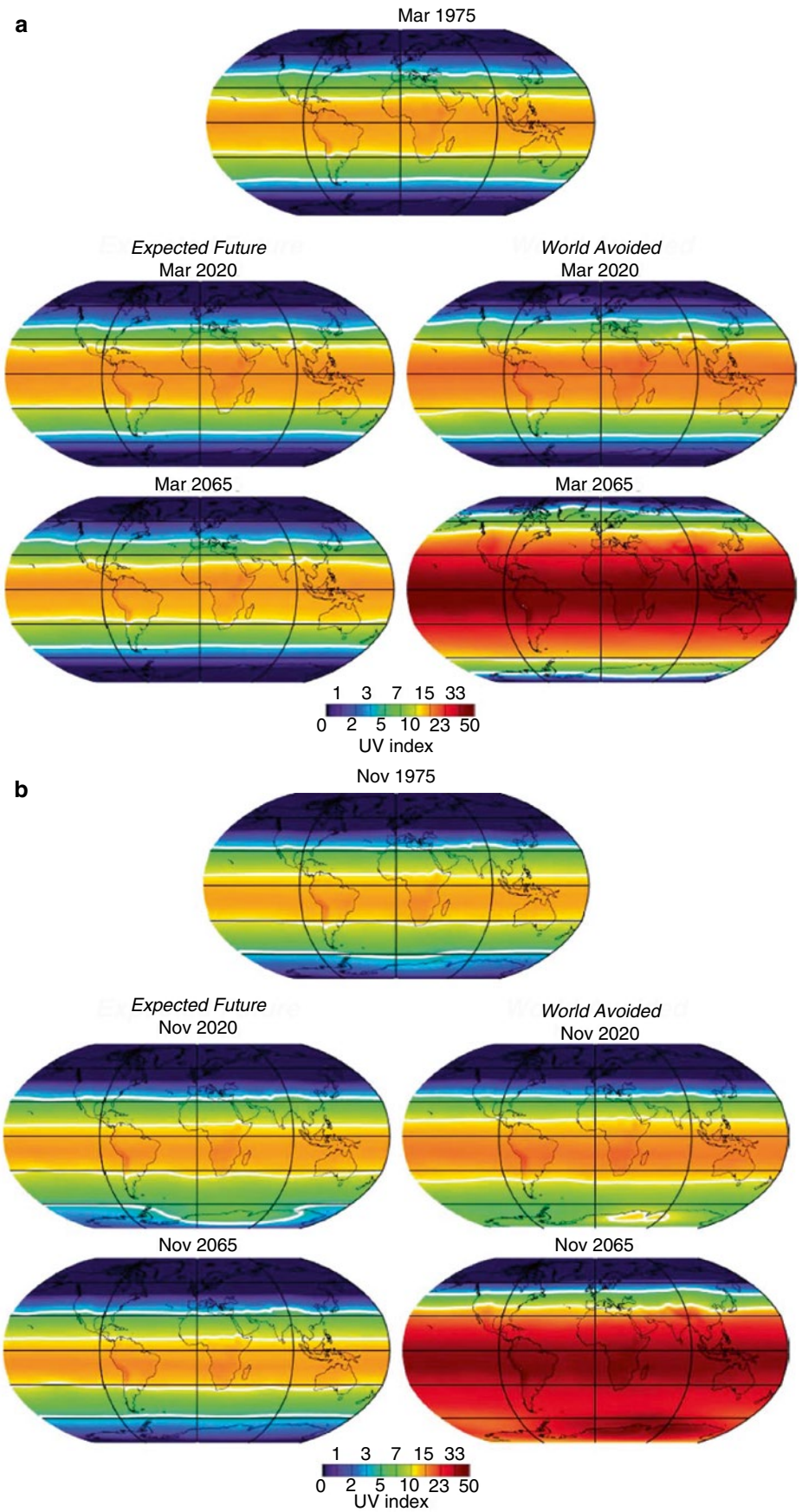

Fig. 22.5 (**a**) Projected changes in UV index in March under adherence to the Montreal Protocol (*left*) and without the Montreal Protocol (*right*). Effects of changes in cloud cover are not taken into account (From Newman and McKenzie 2011). (**b**) Same as in Fig. 22.5a, except that predicted changes are for November (changes in cloud cover have not been taken into account)

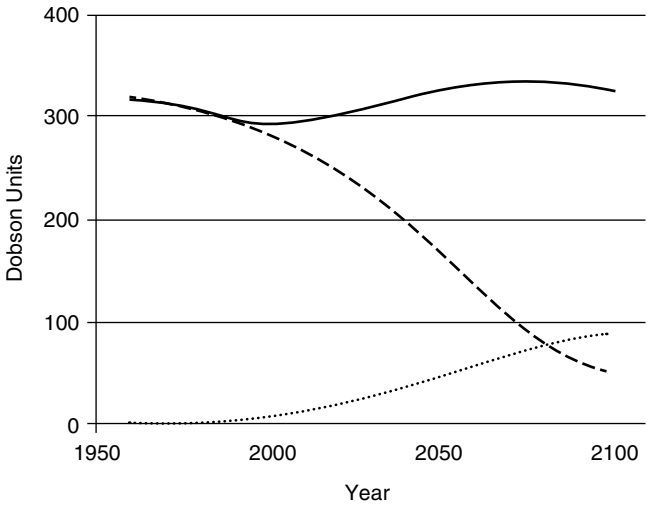

Fig. 22.6 Predicted changes of the global average of ozone without (*dashed*) and with (*solid*) the Montreal Protocol. The *dotted curve* shows percent ozone saved by the Montreal Protocol (Redrawn from Egorova et al. (2013))

22.5.1 Effects of Ultraviolet Radiation on DNA

Ultraviolet radiation directly absorbed by DNA (which may be UV-B under natural conditions but also UV-C under experimental or otherwise artificial circumstances) can elicit a number of different lesions, but the great majority are either dimerization or adduct formation, affecting only adjacent pyrimidine bases (thymine and cytosine) on one DNA strand. The dimerization products are referred to as cyclobutane pyrimidine dimers (CPDs) and the adducts, properly termed 6–4[pyrimidine-2′-one] pyrimidines, are often called (6–4) photoproducts (Fig. 22.9).

Ultraviolet radiation transforms the (6–4) photoproducts to "Dewar photoisomers." This transformation can take place with UV-A (Takeuchi et al. 1998), UV-B, or UV-C radiation (Ravanat et al. 2001). As shown in Figs. 22.9 and 22.10, several diastereoisomers of CPDs are theoretically possible, but only the cis-syn type is, in fact, formed in double-stranded DNA. In single-stranded or denatured DNA also the trans-syn form can be generated, but in low yield. Pyrimidine bases may react to form CPDs as well as (6–4) photoproducts in the combinations TT, TC, and CT; for CPDs also CC is possible. The biological effects are very variable. In some cases replication is stopped at a lesion, in other cases replication continues, resulting either in a mutation (e.g., a change from thymine to cytosine, Jiang and Taylor 1993) or a normal DNA strand. Only specialists in the field can keep track of this, since the same type of lesion may have different consequences in different organisms (e.g., Gibbs et al. 1993). The reader is referred to Ravanat et al. (2001) as an introduction to the literature.

CPDs are the most common UV-induced lesions in DNA. Under UV-C (254 nm) radiation 2–10 CPDs are formed

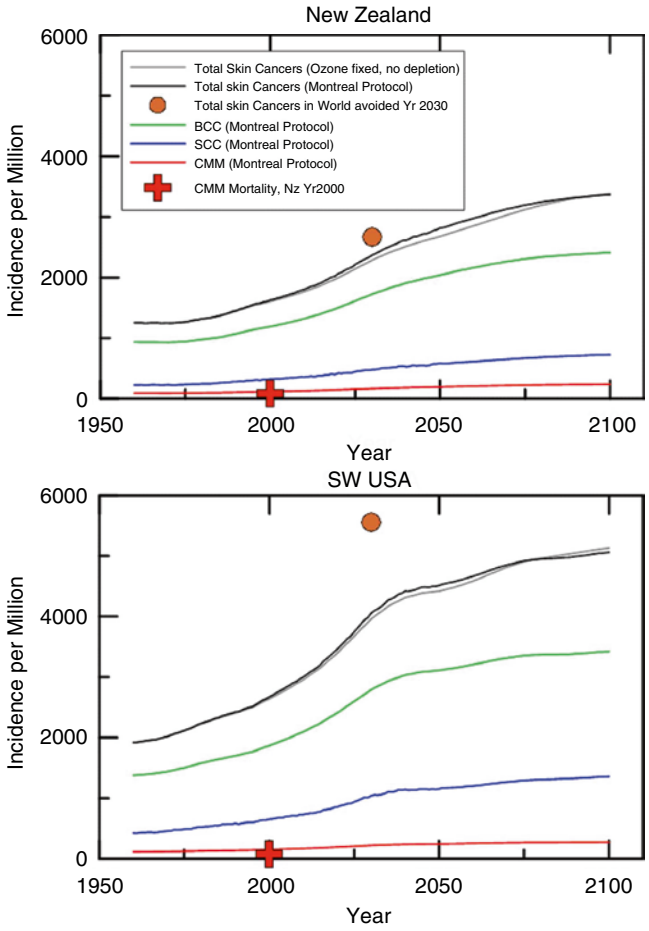

Fig. 22.7 Projected changes in skin cancer incidence rates for (**a**) New Zealand, where the current mortality rates from melanoma skin cancer are the highest in the world, and (**b**) for Southwestern United States, where projected increases in the "World Avoided" are largest (From van Dijk et al. 2013). Incidence rates for all forms of skin cancer are expected to increase markedly over the remainder of the twenty-first century, due mainly to changes in demographics (i.e., aging population). *BCC* basal cell carcinoma, *SCC* squamous cell carcinoma, *CMM* (sometimes designated MM) malignant melanoma; see Sect. 24.5. The difference between the gray and black curves shows the effects of ozone depletions that have already occurred. Because of the success of the Montreal Protocol, the effect is small, and peaks around the middle of the century, about 50 years after the maximum ozone depletion, occurred. The brown symbols (*circles*) show the estimated total skin cancer rates that would have occurred by 2030 in the "World Avoided." Note that because of the longtime lag between exposure and diagnosis, this represents the effects of ozone changes relatively early on (around year 2000) in the World Avoided scenario. In that scenario, ozone depletion accelerates rapidly after 2050 (Newman and McKenzie 2011), which would have led to much more extreme incidence rates by 2100. The red crosses (From Sneyd and Cox 2006) show the most recently published mortality rate for melanoma in New Zealand. The authors acknowledge Arjen van Dijk for providing us with the outputs from the model runs used for production of this figure. Figure adapted from Williamson, CE, et al. (2014), Solar ultraviolet radiation in a changing climate. Nature Climate Change 4: 434–441, doi:10.1038/nclimate2225

per million bases per J/m2. As UV-B is more weakly absorbed by DNA, it is not surprising that the same result requires about two orders of magnitude more UV-B. CPDs occur at

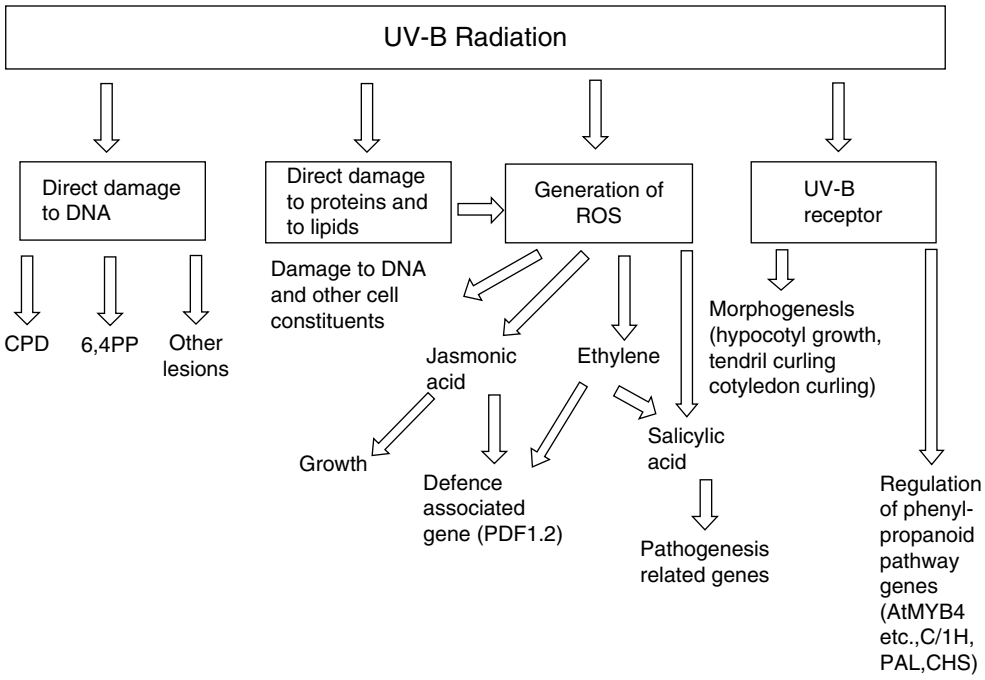

Fig. 22.8 Overview of molecular effects of UV-B radiation on plants. ROS stands for reactive oxygen species (such as HO*, H_2O_2, O_2^-, and $^1O_2$). The UV-B receptor identified so far is the protein UVR8 (see Sects. 12.3.3, 13.1, and 14.3.3)

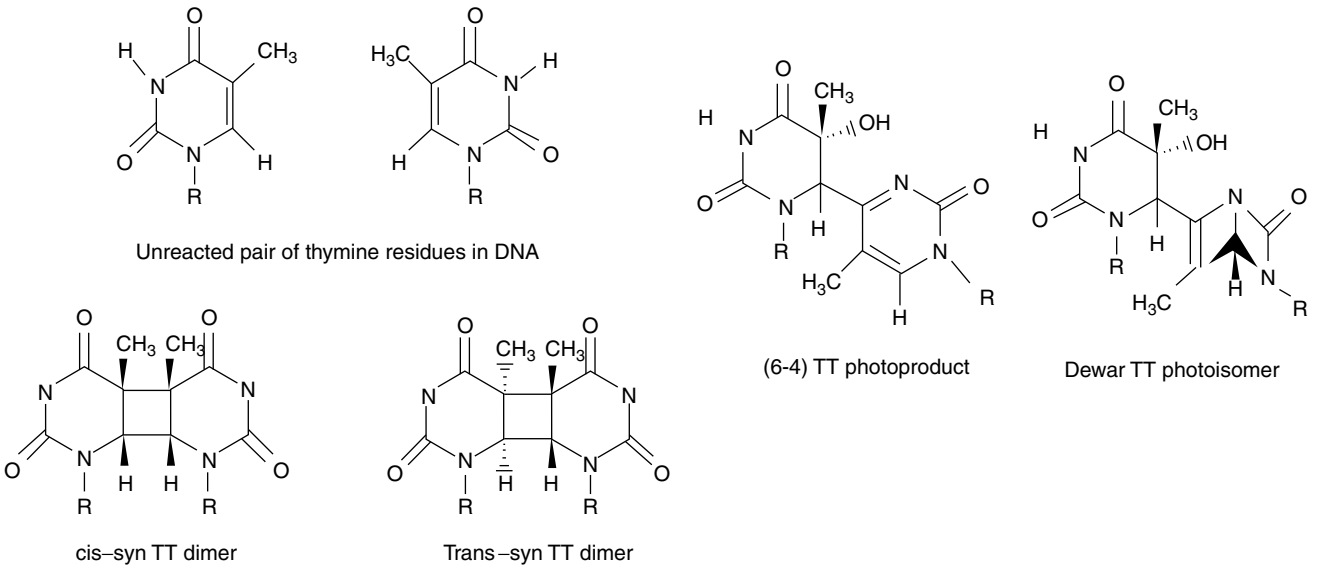

Fig. 22.9 Thymine residues in DNA and the most common types of lesion due to ultraviolet radiation. Dimers and (6–4) photoproducts arise from thymine by the action of UV-B or UV-C radiation, while Dewar photoisomers are formed from (6–4) photoproducts under the influence of UV-A radiation. Since cytosine (C) reacts in a similar way, and also can react with thymine, forming TT, TC, and CT dimers, there are in fact a multitude of possible lesion types, all with differently serious consequences for the organism

higher frequencies than (6–4) photoproducts. Base order is important for UV susceptibility. Pyrimidine pairs with T (thymine) on the 5′-side, i.e., TT and TC, are about tenfold more reactive than those with C (cytosine) on the 5′-side (CT and CC). C at the 3′-side favors (6–4) photoproduct formation. For more details see Ravanat et al. (2001) and Yoon et al. (2000). In diatoms the frequency of (6–4) photoproducts was, on average, 85 % of that of CPDs (Karentz et al. 1991), but in most other organisms, it seems to be lower. CPDs, (6–4) photoproducts, and Dewar photoisomers block DNA replication and are a main cause of UV-induced cancer.

Another kind of lesion affecting cytosine is photohydration followed by deamination to yield uracil hydrate.

Purine bases in DNA may also be altered by ultraviolet radiation. Thus, adenine may combine with either an adjacent adenine or with a thymine residue. This occurs with very low

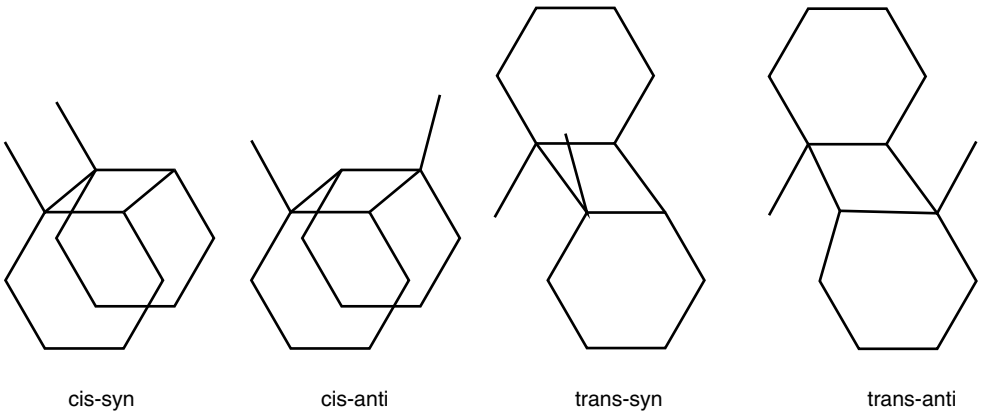

Fig. 22.10 Perspective drawings of the four different diastereoisomers that are possible for a cyclobutane dimer. Due to steric constraints, only the syn forms can be generated in DNA, and of these the trans-syn occurs only in single-stranded DNA. The *lines* indicate methyl groups (Redrawn after Ravanat et al. (2001))

yield but may be biologically important since it is not as easily repaired as the CPDs and (6–4) photoproducts. At least the adenine-thymine adduct is also highly mutagenic (Zhao and Taylor 1996).

DNA bases may also suffer photooxidative damage, and in this respect guanine is particularly sensitive. This photooxidation may take in various ways, and the frequency of various pathways has not yet been established. A direct photon hit in a base may expel an electron, and the electron hole can then migrate along the DNA chain until it encounters a guanine residue, via interaction with water, resulting in 2,6-diamino-4-hydroxy-5-formamidopyrimidine. Deprotonation instead of hydration may also occur and gives another product. Another possibility is that a pyrimidine or purine base after photoexcitation enters a triplet excited state and reacts with oxygen, resulting in generation of singlet oxygen (see Chap. 1). The singlet oxygen then attacks a DNA base, preferably guanine. In this way 8-oxo-7,8-dihydro-2′-deoxyguanosine is formed. Finally, singlet oxygen and other reactive oxygen species (see Chap. 1 and below) formed after photoexcitation of other chromophores may also attack DNA in various ways. It is not known with certainty which cellular chromophores are most important for such processes, but flavines are among the likely candidates. In any case UV-A is more important than UV-B, partly because its fluence rate in daylight is higher and partly because it penetrates further into organisms and natural waters.

Lesions in addition to those mentioned can be induced by direct action of the radiation on DNA. They occur at lower frequency, but some of them may have some importance because they cannot be repaired by the rapid action of photolyases, only by the slower-acting light-independent, "dark" repair systems.

22.5.2 Photolyases and Photoreactivation

Most prokaryotic and eukaryotic organisms are equipped with two kinds of photolyases, enzymes that under the influence of light repair these lesions. In older literature they are called photoreactivating enzymes. The physiological

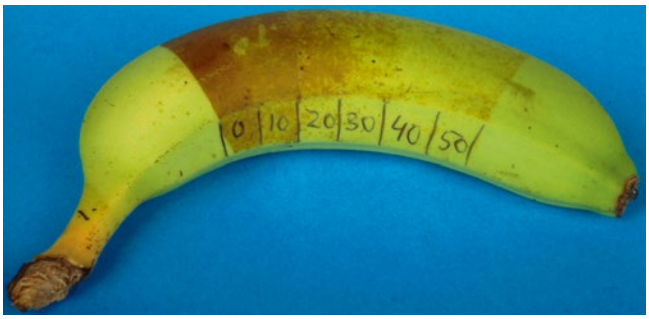

Fig. 22.11 This banana, while still unripe, was first irradiated for 2 min with UV-C radiation (254 nm, W/m^2), except for the ends, which were wrapped in aluminum foil during irradiation. It was then irradiated with white light for the number of minutes indicated on the different sections. Finally it was allowed to ripen in darkness. Where the epidermal cells have been damaged by ultraviolet radiation, they have turned brown, while in other areas they have become yellow during ripening. White light after the ultraviolet has an ameliorating effect. This experiment, which is recommended as a student experiment (see Chap. 24), is in principle the same as that by which photoreactivation was discovered by Hausser and von Oehmcke (1933) (Photo L.O. Björn)

effects of photoreactivation were observed by Hausser and Oehmcke (1933) (see Fig. 22.11) long before the role of DNA was known. Other early publications on the subject include Dulbecco (1949) and Kelner (1949). Recent reviews have been written by Sancar (2003), Weber (2004), and Essen and Klar (2006). One main type of photolyase repairs the CPDs; the other type repairs (6–4) photoproducts. If a (6–4) photoproduct has been converted to a Dewar photoisomer, it can no longer be repaired by photolyase action. Production of photolyases are often stimulated by ultraviolet radiation (e.g., Berrocal-Tito et al. 1999)

The photolyases are of interest not only from the viewpoint of DNA repair, but also because they have played a role in the evolution of other photobiological systems (see Sect. 11.2.1.5 in Chap. 11 and Deisenhofer 2000). Since photolyases are so widespread among organisms and related types occur in distantly related organismal groups, and also because the need for DNA repair probably was very great before the emergence of

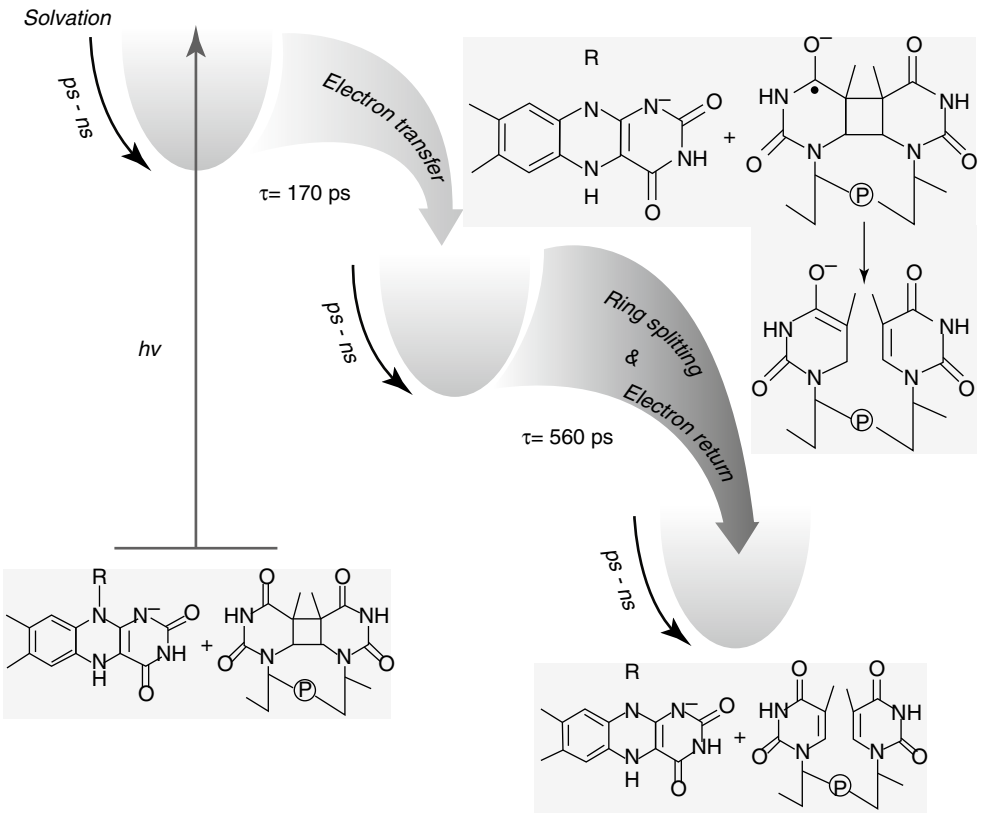

Fig. 22.12 The reaction mechanism in dimer splitting by CPD photolyase. Reaction times (τ) are given in ns (10–9 s) and ps (10–12 s) (Slightly modified from Kao et al. (2005))

the ozone layer, they are thought to have evolved very early. In addition to amino acid sequence and the specificity for different lesion types, photolyases differ also in the chromophore constitution and therefore also in the action spectra (Sect. 11.2.1.5 for photorepair. All photolyases (except "deoxyribozyme photolyase"; see below) contain a flavin (FAD) as the main chromophore but most of them also an accessory chromophore. This can be methenyltetrahydrofolate (Henry et al. 2004; Selby and Sancar 2012), FMN (Ueda et al. 2005; Klar et al. 2006), 7,8-dimethyl-8-hydroxy-5-deazaflavin or phosphoglutamyl-7,8-didemethyl-8-hydroxy-5-deazaflavin (Glas et al. 2009), or 6,7-didemethyl-8-ribityllumazine (Zhang et al. 2013). See also Kiontk et al. (2014).

Based on amino acid sequences, the evolution of the photolyase/cryptochrome family of proteins is thought to have proceeded as follows (Todo 1999). An ancestral gene encoded a CPD photolyase and duplicated very early to form several copies. One of the copies evolved to become a class II CPD photolyase gene, which now occurs only in eukaryotes. Another copy evolved to become class I CPD photolyase gene. One copy gave rise to several related genes coding for (6–4) photolyase and plant and animal cryptochromes and Class III photolyases (Özturk et al. 2008) See also Chap. 13.

CPD photolyase splits CPDs by transferring an electron from the flavin chromophore, which has either been directly excited by light or by energy transfer from the antenna chromophore. The negatively charged cyclobutane ring of the dimer then splits, after which the electron is returned to the flavin (Fig. 22.12). Yamada and Aoki (2006) have tried to study the reaction mechanism in even greater detail in an artificial photolyase.

A quite different kind of DNA photorepair by a "deoxyribozyme photolyase" activity without participation of protein has been described by Chinnapen and Sen (2004, 2007), and Halldal (1961) has described photoreactivation in vivo (by direct photochemical splitting of lesions) by 223-nm radiation, a process without ecological significance under present-day conditions.

22.5.3 Spore Photoproduct and Spore Photoproduct Lyase

Bacterial spores are exceptionally resistant to ultraviolet radiation. This is partly due to low water content but also to the fact that their DNA is in a special state which prevents formation of the otherwise most common UV lesion, CPD. Their DNA is held in a special "A-like" configuration by binding to special proteins (Setlow 1992). Another type of lesion, spore photoproducts (Fig. 22.13), is produced from thymidine pairs in DNA by UV but at a lower rate than CPDs are formed in vegetative cells.

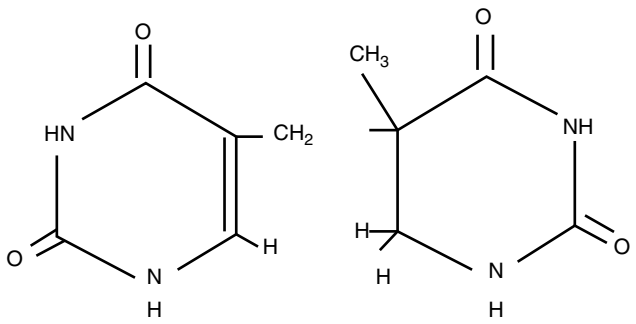

Fig. 22.13 Structure of spore photoproduct

Spore photoproducts cannot be repaired as long as the spore remains in its resting state, but it is essential that it is repaired very quickly when the spore starts to germinate, before extensive DNA replication takes place. This is achieved by a special lyase, which does not require light and has a structure quite different from the photolyases (Fig. 22.14). It contains an iron-sulfur center that reduces S-adenosyl-L-methionine (SAM) in the enzyme. The resulting radical abstracts a hydrogen atom from the spore photoproduct to create a radical with the original thymine pair configuration. Finally, the hydrogen atom is returned via tyrosine and cysteine groups in the enzyme and restores intact DNA.

22.5.4 Formation and Effects of Reactive Oxygen Species

Under the common name of reactive oxygen species (ROS), we lump together a number of oxygen-containing chemical species which arise in organisms by a variety of reactions. Experts dealing with effects of ionizing radiation, such as radiation arising from radioactive decay of atomic nuclei, have been familiar with them for a long time. In photobiology, somewhat surprisingly, they are more important when we are dealing with effects of the less energetic UV-A photons than in the UV-B and UV-C fields, where direct radiation effects on DNA and other macromolecules dominate the picture. This is because the cell contains a number of chromophores which, when excited by UV-A photons, can give rise to ROS. Murphy (1990) and Murphy and Huerta (1990) found that UV-C irradiation of plant cells can give rise to hydrogen peroxide, probably by another mechanism as that described below for UV-B.

According to A.-H.-Mackerness et al. (2001), the main mechanism by which ultraviolet radiation increases the generation of ROS is indirect, by increasing the activity of NADPH oxidase and peroxidases. The generation of ROS by NADPH oxidase is well known from the vertebrate defense against bacterial infection, and an "oxidative burst" similar to that generated in vertebrate neutrophils (a kind of blood corpuscles) takes place also in the plant's defense against infection (review by Lamb and Dixon 1997). NADPH oxidase functions according to the reaction formula $2\ O_2 + NADPH == > 2\ O^{2-} + NADP + H^+$.

The superoxide anion, O_2^- so formed, is very reactive and may give rise to hydrogen peroxide:

$$H^+ + O_2^- ==> HO_2^{\bullet}$$
$$^{\bullet}HO_2 + {}^{\bullet}HO ==> H_2O_2 + O_2$$
$$^{\bullet}HO_2 + O_2 + H_2O ==> H_2O_2 + O_2 + OH^-.$$

In the presence of iron as a catalyst, the most reactive of all ROS, the hydroxyl radical, $^{\bullet}OH$, may be generated from superoxide anion and hydrogen peroxide:

$$O_2^- + Fe^{3+} ==> O_2 + Fe^{2+}$$
$$Fe^{2+} + H_2O_2 ==> Fe^{3+} + OH^- + {}^{\bullet}OH.$$

Peroxidase can contribute to the formation of O_2^- by first oxidizing NADH with H_2O_2 as an oxidant. This results in formation of a $^{\bullet}$NAD radical (2 mol per mol of hydrogen peroxide), which reduces O_2 to O_2^-, a reaction stimulated by monophenols and Mn^{2+}. If the superoxide, after protonation, dismutates to form hydrogen peroxide as shown above, more hydrogen peroxide is generated than was originally consumed.

Enzyme systems and antioxidants protecting against effects of ROS are often increased in response to ultraviolet irradiation.

22.5.5 Effects of Ultraviolet Radiation on Lipids

Lipids containing unsaturated fatty acids are particularly susceptible by photooxidation. Such attacks may be initiated in two different ways (see Girotti 2001 for a review).

Type I photooxidation is started by the formation of a radical when photon absorption in a sensitizer (S) results either in expulsion of an electron resulting in a radical (which can abstract an electron or a hydrogen atom from a lipid molecule) or in formation of a triplet excited state ($^3S^*$). In the latter case, the following reactions can take place (LH symbolizing a lipid molecule and RH another reductant such as ascorbate, glutathione, or a membrane component other than the lipid):

$$(1)\ {}^3S^* + RH ==> S^{-\bullet} + R^{\bullet} + H^+$$
$$(2)\ S^{-\bullet} + O_2 ==> S + O_2^-$$
$$(3)\ S^{-\bullet} + O_2^- + 2H^+ ==> H_2O_2$$
$$(4)\ H_2O_2 + Fe^{2+} ==> OH^- + HO^{\bullet} + Fe^{3+}$$
$$(5)\ LH + HO^{\bullet} ==> L^{\bullet} + H_2O$$
$$(6)\ L^{\bullet} + O_2 ==> LOO^{\bullet}$$
$$(7)\ LOO^{\bullet} + LH ==> LOOH + L^{\bullet}.$$

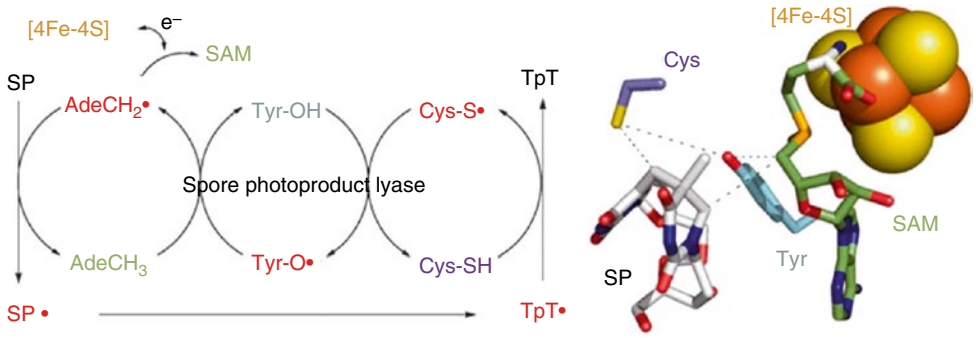

Fig. 22.14 Spore photoproduct lyase action(Reprinted with permission from Yang et al. (2013))

Reaction (1) above results in two radicals: S^{-*} and R^{*}. Either of these could initiate a peroxidative chain reaction (6–7), creating new radicals via a two-step reduction of oxygen (2–3), and a Fenton reaction (4), generating the highly reactive hydroxy radical ($HO^{\bullet}$) that readily attacks the lipid, eventually generating lipid peroxide (LOOH). A product also generated in such peroxidations is malonyl aldehyde, which is often used as an indicator to monitor peroxidative lipid breakdown. Another characteristic is generation of light ("ultraweak radiation"; see Chap. 26), which has been used to construct an action spectrum for lipid breakdown in plant leaves by ultraviolet radiation (Cen and Björn 1994). It should be pointed out that if suitable sensitizers are present in the appropriate compartments, this type of photooxidation can be mediated also by visible light. In addition to unsaturated fatty acids, other lipids, like cholesterol, can be broken down by essentially the same type of process.

The oxygen appearing in the above schemes is ordinary (triplet) oxygen. In a type II photooxidation, singlet-excited oxygen ($^1O_2$, see Chap. 1) is first generated by energy transfer from a sensitizer, which, after photoexcitation to a singlet-excited state, has reached the triplet state. The singlet oxygen then directly reacts with the double bond of an unsaturated fatty acid, and oxygen is added to form a peroxide: $LH + {}^1O_2 ==> LOOH$.

There are many experiments showing deleterious effects of ROS generated by ultraviolet radiation (mostly UV-A but also UV-B), and in many cases hydrogen peroxide is blamed for the effect (e.g., Petersen et al. 2000). Not surprisingly the H_2O_2-degrading enzyme catalase has been shown to play a protective role. But it appears that catalase sometimes is to blame for the generation of ROS (Heck et al. 2003).

22.5.6 Photodestruction of Proteins

Proteins may be affected by ultraviolet radiation in various ways. Enzymes in which sulfhydryl groups are essential for the function are sensitive to photooxidative damage. One of the most sensitive proteins is photosystem II, a protein complex having a key role in oxygenic photosynthesis. In short-term experiments on photosynthesis, this was frequently found to be the most ultraviolet-sensitive link. However, it seems that long-term, ecologically relevant inhibition of photosynthesis by UV-B radiation has other causes (see below).

Proteins can be photochemically cross-linked to adjacent nucleic acids, which is one more mechanism by which ultraviolet radiation can affect DNA. Enzymes may be inactivated also by visible light if they absorb it (e.g., Björn 1969) or via sensitizers which absorb visible light.

22.5.7 UV Absorption Affecting Regulative Processes

Many organisms have special receptors for ultraviolet radiation, which enable them to regulate various processes in accordance with ambient radiation levels, or even to locate environments of higher or lower radiation, or to locate sources of radiation. Most of these, including receptor cells in the eyes of many animals, respond only to UV-A radiation. However, at least some plants and some algae possess receptors for UV-B, and in humans trans-urocanic acid (see Chap. 12) can probably be regarded as a molecular UV-B photoreceptor, even if we presently do not understand the significance. However, many processes are regulated by UV-B, seemingly without any photoreceptors specifically evolved for regulation. Thus, many genes are regulated in both plants and animals via photon absorption in DNA. It is too early to say whether this is, in general, to be regarded as a stress response to DNA damage inflicted by the radiation.

In other cases, regulation proceeds via the formation of ROS (A.-H.-Mackerness et al. 1999, 2001, and literature cited therein). This seems to be the case with the downregulation by increased UV-B of several genes of importance for photosynthesis. Reactive oxygen species also affect a number of hormone systems (Fig. 22.7).

The specific UV-B receptor in plants, with an action maximum at 295 nm, has now been identified as the protein UVR8 (Chap. 13). It regulates growth processes and the

synthesis of flavonoids and other substances. Flavonoids serve as UV-B-absorbing filters and also have other functions in the plants.

It may be wrong, however, to regard the regulation by reactive oxygen species and regulation by an UV-B receptor as two different pathways. As described in Sect. 22.5.4, a major way for generation of ROS may be the increase in activities of NAD oxidase and of peroxidase. This increase may be achieved via the UV-B receptor.

22.5.8 UV-Induced Apoptosis

Induction of apoptosis (programmed cell death), because of its medical importance, has been studied most thoroughly in mammals but is known to occur in other eukaryotes as well. Apoptosis is a normal process in plant development, for instance, in xylem differentiation, and induction of apoptosis by UV-C has also been observed in plants (Danon and Gallois 1998). In the flagellate *Euglena*, induction of an apoptosis-like process was observed by Scheuerlein et al. (1995).

According to Godar (1999a, b), several mechanisms for apoptosis caused by UV-A radiation in the wavelength range 340–400 nm can be distinguished. Two of these depend on the generation of ROS. Formation of singlet oxygen results in "immediate pre-programmed cell death," which takes place in less than 20 min, does not require protein synthesis, and depends on the opening of a "megapore" in the mitochondrial membrane, which releases chemical apoptosis signals into the cytosol. Another pathway for "immediate" apoptosis depends on the formation of superoxide anion, which probably is transformed to hydroxyl radical before interacting with another part of the mitochondrial megapore, which releases cytochrome c. The presence of cytochrome c in the cytosol then causes apoptosis. A third, slower ("intermediate") kind of apoptosis is caused by absorption of radiation in the plasma membrane, causing cross-links in the "Fas receptor" there, which via formation of "caspases" (apoptosis-signaling proteins) lead to opening of the mitochondrial megapore. Finally, there are several forms of "delayed" apoptosis, caused by lesions in DNA. At least some of these signaling channels also go via opening of the mitochondrial megapore. For UV-B-induced apoptosis, CPD formation in DNA can be involved, since Nishigaki et al. (1998) have shown that photorepair of CPDs can prevent UV-induced apoptosis.

22.6 Ultraviolet Effects on Inanimate Matter of Biological Relevance

We have already described how ultraviolet radiation affects the composition of the upper stratosphere. It also has effects on the troposphere. Among other processes, it contributes to the formation of smog. Increased UV-B in the troposphere leads to increased concentration of hydroxyl radical, which in turn results in increased removal of organic compounds and oxides of sulfur and nitrogen. These effects are probably more beneficial than negative for life in general. On the other hand, concentrations of hydrogen peroxide, organic peroxides, and ozone in the troposphere increase when UV-B radiation increases. The overall effect on air quality is probably negative, and various organisms are affected to very different degrees. Tropospheric ozone in particular is clearly a problem for vegetation in many parts of the world.

In the aquatic environment, UV-B decomposes dissolved organic matter, thus making the water more transparent and increasing penetration of ultraviolet radiation, as well as making the organic substances more available for bacterial growth. Photochemical reduction of iron and manganese is an important process in some aquatic ecosystems (reviewed by Wu and Deng 2000). For this, UV-A, and to some extent visible light, is more important than UV-B. UV-A and UV-B can also decrease availability of iron by chelating agents, which is a considerable problem in the use of artificial iron fertilization in some countries.

In the terrestrial environment, ultraviolet radiation affects dead plant matter (litter) in a complex way. The chemical composition of the litter is affected already in the living state: More secondary substances are usually formed in plant parts under increased radiation, making the matter derived therefrom more resistant. After litter has formed, organic compounds in it are photochemically broken down by ultraviolet radiation, provided they are sufficiently exposed. The activity of some litter-decomposing fungi, on the other hand, is hampered by ultraviolet radiation. In some investigations the overall effect was that organic carbon as well as nitrogen disappeared more rapidly under increased UV-B radiation (Gehrke et al. 1995; Paul et al. 1999), while in other cases decomposition was decreased by UV-B radiation (Moody et al. 2001 and references therein). The rate of litter breakdown is very important in some environments, since it may be the most important process making plant nutrients available for new growth.

22.7 UV-B Radiation in an Ecological Context

As we have seen, UV-B radiation can act destructively on DNA and other cellular constituents, but it can also act in a regulating way, and it modifies the physical environment. In the early days of research regarding UV-B effects on organisms and ecosystems, there was an overemphasis on the direct, destructive effects of UV-B on organisms. Nowadays, most researchers in the field are of the opinion that the important effects of UV-B change resulting from changes in the ozone layer and cloudiness will not be these effects but modulations in the way organisms influence one another.

The literature on this is voluminous. We shall here only briefly give some examples and refer the interested reader to recent reviews, books, and special journal issues devoted to the subject (e.g., Björn 1996; Helbling et al. 2001a; Rozema et al. 1997a, b, 2001, 2002; Hessen 2002a).

22.7.1 Aquatic Life

Few biological effects of the increase in UV-B that has resulted from ozone depletion have been directly recorded, so most effects are inferred from experimental manipulation of the radiation level. Direct detection of ozone depletion effects is hampered by the lack of baseline data, i.e., lack of information of the situation prior to ozone depletion. In the Southern Ocean, one can clearly monitor how photosynthesis decreases when the ozone hole sweeps over the monitored area (Smith et al. 1992). Different phytoplankton species are affected to very different extents.

Even if the effects of ozone depletion are difficult to monitor in most water bodies, the impact of UV-B in situ can be inferred from the vertical distribution of photosynthesis, as photosynthesis is partly inhibited in the upper layers where the UV-B radiation is strongest (e.g., Helbling and Willafañe 2002). The degree of vertical mixing of water, which varies with location and season, is important in this context. During the seasons most important for UV-B effects, the upper mixed layer is shallow in antarctic waters (mean depth 50 m), while in the Arctic it varies between 100 and 300 m. When arctic phytoplankton become exposed to UV-B, they are therefore to a higher degree "dark adapted" than antarctic phytoplankton and, therefore, on average, more sensitive (Helbling and Willafañe 2002).

In coastal waters, and in freshwater bodies in particular, UV-B does not penetrate as far as in the open sea and therefore affects only a shallow layer. This can still be of importance, as larvae of many organisms important for the food web live near the surface in these waters. The food web in aquatic ecosystems is generally more complex than in terrestrial ecosystems, and organisms at each trophic level, with the possible exception of mammals and birds, can be affected by UV-B at some stage of development.

One might suspect that the smaller a unicellular organism is, the more susceptible it would be to UV-B radiation. A small organism has less possibility than a larger one to protect the most sensitive parts (especially its DNA) by shielding layers containing radiation-absorbing substances. Some evidence in this direction was presented by Karentz et al. (1991), who compared DNA damage and survival for a number of planktonic diatom species of different size exposed to UV-B radiation. Although the data were scattered, there was a clear tendency for fewer DNA lesions in species with a small surface area: volume ratio (as a large cell has in comparison with a small one, although there is also a shape factor involved). They also (but comparing only four species) showed a negative correlation between survival and frequency of DNA lesions. Such a size-selective effect of UV-B could have serious consequences for consumer organisms, who may simply find the surviving prey too big for consumption. In fact, van Donk et al. (2001) found UV-B irradiation to decrease the fraction of phytoplankton, which was considered "*Daphnia*-edible."

Several other authors have also mentioned a higher tolerance among larger species. But this relationship cannot be upheld when distantly related organisms are compared, and its generality is questionable even when organisms within the same group are compared. Thus Peletier et al. (1996) found no relationship between cell size and UV-B sensitivity among benthic diatoms. Laurion and Vincent (1998) conclude that cell size is not a good predictor of UV-B sensitivity and that, in particular, the cyanobacteria-dominated picophytoplankton is less sensitive than would be assumed on the basis of a size-sensitivity relation. Also, Helbling et al. (2001b) find that picoplankton is more resistant than a cell size relationship would predict.

In the case of marine Prymnesiophyceae, it was found (Mostajir et al. 1999b) that prolonged exposure to UV-B caused an increase in cell size, which possibly diminished the risk of genetic damage, but above all changed the availability and quality of these organisms as food for grazers. Most organisms (including ourselves) have pigments which protect against ultraviolet radiation (the human skin pigment melanin protects in both optical and chemical ways, as do also some plant pigments; Rozema and Björn 2002). In cyanobacteria and many (but not all types of) algae, so-called mycosporine-like amino acids (MAAs) constitute an important group of UV-protecting pigments. In general, however, they protect mainly against UV-A, rather than UV-B radiation (Sinha et al. 1998, 2001; Bishof et al. 2002). Although they are produced by cyanobacteria and some algae and fungi, they are taken up by grazing animals and used also by them as protecting pigments (Sinha et al. 1998). For many aquatic animals, carotenoids serve as important protectants (Hessen 2002b).

Despite the many negative effects of UV-B radiation, it is frequently found that concentrations of various aquatic organisms are increased when UV-B levels are increased. For both bacteria and phytoplankton species, this can be due to a greater sensitivity of the predators, and therefore a decline in predation (Mostajir et al. 1999a). For bacteria it can also be due to increased availability of nutrients when dissolved organic matter is decomposed by the radiation (Herndl et al. 1997).

22.7.2 Terrestrial Life

As in the case of aquatic life, few biological effects of the increase in UV-B that has resulted from ozone depletion

have been directly recorded, so the majority of effects are inferred from experimental manipulation of the radiation level, e.g., Björn et al. (1997). Only in Antarctica, and in Tierra del Fuego, where the ozone hole provides a great increase in radiation level, can a direct biological impact of ozone depletion be recorded. Thus Rousseaux et al. (1999) found that CPD frequency in DNA in plant leaves tracked variations in ambient UV-B in Tierra del Fuego. Several researchers have been inspired to do research on the two higher plant species in Antarctica. The 4-year study of Day et al. (2001) provides data to allow the conclusion that the ozone hole has had an impact on plant life there. These researchers compared plants under UV-B-transmitting and UV-B-excluding filters. Since the "natural" (prehole) UV-B level is so low, the plants under UV-B-excluding filters were probably developed in a way very similar to prehole plants. Many morphological differences between plants exposed to the two treatments were noted. There was some evidence that effects accumulated over the years. See Day (2001) for a review of related literature.

Experiments with exclusion of ambient UV-B from natural ecosystems have also been conducted in Tierra del Fuego (Ballaré et al. 2001), and there are many exclusion studies carried out elsewhere showing that the ambient ultraviolet radiation, even in regions of the world where the ozone depletion has not been severe, is an important environmental factor for many terrestrial (as for aquatic) organisms. In most cases there is little or no direct inhibition of photosynthesis and biomass production by plants. The important effects instead arise in the interaction between organisms. Thus morphological changes in plants can lead to changes in the interspecies competition for light (Barnes et al. 1988). Changes in UV-B often result in changes in herbivory. In most cases increased UV-B leads to decreased herbivory due to changes in chemical composition of the plants (Gwynn-Jones 1999 and reports cited therein). However, other cases are also known: Herbivory may be increased by increased UV-B (Lavola et al. 1998; Buck and Callaghan 1999), and it seems that some insects can perceive UV-B and react directly on changes (Buck and Callaghan 1999). Also, interactions between microorganisms and other organisms can be changed by changes in UV-B, although the conclusion of Paul (2000) is that it is not probable that ozone depletion will cause any substantial change in the incidence or severity of crop diseases.

22.8 Effects on Human Eyes

Most medical effects of ultraviolet radiation take place via the skin; such effects will be dealt with in Chap. 24. The only medical effect of ultraviolet radiation that shall concern us in the present chapter will therefore be those on the eyes.

According to Boottner and Welter (1962), different wave bands of ultraviolet radiation incident on the cornea are absorbed in the various tissues of the eye as shown in Table 22.1. The values in Table 22.1 should be regarded only as approximate values. Especially the lens transmission (Fig. 22.15) varies between individuals, and it is normal that it decreases with age (even if no cataract develops), and this decrease affects also the blue wave band, and thus decreases the eye's sensitivity to blue light. For further information on transmission of ocular media, see Polo et al. (1997).

Because it does not penetrate any further, UV-C radiation can directly affect only the cornea and conjunctiva and the most common type of UV-C radiation (254-nm radiation from low-pressure mercury lamps) only the outermost part of the cornea.

UV-C radiation is, in a way, the least dangerous kind of ultraviolet radiation as far as the eyes are concerned, since the person who has been exposed will very quickly be aware of it and will in the future avoid exposure. Within 2–3 h after the radiation exposure, very unpleasant symptoms will develop. It feels as if the eyelids are covered with sandpaper on the inside. If the exposure has not been very severe, the pain will disappear in a couple of days. The scientific name for this is photokeratitis, and it can also be caused by UV-B

Table 22.1 Percentage of radiation incident on the cornea over the pupil that is absorbed in various parts of the eye

Wavelength, nm	Cornea	Aqueous layer	Lens	Vitreous body
280	100	0	0	0
300	92	6	2	0
320	45	16	36	1
340	37	48	48	1
360	34	52	52	2

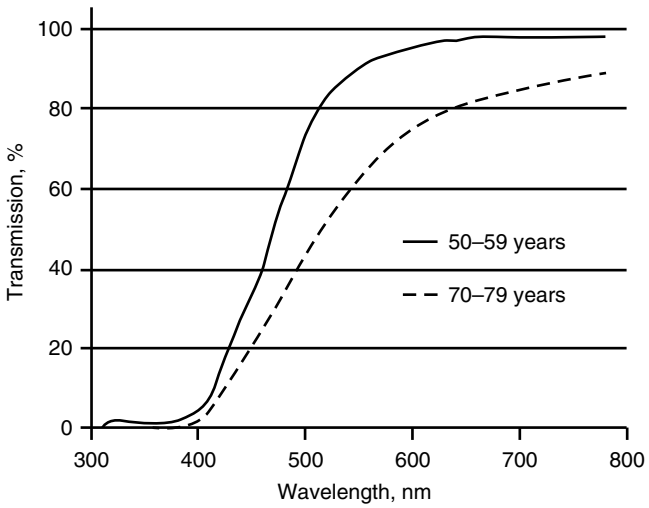

Fig. 22.15 Average spectral transmission of a human lens for two age groups (Redrawn and simplified after Artigas et al. (2012))

radiation in daylight. Well-known forms of photokeratitis are "snow blindness" and "welder's flash." According to Podskochy et al. (2000), photokeratitis is caused by UV-induced apoptosis of cornea cells, resulting in a speeding up of the cell shedding (Ren and Wilson 1994), which normally takes place at a lower rate. This exposes subsurface nerve endings, which causes the gritty feeling and the pain. The action spectrum for ultraviolet damage to the cornea was determined by Pitts et al. (1977).

Cataract is a common and serious group of diseases, which lead to opacity of the lens and ultimately to blindness. Cataracts are usually divided into cortical, nuclear, and posterior subcapsular cataracts. Of these, nuclear cataracts do not seem to be caused by UV exposure, while the two other forms are (Taylor 1994; see also Zigman 1995). In the United States, the probability of cataract surgery increases by 3 % for each degree decrease of latitude (Javitt and Taylor 1994). Such surgery involves removal of the lens and often replacement of it with an artificial (acrylate) lens. Nowadays a lens material is chosen that absorbs ultraviolet radiation efficiently, so radiation exposure of the inner parts of the eye will not be increased after the operation.

Action spectra for cataract induction in lenses of rat and swine have been determined by Merriam et al. (2000) and Oriowo et al. (2001). The highest sensitivity occurs around 295–300 nm, i.e., in the middle of the UV-B band.

UV-related cancer forms, such as melanoma (Michalova et al. 2001) and squamous cell carcinoma, affect not only the skin but also the eye. Newton et al. (1996) estimate that the incidence of squamous cell carcinoma of the eye doubles for a 50° increase in latitude (from the United Kingdom to Uganda), but genetic factors have not been taken into account in this estimate.

Pterygium is an outgrowth of the conjunctiva over the cornea. It is strongly related to sun exposure (Threlfall and English 1999; see also literature cited by Longstreth et al. 1998), but the spectral dependence is not known.

Regarding the role of ultraviolet light (and visible sunlight) in eye disease, the reader is also referred to WHO (1994), Taylor (1994), Young (1994), Sliney (1997), Scott (1998), and Longstreth et al. (1998).

References

A.-H.-Mackerness S, Jordan BR, Thomas B (1999) Reactive oxygen species in the regulation of photosynthetic genes by ultraviolet-B radiation (UV-B: 280–320 nm) in green and etiolated buds of pea (Pisum sativum L.). J Photochem Photobiol B 148:180–188

A.-H.-Mackerness S, John CF, Thomas B (2001) Early signaling components in ultraviolet-B responses: distinct roles for different reactive oxygen species and nitric oxide. FEBS Lett 489:237–242

Artigas JM, Felipe A, Navea A, Fandiño A, Artigas C (2012) Spectral transmission of the human crystalline lens in adult and elderly persons: color and total transmission of visible light. Investig Ophthalmol Visual Sci 53:4076–4084

Ballaré CL, Rousseaux MC, Searles PS, Zaller JG, Giordano CV, Robson TM, Caldwell MM, SDala OE, Scopel AL (2001) Impact of solar ultraviolet-B radiation on terrestrial ecosystems of Tierra del Fuego (southern Argentina) – an overview of recent progress. J Photochem Photobiol B 62:67–77

Barnes PW, Jordan PW, Gold WG, Flint SD, Caldwell MM (1988) Competition, morphology, and canopy structure in wheat (Triticum aestivum L.) and wild oats (*Avena fatua* L.) exposed to enhanced ultraviolet-B radiation. Funct Ecol 2:319–330

Benedick RE (1998) Ozone diplomacy: new directions in safeguarding the planet (enlarged edition). Harvard University Press, Cambridge, MA

Berrocal-Tito G, Saetz-Baron L, Eichenberg K, Horwitz BA, Herrera-Estrella A (1999) Rapid blue light regulation of a *Trichoderma harzianum* photolyase gene. J Biol Chem 274:14288–14294

Bischof K, Hanelt D, Wiencke C (2002) UV radiation and arctic marine macroalgae. In: Hessen DO (ed) UV radiation and arctic ecosystems. Springer, Berlin, pp 225–243

Björn LO (1969) Photoinactivation of catalases from mammal liver, plant leaves and bacteria. Comparison of inactivation cross sections and quantum yields at 406 nm. Photochem Photobiol 10:125–129

Björn LO (1996) Effects of ozone depletion and increased UV-B on terrestrial ecosystems. Int J Environ Stud 51(3(A)):217–243

Björn LO, McKenzie RL (2007) Attempts to probe the ozone layer and the UV-B radiation levels of the past. Ambio 36:366–371

Björn LO, Callaghan TV, Johnsen I, Lee JA, Manetas Y, PaJørgensen HS, Gehrke C, Gwynn-Jones D, Johanson U, Kyparissos A, ul ND, Sonesson M, Wellburn A, Coop D, Heide-Lenzou E, Nikolopoulos D, Petropoulou Y, Stephanou M (1997) The effects of UV-B radiation on European heathland species. Plant Ecol 128:252–264

Boettner EK, Wolter JR (1962) Transmission of the ocular media. Investig Ophthalmol 1:776–783

Buck N, Callaghan TV (1999) The direct and indirect effects of enhanced UV-B on the moth caterpillar *Epirrita autumnata*. Ecol Bull 47:68–76

Cen Y-P, Bjorn LO (1994) Action spectra for enhancement of ultraweak luminescence by ultraviolet radiation (270–340 nm) in leaves of *Brassica napus*. J Photochem Photobiol B 22:125–129

Chinnapen DJ, Sen D (2004) A deoxyribozyme that harnesses light to repair thymine dimers in DNA. Proc Natl Acad Sci U S A 101:65–69

Chinnapen DJ, Sen D (2007) Towards elucidation of the mechanism of UV1C, a deoxyribozyme with photolyase activity. J Mol Biol 365:1326–1336

Crutzen PJ (1970) Influence of nitrogen oxides on atmospheric ozone content. Quart J Roy Meteor Soc 96:320–325

Dameris M (2010) Climate change and atmospheric chemistry: how will the stratospheric ozone layer develop? Angew Chem Int Ed 49:8092–8102. doi:10.1002/anie.201001643

Daniel JS, Fleming EL, Portmann RW, Velders GJM, Jackman CH, Ravishankara AR (2010) Options to accelerate ozone recovery: ozone and climate benefits. Atmos Chem Phys 10:7697–7707, 1680-7324/acp/2010-10-7697

Danon A, Gallois P (1998) UV-C radiation induces apoptotic-like changes in *Arabidopsis thaliana*. FEBS Lett 437:131–136

Day TA (2001) Multiple trophic levels in UV-B assessments—completing the ecosystem. New Phytol 152:183–185

Day TA, Ruhland CT, Xiong FS (2001) Influence of solar ultraviolet-B radiation on Antarctic terrestrial plants: results from a 4-year study. J Photochem Photobiol B 62:78–87

Deisenhofer J (2000) DNA photolyases and cryptochromes. Mutat Res 460:143–149

Dulbecco R (1949) Reactivation of ultraviolet-inactivated bacteriophage by visible light. Nature 163:949–950

Egorova T, Rozanov E, Gröbner J, Hauser M, Schmutz W (2013) Montreal Protocol Benefits simulated with CCM SOCOL. Atmos Chem Phys 13:3811–3823

Essen LO, Klar T (2006) Light-driven DNA repair by photolyases. Cell Mol Life Sci 63:1266–1277
Gehrke C, Johanson U, Callaghan TV, Chadwick D, Robinson CH (1995) The impact of enhanced ultraviolet-B radiation on litter quality and decomposition processes in *Vaccinium* leaves from the Subarctic. Oikos 72:213–222
Gibbs PEM, Kilbey BJ, Banerjee SK, Lawrence CW (1993) The frequency of and accuracy of replication past a thymine-thymine cyclobutane dimer are very different in *Saccharomyces cerevisiae* and Escherichia coli. J Bacteriol 175:2607–2612
Girotti A (2001) Photosensitized oxidation of membrane lipids: reaction pathways, cytotoxic effects, and cytoprotective mechanisms. J Photochem Photobiol B 63:103–113
Glas F, Maul MJ, Cryle M, Barends TRM, Schneider S, Kaya E, Schlichting I, Carell T, Sancar A (2009) The archeal cofactor F0 is a light-harvesting antenna chromophore in eukaryotes. Proc Natl Acad Sci U S A 106:11540–11545
Godar DE (1999a) Light and death: photons and apoptosis. J Invest Dermatol Symp Proc 4:17–23
Godar DE (1999b) UVA1 radiation triggers two different final apoptotic pathways. J Invest Dermatol 112:3–12
Gwynn-Jones D (1999) Enhanced UV-B radiation and herbivory. Ecol Bull 47:77–83
Hada M, Iida Y, Takeuchi Y (2000) Action spectra of DNA photolyases for photorepair of cyclobutane pyrimidine dimers in sorghum and cucumber. Plant Cell Physiol 41:644–648
Halldal P (1961) Photoreactivation at 223 mμ in *Platymonas*. Physiol Plant 14:890–895
Hausser KW, v. Oehmcke H (1933) Lichtbräunung an Fruchtschalen. Strahlen- Therapie 48:223–229
Heck DE, Vetrano AM, Mariano TM, Laskin JD (2003) UVB Light stimulates production of reactive oxygen species. Unexpected role for catalase. J Biol Chem 278:22432–22436
Helbling EW, Willafañe VE (2002) UV radiation effects on phytoplankton primary production: a comparison between Arctic and Antarctic marine ecosystems. In: Hessen DO (ed) UV radiation and arctic ecosystems. Springer, Berlin, pp 203–226
Helbling W, Ballaré CL, Villafañe VE (2001a) Impact of ultraviolet radiation on aquatic and terrestrial ecosystems, pp. ix + 122. J Photochem Photobiol B 62:1–122
Helbling EW, Buma AGJ, de Boer MK, Villafañe VE (2001b) In situ impact of solar ultraviolet radiation on photosynthesis and DNA in temperate marine phytoplankton. Mar Ecol Prog Ser 211:43–49
Henry AA, Jimenez R, Hanway D, Romesberg FE (2004) Preliminary characterization of light harvesting in *E. coli* DNA photolyase. ChemBioChem 2004(5):1088–1094
Herndl GJ, Brugger A, Hager S, Kaiser E, Obernosterer I, Reitner B, Slezak D (1997) Role of ultraviolet-B radiation on bacterioplankton and the availability of dissolved organic matter. Plant Ecol 128:42–51
Hessen DO (ed) (2002a) UV radiation and arctic ecosystems. Springer, Berlin
Hessen DO (2002b) UV radiation and arctic freshwater zooplankton. In: Hessen DO (ed) UV radiation and arctic ecosystems. Springer, Berlin, pp 158–184
IPCC (2005) IPCC/TEAP special report: safeguarding the ozone layer and the global climate system: issues related to hydrofluorocarbons and perfluorocarbons, Summary for policymakers. IPCC, Geneva
Javitt JC, Taylor HR (1994) Cataract and latitude. Doc Ophthalmol 88:307–325
Jiang N, Taylor J-S (1993) In vivo evidence that UV-induced C→T mutations at dipyrimidine sites could result from the replicative bypass of cis-syn cyclobutane dimers or their deamination products. Biochemistry 32:472–481
Kao Y-T, Saxena C, Wang L, Sancar A, Zhong D (2005) Direct observation of thymine dimer repair in DNA by photolyase. Proc Natl Acad Sci U S A 102:16128–16132
Karentz D, Cleaver JE, Mitchell DL (1991) Cell-survival characteristics and molecular responses of antarctic phytoplankton to ultraviolet radiation. J Phycol 27:326–341
Kelner A (1949) Effect of visible light on the recovery of *Streptomyces griseus* conidia from ultraviolet-injury. Proc Natl Acad Sci U S A 35:73–79
Kiontke S, Gnau P, Haselberger R, Batschauer A, Essen L-O (2014) Antenna chromophoreusage by Class IIphotolyases. J BiolChem 289:19659–19669
Klar T, Kaiser G, Hennecke U, Carell T, Batschauer A, Essen L-O (2006) Natural and non-natural antenna chromophores in the DNA photolyase from *Thermus thermophilus*. ChemBioChem 7: 1798–1806
Kuttippurath J, Godin-Beekmann S, Lefèvre F, Nikulin G, Santee ML, Froidevaux L (2012) Record-breaking ozone loss in the Arctic winter 2010/2011: comparison with 1996/1997. Atmos Chem Phys 12:7073–7085
Labitzke K, van Loon H (1997) Total ozone and the 11 year-sunspot cycle. J Atmos Solar-Terr Phys 59:9–19
Lamb C, Dixon RA (1997) The oxidative burst in plant disease resistance. Annu Rev Plant Physiol Plant Mol Biol 48:251–275
Laurion I, Vincent WF (1998) Cell size versus taxonomic composition as determinants of UV-sensitivity in natural phytoplankton communities. Limnol Oceanogr 43:1774–1779
Lavola A, Julkunen-Tiitto R, Roinenen H, Aphalo P (1998) Host-plant preference of an insect herbivore mediated by UV-B and CO2 in relation to plant secondary metabolites. Biochem Syst Ecol 26:1–12
Lean J, Rind D (1999) Evaluating sun-climate relationships since the little ice age. J Solar-Terr Phys 61:25–36
Longstreth J, de Gruijl FR, Kripke ML, Abseck S, Arnold F, Slaper HI, Velders G, Takizawa Y, van der Leun JC (1998) Health risks. J Photochem Photobiol B 46:20–39
Lumsden P (ed) (1997) Plants and UV-B: responses to environmental change, vol 64, Society for experimental biology seminar series. Cambridge University Press, Cambridge
McKenzie RL, Aucamp PJ, Bais AF, Björn LO, Ilyas M, Madronich S (2011) Ozone depletion and climate change: impacts on UV radiation. Photochem Photobiol Sci 10:182–198. doi:10.1039/C0PP90034F
Merriam JC, Löfgren S, Michael R, Söderberg P, Dillon J, Zheng L, Ayala M (2000) An action spectrum for UV-B radiation and the rat lens. Investig Ophthalmol Visual Sci 41:2642–2647
Michalova K, Clemett R, Dempster A, Evans J, Allardyce RA (2001) Iris melanomas: are they more frequent in New Zealand? Brit J Ophthalmol 85:4–5
Molina MJ, Rowland FS (1974) Stratospheric sink for chlorofluoromethanes. Chlorine atomic-catalyzed destruction of ozone. Nature 249:810–812
Moody SA, Paul ND, Björn LO, Callaghan TV, Lee JA, Manetas Y, Rozema J, Gwynn-Jones D, Johanson U, Kyparissis A, Oudejans AMC (2001) The direct effects of UV-B radiation on *Betula pubescens* litter decomposing at flur European sites. Plant Ecol 154:29–36
Morgenstern O, Braesicke P, Hurwitz MM, O'Connor FM, Bushell AC, Johnson AC (2008) The world avoided by the Montreal. Protocol Geophys Res Lett 35:L16811. doi:10.1029/2008GL034590
Mostajir B, Sime-Ngando T, Demers S, Belzile C, Roy S, Gosselin M, Chanut JP, de Mora S, Fauchot J, Vidussi F, Levasseur M (1999a) Ecological implications of changes in cell size and photosynthetic capacity of marine Prymnesiophyceae induced by ultraviolet-B radiation. Mar Ecol Progr Ser 187:89–100
Mostajir B, Demers S, de Mora S, Belzile C, Chanut JP, Gosselin M, Roy S, Villegas PZ, Fauchot J, Bouchard J, Bird D, Monfort P, Levasseur M (1999b) Experimental test of the effect of ultraviolet-B radiation in a planktonic community. Limnol Oceanogr 44:586–596
Murphy TM (1990) Effect of broadband and visible radiation on hydrogen peroxide formation by cultured rose cells. Physiol Plant 80:63–68

Murphy TM, Huerta AJ (1990) Hydrogen peroxide formation in cultured rose cells in response to UV-C radiation. Physiol Plant 78:247–253

Newman PA, McKenzie R (2011) UV impacts avoided by the Montreal protocol. Photochem Photobiol Sci 10:1152–1160

Newman PA, Oman LD, Douglass AR, Fleming EL, Frith SM, Hurwitz MM, Kawa SR, Jackman CH, Krotkov NA, Nash ER, Nielsen JE, Pawson S, Stolarski RS, Velders GJM (2009) What would have happened to the ozone layer if chlorofluorocarbons (CFCs) had not been regulated? Atmos Chem Phys 2009(9):2113–2128

Newton R, Ferlay J, Reeves G, Beral V, Parkin DM (1996) Effect of ambient solar ultraviolet radiation on incidence of squamous-cell carcinoma of the eye. Lancet 347:1450–1451

Nilsson A (1996) Ultraviolet reflections: life under a thinning ozone layer. Wiley, Chichester

Nishigaki R, Mitani H, Shima A (1998) Evasion of UVC-induced apoptosis by photorepair of cyclobutane pyrimidine dimers. Exp Cell Res 244:43–53

Nolin J (1995) Ozonskiktet och vetenskapen. Almqvist and Wiksell, Stockholm

Oriowo OM, Cullen AP, Chou BR, Sivak JG (2001) Action spectrum and recovery for in vitro UV-induced cataract using whole lenses. Investig Ophthalmol Visual Sci 42:2596–2602

Öztürk N, Kao Y-T, Selby CP, Kavakl IH, Partch CL, Zhong D, Sancar A (2008) Purification and characterization of a Type III Photolyase from *Caulobacter crescentus*. Biochemistry 2008:10255–10261

Paul DD (2000) Stratospheric ozone depletion, UV-B radiation and crop disease. Environ Pollut 108:343–355

Paul ND, Callaghan TV, Moody S, Gwynn-Jones D, Johanson U, Gehrke C (1999) UV-B impacts on decomposition and biogeochemical cycling. In: Rozema J (ed) Stratospheric ozone depletion: the effects of enhanced UV-B radiation on terrestrial ecosystems. Backhaus, Leiden, pp 117–133

Peletier H, Gieskes WWC, Buma AGJ (1996) Ultraviolet-B radiation resistance of benthic diatoms isolated from tidal flats in the Dutch Wadden Sea. Mar Ecol- Progr Series 135:163–168

Petersen AB, Gniadecki R, Vicanova J, Thorn T, Wulf HC (2000) Hydrogen peroxide is responsible for UVA-induced DNA damage measured by alkaline comet assay in HaCaT keratinocytes. J Photoch Photobiol B: Biol 59:123–131

Pitts DG, Cullen AP, Hacker PD (1977) Ocular effects of ultraviolet radiation from 295 to 365 nm. Investig Ophthalmol 16:932–939

Podskochy A, Gan L, Fagerholm P (2000) Apoptosis in UV-exposed rabbit corneas. Cornea 19:99–103

Polo V, Pinilla I, Abecia E, Larrosa JM, Pablo LE, Honrubia FM (1997) Assessment of the ocular media absorption index. Int Ophthalmol 20:1–3

Ravanat J-L, Douki T, Cadet J (2001) Direct and indirect effects of UV radiation on DNA and its components. J Photochem Photobiol B 63:88–102

Reid GC (1999) Solar variability and its implications for the human environment. J Atmosph Solar-Terr Phys 61:3–14

Ren HW, Wilson G (1994) The effect of ultraviolet-B irradiation on the cell shedding rate of the corneal epithelium. Acta Ophthalmol 72:447–452

Rousseaux JC, Ballaré CL, Giordano CV, Scopel AL, Zima AM, Szwarccberg- Bracitta M, Searles PS, Caldwell MM, Diaz SB (1999) Ozone depletion and UV-B radiation: impact on plant DNA damage in southern South America. Proc Natl Acad Sci U S A 96:15310–15315

Rowland FS, Molina MJ (1974) Stratospheric ozone destruction catalyzed by chlorine atoms from photolysis of chlorofluoromethanes. Trans Am Geophys Union 55:1153–1153

Rozema J (ed) (1999) Stratospheric ozone depletion: the effects of enhanced UV-B radiation on terrestrial ecosystems. Backhuys, Leiden

Rozema J., Björn L.O (eds) (2002) Special issue: evolution of UV-B absorbing compounds in aquatic and terrrestrial plants. J Photochem Photobiol B 66:1–87

Rozema J, van de Staaij J, Caldwell MM, Björn LO (1997a) UV-B as an environmental factor in plant life: stress and regulation. Trends Ecol Evol 12:22–28

Rozema J, Gieskes WWC, van de Geijn SC, Nolan C, de Boois H (eds) (1997b) UV-B and biosphere. Kluwer, Dordrecht

Rozema J, Manetas Y, Björn LO (eds) (2001) Responses of plants to UV-B radiation. Kluwer Academic Publishers, Dordrecht

Sancar A (2003) Structure and function of DNA photolyase and cryptochrome blue-light photoreceptors. Chem Rev 103:2203–2237

Scheuerlein R, Treml S, Thar B, Tirlapur UK, Häder D-P (1995) Evidence for UV-B-induced DNA degradation in *Euglena gracilis* mediated by activation of metal-dependent nucleases. J Photochem Photobiol B 31:113–123

Scott BR (1998) Ultraviolet radiation effects upon the eye: problems of dosimetry. Radiat Prot Dosim 76:277–277

Selby CP, Sancar A (2012) The second chromophore in Drosophila photolyase/cryptochrome family photoreceptors. Biochemistry 51:167–171

Setlow P (1992) DNA in dormant spores of Bacillus species is in an A-like conformation. Molec Microbiol 6:563–567

Sinha RP, Klisch M, Gröninger A, Häder D-P (1998) Ultraviolet-absorbing Ultraviolet-absorbing/screening substances in cyanobacteria, phytoplankton and macroalgae. J Photochem Photobiol B 47:83–94

Sinha RP, Klisch M, Gröniger A, Häder D-P (2001) Responses of aquatic algae and cyanobacteria to solar UV-B. Plant Ecol 154:221–236

Sliney DH (1997) Ultraviolet radiation effects upon the eye: problems of dosimetry. Radiat Prot Dosim 72:197–206

Smith CC, Prézelin BB, Baker KS, Bidigare RR, Boucher NP, Coley TL, Karentz D, MacIntyre S, Matlick HA, Menzies D, Ondrusek M, Wan Z, Waters KJ (1992) Ozone depletion: ultraviolet radiation and phytoplankton biology in Antarctic waters. Science 255:952–959

Sneyd MJ, Cox B (2006) The control of melanoma in New Zealand. New Zealand Med J 119, 1242 (11 pp)

Takeuchi Y, Murakami M, Nakajima N, Kondo N, Nikaido O (1998) The photorepair and photoisomerization of DNA lesions in etiolated cucumber cotyledons after irradiation by UV-B depends on wavelength. Plant Cell Physiol 39:745–750

Taylor HR (1994) Ocular effects of UV-B exposure. Doc Ophthalmol 88:285–293

Threlfall TJ, English DR (1999) Sun exposure and pterygium of the eye: a dose–response curve. Am J Ophthalmol 128:280–287

Todo T (1999) Functional diversity of the DNA photolyase/blue light receptor family. Mutat Res 434:89–97

Ueda T, Kato A, Kuramitsu S, Terasawa H, Shimada I (2006) Identification and characterization of a second chromophore of DNA photolyase from *Thermus thermophilus* HB27. J Biol Chem 280:36237–36243

UNEP (2011) Environmental effects of ozone depletion and its interactions with climate change: 2010 assessment. Photochem Photobiol Sci 10(2). doi:10.1039/c1030pp90041a

van der Leun J, Tang X, Tevini M et al (1995) Environmental effects of ozone depletion: 1994 assessment. Ambio 24:137–197

van der Leun J, Tang X, Tevini M et al (1999) Environmental effects of ozone depletion: 1998 assessment. J Photochem Photobiol B 46:1–108

van der Leun J, Tang X, Tevini M et al (2003) Environmental effects of ozone depletion and its interactions with climate change: 2002 assessment. Photochem Photobiol Sci 2(i-xxiv):1–72

van der Leun J, Bornman JF, Tang X et al (2007) Environmental effects of ozone depletion and its interactions with climate change: 2006 assessment. Photochem Photobiol Sci 6:208–330

van Dijk A, Slaper H, den Outer PN, Morgenstern O, Braesicke P, Pyle JA, Garny H, Stenke A, Dameris M, Kazantzidis A, Tourpali K, Bais AF (2013) Skin cancer risks avoided by the Montreal protocol—worldwide modeling integrating coupled climate-chemistry models with a risk model for UV. Photochem Photobiol 89:234–246

van Donk E, Faafeng BA, De Lange HJ, Hessen DO (2001) Differential sensitivity to natural ultraviolet radiation among phytoplankton species in Arctic lakes (Spitsbergen, Norway). Plant Ecol 154:213–223

Velders GJM, Andersen SO, Daniel JS, David W, Fahey DW, Mack McFarland M (2007) The importance of the Montreal protocol in protecting climate. Proc Natl Acad Sci U S A 104:4814–4819

Velders GJM, Fahey DW, Daniel JS, McFarland M, Andersen SO (2009) The large contribution of projected HFC emissions to future climate forcing. Proc Natl Acad Sci U S A 106:10949–10954

Velders GJM, Ravishankara AR, Miller MK, Molina MJ, Alcamo J, Daniel JS, Fahey DW, Montzka SA, Reimann S (2012) Preserving Montreal protocol climate benefits by limiting HFCs. Science 335:922–923

Wargent JJ, Jordan BR (2013) From ozone depletion to agriculture: understanding the role of UV radiation in sustainable crop production. New Phytol 197:1058–1076

Weber S (2004) Light-driven enzymatic catalysis of DNA repair: a review of recent biophysical studies on photolyases. Biochim Biophys Acta 1707:1–23

WHO (1994) Environmental health criteria 160: ultraviolet radiation. World Health Organisation, Geneva

Williamson CE, Zepp RG, Lucas RM, Madronich S, Austin AT, Ballaré CL, Norval M, Sulzberger B, Bais AF, McKenzie RL, Robinson SA, Häder D-P, Paul ND, Bornman JF (2014) Solar ultraviolet radiation in a changing climate. Nat Climate Change 4 (in press). doi:10.1038/NCLIMATE2225

Wu F, Deng NS (2000) Photochemistry of hydrolytic iron (III) species and photoinduced degradation of organic compounds. A mini review. Chemosphere 41:1137–1147

Xu Y, Zaelke D, Velders GJM, Ramanathan V (2013) The role of HFCs in mitigating 21st century climate change. Atmos Chem Phys 13:6083–6089. doi:10.5194/acp-13-6083-2013

Yamada Y, Aoki S (2006) Efficient cycloreversion of cis, syn-thymine photodimer by aZn2+−1,4,7,10-tetraazacyclododecane complex bearing a lumiflavin and tryptophan by chemical reduction and photoreduction of a lumiflavin unit. J Biol Inorg Chem 11:1007–1023

Yang L, Nelson RS, Benjdia A, Lin G, Telser J, Stoll S, Schlichting I, Li L (2013) A radical transfer pathway in spore photoproduct lyase. Biochemistry 52:3041–3050

Yoon J-H, Lee C-S, O'Connor TR, Yasui A, Pfeifer GP (2000) The DNA damage spectrum produced by simulated sunlight. J Mol Biol 299:681–693

Young RW (1994) The family of sunlight-related eye diseases. Optom Vision Sci 71:125–144

Young AR, Björn LO, Moan J, Nultsch W (eds) (1993) Environmental UV photobiology. Plenum Press, New York, pp xxi–479

Zhang F, Scheerer P, Oberpichler I, Lamparter T, Krauß N (2013) Crystal structure of a prokaryotic (6–4) photolyase with an Fe-S cluster and a 6,7-dimethyl-8-ribityllumazine antenna chromophore. Proc Natl Acad Sci U S A 110:7217–7222

Zhao X, Taylor J-S (1996) Mutation spectra of TA, the major photoproduct of thymidylyl-(3′5′)-deoxyadenosine, in Escherichia coli under SOS conditions. Nucleic Acids Res 24:1561–1565

Zigman S (1995) Environmental near-UV radiation and cataracts. Optom Vision Sci 72:899–901

Vitamin D: Photobiological and Ecological Aspects

23

Mary Norval and Lars Olof Björn

Abbreviations

1,25(OH)2D	1,25-dihydroxyvitamin D
25(OH)D	25-hydroxyvitamin D
IFN	Interferon
IL	Interleukin
LC-MS/MS	Liquid chromatography-tandem mass spectroscopy
MS	Multiple sclerosis
PTH	Parathyroid hormone
TNF	Tumour necrosis factor
UV	Ultraviolet
VDR	Vitamin D receptor

23.1 Introduction

Some of us remember how we were forced to swallow a spoonful of cod liver oil every day and were told that it contained vitamin D and that we had to eat it to get good bones. At that time, we did not wonder why it was in the cod or how it got there.

The early research history relating to vitamin D has been recounted many times, for instance, by DeLuca (1997), and only a short summary will be given here. Rickets was first described in England by Whistler (1645) and Glisson (1650). In the next century, Sniadecki established a connection between skeleton malformation and lack of sunlight among children in Warsaw (Mozolowski 1939). The disease became known as the English disease in many countries. Mellanby (1918) demonstrated that rickets (Fig. 23.1) could be prevented in dogs by supplementing their diet with cod liver oil, and Hess and Unger (1921) showed that rickets could be cured by sunlight. Hess and Weinstock (1924) and Steenbock and Black (1924) showed that the exposure of lettuce and several other foodstuffs to radiation from a mercury vapour lamp would render them antirachitic.

Several treatises on medical aspects of vitamin D are available, e.g. DeLuca (1997), Feldman, Glorieux and Pike (2005), Holick (2010), Bouillon et al. (2004), Lips (2006), and Norman (2006). Many later reviews deal with various special aspects of vitamin D, such as the molecular mechanisms of action (Haussler et al. 2013). Here vitamin D will be considered broadly covering not only medical aspects but also photochemistry, its role in non-human organisms, and evolutionary, ecological, and biogeographical aspects.

23.2 Chemistry and Photochemistry of Provitamin and Vitamin D

There are at least two kinds of vitamin D (also called calciferol), i.e. vitamin D_2 (ergocalciferol) and vitamin D_3 (cholecalciferol), with slightly different structures (Fig. 23.2). The reason that there is no vitamin D_1 is that the product first given this name turned out not to be a single compound but a mixture. In some non-mammal vertebrates, other compounds act in a similar way as vitamins D_2 and D_3 (Holick 1989), but they have not been chemically defined. In most organisms, the synthesis of vitamin D requires UV-B radiation. Exceptions to this rule will be described later. Vitamin D is formed from the provitamins (provitamin D_2, also called ergosterol, and provitamin D_3, also called 7-dehydrocholesterol). UV-B radiation can photoisomerise the provitamins to the corresponding previtamins, either in vivo without the mediation of any enzyme or in solution. The previtamins are slowly converted by a nonenzymatic and non-photochemical reaction to the vitamins (Fig. 23.2).

M. Norval (✉)
Biomedical Sciences, University of Edinburgh Medical School, Edinburgh, Scotland, UK
e-mail: m.norval@ed.ac.uk

L.O. Björn
School of Life Science, South China Normal University, Guangzhou, China

Department of Biology, Lund University, Lund, Sweden
e-mail: Lars_Olof.Bjorn@biol.lu.se

L.O. Björn (ed.), *Photobiology: The Science of Light and Life*,
DOI 10.1007/978-1-4939-1468-5_23,

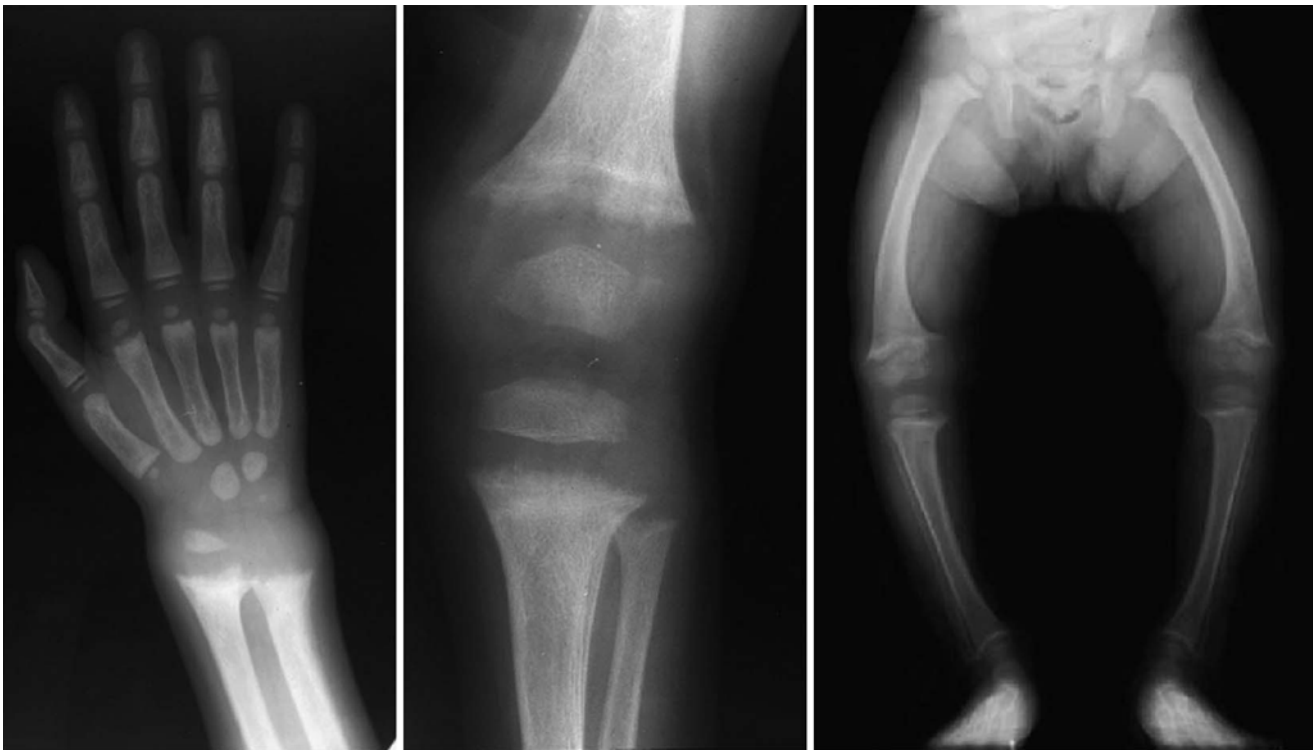

Fig. 23.1 X-ray plates showing signs of vitamin D deficiency (rickets): incomplete bone formation in the wrist and knee and malformed legs in a child (Courtesy Dr. Michael L. Richardson, University of Washington Department of Radiology)

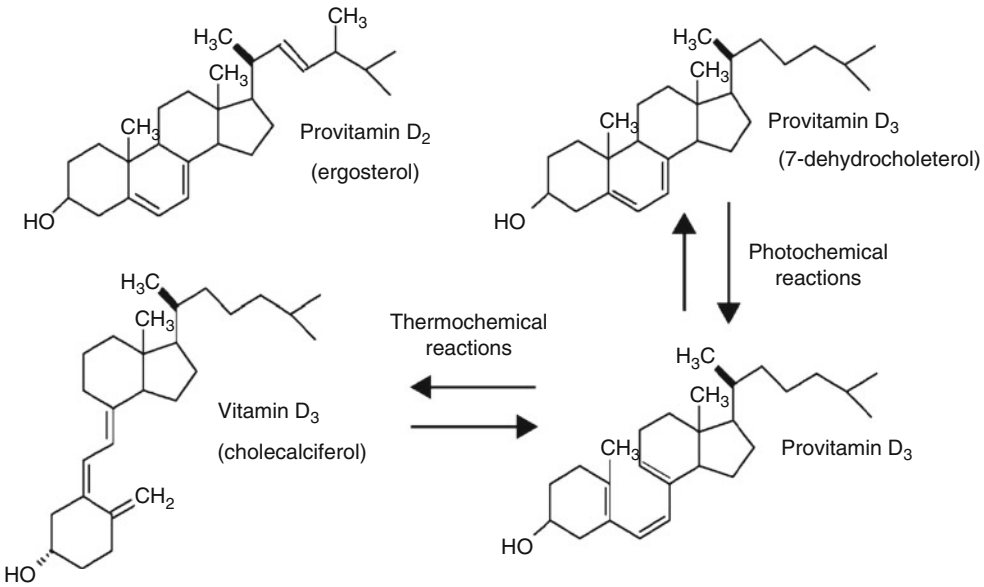

Fig. 23.2 The structure of the two types of provitamin D: the reversible photoconversion of provitamin D_3 to previtamin D_3 and the reversible thermochemical conversion of previtamin D_3 to vitamin D_3

Provitamin D_3 is synthesised in the upper layers of the human skin. Exposure to sunlight converts it to previtamin D_3, which is in turn converted to vitamin D_3. Since a vitamin is defined as a substance necessary for health which cannot be synthesised by the body and must be ingested with the food, vitamin D is, strictly speaking, not a vitamin. Since, however, exposure to sunlight can be insufficient for maintaining health and deficiency can be prevented by vitamin D in food, the vitamin status is defendable.

The recommended daily intake of vitamin D has been gradually raised, for instance, during 2013 in Sweden from 7.5 to 10 μg/day (and from 10 to 20 μg/day for the elderly).

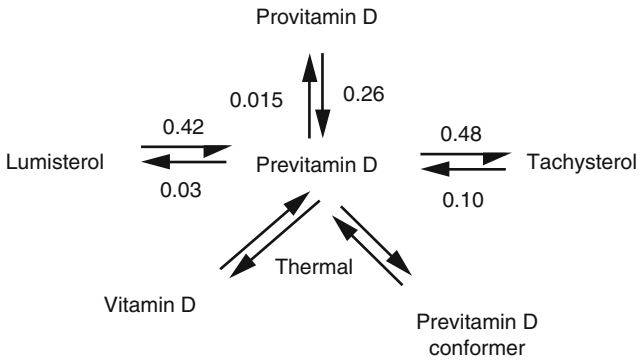

Fig. 23.3 The reversible conversions of previtamin D with quantum yields of the photochemical reactions. Previtamin D can also be photochemically converted to various compounds termed toxisterols (not shown) (From Havinga (1973), modified)

This is insufficient for prevention of deficiency if exposure to UV-B radiation does not supplement the intake. It was found, e.g. that Moslems in Denmark were still deficient after taking 15 μg/day (Glerup et al. 2000). Attempts to avoid the need for UV exposure by high daily intake (over 50 μg daily) cannot be recommended, as this can lead to vitamin D intoxication. Exposure even to high daily fluence of UV-B radiation can never lead to vitamin D overdosage, as will be explained below.

As mentioned, the vitamin D precursor previtamin D is formed from provitamin D by a photochemical reaction (Figs. 23.2 and 23.3) driven by UV radiation (UV-B in the natural condition, but UV-C can also be used artificially). But this is far from the only UV-driven reaction in the vitamin D context. The basic photochemistry of the vitamin D system was summarised by Havinga (1973). Previtamin D is also sensitive to UV radiation and can undergo three different photoreversible photochemical reactions. It can be either reconverted to provitamin D or converted to lumisterol or tachysterol and further irreversibly to products known under the common name of toxisterols (Boomsma et al. 1975). Vitamin D is sensitive to UV radiation and can be photoconverted to three compounds: *5,6-trans*-vitamin D_3, suprasterol 1, and suprasterol 2 (Webb et al. 1989).

Havinga (1973) states that the quantum yields are independent of wavelength or at least have the same values at 254 and 313 nm. There is, however, as will be detailed below, an important exception to this rule. Although some literature sources give values slightly different from those of Fig. 23.3, there is no indication of differences in quantum yield between the D_2 and D_3 series.

Provitamin D_3 is present in mammalian skin not only in free form but also esterified with fatty acids, and the esterified provitamin is transformed to esterified vitamin D_3 upon exposure to UV radiation (Takada 1983). In fact, most of the provitamin and vitamin D in rat skin is in the esterified form.

A number of authors (reviewed by Dmitrenko et al. 2001) have found curious behaviour for the quantum yield of the photochemical ring closure of previtamin D (ring closure results in either conversion back to provitamin D or to formation of lumisterol, which has the same structure as provitamin D except for the direction of a methyl group, which is up for previtamin D in Fig. 23.2, down for lumisterol). This quantum yield increases slowly with wavelength from 295 to 302 nm but then doubles from 0.08 at 302 nm to 0.16 at 305 nm and then increases steadily to 0.29 at 325 nm. The quantum yield of *cis-trans* isomerisation to tachysterol decreases correspondingly over the same wavelength range. Various explanations for this behaviour have been advanced (see Dmitrenko et al. 2001 for further literature).

There are more complications to this photochemical system, which at first glance looks rather simple. It was found that the thermochemical step forming vitamin D, following the photochemical conversion of provitamin D, takes place more quickly in cells than in solutions (Tian et al. 1993; Holick et al. 1995). The reason for this is the existence of the conformer of previtamin D (lower right, Fig. 23.3 Dmitrenko et al. 2001). In solution, this is the preferred conformer, and it cannot be converted directly to vitamin D. In membranes, both natural and artificial liposome membranes (Tian and Holick 1999), the previtamin is held in the active, vitamin-producing conformer (cf. Saltiel et al. 2003). The same effect can be achieved by complexing the previtamin with β-cyclodextrin (Tian and Holick 1995).

Provitamins, previtamins, and vitamin D occur not only in free form but as glycosides in plants and in mammal skin also as fatty acid esters (Takada 1983). In rat skin, at least 80 % of the provitamin D_3 is esterified, and upon exposure of the skin to UV radiation, the provitamin D_3 ester is converted to vitamin D_3 ester.

The action spectrum for conversion of provitamin D_3 to previtamin D_3 in human skin has been determined by MacLaughlin et al. (1982). It has a single peak at about 297 nm that roughly corresponds to the long-wavelength absorption band of provitamin D_3 dissolved in *n*-hexane (Fig. 23.4). A digitised version with a long-wavelength extrapolation to 329.5 nm, having a maximum value at 297.5 nm (Bouillon et al. 2006), has been adopted by CIE (Comité International de l'Éclairage) as an official reference spectrum. This spectrum should be regarded as tentative, and there is reason to use it with caution (Norval et al. 2010). The absorption spectrum for provitamin D_3 is three-peaked, but the two short-wave absorption bands are lacking in the action spectrum. Two circumstances could contribute to this lack: (1) the stratum corneum of the skin could filter the shorter wavelength components, and (2) since at the shorter wavelengths both provitamin and previtamin absorb but at the longer wavelengths (around 295 nm) only provitamin and

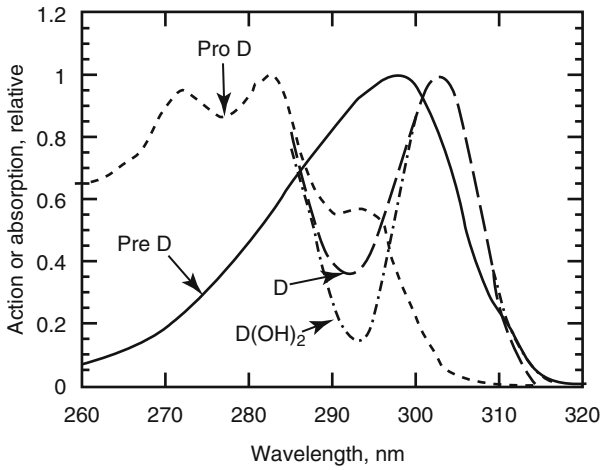

Fig. 23.4 Absorption spectrum for provitamin D_3 (Pro D), action spectrum for photosynthesis of previtamin D_3 (Pre D) according to MacLaughlin et al. (1982), and action spectra for photosynthesis of vitamin D_3 (D) and 1α,25-dihydroxyvitamin D_3 ($D(OH)_2$) according to Lehmann et al. (2001)

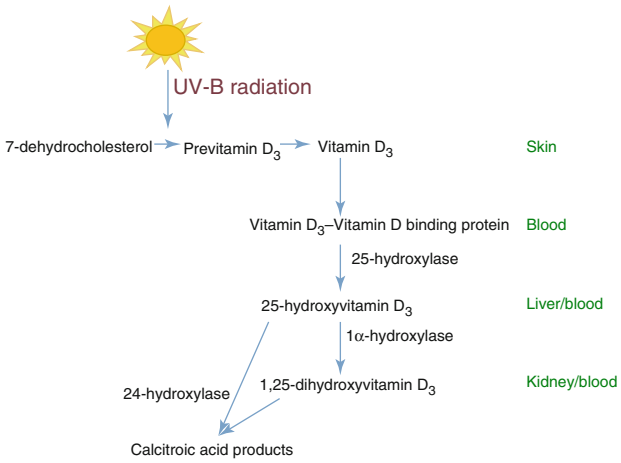

Fig. 23.5 Metabolic pathway leading to the synthesis of the active form of vitamin D_3, 1,25-dihydroxyvitamin D_3, following solar UV-B irradiation of the skin

tachysterol, the conversion of provitamin to previtamin is favoured at long wavelengths, while at shorter wavelengths the back and side reactions of previtamin are important competitors. Probably, under the conditions in which the action spectrum was determined, the first reason is more important.

Lehmann et al. (2001) measured the action spectra for formation of vitamin D_3 as well as $1,25(OH)_2D_3$ (1α,25-dihydroxyvitamin D_3) from provitamin D_3 in "artificial skin" containing cultured human keratinocytes. Remarkably, this action spectrum is displaced about 5 nm towards longer wavelength (peaking at about 302 nm) compared to the spectrum determined by MacLaughlin et al. (1982). Although no wavelength below 285 nm was tested, the spectrum indicates a rise from 293 nm towards shorter wavelengths. The minimum at approximately 293 nm is deeper than would be expected from the provitamin D_3 absorption spectrum. Takada et al. (1979) investigated the spectral dependence of vitamin D_3 formation in shaved cat skin. They found a maximum at 303 nm, similar to Lehmann et al. (2001). Their long-wavelength tail extends all the way to 340 nm. However, their spectrum must be regarded as very approximate, since it is plotted as effect at constant fluence, and the spectral bandwidth of the radiation is not stated. As the spectra of MacLaughlin et al. (1982) and Lehmann et al. (2001), it is plotted on an energy rather than photon basis and, therefore, not expected to match an absorption spectrum exactly. Knudson and Benford (1938) compared the effectiveness of different UV wavebands in preventing rickets in shaved rats. They found a peak at approximately the same wavelength as MacLaughlin et al. (1982) but also a (higher) peak at about 280 nm.

23.3 Production of the Active Form of Vitamin D in Humans

Exposure to the UV-B component in sunlight induces the production of previtamin D_3 from 7-dehydrocholesterol in the membranes of keratinocytes in the epidermis (Fig. 23.5). Vitamin D_3 (cholecalciferol) is then formed by a thermochemical reaction. Vitamin D_3 attaches to the vitamin D-binding protein (Gc-globulin) and enters the blood stream. In the liver it undergoes hydroxylation by the 25-hydroxylase enzyme, CYP27A1, to produce 25-hydroxyvitamin D_3 [$25(OH)D_3$] (calcidiol). A second hydroxylation step takes place in the kidney by the enzyme 1α-hydroxylase enzyme, CYP27B1, to form $1,25(OH)_2D_3$ (calcitriol) which is the active form of vitamin D. $1,25(OH)_2D_3$ can interact with the nuclear vitamin D receptor (VDR) present in many cell types in the body, thus affecting the transcription of more than 2,000 genes. $1,25(OH)_2D_3$ also induces rapid response signalling through a specific membrane receptor, recently identified as a protein disulfide isomerase, Pdia3 (Doroudi et al. 2014). The amount of circulating $1,25(OH)_2D_3$ is tightly regulated by negative feedback control through induction by the hormone of 24-hydroxylase which catabolises both $25(OH)D_3$ and $1,25(OH)_2D_3$ into various calcitonic acid products. There is limited evidence that $1,25(OH)_2D_3$ can be formed entirely in the epidermis following exposure to UV-B radiation.

The quantity of solar UV-B radiation reaching the Earth's surface varies hugely depending on many factors including the solar zenith angle. This is highest in the summer months and decreases to 5 % of this value at mid-latitudes in the winter and is zero at higher latitudes. One recent study

illustrates clearly how the solar UV-B irradiation affects the vitamin D status of a population. In the USA, the peak in vitamin D levels was found in August and the trough in February, a lag of 8 weeks after the peak and trough respectively in ambient UV-B (Kasahara et al. 2013). The solar zenith angle also explains why at least 50 % of the daily UV radiation is found in the 4 h period around local noon. Other environmental variables are ozone, cloud cover, air pollution, altitude, and surface reflection, such as from snow or choppy water. There are also large differences between individuals in their ability to produce active vitamin D following a given dose of solar UV-B. These include skin type, age, amount of clothing worn and head cover, use of sunscreen, body mass index, serum cholesterol level, polymorphisms in VDR and enzymes of the vitamin D pathway, and baseline 25(OH)D. For example, to synthesise the same amount of previtamin D_3, about a sixfold higher dose of UV-B is required for black skin compared with fair skin (due to absorption by melanin) (Clemens et al. 1982), and a twofold higher dose is required for an 80-year-old compared with a 20-year-old (due to the reduction in 7-dehydrocholesterol in older skin) (MacLaughlin and Holick 1985).

23.4 Vitamin D Status and Optimal Levels for Sufficiency

The assessment of vitamin D status is routinely carried out by measurement of the concentration of 25(OH)D in serum or plasma. The methods include chemiluminescence and radioimmunoassay, but these are recognised to lack accuracy, reproducibility, and sensitivity (Lai et al. 2012). Liquid chromatograph-tandem mass spectroscopy (LC-MS/MS) can distinguish between $25(OH)D_2$ (produced after consuming plants and vitamin D_2 supplements) and $25(OH)D_3$ and is rapidly becoming the method of choice. A vitamin D standardisation programme is underway using LC-MS/MS to ensure consistency in the measurements of 25(OH)D globally.

There is no consensus at present on the reference values that define a "satisfactory" vitamin D status, and indeed, the optimal range may differ between the skeletal and nonskeletal functions of vitamin D and between one individual and another. In the 1990s, the threshold for deficiency was frequently defined as <25 nmol/L 25(OH)D. In 2010, the US Institute of Medicine defined sufficiency as a serum concentration of 50 nmol/L or above for both adults and children (Institute of Medicine 2011). Others working in the area recommend much higher levels. For example, the Vitamin D Council advocates at least 125 nmol/L 25(OH)D (www.vitamindcouncil.org/about-vitamin-d/vitamin-d-deficiency/). Concentrations higher than 250 nmol/L may be harmful.

Some surveys suggest that there has been a decline in vitamin D status in populations in recent years. Thus there was a reduction from 75 nmol/L in 1988–1994 to 60 nmol/L in 2001–2004 in the large National Health and Nutritional Examination Survey in the USA (Ginde et al. 2009a). Epidemiological studies in several parts of the world indicate that an insufficient vitamin D status may be widespread, even in sunny countries. For example, 31 % of a large representative adult population in Australia, 21.4 % of women of child-bearing age in Oman, and 57 % of women and 49 % of men, aged 65 and above, in England all had 25(OH)D levels <50 nmol/L. Efforts have been made to construct models using the action spectrum from the conversion of 7-dehydrocholesterol to previtamin D_3 in the human skin to predict how much sun exposure an individual requires under different climate conditions to ensure a satisfactory vitamin D status (McKenzie et al. 2009, 2011; Diffey 2010). This approach has been supplemented by actual measurement of 25(OH)D levels in volunteers with different skin types, exposed to the simulated sunlight present at particular latitudes at different times of the year (Rhodes et al. 2010).

23.5 Vitamin D and Bone Health

Vitamin D deficiency has been known for many years to lead to abnormal skeletal development in utero and in children and to poor bone health in adults. The disease that results from the deficiency in children is called rickets in which bone deformities are found due to chondrocyte disaggregation and skeletal mineralisation defects. It is estimated that 25(OH)D levels lower than about 20 nmol/L can lead to rickets. Supplementation with vitamin D is recommended for infants aged 0–12 months. In adults, osteomalacia can result from vitamin D deficiency, with defective mineralisation of the collagen matrix and hence reduced structural support and increased risk of fracture. Osteoporosis can also occur in the elderly with an increased risk of fracture. Osteoblast activity is reduced and bone mineralisation is defective. Although various studies have not produced consistent results, they suggest that 25(OH)D levels above 75 nmol/L are required for protection against osteomalacia and osteoporosis (reviewed in Wacker and Holick 2013).

Vitamin D has a critical role in calcium and phosphorus metabolism, ensuring adequate levels of both for various metabolic functions and bone mineralisation. $1,25(OH)_2D$ significantly increases the absorption of both calcium and phosphorus from the intestine, the former by increasing the expression of an epithelial calcium channel and a calcium-binding protein. Vitamin D also acts indirectly on calcium and phosphorus levels via the regulation of parathyroid hormone (PTH). Low levels of 25(OH)D are associated with

low levels of serum-ionised calcium, a situation which leads to increased PTH levels. Higher 25(OH)D levels with associated higher calcium levels have the reverse effects on PTH. Both PTH and $1,25(OH)_2D$ stimulate osteoblasts to mobilise calcium stores. Further details can be found in Lips and van Schoor (2011) and Sai et al. (2011).

23.6 Nonskeletal Effects of Vitamin D and Potential Protection Against a Variety of Human Diseases

23.6.1 Immunomodulation Induced by Vitamin D

Increasing evidence has been obtained in recent years that vitamin D has multiple effects on the immune system, some stimulatory and some inhibitory. These could have relevance for the control of several human diseases and have been the subject of intense investigations in recent years.

Innate immunity involves a range of mechanisms that are often of most benefit at the initiation of a disease. Several innate immune responses are stimulated by $1,25(OH)_2D$. One important effect is to promote the expression of the cathelicidin gene in macrophages which leads to the production of cathelicidin (Liu et al. 2007). This peptide has antimicrobial activity against intracellular bacteria. $1,25(OH)_2D$ induces autophagy in monocytes and macrophages via the induction of cathelicidin which then activates transcription of the autophagy-related genes (Yuk et al. 2009). Autophagy is the process whereby a cell self-digests through the action of enzymes within the same cell, thus preventing the survival of intracellular bacteria and viruses. Low levels of vitamin D result in impaired development of invariant natural killer T cells, a consequence that is particularly apparent if the deficiency occurs in utero (Cantorna et al. 2012). The invariant natural killer T cells are involved in many immunological processes; they recognise lipids and glycolipids rather than the peptide-MHC complexes recognised by other T cell subsets, and, on activation, produce a range of immunostimulatory mediators including interferon (IFN)-γ, interleukin (IL)-2, and tumour necrosis factor (TNF)-α.

In contrast to the mainly positive effects of vitamin D on innate immune responses, the majority of adaptive immune responses are downregulated by $1,25(OH)_2D$. It inhibits the number and function of T regulatory cells, promotes the production of immunosuppressive cytokines such as IL-4 and IL-10 while having the reverse effect on the immunostimulatory cytokines such as IL-2, suppresses the differentiation and maturation of dendritic cells and their ability to present antigens, and inhibits the differentiation and maturation of B cells and their production of immunoglobulins (reviewed in Van Etten and Mattieu 2005).

Due to these varying responses, elucidating the role of vitamin D in the immune control of various diseases in humans is not an easy task, particularly when further complexities are considered, such as various VDR polymorphisms which might confer additional susceptibility and the independent immune function of the vitamin D-binding protein. Several disease categories in which vitamin D may play an important role by modulating the immune response have been described. These cover a wide range of common conditions. The evidence frequently relies on the group of patients with the disease having a lower 25(OH)D level than the group of controls. However, few of these studies are prospective and therefore cannot distinguish whether the low status is a consequence of the disease or is a significant risk factor. Clinical trials using vitamin D supplements to prevent the disease or, more commonly, as a treatment have yielded inconsistent results thus far. In addition, it is difficult and frequently impossible to separate the effects of solar UV radiation from the effects of vitamin D in human subjects (Hart and Gorman 2013). Therefore this area is one of uncertainty at present in which there is vigorous research interest and activity.

Diseases where vitamin D may be protective include various microbial infections, autoimmune diseases, internal cancers, mental disorders, cardiovascular diseases, all-cause mortality, and asthma. As examples, information relating to the role of vitamin D in infectious and autoimmune diseases is outlined in Sects. 23.6.2 and 23.6.3, respectively.

23.6.2 Vitamin D and Risk of Infectious Diseases

Many infectious diseases, especially those caused by viruses infecting the respiratory tract (e.g. respiratory syncytial virus, rhinovirus, coronavirus, influenza, and parainfluenza), have a seasonal incidence with a peak in the winter months. Although there could be several explanations for this, including increased survival and transmission of viruses at low temperature and humidity, one suggestion, first made more than 30 years ago (Hope-Simpson 1981), attributed the pattern to the lower level of vitamin D in the winter months as the solar UV-B radiation declines. As outlined in Sect. 23.6.1, many aspects of innate immunity which are important in protection against viral infection of the respiratory tract are diminished by insufficient vitamin D. In particular, the reduced production of antimicrobial peptides by neutrophils, macrophages, and natural killer cells of the respiratory tract and by epithelial cells may be important as well as the lack of autophagy in macrophages. In addition, the action of vitamin D in suppressing the cytokine "storm" that is a feature of many respiratory infections may be vital (de Jong et al. 2006).

Observational evidence has been obtained from a variety of settings and countries in which 25(OH)D levels have been correlated with the occurrence of respiratory viral infections. In most cases, the lower the concentration of 25(OH)D, the higher the risk of respiratory infection (Ginde et al. 2009b; Sabetta et al. 2010; Berry et al. 2011). However, it should be noted that in almost all of these studies, the population already had symptoms of the infection at the time of the 25(OH)D assessment. Thus whether a low vitamin D status contributes to the risk of a symptomatic infection or is a consequence of the infection cannot be distinguished. About eight prospective randomised double-blind trials have taken place which examined whether vitamin D_3 supplements can prevent respiratory infections. No consistent difference in the risk of respiratory infection between those taking the supplement and those given a placebo was found (reviewed in Bergman et al. 2013). However, one study reported that a benefit was apparent if the starting level of 25(OH)D was deficient (Camargo et al. 2012). Further trials are underway currently.

In tuberculosis, the causative bacterium, *Mycobacterium tuberculosis*, persists in macrophages, and therefore, the promotion of antimicrobial peptides and autophagy by $1,25(OH)_2D$ may represent important factors in protection against persistence of the organism or its activation. In the nineteenth century, cod liver oil, which contains the highest level of vitamin D_3 of any food, was used in Europe to prevent childhood diseases such as tuberculosis. It was superseded by heliotherapy (sun exposure) and phototherapy (exposure to artificial light sources) before the development of antibiotics in the second half of the twentieth century. Thus a possible link between vitamin D deficiency and susceptibility to tuberculosis or disease progression has a long history. More recent studies consistently report that subjects with tuberculosis have insufficient 25(OH)D levels or lower levels than control subjects (reviewed in Ralph et al. 2013). It is clearly difficult to investigate whether vitamin D status influences susceptibility to infection with *M. tuberculosis* and development of active disease from latency or response to treatment. In particular, whether a low 25(OH)D level is a consequence of the disease or a risk factor for, it needs to be distinguished. This can only be examined in prospective studies. Clinical trials using vitamin D supplements to prevent progression from latent to active tuberculosis have not been undertaken as yet, but other trials in which the supplements were administered to treat active disease have yielded predominantly negative results. The reasons that these trials do not support the observational findings include the possibilities that suboptimal doses of the supplement were used or that they did not lead to a sufficient increase in $1,25(OH)_2D$ or that host determinants were not taken into account such as expression of the hydroxylases and the vitamin D-binding protein and polymorphisms in the VDR (Ralph et al. 2013).

23.6.3 Vitamin D and Risk of Autoimmune Diseases

It has been recognised for many years that the frequency of several autoimmune diseases is associated with latitude so that the further from the Equator, the higher the prevalence. Such a gradient has been shown most convincingly for multiple sclerosis (MS) but is also found to a lesser degree for type 1 diabetes mellitus, rheumatoid arthritis, and Crohn's disease. Although the aetiology of these diseases is multifactorial with a clear genetic susceptibility, there is evidence that one environmental risk factor might be low exposure to solar UV radiation leading to insufficient vitamin D. As outlined in Sect. 23.6.1 above, $1,25(OH)_2D$ has effects on the immune system that could help to prevent autoimmunity. In brief, it can counteract autoimmune inflammation, induce the differentiation of T regulatory cells that promote self-tolerance, inhibit the differentiation of dendritic cells and their ability to present antigen, and increase the production of immunosuppressive cytokines.

Of the autoimmune diseases and their possible link with vitamin D, most information has been published for MS. In MS, there is immune-mediated destruction of myelin-producing cells and axonal loss in the central nervous system, and it is the most frequent disabling neurological disorder of young adults. The latitudinal gradient for MS was first noted more than 50 years ago (Acheson and Bachrach 1960) and has been validated in more recent reports, including a comprehensive meta-analysis of global data in 2011 (Simpson et al. 2011). A similar latitudinal variation in the incidence of the common precursor of MS, called first central nervous system demyelinating events, has also been found (Taylor et al. 2010). Low ambient UV radiation or low sun exposure in childhood may be particularly significant in increasing the risk of MS in later life. Also, the month of birth has an important effect on the risk of MS development in the offspring; an increased risk for those born in the spring when maternal 25(OH)D levels are likely to be low and a decreased risk for those born in the late autumn/early winter when maternal 25(OH)D levels are likely to be higher (Dobson et al. 2013). In two large cohort studies in the USA, a higher vitamin D intake in the form of supplements and higher serum 25(OH)D levels were both linked to a decreased risk of MS (Munger et al. 2004; Munger et al. 2006). There was a particularly strong inverse relationship if the higher 25(OH)D level occurred before the age of 20 years. Furthermore the relapse rates for MS correlate inversely with serum 25(OH)D levels.

With regard to treatment of MS, several clinical trials have assessed vitamin D_3 as a supplement, sometimes in association with IFN-β. The results thus far have been inconsistent (Soilu-Hanninen et al. 2012; Kampman et al. 2012; James et al. 2013), but none have shown more than a very

modest benefit. Such studies are difficult and costly to undertake due to the low incidence of MS, the length of follow-up that is required, the need for a placebo group and for monitoring radiological, clinical, and immunological parameters, and uncertainties regarding the optimal dose of the supplement and how frequently it should be taken. However, there remains the intriguing possibility of using vitamin D supplements as an inexpensive, safe, and easy to administer treatment to improve current therapies in MS.

23.7 Evolutionary Aspects

Why has nature chosen, for the hormonal regulation of calcium metabolism and other bodily functions, a substance requiring the uncertain exposure to UV radiation for its synthesis? The answer to this question is not obvious and requires probing into several evolutionary aspects.

One explanation, proposed by Chevalier et al. (1997), is that the formation of $1,25(OH)_2D$ from 7-dehydrocholesterol was originally a catabolic pathway, which then became regulatory. Arguments for this are, first, that vitamin D and related substances are rather toxic, and, secondly, that P450-type enzymes are involved both in hydroxylations that lead to detoxification and solubilisation of known toxins and in several hydroxylation steps of vitamin D and its analogues (see reviews of the vitamin D-related hydroxylations by Jones (1999) and Okuda and Ohyama (1999)).

One way of probing into the past is to compare amino acid sequences in proteins of living organisms. It is believed that the VDR belongs to a class of nuclear receptors of very ancient origin. The nuclear receptor class can be divided into several subclasses, and the divergence into these subclasses occurred at least 600 Ma ago (Bertrand et al. 2004). The closest known relative to the VDR is the ecdysone receptor in insects. One way of tracing the origin of the vitamin D regulation system would be to track the evolution of the VDR more in detail, but such a study has not been undertaken thus far.

In terrestrial vertebrates, i.e. birds, reptiles, and amphibians, the role of vitamin D is similar to that in mammals, although birds are not able to use vitamin D_2 efficiently and other provitamins and vitamin D than D_2 and D_3 may exist in lizards and frogs (Holick 1989) (see Sect. 23.10 below for the relative efficiency of vitamin D_3 and vitamin D_2 in humans). Further back in evolutionary history, the evidence starts to become more "fishy".

Several investigations show that various saltwater fish can thrive without vitamin D, and this is true also for at least one freshwater fish species (Ashok et al. 1998, 1999). There are, however, an even larger number of studies that indicate a function for vitamin D in other fish species (Barnett et al. 1979; Brown and Robinson 1992; Larsson 1999 and sources cited therein). It is also not clear why regulation would be unnecessary as a mechanism to avoid too high a calcium concentration in the cytosol is required.

The first vertebrates were the jawless Heterostraci and Osteostrachi, whose bodies were covered by bony plates. They were followed in evolution by the first true fishes, the shark-like Placodermi. These, belonging to the Elasmobranchiomorphi (cartilaginous fishes), had no bones inside their bodies, but they were also covered with a bony armour. Is it possible that the deposition of calcium phosphate and calcium carbonate early in evolution served as a protection against UV radiation, and that its deposition was regulated by radiation? This suggestion could be tested by finding out if the thickness of the armour varied with latitude (and thus with UV-B exposure) while taking continental drift and polar migration into account.

Even the earliest vertebrates mentioned lived less than 550 million years ago, at a time when the protecting ozone shield is thought to have afforded almost the same protection as today (see Chap. 16). The nuclear VDR has been found in a jawless fish (Whitfield et al. 2003), but could the regulation of calcium metabolism by vitamin D be of even more ancient origin than the vertebrates? Several investigations point in this direction.

In one type of coral (incidentally a relative of the red coral used for gems), UV radiation favours the development of normal spicules, structures containing collagen and calcium carbonate. The animal also produces $1,25(OH)_2D$ in a UV-dependent manner (Kingsley et al. 2001).

The most compelling evidence, however, for the ancient origin of vitamin D as a calcium regulator comes from experiments with snails. In these animals, certain vitamin D-like compounds elevate intracellular exchangeable calcium and suppress alkaline phosphatase activity, leading to the conclusion that snails adapt to light conditions via the vitamin D endocrine system (Kriajev and Edelstein 1994, 1995; Kriajev et al. 1994). The evolutionary lines leading to molluscs and to vertebrates are estimated, with some uncertainty, to have diverged about 720 million years ago. If further evidence of vitamin D regulation in copepods, corals, and coccolithophorids is found, a much older age for the regulation system would have credence. If it is assumed that the vitamin effects in plants (see Sect. 23.11.) have an evolutionary origin in common with the regulation of calcium metabolism in animals, then this origin lies more than a one and a half billion years ago (Nei et al. 2001).

There remains the unlikely possibility of convergent evolution that distantly related organisms have independently selected vitamin D as their calcium regulator. If this is the case, why is vitamin D the best choice?

Calcium carbonate itself is a poor absorber of UV radiation, and therefore, it is not efficient as a radiation shield. Even a cm-thick layer absorbs only half of the incident radiation at the DNA absorption maximum (260 nm), as calculated from data for clear calcite crystals (Washburn et al. 1929). However, the scattering effect of calcium carbonate

needs to be added and, most importantly, the absorption by proteins and other substances always associated with calcium carbonate shells and other calcified structures.

If the reason for the choice of the UV-sensitive vitamin D system is not regulation of UV shielding, what could it be? The human immune system is altered by UV radiation (see Chap. 24), but the evolutionary pressure that has selected for this modulation is obscure. It is likely to be relevant, since it occurs through different mechanisms, among others UV absorption in urocanic acid and absorption in DNA. Could it be that the original function of the vitamin D system was to modulate the immune defence, a function that to some extent seems still to exist?

23.8 Vitamin D_2 Compared with Vitamin D_3

The form of vitamin D used in major preparations of prescriptions in North America was for a long time vitamin D_2 (Houghton and Vieth 2006), probably because it can be produced at a lower cost, and the process was patented early. This is now changing. Recently, there has been much interest in comparing the effects of vitamin D_2 and vitamin D_3 in human nutrition (Horst et al. 2000). When administered *over a prolonged time*, both are equally well taken up and converted to 25(OH)D circulating in the blood stream and also hydroxylated a second time to $1,25(OH)_2D$. Tsugawa et al. (1999) found that the D_2 form of $1,25(OH)_2D$ binds equally well as the D_3 form to the VDR. However, this experiment used calf VDR, and the results may not apply to the polymorphic forms of the human receptor. The D_2 forms are not converted to the corresponding D_3 forms (Holick et al. 2008; Biancuzzo et al. 2013). Some of the vitamin D, D_2, as well as D_3 is also converted to 1,24,25-hydroxylated forms. While $1,24,25(OH)_3D_3$ can bind to the VDR and exert biological activity, $1,24,25(OH)_3D_2$ is inactive (see Houghton and Vieth 2006 for this and related topics), and this results in vitamin D_2 having less overall activity than vitamin D_3. It should be noted that differences in effects between D_2 and D_3 forms are not as large in humans as in rats and birds.

When vitamin D is given as a *single large dose*, the increase in circulating $25(OH)D_2$ initially rises in the same way as does the D_3 form, but after 3 weeks, the level starts to fall in the case of hydroxyvitamin D_2 but continues to rise and only falls after 15 weeks in the case of hydroxyvitamin D_3 (Armas et al. 2004).

23.9 Distribution of Provitamin and Vitamin D in the Plant Kingdom

Among microalgae, several (but not all) species of the green algae *Chlorella* (Patterson 1971) and *Chlamydomonas reinhardtii* (Patterson 1974) contain ergosterol. This provitamin has also been found in the diatom *Skeletonema menzelii*, the coccolithophorid *Emaliana huxleyi* (Holick 1989), and the chrysophycean *Ochromonas danica* (Gershengorn et al. 1968). In addition, there have been numerous investigations on phytoplankton of mixed composition. In one instance, a correlation with the probable UV exposure was established, using season as a proxy for irradiation (Takeuchi et al. 1991; see also Tables 1a and 1b in Björn and Wang 2001). Among macroalgae, not only ergosterol but also provitamin D_2 and vitamins D_2 and D_3 have been found in the brown alga *Fucus vesiculosus* grown under natural conditions with a higher content of the vitamins at a lower (southern Sweden) than at a higher (northern Norway) latitude. Provitamin D_3 is present in the gametophyte of the red alga *Chondrus crispus*, while the sporophyte of the same species contains the isomer 22-dehydrocholesterol.

Higher plants generally contain provitamins and vitamins D_2 and D_3 in their leaves (Napoli et al. 1977; Rambeck et al. 1981; Horst et al. 1984; Prema and Raghuramulu 1996; Boland et al. 2003). In general, vitamins are present only after exposure to UV radiation (Hess and Weinstock 1924; Skliar et al. 2000; Björn and Wang 2001 and references cited therein) although there are exceptions (see Sect. 23.13). Some plants even form the hydroxylated forms of vitamin D (Napoli et al. 1977; Skliar et al. 2000; Gil et al. 2007).

23.10 Physiological Effects of Provitamin and Vitamin D in Plants and Algae

Fries (1984) showed that growth of the green macroalga *Enteromorpha compressa*, the red alga *Nemalion helminthoides*, and the brown alga *Fucus spiralis* is stimulated by vitamins and provitamin D. Vitamin D_3 applied to herbaceous and woody plants stimulates initiation of adventitious roots (Buchala and Schmid 1979; Jarvis and Booth 1981; Moncousin and Gaspar 1983). Vitamin D at a nanomolar concentration inhibits root elongation in *Phaseolus vulgaris* and promotes germination of light-sensitive lettuce seed in darkness (Buchala and Pythoud 1988). Vitamin D_3 induces the synthesis of the calcium-binding signalling protein calmodulin in bean roots (Vega and Boland 1986).

23.11 Roles of Provitamin and Vitamin D in Plants

Solanum glaucophyllum, the waxy leaf nightshade, endemic in several South American countries, forms such large amounts of the active vertebrate hormone form, $1,25(OH)_2D_3$, that grazing animals develop calcinosis and can die (see Curino et al. 1998; Boland et al. 2003 for literature). In this case, a protective function of vitamin D for the plant is assumed.

There are some indications that vitamin D and its hydroxylated forms are involved in calcium metabolism in plants. Thus Aburjai et al. (1997) found that calcium deprivation increased the concentrations of vitamin D and 25(OH)D in cell cultures of *Solanum malacoxylon*, while results for $1,25(OH)_2D_3$ were not clear due to analytical difficulties. Burlini et al. (2002) showed that the concentration of $1,25(OH)_2D_3$ increased when calcium ions were removed from the medium. Conversely, Habib and Donnelly (2005) claimed that the calcium content of potato plants (*Solanum tuberosum*) was increased by either exposure to UV radiation or administration of vitamin D. This finding needs confirmation by independent investigators. Vega and Boland (1988, 1989) and Milanesi and Boland (2006) have pointed to the similarity between the vertebrate VDR and proteins present in *Phaseolus vulgaris* and *Solanum glaucophyllum*.

23.12 Biogeographical Aspects

Human complexion tends to be darker the higher the UV radiation in the environment. This is an inherited ("racial") trait that has evolved independently in Europe and Asia (Norton et al. 2007), but many individuals can acclimatise phenotypically to some extent (i.e. the skin forms pigment in response to UV radiation; see Chap. 24 and Cui et al. 2007). UV radiation can cause skin cancer and other problems, and these effects are particularly frequent for people poorly adapted for the high environmental radiation they are exposed to, such as people of European origin living in South Africa and Australia. Thus, clearly, the pigment works as protection against high radiation. It has been proposed (Branda and Eaton 1978; Jablonski and Chaplin 2000) that pigmentation is important for photoprotection of folic acid, but in vivo, this substance is photoprotected in another way (Vorobey et al. 2006). Although vitamin D is toxic at too high a concentration, it has been shown by Holick et al. (1981) that skin pigment is not necessary to prevent its overaccumulation; the photochemical system is self-regulating. The reason for this is the low rate of conversion of previtamin to vitamin, in combination with the photochemical side and back reactions of previtamin D. Thus, toxicity can occur only following excessive intake (e.g. Koutkia et al. 2001).

There is, however, another connection between skin type and vitamin D. All humans are thought to originate from Africa and presumably are all descendants of black-skinned people, although at a prehuman furred stage, lighter skin is possible as found in chimpanzees (Jablonski and Chaplin 2000). But with migration to higher and higher latitudes, the skin colour became paler (Fig. 23.6). The selection pressure for this is clear: avoidance of vitamin D deficiency

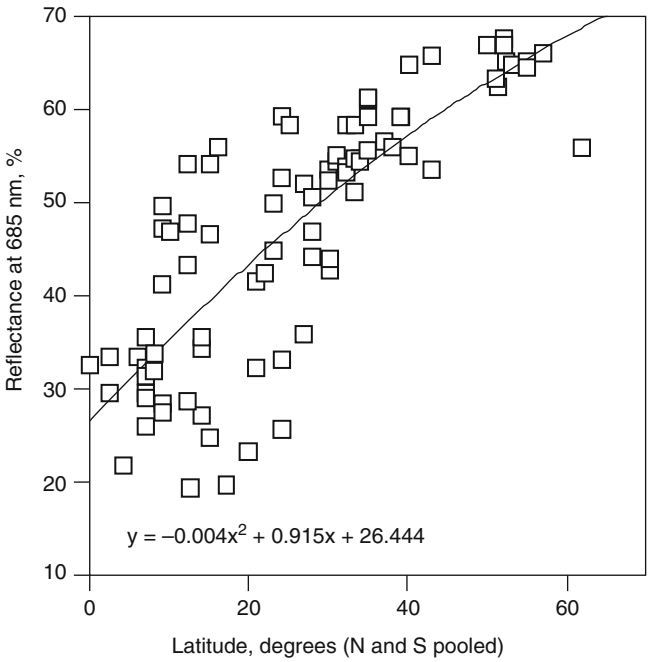

Fig. 23.6 The relation between skin colour (reflectance at 685 nm) and latitude for 85 samples of "indigenous populations" from different parts of the world. Darker skin colour is lower in the diagram, and on the abscissa, 0 stands for the equator. In the regression equation at the bottom of the graph, *y* stands for reflectance in percent and *x* for latitude in degrees. There is a clear trend of darker skin colour towards the equator. The great variation around the regression curve has several causes. Even "indigenous populations" have migrated and settled in their present regions within a time span which is often too short to allow complete adaptation to the environment. The way of life also modulates the need for sunlight. Thus, the square at the highest latitude (a little above 60°) lies far below the regression curve. It represents Inuits in southern Greenland. It is thought that they, due to their vitamin D-rich food from the sea, have a lesser need for vitamin D from photochemical conversion in the skin than most other populations (Data adapted from those compiled by Jablonski and Chaplin (2000))

(Clemens et al. 1982). African people who have emigrated north in historic time are known to suffer from just such a deficiency (Shewakramani et al. 2001). Inuits may have more pigment than would be predicted from their northern habitat; their traditional food is from the sea and mostly rich in vitamin D (because the sea currents bring vitamin D from lower and more sunny latitudes), so they have not been exposed to the same selection pressure as people with more terrestrial habits.

Jablonski and Chaplin (2000) found that in all human populations where data were available, the complexion of women is lighter than that of men. It may be difficult to separate out the acclimation component due to different lifestyles, but the authors believe that it could be an adaptation to the greater need for calcium and vitamin D during pregnancy and lactation.

The question remains: How do non-human terrestrial vertebrates manage at high latitudes? As they are often covered with hair or plumage or are "cold-blooded" (poikilothermic), they would have difficulties in producing their own vitamin D by having either inefficient photochemical conversion of pro- to previtamin or inefficient thermochemical conversion of previtamin to vitamin. In fact, amphibians, and reptiles in particular, decline in frequency with increasing latitude. The arctic dinosaurs may, in fact, have been homeothermic (thermoregulating).

According to an old and abandoned theory, birds produce provitamin D in their uropygial gland and distribute it over their plumage when preening. This converts to vitamin D on exposure to sunlight and is ingested at the next preening. Later investigations with more modern methods of analysis have failed to establish with certainty that provitamin D is in the uropygial secretion. There is a single study, using the best analytical methods available at the time, which demonstrated the presence of provitamin D_3 in the uropygial gland of domestic fowl (*Gallus*) (Uva et al. 1978). Such an investigation needs to be repeated using high-performance liquid chromatography, nuclear magnetic resonance, and absorption spectroscopy, since the identification of provitamin D_3 among all the steroids present in uropygial secretion is not straightforward. If its presence can be established, the analysis could be extended to other kinds of birds. It should also be mentioned that Holick (1989; referring to unpublished observations by himself and M.A. St. Lezin) found no provitamin D_3 in chicken feathers. On the other hand, it is well established that fowl can use UV absorbed by the head and legs to improve their vitamin D and calcium status and egg production. It is assumed that birds like arctic owls and ptarmigans are totally dependent on vitamin D in the food for covering their requirements. Birds cannot efficiently use vitamin D_2 only D_3.

For arctic mammals, like reindeer, the situation is critical. Reindeer need large quantities of calcium, not only for the skeleton but also for the yearly production of antlers. They are covered with hair and do not have a uropygial gland, so they rely heavily on food for their vitamin D. The critical time is the dark winter, and the most important winter food is reindeer lichen. We (Wang et al. 2001) investigated one species of reindeer lichen from different latitudes (Fig. 23.7) and found that it contained both vitamins D_2 and D_3, in a strongly latitude-dependent manner, with the lowest values in northern Scandinavia even by the end of the summer. Still, 10 g of the lichen from northern Scandinavia would provide a human with the necessary daily amount, but would humans eat lichen? Wild reindeer survive, even on Spitsbergen island at 78°N, where the vitamin D content in their food must be lower than this. Could there be another source? It would perhaps be worth looking at what the rumen bacteria can produce.

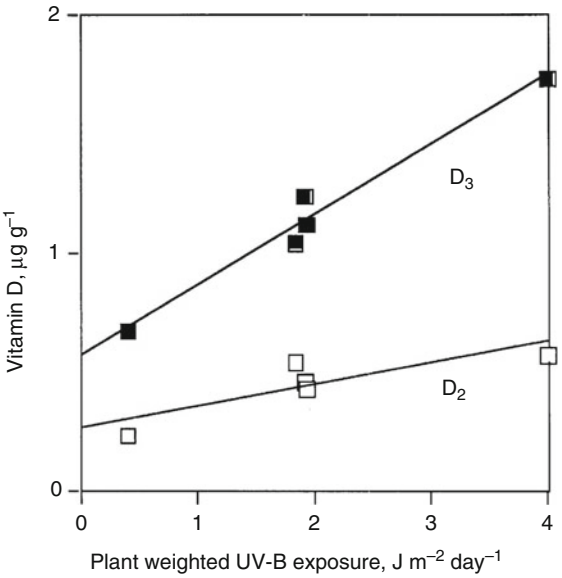

Fig. 23.7 Vitamins D_2 and D_3 contents in the reindeer lichen *Cladina arbuscula* at different latitudes (northern Finland, 67°N, to Greece, 40°N) (From Wang et al. (2001))

23.13 Non-photochemical Production of Vitamin D

Vitamin D can be produced non-photochemically. Curino et al. (1998, 2001) have shown that cells of *Solanum glaucophyllum* grown in culture in darkness form $1,25(OH)_2D_3$, albeit at lower concentrations than the plant under sun-exposed field conditions. The mechanism is not known, but one has been proposed by Norman and Norman (1993) to explain how animals like subterranean mole rats, living in darkness, can obtain their requirement from underground plant parts. It is, however, (1) doubtful whether these animals need vitamin D (Pitcher and Buffenstein 1995 and literature cited there) and (2) unlikely that their diet is really completely vitamin D-free, as we have found small amounts of vitamins D_2 and D_3 in carrot roots not exposed to UV radiation (Wang and Björn, unpublished). The same holds for nocturnal animals (Opperman and Ross 1990; Kwiecinski et al. 2001). Larsson (1999) has erroneously claimed that Opperman and Ross (1990) found that the nocturnal fruit-eating bat *Rousettus aegyptiacus* can form 7-dehydrocholesterol from mevalonate.

References

Aburjai T, Bernasconi S, Manzocchi LA, Pelizzoni F (1997) Effect of calcium and cell immobilization on the production of cholecalciferol and its derivatives by *Solanum malacoxylon* cell cultures. Phytochemistry 46:1015–1018

Acheson ED, Bachrach CA (1960) The distribution of multiple sclerosis in U.S. veterans by birthplace. Am J Hyg 72:77–88

Armas LAG, Hollis BW, Heaney RP (2004) Vitamin D2 is much less effective than vitamin D3 in humans. J Clin Endocrinol Metab 89:5387–5391

Ashok A, Rao DS, Raghuramulu N (1998) Vitamin D is not an essential nutrient for rora (*Labeo rohita*) as a representative of freshwater fish. J Nutr Sci Vitaminol 44:195–205

Ashok A, Rao DS, Chennaiah S, Raghuramulu N (1999) Vitamin D2 is not biologically active for rora (*Labeo rohita*) as vitamin D3. J Nutr Sci Vitaminol 45:21–30

Barnett BJ, Cho CY, Slinger SJ (1979) The essentiality of cholecalciferol in the diets of rainbow trout (*Salmo gairdneri*). Comp Biochem Physiol 63A:291–297

Bergman P, Lindh AU, Bjorkhem-Bergman L, Lindh JD (2013) Vitamin D and respiratory tract infections: a systematic review and meta-analysis of randomized controlled trials. PLoS One 8:e65835

Berry DJ, Hesketh K, Power C, Hypponen E (2011) Vitamin D status has a linear association with seasonal infections and lung function in British adults. Br J Nutr 106:1433–1440

Bertrand W, Brunet FG, Escriva H, Parmentier G, Laudet V, Robinson-Rechavi M (2004) Evolutionary genomics of nuclear receptors: From twenty-five ancestral genes to derived endocrine systems. Mol Biol Evol 21:1923–1937

Biancuzzo RM, Clarke N, Reitz RE, Travison TG, Holick MF (2013) Serum concentrations of 1,25-dihydroxyvitamin D_2 and 1,25-dihydroxyvitamin D_3 in response to vitamin D_2 and Vitamin D_3 supplementation. J Clinic Endocrinol Metab 98:973–979

Björn LO, Wang T (2001) Is provitamin D a UV-B receptor in plants? Plant Ecol 154:3–8

Boland R, Skliar M, Curino A, Milanesi L (2003) Vitamin D compounds in plants. Plant Sci 164:357–369

Boomsma F, Jacobs HJC, Havinga E, van der Gen A (1975) Studies of vitamin D and related compounds, part 24. New irradiation products of pre-vitamin D3. Tetrahedron Lett 7:427–430

Bouillon R, Eisman J, Garabedian M, Holick MF, Kleinschmidt J, Suda T, Terenetskaya I, Webb A (2006) Action spectrum for production of previtamin D3 in human skin, CIE Technical Report 174, Commission Internationale de l'Éclairage (CIE) Central Bureau, Vienna, Austria.

Bouillon R, Norman AW, Pasqualini JR (eds) (2004) Vitamin D: proceedings of the 12th workshop on vitamin D, July 6–10, 2003. Maastricht, the Netherlands. Elsevier, Amsterdam. (Reprinted from J. Steroid Biochem Mol Biol 89–90)

Branda RF, Eaton JW (1978) Skin color and nutrient photolysis: an evolutionary hypothesis. Science 201:625–626

Brown PB, Robinson EH (1992) Vitamin D studies with channel catfish (*Ictalurus punctuatus*) reared in calcium-free water. Comp Biochem Physiol 103A:213–219

Buchala AJ, Pythoud F (1988) Vitamin D and related compounds as plant growth substances. Physiol Plant 74:391–396

Buchala AJ, Schmid A (1979) Vitamin D and its analogues as a new class of plant growth substances affecting rhizogenesis. Nature 280:230–231

Burlini N, Bernasconi S, Manzocchi LA (2002) Effects of elicitors and Ca2+ deprivation on the levels of sterols and 1,25-dihydroxy vitamin D-3 in cell cultures of *Solanum malacoxylon*. Funct Plant Biol 29:527–533

Camargo CA Jr, Ganmaa D, Frazier AL, Kirchberg FF, Stuart JJ, Kleinman K, Sumberzul N, Rich-Edwards JW (2012) Randomized trial of vitamin D supplementation and risk of acute respiratory infection in Mongolia. Pediatrics 130:e561–e567

Cantorna MT, Zhao J, Yang L (2012) Vitamin D, invariant natural killer T-cells and experimental autoimmune disease. Proc Nutr Soc 71:62–66

Chevalier G, Baudet C, AvenelAudran M, Furman I, Wion D (1997) Was the formation of 1,25-dihydroxyvitamin D initially a catabolic pathway? Med Hypotheses 48:325–329

Clemens TL, Adams JS, Henderson SL, Holick MF (1982) Increased skin pigment reduces the capacity of skin to synthesise vitamin D3. Lancet 319:74–76

Cui R, Widlund HR, Feige E, Lin JY, Wilensky DL, Igras VE, D'Orazio J, Fung CY, Schanbacher CF, Granter SR, Fisher DE (2007) Central role of p53 in the suntan response and pathologic hyperpigmentation. Cell 128:853–864

Curino A, Skliar M, Boland R (1998) Identification of 7-dehydrocholesterol, vitamin D3, 25(OH)-vitamin D3 and 1,25(OH)2-vitamin D3 in *Solanum glaucophyllum* cultures grown in absence of light. Biochim Biophys Acta 1425:485–492

Curino A, Milanesi L, Benassati S, Skliar M, Boland R (2001) Effect of culture conditions on the synthesis of vitamin D3 metabolites in *Solanum glaucophyllum* grown in vitro. Phytochemistry 58:81–89

De Jong MD, Simmons CP, Thanh TT et al (2006) Fatal outcome of human influenza A (H5N1) is associated with high viral load and hypercytokinemia. Nat Med 12:1203–1207

DeLuca (1997) Historical overview. In: Feldman D, Glorieux FH, Pike JW (eds) Vitamin D. Academic, New York, pp 3–12

Diffey DL (2010) Is casual exposure to summer sunlight effective at maintaining adequate vitamin D status? Photodermatol Photoimmunol Photomed 26:172–176

Dmitrenko O, Frederick JH, Reischl W (2001) Previtamin D conformations and the wavelength-dependent photoconversions of previtamin D. J Photochem Photobiol A: Chemistry 139:125–131

Dobson R, Giovannoni G, Ramagopalan S (2013) The month of birth effect in multiple sclerosis: systematic review, meta-analysis and effect of latitude. J Neurol Neurosurg Psychiatry 84:427–432

Doroudi M, Chen J, Boyan BD, Schwartz Z (2014) New insights on membrane mediated effects of 1α,25-dihydroxy vitamin D3 signaling in the musculoskeletal system. Steroids 81:81–87

Feldman D, Glorieux FH, Pike JW (eds) (2005) Vitamin D. 2nd ed. Academic Press, New York

Fries L (1984) D-vitamins and their precursors as growth regulators in axenically cultivated marine macroalgae. J Phycol 20:62–66

Gershengorn MC, Smith ARH, Goulston G, Goad LJ, Goodwon TW, Haines TH (1968) The sterols of *Ochromonas danica* and *Ochromonas malhamensis*. Biochemistry 7:1698–1706

Gil S, Dallorso M, Horst R (2007) Screening of vitamin D activity (VDA) of *Solanum glaucophyllum* leaves measured by radioimmunoassay (RIA). J Steroid Biochem Mol Biol. doi:10.1016/j.jsbmb.2006.11.008

Ginde AA, Lui MC, Camargo CA Jr (2009a) Demographic differences and trends of vitamin D insufficiency in the US population, 1988–2004. Arch Intern Med 169:626–632

Ginde AA, Mansbach JM, Camargo CA Jr (2009b) Association between serum 25-hydroxyvitamin D level and upper respiratory tract infection in the Third National Health Nutrition Examination Survey. Arch Intern Med 169:384–390

Glerup H, Mikkelsen K, Poulsen L, Hass E, Overbeck S, Thomsen J, Charles P, Eriksen EF (2000) Commonly recommended daily intake of vitamin D is not sufficient if sunlight exposure is limited. J Intern Med 247:260–268

Glisson F (1650) De Rachitide sive morbo puerili, qui vulgo The Rickets diciteur http://books.google.se/books?id=mtOLP7AI8v4C&printsec=frontcover&hl=sv#v=onepage&q&f=false

Habib A, Donnelly DJ (2005) Stimulation of Ca2+ uptake into micropropagated potato plantlets by UV light and vitamin D_3. Am J Potato Res 82:191–196

Hart PH, Gorman S (2013) Exposure to UV wavelengths in sunlight suppresses immunity. To what extent is UV-induced vitamin D_3 the mediator responsible? Clin Biochem Rev 34:3–13

Haussler MR, Whitfield GK, Kaneko I, Haussler CA, Hsieh D, Hsieh J-C, Jurutka PW (2013) Molecular mechanisms of vitamin D action. Calcif Tissue Int 92:77–98

Havinga E (1973) Vitamin D, example and challenge. Experientia 29:1181–1193

Hess AF, Unger LG (1921) Cure of infantile rickets by sunlight. JAMA 77:39

Hess AF, Weinstock M (1924) Antirachitic properties imparted to inert fluids and green vegetables by ultraviolet irradiation. J Biol Chem 62:301–313

Holick MF (1989) Phylogenetic and evolutionary aspects of vitamin D from phytoplankton to humans. In: Pang PKT, Schreibman MP (eds) Vertebrate endocrinology: fundamentals and biomedical implications, vol 3. Academic, Orlando, pp 7–43

Holick MF (1999) Evolution, biologic functions, and recommended dietary allowances for vitamin D. In: Holick MF (ed.) Vitamin D: Physiology, molecular biology, and clinical applications. Humana Press, Totowa, pp. 1–16.

Holick MF (ed) (2010) Vitamin D: physiology, molecular biology, and clinical applications, 2nd edn. Humana Press, Totowa. ISBN 978-1-60327-303-9; e-ISBN 978-1-60327-303-9'; doi:10.1007/978-1-60327-303-9

Holick MF, MacLaughlin JA, Doppelt SH (1981) Regulation of cutaneous previtamin D3 photosynthesis in man: skin pigment is not an essential regulator. Science 211:590–592

Holick MF, Tian XQ, Allen M (1995) Evolutionary importance for the membrane enhancement of the production of vitamin D3 in the skin of poikilothermic animals. Proc Natl Acad Sci U S A 98:3124–3126

Holick MF, Biancuzzo RM, Chen TC, Klein EK, Young A, Bibuld D, Reitz R, Salameh W, Ameri A, Tannenbaum AD (2008) Maintaining circulating concentrations of 25-hydroxyvitamin D. J Clin Endocrinol Metab 93:677–681

Hope-Simpson RE (1981) The role of season in the epidemiology of influenza. J Hyg (Lond) 86:35–47

Horst RL, Reinhardt TA, Russell JR, Napoli JL (1984) The isolation and identification of vitamin D2 and vitamin D3 from *Medicago sativa* (alfalfa plant). Arch Biochem Biophys 231:67–71

Horst RL, Prapong S, Reinhardt TA, Koszewski NJ, Knutson J, Bishop C (2000) Comparison of the relative effects of 1,24-dihydroxyvitamin D_2, [1,24-(OH)2D2], 1,24-dihydroxyvitamin D_3 [1,24-(OH)2D3], and 1,25-dihydroxyvitamin D3 [1,25-(OH)2D3] on selected vitamin D-regulated events in the rat. Biochem Pharmacol 60:701–708

Hossein-nezhad A (2013) Vitamin D for health: a global perspective. Mayo Clin Proc 88:720–755

Houghton LA, Vieth R (2006) The case against ergocaciferol (vitamin D2) as a vitamin supplement. Am J Clin Nutr 84:694–697

Institute of Medicine (US) committee to review dietary reference intakes for vitamin D and calcium (2011) Ross AC, Taylor CL, Yaktine AL, Del Valle HB (eds) Dietary reference intakes for calcium and vitamin D. National Academies Press, Washington DC

Jablonski NG, Chaplin G (2000) The evolution of human skin coloration. J Hum Evol 39:57–106

James E, Dobson R, Kuhle J, Baker D, Giovannoni G, Ramagopalan SV (2013) The effect of vitamin D-related interventions on multiple sclerosis relapses: a meta-analysis. Mult Scler J 19:1571–1579

Jarvis BC, Booth A (1981) Influence of indole-butyric acid, boron, myo-inositol, vitamin D2 and seedling age on adventitious root development in cuttings of *Phaseolus aureus*. Physiol Plant 53:213–218

Jones G (1999) Metabolism and catabolism of vitamin D, its metabolites and clinically relevant analogs. In: Holick MF (ed) Vitamin D: physiology, molecular biology, and clinical applications. Humana Press, Totowa, pp 57–84

Kampman MT, Steffensen LH, Mellgren SI, Jorgensen L (2012) Effect of vitamin D3 supplementation on relapses, disease progression, and measures of function in persons with multiple sclerosis: exploratory outcomes from a double-blind randomised controlled trial. Mult Scler 18:21144–21151

Kasahara AK, Sungh RJ, Noymer A (2013) Vitamin D (25OHD) serum seasonality in the United States. PLoS One 8:e65785

Kingsley RJ, Corcoran ML, Krider KL, Kriechbaum KL (2001) Thyroxine and vitamin D in the gorgonian *Leptogorgia virgulata*. Comp Biochem Physiol A 129:897–907

Knudson A, Benford F (1938) Quantitative studies of the effectiveness of ultraviolet radiation of various wave-lengths in rickets. J Biol Chem 124:287–299

Koutkia P, Chen TC, Holick MF (2001) Vitamin D intoxication associated with an over-the-counter supplement. N Engl J Med 345:66–67

Kriajev L, Edelstein S (1994) Vitamin D metabolites and extracellular calcium currents in hemocytes of land snails. Biochem Biophys Res Commun 204:1096–1101

Kriajev L, Edelstein S (1995) Effect of light and nutrient restriction on the metabolism of calcium and vitamin D in land snails. J Exp Zool 272:153–158

Kriajev L, Otremski I, Edelstein S (1994) Calcium shells from snails: response to vitamin D metabolites. Calcified Tissue Int 55:204–207

Kwiecinski GG, Lu ZR, Chen TC, Holick MF (2001) Observations on serum 25-hydroxyvitamin D and calcium concentrations from wild-caught and captive neotropical bats, *Artibeus jamaicensis*. Gen Comp Endocrinol 122:225–231

Lai JK, Lucas RM, Banks E, Ponsonby AL (2012) Variability in vitamin D assays impairs clinical assessment of vitamin D status. Intern Med J 42:43–50

Larsson D (1999) Vitamin D in teleost fish: non-genomic regulation of intestinal calcium transport. Diss. Göteborg Univ., Dept of Zoophysiology Göteborg, Sweden. ISBN 91-628-3681-1

Lehmann B, Genehr T, Pietzsch J, Meurer M (2001) UVB-induced conversion of 7-dehydrocholesterol to 1α,25-dihydroxyvitamin D3 in an in vitro human skin equivalent model. J Invest Dermatol 117:1179–1185

Lips P (2006) Vitamin D physiology. Prog Biophys Mol Biol 92:4–8

Lips P, van Schoor NM (2011) The effects of vitamin D on bone and osteoporosis. Best Pract Res Clin Endocrinol Metab 25:585–591

Liu PT, Stenger S, Tang DH, Modlin RL (2007) Cutting edge: vitamin D-mediated human antimicrobial activity against Mycobacterium tuberculosis is dependent on the induction of cathelicidin. J Immunol 179:2060–2063

MacLaughlin J, Holick MF (1985) Aging decreases the capacity of human skin to produce vitamin D3. J Clin Invest 76:1536–1538

MacLaughlin JA, Anderson RR, Holick MF (1982) Spectral character of sunlight modulates photosynthesis of previtamin D3 and its photoisomers in human skin. Science 216:1001–1003

McKenzie RL, Aucamp PJ, Bais AF, Bjorn LO, Ilyas M, Madronich S (2011) Ozone depletion and climate change: impacts on UV radiation. Photochem Photobiol Sci 10:182–198

McKenzie RL, Liley JB, Björn LO (2009) UV radiation: Balancing risks and benefits. Photochem Photobiol 85:88–98.

Mellanby E (1918) The part played by an "accessory factor""in the production of experimental rickets. J Physiol (Lond) 52:11–14

Milanesi L, Boland R (2006) Presence of vitamin D-3 receptor (VDR)-like proteins in *Solanum glaucophyllum*. Physiol Plant 128: 341–350

Moncousin C, Gaspar T (1983) Peroxidase as a marker for rooting improvement of *Cynara scolymus* L. cultured in vitro. Biochem Physiol Pflanzen 178:263–271

Mozolowski W (1939) Jedrzej Sniadecki (1768–1838) on the cure of rickets. Nature 143:121

Munger KL, Zhang SM, O'Reilly E, Hernan NS, Olek MJ, Willett WC, Ascherio A (2004) Vitamin D intake and incidence of multiple sclerosis. Neurology 62:60–65

Munger KL, Levin LI, Hollis BW, Howard NS, Ascherio A (2006) Serum 25-hydroxyvitamin D levels and risk of multiple sclerosis. J Am Med Assoc 296:2832–2838

Napoli JL, Reeve LE, Eisman J, Schnoes HK, DeLuca HF (1977) *Solanum glaucophyllum* as source of 1,25-dihydroxyvitamin D3. J Biol Chem 252:2580–2583

Nei M, Xu P, Glazko G (2001) Estimation of divergence times from multiprotein sequences for a few mammalian species and several distantly related organisms. Proc Natl Acad Sci U S A 98:2497–2502

Norman AW (2006) Minireview: vitamin D receptor: new assignments for an already busy receptor. Endocrinology 147:5542–5548

Norman TC, Norman AW (1993) Consideration of chemical mechanisms for the nonphotochemical production of vitamin D3 in biological systems. Bioorg Med Chem Lett 3:1785–1788

Norton HL, Kittles RA, Parra E, McKeigue P, Mao X, Cheng K, Canfield VA, Bradley DG, McEvoy B, Shriver MD (2007) Genetic evidence for the convergent evolution of light skin in Europeans and East Asians. Mol Biol Evol 24:710–722

Norval M, Björn LO, de Gruijl FR (2010) Is the action spectrum for the UV-induced production of previtamin D_3 in human skin correct? Photochem Photobiol Sci 9:11–17

Okuda K-I, Ohyama Y (1999) The enzymes responsible for metabolizing vitamin D. In: Holick MF (ed) Vitamin D: physiology, molecular biology, and clinical applications. Humana Press, Totowa, pp 85–107

Opperman LA, Ross FP (1990) The adult fruit bat (Rousettus aegypticus) expresses only calbindin-D9K (vitamin D-dependent calcium-binding protein) in its kidney. Comp Biochem Physiol B Biochem Mol Biol 97:295–299

Patterson GW (1971) The distribution of sterols in algae. Lipids 6:120–127

Patterson GW (1974) Sterols of some green algae. Comp Biochem Physiol B 47:453–457

Pitcher T, Buffenstein R (1995) Intestinal calcium-transport in mole rats (*Cryptomys damarensis* and *Heterocephalus glaber*) is independent of both genomic and non-genomic vitamin D mediation. Exp Physiol 80:597–608

Prema TP, Raghuramulu N (1996) Vitamin D3 and its metabolites in the tomato plant. Phytochemistry 42:617–620

Ralph AP, Lucas RM, Norval M (2013) Vitamin D and solar ultraviolet radiation in the risk and treatment of tuberculosis. Lancet Infect Dis 13:77–88

Rambeck WA, Kreutzberg O, Bruns-Droste C, Zucker H (1981) Vitamin D-like activity of *Trisetum flavescens*. Zschr Pflanzenphysiol 104:9–16

Rhodes LE, Webb AR, Fraser HI, Kift R, Durkin MT, Allan D, O'Brien SJ, Vail A, Berry JL (2010) Recommended summer sunlight exposure levels can produce sufficient (>or = 20 ng ml(-1)) but not the proposed optimal (>or = 32 ng ml(-1)) 25(OH)D levels at UK latitudes. J Invest Dermatol 130:1411–1418

Sabetta JR, DePetrillo P, Cipriano P, Smardin J, Burns LA, Landry ML (2010) Serum 25-hydroxyvitamin d and the incidence of acute viral respiratory tract infections in healthy adults. PLoS One 5:e11088

Sai AJ, Walters RW, Fang X, Gallagher JC (2011) Relationship between vitamin D, parathyroid hormone and bone health. J Clin Endocrinol Metab 96:E436–E446

Saltiel J, Cires L, Turek AM (2003) Conformer-specific photoconversion of 25- hydroxytachysterol to 25-hydroxyprevitamin D3: role in production of vitamin Ds. J Am Chem Soc 125:2866–2867

Schwartz GG, Skinner HG (2007) Vitamin D status and cancer: new insights. Curr Opin Clin Nutr Metab Care 10:6–11

Shewakramani S, Rakita D, Tangpricha V, Holick MF (2001) Vitamin D insufficiency is common and under-diagnosed among African American patients. J Bone Miner Res 16:S512

Simpson S Jr, Blizzard L, Otahal P, van der Mei I, Taylor B (2011) Latitude is significantly associated with the prevalence of multiple sclerosis: a meta-analysis. J Neurol Neurosurg Psychiatry 82:1132–1141

Skliar M, Curino A, Milanesi E, Benassati S, Boland R (2000) *Nicotiana glauca*: another plant species containing vitamin D3 metabolites. Plant Sci 156:193–199

Soilu-Hanninen M, Aivo J, Lindstrom BM, Elovaara I, Sumelahti ML, Farkkila M, Lienari P, Atula S, Sarasoja T, Herrala L, Keskinarkaus I, Kruger J, Kallio T, Rocca MA, Filippi M (2012) A randomised, double-blind, placebo controlled trial with vitamin D3 as an add on treatment to interferon β-1b in patients with multiple sclerosis. J Neurol Neurosurg Psychiatry 83:565–571

Steenbock H, Black A (1924) The induction of growth-promoting and calcifying properties in a ration by exposure to ultra-violet light. J Biol Chem 61:405–422

Takada K (1983) Formation of fatty acid esterified vitamin D3 in rat skin by exposure to ultraviolet radiation. J Lipid Res 24:441–448

Takada K, Okano T, Tamura Y (1979) A rapid and precise method for the determination of vitamin D_3 in rat skin by high-performance liquid chromatography. J Nutr Sci Vitaminol 25:385–398

Takeuchi A, Okano T, Tanda M, Kobayashi T (1991) Possible origin of extremely high contents of vitamin D3 in some kinds of fish liver. Comp Biochem Physiol 100A:483–487

Taylor BV, Lucas RM, Dear K, Kilpatrick TJ, Pender MP, van der Mei IA, Chapman C, Coulthard A, Dwyer T, McMichael AJ, Valery PC, Williams D, Ponsonby AL, Lim L (2010) Latitudinal variation in the incidence and type of first central nervous system demyelinating events. Mult Scler 16:398–406

Tian WQ, Holick MF (1995) Catalyzed thermal isomerization between previtamin D3 and vitamin D_3 via β-cyclodextrin complexation. J Biol Chem 270:8706–8711

Tian WQ, Holick MF (1999) A liposomal model that mimics the cutaneous production of vitamin D_3. J Biol Chem 274:4174–4179

Tian XQ, Chen TC, Matsuoka LY, Wortsman J, Holick MF (1993) Kinetic and thermodynamic studies of the conversion of previtamin D3 to vitamin D3 in human skin. J Biol Chem 268:14888–14892

Tsugawa N, Nakagawa K, Kawamoto Y, Tachibana Y, Hayashi T, Ozono K, Okaono T (1999) Biological activity profiles of 1α,25-dihydroxyvitamin D_2, D_3, D_4, D_7, and 2-epi-1α,25-dihydroxyvitamin D_2. Biol Pharm Bull 22:371–377

Uva BM, Ghiani P, Deplano S, Madich A, Vaccari M, Vallarino M (1978) Occurrence of 7-dehydrocholesterol in the uropygial gland of domestic fowls. Acta Histochem 62:237–243

Van de Peer Y, Baldauf SL, Doolittle WF, Meyer A (2000) An updated and comprehensive rRNA phylogeny of (crown) eukaryotes based on rate-calibrated evolutionary distances. J Mol Evol 51:565–576

Van Etten E, Mathieu C (2005) Immunoregulation by 1,25-dihydroxyvitamin D3: basic concepts. J Steroid Biochem Mol Biol 97:93–101

Vega MA, Boland RL (1986) Vitamin D-3 induces the novo synthesis of calmodulin in *Phaseolus vulgaris* root segments in vitro. Biochim Biophys Acta 881:364–374

Vega MA, Boland RL (1988) Presence of sterol-binding sites in the cytosol of French-bean (*Phaseolus vulgaris*) roots. Biochem J 250:565–569

Vega MA, Boland RL (1989) Partial characterization of the sterol binding macro-molecule of *Phaseolus vulgaris* roots. Biochim Biophys Acta 1012:10–15

Vorobey P, Steindal AE, Off MK, Vorobey A, Johan Moan J (2006) Influence of human serum albumin on photodegradation of folic acid in solution. Photochem Photobiol 82:817–822

Wacker M, Holick MF (2013) Sunlight and vitamin D: A global perspective for health. Dermato-Endocrin 5:51–108

Wang T, Bengtsson G, Kärnefelt I, Björn LO (2001) Provitamins and vitamins D2 and D3 in *Cladina* spp. over a latitudinal gradient: possible correlation with UV levels. J Photochem Photobiol B 62:118–122

Washburn EW, Washburn EW et al (eds) (1929) International critical tables of numerical data, physics chemistry and technology, vol 5. McGraw-Hill, New York, p 270

Webb AR, de Costa B, Holick MF (1989) Sunlight regulates the cutaneous production of vitamin D3 by causing its photodegradation. J Clin Endocrinol Metab 68:882–887

Whistler D (1645) Morbo puerili Anglorum, quem patrio idiomate indigenae vocant The Rickets. Lugduni Batavorum 1–13

Whitfield GK, Dang HTL, Schluter SF, Bernstein RM, Bnag T, Manzon LA, Hsieh G, Domnguez CE, Youson JH, Haussler MR, Marchalonis JJ (2003) Cloning of a functional vitamin D receptor from the lamprey (*Petromyzon marinus*), an ancient vertebrate lacking a calcified skeleton and teeth. Endocrinology 144(6):2704–2716

Wickelgren I (2007) A healthy tan? Science 315:1214–1216

Yuk JM, Shin DM, Lee HM, Yang CS, Jin HS, Kim KK, Lee ZW, Lee SH, Kim JM, Jo EK (2009) Vitamin D3 induces autophagy in human monocytes/macrophages via cathelicidin. Cell Host Microbe 6:231–243

Zarowitz BJ (2008) The value of vitamin D_3 over vitamin D_2 in older people. Geriatr Nurs 29:89–91

The Photobiology of Human Skin

24

Mary Norval

24.1 Introduction

The skin is the largest organ of the body and the one which is most exposed to external insults, such as chemicals, infecting microorganisms, and mechanical trauma. These insults include UV radiation from the sun. The structure of the skin is complex: it is composed of three basic layers—the epidermis, dermis, and subcutis—each comprising a variety of cell types. It has been recognized that the skin contains its own immune system, first called skin-associated lymphoid tissues, which generally acts very effectively to deal with any local disturbances. It is now termed the skin immune system. However, UV radiation poses two unique and potentially dangerous consequences for the skin. It induces genotoxic changes, mutations leading on some occasions to the development of skin cancers, and it can also suppress cell-mediated immune responses to a variety of antigens. The reason for the latter change may be to prevent excessive inflammation in sun-exposed skin, but if it occurs at the same time as, say, an infection or oncogenesis, then there may be disadvantages for the host. Solar UV radiation does not always cause harm in the skin, and one case where it is beneficial is in promoting the synthesis of vitamin D, essential for calcium metabolism, a healthy skeleton, and multiple immunological effects. This aspect is covered in detail in Chap. 23.

The following section outlines the structure of the skin and describes the skin immune system, with use of contact and delayed-type hypersensitivity as examples. Consideration is then given to UV radiation in the context of cutaneous pigmentation, sunburn, and photoageing. Sections on photocarcinogenesis and UV-induced immunomodulation follow, and the final part of the chapter outlines some photosensitivity disorders that can occur in human subjects.

M. Norval
Biomedical Sciences, University of Edinburgh Medical School, Edinburgh, Scotland, UK
e-mail: m.norval@ed.ac.uk

24.2 The Structure of Skin and the Skin Immune System

24.2.1 Skin Structure

The outermost layer of the skin is the epidermis, which is separated from the dermis by a basement membrane, and the layer underlying the dermis is the subcutis. UV-B rays (280–315 nm) penetrate into the epidermis and UV-A rays (315–400 nm) deeper into the dermis. These layers are transversed vertically by the skin appendages, such as the sweat glands, hair follicles, and sebaceous glands. The appendages are rarely affected by UV radiation and are not considered in this chapter.

The epidermis is composed mainly of keratinocytes that are formed in the basal layer and migrate upward to terminally differentiate at the skin surface. It takes about 4 weeks to complete this process. The appearance of the keratinocytes at each stage divides the epidermis into four layers: (1) the basal layer where the cells divide intermittently, giving rise to one daughter cell remaining in the basal layer and one which begins to differentiate and move upwards; (2) the prickle cell layer, so-called as the keratinocytes have distinct interconnecting junctions; (3) the granular layer where the keratinocytes begin to flatten and contain keratohyalin granules and degenerating organelles; and (4) the stratum corneum where the keratinocytes die and are sloughed off. The thickness of each layer depends on the location in the body. Other important cell types contained within the epidermis are the melanocytes and the Langerhans cells. The former give the skin its colour and are found mainly at the dermato-epidermal junction. The latter are dendritic cells whose processes form a network throughout the epidermis. There are also scattered lymphocytes. Figure 24.1 illustrates the cellular structure of the epidermis.

The dermis is very different from the epidermis, consisting of collagen fibres with fibroblasts and elastic tissue throughout. There are blood vessels, nerve fibres, and some smooth

L.O. Björn (ed.), *Photobiology: The Science of Light and Life*,
DOI 10.1007/978-1-4939-1468-5_24,

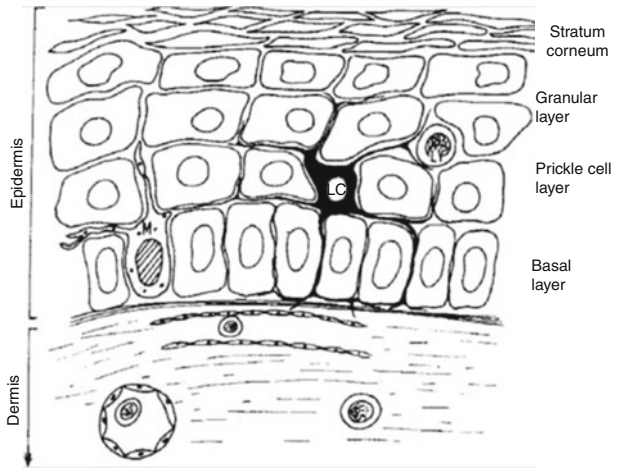

Fig. 24.1 Diagram of the epidermis indicating the keratinocyte layers and a representative Langerhans cell (LC), melanocyte (*M*), and lymphocyte (*LY*). Part of the dermis is also shown illustrating collagen fibres and small blood vessels

Table 24.1 Major resident cells of the skin immune system

Skin layer	Cell type	Function (s)
Epidermis	Keratinocytes	Production of cytokines and hormones
	Langerhans cells	Processing and presentation of antigens and regulatory functions
	Melanocytes	Production of α-melanocyte-stimulating hormone
	T cells	Effector and regulatory functions
Dermis	Mast cells	Production of inflammatory mediators
	Endothelial cells	Regulation of cell migration
	Dendritic cells	Processing and presentation of antigens
	Nerve cells	Production of neuroendocrine hormones and neuropeptides
	T cells	Effector and regulatory functions

muscle, together with small numbers of dendritic cells and tissue macrophages. Mast cells are also present which contain histamine and other inflammatory mediators.

24.2.2 The Skin Immune System

The skin immune system consists of contributions from many skin types, some resident in the epidermis or dermis, and others highly mobile, frequently connecting the cutaneous environment with the blood or lymph (reviewed in Bos 2005). The major populations of resident cells are shown in Table 24.1.

The Langerhans cells were thought until recently to have the important function of initiating the pathways contained within the skin immune system, by acting as the major antigen-presenting cells of the skin. However, there is new evidence that their main role could be activation of regulatory cells in local lymph nodes (Romani et al. 2012). In addition to the Langerhans cells, there are dendritic cells resident in the dermis and other dendritic cells recruited as monocytes from the blood. Both of these cell types can also act as antigen-presenting cells. On contact with an antigen, they internalize it, often by phagocytosis, and process it into smaller peptides for presentation on the cell surface. There are associated changes locally due to a variety of cytokines expressed by the local keratinocytes, including tumour necrosis factor (TNF)-α and interleukin (IL)-1β, and neuromediators expressed by nerves. In response to these substances, the antigen-bearing dendritic cells migrate from the skin. They move down the afferent lymph and enter into the draining lymph node. This process takes around 18 h following cutaneous application of a contact sensitizer. During the migration, the dendritic cells mature into effective antigen-presenting cells, as indicated by the changed expression of various adhesion and co-stimulatory molecules on their surfaces. In the paracortical area of the lymph node, they then present the processed antigenic peptides to antigen-specific T cells. These T cells are stimulated to proliferate and to express a particular cytokine profile, some with immunostimulatory properties, such as interferon (IFN)-γ and some with immunosuppressive properties, such as IL-10. The cytokine profile of the T cells that are activated largely determines the type of immune response generated and its efficiency. In some instances, the activated T cells home preferentially to the skin as they express particular surface markers. They leave the lymph node in the efferent lymph, enter the bloodstream through the thoracic duct, and migrate via the blood to the site of antigen application. They extravasate through the high endothelial venules and enter the dermis or epidermis to act as effector cells locally.

24.2.3 Contact and Delayed-Type Hypersensitivity

Contact hypersensitivity (CHS) is frequently used to assess immune responses in the skin under experimental conditions. In mice, a range of sensitizing compounds is employed for such tests such as 2,4-dinitrochlorobenzene and oxazolone, and in humans nickel is a frequent contact allergen. In brief, CHS is divided into two phases: the first is induction/sensitization (afferent), and the second is elicitation/challenge (efferent). They are followed by a regulation/resolution phase. During sensitization, small, structurally simple haptens are placed on the skin. Haptens on their own are incapable of generating immune responses, but they react with proteins locally in the skin to create immunologically relevant hapten-derivatized proteins. The first response is release of inflammatory mediators by resident skin cells and of neuromediators by sympathetic nerves. Recruitment of monocytes from the blood also occurs rapidly which differentiate into dendritic cells locally. These events are followed by the activation and migration of the hapten-bearing

Table 24.2 Contact hypersensitivity: outline of sequence of events in induction/sensitization (afferent) and elicitation/challenge (efferent) phases

Induction/sensitization	Elicitation/challenge
First skin contact with hapten, formation of hapten-derivatized protein	Second skin contact with the same antigen
Local production of inflammatory mediators and neuromediators	Recruitment of hapten-specific T cells from blood to skin and activation of hapten-specific T cells locally
Migration of hapten-bearing dendritic cells from the skin to the draining lymph node	Production of a range of immune mediators and mast cell degranulation
Arrival of mature hapten-bearing dendritic cells in the draining lymph nodes	Infiltration of neutrophils, natural killer cells, and T regulatory cells
Antigen presentation by these dendritic cells to antigen-specific T cell subsets	
Proliferation of CD8+ T cells and CD4+ T regulatory cells in the lymph node	
Circulation of these T cells in the blood	

epidermal Langerhans cells, dermal dendritic cells, and recruited dendritic cells to the draining lymph node via the afferent lymphatics. In the paracortical area of the draining lymph node, these dendritic cells are mature and activate hapten-specific CD8+ and CD4+ T cells: the proliferation of these T cells is controlled by hapten-specific CD4+ T regulatory cells. The stimulated T cell subsets then migrate to the blood and circulate throughout the body. In the elicitation phase, rechallenge by topical application of same contact sensitizer occurs but on a different body site from the first occasion. Again, there is local inflammation induced with activation of mast cells and release of mediators by resident skin cells. Hapten-specific T cells are recruited from the blood and CD8+ T cells are activated locally in the skin, with production of a range of inflammatory mediators including interferon (IFN)-γ, TNF-α, and IL-17. These induce a massive infiltration of neutrophils, natural killer cells, and T regulatory cells into the skin site. Such changes can be quantified at 24–72 h postchallenge either by a colour change in the skin, as is frequently used in human studies, or by swelling, such as of an ear, in the case of mice. Regulation/resolution of the inflammatory response is an active immune process mediated by specific T regulatory cells and possibly other cell types in addition. A summary of the sequence of events in CHS is shown in Table 24.2, and the subject is reviewed in full in Vocanson et al. (2009).

Delayed-type hypersensitivity (DTH) has the same endpoints as CHS but, in contrast to CHS, the antigens are complex. In natural circumstances and in some animal models, these antigens are often derived from infectious microorganisms or developing tumours. Under experimental conditions, they are frequently injected subcutaneously or intradermally. They are therefore taken up by dermal dendritic cells and are processed and presented differently from the simple haptens applied epicutaneously. One human example is the Mantoux test, used to assess tuberculosis immunity and exposure status, where protein-purified derivative is injected intradermally and the extent of induration at the test site measured two to three days later.

Table 24.3 Selected skin responses to UV radiation: the peak wavelength is the wavelength of maximum responsiveness

Process	Peak, nm	Reference
Induction of squamous skin cancer (mouse)	293	de Gruijl et al. (1993)
Induction of squamous skin cancer [SKUP] (human)	293	de Gruijl (1995)
Local suppression of memory immune responses (human)	300 and 370	Damian et al. (2011)
Immediate pigment darkening (human)	350	Irwin et al. (1993)
Melanogenesis (human)	290	Parrish et al. (1982)
Erythema (human)	300	McKinley and Diffey (1987)
Decrease in epidermal Langerhans cell numbers (mouse)	270–290	Noonan et al. (1984)
Systemic suppression of contact hypersensitivity (mouse)	260–280	De Fabo and Noonan (1983)
Induction of cyclobutane pyrimidine dimers (mouse)	290	Cooke and Johnson (1978)
Isomerization from trans to cis-urocanic acid (mouse)	300–315	Gibbs et al. (1993)
Isomerization from trans to cis-urocanic acid (human)	280–310	McLoone et al. (2005)
Formation of previtamin D3 from 7-dehydrocholesterol (human)	295–300	MacLaughlin et al. (1982)
T cell apoptosis	290	Novak et al. (2004)
Induction of TNF–α in epidermis (human)	300	Walker and Young (2007)

24.2.4 Effect of Solar UV Radiation on the Skin: Action Spectra

Exposure of skin to solar UV radiation results in a number of effects which are outlined in Sects. 24.3–24.7. In some instances the wavelength of the radiation promoting an individual effect with maximal efficiency has been derived from the action spectrum; these results are shown in summary form in Table 24.3, with more detail in the text.

24.3 Pigmentation and Sunburn

24.3.1 Pigmentation and Phototypes

Skin colour is determined by cutaneous pigments, particularly melanin; by blood circulating through the skin; and by the thickness of the stratum corneum. Melanin is synthesized by the melanocytes and is released by exocytosis as granules (melanosomes), which are then taken up by the adjacent keratinocytes. Melanin is present in at least two forms: eumelanin, a brown polymer predominating in darkly pigmented skin, and pheomelanin, a reddish-yellow pigment found in lighter skin types. The production of melanin is influenced by genetic factors, hormones, and exposure to UV radiation. Racial variation in skin colour—black, brown, yellow, and white—is not determined by the absolute number of melanocytes but by their activity in producing melanosomes. As might be expected, the melanosomes are larger and more numerous in black-skinned people. On exposure of the skin to UV radiation, the melanocytes are stimulated to produce melanin, which gives the skin its tan. Individuals vary enormously in this response. Those with fair nonpigmented skin, who cannot or are hardly able to synthesize melanin in response to sun exposure, suffer more cutaneous damage than those who tan, mainly because more UV radiation reaches the dermis. Similarly, the ability to tan correlates with less risk of burning after solar UV. There are six phototypes, originally recognized by Fitzpatrick (1988), as shown in Table 24.4.

24.3.2 Sunburn and Minimal Erythema Dose

Sunburn is recognized by erythema and blistering and is caused most effectively by radiation of wavelengths around 300 nm in the UV-B waveband. It is a delayed response, being maximal 8–24 h after exposure, and it gradually resolves with subsequent skin dryness and peeling. Solar lentigines or freckles can be formed after only one or two episodes of acute solar burning and are often seen on the shoulders, particularly of men. Factors involved in the vasodilatation which characterizes sunburn include direct effects of UV on the vascular endothelium, especially endothelial cell enlargement; the loss of epidermal Langerhans cells; the release of epidermal inflammatory mediators such as TNF-α; and the secretion of vasoactive substances from mast cells, for example, histamine and prostaglandins (Gilchrest et al. 1981).

In sunburned skin, so-called sunburn cells are seen in the epidermis. They are thought to represent apoptotic keratinocytes and are characterized by a glassy eosinophilic cytoplasm and a pyknotic nucleus (Young 1986). They are induced in a UV-dose-dependent manner, most efficiently by radiation towards the lower end of the UV-B waveband, and are found maximally at 24 h postirradiation. They are removed either by desquamation or by keratinocyte-mediated phagocytosis.

It is sometimes required to ascertain the minimal erythema dose (MED) of an individual for medical or experimental purposes. The MED is defined as the smallest dose of radiation that results in just detectable reddening of the skin, usually assessed at 24 h after exposure. It is determined by irradiating the normal, untanned skin, often on the back or the inner upper arm, with a graded series of UV doses. The MED for skin type I is about 150–300 effective J/m^2, while for skin type IV it is 450–600 J/m^2, although there is considerable overlap between the phototypes (Harrison and Young 2002). A monochromatic source is frequently used so that the erythemal response can be investigated at several wavelengths, for example, 300, 320, 350, and 400 nm. Several methods are available to determine erythema, such as visually, by reflectance spectrophotometry, or by scanning laser Doppler velocimetry. As the MED is a measure solely of each person's sensitivity to UV radiation, another term, the standard erythema dose (SED), has been proposed to refer to UV exposure from natural and artificial sources. One SED is equivalent to an erythemal effective radiant exposure of 100 J/m^2 (Diffey 2002). An exposure of four SEDs is likely to cause moderate erythema on unacclimated white skin, but produce little or no erythema on previously exposed skin (Diffey 2002).

Table 24.4 Classification of skin phototypes (Fitzpatrick 1988)

Phototype/ethnicity	UV sensitivity	Sunburn/tan
I – White Caucasian	Extremely sensitive	Always burns, never tans
II – White Caucasian	Moderately sensitive	Burns readily, tans slowly and with difficulty
III – White Caucasian	Moderately sensitive	Can burn after high exposure, tans slowly
IV – White Caucasian, often southern Mediterranean	Relatively tolerant	Burns rarely, tans easily
V – Brown, Asian/middle Eastern	Variable	Can burn easily, difficult to assess as pigment is already present
VI – Black, Afro-Caribbean	Relatively insensitive	Rarely burns

24.4 Photoageing

Photoageing, also termed extrinsic skin ageing or premature skin ageing, is associated with chronically sun-exposed skin. It can be distinguished to some extent from the more subtle changes which occur during intrinsic ageing due to the passage of time on sun-protected body sites (Taylor et al. 1990).

Animal models which have been used to investigate photoageing and its repair include the micro-pig and the hairless mouse. The UV-A waveband induces the majority of the changes observed due to its high penetration into the dermis with effects on the extracellular matrix. Photoageing is found on the body sites most frequently exposed to sunlight, such as the face and the back of the hands and neck. The last site was first recognized over a hundred years ago, and the condition called "farmer's neck"—the heavily wrinkled nape of the neck—was seen in farmers and sailors who worked outdoors predominantly. The involvement of the endocrine system and other environmental factors, such as smoking and malnutrition, can act to accelerate photoageing.

The characteristic features of photoageing include coarse and fine wrinkles, age spots (actinic lentigines containing increased numbers of dermal melanocytes), mottled hyperpigmentation and freckles, elastosis, leathery and thickened skin with surface roughness, and actinic keratoses, which are small scaly lesions, often multiple and persistent. In contrast unexposed skin or intrinsically aged skin is pale, smooth, and relatively unwrinkled.

The changes in photoaged skin are mainly due to effects on the dermal proteins which form the extracellular matrix. In brief, fibrillar collagen confers tensile strength, elastic fibres confer resilience (recoil), and proteoglycans confer hydration. The first stages of process are inflammatory, where mast cells, monocytes, and neutrophils invade the dermis (Lavker and Kligman 1988). Proteolytic enzymes including elastase and matrix metalloproteinases (MMPs) are produced by the neutrophils and lead to the degradation of elastin. In addition, reactive oxygen species and DNA damage, particularly in the mitochondria, result from the UV radiation, and they induce the increased production of the MMPs in keratinocytes (epidermis) and fibroblasts (dermis). Particular MMPs cleave collagen, thus contributing to the degradation of the extracellular matrix. On each exposure to UV, collagen catabolism is induced, followed by repair, but the repair process is not absolute, and, over time, a net loss in collagen occurs, with further degradation of the extracellular matrix and the skin becoming more fragile as a result (Fisher et al. 1997). Loss of collagen within the papillary dermis probably leads to the wrinkled appearance. Fibrillin, which connects the papillary dermal elastic fibre network to that of the deeper dermis, is not expressed. An increase in dermal elastin is found in the deep to mid-dermis where the fibres are not laid down in an orderly fashion but are amorphous and severely truncated. Glycosaminoglycans, such as hyaluronate, are deposited in the dermis. The dermal vasculature is reduced in both size and density and is more liable to damage from trauma. Both the epidermis and dermis have lower levels of antioxidant enzymes leading to the accumulation of oxidized and cross-linked proteins. The epidermis is initially increased in thickness but then becomes atrophic. The melanin content varies from none to increased in different areas. There is also impaired wound healing. These changes in photoaged skin are reviewed in Kohl et al. (2011). It should be noted that recent evidence suggests that UV radiation could directly degrade some of the proteins in the extracellular matrix rather than via the generation of the MMPs. Elastic fibres, such as fibronectin and fibrillin, may be particular susceptible in this regard as they are highly enriched in UV-absorbing amino acid residues including cysteine (Naylor et al. 2011).

One of the main concerns regarding photoageing is that it is related to the risk of developing basal cell carcinoma (BCC) and squamous cell carcinoma (SCC) (see next section). Solar elastosis of the back of the neck is one of the most accurate predictors for either of these cutaneous tumours.

24.5 Photocarcinogenesis

The three skin tumours associated with sun exposure are malignant melanoma (MM), arising from the melanocytes in the epidermis, and SCC and BCC, together called the nonmelanoma skin cancers (NMSCs). Both SCCs and BCCs arise from keratinocytes, also in the epidermis, the latter probably from a pluripotential epidermal stem cell. Skin cancer is the most common form of cancer in fair-skinned individuals.

24.5.1 Nonmelanoma Skin Cancer

Exposure to solar UV radiation represents the major environmental risk factor for NMSC. This is demonstrated by the increasing incidence of NMSC in white populations of similar ethnicity with decreasing latitude. In addition positive correlations have been demonstrated between the incidence/mortality of NMSC and solar UV irradiation in the same location. In most studies, outdoor workers have a higher incidence of NMSC than indoor workers. In addition, the body sites where the tumours most frequently occur, the face and neck, indicate the importance of sun exposure in their aetiology.

However the pattern of exposure for the two types of NMSC is somewhat different: for SCC the risk increases with increasing cumulative lifetime dose of UV radiation (Kricker et al. 1994), but for BCC the relationship is more complex, and, although the cumulative dose of UV matters, exposure early in life or intermittent intense exposure such as may be experienced by sunbathing or outdoor recreational activities may be equally important (Kricker et al. 1995). A study in Queensland has revealed that sunscreens applied daily over a period of 4.5 years could prevent the development

Fig. 24.2 Squamous cell carcinoma at the corner of the mouth shown as a crusted lesion with ulcerated centre

Fig. 24.3 Basal cell carcinoma on the side of the nose showing a raised rolled edge and translucent appearance

of SCC (with a tendency, although not statistically significant, towards decreasing the incidence of BCC) and that the dose of solar UV experienced as recently as in the past 5 years can affect the risk of developing SCC (Green et al. 1999). The beneficial effect of the sunscreens is long lasting, up to at least 8 years after the end of a trial in which they had been applied daily to the head, neck, hands, and forearms (van der Pols et al. 2006).

SCCs are found as persistent red, crusted lesions on sun-exposed areas of the body, most frequently on the face and scalp (Fig. 24.2). They metastasize more readily than BCCs and are sometimes fatal. The incidence of SCCs is about 25 % that of BCCs in immunocompetent subjects, but SCCs are 15 times more common than BCCs in immunosuppressed subjects, such as those receiving organ transplants. SCCs are found frequently in such patients, with the incidence rising in direct proportion to the time since transplantation, and there is an association with papillomavirus infection (see Sect. 24.6.3). For example, in a study of renal allograft recipients in Edinburgh more than twenty years ago, 20 % had papillomas and 2 % had SCCs by 5 years posttransplantation, while 77 % had papillomas and 13 % had SCCs by 22 years posttransplantation (Barr et al. 1989). However the drugs used before 1990 had adverse effects on UV-induced DNA damage and repair in skin cells. Newer immunosuppressive drugs with a different mode of action are likely to reduce the risk of SCC development.

BCCs present as raised translucent nodules (Fig. 24.3) which develop slowly over a period of months or years. A common site is the central area of the face, often around the eyes, particularly the inner canthus where the upper and lower eyelids meet. BCCs occur increasingly on the trunk and upper arms in recent years, a trend attributed to the fashion for intentional body tanning. BCCs are sometimes called rodent ulcers as they have the property of relentless local spread and destruction of large areas of the skin, cartilage, and even bone, if left untreated. They can be cured by surgery or radiotherapy and rarely recur.

Both BCCs and SCCs are very common although exact figures are almost impossible to obtain as frequently such tumours are unrecognized, or untreated, or treated without obtaining a histological diagnosis. Many reports indicate an increasing annual incidence of BCC and SCC in both temperate countries and in places nearer the equator with fair-skinned populations. For example, the incidence of BCC increased by 3 % per year from 1886 to 2003 in the UK (Bath-Hextall et al. 2007), and the incidence of SCC increased fourfold from 1960 to 2004 in Sweden (Dal et al. 2008). The highest recorded incidences of NMSC are in Australia—in 2002 the incidence was five times greater than the incidence of all other cancers combined (Staples et al. 2006). Forecast modelling of SCC and BCC in the Netherlands predicts that the rates of both will double by 2015 compared with the rates in 2000 (de Vries et al. 2005).

NMSC has a much higher incidence in white than in nonwhite individuals, and those with skin type I are at particular risk. The photoprotection offered by melanin in the epidermis provides an explanation of why the number of cases is fewer in those with pigmented skin. This endogenous sun protection factor has been estimated as up to 13.4 in African Americans (Halder and Bridgeman-Shah 1995). In people with evidence of long-term cutaneous sun damage, such as elastosis of the neck and a large number of solar keratoses, there is also a raised risk of both SCC and BCC. The involvement of DNA damage in the induction of NMSC is shown most clearly in patients with the rare genetic disorder xeroderma pigmentosum (XP), in which there is a defect in the ability to repair DNA following UV exposure and a clinical hypersensitivity to UV radiation (see Sect. 24.7.1). These individuals are at greatly increased risk (5,000 times) of developing NMSC compared with normal people, and

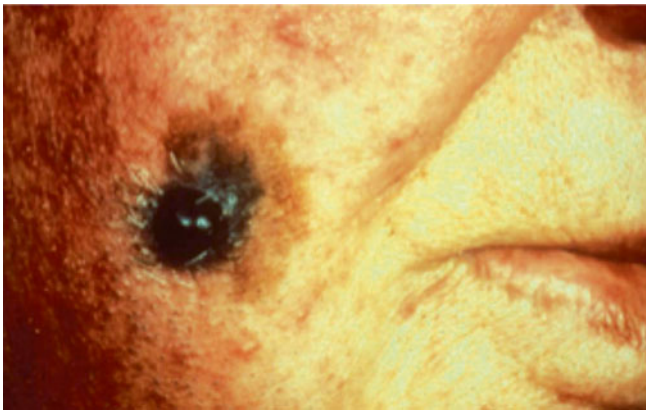

Fig. 24.4 Cutaneous melanoma on the cheek

almost all of the tumours are on constantly exposed sites (Kraemer et al. 1987). A practical and important study indicates that application of a cream containing a DNA repair enzyme to sun-exposed areas of the body reduced the rates of actinic keratosis (a precursor lesion to NMSC) and skin cancer in patients with XP, compared with a placebo cream (Yarosh 2004).

Several UV-B-specific mutations are recognized in BCCs and SCCs, such as in the p53 gene and the PTCH gene (see Sect. 24.5.3). Other UV-related genetic factors are involved in photocarcinogenesis in addition, including mutations in the genes involved in the repair of DNA damage, alterations in DNA methylation, and variants in the melanocortin 1 receptor gene and in the gene coding for the vitamin D receptor (see Sect. 23.3). Several immunological responses are also key following UV irradiation, for example, the extent of UV-induced immunosuppression (see Sect. 24.6.2) and the relative proportion of CD4+ and CD8+ T cells. SCC is about 2.2-fold and BCC about 1.6-fold more common in men than in women, indicating a gender imbalance. This could be due to higher sun exposure in men who tend to have more outdoor occupations and recreational activities than women and who expose a larger area of their skin and are less likely to use sunscreens. Furthermore evidence from animal studies suggests that females could be protected against photocarcinogenesis to some extent by the local synthesis of oestrogens.

24.5.2 Malignant Melanoma

Although MM is much less common than BCC or SCC, it causes 80 % of the deaths associated with skin cancer. The most frequent type (about 70 % of all cases) is called superficial spreading, found most often in middle-aged individuals and seen as small brown or black lesions characterized by irregular lateral edges (Fig. 24.4). It is likely to be the noninvasive precursor lesion to invasive and metastatic melanoma. Other types are nodular (found in elderly people and developing rapidly on parts of the body not frequently exposed to the sun), lentigo maligna (found in elderly people and developing slowly from pigmented areas of skin that get the most sun exposure), and acral lentiginous (rare but the most frequent type in dark-skinned people, occurring on the palms and soles). Survival after surgical removal of a primary melanoma is directly related to the thickness of the tumour, which signals how far the melanocytes have invaded into the underlying dermis.

In many areas of the world, the incidence of cutaneous melanoma increases as the latitude decreases. The annual incidence in Europe and the USA is between 5 and 24 per 100,000 and in Australia, New Zealand, and South Africa, areas with higher ambient UV radiation, is more than 70 per 100,000. Many studies in various countries have indicated that the incidence of MM has increased by between 1 and 3 % per year over the past 50 years.

For example, in the UK between 1975 and 2000, MM showed the largest increase in incidence rate of all the major tumours. In the USA in 2011, invasive MM was the fifth most frequent cancer diagnosed in men, the seventh in women, and the third in adolescents and adults aged 15–39 years. Future forecasts predict that the incidence rate will not decrease for about another 20 years, by which time it will be double that found in 2004 (Diffey 2004). However, in a few instances the annual incidence has stabilized especially in people under the age of 40 years. This could be due to intensive public health campaigns which promote sun awareness, the use of personal photoprotection, and the early diagnosis of suspicious pigmented skin lesions. While the mortality rate of MM rose sharply in the second half of the last century, in the past 20 years or so deaths from MM have not increased in line with incidence and have even stabilized in some countries. This may be due to early detection and the predominance of thin melanomas (early stage) diagnosed in recent years that respond to treatment with high survival rates.

The strongest risk factor for MM discovered to date is large numbers of atypical nevi (moles) (Walls et al. 2013). It is possible that at least some MM arise from pre-existing benign melanocytic nevi, presumably by further genetic changes. Indeed the development of MM is consistent with a two-hit model where early UV exposure may initiate some premalignant changes and then further irradiation later in life may lead to progression (Basta et al. 2011). There is an association between early childhood solar exposure and the development of nevi, particularly episodes of sunburn or intense sun exposure, and the number of nevi is also determined, in part, by genetic factors. Studies which attempt to correlate cumulative UV exposure in white populations with the rise in the number of cases of MM have not yielded consistent results. The consensus view at present is that intermittent recreational exposure to the sun resulting in sunburn,

particularly in early life, may be critical (Elwood and Jopson 1997; Rosso et al. 1998). Certainly there are lifestyle trends in recent decades, such as the fashion to be tanned; many people holidaying in the sun, especially with the advent of cheap charter flights; and minimal clothing being socially acceptable, all of which could lead to intense solar radiation exposure of untanned skin. The age at which acute solar exposure is experienced is important, and, in general, as for the development of nevi, there is a greater risk in childhood compared with adult UV irradiation. The involvement of sun exposure as a factor in MM is emphasized as it has been shown recently that regular sunscreen use can reduce the development of new primary and invasive melanomas (Green et al. 2011).

24.5.3 Animal Studies of Photocarcinogenesis

Many animal studies have investigated the induction of SCC, BCC, and MM and their association with UV exposure. Mice, particularly hairless mice, have been used most frequently and protocols where irradiation is given daily for weeks or months. SCCs are most readily formed in rodents and BCCs very rarely. Quantitative experiments in hairless mice have revealed the action spectrum and dose dependence for the induction of SCC (de Gruijl et al. 1993). Radiation of wavelengths around 290 nm is the most effective, but there is also a second, lesser peak in the UV-A waveband at about 390 nm. Experiments in transgenic mice have revealed the type of UV-induced DNA damage that leads to SCC (Jans et al. 2005). Mutations in the tumour suppressor gene, p53, are implicated as early events, and microscopic clusters of epidermal cells with strong expression of mutant p53 are thought to be potential precursors of SCC (Kramata et al. 2005; Rebel et al. 2005). For BCC, UV-induced mutations in the sonic hedgehog signalling pathway, particularly of the PTCH gene, are thought to be important in the initiation of the tumour (Daya-Grosjean and Sarasin 2000; Reifenberger et al. 2005). This pathway plays a role in embryonic development and is involved in oncogenic transformation.

UV radiation does not induce MM in rodents unless administered at the same time as chemical carcinogens. In recent years some transgenic mouse models have been developed to avoid this problem. The hepatocyte growth factor/scatter factor mouse represents one such model which, unlike wild-type mice, has melanocytes in the epidermis and in trunk skin at the dermal/epidermal junction. In response to UV-B irradiation of these mice as neonates, lesions developed in similar stages as in human melanoma (de Fabo et al. 2004). It was shown subsequently that macrophages, recruited to the neonatal skin by the exposure, produced IFN-γ which then promoted the growth of the melanocytes (Zaidi et al. 2011). Further work using albino and black strains demonstrated two possible pathways for melanoma induction: one was initiated by UV-B, independent of melanin, and was due to direct DNA damage, while the other was initiated by UV-A, requiring the presence of melanin and was due to oxidative DNA damage in melanocytes (Noonan et al. 2012). The UV-B waveband was a more effective driver of melanomagenesis than the UV-A waveband at initiating the melanoma. The majority of the mutations in the genomes of human melanoma have UV-B signatures, reinforcing this conclusion.

24.6 Immunosuppression

24.6.1 UV-Induced Immunosuppression

In addition to the mutagenic properties of UV, irradiation also leads to suppression of cell-mediated immune responses and of some antibody responses. The evolutionary advantage of this might be to inhibit chronically inflamed responses in the skin, due to the formation of neoantigens resulting from UV-induced DNA damage. It could also be a side effect of the release of mediators that enable repair of the damaged DNA. Immunomodulation was first recognized in the 1970s when exposure to mice to UV radiation shortly before implantation of tumour cells resulted in downregulation of T cell responses to the tumour antigens, thus allowing growth of the tumour (Fisher and Kripke 1977). A variety of antigens in addition to tumour cells have been tested since these early days, including microorganisms, haptens, and alloantigens, all giving similar results. Where possible to assess, the same downregulation in immunity occurs in irradiated human subjects as in mice and other animal models. Suppression of primary immune responses has been demonstrated where a novel antigen is applied within a few days of the UV exposure. Where an immune response has already been generated to an antigen, UV radiation can suppress the memory/recall response when the same antigen is reapplied at a future date within a short period after UV exposure. The suppression is considered local if the antigen is applied to a body site that has been directly exposed to the UV radiation. It is considered systemic if the antigen is applied to a distant site that has not been directly exposed to the UV radiation. Inflammation due to the UV exposure could contribute to the systemic effects as, in general, the doses required are higher than those required for the local effects. It is not clear what UV wavelengths are most effective at inducing immunosuppression, especially as most studies have been done in vitro or in highly manipulated, sometimes transgenic mouse strains and with artificial lamps emitting a range of UV spectra. However an action spectrum for the suppression of memory responses to nickel in human subjects using a solar simulator showed two peaks, one within the UV-B waveband

Table 24.5 Cutaneous chromophores involved in the initiation of the pathway leading to suppression of cell-mediated immunity following ultraviolet radiation

Chromophore	UV-induced change in structure	Mechanism of action/ immune mediators
DNA	Cyclobutane pyrimidine dimers; 6–4 photoproducts; ROS-induced base oxidation	Oxidative stress; release of PAF and PGE2; upregulation of IL-6, IL-10, IL-33, TNF-α; downregulation IL-12
Trans-urocanic acid	Cis-urocanic acid	Intracellular ROS; oxidative DNA damage; activation serotonin receptors; PAF, PGE2, and cytokine release; antigen presentation impaired; stimulation of neuropeptides; mast cell degranulation
Membrane phospholipids	Oxidative stress; lipid peroxidation	Receptor clustering; PAF and cytokine production
7-Dehydrocholesterol	Previtamin D	Upregulation of antimicrobial peptides; DNA repair; downregulation of many acquired immune responses

IL interleukin, *PAF* platelet-activating factor, *PGE2* prostaglandin E2, *ROS* reactive oxygen species, *TNF* tumour necrosis factor

at 300 nm and the second within the UV-A waveband at 370 nm (Damian et al. 2011). Indeed there may even be interaction between wavebands, illustrating the complexity of the process.

A cascade of reactions is initiated when the skin is exposed to UV radiation, and here only a brief overview is given. Further details can be found in Schwarz and Schwarz (2011), Ullrich and Byrne (2012), and Gibbs and Norval (2013). Exactly what happens may depend on the UV radiation (dose, intensity, wavelength, frequency of exposure), the antigen in question (type, quantity, route of administration, host species, and strain), and what aspect of the immune response is being monitored (primary, memory, innate, adaptive, body site).

Due to the poorly penetrating power of UV, the initiating event is thought to be absorption at the body surface by chromophores, which change their structure as a result, leading to the production of various immune mediators locally. Several such chromophores have been identified, the main ones being DNA (Schwarz and Schwarz 2011; Vink et al. 1998), trans-urocanic acid (trans-UCA) (Gibbs et al. 2008), membrane phospholipids (Yao et al. 2009), and 7-dehydrocholesterol (Dixon et al. 2010). Details of their change in structure and the consequences are shown in Table 24.5.

As a result of the mediators produced, several cell populations in the skin and elsewhere in the body are changed. First the network of dendritic Langerhans cells (see Sects. 24.2.2 and 24.2.3) in the epidermis is lost, and a proportion migrates to the T cell areas of the draining lymph nodes. There they are poor at producing IL-12, a cytokine that is important for effective antigen presentation (Schwarz et al. 2005). They are able to activate natural killer T cells which produce the immunosuppressive cytokine IL-4 (Fukunaga et al. 2010). In addition there is evidence that they can induce T regulatory cells which, on antigen-specific activation, release IL-10, another immunosuppressive cytokine (Schwarz et al. 2010). Other results indicate that the Langerhans cells might not play a major role in UV-induced immunosuppression but that the dermal dendritic cells might fulfil this function (Wang et al. 2009). These cells are known to suppress CD8+ T cell responses to proteins and haptens. Mast cells are also involved at this stage. Following UVR, their number in the skin increases rapidly as a result of being attracted by IL-33 produced by keratinocytes and dermal fibroblasts (Byrne et al. 2008). They then travel to the B cell areas of the draining lymph nodes where they stimulate B regulatory cells to produce IL-10. The IL-10 can also downregulate T cell-dependent antibody production by suppressing T follicular helper function in the draining lymph nodes (Chacon-Salinas et al. 2011). Finally a special population of macrophage/monocytes infiltrates the skin very soon after UVR, and these cells can be triggered to migrate to the draining lymph nodes on exposure to an antigen where they release IL-10 (Toichi et al. 2008). Thus the immune responses to an antigen applied to an irradiated body site during this time of multiple cellular and mediator changes are significantly suppressed.

The pathways that might be involved in systemic immunosuppression are not clear at present. Here the applied antigen will end up in lymph nodes that did not drain the irradiated site or will be carried there by dendritic cells not affected by the UV radiation. Various scenarios are possible. First, the IL-4 produced by activated natural killer T cells and the IL-10 produced by T and B regulatory cells in the lymph nodes draining the irradiated skin are released systemically and thus may alter the generation of the immunity elsewhere in the body. Second, other mediators such as various complement components, histamine, prostaglandins, TNF-α, and IL-10 generated in irradiated skin may affect the migration of dendritic cells to the lymph nodes. Third, dendritic progenitor cells may be involved as such cells prepared from the bone marrow of irradiated mice induce tolerance and have suppressor activity due to prostaglandin produced by irradiated skin or by mesenchymal stem cells in the bone marrow (Ng et al. 2010).

It should be noted that UV radiation can lead to the upregulation of some antimicrobial peptides in the skin, possibly

through a vitamin D pathway. Antimicrobial peptides represent an important part of the innate immune system, particularly in the initial defence against microbial infection. This aspect is described in Sect. 23.6.1.

24.6.2 UV-Induced Immunosuppression and Tumours

Skin cancers, induced by chronic UV exposure of mice, are highly antigenic, and the human equivalent is likely to be just as antigenic. It is hypothesized that a neoantigen is formed in the skin by UV at a time when the antigen-presenting cells are altered, resulting in the activation of T cells, which suppress the normal immune responses to the tumour antigens (Kripke 1981). Therefore, the interference in the normal host defence mechanisms by UV may be critical. This can be seen most clearly in immunosuppressed individuals who are at significantly increased risk of developing cutaneous malignancies, particularly SCCs and whose tumours arise almost entirely on sun-exposed body sites. Furthermore, the work on XP patients described in Sect. 24.5.1. provides compelling evidence to suggest that UV-induced immunosuppression is a crucial factor in the generation of NMSC. It is also recognized that T regulatory cells infiltrate SCCs and surround BCCs and are likely to produce the immunosuppressive cytokine IL-10 locally. Various murine models confirm the role of the immune system in protection against skin cancers. For example, preirradiation of mice at one site led to enhanced primary tumour growth at a second irradiated site, with the promotion phase of carcinogenesis being most affected (de Gruijl and van der Leun 1982). In addition, mice which had received T regulatory (suppressor) cells prepared from UV-irradiated animals during the course of chronic UV exposure developed skin tumours earlier than mice receiving T cells from control unirradiated mice. Most convincingly, the induction of SCCs in mice as a result of chronic UV exposure can be inhibited by treating the mice throughout with a cis-UCA monoclonal antibody or a PAF receptor antagonist or a serotonin receptor antagonist (reviewed in Norval and Halliday 2011).

Skin phototype may be an important variable as it has been revealed that people with skin types I/II (see Sect. 24.3.1) demonstrate an increased susceptibility to UV-induced immunosuppression compared to people with skin types III/IV (Kelly et al. 2000). This may help to explain why the former group is at higher risk of developing skin cancer than the latter group. Finally mast cells are also involved, as demonstrated by a correlation between their density and skin cancer in human subjects: the higher the number, the higher the risk of BCC and MM. This association may be due to their production of a range of immunosuppressive factors on activation by irradiation and by their stimulation of B regulatory cells after migration to the draining lymph nodes in response to UV radiation (Grimbaldeston et al. 2006).

24.6.3 UV-Induced Immunosuppression and Microbial Infection Including Vaccination

Investigations into the impact of UV radiation on human infectious diseases are relatively few. However about 20 models of infection in rodents have been examined in terms of UV and immunity, with the organisms ranging from viruses through bacteria and yeasts to worms. In practically all cases, suppression of immunity resulted, together with a decreased ability to clear the infectious agent and sometimes increased severity of symptoms or even death. Calculations have been made to relate the results obtained in the animal models to the human situation, and Garssen et al. (1996) concluded that people could receive sufficient solar UV in about 100 min or less at midlatitudes around noon to suppress their immune responses by 50 %. Therefore, on the basis of this study, sunlight irradiance is likely to be biologically relevant to the effectiveness of the human immune response against microbial agents. Questions then arise concerning many infectious diseases, particularly persistent infections where the organisms are not cleared from the body following the primary infection: these can lead to severe symptoms on reactivation or to oncogenesis.

However, in reality, there are few convincing examples to date where solar UV radiation adversely affects the pathogenesis of human infections (reviewed in Norval 2006). The first is herpes simplex virus (HSV), which causes cold sores. Here exposure to solar UV radiation is recognized as a common triggering factor for reactivation of the virus from latency. The irradiation is likely to have dual effects: by activating promoters of HSV as a result of damage to nerve endings and by causing downregulation of the HSV-specific immune response in the skin, thus allowing viral replication and formation of the vesicular lesions. The second is particular human papillomavirus (HPV) types, which have been found in SCCs in immunosuppressed individuals and more recently in some immunocompetent people also. Such types are likely to have developed a range of immune evasion mechanisms, and these, together with the local UV-induced immunosuppression, may alter the balance between the virus and the host in favour of carcinogenesis. A possible third example is the recently discovered involvement of polyoma virus in Merkel cell carcinoma, a rare tumour, although increasing in incidence recently, with a very poor prognosis. It arises on sun-exposed body sites in elderly and immunosuppressed people. No investigations have been carried out thus far into any role in the oncogenic process for UV-induced suppression of immune responses to the polyoma virus.

If UV radiation downregulates the immune response to a microorganism, then the efficacy of vaccination could be significantly reduced by the exposure, resulting in a higher chance of symptomatic infection if the organism is encountered at a future date. This possibility has not been extensively investigated thus far for human vaccines, but limited published results indicate that a less effective immune response is generated if the vaccine is administered in the summer compared with the winter and in tropical compared with temperate regions (reviewed in Norval and Woods 2011). Although many aspects of life change with latitude, the higher sun intensity in the summer and at low latitudes, leading to UV-induced immunosuppression, could explain these findings. Only one large-scale experimental study has been carried out which involved administration of hepatitis B subunit vaccine to irradiated and unirradiated volunteers. Although no difference between the two groups in antibody or T cell responses to the vaccine was found, suppression had occurred in particular subsets of the irradiated group, divided on the basis of cytokine polymorphisms and epidermal UCA content (reviewed in Norval and Woods 2011). Further studies are required to examine the situation for the common vaccines, particularly those such as measles and tuberculosis, that are administered in tropical as well as in temperate climates.

24.7 Photodermatoses

The photodermatoses represent a diverse group of conditions associated with abnormal skin responses to UV and/or visible radiation. These diseases have differing aetiologies and symptoms and can be divided into four main categories, each of which is described briefly below.

24.7.1 Genodermatoses: Xeroderma Pigmentosum

The first photodermatosis group contains the genodermatoses, which are usually inherited. One example of this group, already mentioned above, is XP, a rare autosomal recessive disorder where the repair of DNA after UV exposure is defective, most frequently because of a mutation in the nucleotide excision repair process (reviewed in Knoch et al. 2012). The subjects suffer from extreme photosensitivity, burning after even minimal sun exposure. They are at greatly increased risk of developing all forms of skin cancer, but especially SCC and BCC. In former times they died before the age of 30 from a metastatic malignancy, usually SCC or MM. More recently, better sun protection is offered, and their life expectancy has increased.

Fig. 24.5 Polymorphic light eruption showing multiple small papules

24.7.2 Idiopathic Photodermatoses: Polymorphic Light Eruption

The second group is the idiopathic photodermatoses, comprising a variety of diseases that all thought have an immunological basis. One of the most common is polymorphic light eruption (PLE), estimated to affect 5–20 % of the population. It has been demonstrated from family histories that PLE has a major genetic component with contributing environmental components, mainly sunlight exposure. PLE is manifest as an intermittent pruritic skin eruption which occurs several hours after sun exposure and takes the form of multiple small red papules, which resolve without scarring after a few days to weeks (Fig. 24.5). It is most frequent in the spring and early summer or during a sunny holiday, following the first exposure to a high dose of sunlight. After repeated exposure, the lesions are less likely to occur. There is no latitude difference in prevalence suggesting that PLE is triggered by different seasonal patterns of solar UV radiation.

Many years ago it was suggested that a photoallergen could be induced in the skin of PLE patients, which then stimulates a cell-mediated immune response, precipitating the development of the lesions. Such a "self"-photoallergen has not been identified as yet, although an influx of first CD4+ lymphocytes, then CD8+ lymphocytes, is found in the exposed skin, a pattern that mimics a DTH response. The lack of the normal UV-induced immunosuppression in PLE could be due to reduced numbers of neutrophils and macrophages infiltrating the irradiated skin and possibly reduced numbers of T regulatory cells in the winter months (reviewed in Wolf et al. 2009). The varying impact of UV-induced immunosuppression on skin diseases is illustrated by finding that the prevalence of PLE is 7.5 % in subjects with skin cancer compared with 21.4 % in gender- and age-matched controls without skin cancer (Lembo et al. 2008). This illustrates the positive evolutionary advantage of the immunosuppression in protection against PLE balanced against the disadvantage in protection against skin cancer.

24.7.3 Cutaneous Porphyrias

The third group comprises the cutaneous porphyrias, in which there are inherited enzymic defects in heme synthesis leading to the accumulation of photoreactive porphyrins, which then photosensitize the skin. However, the porphyrias are precipitated by visible light (around 410 nm) rather than UV radiation and are not considered further here.

24.7.4 Photoallergic Contact Dermatitis

The fourth group comprises photosensitization by systemic and tropical drugs and by chemicals. Compounds with such properties are increasing in number at the moment with the development of many novel pharmaceutical agents. When these substances get into the skin, they can act as chromophores to absorb UV, thus becoming either phototoxic or triggering a range of biochemical or immunological responses in a proportion of individuals. (Phototoxicity is considered in Chap. 21.) At low concentrations, some drugs and chemicals cause topical photoallergic contact dermatitis where an eczematous eruption occurs on UV-exposed skin sites, activated mainly by UV-A. The drug is converted to a photoproduct, which then binds to proteins or to cells in the skin, forming a novel antigen which then triggers a DTH response. More than one and frequently many exposures to the photoallergen in the presence of UV are required before this response is induced. As one example, 4-para-aminobenzoic acid has been implicated in photoallergic reactions, and its inclusion in sunscreen preparation has declined as a result. Photoallergic contact dermatitis can be diagnosed by duplicate photopatch testing of subjects, in which the substance is assessed with and without exposure to UV-A. The structural features of some classes of chemicals which make them active as photoallergens have been identified (Barratt 2004).

References

Barr BB, Benton EC, McLaren K, Bunney H, Smith IW, Blessing K, Hunter JAA (1989) Human papillomavirus infection and skin cancer in renal allograft recipients. Lancet 1:124–129

Barratt MD (2004) Structure-activity relationships and prediction of the phototoxicity and phototoxic potential of new drugs. Altern Lab Anim 32:511–524

Basta NO, James PW, Craft AW, McNally RJ (2011) Seasonal variation in the month of birth in teenagers and young adults with melanoma suggests the involvement of early-life UV exposure. Pigment Cell Melanoma Res 24:250–253

Bath-Hexall F, Leonardi-Bee J, Smith C, Meal A, Hubbard R (2007) Trends in incidence of skin basal cell carcinoma. Additional evidence from a UK primary care database. Int J Cancer 121:2105–2108

Bos JD (2005) Skin immune system (SIS), 3rd edn. CRC Press, New York

Byrne SN, Limon-Flores AY, Ullrich SE (2008) Mast cell migration from the skin to the draining lymph nodes upon ultraviolet irradiation represents a key step in the induction of immune suppression. J Immunol 180:4648–4655

Chacon-Salinas R, Limon-Floresm AY, Chavez-Blanco AD, Gonzalez-Estrada A, Ullrich SE (2011) Mast-cell derived IL-10 suppresses germinal center formation by affecting T follicular helper cell function. J Immunol 186:25–31

Cooke A, Johnson BE (1978) Dose response, wavelength dependence and rate of excision of ultraviolet radiation-induced pyrimidine dimers in mouse skin DNA. Biochim Biophys Acta 517:24–30

Dal H, Boldemann C, Lindelof B (2008) Trends during a half century in relative squamous cell carcinoma by body site in the Swedish population: support for accumulated sun exposure as the main risk factor. J Dermatol 35:55–62

Damian DL, Matthews YJ, Phan TA, Halliday GM (2011) An action spectrum for ultraviolet-radiation-induced immunosuppression in humans. Br J Dermatol 164:657–659

Daya-Grosjean L, Sarasin A (2000) UV-specific mutations of the human patched gene in basal carcinomas from normal individuals and xeroderma pigmentosus patients. Mutat Res 450:193–199

De Fabo EC, Noonan FP (1983) Mechanism of immune suppression by ultraviolet irradiation in vivo. I. Evidence for the existence of an unique photoreceptor in skin and its role in photoimmunology. J Exp Med 158:84–98

De Fabo EC, Noonan FP, Fears T, Merlino G (2004) Ultraviolet B but not ultraviolet A radiation initiates melanoma. Cancer Res 64: 6372–6376

de Gruijl FR (1995) Action spectrum for photocarcinogenesis. Recent Results Cancer Res 139:21–30

de Gruijl FR, van der Leun JC (1982) Systemic influence of pre-irradiation of a limited area on UV-tumorigenesis. Photochem Photobiol 35:379–383

de Gruijl FR, Sterenborg HJ, Forbes PD, Davies RE, Cole C, Kelfkens G, van Weelden H, Slaper H, van der Leun JC (1993) Wavelength dependence of skin cancer induction by ultraviolet irradiation of albino hairless mice. Cancer Res 53:53–60

de Vries E, van de Poll-Franse LV, Louwman WJ, de Gruijl FR, Coebergh JWW (2005) Prediction of skin cancer incidence in the Netherlands up to 2015. Br J Dermatol 152:481–488

Diffey BL (2002) Sources and measurement of ultraviolet radiation. Methods 28:4–13

Diffey BL (2004) The future incidence of cutaneous melanoma within the UK. Br J Dermatol 151:868–872

Dixon KM, Sequeira VB, Camp AJ, Mason RS (2010) Vitamin d-fence. Photochem Photobiol Sci 9:564–570

Elwood JM, Jopson J (1997) Melanoma and sun exposure: an overview of published studies. Int J Cancer 73:198–203

Fisher MS, Kripke ML (1977) Systemic alteration induced in mice by ultraviolet light irradiation and its relationship to ultraviolet carcinogenesis. Proc Natl Acad Sci USA 74:1688–1692

Fisher GJ, Wang ZQ, Datta SC, Varani J, Kang S, Vourhees JJ (1997) Pathophysiology of premature skin ageing induced by ultraviolet light. N Engl J Med 337:1419–1428

Fitzpatrick TB (1988) The validity and practicality of sun-reactive skin types I through VI. Arch Dermatol 124:869–871

Fukunaga A, Khaskhely NM, Ma Y, Sreevidya CS, Taguchi K, Nishigori C, Ullrich SE (2010) Langerhans cells serve as immunoregulatory cells by activating NKT cells. J Immunol 185:4633–4640

Garssen J, Goettsch W, de Gruijl F, Slob W, Van Loveren H (1996) Risk assessment of UVB effects on resistance to infectious diseases. Photochem Photobiol 64:269–274

Gibbs NK, Norval M (2013) Photoimmunosuppression: a brief overview. Photodermatol Photoimmunol Photomed 29:57–64

Gibbs NK, Norval M, Traynor NJ, Wolf M, Johnson BE, Crosby J (1993) Action spectra for the trans to cis photoisomerisation of uro-

canic acid in vitro and in mouse skin. Photochem Photobiol 57:584–590
Gibbs NK, Tye J, Norval M (2008) Recent advances in urocanic acid photochemistry, photobiology and photoimmunology. Photochem Photobiol Sci 7:655–667
Gilchrest BA, Soter NA, Stoff JS, Mihm MC (1981) The human sunburn reaction: histologic and biochemical studies. J Am Acad Dermatol 5:411–422
Green A, Williams G, Neale R, Hart V, Leslie D, Parsons P, Marks GC, Gaffney P, Battistutta D, Frost C, Lang C, Russell A (1999) Daily sunscreen application and betacarotene supplementation in prevention of basal-cell and squamous-cell carcinoma of the skin: a randomised controlled trial. Lancet 354:723–729
Green AC, Williams GM, Logan V, Strutton GM (2011) Reduced melanoma after regular sunscreen use: randomized trial follow-up. J Clin Oncol 29:257–263
Grimbaldeston MA, Finlay-Jones JJ, Hart PH (2006) Mast cells in photodamaged skin: what is their role in skin cancer? Photochem Photobiol Sci 5:177–183
Halder RM, Bridgeman-Shah S (1995) Skin cancer in African Americans. Cancer 75:s667–s673
Harrison GI, Young AR (2002) Ultraviolet radiation-induced erythema in human skin. Methods 28:14–19
Irwin C, Barnes A, Veres D, Kaidbey K (1993) An ultraviolet action spectrum for immediate pigment darkening. Photochem Photobiol 57:504–507
Jans J, Schul W, Sert YG, Rijksen Y, Rebel H, Eker AP, Nakajima S, van Steeg H, de Gruijl FR, Yasui A, Hoeijmakers JH, van der Horst GT (2005) Powerful skin cancer protection by a CPD-photolyase transgene. Curr Biol 15:105–115
Kelly DA, Young AR, McGregor JM, Seed PT, Potten CS, Walker SL (2000) Sensitivity to sunburn is associated with susceptibility to ultraviolet radiation-induced suppression of cutaneous cell-mediated immunity. J Exp Med 191:561–566
Knoch J, Kamenisch Y, Kubisch C, Berneburg M (2012) Rare hereditary diseases with defects in DNA-repair. Eur J Dermatol 22:4430455
Kohl E, Steinbauer J, Landthaler M, Szeimies R-M (2011) Skin ageing. J Eur Acad Dermatol Venereol 25:873–884
Kraemer KH, Lee MM, Scotto J (1987) Xeroderma pigmentosum. Cutaneous, ocular, and neurologic abnormalities in 830 published cases. Arch Dermatol 123:241–250
Kramata P, Lu YP, Lou YR, Singh RN, Kwon SM, Conney AH (2005) Patches of mutant p53-immunoreactive epidermal cells induced by chronic UVB irradiation harbor the same p53 mutations as squamous cell carcinomas in the skin of hairless SKH-1 mice. Cancer Res 65:3577–3585
Kricker A, Armstrong BK, English DR (1994) Sun exposure and non-melanocytic skin cancer. Cancer Causes Control 5:367–392
Kricker A, Armstrong BK, English DR, Heenan PJ (1995) Does intermittent sun exposure cause basal cell carcinoma? A case–control study in Western Australia. Int J Cancer 60:489–494
Kripke ML (1981) Immunologic mechanisms in UV radiation carcinogenesis. Adv Cancer Res 34:69–106
Lavker RM, Kligman AM (1988) Chronic heliodermatitis: a morphologic evaluation of chronic actinic dermal damage with emphasis on the role of mast cells. J Invest Dermatol 90:325–330
Lembo S, Fallon J, O'Kelly P, Murphy GM (2008) Polymorphic light eruption and skin cancer prevalence: is one protective against the other? Br J Dermatol 159:1342–1347
MacLaughlin JA, Anderson RR, Holick MF (1982) Spectral character of sunlight modulates photosynthesis of previtamin D3 and its photisomers in human skin. Science 216:1001–1003
McKinlay AF, Diffey BL (1987) A reference action spectrum for ultraviolet induced erythema in humans skin. In: Passhier WF, Bosnjakovic BF (eds) Human exposure to ultraviolet radiation: risks and regulation. Elsevier, Amsterdam, pp 45–52
McLoone P, Simics E, Barton A, Norval M, Gibbs NK (2005) An action spectrum for the production of cis-urocanic acid in human skin. J Invest Dermatol 125:1071–1074
Naylor EC, Watson RE, Sherratt MJ (2011) Molecular aspects of skin ageing. Maturitas 69:249–256
Ng RL, Bisley JL, Gorman S, Norval M, Hart PH (2010) Ultraviolet irradiation of mice reduces the competency of bone marrow-derived $CD11c^+$ cells via an indomethacin-inhibitable pathway. J Immunol 185:7207–7215
Noonan FP, Bucana C, Sauder DN, De Fabo EC (1984) Mechanism of systemic immune suppression by UV radiation in vivo. II. The UV effects on number and morphology of epidermal Langerhans cells and the UV-induced suppression of contact hypersensitivity have different wavelength dependencies. J Immunol 132:2408–2416
Noonan FP, Zaidi MR, Wolnicka-Glubisz A, Anver MR, Bahn J, Wielgus A, Cadet J, Douki T, Mouret S, Tucker MA, Popratiloff A, Merlino G, De Fabo EC (2012) Melanoma induction by ultraviolet A but not ultraviolet B radiation requires melanin pigment. Nat Commun 3:884
Norval M (2006) The effects of ultraviolet radiation on human viral infections. Photochem Photobiol 86:1495–1504
Norval M, Halliday GM (2011) The consequences of UV-induced immunosuppression for human health. Photochem Photobiol 87:965–977
Norval M, Woods GM (2011) UV-induced immunosuppression and the efficacy of vaccination. Photochem Photobiol Sci 10: 1267–1274
Novak Z, Berces A, Ronto G, Pallinger E, Dobozy A, Kemeny L (2004) Efficacy of different UV-emitting light sources in the induction of T-cell apoptosis. Photochem Photobiol 79:434–439
Parrish JA, Jaenicke KF, Anderson RR (1982) Erythemas and melanogenesis action spectra of normal human skin. Photochem Photobiol 36:187–191
Rebel H, Kram N, Westerman A, Banus S, van Kranedn HJ, de Gruijl FR (2005) Relationship between UV-induced mutant p53 patches and skin tumors, analysed by mutation spectra and by induction kinetics in various DNA-repair-deficient mice. Carcinogenesis 26:2123–2130
Reifenberger J, Wolter M, Knobbe CB, Kohler B, Schonicke A, Scharwachter C, Kumar K, Blaschke B, Ruzicka T, Reifenberger G (2005) Somatic mutations in the PTCH, SMOH, SUFUH and TP53 genes in sporadic basal cell carcinomas. Br J Dermatol 152:43–51
Romani N, Brunner PM, Stingl G (2012) Changing views of the role of Langerhans cells. J Invest Dermatol 132:872–881
Rosso S, Zanetti R, Pippioni M, Sancho-Garnier H (1998) Parallel risk assessment of melanoma and basal cell carcinoma: skin characteristics and sun exposure. Melanoma Res 8:573–583
Schwarz T, Schwarz A (2011) Molecular mechanisms of ultraviolet-radiation-induced immunosuppression. Eur J Cell Biol 90:560–564
Schwarz A, Maeda A, Kernbeck K, van Steeg H, Beissert S, Schwarz T (2005) Prevention of UV radiation-induced immunosuppression by IL-12. J Exp Med 201:173–179
Schwarz A, Noordegraaf M, Maeda A, Torii K, Clausen BE, Schwarz T (2010) Langerhans cells are required for UVR-induced immunosuppression. J Invest Dermatol 130:1419–1427
Staples MP, Elwood M, Burton RC, Williams JL, Marks R, Giles GG (2006) Non-melanoma skin cancer in Australia: the 2002 national survey and trends since 1985. Med J Aust 184:6–10
Taylor CR, Stern R, Leyden JJ, Gilchrest BA (1990) Photoageing, photodamage and photoprotection. J Am Acad Dermatol 22:1–15
Toichi E, Lu KQ, Swick AR, McCormick TS, Cooper KD (2008) Skin-infiltrating monocytes/macrophages migrate to draining lymph nodes and produce IL-10 after contact sensitizer exposure to UV-irradiated skin. J Invest Dermatol 128:2705–2715
Ullrich SE, Bryne SN (2012) The immunologic revolution: photoimmunology. J Invest Dermatol 132:896–905

Van der Pols JC, Williams GM, Pandeya N, Logan V, Green AC (2006) Prolonged prevention of squamous cell carcinoma of the skin by regular sunscreen use. Cancer Epidemiol Biomarkers Prev 15: 2546–2548

Vink AA, Schreedhar V, Roza L, Krutmann J, Kripke ML (1998) Cellular target of UVB-induced DNA damage resulting in local suppression of contact hypersensitivity. J Photochem Photobiol B Biol 44:107–111

Vocanson M, Hennino A, Rozieres A, Poyet G, Nicolas J-F (2009) Effector and regulatory mechanisms in allergic contact dermatitis. Allergy 64:1699–1714

Walker SL, Young AR (2007) An action spectrum (290–300 nm) for TNFα protein in human skin in vivo suggests that basal-layer epidermal DNA is the chromophore. Proc Natl Acad Sci U S A 104:19051–19054

Walls AC, Han J, Li T, Qureshi AA (2013) Host risk factors, ultraviolet index of residence, and incident malignant melanoma in situ among US women and men. Am J Epidemiol. doi:10.1093/aje/kws335

Wang L, Jameson SC, Hogquist KA (2009) Epidermal Langerhans cells are not required for UV-induced immunosuppression. J Immunol 183:5548–5553

Wolf P, Byrne SN, Gruber-Wackernagel A (2009) New insights into the mechanisms of polymorphic light eruption: resistance to ultraviolet radiation-induced immune suppression as an aetiological factor. Exp Dermatol 18:350–356

Yao Y, Wolverton JE, Zhang Q, Marathe GK, Al-Hassani M, Konger RL, Travers JB (2009) Ultraviolet B radiation generated platelet-activating factor agonist formation involves EGF-R-mediated reactive oxygen species. J Immunol 182:2842–2848

Yarosh DB (2004) DNA repair, immunosuppression, and skin cancer. Cutis 74(Suppl 5):10–13

Young AR (1986) The sunburn cell. Photodermatology 4:127–134

Zaidi MR, David S, Noonan FP, Graff-Cherry C, Hawley TS, Walker RL, Feigenbaum L, Fuchs E, Lyakh L, Young HA, Hornyak TJ, Arnheiter H, Trinchieri G, Meltzer PS, Merlino G (2011) Interferon-γ links ultraviolet radiation to melanomagenesis in mice. Nature 469:548–553

Light-Promoted Infection

25

Lars Olof Björn

25.1 Introduction

Ultraviolet radiation, and also visible light, can kill bacteria and other microorganisms. This is not surprising and scientifically not very interesting, but may be practically very important, as in the case of the bacterium causing tuberculosis, *Mycobacterium tuberculosis*. Niels Finsen, the first photobiologist to be awarded a Nobel Prize (1903), found a method to heal a form of tuberculosis called *lupus vulgaris* using light.

Ultraviolet radiation downregulates immune defense (Chap. 20) and, in this way, may promote infection. On the other hand, ultraviolet radiation makes possible the synthesis of vitamin D, which may counteract some infections, such as tuberculosis. These mechanisms are rather indirect, and we shall focus here infection-promoting effects via photoreceptors in the microorganisms themselves.

Several bacterial and fungal infections are promoted by light. We shall give examples illustrating a variety of mechanisms for these light effects. As has been pointed out by Liu and Nizet (2009), many pathogenic microorganisms have distinct colors, often reflected in their names: *Staphylococcus aureus*, *Pseudomonas aeruginosa* (aeruginosa refers to the green color of corroded copper, Latin "aerugino", Swedish "ärg"), *Chromobacterium violaceum*, etc. In many cases it has been shown that the pigment is necessary for virulence, but the connection between pigmentation and virulence is seldom understood. We shall start our review with an organism, *Cercospora*, where the virulence mechanism and the role of a light-absorbing compound that it produces are simple and clearly understood. In other cases where light plays a role in virulence and pathogenesis, the mechanism is more complicated and involves specific light receptors.

L.O. Björn
School of Life Science, South China Normal University, Guangzhou, China

Department of Biology, Lund University, Lund, Sweden
e-mail: Lars_Olof.Bjorn@biol.lu.se

25.2 Fungi: Ascomycota

Cercospora is a genus with many parasitic species, each one specialized for a specific host plant. These host plants include many economically important crop plants, such as legumes, maize, tobacco, sugar beet, and banana. For a number of plants, it has been shown that fungal infection is more severe under strong light than under low light (Daub and Ehrenshaft 2000). The fungus produces cercosporin (Fig. 25.1), a photodynamically active compound (see Chap. 21). In this case we are dealing with a mixed type I/type II photosensitization, resulting in the production of both superoxide anion and singlet oxygen, the latter thought to be more important (Daub and Ehrenshaft 2000). This results in membrane damage by peroxidation of lipids and leakage through the plant cell membranes (Fig. 25.2), weakening the resistance and promoting fungal invasion. An action spectrum for killing of tobacco cells in a solution of cercosporin (Daub 1982) follows the absorption spectrum of cercosporin (Fig. 25.3).

Some species of *Cercospora* contain also other substances with a similar photodynamic effect. A number of other parasitic fungi, including the bamboo pathogens *Shiraia bambusicola* and *Hypocrella bambusae*, *Alternaria* and *Elsinoe* species, *Stemphylium botryosum*, *Dothistroma pini*, and several *Cladosporium* species, produce additional substances with photodynamic action that probably give these fungi a similar advantage (Daub et al. 2005).

Research has been carried out to understand how the fungi protect themselves from photodynamic damage. There is strong evidence that pyridoxine (vitamin B6) acts as an important protectant (Daub and Ehrenshaft 2000). A gene

L.O. Björn (ed.), *Photobiology: The Science of Light and Life*,
DOI 10.1007/978-1-4939-1468-5_25, © Springer Science+Business Media New York 2015

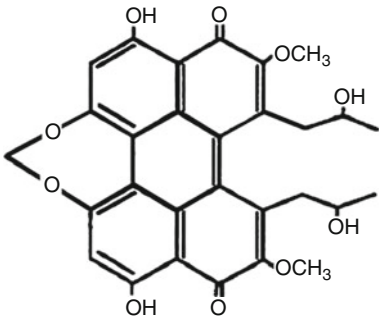

Fig. 25.1 Structure of cercosporin

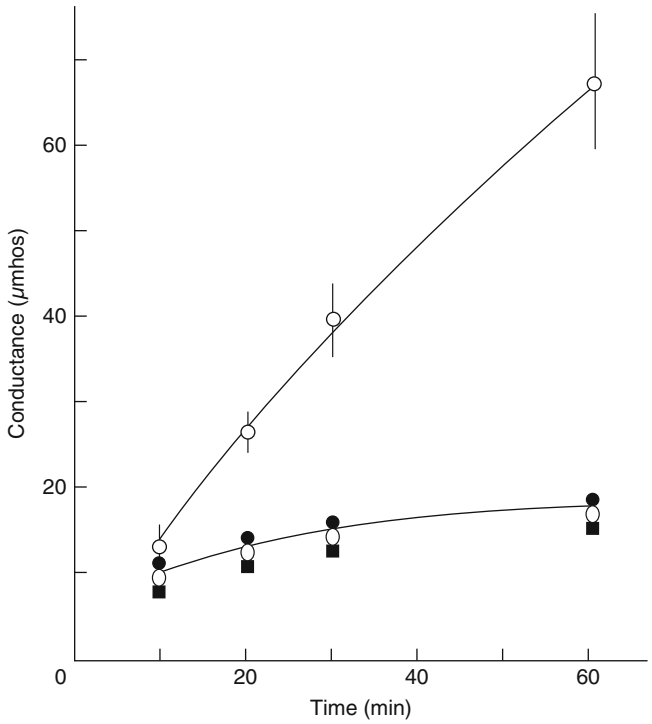

Fig. 25.2 Ion leakage from maize roots treated with cercosporin. *Empty circles*, in light; *filled symbols*, in darkness (From Macrì and Vianello 1979)

called *CRG1*, encoding a transcription factor, is essential for resistance (Chung et al. 2003a, b).

Fusarium oxysporum has many strains with differing lifestyles, many living as saprophytes, some causing fusarium wilt in plants. Some strains are also pathogenic to various animals, from arthropods to mammals. The fungus harbors several photoreceptors (Avalos and Estrada 2010), of which one, the LOV-domain containing white collar-1, is necessary for virulence in mice, but not in plants (Ruiz-Roldán et al. 2008). When a functional gene for white collar-1 is absent, expression of some other photoreceptor genes is repressed (Avalos and Estrada 2010). No experiments have been carried out regarding a possible light effect on virulence.

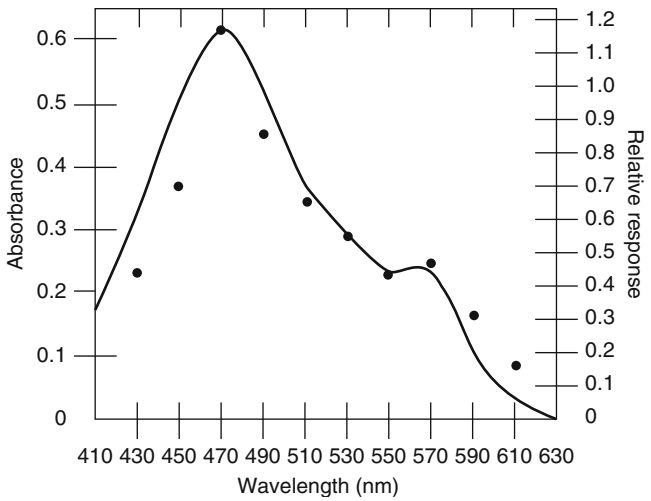

Fig. 25.3 Absorption spectrum (—) of cercosporin and action spectrum for killing of tobacco cells by cercosporin (•) (From Daub 1982)

25.3 Fungi: Basidiomycota

The pathogenic basidiomycete *Cryptococcus neoformans* is equipped with two white collar genes similar to that in *Fusarium oxysporum* (Idnurm and Heitman 2005). Deletion of either one of these genes results in reduced virulence in mice. Idnurm and Heitman (2005) draw the conclusion that "a role for blue/UV light in controlling development is an ancient process that predates the divergence of the fungi into the ascomycete and basidiomycete phyla." We should, however, keep the possibility of lateral gene transfer in mind.

25.4 Alphaproteobacteria of Order Rhizobiales

Brucella is a genus of Gram-negative bacteria with many species infecting various mammals: rodents, carnivores, seals, ungulates, whales, monkeys, and man (Audic et al. 2011). Wild-type *Brucella* is 10 times more virulent after exposure to visible light than bacteria that were never exposed to light (Swartz et al. 2007). This effect has been shown to be due to activation of a LOV histidine kinase (regarding LOV, see Chap. 11), but exactly how this activation leads to increased virulence is not understood. This type of kinase is very widespread among bacteria, so perhaps this effect of light is more common than yet discovered.

Rhizobium leguminosarum is a soil bacterium that infects root hairs and induces the formation of nitrogen-fixing nodules on leguminous plants. Like its relative *Brucella*, it is equipped with a LOV photosensing protein. Illumination of bacterial cultures before inoculation of pea roots increases the number of nodules per plant and the number of intranodular bacteroids (Bonomi et al. 2012). Light can be

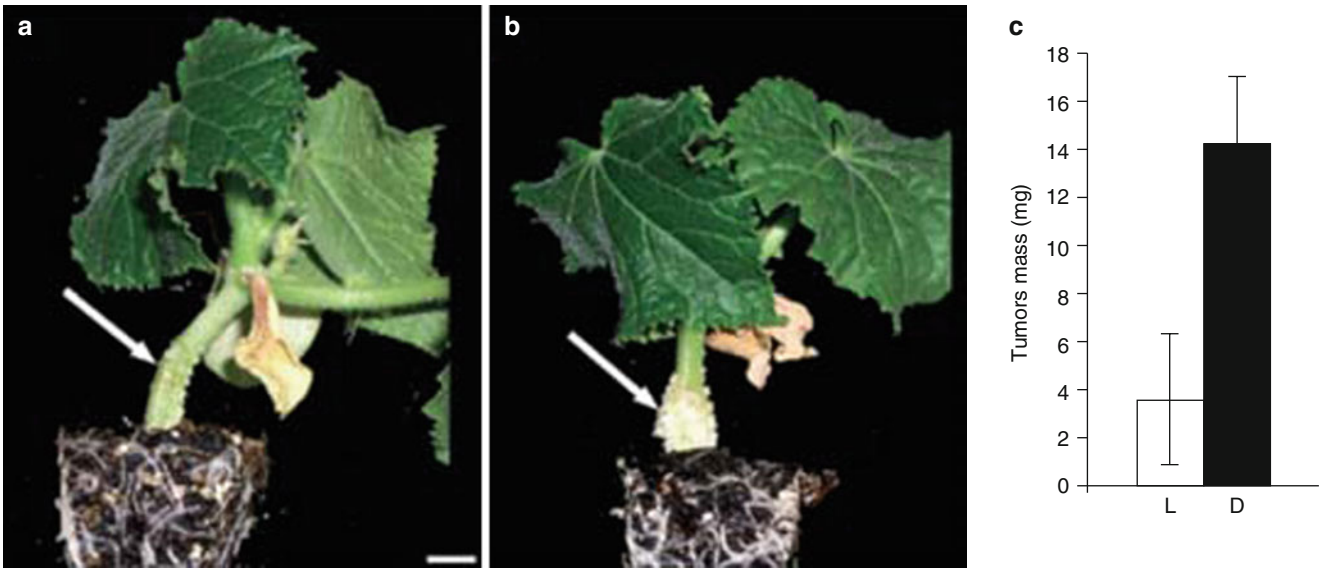

Fig. 25.4 *Agrobacterium tumefaciens* tumor on *Cucumissativus* after incubation in light (**a**) or darkness (**b**). The difference between tumour weight in light (L) and dark (D) is shown in panel (**c**). (From Oberpichler et al. 2008)

conducted down the roots (Sun et al. 2003, 2005), and one can imagine that bacteria in the root zone can perceive and react to light.

Surprisingly Oberpichler et al. (2008) found a different behavior for *Agrobacterium tumefaciens*, which belongs to the same order as *Rhizobium*. Illumination decreases infectivity and other processes related to it, as expression of flagella genes, motility and adhesivity (Fig. 25.4). The same authors found that light decreases growth (colony size) in *Agrobacterium tumefaciens* as well as in *A. vitis*, *Rhizobium leguminosarum*, and *R. radiobacter* (Fig. 25.3).

Agrobacterium is equipped with two sensors for long-wavelength red light (bacteriophytochromes) (Lamparter et al. 2002, Karniol and Vierstra 2003), and possibly other light sensors (Obepichler et al. (2006, 2011)), but what kind of light that elicits the effects described has not been investigated.

25.5 Gammaproteobacteria

Acinetobacter baumannii is a human pathogen. We know of no experiments with human cells infected with this organism, but when *Acinetobacter baumannii* was cocultured with the fungus *Candida albicans*, the filaments of the latter were killed by blue-light irradiation. The light effect seems to be mediated by a flavoprotein in the bacterium (Mussi et al. 2010). In this case it is not a LOV protein, but a protein with another flavine domain (BLUF).

Xanthomonas axonopodis is a plant pathogen. It contains a photosensing protein of the kind referred to as BLUF (blue-light sensing using FAD), which is necessary for virulence, as is light (Kraiselburd et al. 2012).

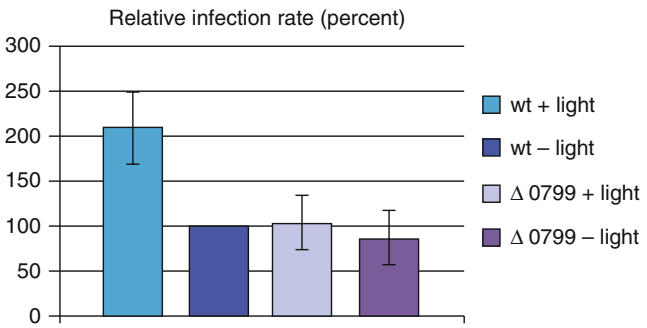

Fig. 25.5 Effect of light on relative infection rate (vertical axis) in Caco-2 enterocyte-like cells were infected with wild type of *Listeria cytogenes* and its isogenic Δ 0799 mutant, deficient in the Lmo blue-light receptor. Prior to infection the bacteria were either exposed for 10 min to blue light or kept in the dark (From Ondrusch and Kreft 2011)

25.6 Firmicutes

Listeria is a genus of Gram-positive rodlike bacteria which may contaminate food. *Listeria monocytogenes* causes serious infection in humans, with high mortality. Like *Brucella* it contains a LOV photoreceptor, but also a red-sensitive photoreceptor. Ondrusch and Kreft (2011) tested the infectiveness of *L. monocytogenes* on cultured human colon epithelial cells (Caco-2 cells) with or without 10 min preirradiation with blue light. The blue light doubled the infection rate with the wild-type *Listeria*, but not when similar *Listeria* mutated in the *Lmo0799* gene were used (Fig. 25.5). *Lmo0799* is the gene for the LOV blue-light receptor in this organism. It was also noticed that the expression of a number of genes was increased by blue light. The photoreceptor has been further characterized by Chan et al. (2013), and other aspects of its action have been described by Tiensuu et al. (2013).

The LOV receptor that helps *Listeria* to take advantage of light is also an Achilles heel. With all likelihood it is the photodynamic potency of the flavin moiety of the photoreceptor that makes it possible to kill *Listeria* with strong blue light (Endarko et al. 2012).

Red light increases growth, swarming motility, and biofilm formation of *Bacillus amyloliquefaciens* JBC36, while blue light had an inhibiting effect (Yu et al. 2013).

References

Audic S, Lescot M, Claverie J-M, Axel Cloeckaert A, Zygmunt MS (2011) The genome sequence of Brucella pinnipedialis B2/94 sheds light on the evolutionary history of the genus Brucella. BMC Evol Biol 11:200, 2011

Avalos J, Estrada AF (2010) Regulation by light in *Fusarium*. Fungal Genet Biol 47:930–938

Bonomi HR, Posadasa DM, Parisa G, del Carmen Carrica M, Frederickson M, Pietrasanta LI, Bogomolni RA, Zorreguieta A, Goldbauma RA (2012) Light regulates attachment, exopolysaccharide production, and nodulation in *Rhizobium leguminosarum* through a LOV-histidine kinase photoreceptor. Proc Natl Acad Sci U S A 109:12135–12140

Chan RH, Lewis JW, Bogomolni RA (2013) Photocycle of the LOV-STAS protein from the pathogen *Listeria monocytogenes*. Photochem Photobiol 89:361–369

Chung K-R, Daub ME, Ehrenshaft M (2003a) Expression of the cercosporin toxin resistance gene (CRG1) as a dicistronic mRNA in the filamentous fungus *Cercospora nicotianae*. Curr Genet 43: 415–424

Chung K-R, Daub ME, Kuchler K, Schüller C (2003b) The CRG1 gene required for resistance to the singlet oxygen-generating cercosporin toxin in *Cercospora nicotianae* encodes a putative fungal transcription factor. Biochem Biophys Res Commun 302:302–310

Daub ME (1982) Cercosporin, a photosensitizing toxin from *Cercospora* species. Phytopathology 72:370–374

Daub ME, Ehrenshaft M (2000) The photoactivated *Cercospora* toxin cercosporin: contributions to plant disease and fundamental biology. Annu Rev Phytopathol 38:461–90

Daub ME, Herrero S, Chung K-R (2005) Photoactivated perylenequinone toxins in fungal pathogenesis of plants. FEMS Microbiol Lett 252(2005):197–206

Endarko E, Maclean M, Timoshkin IV, MacGregor SJ, Anderson JG (2012) High-intensity 405 nm light inactivation of *Listeria monocytogenes*. Photochem Photobiol 88:1280–1286

Idnurm A, Heitman J (2005) Light controls growth and development via a conserved pathway in the fungal kingdom. PLoS Biol 3:e95

Karniol B, Vierstra RD (2003) The pair of bacteriophytochromes from *Agrobacterium tumefaciens* are histidine kinases with opposing photobiological properties. Proc Natl Acad Sci U S A 100:2807–2812

Kraiselburd I, Alet AI, Tondo ML, Petrocelli S, Daurelio LD, Monzón J, Ruiz OA, Losi A, Orellano EG (2012) A LOV protein modulates the physiological attributes of *Xanthomonas axonopodis* pv. citri relevant for host plant colonization. PLoS One 7(6):e38226

Lamparter T, Michael N, Mittmann F, Esteban B (2002) Phytochrome from *Agrobacterium tumefaciens* has unusual spectral properties and reveals an N-terminal chromophore attachment site. Proc Natl Acad Sci U S A 99:11628–11633

Liu GY, Nizet V (2009) Color me bad: microbial pigments as virulence factors. Trends Microbiol 17:406–413

Macrì F, Vianello A (1979) Photodynamic activity of cercosporin on plant tissues. Plant Cell Environ 2:267–271

Mussi MA, Gaddy JA, Cabruja M, Arivett BR, Viale AM, Rasia R, Actis LA (2010) The opportunistic human pathogen *Acinetobacter baumannii* senses and responds to light. J Bacteriol 192:6336–6345

Oberpichler I, Molina I, Neubauer O, Lamparter T (2006) Phytochromes from *Agrobacterium tumefaciens*: difference spectroscopy with extracts of wild type and knockout mutants. FEBS Lett 580:437–442

Oberpichler I, Rosen R, Rasouly A, Vugman M, Ron EZ, Lamparter T (2008) Light affects motility and infectivity of *Agrobacterium tumefaciens*. Environ Microbiol 10:2020–2029

Oberpichler I, Pierik AJ, Wesslowski J, Pokorny R, Rosen R et al (2011) A photolyase-like protein from *Agrobacterium tumefaciens* with an iron-sulfur cluster. PLoS One 6:e26775

Ondrusch N, Kreft J (2011) Blue and red light modulates SigB-Dependent gene transcription, swimming motility and invasiveness in *Listeria monocytogene*s. PLoS One 6(1):e16151

Ruiz-Roldán MC, Garre V, Guarro J, Mariné MA, Roncero MIG (2008) Role of the white collar 1 photoreceptor in carotenogenesis, UV resistance, hydrophobicity and virulence of *Fusarium oxysporum*. Eukaryot Cell 7:1227–1230

Sun Q, Yoda K, Suzuki M, Suzuki H (2003) Vascular tissue in the stem and roots of woody plants can conduct light. J Exp Bot 54:1627–1635

Sun Q, Yoda K, Suzuki H (2005) Internal axial light conduction in the stems and roots of herbaceous plants. J Exp Bot 56:191–203

Swartz TE, Tseng T-S, Frederickson MA, Paris G, Comerci DJ, Rajashekara G, Kim J-K, Mudgett MB, Splitter GA, Ugalde RA, Goldbaum FA, Briggs WR, Bogomolni RA (2007) Blue-light–activated histidine kinases: two-component sensors in bacteria. Science 317:1090–1093

Tiensuu T, Andersson C, Rydén P, Johansson J (2013) Cycles of light and dark co-ordinate reversible colony differentiation in *Listeria monocytogenes*. Mol Microbiol 87:909–924

Yu S-M, Lee YH (2013) Effect of light quality on *Bacillus amyloliquefaciens* JBC36 and its biocontrol efficacy. Biol Control 64:203–210

Bioluminescence

26

Lars Olof Björn and Helen Ghiradella

26.1 Introduction

Apart from the fluorescence and phosphorescence introduced in Chap. 1, three kinds of light emission from a living organism may take place:

1. Photosynthetic *delayed light emission*, also called *delayed fluorescence* or *afterglow*. This is weak red light emitted by all green plants and algae. The intensity is so low, and the light of such long wavelength, that we cannot see it, but it is easily measured. It is due to reversion of the first steps of photosynthesis.
2. *Ultraweak light emission* takes place in all organisms. It is due to various processes, mostly (but not always) involving molecular oxygen. It is regarded as a by-product of metabolic activity and has no biological function in itself. It is even weaker than delayed light emission, and although it is often of shorter wavelength, it cannot be seen; rather sophisticated equipment is needed for its measurement. It can be exploited for studying what is going on in cells in a noninvasive and nondestructive way.
3. *Bioluminescence* is the best known of the biological luminescence phenomena, mostly because it can be observed using only one's eyes. We shall devote most of this chapter to bioluminescence. Although photosynthetic delayed light emission and ultraweak light emission are not, in our terminology, bioluminescence, sections at the end of this chapter will deal with these phenomena.

L.O. Björn (✉)
School of Life Science, South China Normal University, Guangzhou, China

Department of Biology, Lund University, Lund, Sweden
e-mail: Lars_Olof.Bjorn@biol.lu.se

H. Ghiradella
Department of Biology, University at Albany, Albany, NY, USA
e-mail: hghff@albany.edu

In addition to the more recent literature cited in this chapter, we would like to mention the book by Harvey (1952) as an excellent summary of the older bioluminescence literature. Extensive reviews of marine bioluminescence are provided by Hastings (1966); Tett and Kelly (1973); Herring (1982, 2002, pp. 188–216); Marcinko et al. (2013); Wilson and Hastings (2013).

26.2 Evolution and Occurrence Among Organisms

Although most species are nonbioluminescent, most phyla have bioluminescent representatives. Among the exceptions are true plants and higher vertebrates (i.e., amphibians, reptiles, birds, and mammals).

Comparison of the biochemical systems involved clearly shows that bioluminescence has evolved multiple times. At least 30 independently evolved systems are still extant (Hastings 1983; Wilson and Hastings 1998; Waldenmaier et al. 2012). Still, most bioluminescence systems share some common features, as we shall see in the section on biochemistry. Rees et al. (1998) and Dubuisson et al. (2013) have proposed that bioluminescence has evolved from antioxidant systems.

Thus bioluminescence occurs among bacteria, fungi, dinoflagellates, protozoa, sponges, cnidaria, ctenophores (comb jellies), molluscs, annelids, crustaceans, insects, bryozoa, echinoderms, and fish. The majority of bioluminescent species live in the sea, although there are also many bioluminescent insects (all terrestrial), especially beetles. It has been estimated that 60–80 % of the fish species in the deep sea are bioluminescent. Table 26.1 shows the distribution in more detail.

Since bioluminescent microorganisms exist, one must be careful not to confuse microbial luminescence with luminescence of the host. Many fish and mollusc species that have been regarded as bioluminescent organisms have been shown to glow by the light of symbiotic bacteria. There are,

L.O. Björn (ed.), *Photobiology: The Science of Light and Life*,
DOI 10.1007/978-1-4939-1468-5_26,

Table 26.1 Systematic distribution of bioluminescence

Phylum	Approximate number of genera with bioluminescence
Bacteria	5
Pyrrophyta	11
Protozoa	9
Porifera	1
Cnidaria	66
Ctenophora	15
Rhynchocoela	1
Nematoda	1
Mollusca	74
Annelida	40
Arthropoda	207
Bryozoa	1
Echinodermata	47
Chordata	208

Source: Adapted from Campbell (1988)

however, also cases of true fish and mollusc bioluminescence.

It is probable that bioluminescence first appeared during the "Cambrian explosion", when the evolution of eyes had made it meaningful. Molecular oxygen is required for all known bioluminescence mechanisms, but the required oxygen partial pressure (or equivalent chemical activity) is much lower than that of the contemporary atmosphere.

26.3 Biological Roles: What Is Bioluminescence Good For?

In some cases the advantage to the organisms of bioluminescence is quite clear, in other cases quite obscure. An old hypothesis for explaining bioluminescence in cases where no other explanation could be found is that it takes care of big energy quanta, which could act destructively, and converts them to harmless photons (McElroy and Seliger 1962; Seliger and McElroy 1965). The energy in a bioluminescence photon is an order of magnitude greater than the energy bound in a high-energy phosphate bond in, e.g., ATP. The evolution of bioluminescence could have been triggered by the appearance of free oxygen, causing formation of dangerous peroxides. As we shall see, peroxides play a role in most bioluminescent systems. It has also been pointed out (Seliger and McElroy 1965) that bioluminescent reactions, although depending on the presence of oxygen, require only very low partial pressures, corresponding to conditions in the distant past when organisms would first have had to adapt to this dangerous triplet molecule. More recently Rees et al. (1998) present evidence for antioxidant activity in coelenterazine, a common marine luciferin, and Lyzen and Wegrzyn (2005) demonstrate similar protective effects in bacterial luciferases. Barros and Bechara (2000) further discuss the protective effect of an insect luciferase, with special regard to a beetle larva.

In those cases when we can clearly see a present-day biological role for bioluminescence, we can divide the advantages gained into five main categories: (1) reproduction, (2) protection from predation (defense, camouflage or aposematic signaling), (3) food acquisition, (4) protection from reactive oxygen species (ROS), and (5) DNA repair by means of activation of photolyase repair enzymes. We shall give examples of each of them.

26.3.1 Reproduction

The best-known examples of bioluminescence having a role in the propagation of the species are found among the beetles of the family Lampyridae (true fireflies and glowworms), although bioluminescence also occurs in several other beetle families. In glowworms only the female glows brightly (with a steady light) and by this attracts the male, and the same is the case in some firefly species. In other fireflies, a sophisticated "light conversation" between males and females has evolved, with a different "language" for each species. Males send out an "interrogation" flash, and females respond. Species specificities are obtained both by the time course of the flash on a half-second time scale and by the time delay between "interrogation" and "answer." Some details of this, with references are given by Seliger and McElroy (1965).

The competitive value of various flashing abilities has been investigated by Branham and Greenfield (1996), Vencl et al. (1994), and Vencl and Carlson (1998). For one species, Branham and Greenfield (1996) found that the flash rate, rather than the flash length or flash intensity, determined the female's preference.

An intriguing phenomenon is the synchronous flashing of the males of some fireflies. These males often collect in a tree, and the whole tree flashes "in step" (Buck and Buck 1976; Buck 1988). Species differences and various ideas about how this synchronized flashing comes about, as well as how it aids the reproduction of the species, are discussed with many references by Buck (1988). For newer investigations on the phenomenon, we refer the reader to Moiseff and Copeland (2000). Another example of luminescence intensity being synchronized among individuals is that of the cave-dwelling Tasmanian glowworm *Arachnocampa tasmaniensis*, which exhibit 24-h rhythm even in the distant parts of the cave where no daylight reaches (Merritt and Clarke 2011).

There is also a multitude of deep-sea animals which use bioluminescence for finding a mate in the dark abyss, and here new discoveries are certainly going to be made for some time to come. Among the more interesting cases is the

dragonfish, which uses light of a wavelength so long (maximum 702 nm) that it cannot be perceived by other organisms on which the dragonfish preys (Herring 2002).

There is little solid information on the role of bioluminescence in fungi (Cassius et al. 2013). Bioluminescence has been reported in about 40 species of fungi, of which nearly two thirds belong to the genus *Mycena*. Other genera with luminescent members are *Panellus*, *Armilariella*, *Lampteromyces*, *Pleurotus*, *Omphalia*, and *Omphalotus. Panellus stipticus* is a brightly luminescent fungus, common in North America, which has served as material for several investigations. It has been speculated that luminescent fungi attract insects which aid in dispersal of spores (O'Kane et al. 1990a; Bermudes et al. 1992, and many others). However, in many fungi, only the mycelium, and not the fruiting bodies, luminesces.

26.3.2 Protection from Predation

One of the best-known examples of bioluminescence, described by Aristotle, is the "fire of the sea" caused by dinoflagellates such as *Noctiluca* and *Gonyaulax*. Its survival value remained obscure for a long time, but it has now been shown that it protects from grazing by copepods (Esaias and Curl 1972; Buskey and Swift 1983).

In different animal groups, there are examples of how bioluminescence can protect by diverting the attacker's attention away from the prospective prey. Some squid, when attacked, give off a luminescent secretion which confuses the attacker, and luminescent secretion from a shrimp (Inouye et al. 2000) may serve a similar purpose. A kind of marine annelid called a scale worm is covered on the dorsal side by scales which first emit flashes when the animal is attacked and then are shed, still glowing (Herrera et al. 1974). Its light-emitting protein may have use for detection of superoxide anions (Bassot and Nicolas 1995).

By aposematic coloration, we mean easily recognized bright color patterns like the black-yellow banding of wasps, spots on ladybugs, and stripes on coral snakes, which warn a predator of nasty consequences of an attack (and frequently are mimicked by species which do not have any other protection). It was shown by Underwood et al. (1997) that bioluminescence of firefly larvae serves a similar purpose. The bioluminescence of the millipede *Motyxia sequoiae* also has an aposematic function (Marek et al. 2011). Luminescence of cockroaches is thought to be mimicry of non-palatable click beetles (Vršanský et al. 2012).

Somewhat surprisingly, bioluminescence can also be used for camouflage in two different ways. Fish can be either luminescent by themselves or can harbor luminescent bacteria. Some fish of both categories use bioluminescence for counterillumination and "disruptive illumination" (McFall-Ngai and Morin 1991), to avoid perception of their shape and size. Most fish are lighter on the ventral than on the dorsal side, and this can be regarded as minimizing their visibility: from above, they look dark like the background depth, and from below, they look bright like the sky above. This cannot give complete protection; they still look rather dark against a bright sky. But some fish, by bioluminescence, do match both the intensity and the angular distribution of the downwelling surface light (Denton et al. 1972). The spectral match is also very good (Denton et al. 1985), and the intensity is regulated according to ambient light (McFall and Morin (1991).

An intriguing function might be what is commonly called the "burglar alarm" hypothesis (Fleisher and Case 1995; Mensinger and Case 1992, and papers cited in these). Bioluminescent organisms such as the dinoflagellate, *Noctiluca*, respond to predation, or even movement, by flashing, thereby increasing the visibility of actual or potential predators to secondary predators, and thus protecting themselves.

26.3.3 Food Acquisition

The deep-sea anglerfish *Linophryne arborifera* uses a bait with luminescent bacteria. Female fireflies of the genus *Photuris* reply to the "interrogating flashes" from males of other fireflies, lure them to approach, and eat them (Lloyd 1984a). Most sly and cunning of them all are the females of *Photuris versicolor*, who know firefly languages sufficiently well to be able to prey on 11 different species (Lloyd 1984b), but male *Photuris*, in turn, outsmart the females by mimicking their prey in order to mate (Lloyd 1980). Lloyd and Wing (1998) further exemplify the dangers of being luminescent. In other cases, luminescent fireflies rely for their catch on the more unspecific attraction of insects to light.

In addition to beetles, among bioluminescent insects one finds fungus gnats, members of the order Diptera. About a dozen of more than 3,000 species in the family have larvae which use bioluminescence in different ways to catch prey. Particularly famous are the larvae in the Te Ana-au caves on the South Island of New Zealand. The gnat larvae sit on the roof and deploy luminescent and sticky "fish lines," which attract other insects which are caught and devoured. Willis et al. (2011) found that using light to lure prey is an energetically "cheap" predatory strategy compared to spiders' web construction.

In many cases, marine animals are aided in their vision by their own luminescence, which functions mainly in the service of food acquisition. Several fish species, such as *Aristosmonias scintillans* and *Pachystomias microdon* in the deep sea, and *Photoblepharon palpebratus* and *Anomalops katoptron* in shallow waters, have luminescent organs in proximity to their eyes. The dragonfish, which are so remarkable that we shall return to them later, also belong to those for which vision is aided by their own bioluminescence, as are the shrimp-like euphausiids.

26.3.4 Protection from Reactive Oxygen Species

Rees et al. (1998) investigated the properties of coelenterazine, a common marine luciferin, and documented its strong antioxidant properties. They proposed that during the early stages of their evolution, the primary function of these systems would have been detoxification of oxygen and other ROS at a time in which environmental oxygen levels were rising (modern surface waters are rich in superoxide [SO] and hydrogen peroxide). Along the way, these organisms would have developed effective ways of handling these potentially toxic and high-energy systems, and as they colonized the less oxidatively stressful deeper levels of the seas (less light, including UV, less oxygen, and slower metabolisms), their systems would be pre-adapted to produce light for other purposes (as these authors note, all bioluminescent reactions are high energy and require involvement of oxygen or its activated species).

Studies of luminescence in bacteria (Gonzales-Flecha and Demple 1994; Katsev et al. 2004; Lyzen and Wegrzyn 2005; Szpilewska et al. 2003) have reinforced and extended this view. There has long been speculation about the role of luminescence in bacterial life, besides its role in those symbionts, which presumably gain shelter, food, and possibilities of a future life.

Luminous bacteria occur in the genera *Vibrio*, *Photobacterium*, *Lucibacterium*, *Alteromonas*, and *Xenorhabdus*; most investigations deal with either the first or second of these. The cited studies demonstrate that wild-type (=luminescent) bacteria of *Vibrio harveyi* and other strains are able to survive UV irradiation or exposure to hydrogen peroxide better than nonluminescent *lux* mutants and, further, that this wild-type resistance can be conferred to *E. coli* via constructs between the *lux genes* and the promoter of a stress-response gene. Gonzales-Flecha and Demple found that in *E. coli*, the bacterial luciferase was producing superoxide as a by-product, and they urge caution in using this construct system to report oxidative stress in bacteria that normally do not produce such luciferase. It is highly probable, given the connection between ROS and bioluminescence, that other such systems will show similar effects.

26.3.5 DNA Repair

Many of the above luminescent bacteria display a behavior called "quorum sensing," in which the bioluminescent systems are not expressed until the colony reaches a certain density (Swift et al. 1998). A common interpretation is that this may deter predators from disturbing a colony that has gained a beachhead in a food item. But many luminescent bacteria luminesce at extremely low density, and in addition to possible detoxification of ROS, evidence now suggests strongly that this solo luminescence may function in activation of photolyase enzymes in DNA repair (Czyz et al. 2000, Kosakiewicz et al. 2005). In *V. harveyi* (nonluminescent), *lux* mutants irradiated with UV light and then cultured in the dark did not survive as well as the (luminescent) wild type or as *lux* mutants returned to light after irradiation; this result has been generalized to other strains of bacteria as well. In short, bacteria living in relatively dark levels of the ocean may be achieving photoreactivated DNA repair by producing their own "photo." Experiments by Walker et al. (2006) do not support the theory that bioluminescence protects DNA. However, given that bioluminescence in these organisms may be extremely expensive metabolically (requiring about 20 % of cellular energy; Kozakiewicz et al. 2005), its use for protection against ROS and for DNA repair would certainly be a strong factor for its evolution and conservation. Indeed, cells are able to handle and manipulate many types of ROS. We will meet another such system later.

26.4 Mechanisms of Light Production

As mentioned earlier, bioluminescence has evolved several times, and it is not surprising therefore that there are many different mechanisms (Hastings and Tu 1995). The different mechanisms do, however, have in common that they all require oxygen at some stage. Many of them also involve a peroxide—either a hydroperoxide or a cyclic peroxide. They involve catalysis by an enzyme called luciferase, but luciferases from different organisms are different (the outcome of comparisons of luciferase sequences is the main reason for the statement that bioluminescence in extant taxa probably has evolved about 30 times). Luciferase action on a relatively low molecular weight organic compound called luciferin results in an excited state of a pigment, which either emits light directly or transfers excitation energy to another emitter.

Bacterial luminescence is based on peroxidation of flavin mononucleotide (FMN) and oxidation of a long-chain aldehyde to carboxylic acid, so flavin mononucleotide can be said to be the luciferin in this case. The reaction scheme is shown in Fig. 26.1. The flavin molecule is here drawn isolated but is, in fact, bound to the luciferase. The emission may be either the blue-green emission from FMN or be from an accessory chromoprotein to which the excitation is transferred. There are several such proteins known for different bacteria (Eckstein et al. 1990; Lee et al. 1991), but the mechanisms for light emission are not completely understood. Some bacteria can emit radiation with different spectra.

Fungal bioluminescence is relatively little explored, and in most investigations, spectral analysis of the emitted light suffers from deficient methods and equipment. The most reliable spectrum so far was published by O'Kane et al. (1990b). They found an emission maximum (on a photon per wavelength interval basis) of about 525 nm. Shimomura

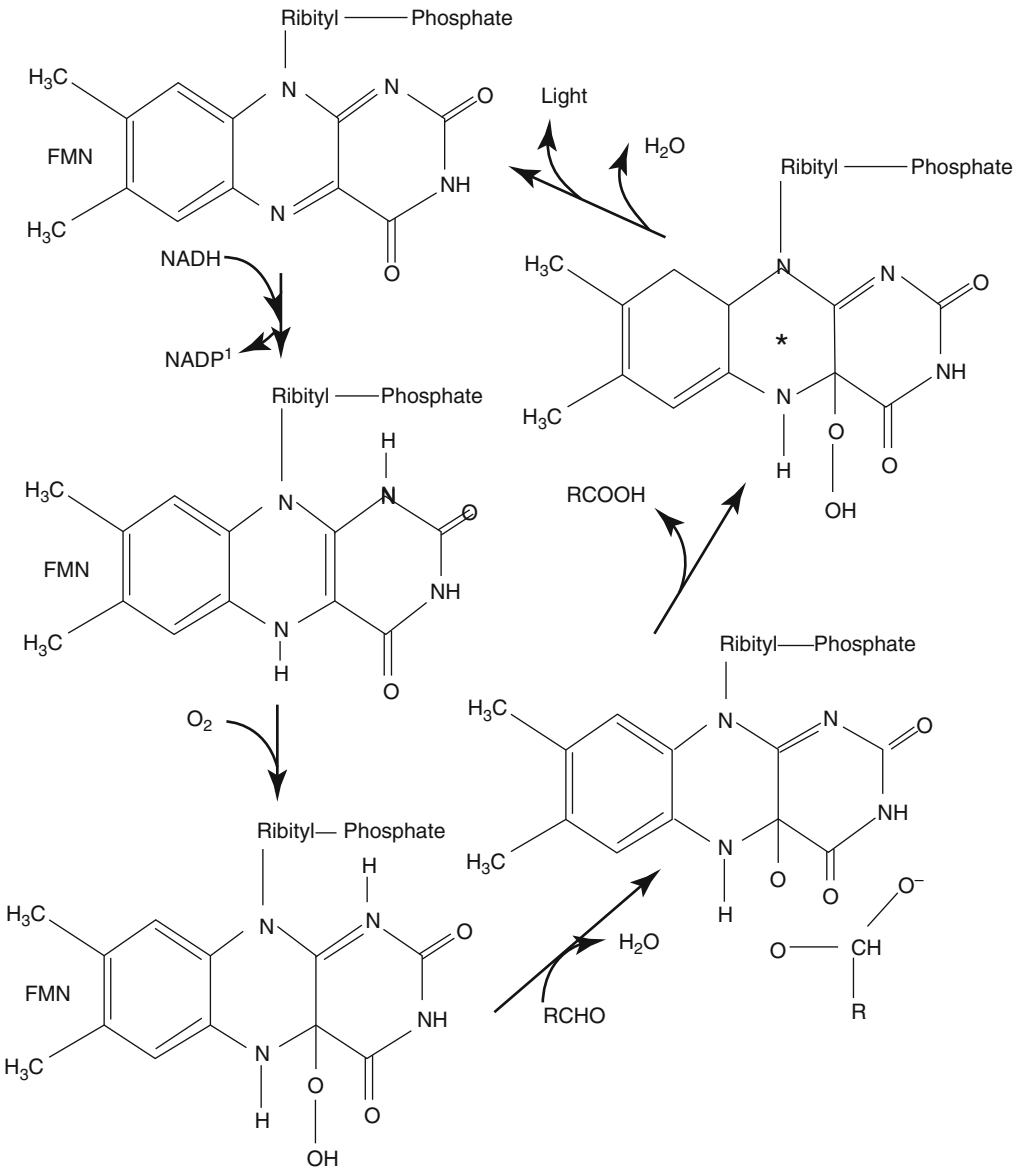

Fig. 26.1 Reactions involved in bacterial bioluminescence

(1980, 1989, 1992) favors the view that the emission is caused by a reaction between hydrogen peroxide, a low-molecular amine, and panal (sesquiterpene aldehyde). However, as O'Kane et al. (1990b) point out, such a conclusion cannot be based on spectral data, since chemiluminescence of the latter system in vitro has emission maxima ranging from 485 to 570 nm, depending on conditions. Several other emitters have been proposed in fungal bioluminescence, one of which is riboflavin (Isobe et al. 1987).

Dinoflagellates have different luciferins depending on the species. In the most studied organism, *Gonyaulax polyedra*, it is a tetrapyrrole-like substance with an extra ring (Nakamura et al. 1989), clearly derived from chlorophyll (Fig. 26.2), but in another species, *Pyrocystis lunula*, it is quite different (Nakamura et al. 1989). The bioluminescence of *Gonyaulax* differs from that of most bioluminescent organisms in that no peroxide seems to be involved. Another remarkable thing is that the spectrum of luminescence agrees with the fluorescence spectrum of unreacted luciferin (Hastings 1978), while the postulated emitter is nonfluorescent. Therefore, the mechanism sketched in Fig. 26.2 must be regarded as tentative.

For light emission by the firefly luciferin/luciferase reaction (Fig. 26.3), prior adenylation of the luciferin by reaction with ATP is required. Both luciferin and luciferase are located in the peroxisomes in one part of the cell, while another part of the cell is full of ATP-generating mitochondria.

Although different beetles can produce light with different colors from green to red, they all seem to possess the same kind of luciferin. The differences in wavelength distribution are probably due to differences in luciferase. Possibly

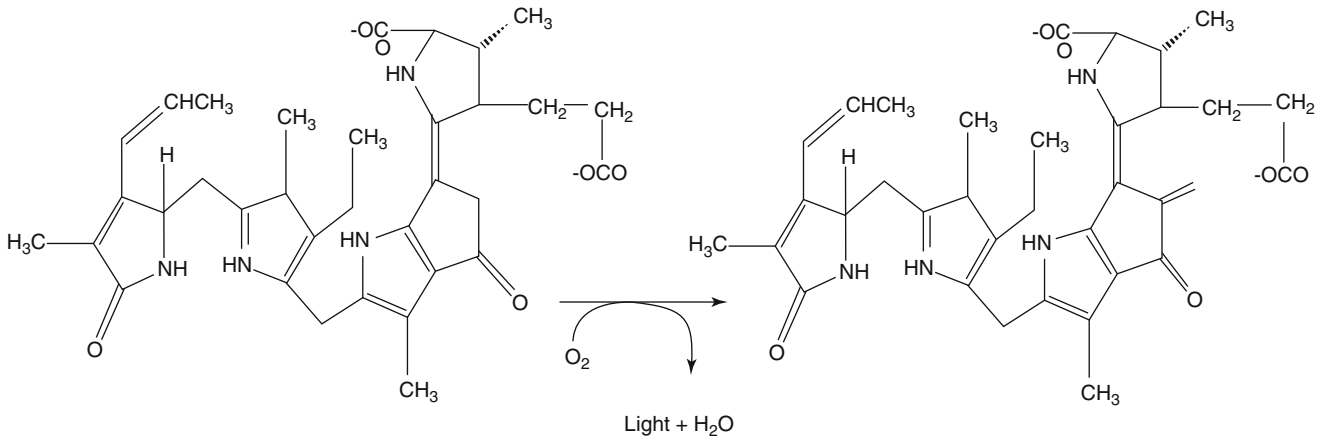

Fig. 26.2 Bioluminescence reaction in the dinoflagellate *Gonyaulax*

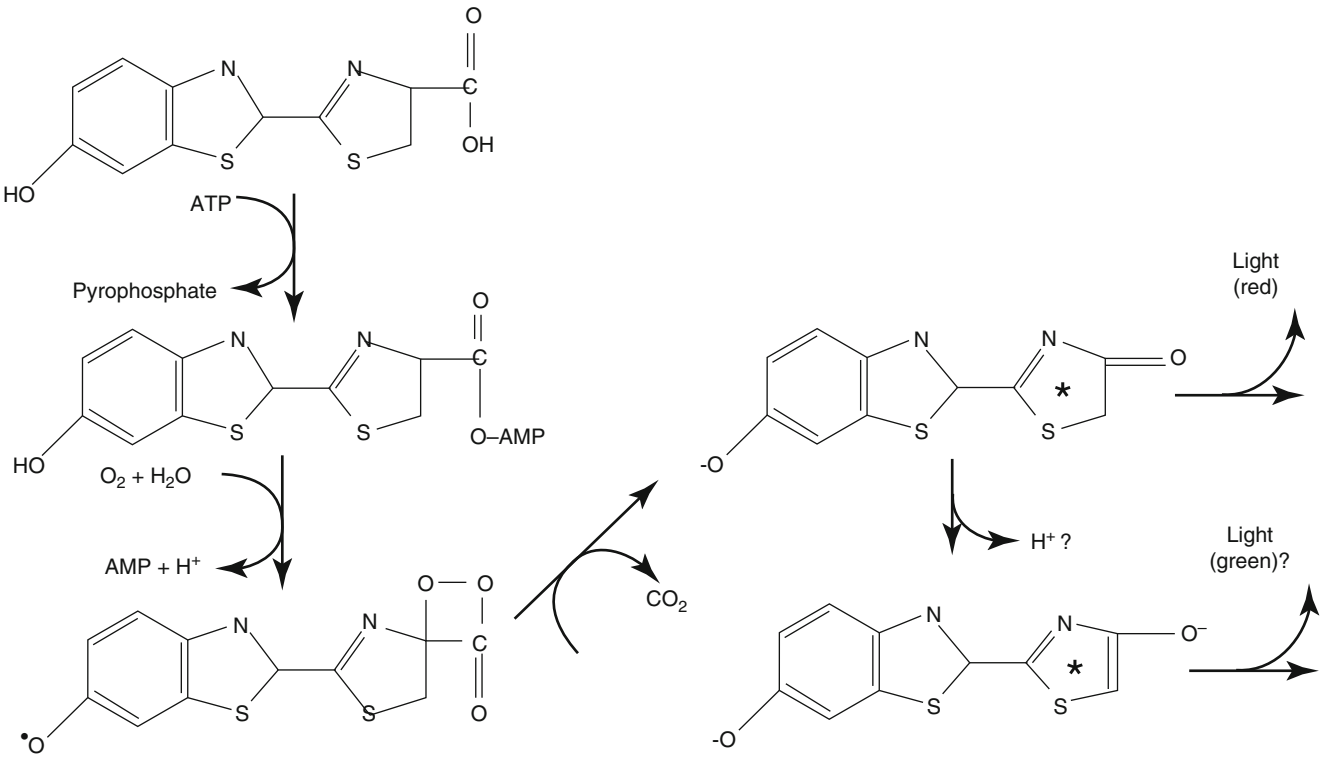

Fig. 26.3 Reactions leading to luminescence in fireflies and other beetles. The luciferin and its derivatives remain bound to luciferase throughout the reaction sequence. The *asterisk* indicates an excited state. The diagram is essentially according to Wilson and Hastings (1998)

there are two different molecular species involved as emitters, as sketched in Fig. 26.3.

As for color of emitted light, the most remarkable animal is the larva in the beetle family Phengodidae (*Phrixothrix vivianii* and *Euryopa* species), the so-called railroad worms (Viviani and Bechara 1997; Viviani and Ohmiya 2000). These carry both red lanterns (on the head) and yellow-green ones (on the sides) on the same individual. Color pictures of these magnificent animals are available at several Internet sites, e.g., http://www.lifesci.ucsb.edu/~biolum/forum/vviviani2.html.

The mechanism of bioluminescence in dipterans differs from that of beetles but is as yet little explored.

In addition to *Vargula* (see below), among crustaceans the euphausiids are worth special mention because of their strong light and sophisticated lantern optics. They are shrimp-like animals but distinct from true shrimps and not members of the group Decapoda. Like the dinoflagellate *Gonyaulax*, they have a tetrapyrrole chlorophyll derivative as a light-emitting chromophore, but the macrocycle of the chlorophyll molecule is split open at another site. Their

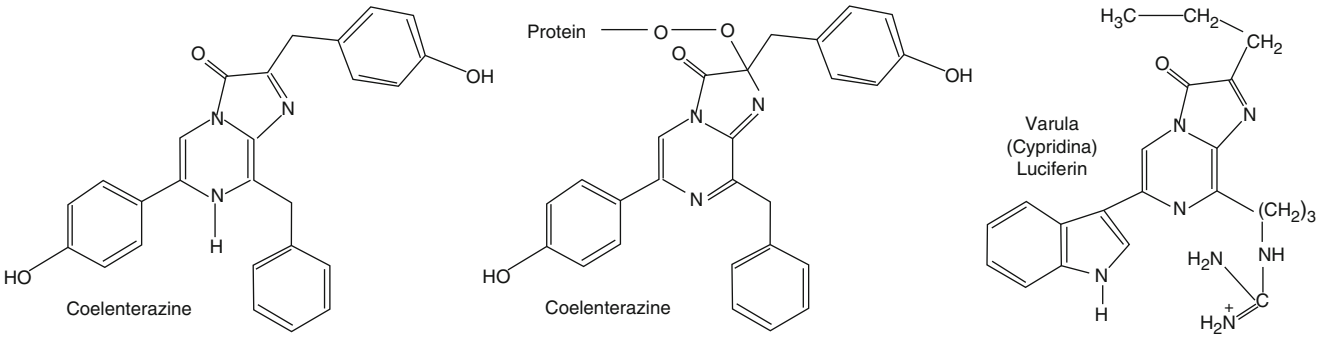

Fig. 26.4 Coelenterazine and related chromophores

lanterns are equipped both with a reflective backing and a lens system to direct the light. Those lanterns which are located on the eye stalks just above the eyes certainly serve as an aid to vision.

The structure of the luciferin typical of the coelenterates, i.e., cnidaria and ctenophores (coelenterazine), has great similarities to the prosthetic group of a light-generating chromoprotein, aequorin, of the jellyfish *Aequorea*. The luciferin of the squid *Watasenia* is coelenterazine with the hydroxy groups replaced by sulfate groups. The luciferin of the crustacean (ostracod) *Vargula* (formerly known as *Cypridina*) is also structurally related to these chromophores (Fig. 26.4).

The luciferins of coelenterates and of *Vargula* function together with luciferases and also require oxygen for the light-emitting reactions to take place. Earlier it was thought that the bioluminescence of *Aequorea* (Fig. 26.5) was something in principle different, since the chromoprotein aequorin extracted from it would glow in vitro when calcium ion was added, without the need for molecular oxygen. However, it is now realized that aequorin is an enzyme–substrate (luciferase–luciferin) complex which requires oxygen for formation and is stable in the absence of calcium ions.

Just like some bacteria, some animals also have accessory light-emitting chromoproteins, proteins different from the luciferin–luciferase complexes. This is the case with *Aequorea* (Fig. 26.6) and also the sea pansy *Renilla* (Pennatulacea, relatives of corals). Excitation energy is transferred by the Förster mechanism from the excited reaction product of the luciferin to the covalently bound chromophores of these accessory proteins.

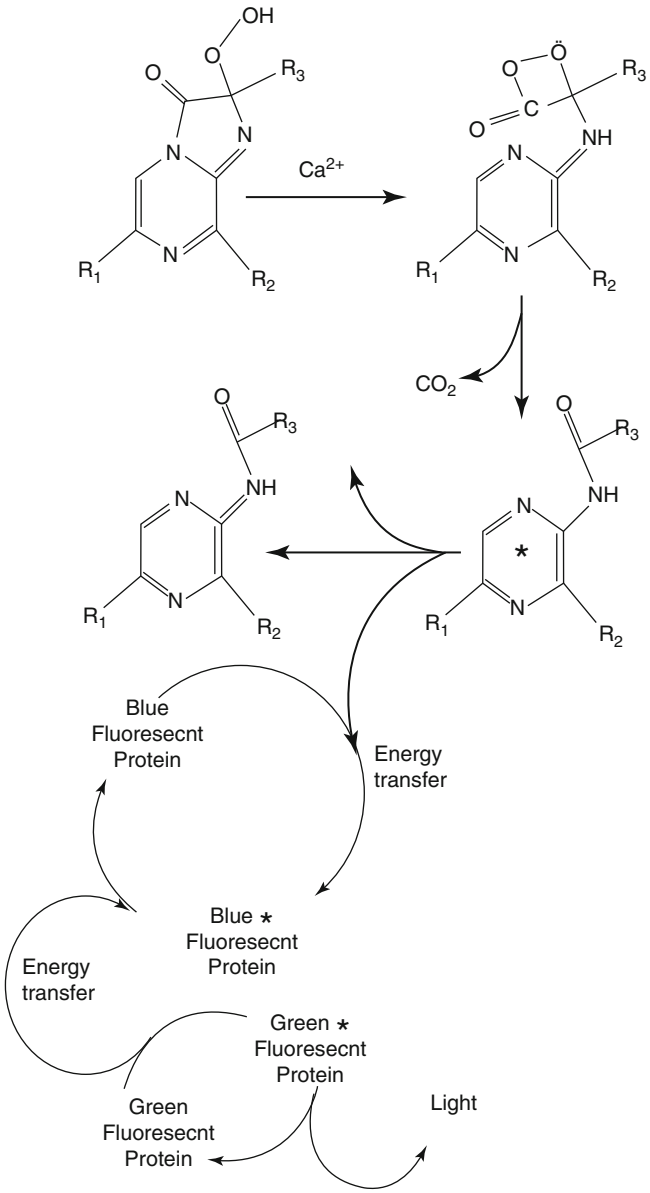

Fig. 26.5 *Aequorea* bioluminescence. The *asterisk* indicates an excited state

26.5 Dragonfishes: Long-Wave Bioluminescence and Long-Wave Vision

Even the dark deep-sea harbors creatures of great interest to photobiologists. Dragonfishes are worth our attention for two reasons: their bioluminescence and their vision. Both operate

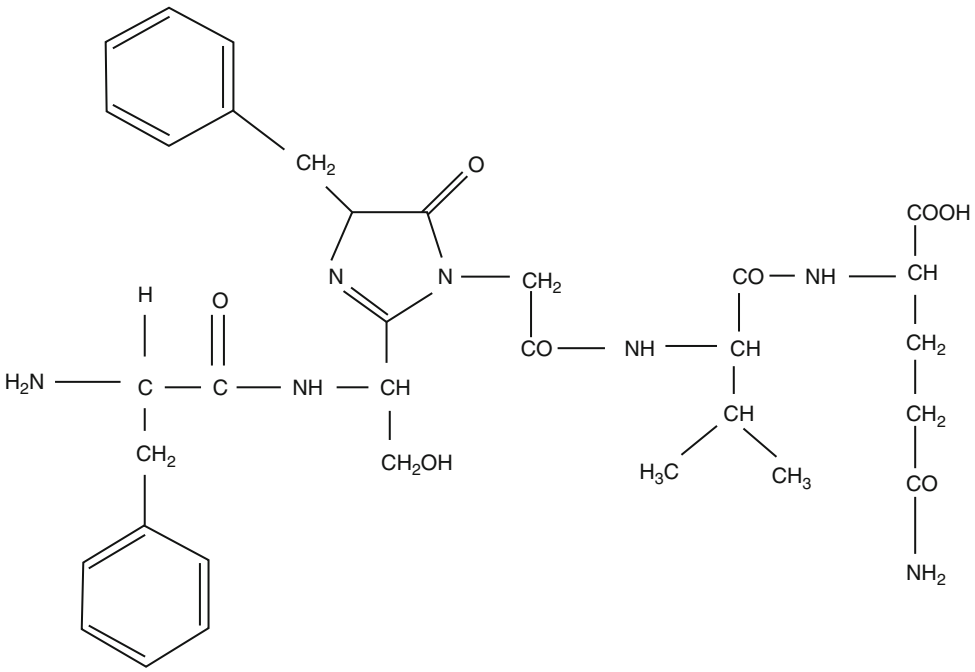

Fig. 26.6 Structure of the chromophore of the green fluorescent protein from *Aequorea* according to Cody et al. (1993). A slightly different structure has been published by Shimomura (1979). The fluorescence spectrum has a narrow band peaking at 509 nm

at the long-wavelength limit of our own perceptual abilities, at wavelengths of around 700 nm (Partridge and Douglas 1995).

Three genera, *Aristomias*, *Malacosteus*, and *Pachystomias*, emit both blue light from organs behind the eyes and far-red light from organs below the eyes (Widder et al. 1984; Douglas et al. 2000). It is possible that the basic luminescence system is the same in both blue-emitting and far-red-emitting organs and that the latter are equipped with secondary emitters to which excitation energy is transferred from the luciferin. If this is the case, probably also an intermediary pigment is required to span the spectrum from the 479-nm (A. *scintillans*) or 469-nm (M. *niger*) primary emitter to the final 703-nm (A. *scintillans*) or 660-nm (*M. niger*) emitter, to make possible sufficiently large overlap integrals for Förster energy transfer to take place. *M. niger* has a short-wavelength cutoff filter in front of the light emitter to shift the emission maximum from 660 to 702 nm (Widder et al. 1984; Denton et al. 1985).

What could the pressure be to drive evolution of emission maxima in both these fishes to such long wavelengths, using different methods? This for a long time was an enigma. Water absorbs such radiation rather efficiently, so its range cannot be very large. And, above all, what could its use be? It was hard to believe that any visual pigment could exist to permit the fish to see such long-wave radiation.

But in the difficulty of constructing a retinal-based visual pigment with such long-wavelength absorption lies the explanation for the advantage. The dragonfish can use its far-red torch to watch its prey without being observed by other animals. But still, to have any use for the light, it must be able itself to perceive it. And how it manages to do that is the most remarkable fact about this fish.

The genera *Aristomias* and *Pachystomias* use a "conventional" method. They have managed to tune a rhodopsin by "protein engineering" to get an absorption band peaking at 588–595 nm or even 650 nm (Bowmaker et al. 1988; Douglas et al. 1998a, b, 2000). This is quite a feat, considering that essentially the same chromophore, in a different protein environment, is used by other animals for UV receptors with sensitivity peaks around 360 nm. The tail of the 588-nm pigment extends above 700 nm and would give some sensitivity overlapping the bioluminescence spectrum. However, in addition to rhodopsins (retinal-based visual pigments), fishes (and also dragonfishes) usually contain porphyropsins (3,4-dehydroretinal-based pigments) with the same opsin-type protein moiety. Although Douglas et al. (2000) were unable to find the porphyropsin analogue of the 588-nm rhodopsin, they speculate that *A. tittmanni* is equipped with it. They calculate the absorption peak to be at 669 nm and show that it would match the bioluminescence almost perfectly.

But *Malacosteus* has not succeeded with this "protein engineering." It has only two "conventional" visual pigments, with peaks at 520 and 540 nm. But it has another trick up its sleeve.

Not only is it difficult to construct a retinal-based pigment with an absorption maximum above 650 nm, but there are, in fact, very few types of organic substances which absorb at such long wavelengths. One well-known type widespread in the biosphere is chlorophyll. Bacterial variants of this may have absorption peaks even above 1 μm.

And this type of pigment is just what *M. niger* uses for its vision. Chlorophyll from photosynthetic bacteria at the base of the food chain has been converted to a mixture of pheophorbides and deposited in the outer segments of the photoreceptor cells in close contact with the 520- and 540- nm pigments. It seems either that in some way energy can be transferred from pheophorbide to these pigments (Douglas et al. 1998b, 1999 speculate that this could take place via the triplet state of the rhodopsin or porphyropsin) or that pheophorbide can act in place of ordinary visual pigments.

A well-illustrated description of the dragonfish light organs and further references are provided by Kenaley (2010); Kenaley et al. (2014).

26.6 Control of Bioluminescence

Even in bacteria, bioluminescence is regulated; bacteria do not glow unless the cell density is high, as it is, for instance, in the organs where some squids and fishes harbor luminescent bacteria. Fascinating details of how quorum sensing (density sensing) takes place and how host animals can control bacterial luminescence in their light organs are currently being revealed (McFall-Ngai et al. 2011; Miyashiro and Ruby 2012).

A common feature for many bioluminescent systems is that the light intensity decreases when ambient light increases. This indicates both that the light has some function in itself (not primarily serving to divert excess energy) and that bioluminescence is energetically and metabolically demanding and that an organism cannot afford to waste the resources. In a couple of cases, action spectra have been constructed for the inhibition of luminescence (Esaias et al. 1973; Li et al. 1996; Fig. 26.7), but the chromophore corresponding to this spectrum is unknown, as is the mechanism of inhibition.

There are many interesting findings regarding regulation of bioluminescence. These range from such relatively short-term events as the rapid flashing of fireflies and dinoflagellates, and circadian rhythms, to long-term effects of environment and nutrient status and from organismal to subcellular levels. We must refrain from descriptions of most of this here, and the reader is referred to the treatises by Campbell (1988), Ulitzur and Dunlap (1995), Hosseini and Nealson (1995), and Wilson and Hastings (1998). A few words will be devoted to recent findings about one of the best investigated cases, firefly bioluminescence.

Most fireflies flash with precise timing in a species-specific way and rapidly respond to flashes from other fireflies. Obviously they must have very tight control of their so-called photocytes, the light-emitting cells. How this control is possible has been an enigma, since in some case they have no direct nerve connections. As we have seen, the

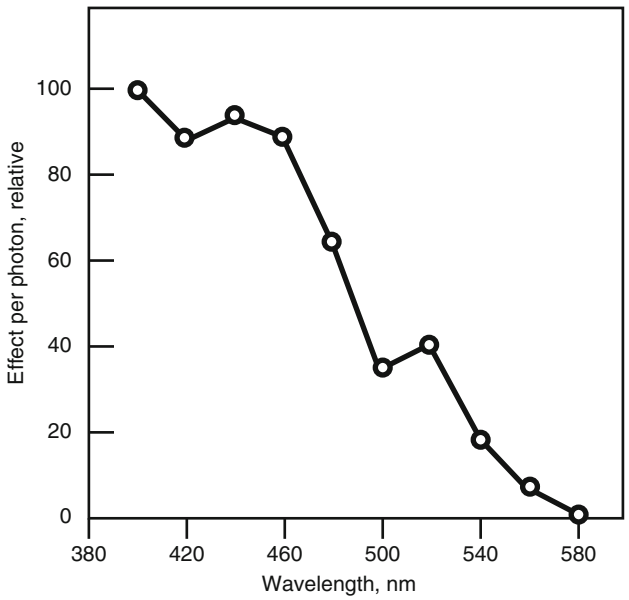

Fig. 26.7 Action spectrum for the inhibition of bioluminescence of the dinoflagellate *Protoperidinium depressum* (Redrawn from Li et al. (1996))

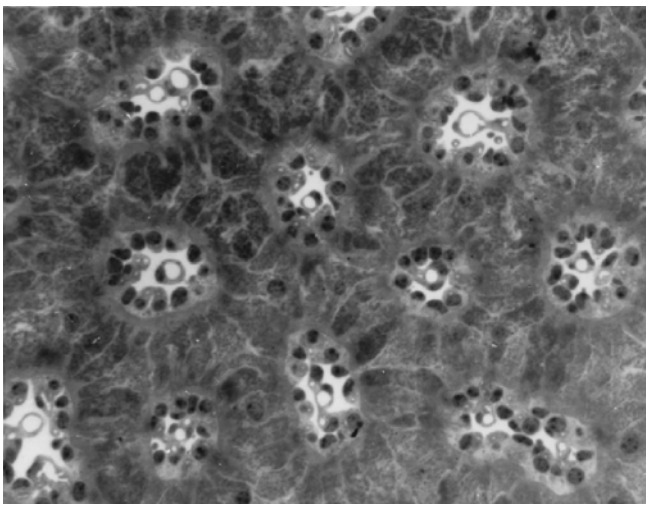

Fig. 26.8 A section through the light-emitting organ of the firefly *Photuris* sp, showing tracheae surrounded by cylindrical tracheal end organs and photocytes. The photocytes stretch rosette-fashion from one cylinder to the next (see the following figures) (From Ghiradella 1998)

light-emitting process requires oxygen, and the photocytes are located in close proximity to the profusely branched tracheae (Figs. 26.8, 26.9, and 26.10). Trimmer et al. (2001) suggest that the signaling takes place along the same path as the supply of oxygen, using the gaseous hormone nitrogen monoxide (NO). This hormone, coined "molecule of the year" by *Science* in 1992, is also important in human physiology, but in humans and most other animals, it is transported in the dissolved state. According to this model, the fireflies

take advantage of the fact that it is a small molecule diffusing very rapidly in the gaseous phase. The nitrogen monoxide is produced in the terminal cells of the tracheal system, where the nerve projections end, and in some of the peripheral (and mitochondria-rich) parts of the photocytes (Fig. 26.10).

This model, as many earlier ones, depends on oxygen as the controlling molecule and builds on earlier suggestions that the mitochondria that occupy the photocyte borders between the branches of the tracheal system and the photocyte interiors (where the light is actually produced) may serve as "gate keepers," using up incoming oxygen before it can penetrate into the photocyte. NO reversibly shuts down mitochondrial action, which in this case would then "open the gate" and allow free passage of oxygen. However, the model does not account for important morphological and physiological features of the lantern, especially the presence in the photocyte interior of huge numbers of peroxisomes, organelles particularly adept at handling peroxides and other ROS.

Ghiradella and Schmidt (2004) propose that to complete the flash reaction (and thus control the flash) the photocyte is in fact using *hydrogen peroxide*, produced in its peroxisomes from incoming oxygen, rather than the oxygen itself. This new proposal has required reworking of the current chemical model, which was generated by superb scientists but working at a time and in a climate in which it was not believed that cells can in fact control and manipulate reactive oxygen species (ROS). We are learning that they can (Apel and Hirt 2004), and our new knowledge of the capabilities of cells suggests that many models, these included, are ripe for reexamination and revision.

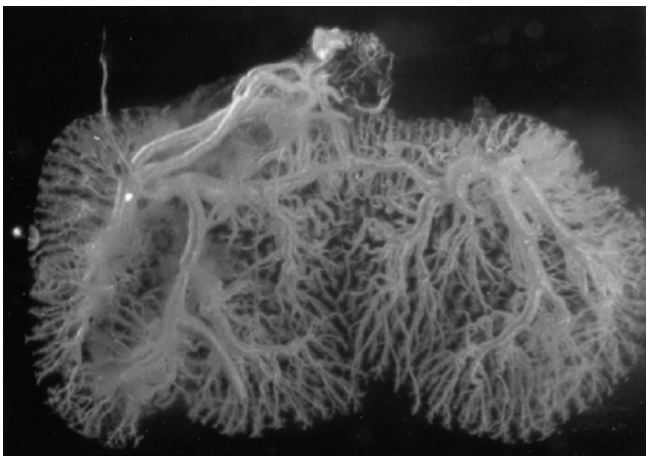

Fig. 26.9 Preparation of isolated tracheae from a light-emitting organ of a firefly, showing the repeated ramification (From Ghiradella 1998)

26.7 Human Exploitation of Bioluminescence

Warfare is perhaps not an application one would guess at for bioluminescence. Japanese soldiers are said to have used dried *Vargula* for reading maps during World War II. When

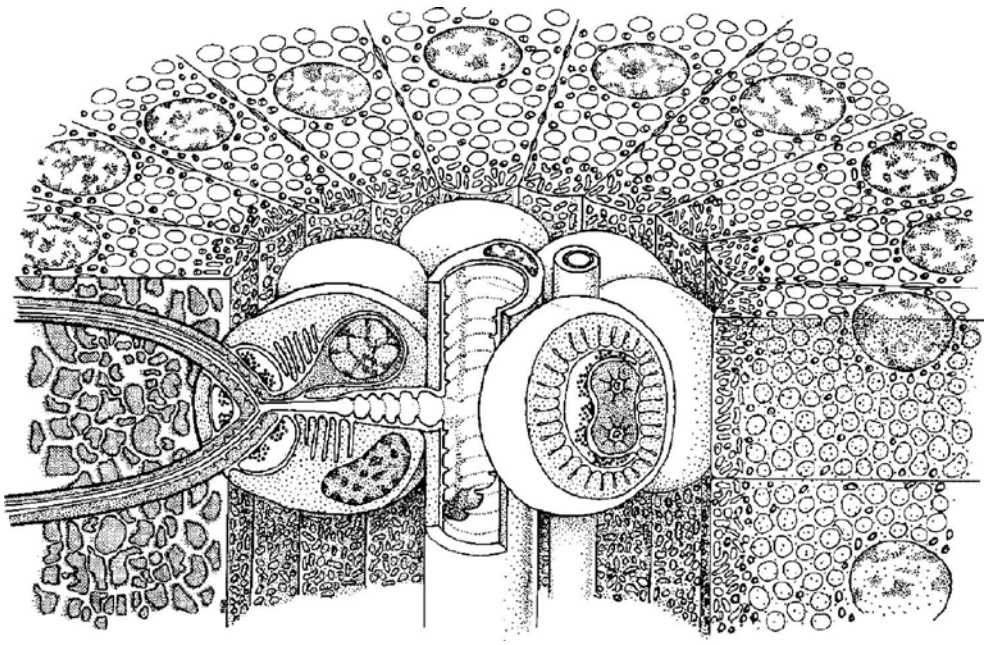

Fig. 26.10 Diagrammatic view of part of a firefly lantern. At center, the main trachea (parallel to a nerve) is connected to a cluster of tracheal end organs. At left is shown a longitudinally sectioned end organ with its tracheolar branches and the webbed intercellular border of an associated photocyte. To the right is shown a transversely sectioned end organ. In the upper part of the picture is a half-circle of cross sections of photocytes (From Ghiradella 1998)

moistened, these dried animals emitted sufficient light for the purpose.

The cloned gene of the fluorescent accessory protein of *Aequorea* ("green fluorescent protein") has found wide application in molecular biology as a reporter gene. It has even been improved for this function by genetic engineering (Blinks 1989; Cubitt et al. 1995a; Heim et al. 1995; Heath 2000; Deo and Daunert 2001).

The "arrested" luciferin–luciferase complex of *Aequorea* can be used for extremely sensitive assays of calcium ion. Using this protein, it is even possible to map the concentration of calcium ions inside cells. The protein can be introduced into the cells under study by different methods. If the aequorin gene is cloned into the organism under study, it ends up in the cytoplasm of that organism. The cytoplasm has a low calcium ion concentration most of the time, but one step in many signal transduction chains consists in a sudden elevation of the concentration, and this can be studied by this method (Knight et al. 1991, 1993; Cubitt et al. 1995b; Wood et al. 2000, 2001).

Various other luciferase genes, especially that of the firefly luciferase, are also used for the study of gene regulation. The luciferase gene is fused to the regulator gene under study. A disadvantage is that the organism has to be killed and treated in such a way that ATP and luciferin can be added. This can be circumvented by using instead bacterial luciferase, which can be activated by addition of the vapor of an aldehyde. However, as mentioned above, Gonzáles-Flecha and Demple (1994) warn of at least one case in which the results were ambiguous. In a study aimed at reporting concentrations of redox stress agents, specifically superoxide, they fused the *lux* luciferase genes to the promoter of *soxS*, part of the cell's response system to such agents, and discovered that the alien (to *E. coli*) bacterial luciferase was raising superoxide concentration, thereby complicating the measurements and the interpretation of the results.

The classic use of bioluminescence, however, is the use of a luciferin–luciferase mixture from fireflies as an assay for ATP. The sample to be analyzed is mixed with a luciferin–luciferase mixture or crude firefly lantern extract. Since the luciferase preparations usually also contain an enzyme capable of converting two molecules of ADP to one molecule of AMP and one of ATP (a slower reaction than the luciferase reaction), AMP in the sample will also produce light but with much slower kinetics. Therefore the intensity of the initial flash upon mixing the sample with the reagents is taken as a measure of ATP.

The firefly assay for ATP has found very wide use, and kits for assay are commercially available. This application forms a natural bridge to the next section.

26.8 Photosynthetic Afterglow

In the 1950s, many people were involved in the discovery and study of photosynthetic phosphorylation, and one of the present authors (LOB) had the privilege of working as an assistant to D.I. Arnon during this exciting time. Early in the decade, Strehler and Arnold (1951) had attempted to demonstrate the formation of ATP in a preparation of isolated chloroplasts by mixing the chloroplast suspension with firefly extract. After a period of illumination to let the chloroplasts synthesize ATP, the experimenters shut off all external light and tried to measure bioluminescence from the mixture. They were pleased to find a clear light signal, which rapidly decayed with time (as they expected, because the tiny amount of ATP would soon be consumed by the luciferase reaction). Then they did a control experiment without firefly extract and to their surprise found that the light was as strong as before. This was the discovery of a phenomenon to which several names have been given: afterglow, delayed light emission, delayed fluorescence. Briefly, it is due to the reversion of early steps in photosynthesis: light energy recently converted to chemical, electrical, and proton gradient energy is reconverted to light. Chlorophyll serves as the emitter.

The delayed light emission is due almost exclusively to emission by photosystem 2 (PSII) and consists of several kinetic components. The most rapidly decaying component is due to return of electrons from pheophytin and the quinone called Q_A to the chlorophyll ion in the reaction center, resulting in excited chlorophyll. The slowest component also involves PSI and is best excited using long-wavelength light preferentially absorbed by this system. It is also dependent on molecular oxygen (Björn 1971). Energy for this emission is stored as proton gradient and as ATP and is inhibited not only by such electron transport blockers as DCMU but also by uncouplers. Even before the acceptance of the chemiosmotic theory of Mitchell (1961) study of this long-lived component demonstrated that the membrane system in a chloroplast stores energy as a unit (Björn 1971). Several reviews have been written on delayed light emission; one of the best and most comprehensive is still that by Lavorel (1975). Apart from its use in studies of the mechanism of photosynthesis, delayed light emission has been used for study of plant damage by disease, frost, etc. A special technique for this is "phytoluminography," whereby pictures of plants are produced using only the delayed light (Sundbom and Björn 1977; Björn and Forsberg 1979; Pérez-Bueno et al. 2006; Figs. 26.11 and 26.12).

Photosynthetic cells also exhibit a phenomenon known as thermoluminescence (light emission caused by a temperature rise). It has, as has afterglow and chlorophyll fluorescence, been used for experiments aimed at understanding the mechanism of photosynthesis (DeVault et al. 1983; Tyystjärvi and Vass 2004).

Fig. 26.11 Part of a bean leaf imaged in different ways by its own emitted light: *Left*, Fluorescence light; *center*, fast luminescence (about 0.25 s after the cessation of light incident on the leaf); *right*, slow luminescence (integrated between 30 and 60 s after the cessation of incident light). The leaf veins were injected with DCMU, a substance that interrupts electron transfer between the photosystems, before the picture was taken. This makes photosystem II dissipate energy faster, so fluorescence and fast luminescence become stronger but slow luminescence weaker than from unpoisoned cells further away from the veins (From Björn and Forsberg 1979)

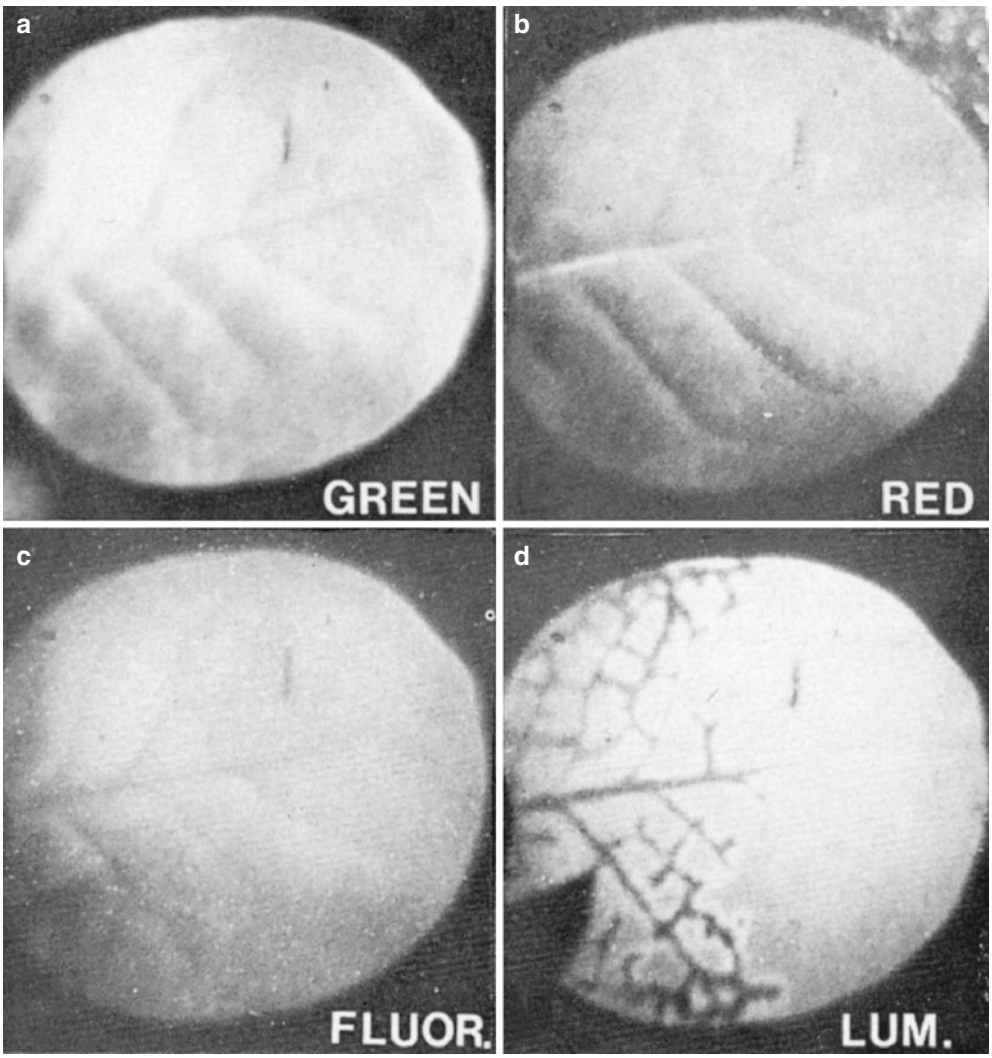

Fig. 26.12 Leaf on a tobacco plant on which another leaf was inoculated with tobacco mosaic virus 6 days before the picture was taken. The virus has spread through the veins to the depicted leaf. Pictures were taken using reflected green (**a**) and red (**b**) light, red fluorescence evoked by blue light (**c**), and light emitted by the leaf after cessation of external illumination (**d**). Only in the last case does the infection become visible at this early stage (From Björn and Forsberg 1979)

26.9 Ultraweak Light Emission

So far we have treated special organisms, which emit bioluminescence, and photosynthetic organisms, which produce delayed light emission due to reversal of photosynthesis. But all other organisms and all cells with active metabolism which have been studied emit very weak light. This is called ultraweak light emission. The ultraweak light emission from green leaves can be studied when the delayed light emission has decayed for about 4 h (at room temperature).

Ultraweak light emission probably has several components with different causes. The main emission from green leaves is of a wavelength exceeding 600 nm and probably is emitted from chlorophyll. In most other cases, the emission is of shorter wavelength. It is believed that a main component stems from peroxidation of unsaturated membrane lipids. However, most cells contain other components which can emit light. For instance, when hydrogen peroxide is decomposed by catalase in the presence of various organic compounds (the plant hormone auxin is one example, pyrogallol another), light is emitted. A number of other causes of ultraweak light emission are listed by Campbell (1988).

If plants are irradiated with UV-B or UV-C radiation, the intensity of ultraweak light emission increases after a long lag period (about 2 days). The reason is probably that the ultraviolet radiation initiates a chain reaction, leading to peroxidation of membrane lipids. An action spectrum for this ultraviolet effect has been determined (Cen and Björn 1994).

Measurement of ultraweak light emission has recently been used for monitoring chemical stress in plants (Bertogna et al. 2013).

Various medical and other applications of measurements of ultraweak light emission are described by Campbell (1988) and Jezowska-Trzebiatowska et al. (1990).

The authors dedicate this chapter to the memory of Woody Hastings and Thérèse Wilson.

References

Apel H, Hirt H (2004) Reactive oxygen species: Metabolism, oxidative stress, and signal transduction. Annu Rev Plant Biol 55:373–399

Barros MP, Bechara EJH (2000) Luciferase and urate may act as antioxidant defeneses in larval Pyrearinus termitilluminans (Elateridae: Coleoptera) during natural development and upon 20-hydroxyecdysone treatment. Photochem Photobiol 71:648–654

Bassot JM, Nicolas MT (1995) Bioluminescence in scale-worm photosomes: the photoprotein polyoidin is specific for the detection of superoxide radicals. Histochem Cell Biol 104:199–210

Bermudes D, Petersen RH, Nealson KH (1992) Low-level bioluminescence detected in *Mycena haematopus* basidiocarps. Mycologia 84:799–802

Bertogna E, Bezerra J, Conforti E, Gallep CM (2013) Acute stress in seedlings detected by ultra-weak photon emission. Photochem Photobiol B Biol 118:74–76

Björn LO (1971) Far-red induced, long-lived afterglow from photosynthetic cells. Size of afterglow unit and paths of energy accumulation and dissipation. Photochem Photobiol 13:5–20

Björn LO, Forsberg AS (1979) Imaging by delayed light emission (phytoluminography) as a method for detecting damage to the photosynthetic system. Physiol Plant 47:215–222

Blinks JR (1989) Use of calcium-regulated photoproteins as intracellular Ca^{2}+ indicators. Methods Enzymol 172:164–203

Bowmaker JK, Dartnall HJA, Herring PJ (1988) Longwave-sensitive visual pigments in some deep-sea fishes: segregation of paired rhodopsins and porphyropsins. J Comp Physiol A163:685–698

Branham MA, Greenfield MD (1996) Flashing males win mate success. Nature 381:745–746

Buck J, Buck E (1976) Synchronous fireflies. Sci Am 234:74–85

Buck J (1988) Synchronous rhythmic flashing of fireflies. II. Q Rev Biol 63:265–289

Buskey EJ, Swift E (1983) Behavioural responses of the coastal copepod Acartia hudsonica to simulated dinoflagellate bioluminescence. J Exp Biol Ecol 72:43–58

Campbell AK (1988) Chemiluminescence: principles and applications in biology and medicine. Ellis Horwood, Chichester, p 608. ISBN ISBN 3-527-26342-X

Cassius V. Stevani CV, Oliveira AG, Mendes LF, Ventura FF, Waldenmaier HE, Carvalho RP, Pereira TA (2013) Current status of research on fungal bioluminescence: Biochemistry and prospects for ecotoxicological application. Photochem Photobiol 89: 1318–1326

Cen Y-P, Björn LO (1994) Action spectra for enhancement of ultraweak luminescence by ultraviolet radiation (270–340 nm) in leaves of Brassica napus. J Photochem Photobiol BL Biol 22:125–129

Cody CW, Prasher DC, Westler WM, Prendergast FG, Ward WW (1993) Chemical structure of the hexapeptide chromophore of the *Aequorea* green-fluorescent protein. Biochemistry 32:1212–1218

Cubitt AB, Heim R, Adams SR, Boyd AE, Gross LA, Tsien RY (1995a) Understanding, improving and using green fluorescent proteins. Trends Biochem Sci 20:448–455

Cubitt AB, Firtel RA, Fischer G, Jaffe LF, Miller AL (1995b) Patterns of free calcium in multicellular stages of *Dictyostelium* expressing jellyfish apoaquorin. Development 121:2291–2301

Czyz A, Wrobel B, Wegrzyn G (2000) *Vibrio harveyi* bioluminescence plays a role in stimulation of DNA repair. Microbiology 146:283–288

Denton EJ, Gilpin-Brown JB, Wright PG (1972) The angular distribution of the light produced by some mesopelagic fish in relation to their camouflage. Proc R Soc Lond B 182:145–158

Denton EJ, Herring PJ, Widder EA, Latz MF, Case JF (1985) The roles of filters in the photophores of oceanic animals and their relation to vision in the oceanic environment. Proc R Soc Lond B 225:63–97

Deo SK, Daunert S (2001) Luminescent proteins from *Aequorea victoria*: applications in drug discovery and in high throughput analysis. Fresenius J Anal Chem 369:258–266

DeVault D, Govindjee, Arnold D (1983) Energetics of photosynthetic glow peaks. Proc Natl Acad Sci U S A 80:983–987

Douglas RH, Partridge JC, Marshall NJ (1998a) The eyes of deepsea fish I: lens pigmentation, tapeta and visual pigments. Prog Retin Eye Res 17:597–636

Douglas RH, Partridge JC, Dulai KS, Hunt DM, Mullineaux CWT, Hynninen PH (1998b) Dragon fish see using chlorophyll. Nature 393:425

Douglas RH, Partridge JC, Dulai KS, Hunt DM, Mullineaux CW, Hynninen PH (1999) Enhanced retinal longwave sensitivity using a chlorophyll-derived photosensitiser in *Malacosteus niger*, a deep-sea dragon fish with far red bioluminescence. Vision Res 39:2817–2832

Douglas RH, Mullineaux CW, Partridge JC (2000) Long-wave sensitivity in deep-sea stomiid dragonfish with far-red bioluminescence: evidence for a dietary origin of the chlorophyll-derived retinal photosensitizer of *Malacosteus niger*. Philos Trans R Soc Lond B 355:1269–1272

Dubuisson M, Marchand C, Rees J-F (2013) Firefly luciferin as antioxidant and light emitter: the evolution of insect bioluminescence. Luminescence 19:339–344

Eckstein J, Cho KW, Colepicolo P, Ghisla S, Hastings JW, Wilson T (1990) A time-dependent bacterial luminescence emission spectrum in an in vitro single turnover system: energy transfer alone cannot account for the yellow emission of *Vibrio fischeri* Y-1. Proc Natl Acad Sci U S A 87:1466–1470

Esaias WE, Curl HC (1972) Effect of dinoflagellate bioluminescence on copepod ingestion rates. Limnol Oceanogr 17:901–906

Esaias WE, Curl HC Jr, Seliger HH (1973) Action spectrum for a low intensity rapid photoinhibition of mechanically stimulable bioluminescence in the marine dinoflagellates *Gonyaulax catenella*, *Gonyaulax acatenella* and *Gonyaulax tamarensis*. J Cell Physiol 82:363–372

Fleisher KJ, Case JF (1995) Cephalopod predation facilitated by dinoflagellate luminescence. Biol Bull 189:263–271

Ghiradella H (1998) The anatomy of light production: the fine structure of the firefly lantern. In: Harrison FW, Locke M (eds) Microscopic anatomy of invertebrates, vol. 5 Insecta. Wiley-Liss, New York, pp 363–381

Ghiradella H, Schmidt JT (2004) Fireflies at one hundred plus: a new look at flash control. Integr Comp Biol 44:203–212

Gonzales-Flecha B, Demple B (1994) Intracellular generation of superoxide as a by-product of *Vibrio harveyi* luciferase expressed in *Escherichia coli*. J Bacteriol 176:2293–2299

Harvey EN (1952) Bioluminescence. Academic, New York

Hastings JW (1978) Bacterial and dinoflagellate luminescent systems. In: Herring PJ (ed) Bioluminescence in action. Academic, London, pp 129–170

Hastings JW (1983) Biological diversity, chemical mechanisms, and the evolutionary origins of bioluminescent systems. J Mol Evol 19:309–321

Hastings JW (1996) Chemistries and colors of bioluminescent reactions: a review. Gene 173:5–11

Hastings JW, Tu D (eds) (1995) Symposium-in-print: molecular mechanisms in bioluminescence. Photochem Photobiol 62:597–673

Heath MC (2000) Advances in imaging the cell biology of plant-microbe interactions. Annu Rev Phytopathol 38:443–459

Heim R, Cubitt AB, Tsien RY (1995) Improved green fluorescence. Nature 373:663–664

Herrera AA, Hastings JW, Morin JG (1974) Bioluminescence in cell-free extracts of scale-worm Hamrmothoe (Annelida: Polynoidae). Biol Bull 147:480–481

Herring PJ (1982) Aspects of the bioluminescence of fishes. Oceanogr Mar Biol Annu Rev 20:415–470

Herring P (2002) The biology of the deep ocean. Oxford University Press, Oxford

Hosseini P, Nealson KH (1995) Symbiotic luminous soil bacteria: unusual regulations for an unusual niche. Photochem Photobiol 62:633–640

Inouye S, Watanabe K, Nakamura H, Shimomura O (2000) Secretional luciferase of the luminour shrimp *Opiophorus gracilirostris*: cDNA cloning of a novel imidazopyrazinone luciferase. FEBS Lett 481:19–25

Isobe M, Uyakul D, Goto T (1987) *Lampteromyces* bioluminescence—1. Identification of riboflavin as the light emitter in the mushroom L. japonicus. J Biolumin Chemilumin 1:181–188

Jezowska-Trzebiatowska B, Kochel B, Slawinski J, Strek W (eds) (1990) Biological luminescence. World Scientific, Singapore

Katsev AM, Wegrzyn G, Sziplewska H (2004) Effects of hydrogen peroxide on light emission by various strains of marine luminescent bacteria. J Basic Microbiol 44:178–184

Kenaley CP (2010) Comparative innervation of cephalic photophores of the loosejaw dragonfishes (Teleostei: Stomiiformes: Stomiidae): evidence for parallel evolution of long-wave bioluminescence. J Morphol 271:418–437

Kenaley CP, DeVaney SC, Fjeran TT (2014) The complex evolutionary history of seeing red: Molecular phylogeny and the evolution of an adaptive visual system in deep-sea dragonfishes (Stomiformes: Stomidae). Evolution 68:996–1013

Knight MR, Campbell AK, Smith SM, Trewavas AJ (1991) Transgenic plant aequorin reports the effects of touch and cold-shock and elicitors on cytoplasmic calcium. Nature 352:524–526

Knight MR, Read ND, Campbell AK, Trewavas AJ (1993) Imaging dynamics in living plants using semisynthetic recombinant aequorins. J Cell Biol 121:83–90

Kozakiewicz J, Gajewska M, Lyzen R, Czyz A, Wegrzyn G (2005) Bioluminescence-mediated stimulation of photoreactivation in bacteria. FEMS Microbiol Lett 250:105–110

Lavorel J (1975) Luminescence. In: Govindjee (ed) Bioenergetics of photosynthesis. Academic, New York, pp 223–317

Lee J, Matheson IBC, Müller F, O'Cane DJ, Vervoort J, Visser AJWG (1991) The mechanism of bacterial bioluminescence. In: Muller F (ed) Chemistry and biochemistry of rlavins and flavoenzymes. CRC Press, Orlando, pp 109–151

Li Y, Swift E, Buskey EJ (1996) Photoinhibition of mechanically stimulable bioluminescence in the heterotrophic dinoflagellate *Protoperidinium depressum* (Pyrrophyta). J Phycol 32: 974–982

Lloyd JE (1980) Male *Photuris* mimic sexual signals of their females' prey. Science 210:669–671

Lloyd JE (1984a) On deception, a way of all flesh, and firefly signaling and systematics. Oxf Surv Evol Biol 1:49–84

Lloyd JE (1984b) Evolution of a firefly flash code. Fla Entomol 67:368–376

Lloyd JE, Wing SR (1983) Nocturnal aerial predation of fireflies by light-seeking fireflies. Science 222:634–635

Lyzen R, Wegrzyn G (2005) Sensitivity of dark mutants of various strains of luminescent bacteria to reactive oxygen species. Arch Microbiol 183:203–208

Marek P, Papaj D, Yeager J, Molina S, Wendy Moore W (2011) Bioluminescent aposematism in millipedes. Curr Biol 21:R680–R681

McElroy WD, Seliger HH (1962) Origin and evolution of bioluminescence. In: Kasha M, Pullman B (eds) Horizons in biochemistry. Academic, New York, pp 91–101

Marcinko CLJ, Painter SC, Martin AP, Allen JT (2013) A review of the measurement and modelling of dinoflagellate bioluminescence. Progress in Oceanography 109:117–129

McFall-Ngai M, Morin JG (1991) Camouflage by disruptive illumination in leiognathids, a family of shallow-water, bioluminescent fishes. J Exp Biol 158:119–137

McFall-Ngai M, Heath-Heckman EA, Gillette AA, Peyer SM, Harvie EA (2011) The secret languages of coevolved symbioses: insights from the *Euprymna scolopes–Vibrio fischeri* symbiosis. Semin Immunol 24:3–8

Mensinger AF, Case JF (1992) Dinoflagellate luminescence increases the susceptibility of zooplankton to teleost predation. Mar Biol 112:207–210

Merritt DJ, Clarke AK (2011) Synchronized circadian bioluminescence in cave-dwelling Arachnocampa tasmaniensis (glowworms). J Biol Rhythms 34–43

Mitchell P (1961) Coupling of phosphorylation to electron and hydrogen transfer by a chemiosmotic type of mechanism. Nature 191:144–148

Miyashiro T, Ruby RG (2012) Shedding light on bioluminescence regulation in Vibrio fischeri. Mol Microbiol 84:795–806

Moiseff A, Copeland J (2000) A new type of synchronized flashing in a North American firefly. J Insect Behav 13:597–612

Nakamura H, Kishi Y, Shimomura O, Morse D, Hastings JW (1989) Structure of dinoflagellate luciferin and its enzymatic and non-enzymatic air-oxidation products. J Am Chem Soc 111:7607–7611

O'Kane DJ, Lingle WL, Porter D, Wambler JE (1990a) Localization of bioluminescent tissues during basidiocarp development in *Panellus stypticus*. Mycologia 82:595–606

O'Kane DJ, Lingle WL, Porter D, Wambler JE (1990b) Spectral analysis of bioluminescence of Panellus stypticus. Mycologia 82:607–616

Partridge JC, Douglas RH (1995) Far-red sensitivity of dragon fish. Nature 375:21–22

Pérez-Bueno ML, Ciscato M, vandeVen M, García-Luque I, Valcke R, Barón M (2006) Imaging viral infection: studies on Nicotiana benthamiana plants infected with the pepper mild mottle tobamovirus. Photosynth Res 90:111–123

Rees J-F, De Wergifosse B, Noiset O, Dubuisson M, Janssens B, Thompson EM (1998) The origins of marine bioluminescence: turning oxygen defence mechanisms into deep-sea communication tools. J Exp Biol 201:1211–1221

Seliger HH, McElroy WD (1965) Light: physical and biological action. Academic, New York

Shimomura O (1979) Structure of the chromophore of *Aequorea* green fluorescent protein. FEBS Lett 1054:220–222

Shimomura O (1980) Chlorophyll-derived bile pigment in bioluminescent euphausiids. FEBS Lett 116:203–206

Shimomura O (1989) Chemiluminescence of panal (a sesquiterpene) isolated from the luminous fungus *Panellus stipticus*. Photochem Photobiol 49:355–360

Shimomura O (1992) The role of superoxide dismutase in regulating the light emission of luminescent fungi. J Exp Bot 43:1519–1525

Strehler B, Arnold W (1951) Light production in green plants. J Gen Physiol 34:809–820

Sundbom E, Björn LO (1977) Phytoluminography: imaging plants by delayed light emission. Physiol Plant 40:39–41

Swift S, Throup J, Bycroft B, Williams P, Stewart G (1998) Quorum sensing: bacterial cell-cell signaling from bioluminescence to pathogenicity. In: Busby SJW, Thomas CM, Brown NL (eds) Molecular microbiology. Springer, Berlin, pp 185–207

Szpilewska H, Czyz A, Wegrzyn G (2003) experimental evidence for the physiological role of bacterial luciferase in the protection of cells against oxidative stress. Curr Microbiol 47:379–382

Tett PB, Kelly MG (1973) Marine bioluminescence. Oceanogr Mar Ann Rev 11:89–173

Trimmer BA, Aprille JR, Dudzinski DM, Lagace CJ, Lewis SM, Michel T, Qazi S, Zayas RM (2001) Nitric oxide and the control of firefly flashing. Science 292:2486–2488

Tyystjärvi E, Vass I (2004) Light emission as a probe of charge separation and recombination in the photosynthetic apparatus: relation of prompt fluorescence to delayed light emission and thermoluminescence. In: Papageorgiou GC, Govindjee (eds) Chlorophyll a fluorescence: a signature of photosynthesis. Advances in photosynthesis and respiration, vol 19. Springer, Dordrecht, pp 363–388 (Govindjee, series and vol. Ed.)

Ulitzur S, Dunlap PV (1995) Regulatory circuitry controlling luminescence autoinduction in *Vibrio fischeri*. Photochem Photobiol 62:625–632

Underwood TJ, Tallamy DW, Pesek JD (1997) Bioluminescence in firefly larvae: a test of the aposematic display hypothesis (Coleoptera:Lampyridae). J Insect Behav 10:365–370

Vencl FV, Blasko BJ, Carlson AD (1994) Flash behavior of female *Photuris versicolor* fireflies (Coleoptera: Lampyridae) in simulated courtship and predatory dialogs. J Insect Behav 7:843–858

Vencl FV, Carlson AD (1998) Proximate mechanisms of sexual selection in the firefly *Photinus pyralis* (Coleoptera: Lampyridae). J Insect Behav 11:191–207

Viviani VR, Bechara EJH (1997) Bioluminescence and biological aspects of Brazilian railroad worms (Coleoptera: Phengodidae). Ann Entomol Soc Am 90:389–398

Viviani VR, Ohmiya Y (2000) Bioluminescence and color determinants of *Phrixothrix* railroad worm luciferases: Chimeric luciferases, site-directed mutagenesis of Arg 215 and guanidine effect. Photochem Photobiol 72:267–271

Vršanský P, Chorvát DI, Fritzsche I, Hain M, Ševčík R (2012) Light-mimicking cockroaches indicate tertiary origin of recent terrestrial luminescence. Naturwissenschaften 99:739–749

Waldenmaier HE, Oliveira AG, Stevani CV (2012) Thoughts on the diversity of convergent evolution of bioluminescence on earth. Int J Astrobiol 11:335–343

Walker E, Bose JL, Stabb EV (2006) Photolyase confers resistance to UV light but does not contribute to the symbiotic benefit of bioluminescence in *Vibrio fischeri* ES114. Appl Environ Microbiol 72:6600–6606

Widder EA, Latz MI, Herring PJ, Case JF (1984) Far red bioluminescence from two deep-sea fishes. Science 225:512–513

Willis RE, Craig R, White CR, Merritt DJ (2011) Using light as a lure is an efficient predatory strategy in *Arachnocampa flava*, an Australian glowworm. J Comp Physiol 181:477–486

Wilson T, Hastings JW (1998) Bioluminescence. Annu Rev Cell Dev Biol 14:197–230

Wilson T, Hastings JW (2013) Bioluminescence: living lights, lights for living. Harvard University, Cambridge, MA, USA

Wood NT, Allan AC, Haley A, Viri-Moussaid M, Trewavas AJ (2000) The characteristics of differential calcium signalling in tobacco guard cells. Plant J 24:335–344

Wood NT, Haley A, Viri-Moussaid M, Johnson CH, van der Luit AH, Trewavas AJ (2001) The calcium rhythms of different cell types oscillate with different circadian phases. Plant Physiol 125: 787–796

Role of Ultraviolet Radiation in the Origin of Life

27

Lars Olof Björn, Shaoshan Li, Qiu Qiu, and Yutao Wang

27.1 The First Thoughts on a Role of Ultraviolet Radiation in the Origin of Life

A prerequisite for the emergence of life was the availability of the chemical compounds of which organisms are constructed. Thus, it is of interest to find out how such compounds can be formed abiotically from simpler molecules. A classic experiment (Miller 1953) showed that amino acids and other biologically important compounds can be formed from simple precursors (water, methane, ammonia, carbon dioxide, and hydrogen) if energy is added in suitable form. Electrical discharge was used in the first experiment. Ultraviolet radiation was then already considered as an energy source but was not used, since it was difficult to generate radiation of appropriate wavelength with sources available at that time (Miller and Urey 1959).

In these early experiments, the conditions were not what we nowadays consider to be realistic approximations of those that led to life. Since it is now known that a large number of organic compounds are present in space outside the Earth, interest has partially shifted from simulation of early Earth conditions to simulation of space conditions and from electric discharge to ultraviolet radiation as the form of energy input. In addition, the first experiments were done with liquid solutions; nowadays experiments are also carried out with reactions taking place on the surfaces of minerals and ice grains.

27.2 Methods for Studying Extraterrestrial Chemistry

A number of methods have been used for the study of extraterrestrial chemistry; these range from a number of spectroscopic methods (Herbst and van Dishoeck 2009) to chemical analysis of samples of meteorites collected on Earth and of samples retrieved from comets (De Gregorio et al. 2011), as well as remote analysis of Martian soil. Spectroscopy reaches far out in space and far back in time and has shown that carbon monoxide already existed 800 Ma after the Big Bang (Bertoldi et al. 2003; similar results by Wang et al. 2011). The photons from these simple molecules have been traveling at a velocity of 299792456.2 m s^{-1} across most of the visible Universe and over most of the time that has elapsed since the Big Bang. In the meantime, we and other more complicated molecular assemblies have evolved, mostly from even simpler particles (protons and electrons). In this evolution, photons have played an important role, as we shall see in the following discussion.

27.3 A Plethora of Organic Compounds Found in Extraterrestrial Space

In closer regions of the Universe, which correspond to more recent times, between one and two hundred different extraterrestrial carbon compounds have been detected (Herbst and van Dishoeck 2009; Wang and Bowie 2012; http://www.astro.uni-koeln.de/cdms/molecules; http://www.astrochymist.org/astrochymist_ism.html; http://en.wikipedia.org/wiki/List_of_molecules_in_interstellar_space), with up to sixty carbon atoms in the molecules (Zhang and Kwok 2011). Of special use

L.O. Björn (✉)
Department of Biology, Lund University, Lund, Sweden

School of Life Science, South China Normal University, Guangzhou, China
e-mail: Lars_Olof.Bjorn@biol.lu.se

S. Li • Y. Wang
School of Life Science, South China Normal University, Guangzhou, China
e-mail: lishsh@scnu.edu.cn; wangyutao@scnu.edu.cn

Q. Qiu
Department of Research and Development, Guangzhou Water Quality Monitoring Center, Guangzhou, China
e-mail: qiuqiuwin2005@126.com

L.O. Björn (ed.), *Photobiology: The Science of Light and Life*,
DOI 10.1007/978-1-4939-1468-5_27, © Springer Science+Business Media New York 2015

is the probing of protoplanetary disks, precursors of planetary systems, since this can give insight into what our own solar system might have contained while the Earth was being formed. Spectroscopic detection of organic material in such a disk (Mandell et al. 2012) has been complemented with model calculations (Throop 2011; Walsh et al. 2012). There has been some discussion as to whether the "biogenic" molecules, for instance, amino acids, have been created in a liquid environment or at low temperature. Temperatures compatible with liquid water could have occurred in or on solid bodies before they aggregated to larger planets, due to the heat from radioactive decay of ^{26}Al (McSween et al. 2002), and at times from the protostar when they come close to it (Ciesla and Sandford 2012). However, the enrichment of deuterium found in meteoritic organic compounds is more compatible with irradiation at low temperature, especially as meteoritic water is deuterium depleted (Throop 2011). Photons absorbed by ice break molecular bonds, producing reactive ions and radicals. If these reactive photoproducts are adjacent to each other, they may react to form new compounds even at very low temperatures. When the irradiated ice is warmed, the photoproducts become mobile and react more readily.

27.4 Information from Space Complemented by Experiments on Earth

In simulations in which they have been exposed to ultraviolet radiation and then warmed (Bernstein et al. 2002; Muñoz Caro et al. 2002; Nuevo et al. 2007, 2008), ices consisting of water containing simple organic compounds have produced a large number of amino acids and other complex organics.

Experiments by Elsila et al. (2007), using an almost 50–50 mixture of 122 and 160 nm radiation, indicated the following main reactions for the formation of glycine and serine from a mixture of water, methanol, hydrogen cyanide, and ammonia; the carbon and nitrogen atoms originating from HCN are indicated by bolding:

$$H_2O + CH_3OH + H\mathbf{C}\mathbf{N} + NH_3 \overset{UV}{\Rightarrow} H_2\mathbf{N} - \underset{\text{Glycine}}{\mathbf{C}H_2} - \mathbf{C}OOH$$

$$H_2O + CH_3OH + H\mathbf{C}\mathbf{N} + NH_3 \overset{UV}{\Rightarrow} H_2\mathbf{N} - \underset{\underset{\text{Serine}}{CH_2OH}}{\mathbf{C}H} - \mathbf{C}OOH$$

This differs from the result expected from the "Strecker mechanism" (Strecker 1850; Bernstein et al. 1999, 2002), in which the amino nitrogen comes from ammonia. As regards serine, the result differs also from a proposed "radical-radical mechanism" (Woon 2002).

27.5 Radiation in the Young Solar System

It is thought that solar systems of our type start out in dense clusters of young stars. Inside a protoplanetary disk, most of the ultraviolet radiation does not come from its own sun, but from neighboring stars. This is because its own sun shines "edge on," and the radiation is quickly attenuated by dust. Neighboring stars, on the other hand, can irradiate the whole disk. Although X-rays are also emitted, ultraviolet photons have a much greater impact on these reactions (Walsh et al. 2012).

The popular "faint young sun" hypothesis states that when it was young, 4.5 Ga ago, our Sun radiated ca 30 % less power than it does now. This, however, is true only for the complete spectrum and for components of longer wavelength. In the shortwave UV region (below 170 nm wavelength), it radiated more than now, as deduced from observation of stars similar to the young Sun (Canuto et al. 1982; Ribas et al. 2010). The reason is nonthermal emission originating from magnetically active regions. Stellar magnetic activity is more pronounced in rapidly rotating young stars and decays roughly with the inverse square root of stellar age (e.g., Skumanich 1972). Most of the ultraviolet radiation in star-forming galaxies emanates from young stars (Law et al. 2011). Most of the shortwave radiation was probably absorbed by even thin planetary atmospheres and did not reach the solid surface (Cnossen et al. 2007). Ciesla and Sandford (2012) have carried out detailed modeling of the radiation to which ice grains are exposed, taking into account their movements inside an accretion disk. They find that the ultraviolet doses and temperature they are exposed to during a million years are similar to those used in the laboratory experiments and conclude that their "results imply that organic compounds are natural by-products of protoplanetary disk evolution and should be important ingredients in the formation of all planetary systems, including our own."

Organic compounds (HCN, C_2H_2) as well as water and carbon dioxide have been spectroscopically observed in several protoplanetary disks (Carr and Najita 2008, 2011; Mandell et al. 2012). HCN and C_2H_2 are considered to be precursors of the nucleotide bases found in meteorites, but these bases themselves have so far not been observed in protoplanetary disks or interstellar matter. UV irradiation of ices containing pyrimidine leads to formation of a large number of pyrimidine derivatives (Nuevo et al. 2009, 2012). Purine derivatives have been found in meteorites (Fig. 27.1), so-called CM2 meteorites.

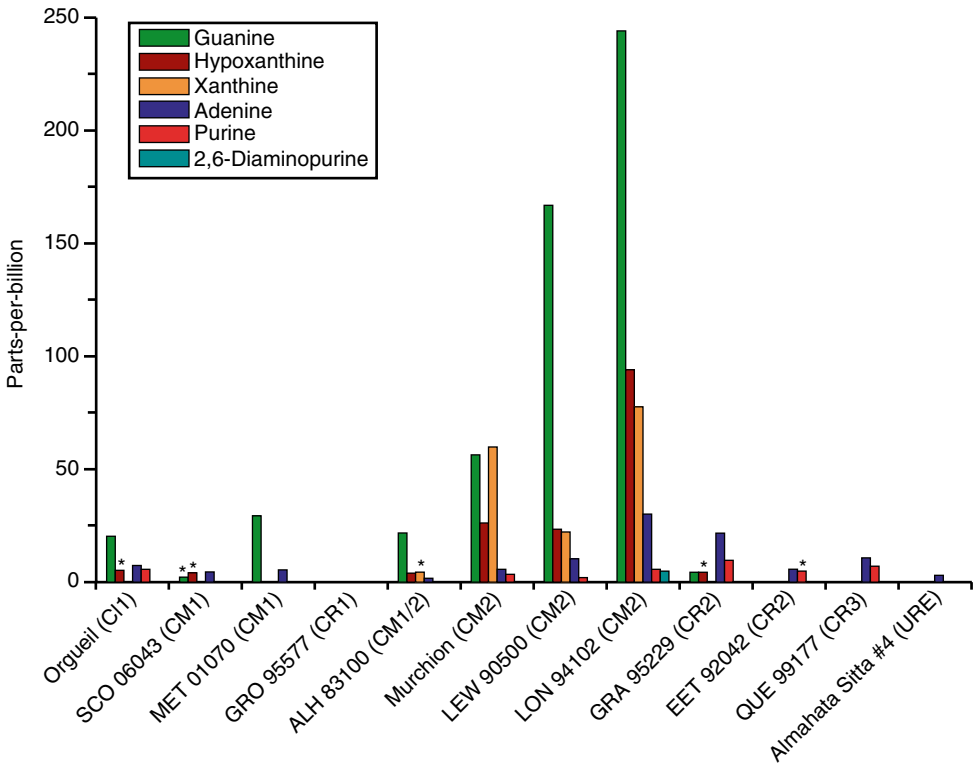

Fig. 27.1 Distribution of guanine, hypoxanthine, xanthine, adenine, purine, and 2,6-diaminopurine in 11 carbonaceous chondrites and one ureilite. The three CM2 carbonaceous chondrites in this study (Murchison, LEW 90500, and LON 94102) contained significantly higher (approximately 4× to 12×) abundances of purine nucleobases as well as greater structural diversity. The * represents a tentative assignment. The meteorites are roughly ordered (*right to left*) according to the degree that they have been altered by water (From Callahan et al. 2011)

Even before a new protostar and an accretion disk are formed, many organic compounds are present in the interstellar medium. Among the most important of these are polycyclic aromatic hydrocarbons (PAHs), which can be found spectroscopically almost anywhere in space (Allamandola et al. 1959, 1985; Allamandola 2011). These can undergo various UV-induced reactions, often with high quantum yields and can often be driven by long-wavelength UV or even by visible light (Klærke et al. 2011; Fu et al. 2012). These reactions therefore may have significance, even in dense clouds where radiation of shorter wavelength is attenuated quickly.

27.6 The Molecular Asymmetry of Life

One of the peculiarities of life on our planet is that many of such building blocks of the organism as amino acids, sugars, and nucleic acids are dissymmetric and different from their mirror images. This property is called homochirality, and it can be investigated using polarized light. The plane of plane-polarized light passing through a solution of the biological version of glucose is turned clockwise ("to the right"), and the same kind of light passing through a solution of one of the amino acids of which proteins are constructed is turned counterclockwise ("to the left"). It is not difficult to understand that it is advantageous for organisms to use only one of two possible enantiomers. This cuts in half the requirement for enzymes that can handle the molecules and reduces the risk for "mistakes" in the metabolism. In the few cases that both enantiomers are used biologically, as are both D- and L-forms of lactic acid, it is in quite different contexts. But the big question that has occupied scientists for more than a hundred years is why the biosphere on our planet uses one particular steric configuration, and not the opposite one. Does it have to do with a chance event in connection with the origin of life or with a specific property of our place in the universe, or does it have to do with basic physics, common to all places in the Universe? At present, the second possibility appears most likely.

Vocabulary

Chiral An adjective used about a kind of molecule that is dissymmetric. For biological molecules chirality usually arises as a consequence of four different atoms or atomic groups being bonded to the same (stereogenic) carbon atom. The term chiral has also been applied to circularly polarized light. Some molecules are chiral, which means that they exist in two geometrical mirror-image forms that cannot be superimposed on each other.

Enantiomer A noun meaning a molecule with specific chirality.

Homochiral An adjective applied to a collection of molecules all having the same chirality, i.e., consisting of only one of two possible enantiomers.

Racemic An adjective applied to a collection of molecules where there is no excess of an enantiomer with a particular chirality.

The first possibility, a chance event on Earth, has seemed less likely after the discovery of non-racemic (not homochiral) amino acids (Engel and Nagy 1982; Cronin and

Table 27.1 Hydroxy acids identified in the Murchison and two CR2 meteorites, in nmol/g

Meteorite			
Hydroxy acid	GRA 95229	LAP 02342	Murchison
D-Lactic	16.8	97.9	39.9 (28.3–58.8)
L-Lactic	17.8	110.6	44.3 (32.0–64.5)

From Pizzarello et al. (2010)

Pizzarello 1997, 1999; Pizzarello and Cronin 2000; Pizzarello et al. 2003) and hydroxy acids (Pizzarello et al. 2010) in three kinds of meteorite. The chirality in all cases had the same sense. We show below data for lactic acid from Pizzarello et al. (2010) (Table 27.1).

Recently (Pizzarello et al. 2012) a survey of carbon-containing meteorites called CR chondrites found in Antarctica revealed very large enantiomeric excesses. If we define L = amount of L-form and D = amount of D-form, then L-form enantiomeric excess expressed as $100\times(L-D)/(L+D)$ in such meteorites is up to 76 for alanine; 95 for serine, threonine, and glutamic acid; 65 for leucine; 90 for aspartic acid; and 45 for proline. The authors conclude that this material must have been formed in a dry and cold environment and not undergone heating in the presence of water. Glabin et al. (2012) found large L excesses of several amino acids in a meteorite from British Columbia and could exclude terrestric contamination by isotope analysis.

A suggestion regarding the cause for the homochirality of life is based on the physical properties of matter, more precisely on the "weak neutral current", a chiral force holding the atomic nucleus together. This can result in a very small energy difference between mirror enantiomers. Chandrasekhar (2008) discusses this theory and comes to the conclusion that at least in its original version this so-called electroweak effect is too small to have had any influence on the choice of chiral sense.

There are also other theories, but the one which has recently gained most support is based on photochemical reactions driven by circularly polarized ultraviolet radiation. A suitable natural source for such radiation has so far not been conclusively found. However, it is likely to exist, since circularly polarized radiation of longer wavelength has been found to originate in star-forming regions of our galaxy. Bailey et al. (1998) and Fukue et al. (2010) demonstrated circularly polarized infrared radiation from the Orion nebula (Fig. 27.2) and Kwon et al. (2013) found even stronger circular polarization (up to 22 %) in radiation from another star-forming region, NGC 6334-V. It is probably the dichroic extinction in the molecular cloud, rather than the scattering, that is the main cause of circular polarization (Lucas et al. 2005). Circularly polarized spectral lines are emitted from regions with magnetic fields, where the lines have been split and polarized by the Zeeman effect. Since

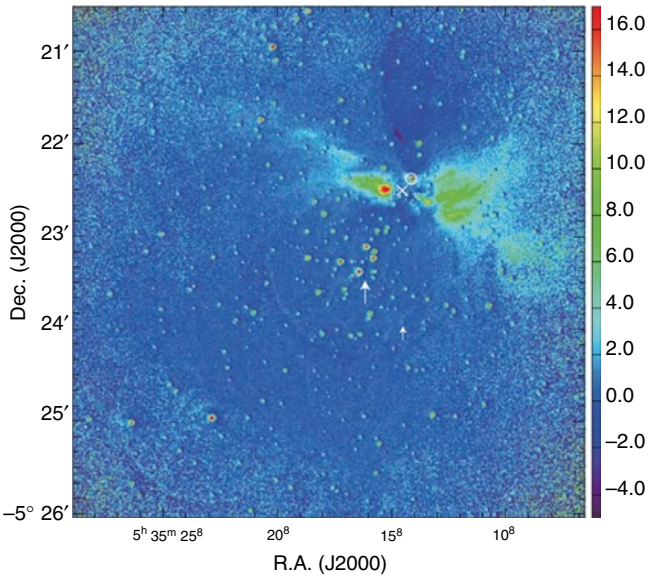

Fig. 27.2 Image of degree of circular polarization (%) in the Ks band (2.14 μm) of the central region of the Orion star-forming region. Image of circular polarization degree. The positions of IRc2 and BN are indicated by a *cross* and a *circle*, respectively, while those of the Trapezium stars and the low-mass young star OMC-1S are denoted by *big* and *small arrows*, respectively. A positive sign for CP indicates that the electric vector is rotated anticlockwise in a fixed plane relative to the observer (From Fukue et al. 2010)

Table 27.2 Measured enantiomeric excesses for ^{13}C-alanine

UV polarization	Photons molec^{-1}	e.e.L (%)	3σ error bars (%)
R-CPL	~5	−1.34	0.40
LPL	~2.5	−0.04	0.42
L-CPL	~2.5	+0.71	0.30

From de Marcellus et al. (2011)
R-CPL right circularly polarized, *LPL* linearly polarized, L-*CPL* left circularly polarized, *e.e.L* excess of L-enantiomer

both magnetic fields and ultraviolet emission are much more intense in young stars than in the present Sun, one might conceive situations where circularly polarized, radiation could also be of some significance. Other with circular polarization were described by Hezareh et al. (2013) and Wiersma et al. (2014).

Irradiation in the laboratory of simulated "cosmic ice" leads to the production of non-racemic alanine, the sign of the enantiomeric excess depending on the sense of circular polarization (de Marcellus et al. 2011).

Polarization-selective photo-destruction of one enantiomer, rather than polarization-selective photosynthesis, is thought to lead to excess of the other enantiomer, which already by prebiotic evolution could lead to its complete domination.

So far, no chiral compound has been detected in the interstellar medium (Møllendal et al. 2012).

The excesses in Table 27.2 are far from homochirality, but mechanisms have been proposed for prebiological increase of enantiomeric excess, once some excess has been achieved (Fletcher et al. 2007; Noorduin et al. 2009; Hein et al. 2011). The first of these mechanisms involves sublimation, the second mechanical action, and the third chemical reactions.

References

Allamandola LJ (2011) PAHS and astrobiology. In: Joblin C, Tielens AGGM (eds) PAHs and the universe. EAS Publications Series, vol 46. EAS, EDP Sciences, Les Ulis, pp 305–317. doi: 10.1051/eas/1146032

Allamandola LJ, Tielens AGGM, Barker JR (1959) Interstellar polycyclic aromatic hydrocarbons – the infrared emission bands, the excitation/emission mechanism, and the astrophysical implications. Astrophys J Suppl 71:733–775

Allamandola LJ, Tielens AGGM, Barker JR (1985) Polycyclic aromatic hydrocarbons and the unidentified infrared emission bands – auto exhaust along the milky way. Astrophys J 290:L25–L28. doi:10.1086/184435

Bailey J, Chrysostomou A, Hough JH, Gledhill TM, McCall A, Clark S, Me«nard F, Tamura M (1998) Circular polarization in star-formation regions: implications for biomolecular homochirality. Science 281:672–674

Bernstein MP, Sandford SA, Allamandola LJ (1999) Life's far-flung raw materials. Sci Am 281(1):42–49

Bernstein MP, Dworkin JP, Sandford SA, Cooper GW, Allamandola LJ (2002) Racemic amino acids from the ultraviolet photolysis of interstellar ice analogues. Nature 416:401–403

Bertoldi F et al (2003) High-excitation CO in a quasar host galaxy at z = 6.42. Astron Astrophys 409:L47–L50. doi:10.1051/0004-6361:20031345

Callahan MP, Smith KE, Cleaves HJ II, Ruzicka J, Stern JC, Glavin DP, House CH, Dworkin JP (2011) Carbonaceous meteorites contain a wide range of extraterrestrial nucleobases. Proc Natl Acad Sci U S A 108:13995–13998

Canuto VM, Levine JS, Augustsson TR, Imhoff CL (1982) UV radiation from the young Sun and oxygen and ozone levels in the prebiological atmosphere. Nature 296:816–820

Carr JS, Najita JR (2008) Organic molecules and water in the planet formation region of young circumstellar disks. Science 319:1504–1506. doi:10.1126/science.1153807

Chandrasekhar (2008) Molecular homochirality and the parity-violating energy difference. A critique with new proposals. Chirality 20:84–95

Ciesla FJ, Sandford SA (2012) Organic synthesis via irradiation and warming of ice grains in the solar nebula. Science 336:452–454. doi:10.1126/science.1217291

Cnossen I, Sanz-Forcada J, Favata F, Witasse O, Zegers T, Arnold NF (2007) Habitat of early life: solar X-ray and UV radiation at Earth's surface 4–3.5 billion years ago. J Geophys Res 112:E02008. doi:10.1029/2006JE002784

Cronin JR, Pizzarello S (1997) Enantiomeric excesses in meteoritic amino-acids. Science 275:951–955

Cronin JR, Pizzarello S (1999) Amino-acid enantiomer excesses in meteorites: origin and significance. Adv Space Res 23:293–299

De Gregorio BT, Stroud RM, Cody GD, Nittler LR, Kilcoyne ALD, Wirick S (2011) Correlated microanalysis of cometary organic grains returned by stardust. Meteorit Planet Sci 46:1376–1396. doi:10.1111/j.1945-5100.2011.01237.x

de Marcellus P, Meinert C, Nuevo M, Filippi J-J, Danger G (2011) Non-racemic amino acid production by ultraviolet irradiation of achiral interstellar ice analogs with circularly polarized light. Astrophys J Lett 727:L27

Elsila JE, Dworkin JP, Bernstein MP, Martin MP, Sandford SA (2007) Mechanisms of amino acid formation in interstellar ice analogs. Astrophys J 660:911–918

Engel MH, Nagy B (1982) Distribution and enantiomeric composition of amino acids in the Murchison meteorite. Nature 296:837–840

Fletcher SP, Jagt RBC, Ben L, Feringa BL (2007) An astrophysically-relevant mechanism for amino acid enantiomer enrichment. Chem Commun 2007:2578–2580

Fu Y, Szczepanski J, Polfer NC (2012) Photon-induced formation of molecular hydrogen from neutral polycyclic aromatic hydrocarbon: 9,10-dihydroanthracene. Astrophys J 744:61, 8 pp. doi:10.1088/0004-637X/744/1/61

Fukue T, Tamura M, Kandori R, Kusakabe N, Hough JH, Bailey J, Whittet DCB, Lucas OW, Nakajima Y, Hashimoto J (2010) Extended high circular polarization in the orion massive star forming region: implications for the origin of homochirality in the solar system. Orig Life Evol Biosph 40:335–346. doi:10.1007/s11084-010-9206-1

Glabin DP, Elsila JE, Burton AS, Callahan MP, Dworkin JP, Hilts RW, Herd CDK (2012) Unusual nonterrestrial L-proteinogenic amino acid excesses in the tagish lake meteorite. Meteorit Planet Sci 47:1347–1364

Hein JE, Tse E, Blackmond DG (2011) A route to enantiopure RNA precursors from nearly racemic starting materials. Nat Chem 3:704–706

Herbst E, van Dishoeck EF (2009) Complex organic interstellar molecules. Annu Rev Astron Astrophys 47:427–480

Hezareh T, Wiesemeyer H, Houde M, Gusdorf A, Siringo G (2013) Non-Zeeman circular polarization of CO rotational lines in SNR IC 443. Astron Astrophys 558:A45, 13 pp

Klærke B, Holm AIS, Andersen LH (2011) UV action spectroscopy of protonated PAH derivatives: methyl substituted quinolines. Astron Astrophys 532:A132. doi:10.1051/0004-6361/201117371

Kwon J, Tamura M, Lucas PW, Hashimoto J, Kusakabe N, Kandori R, Nakajima Y, Nagayama T, Hough JH (2013) Near-infrared circular polarization images of NGC 6334-5. Astrophys J Lett 765:L6, 6 pp

Law K-H, Gordon KD, Misselt KA (2011) Young, ultraviolet-bright stars dominate dust heating in star-forming galaxies. Astrophys J 738:124, 12 pp. doi:10.1088/0004-637X/738/2/124

Lucas PW, Hough JH, Bailey J, Chrysostomou A, Gledhill TM, McCall A (2005) UV circular polarisation in star formation regions: the origin of homichirality? Orig Life Evol Biosph 35:29–60

Mandell AM, Bast J, van Dishoeck EF, Blake GA, Salvk C, Mumma MI, Villanuova G (2012) First detection of near-infrared line emission from organics in young circumstellar disks. Astrophys J 747(92):14 (14 pp)

McSween HY Jr, Ghosh A, Grimm RE, Wilson L, Young ED (2002) Thermal evolution models of asteroids. In: Asteroids III. U. Ariz. Pr., Tucson. (more here?)

Miller SL (1953) A production of amino acids under possible primitive earth. Science 117:528–529

Miller SL, Urey HC (1959) Organic compound synthesis on the primitive earth. Science 130:245–251

Møllendal H, Margulès L, Belloche A, Motiyenko RA, Konovalov A, Menten KM, Guillemin JC (2012) Rotational spectrum of a chiral amino acid precursor, 2-aminopropionitrile, and searches for it in Sagittarius B2(N). Astron Astrophys 538:A51. doi:10.1051/0004-6361/201116838

Muñoz Caro GM, Meierhenrich UJ, Schutte WA, Barbier B, Arcones Segovia A, Rosenbauer H, Thiemann WH-P, Brack A, Greenberg JM (2002) Amino acids from ultraviolet irradiation of interstellar ice analogues. Nature 416:403–406

Noorduin WL, Bode A, van der Meijden M, Meekes MH, van Etteger AF, van Enckevort WJP, Christianen PCM, Kaptein B, Kellogg RM, Rasing T, Vlieg E (2009) Complete chiral symmetry breaking of an

amino acid derivative directed by circularly polarized light. Nat Chem 1:729–732
Nuevo M, Chen Y-J, Yih T-S, Ip W-H, Fung H-S, Cheng C-Y, Tsai H-R, Wu C-YR (2007) Amino acids formed from the UV/EUV irradiation of inorganic ices of astrophysical interest. Adv Space Res 40:1628–1633
Nuevo M, Auger G, Blanot D, D'Hendencourt L (2008) A detailed study of the amino acids produced from the vacuum UV irradiation of interstellar ice analogs. Orig Life Evol Biosph 38:37–56
Nuevo M, Milam SN, Sandford SA, Elsila JE, Dworkin JP (2009) Formation of uracil from the ultraviolet photo-irradiation of pyrimidine in pure H_2O ices. Astrobiology 9:683–695
Pizzarello S, Cronin JR (2000) Non-racemic amino-acids in the Murray and Murchison meteorites. Geochim Cosmochim Acta 64:329–338
Pizzarello S, Zolensky M, Turk KA (2003) Nonracemic isovaline in the Murchison meteorite: chiral distribution and mineral association. Geochim Cosmochim Acta 67:1589–1595
Pizzarello S, Wang Y, Chaban GM (2010) A comparative study of the hydroxy acids from the Murchison, GRA 95229 and LAP 02342 meteorites. Geochim Cosmochim Acta 74:6206–6217
Pizzarello S, Schrader DL, Monroe AA, Lauretta DS (2012) Large enantiomeric excesses in primitive meteorites and the diverse effects of water in cosmochemical evolution. Proc Natl Acad Sci U S A 109:11949–11954
Ribas I, Porto de Mello GF, Ferreira LD, Hébrard E, Selsis F, Catalán S, Garcés A, do Nascimento JD Jr, de Medeiros JR (2010) Evolution of the solar activity over time and effects on planetary atmospheres. II. κ^1 Ceti, an analog of the sun when life arose on earth. Astrophys J 714:384–395
Skumanich A (1972) Time scales for CaII emission decay, rotational breaking, and lithium depletion. Astrophys J 171:565–567
Soares ARM, Taniguchi M, Chandrashaker V, Lindsey JS (2012) Self-organization of tetrapyrrole constituents to give a photoactive protocell. Chem Sci 3:1963–1974
Strecker A (1850) Über die künstliche Bildung der Milchsäure und einen neuen, dem glycocoll homologen Körper. Ann Chem Pharm 75:27–45. doi:10.1002/jlac.18500750103
Taniguchi M, Soares ARM, Chandrashaker V, Lindsey JS (2012) New J Chem 36:1057–1069
Throop HB (2011) UV photolysis, organic molecules in young disks, and the origin of meteoritic amino acids. Icarus 212:885–895
Walsh C, Nomura H, Millar TJ, Yuri Aikawa Y (2012) Chemical processes in protoplanetary disks. II. On the importane of photochemistry and X-ray ionization. Astrophys J 747:114 (19pp)
Wang T, Bowie JH (2012) Can cytosine, thymine and uracil be formed in interstellar regions? A theoretical study. Org Biomol Chem 10: 652–662
Wang R, Wagg J, Carilli CL, Neri R, Walter F, Omont A, Riechers D, Bertoldi F, Menten KM, Cox P, Strauss MA, Fan X, Jiang L (2011) Far-infrared and molecular CO emission from the host galaxies of faint quasars at z ~ 6. Astron J 142:101, 10 pp
Wiersma K, Covino S, Toma K et al. (2014) Circular polarization in the optical afterglow of GRB 121024A. Nature 509:201–203
Woon DE (2002) Pathways to glycine and other amino acids in ultraviolet-irradiated astrophysical ices determined via quantum chemical modeling. Astrophys J 571:L177–L180
Zhang Y, Kwok S (2011) Detection of C_{60} in the protoplanetary nebula IRAS 01005 + 7910. Astrophys J 730:126, 5 pp. doi:10.1088/0004-637X/730/2/126
Ziurys LM, Milam SN, Apponi AJ, Woolf NJ (2007) Nature 447: 1094–1097

Hints for Teaching Experiments and Demonstrations

28

Lars Olof Björn

28.1 Introduction

The following is not meant to represent a complete set of practicals for a photobiology course. I shall try to do just what the title says—give some hints. As a general reference book for photobiological teaching experiments, Valenzeno et al. (1991) merits special mention. Those planning a general photobiology course should consult that book also in addition to the present one. One disadvantage of several of the experiments in the book by Valenzeno et al. (1991) is that one needs advanced equipment which may not be available everywhere, and I have tried to concentrate below on less demanding experiments (although some do need special equipment).

Experiments and demonstrations must, of course, always be adapted to the audience. In the following you will find some which, with suitable adaptations, can be used from elementary school to graduate student levels. From some of them you may even learn something yourself.

I am grateful to former students, Drs. Björn Sigfridsson, Gunvor Björn, and Susanne Widell, for testing some of the descriptions below.

28.2 A Good Start

I shall start with my own pet demonstration, which I have used as an introduction to many courses, which makes students start thinking and which can be a starting point for discussions on the interaction of light with matter, vision, photosynthesis, and phytochrome. It requires a lecture hall which can be efficiently darkened, an overhead projector, a beaker, and an acetone extract of plant leaves. You should also make a cover of cardboard or masonite for the projector, so the light can emerge only from a hole slightly smaller than the bottom of the beaker.

Before the demonstration you should prepare the leaf extract. It is essential that it be very concentrated. The easiest way, if you have the time, is to put leaves into a bottle together with the acetone and let it stand in the cold and dark. A faster way is to grind the leaves with some sand and acetone in a mortar and filter the slurry. You will require about 1 l of extract for a 2-l beaker. Make sure that the extract is clear.

Ask your audience what color plant leaves have and whether they know what makes them have that color. They are likely to answer that plant leaves are green, and in most audiences at least somebody is likely to answer that it is chlorophyll that makes them green. Explain that in your bottle (which should preferably be brown or opaque so as not to show the color of the extract) you have an extract with the pigments of plant leaves and that you are now going to demonstrate the color.

Switch on the overhead projector, put the cardboard mask on, and place the beaker so that it covers the hole in the mask. Turn off the room light completely. Pour a small amount of your extract into the beaker. As expected, a green color will be projected onto the screen.

Pour more and more of the extract into the beaker, and let the (usually very surprised) audience see how the color on the screen goes through a dirty brown to a clear red. Then point to the beaker to make them see the brilliant red chlorophyll fluorescence, and ask them again what the color of chlorophyll is and to think about what color really is: a property of an object or a sensation in our brains.

A few explanations follow:

1. The red color to be seen on the screen is something quite different from the red light radiating in all directions from the solution. The light on the screen, which appears red to us, is really far-red, i.e., light of very long wavelength which chlorophyll cannot absorb. This is the kind of light

L.O. Björn
School of Life Science, South China Normal University, Guangzhou, China

Department of Biology, Lund University, Lund, Sweden
e-mail: Lars_Olof.Bjorn@biol.lu.se

L.O. Björn (ed.), *Photobiology: The Science of Light and Life*,
DOI 10.1007/978-1-4939-1468-5_28,

dominating at the bottom of a dense forest or inside a wheat canopy. It is the kind of light driving phytochrome (a light-sensitive pigment in plants; see Chaps. 11 and 12) from the P_{fr} form to the P_r form.
2. The red light radiating from the solution is energy that has been absorbed and excited chlorophyll molecules and been reradiated as fluorescence when the chlorophyll molecules reverted to the ground state. Chlorophyll in solution fluoresces much more intensely than chlorophyll in the plant, because the plant uses much of the absorbed energy for photosynthesis.
3. For us the color on the screen and the light radiated by the solution look the same, although the wavelength composition is different, because we do not have any light-sensitive pigment in our eyes absorbing at longer wavelength than the one that has an absorption maximum at 552 or 557 nm (depending on the person; see Chap. 9).

You can do a similar demonstration—except that there will be no fluorescence—using colored Perspex or Plexiglass instead of the chlorophyll solution. You start with one layer of green acrylate, showing a green color on the screen, and add additional layers of green acrylate until only far-red light goes through. The version with chlorophyll solution is no doubt the best, but if you are traveling around or have to arrange a demonstration in a hurry, it may be good to have the colored plastic version available. You can also use blue acrylate; in fact any color will end up far red if you add a sufficient amount of acrylate.

28.3 The Wave Nature of Light

The laser pointers now available on the marked make demonstrations of diffraction and interference much easier than they used to be. Pointers with laser diodes can be obtained very cheaply now. Even laser pointers of the same type emit light with slightly different wavelengths, but with the same indistinguishably red color. If you have a couple of such pointers with different spectral tuning, you can therefore easily arrange one more demonstration of the fact that wavelength and color are not the same. It is possible to find some colored plastic, for instance, blue Plexiglass, which transmits light from one pointer but not from the other, although both give light of the same red color.

More importantly, you can easily demonstrate both single-slit diffraction and Young's famous double-slit experiment with using laser pointers. You may be able to cut out sufficiently thin slits in (not too thick) cardboard. Alternatively, you can use black adhesive tape that you stick either on a glass slide or over a hole in a piece of cardboard. Better precision can be obtained by drawing one black line (or for the double-slit experiment, two parallel black lines with a small spacing in between) on white paper, photographing the paper with ordinary negative black-and-white film and using the negative. A number of other items for optical experiments can be purchased from Edmund Scientific.

If you want to demonstrate how a grating works and have not got one from an instrument, you can use a recordable CD or a DVD. The latter has many more lines per mm and thus deflects light more. The curvature of the grooves will not matter with the small spot from a laser pointer. If you have sufficient money for teaching your course, you may want to buy the (much more expensive) laser pointers with green light and UV-A radiation now available to show how the behavior of the beam depends on wavelength.

28.4 Singlet Oxygen

Singlet oxygen for demonstration purposes can be easily generated by mixing hydrogen peroxide (30 %) with solid sodium hypochlorite. If you do this in a darkroom, you will see a rapidly fading red glow. This is the so-called dimol emission of singlet oxygen, which has half the wavelength of emission from isolated singlet oxygen molecules. Dimol emission takes place when the concentration of singlet oxygen is sufficiently high, and the probability is high that two singlet oxygen molecules collide and the excitation energy of both are added to form one photon.

Concentrated hydrogen peroxide is extremely caustic, and mixing it with sodium hypochlorite will cause heating and gas production, so you have to take great care to avoid splashing and especially to protect your eyes. Try it out in a lighted room before you do it in the dark. One good way is to use a Pasteur pipette with a rubber balloon for the hydrogen peroxide, fill it in the light, and put it in a test tube that you hold in one hand together with a test tube with the hypochlorite. To see the dimol emission well, you should first dark-adapt your eyes for 5 min.

28.5 Complementary Chromatic Adaptation of Cyanobacteria

Some cyanobacteria form no phycoerythrin when grown under red light and then appear blue green in color from chlorophyll, phycocyanin, and allophycocyanin. When grown under green light, they change to almost black, because of the presence of phycoerythrin.

The most difficult part of this is to obtain a suitable culture of cyanobacteria. We recommend either *Tolypothrix tenuis* or *Fremyella diplosiphon* (Fujita and Hattori 1960a, b; Diakoff and Scheibe 1973). The American Type Culture Collection (http://www.atcc.org) has *Tolypothrix tenuis* Kutzing 20,335 and many other strains, but at high cost. From Carolina Science and Math (http://www.carolina.com/#), you can buy a set of 15 cultures including a *Tolypothrix* sp. (not tested) for US$ 86.25 (Oct. 2007).

Sammlung Algenkulturen at the University of Göttingen sells *Tolypothrix tenuis* (accession number 94.79) and *Fremyella diplosiphon* (accession number 1,429-1b) to noncommercial customers for 12.50 Euro per culture (early 2007) plus postage. The most complete collection of chromatically adapting cyanobacteria is available at the Institut Pasteur in Paris, http://www.pasteur.fr/recherche/banques/PCC/help/htm. The following culture medium is suitable for *Tolypothrix tenuis* (concentrations in g/l): KNO_3 (3.0), $MgSO_4 7H_2O$ (0.5), Na_2HPO_4 (0.2) or $Na_2HPO_4 12H_2O$ (0.5), $CaCl_2$ (0.02) or $CaCl_2 2H_2O$ (0.027), $FeSO_4 \cdot 7H_2O$ (0.02), and trace elements (B, Mn, Zn, Mo, Cu, Co). Trace element amounts and recipes for other suitable media are listed on the Internet at the above culture collection sites.

Light to adapt to is generated by green and red fluorescent lamps (e.g., Philips TLD 17 and TLD 15, respectively). The red lamps can be wrapped in red (or yellow) cellulose acetate foil to filter off small amounts of blue light given off (particularly at the ends), the green lamps with green (or yellow) foil. If colored fluorescent lamps are hard to obtain, white ones can be used if several layers of appropriate-colored cellulose acetate are wrapped around them. The cultures grow more rapidly if they are bubbled with 5 % carbon dioxide in air, but ordinary air will also do. With added carbon dioxide 1 week should be allowed for sufficient growth—without added carbon dioxide 2 weeks.

For evaluation of the result, you may be content just looking at the cyanobacteria with the naked eye and in the microscope. You can also do in vivo absorption spectra using a "Shibata plate," i.e., a scattering plate, just behind the cuvettes in the spectrophotometer, or use the apparatus described in Chap. 25. For quantitative estimation of the phycobiliprotein pigments, proceed as follows.

Separate the organisms from the culture medium by low-speed centrifugation, and resuspend them in a small amount of 0.01 M phosphate buffer (pH 7.0), and sonicate them. Avoid overheating by precooling the suspension, keeping it in ice during treatment, and sonicating in several short pulses. If you have a French press or equivalent, you can disintegrate the cells more completely by using it. Only grinding in a mortar does not give a very good result. Centrifuge the slurry at 10,000× g for 5 min and then the supernatant for 1 h at 80,000× *g* to obtain a clear phycobiliprotein extract.

Measure the absorbance of the extract (if necessary after dilution) at 565, 620, and 650 nm. The specific absorption coefficients of the phycobiliproteins, in g/l/cm, are as follows:

	Phycoerythrin	Phycocyanin	Allophycocyanin
565 nm	12.6	3.12	1.81
620 nm	0.22	6.77	4.39
650 nm	0.15	1.75	6.54

The absorbance you measure at each wavelength will be the sum of the products of concentration (c) and absorption coefficient (ε) for each of the three pigments times the path-length (L), i.e., $A_\lambda = (c_E \cdot \varepsilon_E + c_C \cdot \varepsilon_C + c_A \cdot \varepsilon_A)\, L$, where subscripts E, C, and A stand for phycoerythrin, phycocyanin, and allophycocyanin, respectively. You will thus have an equation system with three equations and three unknowns, which can be solved for the pigment concentrations.

Instead of continuous light treatments, you can try inductive pulses according to descriptions in the literature. The colored polypeptides can be separated into very beautiful bands by isoelectric focusing.

28.6 What Is Color? The Benham Disk

The Benham disk (or Benham's disk or Benham top) was originally a toy, not even invented by Benham, but described by him in a paper in *Nature* (Anon. 1894). Since then many learned papers have been written about it. A review with 67 references was published by von Campenhausen and Schramme (1995), and publications continue on the subject until recently (e.g., Le Rohellec and Vienot 2001). There is no real consensus about how it works, but in any case it affords a clear demonstration that color and spectral composition of light are not the same. It is a disk with a black-and-white pattern. Surprisingly, you can change the apparent color in different sectors of it just by changing the direction of rotation.

A template for the disk is shown in Fig. 28.1. Copy it (double size) and glue the copy to cardboard, cut it out, and attach it to an electric or hand-driven drill so you can rotate

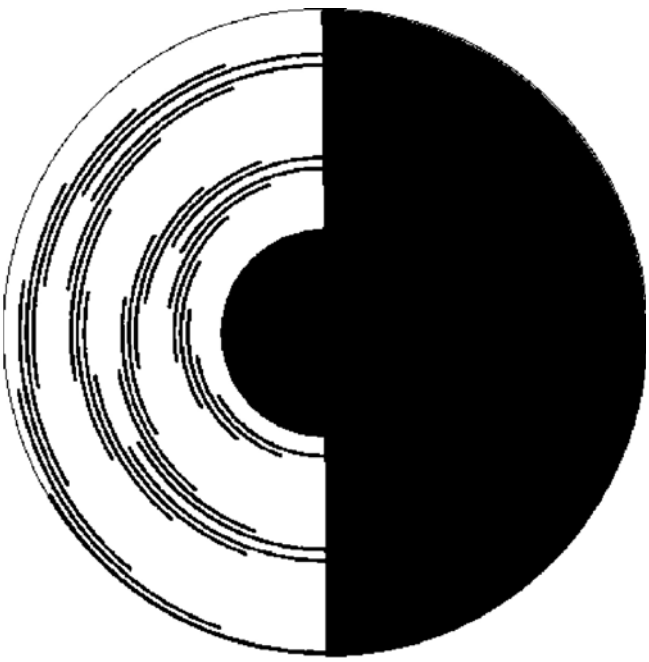

Fig. 28.1 Template for a Benham disk

it around its center. An electric drill with variable speed and the ability to reverse the direction is ideal. The disk in Fig. 28.1 is an example; other versions can be found on the Internet, but one half of the disk should always be black. In my experience, the most vivid colors are obtained if the black sectors in the other half are narrow, like the one shown. It can be instructive to make a disk with stripes of various widths. It is very important that one is able to adjust the speed. If the rotation is too slow or too fast, you will see no color.

One of the first explanations for appearance of the color phenomena was that receptors in the eye for different spectra regions have different time constants. This explanation, however, is no longer regarded to be correct. The contrast between different parts of the image projected on the retina is regarded as an essential ingredient.

28.7 Photoconversion of Rhodopsin

Background Visual pigments in vertebrate eyes are concentrated in cells called rods and cones. The rods are active in "dusk vision," while cones are used for color vision in stronger light. The light-sensitive pigment in rods is rhodopsin, a protein with 11-*cis*-retinal as a chromophore (see Chaps. 10 and 11). Absorption of light triggers a multistep isomerization process, resulting in the separation of protein and chromophore and to bleaching of the initially red color. The first part of the rhodopsin conversion, from rhodopsin to metarhodopsin I, is photoreversible.

Chemicals required for the experiment are as follows (Johnson and Williams 1970):

Sodium phosphate buffer (0.15 M, pH 6.5)
Sucrose solution (40 % w/v dissolved in the phosphate buffer)
Potassium aluminum sulfate ($KAl(SO_4)_2$ 4 % w/v in water)
Hydroxylamine hydrochloride (NH_2OH HCl, 0.05 M in phosphate buffer)
Digitonin (2 % w/v dissolved in phosphate buffer in a heated water bath)

Biological Sample Obtain several (at least eight) cattle eyes from a slaughterhouse, and leave them in the dark for an hour at room temperature. Dissect out the retinas under red light. The retinas can be frozen and preserved for use later.

Extraction of Rhodopsin The preparation is carried out in a cold room under red light. Avoid too much of the working light on the retinas. Put eight retinas in a cold mortar and grind very thoroughly for 20 min. Then add 5–10 ml of the sucrose solution (about three times the volume of the ground retinas). Mix well and transfer the suspension to a transparent centrifuge tube. Carefully layer phosphate buffer (about the same volume) on top, using, for instance, a syringe with a short tubing. Try to keep a sharp interface between the two liquids. Centrifuge at high speed for 30 min. The rod outer segments have about the same density as the sucrose solution and will be enriched at the interface between the liquids.

Carefully suck the rod outer segments into a syringe. Transfer them to a new centrifuge tube, and fill it halfway with buffer. Centrifuge at high speed for 10 min. Discard the supernatant, and repeat the washing procedure. Then add 3 ml $KAl(SO4)_2$, which will fix the rhodopsin. Let stand for 10 min. Precipitate the segments again by 10-min high-speed centrifugation, and wash twice more, but now with water. Add 4 ml of the digitonin solution to the rod segments. Stir thoroughly, and let stand in the cold overnight. This procedure will solubilize the rhodopsin. Centrifuge just before the experiment, which is carried out on the clear supernatant.

Experiment 1. Low Fluence Rate Treatment Under red working light, pipette 600 µL of rhodopsin solution and 150 µL of NH_2OH HCl into a 10-mm spectrophotometer cuvette. Prepare a reference cuvette with 600 µL of buffer plus 150 µL of NH_2OH HCl. Determine the absorbance difference between the cuvettes throughout the range 500–600 nm.

Remove the sample cuvette from the spectrophotometer, and put it about half a meter from a small incandescent lamp, such as a microscope lamp. Illuminate for 30 s and let stand for 2–3 min. In this time, the retinal released from the opsin protein will react with the hydroxylamine, which results in a product with absorption maximum at much shorter wavelength than rhodopsin. Disappearance of intermediates will also be speeded up by the hydroxylamine. Again determine the difference absorption spectrum between sample and reference cuvettes. Repeat the procedure until 80–90 % of the rhodopsin has been bleached. Then switch on normal room light, and bleach the remaining rhodopsin.

Repeat the irradiation experiment with one quarter of the fluence rate. If you cannot measure the light and have not calibrated the filter, and provided you have a small light source (not a fluorescent tube) and a not too white or shiny lab bench, you can approximate this by doubling the distance between the lamp and cuvette.

Compute the ratio $(A_i - A_t)/(A_i - A_e)$ as a measure of converted rhodopsin for each time point: A_i = initial absorbance difference, A_e = final absorbance difference, and A_t absorbance difference for irradiation time t. Compare the result for the two fluence rates, and figure out whether the process follows the Bunsen–Roscoe law ("reciprocity law"). What is the reaction order?

Experiment 2. High Fluence Rate Illumination Repeat the same, but using a photoflash instead as light source. Does this alter the validity of the reciprocity law, and if so, why?

28.8 Photosynthesis of Previtamin D

An experiment to determine the quantum yield of provitamin D_3-to-previtamin D_3 conversion is described by Pottier and Russell (1991). Part of their description concerns the use of the ferrioxalate actinometer, which is already covered elsewhere (Chap. 4) in the present book, as is the theoretical introduction. One difficulty in carrying out the experiment as described by Pottier and Russell (1991) is that the pure previtamin D_3 used for calibration in their experiment is not commercially available. The present description is modified with this in mind.

I shall also take the opportunity to show an unusual way of determining the quantum yield, which sometimes has advantages.

For determination of quantum yield of a photochemical reaction, one usually determines the number of molecules converted and the number of photons absorbed and takes the ratio between the two quantities. Björn (1969b), when faced by the problem of determining the quantum yield of inactivation of an enzyme, could not directly measure the amount of light absorbed by the enzyme, because the enzyme solution was dilute and the amount of light absorbed by it very small. He showed, instead, that the quantum yield equals $^{10}\log(a_o/a_t)/(\varepsilon \cdot t \cdot I)$, where a_o is the concentrations at the start and a_t that after irradiation time t, I the photon fluence rate, and ε the molar absorption coefficient.

In our present case, the photoconversion of provitamin D, we have to keep in mind that the primary product, previtamin D, can undergo a number of photochemical reactions which could disturb our measurement. We avoid them in two ways: by limiting the amount of radiation to keep the amount of product (previtamin D) much lower than the amount of substrate (provitamin D) and by choosing a wavelength at which the substrate absorbs much more strongly than the product, i.e., 294 nm. For an ethanol solution containing 5 μg provitamin D per ml (which is a suitable concentration for experimentation), the absorbance at 294 nm in a 1-cm layer is 0.088. The absorbance of a corresponding solution of previtamin D is only 0.034.

We choose the initial provitamin concentration with the following in mind: it should be high enough to allow accurate spectrophotometry, yet low enough to keep the fluence rate within the sample reasonably uniform. If the absorbance in a 1-cm cuvette is 0.088, then the irradiance at the exit side of the cuvette is $10^{-0.088} = 81.7$ % of that on the illuminated side, i.e., transmission $T = 0.817$ for a thickness $x = 1$ cm. The average irradiance is $\int T^x dx = (T-1)^{10}\log e/^{10}\log T = -0.183/\ln 0.817 = 0.905$. Use of such an average irradiance in the calculations requires that the solution is stirred. For an unstirred solution it is better to mentally divide the solution into, say, 10 (or 100) layers, calculate for each layer separately how the chemical change (and the change in irradiance) takes place, and finally add up the chemical change for the layers. I leave this as an exercise for the reader.

The molecular weight for provitamin D_3 is 384.65 (for provitamin D_2 it is 400.70; this can be looked up in the Handbook of Chemistry and Physics, where the compounds are called $\Delta^{5,7}$-cholestadien-3β-ol and ergosterol, respectively). Thus the molar absorption coefficient ε (for the D_3 form) is $384.65 \cdot 10^6 \cdot 100/5/1{,}000\ m^{-1}\ M^{-1} = 7.7 \cdot 10^4\ m^{-1}\ M^{-1}$ (the factor 10^6 is for converting μg to g, 100 for converting cm to m, and 1,000 for converting ml to l). Thus the quantum yield in our special case is $^{10}\log(a_o/a_t)/(\varepsilon \cdot t \cdot I \cdot 0.905) = {}^{10}\log(a_o/a_t)/(7.7.10^4 \cdot t \cdot I \cdot 0.905)$, with t and I in SI units.

28.9 Photoconversion of Protochlorophyllide

Background The synthesis of chlorophyll *a* proceeds via 5-aminolevulinic acid (ALA), protochlorophyllide, and chlorophyllide *a*. When angiosperms are grown in darkness, the synthesis is arrested at the protochlorophyllide stage. However, there is no major buildup of protochlorophyllide, because the synthesis of ALA is exposed to feedback inhibition by protochlorophyllide and is resumed only when protochlorophyllide is used up. This is the reason that plants do not become visibly green in darkness, even if protochlorophyllide in itself has a green color. When the plant is illuminated, protochlorophyllide is transformed to chlorophyllide by photoreduction, and it is the protochlorophyllide itself, bound to NADPH–protochlorophyllide oxidoreductase (POR, EC 1.6.99.1) that absorbs the active light (Björn 1969a). The reductant is NADPH, which in darkness is bound to the enzyme together with protochlorophyllide.

The transformation of protochlorophyllide to chlorophyllide *a* can be monitored spectrophotometrically directly in living leaves, since the weak light beam in the spectrophotometer does not noticeably affect the process. A single flash from an electronic photoflash, on the other hand, transforms a large part of the protochlorophyllide present.

Spectrophotometer You will need a good split-beam spectrophotometer (or a single-beam spectrophotometer with computer that can store a reference signal). For this you should make a special leaf holder. If you use bean leaves (see below), the leaf holder should consist of two glass plates and some kind of clamp holding the plates together, so you can position the leaves between the plates, covering the measuring beam. The details depend on the spectrophotometer. One of the glass plates should be scattering (ground surface or milky glass), or you must add a special Shibata plate to scatter light after passage of the sample and reference.

If you use grass leaves, you can use the standard cuvette holder (except that you need to add a Shibata plate). Instead of a cuvette you use a square rod of Plexiglas or Perspex

(1 cm×1 cm×4 cm) in which you have drilled nine holes (1.5-mm diameter) along the 4-cm direction. Five of the holes are in a row, with 1 mm in between. The remaining four holes are in another row, such that the holes are in between the holes in the first row. Figure 28.2 gives an idea of what the grass leaf holder looks like from above. You may need to adjust the dimension to the kind of grass you use; maize needs larger holes.

Experimental Procedure You can use either bean or wheat plants (or some other grass). All steps in which you handle your plants or leaves after sowing should be carried out in dim green working light. Your eyes, fortunately, are most sensitive to this light, whereas the process you want to study has a sensitivity minimum in the green spectral region.

If you use bean plants, soak the beans in dilute hydrogen peroxide (initial concentration 1–2 %) overnight, and then remove the seed coats. The hydrogen peroxide serves both to kill some mold spores and to facilitate peeling by producing gas under the seed coats. Sow the beans directly in vermiculite or sand that has been heated to kill microorganisms, or pregerminate on filter paper, and then sow under green light. Let the plants grow (about 5–7 days) until the first true leaves (between the cotyledons) have become a little longer than the cotyledons. If you wait until the plants have become much older, only part of the protochlorophyll(ide) will be immediately phototransformable.

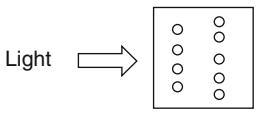

Fig. 28.2 Sketch of holder for grass leaves in spectrophotometer

If you use grass leaves, after sowing a few dozen caryopses, allow the plants to grow in darkness until you (by inspection under green light) see that the leaves have just emerged from the coleoptiles. They will still remain tightly rolled together unless you have used too much of your inspection light (unrolling is a phytochrome-controlled reaction). Collect nine leaves, cut out 5 cm of the middle portion, and put them in the holes in your leaf holder. No matter what kind of leaf you use, it is important that the leaves completely cover the whole measuring beam in the spectrophotometer.

Record a spectrum for the unirradiated leaves from 500 to 720 nm. Do not worry about absolute absorbance; it is the shape of the spectrum that is of interest. To balance the split-beam spectrophotometer with the leaves on the sample side, you may need to put something "neutral" in the reference beam. One or a few pieces of filter paper serve well.

When you have recorded the "dark" spectrum, irradiate in a suitable way, for instance, with a photoflash. Record a new spectrum. If you want to produce a good-looking series of spectra, as in Fig. 28.3, it is important that you work fast, since the Shibata

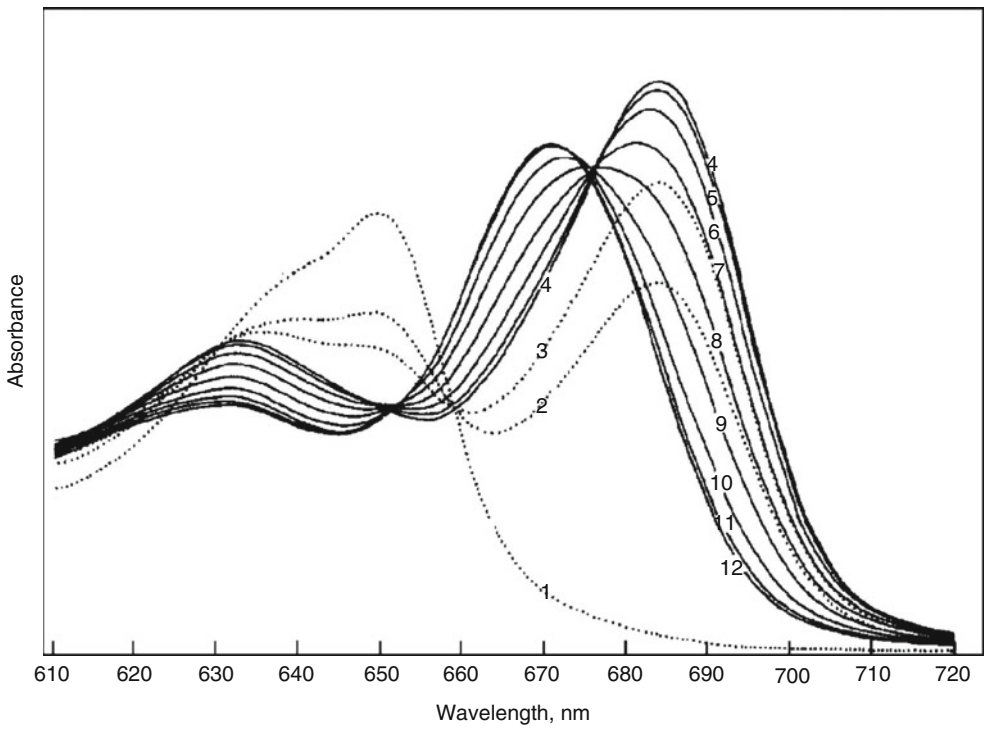

Fig. 28.3 Absorption spectra for dark-grown bean leaves, before illumination (*curve 1*), after 1, 2, and 10 exposures to a photographic flash (*curves 2–4*), and after incubation for various times in darkness after the light exposures (*curves 5–12*). The first curve represents mainly the absorption of the protochlorophyllide–NADPH–enzyme complex, which is changed to a chlorophyllide *a*–$NADP^+$–enzyme complex by illumination. During the following dark incubation, the chlorophyllide is released from the enzyme, attaches to another protein, and is esterified to chlorophyll *a*. More sophisticated experiments reveal several spectral shifts

shift from the initial chlorophyllide *a*–enzyme complex starts at once (rate depending on age of leaves and other factors).

This experiment can be modified in a number of ways. The protochlorophyllide–enzyme complex ("protochlorophyllide holochrome") can be extracted and the conversion studied in solution, and fluorescence spectroscopy can be used in place of absorption spectroscopy (Björn 1969a).

In case you do not have access to an advanced research spectrophotometer, it should be possible to adapt this experiment for the home-built apparatus described in Chap. 25.

28.10 Separation of Chloroplast Pigments

There are many ways of carrying out this experiment, but I have my definite favorite. It is to use a cylindrical chromatography paper, as described below.

Pigment Extraction Choose a plant species that does not have extremely acid cell sap, which will result in conversion of chlorophyll to pheophytin. We have used, among others, spinach, bean, and stinging nettle. Extract a leaf using a small amount of 100 % acetone. We have usually done this in a mortar with sand, and then one has to filter or centrifuge to get a clear extract. I have read that other people, with good result, have just left the leaf with acetone in a bottle in the dark for a day or two, so if you do not want to do the whole experiment in one day, this saves some work and dishwashing.

The acetone extract may be applied as it is to the chromatogram, but then you cannot put on very much of it without getting into trouble. It is better to mix it with a little (one-tenth the volume of the extract or so) light petroleum (or hexane) and add water (about the same volume as the original extract) to separate into two layers. Discard the lower (aqueous) layer (the most convenient way is to suck up the upper layer using a Pasteur pipette and transfer the liquid to a clean test tube), add water again, shake, and let separate. If you have difficulty getting a clean phase boundary, add some sodium chloride. Pipette the organic, dark green phase to a clean test tube.

Chromatography Get a glass jar with a tightly fitting lid (it is very important that it fits tightly). You may find one in your home that has contained mayonnaise or some other food product. A suitable size is 150 mm high and 70 mm wide. Cut out a rectangular paper of a size that can produce a cylinder that fits inside the jar without touching the walls or the lid, but do not fold it into a cylinder yet. Avoid touching the paper with your fingers.

Pour into the jar a mixture of 90 % (v/v) petroleum ether and 10 % (v/v) acetone. You should have a layer about 10 mm deep at the bottom of the jar. Put on the lid.

Use a Pasteur pipette to apply your pigment extract along a line parallel to and 15–20 mm from a side of the paper that will form the base of your cylinder.

The paper edge should rest on a test tube or glass rod or stick out over the edge of the lab bench, so it is free in the air (or put the paper in a book, with the edge sticking out). With some practice you will be able to produce a nice green line. You should let the tip of the pipette move quickly across the paper to avoid big blobs. Try not to scratch the paper with the tip of the pipette. If the extract is in light petroleum or hexane, it will dry quickly, and you can in a short time repeat the application until you have quite a lot of pigment on the line. But do not apply so much that you clog the pores in the paper.

Now shape the paper into a cylinder with the green line at the bottom. Staple it together along the edges perpendicular to the bottom edge in such a way that the edges do not touch (if they do, the liquid will rise in the paper in an irregular way). Open the jar briefly and put down your paper cylinder, green line down. Put on the lid immediately to avoid liquid evaporating from the paper. Do not move the jar until you finish the experiment. Wait and enjoy the result!

This chromatography is mainly a liquid/liquid distribution of substances according to lipophily/hydrophily between the moving hydrocarbon and stationary water molecules hydrogen-bonded to the OH groups in the cellulose.

Within a few minutes you can see the pigments separating into several bands: A yellow band almost at the rising liquid front indicates carotenes. They do not stick to the water adsorbed on the paper because they contain only carbon and hydrogen. Next comes another yellow band, the oxygen-containing xanthophylls. Lower down follow chlorophylls *a* and *b*, in that order, because chlorophyll *a* has a lipophilic methyl group, whereas chlorophyll *b* has an aldehyde group.

Spectrophotometry When the liquid front has almost reached the top of the paper after half an hour or so, take it out and let it dry. This experiment is easily done as a demonstration during a lecture, in which case you can conclude it by cutting strips of the paper and sending them around in the audience for inspection. If it is done as a student experiment, it can be concluded by determining the absorption spectra of the various pigments. If you have a handheld reflection spectrophotometer such as the Colortron (see next section), or the device described in Chap. 25, this can be done in a couple of minutes directly on the paper. Otherwise the chromatogram can be eluated with acetone. Cut out the strips with the various pigments. If you dip an end into acetone, the acetone will rise and carry all of the pigment with the front, so you can easily concentrate the pigment and dissolve it in a small amount of acetone. You will easily get a concentration high enough and of sufficient volume for a standard spectrophotometer cuvette from a single chromatogram.

28.11 Light Acclimation of Leaves: The Xanthophyll Cycle

We have used a simple handheld reflectance spectrophotometer (Colortron and a later model, Colortron II) for a number of biological experiments. It has already been mentioned in connection to photoreactivation (Sect. 28.12) and spectrophotometry of paper chromatograms (Sect. 28.10). These excellent and cheap (about US$ 1,000) instruments (originally marketed by Light Source, Inc.) are, unfortunately, no longer available. Other companies sell other instruments of a similar type that should also work. Such instruments can certainly also be used to evaluate complementary chromatic adaptation (Sect. 24.5), changes in skin color, changes in leaf color during senescence or nutrient deficiency, and a large number of other experiments. A very simple but interesting experiment, relating to the light acclimation of leaves and the xanthophyll cycle, can also be carried out.

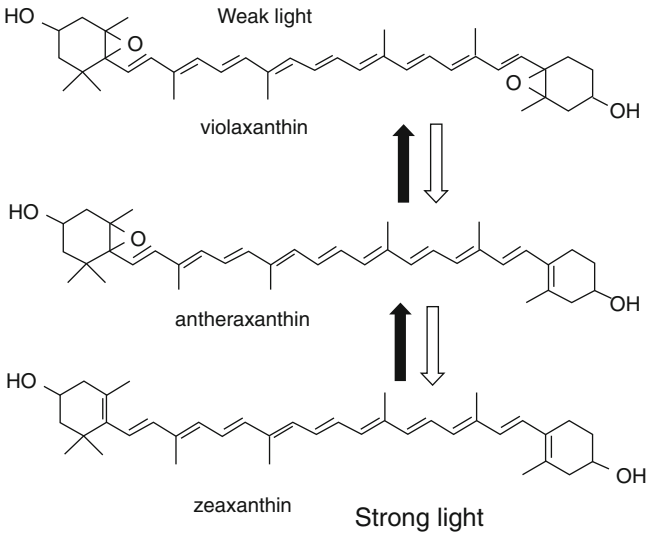

Fig. 28.4 The xanthophyll cycle in higher plants (also called the violaxanthin cycle). In some algae an analogous cycle with other carotenoids takes place

28.11.1 Introduction to the Xanthophyll Cycle

We start with an introduction to the xanthophyll cycle (see also Sect. 16.9).

Daylight is highly variable, and the plant must be able to adjust to strong as well as weak light. When the rate of light absorption by the photosynthetic system exceeds the rate with which carbon dioxide can be assimilated, or other assimilatory reactions can be carried out, there is risk for damage to the plant. One thing that may happen when carbon dioxide cannot be reduced by the electrons transported through the electron transport chain is that *electrons* may end up on molecular oxygen and reduce it to superoxide anion. The plant has superoxide dismutase to take care of this. However, the electron transport chain itself may be overloaded, so that the excitations in the pigment system cannot be used up for electron transport at all. What may then happen is that the *energy* is transferred to oxygen molecules, resulting in a form of excited oxygen called singlet oxygen (actually there is more than one kind of singlet oxygen). Singlet oxygen is very reactive and may cause damage. The plant needs a way of disposing of excitation energy, but this should operate only when there is an excess. In weak light the plant needs all the energy it can collect.

One way for the plant to regulate the dissipation of excess energy absorbed by the photosynthetic system is by adjusting the amount of violaxanthin and zeaxanthin through the reactions of the xanthophyll cycle. In this cycle, violaxanthin is converted to zeaxanthin via the intermediate antheraxanthin, a reaction (so-called deepoxidation) catalyzed by the enzyme violaxanthin de-epoxidase. The reverse reaction (epoxidation of zeaxanthin to violaxanthin) can also take place (Fig. 28.4). De-epoxidation takes place in strong light, epoxidation in weak light or darkness.

Both zeaxanthin and violaxanthin have long conjugated double-bond systems. The important difference between them is that the zeaxanthin molecule has a longer conjugated system (11 double bonds vs. 9 for violaxanthin). This causes the lowest excited state in the zeaxanthin molecule to be at a lower level than the lowest excited state of violaxanthin. It so happens that the lowest energy levels of the chlorophyll *a* molecule are just between that of zeaxanthin and that of violaxanthin.

I must here introduce a small complication. If you do not understand this paragraph, do not worry, since it is not important for an understanding of the plant's physiology. Xanthophylls, like zeaxanthin and violaxanthin, are yellow because they have energy levels low enough for blue light photons to be absorbed and excite them to an excited state. These energy levels cause the bands in the blue part of the absorption spectrum. Xanthophylls possess these energy levels because they have long conjugated bond systems. However, these are *not* the energy levels we are talking about in explaining the xanthophyll cycle. There are even lower energy levels, corresponding to red light. They do not, however, show up in the absorption spectra, because the transition to this state from the ground state is forbidden. Like most of quantum mechanics, we shall, as biologists specializing in another branch of science, just have to accept this.

Let's now return to the main line of thought. Since the lowest excited state of violaxanthin is slightly higher than the lowest excited state of chlorophyll *a*, energy from an excited violaxanthin molecule may be transferred to a chlorophyll *a* molecule, provided it is close enough. In other words, violaxanthin can act as an antenna pigment.

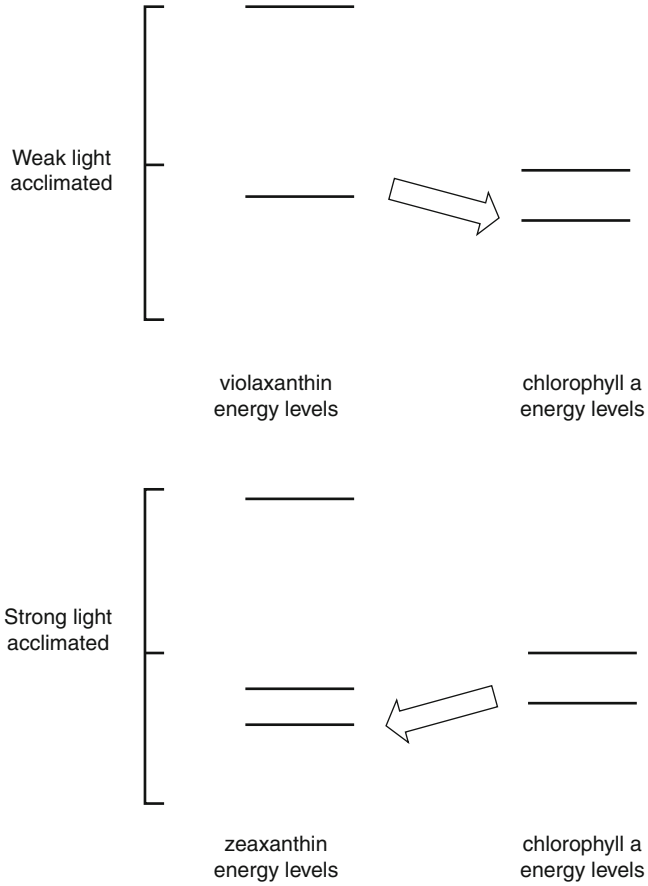

Fig. 28.5 Energy levels in violaxanthin, chlorophyll *a*, and zeaxanthin. For violaxanthin the lowest excited state is higher, for zeaxanthin lower than the lowest (singlet) excited state in chlorophyll. The *arrows* show direction of energy transfer (Simplified from Frank et al. (1994))

Zeaxanthin, on the other hand, cannot act as an antenna pigment for chlorophyll *a*, since its lowest energy level is lower than the lowest energy level of chlorophyll *a*. On the contrary, it can accept energy from an excited chlorophyll *a* molecule, provided it is close enough (Fig. 28.5).

We are more accustomed to describing the photosynthetic pigments in terms of the positions of their absorption maxima than in terms of energy levels. This is OK as long as we remember that energy is inversely proportional to wavelength. The reaction center pigment in photosystem I is referred to as P700, because its (long-wavelength) absorption peak is at 700 nm and that of photosystem II is called P680 for the corresponding reason. These wavelengths correspond to energies of 1.77 and 1.82 eV, respectively. The antenna pigments have peaks at shorter wavelength, corresponding to higher energy. This is the reason that energy can flow from antenna pigments to reaction centers, while some of the energy is degraded to heat, giving an overall positive entropy change.

The lowest energy level (1.89 eV) of violaxanthin corresponds to 655 nm, allowing this pigment to donate energy to any pigment with an absorption peak at longer wavelength. This includes all forms of protein-bound chlorophyll *a*. The lowest energy level (1.76 eV) of zeaxanthin corresponds to 704 nm. It allows it to accept energy from any antenna chlorophyll *a*.

For the intermediate xanthophyll, antheraxanthin with ten conjugated double bonds, the lowest energy level corresponds to 680 nm. It therefore can accept energy from photosystem II antenna pigments on the same terms as the reaction center, but donate energy to photosystem I.

The xanthophyll cycle can thus function as a safety valve for the photosynthetic system when it is overloaded with energy. The valve opens when zeaxanthin is formed from violaxanthin. The energy received by zeaxanthin is degraded to small quanta (heat), which is less dangerous than the large energy quanta that can break bonds and cause chemical reactions.

This is just half the truth, though. There are energy sinks other than zeaxanthin in the photosynthetic system. Violaxanthin has a third important function in addition to being an antenna pigment and a source of zeaxanthin. It is able to inactivate the other (not yet characterized) energy sinks. The xanthophyll cycle thus regulates the electron pumping by the photosystems in a threefold way.

Violaxanthin deepoxidase has a pH optimum of about five, and it is likely that deepoxidation is activated by the proton uptake into the thylakoids that occurs in light, and the "trigger point" is the pH that is just a little bit lower than that required for ATP synthesis.

The acidification of the thylakoids and the conversion of violaxanthin to zeaxanthin that take place when the plant is subjected to excess light cause secondary changes in the antenna pigments. The structure is changed, which can be seen as increased light-scattering power. This is a contributing factor to the signals that we shall monitor in our experiment.

The xanthophyll cycle pigments are present both in photosystem I and photosystem II antennas (chlorophyll *a*/*b*-*binding* proteins) and also dissolved in the thylakoid membrane lipid. In addition, violaxanthin occurs in the envelope membrane. All violaxanthin in the plant is not available to the deepoxidase, and the available fraction seems to increase with increasing reduction of the plastoquinone pool. This may be an important point for us who are interested in effects of UV-B radiation on plants. UV-B inhibits photosystem II more than photosystem I and thus presumably leads to a more oxidized plastoquinone pool, resulting in less substrate for the xanthophyll cycle. UV-B may also inhibit the deepoxidase, and both these changes may lead to a decrease in the ability of the plant to protect the photosystem against overloading by excess light. One of the experiments we can carry out is to look just at how UV-B affects the deepoxidation.

The pool of xanthophylls that can participate in the xanthophyll cycle also increases when the plant prepares for the winter. There is a big need for safety valve function during the spring, when the plant may be subjected to strong light at the same time that the temperature is so low that carbon dioxide assimilation is impaired. The pool is larger in plants adapted or acclimated to strong light than in shade plants.

Finally, a different role has also been proposed for zeaxanthin and the xanthophyll cycle: as a blue light-sensing system in stomatal regulation and phototropism.

28.11.2 Experiment

Gamon et al. (1990) described a principle for sensing of the xanthophyll cycle state by monitoring reflectance at 530 nm. The method described here employs the same principle. The advantage with our variant is that it uses equipment that is cheap, battery operated, and portable. Although leaves picked from plants were used for the examples shown here, the method has potential of being nondestructive, as there seems to be nothing preventing measurements to be made on attached leaves.

A leaf is kept in darkness for at least 10 min. The reflectance spectrum is then recorded. If a Colortron instrument is used, this simply means pressing the instrument, connected to a Macintosh or PC with the appropriate software running, against the leaf. In a few seconds the spectrum from 390 to 700 nm is then automatically stored in the computer, using the two lamps built into the instrument as light sources. We have built a simple leaf holder, so a leaf can be placed in front of the instrument in a repeatable way. After the first spectrum is stored, the leaf is exposed to strong light (PAR) for 0.5–7 min, and the spectrum again recorded. The spectra can be viewed with the original software, but in this case they are best transferred to another program (we have used CricketGraph III or KaleidaGraph for the purpose; see Figs. 28.6 and 28.7), in which the light–dark difference spectra can be computed and displayed; Excel can of course also be used. An alternative is to not follow the directions for calibrating the spectrophotometer using the "100 % reflectance standard" supplied, but to use the dark-adapted leaf as reference, against which the illuminated leaf is compared. One can easily investigate the kinetics using a series of irradiations. Best (Figs. 28.6 and 28.7) is to plot the logarithm of the ratio of reflectances in order to have an analogue to the absorbance used in transmission measurements.

The result of this experiment is that the reflectance in the green region, especially near 530 nm, is decreased by the radiation. This change is caused by conversion of violaxanthin to zeaxanthin, which causes rearrangements in the thylakoid membranes with concomitant changes in light scattering. One can also see an apparent reflectance decrease in the red region. This, however, is not a true reflectance decrease, but signals the quenching of fluorescence associated with it.

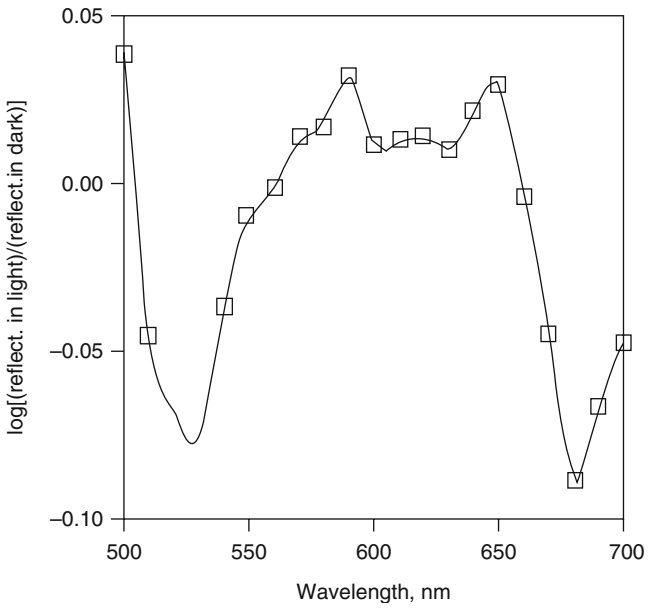

Fig. 28.6 Light/dark difference reflectance spectrum of a *Prunus laurocerasus* leaf measured with Colortron. The dip at 530 nm signals the xanthophyll changes and the dip at 680 nm the quenching of chlorophyll fluorescence associated with it. CricketGraph was used for plotting the data

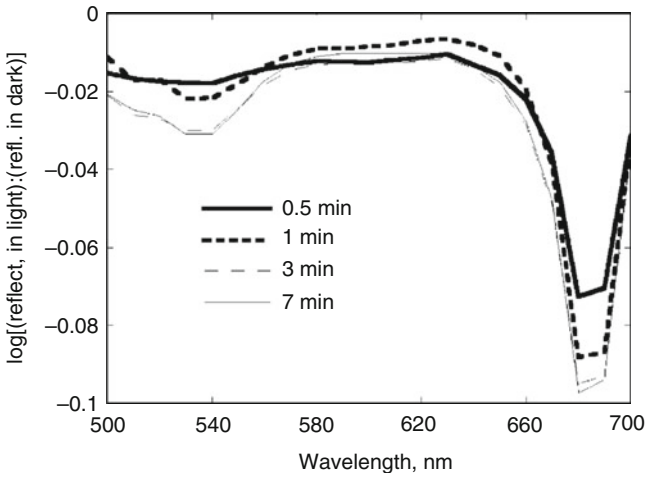

Fig. 28.7 Experiment similar to that in Fig. 28.6, but with several irradiation times and with leaves of *Vaccinium vitis-idaea* as experimental material. As can be seen from a comparison of the two figures, the relation between the scattering and the fluorescence change varies among species. It can also be seen here that the change is complete after 3 min in strong light

This measurement is in principle similar to that explored by Gamon et al. (1990) as a method for remote sensing of photosynthetic efficiency of plants and later in more detail by Gamon et al. (1992, 1997), Gamon and Surfus (1999),

Penuelas et al. (1995, 1997), Filella et al. (1996), Nichol et al (2000), and Barton and North (2001).

I have also successfully adapted the home-built spectrophotometer (Chap. 29) for this experiment, using a green light laser pointer as source for actinic and fluorescence excitation light and for reflectance measurement. The modified spectrophotometer and experiments with it have been described by Björn and Li (2013).

28.12 Ultraviolet Radiation Damage and Its Photoreactivation

This exercise can be carried out as a demonstration, but is recommended as a practical for students. In its simplest form it is a direct repeat of the classical first demonstration of photoreactivation by Hausser and Oehmcke (1933) and is evaluated visually. With relatively cheap equipment, also useful for other experiments, it can be evaluated quantitatively.

You will need a low-pressure (germicidal) mercury lamp, a strong lamp, preferably medium-pressure mercury with fluorescent coating (or other lamp with sufficient emission in the blue and UV-A) for photoreactivating light; a big jar or (preferably) small plastic aquarium; and a few unripe (green) bananas. You should also have goggles for protecting your eyes from the UV-C radiation from the mercury lamp.

Mount the germicidal lamp so you can irradiate the bananas at a distance of about 20–30 cm (not critical, but suitable exposure times vary with distance). Mount the photoreactivation lamp with the aquarium below it, and some space below the aquarium. The bananas can be irradiated for photoreactivation in the space below the aquarium. The purpose of the aquarium (which should be filled with clear water) is to remove infrared radiation and avoid heating of the bananas by the strong lamp. If you find it more convenient, it is also possible to mount the bananas in the water in the aquarium, but there should be at least 10 cm of water above them.

If green bananas are exposed to the bactericidal radiation (mainly 253.7 nm) only (about 1–2 min, but depending on the lamp, the distance, and the bananas), and then left to ripen during a couple of days at room temperature, they will turn brown instead of yellow. If they are exposed to photoreactivating light (15–60 min required depending on lamp, and distance) immediately after the ultraviolet radiation, the browning is prevented, and they will turn yellow during ripening. You can use, e.g., aluminum foil to shade different parts of the banana during exposure, and so expose different parts for different times, and get many combinations of damaging and reactivating exposures on the same banana. The result can be evaluated visually or by reflectance spectrophotometry (Figs. 28.8 and 28.9) or photographically.

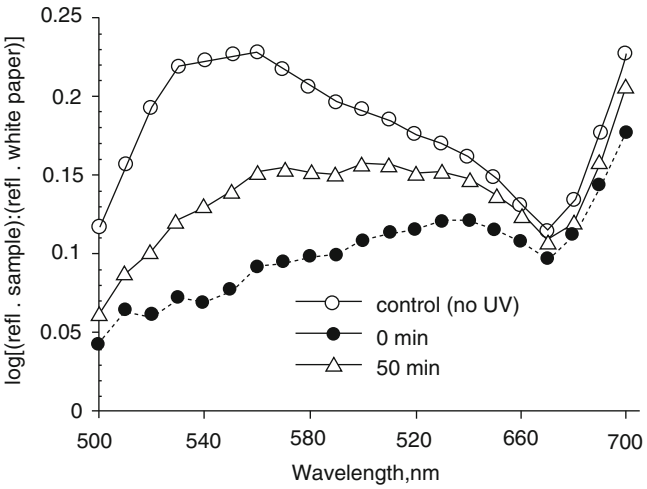

Fig. 28.8 Reflectance spectra of bananas measured with Colortron. The top curve is an average spectrum for five bananas which were not exposed to ultraviolet radiation, the two others for bananas exposed to UV-C radiation for 2 min. The bananas for the middle curve, in addition, received 50 min of white light immediately after UV-C irradiation. In this case spectra were measured 2 days after irradiations, when the bananas were still green. If the UV-C irradiation is decreased, more complete approach to the control curve can be achieved by white light irradiation

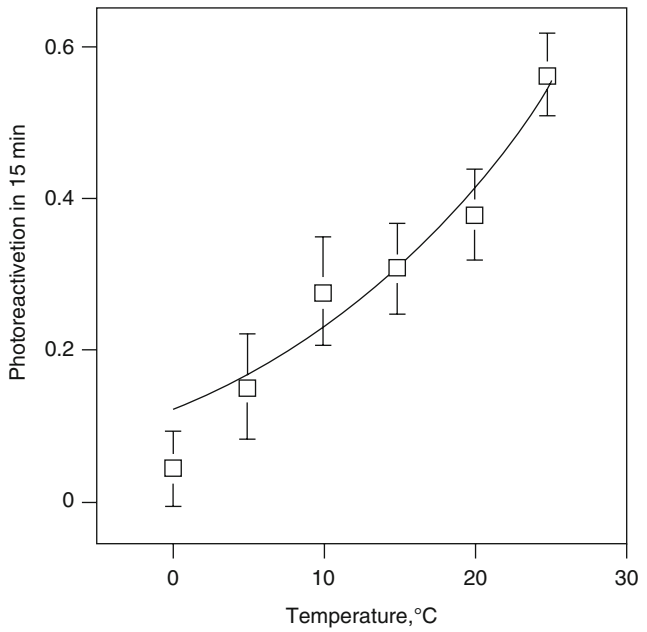

Fig. 28.9 A study of the temperature dependence of photoreactivation of the UV-C-induced darkening of bananas. The experiment was carried out as in Fig. 22.11, except that the bananas were kept in water of different temperature during white light irradiation. The UV-C irradiation lasted 1 min, and the reactivation time was only 15 min. The reflectance at 570 nm was monitored and photoreactivation expressed as fractional approach to the control curve. The curve in the diagram here is an Arrhenius plot fitted to the data with the zero degree data omitted

A simple spectrophotometer for reflectance measurements, such as Colortron (see Sect. 28.11), can be used to evaluate "color changes" (or more correctly: reflectance changes) quantitatively. You can also adapt a spectrophotometer intended for transmission measurements by attaching a Y-shaped light conductor to it. One arm of the conductor picks up light from the monochromator, the other arm delivers it to the photomultiplier, and the base of the Y is placed at a distance of about 5 mm from the banana. Light conductors of this kind can be obtained, e.g., from Oriel. It is best to plot the logarithm of the reflectance of the sample relative to a white standard (Figs. 28.8 and 28.9), but the easiest way is to photograph the banana with a digital camera under standardized illumination conditions, and then evaluate the picture with a program for image analyzes such as Image J.

28.13 Ultraviolet Damage to Microorganisms

Any actively swimming microorganism can be used to repeat in a simplified form Hertel's (1905) classical experiment, using UV-C radiation (254 nm) from a germicidal lamp to stop the movement. Note that a visible effect takes time to develop, so it is in many cases sufficient to irradiate for a minute, and then wait. (Take care to protect your eyes!) We have used *Euglena gracilis* for the purpose. In addition to stopping the movement, the radiation causes this organism to change shape, and with sufficient radiation the color will also eventually change from green to yellow. This is a very simple experiment to carry around if you are a "traveling teacher," as I have sometimes been. See also Delpech (2001) and either Valenzeno et al. (1991) or Smith (1977). Another educational photoreactivation experiment is described by Delpech (2001).

28.14 Photomorphogenesis in Plants and Related Topics

For those readers who know German, I recommend the book by Schopfer (1970), in which a number of class experiments on plant photomorphogenesis are described in detail. I do myself have three favorite experiments, the first two of which are in principle similar to experiments in Schopfer's book. Many experiments, such as basic observations on phototropism, solar tracking leaves, phototaxis, etc., are so simple that they do not need to be described here. For those who feel they need some guidance, see Valenzeno et al. (1991) for phototropism and phototaxis and Vogelmann and Björn (1983) for sun tracking.

28.14.1 Photomorphogenesis of Bean Plants

Prepare sources for red and far-red light as follows. For red light, wrap a red fluorescent lamp in red cellulose acetate film to remove traces of blue light. If you cannot obtain a red fluorescent lamp, use a white one with red acetate film. For far-red light, use an incandescent lamp (25–40 W) behind one layer (3 mm) of red and one layer (3 mm) of blue Plexiglass (many other colored plastic filters will also work). You can use a standard photographic darkroom lamp in which you change the filter for the far-red irradiation, or you can build your own lamp and filter holder; just make sure that only far-red light escapes to your experimental darkroom or cabinet. Do not leave the incandescent lamp on when not in use, since it gives off heat which may damage the filter.

Soak red beans (*Phaseolus vulgaris*) overnight in water, peel off the seed coats, and sow in (at least) five pots with soil (or sow seeds directly without soaking and peeling, although the result will be more variable then). Place one pot in a greenhouse or other suitable place where the plants can continue development under normal light conditions. Put the other pots in a completely dark place, where you can inspect them using dim green light from a green fluorescent lamp (preferably wrapped in green or yellow cellulose acetate film to remove traces of blue light), and water when necessary (not too much, which may result in mold development). Do not unnecessarily expose the plants even to the green safelight. It is not ideal to use an incandescent lamp with a green filter as safelight, since it will emit a lot of far-red light, to which the plants are sensitive, even if you do not see it yourself. When the seedlings have reached a few cm in height, expose one pot to red, one pot to far red, one pot to red followed by far-red light, and keep one pot as dark control. Each exposure should be for 10 min. Let all bean plants continue their development in darkness, except that you repeat the light treatments on each of the two following days. After the 3 days of light treatment, let the plants develop for two more days, after which they can be inspected in full room light and compare the plumular hook angles (Withrow et al. 1957) and the pigmentation. As a variant, you can do a similar experiment with peas (Björn and Virgin 1958).

28.14.2 Regulation of Seed Germination by Phytochrome

The red and far-red light sources for this experiment can be the same as in the bean plant experiment. As plant material most educators have used lettuce seeds of a variety called Grand Rapids, available from many sources (see the Web). However, even different lots of seeds obtained from a particular source do not react uniformly, depending on temperature prehistory and other factors (Frankland and Taylorson 1983;

Cone and Kendrick 1986). If you find that seeds germinate independently of light treatment, try one of the following pretreatments:

1. Hydrate the seeds in the dark, expose them for 10 min to far-red light, and dry them again for class use (recommendation by John Hoddinott, University of Alberta).
2. Try doing the experiment at a high temperature (25–28 °C) rather than normal room temperature (recommendation by Brad Goodner, University of Richmond). When you have got a good lot, keep it in a closed container in your freezer for future use, preferably in small portions, so you do not have to refreeze.

The above advice was found on an Internet chat site at http://www.clemson. edu/biolab/phyt.html. One participant (Jon Monroe), who points out that Grand Rapids is no longer as good for the experiment as it used to be, because suppliers treat the seeds to ensure complete germination, used seeds from the Harris Seed Company (http://commercial.harrisseeds.com/), while Ross Koning at Eastern Connecticut State University recommends "Salad Bowl" lettuce from Agway (http://www.seedway.com/catalog). Dan Tennessen at Cornell University suggests trying seeds of *Poa pratensis* (bluegrass) and *Lepidium virginianum* (peppergrass). For the experiment, cover the bottoms of 12 small petri dishes with a double layer of filter paper, and cut to size so it is flat on the bottom. Pour distilled water into the dishes and pour it off again, so the paper is moist but no longer dripping. Place 50 seeds in rows in each dish. Cover the dishes with aluminum foil. After letting the seeds imbibe for 1–3 h in the dark, irradiate with your red (R) and far red (FR) as follows: each time for 5 min, or leave as dark control. Do duplicates of each treatment.

Irradiation sequences: R, FR, R + FR, R + FR + R, R + FR + R + FR.

Leave in complete darkness (wrapped in aluminum foil) for 2 days, and then evaluate the result.

As an alternative to seeds, fern spores can be used for a red/far-red germination experiment. The procedure for preparing and sowing spores described in the next experiment can be used for this.

28.14.3 Effects of Blue and Red Light on Development of Fern Prothallia

Collection of Fern Spores When fern spores are about to be released (late August in northern Europe), collect spore-bearing leaves and put them on a white paper, sporangia side down. Haupt and Björn (1987) used *Dryopteris filix-mas*, but some other species should also work. After a couple of days, most spores have fallen out on the paper and form a beautiful imprint of the leaf. By holding the paper at a slight angle and gently tapping it, it is easy to separate spores from empty sporangia and other debris. This is easily done manually, but if you like gadgets you can use the handle of an electric toothbrush to vibrate the paper.

Nutrient Medium. (according to Etzold 1965, amounts in g/l) NH_4NO_3 (0.2), K_2HPO_4 (0.1), $MgSO_4{\cdot}7H_2O$ (0.1), and $CaCl_2{\cdot}2H_2O$ (0.1); add a couple of drops of a solution of $FeCl_3$ (1 % w/w) per liter. Adjust pH to 6.0–6.3 with HCl. Add 5 g of agar per liter and heat to dissolve the agar. Transfer the medium to Erlenmeyer flasks, plug with cotton, and autoclave for 10 min at 1 atm overpressure. Let cool to about 40 °C, and pour the medium into sterile 9-cm plastic petri dishes. The dishes can be stored in the dark at 5 °C until use.

Sterilization and Sowing of Spores Pour a few (about 20) drops of dilute (5 % w/v) sodium hypochlorite solution (or corresponding concentration of commercial bleach) into a small glass cup. Put a small amount of spores (as much as the outermost mm of the tip of a knife or spatula can hold) on the solution, and stir with a glass rod until all spores are in the solution. After 3–4 min you can start to sow your petri plates with the suspension using a sterile inoculation loop. Put the loop under the spores and lift, so you get a drop with spores in the loop. Streak out the drop on a plate, and repeat with more plates (you need at least four plates). The spores can remain in the hypochlorite solution for some time without being damaged. After transfer to the agar, the hypochlorite will be sufficiently diluted and need not be removed.

Irradiation and Development Put two plates under blue light and two under red light (best to use colored fluorescent lamps, but white fluorescent lamps with colored cellulose acetate film will probably also work well). After about 6 days the spores should have germinated. Study the development for 1 week. When you see that the prothallia have started to grow, you can transfer one plate from red light to blue light and one from blue light to red light. Under red light the prothallia will grow as filaments, under blue light as plates.

If you run a dark control, you will find that the spores do not germinate. You can do red/far-red reversion experiments as on the seeds in the previous experiment.

28.15 Spectrophotometric Studies of Phytochrome In Vivo

Photobiology practicals in our own photobiology courses have included purification of phytochrome and in vitro experiments with the purified phytochrome, but this may be too laborious to set up in a laboratory not doing research on phytochrome. The following is a simple experiment to carry

through, but requires a good dual wavelength spectrophotometer such as Aminco DW-2. It may be possible to adapt the experiment for an ordinary double-beam single-wavelength computerized spectrophotometer of good quality, but I have not tried this.

The aim of the experiment is to demonstrate spectrophotometrically the in vivo transformations between the red-absorbing (P_r) and far-red-absorbing (P_{fr}) forms of phytochrome: P_r ==>P_{fr} (under red light) and P_{fr} ==>P_r (under far-red light).

Plant Material Oats or wheat is sown in moist vermiculite (mica) in plastic or metal trays (a total of 0.25 m^2 required). The trays are incubated in complete darkness at 20–25 °C for about 4 days. When the seedlings have emerged, and preferably before the leaves have broken through the coleoptiles, the shoots are harvested. Harvesting and the following manipulations should be carried out using dim green working light. About 50 plants are required for an experiment.

Sample Preparation The coleoptiles are cut open so the leaves in them can be removed. This procedure is rather time-consuming and not absolutely necessary if you just want to demonstrate the presence of phytochrome. For quantitative experiments it is of advantage to get rid of the leaves, which are rich in protochlorophyllide. This is also photoconvertible, which obscures the phytochrome signal.

The coleoptiles are collected in a petri dish with water, so they do not dry out. When you have enough coleoptiles, arrange them in a bundle which you cut across with a razor or scalpel in the middle to get two bundles with a sharp delimitation. Join them with the cut ends in the same direction, and press them into a water-filled spectrophotometer cuvette in such a way that you avoid air bubbles between the coleoptiles. There is no need to crush an expensive cuvette trying to squeeze in the coleoptiles; you might as well use a cheap plastic one. We have also with good results used small round glass test tubes, which fit the cuvette holder of the spectrophotometer.

Measurement Switch the spectrophotometer to dual-wavelength mode, and set the monochromators to measure the absorbance difference between 660 and 730 nm (or, preferably, between 660 and 800 nm in one series of measurement and 730 and 800 nm in another series of experiments). If you have not removed the leaves, it is best to focus on measuring the P_{fr} changes only by recording the absorbance difference between 730 and 800 nm. Using the Aminco DW-2 and DW-2a spectrophotometers, we have set full scale to 0.01 absorbance units and the damping to medium.

After taking a reading, irradiate the sample with strong red light for one minute and take a new reading. Then do the same with far-red light and take a new reading. If this works you can continue the experiments in a variety of ways, studying reaction kinetics and action spectra, for instance. We have also let students take coleoptiles outside to different environments, above and below tree canopies, etc., and then bring the coleoptiles back to the laboratory (on ice) for evaluation of the phytochrome state.

The phytochrome-transforming irradiation can either be carried out with the sample cuvette still in the spectrophotometer, using a xenon lamp–monochromator combination, or after removal from the spectrophotometer. In the former case, the photomultiplier should be protected with a piece of sheet metal during irradiation, and if the spectrophotometer does not switch the photo-multiplier voltage off automatically, this should be done manually. In the latter case, we have used light sources similar to those used for photomorphogenesis and germination experiments. In this case it is important to handle the cuvette carefully so the coleoptiles or any air bubble present does not change position, so as not to touch the places where the measuring beam is to enter and exit and to put the cuvette back with the original orientation.

As an alternative to coleoptiles, the epicotyls (internodes between cotyledons and first two leaves) of dark-grown pea plants serve very well. This circumvents the time-consuming task of removing leaves.

28.16 Bioluminescence

28.16.1 Fireflies

If you do not have bioluminescent insects where you live, or if the season is not the right one, you can buy dried fireflies from one of several suppliers, such as Sigma Chemical Co. (St. Louis, MO) or Worthington Chemical Corp. (Freehold, NJ). The simplest experiment you can do is to wet the abdomen of such a dead insect with ATP solution (dissolve 10 mg ATP in 10 ml 0.1 M phosphate buffer, pH 7.6, containing 1 mM $MgCl_2$) and watch it glow. If you remove oxygen by flushing with nitrogen, the glow disappears. Other experiments can be carried out with extracts of the fireflies containing luciferin and luciferase. For extraction of the fireflies in a mortar with sand, use a solution of 0.4 g glycine and 0.1 g ammonium bicarbonate in 100 ml distilled water. You can also buy ready-made, dried firefly extract, which only needs reconstitution with water. If you can get living bioluminescent insects, it would be interesting to try repeating the new observation of the role of nitrogen monoxide (Trimmer et al. 2001), but I have not done this myself.

28.16.2 Bacteria

A culture of luminescent *Photobacterium phosphoreum* can be purchased from a culture collection, such as the American Type Culture Collection (http://www.atcc.org), but the cost is considerable. It is, however, not very difficult to get luminescent bacteria to grow on old decaying fish (if you can stand the smell), preferably fish from the sea (Lee 1977, 1991).

28.17 Miscellaneous Teaching Experiments and Demonstrations

Here are a few ideas which I have not tried myself, but which appear worth exploring:

1. Gelatin optics. Many interactions between light and matter can be demonstrated using gelatin. Knotts (1996) has published a rather detailed description, and variations of this are available from various Internet sites—search, for instance, for "gelatin optics" or "edible optics" or "optics fun with gelatin." The main thing to remember is that the gelatin gel should be prepared three times more concentrated as most cooking recipes require. From such gels you can prepare lenses, prisms, and fiberoptics. Demonstrations of refraction and reflection (including total reflection) can be carried out using a laser pointer as light source. The slight scattering in the gel makes the light rays visible. Knotts (1998) reviewed several books for elementary optics experimentation.
2. Optical tweezers for students are described by Smith et al. (1999).
3. Quantum dots. Several student experiments for production of quantum dots by the wet method have been worked out, both for CdS and for CdSe quantum dots (Kippeny et al. 2002; Boatman et al. 2005; Winkler et al. 2005). All of the methods involve dangerous chemicals, and a qualified chemist to lead the exercises is required, as well as proper disposal of chemicals. The method of Boatman, Lisensky, and Nordell for CdSe quantum dots is probably the safest.
4. An exercise about the ozone layer is found at NASA's site: "Ozone over your head," http://edmall.gsfc.nasa.gov/inv99Project.Site/Pages/trl/inv3-1.html.

References

Anon. (1894) Artificial spectrum top. Nature 51:113–114

Barton CVM, North PRJ (2001) Remote sensing of canopy light use efficiency using the photochemical reflectance index: model and sensitivity analysis. Remote Sensing Environ 78:264–273

Björn LO (1969a) Action spectra for transformation and fluorescence of protochlorophyll holochrome from bean leaves. Physiol Plant 22:1–17

Björn LO (1969b) Photoinacivation of catalases from mammal liver, plant leaves and bacteria. Comparison of inactivation cross sections and quantum yields at 406 nm. Photochem Photobiol 10:125–129

Björn LO, Li S (2013) Teaching about photosynthesis with simple equipment: analysis of light-induced changes in fluorescence and reflectance of plant leaves. Photosynth Res 116:349–353

Björn LO, Virgin HI (1958) The influence of red light on the growth of pea seedlings. An attempt to localize the perception. Physiol Plant 11:363–373

Boatman EM, Lisensky GC, Nordell KJ (2005) A safer, easier, faster synthesis for CdSe quantum dot nanocrystals. J Chem Educ 82:1697–1699

Cone JE, Kendrick RE (1986) Photocontrol of seed germination. In: Kendrick RE, Kronenberg GHM (eds) Photomorphogenesis in plants. Martinus Nijhoff/Junk Publishers, Dordrecht, pp 443–463

Delpech R (2001) Using *Vibrio natriegens* for studying bacterial population growth, artificial selection, and the effects of UV radiation and photo-reactivation. J Biol Educ 35:93–97

Diakoff S, Scheibe J (1973) Action spectra for chromatic adaptation in Tolypothrix tenuis. Plant Physiol 51:382–385

Etzold H (1965) Der Polarotropismus und Phototropismus der Chloronemen von *Dryopteris filix-mas* (L.). Schott Planta 64: 254–280

Filella I, Amaro T, Araus JL, Penuelas J (1996) Relationship between photo-synthetic radiation-use efficiency of barley canopies and the photochemical reflectance index (PRI). Physiol Plant 96:211–216

Frank HA, Cua A, Chynwat V, Young A, Gosztola D, Wasielewski MR (1994) Photophysics of the carotenoids associated with the xanthophyll cycle in photosynthesis. Photosynth Res 41:389–395

Frankland B, Taylorson RB (1983) Light control of seed germination. In: Shropshire Jr. W, Mohr H (eds) Encyclopedia of Plant Physiology, New Series, 16A. Springer, Berlin, pp 428–456

Fujita Y, Hattori A (1960a) Formation of phycoerythrin in preilluminated cells of *Tolypothrix tenuis* with special reference to nitrogen metabolism. Plant Cell Physiol 1:281–292

Fujita Y, Hattori A (1960b) Effect of chromatic lights on phycobilin formation in a blue-green alga, *Tolypothrix tenuis*. Plant Cell Physiol 1:293–220

Gamon JA, Surfus JS (1999) Assessing leaf pigment content and activity with a reflectometer. New Phytol 143:105–117

Gamon JA, Field CB, Bilger W, Bjorkman O, Fredeen AL, Peñuelas J (1990) Remote-sensing of the xanthophyll cycle and chlorophyll fluorescence in sunflower leaves and canopies. Oecologia 85: 1–7

Gamon JA, Peñuelas J, Field CB (1992) A narrow-waveband spectral index that tracks diurnal changes in photosynthetic efficiency. Remote Sensing Environ 41:35–44

Gamon JA, Serrano L, Surfus JS (1997) The photochemical reflectance index: an optical indicator of photosynthetic radiation use efficiency across species, functional types, and nutrient levels. Oecologia 12:492–501

Haupt W, Björn LO (1987) No action dichroism for light-controlled fern-spore germination. J Plant Physiol 129:119–128

Hausser KE, von Ohmcke HV (1933) Lichtbräunung an Fruchtschalen. Strahlentherapie 48:223–229

Hertel E (1905) Ueber physiologische Wirkung von Strahlen verschiedener Wellenlänge. Zschr Allgem Physiologie 5:95–122

Johnson RH, Williams TP (1970) Action of light upon the visual pigment rhodopsin. J Chem Edu 47:736–739

Kippeny T, Swafford LA, Rosenthal SJ (2002) Semiconductor nanocrystals: a powerful visual aid for introducing the particle in a box. J Chem Edu 79:1094–1100

Knotts ME (1996) Optics fun with gelatin. Optics and photonics news, Apr 1996, pp 50–51. Available from http://www.opticsforkids.org/resources/GO_3.pdf

Knotts ME (1998) Books for optics experimenters. Optics and Photon News 9:50–51

Le Rohellec J, Vienot F (2001) Interaction of luminance and spectral adaptation upon Benham subjective colors. Color Res Appl 26:S174–S179

Lee J (1977) Bioluminescence. In: Smith KC (ed) The science of photobiology, Chapter 14. [Reprinted in D.P. Valenzeno et al. (eds) (1991) Photobiological techniques. Plenum, New York, pp 359–360]

Lee J (1991) Experiment 33: bacterial bioluminescence. In: Valenzeno DP (ed) Photobiological techniques. Plenum, New York, pp 317–320

Nichol CJ, Hümmrich KF, Black TA, Jarvis PG, Walthall CL, Grace J, Hall FG (2000) Remote sensing of photosynthetic light-use efficiency of boreal forest. Agric Forest Meteorol 101:131–142

Peñuelas J, Filella I, Gamon JA (1995) Assessment of photosynthetic radiation-use efficiency with spectral reflectance. New Phytol 131:291–296

Peñuelas J, Llusia J, Pinol J, Finella I (1997) Photochemical reflectance index and leaf photosynthetic radiation-use efficiency assessments in Mediterranean trees. Int J Remote Sensing 18:2863–2868

Pottier RH, Russell DA (1991) Quantum yield of a photochemical reaction. In: Valenzeno DP, Pottier RH, Mathis P, Douglas RH (eds) Photobiological techniques. Plenum Publishing Corp, New York, pp 45–52

Schopfer P (1970) Experimente zur Pflanzenphysiologie. Rombach Verlag, Freiburg

Smith KC (ed) (1977) The science of photobiology. Plenum, New York

Smith SP, Bhalotra SR, Brody AL, Brown BL, Boyda EK, Prentiss M (1999) Inexpensive optical tweezers for undergraduate laboratories. Am J Phys 67:26–35

Trimmer BA, Aprille JR, Dudzinski DM, Lagace CJ, Lewis SM, Michel T, Qazi S, Zayas RM (2001) Nitric oxide and the control of firefly flashing. Science 291:2486–2488

Valenzeno DP, Pottier RH, Mathis P, Douglas RH (eds) (1991) Photobiological techniques. Plenum Publishing Corporation, New York

Vogelmann TC, Björn LO (1983) Response to directional light by leaves of a sun-tracking lupine (*Lupinus succulentus*). Physiol Plant 59:533–538

von Campenhausen C, Schramme J (1995) 100 years of Benham top in color science. Perception 24:695–717

Winkler LD, Arceo JF, Hughes WC, DeGraff BA, Augustine BH (2005) Quantum dots: an experiment for physical or materials chemistry. J Chem Educ 82:1700–1702

Withrow RB, Klein WH, Elstad VB (1957) Action spectra of photomorphogenetic induction and its inactivation. Plant Physiol 32:453–462

The Amateur Scientist's Spectrophotometer

29

Lars Olof Björn

29.1 Introduction

A spectrophotometer is a very useful instrument for many types of chemical and biological measurements. The most common types are designed for measuring light absorption in solutions, but there are also spectrophotometers with which you can take measurements on living tissues or even single cells, and there are reflectance spectrophotometers for measurements on surfaces and many other special types. A common property is that they are expensive. Here we shall see that it is easy to build a low-cost spectrophotometer. It is not a precision instrument, but it is sufficient for many demonstrations and teaching experiments. It is an elaboration of a design for a spectroscope described by Wakabayashi and Hamada (2006).

A spectrophotometer has the following main parts: a lamp, a dispersing element (usually a reflecting grating; see Chap. 3) that divides the light into spectral components, a place to put the sample, a light detector, and some device for reading or recording the result. In addition, there is usually a number of lenses and mirrors. The most expensive parts are the grating and the light detector; the recording system may also be expensive.

A reflecting grating is a mirror with many fine parallel grooves ruled into it. For our low-cost spectrophotometer, we shall use a DVD as a grating. Perhaps you have an old one with a movie that you have seen enough of. It is all right if it is scratched and useless for watching your movie, if it is just OK in a small sector, because that is all we will use. Otherwise you will have to buy a movie DVD, and if so this may be your major investment in the project. Some of the DVDs (DVD-R or DVD-RW) that you buy for making your own recording are not suitable because they have a lacquer that will show up as a dark band in the red region of the spectrum. Some other types of DVDs are also unsuitable. Check that the reflection from the DVD does not look colored (except for the rainbow type reflection you see in some directions). CDs can be used with modifications of the present description, but give much lower resolution, since they have only 625 grooves per mm, as compared to 1,350 grooves per mm for a DVD. A CD also has to be mounted in a slightly different way from a DVD.

You might already have the other expensive component of your spectrophotometer, the light detector, because for this we shall use a digital camera. It does not have to be a very fancy type. The one that I have used (Fujifilm F601 Zoom) has only three megapixels, which is considered little nowadays. I do not even use the highest resolution of 6 Mb per picture, but only half of that, to save computer memory. Even this gives me a nominal spectral resolution of 3.515 pixels per nm, which is much better than what the primitive optics allows me to take full advantage of anyway. But the camera should allow for manual exposure, so that it does not automatically set stop and/or exposure time.

A third component that could be expensive is the recording system, and for this we shall use a personal computer, which you probably already own or have access to.

29.2 Construction

Start by making a cardboard box according to Fig. 29.1. When the box is finished and the glue has dried, you can insert the DVD in the slot, ruled side up. Push it right into the corner of the box (part of it will stick out, and if you wish you can cut that part away). To reduce stray light, one potential problem, a mask of black paper should be put on top of the DVD to leave uncovered only that part which we wish to use optically. Figure 29.2 shows a template of the mask.

On a piece of plywood or other board, assemble the cardboard box, a suitable lamp (I use a quartz-iodine lamp with

L.O. Björn
School of Life Science, South China Normal University, Guangzhou, China

Department of Biology, Lund University, Lund, Sweden
e-mail: Lars_Olof.Bjorn@biol.lu.se

L.O. Björn (ed.), *Photobiology: The Science of Light and Life*,
DOI 10.1007/978-1-4939-1468-5_29,

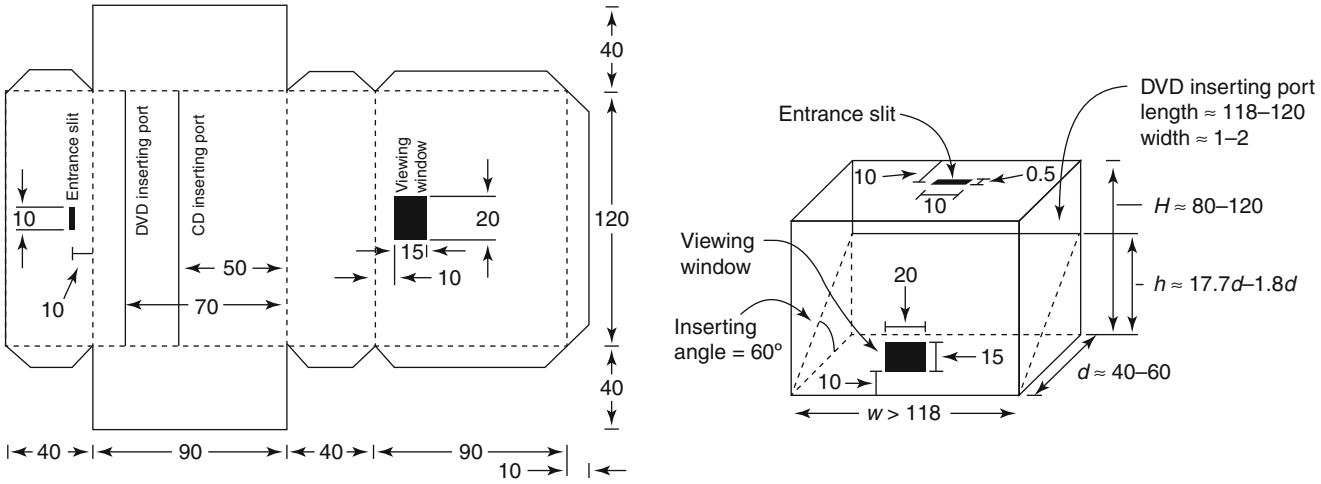

Fig. 29.1 Construction of the light-dispersing unit box (spectroscope) of the spectrophotometer. Measures are given in mm. The best material to use is black cardboard. If you use another cardboard, paint the inside of the box with black paint that is as dull as possible. In one trial I used a black marker pen which worked, but this is not ideal since it results in a surface that is a little shiny. The rectangle marked "viewing window" should be cut out, as well as a slot for insertion of the DVD and a 10 mm by 0.5 mm entrance slit. In this figure a slot for a CD is also indicated, but if you are going to use only a DVD (recommended), do not cut out this slot since it may lead to stray light problems (From Wakabayashi and Hamada 2006, with permission)

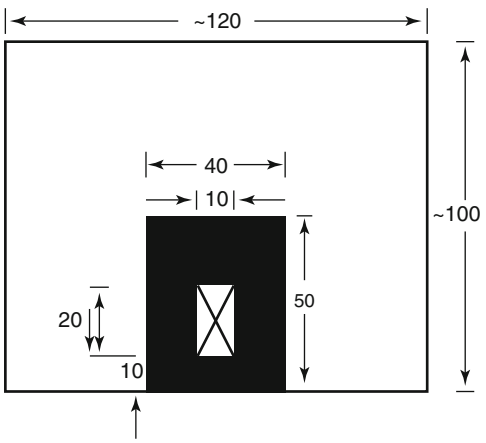

Fig. 29.2 Dimensions of the black paper mask to cover the DVD. The whole paper is 120 mm by 100 mm, the hole 10 mm by 20 mm, at a distance of 10 mm from the edge of the paper

built-in "cold mirror," i.e., a mirror which lets infrared radiation through but reflects visible light) and your camera. To get the proper height relations between my lamp and the cardboard box, I put two extra plywood pieces and an aluminum sheet between the box and the baseboard. I let a little of the aluminum sheet protrude in front of the plywood support and made a hole in it for a screw that fixed the camera. I also mounted a sheet of brass with a hole in it to screen out unwanted light from the lamp and covered the box, including the protruding part of the DVD with duct tape. The cardboard box and the completed assembly are shown in Figs. 29.3 and 29.4.

29.3 Calibration of Wavelength Scale

The most convenient way to calibrate the wavelength scale is to use a mercury lamp. Just remove the ordinary lamp, and point the slit toward a mercury lamp; a streetlamp may do. (The first time I went outdoors and pointed my strange gadget toward a streetlamp, a lady passing by, worried about my mental health, asked whether I was all right or needed help.) Figure 29.5 shows to the left part of the picture obtained in this way. With more exposure it is also possible to show weaker emission lines, but then the closer lines, like 577 and 579 nm, can no longer be resolved.

For quantitative work with spectra, a computer program, ImageJ, is available for download without charge from the Internet. To download it, go to http://rsb.info.nih.gov/ij/, where you can read some general information, and then click on "download" to get to http://rsb.info.nih.gov/ij/download.html, where you can download ImageJ for your particular computer platform. In the following I shall show how to use the Macintosh OS-X version, but it is probably no different with another computer. The program was written for another purpose, and I got the idea of using it for spectral analysis from Kohl et al. (2006).

The first thing I see when I load a picture from the camera into the ImageJ program is the color picture with the spectrum. In the example shown in Fig. 29.5, I used a UV-B lamp (Philips TL12 fluorescent lamp with mercury lines). In this case I also captured the violet mercury line (404.7 nm), but due to overexposure the two yellow lines (577 and 579 nm) are not separated. The red lines are not visible, probably because the mercury vapor in this lamp has a lower pressure

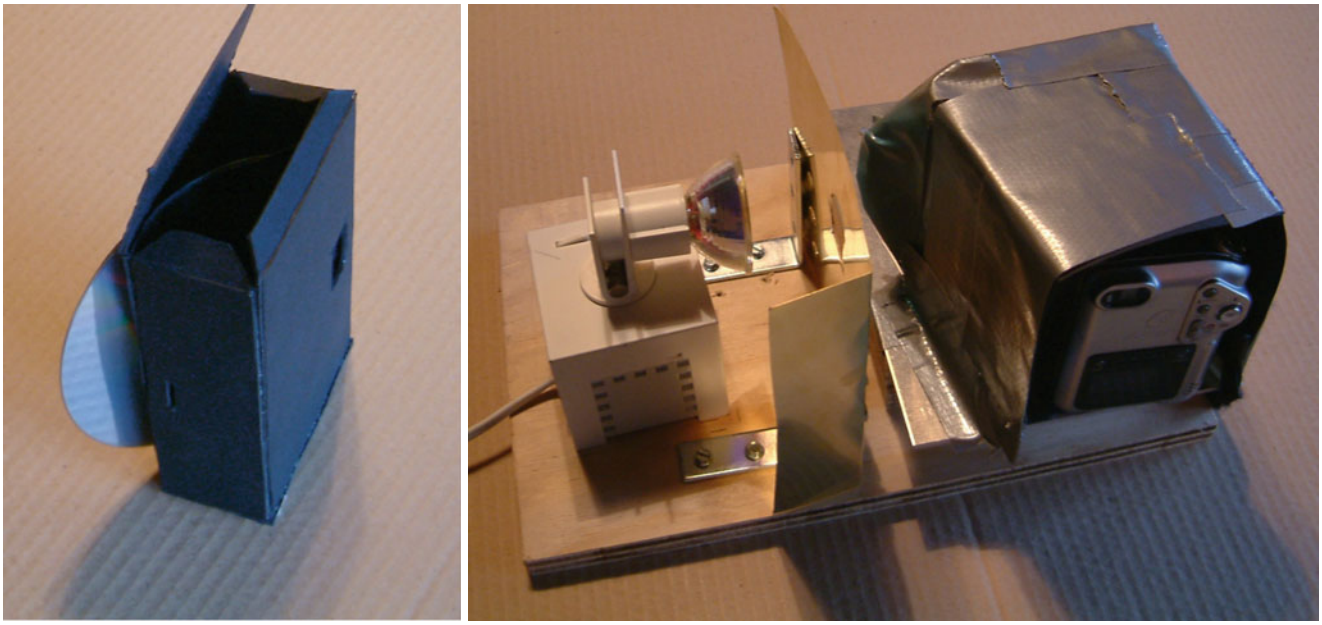

Fig. 29.3 The finished cardboard box with DVD inserted, just before gluing on the lid (*left*), and the completed assembly (*right*)

Fig. 29.4 The almost completed spectrophotometer with lamp switched on. You can see the spectrum displayed on the camera screen. The only thing that is lacking now is a sample. This should be placed between the brass screen and the entrance slit on the box, according to the nature of the sample. A plant leaf could be attached with Scotch tape directly over the entrance slit, while a cuvette with solution has to stand on some support or placed in a holder. Using the kind of lamp shown here, which turned out to be unnecessarily strong (20 W rating), the light should not be switched on too long to avoid heating the box too much (fire risk)

than in the street lamp. That the violet line did not appear in the spectrum of the street lamp is probably due to absorption in the weatherproof cover of that lamp. The blue to the far right in the spectrum is the second order of the 404.7-nm line, with a position corresponding to 2×404.7 nm $= 809$ nm in the first-order spectrum. Also, this value can be used for the wavelength calibration.

Moving the cursor over the picture with the mouse button down, you can select a rectangle in the picture delimiting the area you wish to analyze. In doing so, select a part of the spectrum which is central in a vertical direction, so you avoid including too much of the curvature of the lines. Also be careful to include everything in the horizontal direction, so you start with the leftmost line of pixels and end with the rightmost one. Otherwise it will not be possible to compare different spectra. The next thing to do is to pull down the menu under "Analyze" and select "Plot profile" (Figs. 29.5 and 29.6). Then the spectral plot of "gray value" versus "Distance (Pixels)" pops up.

When you move the cursor over this picture, both the horizontal and vertical coordinates are displayed. If you position the cursor at the various peaks you see, you can read and note their horizontal pixel coordinates (x values). Since there are relatively few peaks in this spectrum, and you can see their colors in the color picture, it is not difficult to relate them to wavelength values for mercury found in a table. Enter the pixel numbers and their corresponding wavelengths in a table in Excel or a similar program. If you do not have one, you can download "Open Office" without charge from the Internet. To the right in Fig. 29.6, we have done this, produced a plot of the table in Excel, and added a linear trend line and a trend equation. It is this trend equation that you will use for calibrating the wavelength in other spectra.

As you can see, the wavelength calibration turns out to be surprisingly linear, considering the very simple optics used. The equation $y = 2{,}864\times + 233.72$, with x as the pixel number and y as the wavelength in nm, is what you use to convert

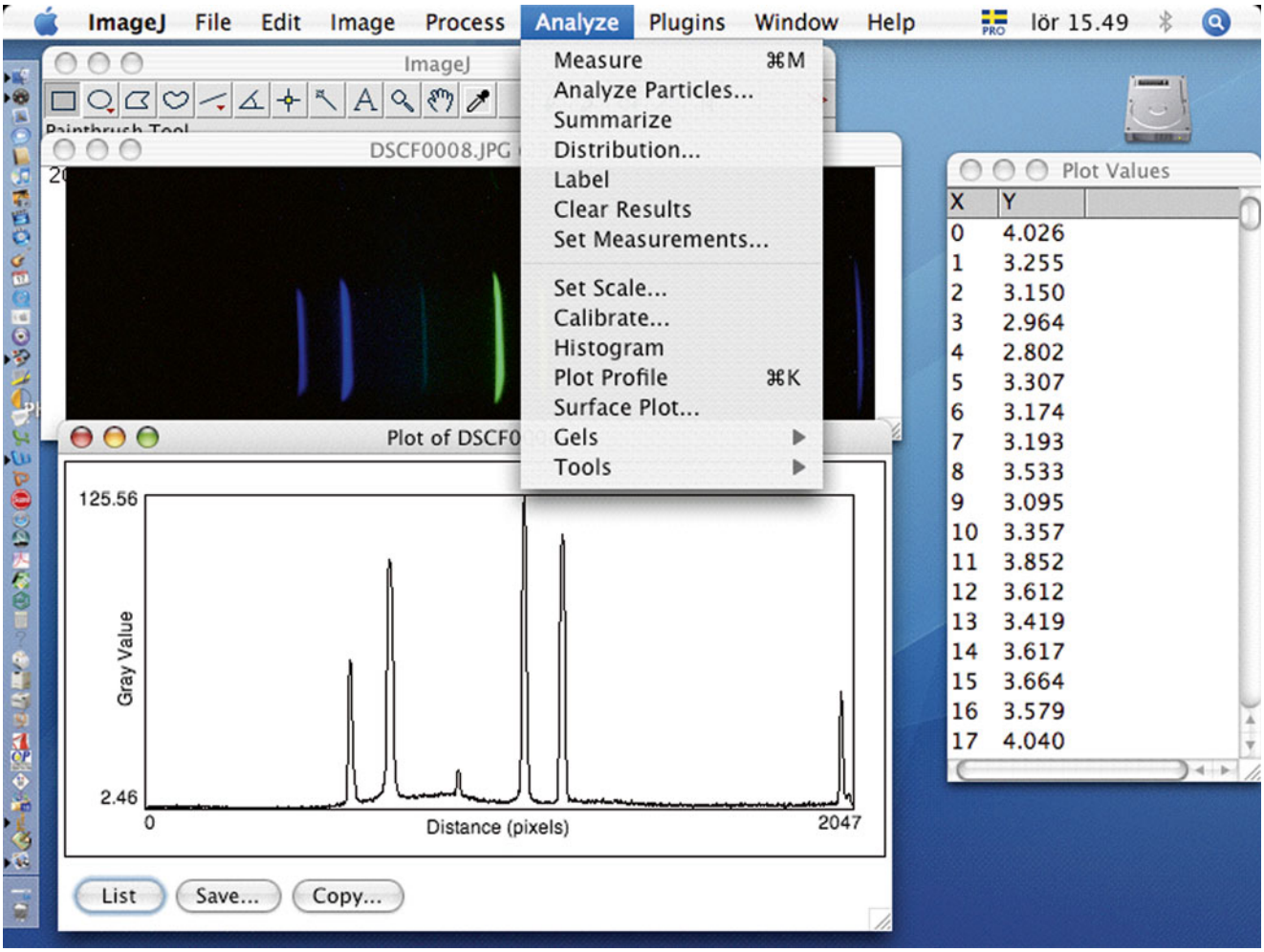

Fig. 29.5 Appearance of Macintosh computer screen during work with ImageJ for wavelength calibration using a mercury spectrum

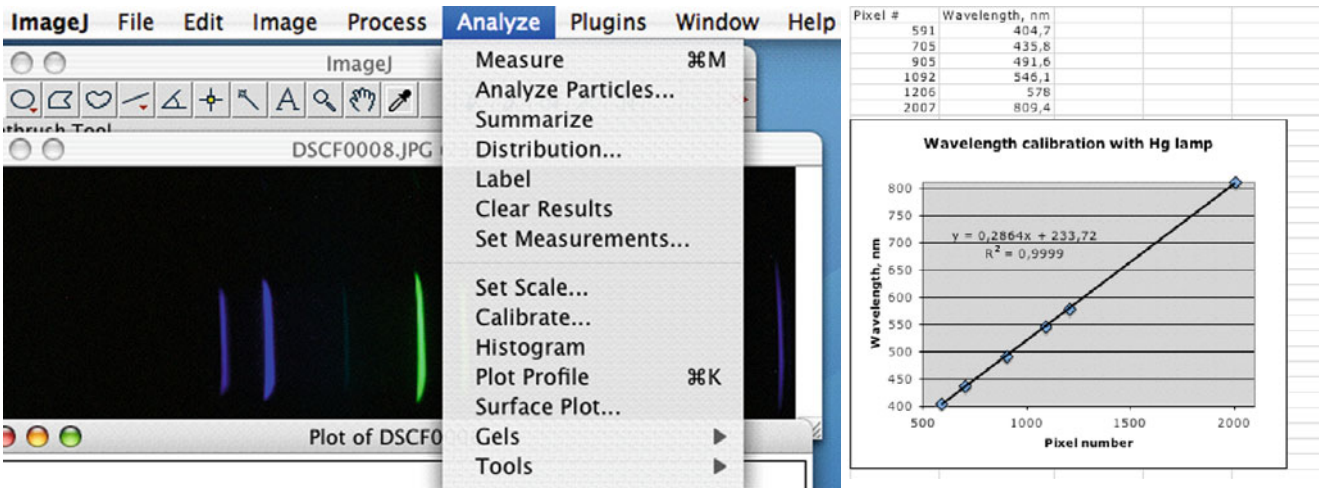

Fig. 29.6 How to pull down the menu for selecting “Plot Profile” and make a wavelength calibration table and calibration plot in Excel

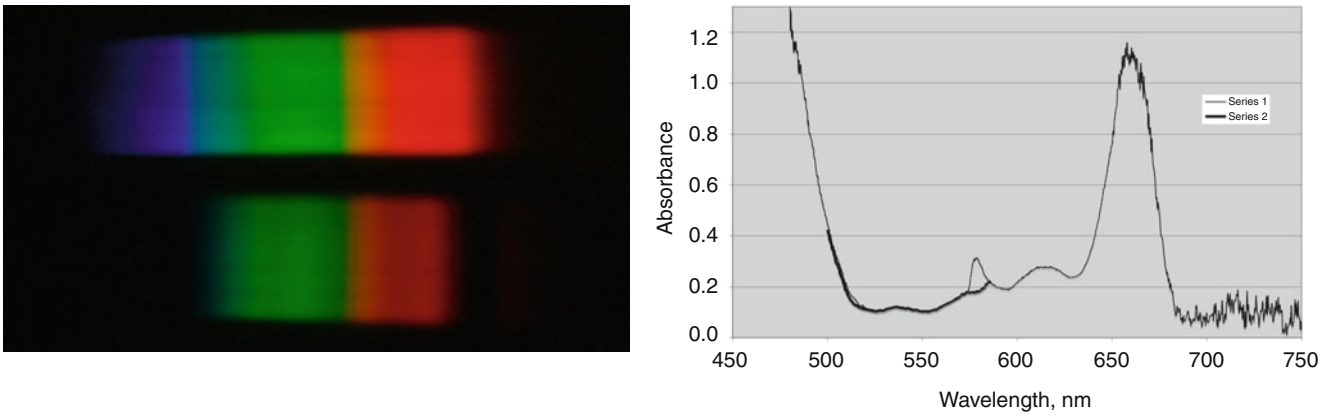

Fig. 29.7 Reference spectrum without sample (*upper left*) and with plant leaf extract (*lower left*). To the right is shown the corresponding plot of the absorbance of a plant leaf extract in acetone. For the thin curve, all three camera color channels (*blue, green, and red*) were used. The bump at 580 nm is an artifact. It coincides with the steepest portion of the reference spectrum (the segment from C to D in Fig. 25.12), where the red channel takes over from the green one. If only the green channel is used for this region (*thick curve*), the bump disappears. See inset for a color version of the spectra

pixel numbers in other spectra to wavelength in nm. The constant term in the right member depends on the position of the camera. Since you may wish to use the camera for other purposes between calibration and other measurements, you must either devise some way of repositioning the camera exactly or use a trick to be described below.

Before we lose Fig. 29.5 from sight, I should explain that the table in the panel to the right is only the beginning of a 2,047-line table of the complete spectral plot that you obtain by selecting "List" below the spectral plot. It is not necessary for the wavelength calibration, but we will soon use this facility for computations on measured spectra.

29.4 Measurement and Manipulation of Spectra

We now come to the real measurements. Suppose we wish to measure the absorption spectrum of an acetone extract of a plant leaf. Before positioning the sample itself, we must take a reference spectrum of the lamp (the quartz-iodine lamp shown in Figs. 29.4 and 29.5, or whatever lamp we have chosen to use). If we wish to be careful, we can insert a cuvette with acetone in front of the entrance slit to get just the absorption of the plant constituents in the end. We then get a spectrum like the upper one shown in Fig. 29.7. The lower spectrum is made with the plant extract in the cuvette.

Initially follow the same procedure as for the wavelength calibration: open the picture in ImageJ, select the rectangular portion we wish to use, pull down the "Analyze" menu, and select "Plot Profile." Then choose "List" under the spectral plot, and display all the pixel positions of the spectral plot. The first column in this is the horizontal pixel position, the second one the gray value, or more appropriately the brightness of the corresponding portion of the spectrum. These values are then transferred to Excel or another spreadsheet program. Users of commas rather than periods in decimal numbers can easily change from one to the other by first copying the values into Word, using the "replace all" facility of this program, and then copying the values into Excel. Using Word as an intermediate for changing "." to "," seems more reliable than changing directly in Excel.

In Excel, you can change the horizontal pixel positions to wavelength values using your calibration equation. Then you can divide the sample column by the reference column to get transmittance values, and you can take minus the logarithm of this to get the absorbance. We show the result of these manipulations in Fig. 29.11.

A few more remarks relating to this measurement: in cases such as these, when you compare the brightness of two spectra, it is important to use the same camera stop and exposure time values for the spectra to be compared. This means that you cannot use the camera's facility for automatic exposure. For the above measurement I used the least possible exposure, i.e., f/8 and 1/1,600 s exposure time. In some cases, if you have very dense samples to compare to a bright control spectrum, it might be better to use different settings, but you must then take this into account to get the correct absorbance value.

In order to be able to remove the camera between wavelength calibration and measurement of a sample, and not have to reposition it very exactly, I used a special trick. It turned out that with my camera and the lamp I used, the reference spectrum without sample had several very easily recognizable and useful features, as shown in Fig. 29.8.

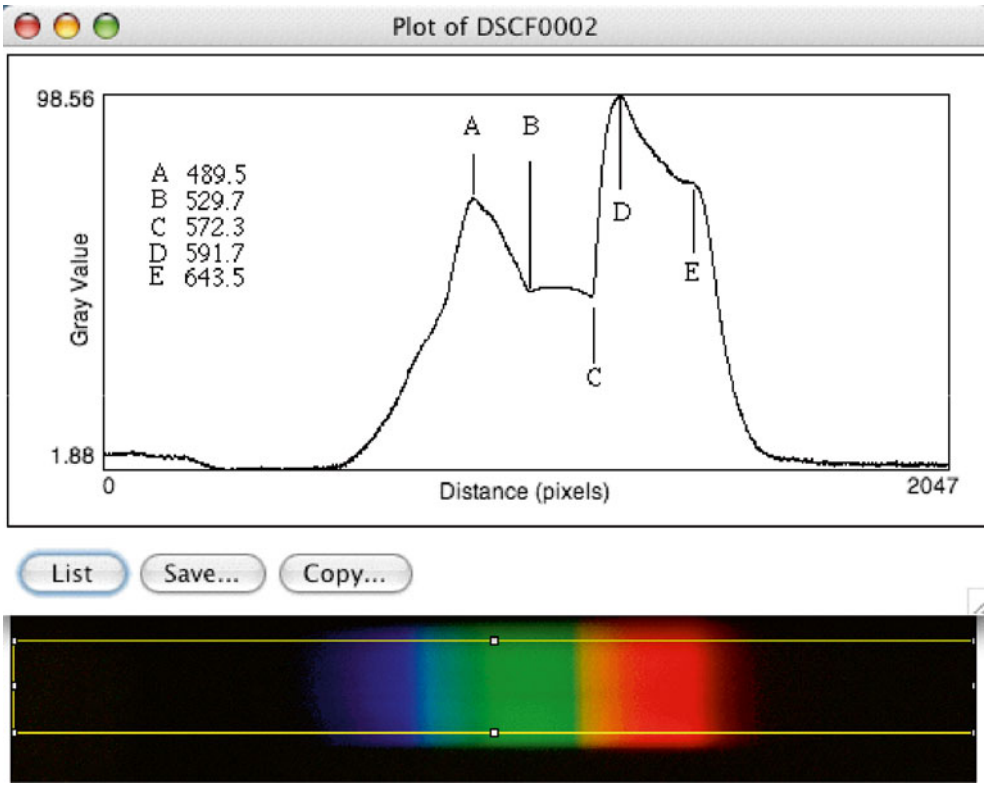

Fig. 29.8 Appearance of my control spectrum without sample. Once the wavelengths for points A, B, C, D, and E have been determined, these points can be used to convert pixel positions to wavelength values without having to record a mercury spectrum every time

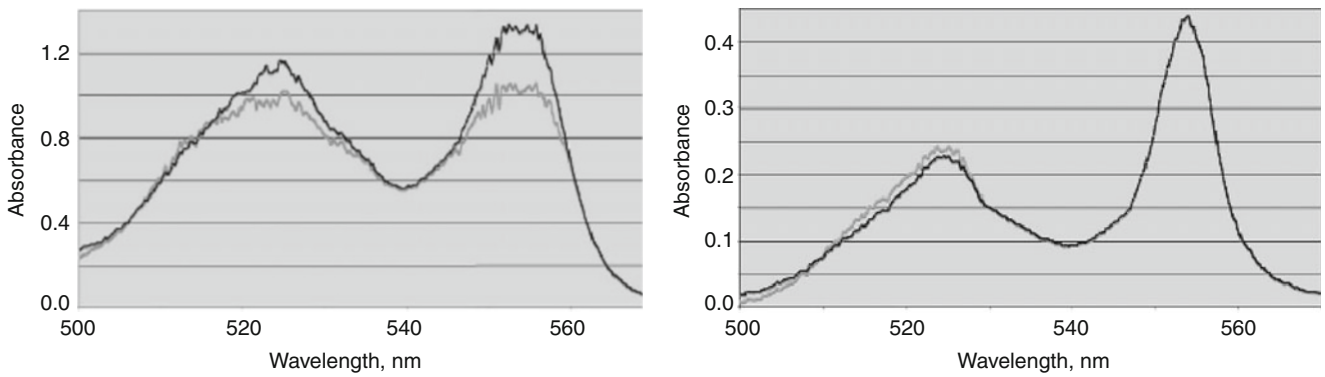

Fig. 29.9 (*Left*) Absorption spectrum of the a and b band region of reduced cytochrome *c* (in phosphate buffer, pH 7, and reduced with dithionite) measured with all three color channels (*gray curve*) or the green channel only (*black curve*). The absorbance is too high for the spectrophotometer to cope with. (*Right*) The same, except more dilute solution of reduced cytochrome *c*. There is a wavelength error of about 4 nm (the literature value for the peak is 550 nm), which is about what one can expect

One more facility of the ImageJ program may be useful in some cases. The color picture of the spectrum can be divided into RGB (red-green-blue) components, and each of these three pictures can be evaluated separately. In some cases, some parts of the spectrum can be over- or underexposed, and then it may still be possible to retrieve useful values by such a decomposition.

In Fig. 29.7, a case is shown where a single color channel (the green channel) seems to give a better result in a certain spectral region than the three channels combined. One can also expect that using only one channel at a time will decrease the effect of scattered light. Such scattered light is a problem in spectrophotometry when measuring samples in spectral regions of high absorbance, when other regions have low absorbance. The left graph in Fig. 29.9 gives an example of how using all the color channels in such a case gives lower absorption peaks than a single channel; in such cases one should use only a single channel. With a more dilute solution and lower absorbance (more favorable measurement conditions), we do not have this effect (right graph). To perform a decomposition for selecting the correct channel, pull down the “Image” menu

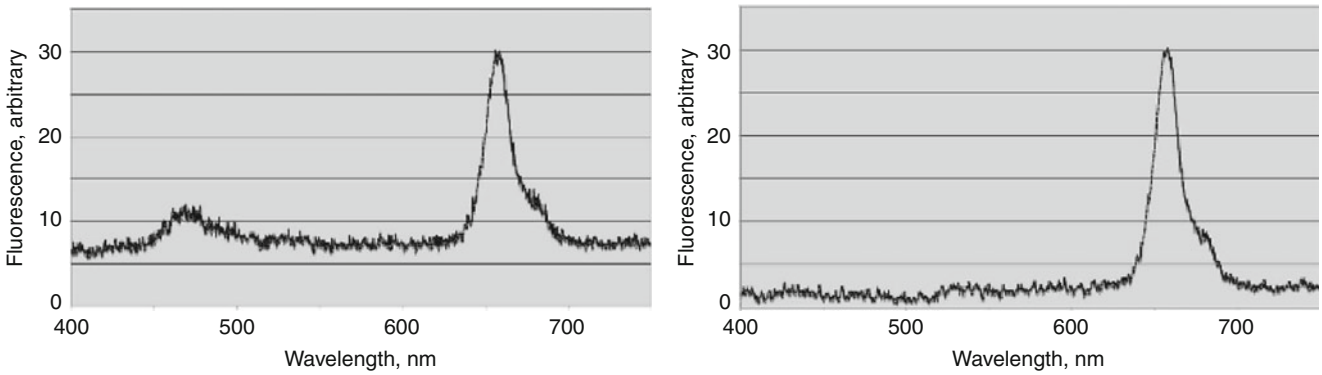

Fig. 29.10 Fluorescence of an acetone extract of a plant leaf excited by light from a blue light-emitting diode (469 nm). With such excitation most of the fluorescence comes from chlorophyll *b*. For the left panel all three color channels of the camera were used, for the right one the red channel only. The spectra are not corrected for wavelength dependence of the camera sensitivity, and because of rapid decline of sensitivity above 640 nm, only the short-wavelength portion of the spectrum is visible. The easiest way for an amateur to make an approximative sensitivity calibration would be to use the sun when it is high in the sky

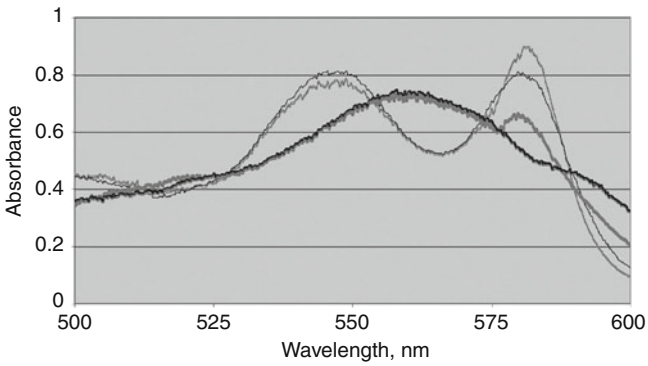

Fig. 29.11 Blood diluted in oxygenated water (i.e., spectrum of oxyhemoglobin, thin lines) and after removal of oxygen with dithionite (i.e., spectrum of hemoglobin, thick lines). Either all three color channels were used (*gray lines*) or only the green channel (*black lines*), and we see here again the artifactual elevation at 585 nm when all channels are used (c.f. Fig. 29.7). With other digital cameras, other similar artifacts may occur at other wavelengths

and choose "Color," and in the menu that pops up, then choose "RGB Split."

It is also possible to use the same equipment for spectrofluorimetry, using a different light source. I used a blue light-emitting diode, with emission centered at 469 nm and the same acetone extract as used for the absorption spectrum. This light did not interfere with the fluorescence recording, but to get rid of the blue light signal completely, one can use only the red light channel for plotting the fluorescence. This also improves the signal-to-noise ratio considerably (Figs. 29.10 and 29.11). My camera does not have a good sensitivity above 640 nm, so it is not particularly good for this purpose. The red and infrared sensitivity differs between camera models. To test a camera for infrared sensitivity, you can use an infrared remote control, for instance, one used for TV. You should use a filter to block short-wave radiation from the second-order spectrum if you are particularly interested in the long-wavelength region.

The best results were obtained with the sample very close to the slit. Since light-emitting diodes with a number of peak wavelengths are now available, it should also be possible to determine rough excitation spectra with this device and to analyze mixtures of fluorescent substances. Using 532 nm excitation light from a "green" laser pointer, I have recorded light-induced fluorescence and reflectance changes in plant leaves.

29.5 Suggestions for Further Experimentation

There are many experiments that one can perform with this simple equipment or simple modifications of it. With the lamp I used, it is a bit difficult to get proper exposure in the blue part of the spectrum. A more appropriate spectrum would probably be obtained from a photographic flashlight, but my camera lacks the possibility to synchronize an external flash. Otherwise this could protect sensitive samples from excessive light, since the measurement light is required only for about a millisecond.

Many cameras can take a series of pictures in rapid succession. Using this it should be possible to study rapid spectral changes, such as those that rhodopsin and phytochrome undergo upon illumination. If you wish to do such experiments, you should equip your lamp (or sample compartment) with some kind of shutter, so that you start exposing your sample only when you start recording spectra. For showing spectra to a large auditorium, you can use a video camera instead of an ordinary digital camera.

Recording such spectra of scattering samples as plant leaves or yeast suspensions is more difficult than clear samples,

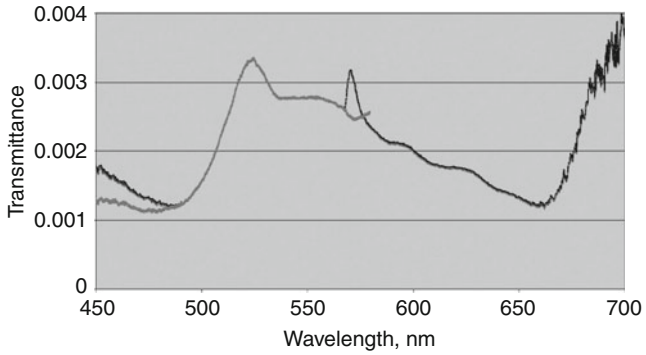

Fig. 29.12 Transmission spectrum of a leaf of *Abutilon hybridum*. This leaf is neither very thin nor very thick. All three color channels were used for the range 450–700 nm (*black line*), and from 450 to 580 the spectrum was also recorded using blue and green channels only. The two methods deviate in the 450–470-nm and the 570–580-nm bands. An exposure time of 1/1,600 s was used for the reference and 1/2 s for the sample, in both cases with stop 8. No extra light baffles were used

because light is scattered in unwanted directions. However, it should be possible to record also spectra of such samples if you insert light baffles of black paper or cardboard in the box, to prevent as much scattered light as possible from reaching the DVD surface. There should be no risk that the measurement light is too weak, since the exposure time of the camera can be increased. Figure 29.12 shows an example of what can be measured without extra light baffles. Note again the artifact near 580 nm appearing when the red channel is included. Note that this graph does not show all light that penetrates through the leaf, only that which propagates in the direction of the camera (via the DVD). A better approximation of the total transmitted light can perhaps be obtained if a piece of filter paper or similar scattering, nonabsorbing material, is inserted between the leaf and the slit and also used for the reference measurement.

Upon reduction, oxygenation, or pH changes, many substances, like cytochrome *c* and hemoglobin, undergo absorption changes that you should be able to observe (certainly in solution, and in some cases even in vivo). For a procedure for preparing a solution of cytochrome *c* from yeast, see the original paper by Keilin (1930), but you can scale it down at least ten times (i.e., extract 100 g or less of yeast instead of 1 kg).

If you are interested in computer programming, it should be possible to modify the ImageJ program so that spectra can be immediately displayed on the computer screen when a sample is put in place. Many "plug-ins" for ImageJ are already available in the public domain.

Some simple chemical experiments are suggested by Wakabayashi et al. (1998). Information about CDs and DVDs is provided by Birkett (2002).

If the slit of the apparatus is illuminated with sunlight or skylight, one can record some Fraunhofer absorption lines. I could catch lines for hydrogen (434, 486, and 656 nm), magnesium (517 nm), and sodium (589 nm) in the Sun and the molecular band of oxygen (688 nm) in the terrestrial atmosphere. A use of Fraunhofer lines in biological research is to measure chlorophyll fluorescence from plants at these wavelengths, where disturbing daylight is very weak (Liu et al. 2005, Corp et al. 2006). For satellite measurements only the lines from the solar atmosphere can be used.

An adaptation of the apparatus that allows the study of photochemical reactions in a living leaf has been published by Björn and Li (2013).

References

Birkett D (2002) The chemistry of optical discs. J Chem Educ 79: 1081–1087

Björn LO, Li S (2013) Teaching about photosynthesis with simple equipment: analysis of light-induced changes in fluorescence and reflectance of plant leaves. Photosynth Res 116:349–353. doi:10.1007/s11120-013-9858-6

Corp LA, Middleton EM, McMurtrey JE, Entcheva Campbell PK, Butcher LM (2006) Fluorescence sensing techniques for vegetation assessment. Appl Optics 45:1023–1033

Keilin D (1930) Cytochrome and intracellular oxidase. Proc Roy Soc London B 106(749):418–444

Kohl SK, Landmark JD, Stickle DF (2006) Demonstration of absorbance using digital color image analysis and colored solutions. J Chem Educ 83:644–646

Liu L, Zhang Y, Wang J, Zhao C (2005) Detecting solar-induced chlorophyll fluorescence from field radiance spectra based on the Fraunhofer line principle. IEEE Transact. Geosci. Remote Sens 43:827–832

Wakabayashi F, Hamada K (2006) A DVD spectroscope: a simple, high-resolution classroom spectroscope. J Chem Educ 83:56–58

Wakabayashi F, Hamada K, Sone KJ (1998) CD-ROM spectroscope: a simple and inexpensive tool for classroom demonstrations on chemical spectroscopy. J Chem Educ 75:1569–1570

Index

L.O. Björn (ed.), *Photobiology: The Science of Light and Life*,
DOI 10.1007/978-1-4939-1468-5, © Springer Science+Business Media New York 2015